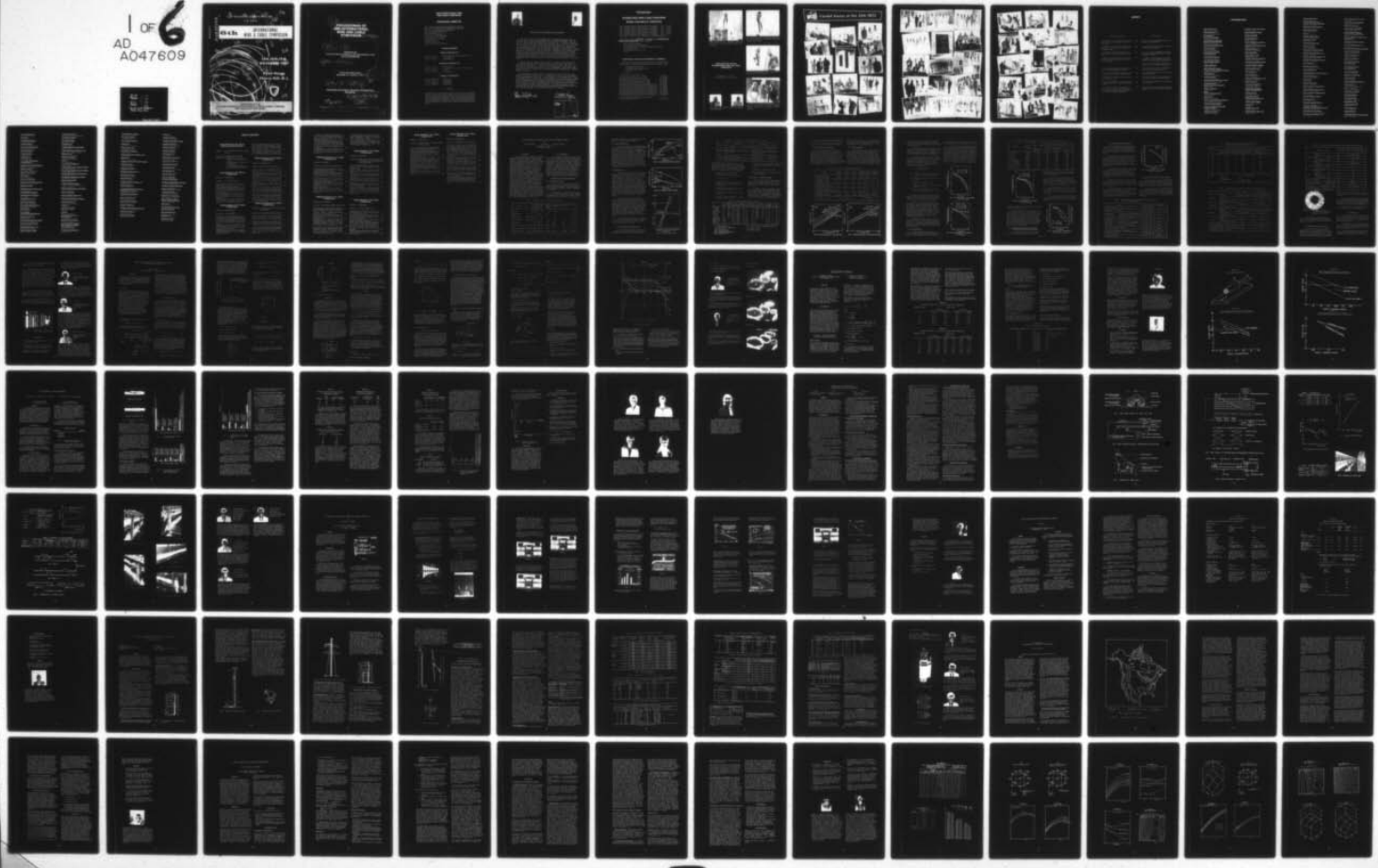


AD-A047 609 ARMY COMMUNICATIONS RESEARCH AND DEVELOPMENT COMMAND --ETC F/G 9/1
PROCEEDINGS OF INTERNATIONAL WIRE AND CABLE SYMPOSIUM (26TH) CH--ETC(U)
NOV 77 E F GODWIN

UNCLASSIFIED

1 OF 6
AD
A047609

NL



ADA 047609

cm PROCEEDINGS
of the

6th

INTERNATIONAL
WIRE & CABLE SYMPOSIUM

15th, 16th, 17th
NOVEMBER 1977

Hyatt House
Cherry Hill, N.J.



SPONSORED BY THE
U.S. ARMY COMMUNICATIONS RESEARCH & DEVELOPMENT COMMAND
FORT MONMOUTH, NEW JERSEY

⑥

PROCEEDINGS OF 26th INTERNATIONAL WIRE AND CABLE SYMPOSIUM (26th)

⑦ Final rept.

Sponsored by
Communications Research and Development Com-
mand (CORADCOM)

⑧ Elmer F. Godwin

Cherry Hill, New Jersey
November 15, 16 and 17, 1977.



⑩ Nov 77 ⑪ 478P.

APPROVED FOR PUBLIC RELEASE; DISTRIBUTION
UNLIMITED

⑫ 11162705AH94

New
⑬ 410489

⑭ ⑮

Army Communications Research and Development
Command, Fort Monmouth, NJ

HB

26th INTERNATIONAL WIRE AND CABLE SYMPOSIUM

SYMPORIUM COMMITTEE

Elmer F. Godwin, Chairman, USA CORADCOM (201) 544-2770
Milton Tenzer, Co-Chairman, USA CORADCOM (201) 544-4834
Adolf Asam, ITT Electro-Optical Products Division
Marta Farago, Northern Telecom Ltd.
F. M. Farrell, 3M Company
Irving Kolodny, General Cable Corp.
Sherman Kottle, Dow Chemical U.S.A.
Trish McGillen, Icore International
Joe Neigh, AMP Inc.
Frank Short, Belden Corp.
George H. Webster, Bell Laboratories

TECHNICAL SESSIONS

Tuesday, 15 November 1977

9:30 a.m. Session I: Tutorial—Metrication—Smooth Change or Crisis
2:00 p.m. Session II: Cable Materials I
2:00 p.m. Session III: Cable Applications

Wednesday, 16 November 1977

9:00 a.m. Session IV: Cable Materials II
9:00 a.m. Session V: Cable Manufacture & Aluminum Telephone Cable
2:00 p.m. Session VI: Filled Cable
2:00 p.m. Session VII: Fire Retardancy

Thursday 17 November 1977

9:00 a.m. Session VIII: Fiber Optics I
9:00 a.m. Session IX: Cable Design I
2:00 p.m. Session X: Fiber Optics II
2:00 p.m. Session XI: Cable Design II

PAPERS

Responsibility for the contents rests upon the authors and not the symposium Committee or its members. After the symposium all the publication rights of each paper are reserved by their authors, and requests for republication of a paper should be addressed to the appropriate author. Abstracting is permitted, and it would be appreciated if the symposium is credited when abstracts or papers are republished. Requests for individual copies of papers should be addressed to the authors.

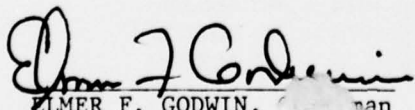


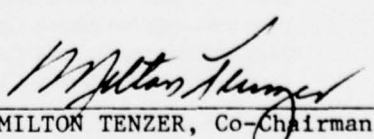
MESSAGE FROM THE CHAIRMAN AND CO-CHAIRMAN

Once again it is your chairman's and co-chairman's pleasant duty to welcome you to another International Wire and Cable Symposium. This is the 26th annual session and the third at Cherry Hill. Official registration at last year's silver anniversary meeting was a record 1614, eclipsing the previous year's high mark by over 15%, the largest such increase in the symposium's history. Non United States attendance also marked a new high of 170 registrants from 27 different countries. Ten of these countries presented a total of 23 technical papers. Representatives from United States government agencies presented or co-authored six papers. The remaining papers, approximately 50% of the total, came from United States industrial organizations. We can be justly proud of attracting such a representative cross section of wire and cable expertise from all over the world.

Judging from the response to the call for papers, the participation and interest in this year's symposium will at least equal last year's enthusiastic experience. A total of 58 technical papers covering a broad spectrum of wire and cable subjects will be presented. This year's symposium opens with a timely tutorial session entitled "Metrication - Smooth Change or Crisis".

The symposium committee agreed to extend the term of office of its members from three to four years. Consequently, there are no retirements of committee members this year. The chairman and co-chairman wish to take this opportunity to express their appreciation to all the committee members and to representatives of government activities and the many individual organizations for their sustained efforts and cooperation in contributing to the present success of this symposium. The future success of this symposium and the mutually beneficial rewards derived therefrom depend on the continued support of all associated with this endeavor.


ELMER F. GODWIN, Chairman


MILTON TENZER, Co-Chairman

| | | | |
|-----------------------------|--|-----------------------------|--|
| ACCESSION No. | | FILE SECTION | |
| DATE RECEIVED | | DATE ISSUED | |
| RECEIVED BY | | BY | |
| DISTRIBUTION/MATERIAL CODES | | DISTRIBUTION/MATERIAL CODES | |
| DRAFT | | DRAFT | |
| SPECIAL | | SPECIAL | |

A

PROCEEDINGS

INTERNATIONAL WIRE & CABLE SYMPOSIUM

BOUND—AVAILABLE AT CORADCOM

20th International Wire & Cable Symposium Proceedings — 1971 — \$ 4.00
21st International Wire & Cable Symposium Proceedings — 1972 — \$ 6.00
22nd International Wire & Cable Symposium Proceedings — 1973 — \$ 7.00
23rd International Wire & Cable Symposium Proceedings — 1974 — \$ 8.00
24th International Wire & Cable Symposium Proceedings — 1975 — \$10.00
°26th International Wire & Cable Symposium Proceedings — 1977 — \$10.00
°Extra Copies—1-3 \$10.00; next 4-10 \$9.00; next 11 and above \$5.00 each.

Make check or bank draft **PAYABLE** in **US dollars** to the **INTERNATIONAL WIRE & CABLE SYMPOSIUM** and forward request to:

Mr. E. F. Godwin, Chairman
International Wire & Cable Symposium
US Army Communications Research & Development Command
ATTN: DRSEL-TL-ME
Fort Monmouth, New Jersey 07703
U.S.A.

PHOTOCOPIES—AVAILABLE AT DEPARTMENT OF COMMERCE

Photocopies are available for complete sets of papers for 1964 and 1966 thru 1976. Information on prices and shipping charges should be requested from the:

US Department of Commerce
National Technical Information Service
Springfield, Virginia 22151
U.S.A.

Include title, year, and "AD" number.

| | |
|---|--------------|
| 13th Annual Wire & Cable Symposium (1964) | — AD 787164 |
| 15th Annual Wire & Cable Symposium (1966) | — AD A006601 |
| 16th International Wire & Cable Symposium (1967) | — AD 787165 |
| 17th International Wire & Cable Symposium (1968) | — AD 787166 |
| 18th International Wire & Cable Symposium (1969) | — AD 787167 |
| 19th International Wire & Cable Symposium Proceedings 1970 | — AD 714985 |
| 20th International Wire & Cable Symposium Proceedings 1971 | — AD 733399 |
| 21st International Wire & Cable Symposium Proceedings 1972 | — AD 752908 |
| 22nd International Wire & Cable Symposium Proceedings 1973 | — AD 772914 |
| 23rd International Wire & Cable Symposium Proceedings 1974 | — AD A003251 |
| 24th International Wire & Cable Symposium Proceedings 1975 | — AD A017787 |
| 25th International Wire & Cable Symposium Proceedings 1976 | — AD A032801 |
| Kwix Index of Technical Papers, International Wire and Cable Symposium (1952-1975) | — AD A027558 |



Guest speaker, Mr. John L. Swigert, Jr., Executive Director of the House Committee for Science and Technology.



Dr. C. G. Thornton, Director, Electronics Technology and Devices Laboratory, Fort Monmouth, welcoming attendees at the banquet.

HIGHLIGHTS OF THE 25th INTERNATIONAL WIRE AND CABLE SYMPOSIUM

November 16, 17, 18, 1976
Cherry Hill Hyatt House, Cherry Hill, N.J.



James Kanely and Joseph M. Flanigan, Retiring IWCS Committee Members.



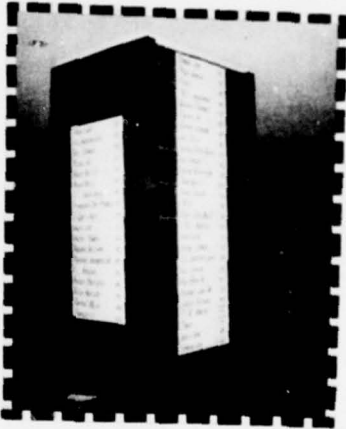
Former committee members F. Horn and M. Lipton attending Silver Anniversary Jubilee.

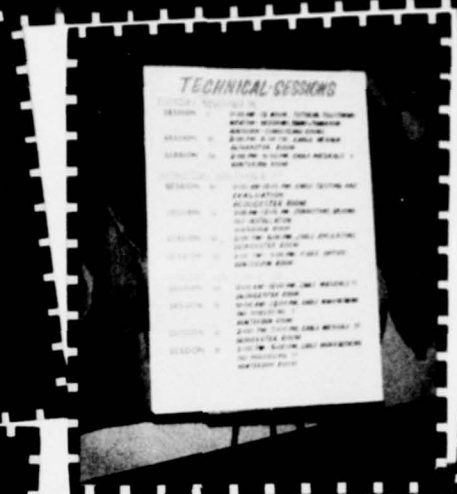


T. S. Choo, 3M Company, Outstanding Technical Paper; and J. Wimsey, US Airforce, Best Presentation, receiving awards from E. F. Godwin, Symposium Chairman.



Candid Scenes at the 25th IWCS







AWARDS

Outstanding Technical Paper

- H. Lubars and J. A. Olszewski, General Cable Corp—"Analysis of Structural Return Loss in CATV Coaxial Cable"
- J. B. McCann, R. Sabia and B. Wargotz, Bell Laboratories—"Characterization of Filler and Insulation in Waterproof Cable"
- D. E. Setzer and A. S. Windeler, Bell Laboratories—"A Low Capacitance Cable for the T2 Digital Transmission Line"
- R. Iyenger, R. McClean and T. McManus, Bell Northern Research—"An Advanced Multi-Unit Coaxial Cable for Tool PCM Systems"
- J. B. Howard, Bell Laboratories—"Stabilization Problems with Low Density Polyethylene Insulations"
- Dr. H. Martin, Kabelmetal—"High Power Radio Frequency Coaxial Cables, Their Design and Rating"
- D. Doty, AMP Inc.—"Mass Wire Insulation Displacing Termination of Flat Cable"
- T. S. Choo, Dow Chemical U.S.A.—"Corrosion Studies on Shielding Materials for Underground Telephone Cables"
- N. J. Cogelia, Bell Telephone Laboratories and G. K. Lavoie and J. F. Glahn, US Department of Interior—"Rodent Biting Pressure and Chemical Action and Their Effects on Wire and Cable Sheath"

Best Presentation

- 1968 N. Dean, B.I.C.C.—"The Development of Fully Filled Cables for the Distribution Network"
- 1969 J. D. Kirk, Alberta Government Telephones—"Progress and Pitfalls of Rural Buried Cable"
- 1970 Dr. O. Leuchs, Kable and Metalwerke—"A New Self-Extinguishing Hydrogen Chloride Binding PVC Jacketing Compound for Cables"
- 1971 S. Nordblad, Telefonaktiebolaget LM Ericsson—"Multi-Paired Cable of Nonlayer Design for Low Capacitance Unbalance Telecommunication Network"
- 1972 N. Kojima, Nippon Telegraph and Telephone—"New Type Paired Cable for High Speed PCM Transmission"
- 1973 S. Kaufman, Bell Laboratories—"Reclamation of Water-Logged Buried PIC Telephone Cable"
- 1974 R. J. Oakley, Northern Electric Co., Ltd.—"A Study into Paired Cable Crosstalk"
- 1975 G. H. Webster, Bell Laboratories—"Material Savings by Design in Exchange and Trunk Telephone Cable"
- 1975 J. E. Wimsey, United States Airforce—"The Bare Base Electrical Systems"
- 1976 Michael DeLucia, Naval Ship Research and Development Center—"Highly Fire-Retardant Navy Shipboard Cable"

CONTRIBUTORS

- Abbey Plastics Corp.** Hudson, Massachusetts
Abbott Industries, Inc. Leominster, Massachusetts
AFA Industries
Arnold Field Associates Hackensack, New Jersey
Allied Chemical Corporation Specialty Chemicals Division Morristown, New Jersey
American Hoechst Corporation Somerville, New Jersey
AMP Incorporated Harrisburg, Pennsylvania
The Anaconda Company Aluminum Division Louisville, Kentucky
The Anaconda Company Overland Park, Kansas
The Anaconda Company Wire and Cable Division Marion, Indiana
Andrew Corporation Orland Park, Illinois
ARCO Chemical Company
Division of Atlantic Richfield Company Philadelphia, Pennsylvania
ARCO Polymers Philadelphia, Pennsylvania
Arvey Corporation Jersey City, New Jersey
Austral Standard Cables Pty. Limited Melbourne, Victoria, Australia
Autometrix Division
Systems Research Laboratories Dayton, Ohio
Belden Corporation Geneva, Illinois
Bendix Electrical Components Div. Sidney, New York
Berk-Tek, Inc. Reading, Pennsylvania
BICC Telecommunication Cables Ltd. Prescot, Merseyside, England
Borden Chemical Company Leominster, Massachusetts
Boston Insulated Wire and Cable Company, Limited Hamilton, Ontario, Canada
Brand-Rex Company Willimantic, Connecticut
Buchanan Crimp Tool Products Union, New Jersey
Burgess Pigment Company Sandersville, Georgia
Burndy Corporation Norwalk, Connecticut
BUSS-CONDUX, Inc. Elk Grove, Illinois
Cable Consultants Corporation Larchmont, New York
Cables de Comunicaciones, S.A. Zaragoza, Spain
Cablewave Systems Inc. North Haven, Connecticut
Cabot Corporation Boston, Massachusetts
Camden Wire Co., Inc. Camden, New York
Campbell Technical Waxes Ltd. Crayford, Kent, England
Canada Wire and Cable Limited Winnipeg, Manitoba, Canada
Canadian Industries Limited Brampton, Ontario, Canada
Carlew Chemicals Ltd. Montreal, Quebec, Canada
R. E. Carroll, Inc. Trenton, New Jersey
Cary Chemicals, Inc. Edison, New Jersey
Central Tool & Machine Co., Inc. Bridgeport, Connecticut
Chase & Sons, Inc. Randolph, Massachusetts
Cimco Wire & Cable Inc. Allendale, New Jersey
Cities Service Company Chester Cable Operations Chester, New York
C&M Corporation Wauregan, Connecticut
Colorite Plastics Co.
Division Dart Industries, Inc. Ridgefield, New Jersey
Comm/Scope Company Catawba, North Carolina
Coneica, S.A. El Salvador
CONOCO Chemicals Houston, Texas
Dainichi-Nippon Cables, Ltd. Osaka, Japan

| | |
|--|---|
| Dardanio Manuli S.p.A. | The Furukawa Electric Co., Ltd. |
| Brugherio (MI), Italy | Tokyo, Japan |
| Davis-Standard Division of Crompton & Knowles Corporation | Gavitt Wire & Cable Company |
| Pawcatuck, Connecticut | Brookfield, Massachusetts |
| DCM International Corporation | Gem Gravure Co., Inc. |
| San Leandro, California | West Hanover, Massachusetts |
| Delphi Electronics Inc. | General Cable Corporation |
| Folcroft, Pennsylvania | Colonia, New Jersey |
| Disco Inc. | General Electric Company |
| Ringwood, New Jersey | Silicone Products Department |
| Dodge Fluorglas Division | Waterford, New York |
| Hoosick Falls, New York | General Telephone Company of the Northwest, Inc. |
| Dow Chemical USA | Everett, Washington |
| Midland, Mich. | BF Goodrich Chemical Division |
| Dow Corning Corporation | Cleveland, Ohio |
| Midland, Michigan | W. L. Gore & Associates, Inc. |
| Du Pont Company | Newark, Delaware |
| Wilmington, Delaware | Great American Chemical Corporation |
| Dussek Bros. (Canada) Limited | Fitchburg, Massachusetts |
| Belleville, Ontario, Canada | GTE Service Corporation |
| Eastman Chemical Products, Inc. | Stamford, Connecticut |
| Kingsport, Tennessee | Harbour Industries, Inc. |
| Economy Cable Grip Company, Inc. | Shelburne, Vermont |
| South Norwalk, Connecticut | Hardman Incorporated |
| Edmands Div. Wanskuck Company | Belleville, New Jersey |
| Providence, Rhode Island | Hatco Chemical Division |
| Elco Corporation | W. R. Grace & Co. |
| El Segundo, California | Fords, New Jersey |
| Electroconductores C.A. | Hatco Plastics Division |
| Las Palmas Caracas-Venezuela | W. R. Grace & Co. |
| Emery Industries, Inc. | Brooklyn, New York |
| Cincinnati, Ohio | Hercules Incorporated |
| Engelhard Minerals & Chemical Corp. | Wilmington, Delaware |
| Edison, New Jersey | Hercules Inc./Scott Wise |
| The Entwistle Company | Crowley, Louisiana |
| Hudson, Massachusetts | Hewlett-Packard |
| Essex Group | Palo Alto, California |
| Decatur, Illinois | High Voltage Engineering Corp. |
| Etudes & Fabrications | Burlington, Mass. |
| New York, New York | Hitachi Cable, Ltd. |
| Exxon Chemical Company U.S.A. | Chiyoda-ku, Tokyo 100, Japan |
| Houston, Texas | Huber + Suhner Ltd. |
| Fabricon Manufacturing Limited | Pfaeffikon ZH, Switzerland |
| Trenton, Ontario, Canada | Hudson Wire Company |
| Felten & Guilleaume Carlswerk AG | Ossining, New York |
| Koln, Germany | ICI United States Inc. |
| Firestone Plastics Company | Wilmington, Delaware |
| Pottstown, Pennsylvania | Icore Wire & Cable |
| FMC Corporation | Santa Barbara, California |
| Philadelphia, Pennsylvania | Independent Cable |
| Formulabs Industrial Inks, Inc. | Hudson, Massachusetts |
| Escondido, California | Indeco Peruana, S.A. |
| Foster Grant Company, Inc. | Lima, Peru |
| Subsidiary of American Hoechst Corp. | Inmont Corporation |
| Leominster, Massachusetts | St. Louis, Missouri |
| Franklin Plastics Corporation | Insulated Wire, Inc. |
| Bound Brook and Kearny, New Jersey | Union, New Jersey |
| The Fujikura Cable Works, Ltd. | International Wire Products Company |
| Tokyo, Japan | Wyckoff, New Jersey |

| | |
|---|--|
| ITT Cable-Hydrospace | Providence (Rumford), Rhode Island |
| San Diego, California | |
| ITT Cannon | Ramsey, New Jersey |
| Santa Barbara, California | |
| ITT Surprentant Division | Olex Cables Limited |
| Clinton, Massachusetts | Melbourne, Australia |
| Judd Wire Division | Omega Wire Inc. |
| Turners Falls, Massachusetts | Camden, New York |
| Kenrich Petrochemicals, Inc. | OY NOKIA AB Finnish Cable Works |
| Bayonne, New Jersey | Helsinki, Finland |
| Lamart Corporation | Pacific Electric Wire & Cable Co., Ltd. |
| Clifton, New Jersey | Taipei, Taiwan, Republic of China |
| Lamotite Products | PENN Color, Inc. |
| Cleveland, Ohio | Doylestown, Pennsylvania |
| Laribee Wire, Inc. | Pennwalt Corporation |
| Camden, New York | Philadelphia, Pennsylvania |
| S. A. Lignes Telegraphiques et Telephoniques | Penreco |
| Conflans Sainte Honorine, France | Butler, Pennsylvania |
| Madison Wire & Cable Corporation | A. E. Petsche Company, Inc. |
| Worcester, Massachusetts | Arlington, Texas |
| Maillefer Company | Phelps Dodge Communications Company |
| South Hadley, Massachusetts | White Plains, New York |
| Mark Mor Tool & Die Inc. | Phelps Dodge Copper Products Company |
| Allenwood, New Jersey | Elizabeth, New Jersey |
| 3M Company | Phelps Dodge International Corporation |
| St. Paul, Minnesota | New York, New York |
| Micro-Tek Corporation | Philadelphia Insulated Wire Company |
| Cinnaminson, New Jersey | Moorestown, New Jersey |
| Mohawk Wire & Cable Corporation | Phillips Cables Limited |
| Leominster, Massachusetts | Brockville, Canada |
| Monsanto Company | Phillips Chemical Company |
| Akron, Ohio | (A Division of Phillips Petroleum Co.) |
| Monsanto Industrial Chemicals Co. | Bartlesville, Oklahoma |
| St. Louis, Missouri | Pirelli USA Representative Corporation |
| The Montgomery Company | New York, New York |
| Windsor Locks, Connecticut | Plastoid Corporation |
| Samuel Moore and Company | New York, New York |
| Aurora, Ohio | Plymouth Rubber Company, Inc. |
| H. Muehlstein & Co., Inc. | Canton, Massachusetts |
| Greenwich, Connecticut | Plymouth Wire and Cable Company |
| Nesor Alloy Corporation | Worcester, Massachusetts |
| West Caldwell, New Jersey | Polymer Services, Inc. |
| New England Printed Tape Co. | East Brunswick, New Jersey |
| Pawtucket, Rhode Island | Prodelin Inc. |
| NKF Kabel B.V. | Hightstown, New Jersey |
| Delft, Netherlands | Radix Wire Company |
| N.L. Industries | Euclid, Ohio |
| Plastics & Specialty Chemicals | Raychem |
| Hightstown, New Jersey | Menlo Park, California |
| Nokia Electronics, Inc. | Reichhold Chemicals, Inc. |
| Atlanta, Georgia | Cooke Division |
| Nonotuck Manufacturing Company | Hackettstown, New Jersey |
| South Hadley, Massachusetts | Reliable Electric Company |
| North Anson Reel Company | Franklin Park, Illinois |
| North Anson, Maine | Rexene Polyolefins Company |
| Northeast Wire Company, Inc. | Rexene Styrenics Company |
| Holyoke, Massachusetts | (Dart Industries, Inc.) |
| Northern Telecom Limited | Paramus, New Jersey |
| Lachine, Quebec, Canada | The Rochester Corporation |
| | Culpeper, Virginia |

| | |
|--|--|
| The Rockbestos Company | Teldor Ltd. |
| New Haven, Connecticut | D.N. Jezreel, Israel |
| John Royle and Sons | Teledyne Thermatics |
| Paterson, New Jersey | Elm City, North Carolina |
| S.A. Telecommunications | Teledyne Western Wire & Cable |
| Paris, France | Los Angeles, California |
| Sartomer Co. | Telephone Cables Ltd. |
| Westchester, Pennsylvania | Dagenham, Sussex, England |
| Schulz Controls, Inc. | Tenneco Chemicals |
| New Haven, Connecticut | Piscataway, New Jersey |
| Shell Chemical Company | Tensolite Company |
| Houston, Texas | Buchanan, New York |
| Showa Electric Wire & Cable Co., Ltd. | TFE Industries, Inc. |
| Kawasaki, Japan | Warwick, R.I. |
| Siemens AG | Thermax Wire Corporation |
| Munchen, West Germany | Flushing, New York |
| Southwest Chemical & Plastics Company | Times Wire & Cable Co. |
| Seabrook, Texas | Wallingford, Conn. |
| Southwire Company | Torpedo Wire & Strip, Inc. |
| Carrollton, Georgia | Pittsfield, Pennsylvania |
| Spargo Wire Company | Trea Industries, Inc. |
| Rome, New York | North Kingstown, Rhode Island |
| Springborn Laboratories, Inc. | Ube Industries, Ltd. |
| Enfield, Connecticut | Chiyodaku, Tokyo, Japan |
| Sterling/Davis Electric | Union Carbide Corp. |
| Wallingford, Connecticut | New York, New York |
| Storm Products Co. | US Steel Corporation |
| Inglewood, California | Electrical Cable Division |
| Sumitomo Electric Industries, Ltd. | Worcester, Massachusetts |
| Yokohama, Japan | Wardwell Braiding Machine Company |
| Sun Chemical Corp. | Central Falls, Rhode Island |
| Paterson, New Jersey | The Ware Chemical Corporation |
| Sun Petroleum Products Company | Stratford, Connecticut |
| (A Division of Sun Oil Co.) | Weber & Scher Mfg. Co., Inc. |
| Philadelphia, Pennsylvania | Newark, New Jersey |
| Superior Cable Corporation | G. Whitfield Richards Co. |
| Hickory, North Carolina | Philadelphia, Pennsylvania |
| Albert H. Surprenant, Inc. | Whitmor Wire & Cable Corp. |
| Jaffrey, New Hampshire | North Hollywood, California |
| Syncro Machine Company | Wilson Products Company |
| Perth Amboy, New Jersey | Division Dart Industries, Inc. |
| Synthetic Thread Co. | Neshanic, New Jersey |
| Bethlehem, Pennsylvania | Wire Journal |
| Tamaqua Cable Products Corporation | Guilford, Connecticut |
| Schuylkill Haven, Pennsylvania | Witco Chemical Corporation |
| Technical Coatings Co. | Sonneborn Division |
| Nutley, New Jersey | New York, New York |
| Teknor Apex Company | Woven Electronics Div. |
| Pawtucket, Rhode Island | Mauldin, South Carolina |
| | Wyre-Wynd, Inc. |
| | Jewett City, Connecticut |
| | Wyrrough and Loser |
| | Trenton, New Jersey |

TABLE OF CONTENTS

**Tuesday, November 15, 1977—9:30 am
Hunterdon and Cumberland Rooms**

SESSION I: Tutorial—Metrication—Smooth Change or Crisis

Chairperson: Joe Neigh, AMP, Incorporated
Panel Members: Walter Short, Crouse-Hinds
 John Haas, Navy, DOD Metrication Panel
 Wilson McGruder, REA, Department of Agriculture
 Jim Eagan, AMP, Incorporated
 Bruce Tyrrell, Northern Telecom, Ltd.

**Tuesday, November 15, 1977—2:00 pm
Gloucester Room**

SESSION II: Cable Materials I

Chairperson: F. Farrell, 3M Company

NEW POLYMETHYL PENTENE-1 INSULATED ELECTRONICS WIRES, M. Okada, A. Kusui, H. Takemori, *Dainichi-Nippon Cables, Ltd., Osaka, Japan*
 BUBBLE-FORMATION MECHANISM IN THE EXTRUSION PROCESS OF FOAMED PLASTIC INSULATION, K. Orimo and T. Shimano, *The Furukawa Elec. Co., Ltd., Tokyo, Japan*
 EFFECTIVE RODENT SHIELDS AND CABLE ELECTRICAL PERFORMANCE, H. M. Hutson, *Rural Electrification Administration, and K. W. Brownell, Jr., Brand-Rex Co.*
 THE PERFORMANCE OF CABLE RECLAMATION, S. Kaufman, R. Sabia, J. L. Williams, *Bell Laboratories, and M. Brauer, T. F. Kropinski, NL Industries*

**Tuesday, November 15, 1977—2:00 pm
Hunterdon Room**

SESSION III: Cable Applications

Chairperson: Joe Neigh, AMP, Inc.

PATTERN BELT, A NEW INDUCTIVE WIRE FOR POSITION DETECTION OF LINEAR MOTOR VEHICLES, T. Sasaki, *Japanese National Railways, Tokyo, Japan*, T. Aono, *Japanese National Railways, Hukuoka, Japan*, and T. Asai, T. Hoshikawa, *Hitachi Cable, Ltd., Hitachi, Japan*
 AN IMPROVED ETFE BASED CABLE FOR AEROSPACE AND INDUSTRIAL APPLICATIONS, E. Bascou and M. Marechal, *FILOTEX, Manufacture de Fils et Câbles Electriques, Draveil, France*
 WIRE INSULATION DESIGNED FOR TELECOMMUNICATIONS EQUIPMENT, A. F. Faber, *Philadelphia Insulated Wire Co., Inc.*

| | |
|---|----|
| MULTI-PAIR SUBSCRIBER CABLES FOR VERTICAL INSTALLATION IN HIGH-RISE BUILDINGS, K. Mori, <i>Nippon Telegraph and Telephone Public Corporation, Tokyo, Japan</i> , and R. Yashiro, T. Umetsu, <i>The Fujikura Cable Works, Ltd., Tokyo, Japan</i> | 53 |
| GEO-TELEPHONY: THE INSTALLATION OF SUBSURFACE TRANSMISSION MEDIA, F. A. Huszarik, <i>Transmission Media Development, Bell-Northern Research</i> | 62 |

**Wednesday, November 16, 1977—9:00 am
Gloucester Room**

SESSION IV: Cable Materials II

Chairperson: Sherman Kottle, Dow Chemical

| | |
|--|-----|
| OXIDATIVE STABILITY OF HIGH DENSITY POLYETHYLENE, K. D. Kiss and E. G. Malawer, <i>Phelps Dodge Communications Co.</i> | 68 |
| A BIFUNCTIONAL ANTIOXIDANT/METAL DEACTIVATOR FOR POLYOLEFIN WIRE INSULATION, A. Patel, <i>CIBA-GEIGY Corp.</i> | 83 |
| NEW COPPER DEACTIVATORS FOR POLYOLEFINS, K. Yamaguchi, T. Yoshikawa, N. Sakamoto, S. Ohtomo, K. Kanda, S. Oh-e and T. Imaoka, <i>Ube Industries, Ltd., Tokyo, Japan</i> | 87 |
| SULFIDE TREEING: A DILEMMA FOR TELECOMMUNICATION CABLES, B. D. Gesner, <i>Bell Labs</i> | 94 |
| ORGANIC COLORANTS FOR CCP CABLE INSULATION, Hiroshi Ohshima and Senkichi Kawakubo, <i>Musashino Electrical Communication Laboratory, Nippon Telegraph and Telephone Public Corp., Tokyo, Japan</i> | 102 |
| ELECTRICAL PROPERTIES OF POLYPROPYLENE HOMO- AND COPOLYMERS AT HIGH FREQUENCIES, D. H. Buerkle, J.-C. Rebeille, <i>ATO Chimie -Usine de Mont, Orthez, France</i> and J.-C. Bobo, B. L. Hochon, <i>Laboratoires de MARCOUSSIS, Cie Générale d'Électricité, MARCOUSSIS, France</i> | 110 |

**Wednesday, November 16, 1977—9:00 am
Hunterdon Room**

SESSION V: Cable Manufacture & Aluminum Telephone Cable

Chairperson: George Webster, Bell Laboratories

| | |
|---|-----|
| DYNAMIC WATERPROOF FILLING PROCESS MONITOR, J. A. Hudson and A. K. Long, <i>Cable & Wire Product Engineering Control Center, Western Electric Co.</i> | 119 |
| HIGH-SPEED SZ TWISTING AND STRANDING MACHINES USING STRAIGHT ACCUMULATORS, Dieter Vogelsberg, <i>Siemens AG, Neustadt/Coburg, Germany</i> | 127 |
| LEAKY COAXIAL CABLE WITH HELICAL MEMBRANE POLYETHYLENE INSULATION BY DIRECT EXTRUSION, Y. Saito, H. Kumamaru, K. Sakamoto, and S. Shimada, <i>Sumitomo Electric Industries, Ltd., Yokohama, Japan</i> | 134 |

| | |
|--|-----|
| EC GRADE FULLY ANNEALED ALUMINUM CONDUCTORS IN PAPER INSULATED TELEPHONE CABLE, R. J. Lewis and N. W. Peters, <i>Telecom Australia, Headquarters, Melbourne, Australia</i> | 141 |
| STAIRCASE TO ALUMINUM—THE BRITISH POST OFFICE PROGRAM FOR A NEAR-COMPLETE SUBSTITUTION OF ALUMINUM FOR COPPER CONDUCTORS IN LOCAL LOOP CABLES, H. J. C. Spencer, <i>British Post Office Telecommunications Headquarters, London, England</i> | 149 |
| ALUMINUM ALLOY CABLE CONDUCTORS—A PROVEN SUBSTITUTE FOR COPPER, D. R. Bissell, <i>Post Office Telecommunications Headquarters, London, England</i> | 156 |

**Wednesday, November 16, 1977—2:00 pm
Gloucester Room**

SESSION VI: Filled Cable

Chairperson: I. Kolodny, General Cable Corp.

| | |
|---|-----|
| LIFE PREDICTION OF INSULATIONS FOR FILLED CABLES IN PEDESTAL TERMINALS, G. A. Schmidt, <i>General Cable Corp., Research Center</i> | 161 |
| IMMUNITY TO WATER OF FOAM, FOAM-SKIN AND SOLID INSULATED FILLED TELEPHONE CABLES, J. A. Olszewski, <i>Research Center, General Cable Corp.</i> | 182 |
| ANALYSIS AND CONTROL OF CAPACITANCE UNBALANCE TO GROUND IN FILLED CABLE, Joaquin Prósper, <i>Cables de Comunicaciones S.A.</i> | 188 |
| THE MANUFACTURING CAUSES OF CAPACITANCE UNBALANCE TO GROUND IN FILLED TELECOMMUNICATIONS CABLE, W. M. Flegal and B. C. Vrieland, <i>Western Electric Co.</i> | 197 |
| A NEW GENERATION OF FILLED CORE CABLE, T. K. McManus, <i>Northern Telecom Canada Ltd., Montreal, Quebec, Canada, and R. Beveridge, Sask. Tel., Regina, Saskatchewan</i> | 204 |

**Wednesday, November 16, 1977—2:00 pm
Hunterdon Room**

SESSION VII: Fire Retardancy

Chairperson: Marta Farago, Northern Telecom, Ltd.

| | |
|--|-----|
| DEVELOPMENT OF FLAME RESISTANT CABLES FOR NUCLEAR POWER PLANT AND THEIR QUALIFICATION TEST RESULTS, J. Matsuo, M. Hanai, Y. Yamamoto, T. Sakurai, I. Nishikawa, <i>Showa Electric Wire & Cable Co., Ltd. Kawasaki, Japan</i> | 216 |
| SPECIAL TELEPHONE CABLES AGAINST FIRE HAZARDS, G. Beretta and P. Calzolari, <i>Industria Pirelli S.p.A., Milan, Italy</i> | 228 |
| PERFORMANCE OF FLUOROPOLYMER WIRE AND CABLE INSULATION IN LARGE SCALE TESTS FOR FLAMMABILITY, SMOKE, CORROSIVE OFF-GASES AND CIRCUIT INTEGRITY, E. W. Fasig, Jr., D. B. Allen, and J. C. Reed, <i>E. I. du Pont de Nemours & Co., Inc.</i> | 239 |
| THE EVALUATION OF COMMUNICATIONS CABLE FLAMMABILITY USING THE RELEASE RATE-APPARATUS, E. J. Gouldson, G. R. Woollerton, <i>Northern Telecom Limited, Montreal, Quebec, and E. E. Smith, H. C. Hershey, Ohio State University</i> | 249 |

| | |
|---|-----|
| INTERLABORATORY EVALUATION AND CORRELATION STUDIES WITH THE ARAPAHOE AND NBS SMOKE CHAMBERS, C. J. Sparkes, J. J. Kracklauer, and R. E. Legg, <i>Arapahoe Chemicals, Inc.</i> | 261 |
| EFFECTIVE METHODS OF RETARDING FIRE PROPAGATION THROUGH CABLE PENETRATIONS IN TELEPHONE EXCHANGES, R. L. Medynski, <i>Bell-Northern Research, Montreal, Quebec</i> | 269 |

**Thursday, November 17, 1977—9:00 am
Gloucester Room**

SESSION VIII: Fiber Optics I

Chairperson: Milton Tenzer, US Army Communications Research and Development Command (CORADCOM)

| | |
|---|-----|
| DESIGN AND PERFORMANCE OF AN OPTICAL CABLE, M. J. Buckler, M. R. Santana and S. C. Shores, <i>Bell Laboratories</i> | 276 |
| OPTICAL FIBER CABLE PLACING TECHNIQUES—LONG SECTION LENGTHS, R. Soyka, <i>GTE California</i> | 281 |
| APPLICATION OF OPTICAL TRANSMISSION IN OUTSIDE PLANTS, E. E. Basch and R. A. Beaudette, <i>GTE Laboratories Inc.</i> | 287 |
| INSTALLATION OF AN OPERATIONAL TWO-KILOMETER FIBER OPTIC CABLE, G. J. Wilhelm, J. C. Smith, and G. W. Bickel, <i>ITT Electro-Optical Products Division</i> | 293 |
| REINFORCED SINGLE FIBER CABLES FOR OPTICAL DATA LINK APPLICATIONS, L. L. Blyler, Jr. and A. C. Hart, Jr., <i>Bell Laboratories</i> | 300 |
| SOME FIELD APPLICATIONS OF FIBER OPTIC CABLE SYSTEMS, D. F. Hemmings, J. B. Wise, <i>Canada Wire & Cable Co. Ltd., Toronto, Ontario, Canada, and F. R. McDevitt, Harris Corp., Electronic Systems Division, Melbourne, Fla.</i> | 307 |

**Thursday, November 17, 1977—9:00 am
Hunterdon Room**

SESSION IX: Cable Design I

Chairperson: Frank Short, Belden Corp.

| | |
|--|-----|
| A NEW CABLE JACKET DESIGN WITH BUILT-IN AXIAL STRESS RELIEF, W. Lynen and R. Ney, <i>Lynenwerk K.G., Eschweiler, West Germany</i> | 312 |
| STATE OF THE ART TEST FOR MECHANICALLY INDUCED NOISE VOLTAGE IN ELECTRONIC CABLE, J. W. Kincaid, Jr., <i>Belden Corp.</i> | 321 |
| A STUDY COMPARING PAIRS AND QUADS, Valentin Abadia, <i>Cables de Comunicaciones S.A.</i> | 329 |
| ON THE COMPUTATION OF PRIMARY PARAMETERS OF CIRCUITS IN TWISTED MULTIWIRE CABLES, V. Belevitch, <i>MBLE Res. Lab., Brussels, Belgium</i> , G. C. Groenendaal, <i>Philips Res. Labs, Eindhoven, Netherlands</i> , and R. R. Wilson, <i>NKF Kabel BV, Delft, Netherlands</i> | 338 |
| PARAMETRIC Design of flexible coaxial cables based on a new multiwire impedance theory, G. H. Nowak, <i>ITT Cable-Hydrospace</i> | 343 |

Thursday, November 17, 1977—2:00 pm
Gloucester Room

SESSION X: Fiber Optics II

Chairperson: Adolf R. Adam, ITT Electro-Optical Products Division

- DUCTILE PLASTIC OPTICAL FIBERS WITH IMPROVED VISIBLE AND NEAR INFRARED TRANSMISSION, *H. M. Schleinitz, E. I. du Pont de Nemours & Co.* 352
 STRESS STRAIN AND OPTICAL TRANSMISSION DATA ON PLASTIC CLAD SILICA FIBER OPTIC CABLES WITH AND WITHOUT CONNECTORS, *G. C. Adams, E. I. du Pont de Nemours & Co.* 356
 DESIGN CONSIDERATIONS FOR SINGLE FIBER CONNECTORS, *W. L. Schumacher, AMP Inc.* 362
 INFLUENCE OF JACKETING ON THE TRANSMISSION LOSS OF LOW-LOSS OPTICAL FIBERS, *B. Hillerich, P. Rautenberg, D. S. Parmar, P. Schlang, AEG-Telefunken Kabelwerke AG, Mulheim, W. Germany* 367
 ON SITE LOCATION OF OPTICAL FIBER DEFECTS AND EVALUATION OF TRANSMISSION LOSS, *B. Hillerich, AEG-Telefunken Kabelwerke AG, Mulheim, W. Germany* 373
 EXPERIENCE TO-DATE WITH OPTICAL FIBER CABLES, *G. Bahder and J. A. Olszewski, General Cable Corp.* 380

Thursday, November 17, 1977—2:00 pm
Hunterdon Room

SESSION XI: Cable Design II

Chairperson: Trish McGillen, Icore International

- ACTIVE PROTECTION DEVICE FOR SUPPRESSION OF INDUCED LONGITUDINAL VOLTAGES IN TELECOMMUNICATION CABLES IN THE FREQUENCY RANGE FROM 16 TO 3,400 Hz, *W. Baum, Baum-Elektrophysik GmbH, Nuernberg, West Germany, A. Silberhorn, Deutsche Bundespost, Darmstadt, West Germany, M. Still, Kabel-und Metallwerke Gutehoffnungshuette A.G. (Kabelmetal), Hannover, West Germany* 385
 CROSSTALK CONSIDERATIONS IN PAIRED COMMUNICATION CABLES FOR PCM USE, *R. Hauschildt, Phillips Cables Ltd., Brockville, Canada* 398
 PARAMETERS AFFECTING NEAR-END CROSSTALK IN SCREENED CABLES, *J. P. Savage, Bell Laboratories, and T. G. Hardin, Western Electric Co., Inc., Norcross, Ga.* 420
 CALCULATION OF CROSSTALK IN BALANCED PAIR CABLES BY MEANS OF SIMULATION, *Nils Holte, Electronics Research Laboratory, Trondheim, Norway* 428
 A STATISTICAL METHOD FOR DETERMINING CUSTOMER NOISE DUE TO WIRE PAIR UNBALANCES, *D. S. Wilson, Bell Laboratories* 440
 DETERMINING MAGNITUDE OF CABLE CAPACITANCE AND RESISTANCE UNBALANCE FROM LONGITUDINAL BALANCE MEASUREMENTS, *M. L. Brewer, Rural Electrification Administration, Washington, D. C.* 454

NEW POLYMETHYL PENTENE-1 INSULATED ELECTRONICS WIRES

By

Masaaki Okada,

Akio Kusui,

Hayashi Takemori

Dainichi-Nippon Cables, Ltd.

Osaka, Japan

Abstract

Polymethyl Pentene-1 (PMP) was originally developed by Imperial Chemical Industries, Ltd. With its low loss characteristics, high insulation resistance, high dielectric strength and high melting point, this polymer was examined for use as electronics wire insulations but was found unsuited for wire insulations because of its low flexibility. Mitsui Petrochemical Industries, Ltd. recently started to exclusively produce the polymer and improved the polymer with its accumulated polymerization techniques. Focusing attention on Mitsui's new PMP, Dainichi-Nippon Cables, Ltd. has conducted research on new PMP to explore its application to electronics wires. Mitsui's improved resin has satisfactory flexibility at ambient temperature as well as the outstanding characteristics inherent in the polymer. Dainichi's research has been directed also to cold flexible PMP, flame retardant PMP and foamed PMP and matured to various electronics wires of excellent properties. Cables insulated with the natural polymer are comparable to fluorocarbon polymer insulated wires in electrical properties and superior to XLPE in heat resistance. Those insulated with flame retardant type PMP compounds have the flame retardancy of UL Specification, "FR-1". The use of suitable chemical blowing agents gives satisfactory insulation. The wires insulated with new PMP are expected to have a service temperature of about 130°C.

1. Introduction

In many fields particularly for use as electronics wire insulations, it has been strongly desired to provide new inexpensive materials having high electrical properties and retaining form stability at temperatures of up to 200°C or higher. Fluorocarbon polymers, although excellent insulation materials for wires, are expensive and are therefore still in limited use. With attention centered towards the improved high-melting polyolefine, polymethyl pentene-1 (PMP), provided by Mitsui Petrochemical Industries, Ltd. in place of ICI,¹ we started research on applications of the new resin to electronics wires and developed cold flexible wires, flame retardant wires and foam insulated wires.

2. Properties of Polymethyl Pentene-1

2.1 Initial Characteristics

Table 1 shows the initial characteristics at ambient temperature of natural PMP and flame retardant PMP in comparison with those of irradiation crosslinked polyethylene (XLPE), crosslinked PVC and ETFE.

Natural, PMP is approximately equivalent to XLPE in mechanical properties, close to ETFE in melting point and equivalent or superior to XLPE and ETFE in electrical properties. Flame retar-

Table 1 Typical Properties of PMP and Other Insulants

| Properties at 23°C | ASTM test method | Natural PMP | Flame retardant polyethylene PMP | Crosslinked PVC | Crosslinked PVC | ETFE |
|-------------------------------------|------------------|---------------------|----------------------------------|---------------------|----------------------|---------------------|
| Density | D792 | 0.84 | 1.1 | 0.92 | - | 1.74 |
| Melting point °C | - | 230 | 230 | - | - | 268 |
| Yield Stress kg/mm ² | D638 | 2.0 | - | 1.0 | - | 2.0 |
| Tensile Strength kg/mm ² | D638 | 1.6 | 1.4 | 1.8 | 3.1 | 4.4 |
| Elongation % | D638 | 310 | 350 | 400 | 220 | 430 |
| Volume resistivity ohm-cm | D257 | >1x10 ¹⁷ | 5x10 ¹⁶ | >1x10 ¹⁷ | 3x10 ¹⁴ | >1x10 ¹⁷ |
| Dielectric constant 1 KHz | D150 | 2.1 | 2.3 | 2.3 | 4.2 | 2.6 |
| Dissipation factor 1 KHz | D150 | 2x10 ⁻⁴ | 10x10 ⁻⁴ | 2x10 ⁻⁴ | 600x10 ⁻⁴ | 8x10 ⁻⁴ |

dant PMP is superior to crosslinked PVC and comparable to ETFE in electrical properties.

2.2 Cold Flexible PMP

Mitsui's new PMP has remarkably improved flexibility at ambient temperature as compared with the ICI grade. But the insulation is required to sufficiently flexible also at lower temperatures for use in certain areas of application. To fulfill such a requirement, we improved natural PMP with use of additional materials. Figures 1 and 2 respectively show variations in the elongation and tensile strength of typical compounds at varying temperatures. These Figures reveal that whereas cold flexible PMP retains the properties of the natural resin at ambient temperature or higher, the resin possesses greatly enhanced flexibility at lower temperatures. In fact, cold flexible PMP has stable good mechanical properties at -10°C to 150°C.

2.3 Thermal Life

To determine the service temperature and thermal life at varying temperatures of new PMP insulated wires, wire specimens were subjected to accelerated aging in an air oven. The results are given in Figure 3 in which the thermal life is shown according to Arrhenius plot. The aged specimen was helically wound around itself, and the time when cracks were found in the specimen minus 1 day was taken as the life of the specimen, because cracking indicates aging more manifestly than the deterioration in electrical properties which progresses with slow changes and because resistance to cracking is practically a most critical property. The temperature corresponding to a life of 40,000 hours (1,667 days) was taken as the service temperature. The wire specimens tested are listed in Table 2.

The bare copper wire insulated with natural PMP had a service temperature of 125°C, and the silver coated copper wire and nickel coated copper wire with the natural PMP 133°C. This indicates that despite the high resistance of the new PMP against thermal aging, copper catalyzed oxidative degradation causes accelerated aging, which however can be inhibited by the silver or nickel coating on the conductor. At the same temperature, the copper deactivator containing PMP gave the bare copper wire approximately two times the thermal life obtained in the absence of the deactivator.

The new PMP insulated wires, are expected to have a service temperature of 130°C or higher for use as novel thermally resistant electronics wires of high electrical properties.

3. PMP Dielectric Coaxial Cables

In an attempt to make the best use of the outstanding heat resistant properties and dielectric properties of new PMP for the development of

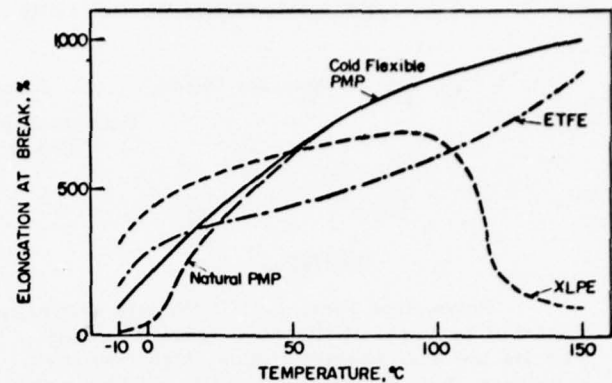


Figure 1 Ultimate Elongation at Various Temperature

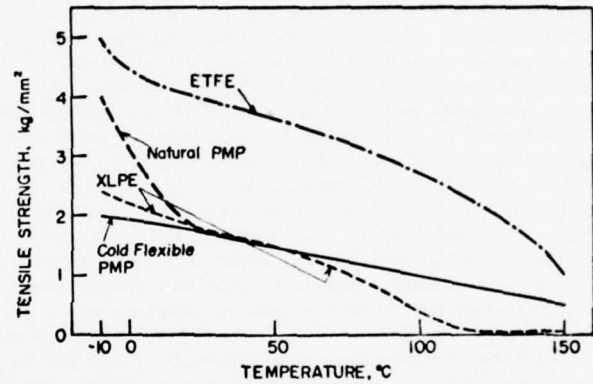


Figure 2 Tensil Strength at Various Temperature

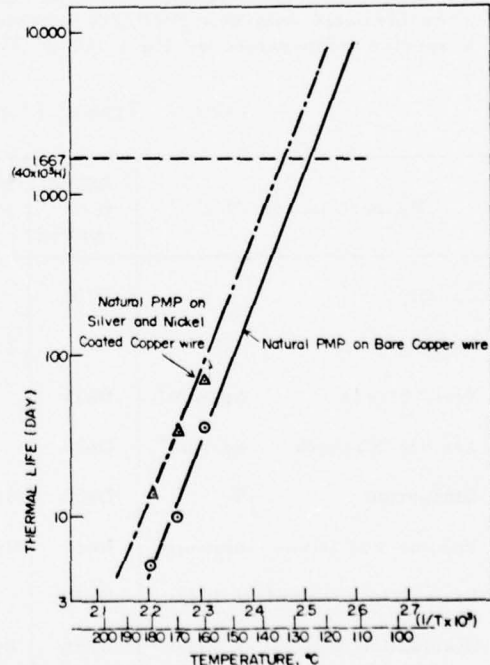


Figure 3 Thermal Life of New PMP Insulant

Table 2 Wire Specimens for Thermal Life Test of PMP

| Specimens | Conductor | | Insulation | |
|-----------|----------------------|----------------|--------------------------------------|----------------|
| | Material | Outer Dia.(mm) | Material | Outer Dia.(mm) |
| No. 1 | Bare Copper | 1.0 | Natural PMP | 3.0 |
| No. 2 | Bare Copper | 1.0 | Copper deactivator containing PMP | 3.0 |
| No. 3 | Silver Coated Copper | 1.0 | Natural PMP | 3.0 |
| No. 4 | Nickel Coated Copper | 1.0 | Natural PMP | 3.0 |

coaxial cables which are serviceable in an intermediate temperature range between the service temperatures of polyethylene and of fluoropolymers, we prepared specimens of PMP dielectric coaxial cables of the following types and tested the specimens for the evaluation of various properties.

- (1) Solid-dielectric flexible cables.
- (2) Solid-dielectric semi-rigid cables.

Our objects were:

- (1) Manufacture of heat resistant coaxial cables at low costs and with high performance.*
- (2) Increase in the power rating of radio-frequency coaxial cables.*
- (3) Improvement in solderability for easier connection.*
- (4) Increase in the phase stability of radio-frequency coaxial cables.*

(5) Improvement in the temperature dependence of the insulating properties of coaxial cables.*

(6) Reduction in the weight of cables.

(*) Polyethylene dielectric coaxial cables wire taken as standard.

3.1 Structures of Cable Specimens

Table 3 briefly shows the structures of PMP coaxial cable specimens as well as those of specimens of polyethylene coaxial cable, XLPE coaxial cable and PTFE coaxial cable tested for comparison.

Fortunately PMP has a dielectric constant which is approximate to and intermediate of the corresponding values of polyethylene and PTFE. This ensures a great convenience in that a PMP coaxial cable can be designed with substantially the same structure and dimensions as the polyethylene or PTFE coaxial cable of corresponding size.

Table 3 Structures of PMP Coaxial Cables and Other Specimens

| | Inner Conductor | | | Dielectric | | Outer Cond. | | Jacket | | Nominal Impedance (ohms) | Approx. kg/100m |
|--------------|-----------------|--------|----------|------------|----------|-------------|----------|--------|----------|--------------------------|-----------------|
| | Mat.* | Strand | O. D(mm) | Mat.* | O. D(mm) | Mat.* | O. D(mm) | Mat.* | O. D(mm) | | |
| 1.5D-PMPV | C | 7/0.18 | 0.54 | PMP | 1.6 | C | 2.1 | PVC | 2.9 | 50 | 1.4 |
| 3D-PMPV | C | 7/0.32 | 0.96 | PMP | 2.9 | C | 3.6 | PVC | 5.2 | 50 | 4.2 |
| 5D-PMPV | C | 1 | 1.40 | PMP | 4.6 | C | 5.3 | PVC | 7.1 | 50 | 7.7 |
| RG-8/U-PMPV | C | 7/0.72 | 2.17 | PMP | 7.0 | C | 7.9 | PVC | 10.2 | 50 | 15.5 |
| 1.5D-2VX | C | 7/0.18 | 0.54 | XLPE | 1.6 | C | 2.1 | PVC | 2.9 | 50 | 1.4 |
| 3D-2V** | C | 7/0.32 | 0.96 | LDPE | 3.0 | C | 3.7 | PVC | 5.3 | 50 | 4.4 |
| 8D-2V** | C | 7/0.8 | 2.40 | LDPE | 7.8 | C | 8.7 | PVC | 11.1 | 50 | 19.5 |
| MX50-2.2PMP | SCW | 1 | 0.51 | PMP | 1.7 | CT | 2.2 | - | - | 50 | 1.7 |
| MX50-3.6PMP | SCW | 1 | 0.91 | PMP | 3.0 | CT | 3.6 | - | - | 50 | 3.8 |
| MX50-2.2** | SCW | 1 | 0.51 | TFE | 1.7 | CT | 2.2 | - | - | 50 | 2.0 |
| MX50-3.6**** | SCW | 1 | 0.91 | TFE | 3.0 | CT | 3.6 | - | - | 50 | 4.6 |

(*) C : Bare Copper Wire
 SC : Silver-coated Copper Wire
 SCW : Silver-coated Copper-clad Steel Wire
 CT : Tubular Copper
 PMP : Polymethyl Penten-1
 TFE : Polytetrafluoroethylene
 XLPE : Irradiation Crosslinked Polyethylene
 LDPE : Low-Density Polyethylene
 PVC : Polyvinylchloride

(**) Specified under Japanese Industrial Standard "JIS C 3501"

(***) Equivalent RG-405/U

(****) Equivalent RG-402/U

3.2 Properties of PMP Coaxial Cable Specimens

The PMP coaxial cable specimens were tested with the results summarized in Table 4.

3.2.1 Attenuation Characteristics

Figures 4 and 5 show the frequency dependence of attenuation of PMP coaxial cable specimens. The properties of flexible cable specimens given in Figure 4 are close to those of the polyethylene cable. The properties of semi-rigid cable specimens indicated in Figure 5 are apparently inferior to those of the PTFE cable owing to the difference in dissipation factor between these two materials. With an improvement expected in the dissipation factor of the PMP resin, the

difference will be reduced. In view of the attenuation characteristics of Figure 5, the PMP resin used appears to have a dissipation factor of about 6×10^{-4} in the radio frequency range.

3.2.2 Phase Stability

Radio-frequency coaxial cables for use in highly phase-sensitive electronic systems such as array-antenna systems must have good phase stability against variations in temperature, that is the cables must not involve marked variations in electrical length due to changes in cable temperature. Air-spaced semi-rigid cables generally have a satisfactory coefficient of phase stability of about 10 ppm/ $^{\circ}\text{C}$, and special phase compensated cables are available with extremely high stability of about

Table 4 Test Results of PMP Coaxial Cables

| Test | 1.5D-PMPV | 3D-PMPV | 5D-PMPV | RG-8/U-PMP | MX50-2.2PMP | MX50-3.6PMP |
|--|-------------------|------------------|------------------|------------------|-------------------|------------------|
| Dielectric Strength, () kV rms, 1 min. | (2) Passed | (2) Passed | (5) Passed | (5) Passed | (2.5) Passed | (5) Passed |
| Capacitance, PF/m at 1 KHz, at 20°C | 98.0 | 96.3 | 96.9 | 95.1 | 98.8 | 99.0 |
| Characteristic Imp., ohms, at 300 to 400 MHz | 49.0 | 49.8 | 49.7 | 50.3 | 49.0 | 48.9 |
| Propagation Velocity, percent, at 300 to 400 MHz | 69.3 | 69.5 | 69.3 | 69.7 | 68.9 | 68.8 |
| Cold Bend, at -25°C, Mandrel Dia. () mm | (10) Passed | (20) Passed | (30) Passed | (70) Passed | (10) Passed | (20) Passed |
| Attenuation, at 20°C | Refer to Figure 4 | | | | Refer to Figure 5 | |

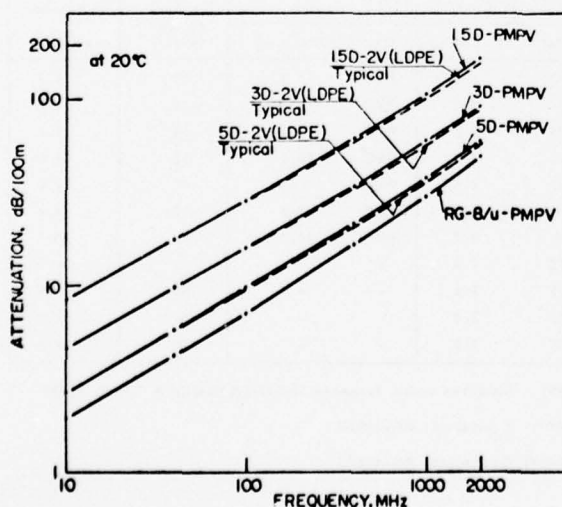


Figure 4 Attenuation Characteristics of PMP Coaxial Cables

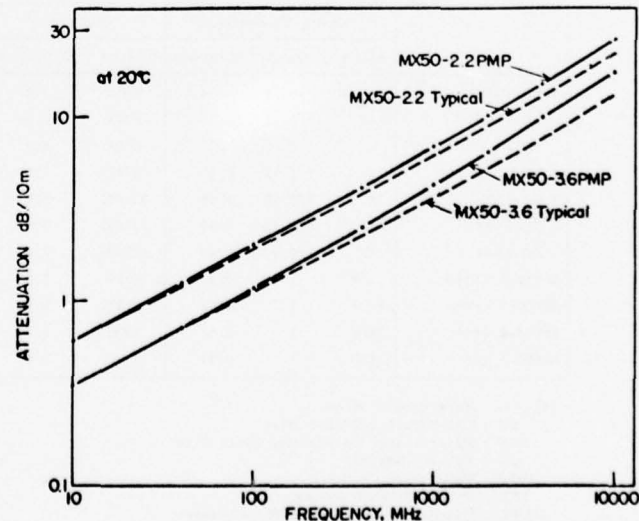


Figure 5 Attenuation Characteristics of PMP Semi-rigid Coaxial Cables

1 ppm/ $^{\circ}\text{C}$ over selected temperature ranges.^{2,3} With air-spaced cables, however, care should be taken of the phase variations which will arise from the gas pressure.²

Solid polyethylene dielectric flexible coaxial cables were reported to have a coefficient of phase stability of about (-)200 to about (-)400 ppm/ $^{\circ}\text{C}$, hence poor stability.⁴ This was substantiated also by the test results obtained in our laboratory.

The specimens were tested for coefficient of phase stability by placing an open circuit ended specimen in a heating chamber and measuring the variation with temperature of the resonance frequency of the specimen to determine the variation of electrical length. Equation (1) gives the coefficient of phase stability.

$$K = \frac{L_e \times V_p \times 10^6}{T \times L} \quad (1)$$

K = Coefficient of change in electrical length, in parts per million per $^{\circ}\text{C}$ (ppm/ $^{\circ}\text{C}$).

L_e = Change in electrical length of specimen, in meters.

T = Change in temperature, in $^{\circ}\text{C}$.

L = Length of the specimen inside the heating chamber, in meter.

V_p = Velocity of propagation of the dielectric core, expressed as a fraction.

Figures 6 to 8 show the electrical length variations (mm) of specimens per mechanical unit length (1 m). Listed in Table 5 are the coefficients of phase stability of the specimens calculated.

Figure 6 reveals that the temperature dependence of the electrical length of the polyethylene flexible coaxial cable is markedly negative, the coefficient of phase stability thereof being about (-)300 ppm/ $^{\circ}\text{C}$ at 70°C to 80°C. Figures 7 and 8 indicate the temperature dependence of the electrical length of PMP coaxial cables. The PMP flexible coaxial cables have a coefficient of phase stability of about 70 ppm/ $^{\circ}\text{C}$ at 70°C to 80°C, namely approximately 1/4 the coefficient of the polyethylene coaxial cables.

The PMP semi-rigid coaxial cables have a coefficient of phase stability of about (-)20 ppm/ $^{\circ}\text{C}$ at 0°C to 80°C and are of extremely stable characteristics. In a high-temperature range about 100°C, the PMP cables are comparable to the PTFE semi-rigid coaxial cable.

3.2.3 Power Rating

The power rating of solid polyethylene dielectric flexible coaxial cables is usually expressed in terms of permissible transmission power at

ambient temperature of 40°C or 50°C with the highest temperature of the inner conductor at 85°C.

In view of the fact that the PMP material has about 1/2 the thermal conductivity of polyethylene and assuming that the PMP coaxial cable dielectric has twice the heat resistance of polyethylene coaxial cable dielectric and that the highest temperature of the inner conductor is 130°C, PMP coaxial cables appear to have about 90% higher power rating at ambient temperature of 50°C than polyethylene coaxial cables of the same size. With an increase in ambient temperature, the power rating of PMP cables decreases at a lower rate than that of polyethylene cables; as a result for

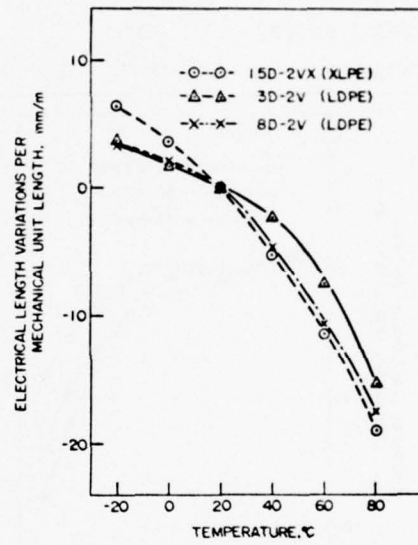


Figure 6 Electrical Length Variations at Various Temperatures of Polyethylene Coaxial Cables

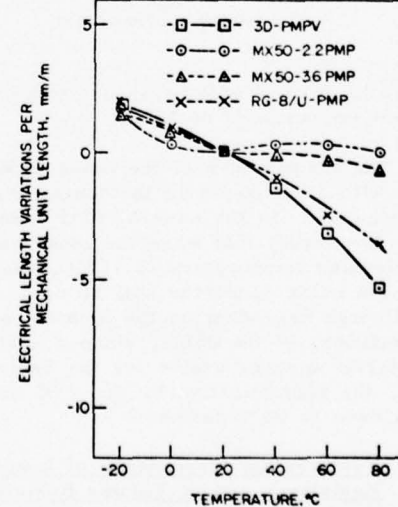


Figure 7 Electrical Length Variations at Various Temperatures of PMP Coaxial Cables

Table 5 Phase Stability of PMP Coaxial Cables and Other Specimens

| Cable Type | Dielectric Material | Coefficients of Phase Stability, ppm/°C | | | |
|-------------|---------------------|---|----------|----------|----------|
| | | Temperature Range, °C | | | |
| | | 0 to 20 | 20 to 40 | 40 to 60 | 70 to 80 |
| 1. SD-2VX | XLPE | - 120 | - 180 | - 200 | - 300 |
| 3D-2V | LDPE | - 60 | - 80 | - 170 | - 300 |
| 8D-2V | LDPE | - 70 | - 160 | - 200 | - 260 |
| 3D-PMPV | PMP | - 30 | - 45 | - 65 | - 75 |
| RG-8/U-PMP | PMP | - 35 | - 35 | - 45 | - 50 |
| MX50-2.2PMP | PMP | - 10 | - 10 | ± 5 | - 15 |
| MX50-3.6PMP | PMP | - 30 | - 5 | - 10 | - 20 |
| MX50-3.6 | TFE | - 35 | - 20 | - 25 | - 35 |

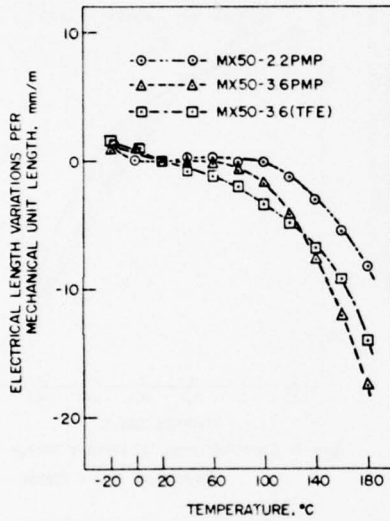


Figure 8 Electrical Length Variations at Various Temperature of PMP Semi-rigid Coaxial Cables

example, the former will be about 340% of the latter at ambient temperature of 70°C.

The temperature of the cable jacket will increase with an increase in the temperature of the inner conductor. In the case of PMP coaxial cables, however, we expect that when the inner conductor has an elevated temperature of 130°C, the temperature of the outer conductor will be up to about 105°C although dependent on the ambient or installation conditions of the cable, since a heat resistant PVC material appears usable for the cable jacket. However, the contamination by the PVC material will than have to be considered.

3.2.4 Temperature Dependence of Insulation Resistance and of Volume Resistivity

It is usually required that coaxial cables for use in measuring instruments and electronic

systems handling d.c. signals of microampere order have high insulation resistance and good temperature dependence.

A specimen of PMP coaxial cable and comparison specimens of coaxial cables were examined for the temperature dependence of insulation resistance. The temperature dependence of volume resistivity of each insulation was also calculated. Figure 9 shows the results.

The volume resistivity of PMP has very good temperature dependence and is in the order of 10^{16} ohms-cm at 140°C. This indicates that PMP coaxial cables are useful for the applications mentioned.

Care should be taken of XLPE cables for such uses since the charge on the insulation due to irradiation might disturb the stability of insulation resistance.

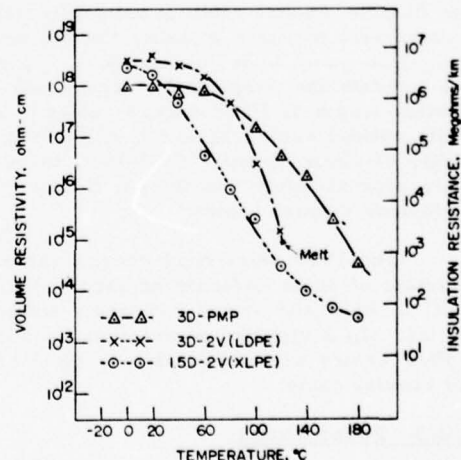


Figure 9 Insulation Resistance at Various Temperature of PMP Coaxial Cable and other Specimens

4. PMP Insulated Hook-Up Wires

Heat resistant PVC wires, crosslinked PVC wires, flame retardant XLPE wires and fluorocarbon resin wires are presently available for use in electronics systems as insulated hook-up wires and are selectively used for particular purposes.

Fluorocarbon resin wires are heat resistant at temperatures of up to 150°C to 260°C and generally have high flame retardance but are invariably expensive. PVC and XLPE wires usually have heat resistance of the order of 105°C. Thus only few kinds of heat resistant wires are now available in an intermediate temperature range of 125°C to 150°C.

In an attempt to use PMP as a heat resistant wire insulation serviceable in the intermediate temperature range, flame retardant PMP was developed, and hook-up wire specimens were prepared with the use of the compound and tested in comparison with XLPE wires and crosslinked PVC wires.

Tables 6 and 7 and Figure 10 chiefly show the test results achieved by flame retardant PMP insulated hook-up wire specimens having a conductor size of 0.51 mm (AWG 25) and an insulation thickness of 0.42 mm.

The flame retardant PMP insulated hook-up wire fulfills the requirements specified in UL Sub. 758 and has good heat resisting properties as evidenced by the temperature dependence of insulation resistance shown in Figure 10, and the chisel cut-through test results given in Table 7.

Table 6 Test Results of Flame Retardant PMP Hook-up Wire
(0.51mm - 0.42mm Thick.)

| Test | Test Method | Test Results | |
|---|----------------------------------|--------------------|----|
| Tensile Strength , kg/mm ² , at 23°C | ASTM D 638 | 1.4 | |
| Elongation, % , at 23°C | ASTM D 638 | 350 | |
| Heat Aging 7 days at 158°C | Retention of Tensile Strength, % | UL Sub. 758 | 90 |
| | Retention of Elongation, % | UL Sub. 758 | 70 |
| Deformation , at 158°C, 500g, % | UL Sub. 758 | 24 | |
| Heat Shock , at 158°C, 1 hr, 1/2"D mandrel | UL Sub. 758 | Passed | |
| Cold Bend , at -10°C, 1/8"D mandrel | UL Sub. 758 | Passed | |
| Vertical Flame Test "FR-1" | UL Sub. 758 | Passed | |
| Chisel Cut-through Test (Penetration Test) | UL Sub. 758 | Refer to Table 7 | |
| Solder Resistant Test | MIL-W-16878D | Passed | |
| Insulation Resistance | — | Refer to Figure 10 | |

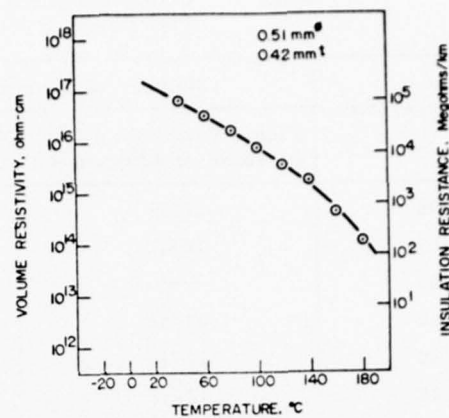


Figure 10 Insulation Resistance at Various Temperature of Flame Retardant PMP Hook-up Wire

5. Foamed PMP Dielectric Shielded Cables

Low-capacitance and good solderability are usually required of shielded cables for the internal wiring of audio amplifiers, tape recorders and other sound systems. At present, foamed XLPE dielectric shielded cables are mainly used for such purposes.

To investigate the use of new PMP in this field, research was made on the chemical expansion of new PMP and successfully achieved an expansion ratio of about 35% which gives an effective dielectric constant corresponding to that of about 40% expanded polyethylene.

Table 7 Chisel Cut-through Test Results Flame Retardant PMP Hook-up Wire and Other Specimens

| Test Temperature °C | Number of Specimens Passing/Number of Specimens Tested | | |
|------------------------|--|--|--|
| | Flame Retardant PMP 0.51mm, 0.42mm thick. | Crosslinked Polyethylene 0.51mm, 0.5mm thick. | Crosslinked PVC 7/0.254mm, 0.5mm thick. |
| 90 | 12/12 | 12/12 | 12/12 |
| 100 | 12/12 | 10/12 | 12/12 |
| 105 | — | 0/12 | — |
| 110 | 12/12 | 0/12 | 12/12 |
| 120 | 12/12 | 0/12 | 12/12 |
| 125 | 12/12 | — | 0/12 |
| 130 | 4/12 | — | 0/12 |
| 135 | 0/12 | — | — |
| 140 | 0/12 | — | — |
| (Note) | Chisel : 90°, 5 mils radius edge | | |
| | Load Weight : 350 g | | |
| | Cut-through Time : < 10 min. Failed | | |
| | | > 10 min. Passed | |

Table 8 Structures and Test Results of Foamed PMP Shielded Cable

| | | 0.51 - PMFSV | 7/0.16 - PMFSV |
|--|--------------------|------------------------|------------------------|
| Inner Conductor | Material | Tin-coated Copper Wire | Tin-coated Copper Wire |
| | Strand | 1 | 7/0.16 |
| | Outer Diameter, mm | 0.51 | 0.48 |
| Dielectric | Material | Foamed PMP | Foamed PMP |
| | Outer Diameter, mm | 1.35 | 2.12 |
| Shield | Material | Tin-coated Copper Wire | Tin-coated Copper Wire |
| | Type of Shield | Spiral Wrapped | Spiral Wrapped |
| | Outer Diameter, mm | 1.55 | 2.36 |
| Jacket | Material | PVC | PVC |
| | Outer Diameter, mm | 2.1 | 3.0 |
| Dielectric Strength, 0.5kV rms, 1 min. | | Passed | Passed |
| Insulation Resistance, Megohms/km | | > 1000 | > 1000 |
| Capacitance, PF/m, at 1 KHz | | 92 | 61 |

Table 9 Structures and Test Results of PMP Insulated Computer Cable

| Number of Paires | | Center Layer | 1st Layer | 2nd Layer |
|------------------------------------|----------------------|------------------|-----------|-----------|
| | | 2 | 6 | 12 |
| Conductor | Material | Bare Copper Wire | | |
| | Size mm ² | 0.5 (20/0.18mm) | | |
| | Outer Diameter mm | 0.9 | | |
| Insulation | Material | Colored PMP | | |
| | Thickness mm | 0.4 | | |
| | Outer Diameter mm | 1.7 | | |
| Jacket | Material | PVC | | |
| | Thickness mm | 1.6 | | |
| | Outer Diameter mm | 19.5 | | |
| Dielectric Strength 1kV rms, 1min. | | Passed | | |
| Insulation Resistance Megohms/km | | >1000 | | |
| Capacitance nF/km, 20°C, at 1 KHz | | 46.1 (average) | | |
| Conductor Resistance ohms/km, 20°C | | 33.3 | | |

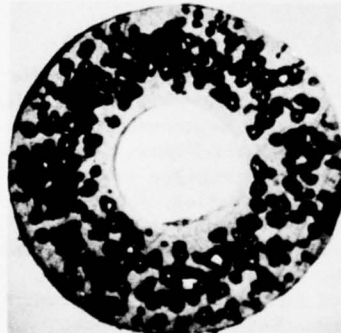


Figure. 11 Micrograph of Cross Section of Foamed PMP Dielectric (conductor : 0.51 mm)

Listed in Table 8 are the structures of cable specimens and the test results obtained. Figure 11 is a photograph showing a foamed PMP dielectric in section.

6. PMP Insulated Computer Cables

Multi-conductor cables incorporated in computers for controlling industrial processes are frequently used in a high-temperature environment and must therefore be resistant to heat. Mainly used in such an environment are cables including a core of heat resistant PVC insulated wires or of

XLPE insulated wires. Fluorocarbon resin wires are also used where still higher heat resistance is required.

For the use of PMP in this field, specimens were prepared of PMP insulated PVC jacketed computer cable incorporating 20 pairs of 0.5mm² conductors using colored PMP. Flame retardant PMP is considered to be also useful in this application.

Table 9 gives the structures of the cable specimens and the test results obtained.

7. Conclusions

It was confirmed that new PMP is a noteworthy material usable for a wide variety of electronics and mechanical properties and outstanding heat resistance with its service temperature expected to be about 130°C.

New PMP based, cold flexible PMP developed in our laboratory has greatly increased flexibility at low temperatures while retaining the good properties inherent in new PMP.

Our research was directed also to flame retardant PMP and matured to a formulation conforming to the requirements of UL Sub. 758.

Various electronics wire specimens were test produced with use of the PMP resins as insulations and tested for evaluation.

The results show that PMP coaxial cables are substantially equivalent to polyethylene coaxial cables in attenuation performance and are comparable to fluorocarbon resin coaxial cables in phase stability and insulation resistance at varying temperatures. PMP coaxial cables can be expected to have about two times and about three times the power rating of polyethylene coaxial cables at ambient temperatures of 50°C and 70°C respectively, although the power rating is dependent on the ambient temperature specified. Flame retardant PMP wires are equivalent or superior to XLPE wires in electrical properties and heat resistance.

Further research was conducted on the chemical expansion of new PMP and succeeded in extruding about 35% expanded PMP corresponding to about 40% expanded polyethylene. The foamed PMP was used for low-capacitance shielded cables.

With the various features described, new PMP wires are expected to be used in the field ranging from crosslinked polyethylene or PVC insulated wires, up to part of fluorocarbon resin wires.

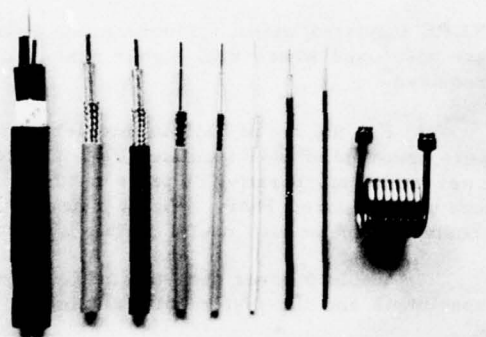


Figure. 12 Photograph of PMP Coaxial cable and PMP Computer cable

References

- (1) Modern Plastics Encyclopedia 1976-1977 vol 53 No. 10A P. 78, P. 473.
- (2) S. Morisada, T. Kuroe, A. Kusui, "Phase Stabilized Coaxial Cable", Dainichi-Nippon Cables Review, No. 38 March, 1968.
- (3) Andrew Co., General Edition Catalog 27 Antenna/Transmission Lines, P. 55.

- (4) G. Rodriguez, "Phase Stability of Typical Navy Radio Frequency Coaxial Cables", 14th International Wire & Cable Symposium, Atlantic City, New Jersey, Dec. 1965 (U.S. Naval Applied Science Laboratory).



Masaaki Okada

Dainichi-Nippon Cables, Ltd.
Marunouchi Chiyoda-ku,
Tokyo,
Japan

Masaaki Okada, born in 1935, graduated from Kyoto University majoring industrial chemistry in 1957 and immediately joined Dainichi where he has been engaged in the research and development of plastic materials and related products. He is now a Senior Research Engineer in Material Laboratory of his company. He is also a member of the Society of the Plastics Engineers.



Akio Kusui

Dainichi-Nippon Cables, Ltd.
1, Kaichiku, Ikejiri,
Itami, Hyogo,
Japan

Akio Kusui, born in 1935. He was graduated from Osaka Yodogawa Technical High School majoring Electrical Engineering in 1954 and immediately joined Dainichi-Nippon Cables, Ltd. Past 23 years, he has been engaged in the development work on Telephone cables, Radio-frequency Coaxial Cables, UHF-TV antennas, and filters. He is now a Senior Research Engineer in Telecommunication Research Department of his company. He is also a member of the Institute of Electronics and Communication Engineers of Japan.



Hayashi Takemori

Dainichi-Nippon Cables, Ltd.
Higashimukaijima
Amagasaki,
Japan

As a material engineer Hayashi Takemori has been with Dainichi-Nippon Cables, Ltd. since 1957. These twenty years he has been mainly engaged in research and development of materials for electrical cables. Recently his interest has been directed to insulated wires for electrical and electronics equipments. In this study, he was responsible for the material and product evaluation, formulation developments, and extrusion processes.

BUBBLE-FORMATION MECHANISM IN THE EXTRUSION PROCESS OF FOAMED PLASTIC INSULATION

K. Orimo T. Shimano
The Furukawa Elec. Co., Ltd., Tokyo, Japan

SUMMARY:

This report describes a theoretical study of the bubble-forming mechanism of chemical and physical blowing. It is made clear that they have something in common with each other in view of the nucleation phenomenon. Nucleation energy is calculated, and the energy-contributing factors are discussed.

I. Introduction

The electrical properties of plastic cable are of a higher efficiency when the insulating material is made of a foam-like mass, i.e., matrix of air-filled bubbles. From this common knowledge, serious research into the production of such a material was begun in many cable manufacturing companies worldwide as early as two or three decades ago. Until now, although progress in the understanding of the plastic foam mechanism has been made by R.H. Hansen et al., there still have remained many relatively unknown areas. With this in mind, we are led to believe that more advanced foaming extrusion techniques will be yet developed in the future. Our research, therefore, has also been directed towards reaching a clearer understanding of the plastic foam mechanism, and thereby at the same time developing a better extrusion technique for the purpose of foam cable production.

II. The bubble-forming mechanism using a chemical foaming agent

1. Summary of research system

Our research system centers on foamed plastic used for the extrusion covering of electric cable. Fig. 1

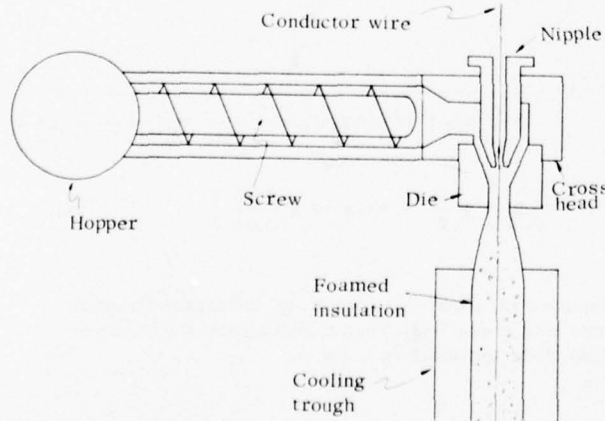


Figure 1.

illustrates the wire-covering process, which involves placement of a plastic compound (containing a foaming agent) into the extruder hopper, the mixing and melting, and its discharge from the front end of the extruder directly into the crosshead. From this point the plastic flow turns 90° into the direction of the running conductor. Under usual conditions, a plastic pressure of between 200~500 kg/cm² is maintained in the cross-head. For this reason, the gas created by decomposition of the foaming agent is evenly diffused throughout the plastic. Then, after the plastic has passed through the die and the pressure has been concurrently reduced to the atmospheric level, the foaming process takes place. Following this, the insulated wire is cooled in a water trough and taken up on reels.

2. Foaming mechanism

The quality of the foam is determined by a number of factors, for example, the amount of bubbles, the expansion rate, etc. The relationship between these factors and the temperature of the plastic at the crosshead is shown in figures 2 and 5. The phenomena seen in these figures as well as reference to reports by R.H. Hansen et al., have led us propose the following mechanism: a portion of the foaming agent particles decompose in a short time period (Δt) just before leaving the die, and these very particles only become the nuclei for the foaming process, that is, the loci where gas collects to form the bubbles. This hypothesis will be discussed in more detail in this report.

(1) Number of bubbles

It is obvious that the quality of the foam depends upon the decomposition properties of the agent. It is also well known that when temperature is increased steadily, the decomposition rate for unit time follows a Gaussian distribution pattern. Therefore the following equations are given:

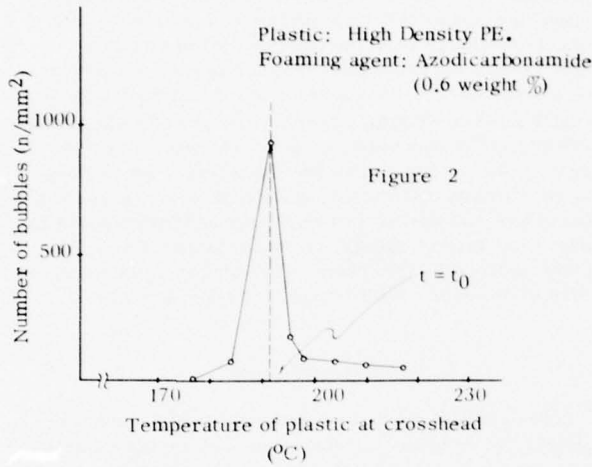
$$x = \frac{h}{\sqrt{\pi}} \exp \left\{ -h^2 (t - t_0)^2 \right\} \quad (1)$$

$$y = M \frac{h}{\sqrt{\pi}} \int_{-\infty}^t \exp \left\{ -h^2 (t - t_0)^2 \right\} dt \quad (2)$$

where t is time and is equivalent to temperature because it is increased steadily, x is the decomposition rate for unit time at time t , y is the total amount of derived gas until time t , M is the amount of gas given off from the unit weight of the agent and h is $\frac{1}{2} \lambda$ where λ is the standard deviation. Therefore, if the above mentioned mechanism is correct, the number of bubbles per unit volume of plastic should be as follows:

$$\begin{aligned} m &= \frac{\beta \rho}{\alpha} \frac{h}{\sqrt{\pi}} \int_{t-\Delta t}^t \exp \left\{ -h^2 (t - t_0)^2 \right\} dt + mq \\ &\approx \frac{\beta \rho}{\alpha} \frac{h}{\sqrt{\pi}} \Delta t \exp \left\{ -h^2 (t - t_0)^2 \right\} \end{aligned} \quad (3)$$

where m is number of bubbles, α is the average weight of one particle of the agent, β is weight percentage of the agent in the plastic, ρ is the plastic density and m_0 is the number of bubbles formed between the point where plastic exits from the die and the point of entry into the cooling trough and is comparatively small because the intervening space between said die and trough is not instrumental in determining the number of bubbles. This equation explains the phenomenon illustrated in figure 2.



(2) Foam expansion rate

If there is no escape of gas from the plastic, the expansion rate will rise with increases in temperature. There is, in fact, however, always some gas escape. Therefore, the amount of escaping gas must be taken into consideration. When nuclei distribution in the plastic is uniform and the number of nuclei in a unit volume is indicated by ε , and when the gas in a minute volume passes through the distance r and continues through the spherical shell of dr thickness, the gas before passing through dr is $y(r)$, and after passing through dr is $y(r+dr)$, their relation being expressed by

$$y(r)(1 - \xi \varepsilon dr) = y(r+dr) \quad (4)$$

where ξ is constant. Accordingly,

$$y(r) = y(0) \exp(-\xi \varepsilon r) \quad (5)$$

Therefore, when the gas and nuclei distribute uniformly in a hemispherical form as in fig. 3, the quantity of gas y_e passing through the unit area near the center of the flat surface is expresses by

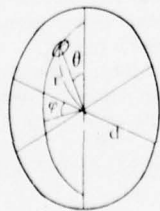


Figure 3.

$$y_e = \int_{r=0}^d \int_{\theta=0}^{\pi} \int_{\varphi=0}^{2\pi} \frac{c}{4\pi} \sin^2 \theta \sin \varphi e^{-\xi \varepsilon r} dr d\varphi d\theta \\ = \frac{c}{4\xi \varepsilon} \{ 1 - \exp(-\xi \varepsilon d) \} \quad (6)$$

where c is gas concentration. Therefore, under the condition of $\xi \varepsilon d \gg 1$,

$$y_e \approx A \cdot \frac{c}{\varepsilon} \quad (7)$$

where $A = \frac{1}{4\xi}$. When wire is actually being coated, the integral area of equation (6) above is negligible. However, when $\xi \varepsilon$ is large enough, the gas escaping through the surface ΔS can be calculated by integrating radius ℓ which is fairly small compared with L (fig. 4), thereby enabling the use of equation (7). Therefore the expansion rate of insulation γ is expressed as

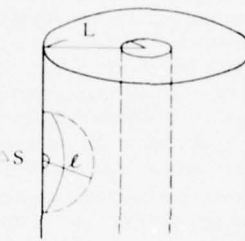


Figure 4.

$$\gamma = 1 - \frac{1}{By(1 - \frac{A}{m}) + 1} \quad (8)$$

$$\left[B = \frac{R \cdot T}{Vm P} \beta \rho \right]$$

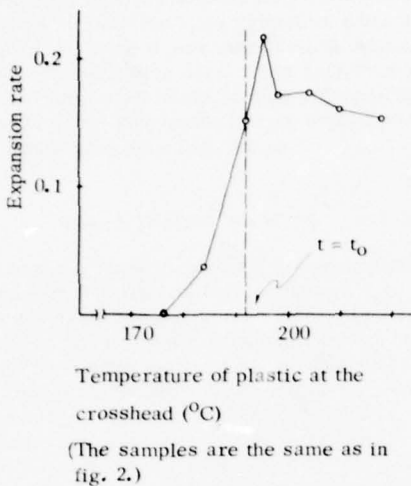
where R is the gas constant, T is absolute temperature, V_m is 22,400 cc and P is the gas pressure in the bubbles. From equations (2), (3) and (8),

$$\gamma = 1 - \frac{1}{B' \int_{-\infty}^t \exp\{-h^2(t-t_0)^2\} dt (1 - \frac{A'}{\exp\{-h^2(t-t_0)^2\}}) + 1} \quad (9)$$

$$\left[B' = B \frac{h}{\sqrt{\pi}}, \quad A' = A \frac{\alpha \sqrt{\pi}}{\beta \rho h} \right]$$

Equation (9) shows that when $t > t_0$, the maximum expansion rate is reached. The result suggests the relationship of the temperature in fig. 5.

Figure 5.



III. Examination of the nucleus

1. Bubble stability

In the production of foam plastic, the bubbles become stabilized upon solidification of the plastic when it is immersed in the cooling trough. But the question arises as to what happens to the bubbles when the plastic is not exposed to any cooling process. In case the viscosity of the plastic is very low, buoyancy will allow the bubbles to escape readily. On the other hand, if the viscosity is a high value as in our case, the easy escape of bubbles will not occur.

We are now assuming that the surface tension of plastic is σ , that plastic is compressed by a certain gas with the pressure P , and that the gas in the plastic reaches equilibrium at concentration C .

In such a system, a bubble of the radius r existing in the plastic will be compressed by the pressure $2\sigma/r$ created by the surface tension and the pressure P . Under these conditions, the gas in the bubble will dissolve into the plastic and the bubble will eventually vanish because the gas pressure in the bubble is greater than equilibrium pressure P by $2\sigma/r$ with the concentration C . As r becomes smaller, its reducing velocity is much accelerated, meaning that bubbles can not exist in plastic for any considerable length of time. If this is so, then by what method can bubbles possibly be grown? In any case, it is certainly necessary that the system be in such a condition that the gas will diffuse into the bubble from the plastic.

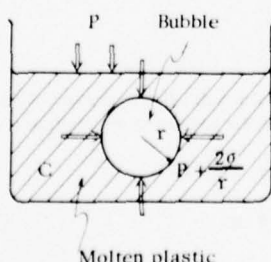


Figure 6.

For this purpose it is essential that the gas pressure within the bubble be less than the equilibrium pressure P in the gas concentration C . Such a state is accomplished by reducing the pressure P while maintaining the gas concentration, that is, by suddenly reducing the pressure P for a very short time. During that brief period, the bubble is supposed to grow rapidly until its inner pressure becomes $P + \frac{2\sigma}{r} - \Delta P$ where ΔP is the reduction value of the pressure P and r is the radius of the bubble after growth.

Subsequent to this period, in case $\frac{2\sigma}{r} - \Delta P < 0$, the gas dissolved into the plastic continues diffusing into the bubble, causing it to grow large. However, in case $\frac{2\sigma}{r} - \Delta P > 0$, the bubble will vanish. Since, a growing bubble is not in a stationary state, as mentioned above, after some time no bubble will be able to exist in the plastic.

2. Nucleation

As explained above, it is understood that as long as a bubble exists in the plastic already, it can be caused to expand. Now, however, we wish to discuss how a bubble can originally be created in plastic which initially contains none. It will be most desirous that a minute bubble having a radius greater than a certain value determined by the state of gas and plastic is created by the fluctuation of kinetic energy of plastic molecules, thereby resulting in the growth of the bubble. In other words, if a minute bubble having radius r has been created by the fluctuation, the bubble will grow when $r > \frac{2\sigma}{\Delta P}$ but will disappear if $r < \frac{2\sigma}{P}$. Next, calculation of the probability q that the value $r > \frac{2\sigma}{\Delta P}$ will be created by the fluctuation, is carried out in order to establish the condition under which a nucleus can be easily created.

The following system discussed is that of a super-saturated state in which, after making gas dissolve in plastic to the equilibrium concentration C at pressure P_0 , this pressure is suddenly lowered to P , a artificially created new environmental pressure. (The system probably resembles the state which exists at the moment when the plastic leaves the die in chemical and physical extrusion foaming.) In such a system, the energy dW being used in making the bubble increase from the radius r to $r + dr$ must be calculated. First, the compressing force of the bubble F is

$$F = P_1 + \frac{2\sigma}{r} - P_2 = \frac{2\sigma}{r} - \Delta P \quad (10)$$

P_2 is the gas pressure in the bubble. In an unstable condition, i.e., when the bubble is growing or shrinking, it is not clear whether $P_2 = P_0$ or not. However, P_2 will be near P_0 because the gas diffusion into the bubble will reach equilibrium in a very short time due to the very small size of the bubble.

Accordingly,

$$dW = F dV = \left(\frac{2\sigma}{r} - \Delta P \right) 4\pi r^2 dr \quad (11)$$

where V is the volume of the bubble.

Therefore,

$$W = \int_0^r \left(\frac{2\sigma}{r} - \Delta P \right) 4\pi r^2 dr = 4\pi r^2 \left(\sigma - \frac{\Delta P r}{3} \right) \quad (12)$$

and the relation of r and W is illustrated in fig. 7. According to this figure and the above discussion, it is clear that the growth or disappearance of the minute bubble is dependent upon whether or not the bubble radius is greater than $\frac{2\sigma}{\Delta P}$. In other words, for any bubble to become a nucleus, it is necessary for the bubble to possess energy greater than $E = \frac{16\pi\sigma^3}{3\Delta P^2}$, the equation designated as the nucleation energy value. Therefore the probability q of the nucleus being created is

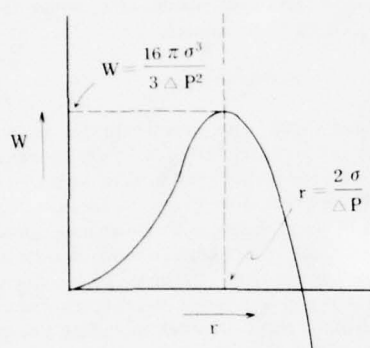


Figure 7.

$$q = \exp \left(-\frac{E}{kT} \right) = \exp \left(-\frac{16\pi\sigma^3}{3kT\Delta P^2} \right) \quad (13)$$

where k is Boltzmann's constant and T is absolute temperature. This equation shows that the nucleus is created more readily with higher values of ΔP and T and lesser values of σ . As we understand already, the bubble is created by gas which having dissolved in plastic in a supersaturated state, gathers at the nucleus created by the fluctuation of kinetic energy of plastic molecules.

IV. Nucleating agent

1. Nucleus in chemical foaming

We have up to now discussed a system containing only gas and plastic. In such a condition, however, the number of bubbles is usually meager and therefore, in fact, it is not possible to produce foamed insulation. In comparison as stated previously, a foamed substance produced by using a chemical foaming agent consists of many small bubbles. As we have reported in chapter II, the chemical foaming agent itself can become the nucleus. We wish to discuss this fact while considering the results mentioned in chapter III.

In a plastic matrix in the vicinity of foaming agent particles which have just decomposed or are decomposing the temperature is higher, the surface tension is less, and the gas concentration is higher than at other places in the plastic. Accordingly, the probability of nucleation near these foaming agent particles will be higher than at a

greater distance from them. Thus, a foam substance having uniformly distributed little bubbles might be difficult to produce, should a nucleating agent not exist in the plastic and gas solution. Considering this, it should be expedient to utilize a nucleating agent in the production of a foamed substance of superior quality, and in the chemical foaming process, this desired quality is achieved with a foaming agent which itself acts as the good nucleating agent.

2. Required properties of nucleating agent

A nucleating agent is a substance which tends to increase the likelihood of nucleation, that is, causing a temperature increase, an increase of the difference between gas pressure in the bubble and environmental pressure, and as well, as decrease in surface tension. In a system without the agent, a bubble grows from an originally very minute sphere. On the other hand, a bubble created by a nucleating agent, first appears to develop semi-spherically on the surface of the agent particle, and then grow successively into a spherical shape with the agent particle visibly attached to the bubble surface. (See photographs 1 to 3.) It would seem interesting, therefore, to discuss bubble growth on an extraneous substance. When considering such a problem, the interface energy between the plastic and the extraneous substance appears to be of great importance. A bubble will grow along the interface because the energy is normally less than the surface energy of plastic. The probability of nucleation at the interface may, in fact, be higher than at other places in the plastic due to this lower interface energy value.

(1) Effect of contact angle of the extraneous substance with plastic

We wish to discuss the probability of nucleation in a case where the interface is flat and the system is the same as in III-2. At first the quantity of work dW_n needed to make a bubble having radius r grow into $r + dr$ must be determined in order to derive the amount of energy W_n required for creation of a bubble having radius r in such a system.

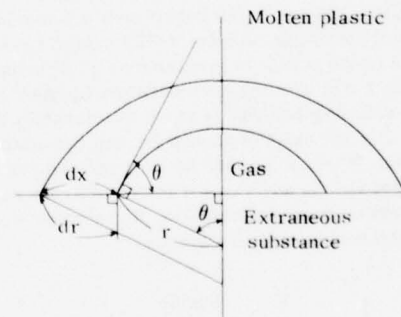


Figure 8.

When r grows to $r + dr$, the increase of area ΔS_{n1} at the interface of the extraneous substance and gas is as follows:

$$\Delta S_{n1} = 2\pi r \sin\theta dx$$

$$= 2\pi r \sin^2\theta dr \quad (14)$$

Where $\theta = \pi$ is the contact angle, and the increase of area ΔS_{n2} at the interface of gas and plastic is

$$\Delta S_{n_2} = \int_0^\theta 2\pi(r+dr)^2 \sin\theta d\theta - \int_0^\theta 2\pi r^2 \sin\theta d\theta \\ = 4\pi r(1-\cos\theta) dr \quad (15)$$

Therefore,

$$dW_n = \{\Delta S_{n_1}(1-\cos\theta) + (\Delta S_{n_2} - \Delta S_{n_1})\}(\sigma - \frac{\Delta P r}{2}) \\ = 4\pi r^2(\frac{2\sigma}{r} - \Delta P) dr \left(\frac{2-3\cos\theta+\cos^3\theta}{4} \right) \\ = f(\theta) \cdot 4\pi r^2(\frac{2\sigma}{r} - \Delta P) dr \\ \left[f(\theta) = \frac{2-3\cos\theta+\cos^3\theta}{4} \right] \quad (16)$$

From equations (11) and (16),

$$dW_n = f(\theta) dW \quad (17)$$

As $0 \leq f(\theta) \leq 1$, we understand easily that W_n is always smaller than W , meaning that the bubble is more easily created on the surface of the extraneous substance than at any other place.

(2) Structural effect of extraneous substance

In order to consider the structural effect of the extraneous substance, growth of the bubble must be seen from the peak of a cone with a vertical angle of 2φ (fig. 9).

This system is the same as in JJJ-2. The increase ΔS_{m_1} of the interface between the gas and the extraneous substance when r becomes $r+dr$ is

$$\Delta S_{m_1} = 2\pi r \sin\theta dx \\ = 2\pi r \sin^2\theta dr \quad (18)$$

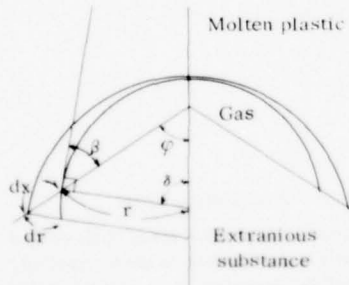


Figure 9.

and the increase ΔS_{m_2} of the interface between the gas and the molten polymer is

$$\Delta S_{m_2} = \int_0^\delta 2\pi(r+dr)^2 \sin\delta d\delta - \int_0^\delta 2\pi r^2 \sin\delta d\delta \\ = 4\pi r(1-\cos\delta) dr = 4\pi r \{1-\sin(\varphi-\theta)\} dr \quad (19)$$

Therefore,

$$dW_m = \{\Delta S_{m_1}(1-\cos\theta) + (\Delta S_{m_2} - \Delta S_{m_1})\}(\sigma - \frac{\Delta P r}{2}) \\ = 4\pi r^2(\frac{2\sigma}{r} - \Delta P) dr \frac{1}{4} \{2-2\sin(\varphi-\theta)-\cos^2(\varphi-\theta)\frac{\cos\theta}{\sin\varphi}\} \\ = f(\theta, \varphi) 4\pi r^2(\frac{2\sigma}{r} - \Delta P) dr \quad (20)$$

$$\left\{ \begin{array}{l} f(\theta, \varphi) = \frac{1}{4} \{2-2\sin(\varphi-\theta)-\cos^2(\varphi-\theta)\frac{\cos\theta}{\sin\varphi}\} \\ 0 \leq f(\theta, \varphi) \leq 1, \\ \text{on condition:} \\ \frac{\pi}{2} - \varphi \leq \theta \leq \frac{\pi}{2} + \varphi \quad (0 \leq \varphi \leq \frac{\pi}{2}), \quad (1) \\ \varphi - \frac{\pi}{2} \leq \theta \leq \frac{3\pi}{2} - \varphi \quad (\frac{\pi}{2} \leq \varphi \leq \pi). \quad (2) \end{array} \right. \quad (21)$$

Thus, comparing Eq. (11) with Eq. (20)

$$dW_m = f(\theta, \varphi) dW \quad (21)$$

Now we plot the values of the function $f(\theta, \varphi)$ for the variables θ and φ (fig. 10). The section which satisfies both conditions 1 and 2 is the range enclosed by the thick line in the figure. This illustrates that more energy is necessary when φ is smaller; in other words, it is easier to grow a bubble from the interior surface of an open depression in the extraneous substance.

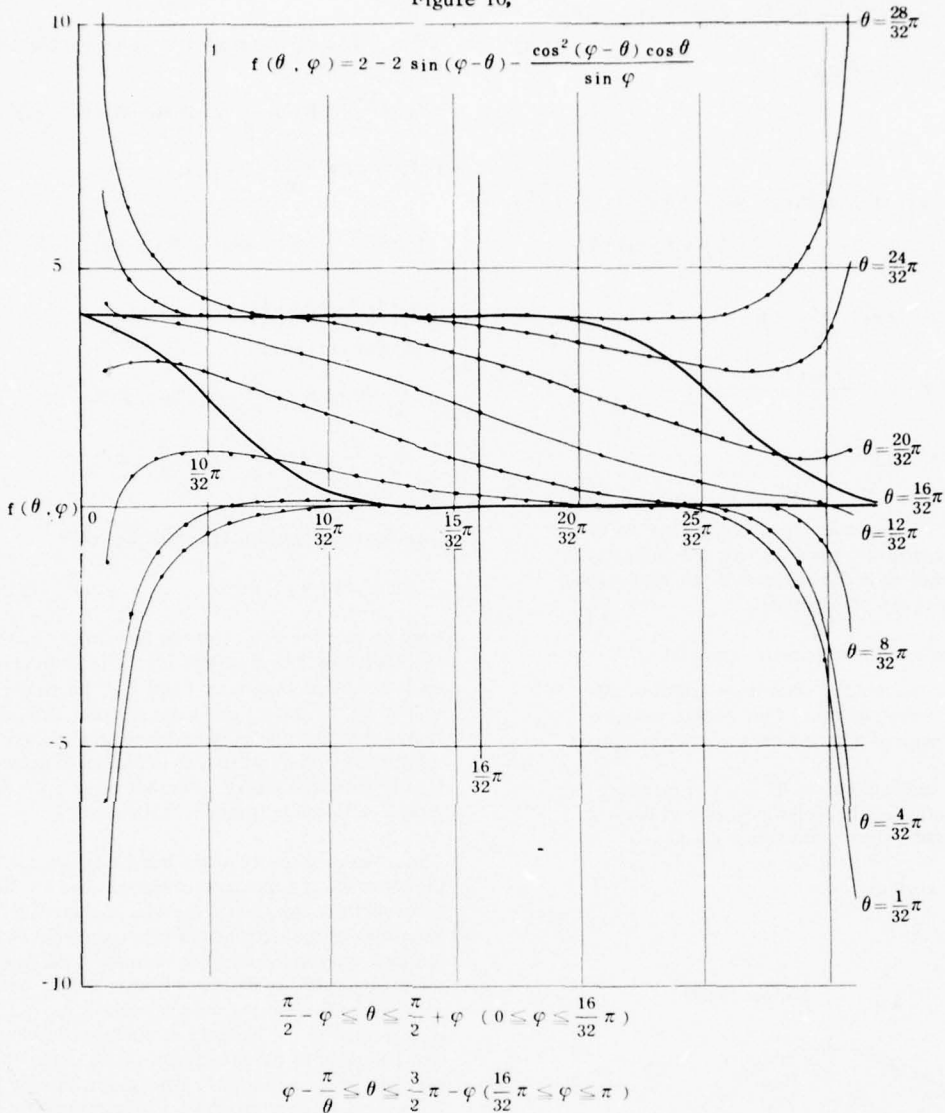
Thus, the probability of nucleation at the surface of the extraneous substance is higher than at other places within the plastic matrix. As for the structure of the extraneous substance, the more hollows and the greater the diameter, the higher the probability for the growth of bubbles. Specially regarding diameter of the extraneous particles, and with a mind to the quantity of such particles which will be added to the plastic, in mind, it is supposed that an optimum diameter does exist, simply because a lesser diameter provides a larger specific surface area.

V. Conclusion

It is hoped that the above discussion has helped to give a clearer understanding of the properties and primary function of the nucleating agent. That is to say, a good nucleating agent is a substance which decreases the nucleation energy. Factors to be considered regarding this energy include the following:

- (1) Surface tension of plastic (σ)
A lesser surface tension encourages growth of a nucleus.
- (2) Temperature of plastic (T)
A higher temperature encourages growth of a nucleus.
- (3) The difference between the gas pressure inside the bubble and the external pressure (ΔP).
The difference between the gas pressure inside the bubble and the external pressure (ΔP).

Figure 10,



A higher pressure difference ΔP encourages the growth of a nucleus. This pressure difference can be increased by the following methods:

- (i) by increasing the **inner pressure** of the bubble.
- (ii) by decreasing the **external pressure**.

As for (i), in a case where the gas concentration in the plastic must be constant, as, for example, when the expansion ratio is constant, it is better to dissolve the almost insoluble gas into the plastic at high pressure. And as for (ii), a condition might be provided in which the extruded plastic from the die is immediately put into a vacuum state.

- (4) Contact angle between the nucleating agent and the plastic.

A larger contact angle will encourage the growth of a nucleus.

(5) Structure of the nucleating agent.

Those particles that have many hollows and larger diameters will more readily cause nucleation. As mentioned before, however, it is predicted that there exists an optimum diameter of the agent.

These are probably not the only factors related to nucleation energy. Especially during actual production of foaming goods, when plastic is in a flowing state, the presence of other determining elements can not be ruled out. But, at least, it is clear that if a good nucleating agent is to be found, emphasis must be placed on the results obtained in the above discussion.

VI. References

- (1) R.H. Hansen, SPE Journal, 18, 1, 77, Jan. 1962
- (2) P.S. Epstein, M.S. Plesset, The Journal of Chemical Physics, 18, 11, 1505, 1950

(AUTHORS BIOGRAPHIES)



KATSUMI ORIMO
The Furukawa Electric
Co., Ltd.
6-1 Marunouchi 2-Chome,
Chiyoda-ku, Tokyo,
Japan

Mr. Orimo graduated from Kyoto University in 1960 with a B. Sc. in Applied Chemistry.

Upon graduation he jointed the Furukawa Electric Co., Ltd. and has been engaged in the research and development of plastic materials and manufacturing methods for telephone cables.

Mr. Orimo is now the head of the Material Research Section of the Telecommunication Laboratory at The Furukawa Electric Co., Ltd., and is also a member of the Society of Materials Science of Japan.



TAKASHI SHIMANO
The Furukawa Electric
Co., Ltd.
6-1 Marunouchi 2-Chome,
Chiyoda-ku, Tokyo,
Japan

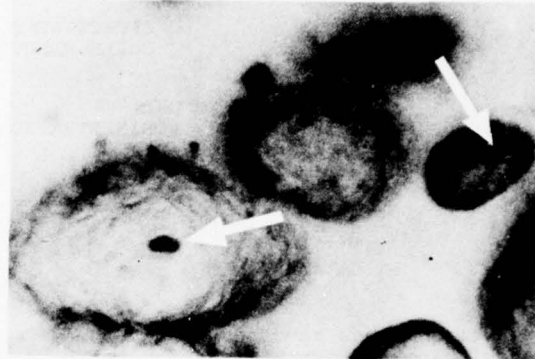
Mr. Shimano graduated from Tokyo Kyoiku University with a B. Sc. in Physics in 1969.

Thereafter he jointed The Furukawa Electric Co., Ltd. and has been engaged in the research and development of plastic materials and manufacturing methods for telephone cables.

Mr. Shimono is now a member of the Material Research Section of the Telecommunication Laboratory at The Furukawa Electric Co., Ltd.

Nucleus in each bubble

Photograph 1



Photograph 2



Photograph 3



EFFECTIVE RODENT SHIELDS AND CABLE ELECTRICAL PERFORMANCE

HARRY M. HUTSON
RURAL ELECTRIFICATION ADMINISTRATION
WASHINGTON, DC

DR. KENNETH W. BROWNELL, JR.
BRAND-REX COMPANY
WILLIMANTIC, CONNECTICUT

Abstract

Investigations have shown that when designing a rodent shield for telecommunications cables, a critical balance must be maintained between good electrical parameters and adequate protection against gopher attack. Improperly isolated ferrous materials have a deleterious effect on carrier frequency attenuation. Data are presented showing the cause for recent changes concerning gopher shielding materials in REA cable specifications.

Introduction

In 1976 and 1977 there has been a great deal of controversy generated in the area of the proper shield material selection for rodent shielded telecommunications cables and buried wires. This paper shall highlight this controversy and attempt to minimize the resulting confusion by presenting the data which have been utilized as the basis for decision making at the REA. The paper deals first with the effects on carrier frequency attenuation caused by 5 mil and 6 mil copper-clad ferrous stainless steel. The paper concludes with a section detailing the rationale behind the recent increase in the required thickness of copper alloy 194 for small pair count buried cables.

Section I: Electrical Effects of Ferrous Shield Materials

Basic Theory

If a conductive shielding material is brought into the proximity of a conductor carrying an a.c. current, as shown in Figure I-1, the magnetic field of the conductor causes a small current to be generated in the shield. This current is in such a direction as to oppose the current causing it to be generated.

Therefore, it causes a non-uniform distribution of conductor current when the frequency of interest is high enough to be in the conductor's skin effect range. This phenomena increases the a.c. resistance of the conductor as the shield is brought into closer proximity in much the same manner as does bringing balanced pair conductors closer together.¹

This shield proximity effect can be extended to twisted pair cables and is quantified in the third term of Equation I-1.²

$$R = 2R_e + 2\zeta_1 R_e + 8 \left[\frac{v^2}{1 - v^4} - \zeta_o \right] R_s \quad I-1$$

WHERE:

R = a.c. resistance

$$R_e = \frac{K}{d^2} \sqrt{\frac{f_{\text{KHz}}}{\rho_{\text{cond}}}}$$

$$R_s = \frac{K\rho}{D(D_1 - D)} \left[h \left(\frac{\sinh 2h + \sin 2h}{\cosh 2h - \cos 2h} \right) - \frac{K_1}{D} \left[\frac{3}{D_1} + \frac{1}{D} \right] \right]$$

K, K₁, S₁, V and ζ are dimensional constants

D = inner diameter of shield

D₁ = outer diameter of shield

d = diameter of conductor

$$h = 7.98 \sqrt{\frac{\mu_r f_{\text{KHz}}}{\rho_{\text{shield}}}} (D_1 - D)$$

μ_r = relative permeability of the shield

ρ = resistivity

It is obvious from Equation I-1 that as the permeability of the shield material is increased so is the proximity effect on the twin pair a.c. resistance for the same cable geometry.

The shields of interest in this study are constructed from copper clad stainless steel (CCS). The CCS which has been primarily utilized in the independent telecommunications industry for buried wire is 3.4 mils of 430 series stainless steel metallurgically bonded between two layers of 0.8 mils of pure copper (5 mil CCS). For buried cables, the accepted laminate is 2 mils of 430 series stainless steel metallurgically bonded between two layers of 2.0 mils of pure copper (6 mils CCS).

The calculation of the effective shield permeability and resistivity at each frequency of interest would be a tedious task due to the non-uniform cross section of the material. One would predict that 6 mil CCS would have less proximity effect on a.c. resistance than 5 mil CCS for the equivalent geometry, due to the increased thickness of the inner copper layer. However, skin effect calculations would indicate that a 2 mil layer of copper would not be adequate to cause

the majority of the shield current to flow in the copper.

To resolve this problem, filled wires were constructed with identical cores being shielded with aluminum and 5 mil CCS and filled cables were constructed with identical cores being shielded with 5 mil copper, 6 mil alloy 194 and 6 mil CCS. Conductor resistance and pair attenuation were calculated from short circuit impedance and open circuit admittance measurements of these constructions. These data are presented in the following section.

Shield Proximity Effects on Attenuation

Data taken on the equivalent 2 pair 22 gauge filled wires are presented in Table I-1.

Data taken on an outer layer pair of the equivalent 12 pair 22 gauge filled cables are presented in Table I-2.

TABLE I-1

PROXIMITY EFFECTS OF 5 MIL CCS ON FILLED WIRE ATTENUATION

| FREQUENCY (KHz) | SHIELD TYPE | | | |
|-----------------|--------------------------|------------------|--------------------------|------------------|
| | ALUMINUM | | 5 MIL CCS | |
| | R (Ω/mi) | α (dB/Mi) | R (Ω/mi) | α (dB/mi) |
| 1 | 170.5 | 1.69 | 176.9 | 1.69 |
| 50 | 182.8 | 6.32 | 199.6 | 6.56 |
| 112 | 207.9 | 7.43 | 236.2 | 8.13 |
| 200 | 252.4 | 9.16 | 284.6 | 9.95 |
| 300 | 302.0 | 11.14 | 337.7 | 12.04 |

TABLE I-2

PROXIMITY EFFECTS OF 6 MIL CCS ON FILLED CABLE ATTENUATION

| FREQUENCY (KHz) | SHIELD TYPE | | | |
|-----------------|--------------------------|------------------|--------------------------|------------------|
| | COPPER | | ALLOY 194 | 6 MIL CCS |
| | R (Ω/mi) | α (dB/mi) | R (Ω/mi) | α (dB/mi) |
| 10 | 185.0 | 5.02 | 184.7 | 5.02 |
| 50 | 195.3 | 6.98 | 196.1 | 7.02 |
| 80 | 208.1 | 7.65 | 208.7 | 7.67 |
| 350 | 346.4 | 13.44 | 350.0 | 13.60 |
| 772 | 496.4 | 19.94 | 498.6 | 20.09 |
| 1000 | 558.8 | 22.86 | 561.6 | 23.07 |

The data in Table I-1 indicate the deleterious effects that 5 mil CCS can have on filled wire analog carrier attenuation if the shield is not far enough removed from the twisted pairs. The data in Table I-2 indicate the absence of these deleterious effects when 6 mil CCS is employed as a rodent shield for filled cables. This is due to the shielding effectiveness of the 2 mil inner coating of copper on the 6 mil CCS product.

Section II: Thickness Selection of Rodent Shields

History

Electrolytic tough pitch (ETP) copper 10 mils thick has been utilized in the telecommunications industry over the past 15 years without a reported complaint of rodent damage to the cable core. Several studies have been conducted at the U. S. Fish and Wildlife facility in Denver, Colorado, which give 10 mil ETP copper a mean score of 2.7 in gopher resistance.³ In 1976 a report was issued to the REA from the field as to the apparent lack of puncture resistance afforded by 194 alloy⁴, and at the same time two valid field complaints were received on rodent damage to small diameter alloy 194 shielded cables.

Test Program and Data

A test program was opened at Denver. In these tests, a sheet of steel with a hole two inches in diameter was placed at the end of each of 10 cages. Samples of the cable were placed across the hole with

care being taken as to shield overlap orientation. The following rating scheme was used to evaluate damage:

0. No damage
1. Slight Damage - Outer Jacket
2. Outer Jacket Penetrated
3. Shield Penetrated
4. Conductors Damaged
5. Cable Severed

The cables tested are summarized in Table II-1. Care was taken to conduct one test with the shield overlap turned away from the animal and two tests with the shield overlap facing the animal.

A summary of the data for the 0.42 inch cables tested is presented in Figure II-1.

A summary of the data for 6.0 mil 194 alloy and 5.0 mil ETP copper for the cable diameters tested is presented in Figure II-2.

A summary of the data for the 5.0 mil ETP copper shielded cables illustrating the effect of making the shield overlap accessible to the rodent is presented in Figure II-3.

Specification Requirements

It has been decided by the REA that any new shield material submitted for approval must have a gopher rating of less than 2.7

TABLE II-1
CABLES TESTED FOR RODENT ATTACK

| OVERALL CABLE DIAMETER (IN) | SHIELD TYPE | SHIELD NOMINAL THICKNESS (MILS) |
|-----------------------------|-------------|---------------------------------|
| 0.42 | CCS | 5.5, 6.0 |
| 0.42 | 194 Alloy | 5.5, 6.0, 6.5, 7.0, 7.5 |
| 0.42 | 196 Alloy | 5.5, 6.0, 6.5, 7.0, 7.5 |
| 0.42 | ETP Copper | 5.0, 8.0, 10.0 |
| 0.63 | 194 Alloy | 6.0 |
| 0.75 | 194 Alloy | 6.0 |
| 0.75 | ETP Copper | 5.0 |
| 1.00 | 194 Alloy | 6.0 |
| 1.5 | 194 Alloy | 6.0 |
| 1.5 | ETP Copper | 5.0 |
| 2.0 | ETP Copper | 5.0 |

for cable overall diameters less than 1.25 inches. Due to higher financial liability a rating of 2.0 is the standard for cables with an overall diameter greater than 1.25 inches. This desired value is superimposed on Figure II-1 and Figure II-2.

Figure II-1 demonstrates that 6 mil alloy 194 does not possess a low enough gopher rating to allow its continued use below 0.60 inch overall cable diameter. Therefore, a change was effected September 1, 1976, requiring 7 mil alloy 194 for cables with an overall diameter of 0.60 inches and below. Figure II-2 demonstrates the adequacy of 6 mil alloy 194 for cable sizes above 0.60 inches overall. This is further exhibited when one considers that 6 mil alloy 194 has been utilized for five years with no reported field complaints for rodent caused cable failures for diameters in excess of 0.60 inches.

Conclusions

It has been demonstrated with theory and data that ferrous shields with non-ferrous liners with less than the conductivity equivalence of 2 mils of copper can have deleterious effects on carrier frequency attenuation of twisted pair telephone cable (wire) if proper care in cable (wire) design is not taken.

Data have been presented which justify the increase of shield thickness required when alloy 194 is utilized on cables under 0.60 inches in overall diameter.

Acknowledgements

The authors wish to acknowledge the data contributed by Superior Cable Corporation which are utilized in Table II-2 of this paper. They also acknowledge the data, shield materials, and test results provided by Texas Instruments Incorporated, Olin Brass, and American Brass.

References

1. H. H. Skilling, Electric Transmission Lines, McGraw Hill Book Company, Inc., New York, 1951, p. 308.
2. Bell Telephone Laboratory Technical Library, Outside Plant Design Department, "Notes on Cable Development and Design".
3. R. Babioan, S. R. Hartley, and E. D. Hyman, "High Strength Corrosion Resistant Clad Metal Shielding for Telephone Wire and Cable", 23rd International Wire and Cable Symposium, Atlantic City, NJ, December, 1974.
4. R. C. Jerner and J. A. Harcourt, "Evaluation of Puncture Resistant Property", Unpublished document.

Biography

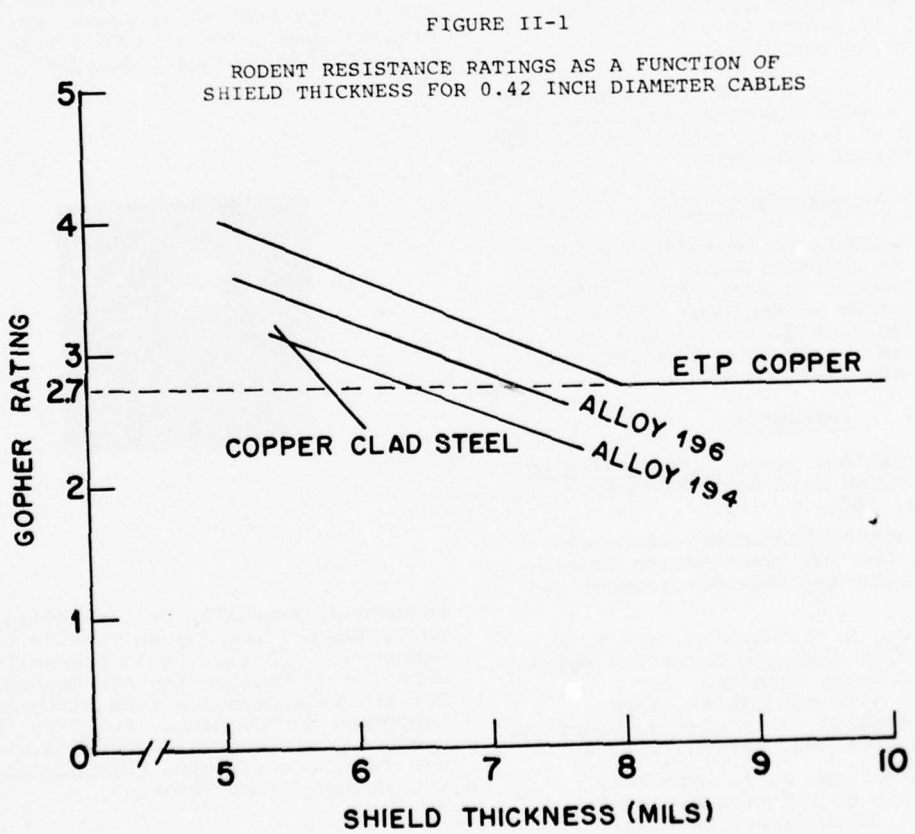
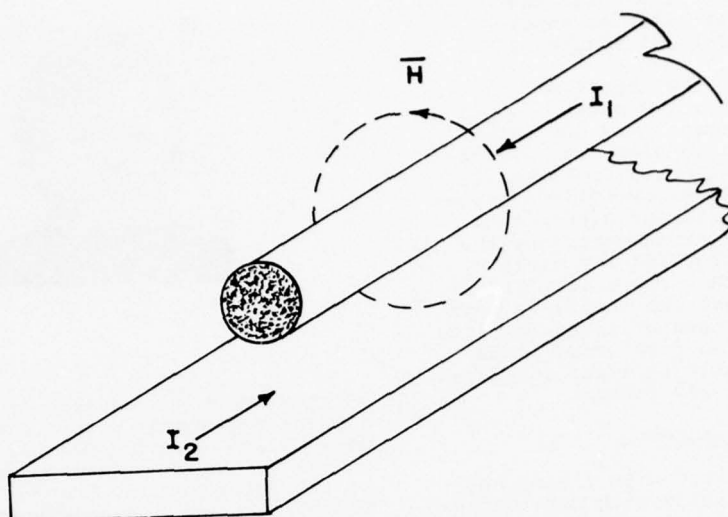


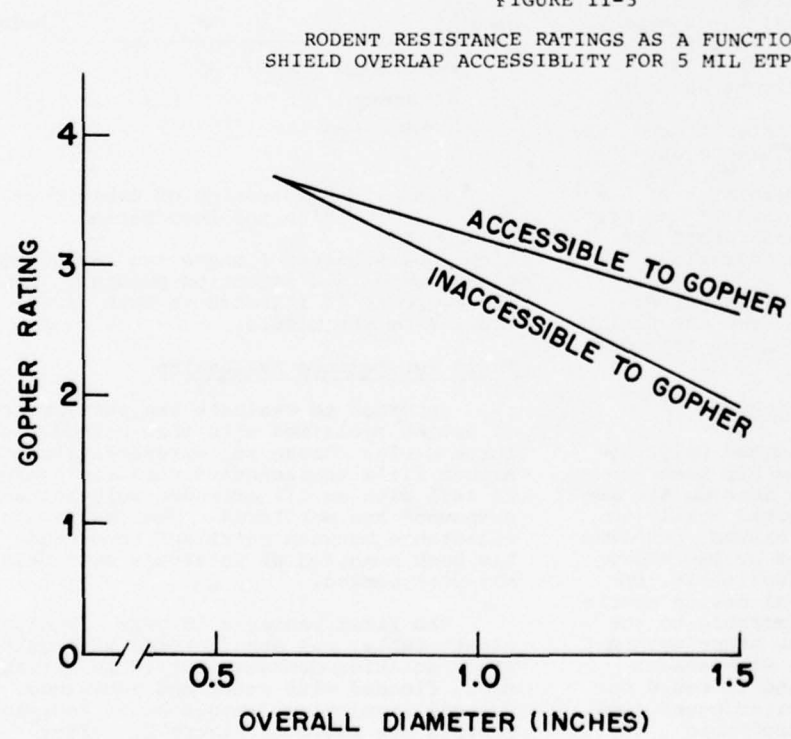
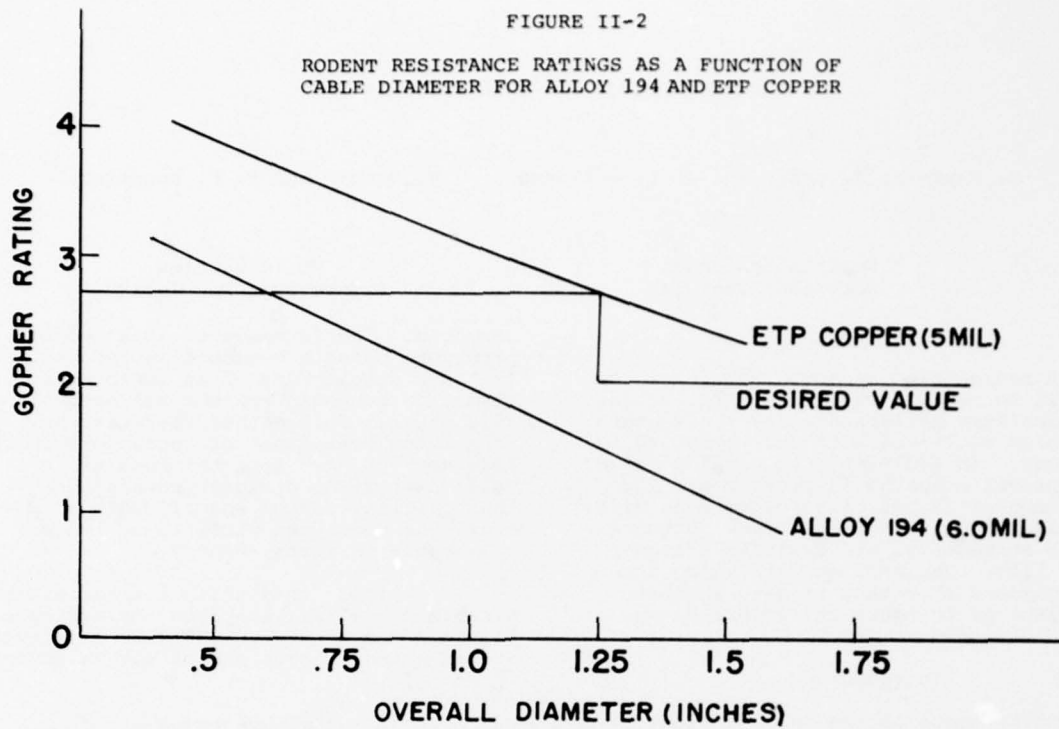
Harry M. Hutson graduated from John Hopkins University with a B.S.E.E. degree in 1970 and attended Georgia Tech in 1971 and 1972. He is presently on the staff of the Outside Plant Branch of REA's Telephone Operations and Standards Division. Most of his work has been in the field of outside plant cable developments. Mr. Hutson, who has been with the REA for the past three years, was previously associated with Bell Telephone Laboratories, Atlanta, Georgia.



Kenneth W. Brownell, Jr., received his Ph.D. degree from the University of Tennessee in 1975. He is presently the Director of Engineering and Development for the Telecommunications Division of the Brand-Rex Company. Prior to this present position he served as a research and development engineer at Superior Continental Corporation.

FIGURE I-1
SHIELD PROXIMITY EFFECTS





THE PERFORMANCE OF CABLE RECLAMATION

S. Kaufman, R. Sabia and J. L. Williams

M. Brauer and T. F. Kropinski

Bell Laboratories
Norcross, Georgia

NL Industries
Hightstown, New Jersey

Abstract

A reclamation compound was developed in 1971 to reclaim waterlogged PIC cables. The excellent performance, over six years, of cables reclaimed with this compound is reviewed. In addition, the development of an improved compound is presented. The new compound is not based on toluene diisocyanate, does not stress crack polycarbonate connectors, and exhibits a longer shelf life. Reclamation data using the new compound show that it also exhibits excellent performance characteristics.

Introduction

Maintenance of the outside plant is a major concern of the operating telephone companies. Due to the large investment in the plant, methods and materials for rehabilitating the outside plant offer the operating companies significant savings.

In 1971, methods and materials for reclaiming waterlogged polyethylene insulation (PIC) cable were introduced.¹ This was accompanied by the development of additional methods,^{2,3} materials⁴ and test sets⁵ to troubleshoot, rehabilitate and reclaim cables, coils and pedestals.

This paper will review the performance of cable reclamation over the past six years and present data on an improved reclamation compound.

Cable Reclamation

Reclamation of waterlogged polyethylene insulated (PIC) cables has been reviewed.^{1,2} Presently, two methods are being used. One method, limited mostly to flooded but undamaged PIC cables, involves purging of water using high pressure dry air. This method, where applicable, restores the cable to original design specification but leaves it vulnerable to subsequent water reentry. The other method is applicable to PIC cable with sheath damage (e.g., lightning) and is based on the concept of purging a waterlogged cable and gelling in-place a hydrophobic

compound.¹ Performance of this second procedure using a compound introduced in 1971 and development of an improved reclamation compound are the subjects of this paper. This method restores the insulation resistance of conductors which have not corroded open but results in a cable exhibiting a higher capacitance than original design specification. However, the reclaimed cable is no longer vulnerable to water reentry.

A typical field setup for reclaiming a cable by gelling in-place the hydrophobic compound is shown in Figure 1. Plugs are injected at each end of the cable sec-

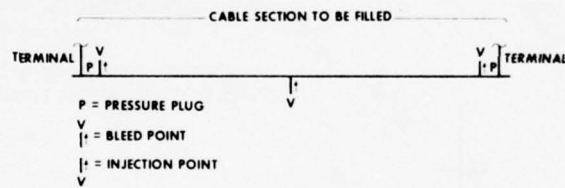


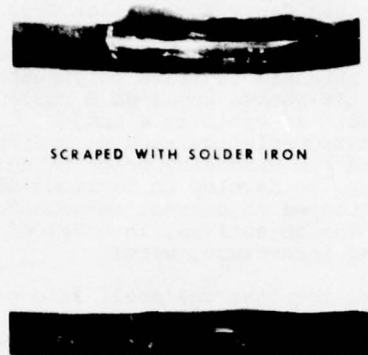
Fig. 1 - Preparation of Cable Section for Reclamation

tion, and pressure flanges are installed at the bleed and injection points. Then the compound is injected in both directions from the middle.

Field Performance Evaluation

In order to evaluate the performance of cables reclaimed with this method, three cables chosen as representative of severe field environments were reclaimed in 1971 with an oil extended polyurethane compound¹ and monitored. The insulation resistance between pairs and to ground has been measured at intervals over this six-year period.

The first cable, a 50 pair, 19 gauge alpeth cable, was manufactured with multiple insulation damages, buried in a swamp area, flooded with water and reclaimed. Typical insulation damages at 50 foot intervals are shown in Figure 2. After



SCRAPED WITH SOLDER IRON

CRIMPED WITH ROUND NOSE PLIERS

Fig. 2 - Two Types of Insulation Damages

gelling of the reclamation compound, the buried cable jacket was violated at 100-foot intervals. Full of water, this test cable exhibited 35 out of 50 pairs with insulation resistance values of 10^7 ohms or less. The performance after reclamation is shown in Figure 3, with all pairs at 10^8 ohms or better after six years.

The second cable was a working 19 gauge alpeth cable buried in a high lightning area. Adjacent buried sections had already been replaced with aerial cable. Faced with continuing trouble reports, the operating company agreed to reclaim the remaining buried sections. Some of the pairs were made available for monitoring long term performance, Figure 4. After six years, all monitored pairs are 10^6 ohms or better, which is satisfactory for voice use.

The third cable was a 400 pair, 22 gauge alpeth working cable buried in a wet area. It had a history of trouble reports and transposed pairs. The performance after reclamation is summarized in Figure 5. After six years, all pairs are 10^7 ohms or better.

Field Problem Reports

Cable reclamation is a success as evidenced by the field performance over six years and the widespread acceptance by telephone companies. Complaints associated with cable reclamation have been few. Only four cases have come to our attention and none of these has indicated a lack of performance by the reclamation compound.

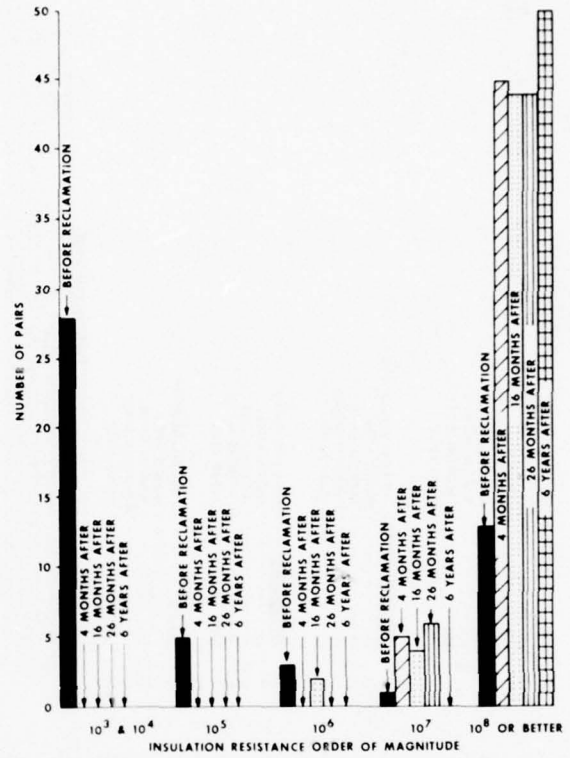


Fig. 3 - Reclamation Performance of Test Cable

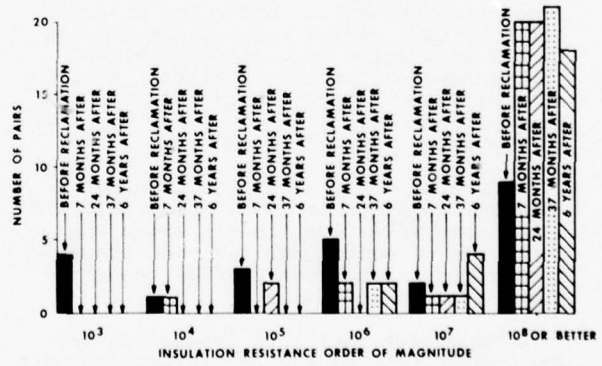


Fig. 4 - Performance of Working Cable Reclaimed in High Lightning Area

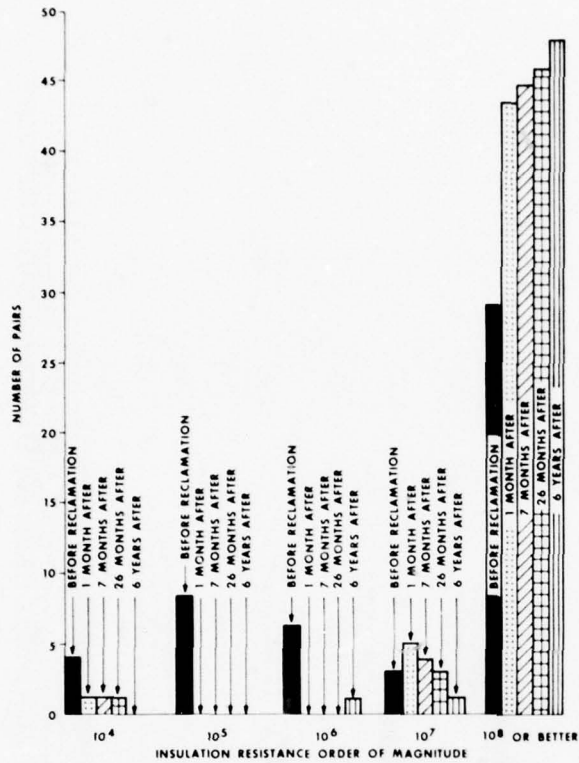


Fig. 5 - Performance of a Working Cable Reclaimed in a Wet Area

In one cable, an existing encapsulated splice was used as the plug at a bleed point, per Figure 1. Water, trapped between the bleed point and the splice, penetrated the splice under the injection pressure used during reclamation and led to low insulation resistance problems. The recommendation now in similar circumstances is to inject a plug adjacent to the splice to act as the primary barrier to any water trapped in the cable.

Another cable after reclamation exhibited two pairs at 10^3 ohms. Field and laboratory investigations in which the cable was dissected and analyzed traced the problem to cuprous sulfide trees^{6,7} which shorted the pairs.

Excessive, multiple insulation damages which escaped factory inspection were the causes for the poor reclamation of the last two cables. In one cable corrosion of the conductors was too advanced prior to reclamation. The other cable used a spun bonded polyester core wrap which if wet cannot be dried under field conditions. Exposed conductors in contact with the wet

core wrap continued to exhibit low insulation resistance after reclamation.

An Improved Cable Reclamation Compound

The original reclamation compound¹ is an oil extended two-part polyurethane compound. It became known as B reclamation compound. It exhibits a number of desirable characteristics such as hydrophobicity and low viscosity prior to gelling. A program to develop an improved compound was initiated to correct certain deficiencies. The objectives, in order of decreasing importance, were:

- (1) to increase the shelf life of the compound,
- (2) to remove the need of a prepurge compound,
- (3) to eliminate toluene diisocyanate from the prepolymer,
- (4) to decrease the volatility of the gelled compound, and
- (5) to develop a compound which did not dissolve or stress crack polycarbonate materials.

The new formulation has replaced the original compound and is marketed as C reclamation compound. It meets all objectives listed above. Furthermore, C reclamation compound has essentially the same handling characteristics as B reclamation compound.

The basic chemistry of the new compound is described in the patent literature.⁸ A reenterable encapsulant⁹ introduced in 1975 also employs this technology. By suitable choice of components and concentrations, the shelf life, viscosity, gel time, volatility, as well as the stress cracking activity of the compound can be controlled.

B reclamation compound exhibited a shelf life of about 6-12 months. This was a severe limitation, since the viscosity and, hence, pumping time increase as the shelf life is approached. The aging characteristics of C reclamation compound have been studied over a four-year period, Table I. These data indicate that properly sealed containers of the compound do not experience significant increases in viscosity, and that the gel time is quite stable even after 46 months.

Table I

Effect of Aging on the Gel Time of C Reclamation Compound

| <u>Months</u> | <u>Gel Time*</u> <u>(hrs)</u> | <u>Viscosity (cps)</u> | |
|---------------|----------------------------------|------------------------|----------------|
| | | <u>Part I</u> | <u>Part II</u> |
| 0 | 23 | 19 | 16 |
| 7 | 19 | | |
| 18 | 20 | | |
| 46 | 22 | 22 | 24 |

*Gel time is defined here as the time to reach 1000 centipoises using a Brookfield Viscometer and a number 1 spindle at 6 rpm and 25°C.

After mixing, the viscosity increases exponentially up to gel formation, Table II. Since at a given pressure, the pumping time is proportional to the viscosity,¹ the reclamation procedure requires careful planning so that, in general, no section will require more than two hours of pumping. During this period the viscosity of C reclamation compound increases by a factor of 2 to 3.

Table II

Viscosity of C Reclamation Compound As it Gels (Mixed at 25°C)

| <u>Time (hrs)</u> | <u>Viscosity (cps)</u> |
|-------------------|------------------------|
| 0 | 20 |
| 1 | 35 |
| 5 | 70 |
| 10 | 120 |
| 15 | 210 |
| 20 | 440 |
| 22 | 1000 |

In keeping with the concept that reclamation of a cable section will require about 2 hours of pumping time, the gel time may be set. Thus, the gel time typically is about 23 hours at 25°C, Tables I and II. However, the gel time of production lots may vary between 15 and 40 hours. It is also strongly dependent on temperature. The importance of keeping the compound and pump well shaded and cool is illustrated in Table III or the compound may gel in the pump on sunny, hot days.

Table III

Temperature Dependence of C Reclamation Compound

| <u>Temperature °C</u> | <u>Initial Viscosity (cps) of Mixture</u> | <u>Gel Time (hrs)</u> |
|-----------------------|---|-----------------------|
| 15 | 28 | 40 |
| 25 | 19 | 23 |
| 35 | 15 | 13 |

The cable reclamation time is dependent on the viscosity of the compound. The low viscosity components used in the compounds necessarily exhibit high volatilities. The volatility of B reclamation compound was acceptable since it was used in a buried application. The data, after six years in the field, support this engineering decision. The volatility of C reclamation compound is approximately half that of B reclamation compound. Further improvements were not warranted based on the field performance.

B reclamation compound dissolves polycarbonate connectors. Thus, buried cable splices and splices in aboveground terminals had to be protected during cable reclamation. A design objective for the new compound was that it would not dissolve or stress crack polycarbonate connectors. A test was designed⁹ in which an annealed polycarbonate flexure bar was strained to 0.75% and exposed to the compound at room temperature for 30 days. The requirement was that the bar should not craze or crack during or after curing. C reclamation compound passed this test with no visible degradation. The test was continued for one year with still no visible signs of degradation.

Selected physical properties of the reclamation compounds are presented in Table IV. The densities of each part in either compound are essentially the same, so that the proper mix ratio of 1:1 can be obtained on either a weight/weight or volume/volume basis. Also, the pour point of both parts is well below normal operating temperature. The difference in densities between the B and C reclamation compounds is reflected in the cable reclamation process, i.e., when water and compound are being purged out of the cable, C reclamation floats while B reclamation compound sinks. Thus, when reclaiming a cable, water is purged out followed by a mixture of compound and water which separates out. When phase separation stops, the reclamation process is completed.

Table IV
Physical Properties of
Reclamation Compounds

| | B Compound | | C Compound | |
|---------------------|------------|---------|------------|---------|
| | Part I | Part II | Part I | Part II |
| Density (g/cc) | 1.02 | 1.00 | 0.844 | 0.845 |
| Pour Point (°C) | 8 | -36 | 5 | 6 |
| Flash Point (°C) | 129 | 132 | 127 | 131 |

The electrical properties of C reclamation compound, Table V, are slightly superior to B reclamation compound

Table V
Electrical Properties (25°C)

| | C Compound | B Compound |
|---|----------------------|----------------------|
| Dielectric Constant @ 1 kHz | 2.6 | 2.6 |
| Dissipation Factor @ 1 kHz | 0.001 | 0.005 |
| Volume Resistivity at 100 vdc (ohm-cm) | 1.6×10^{13} | 1.5×10^{11} |

The gelled reclamation compounds are soft gels with very low tear strengths. Thus, in those cases where a reclaimed cable has to be spliced (for example, if it is cut), entry is not a problem. However, since low density polyethylene insulation is softened by these compounds, handling with care is required to avoid excessive elongation of the insulation and to insure a good splice.

In evaluating the performance of C reclamation compound, a 50 pair, 26 AWG alpeth cable with deliberate insulation damages, Figure 2, was manufactured per Table 2.

Table 2
Types of Insulation Damages

| Pair Number | Condition |
|-------------|--------------------------------|
| 1-20 | Scraped with hot solder iron |
| 21-25 | Not intentionally damaged |
| 26-45 | Crimped with round-nose pliers |
| 46-50 | Not intentionally damaged |

The cable was divided into three 300-foot sections. After filling with water, all three sections were reclaimed with C reclamation compound as discussed below.

The need of a prepurge compound¹⁰ was evaluated, using two experimental cables. The prepurge compound is polypropylene glycol. It is miscible with water and B reclamation compound but is not miscible with C reclamation compound. It was introduced since data and visual examination indicated that if pumped into a waterlogged cable ahead of the reclamation compound, it improved the purging of water out of the cable. This was accomplished at the expense of increased pumping time. Cable reclamation results indicated that with C reclamation compound, the use of polypropylene glycol is not necessary and its use has been eliminated.

The performance of the third cable reclaimed with C reclamation compound is summarized in Figures 6 and 7. After 18 months, all pairs of one of the intentionally damaged cables, which was reclaimed while buried in a cable test lot, exhibited volume resistivities in excess of 10^8 ohms, Figure 6. The change in capacitance with time may reflect compound components being absorbed by the insulation, migrating to the conductor-insulation interface and changing the effective dielectric constant. Cables reclaimed with B reclamation compound and monitored for only seven months

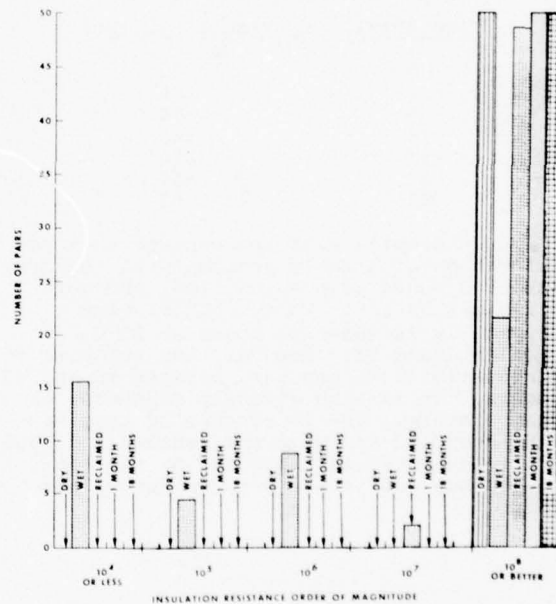


Fig. 6 - Insulation Resistance Data of Cable Reclaimed with Improved Reclamation Compound

show similar trends. This change is not important for voice transmission.

In addition to the above experiments, C reclamation compound was used on field trials with two operating companies. These trials were successful and concluded the evaluation program.

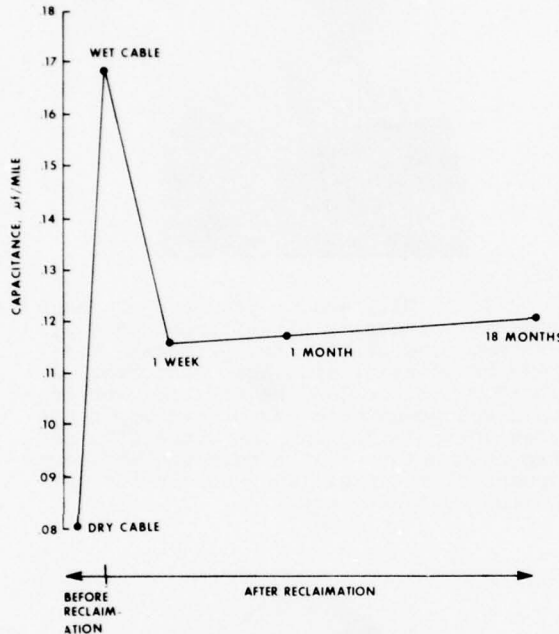


Fig. 7 - Capacitance Before and After Reclamation

Conclusion

Reclamation of waterlogged cables by pumping into the cable a compound which displaces water and gels in place is a widely accepted practice. The performance of cables reclaimed by this method in 1971 using B reclamation compound has been excellent. No failures attributable to the compound have been reported. An improved reclamation compound has been introduced. It is not based on toluene diisocyanate, exhibits an extended shelf life and does not attack polycarbonate connectors. Insulation resistance data have been presented which show that a cable reclaimed with C reclamation compound has performed over a period of 18 months as well as cables reclaimed with B reclamation compound.

Acknowledgement

This paper was made possible by the contributions of numerous persons, especially R. Walker.

References

1. S. Kaufman and R. Sabia, Proceedings of the 21st International Wire and Cable Symposium, 1972.
2. N. E. Hardwick, III, Proceedings of the 23rd International Wire and Cable Symposium, 1974.
3. Methods and materials for reclaiming (leaking) coil cases and rehabilitating pedestals have been recently introduced.
4. J. W. Shea, Proceedings of the 21st International Wire and Cable Symposium, 1972.
5. New automated test sets for sheath fault location and for detection of water in cables have been introduced.
6. Fukuda et al, Proceedings of the 21st International Wire and Cable Symposium, 1972.
7. B. D. Gesner, this Symposium.
8. U. S. Patent 4008 197 assigned to NL Industries.
9. M. Brauer and R. Sabia, Proceedings of the 24th International Wire and Cable Symposium, 1975.
10. Bell System Practice.



Stanley Kaufman is the Supervisor of the Materials Chemistry Group at Bell Telephone Laboratories in Norcross, Georgia. He received a B.S. in Physics from the City College of the City University of the City of New York, and a Ph.D. in Chemistry from Brown University. Before joining Bell Laboratories in 1970, he was a research scientist at the Uniroyal Research Center.



J. L. Williams, a graduate of Johns Hopkins University of Baltimore (B.S.), was employed by the Glen L. Martin Company prior to joining Bell Laboratories in 1962. Since 1962 he has been working on development of closures and apparatus used in cable joining and since 1975 he has been active in the research and development of materials and methods for use in the outside plant.



Raffaele Sabia, a graduate of St. Francis Collete of Brooklyn (B.S.) and Polytechnic Institute of Brooklyn (Ph.D.), was employed by the Polymer Chemical Division of W. R. Grace prior to joining Bell Telephone Laboratories in 1963. Since 1963 he has been active in the research and development of materials for application in the wire and cable area. Since 1967 he has been supervisor of the Chemical Engineering Group in the Transmission Media Laboratory.



Melvin Brauer received his B.A. Degree from Hunter College and did graduate work at this college. Prior to joining NL Industries in 1972 he was employed by Hercules Incorporated as a propellant development chemist. Since 1973 he has been exclusively involved in the development of potting, encapsulation and cable reclamation compounds. He has two patents pending in connection with this work.



Ted Kropinski received his B.S. Degree from Rutgers University and his M.S. from The New Jersey Institute of Technology. Prior to joining NL Industries in 1965, he was employed by the U. S. Envelope Company as an adhesive chemist. At NL Industries his work involves the development of polyurethane adhesives, coatings, and elastomers. Since 1972 he has been Section Leader for the urethane laboratory. He has written two papers and has several patents pending.

PATTERN BELT, A NEW INDUCTIVE WIRE FOR
POSITION DETECTION OF LINEAR MOTOR VEHICLES

T. Sasaki

Japanese National Railways
Tokyo, Japan

T. Aono

Japanese National Railways
Hukuoka, Japan

T. Asai

T. Hoshikawa

Hitachi Cable, Ltd.
Hitachi, Japan

ABSTRACT

A new inductive wire cable designed for position detection of linear motor vehicles was developed and installed along JNR's test track in Miyazaki, Japan. The cable is formed by laying transpositioned multipair inductive wires in a fixed pattern on a common plastic belt. In the course of the development work, problems involving dimensional stability and crosstalk between different circuits -- particularly important problems affecting performance -- were resolved. As a result, high precision position detection of linear motor vehicles will be possible.

1. INTRODUCTION

Linear motor vehicles, viz., vehicles for magnetically levitated ground transportation, are now attracting attention as a pollution-free means of rapid transit. They produce very little noise or vibration because they operate without contacting any object, whereas conventional railway vehicles run on wheels contacting the rail track, with the pantograph contacting the power line. Moreover, linear motor vehicles are thought to be capable of speeds up to 500 km per hour, by far exceeding the acknowledged limit of 300 kph for conventional railways. The Japanese National Railways (JNR) began research work on magnetically levitated ground transportation around 1962.¹ Since April 1977, experiments have been conducted on a part of test track in Miyazaki Prefecture, Japan. Fig. 1 is a sectional diagram of the linear motor vehicle used in the experiments.

A key point in forming a safety control system for the linear motor vehicle lies in securing position detection of the vehicle. In the case of linear motor drive, requirements for position detection are different from those in conventional vehicles, in the following respects:

- Since the linear motor vehicle is levitated, the rail cannot be used for position detection as it is for conventional vehicles.
- To secure good efficiency of the linear motor, position detection for controlling the feeder section switch is required in order that current may flow only in the ground coils near the vehicle.

The linear motor for the JNR's test track in Miyazaki is a linear synchronous motor. In this case,

- Position detection must be made so that synchronous operation of the linear motor will be possible by switching the ground coil current synchronously with the on-board magnet position. For high-speed operation in the range of 500 kph, position detection must be made at high accuracy.

In an effort to meet the above requirements, the possibility of using induction radio techniques for position detection was investigated, and it was concluded that a detection system utilizing transpositioned multi-pair inductive wires is applicable for that purpose. We arranged transpositioned multipair inductive wires on a plate core and covered it with a sheath, to produce a flat cable. This cable can be installed in the same way as any conventional cable. From its appearance, the new cable was named "pattern belt."

Fig. 2 shows a position detecting system based on transpositioned multipair inductive wires (pattern belt).

The pattern belt is installed along the linear motor vehicle track in a way that it is held in a specified position relative to the ground coils. A 180 kHz signal transmitted from the on-board antenna is received by the pattern belt through which it proceeds to the central receiving equipment (position detecting equipment), where the vehicle position and speed are detected. Based on that information, ground coil current is controlled. Fig. 3 shows the relative position of on-board antenna and pattern belt.

2. VEHICLE POSITION DETECTION BY PATTERN BELT

Configuration of Pattern Belt

Fig. 4 is a block diagram of a linear motor vehicle position detecting system using transpositioned multipair inductive wires. Six pairs of inductive wires are arranged one on top of the other on the same plate core, so that each inductive pair is held in a specified position relative to the corresponding ground coil (U_1, V_1 of W_1). Each pair forms a loop at the point of the corresponding ground coil. The loops are in transposition.

Principle of Position Detection

As is shown in Fig. 2, the pattern belt is divided into several blocks over the entire route, and the blocks are connected by cable to the central receiving equipment through repeaters.

Fig. 4 explains the principle with regard to the U_1 pair. As the on-board transmitting antenna moves, a voltage corresponding to coil position is received. This voltage undergoes amplification, detection and comparison. The moment the comparator input level reaches the threshold level is regarded as the moment the vehicle passes the coil corresponding to the U_1 pair. In this way, position detection is made.

Feeder section can be detected by counting the output for the coil position detection in a unit feeder section. A method of using the pattern belt to detect vehicle position as continuous analog values is being studied.²

3. CONSTRUCTION OF PATTERN BELT

Cable of Transpositioned Multipair Inductive Wires

Many pairs of transpositioned inductive wires mean many signals of antenna position; hence a higher detecting accuracy can be expected. It is not practical to install the pairs separately since this would increase the number of inductive wires. The wires were arranged in a specified pattern on a common belt-like plate core, which was then wrapped in a common sheath. The product was named pattern belt. In making the cable, attention was paid to the following requirements:

- As installed inductive wires must be held in a specified position dimensionally relative to the ground coils of the linear motor, variation of longitudinal dimensions due to variation of temperature, tension and other factors during

- manufacture or after installation must be minimized.
- (2) Using many pairs of inductive wires results in greater possibility of crosstalk or noise between different pairs. Therefore, an installation pattern subject to minimum electrical coupling between pairs must be selected.
 - (3) The cable must allow easy installation by conventional cable techniques.
 - (4) The cable must be strong enough to withstand wind pressure and vibration generated by high-speed operation of the linear motor vehicle.
 - (5) The cable must have sufficient weatherability to prevent deterioration of inductive wires due to exposure to the elements.

Fig. 5 and Table 1 show the construction of a newly developed pattern belt that meets the requirements listed above. Twisted pairs of inductive wires with loops at specified points are placed on a belt-like FRP core plate and fixed in place by using hole notches provided on both edges of the core plate. The core plate is then jacketed in a common sheath supported by suspension wires running along both edges.

Material for Core Plate

Variation of the length of the pattern belt due to temperature, tension and other factors will affect the accuracy of position detection. Suppose that expansion and contraction of the pattern cable of inductive wires must be limited to ± 10 cm. The cable used on the test track in Miyazaki was made in unit lengths of 120 m in consideration of ease of transportation and installation. Therefore, the allowable expansion and contraction is $\pm 10\text{cm}/120\text{m}$, viz. $\pm 0.085\%$ (8.5×10^{-4}).

In securing dimensional stability of the pattern cable of inductive wires, selection of the proper material for the core plate is the most important consideration. Even if the hole notches in the core plate (Fig. 5) are made accurately and the inductive wires are installed with high precision, the unusually rigid requirement of $\pm 0.085\%$ cannot be met if the core plate should expand or contract due to the heat in the extrusion process, the tension at installation, the temperature variation following installation, or to other reasons.

A metal plate has a small coefficient of expansion, but is not suited for a core plate for inductive wires because it shields radio waves. The core plate must have a suitable flexibility in order that the cable may be wound on a drum during manufacture of after completion, and that the completed cable may be handled with ease during installation.

After examining various materials with these conditions in mind, it was found that a core plate of FRP would be the best choice.

Table 2 shows the measured Young's modulus and coefficient of linear expansion of the FRP core plate used in the pattern belt illustrated in Fig. 5, as compared with those of a high-density PE core plate. As is shown in Table 2, deviation of length in cables of the two materials subjected to a tension of about 900 kg was only 0.025% for FRP as against 0.48% of high-density PE.

FRP resists elongation even at high temperatures and is effective in minimizing deviation of length due to heat during manufacture and use. It is also useful as a tension member.

Strain during manufacture often remains in plastic materials. Consequently, they occasionally show thermal contraction, which leads to deviation of length. Fig. 6 shows thermal contraction of an FRP plate (2 x 120 mm) and a high-density PE plate (3 x 130 mm) as observed in a heat cycle test. FRP shows a small thermal contraction, which makes it ideal for a core plate.

4. CHARACTERISTICS OF PATTERN BELT

Crosstalk Coupling Between Inductive Pairs

In using transpositioned multipair inductive wires over a long distance, crosstalk between different inductive pairs poses a problem. With strong coupling and intense crosstalk between pairs reception level would vary, making accurate position detection difficult. The relationship between cross-talk and installation pattern of inductive pairs was considered.

In a pattern belt of six pairs of transpositioned inductive wires trially manufactured in the early stage of our development work, the inductive wires were arranged as in Pattern I in Fig. 7 (a). In this case, major causes of crosstalk between different inductive pairs were, in the order of seriousness: (i) coupling between adjacent loops, (ii) coupling between loop and lead, and (iii) coupling between leads.

With the inductive wires arranged as in Pattern II in Fig. 7 (b), coupling between pairs was vastly reduced. The differences from Pattern I are (i) each loop is made shorter, (ii) the lead part of inductive wires is twisted, and (iii) twisting pitch is varied from pair to pair.

Table 3 shows crosstalk loss between inductive pairs in Patterns I and II. It will be noted that far-end crosstalk loss (FXT) in Pattern II is 16 dB better in both mean and minimum values.

Possible methods of stacking twisted inductive wires on the core plate are shown by Patterns II-a and II-b in Fig. 8 (c). At an operating frequency of 180 kHz, the required crosstalk loss is presumed to be at least 25 dB/km. To verify the possibility of realizing this, we measured crosstalk loss frequency characteristics using a sample of about 70 m length. The results are shown in Fig. 8. If the length dependence of crosstalk may be assumed to deteriorate at the rate of $20 \log L$ as a general tendency, then a crosstalk loss of at least 49 dB will be needed for 70 m. In both Patterns II-a and II-b, this requirement is easily met. In Pattern II-a, however, crosstalk suddenly deteriorates as frequency increases, so that there is a danger of intense crosstalk where long distances are involved. It was, therefore, concluded that Pattern II-b is a better choice as the construction of inductive wires.

Transmission Properties of Pattern Belt

Table 4 shows some transmission properties of the pattern belt.

For use on the Miyazaki test track both the on-board signal generator and antenna were newly developed. Fig. 9 gives some measured coupling losses between on-board antenna and pattern belt. At the Miyazaki test site, the antenna and pattern belt are arranged about 520 mm apart as in Fig. 3, so that coupling loss is 54 dB (180 kHz) according to Fig. 9. From Fig. 9, it will be seen that, at around $h=520$ mm, variation of coupling loss with a variation of spacing between antenna and pattern belt is about 0.35 dB/10mm.

5. INSTALLATION OF PATTERN BELT

For transportation, each pattern belt, made in a unit length of 120 m, is wound on a cable drum (as ordinary cable drum modified for pattern belts). Installation is accomplished by almost the same procedure as for ordinary cables. In installation, the two suspension wires on both edges of the pattern belt can be utilized as tension members. Fig. 10 shows installation of Pattern Belt.

Installation of Pattern Belt

The greatest difficulty encountered in installing a pattern belt is the fact that the proper relative position between the pattern of inductive

pairs and the ground coils must be secured at all points along the route. The position must be maintained within the range of allowable error not only at the time of installation but also at all times thereafter even under temperature changes and vibrations due to passing vehicles.

To make this possible, the sheath was marked in advance to show positions of loops of certain couples of inductive wires and, at cable installation, these guide marks were aligned with the ground coils. Also, cable installation hardware was designed especially to withstand any increase of tension in supports that may be caused by temperature changes and wind pressure from passing vehicles.

The following three types of installation hardware were used:

- a. Suspension hardware (Fig. 11)
- b. Strain hardware (Fig. 12)
- c. Dead-end hardware (Fig. 13)

Cable Jointing

Pattern belts are jointed to form a repeater block (Fig. 2). In jointing work, care was taken not to disrupt the loop shape and positions of the pairs of inductive wires in the longitudinal direction. Also, to reinforce the joints and prevent water leakage there, they were covered with a polyethylene sleeve with an elliptical section, which was welded to the polyethylene sheath of the pattern belt. Fig. 14 and 15 show a joint and a termination, respectively.

6. CONCLUSIONS

A pattern belt was developed and shown to have high dimensional stability, which is required in position detection of linear motor vehicles. Crosstalk between different inductive pairs in the pattern belt was found to pose no problem. The pattern belt can be installed in almost the same way as conventional cables. The advantages of a cable of transposed multipair inductive wires can thus be given full play.

The cable, installed along JNR's test track under construction in Miyazaki, is now undergoing field application tests. The authors are confident that it will prove to be applicable for practical purposes.

REFERENCES

1. K. Miyazaki, "The State of Development by JNR of Magnetically Levitated Ground Transportation (MLCT)", Japanese Railway Engineering Vol. 16 No. 3 & 4, 1976.
2. T. Sasaki, E. Itakura, Y. Yokota, "Continuous Type Train Location Detection with Inductive Wires", Railway Technical Research Report No. 896, 1974.

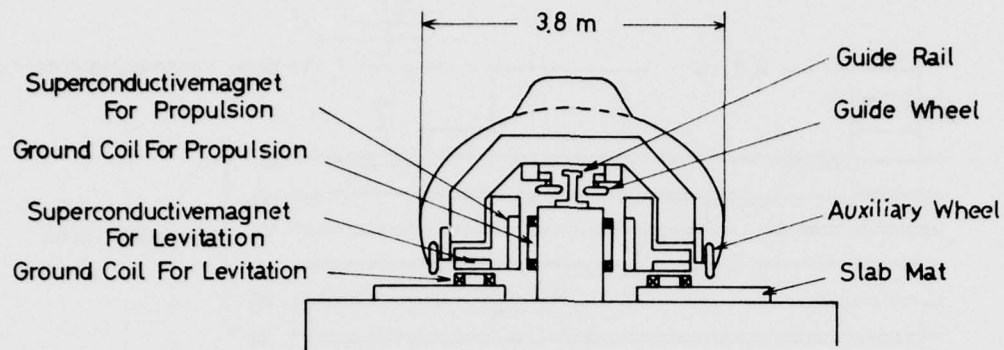


Fig. 1 Linear Motor Vehicle For JNR's Test Track

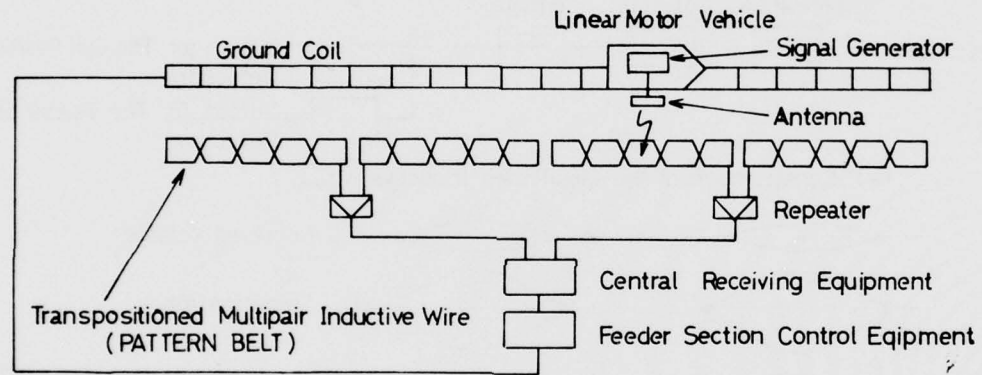


Fig. 2 Position Detecting System by Transpositioned Inductive Wires

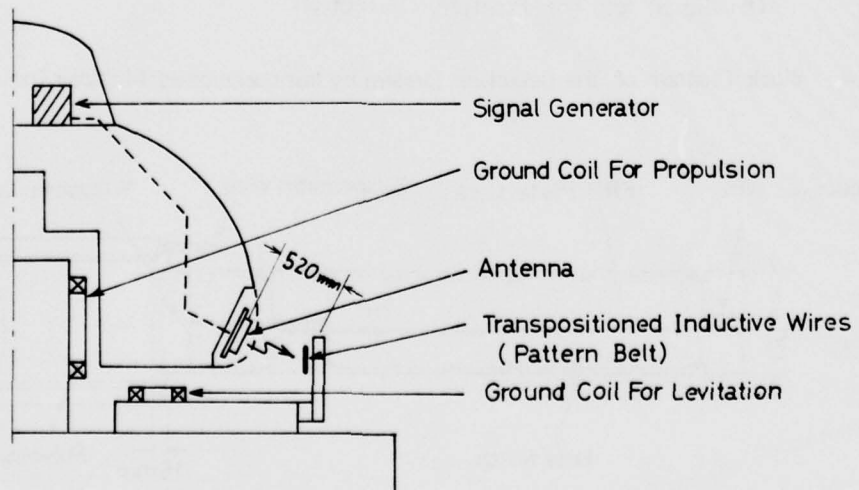
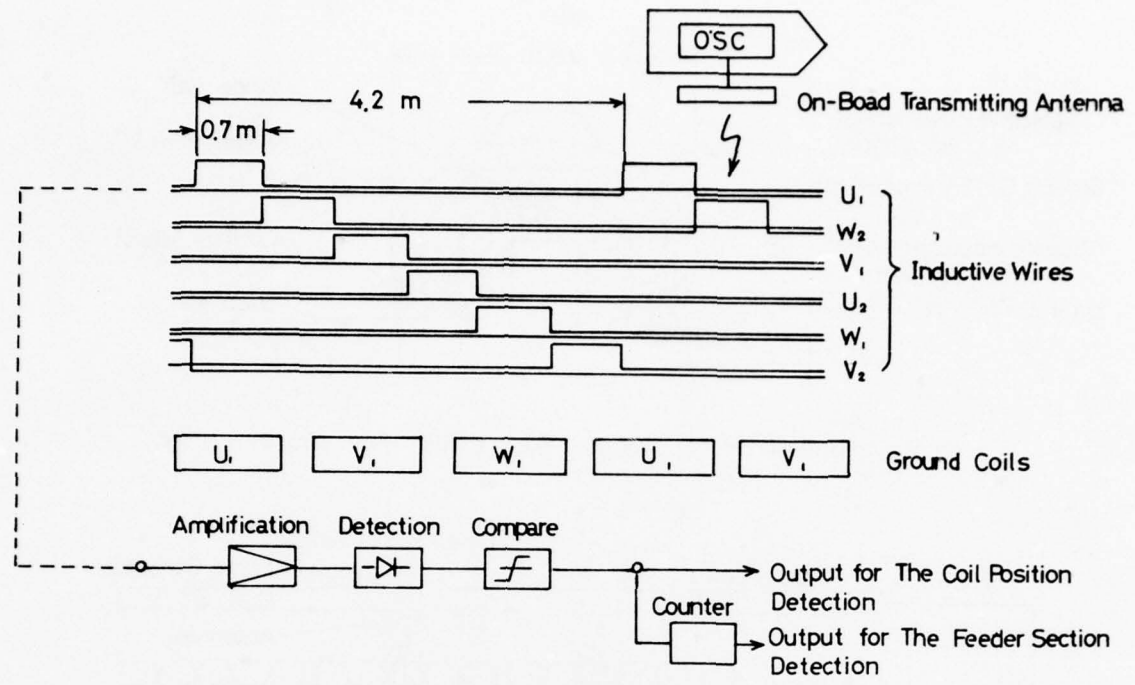
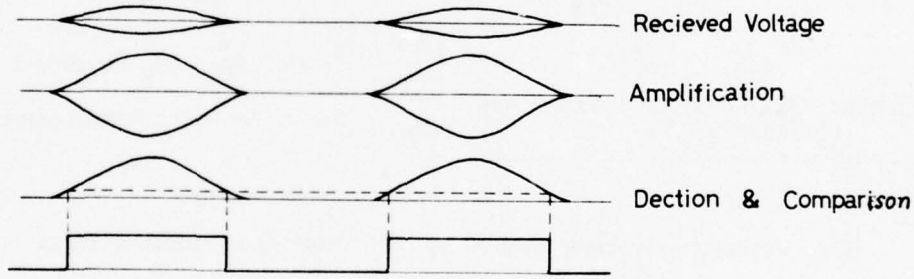


Fig. 3 Installation of Pattern Belt



(a) Construction of Transpositioned Inductive Wires



(b) Signal for The Position Detection

Fig.4 Block Diagram of The Detecting System by Transpositioned Multipair Inductive Wires

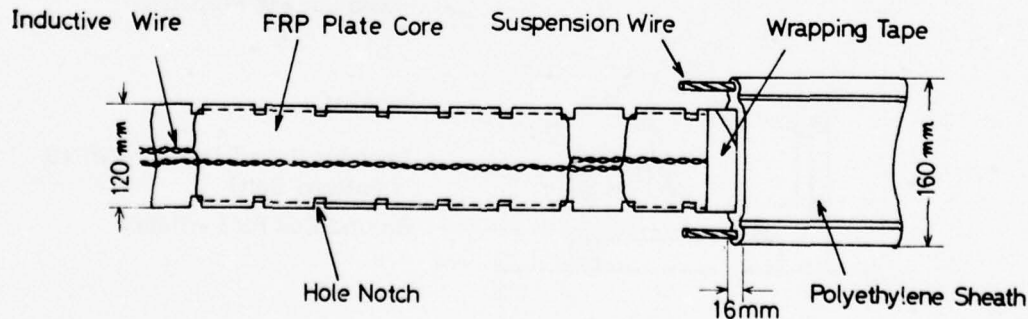


Fig.5 Physical Structures of Pattern Belt

Table 3 Crosstalk Loss

| Pattern | Crosstalk | Mean(dB) | Min. (dB) |
|---------|-----------|----------|-----------|
| I | NXT | 67 | 56 |
| | FXT | 73 | 63 |
| II | NXT | 90 | 80 |
| | FXT | 89 | 79 |

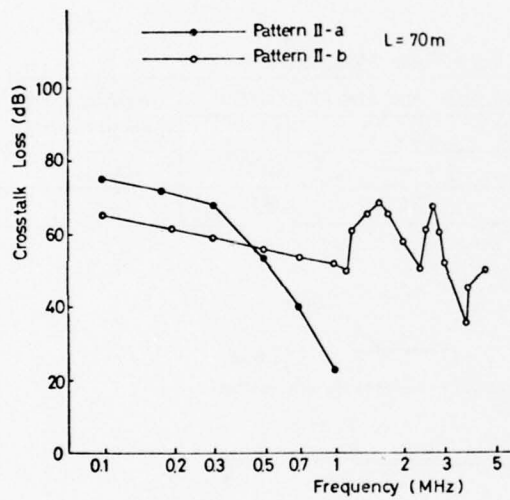


Fig. 8 Crosstalk Loss Frequency Characteristics

| Table 4 Transmission Properties of Pattern Belt | | |
|---|----------|------------------|
| Item | Unit | Measured Value |
| Measured Frequency | KHz | 180 |
| Attenuation | dB/km | 3.6 |
| Crosstalk Loss | dB/km | Not less than 43 |
| | dB/km | Not less than 44 |
| Characteristic Impedance | Ω | Approx. 170 |

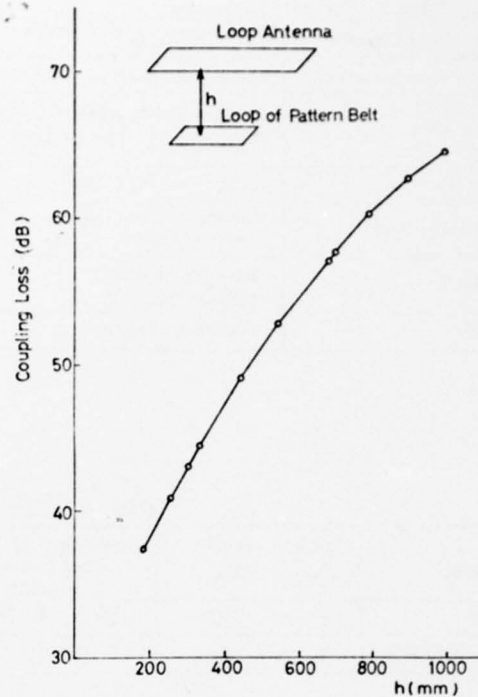


Fig. 9 Coupling Loss (Antenna-Pattern Belt)

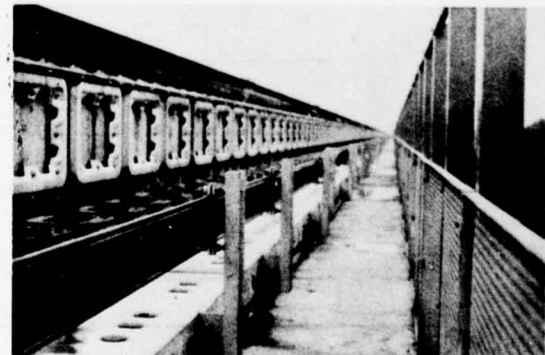


Fig. 10 Installation of Pattern Belt

Table 1 Physical Construction

| | | |
|-----------------|------------|---|
| Inductive Wire | Conductor | Stranded annealed tinned copper wire 0.9mm ² |
| | Insulation | Coloured polyolefin |
| Plate Core | | Fiberglass Reinforced Plastic(FRP) Thick. x Width. 2mm x 120mm |
| Wrapping | | Plastic or Cloth tape |
| Suspension Wire | | Galvanized steel wires number / mm : 7/ 2.9 |
| Jacket | | Black polyethylene Nominal thick. : 3mm |
| Weight | | Approx. 2.3Kg/m |

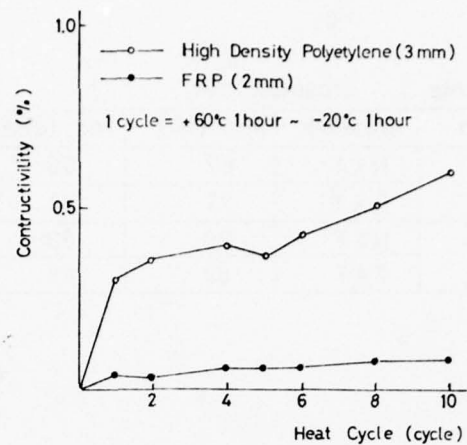


Fig.6 Thermal Contraction of FRP Plate

Table 2 Comparison of Core Plate Material

| Material | Thick. x Width (mm) (mm) | Coefficient of Linear Expansion (1/°C) | Young's Modulus (kg/mm ²) | | | Deviation of Length (%) |
|-----------------|-----------------------------|--|---------------------------------------|-------|--------|----------------------------|
| | | | 15 °C | 60 °C | 110 °C | |
| FRP | 2 x 120 | 0.8×10^{-5} | 840 | — | 600 | 0.025 |
| High Density PE | 3 x 120 | 17×10^{-5} | 49 | 14.3 | 8.9 | 0.48 |

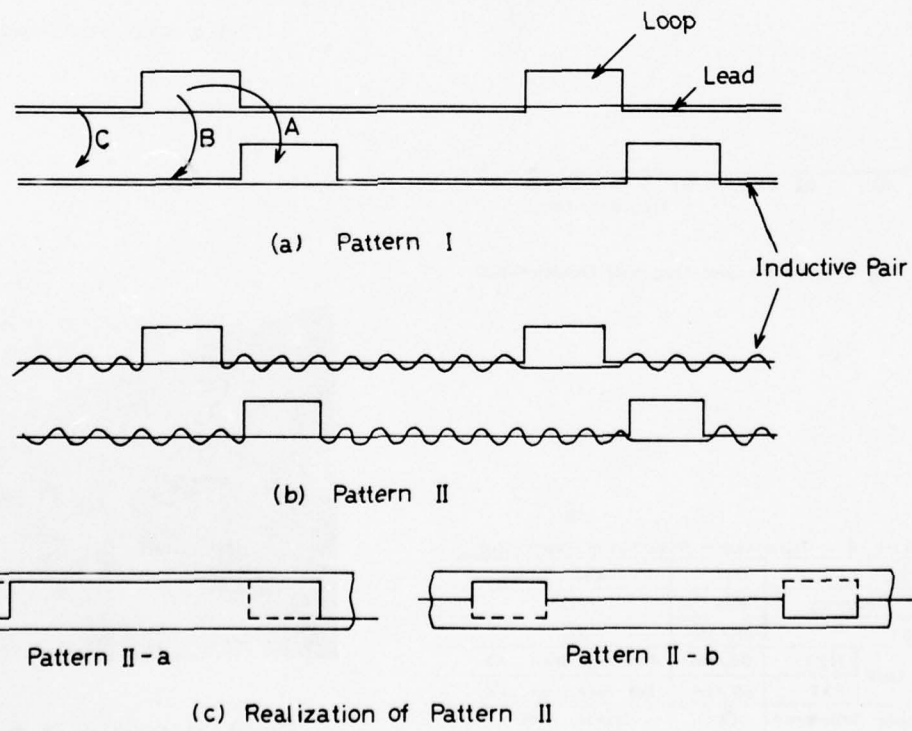


Fig. 7 Constructions of Inductive Wirers

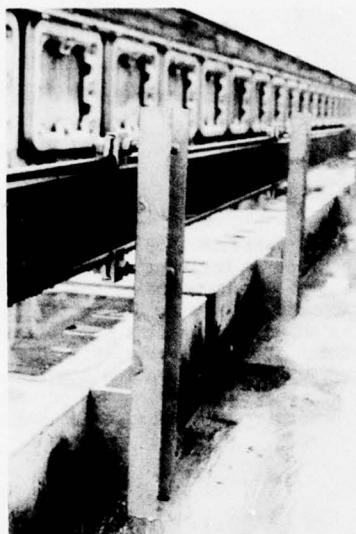


Fig. 11 Suspension of Pattern Belt



Fig. 12 Strain of Pattern Belt

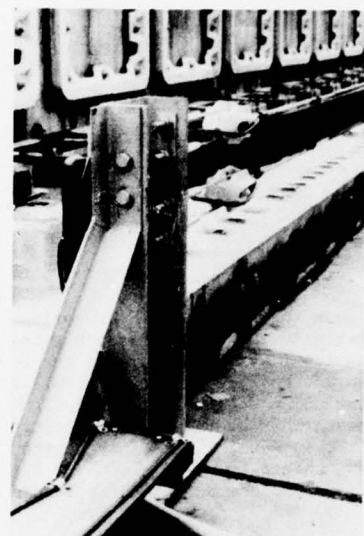


Fig. 13 Dead-end of Pattern Belt

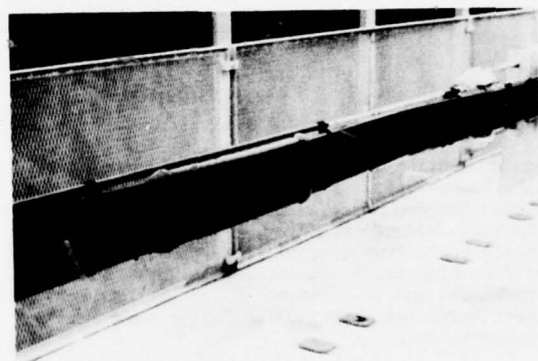


Fig. 14 Jointing of Pattern Belt

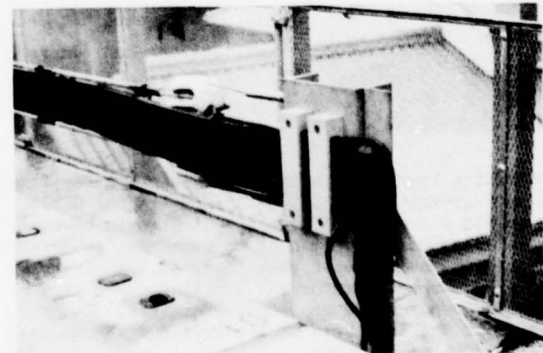


Fig. 15 Terminating of Pattern Belt



Toshiaki Sasaki
Railway Technical Research
Institute, Japanese
National Railway
2-8-38 Hikari-cho,
Kokubunji-shi
Tokyo, Japan



Takeshi Hoshikawa
Hitaka Works,
Hitachi Cable, Ltd.
5-1 Hitaka-cho, Hitachi-shi
Ibaraki-ken, Japan

Graduated from the Electronic Engineering Department, Tohoku University in 1962, thereupon joining the Japanese National Railway, where he has been engaged in research and development work on railway signal systems, including engineering and design work. Now, as chief researcher at the Railway Technical Research Institute, he is working on safety control systems for railway vehicles. He is a member of the Institute of Electronics and communication Engineers of Japan.

He joined Hitachi Cable in 1965 after completing a course in the Electric Engineering Department, Nagoya University. Every since he has devoted himself to development and design of communication cables. He is an engineer at the Communication System Department of Hitaka Works, Hitachi Cable. He is in charge of design of cables for broad band transmission systems. He is a member of the Institute of Electric and Communication Engineers of Japan.



Tatsuo Aono
Moji Electrical Construction Bureau, Japanese
National Railways
7-30 Minato-cho, Moji-ku
Kitakyushu-shi
Fukuoka-ken, Japan

Upon graduation from the Electric Engineering Department, Nagoya Institute of Technology, in 1959, he entered the Japanese National Railways, where his work has concerned planning, engineering and maintenance of railway electric communications. He is now Vice Director of the Moji Electrical Construction Bureau and is involved in the construction of a test track for magnetically levitated ground transportation.



Takahiro Asai
Research Laboratory,
Hitachi Cable, Ltd.
5-1, Hitaka-cho, Hitachi-shi,
Ibaraki-ken, Japan

Graduating from the Electronic Engineering Department, Tokyo University in 1965, he joined Hitachi Cable, where his research and development efforts have been directed at communication cable transmission systems. At present, he is chief researcher at the Hitachi Cable Research Laboratory, taking charge of work on high-frequency cable application systems. He is a member of the Institute of Electric and Communication Engineers of Japan.

AN IMPROVED ETFE BASED CABLE FOR AEROSPACE AND INDUSTRIAL APPLICATIONS

BY

E. BASCOU and M. MARECHAL

F I L O T E X
Manufacture de Fils et Câbles Electriques
140, rue E. Delacroix
91210 DRAVEIL (FRANCE)

ABSTRACT

A new ETFE based cable insulation, having a polyimide topcoat, appears as one of the best compromises on characteristics and price for use in Aerospace, Electronics, Nuclear, and Rapid Transit areas. Such cables maintain good handling characteristics and demonstrate significantly improved mechanical, thermal, overload, flame, and radiation resistance over straight ETFE cables.

INTRODUCTION

The market for wires and cables, produced for Specific Applications such as Aeronautics, Electronics, Rapid Transit and Nuclear Plants, has been moving most quickly those last years. This trend is related to real needs of the Industry, which has to cut prices and weights while always improving the characteristics of its equipments, in order to better compete at an International level.

The T/H cable construction, we are introducing here, has been developed according to those considerations and it appears as one of the best compromise on price and characteristics among all cable constructions now available. Nevertheless, we must point out that T/H cables are not a quite new development, and have already been chosen for a French Commercial Plane.

T/H CABLE CONSTRUCTION

The T/H hook-up wire, we wish to present, has an extruded ETFE insulation with a polyimide topcoat, both insulating layers being in intimate contact. No air gap must remain between the ETFE and polyimide layers, which can be easily obtained through our production procedures. Let us insist on the fact that air gaps must be avoided on dual layer insulations, mainly at low radial thicknesses as air gaps will lower the insulation Corona Ignition Voltage (fig. 1).

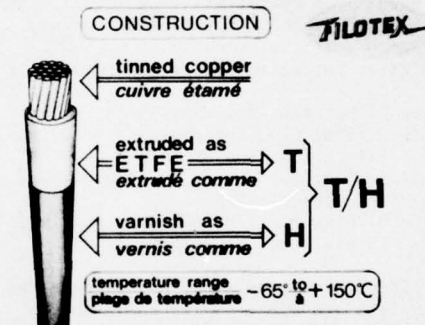


Figure 1

The thickness of the polyimide topcoat is close to 25 µm or 1 mil, 20 µm being the minimum figure, sufficient to improve ETFE characteristics to the level we shall detail.

Such a topcoat may be applied on ETFE insulations as low as 0.15 mm or 6 mils in thickness. Of course, the polyimide topcoat thickness might be increased to 1.5 or 2 mils for Specific Applications.

This type of insulation can be applied on any bare or coated conductor, including tin, silver and nickel protections on copper.

In fact, we shall only consider here T/H cables with tinned copper conductors as this construction is quite consistent with the rating of such cables, which is theoretically restricted to 150° C as any ETFE based cable.

GENERAL T/H CABLE CHARACTERISTICS

When compared to conventional or "old-fashion" cables such as those based on PVC, Polyolefins or Elastomers, T/H cables introduce the tremendous improvements of those well-known new chemical insulating products, which appeared those very last years, ETFE and Polyimides being among the best examples.

The most important improvements introduced by T/H cables concern :

A - Weight and space saving, similar electrical and mechanical characteristics levels being achieved through lower wall thicknesses. For a 600 Volts rated cable in Gage 20, insulation thickness varies approximatly :

- . from 0.5 mm min. for elastomers
- . to - 0.35 mm min. for plain or irradiated Polyolefins and PVC/PA.
- 0.25 mm for plain, irradiated ETFE and possibly T/H.
- 0.20 mm for T/H and fully polyimide insulations, referenced as K/H.

The difference in wall thickness leads to the weight and space saving shown on the following graphs (fig. 2).

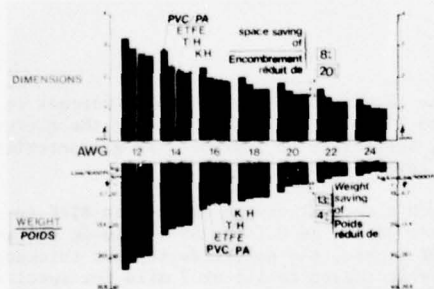


Figure 2

and which are, in 20 AWG size, of :

- 8 % for T/H and K/H in 8 mils over ETFE, and 20 % over PVC/PA, for space saving.
- 4 % for T/H over ETFE, and 13 % over PVC/PA, for weight saving.

B - Safety and reliability through all service life will also be enhanced by T/H cables.

Surely, one of the main drawbacks of conventional cables is their poor behaviour in fires or under overloads, which can be characterized by the following cable properties :

- . flame behaviour
- . smoke emission
- . circuit integrity
- . corrosivity

- Reliable cables have to be self-extinguishing and must not propagate flame, so they have to meet FAR 25 and UL 94 - VO requirements, which can be related to a 27 minimum LOI value.

So it appears most interesting to compare LOI figures of the different cable constructions considered and which appear to be :

27.5 for a good flame retardant PVC/PA

30 for ETFE

> 50 for T/H

> 50 for K/H

How LOI values relate to flame behaviour can easily be understood through the following test, in which we have submitted to an identical flame 2 different cables, of the same 20 AWG size. As the LOI figure of the PVC/PA sample is very close to the 27 limit, the burning time and burnt length, after flame removal, are much higher than on the T/H sample (fig. 3).

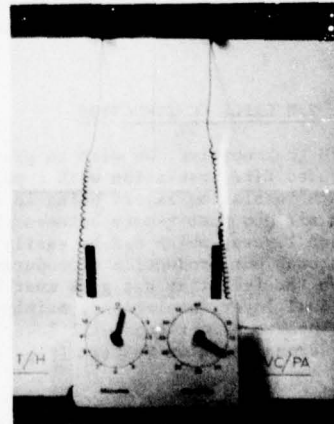


Figure 3

- Smoke emission is another most important characteristic, as heavy fumes appear to be a psychological but also a real danger, each time public is involved. Those questions are so very well-known nowadays that we believe necessary to only show tests comparing smoke emitted from the different cable constructions considered, on the same 20 AWG size and under the identical 50 Amps overload.

In a first test series, we compare PVC/PA to ETFE, which is self explanatory on fig. 4. Remember that polyolefins would emit about the same smoke volume as PVC/PA, elastomers being far worse.

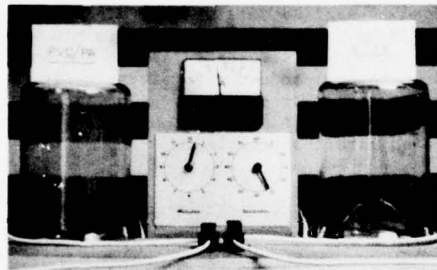


Figure 4

In a second test series, where plain ETFE is compared to T/H, this last cable construction appears as a significant improvement, delaying smoke emission and preventing the thermoplastic ETFE from flowing (fig. 5).

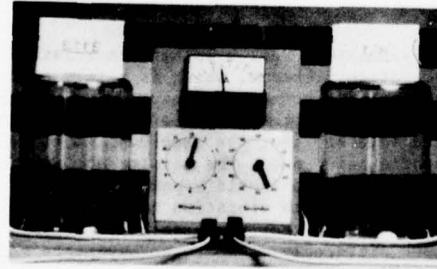


Figure 5

This only characteristic is most important as it shows that, in bundles, T/H cables will maintain circuit integrity even under large overloads.

A last test series compares T/H to K/H or fully polyimide cables, which are the best known cables for safety considerations. K/H shows the lowest possible smoke emission and ensures complete circuit integrity, the whole insulation being non thermoplastic (fig. 6).

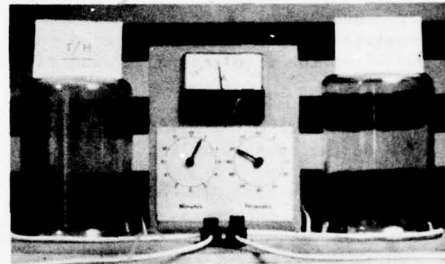


Figure 6

- Corrosivity also must be considered as a very big danger, not so very much towards people, but mainly towards equipments which might be impaired through corrosion of electrical contacts. Different test methods have been developed, the better known being the Copper Mirror test, which cannot be considered as reflecting exactly what occurs in fires, the test temperature being rather low.

Another method, more realistic, has recently been introduced in the French Specification UTE-C-20.453. It takes into account the corrosivity of the decomposition gases, which is tested through the change in resistivity of a bare copper wire. Plain ETFE, T/H and K/H cables meet both test requirements which is not the case for PVC and most flame-retardant polyolefins and elastomers.

C - Chemical resistance is the third main improvement introduced by ETFE and Polyimide based insulations over conventional ones.

ETFE is almost as good as PTFE and FEP, while Polyimides will only encounter some attack in alkaline media. As concerns T/H cables, they will show the same chemical behaviour as those ETFE insulated, a possible attack in alkaline media of the T/H polyimide topcoat keeps the cables full ETFE protection.

COMPARATIVE T/H CABLE CHARACTERISTICS

Having briefly shown the interest of the newer and somewhat more sophisticated cable construction over conventional cables, we now believe of interest to directly compare to each other, on 20 AWG sizes the insulations considered, which are :

- . plain ETFE to MIL-W-22759/16
- . T/H at the same 10 mil or 0.25 mm wall thickness.
- . K/H to MIL-W-81381/12, of an 8 mil or 0.20 mm wall thickness.

A - We shall start with a quick comparison of their mechanical properties :

- as concerns cut-through, we have performed tests at ambient and at the rated 150° C temperature, the results being shown fig. 7. The tests have been performed in accordance with AECMA* Pr. EN 2084 Specification, using a 0.45 mm needle.

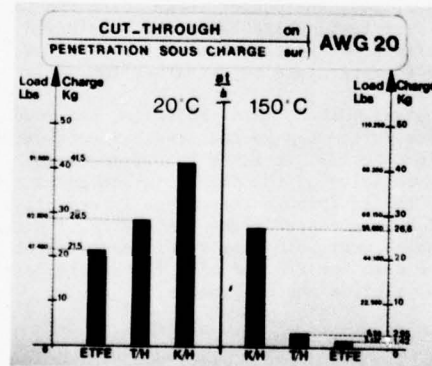


Figure 7

* Association Européenne des Constructeurs de Matériel Aérospatial.

No doubt polyimide insulations are far better than any other one, in this respect, mainly at high temperature, but you can appreciate how the polyimide topcoat on T/H significantly improves ETFE performance, being :

- . 30 % higher at 20° C
- . twice ETFE figure at 150° C

- Scrape abrasion resistance appears surely as one of the most important characteristic, both during cable installation and in service, when a high level of vibration may occur.

To simulate installation abuse, we have performed the test specified in AECMA Pr. EN 2084 Specification, in which a 1.5 kg load is applied on a 0.45 mm needle using the same equipment as defined in MIL-W-81381. The number of strokes to abrade the insulation down to the conductor is given in fig. 8 and shows the important improvement introduced by T/H over ETFE and K/H, abrasion resistance being more than doubled.

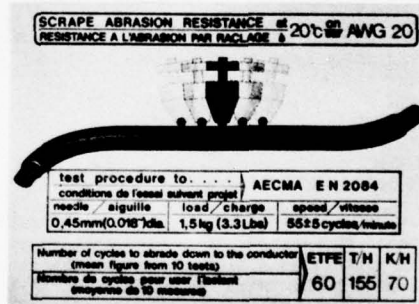


Figure 8

To simulate abrasion in service related to vibration problems, which is mainly an Aeronautics concern, we have drawn Fig. 9, the curves of the number of strokes versus the load applied, the same 0.45 mm abrading needle being used. The results obtained at the lower load levels appear to be very consistent with vibration test results, which showed that those abrasion curves must preferably come to an asymptote and not have an important slope.

We wish to say that this most interesting test procedure has been developed by Avions Marcel Dassault Technical Department.

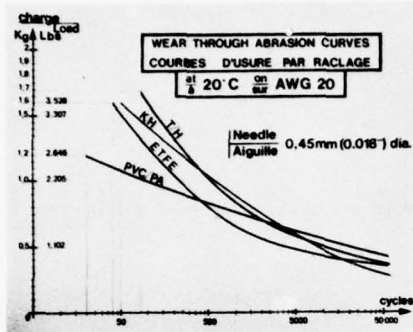


Figure 9

Let us add that the figures, at the higher loads, appear of no real interest in this respect, so hard insulations are surely not the best ones. You may notice how T/H performs well.

Notch sensitivity has been a problem for some specific and rather stiff insulations, which could be related to some stress-cracking sensitivity - but all the cable insulations we are considering here are not notch sensitive.

Flexibility and Stripping are handling characteristics which must not be neglected.

T/H can be stripped as easily as plain ETEFE or conventional insulations.

No problem for stripping K/H cables if the right blades are used.

Flexibility is not so very easy to represent, but we have developed a procedure which we believe to give a very good picture of the comparative flexibilities of cables of a same gage.

A cable loop of a given and constant diameter is squeezed by a load, and the loop deflection measured.

The higher flexibility corresponds to the bigger deflection for a given load or to the lower load for a given deflection.

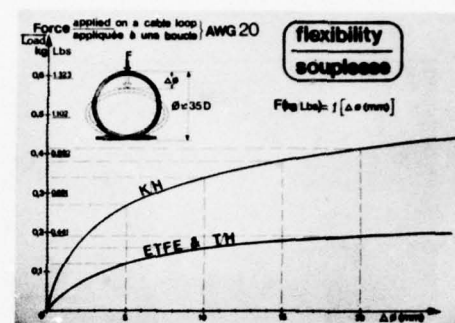


Figure 10

The curves, figure 10, of the deflection level versus the load applied to the cable loop are very significant, T/H being as flexible as ETEFE.

B - We now come to electrical properties, which are quite good, even excellent, for any of those 3 cable types.

- Insulation resistance curves versus temperature are shown, Figure 11, just as an information, as this characteristic does not appear to be a real problem in use, even with PVC/PA cables.

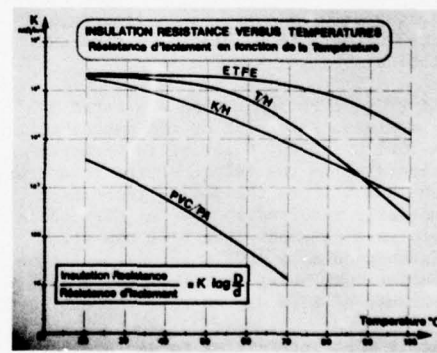


Figure 11

- Circuit integrity under overloads has become, those last months, a main requirement for many customers of the Aircraft, Rapid Transit and other Industrial areas.

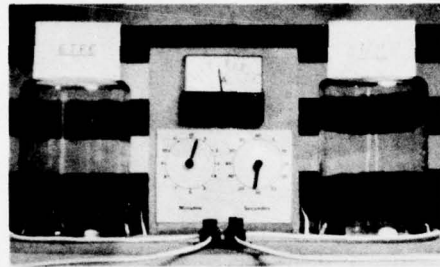


Figure 12

As can be seen fig. 12, under even large overloads, the polyimide topcoat on T/H cables prevents the thermoplastic ETFE from flowing off the conductor, which prevents shorts from occurring in bundles.

Of course, K/H cables are the best ones as concerns circuit integrity.

C - Now the true life of a cable in service is very much dependent on its thermal properties.

All those new cable insulations, which are ETFE or Polyimide based, withstand much lower cold bend temperatures than PVC cables, tests performed at -65°C leading, for such insulations, to no cracks on good quality cables.

If PVC and PVC/PA cables are rated 105°C as a maximum, Polyimide or K/H cables will have a 150°C to 200°C rating temperature according to the nature of the conductor used, while 150°C is the rating temperature normally referred to for any ETFE cable. But you must remember that ETFE was first introduced as a 180°C rated insulation, this temperature being then lowered to 150°C because of ETFE degradation through oxydation.

It is most interesting to see how the polyimide topcoat on T/H cables improves ETFE thermal life, as appears clearly on the curves, figure 13, giving the true thermal life of the 3 cable insulations considered.

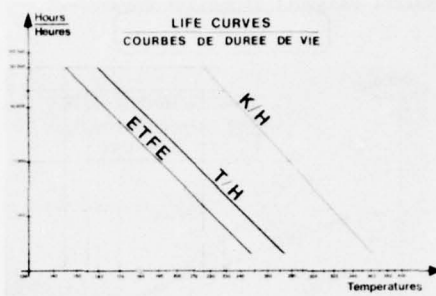


Figure 13

This polyimide topcoat really acts as a barrier between ETFE and air, lowering significantly ETFE degradation.

Those comparative life curves were obtained through aging tests performed at oven temperatures ranging from 175°C to 250°C , on wire samples wrapped in pigtailed. The requirements on the aged samples were :

- . no insulation or lacquer cracking
- . insulation resistance maintained
- . no breakdown at 2.5kV .

We wish to add that insulations crosslinked through irradiation will never have better thermal lives than the relevant plain insulations, even if at high temperatures they appear much improved. For instance, the slope of the life curve of an irradiated ETFE will be completely different from the ones shown Figure 12, leading, maybe, to a 150°C temperature rating.

This only example explains why short term aging tests are insufficient to predict the true life of a cable some long term aging tests having absolutely to be performed.

D - This polyimide topcoat on T/H cables also explains why they show a real improved radiation resistance, ETFE degradation occurring partly through oxydation on conventional ETFE cables. So T/H cables pass the LOCA test but more testing has to be run to study the real maximum radiation dosage such cables may withstand. It might be interesting to point out that, when submitted to a few Mrads, polyimides will no more be attacked by alkalis, so T/H cables will normally keep their topcoat during LOCA.

E - What is often considered as a drawback for polyimides is related to their natural amber colour, which cannot lead to a white finish. This applies to T/H and K/H cables, which anyhow can be produced in sufficiently light colours to make their identification easily legible. Also, if a white finish is a need, a white coating can be applied, introducing no real modification in the cable characteristics.



CONCLUSION

T/H cables appear to be one of the best compromise on price and characteristics for Aeronautics, Electronics, Rapid Transit, Nuclear Plants and surely other Industrial applications.

Normally applied in thicknesses ranging from 6 to 15 mils, those ETFE/polyimide insulations show :

- . possible weight and space saving
- . good mechanical properties
- . enhanced electrical and thermal performance over other ETFE based insulations.
- . interesting radiation resistance
- . easy handling.

As concerns safety, just remember that such cables :

- . meet FAA and UL most stringent flame requirements.
- . maintain circuit integrity.

Edith BASCOU was born in PARIS (France) in 1925. She was graduated as an Electrochemical Engineer from Grenoble Institut National Polytechnique in 1947.

She first joined the French Atomic Energy up to 1951.

From 1951 to 1957, she was in charge with an electroplating unit and with development of electrical equipment at Etablissements SOULE, Bagnères de Bigorre (France).

Since then, she joined FILOTEX Wire and Cable Manufacturing Co. where she is now responsible of the Research/Development Division.



Michel MARECHAL was born in FRANCE in 1941. He was graduated as an Electrotechnics Engineer from "Conservatoire National des Arts et Métiers" of PARIS in 1971.

He first worked at C.N.R.S. (Scientific Research French National CENTER) and since his graduation he has in charge of FILOTEX Research Laboratory.

WIRE INSULATION DESIGNED FOR TELECOMMUNICATIONS EQUIPMENT

A.F. Faber

PHILADELPHIA INSULATED WIRE COMPANY INC.
MOORESTOWN, N.J. 08057

OBJECTIVES

The initial application of the liquid approach is addressed to this particular product with the challenge to meet the following requirements.

1. The product must be capable of termination by automatic machinery.
2. Cut-thru resistance to sharp edges of posts is a prime requirement to prevent wiring faults in service.
3. To allow density of wiring, insulation must not be stiff.
4. Dielectric constant should not exceed 3.4 (preferably lower) at all frequencies. Humidity should not seriously increase the dielectric constant.
5. Insulation should be capable of soldering with no shrink-back or flare.
6. The insulation must be self-extinguishing to flame by usual testing, but more recently should exceed 28% oxygen index.
7. Economics, while pricing is very competitive, recognition is given to quality by customers.

The above considerations are probably the most important. Others will be noted.

PRODUCTS DEVELOPED

The first product brought to a commercial reality is a 3 layer composite insulation. Against the conductor is a 2 mil wall of flexible urethane. Over this is served a 1 mil wall of polyester fibers. The final topcoat is a methacrylate resin cross-linked with a polyvinyl chloride. The total final wall is 4.5 mil held to better than 70% concentricity.

INTRODUCTION

As wire insulation engineers, did you ever consider an approach other than stuffing solid resin out of little holes? Do you realize that the extruder places its own requirements on the material before the insulation requirements can be considered?

The following will describe the use of resins in liquid form to achieve an insulation with a unique combination of physical and electrical properties.

In the period following 1965, major design changes were made described by the magic word "miniaturization". In the electronic industry this meant a change in wire size from 26 gauge to 30 gauge. Today, 30 gauge wire for backplane application is not new, but the schools of thought on properties required are diverse.

The liquid resins are applied as multiple coats, die wiped, and oven cured. The manufacturing techniques are related to those used in the magnet wire industry with modifications appropriate to the difference in materials used. Two very important attributes of magnet wire manufacturing are the close dimensional tolerances (taken for granted) and very economical application of manpower, energy and overhead costs. "Insulated" wire and "magnet" wire are two different worlds. Very few engineers and managers have the opportunity to appreciate the accomplishments of the "other" industry.

With magnet wire, for example, dimensional tolerances of finished diameter which must include wire drawing variations as well as insulation are held within 0.0003 inch total. The 3 layer composite construction will hold plus or minus 0.001 inch regularly. A one-material insulation can hold within 0.0005 inch total variation.

Important differences of this operation compared with magnet wire will be mentioned. Magnet wire enamels are usually formulated with a solid content below 45%, while the methacrylate is above 80%, and will probably become 100%. Since the cost of any diluent or solvent is a direct loss up the exhaust stack and an air pollution liability, the advantage of high solids is obvious.

Normal insulation thickness of magnet wire is in the range of 0.0005 wall to 0.001 wall compared with this "insulated" product at 0.0045 nominal wall.

Insulated wire must be strippable but this is not permitted as magnet wire.

Electrical pin-holes are permitted on magnet wire but constitute a "fault" for "insulation" and must be removed.

MATERIALS SYSTEM NO. 1 USING URETHANE

The urethane has excellent wet electricals and is tough but flexible. The oxygen index is low, by itself the urethane would not be acceptable.

The served polyester fibers help to achieve a high cut-thru, but without adding stiffness. The mechanics may be likened to a filament-wound cylinder.

The unique (and proprietary) formulation of methacrylate compound contributes to all properties. The oxygen index of this material alone exceeds 32% and helps to achieve 24-1/2% for this composite using urethane. The methacrylate used as a single component insulation has good properties and could be marketed at a very competitive price.

Table No. 1 is given to show typical values of electrical and physical properties.

MATERIALS SYSTEMS NO. 2

The objective of this development program was to achieve an insulation with oxygen index exceeding 29%. Since tests of wire samples with only methacrylate gave an index exceeding 32%, it was obvious that the urethane and the polyester fibers had low values of oxygen index which were not acceptable. Many attempts to improve the urethane using flame retardants produced no improvement, or at best very little. A reduction of wall thickness of urethane with attendant increase of methacrylate managed to achieve 26%. The use of polyester fibers reduced the index of the 100% methacrylate from 32% to 29% which still exceeds the 28% objective. Fortunately, a reformulation of the methacrylate made it possible to maintain the 1400 gram cut-thru requirement, with a margin of safety.

The testing for oxygen index as described in ASTM-2863 was followed except that all 30 gauge wire samples were used including the conductor. The results are not the same as testing for insulation materials alone.

Cut-thru testing follows procedure specified in MW-81822 specification. This author has determined from experience that the radius of the test blade must be ground using a high quality jig boring machine to "generate" the precise form (in the manner of cutting gear teeth). An optical comparator or shadowgraph is not satisfactory. The load is applied gently by pouring lead shot into a container precisely located to the blade. By following the above procedure, consistent results and evaluation can be obtained.

Obtaining a value for dielectric constant followed the ASTM D-3032 test procedure using a mercury filled steel U-tube apparatus. Table II is given to show measured values of capacitance and other measurements used to calculate the constant K. Details of testing 30 gauge wire samples of other materials is also given.

CONCLUSION

It appears that the combination of all properties desired to meet the needs of backplane wiring are mutually exclusive for any one material and that a composite must be used. Many wire insulations are designed using several components which make their individual and unique contribution to the final product. A composite with a total wall of 0.005 inch dictates the liquid approach.

But further, it is hoped that this development is only the beginning. The liquid approach makes possible the consideration of other chemistry not yet tried as wire insulation.

TABLE NO. 1

PROPERTIES & PERFORMANCE DATA

CONSTRUCTION: Urethane and Polyester Fibers and Methacrylate

PRODUCT DETAILS:

| | | |
|----------------|--------------------------------|-------------------------|
| Catalog No. | F-180 | F-120 |
| Conductor | Silver-plated soft OFHC copper | Tinned soft OFHC copper |
| Conductor Size | 30 gauge | 30 gauge |
| Finished O.D. | .0195" | .0340" |

ELECTRICAL PROPERTIES:

| | | |
|--|--|--|
| Insulation Dielectric Constant | 3.4 max. | 3.4 max. |
| Insulation Power Factor, 1 KC | .05 max. | .05 max. |
| Insulation Surface Resistivity | 100 megohms min. | 100 megohms min. |
| Dielectric Strength (after 1 hr. water soak) | Hold 2 KV 1 minute, breakdown over 5.0 KV | Holds 2 KV 1 minute, breakdown over 5.0 KV |
| Insulation Resistance (500 V DC for 1 minute after 1 hr. water soak) | 500 megohms min./M ft. | 500 megohms min./M ft. |
| Insulation Heat Resistance (after 48 hrs. at 95°C) | No shrink back of insulation. Wrap on .060" diam. mandrel, then water soak 1 hr., hold 2 KV 1 minute. | No shrink back of insulation. Wrap on .105" diam. mandrel, then water soak 1 hr., hold 2 KV 1 minute. |
| Insulation Cold Bend (after 4 hrs. at -54°C) | Wrap on 1" diam. mandrel, then water soak 1 hr., hold 2 KV 1 minute. | Wrap on 1" diam. mandrel, then water soak 1 hr., hold 2 KV 1 minute. |

PHYSICAL PROPERTIES:

| | | |
|---|--|--|
| Temperature Rating | 105°C. | 105°C. |
| Insulation Tensile Strength | 10,000 psi min. | 10,000 psi min. |
| Insulation Elongation | 35% min. | 50% min. |
| Insulation Stripping Force (1-5/8" lengths) | .5 lb. min./2.5 lb. max. | 1.0 lb. min./4.0 lb. max. |
| Insulation Cut-Thru (90° chisel, .003" radius) | Hold 1400 gms. 1 hr., then 500 V. AC for 1 minute. | Hold 2250 gms. for 1 hr., then 500 V. AC for 1 minute. |
| Flammability | Self-extinguishing, 10 sec. | Self-extinguishing, 10 sec. |
| Oxygen Index | 24-1/2% | 24-1/2% |
| Insulation Cold Flow (90° chisel, .003" radius) | Hold 1000 gms. 96 hrs., then 500 V. AC for 1 minute. | Hold 1750 gms. 96 hrs. then 500 V. AC for 1 minute. |
| Resistance to Soldering | 1/64" max. shrink back | 1/64" max. shrink back |
| Insulation Fungus Resistance | Fungus Resistant | Fungus Resistant |

TABLE NO. II

SUMMARY OF COMPARATIVE PROPERTIES

DIELECTRIC CONSTANT OF 30 AWG INSULATED WIRE

| | C Capacitance per mil in pF @ 1 MHz | d | L inches | Outside Diameter D2 inches | Conductor Diameter D1 inches | Cv in Pf | K |
|---|---|-------|-------------|-------------------------------------|---------------------------------------|-------------|------|
| <u>ETFE</u> | | | | | | | |
| {Ethylene - Tetrafluoroethylene} violet | 564.9 | .0095 | 87.5 | .0184 | .0100 | 202.76 | 2.79 |
| --Rough clear | 458.2 | .0087 | 87.5 | .0200 | .0100 | 178.37 | 2.57 |
| Polyester Tape | 623.2 | .0298 | 87.5 | .0205 | .0100 | 172.24 | 3.62 |
| Methacrylate | | | | | | | |
| Cross-linked with | | | | | | | |
| Polyvinyl Chloride | 541.2 | .0190 | 87.5 | .0207 | .0100 | 169.94 | 3.18 |
| PVF ₂ | | | | | | | |
| Polyvinylidene | | | | | | | |
| Fluoride | 1563.9 | .2226 | 87.5 | .0197 | .0102 | 187.85 | 8.33 |

Notes:

1. Capacitance measured with HP-4217 @ 1MHz digital LCR meter (SID 3302632L31) using Mercury U-tube electrode system per ASTM D 3032
2. $Cv = \frac{.6137L}{\log \frac{D2}{D1}}$ $K = \frac{C}{Cv}$ {Equations used from ASTM D-150}
3. d is the dissipation factor.
4. The Oxygen Index was measured using 5 mils of insulation on a 30 gauge wire sample.

| Oxygen Index ASTM 2863 | Cut-Thru MW 81822 Load-Grams |
|------------------------------|------------------------------------|
|------------------------------|------------------------------------|

ETFE

| | | |
|-----------------------------------|-------|------|
| Ethylene - Tetrafluoroethylene | | |
| --Rough | 27% | 800 |
| --Smooth | 27% | 800 |
| Polyester Tape | 26% | 1400 |
| Methacrylate | | |
| Cross-linked with | | |
| Polyvinyl Chloride | 29% | 1400 |
| PVF ₂ | | |
| Polyvinylidene | | |
| Fluoride | (44%) | 850 |

Note: Table No. II refers to Methacrylate Systems No. 2

ACKNOWLEDGEMENTS

1. Mr. F.H. Miller, Development Engineer
Western Electric
Springfield, New Jersey
2. Mr. John Ware
Ware Chemical Corp.
3. Mr. Ralph Poirot, Senior Chemist
Acme Chemicals & Insulation Division
Allied Products Corp.
4. Mr. James Pezza, Vice President
Bridgeport Insulated Wire Co.
5. Philadelphia Insulated Wire Company
Management associates
6. Many good friends in the wire
industry

REFERENCE

Mr. James R. Austin, Senior Staff Engineer
Western Electric, "Heat Resisting High
Tensile Strength Plastic Insulation for
Wire" - Wire Journal, May, 1974.



A.F. Faber is a Consulting Engineer to the
Philadelphia Insulated Wire Company, 333 New
Albany Road, Moorestown, New Jersey 08057.
Prior to this, he was General Manager of
Unicable Inc., which company was created to
manufacture products described in this paper.
He has thirty years experience in insulated wire
and magnet wire with positions of responsibility
in engineering to general management. Mr. Faber
holds a BSME Degree and Graduate ME Degree from
Princeton University.

MULTI-PAIR SUBSCRIBER CABLES FOR VERTICAL INSTALLATION
IN HIGH-RISE BUILDINGS

K. Mori
Nippon Telegraph and
Telephone Public Corporation
Tokyo, Japan.

R. Yashiro
T. Umetsu
The Fujikura Cable Works, Ltd.
Tokyo, Japan

Summary

Multi-pair telephone cables for vertical installation are necessary in high-rise buildings with large numbers of telephone subscribers. Requirements for such cables differ from those for underground or aerial cables. This paper describes the development of the self-supporting type vertical cable with anti-slippage dam, and its method of installation.

Introduction

It has been ten years since the first high-rise building was constructed in Japan. In 1964, the 31-meter building height restriction was altered to a restiction of a building's volume in relation to its area. And in 1967, the 145-meter 36-floor Kasumigaseki Building was constructed. After that, many buildings of more than 100meters in height were constructed in the Tokyo and Osaka areas.

These high-rise buildings are offices or hotels and accomodate more than 10,000 people. Compared with small buildings, the number of telephones installed is large, and several multi-pair subscriber cables to the telephone office are thus necessary.

Utilities such as air conditioning, power supply, and telephone equipment are installed jointly for some floors. Vertical multi-pair subscriber cables are required to link the telephone equipment with underground cables to the telephone office.

In the early days, conventional Stalpeth sheathed cables were installed as vertical cables. Through the installation of Stalpeth sheathed cable, requirements for the vertical cables were discovered and the new vertical multi-pair subscriber cable was developed and has been put into use.

Vertical Installation of Stalpeth Cable

When vertical multi-pair cables were required, it was settled that the laying method was to be developed for conventional cable instead of the new vertical cable development. The laying method for Stalpeth sheathed cable was practically established in two installations.

Installation in the Kasumigaseki Building¹
Basic investigation for vertical laying

was carried on before the installation in the first high-rise building, the Kasumigaseki Building, Tokyo. In November of 1967, four pieces of 0.4mm 1,000pairs, paper insulated, star quaded, unit type, and Stalpeth sheathed telephone cable were laid vertically.

Cable Laying Method The cable diagram of the building is shown in Fig. 1. Two cables were installed between the 3rd basement and the 36th floor and two others between the 3rd basement and the 13th floor. Since cable could only be brought into the 1st basement, laying was complicated.

The first two cables were pulled up to the 36th floor by winch, with wire attached to the pulling eye at the running end of the cable. For the laying of the horizontal length at the 36th floor, net type cable grips were attached at intervals of 24meters and then, the cable grip wires were jointed to a delta-shaped coupler, and pulled up with the coupler about 27meters more.

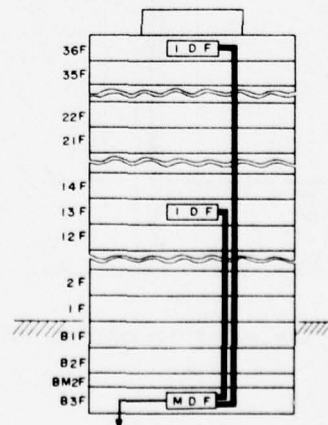


Fig. 1 Cable diagram of the Kasumigaseki Building

Details are shown in Fig. 2. The delta-shaped coupler was used due to the fact that, when the cable is pulled up to the horizontal with the pulling eye, the cable is damaged at the curved point and also, the holding force of net type cable grip is not enough to hold the cable at a single point. Where it curves to the horizontal, a curved roller with many rollers lined in a 90degree circular arc iron is used. After the vertical length between the 1st basement and the 36th floor was secured with cable clamps, the remained cable length was unwound from the cable drum, and then laid hand to hand.

The other two cables were pulled up to whole vertical length, because they are shorter than the length of vertical shaft to the 36th floor, and then hung down as far as reach the running top of the cable to 3rd basement MDF. Then the vertical length between the 3rd basement and the 13th floor was secured. The horizontal length at the 13th floor was laid hand to hand.

When laying cables in high-rise buildings, how to lay the horizontal length of cables for the highest floor, the lowest floor, and intermediate floor is a problem.

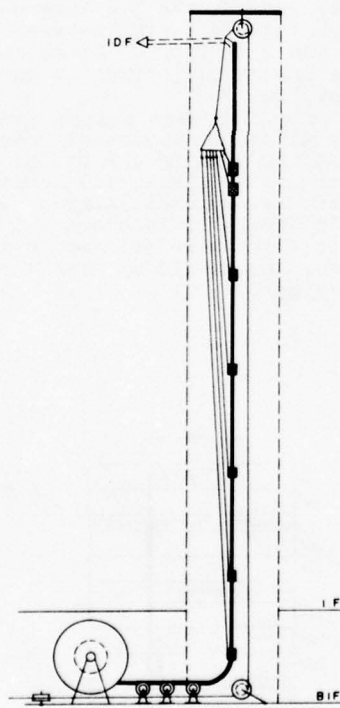


Fig. 2 Laying of horizontal cable

Cable Clamp The cable clamp, shown in Fig. 3, was used for setting the cable to the cable rack. The cable was clamped at one point on each floor. When the bolt is screwed to attach this clamp to the cable, the cable sheath is in danger of rippling, so that clamp can not stop the slip between the sheath and cable core, but only grips the cable sheath.

Slip between Sheath and Cable Core The cable sheath and the cable core are joined by shrinking of the sheath and various deformations from the perfect circle along the cable length. The force of the joint is determined by the draw-out force, meaning the maximum draw-out force of the cable core from the sheath along the cable axis. This value, however, is not applied directly to the vertically laid cable for a long time. When the cable is vibrated, slippage occurs between the core and the sheath, even if it does not occur when the cable is held vertically for a short time. Also in the case of a cable that had been held vertically outdoors for 20months as shown in Fig.4, the slippage was 40mm for straightly laid cable and 19mm for inverted L shaped cable. This shows that the draw-out value does not apply directly to the design, though the outdoor experiment has severe temperature changes compared with the indoor.

In accordance with the results of the experiment, a slip-stoppage dam was installed in the cable after laying, where the cable sheath was partially cut off and epoxy resin was poured into it. The cable to the 36th floor has two dams and the cable to the 13th floor has one.

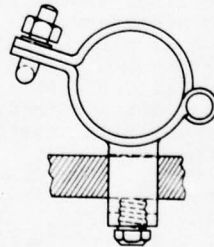


Fig. 3 Clamp for vertical cable

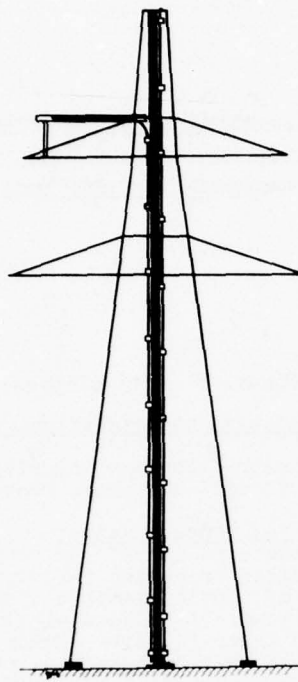


Fig. 4 The experiment for vertical laying

Installation in the World Trade Center

In October 1970, eight pieces of 0.4mm 1,000pairs, paper insulated, star quadded, unit type, and Stalpeth sheathed telephone cable were installed in the 2nd high-rise building, the World Trade Center Building (Hamamatsu-cho, Tokyo). Due to the experience of installation in the Kasumigaseki Building, several new tools were introduced.

Cable Laying Method The cable diagram of the building is shown in Fig. 5. Two cables were installed between the 3rd basement and the 40th floor and the five others were between the 3rd basement and the 13th floor. The cable could be brought into only the 2nd basement.

For the pulling of cable to the 40th floor, a wire consisting of 23meters long wires with a swivel at one end connected to one continuous length, was used. Newly developed plastic cable grips were attached to the cable at 23meter interval instead of the net type cable grips that take a great deal of time to attach. Then the grips were connected to the wire coupler. The operations were repeated as the cable was being pulled up. Details are shown in Fig. 6. Also, three triangularly distributed pulleys were used to make the swivel turn around the pulleys at the top (Fig. 7), as large pulley for cable guide at curve in place of curved roller, which is too heavy to handle, and so on.

For the horizontal length at the 3rd basement which was relatively long, cable was pulled up until the running top of cable was uncoiled from the drum, and then it was hung down to the 3rd basement.

Two different methods were adopted for cable laying to the 13th floor. Two shorter horizontal lengths at the basement were pulled up over the 13th floor with a pulling eye, and then hung down to the 3rd basement. The cable was clamped and the horizontal length at the 13th floor was laid hand to hand. The other three lengths were too long to pull up into the shaft, because the horizontal length at the basement was long. The cables were brought into the 13th floor and hung down to the basement. A drum shaped cable laying wheel equipped with a brake was used

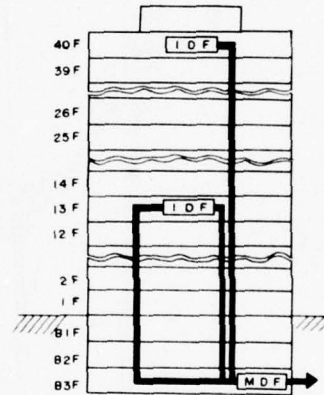


Fig. 5 Cable diagram of World Trade Center

Requirements for Vertical Cables

It was found from experience with the laying of conventional Stalpeth sheathed cable that the following characteristics are required for vertical cables in the building.

- (1) Cable strength must be sufficient for vertical installation of 300meters in height.
 - (2) Cable construction must be suitable for vertical clamping.
 - (3) The draw-out force of cable core from sheath must be sufficient for vertical installation.
 - (4) Good flexibility.
 - (5) Cable must have ability to be laid in 75mm diameter pipe.
 - (6) Cable must be electrostatically screened.
 - (7) Cable sheath must be flame resistant.
 - (8) Electrical characteristics must be equivalent to those of the conventional Stalpeth sheathed cable.
- As for (1), the maximum building height may be 250meters regarding cost and facility in Japan. Maximum vertical length of cable may be 300meters in regarding allowance.

As for (2), it is required that the torque of the bolt has to be rigidly controlled for Stalpeth sheathed cable and also the problem of the short interval of the clamp metal for its unsatisfactory clamping force. As for (3), it is necessary that the cable components are secured tightly enough against each other to ensure that slippage does not occur. As for (4), the cable shaft of a building is usually narrow making and bending. As for (5), shaft may be connected to pipes. As for (6), power cables are laid in the same shaft.

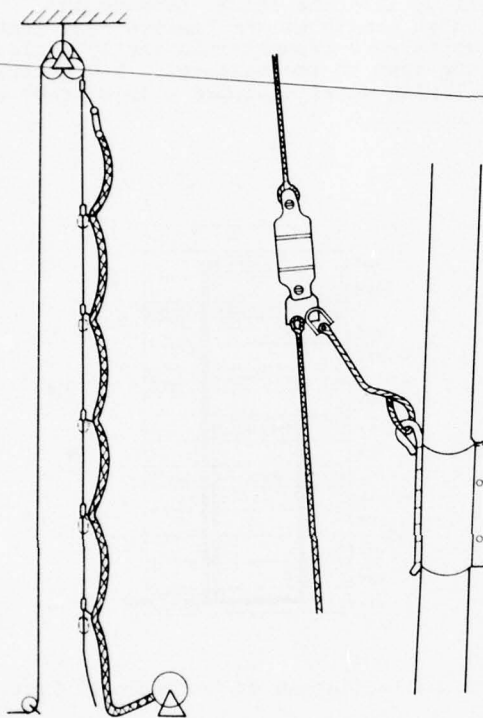


Fig. 6 Cable laying

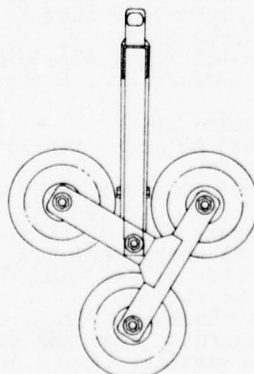


Fig. 7 Three pulleys

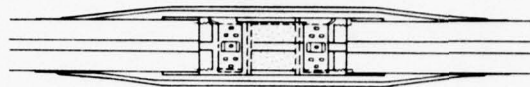


Figure 8 Anti-slipage dam
Development of Vertical Cable

Cable construction was investigated and developed to meet the above requirements.

Necessity for Tension Member

Due to the strength of the copper wire, a tension member is needed for vertical cables. The types of tension members investigated are as follows; (1) Figure-eight type, (2) Center type, (3) Wire armour type. Each type of cable was designed and calculated in terms of the cable diameter, weight, and dimensions of cable drum, for foamed polyethylene or solid polyethylene insulation, aluminum screened and PVC sheathed cables. Conductor diameter is fixed to 0.4mm, the smaller diameter for easy terminating. The results are shown in Table 1.

Let us discuss the relation between the strength of copper conductors and the cable tension during the laying and after securing. During cable laying, the cable is hung with a pulling eye. The permitted tension for the pulling eye is 880kgs in case of 1,000pairs; 0.2% deformation strength of copper conductor is 7kgs/sq.mm and the conductor holding rate of the pulling eye is 50%. The cable weight of 1,000pairs without messenger wire is 980kgs/300meters. Therefore, a cable of 300meters length can not be hung with a pulling eye. For long term tension, creepage of material, especially copper must be considered. Creep tests on copper shows that load for 0.1% deformation in 50years is 2.3kgs/sq.mm. Therefore, the permitted weight for 1,000 pairs cable is 578kgs and is equal to cable weight of 178meters and cable core weight of 213meters.

Therefore, it is required that the cable itself have a tension member or, that during the laying, a tension member is laid parallel to the cable and clamped at various points.

Clamping Method

There are 2 methods for securing the cable in the shaft. Single point fixing at the top and several point fixing along the vertical shaft. In case of single

fixing, a cable holding device is needed in the building and application of this method has limitations. Also, flexible cable such as telephone cable follows the building's sway and do not need single point fixing. Thus the several point fixing method is adopted. When the cable is fixed, it is squeezed. Robust construction, stronger than Stalpath sheathed cable, is necessary for clamp compression. But we were unable to develop the cable construction with a good anti-compression sheath and good flexibility. Therefore, the cable construction with the fixing member is necessary.

Other Requirements in Cable Laying

There are some other requirements for cables in cable laying. The cable drum may be brought into the basement, where the motor pool is located. The entrance to the basement must have slope of minimum 2.0 meters in height and the flange diameter of the drum less than 2.0 meters is desired. From the experience with cable laying, it was found that the winch must be secured at the top, because the wire rope is only hung down for the cable pulling-up and not entangled. But in such case, the winch may be small and less powerful. And cable weight less than 2 tons is desirable.

According to Table 1, the wire armoured type is too heavy. The center type has a clamping problem. So the figure-eight self-supporting type cable having 1,000 pairs may be most suitable.

Slippage between Cable Components

The draw-out force of the cable core from sheath for conventional cable is obtained as shown in Table 2. Draw-out force is different for different cable types, depending on insulation material, number of pairs, and sheath. Results show that a non-screened sheath over the cable core is good, because of its tightly fitting sheath to the cable core, but vertical cables require the screen. Considering this, various type of laminated aluminum sheathed cables were trial manufactured and tested for draw-out force and flexibility. The types of cables tested are shown in Table 3. Tests for draw-out force are made on lengths of 50cms and at tensile speed of 100mm per minute. Bending moment of the cable is the product of force from bending the cable along the disk and cable length. Results are shown in Table 4. It is obvious from Table 4 that slippage occurs between the outer unit and core wrapping. Also, the bending moment and draw-out force are so closely related that cable construction with high draw-out force and good flexibility can not be developed. In addition, it is found that the aluminum PVC laminated sheath is fragile at low temperature. Cables are usually laid in buildings under construction and require the same temperature characteristic as outdoor cables. Therefore, the aluminum PVC laminated sheathed cable is unsuitable for use as vertical cable.

Finally aluminum screened PVC sheath is adopted due to the test result and for slip, an anti-slippage dam is made in the cable at intervals.

Anti-slippage Dam

Anti-slippage dam is installed for the

purpose of stopping the slippage of components. On the other hand, flexibility of cable at the dam become worse. Therefore, it is desirable that the number of dam is as few as possible.

The dam requires sufficient strength to hold the cable core weight. In the case of Stalpath sheathed cable, the dam was installed after cable laying. A lead sleeve was set to the cable and epoxy resin was poured in it. The lead sleeve was squeezed and secured to the cable rack. Therefore, the cable core weight is held at the dam. For the vertical cable, the cable core is attached to the messenger wire, and the core weight is held by messenger wire that is secured to cable rack by clamping metals. Therefore, the core weight is held by several points and the dam is not a special point in cable clamping.

Epoxy resin mixed with polyethylene powder is used to attach the core to the messenger wire. Perforated reinforce rings are buried in the resin at both sides of dam, because the resin is weak for tensile force.

The vertical cable dam is pre-fabricated in the factory. In such case, the dam is coiled on the cable drum and laid through a curve-riched shaft, and requires flexibility. The dam is wrapped with self-adhesive rubber tapes and covered with a heat-shrinkable tube. It has good flexibility because the rubber tape is well-deformed. The dam construction is shown in Fig. 8.

Test results for the dam are shown in Table 5. The dam is made at intervals of maximum 80meters along the vertical length of the cable. Long term loading tests show the satisfactory strength for such cable length.

Table 5 Test Result of Dam

| Item | Result |
|----------------------------------|-------------------------------------|
| Tensile test | 1000kgs |
| Tensile test after heat-cycling | 1000kgs (-60°C - -20°C 10cycles) |
| Long term loading test | Good (300kgs for 20months) |
| Bending test | Good (10d* radius at -10°C) |
| 90° curved pipe run through test | Good (at -10°C) |
| Twisting test | Good (720degree for 2meters sample) |

d: cable diameter

Sheath

We studied flame resistance and creepage of the sheath material.

Flame resistance General characteristics, flammability, smoke generation properties, type of gas, and ignition point were investigated on sheath materials such as PVC general purpose, PVC hard grade, flame-retardant PE non-burning grade, and self-extinguishing grade. The general characteristics are shown in Table 6. Flammability and smoke density are tested in accordance with ASTM D635 and D2863. The results are shown in Table 7. The smoke density is PVC flame-retarded PE. Polyethylene burns perfectly with low smoke. Ignition point is tested by heating plate method. The results are shown in Table 8. Analysis of generated gas was carried on with gas detector.

Table 1 Cable Construction Having Tension Member

| Tension member | Number of pairs | Insulation material | Cable diameter (mm) | Cable height (mm) | Cable weight (kgs/300m) | Flange diameter of cable drum |
|------------------------|-----------------|---------------------|---------------------|-------------------|-------------------------|-------------------------------|
| Without messenger wire | 1,000 | PEF | 43.5 | - | 980 | 1600 |
| | | PE | 50.5 | - | 1080 | 1800 |
| | 1,800 | PEF | 55.5 | - | 1660 | 2000 |
| | | PE | 64.5 | - | 1820 | 2200 |
| | 2,400 | PEF | 62.5 | - | 2160 | 2200 |
| | | PE | 73.0 | - | 2360 | 2400 |
| Figure eight type | 1,000 | PEF | 43.5 | 56.5 | 1060 | 1800 |
| | | PE | 50.5 | 63.5 | 1150 | 2000 |
| | 1,800 | PEF | 55.5 | 70.5 | 1780 | 2200 |
| | | PE | 64.5 | 79.5 | 1940 | 2400 |
| | 2,400 | PEF | 62.5 | 78.5 | 2300 | 2400 |
| | | PE | 73.0 | 88.5 | 2500 | 2600 |
| Wire armour | 1,000 | PEF | 55.0 | - | 1900 | 1950 |
| | | PE | 61.5 | - | 2120 | 2200 |
| | 1,800 | PEF | 67.0 | - | 2810 | 2400 |
| | | PE | 77.0 | - | 3390 | 2600 |
| | 2,400 | PEF | 75.0 | - | 3690 | 2600 |
| | | PE | 85.5 | - | 4130 | 2600 |

PE: solid polyethylene

PEF: foamed polyethylene

Table 2 Draw-out Force of Conventional Cables

| Cable | | | Cable weight (kgs/m) | Draw-out force (kgs/m) | Draw-out/cable weight force |
|------------------|------------|----------|----------------------|------------------------|-----------------------------|
| Conductor | Insulation | Sheath | | | |
| 0.32mm 3600pairs | PEF | Stalpeth | 12.2 | 15.5 | 1.27 |
| 0.4 1000 | Paper | Stalpeth | 3.5 | 21.5 | 6.15 |
| 0.4 2400 | Paper | Stalpeth | 7.8 | 23.3 | 3.00 |
| 0.5 1800 | Paper | Stalpeth | 8.9 | 34.0 | 3.80 |
| 0.65 1000 | Paper | Stalpeth | 8.4 | 22.3 | 2.66 |
| 0.4 100 | PE | PE | 0.37 | 77.0 | 208 |
| 0.4 200 | PE | PE | 0.69 | 77.5 | 112 |
| 0.9 30 | PE | PE | 0.52 | 144 | 277 |
| 0.4 100 | PE | Alpeth | 0.51 | 10.7 | 21.0 |
| 0.4 200 | PE | Alpeth | 0.81 | 22.0 | 27.2 |

Table 3 Trial Manufactured Cable

| 0.4mm 1000pairs polyethylene insulated cable | | | | | |
|--|--------------------|--------------------------|--------------|-----------------------------|----------------|
| Cable No. | Wrapping over unit | Wrapping over cable core | Inner sheath | Plastic coating on aluminum | Messenger wire |
| 1 | Non | Helix of rubber | PE | On side | |
| 2 | Non | Helix of cotton | PE | On side | |
| 3 | Non | Helix of PE | PE | Both side | |
| 4 | Non | Helix of rubber * | PE | Both side | |
| 5 | Non | Helix of rubber | Non | One side | |
| 6 | Non | Helix of PE | Non | Both side | |
| 7 | Non | Helix of PE | Non | Both side | |
| 8 | PE | Helix of PE | PE | Both side | |
| 9 | Non | Helix of cotton | Non | One side | |
| 10 | Non | Helix of rubber * | Non | One side | |

*: Friction riched rubber

Table 4 Draw-out Force and Bending Moment

| Cable No. | | Draw-out force | | Bending moment |
|-----------|------------------------------|--------------------------|------------------------|----------------|
| | Outer unit -Core wrapping | Core wrapping -Sheath | Inner -Outer sheath | |
| 1 | 140kgs/50cm | 152kgs/50cm | 199kgs/50cm | 7.0kgs-m |
| 2 | 150 | 152 | 150 | 8.2 |
| 3 | 190 | Rupture | Rupture | 7.9 |
| 4 | 350 | 442 | Rupture | 9.2 |
| 5 | 215 | 260 | - | 5.2 |
| 6 | 53 | Rupture | - | 5.9 |
| 7 | 53 | Rupture | - | 4.6 |
| 8 | Rupture | Rupture | Rupture | 10.7 |
| 9 | 119 | 102 | - | 4.4 |
| 10 | 332 | 347 | - | 6.1 |

Table 6 General Characteristics of Sheath

| Test Item | PVC | | | PE | | |
|-----------------------------|--|------------|-------------|-----------------|--------------------|--------------------|
| | General | Hard grade | Spec. value | General purpose | Flame-retardant PE | Non-burn. Self-ex. |
| Tensile test | 100% modulus (kg/cm ²) | 1.1 | 1.5 | Min. 1.5 | - | - |
| | Tensile strength (kg/cm ²) | 2.0 | 2.2 | Min. 2.0 | 1.8 | 1.5 |
| | Elongation (%) | 340 | 300 | Min. 180 | 650 | 555 |
| Tensile * test after ageing | Tensile strength (%) | 95 | 105 | Min. 70 | 107 | 92 |
| | Elongation (%) | 90 | 95 | Min. 60 | 101 | 90 |
| Density | 1.28 | 1.42 | - | 0.93 | 1.24 | 1.08 |
| Melt Index | - | - | - | 0.20 | 0.82 | 0.28 |
| Cold bend (°C) | -30 | -20 | Max. -15 | -60 | -35 | -60 |

Table 7 Flammability Test and Amount of Smoke

| Material | Flammability | | Smoke density | |
|------------------------|------------------|--------------|-------------------------|--|
| | D-635-68 | Oxygen Index | Light transmittance (%) | Absorbance of light (M ⁻¹) |
| PVC, general purpose | Non-burning | 25.0 | 28 | 1.11 |
| PVC, hard grade | Non-burning | 33.5 | 20 | 1.40 |
| PE, general purpose | Burning | 19.0 | 99 | 0.008 |
| PE, non-burning | Non-burning | 26.5 | 73 | 0.27 |
| PE, self-extinguishing | Self-extinguish. | 26.0 | 87 | 0.12 |

Table 8 Ignition Point

| Material | Ignition point (°C) |
|--------------------|---------------------|
| PE general purpose | 300-350 |
| PE non-burning | 400 (Smoke 320-350) |
| PVC | 500 (Smoke 320-350) |

The results are shown in Table 9. After all, PVC is used for vertical cable

Creepage The cable is clamped at messenger with PVC sheath. The sheath over the messenger is compressed with clamp metals. Also, the sheath over the cable core supports the weight. Therefore, the PVC used for the vertical cable requires the high tensile strength and high creep-resistance as shown in Table 6.

Detail Construction of Vertical Cable

Vertical cable satisfying the above requirements is the constructed as shown in Table 10 and Fig. 9.

Table 9 Composition of Generated Gas

| Gas | PVC | | General purpose | PE | | Flame-retarded PE Non-burning Self-extinguishing | 0.2 2.8 0.0008 0.18 0 0.0008 0 0.0025 0 0.0005 | (%) |
|---------------------|-----------------|------------|-----------------|-------------|--------------------|--|---|-----|
| | General purpose | Hard grade | | Non-burning | Self-extinguishing | | | |
| | | | | | | | | |
| CO | 0.2 | 0.2 | 0.2 | 0.2 | 0.2 | 0.2 | 0.2 | (%) |
| CO ₂ | 2.45 | >3.0 | 2.8 | 2.8 | >3.0 | | | |
| Cl ₂ | 0.001 | 0.0001 | 0 | 0.0008 | 0 | | | |
| HCl | 10.8 | 20.2 | 0.09 | 0.18 | 0.12 | | | |
| CO, Cl ₂ | 0 | 0 | 0 | 0 | 0 | | | |
| NO ₂ | 0.0002 | 0.0001 | 0 | 0.0008 | 0 | | | |
| H ₂ S | 0.001 | 0 | 0 | 0 | 0 | | | |
| SO ₂ | 0.0014 | 0.06 | 0 | 0.0025 | 0 | | | |
| CS ₂ | 0 | - | 0.001 | 0 | 0.0005 | | | |

Table 10 Construction of Vertical Cable

| Item | Detail |
|------------|--------------------------|
| Conductor | 0.4mm annealed copper |
| Insulation | High density PEF |
| Twisting | Star quad |
| Stranding | Unit type |
| Screen | Corrugated aluminum tape |
| Sheath | PVC |

Demension

| No. of pairs | Overall diameter mm | Cable height mm | Cable weight kg/m |
|--------------|---------------------|-----------------|-------------------|
| 400 | 31 | 43 | 1.6 |
| 600 | 36 | 48 | 2.2 |
| 800 | 41 | 54 | 3.0 |
| 1000 | 46 | 59 | 3.6 |
| 1200 | 50 | 63 | 4.1 |

Cable laying MethodVertical Laying

The cable laying methods that have been adopted are roughly classified to the following three types.

Pulling-up by winch and Pulley The cable is pulled up by a winch, that is set on the ground or in the basement, with a pulley at the top. This method was adopted for a 200meter high-rise building.

Draw-up machine for vertical cable The cable is pulled up with the wire rope draw-up machine for vertical cables. The equipment is to be set at the top, so that preparation is easy and wire removal is not necessary. The wire rope draw-up machine is suitable for narrow shafts.

Cable drawing machine for vertical laying The belt type cable drawing machine is set up at intervals. The cable is sent up by the two rotating belts of the machine. It is useful for laying several pieces of cable with long horizontal length in the same shaft.

Horizontal Laying

For horizontal cable laying the upper horizontal length is laid at first and then the lower horizontal length follows.

Usually, the messenger wire was cut off from the cable at the top floor. The wire was pulled up still more and only the cable was sent to the horizontal rack. There was an exception when using the cable drawing machine. For removal of messenger, good flexibility is obtained and the cable becomes suitable for the bent-riched horizontal rack. In this case, the top of the messenger is secured to the rack with messenger grip. Recently, a standard cable laying method has been established. The method is as follows; the cable is pulled up by divided wires which was used in Stalpath sheathed cable laying. Another hang wire at the top is added for cable hanging when the winch wire returns to the one under the divided wire for horizontal laying in place of three pulleys. The messenger wire is not cut off in this method.

Clamping Metals

For the securing of vertical lengths, the clamping metals shown in Fig. 9 are used. The holding force of clamping metals over the messenger with PVC sheath is about 200kgs. The holding interval is maximum 10meters. Holding force drops when the flooding compound is coated over the messenger.

Splicing and Termination

The vertical cable is connected to the underground cable or terminated at terminal blocks. An auxiliary lead sleeve is used for splicing and gas stoppage for underground cables is effected by pouring in resin. In case of termination, the each insulated conductor is threaded into the PVC pipe for protection. It is necessary to develop tough strength insulation for termination.

Conclusion

Through our many experiments and experiences, cable construction suitable for vertical installation was developed. It has been six years since our first cable laying of vertical cable. During these years, some improvements have been made. About 80 pieces of cable already have been laid and are in service.

Acknowledgment

The authors are indebted to many people within NTT and The Fujikura Cable Works, Ltd. who engaged in the development and laying of

the vertical cable.

Reference

1. T. Miyawaki, R. Aoyama, T. Takada, T. Watanabe, and H. Ishihara Fujikura Technical Review No. 37, 1968
2. S. Kaibuchi and K. Asada Japan Telecommunication Review, January 1976



Fig. 9 Vertical cable

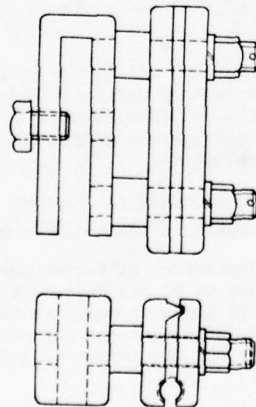


Fig. 10 Clamp metals



Kenji Mori

Nippon Telegraph and Telephone Public Corporation
1-1-6, Uchisaiwai-cho
Chiyoda-ku, Tokyo,
Japan

Kenji Mori is Staff Engineer, Engineering Bureau, NTT, and is now engaged in developmental research on intra-office cables and wires, and gas pressurization systems.

He received B. E. degree in electrical engineering from Tokyo Institute of Technology in 1968, and is a member of the Institute of Electronics and Communication Engineers of Japan



Ryuji Yashiro

The Fujikura Cable Works, Ltd. 1-5-1, Kiba, Koto-ku, Tokyo, Japan

Ryuji Yashiro is General Manager in Telecommunication Cable Engineering Department, the Fujikura Cable Works, Ltd., and has been mainly engaged in the Engineering and manufacturing of telecommunication cable

He received B. E. degree in electrical engineering from Tokyo Metropolitan University in 1953, and is a member of the Institute of Electronics and Communication Engineers in Japan.



Takashi Umetsu

The Fujikura Cable Works, Ltd. 1-5-1, Kiba, Koto-ku, Tokyo, Japan

Takashi Umetsu is Engineer in Engineering Department, Telecommunication Cable Division, the Fujikura Cable Works, Ltd., and engaged in communication cable development and engineering.

He received B. E. degree in telecommunication engineering from Tohoku University in 1968, and is a member of the Institute of Electronics and Communication Engineers of Japan.

GEO-TELEPHONY:
THE INSTALLATION OF SUBSURFACE TRANSMISSION MEDIA

Fred A. Huszarik

Transmission Media Development, Bell-Northern Research

SUMMARY

The increasing requirement for cheaper, faster and more reliable communications has resulted in some outstanding technological advancements in the design of communication transmission systems. The most recent evidence of these advancements is the evolution and installation of the first fiber optic transmission systems. While the design of electronics and major components such as cable is continually being up-dated, one cannot help but wonder about progress at the opposite end of the communications hierarchy, the outside plant installation methods. This author's contention is that although the industry is generally well advanced in terms of transmission systems design, it is not providing communications companies with a total system package which includes innovative installation methods.

This paper analyses this hypothesis by identifying the source of the problem, reviewing the state-of-the-art in cable installation methods and proposing some possible improvements.

THE PROBLEM

By examining the evolution of below-ground cable installation methods one finds that, except for the development of the cable plow, relatively little has changed since the installation of the first communication cables. During the same time communications electronics, cables and apparatus have evolved at an impressive rate, with the result that the construction and maintenance of below-ground cable systems may now very well be the weakest link in the overall transmission system. The importance of below-ground construction methods must not be underestimated. In North America billions of dollars are spent by telephone companies every year on the installation of below-ground systems. In some parts of the continent as many as 90 percent of all new installations are below-ground or 'out-of-sight'. Even more significant is the fact that over the last three years cable installation costs have on the average doubled. Every indication is that this trend will continue.

Two fundamental requirements must be met before cable installation methods can be up-dated and made more cost effective. First, the responsibility for solving the problem must be established.

Traditionally the telephone companies and their contractors have provided the necessary installation methodology and tools. This approach usually has been adequate as long as cable and the supporting apparatus were relatively simple in design and could be easily handled in the rugged construction environment without fear of damage. But with the development of more complex cables and outside plant apparatus the performance of which is increasingly more sensitive to the physical environment, the pressure appears to be more and more on the cable and apparatus manufacturers to provide a total system package including safe and cost-effective installation practices.

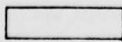
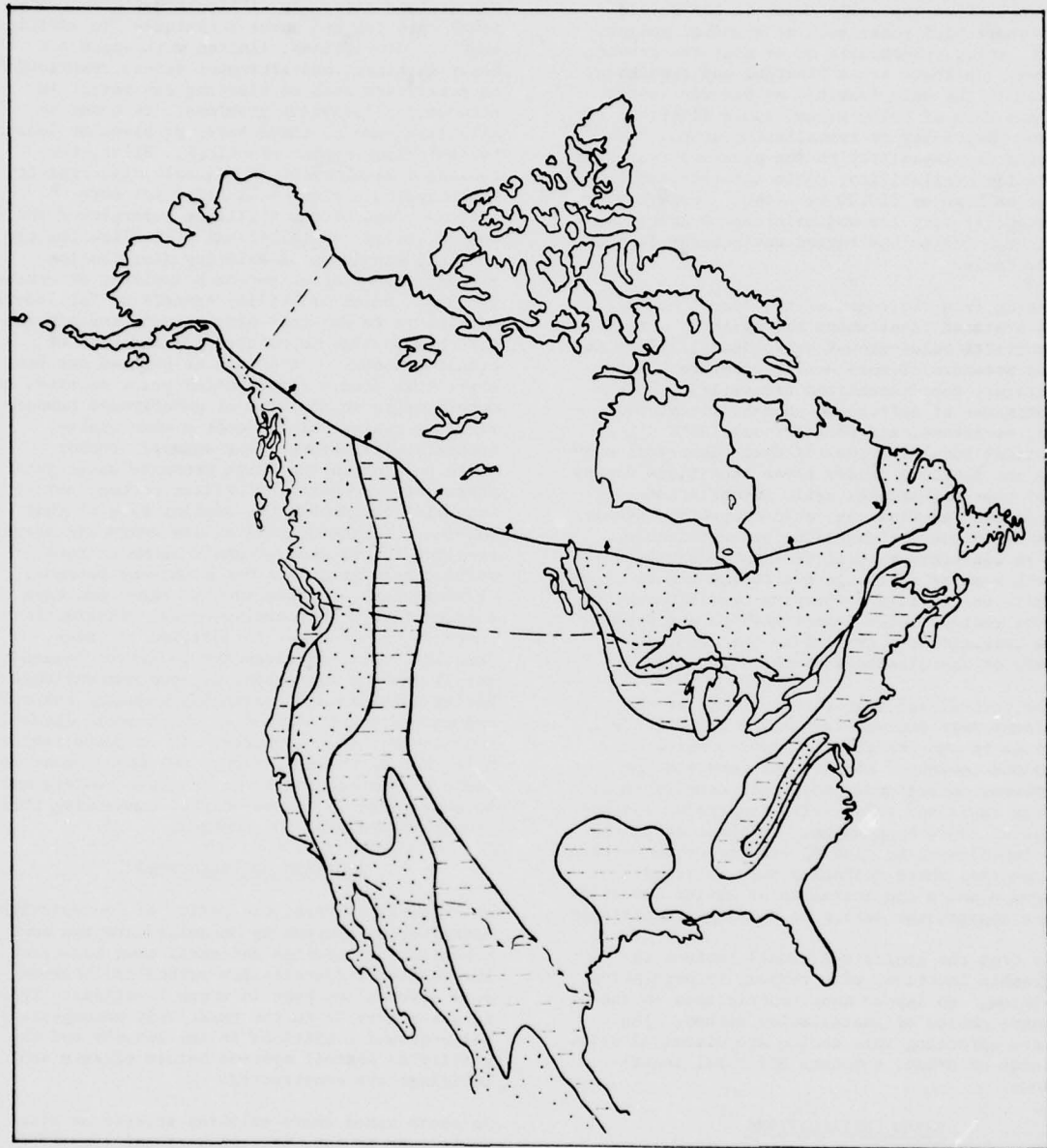
Secondly, a much more comprehensive and factual data base describing the forces acting on cables during and after the installation must be acquired. Surprisingly little is known about the forces imposed on cables during normal construction operations such as plowing, trenching or pulling. Even less is known about long term forces such as soil and rock abrasion, ground pressure and frost action. Without this information one cannot realistically evaluate how good or bad a particular installation method is in terms of assuring the life of the cable. Furthermore, without an accurate characterization of the short and long term environment surrounding the cable, it is difficult to optimize the design of the cable to meet these conditions.

In order to better appreciate the shortcomings of present below-ground cable installation methods and tools two factors stand out from the rest: the geology and geography associated with every installation.

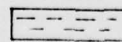
GEOLOGICAL AND GEOGRAPHICAL FACTORS AFFECTING
BELOW-GROUND CABLE INSTALLATION METHODS

Since the utilization of different cable installation techniques is highly dependant on the surficial geology along proposed routes, it is worthwhile to briefly consider the North American geology and its impact on cable installation methods.

As illustrated in Figure 1, more than half of the populated areas of the continent are covered by what would normally be considered to be



GOOD



MODERATELY POOR



POOR



SOUTHERN LIMIT OF PERMAFROST

FIGURE 1 - CABLE BURYING CONDITIONS IN NORTH AMERICA

'poor' or 'moderately poor' burying conditions. Poor conditions typically exist in the shield areas where hard rocks such as granite, gneiss, basalt, etc., predominate at or near the ground surface. In these areas blasting and trenching is usually the only feasible method for installing any form of below-ground cable distribution system. Depending on installation depth, rock hardness, accessibility to the proposed route and contractor availability, cable installation costs can be as high as \$20.00 per foot. Productivity is generally very low and maintenance costs tend to be high due to the rugged environment imposed on the cable.

Extending from the edges of the 'poor' burial areas are conditions which are slightly more conducive to below-ground cable installations due to the presence of more soil overburden. These 'moderately poor' locations are typified by a predominance of soft rocks such as limestone, shale, sandstone, and bouldery soil with occasional long stretches of deep clear soil overlying the bedrock. Under these conditions almost all of the conventional cable installation methods such as blasting, soil trenching, plowing and small diameter tunnelling are applicable. From an engineering point of view these areas present a major challenge due to the almost infinite variability of burying conditions along a major route. Soils investigations and proper route selection are crucial to the economic success of installations at these locations.

In the central and southeastern parts of the continent deep boulder-free soils present few problems to the installation contractor or telephone company. Bedrock outcrops are the exception, consequently good soil conditions allow for the rapid and relatively inexpensive installation of cable by plowing. In these areas the only impediments to plowing are the urban centers and suburbs, where obstacles such as roads, driveways and a concentration of buried utilities have a significant effect on plowing productivity.

Aside from the geological considerations the geographic location, with respect to population densities, can impose many restrictions on the ultimate choice of installation method. The factors affecting this choice are discussed below in terms of urban, suburban and rural installations.

URBAN INSTALLATIONS

In many North American cities and towns regulatory bodies are insisting that all utilities install their outside plant 'out-of-sight'. It seems inevitable that this requirement will become even more common in the near future. Along with the 'out-of-sight' restriction come the logistics problems and extremely high costs associated with excavating ground in an urban environment.

In most large urban centers existing congestion under city streets and the problem of accurately

locating existing plant make the installation of new systems extremely difficult using conventional open cut and cover techniques. In addition, traffic disruptions, limited work space for heavy machinery and stringent safety restrictions on activities such as blasting can result in monumental logistics problems. In order to alleviate some of these basic problems at least two solutions appear practical. First, the continued development of reliable high capacity transmission systems will allow for more efficient use of the available underground space. Second, deeper installations will allow for the physical expansion of existing distribution systems. The latter approach implies, of course, the development of utility tunnels or "utilidors". Suffice it to say that many reports and papers have been published on the pros and cons of utility tunnels. It should be pointed out however, that from a construction point of view, new developments in the area of underground tunnelling are making this concept a more viable economic alternative. For example, recent tests have shown that high pressure water jets assisting a conventional roller cutter, rotary tunneller can double the cutting rate of that machine. Although still in its embryonic stages, research in the area of small diameter rock melting tunnelers has met with some success. Technological advances such as these can have a major impact on reducing tunnel construction costs in the future. In addition to these 'exotic' tools, improvements in cutter designs, metallurgy and automation of more conventional boring machines are constantly reducing the costs and increasing the speed at which small diameter tunnels can be constructed. It is quite conceivable that in the near future the requirement for surface construction in major urban centers will be superceded by 'out-of-sight' tunnelling thirty or more feet below the surface.

SUBURBAN INSTALLATIONS

As in urban centers, the policy of 'out-of-sight' distribution systems is becoming more and more prevalent in suburban and small town locations. The choice of installation method is, however, more diversified than in urban locations. This is due primarily to the relatively uncongested below-ground conditions in the suburbs and the ability to install systems before streets and buildings are constructed.

In those cases where existing streets or sidewalks must be cut, the conventional trenching technique is normally used. One exception to this occurs at major road crossings where boring or tunnelling often becomes a more desirable alternative for two major reasons. First, the tunnelling operation results in minimal disturbance to the steady flow of traffic and therefore enhances both public relations and the safety of the workmen. Second, the problem of pavement removal and replacement is eliminated. Pavement replacement is often a major problem in terms of achieving adequate compaction in the trench to avoid seasonal pavement repair costs. In

good soil conditions such as loose fill or sand, horizontal earth augers provide an efficient and economically attractive technique for crossing roads, sidewalks and driveways. In rocky locations horizontal rock boring machines can drill an 11 inch diameter hole at 20 feet per hour, or a 60 inch diameter hole at an average speed of one foot per hour in solid limestone. These machines drill harder rocks at slower speeds, while maintaining good accuracy at distances up to 500 feet. Research is presently underway to increase the effective drilling distances and accuracy of these small diameter rock boring machines.

In suburban locations where the ground can be easily penetrated and cables are to be buried rather than placed in ducts, the cable plow is by far the most efficient tool that can be used. As well as being the least damaging to the terrain, plowing is by far the least expensive and fastest cable installation method. The major deterrent to plowing in a suburban environment is the frequency with which one encounters obstacles such as driveways, fences, existing utilities and so on. In such problem locations consideration must be given to the use of continuous trenching machines.

Although many urban and suburban centers are located in areas with a reasonable amount of soil cover, bedrock or boulder concentrations are sometimes encountered. This situation can create severe problems, especially in a populated environment. Normal blasting techniques often cannot be applied due to stringent safety regulations. Even if blasting is allowed, restrictions on the size of explosive charge make this excavation method extremely time and money consuming. In suburban locations the alternatives to blasting include the use of pneumatic rock hammers, 'Hoe-rams', rock splitters and rock saws. Although all these devices are effective to varying degrees, none is particularly efficient and all are very costly to operate.

RURAL INSTALLATIONS

A large percentage of below-ground installations occur in rural or relatively unpopulated areas. Even though the option to place systems above ground exists, it is often cheaper to bury. This is particularly true in areas where there is sufficient soil cover to permit plowing.

Plowing is the cheapest, fastest and most environmentally acceptable method of installing cable presently available. Cable plows can bury everything from small diameter drop wire to three inch diameter cable, up to six feet below the surface. Also plows which can bury up to four or five cables at a time are available. These machines can install cable at rates up to approximately one mile/hour with little disturbance to the ground surface and consequently minimal clean-up costs. Even more attractive is the fact that cables can be installed for considerably less than one dollar per foot. Plowing is, however, very sensitive to ground

conditions and is therefore restricted to locations where good, obstacle free soil cover exists.

As mentioned previously less than half of the North American continent consists of what is normally referred to as good plowable terrain. The rest is a mixture of boulders, bouldery till and bedrock which normally must be trenched. Bouldery areas or generally poor soil conditions can often create more problems than bedrock. Wet soils or heavy boulder concentrations can be extremely difficult to excavate. When they are excavated it is often difficult to maintain a good trench profile. Furthermore, considerable care must be taken in placing as well as back-filling cables or structures to prevent damage to the installed plant. The type of trenching equipment used is frequently determined by the soil type. Loose materials with stone sizes less than two or three inches can be excavated with continuous wheel or chain trenchers. Soils containing larger stone sizes or heavily compacted materials usually require back-hoe type excavators. Associated with trenching is the requirement for wide rights-of-way and a considerable clean-up budget.

In some poor soil conditions an alternative to trenching that is becoming more popular is the concept of plowing a protective continuous duct prior to pulling the cable. Although more expensive than direct burial, this method is usually less costly and faster than trenching. Initially a rock ripper is used to create a slot and remove obstacles such as large boulders and tree roots along the proposed route. Once this has been accomplished a cable plow installs a continuous section of flexible polyethylene duct. The duct provides the mechanical protection which is usually supplied by sand padding around a trenched cable. After the duct has been installed and proven, the cable is pulled into the duct. This technique has been used successfully on projects where direct burial by plowing was not feasible due to poor soil conditions and where the more costly trenching method would normally have been used.

The problem of installing outside plant in rural locations where bedrock exists at or near the surface is somewhat less acute since blasting is usually an acceptable excavation method and the aerial placing option is available. Pole line installations are definitely less expensive than blasting a continuous trench. However, for a variety of reasons the amount of rock trenching presently being performed is significant and will probably increase in the future.

At the present time rock trenching on a continuous basis is limited to essentially three methods: breakage and excavation by machine; rock cutting with continuous saws; and, blasting and excavating. Where soft, weathered rocks such as shale, weak limestone and sandstone exist it is often feasible to break and excavate the material with a backhoe. Alternatively, rock rippers can be used to break the material which can then be excavated by backhoe. Cutting with circular rock

saws is becoming a common method of trenching in rock. However, there are some drawbacks with these saws. First, they are normally limited to a 36 inch depth of cut. Second, they have limitations in the type of rock that they can be cut effectively. Third, on long excavations the tooth replacement and general maintenance cost can be extremely high. Despite these limitations, the rock saw can be a useful tool for sections up to 100 feet in length. The third trenching method, blasting and excavating, is the one used most frequently for major rural installations in rock. Blasting is, of course, noisy, dirty, somewhat hazardous and expensive; but in hard rocks it is often the only alternative.

FUTURE CABLE INSTALLATION METHODS

Based on the present approach to installing cables in the different geographic locations discussed above it becomes apparent that better methods and tools are required to handle moderately poor to very poor soil conditions. For these areas at least two technologies have the potential to impact on the construction methods used for future cable installations: high pressure water jetting and rock melting using the 'subterrene'.

High Pressure Water Jetting

Since the mid-1950's waterjets have been effective tools for cutting rock. Laboratory tests have shown that water passing through small diameter (0.1 inch) nozzles at pressures of 50,000 to 100,000 psi. can easily cut into the hardest rock. However, pumping equipment that is capable of reliably maintaining the high pressures required for continuous cutting has only recently become available. During the past four years, a large number of waterjet cutting systems have been placed in industries for cutting a wide range of material. These machines have proved to be reliable and economically beneficial.

There are many ways in which waterjets can be used for cutting rock, and, among them, two stand out as the most effective. In the first method, the waterjet is used to assist or augment a mechanical system. This is done by making narrow slots, from 1/10 to 1 inch deep, in the rock with the waterjet. The slots weaken the rock and significantly reduce the mechanical forces required of the cutters to remove the rock between the slots. This method has been successfully used in waterjet-assisted drilling and tunnel boring projects.

The second method of cutting rock with waterjets is to cut a wide, deep slot in the rock by using a rotating or oscillating nozzle, which can enter the slot. In this way, the slot depth is limited only by the mechanical design of the system and not by the cutting ability of the waterjet. This method requires more energy to remove a volume of rock than the mechanically assisted method, but requires no mechanical loads.

The attractive features of waterjet devices for

utility construction applications include little noise and environmental pollution, safety in populated areas and increased productivity. In addition, since water is the cutting medium, no mechanical cutters need replacing thereby eliminating a major operational expense currently encountered with mechanical rock cutters. Although still in the preliminary stages of development, it is expected that this type of equipment will impact on utility construction as early as 1978.

The Rock Melting Subterrene

The Subterrene is a device which has the capability to melt small diameter holes in most rocks and some types of soil. In general rock and soil are composed of minerals which have a melting point about 1450 K (2150°F). Refractory metals, such as molybdenum and tungsten, have a higher melting point and are used for the penetrator body material. An electrical resistance heater operates the tip at 1800 K (2800°F). The melted rock is formed into a glass lining to seal and support the walls of the bore-hole. Any excess melt is chilled and formed into glass pellets which are extruded through the stem of the system. This concept of rock-melting offers more than just a new method of breaking or disintegrating rock. It provides simultaneously the three major elements of the conventional excavation process:

1. Making the hole or tunnel.
2. Supporting the wall.
3. Removing the debris.

Although this technique offers many advantages for 'out-of-sight' cable installations, there is still considerable research required in the area of penetration speed and penetrator life. Also the problems of safety and below-ground obstacle location require further study before this concept can be used for utility construction.

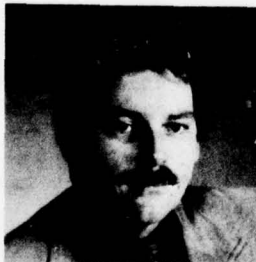
CONCLUSIONS

With the development of more complex outside plant apparatus and cables the manufacturers of these products must adopt a more significant role in providing a total system package which includes installation practices. The first step towards providing cost-effective cable installation practices is to establish a comprehensive data base which describes both the short and long term forces acting on below-ground cables. Based on the present state-of-the-art, available cable installation methods are quite adequate when used in good soil conditions and in an unpopulated environment. However, a large proportion of installations are located in poor soils, rock and restricted heavy machinery areas where the available excavation techniques are both technically and economically inadequate. It is essential that improved excavation tools and methods be developed to meet the social, political, technical and most important, economic require-

ments. Based on the available data, high pressure water jetting and efficient small diameter tunneling are two methods which may provide the capability to meet these requirements in the near future.

REFERENCES

1. First International Symposium on Jet Cutting Technology, BHRA Fluid Engineering, Coventry, England, April 5-7, 1972.
2. H.D. Harris; "Rock cutting with water jets", Presented to 75th Annual General Meeting of the Canadian Institute of Mining and Metallurgy, Vancouver, Canada, April 15-18, 1973.
3. J.H. Olsen; "Jet kerfing experiments on red granite and white marble," Flow Research Report No. 34, Flow Research, Inc., Kent, Washington, U.S.A., April 1, 1974.
4. Second International Symposium on Jet Cutting Technology, BHRA Fluid Engineering, Cambridge, England, April 2-4, 1974.
5. D.L. Sims; "A versatile rock-melting system for the formation of small diameter horizontal glass-lined holes", Los Alamos Scientific Laboratory, Los Alamos, N.M., Report LA-5422-MS (1973).
6. D.L. Sims; "Identification of potential applications for rock-melting subterraneos", Los Alamos Scientific Laboratory, Los Alamos, N.M., Report LA-5206-MS (1973).



Fred Huszarik received his B.Sc. in Civil Engineering in 1972 and his M.Sc. in Geotechnical Engineering in 1974. Since joining Bell-Northern Research in 1973 Fred has been responsible for research on various aspects of telephone outside plant construction methods, tools and materials. Fred holds memberships in the Canadian Society for Civil Engineering, Canadian Geotechnical Society, American Underground Association and the International Society for Soil Mechanics and Foundation Engineering. Since 1976 Fred has been chairman of the IEEE Task Force on Cable Installation Methods.

OXIDATIVE STABILITY OF HIGH DENSITY POLYETHYLENE

K.D. Kiss and E.G. Malawer

Phelps Dodge Communications Company
White Plains, N.Y.

Abstract

The oxidative stability of foamed high density polyethylene is substantially poorer than that of solid insulation containing comparable levels of stabilizers. Laboratory studies show that interaction between the metal deactivator and foaming agent is responsible for the observed difference in the presence of copper conductors. The effect of antioxidant, metal deactivator and foaming agent concentration on stability was quantified. An experimental grid was designed and OIT stabilities of the compositions were determined both in contact with copper and in its absence. The data facilitated the computation of best fitting second order equations. The coefficients of these equations were determined.

Background

Polymer insulated telephone wire insulation has traditionally been made from low density polyethylene (LDPE), high density polyethylene (HDPE), and polypropylene. Within the past two decades there has been considerable interest in the utilization of foamed insulation, to counteract increasing resin cost, provide reduced cable diameter and increase duct fill. The first large volume application of expanded insulation using LDPE appeared in Japan in 1958.¹ Around 1960, a foamable HDPE using azobis-formamide as blowing agent first appeared.²

Subsequently, it was observed that the presence of blowing agent or its reaction products reduces the thermal stability of HDPE insulation as evidenced by lower oxidative induction times (OIT)^{3,4}. Oven aging at 100°C,⁵ 120°C oxygen uptake⁶ and DTA-OIT data equivocally show that foamed HDPE insulation has poorer stability when compared to solid HDPE insulation in the presence of copper. It has also been

shown that the stability of the foam is not reduced appreciably in the absence of copper.

Recently, it has been found that the deleterious effect of the blowing agent (or its decomposition products) on HDPE in the presence of copper could be overcome by increasing the antioxidant concentration.⁷ Another worker has postulated that the cellular structure itself may play a part in reducing stability in the foam by facilitating increased rate of oxygen diffusion into the matrix.⁸

In this work, we quantify the interactions of foaming agent, metal deactivator, and antioxidant, using a three dimensional experimental grid program and show the relationship between the desired level of stability and the lowest possible cost at that level.

Objectives

The objectives of this work were to:

- Quantify the antioxidant - metal deactivator - foaming agent interaction.
- Estimate limiting stability of foamed insulation.
- Establish cost of stability improvement for foamed insulation.
- Demonstrate applicability of predesigned experimental grids to compounding problems.

Experimental Part

Preliminary Investigation

The initial stage of the work included the comparison of OIT stabilities of solid and foamed HDPE in the presence and absence of copper in forms of pelletized compound, insulation and insulation converted into a 7 mil film. The results presented in Figure 1 show that within experimental error

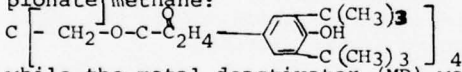
the OIT stabilities are:

- Comparable for solid and foam grades in the absence of copper.
- Comparable for the solid compound in the presence and absence of copper.
- Decreasing to about half of the original level for foam in the presence of copper.
- Decreasing gradually with the sequence of heat processing steps:
pelletization → insulation → compression molding of insulation.

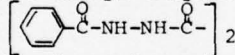
These observations indicate that the deterioration of stability is caused by some interaction of copper and foaming agent either directly or indirectly, e.g. through the deactivation of the metal deactivator. They also suggest that the physical shape of foam is not directly responsible for the lower stability.

Materials

The foamable grade HDPE compound was a commercially available product in pellet form. The solid grade compound was identical to the foamable grade except it contained no foaming agent. The antioxidant (AO) utilized was tetrakis[methylene-3(3'-5'-di-t-butyl-1-4-hydroxyphenyl) propionate]methane:



while the metal deactivator (MD) was N,N'-dibenzal oxaryl dihydrazide:



The experimental compositions were arrived at in two steps. First the masterbatches of antioxidants and metal deactivator were compounded at 1% w/w in solid grade HDPE. These masterbatches were in turn compounded with HDPE to achieve the final formulations specified by the experimental grid.

The foaming agent (FA) level was controlled by using proportional amounts of solid and foamable grade HDPE pellets in the second compounding steps. Exact concentrations of Δ AO, Δ MD and FA in each experimental composition is specified in Table 1.

Procedures

All compounding was performed in a Brabender Plasticorder equipped with a roller 5-type measuring head. Forty gram batches were mixed at 160°C and 50 rpm for 10 minutes.

Each masterbatch and experimental formulation was passed once through a Farrel roll mill equipped with two 6 x 13 inch horizontal rollers. The mill temperature was set at 177°C (350°F). The 15 experimental formulations were then pressed for 3 minutes to 8 mil thick films using a Wabash hydraulic press set at 138°C and 5500 lbs./sq. in. In addition, two experimental controls were prepared by subjecting 40 gram samples of each of the two compounds to all of the aforementioned processing conditions.

The oxidative induction times (OIT) were determined on a Perkin-Elmer model 1B Differential Scanning Calorimeter (DSC).

Sample preparation consisted of punching 3 mm. diameter discs from the 8 mil films to give typical sample sizes of 1.4 to 1.7 mg. The discs were placed in sample pans of both aluminum and pre-oxidized copper and covered with aluminum lids. A fast, manual scan in nitrogen atmosphere brought the temperature to 200°C . After the sample assembly equilibrated at this temperature, the atmosphere was switched to oxygen and the strip-chart recorder was activated. The OIT was taken to be the time from the introduction of the oxygen to the onset of oxidative degradation. All experiments were performed in duplicate and the results averaged. The averages were utilized for statistical treatment.

Experimental Design

In order to gain maximum information from a given number of experiments a statistical approach was elected. This approach consisted of:

- Designing an experimental grid to maximize information with a minimum number of experiments.
- Conducting the experiments to generate responses ("actual" data).
- Selection of mathematical equations which adequately approximate the effects of variables on each of the responses.
- Computation of coefficients for these equations.
- Computation of experimental results ("computed" data) using these coefficients.
- Decision on the acceptability of approximation by comparing "actual" and "computed" data.
- Application of the equations to generate:

Primary effects of variables on responses
Interactions of variables
Correlation of responses

The experimental grid was designed to assess the following variables:

- X_1 = antioxidant concentration, incremental amount in addition to that already present in the compounds, AO, ranging from 0 to 0.1% by weight.
 X_2 = metal deactivator concentration, incremental amount in addition to that already present in the compounds, MD, ranging from 0 to 0.1% by weight.
 X_3 = foaming agent level, FA, relative scale ranging from 0 for solid insulation grade HDPE to 100 for foamable grade HDPE.

The responses of interest were:

- Y_A = Oxidative Induction Time (OIT) in contact with copper measured in minutes.
 Y_B = OIT in the absence of copper, minutes.
 Y_C = Relative cost of added stabilizers on an arbitrary scale ranging from 0 for the commercial compounds to 100 for the combination of 0.1% antioxidant + 0.1% metal deactivator, cents per pound of compound.

The expected non-linear correlation of variables and responses necessitated the use of at least three levels for the variables. A full factorial 3 level design for 3 variables specifies $3^3 = 27$ experiments. Partial factorial grids require fewer experiments at the expense of sacrificing some of the "fit", i.e. resulting in somewhat limited approximation. The grid selected gives an acceptable balance of experimental work and "fit".

The experimental grid (Figure 2) is a 3 variable, multilevel, center weighted, patched orthogonal design and requires 15 experiments. The levels of the variables in each experiment are specified to give a symmetrical 3 dimensional arrangement in which each experiment contributes to the computation of the coefficients uniformly. The variables are on 5 levels (designated as very low, low, medium, high, and very high in Figure 2 and in Table 1) and are expressed in "experimental units". An ex-

perimental unit is specified as the difference between high and medium or between medium and low levels. Using the medium level as 0 the other 4 levels are: -1.215 e.u. for very low, -1.0 for low, +1.0 for high, and +1.215 for very high levels. The levels, experimental units and concentrations of the 3 variables in each experiment are listed in Table 1.

The responses Y_A , Y_B , and Y_C were determined experimentally and used in generating the coefficients of best fitting equations. The assumption was made that in view of the relatively narrow range selected for the variables, a second order equation adequately describes the correlation. The generalized equation for each response is:

$$Y = a_0 + a_1 X_1 + a_2 X_2 + a_3 X_3 + a_{11} X_1^2 + a_{22} X_2^2 + a_{33} X_3^2 + a_{12} X_1 X_2 + a_{13} X_1 X_3 + a_{23} X_2 X_3 \text{ where,}$$

X_1 , X_2 and X_3 are the values for ΔAO , ΔMD and FA concentrations, respectively, in experimental units. The coefficients a_0 to a_{23} were computed for each response separately using the least squares method. These coefficients are listed in Table 2. It should be noted that in the case of relative cost, Y_C , only 3 coefficients are needed to specify the first order equation due to the additive nature of this response.

The coefficients were used to back calculate the predicted or "computed" values for each experiment. Figure 3 and Table 1 compare these "computed" values for each experiment for responses Y_A and Y_B with the "actual" experimental values. The relative cost, Y_C , is the result of calculation, therefore "actual" values are identical to "computed" values. The difference between computed and actual values is a measure of "fit" or applicability of the approximation. Other measures of the "fit" are the standard deviation and the relative error, both listed in Table 2. In case of response Y_A , OIT in copper, at 14.1% relative error the "fit" is considered adequate, especially in view of the notoriously poor reproducibility of this test. At 2.1% relative error for Y_B (OIT in absence of copper) the "fit" is excellent. No relative error can exist for relative cost, (Y_C) since it is the result of calculation.

The "computed" values for the responses were used to calculate the primary ef-

fect of each variable on each response. The data generated is presented graphically in a number of figures, plotting a response against a variable. The mathematical approach facilitates the computing of variable - Variable interactions, which are presented by plotting one variable against another, generating the equal performance contours (Figures 9, 10, 11, 20, and 21) in a two dimensional plot or by the response surfaces presented isometrically (Figure 12, 13, 14, 22, 23, and 26).

Discussion

OIT Stability in Contact with Copper

Primary effects of the three variables, incremental concentrations of antioxidant and metal deactivator, and foaming agent level are presented in Figures 4-8. Figure 4 shows the effect of antioxidant in solid compound. The three curves represent three levels of metal deactivator 0, 0.05 and 0.1% respectively. The proximity of these three curves is indicative of a relatively minor effect of the metal deactivator under these circumstances. The maximum type curve cresting at approximately 0.07% additional antioxidant concentration can be considered as indication of a maximum type correlation. On the other hand, the minor decline in these curves to the right of the maximum point can be interpreted as indication of an asymptotic correlation which is distorted by the forced use of a second order equation. In either case, the antioxidant concentration up to 0.07% incremental value improved the OIT stability in the presence of copper.

Figure 5 is a similar plot for the 50-50 blend of solid and foamable compounds. Compared to the previous Figure, a more significant stability increase with increasing antioxidant concentration can be seen. The correlation can be considered either as maximum cresting at 0.07% or as asymptotic beyond a 0.07% incremental antioxidant level.

The stabilizing effect of both additional antioxidant and additional metal deactivator is even more pronounced in the case of the foaming grade compound (Figure 6). Compared to the previous two figures, the maximum or asymptotic region is shifted to the 0.09% incremental antioxidant concentration.

These curves can be used to define the composition of an additive system resulting in a desired stability level. As an example for the foam grade compound, OIT stabilities in copper can be achieved in the range of 13 to 65 minutes by selecting the corresponding incremental antioxidant and metal deactivator levels. An OIT value of 50 minutes can be obtained by increasing the stabilizer level with any of the following combinations.

0.05% antioxidant + 0.1% metal deactivator

0.042% antioxidant + 0.08% metal deactivator

0.06% antioxidant + 0.08% metal deactivator

0.076% antioxidant + 0.05% metal deactivator

The primary effect of metal deactivator is nearly linear (Figure 7). It has virtually no effect on the solid compound and a very strong effect on the foam either by itself or in combination with antioxidant.

The destabilizing effect of foaming agent is partially compensated for by the addition of either metal deactivator or antioxidant (Figure 8).

Interactions. The mathematical approximation allows the computation of the interactions of the variables. A graphical method to present the interactions is the construction of the equal performance contours in which one variable is plotted against the other keeping the third one constant, as shown in Figures 9, 10, and 11, respectively. In the first one variable X_3 , foaming agent concentration is kept at the zero level. In other words, this figure reflects the equal performance curves in the solid compound. Plotting the other two variables on the two axes of the coordinate system, each point defines a combination of them and the curves represent the equal performance combinations. The saddle type configuration around 0.07% antioxidant concentration results from the maximum type curve found earlier on Figure 4. Similar plots for the 50-50 blend of solid and foam grade compounds and for the foamy grade compound is presented in Figures 10 and 11 respectively. These plots can be used to select compositions for a given performance. As an example, the 50 minutes line in Figure 11 defines all $\Delta A_0, \Delta M_D$ combinations providing this OIT level, including those specified earlier using Figure 6.

The interaction of two variables can be conveniently visualized in the isometric presentation of response surfaces. The bottom plane of Figures 12, 13, and 14 represents the same antioxidant metal deactivator compositions as Figures 9, 10, and 11. The OIT values are plotted on the vertical axis. The sum of the end points of imaginary vertical lines for an infinite number of compositions constitutes the response surface. The relative position of these surfaces shows that in the foaming grade compound, both the antioxidant and the metal deactivator result in significant improvement and the combination of the two additives amplifies this improvement without being synergistic. The similarity of the surface for the 50-50 blend of the two compounds, Figure 13 suggests that relatively minor amount of the foaming agent is capable of interfering with the stability. The relatively high position of the surface for the solid compounds, Figure 12, reflects the higher stability of this compound. Interestingly, the highest point of this surface representing the maximum additive levels is marginally lower than the similar corner for the foamable grade. Since this juxtaposition is not justified by simple logic, we should conclude that the forced use of second order approximation results in minor discrepancies, and the values for this point should be considered as equal.

OIT Stability in the Absence of Copper

The catalytic effect of copper on the OIT stability is assessed by comparing the results described above with those generated in the absence of copper. "Actual" OIT values, Y_B , for compositions 1-15, are listed in Table 1 and are presented in the three dimensional grid system in Figure 15. The coefficients of an assumed second order approximation were determined (Table 2) and used to calculate the "computed" OIT values. (Table 1 and Figure 15).

Primary effects. Antioxidant addition results in OIT improvement both in the solid and in the foam grade compounds (Figures 16 and 17 respectively). Neither the incremental metal deactivator (Figure 18) nor the foaming agent (Figure 19) has a significant effect.

Interactions of variables. The approximately vertical direction and negligible curvature of the equal performance contours

in Figures 21 and 22 are indicative of the absence of interactions both in the solid and in the foam grade compound. This is reflected in the isometric presentation of the response surfaces (Figures 22 and 23) as almost planar surfaces tilted predominantly in the X_1 direction representing incremental antioxidant.

Correlation of responses. The correlation between OIT stabilities in the presence and absence of copper, Y_A versus Y_B is best represented in Figure 24. The numbers in the circle refer to the serial numbers in the compositions. The three types of arrows connect the compositions which are identical in two components and differ only in the third one. Therefore, the arrows of identical type represent the main effect due to the copper. The dotted arrows show the effect of antioxidant. The approximately 45° slope for most of these arrows indicates that increments in the antioxidant are about equally effective as stability increasing agents both in the presence and in the absence of copper. The approximately horizontal solid arrows representing the metal deactivator show that this agent is much more efficient in improving the OIT in the presence of copper than in its absence. The broken arrows pointing mostly downward showing the effect of the foaming agent confirmed the known fact that its primary influence is the decrease in the stability enhanced by the presence of copper.

Relative Cost

The relative cost of incremental additives Y_C is computed only for that of the antioxidant and of the metal deactivator. The cost of 0.1% antioxidant plus 0.1% metal deactivator is considered as 100, and the cost of any other combination is proportionated. By definition, this property can be described with a first order equation requiring only 3 coefficients (Table 2).

Computed values of relative cost for the 15 compositions are presented in Table 1. It is evident that there is no difference between experimental and computed values in this case.

The primary effect of antioxidant and metal deactivator additives on the relative cost is presented in Figure 25. The additive nature of this property manifests itself in a linear correlation both with

the antioxidant and with the metal deactivator concentrations.

The isometric presentation of the response surface (Figure 26) is a tilted plane due to the linear correlation. By definition the low point of this surface is at 0 relative cost corresponding to the absence of incremental additives, and the high point at the maximum level for each additive is 100.

The correlation of responses is presented by the plotting of relative cost against the OIT stability either in the presence or in the absence of copper, Figures 27, and 28 respectively. The three types of arrows connect the compositions which differ in one component only. The upward trend of the dotted arrows for compositions with equal antioxidant levels is indicative of its cost efficiency. The almost horizontal solid lines for the metal deactivator shows no effect on Y_A or Y_B indicating very poor cost efficiency of this additive. The downward orientation of the broken line arrows for equal levels of foaming agent shows the negative effect. The relative position of Figure 27 compared to Figure 28 is indicative of the catalytic effect of copper.

Determination of Most Cost Effective Systems

It was shown earlier that both the stability and the cost of any combination of the additives can be expressed with relatively simple equations. The combination of two appropriate equations makes it possible to compute the composition for any selected stability level at the minimum cost. In the case of two variables a graphical method can be used and is demonstrated in Figure 29. It is basically a combination of Figures 11 and 25, the equal stability contours for foam grade compound in the presence of copper, and the equal cost lines. The line representing 44 min OIT stability. The same technique can be used to determine the tangential points for performances from 42 to 60 minutes. The dotted line connecting these tangential points is the path of the minimum cost compositions for this performance range. For performances below 42 minutes OIT no tangential points are available within the field of investigation. In this area, the minimum compositions are achieved at 0 incremental metal deactivator concentration with the addition of appropriate amounts of antioxidant. This is reflected by the

dotted line along the bottom of Figure 29 progressing from 0 to 0.065% incremental antioxidant. Similarly, performance levels above 60 minutes OIT are achieved by the addition of the maximum metal deactivator level, 0.1%, combined with the appropriate amount of antioxidant. This is represented in Figure 29 by the dotted line in the top right corner.

The same technique was used to determine the minimum cost composition for the 50-50 blend of solid and foamable grade compound. In the case of OIT stability in the presence of copper this is presented with the dotted line in Figure 10. In the case of the solid compound, the minimal cost composition is along the bottom line of Figure 9 showing that the minimum cost compositions can be achieved with the addition of incremental antioxidant only.

The equal performance contours for OIT stability in the absence of copper were presented in Figures 20, and 21. Using the same techniques, it is shown that the minimum cost compositions, represented with dotted lines in each of these figures, can be achieved by addition of incremental antioxidant only up to 0.1%.

Conclusions

- Second order equations can be used to approximate primary effects and interactions of the antioxidant, metal deactivator, foaming agent system on OIT stability in HDPE.
- OIT in contact with copper is greatly decreased by foaming agent.
- This decrease in stability can be compensated for by additives.
- Antioxidant is more efficient than metal deactivator at equal concentration.
- The method presented is suitable to establish minimum cost compositions at desired stability levels.

Acknowledgments

Thanks are due to Dr. M.C. Biskeborn, Mr. R.M. Morgan, Mr. W.J. O'Grady for their stimulating interest and helpful suggestions in this work, and to Ms. J. Amato, Mr. E. Armour, and Mr. C. [unclear] for performing the experimental work.

Their contribution is gratefully acknowledged.

References

1. Rokunohe, M., Oshida, Z., Miyamoto, H., Mizuno, S. and Oketani, T., U.S. Patent No. 3,068,26, December 11, 1962.
2. Pusey, B.B., "Cellular Insulating for Communication Cable", 19th Annual Wire and Cable Symposium, Asbury Park, N.J. November 29-December 1, 1961.
3. Marshall, D.I., Turnipseed, J.M., and Wight, F.R., "Raw Material Inspection for Expandable Polyolefin Insulation", 23rd Annual International Wire and Cable Symposium, Cherry Hill, N.J., November 1974, P. 63.
4. Robinson, M., Society of Plastics Engineers, Technical Papers, Vol., XXI, P. 390 (1975).
5. G.A. Schmidt, G.A., "Life Prediction of Insulations for Filled Cable," 26th Annual International Wire and Cable Symposium, Cherry Hill, N.J., November, 1977.
6. Gesner, B.D., and Harmel, R.J., Society of Plastics Engineers, Technical Papers, Vol. XXI, P. 286 (1975).
7. O'Rell, D.D., and Patel, A., "Oxidative Stability Studies on Cellular High Density Polyethylene Insulation for Communications Wire". 24th Annual International Wire and Cable Symposium, Cherry Hill, N.J. November 18-20, 1975, P. 231.
8. Wight, F.R., "Oxidative Stability of Expanded Polyethylene for Wire and Cable", Journal of Cellular Plastics, November/December 1976, P. 317.



KORNEL D. KISS is the Manager of the Materials Research Laboratory at the Phelps Dodge Cable & Wire Company. He received a B.S. in Chemical Engineering in 1944 and a D.C.E. in 1947 from the Polytechnical University of Budapest. His past experience includes organic and polymer synthesis research, supervision of product and process development on a variety of polymers, polymer aging, degradation and stabilization. He is the author of five textbooks, and the inventor of over 40 patents, about half of them in the additives and polymer stabilization field. His interests include the optimization of insulating materials, thermal analysis, process miniaturization, statistics and laboratory scale simulation of polymer aging.



EDWARD G. MALAWER is a Research Chemist in charge of the Analytical Instrumentation Laboratories of Phelps Dodge Cable & Wire Company. He received a B.S. in Chemistry from the City College of New York in 1970, a Ph.D. in Physical Chemistry from New York University in 1976 and performed a postdoctoral study at the State University of New York, Albany. His areas of interest include instrumental analysis, optical and scanning electron-microscopy, thermal analysis, stabilization, polymer degradation and morphology of solid dielectrics. His thesis involved the characterization of molecular motion in molten salts by Fourier-transform NMR spectrometry, and his work on the development of a DTA system for the teaching laboratory was published in the Journal of Chemical Education.

TABLE 1
Variables and Responses

Variables: X_1 =Antioxidant concentration, % by weight Responses: Y_A =OIT in copper, minutes
 X_2 =Metal Deactivator concentration, % by weight Y_B =OIT in absence of copper, minutes
 X_3 =Forming Agent Level, % formable compound Y_C =Relative Cost
L=Low, M=Middle, H=High, V=Very $\alpha = 1.215$ ΔY =Actual Value-Computed Value

| Exp. No. | VARIABLES | | | | | | | | | RESPONSES | | | | | | | | |
|-------------|-----------------------|--------------|--------------|--------------|--------------|--------------|----------------------|--------------|--------------|---------------------|-------|--------------|------------------|-------|--------------|------|--------------|--|
| | Experimental Units | | | % By Weight | | | Y_A =OIT in Copper | | | Y_B =OIT in Alum. | | | Y_C =Rel. Cost | | | | | |
| | ΔA_O | ΔM_D | ΔF_A | ΔA_O | ΔM_D | ΔF_A | ΔA_O | ΔM_D | ΔF_A | Act. | Comp. | ΔY_A | Act. | Comp. | ΔY_B | Act. | ΔY_C | |
| 1 | L | L | L | -1 | -1 | -1 | 0.009 | 0.009 | 9 | 52.1 | 48.3 | 3.8 | 62.9 | 62.5 | 0.4 | 8.8 | 0 | |
| 2 | H | L | L | 1 | -1 | -1 | 0.091 | 0.091 | 9 | 57.9 | 56.6 | 1.3 | 89.5 | 87.5 | 2 | 42.8 | 0 | |
| 3 | L | H | L | -1 | 1 | -1 | .009 | .091 | 9 | 40.6 | 45.1 | -4.5 | 66.4 | 65.3 | 1.1 | 57.2 | 0 | |
| 4 | H | H | L | 1 | 1 | -1 | .091 | .091 | 9 | 65.5 | 57.7 | 8.1 | 90.2 | 91.9 | -1.7 | 91.2 | 0 | |
| 5 | L | L | H | -1 | -1 | 1 | .009 | .009 | 91 | 17.3 | 20 | -2.7 | 65.5 | 64.5 | 1 | 8.8 | 0 | |
| 6 | H | L | H | 1 | -1 | 1 | .091 | .009 | 91 | 51.2 | 41.6 | 9.6 | 81.6 | 83.1 | -1.5 | 42.8 | 0 | |
| 7 | L | H | H | -1 | 1 | 1 | .009 | .091 | 91 | 37.9 | 33.7 | 4.2 | 59.1 | 58.7 | 0.4 | 57.2 | 0 | |
| 8 | H | B | H | 1 | 1 | 1 | .091 | .091 | 91 | 60.7 | 59.3 | 1.4 | 81.1 | 82 | 0.9 | 91.2 | 0 | |
| 9 | VL | M | M | - α | 0 | 0 | 0 | 0 | 0 | 36.7 | 24.9 | 11.8 | 62.6 | 62.7 | -0.1 | 29.4 | 0 | |
| 10 | VH | M | M | α | 0 | 0 | 0.1 | 0.05 | 50 | 41 | 45.6 | -4.6 | 91.6 | 90.2 | 1.4 | 70.6 | 0 | |
| 11 | M | VL | M | 0 | - α | 0 | .05 | 0 | 50 | 45.4 | 43.2 | 2.2 | 78.1 | 80 | -1.9 | 20.6 | 0 | |
| 12 | M | VH | M | 0 | α | 0 | .05 | .05 | 50 | 56.4 | 52 | 4.4 | 84.2 | 81 | 3.2 | 79.4 | 0 | |
| 13 | M | M | VL | 0 | 0 | - α | .05 | .05 | 0 | 66.6 | 61.5 | 5.1 | 77.5 | 79.2 | -1.7 | 50 | 0 | |
| 14 | M | M | VB | 0 | 0 | α | .05 | .05 | 100 | 47.5 | 45.4 | 2.1 | 77.6 | 74.5 | 3.7 | 50 | 0 | |
| 15 | M | M | M | 0 | 0 | 0 | .05 | .05 | 50 | 47.2 | 45.6 | 1.6 | 79.2 | 80.9 | -1.7 | 50 | 0 | |

TABLE 2
**Coefficients of Second Order Equation
and Measure of Fit**

| DESIGNATION | RESPONSES | | | Coefficient FOR |
|--------------------|-----------|-------|-------|--------------------|
| | Y_A | Y_B | Y_C | |
| Coefficient a_0 | 45.54 | 80.94 | 50 | |
| a_1 | 8.485 | 11.3 | 17 | x_1 |
| a_2 | 3.62 | 0.43 | 24.2 | x_2 |
| a_3 | -6.63 | 1.97 | 0 | x_3 |
| a_{11} | -7.01 | 3.06 | 0 | x_1^2 |
| a_{22} | 1.37 | 0.32 | 0 | x_2^2 |
| a_{33} | 5.314 | 2.75 | 0 | x_3^2 |
| a_{12} | 1.038 | 0.39 | 0 | x_1x_2 |
| a_{13} | 3.31 | -1.58 | 0 | x_1x_3 |
| a_{23} | 4.2 | -1.34 | 0 | x_2x_3 |
| Standard Deviation | 6.45 | 1.71 | 0 | |
| Relative Error, % | 14.1 | 2.1 | 0 | |

Figure 1
**Comparison of Solid and Foam insulations
Compounds**

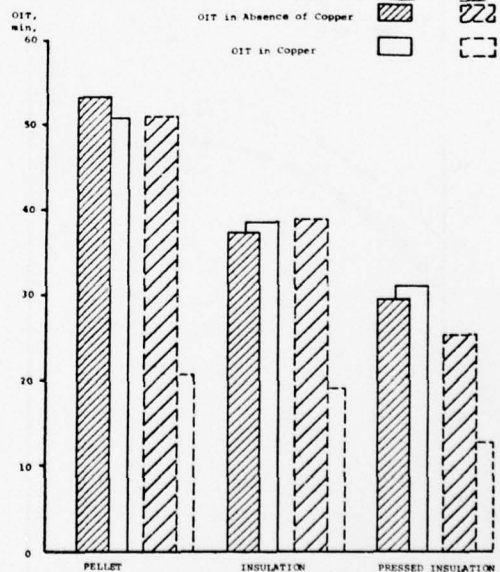


Figure 2
Partial Factorial Grid Design for 3 Variables

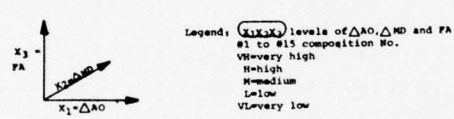
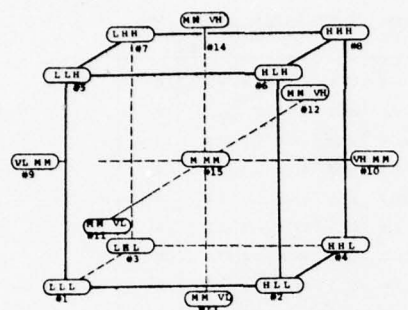


Figure 4
Effect of Antioxidant

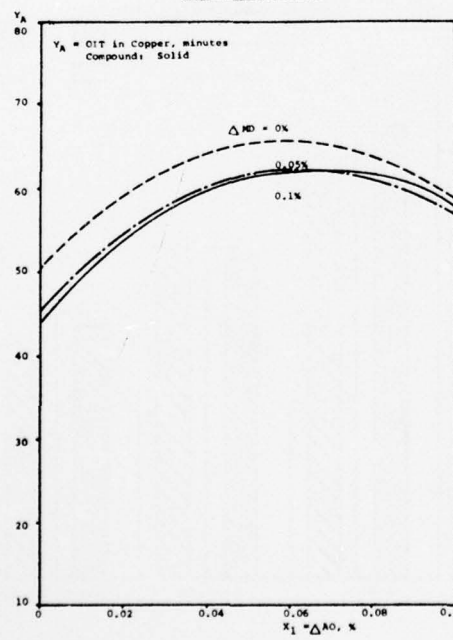


Figure 3
Comparison of "Actual" and "Computed" Values
Display: Y_A , OIT in Copper, minutes

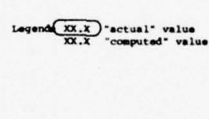
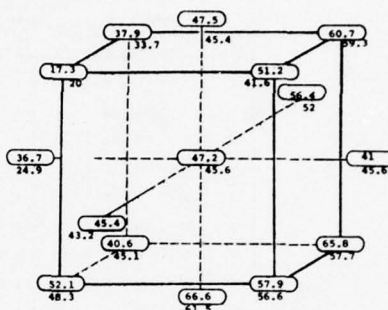
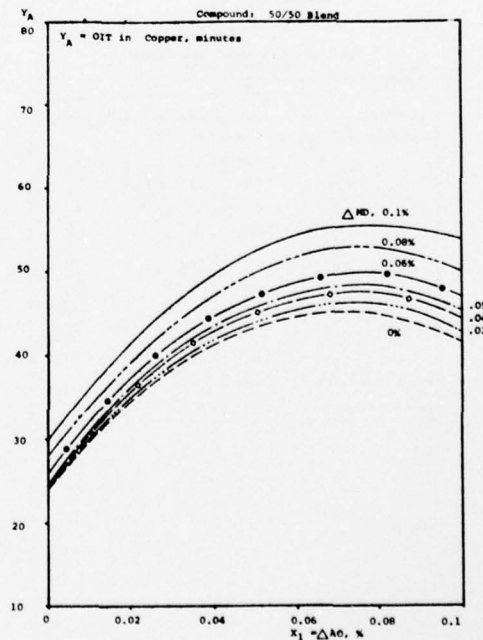
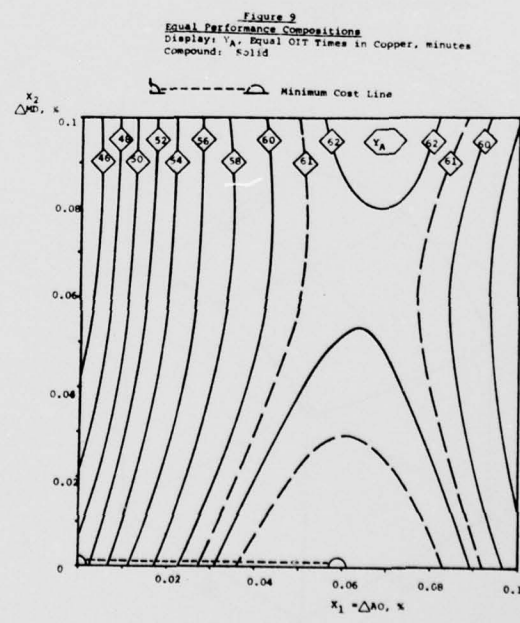
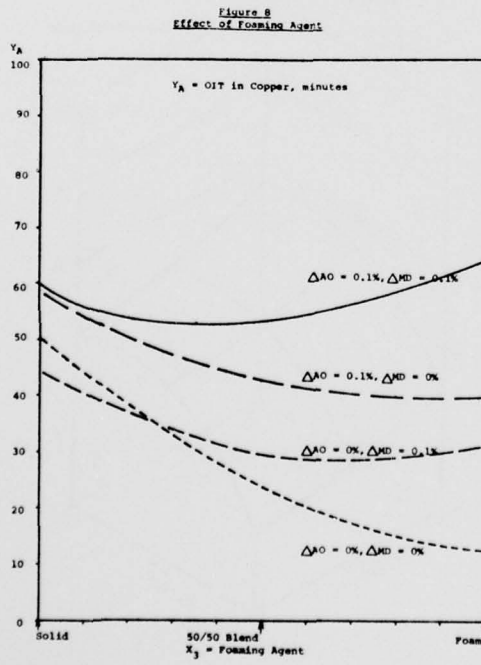
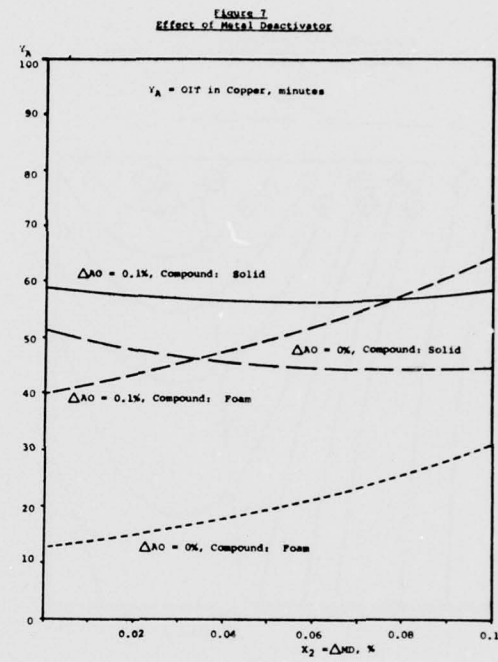
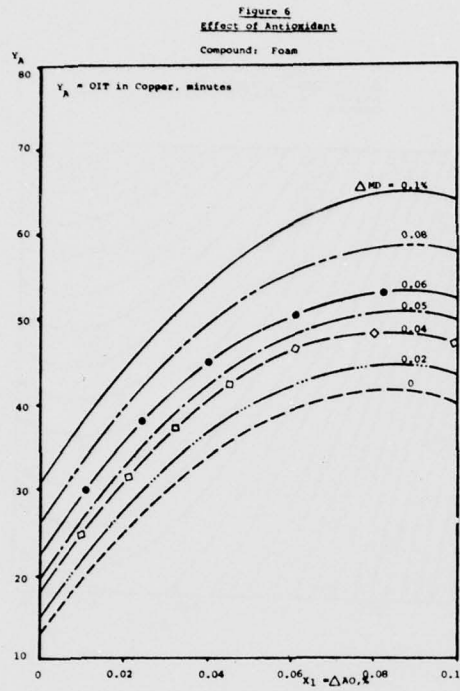
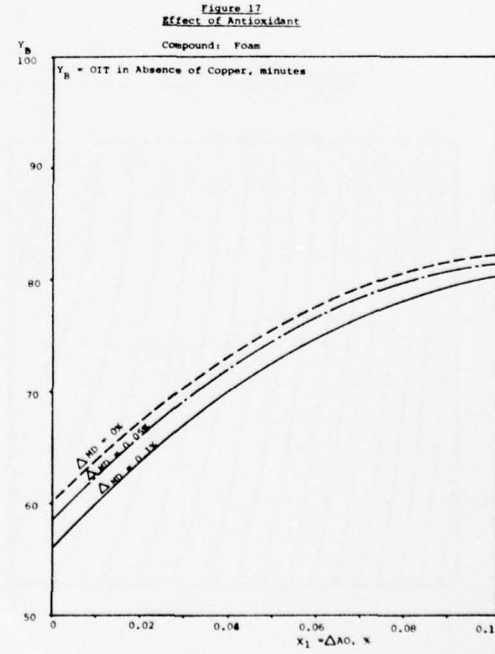
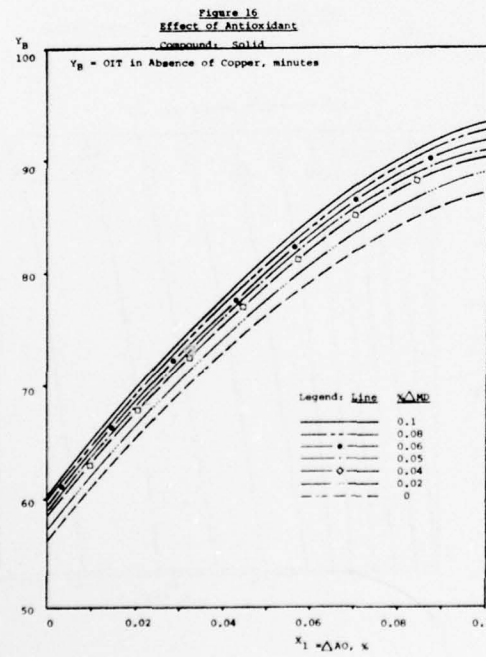
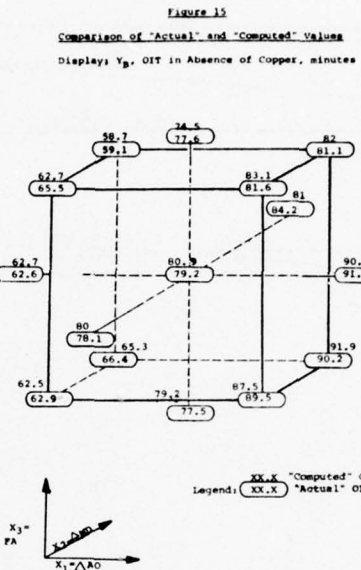
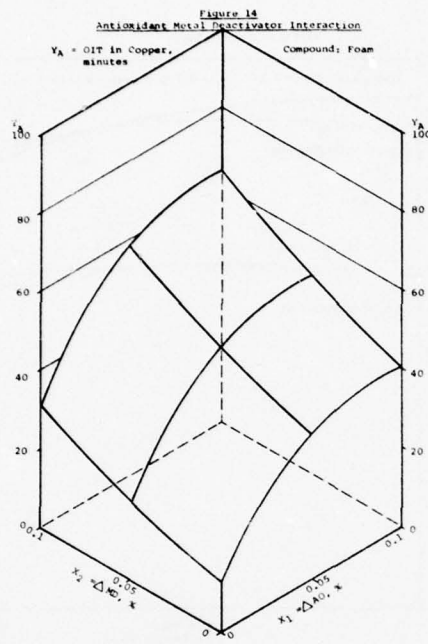
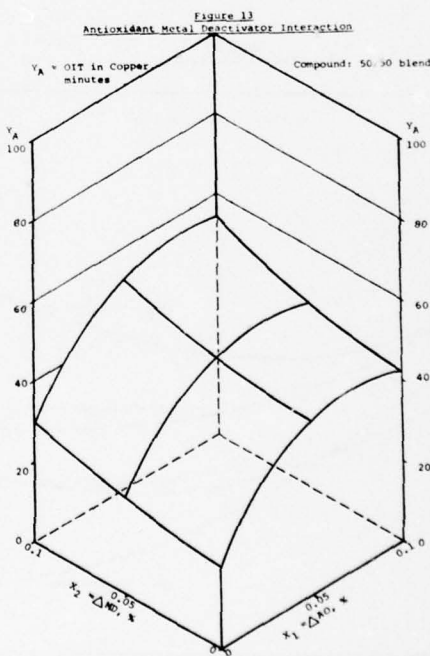
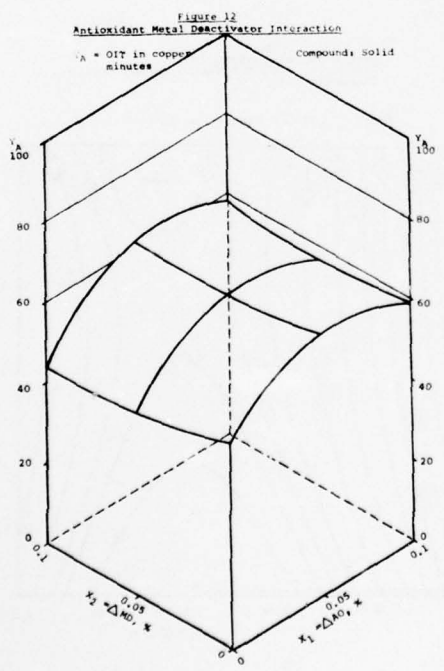
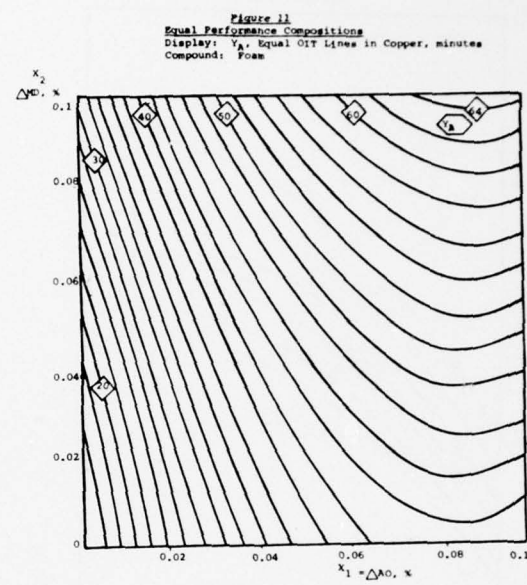
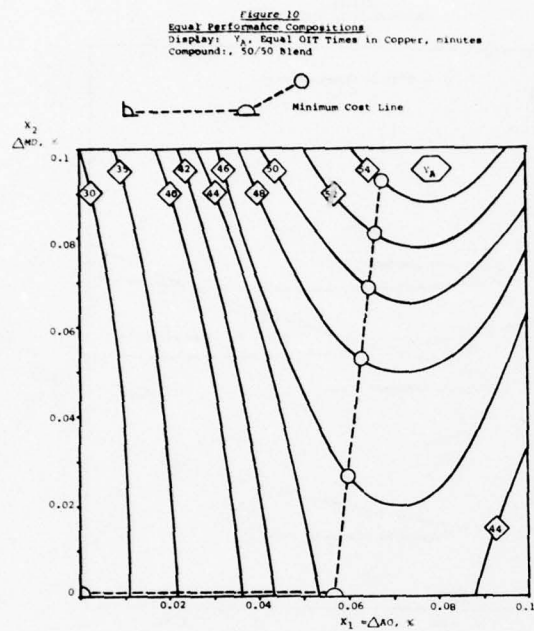


Figure 5
Effect of Antioxidant









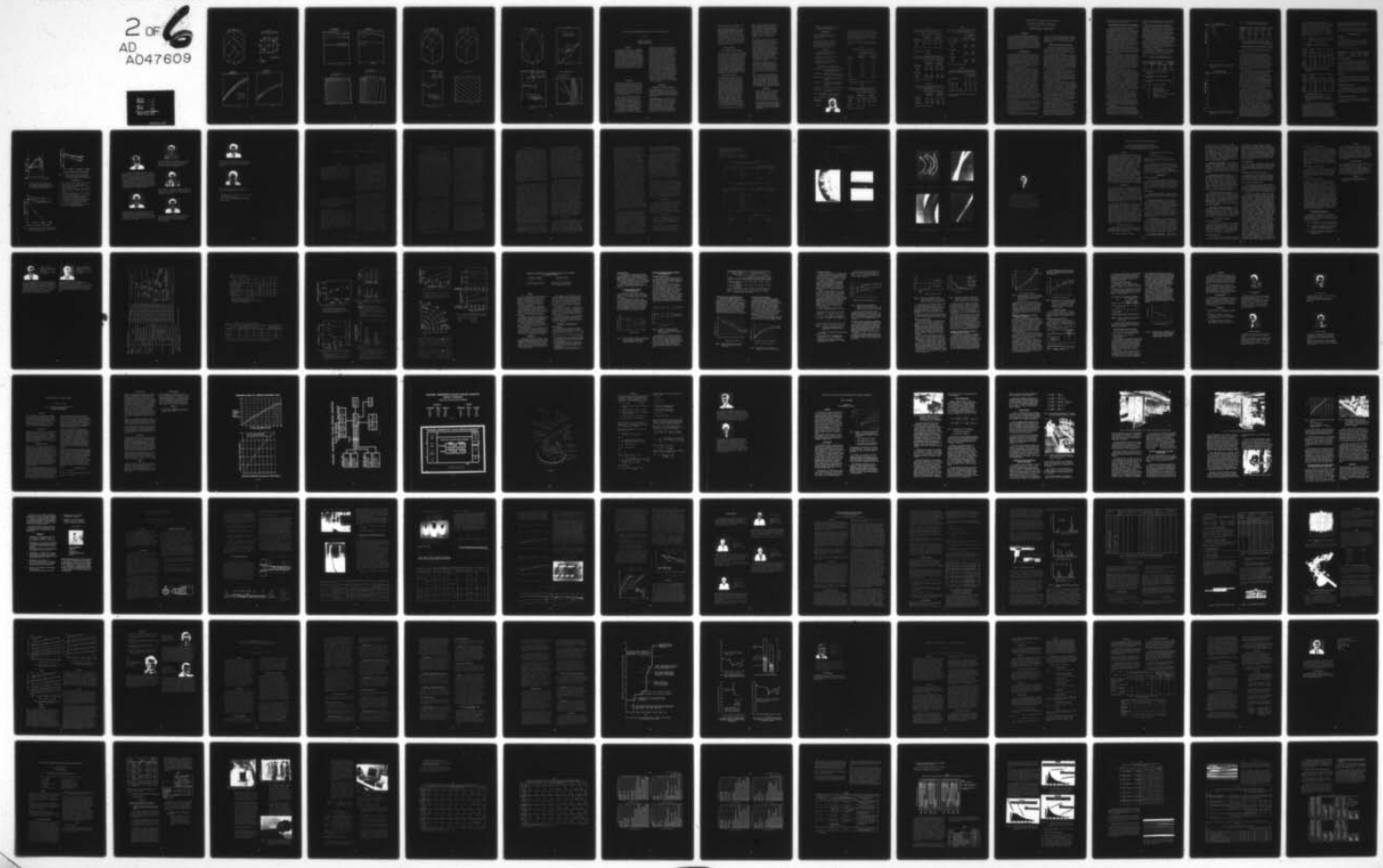
AD-A047 609

ARMY COMMUNICATIONS RESEARCH AND DEVELOPMENT COMMAND --ETC F/G 9/1
PROCEEDINGS OF INTERNATIONAL WIRE AND CABLE SYMPOSIUM (26TH) CH--ETC(U)
NOV 77 E F GODWIN

UNCLASSIFIED

2 of 6
AD A047609

NL



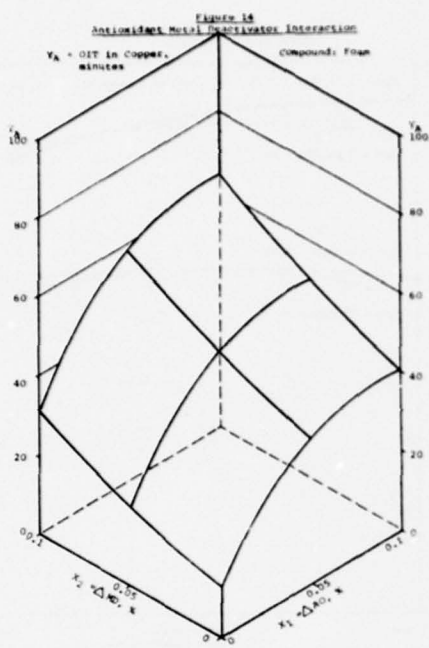


Figure 15
Comparison of "Actual" and "Computed" Values
 $y_B = \text{GIT in Absence of Copper, minutes}$

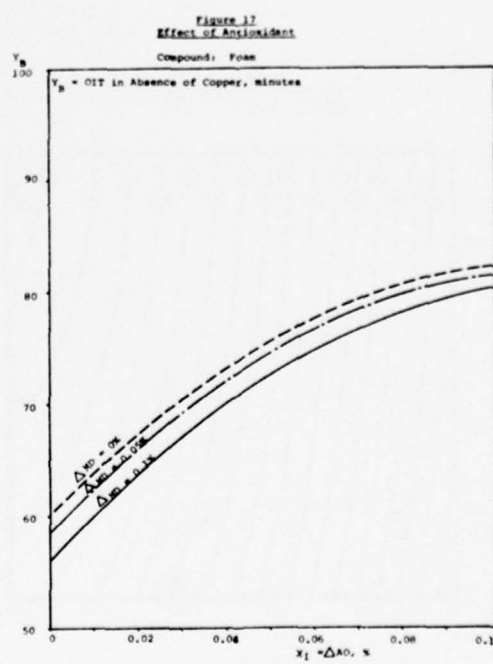
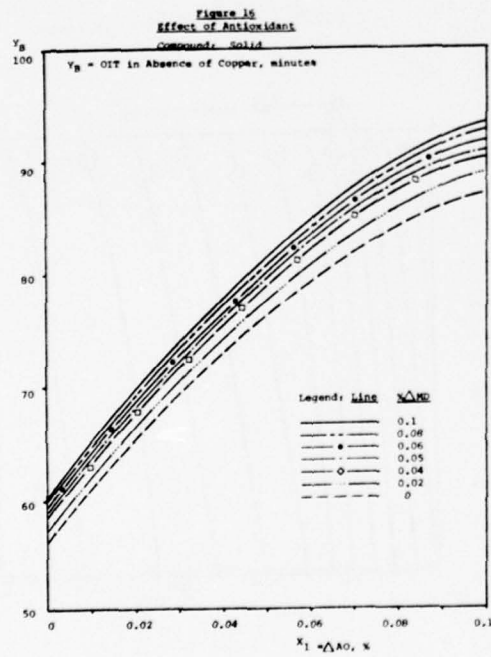
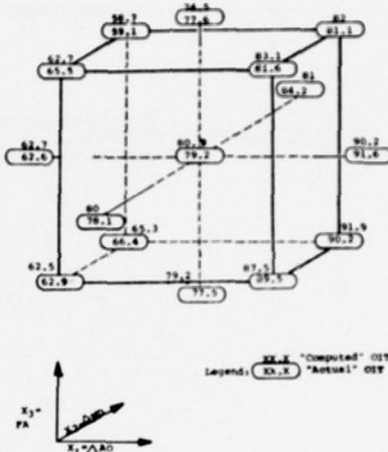


Figure 18
Effect of Metal Deactivators

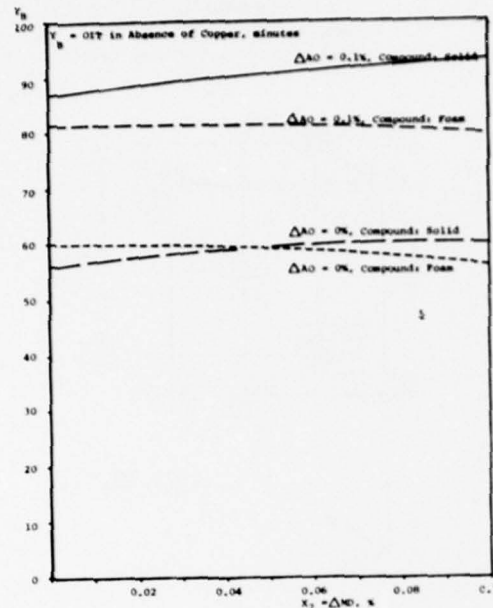


Figure 19
Effect of Foaming Agent

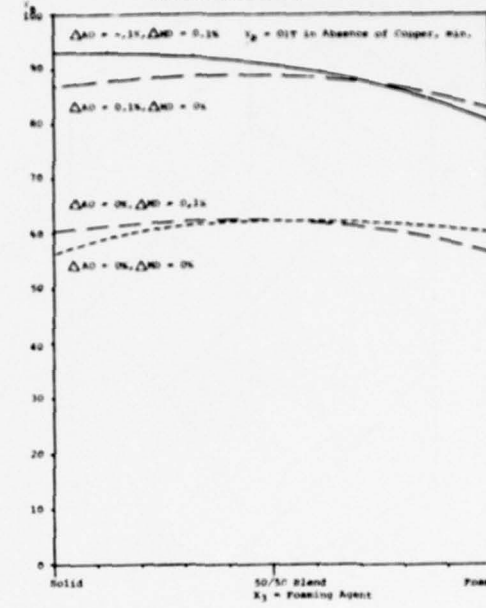


Figure 20
Equal Performance Compositions
Display: Y_0 , equal OIT times in absence of copper, min.
Compound: Solid

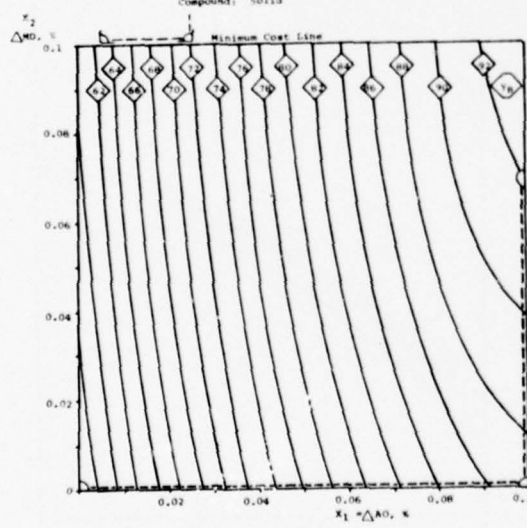
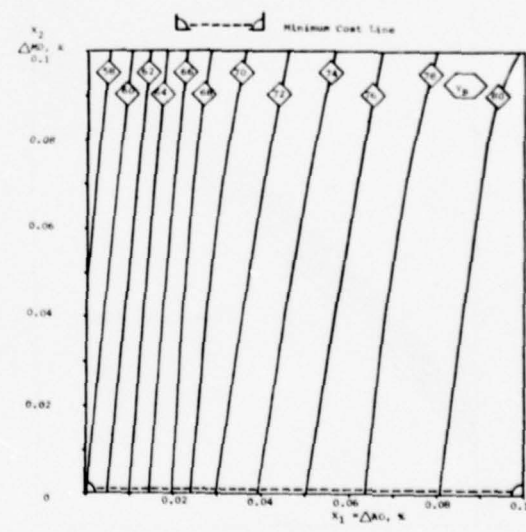


Figure 21
Equal Performance Compositions
Display: Y_0 , OIT in Absence of copper, minutes
Compound: Foam



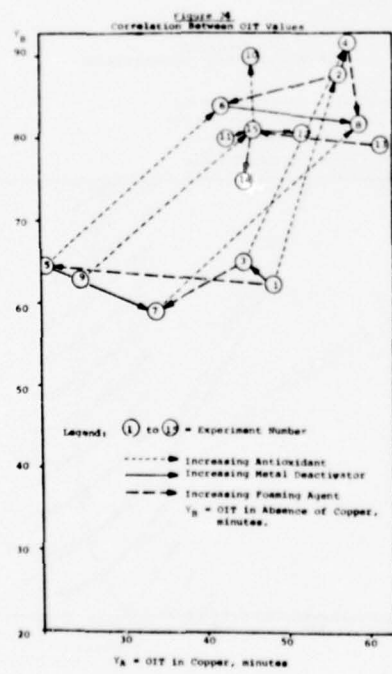
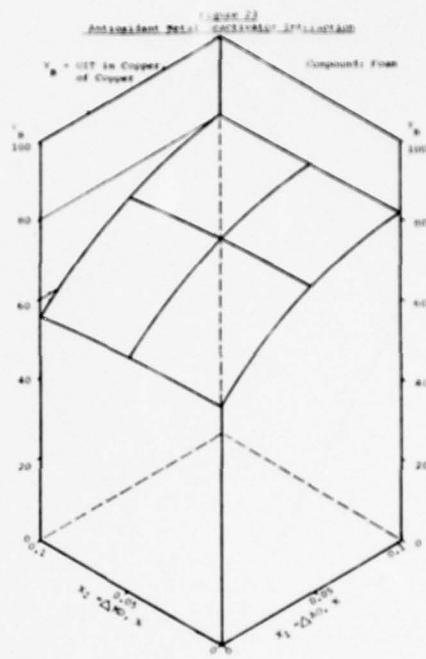
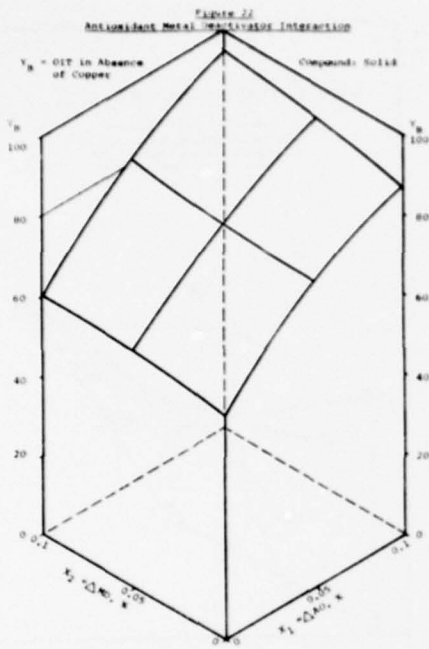
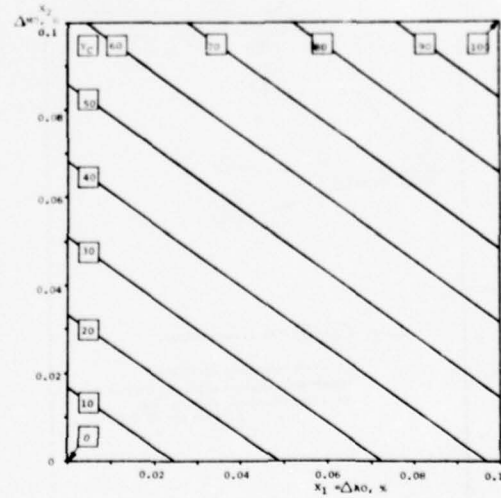
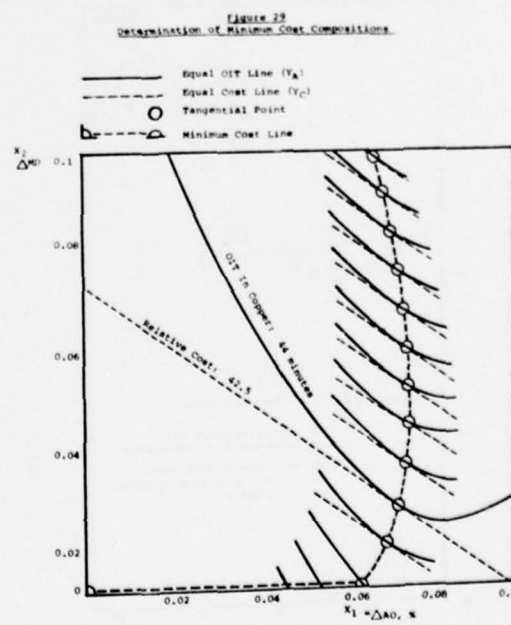
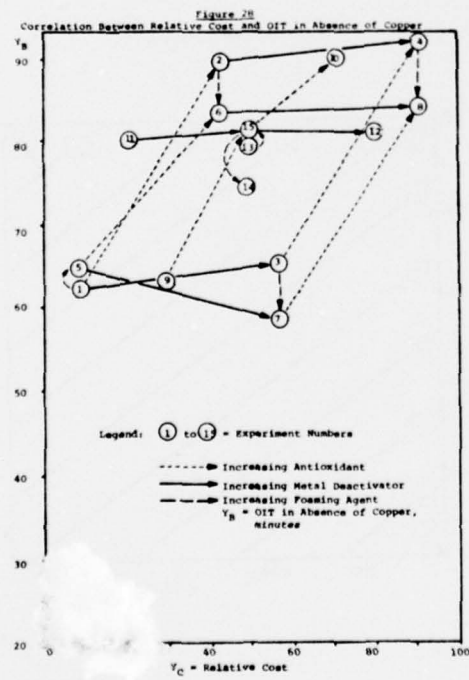
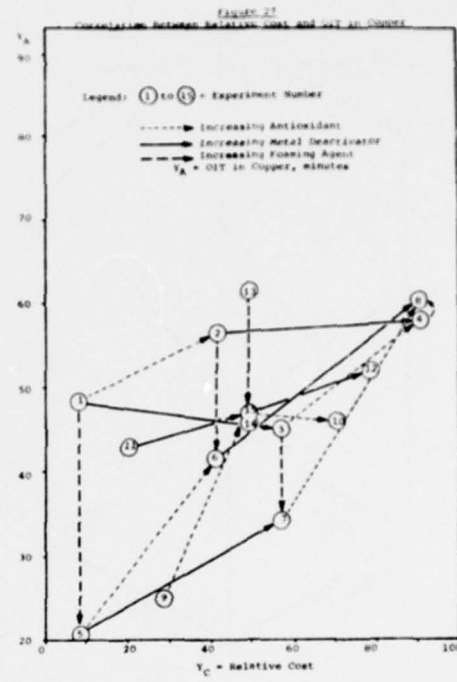
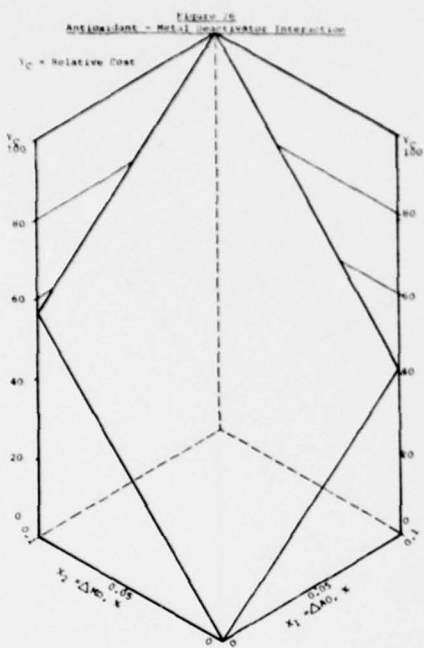


Figure 25
Optimal Performance Contours





A BIFUNCTIONAL ANTIOXIDANT/METAL DEACTIVATOR FOR POLYOLEFIN WIRE INSULATION

A. PATEL

CIBA-GEIGY CORPORATION
Additives Department
Ardsley, New York 10502

ABSTRACT

The outstanding performance of a bifunctional Antioxidant/Metal Deactivator for polyolefin wire insulation is discussed with regard to the performance of the presently used two component stabilizer systems for this application. The data indicate that N,N'-Bis[3-(3', 5'-di-tert-butyl-4'-hydroxyphenyl)-propionyl] hydrazine functions both as an antioxidant and as a metal deactivator. It provides thermal oxidative stability to polypropylene copolymer and high density polyethylene solid and cellular insulation in the presence of copper conductors. The effect of temperature, petrolatum cable filler and processing on the performance of this compound is also discussed.

INTRODUCTION

Polyolefins are extensively used in a wide variety of wire and cable applications where thermo-oxidative degradation can occur. Degradation is manifested as cracking and embrittlement of the wire insulation, thereby exposing the copper conductor. Thermally-induced oxidation and exposure of insulation to petrolatum filler for wire and cable can significantly reduce the useful field life of polyolefin materials.

The most commonly used metal deactivators for either solid or cellular polyolefins wire insulation are N,N'-Bis[3-(3',5'-di-tert-butyl-4'-hydroxyphenyl)-propionyl] hydrazine (MDA-1) and N,N'-Dibenzal Oxalyl-dihydrazide (MDA-2). Presently these metal deactivators are being used in conjunction with antioxidant, Tetrakis[methylene-3-(3',5'-di-tert-butyl-4'-hydroxyphenyl)propionate]methane (AO-1). Previous evaluations in our laboratories indicated that MDA-1 performed both as an antioxidant and as a metal deactivator. Moreover, this compound

appeared to be less sensitive to petrolatum exposure than the present two component stabilizer systems used for stabilization of polyolefin wire insulation. Data published by M. G. Chan and R. A. Powers² (Table 1) also indicated that the formulation containing this bifunctional compound alone exhibited the best oxidative stability performance of copper laminates at 121°C and has retained high stability after petrolatum exposure as compared to several other compounds evaluated. The same published data also indicated that this bifunctional compound, in conjunction with unidentified hydrazine derivative, was the most effective formulation in oxidative stability performance of poly(propylene-ethylene) copolymer wire insulation at 140°C and appeared to be the least sensitive to petrolatum exposure. The above finding can be well supported by our recent results which showed that the use of this bifunctional compound (MDA-1) alone, either in solid or cellular polyolefin wire insulation, offered better oven aging performance than the present two component systems and it appeared to be less sensitive to petrolatum exposure than the two component stabilizer systems.

EXPERIMENTAL

PREPARATION OF INSULATED WIRE SAMPLES

Initial Compounding: The specified stabilizer system plus 1.0% titanium dioxide were dry blended into a minimally stabilized wire grade high density polyethylene and poly(propylene-ethylene) copolymer and extruder compounded at 199°C (390°F).

Solid Insulated Wire: The pellets obtained as above were extruder coated onto 22 AWG copper wire to provide a final insulation thickness of 0.35 mm (14 mil). Extrusions were performed using a 25 mm (1") 24:1 L/D extruder equipped with a constant pitch gradual transition metering screw and a wire coating crosshead. The crosshead temperature $\sim 254^\circ\text{C}$ (490°F) was maintained. The speed of the wire coating line was 39 meters (130') per minute. The copper wire

was preheated using a hot air gun at 260°C (500°F) to assure adequate adhesion.

Cellular HDPE Insulated Wire: The pellets obtained in the initial compounding step were dry blended with 0.5% Celogen AZNP-130 blowing agent and extruder coated onto 22 AWG copper wire using the same extruder as described above. The wire coating cross-head was maintained at 210°C (410°F) and 197 kg/cm² (2800 psi) pressure. The speed of the wire coating line was 27 meters (90') per minute. The copper wire was preheated using a gas flame to assure adequate adhesion. The cellular coating on the wire was 0.35 mm (14 mil) thick.

TESTING PROCEDURES

Petrolatum Exposure and Oven Aging:

"U" shaped lengths of insulated wire samples were quickly dipped (1-2 seconds) into molten petrolatum at 115°C, withdrawn and allowed to cool. The adhering petrolatum represented a weight pick up of about 100% based on the insulation weight. The dipped wire samples were then oven aged at 70°C (158°F) for 10 days, wiped free of petrolatum and formed into pigtailed. The pigtailed were oven aged at 100°C and 120°C for HDPE and 120°C and 140°C for poly(propylene-ethylene) copolymer in forced draft ovens with a minimum airflow and equipped with rotating shelves. The pigtail samples were visually examined periodically for cracking, embrittlement or decomposition. The average failure time of five replicates was recorded.

RESULTS AND DISCUSSIONS

The performance of N,N'-Bis[3-(3'5'-di-tert-butyl-4'-hydroxyphenyl)-propionyl] hydrazine (MDA-1) as a sole stabilizer for solid and cellular polyolefins wire insulation was determined using in-house prepared wire insulation. Oven aging results at 120°C and 100°C of both solid and cellular HDPE wire insulation indicated that this bifunctional compound performed both as an antioxidant and as a metal deactivator (Table 2 and Table 3). Moreover, MDA-1 exhibited better performance to the present two component stabilizer systems, A0-1/MDA-1 and A0-1/MDA-2 and it appeared to be less sensitive to petrolatum exposure than the two component stabilizer systems. These findings confirm the published data² by M. G. Chan and R. A. Powers and indicate that MDA-1 is capable of functioning as a hydrogen donor as well as capable of functioning as a copper deactivator used for polyolefins wire insulation.

The concentration/performance profile for

MDA-1 in cellular HDPE wire insulation at 120°C and 100°C, presented in Table 4, indicates that 0.2% concentration of MDA-1 is a very viable concentration because at this level MDA-1, both before and after petrolatum exposure appears to perform better than the two component stabilizer systems. A lower 0.1% concentration is probably too low a concentration to be useful for this cellular HDPE wire insulation.

The performance of MDA-1 alone and in conjunction³ with A0-1 was also determined in poly(propylene-ethylene) copolymer solid wire insulation. Oven aging results at 120°C and 140°C indicated that a 1:1 blend of MDA-1 with A0-1 at 0.4% total concentration performed better than a 1:1 blend of MDA-2 with A0-1 at the same concentration (Table 5). Here again, 0.4% MDA-1 alone was less sensitive to petrolatum exposure than the present two component stabilizer systems, A0-1/MDA-1 and A0-1/MDA-2. The advantage of MDA-1 is especially evident at the lower oven aging temperatures which are a closer approximation to temperatures encountered in actual use conditions.

Concentration/performance profile for MDA-1 has also been developed in this poly(propylene-ethylene) copolymer wire insulation and it is presented in Table 6. It is interesting to note that substantially improved thermal stability before and after petrolatum exposure can be obtained with higher concentration of MDA-1.

MDA-1 has desirable ancillary properties such as lower melting point than MDA-2 (227 vs. 320°C) and processing stability (Table 7) comparable to the present two component stabilizer system in polypropylene at 260°C (500°F). These ancillary properties make MDA-1 easily processed in polyolefins used in a wide variety of wire and cable applications at processing temperatures of 232°C - 260°C (450° - 500°F).

CONCLUSIONS

1. The use of MDA-1 as a sole stabilizer system at about 0.2% in solid and cellular polyolefin wire insulation offers a viable alternative to the present two component stabilizer systems (A0 + MDA) and it appears to be less sensitive to petrolatum than the two component stabilizer systems.
2. Substantially improved thermal stability of high density polyethylene and poly (propylene-ethylene) copolymer wire insulation can be obtained with high concentration of MDA-1 alone and A0-1/MDA-1 blend.

3. Improved dispersibility and processing properties are advantages for metal deactivator MDA-1 vs. MDA-2.

ACKNOWLEDGMENTS

A special acknowledgment is given to Dr. Peter Klemchuk and Mr. H. Jones for their guidance throughout this investigation.

I would like to express our sincerest thanks to Mr. John Windus and Mr. Patrick Morabito, who performed most of the experimental work and to Mrs. Mary Trojak, whose help in preparing the manuscript was invaluable.

REFERENCES

1. D. D. O'Rell and A. Patel, 24th Int. Wire and Cable Symposium, November 18-20, 1975, p. 231.
2. M. G. Chan, R. A. Powers, 33rd SPE ANTEC, p. 292, May 5-8, 1975.
3. A. DiBattista, J. M. Farber, M. A. Trainor, P. P. Klemchuk, 33rd SPE ANTEC, May 5-8, 1975.

ADDITIVES USED IN THIS PUBLICATION

- Antioxidant-1: Tetrakis [methylene-3(3',5'-di-tert-butyl-4-hydroxyphenyl) propionate] methane.
- Antioxidant-2: Thiodiethylene bis(3,5-di-tert-butyl-4-hydroxy)hydrocinnamate.
- Antioxidant-3: 3:1 Condensate of 3-methyl-6-tert-butylphenol with croton aldehyde.
- Antioxidant-4: 1,3,5-Trimethyl-2,4,6-tris(3,5-di-tert-butyl-4-hydroxyphenyl) benzene.
- Antioxidant-5: Di-β-naphthyl-p-phenylenediamine.
- Antioxidant-6: 4,4'-Thiobis(3-methyl-6-tert-butylphenol).
- MDA-1: N,N'-Bis[3-(3',5'-di-tert-butyl-4'-hydroxyphenyl)propionyl]hydrazine.
- MDA-2: N,N'Dibenzal oxalylidihydrazide.

BIBLIOGRAPHY

A. Patel



Mr. A. Patel received his B.S. degree in Dyes and Intermediates Technology from the University of Bombay (India) in 1965 and his M.S. in Polymer Science from the University of Akron in 1969. He is now a research and development chemist, working on polymer stabilization in the Additives Department, Plastics and Additives Division of C.I.T.A.-GEIQUY CORPORATION.

Mr. Patel is a member of the American Chemical Society and the Society of Plastics Engineers, Inc.

Table 1

OXIDATIVE STABILITIES OF LAMINATES

| Additive* | Average Extrapolated Induction Times (Hours) at 121°C | |
|-----------|---|---------------------|
| | No Petrolatum Exposure | Petrolatum Exposure |
| Alone | <1 | <2 |
| A0-1 | 572±45 | 28±2 |
| A0-2 | 359±35 | 25±0 |
| A0-3 | 252±11 | 27±12 |
| A0-4 | 162±3 | 22±3 |
| A0-5 | 106±30 | 13±2 |
| A0-6 | 360±2 | 116±2 |
| MDA-1 | 1495±16 | 1019±14 |

*0.5 Weight Percent

2 - M. G. Chan, R. A. Powers, 33rd SPE ANTEC, p. 292, May 5-8, 1975.

Table 2

Effectiveness of Antioxidant/Metal Deactivator in 22 AWG HDPE Insulated Wire at 120°C

| 0.1% A0-1 + 0.1% MDA | Hours to Cracking* of Insulation | | | |
|----------------------|----------------------------------|----------|---------------------|----------|
| | No Petrolatum Exposure | | Petrolatum Exposure | |
| | Solid | Cellular | Solid | Cellular |
| MDA-1 | 3,300 | 1,900 | 2,800 | 1,500 |
| MDA-2 | 3,200 | 2,000 | 1,900 | 1,000 |

| 0.2% MDA-1 Only | Hours to Cracking* of Insulation | | | |
|-----------------|----------------------------------|----------|-------|----------|
| | Solid | Cellular | Solid | Cellular |
| MDA-1 | 3,800 | 2,900 | 3,400 | 1,700 |
| MDA-2 | | | | |

*Averages of five replicates

Table 3

Effectiveness of Antioxidant/Metal Deactivator in 22 AWG HDPE Insulated Wire at 100°C

| 0.1% AO-1 + 0.1% MDA-1 | Hours to Cracking* of Insulation | | | |
|---------------------------|----------------------------------|----------|------------------------|----------|
| | No Petrolatum Exposure | | Petrolatum Exposure | |
| | Solid | Cellular | Solid | Cellular |
| MDA-1 | 11,300 | 9,300 | 9,100 | 4,600 |
| MDA-2 | 10,800 | 7,600 | 6,700 | 3,400 |
| 0.2% MDA-1 Only | 12,700 | 10,300 | 9,500 | 4,900 |

*Averages of five replicates

Table 4

Effect of Concentration of MDA-1 on Thermal Stability of 22 AWG HDPE Cellular Insulated Wire

| 0.1% AO-1 + 0.1% MDA | Hours to Cracking* of Insulation | | | |
|-------------------------|----------------------------------|--------|------------------------|-------|
| | No Petrolatum Exposure | | Petrolatum Exposure | |
| | 120°C | 100°C | 120°C | 100°C |
| MDA-1 | 1,900 | 9,300 | 1,500 | 4,600 |
| MDA-2 | 2,000 | 7,600 | 1,000 | 3,400 |
| MDA-1 Only | | | | |
| 0.10% | 1,400 | 5,500 | 700 | 2,700 |
| 0.20% | 2,900 | 10,300 | 1,700 | 4,900 |
| 0.30% | 3,600 | 13,000 | 2,400 | 5,900 |

*Averages of five replicates

Table 5

Effectiveness of Antioxidant/Metal Deactivators in 22 AWG Poly(propylene-ethylene) Solid Insulated Wire

| 0.2% AO-1 + 0.2% MDA | Hours to Cracking* of Insulation | | | |
|-------------------------|----------------------------------|-------|------------------------|-------|
| | No Petrolatum Exposure | | Petrolatum Exposure | |
| | 120°C | 140°C | 120°C | 140°C |
| MDA-1 | 5,100 | 1,300 | 4,200 | 850 |
| MDA-2 | 3,700 | 1,070 | 2,700 | 750 |
| 0.4% MDA-1 Only | 5,200 | 740 | 5,000 | 650 |

*Averages of five replicates

Table 6

Effect of Concentration of Antioxidant/Metal Deactivator in 22 AWG Poly(propylene-ethylene) Solid Insulated Wire at 120°C

| Total Concentration of 1:1 Blend | Hours to Cracking* of Insulation | |
|-------------------------------------|-------------------------------------|------------------------|
| | No Petrolatum Exposure | Petrolatum Exposure |
| AO-1 + MDA-1 | | |
| 0.2% | 3,300 | 2,200 |
| 0.4% | 5,100 | 4,200 |
| 1.0% | 8,200 | 6,800 |
| AO-1 + MDA-2 | | |
| 0.2% | 2,800 | 1,850 |
| 0.4% | 3,700 | 2,700 |
| 1.0% | 6,400 | 5,100 |
| MDA-1 Only | | |
| 0.2% | 3,100 | 2,700 |
| 0.4% | 5,200 | 5,000 |
| 1.0% | 9,000 | 9,200 |

*Averages of five replicates

Table 7

Processing Stability of Antioxidant/Metal Deactivator in Polypropylene at 260°C (500°F)

| Additive | Melt Flow Rates* After Extrusions | | |
|------------------------|--------------------------------------|------|------|
| | 1 | 3 | 5 |
| None | 0.75 | 1.78 | 3.25 |
| 0.2% MDA-1 Only | 0.38 | 0.63 | 0.98 |
| 0.2% MDA-2 Only | 0.61 | 1.95 | 3.46 |
| 0.2% AO-1 Only | 0.36 | 0.62 | 1.02 |
| 0.1% AO-1 + 0.1% MDA-1 | 0.32 | 0.59 | 0.85 |
| 0.1% AO-1 + 0.1% MDA-2 | 0.41 | 0.85 | 1.66 |

*ASTM Designation D1238-65T, Condition L for Polypropylene

NEW COPPER DEACTIVATORS FOR POLYOLEFINS

BY

K. Yamaguchi, T. Yoshikawa, N. Sakamoto,
S. Ohtomo, K. Kanda, S. Oh-e and T. Imaoka.

Ube Industries, Ltd., 7-2, Kasumigaseki
3-chome, Chiyoda-ku, Tokyo, Japan

SUMMARY

It is shown by the statistical analysis on the structure-performance relationship that high melting point, high molecular weight, low solubility and low reactivity to free radicals are the desirable properties for the copper-deactivators for polypropylene in contact with metallic copper. Of a large number of compounds synthesized, four compounds are selected for detailed studies of practical properties relative to copper-deactivators for polyolefin insulation of PIC cables.

INTRODUCTION

The basic action of the copper-deactivator is supposed to lie in lowering redox potential of cupric ion by capturing it into a chelate compound. The copper diminishes thereby its catalytic action upon peroxides, which on decomposition lead to an accelerated auto-oxidation of polyolefins. There are many papers on this subject, but the newest one may be that of Allara et al¹, who studied the catalytic activities of the reaction products obtained from various cupric salts and oxamides.

The second factor that determines the performance of copper-deactivator would be its diffusion property. Chan et al² proved that copper-deactivator added to polyethylene diffuses into the polyethylene-copper interface and deactivates the surface of copper. However, for the long-term stability of insulations, the copper-deactivator should not be lost too rapidly by diffusion. Hansen et al³ and Ohswa et al⁴ proved that the low reactivity of N, N'-diphenyloxamide is due to its high diffusivity.

The third factor is the solubility of copper-deactivator in polymer. It remains to be solved whether or not the high solubility of copper-deactivator is desirable for the long-term stability of insulations. Howard et al⁵ claim that the copper-deactivators which are either completely insoluble or extensively soluble in the polymer are preferable to the compounds with intermediate solubilities.

It can be seen from the present series of experiments that the long-term effect of copper deactivator is not only dependent on the chemical reactivity but also on the physical behavior of molecule in the polymer matrix.

As the continuation of our previous publication⁶, the present study has been made to find copper deactivators with long-term effect for polyolefins occurring in contact with metallic copper.

In the present study, the copper mesh laminate and insulated conductor were used for aging tests so as to obtain more relevant data in relation to their practical performances.

Consideration on the structure-performance relationship for many compounds tested allowed us

to derive the multiple regression equations which can be used for interpreting the behavior of copper-deactivators. They would be helpful in molecular design or prediction of the effect of new copper deactivators.

MULTIPLE REGRESSION ANALYSIS

The first step of multiple regression analysis is to set up the independent variables and the dependent variable. The former consist of two elements: the chemical reactivity indices and the physical parameters of molecule.

In the present study, the orbital data such as electron density, densities of frontier electrons that may participate in radical reactions⁷, and super-delocalizability⁸ at the central atoms of functional groups were referred to as the chemical reactivity indices and were calculated by means of the simple Hückel Molecular Orbital method. As the physical parameters of molecule, molecular weight, length of molecule, solution parameter and molar volume were employed. The melting point was also referred to as an important parameter.

The dependent variable, on the other hand, was represented in this study by the molar efficiency Em (days/m.mole/kg polypropylene) which is a measure of activity of copper-deactivator. Em was calculated from the aging life determined at 150°C with the samples of copper mesh-laminate of polypropylene containing 3,000 ppm copper deactivator and 1,000 ppm Irganox 1010.

The statistical study has been made with eighty six compounds. The multiple regression analysis was applied in two ways. First of all, 86 compounds were all subjected to the analysis. This is designated as Analysis I. In the next place, 37 compounds were picked out of whole samples by a certain criterion to subject them to the similar analysis, which we designate as Analysis II. The compounds employed in Analysis II are characterized by the substituents which, possessing unsaturations, can form conjugated system with their functional group. Diarylhazirines are typical examples. The molecules of this type are assumed to be more rigid than those having saturated alkyl substituents.

In order that the number of independent variables in regression equation might be minimized, while the multiple regression coefficient (*r*) might be greatest, the calculation was carried out by the "stepwise variable in-out" method. In performing calculation, the squared values of independent variables and the product of molecular weight and melting point were also used in addition to the individual independent variables. To know the effect of melting point, the results obtained with data of

melting point were compared with those calculated without reckoning the melting point.

STRUCTURE-PERFORMANCE RELATIONSHIP

The results of computations made by the multiple regression analysis are given in Table I. The multiple regression coefficients (*r*) lie between 0.778 and 0.891. It can be seen that satisfactorily large values of *r* are obtained in either Analysis I or Analysis II. On the whole, however, the latter yields larger coefficients than the former. In both analyses, the coefficients computed with a set of variables including melting point are larger than those calculated with another set of variables only lacking melting point. Speaking in general, the activity of copper-deactivator can be predicted with a higher precision when the samples are confined to the conjugated compounds as in the case of Analysis II, compared with the analysis made with samples consisting of various species of compounds like in Analysis I. The use of melting point as an independent variable enhances the accuracy of prediction in either case.

The result of Analysis I indicates that none of chemical reactivity indices employed accounts for the activities of deactivators. On the contrary, the effects of the physical parameters are clearly significant. Eq. (1) indicates that a high molecular weight is favorable to the copper-deactivator. We may find explanation of this effect in a small diffusion constant due to a large molecular weight. The smaller is the diffusion of deactivator, the longer it stays in polymer matrix maintaining its activity. Consequently, *Em* increases.

It is indicated in the equations that a high melting point is advantageous. This also may be justifiable. When the melt of polypropylene containing a deactivator whose melting point is higher than that of polypropylene is allowed to cool, the deactivator crystallizes prior to polypropylene accelerating its crystallization. As a consequence, the crystallites of deactivator are strongly fixed between the crystalline domains of polypropylene. On the contrary, the deactivator having a low melting point crystallizes after crystallization of polypropylene. As the result, the crystallites of deactivator are concentrated in the amorphous domains of polypropylene where the molecules are readily movable and can migrate out of polymer matrix.

It is reasonable that a small molar volume prefers to a larger molar volume. The compact molecules can be more firmly fixed in a matrix than the bulky molecules. In this meaning, the aromatic groups are better than the alkyl groups with a large number of carbon atoms.

Eq. (2) derived without making use of the data of melting point indicates that *Em* decreases in proportion to the squared value of molecular length. In this respect also, the lengthy alkyl groups are disadvantageous.

Analysis II also shows that high molecular weight and high melting point are profitable to the deactivator. Of interest is the effect of solution parameter which shows in Eq. (3) a positive-signed correlation with *Em*. Since the solution parameters of compounds used are larger than that of polypro-

pylene, Eq. (3) implies that the decrease in solubility is favorable for long life time of copper deactivator.

The second point of interest in Analysis II consists in that the molecular orbital data which were of no use in Analysis I have a considerable significance. The frontier electron density and the superdelocalizability, which are the indices for radical reactions should be as small as possible. It is natural that the effects of orbital data could be observed only in Analysis II, since the simple Hückel Molecular Orbital method employed in this study was originally set up for conjugated molecules.

Figs. 1 and 2 depict the plots of Eqs. (1) and (3), respectively. The present analysis showing quantitatively that high molecular weight, high melting point, low solubility and low reactivity to free radicals are favorable to copper-deactivators would be a guideline for the search of other new copper deactivators for polyolefins.

Through the screening tests and from other points of view, four compounds, i.e., compounds 5, 11, 15 and 16 were sorted out for further evaluations which will be stated in the next section.

Table 1. Multiple Regression Analysis on Copper-Deactivating Efficiency (*Em*).

| Analysis | Number of Compounds | Use of m.p. Data | <i>r</i> | Regression Equation |
|----------|---------------------|------------------|----------|---------------------|
| I | 86 | yes | 0.859 | (1) |
| I | 86 | no | 0.778 | (2) |
| II | 37 | yes | 0.891 | (3) |
| II | 37 | no | 0.834 | (4) |

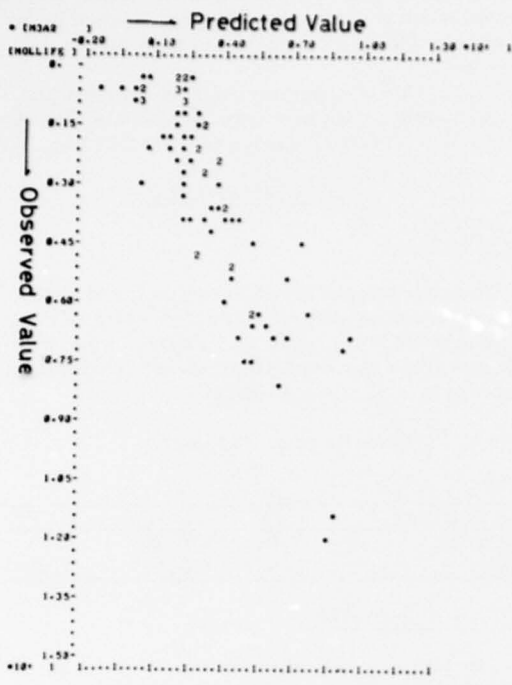
$$Em = 6.71 + 0.000279(mw)(mp) - 0.0649(mp) - 0.0268(mv) \quad (1)$$

$$Em = -6.69 + 0.0592(mw) - 0.00493(length)^2 - 0.0214(mv) \quad (2)$$

$$Em = 11.57 + 0.0361(mw) + 0.0169(mp) + 0.0258(sp) - 11.08f^R \quad (3)$$

$$Em = 17.35 + 0.216(mw) - 185.1f^R - 80.4Sr \quad (4)$$

where mw = molecular weight
 mp = melting point (°C)
 mv = molar volume (cm³/mole)
 sp = solution parameter
 f^R = frontier electron density for radical reaction.
 Sr = superdelocalizability



The synergistic effect in the presence of Irganox 1010 is very remarkable for them, particularly for Compounds 5, 11 and 15, when the CDA/AO ratios are 2,000/2,000 and 3,000/1,000, as can be seen in Fig. 3. On the other hand, the cooperative action is less significant for the conventional copper-deactivators. Since antioxidants are present in all cases in addition to copper-deactivators, the synergistic effect as observed is of practical importance.

Table 3. Effects of Various Copper-Deactivators on Aging Lives (days) of Polyolefins Being in Contact with Metallic Copper.

- a) Polypropylene with Copper Deactivator 2,000 ppm and Irganox 1010 2,000 ppm

| Sample Form | Copper Mesh Laminate | | Cable A *** | | Cable B *** | |
|-------------|----------------------|-----|-------------|-----|-------------|-----|
| | 150 | 130 | 150 | 130 | 150 | 130 |
| 5 | 52 | 297 | 19 | 108 | 20 | 111 |
| 11 | 58 | 252 | 31 | 115 | 26 | 120 |
| 15 | 55 | 265 | 28 | 106 | 23 | 96 |
| 16 | 36 | 308 | 20 | 89 | 19 | 88 |
| MDA-1* | 35 | 201 | 20 | 99 | 20 | 100 |
| MDA-2** | 31 | 200 | 20 | 75 | 13 | 80 |
| Blank | 3 | 38 | 9 | 26 | 5 | - |

- b) High Density Polyethylene with Copper Deactivator 1,000 ppm and Irganox 1010 1,000 ppm

| Sample Form | Copper Mesh Laminate | | Cable A | | Cable B | |
|-------------|----------------------|------|---------|-----|---------|-----|
| | 130 | 100 | 130 | 110 | 130 | 110 |
| 5 | 79 | 500+ | 5 | 81 | 6 | 80 |
| 11 | 22 | 500+ | 8 | 51 | 8 | 42 |
| 15 | 50 | 500+ | 5 | 81 | 8 | 85 |
| 16 | 85 | 500+ | 24 | 133 | 8 | 133 |
| MDA-1 | 63 | 500+ | 9 | 57 | 8 | 92 |
| MDA-2 | 53 | 500+ | 11 | 61 | 11 | 68 |
| Blank | 5 | 56 | 3 | 16 | 3 | 5 |

* Oxalobis (benzalhydrazid)

** N, N'-Bis [3-(3,5-di-tert-butyl-4-hydroxy-phenyl)-propionyl] hydrazine.

*** Cables (26AWG) were molded at a speed of 800 mm/min. (Cable A) and at 1,000 m/min. (Cable B).

In Fig. 4 the effectiveness of copper-deactivator is expressed in terms of the induction period of oxygen absorption of polymer measured at 160°C. The samples employed are the low density polyethylene films which were preliminarily heated at 100°C for various lengths of time while being sandwiched in between two copper plates. The abscissa indicates the time of pre-aging and the ordinate gives the induction period. It can be seen in the figure that the polymer pre-aged for 150 days at 100°C being

kept in contact with copper remains completely unaffected when it contains Compound 5 or 15 by an amount of 1,000 ppm. MDA-2 is also similarly effective.

The result of experiments performed in the similar manner with pre-aged samples of low density polyethylene insulated cables is shown in Fig. 5.

EXPERIMENTALS

Base Polymers

The characteristics of base polymers used for the preparation of samples are given in Table 4. The sample of polypropylene employed was an ethylene-propylene copolymer whose composition is polypropylene 93 : polyethylene 7.

Table 4. Polyolefin Base Polymers.

| Base Polymer | PP | HDPE | LDPE |
|--------------|-------|-------|-------|
| Melt Index | 3.00 | 0.30 | 0.25 |
| Density | 0.920 | 0.947 | 0.926 |

Laminate Preparation

The blending of additives into the polyolefins was done by a Bravender Plastograph which was driven at 60 rpm at 190°C. The copper mesh-laminates of polyolefins were prepared in the following manner. The copper mesh, 60 per inch, was sandwiched in between two polyolefin films and subjected to a heat press to form a laminate of 1 mm thickness. The temperature of press was 190°C.

Aging Test

The aging tests were carried out with strips of the laminates 7 cm long and 1 cm wide. To obtain the aging lives of insulated conductors, the thermal stress cracking tests were conducted using their pigtail specimens.

Biological Degradation Test

The degradation of the compounds by the action of activated sludge was tested at the Chemical Inspection and Testing Institute according to the method described in the regulation of the Government.

Multiple Regression Analysis

Data input and output were done through Dentus Mark III terminal device connected to the Statsyst Analysis System.

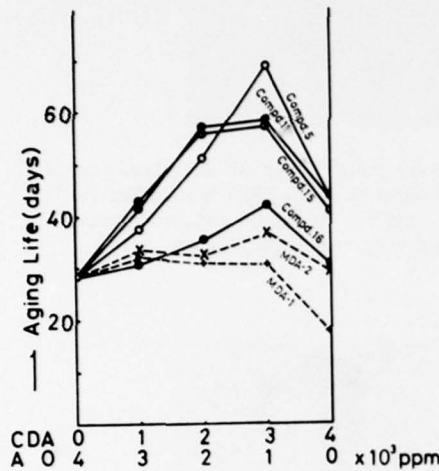


Fig. 3. Aging Life at 150°C of Copper Mesh-Polypropylene Laminate Stabilized by Irganox 1010-Copper Deactivator System in a Combined Amount of 4,000 ppm.

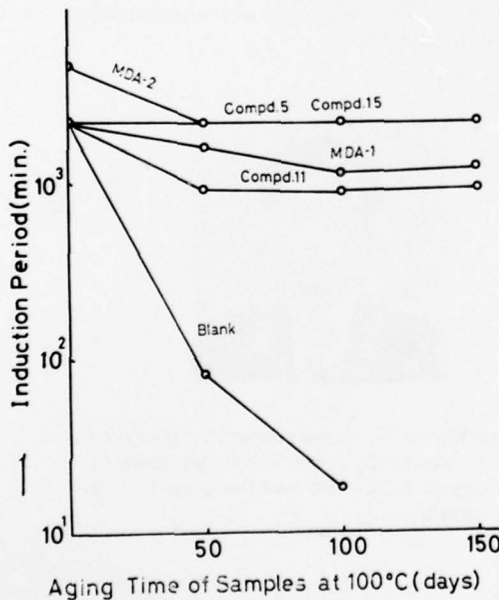


Fig. 4. Change of Induction Period of Oxygen Uptake (160°C) by the Pre-aged Low Density Polyethylene Film (1.0 mm).

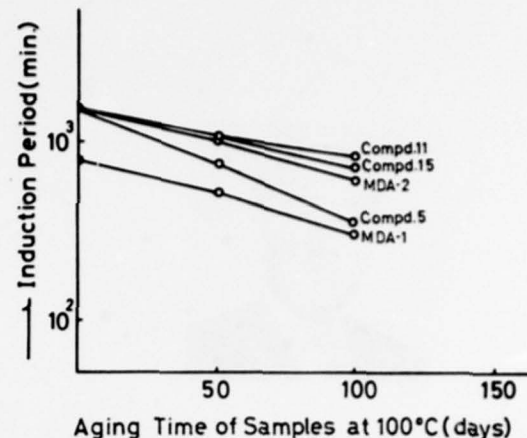


Fig. 5. Change of Induction Period of Oxygen Uptake (160°C) by the Pre-aged Low Density Polyethylene Insulated Conductor.

REFERENCES

- 1) D.L. Allara and M.G. Chan, *J. Polymer Sci. Polymer Chem. Ed.* **14**, 1857 (1976).
- 2) M.G. Chan and D.L. Allara, *Polymer Eng. and Sci.*, **14**, 12 (1974)
- 3) R.H. Hansen, C.A. Russel, T. DeBenedictis, and W.M. Martin, *J. Polymer Sci. A2*, 587 (1964)
- 4) Z. Ohsawa, and K. Matsuzaki, *Kogyo Kagaku Zasshi*, **70**, 2364 (1967)
- 5) J.B. Howard, *Proceedings 21st International Wire and Cable Symposium*, 329 (1972)
- 6) K. Yamaguchi, T. Yoshikawa, H. Kishi, M. Masaki, and N. Sakamoto, *ibid* 97 (1974)
- 7) K. Fukui, T. Yonezawa, and H. Shingu, *J. Chem. Phys.*, **20**, 722 (1952)
- 8) K. Fukui, T. Yonezawa, and C. Nagata, *Bull. Chem. Soc. Japan*, **27**, 423 (1954)



Koji Yamaguchi* received B. S. degree in fuel engineering from Kyoto University in 1949. He joined Ube Industries, Ltd. in the same year and worked for 10 years at the Central Research Laboratory and three years at the Products Development Dept. In 1963 he joined the construction of Ube's first high pressure polyethylene plant in Chiba as the assistant manager in technical department. Since then, he has been the manager of technical department of polyethylene and polypropylene. He is presently the general manager of Ube's Petrochemical Factory in Chiba.



Nagayoshi Sakamoto**, senior chemist, received B. S. in 1965 and M. S. in 1967 from Hiroshima University. He has been engaged in organic synthesis and polymer stabilization.



Susumu Ohtomo* received B. S. degree in industrial chemistry from Yamaguchi University in 1970. He is presently a staff engineer of technical department, petrochemical division.



Toshio Yoshikawa**, senior researcher, received B. S. degree in 1956 in applied chemistry from Nagoya University. He has been engaged in organic synthesis and polymer stabilization. In 1977, he received Ph. D. from Nagoya University for his study on stabilizers of polymers.



Kazusato Kanda**, research staff, received B. S. degree in chemistry from Tokyo Institute of Technology in 1973. He has been working in organic synthesis.



Shunji Oh-e**, research staff, received B.S. in chemistry from Osaka University in 1974. He has been engaged in stabilization of polyolefins and rubbers.



Koji Imaoka**, research staff, graduated from Izumo Technical High School in 1975.

* Ube Industries, Ltd. 7-2, Kasumigaseki 3-chome,
Chiyoda-ku, Tokyo, Japan

** Polymer Research Laboratory, Ube Industries,
Ltd. 8-2, Goi-Minamikaigan, Ichihara City,
Chiba, Japan

SULFIDE TREEING: A DILEMMA FOR TELECOMMUNICATION CABLES

B. D. Gesner

ABSTRACT

A sulfide tree phenomenon has been discovered in buried telecommunication cable containing copper conductors. The sulfide growth leading to electrical breakdown occurs in the absence of an applied voltage and depends on the condensation of water within the cable. Accordingly, sulfide induced electrical breakdown in buried telecommunication cables can be avoided by the use of waterproof cable.

Because of the probability for sulfide generation along the seacoast, sulfiding becomes a distinct possibility whenever a copper containing object is placed directly in sea soil. Kawawata, et al¹ and later Fukuda, et al² have shown us that copper conductor-containing power and control cables placed in sulfide-containing water and soils are subject to copper sulfide growth through insulation. Copper sulfide findings in telecommunication cables have been reported to us over the past several years. All reports have been from coastal areas. In only one instance however had a clear cut case of growth through insulation been established. That one case occurred in a "water-logged" cable. In that cable, water was considered the culprit and hydrogen sulfide a casual and innocuous participant. The persistence, however, of trouble reports in which sulfiding was a common denominator led us to this investigation.

Introduction

The copper sulfiding cases about to be related occurred at the seashore. Sea soil, because it contains decaying organic matter and sulfate-rich water is an ideal breeding place for sulfate-reducing and therefore sulfide-producing bacteria,



Metal tarnishing is a common occurrence wherever hydrogen sulfide comes in contact with certain metals particularly silver and copper. But by no means is metal sulfiding restricted to the seashore. Comparable conditions for sulfate-reducing bacteria activity are as equally probable in swamps and marshes and among sewage as they are at the seashore. Hydrogen sulfide also evolves by other processes as an environmental pollutant from hot springs, from oil fields and from chemical industries. It is expected therefore that the sulfiding problem found at the seashore will repeat itself in other locales.

As the investigation proceeded it became obvious that the design of telecommunication cables and the thinness of conductor insulation provided distinct sulfiding features quite apart from the Kawawata and Fukuda cases. Three visually distinguishable types of sulfiding in fine gauge insulated conductors were uncovered. They are referred to in this text as uniform sulfiding, blotching, and measles. Uniform sulfiding results in a general darkening of the insulation. Blotching appears as randomly distributed patches of darkened insulation. Neither of these conditions cause marked changes in insulation dielectric characteristics. Measling leaves the insulation black-speckled. These measles are the outer growths of copper sulfide trees, whose conductivity obviates the effectiveness of the dielectric. Although the three types are related, one is not necessary for the development of the other. Generally, however, measles is preceded by blotching which in turn is preceded by uniform sulfiding. All three sulfiding types observed in this study were readily reproduced in the laboratory. Uniform sulfiding was the most commonly encountered and most readily reproduced while measles

was the least encountered and required long exposure to reproduce.

Field Observations

Buried air core cables were examined in Fort Pierce, Jacksonville, and Panama City, Florida, and Savannah, Georgia. In all cases the cables unearthed were known to have defective circuits and the conductors were suspected to be sulfided. Fifteen cables were examined. Panama City was the only area in which sulfided conductors were not found. However, the two cables investigated in the Panama City area were from locations fifty miles inland. Even though the probability of hydrogen sulfide formation in this area is low these two locations were investigated on the basis of reports of apparent sulfide corrosion products. The corroded conductors were in fact found in pedestals and the corrosion products were actually copper chlorides. The extent of sulfiding and distribution of type sulfiding among the remaining cables were approximately the same. All thirteen cables had some degree of sulfiding. Measling was detected in four cables, two from Fort Pierce and one each from Jacksonville and Savannah. Measled insulation was found only in PAP cables all of which had been placed after 1972 and within ten miles of the coast. Sulfide ion was absent in soil sample from selected locations in which both measling and uniform sulfiding were encountered. Some comfort was taken in the fact that sulfate and chloride ions were found in these same locations and were in particularly high concentration in the immediate vicinity of rivers and the ocean. However, in all of these investigations we could show nothing more than a potential for sulfide formation at the exposure sites.

The Fort Pierce samples were carefully examined. The dielectric characteristics of these samples are recorded in Table 1 and 2. The blackened deposit in the insulations of each of these samples was identified by X-ray fluorescence analysis and X-ray diffraction patterns as a composite of cuprous oxide and sulfide. Chlorides were not present. Cross-sections of the measled samples (Fig. 1) revealed the same type copper sulfide trees as those reported by Kawawata, et al in contaminated signal cables. Uniformly sulfided samples possessed insulation resistance and breakdown potential comparable to those of freshly manufactured samples. Uniform sulfiding evidently is not disrupting to the dielectric. The measled samples, however, were readily broken down even under the moderate conditions of the insulation resistance test. The conductivity of the sulfide trees and their passage through insulation are sufficient to destroy the dielectric capability of the insulation.

The double jacketed cable from FP-3 posed unique characteristics in terms of

sulfide growth. Unlike Kawawata's samples, the outer polyethylene jacket showed no signs of sulfide growth. The aluminum shield too was unaffected. However, on removal of the outer jacket and aluminum shield black spots about a centimeter in diameter and about 25 centimeters apart were observed underlying the inner jacket (Fig. 2). The areas seemed to arise from within the Reemay core wrap at the nylon thread binder. Removal of the inner jacket confirmed that the blackened areas progressed inward from the Reemay. The inner jacket itself was no more than stained. Careful removal of the Reemay and nylon binder provided a most startling discovery. The blackened areas actually had their source from underlying insulated conductors. Measled insulation was restricted to these areas. In all other areas uniform sulfiding predominated. Blotching occurred occasionally within the whole and more frequently in the vicinity of the black spots. The measled samples from Jacksonville and Savannah had these same black spots underlying the inner polyethylene jacket. The FP-1 cable was entered at a repair point from which it was impossible to determine whether this cable suffered the same black spot phenomenon. However, the evidence strongly suggests that black spotting is the dielectric failure mode in hydrogen sulfide attacked buried telecommunications cables. Finally, a sample removed from the FP-1 cable had a uniform silvery stain along its length. The silvery material was rich in copper sulfide and originated from a split in the insulation. The shape and growth pattern of the stain indicated water had been involved in its formation. Chlorides were not detected in this silvery material. Therefore any water that had entered this cable must not be ground water.

In summary, the sulfiding observed in buried cables occurred in sulfate-rich soils. The tree-like black corrosion products within the insulation consisted of copper sulfide and oxide. The absence of chlorides among the corrosion products indicates that ground water did not enter the cables. Corrosion products that grew through the insulation appeared on the surface as black measles and were electrically conductive. The sulfide measles were found only in double jacketed cables and formed in localized colonies at the Reemay-insulated conductor bundle interface. This black spot effect strongly suggests that the corrosion of the underlying conductors was promoted by the formation of condensed water cells through which the concentration of hydrogen sulfide could be first increased and then maintained at a high level.

Laboratory Observations

Three separate sulfide growth experiments representative of dry, damp and wet conditions were conducted. In all cases simulated cables (Fig. 3) containing conventional 22 and 26 gauge insulated conductors were employed. All cables were exposed to hydrogen sulfide in desiccators. The nominal atmospheres for dry and damp environments are listed in Table 3. To create a wet environment the cores of each cable under the nominal atmosphere for the damp condition were doped with approximately two milliters of tap water. Only air core structures were studied under the dry and wet conditions, whereas both air core and petrolatum - filled structures were studied under the damp condition. Air core structures contained both low density polyethylene and solid or cellular high density polyethylene insulations; petrolatum filled structures contained both polypropylene and cellular high density polyethylene insulation. Each cable contained ten conductors, the insulations of which were colored in the ten colors of the cable color code.

Under dry conditions, after seven days certain of the low density polyethylene insulations appeared darkened. The orange, for instance, appeared light brown and the yellow a dull green. In fifteen days the red took on a crimson hue and the white a dull grey. No other changes occurred in the low density polyethylene insulation through the 100 day course of this experiment. Similar color changes were apparent for the high density polyethylene insulation. However, the changes were much less pronounced. Even after 100 days, for instance, the orange did not appear brown but merely darkened. More important however, the high density polyethylene insulations after 100 days exposure were measled and covered with fine white needle-like crystals (Fig. 4) some as much as 0.6 mm in length and 20 μ thick. In addition some of these crystals appeared to originate from sulfide measles. The measles were most common at bends in the insulated conductor. The white crystalline material melted sharply at 118°C. The scant quantity allowed no further analysis. However, the high density polyethylene insulation had an unusually high concentration of stabilizer (as indicated by differential thermal analysis) a constituent of which melts at 118°C. It appears that the white crystalline material and this stabilizer are one and the same.

Under damp conditions, insulations in filled structures had no more than mild sulfiding throughout the 54 day course of this experiment. Polypropylene insulation was particularly resistant to sulfide growth even in air core structures. The high and

low density polyethylene insulations in air core structures were uniformly sulfided within the first 13 days of this experiment. Blotching particularly in the brown insulation was apparent in 20 days. Measling was apparent after 54 days exposure. The brown insulations pass through a whitened and then black stage as they become measled. Black crystals eventually grow on the insulation surface (Fig. 5). The whitened material is organic, probably the stabilizer additive, and the black crystals consist of cuprous oxide and sulfide. Lead base pigments within the brown insulation may promote the anomalous coloration behaviour. The process under wet conditions is similar to that under damp conditions except that measling occurs much sooner and predominates along areas of the insulation upon which water had condensed (Fig. 6). Dielectric breakdown of pairs after 55 days exposure range from 10 to 800 VDC. Values tended to be greater for thicker insulations regardless of polymer type.

The laboratory simulation under high concentrations of H₂S showed that sulfide measles can be produced under both dry and wet conditions. The measles were once again electrically conductive. The rate of measles growth increases as the concentration of water in the corrosion atmosphere increases. Under wet conditions low and high density polyethylene insulations in air core structures are readily attacked. The attack was particularly harsh on the brown insulation. All insulations in filled structures and polypropylene in an air core structure did not measle. The conductors underlying these insulations were no more than uniformly sulfided. For those cases in which measling did occur, localized spotting within the confines of condensed water droplets was common. Under dry conditions the low density polyethylene insulated conductors underwent mild sulfiding. In this case the brown insulation behaved no differently than the other insulations. In the dry experiment white crystals formed on the surface of the high density polyethylene insulation. Measles were observed at crystal sites and more frequently at bends in this insulation.

Conclusions

Even though field conditions are mild and laboratory conditions severe, there is a striking similarity between certain results from the two. The three modes of sulfiding and their effect on insulation are the same in both. Perhaps, the most significant similarity is the black spot phenomenon in buried cable and the intensification of measling at condensed water sites on the laboratory exposed insulation

under wet conditions. That similarity is the basis for our conclusion that the measling in the cables examined is restricted to liquid water sites. The absence of chlorides in the corrosion products indicates that the water involved in the sulfide corrosion was of such purity that it could have entered only by a condensation process. For instance, humid air entered the cable at above ground access points. As the humid air dispersed through the cable, condensation occurred because of the air temperature drop within the buried cable. If this rationale is correct, the contribution of the double jacketed cable becomes clear. That cable alone among all the cables investigated contained both a nylon string core wrap binder and a Reemay core wrap. Furthermore the double jacketed cable was the only one that contained black spot measled conductors. The hydrophilic nylon string in this cable provides an excellent nucleation site for condensation. The porous Reemay affords an aggregating and holding place for the condensed water droplets. These droplets become reservoirs and concentrating media for hydrogen sulfide. That is a consequence of the ability of hydrogen sulfide to achieve a relatively stable 0.5 percent w/v concentration in the water at cable ambient. Once this concentration is attained it becomes independent of the concentration of hydrogen sulfide gas within the cable core. Because of the constancy and concentration of these aqueous sulfide cells the sulfiding of the underlying conductors is accelererated. The process is similar to that described by Kawawata.¹ However, because of the structure of Kawawata's cables, the sulfide-containing water external to the cable served as one large aqueous sulfide cell. Naturally aqueous sulfide cells can be formed in the cable by the entry of ground water. However, it must not be underemphasized that something as innocuous as humid air can in the presence of hydrogen sulfide cause cable failure.

The laboratory experiments provided as many questions as answers. The rapid deterioration of brown polyethylene insulations under wet exposure conditions could have been promoted by the lead containing molybdate orange pigment. However this pigment is also found in orange and yellow insulations both of which were normal in their behaviour. Except for the brown the change in coloration for insulations under uniform sulfiding conditions is probably due to the underlying black sulfide. The exudation of organic material and particularly the crystal growth on high density polyethylene insulation under dry sulfiding conditions probably occurs by a displacement process. The growth of black crystals probably

follows the same mechanism. If that be the case, however, the type of displaced material and its concentration should play an important role in the treeing phenomenon.

There is a reasonable correlation between the effect of hydrogen sulfide on the insulated conductors and the permeability of hydrogen sulfide gas through the different insulation materials (Table 4). The degree of sulfiding in a given time is greatest for the low density polyethylene insulations and the least for polypropylene. However, the reluctance of the polypropylene insulation to allow more than uniform sulfiding under conditions in which the polyethylenes were severely sulfided probably deserves a further explanation. The permeability differences are not sufficient to suggest the preclusion in one and not in the others. The structural and compositional complexities of the polypropylene certainly play a role. However, a discussion of the nature of that role is beyond the scope of this work.

The variety of environments under which hydrogen sulfide can be formed to an extent sufficient to disrupt the operation of buried cables is still to be established. However, since it appears that liquid water and hydrogen sulfide are partners in the sulfide-measling process the elimination of one or the other from the cable should be sufficient to prevent electrical problems. Since filled cables resist ground-water penetration and are improbable vehicles for water condensation, their use in buried installations should minimize the effects of hydrogen sulfide in the future.

Acknowledgement

I wish to acknowledge Fran Mullin for his efforts in arranging the field trips. His investigation on assessing the extent of sulfide-induced problems in buried cable within the United States will be reported in a separate work. I thank Roman Harmel and John Blee for their analytical assistance on samples from the field and from the laboratory experiments.

REFERENCES

1. Shichiro Kawawata and Jiro Ogura, Chemical Tree Deterioration in the Insulation of Plastics-Insulated Wires and Cables, *Hitachi Review*, 20, No. 2, 55-63 (1971), and references cited therein.
2. Teruo Fukuda, Toyokazu Hisatsune, Hiroshi Nagai, and Morikuni Hasebe, Sulfide Attack to Polyethylene Insulated Control Cable and Development of Sulfide Capture Sheath,

Proceedings of the Twenty First
International Wire and Cable
Symposium, Pages 75-87, December 1972,
and references therein.

3. Reemay is the registered trademark for
the E. I. Dupont de Nemours Companies'
spunbonded polyester sheet material.

Table 1: INSULATION RESISTANCE OF SAMPLES RECOVERED
FROM FORT PIERCE, FLORIDA

| Location | Cable Age (Years) | Condition | Sheath | Insulation Resistance Range at 1000 VDC (OHMS) | |
|----------|----------------------|-----------------------|--------|---|-----------|
| | | | | High Value | Low Value |
| FP-1 | 2 | Measled | PAP | 10^{10} | Breakdown |
| FP-2 | 15 | Uniformly Sulfided | ALPETH | 10^{16} | 10^{10} |
| FP-3 | 4 | Measled | PAP | Breakdown | - |

Table 2: D.C.DIELECTRIC BREAKDOWN OF SAMPLES RECOVERED
FROM FORT PIERCE, FLORIDA

| Location | Cable Age (Years) | Condition | Sheath | Breakdown Potential (kVDC) | |
|----------|----------------------|-----------------------|--------|----------------------------|-----------|
| | | | | High Value | Low Value |
| Control | - | - | - | - | 20 |
| FP-1 | 2 | Measled | PAP | 4 | 11 |
| FP-2 | 15 | Uniformly Sulfided | ALPETH | - | 20 |
| FP-3 | 4 | Measled | PAP | 2 | 1 |
| FP-4 | 4 | Uniformly Sulfided | PAP | 20 | 15 |
| FP-5 | 4 | Uniformly Sulfided | ALPETH | - | 20 |

Table 3: NOMINAL ATMOSPHERIC COMPOSITION FOR EXPERIMENTAL
CABLES

| GASEOUS COMPONENT | NOMINAL CONCENTRATION (VOLUME %) | |
|----------------------|-------------------------------------|-------------------|
| | DRY CONDITION | DAMP CONDITION |
| H ₂ S | 92 | 90 |
| H ₂ O | < 0.2 | 2 |
| Air | > 7.8 | 8 |

Table 4: GAS PERMEABILITIES OF CERTAIN POLYOLEFINS AT
25°C (P X 10¹⁰ IN CGS UNITS)

| GAS | Permeabilities for | | |
|------------------|--------------------|------|-----|
| | LDPE | MDPE | PP |
| O ₂ | 4 | 0.5 | 2 |
| H ₂ O | 90 | 10 | 50 |
| H ₂ S | 40 | 5 | 0.3 |



Figure 1. Cross-section of measled insulation.

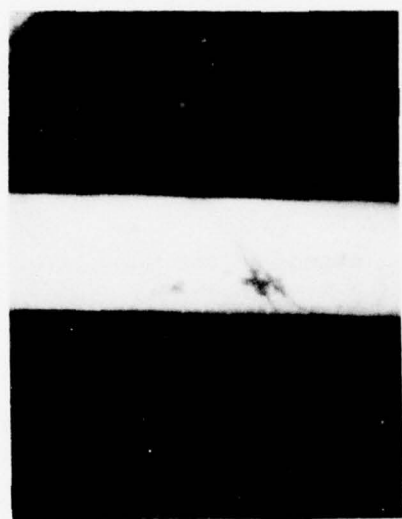


Figure 2. Black-spots underlying cable inner jacket.



Figure 3. Example of simulated cables.

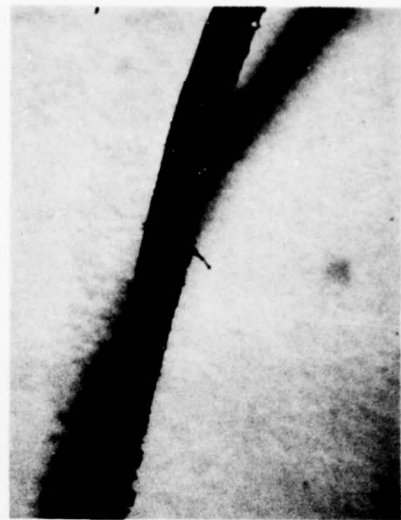


Figure 5. Black crystal growth on an insulated conductor.



Figure 4. Needle-like crystal growth on an insulated conductor.



Figure 6. Water-droplet-measled insulated conductor.



B. D. Gesner received a B.S. in Chemistry from The Bradford Durfee Technological Institute, Fall River, Massachusetts in 1960 and a Ph.D in Physical Organic Chemistry from the University of Idaho in 1963. Since that time he has been a member of the Technical Staff in Bell Laboratories, working in materials chemistry. He is currently Supervisor of the Cable and Wire Group in the Quality Assurance Center of the Bell Laboratories, Holmdel, New Jersey.

ORGANIC COLORANTS FOR CCP CABLE INSULATION

Hiroshi Ohshima and Senkichi Kawakubo
Musashino Electrical Communication Laboratory
Nippon Telegraph and Telephone Public Corporation
Musashino-shi, Tokyo, 180 Japan

Abstract

Colorants containing cadmium pigments have been used for coloring CCP (Color-Coded Polyethylene) cable insulation. Recently, a plan was made to substitute less toxic organic colorants for conventional ones. In selecting suitable colorants, excellent characteristics as colorants for CCP cable insulation and maintenance of conventional color tone were taken into consideration. The most important property needed for CCP cable insulation is oxidative stability, as this cable is used mainly in overhead lines. Further requirements are some resistance against ultraviolet ray needed in splicing, resistance to hydrogen sulfide, considering the application to spa areas, and resistance to petroleum jelly and some solvents, when used for CCP-JF (Jelly-Filled) cable. The effect of these environmental factors on the physical and chemical properties of polyethylene insulation colored by organic colorants, and the types of organic colorants which can be used under such environment are described.

Introduction

In Japan, CCP cable is widely used as a distribution cable. Insulation material for CCP cable is low-density polyethylene color-coded for easy splicing. Insulation colors are blue, yellow, green, red, violet, brown, white and black. The yellow, green and red insulations used to be colored either by cadmium pigment only or by colorants made up of cadmium pigments and other components. Cadmium pigments have excellent color clearness, dispersion in plastic, fastness against light and heat resistance.

Recently, environmental pollution by industrial waste has caused public nuisance and general demand has increased to cease using materials containing cadmium. So now in Japan, there is a tendency to substitute organic pigments with less toxicity for cadmium pigments. For this reason, a plan was made to substitute less toxic organic colorants for the conventional cadmium ones which had been used for coloring CCP cable insulation. This paper reports the effect of colorants on oxidative stability, resistance against ultraviolet ray and other properties of colored insulations as well as proposable organic colorants which can be used for CCP cable insulation.

Selection Principles

The chromatic color pigments investigated are shown in Table 1. In selecting suitable pigments, the following conditions were taken into consideration.

1. No heavy metals contained,

2. Excellent physical and chemical properties,

3. Good supply stability.

Pigments to be examined are organic ones, with the exception for titanium yellow as shown in Table 1.

The colorants were composed of the pigments shown in Table 1, in addition to titanium white and carbon black. Colorants were prepared so that color tones would be as similar to conventional ones as possible. Properties of the new colorants were evaluated in comparison with those of conventional colorants of corresponding colors.

Experimental

Sample Preparation

Samples for this study were made from stabilized low-density polyethylene, which is used for CCP cable insulation, and new colorants or conventional colorants in three colors. Samples were prepared in forms of test sheets and insulated wires. Copper wire diameter is 0.4 mm and insulation thickness is 0.12 mm.

Test Method

Dielectric Properties Dielectric constant and dissipation factor were measured by benzene displacement method at 23°C and at 1 MHz.

Oxidative Stability As CCP cable is used mainly for an overhead line, polyethylene insulated wires are subject to rather high temperature. So, good oxidative stability is necessary for insulation materials. Samples were prepared by wrapping an insulated wire around its own diameter with a weight of 80 grams ("pig-tail test"). Samples were aged in a circulating-air oven at 80°C for 200, 500 and 1000 hours. After aging, the insulated wires were visually examined for crack and discoloration, and insulation densities were measured by density gradient method.

Heat Resistance Heat resistance needed in the manufacturing process was examined with an extrusion plastometer. Five grams of colored polyethylene granules were charged in a cylinder of an extrusion plastometer. This test was carried out at temperature of 265, 280 and 300°C, and heating time of 5, 15 and 30 minutes. After heating, an 8.55 kilogram load was put on a piston and a noodle-like extrudate was obtained. Discoloration of the extrudate was visually examined.

Resistance to Vaseline CCP-JF cable is used as an underground cable, whose core is

filled with a jelly compound to prevent moisture penetration. Therefore, there is a possibility that the colorants should migrate into the jelly compound. Vaseline was used as a substitute for the jelly compound during the experiment. It is a basic component of the jelly compound, and its extraction power is stronger and handling is easier than the jelly compound. Vaseline was put between two test sheets, and the assembly was heated for 72 hours in a circulating-air oven at 60°C. After heating, colorant migration to vaseline was visually examined.

Resistance to Solvents In splicing insulated CCP-JF cable wires, jelly compound adhering to insulated wires is wiped off with solvent, such as kerosene. For this reason, resistance to solvents was also examined. Kerosene and xylene were used as typical test solvents. After immersion for up to 50 days at 50°C, solvent discoloration was visually examined.

Resistance to Ultraviolet Ray Insulated CCP cable wires may be exposed to sunlight during splicing or when a terminal box cover is blown off by strong wind. Therefore, colorants must have some resistance to ultraviolet ray. Samples in the form of test sheet and insulated wire were used. Two types of weather testers were used; open-flame sunshine carbon-arc weather tester and enclosed carbon-arc weather tester. Maximum irradiation time was 600 hours. After irradiation, tensile properties and discoloration were measured.

Resistance to Hydrogen Sulfide In spa areas, it is a matter of great concern that insulations may discolor by hydrogen sulfide. So, resistance to hydrogen sulfide was examined. Sheet samples and insulated wire samples were kept in saturated hydrogen sulfide aqueous solution and hydrogen sulfide gas whose maximum concentration was 300 ppm. Exposure was carried out for up to 600 hours at room temperature. Then, sample discoloration was measured.

Resistance to Chemical Agents Resistance to acid and alkali is generally a good colorant selection criterion. Sheet samples and insulated wire samples were immersed in an aqueous solution of 10% sulfuric acid, 10% hydrogen chloride and 3% sodium hydroxide for up to 15 days at 50°C. After immersion, sample discoloration was measured.

Results and Discussion

Dielectric Properties

The dielectric constants of all colored samples were approximately equal to that of uncolored polyethylene sample. The conventional red sample (colored by cadmium red) showed the largest dissipation factor value among all the samples. On the whole, the sheets colored by new colorants exhibited satisfactory dielectric properties.

Oxidative Stability

An example of density changes in insulations by pig-tail test is shown in Figure 1.

The samples showed an increase in density upon heating. However, colored samples showed almost the same increase in density as that of an uncolored one. The other colored samples also gave a similar result to that in Figure 1. No discoloration and no crack as signs of oxidative deterioration, was observed for any of the samples after aging for 50 days. As a result, it was recognized that oxidative deterioration of polyethylene insulation was not accelerated by conventional and new colorants.

Heat Resistance

Table 2 shows an example of heat resistance. A colorant containing azo lake yellow discolored markedly at 280 and 300°C. Other new colorants and conventional ones showed good heat resistance under all test conditions.

Resistance to Vaseline and Solvents

An example of data is shown in Table 3. Colorants containing insoluble azo and azo lake pigments showed low resistance to vaseline and/or solvents. Other new colorants and conventional ones had good resistance.

Resistance to Ultraviolet Ray

Ultraviolet ray exposure caused samples containing anthraquinone yellow to deteriorate in tensile properties and to discolor markedly. Pertinent data is shown in Figure 2. Other new colorants showed almost the same resistance as that of conventional ones.

Two types of weather testers were used in ultraviolet ray exposure tests. Discoloration and deterioration of tensile properties occurred in different manners with these weather testers. An example of results of ultraviolet ray exposure tests is shown in Figure 3. As is evident from Figure 3, discoloration was larger by enclosed carbon-arc weather tester than by open-flame sunshine carbon-arc weather tester. On the contrary, deterioration in tensile elongation proved to be larger by the latter. In some cases, appearance of sample surfaces irradiated by the weather testers was different for each type of weather tester. For example, fine cracks were generated on the surface of yellow test sheet colored by anthraquinone yellow, titanium yellow and titanium white, after exposure of 600 hours by open-flame sunshine carbon-arc weather tester. By the other tester, such phenomenon was not recognized. It is assumed that the difference in the test results originates from the difference in ultraviolet ray spectrum of these weather testers. Polyethylene is said to be most sensitive to radiation at 300 nm wavelength and virtually unaffected by wavelength above 340 nm. In addition, open-flame sunshine carbon-arc weather tester radiation between 300 and 340 nm is known to be more intense than that of an enclosed carbon-arc weather tester. Samples which showed good resistance to ultraviolet ray in a form of test sheet provided relatively good results also in a form of insulated wire. In case of insulated wires, evaluation among samples was possible within shorter irradiation time than

in case of test sheets.

Resistance to Hydrogen Sulfide

By saturated hydrogen sulfide aqueous solution, colorants containing anthraquinone yellow or poly-Cl-Br-Cu-phthalocyanine discolored to some extent. But, all colorants scarcely discolored when exposed to hydrogen sulfide gas at a maximum concentration of 300 ppm. The data of test sheets is shown in Figure 4. However, yellow samples in the form of insulated wire showed an apparent discoloration because of their low hiding power against copper conductors blackened by hydrogen sulfide gas penetrating through the insulation.

Resistance to Chemical Agents

Discoloration occurred only by 10 % hydrogen chloride on conventional yellow and green colorants containing cadmium yellow. The data is shown in Figure 5. All colorants scarcely discolored in aqueous solution of 10 % sulfuric acid and 5 % sodium hydroxide.

Pigment Combination Effect

Most colorants investigated were prepared by combinations of several chromatic pigments. The reason is that the combination enables easier preparation of colorants at desired color tones. An example of combination effect of pigments is described as follows. Figure 6 shows the variation of hue and chroma of yellow and red sheets made by a combination of two kinds of pigments in Munsell hue circle. As shown in this figure, hue and chroma of colorants containing two chromatic pigments vary widely with content ratio of two kinds of pigments. Results of ultraviolet ray exposure tests are shown in Figure 7. Condensed azo yellow (A), as a component of the yellow colorant, had good resistance to deterioration in tensile properties and discoloration after ultraviolet ray exposure in comparison with condensed azo yellow (B) as another component. Discoloration and deterioration of elongation changed almost linearly with content ratio of two kinds of pigments.

Selection of Colorants for CCP Cable Insulation

Properties obtained on new colorants were evaluated in comparison with those of corresponding conventional colorants. Colorants suitable for CCP cable insulation were selected as follows.

Yellow: colorant containing condensed azo yellow and/or isoindolinone yellow

Green: colorant containing phthalocyanine green, and condensed azo yellow and/or isoindolinone yellow

Red: colorant containing condensed azo red and/or quinacridone red and/or perylene red

Summary

It was planned to substitute less toxic organic colorants for conventional cadmium ones which had been used for CCP cable insulation. In selecting suitable colorants, maintenance of the conventional color tones and excellent characteristics as colorants for the insulation were taken into consideration. As a result of investigation, yellow, green and red colorants, which contain several condensed azo and polycyclic pigments, were selected.

Acknowledgement

The authors would like to thank Mr. K. Matsumae for his guidance on the work. The authors also wish to thank Mr. H. Nakamura for his helpful suggestions on the manuscript, Mr. H. Sato and the persons concerned in the Furukawa Electric Co., Ltd., Sumitomo Electric Industries, Ltd., and Fujikura Cable Works, Ltd., for their cooperation during the work.

Reference

1. F. H. Winslow, W. Matreyek and A. M. Trozzolo, SPE Journal, 28, No. 7, 19 (1972)



Hiroshi Ohshima
Musashino Electrical
Communication Labora-
tory, NTT
Musashino-shi, Tokyo,
180 Japan



Senkichi Kawakubo
Musashino Electrical
Communication Labora-
tory, NTT
Musashino-shi, Tokyo,
180 Japan

Mr. H. Ohshima is Staff Engineer, Engineering Division, Musashino Electrical Communication Laboratory, NTT, and is presently engaged in the development and application of plastics for cable and wire. He once worked on cellular polyethylene insulation. He received his Master of Science degree from Hokkaido University in 1965 and is a member of the Society of Polymer Science, Japan.

Mr. S. Kawakubo is Staff Engineer, Engineering Division, Musashino Electrical Communication Laboratory, NTT. Since joining ECL, he has been engaged mainly in the development and application of plastics for cable facilities. He is a member of the Institute of Electrical Engineers, Japan.

Table 1. Candidate Pigments

| Classification | Color | Pigment | Expected Color Fastness | | | | Pigment Structural Formula Example |
|----------------|---------------------|------------------------------|-------------------------|------|-----|------|------------------------------------|
| | | | Light | Heat | HCl | NaOH | |
| Insoluble azo | Yellow | Mono azo yellow (1)* | ○ | △ | ○ | ○ | (1) |
| | | Dis azo yellow | ○ | △ | ○ | ○ | |
| Azo lake | Yellow | Azo lake yellow | ○ | △ | ○ | ○ | (2) |
| | | Azo lake red (2) | ○ | △ | ○ | ○ | |
| Condensed azo | Yellow | Condensed azo yellow | ○ | ○ | ○ | ○ | (3) |
| | | Condensed azo red (3) | ○ | ○ | ○ | ○ | |
| Green | Red | Phthalocyanine green (4) | ○ | ○ | ○ | ○ | (4) |
| | | Poly-Cl-Br-Cu-phthalocyanine | ○ | ○ | ○ | ○ | |
| Polycyclic | Yellow | Anthraquinone Yellow (5) | ○ | ○ | ○ | ○ | (5) |
| | | Isoindolinone yellow (6) | ○ | ○ | ○ | ○ | (6) |
| Red | Yellow | Quinacridone red (7) | ○ | ○ | ○ | ○ | (7) |
| | | Perylene red (8) | ○ | ○ | ○ | ○ | |
| Inorganic | Titanium yellow (9) | | ○ | ○ | ○ | ○ | (9) |

○ Excellent, ○ Good, △ Poor.

* Numbers in parentheses indicate the corresponding structure in the far right column.

Table 2. Heat Resistance

| Colorant | Time (min.) | Temp. (°C) | | 300 |
|--|-------------|------------|-----|-----|
| | | 265 | 280 | |
| Azo lake yellow and Titanium yellow | 15 | ○ | ✗ | ✗ |
| Dis azo yellow, Mono azo yellow and Titanium white | 5 | ○ | ○ | △ |
| Anthraquinone yellow and Titanium white | 30 | ○ | ○ | ○ |
| Condensed azo yellow and Titanium white | 15 | ○ | ○ | ○ |

- No perceptible discoloration,
 ○ Slight discoloration,
 △ Distinct but not strong discoloration,
 ✗ Intense discoloration.

Table 3. Resistance to Vaseline and Solvents

| Environment \ Colorant | Mono azo yellow, Dis azo yellow and Titanium white | Azo lake yellow and Titanium white | Azo lake red, Condensed azo red and Titanium white |
|------------------------|--|--|--|
| Xylene | ○ | ○ | ✗ |
| Kerosene | ○ | ○ | △ |
| Vaseline | ✗ | ✗ | ✗ |

- No migration, △ Slight migration, ✗ Marked migration.

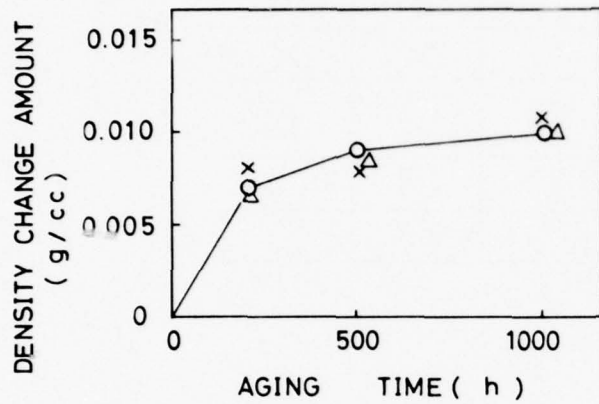


Figure 1. Density changes in insulations by pig-tail test.

○ Uncolored polyethylene sample
 × Red sample (condensed azo red,
 quinacridone red and titanium white)
 △ Red sample (cadmium red)

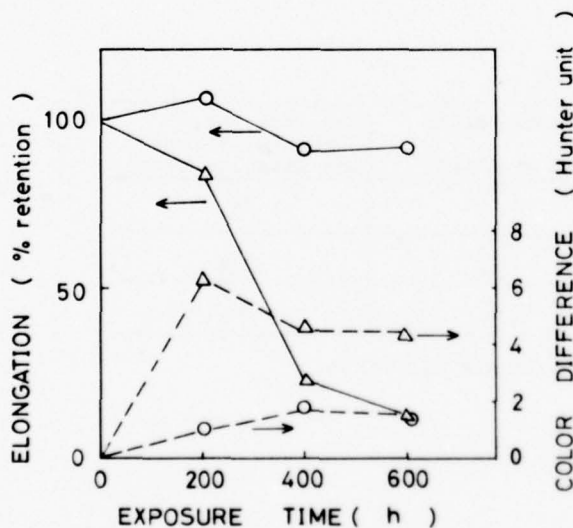


Figure 2. Test sheet elongation and discoloration after ultraviolet ray exposure

○ Yellow sample (cadmium yellow and titanium white)
 △ Yellow sample (anthraquinone yellow, titanium yellow and titanium white)

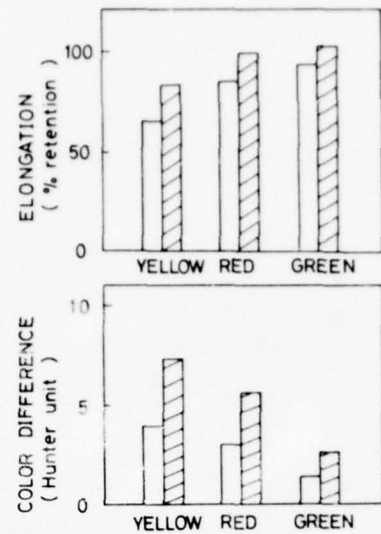


Figure 3. Test sheet elongation and discoloration after 600 hr ultraviolet ray exposure in two types of weather testers.

■ Open-flame sunshine type
 ■ Enclosed carbon-arc type
 Yellow sample (2 kinds of condensed azo yellow and titanium white)
 Green sample (phthalocyanine green, condensed azo yellow and titanium white)
 Red sample (condensed azo red, quinacridone red and titanium white)

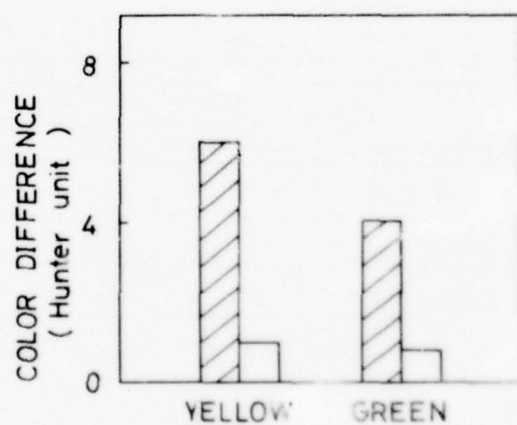


Figure 4. Test sheet discoloration by hydrogen sulfide.

■ in saturated hydrogen sulfide aqueous solution for 600 hrs
 □ in hydrogen sulfide gas at a 30 ppm concentration for 600 hrs
 Yellow sample (anthraquinone yellow and titanium white)
 Green sample (poly-Cl-Br-Cu-phthalocyanine, phthalocyanine green and titanium white)

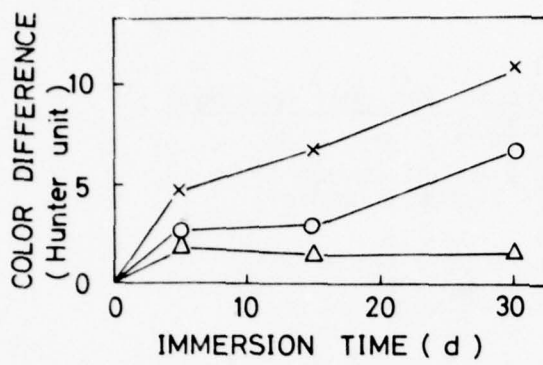


Figure 5. Test sheet discoloration by hydrogen chloride.

○ Yellow sample (cadmium yellow and titanium white)
 × Green sample (phthalocyanine green, cadmium yellow and titanium white)
 △ Red sample (cadmium red)

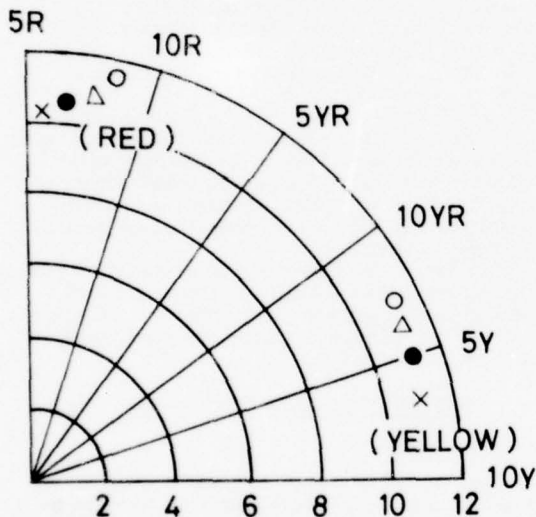


Figure 6. Hue and chroma of test sheet colored by various combinations of pigments.

| Yellow | | (wt.%) | | | |
|--------------------------|----------|--------|----|-----|-----|
| Pigment | Colorant | × | ● | △ | ○ |
| Condensed azo yellow (A) | 100 | 63 | 50 | 0 | 0 |
| Condensed azo yellow (B) | 0 | 37 | 50 | 100 | 100 |

| Red | | (wt.%) | | | |
|-------------------|----------|--------|----|-----|---|
| Pigment | Colorant | × | ● | △ | ○ |
| Condensed azo red | 0 | 6 | 50 | 100 | 0 |
| Quinacridone red | 100 | 94 | 50 | 0 | 0 |

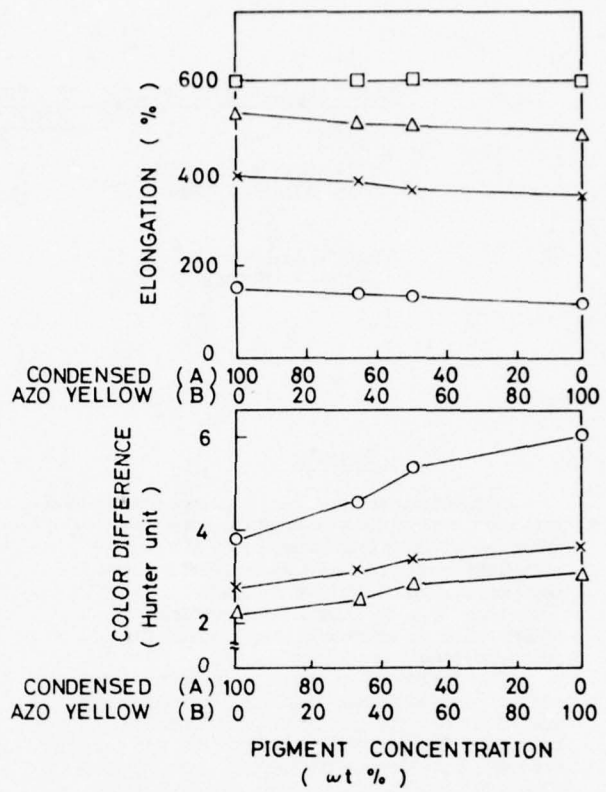


Figure 7. Test sheet elongation and discoloration after ultraviolet ray exposure.

□ Exposure time 0 hrs
 △ 200 hrs
 × 400 hrs
 ○ 600 hrs

ELECTRICAL PROPERTIES OF POLYPROPYLENE HOMO- AND COPOLYMERS
AT HIGH FREQUENCIES

by

Dieter H. BUERKLE
Jean-Claude REBEILLE

Jean-Claude BOBO
Bernard L. HOCHON

ATO Chimie -Usine de Mont
64300 - ORTHEZ - France

Laboratoires de MARCOUSSIS
Cie Générale d'Electricité
91460 - MARCOUSSIS- France

SUMMARY

Dielectric properties of polypropylene and ethylene - propylene copolymers have been measured at frequencies up to 60 MHz. Polypropylene shows decreasing dielectric loss between 0.1 and 60 MHz and loss factors of less than $50 \cdot 10^{-6}$ have been obtained at 60 MHz with an extremely pure, stabilized polypropylene homopolymer.

The influence of atactic polypropylene content and additives has been investigated. The level of catalyst residues turned out to be a main factor with high chloride and titanium content, bringing up dielectric loss to more than $100 \cdot 10^{-6}$. Low cooling rate results generally in higher crystallinity and lower loss factor.

Ethylene - propylene block copolymers show significantly higher losses than homopolymers, whilst ethylene - propylene random copolymers have loss factors only slightly higher than corresponding polypropylene homopolymers.

Both polypropylene homo- and copolymers are even less subject to ageing in saline water solution and direct voltage field than low density polyethylene.

Problems occurring with polypropylene during extrusion of thick insulation, especially void forming tendency, are discussed and solutions using ethylene - propylene random copolymers and modified extrusion techniques are suggested.

INTRODUCTION

During recent years, the tendency in submarine cable system development has been towards higher transmission capacity. Therefore, higher frequencies will be needed than those actually employed, e.g. 30 MHz, as in the last transatlantic cable TAT 6, which has been installed recently, adding another 4000 simultaneous lines to the existing capacity.

These systems comprise, besides the cable, electronic repeaters at a constant distance of about 10 nautical miles. The repeaters amplify the signal and thus compensate the attenuation due basically to the dielectric losses of the cable insulation. For economic reasons it is desirable to have minimum losses in the cable insulation, in order to reduce the necessary number of repeaters.

Considerable work done by a limited number of insulation resin producers, in cooperation with cable manufacturers, lead to low density polyethylene grades, with dielectric loss factors of about $50 \cdot 10^{-6}$ at 30 MHz. However, at higher frequencies all low density polyethylene resins show higher losses.

In order to be prepared for a new generation of submarine cables working at frequencies of 60 MHz or higher, dielectric properties of polypropylene and ethylene - propylene copolymers have been investigated.

MEASUREMENT OF DIELECTRIC LOSSES

Measuring device

The measuring device used was a Q-meter specially adapted to measurements on materials with dielectric losses of less than $50 \cdot 10^{-6}$ at 60 MHz. The precision is about $2 \cdot 10^{-6}$ at 30 and 60 MHz.

The key points of its excellent performances are :

- the incorporation of a high frequency amplifier in the measuring head, which means that corrections for parasite effects at the connections were not necessary.
- the replacement of the tuning condensers by "Varicap" diodes which have variable capacity as a function of the inverse polarisation voltage applied.
- the preparation of a high quality 60 MHz self induction coil with fine silver wires.

Sample preparation

The samples were compression molded discs of 50 mm diameter and 1.2 mm thickness. Molding temperature was 180°C, molding pressure 150 kg/cm², pressure holding time 1 minute (in the case of samples without antioxidants : 170°C, 25 seconds). If not indicated, samples were cooled under pressure to room temperature at a cooling rate of 30°C/min.

Each value indicated in this paper is an average of 5 measurements on samples, after a minimum of 48 hours in standard conditions (23°C, 40% R.H.).

RELATIONSHIP BETWEEN FREQUENCY AND DIELECTRIC LOSS

Polyolefins are essentially non-polar polymers and for this reason show relatively low dielectric losses. However, generally 3 relaxation peaks (α , β , γ) are found depending on frequency and temperature.

Whilst low density polyethylene losses increase with frequency in the 1 to 60 MHz range (fig. 1), polypropylene shows sharply decreasing losses. This may be attributed to a shift of the β -absorption peak towards the lower frequencies and to the absence of a γ -peak (1). Our measurements with polypropylene homopolymers show that loss factors below $50 \cdot 10^{-6}$ are possible with very pure stabilized polypropylene at 60 MHz.

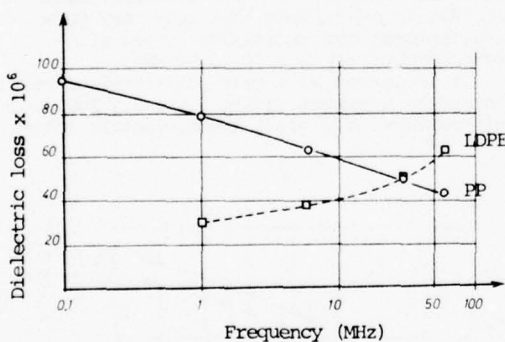


Fig. 1 : Dielectric loss as a function of frequency for PP (LACQTENE P commercial grade for electrical applications) and LDPE (LACQTENE submarine cable grade)

RELATIONSHIP BETWEEN POLYPROPYLENE STRUCTURE AND DIELECTRIC LOSS

Influence of Crystallinity

As propylene is a semi-crystalline polymer, its end use properties are influenced by the total amount of crystallinity and the spherulite size. Both are a function of cooling conditions during sample preparation.

DSC-data show that slow sample cooling conditions lead to more crystalline samples and therefore lower dielectric loss (table 1).

It has generally been admitted that polypropylene continues to change its crystalline structure, even several days after an extrusion or molding step. We therefore thought that dielectric loss could change as a function of time, after compression molding the test samples. However, for polypropylene homopolymer, as for low density polyethylene, we found no significant change of the loss angle on samples measured immediately after compression molding or after up to 3 weeks storage under standard conditions. (fig. 2).

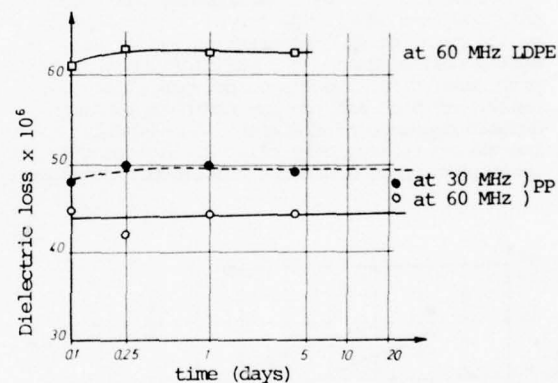


Fig. 2 : Influence of time between sample preparation and measurements on dielectric loss for PP and a submarine cable grade LDPE.

We suppose that the samples cooled after compression molding, at a cooling rate of 30°C/min., which is relatively slow, had already a highly crystalline structure immediately after sample preparation. Quicker cooling should result in less crystalline samples immediately after molding, and might therefore show increasing crystallinity during storage, thus giving decreasing dielectric losses as a function of time.

| Resin | Frequency Cooling rate | Dielectric loss $\times 10^{-6}$ | | | |
|----------------------------------|---------------------------|----------------------------------|----------|-----------|----------|
| | | at 30 MHz | | at 60 MHz | |
| | | 30° C/min | 1° C/min | 30° C/min | 1° C/min |
| PP | | 53 | 50 | 49 | 41 |
| E/P block copolymer (4.8% E) | | 96 | 82 | 92 | 86 |
| E/P random copolymer (1.2% E) | | 62 | 52 | 60 | 51 |

Table 1. : Dielectric loss for PP and E/P copolymers for different cooling rates at 30 and 60 MHz.

Influence of Atactic Polypropylene Content

Commercially available polypropylene contains generally between 92 and 98% of highly crystalline, stereoregular isotactic polypropylene and 2 to 8% of amorphous, waxy atactic polypropylene (APP). The amount of APP depends on the catalyst and the deashing system used during polymerisation and purification of polypropylene. First results on polypropylene with relatively high ash content indicate a considerable decrease of dielectric losses with increasing isotacticity (fig. 3), due to the lower portion of amorphous atactic polypropylene.

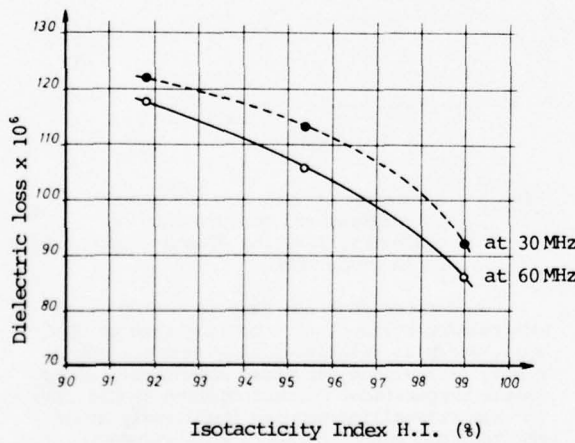


Fig. 3 : Influence of isotacticity index (heptane insolubles) on dielectric loss for PP.

Influence of Catalyst Residues

Polypropylene and ethylene - propylene copolymers are obtained in a polymerisation process where the monomers are activated by a catalyst, generally titanium-tri-chloride ($TiCl_3$) and a catalyst, di-ethyl-aluminium chloride (DEAC). For this reason, all polypropylene resins contain traces of titanium, aluminium and chlorides in various forms, in spite of a more or less efficient deashing operation.

Especially high chloride and titanium levels give a dramatic increase of dielectric losses (fig. 4). It can be seen that only very pure polypropylenes show decreasing losses with frequency going up from 30 to 60 MHz.

It is obvious that only polypropylene resins, produced by a process giving extremely low catalyst residues, will yield low dielectric losses.

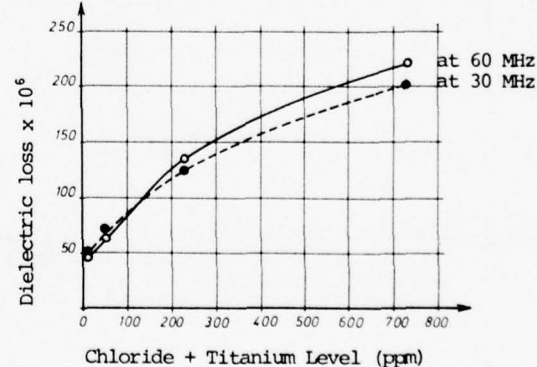


Fig. 4 : Dielectric loss as a function of residual chloride and titanium level in PP.

Influence of Additives

Because of the presence of the methyl groups in the polypropylene polymer chain, polypropylene is relatively sensitive to degradation under the influence of heat, light, oxygen and mechanical stress. High catalyst residue level is an additional reason for degradation.

Therefore, all commercial polypropylene resins are stabilized by radical scavengers (generally hindered phenols) and eventually also by peroxide decomposers. In addition, contact of polypropylene with certain metals, such as copper, accelerates the degradation process, if it is not inhibited by metal deactivators.

Another additive commonly found in polypropylene is calcium stearate. It is generally used for its ability to neutralise chlorides, which in the form of hydrochloric acid could cause corrosion problems on extrusion tools.

We have investigated the influence of these additives on the dielectric loss of polypropylene homopolymers. Previous experience with polyethylene had shown (2) that one of the anti-oxidants with very few effect on electrical properties was 1,3,5-trimethyl-2,4,6-tris [3,5-di-tert-butyl-4-hydroxybenzyl] benzene = IONOX 330.

Table 2 shows that it causes a slight increase of dielectric losses at a 0.1% level.

| Antioxidant level (%) | Dielectric loss $\times 10^{-6}$ | |
|-----------------------|----------------------------------|-----------|
| | at 30 MHz | at 60 MHz |
| 0 | 41 | 40 |
| 0.1 | 52 | 46 |

Table 2 : Influence of antioxidant (IONOX 330) on dielectric loss of PP, MFI 3, Calcium stearate concentration was 0.01%.

Two commercially available metal deactivators have been used :

- Bis (3,5 ditert-butyl-4-hydroxy-phenyl hydrazine propionic) = IRGANOX MD 1024.
- Tris [2-tert. butyl-4-thio (2' methyl-4' hydroxy-5' tert-butyl) phenyl-5-methyl] phenylphosphite = VP OSP 1.

Figure 5 shows that the first metal deactivator tends to give a lower increase of about $4 \cdot 10^{-6}$ at a medium concentration level (0.2%), whilst at 0.5% level the increase is the same for both additives.

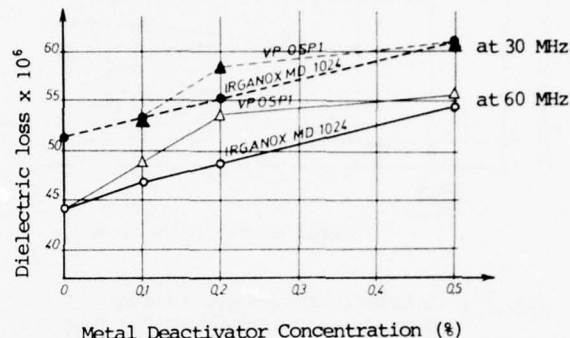


Fig. 5 : Influence of metal deactivators IRGANOX MD 1024 and VP OSP 1 on dielectric loss of PP, MFI 3, with 0.1% IONOX 330 and 0.01% of calcium stearate.

High calcium stearate content causes considerable increase of dielectric loss. It is therefore important to limit the level of this additive, and consequently use only low chloride level, highly purified polypropylene for applications where very low dielectric loss is required.

Influence of Thermal and Mechanical Degradation

As discussed in the previous chapter, polypropylene can be degraded under the influence of heat and shear stress during an extrusion step. A medium stabilized, low catalyst residue polypropylene homopolymer was exposed to subsequent multiple extrusions at 200°C, in a laboratory Buss-Cokneader which develops a high shear action.

Figure 6 shows that a marked increase of dielectric loss is only observed from the third and subsequent extrusion steps at 60 MHz, whilst the increase at 30 MHz is low, even after five extrusions.

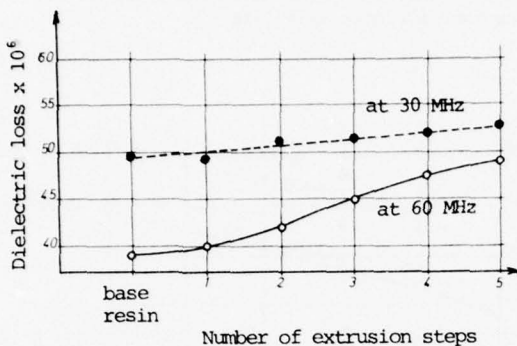


Fig. 6 : Influence of subsequent multiple extrusion steps on dielectric loss of PP, MFI of base resin 2.1, antioxidant IONOX 330 0.1%, calcium stearate 0.01%.

At the same time, we measured a slight melt flow increase from 2.1 for the base resin to 2.3, after five subsequent extrusion steps. This is a simple way of controlling molecular weight decrease by degradation. On the other hand, no significant evolution of the carbonyl group absorption peak in infrared spectroscopy could be found.

We can conclude that intensive mixing during extrusion essentially causes chain scission, thus giving only a slight increase of dielectric losses.

Influence of Water Uptake

Intensive work has been done already on the conditions of water uptake of low density polyethylene and its influence on dielectric properties (2), (3). It has been shown that unexpectedly high cable attenuations can result from water entrapment during the cable manufacturing process. Thus, more water than normally soluble in cold low density polyethylene was found in samples containing very small cavities created during the cooling step of the molten polymer.

Figure 7 shows, as a function of time, the dielectric loss for samples exposed initially either 3 hours or 3 days to steam at 100°C and subsequently kept in both cases at 23°C and 40% relative humidity, before the first measurement.

It appears that steam exposure of the 1.2 mm thick test samples lead to about 10 times higher dielectric loss, immediately after exposure, than found on untreated samples. This increase was in the same order of magnitude after 3 hours and 3 days steam exposure. For the samples exposed only 3 hours, dielectric loss falls quickly to a level of less than $50 \cdot 10^{-6}$, as usual with low catalyst residue polypropylenes.

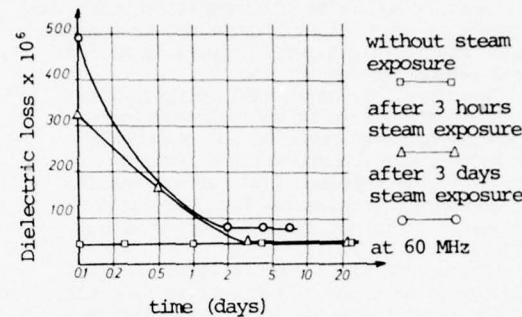


Fig. 7 : Influence of 3 hours or 3 days steam exposure on dielectric loss of PP, MFI 3, containing 0.1% of antioxidant IONOX 330 and 0.01% of calcium stearate.

However, samples submitted to long steam exposure during 3 days, remained at dielectric loss levels of about $80 \cdot 10^{-6}$ after one week. Even after additional vacuum oven drying during 16 hours at 70°C and 10^{-1} Torr, dielectric losses remained still relatively high ($81 \cdot 10^{-6}$ at 30 MHz and $76 \cdot 10^{-6}$ at 60 MHz compared to 83 and 78 respectively without additional vacuum oven drying).

We did not measure the water content of the steam treated samples. Nevertheless, we assume that the very long steam treatment might have caused void formation due to the water being no longer soluble in the polymer during sample cooling. We do not believe that oxidation can have caused the high remaining dielectric losses. If the hypothesis of void formation by non-soluble water is right, DSC-measurements should show a transition at 0°C, corresponding to the heat of fusion of ice in the voids. More extensive work is still necessary in this field.

Influence of Ethylene Content in Ethylene - Polypropylene Block Copolymers

Copolymerisation of ethylene and propylene is very widely used, especially for improving low temperature impact performance of poly-propylene. The so-called block copolymers contain not only blocks of polypropylene homopolymer and high density polyethylene, but also portions having the structure of ethylene - propylene rubber. These three different types of polymer can be found on the same molecular chain, but also very often side by side on different chains in a very homogeneous mixture, as these blends form in situ during the polymerisation stage.

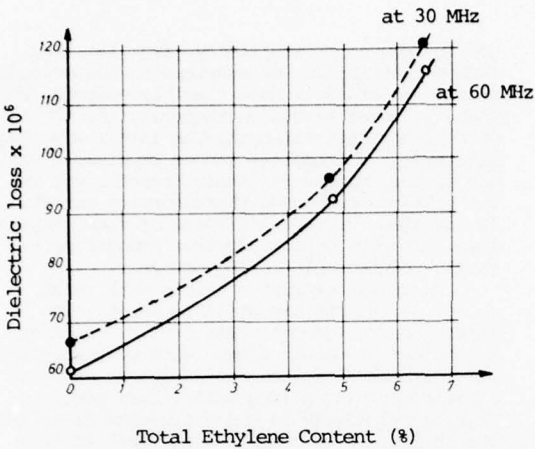


Fig. 8 : Dielectric loss as a function of total ethylene content in E/P block copolymers, MFI 5, antioxidant 2,6-di-tert-butyl-para-cresol (DBPC) 0.1%, calcium stearate 0.1%.

As expected, dielectric loss increases sharply with the total ethylene content of block copolymers (fig. 8). This behaviour is probably linked to the increasing amount of the rubbery ethylene - propylene phase. For the two block copolymers shown in figure 8, we determined by a selective extraction method the total amount of the rubber phase. We found as much as 1.9% for the 4.8% E-copolymer, and 2.6% for the 6.5% E-copolymer.

Influence of Ethylene Content in Ethylene - Propylene Random Copolymers

Ethylene - propylene random copolymers do not contain crystalline polyethylene blocks as block copolymers, but only molecular chains with one (or maximum up to five consecutive) ethylene molecules in a random distribution on the polymer chain, which is basically formed of 97 to 99% of propylene (true random copolymer). In addition to the high amount of true random copolymer, commercially available ethylene - propylene random copolymers contain small portions of ethylene - propylene rubber with relatively low ethylene content.

We assume that, as in ethylene - propylene block copolymers, the ethylene - propylene rubber phase is the reason for the increase of dielectric losses with total ethylene content in ethylene - propylene random copolymers (fig. 9).

A reduction of the ethylene - propylene rubber phase can be achieved by using new highly stereospecific catalyst systems and by partially extracting ethylene - propylene rubber by solvents, during the deashing step after polymerisation. We believe that it is therefore possible to prepare ethylene - propylene random copolymers with about 1 to 2% total ethylene content with dielectric losses only slightly higher than those of polypropylene homopolymers. These investigations are currently under way.

Random copolymers may offer advantages compared to homopolymers during cable extrusion (see chapter "Processing Problems with Polypropylene" below).

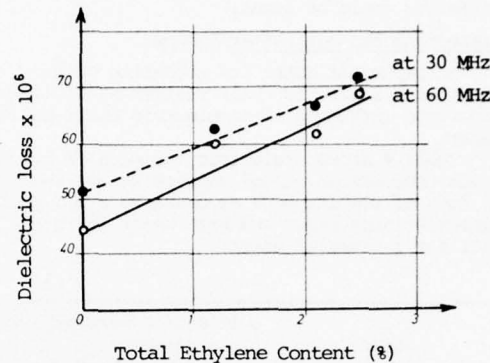


Fig. 9 : Dielectric loss as a function of total ethylene content in E/P random copolymers, MFI 1 - 2, antioxidant IONOX 330 0.1%, calcium stearate 0.1%. The 1.2% E-copolymer contained 0.2% of DBPC instead of IONOX (giving relatively high loss values).

DIELECTRIC STRENGTH

High dielectric strength is an important factor, not only for energy cables, but also for submarine cables, as supply voltages of the repeaters increase with the frequency of the systems.

Dielectric Strength before Ageing

Dielectric strength has been measured for alternative voltage at 50 cycles/sec and a voltage increase of 2.1 KV/sec on 0.3 mm-thick extruded samples between plane electrodes in condensor oil.

Values given in table 3 are averages of at least 20 breakdowns for each resin.

| Resin | Dielectric strength (kV/mm) |
|-------------------------------|-----------------------------|
| PP | 78.2 |
| E/P block copolymer (4.8% E) | 79.1 |
| E/P random copolymer (2.1% E) | 75.2 |
| LDPE (power cable grade) | 78 |

Table 3 : Dielectric strength for PP, E/P copolymers and LDPE.

The dielectric strength of all resins tested were in the same range as that of low density polyethylene, with random copolymers showing slightly lower values. After 12 days storage of the samples under standard conditions, no variation could be found.

Dielectric Strength after Ageing

An important point for submarine cable insulation resins is their resistance to ageing under the influence of an electric field and salt water.

Table 4 shows dielectric strength of 0.5 mm thick compression molded samples before and after 26 days of simultaneous exposure to a 2.5 kV/mm direct voltage field and salt water (30 g of NaCl for 1 liter of water).

| Resin | Dielectric strength (kV/mm) | |
|----------------------------------|--------------------------------|-----------------|
| | before ageing | after ageing |
| PP | 46.5 | 44.6 |
| E/P random copolymer (2.1% E) | 45 | 43.2 |
| LDPE (submarine cable grade) | 49 | 43 |

Table 4 : Dielectric strength before and after ageing in salt water and direct voltage field.

The results show that polypropylene is slightly less subject to ageing in salt water and a direct voltage field than a comparative low density polyethylene.

PROCESSING PROBLEMS WITH POLYPROPYLENE

For thick cable insulation, polypropylene reveals three major disadvantages which are :

- strong tendency to void formation,
- low melt strength and
- high rigidity.

Strong tendency to void formation stems from its highly crystalline character giving very high shrinkage during crystallisation. In addition, its low thermal conductivity creates very high temperature gradients during the cable cooling operation. The relatively low melt strength of polypropylene homopolymers may cause conductor eccentricity and high rigidity can lead to problems in cable laying linked to limited bending radius.

We believe that these difficulties might be overcome by adequate extrusion and cooling techniques and the use of ethylene - propylene random copolymers, which show less tendency to void formation than polypropylene homopolymers,

due to reduced crystallinity (fig. 10). The random distribution of ethylene on the molecular chain also yields a more flexible polymer, thus enabling lower extrusion temperatures, combined with higher melt strength. The latter advantage of ethylene - propylene random copolymers was one of the reasons for their breakthrough in the bottle blowing and thermoforming market. In addition, reduced stiffness at room temperature compared to polypropylene homopolymers should reduce cable laying problems.

Extensive extrusion trials with thick cable insulations are still necessary. The first results indicate that a void free insulation can be obtained even with polypropylene homopolymers at low extrusion speeds and with a die comprising a long cooled land portion. Thus, a relatively high die pressure gives the possibility of compensating for part of the shrinkage during the initial cooling step. Different cooling techniques are under investigation, such as subsequent water baths with decreasing temperature at atmospheric or higher pressure.

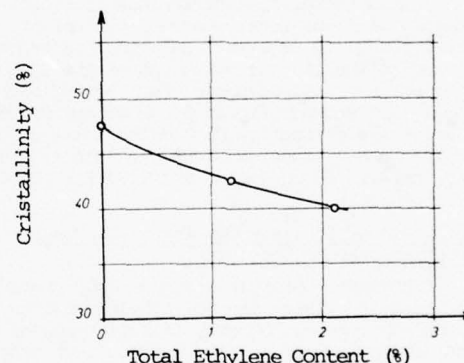


Fig. 10. : Cristallinity as a function of total ethylene content in E/P random copolymers, values based on DSC-data of samples with the same thermal history (quench in water at 0° C).

CONCLUSIONS

It has been shown that polypropylene with very low catalyst residue level has loss factors of less than $50 \cdot 10^{-6}$ at 60 MHz. Polypropylene is therefore an interesting candidate for future submarine cable insulation in systems designed for very high frequencies, provided void forming problems in thick layer insulation can be overcome.

Two complementary ways of solving these extrusion problems have been indicated : one is the use of ethylene - propylene random copolymers reducing crystallinity without affecting the electrical properties too much and the other is the development of a modified extrusion technique particularly suitable for polypropylene.

ACKNOWLEDGEMENTS

The authors wish to thank the personnel of the ATO Chimie and Marcoussis Research Laboratories for their collaboration and especially Gilbert Marie for the preparation of raw materials and helpful discussions, and René Destrée and Daniel D. Decker for the modification of the Q-meter for high frequencies.

REFERENCES

- (1) K.A. Buckingham and W. Reddish, Proceedings IEE, vol. 114, Nr. 11, Nov. 1967, p. 1810 - 1814.
- (2) H. Kishi, Y. Yamazaki, T. Nagasawa, H. Takashima, H. Fujita and I. Tsurutani, 25th International Wire and Cable Symposium 1976, p. 47 - 55.
- (3) J. H. Daane, H.E. Bair, G.E. Johnson, E.W. Anderson, 25th International Wire and Cable Symposium 1976, p. 296 - 301.



Dieter H. BUERKLE
(Speaker)

D. H. Buerkle received his Dipl. Ing. degree in Plastics Technology in 1969 from Technische Hochschule Stuttgart, Germany. He then joined Kabel und Draht GmbH, Mannheim Germany, where he was concerned with cable manufacturing problems. Since 1973 he has worked with ATO Chimie, France, on research on plastics extrusion technology. Since 1975 he has been responsible for polypropylene product development.



Jean-Claude REBEILLE

J. C. Rébeillé received his degree in Chemical Engineering at the University of Strasbourg, France. He then joined ATO Chimie in 1967, where he was involved in fundamental research on polyolefins. He received his Dr. Ing. degree in 1970, from the University of Pau, France. He is now polyolefins research and development manager of ATO Chimie.



Jean-Claude BOBO

J.C. Bobo received his Ph. D. from the University of Paris, France, in 1964. He joined Compagnie Générale d'Electricité in 1966, where he is Head of the Electrical Laboratory.



Bernard L. HOCHON

B.L. Hochon is a graduate of Ecole Supérieure de Physique et Chimie Industrielle de Paris and obtained in 1973 a speciality degree in Polymer Science from the University of Paris, France. He then joined the research center of Compagnie Générale d'Electricité, where he is concerned with cable insulation studies (material properties and processing).

DYNAMIC WATERPROOF FILLING PROCESS MONITOR

J. A. HUDSON; A. K. LONG

CABLE & WIRE PRODUCT ENGINEERING CONTROL CENTER
WESTERN ELECTRIC COMPANY
NORCROSS, GEORGIA 30071

ABSTRACT

Due to the absence of an in-process waterproof filling monitor for waterproof cable, a problem in the past has been to determine the filling effectiveness before a considerable amount of faulty cable is manufactured. This on-line monitoring system, including a microprocessor, periodically measures the mutual capacitance along with accumulated footage and relates this data to determine filling effectiveness.

INTRODUCTION

Communications multipair cable is made waterproof during the manufacturing process by filling the pair interstices of the cable with a waterproof compound similar to petroleum jelly. At Western Electric this compound is applied to the cable in tandem with and immediately before the sheathing process by passing the cable core through a chamber where the compound is at its melt temperature and under pressure.

PROBLEM AND SOLUTION

Obviously it is difficult to determine whether the filling process is completely filling the cable, since the cable is immediately sheathed and jacketed. Manufacturing has traditionally relied on testing finished cable end samples to determine this completeness by measuring the volume of filling material in a sample or measuring its restriction to water flow. The Dynamic Waterproof Filling Process Monitor (DWPFM) uses a technique which is based on the fact that as filling compound is applied to a cable pair, the mutual capacitance increases by an amount proportional to the amount of compound applied. This mutual capacitance is measured on an inside and an outside pair during the filling process and then related to the processed footage.

The mutual capacitance increase described above is due to the increase in dielectric constant when the air with a relative constant of 1.0 is replaced with a compound with a relative dielectric constant of 2.23. This increase in capacitance as the cable is filled is illustrated by the curve in Figure 1. The flat areas on the curve illustrate lengths where the process was not filling the cable. Since other process factors including tension and com-

pression also effect the mutual capacitance, a pair on the inside of the cable core which is usually the more difficult to fill is compared to a pair on the outside which is usually not difficult to fill. This tends to cancel out other variation factors which are assumed to be approximately equal for the two pairs. The processed footage information is determined by accumulating incremental length pulses from a transducer inherent to the sheathing line.

The filling is evaluated and compared with a quantity called Relative Filling Effectiveness (RFE). This quantity is derived from relating the amount of increase in capacitance to the processed footage and is a measure of the percent of fill immediately surrounding the pair being measured. Appendix 1 is a derivation of this relationship based on relative dielectric constants of composite materials. Figure 2 is a curve showing RFE as a function of the percent difference in mutual capacitance between an outside pair and a standard average filled cable value or between an inside and an outside pair. This curve is a plot of the equation derived in Appendix 1.

Several experimental cables were filled at various levels of fill to correlate the monitor technique results with other conventional tests. The monitor RFE results did not correlate with the volume measurement percent fill or the delta capacitance tests. These tests have since been discontinued on most cables. The monitor RFE results did correlate with the core flow tests, which is a test which exposes a three-foot sample of finished filled cable to an actual head of water. It was determined from these experimental cables that samples from lengths of cable with RFE values shown below produced the corresponding core flow results:

| <u>RFE</u> | <u>Core Flow Results</u> |
|------------|--------------------------------------|
| 90 - 100 | All Passing |
| 80 - 90 | Marginal: Some Passing, Some Failing |
| Below 80 | All Failing |

IMPLEMENTATION

Figure 3 is a general block diagram of the monitor system. A microprocessor was selected for this monitor to provide data acquisition control and for computations involved in the analysis and presentation of the results. The data from measuring mutual capacitance on two pairs, the line speed data and the operator instructions to the monitor are processed by the microprocessor and results are displayed to the operator on console front panel displays and a recorder printout. The displayed result is the RFE for both the inside and outside pairs as a function of the processed footage. Figure 4 is an example of the recorded printout showing first the RFE for the total amount of cable processed up to that point for an outside and an inside pair and secondly the RFE values for the last 40 feet which has gone through the process. These values are updated and printed out each 10 feet.

Figure 5 is a front view of the monitor console showing the LED displays and operator push-button controls. The production operator has only limited control of the monitor to start the test on either of two payoffs, restart the test or stop the test.

Figure 6 shows the data coupler assembly mounted on a cable payoff stand. As shown a contactless magnetic coupling system is used to transfer power into and signals out of the measurement-transmitter circuits which are mounted on the rotating core truck brake arm.

APPLICATIONS

Presently, these DWFPMS systems are used primarily as engineering tools to evaluate changes to and new designs of the filling process facilities, maximizing line speed, evaluating changes in filling chamber pressure and temperature and most importantly for evaluating the effectiveness in filling new designs of larger pair size cables which are being run for the first time. The filling effectiveness is stable once the proper operating parameters of temperature, pressure and line speed are established for a particular design of cable.

The monitor displays immediate results to the operator to prompt changes during the process and records the results as a function of length. The recorded results also serve as a permanent profile of the cable if there is a need to cut out marginal lengths of the finished cable.

SUMMARY

A system has been built for in-process monitoring of the effectiveness of waterproof filling process facilities. These systems are being used as engineering tools in the design of process facilities, the design of new waterproof cables, and are helping to provide quality waterproof cable for the Bell System.

ACKNOWLEDGEMENTS

We acknowledge the assistance and advice of Mr. R. A. Levandoski of our engineering organization in the development of this system. We also acknowledge the assistance of other engineering and operating personnel at the Cable and Wire PECC as well as the Atlanta and Omaha Manufacturing Works in the development and prove-in of the system. Ursula Werl's assistance in typing and proofreading of the manuscript is appreciated.

REFERENCES

1. T. F. McIntosh, "Electrical Design of PIC Multipair Cable," Memorandum for File, Case 39603-49, July 2, 1973.

CAPACITANCE OF CABLE AS A FUNCTION OF WATERPROOF FILLING

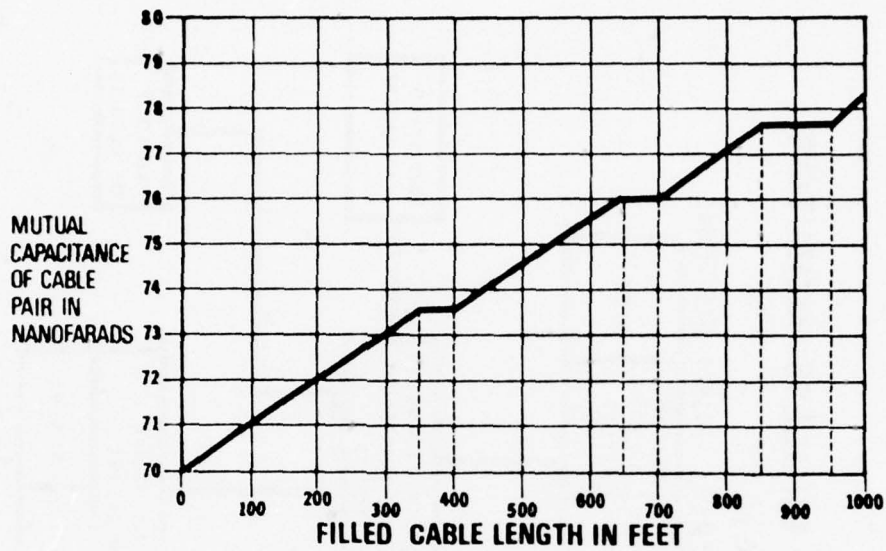


FIGURE 1.

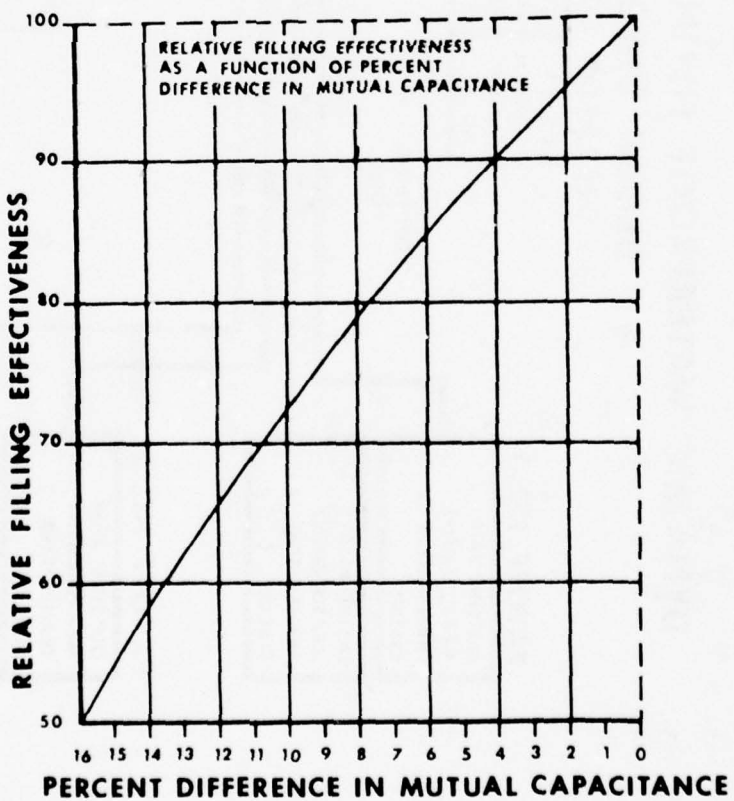


FIGURE 2.

**DYNAMIC WATERPROOF FILLING PROCESS MONITOR
BLOCK DIAGRAM**

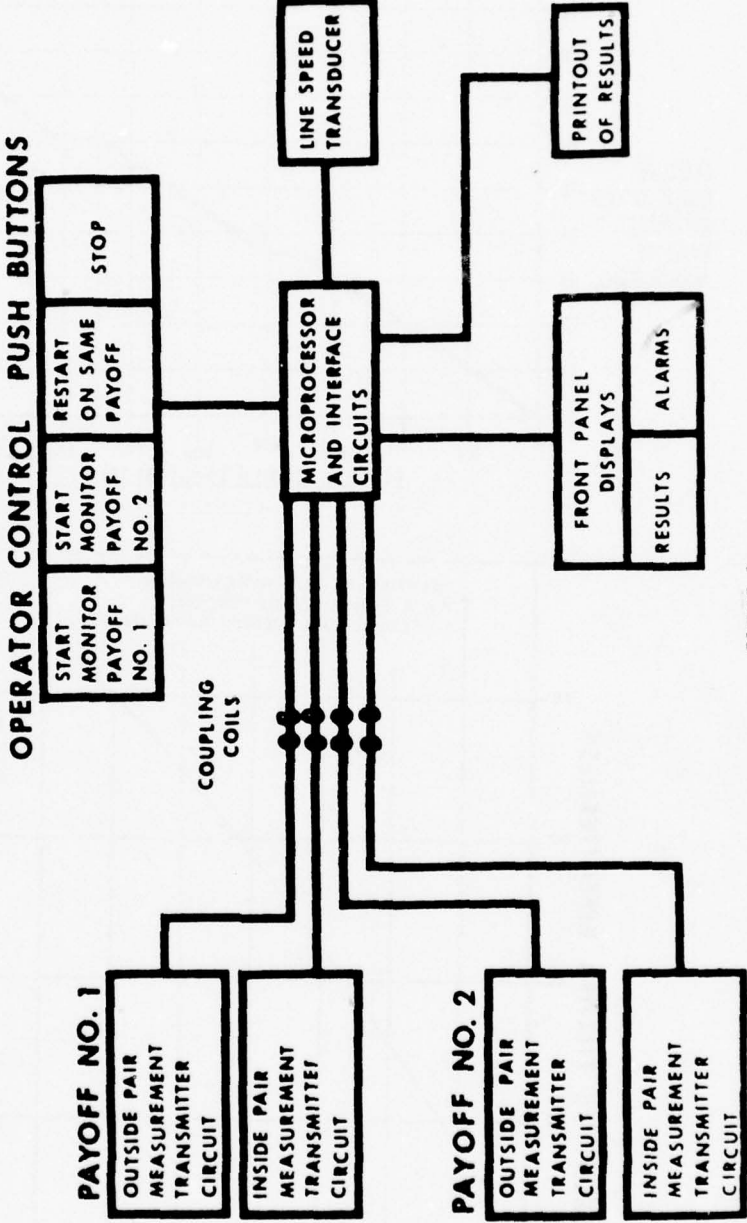


FIGURE 3.

DYNAMIC WATERPROOF FILLING PROCESS MONITOR
RESULTS PRINTOUT
RELATIVE FILLING EFFECTIVENESS

| OUTSIDE | | | INSIDE | | |
|---------|-------|--------|---------|-------|--------|
| FOOTAGE | TOTAL | SAMPLE | FOOTAGE | TOTAL | SAMPLE |
| 10 | 100 | 99 | 10 | 95 | 90 |
| 20 | 98 | 98 | 20 | 94 | 98 |
| 30 | 99 | 100 | 30 | 93 | 96 |
| 40 | 99 | 100 | 40 | 93 | 100 |

FIGURE 4.

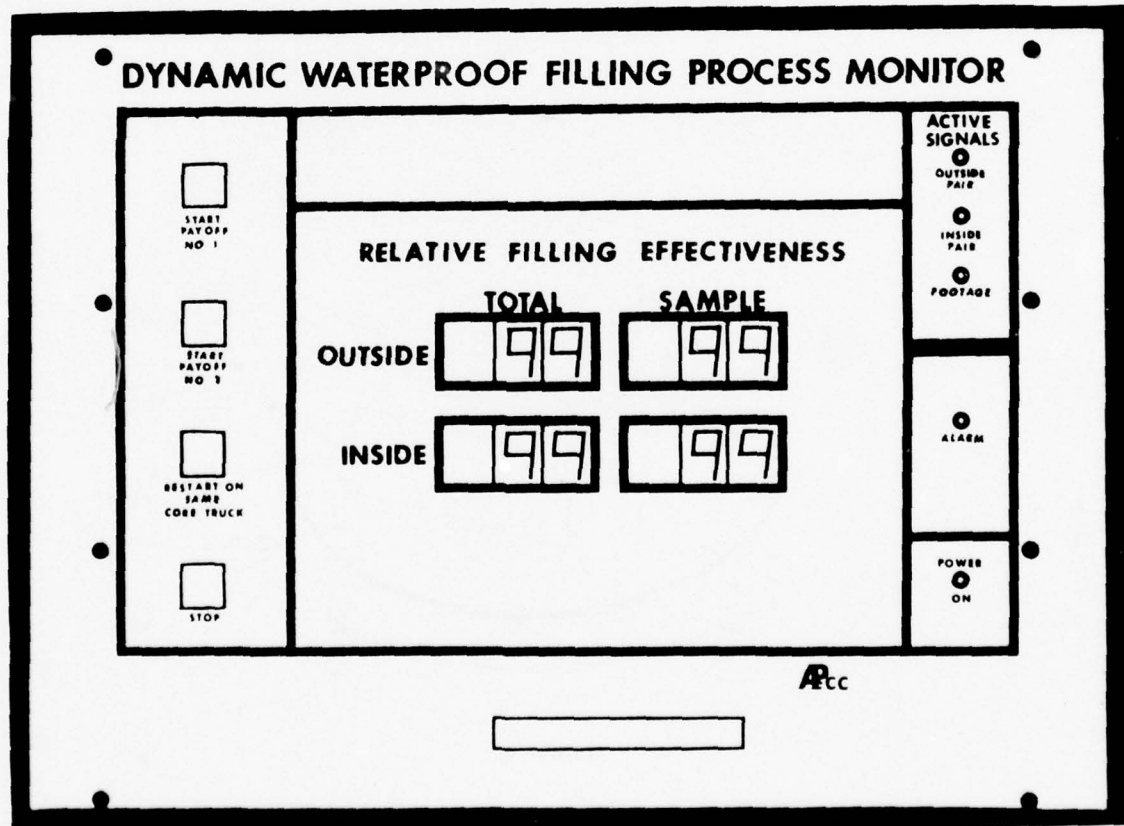


FIGURE 5.

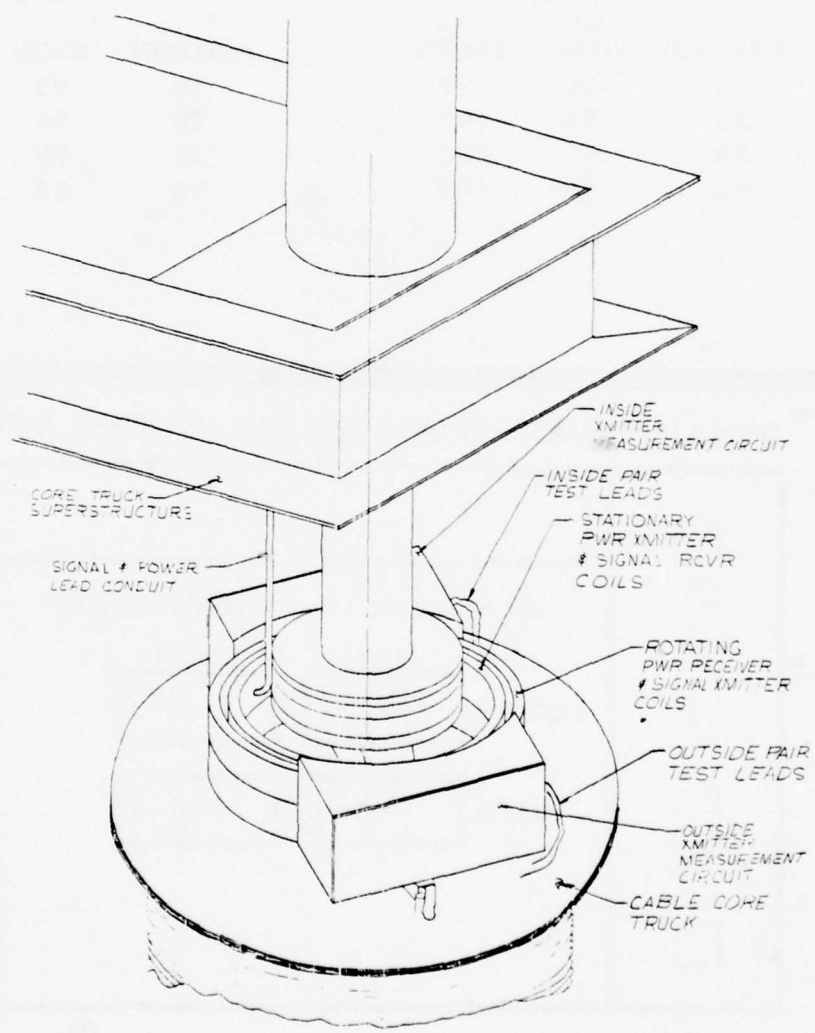


FIGURE 6.

APPENDIX I

Derivation of Relative Filling Effectiveness (RFE) as a function of percent difference in mutual capacitance of a pair to a standard value or to difference in inside and outside pairs. From Reference No. 1 we get the following equation:

$$E = E_I V_I + E_F V_F \quad \text{where:}$$

E_F = Relative Dielectric Constant of Composite Material

E_F = Relative Dielectric Constant of Filling

E_I = Relative Dielectric Constant of Conductor Insulating Material

V_I = Relative Volume of Insulating Material

V_F = Relative Volume of Filling Material

(1)

For filled cable E , V_I and V_F are unknown in general. E can be measured for 100% fill and no fill situations. E_F is known for 100% fill and no fill situations. E_I is known.

So V_F and V_I can be determined by substituting known values of E_I , E_F .

$$V_F = \frac{E_I - RE_I}{RE_F \text{ max.} - RE_I + E_I - EF \text{ min.}}$$

where:

$$R = \frac{E_I}{E_2} = \frac{\text{Mutual Capacitance With No Fill}}{\text{Mutual Capacitance With 100% Fill}}$$

E_F max. = E_F With 100% Fill

E_F min. = E_F With No Fill

then:

$$V_I = 1 - V_F$$

Now solving equation Number 1 for E_F :

$$E_F = \frac{E - E_I \left[1 - (E_I - RE_I) / (RE_F \text{ max.} - RE_I + E_I - EF \text{ min.}) \right]}{E_I - RE_I / (RE_F \text{ max.} - RE_I + E_I - EF \text{ min.})}$$

and differentiating:

$$\Delta E_F = \frac{\Delta E (RE_F \text{ max.} - RE_I + E_I - EF \text{ min.})}{(E_I - RE_I)}$$

Then substituting values for a specific type of multipair cable:

$$E_I = 2.24$$

$$E_F \text{ max.} = 2.22$$

$$E_F \text{ min.} = 1.00$$

Mutual capacitance measured for no fill = 69.25 nanofarads

Mutual capacitance measured for 100% fill = 82.27 nanofarads

then $R = .842$

$$\text{and } \% \Delta E_F = \% \Delta E (3.456)$$

(2)

Now we have the percent change in the relative dielectric constant of the fillable area of the cable as a function of the percent difference in the composite relative dielectric constant.

Now we will use the following equation from Reference No. 1 to derive the Relative Filling Effectiveness as a function of the $\% \Delta E_F$.

$$\frac{(E_F - E_F \text{ max.})}{(E_F + 2 E_F \text{ max.})} = \left(1 - \frac{RFE}{50} \right) \frac{(1 - E_F \text{ max.})}{(1 + 2 E_F \text{ max.})}$$

or:

$$RFE = 100 \left[1 - \frac{(E_F - E_F \text{ max.}) (1 + 2 E_F \text{ max.})}{(E_F + 2 E_F \text{ max.}) (1 - E_F \text{ max.})} \right] \quad (3)$$

Now using Equation No. 2 we have:

$$E_F = E_F \text{ max.} \left(1 - \frac{3.456 \% \Delta E}{100} \right)$$

Substituting this into Equation No. 3, along with E_F max. = 2.22, we can simplify to:

$$RFE = 100 - 50 \left[\frac{1}{\frac{19.465 - .224}{\% \Delta E}} \right]$$



J. A. Hudson is a development engineer at the Western Electric Company's Cable and Wire Product Engineering Control Center. He received his BS and MS degrees in electrical engineering from the Georgia Institute of Technology in 1965 and 1967. Since joining Western Electric in 1970, he has done both analog and digital hardware design. For relaxation, he enjoys tennis and backpacking.



A. Kyle Long is a senior development engineer at the Western Electric Company's Cable and Wire Product Engineering Control Center, where he has been involved with the development of test sets for the electrical and physical parameters of cable. He received his BS degree in electrical engineering from the University of Tennessee in 1964 and served two years in the Army Signal Corp before joining Western Electric in 1966. He is married with four children. His hobbies include fishing and sports.

High-Speed SZ Twisting and Stranding Machines Using Straight Accumulators

Dieter Vogelsberg

Siemens AG
Neustadt/Coburg, Germany

Summary

On the basis of a new SZ method it has been possible to construct very simple twisting strander lines operating at the same manufacturing speed as conventional pair or quad twisting machines. The new method is characterized by a straight accumulator with a twisting support at each end rotating alternately. The mechanical stress to which the wire pairs or quads are subjected in the twisting operation -which proceeds at a rate of approximately 3000 twists per minute- is scarcely greater than when the conductors are simply pulled off the supply reels. Using a machine constructed for various unit designs, up to 13 conductor pairs or quads can be produced side by side and stranded to form a unit.

Introduction

For economic reasons, increasing use is being made of twisting strander lines for manufacturing communication cables. With this equipment it is possible for complete units consisting of, say, 10 pairs or 5 star quads to be manufactured from individual wires in a single operation. Special advantages are offered by twisting strander lines in which the pay-off reels or pair packs are stationary and can be changed while the machine is operating. These strander lines have very small down-times and hence a high overall efficiency, especially when double pay-off strands are used, permitting continuous pay-off operation (Fig. 1).

A prerequisite for this mode of operation is SZ twisting of the wire pairs or star quads, i.e. stranding with a periodic reverse of lay. Suitable methods

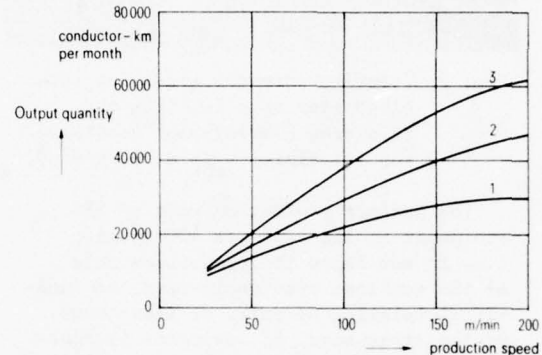


Fig. 1 Output of twisting strander lines (10-pair or 5-quads units with 0.4 mm conductor diameter, 3-shift operation)
1 with single pay-off stand
2 with double pay-off stand
3 with double pay-off stand and continuous pay-off operation

and equipment were described in the 1971 and 1974 symposia, and they have proven successful in years of current production 2,3.

At Siemens, for instance, all local feeder and distribution cables for the Deutsche Bundespost are manufactured with combined twisting and stranding machines using "breathing" accumulators 3 (Fig. 2).

Our experience has shown that the quality of cables manufactured with SZ equipment is just as good as that of cables twisted according to conventional methods. There are also no known disadvantages as regards practical application and installation.

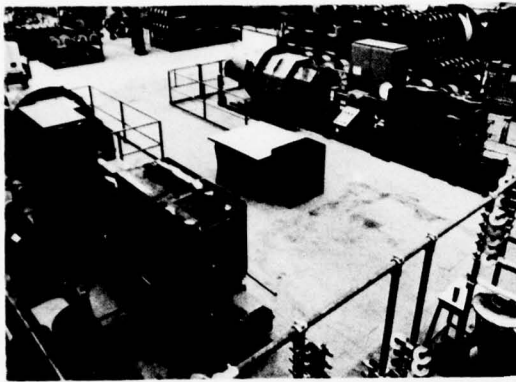


Fig. 2 Twisting strander lines for combined star quad twisting and stranding ("breathing" accumulator principle, $v_{max} = 100 \text{ m/min}$)

The maximum production rate of SZ equipment in the past was 100 m/min., i.e. it was below the production rate of the machines previously used for individual twisting of pairs or star quads. On the other hand, SZ equipment is smaller and lighter than conventional twisting and stranding machines, and this suggested that the potential of SZ twisting and stranding had so far not been fully exploited. Consequently, plans were made to develop a new generation of SZ equipment designed to match the operation speed of conventional individual twisting machines and so reduce the amount of equipment required for manufacturing local cables.

A reduction in the amount of equipment is of particular interest in cases where—as in the U.S.A. or France, for instance—25 pairs or 14 star quads are to be simultaneously produced and stranded to form a unit.

This paper describes how the problem was solved. It resulted in a new SZ method which is suitable for wire pairs and star quads alike. A very effective twisting and stranding process has been achieved by simple means, and the mechanical strain to which the individual wires are subjected is not greater than when they are simply pulled off supply reels. The equipment constructed on the basis of the new method is particularly easy to operate, requires little maintenance, and operates

at twice the speed of the first generation of SZ equipment.

Basic considerations

Every SZ setup includes at least one accumulator which can store as many twists as are contained in a finished section of the twisted element having a constant direction of lay¹. The accumulator may be a roller-type accumulator, or it may be a straight or linear accumulator in which the elements being twisted are drawn along a straight path in the air (Fig. 3).

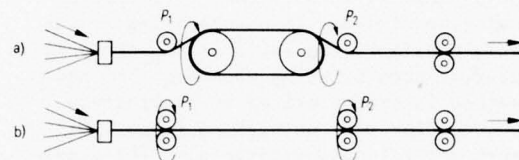


Fig. 3 Accumulators for SZ processes

- a) roller-type accumulator
- b) straight accumulator

With the aid of the two rotating twisting supports P_1 and P_2 , the elements are twisted as they enter the accumulator and as they leave it. The two twisting processes act in opposite directions.

In order to realize SZ twisting, one of the process parameters involved is changed, preferably periodically, in such a way that the two opposite twisting processes at the entrance and exit of the accumulator do not cancel each other out but complement each other such that the number of twists per length in the finished twisted element is other than zero. SZ twisting can be realized by altering the rotation of a twisting support or changing its position, or by altering the relative rate at which the elements enter or leave the accumulator.

For high-speed SZ twisting and stranding, the straight accumulators illustrated in Fig. 3b are now considered the most suitable because they impose low centrifugal stress on the twisted elements. The length of the accumulators depends on the reversal distance, which may only be a few meters for

pairs or star quads. Straight accumulators of this length are easy to realize.

In some known versions of this type of accumulator the two twisting supports P_1 , P_2 have been combined to form a single support at the end of the accumulator section 4,5. In such cases, an abrupt alternation takes place in only one of the two twisting processes involved.

The new method

In order to achieve particularly effective twisting we use two separate twisting supports as shown in Fig. 3b 6. Both change their rotation synchronously at intervals corresponding to the length of the straight accumulator.

In this way both twisting processes are alternated abruptly at the entrance and exit of the accumulator. When the twisting supports are operating at the maximum rotation rate, and assuming comparable boundary conditions, the number of twists is twice that obtained with alternative solutions using only one rotating twisting support.

Even if these facts are not exploited to achieve faster pull-off rates, one has the advantage of being able to choose shorter pitches of lay which result, among other things, in improved crosstalk or bending properties of a cable.

The use of double twisting supports also results in a virtually constant pitch of lay in the twisted element, as in conventional twisting methods. Where communication cables are concerned, this makes it easier to solve decoupling problems. All experience relating to balancing of large-pair-count units can readily be applied to the makeup of SZ twisted and stranded cables.

Five-fold twisting equipment for pairs or star quads

Fig. 4 shows how the new method is applied for parallel production of 5 pairs or star quads, the twisting supports being represented by symbols. The individual insulated conductors run into a twisting closer and are twisted once alternately by the first twisting support. Each twisted element is drawn a few meters through the air. At the end of the accumulator the conductors are twisted again, in the opposite direction. The completed pairs

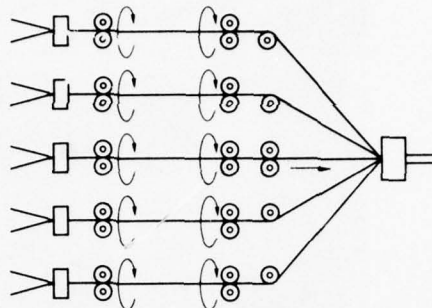


Fig. 4 5-fold twisting equipment with straight accumulators (double-twister principle)



Fig. 5 Pay-off stand and 5-fold twisting equipment with straight accumulators ($v_{\max} = 200 \text{ m/min}$)

or star quads are fed to a unit stranding machine (not shown here) which can operate either with constant lay or according to the SZ principle.

Fig. 5 shows this five-fold twisting equipment together with the pay-off stands. It is designed for conductor diameters of 0.3 to 0.8 mm.

The twisting supports are mounted in groups of five in stands. The alternating

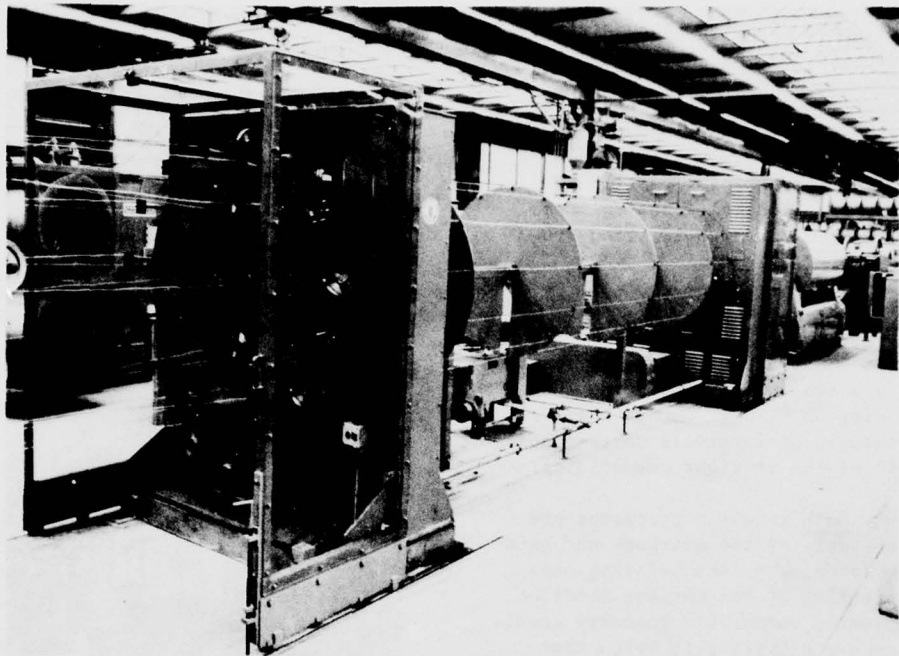


Fig.6 13-fold twisting equipment with straight accumulators (entrance side)

drive is performed by means of electromagnetic clutches which have worked well in machine tool applications with a high switching frequency and which guarantee a high degree of operational reliability.

The electromagnetic clutches of different twisted elements are switched over at different times so that the reversal points of different pairs or quads do not lie in the same cross-section of the completed unit.

Within each straight accumulator there are simple guides fitted in circular disks to prevent transverse vibrations of the twisted elements.

The completed pairs or quads pass over the white guiding rollers (see bottom of Fig. 5) to the following unit stranding machine. The maximum rotational speed of the twisting supports is 4000 min^{-1} . Without any great difficulty, therefore, a rate of approximately 3000 twists per minute can be achieved. The maximum production rate is about 200 m/min. When an appropriate rotational speed program is selected, the pairs or quads produced at a uniform speed have different pitches of lay in a range which corresponds roughly to that of conventional manufacture.

In the case of the combined star quadding and stranding operation, the capacitance unbalance quality was found to correspond to that of the time-proven system using "breathing" accumulators 3. The specifications of the Deutsche Bundespost according to 72 GU 1 to 4 for local feeder and distribution cables with a conductor diameter of 0.4 to 0.8 mm are reliably met. If necessary, the unbalance level can be improved by selecting particularly short pitches of lay.

13-fold twisting equipment for pairs or star quads

Many cable specifications call for units consisting of far more than five twisted elements. Units with 10, 12, 13 or 25 conductor pairs, or 7 or 14 star quads, may be required.

To permit cost-effective manufacture of such units with a conductor diameter of 0.4 to 0.9 mm, a 13-fold twisting equipment has been developed according to the new double-twister method (Fig. 6, 7). If more than 13 twisted elements are required in one unit, the equipment is used in two operations, or two such machines are set up in tandem. All 13 twisting devices are mounted in a circle.

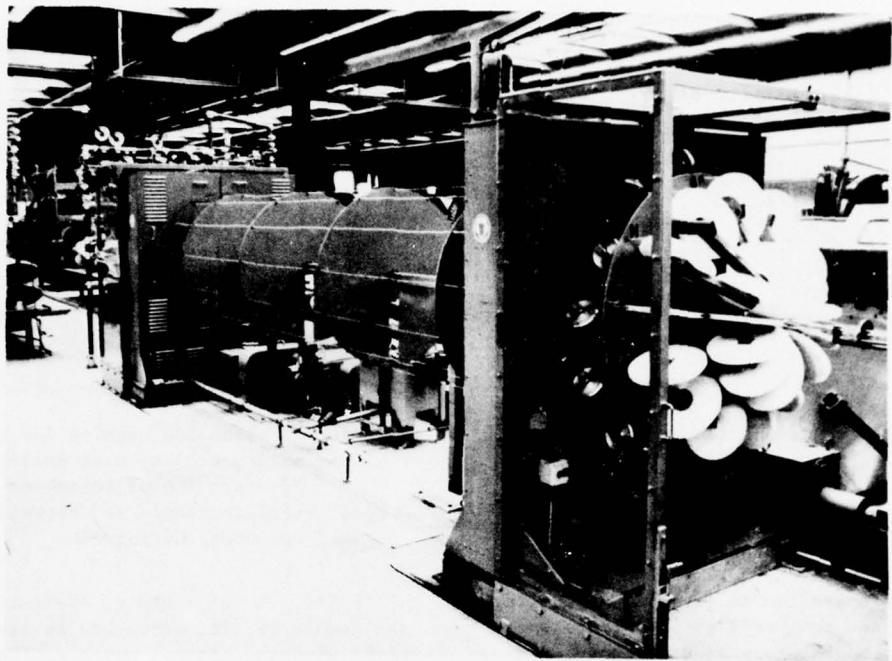


Fig. 7 13-fold twisting equipment (exit side)

The twisting supports are driven via electromagnetic clutches, as in the case of the five-fold machine. The equipment has electronic control facilities so that the twisting program for the different twisting devices can be selected according to the makeup of the unit. These facilities also supervise the rotational speeds of the different twisting supports. In the event of a deviation from the specified nominal values, the entire equipment is stopped. This also applies when a conductor breaks.

Once-looped rollers have proved most suitable for use as twisting supports, assuring non-slip transmission of force between the twisting support and the wire passing through (Fig. 8). The rollers are arranged eccentrically and by guiding the conductors with only few deflections they guarantee that the mechanical strain on the conductor materials is very low. The mean increase in resistance to which copper or aluminum conductors with a diameter of 0.5 mm, for instance, are subjected when passing through the machine is only 1 to 2 %.

Depending on the unit design, either one or two layers are formed from the finished pairs or star quads. The deflection system at the end of the SZ equipment (the white rollers

on the right in Fig. 7) is adjusted accordingly.

As with the five-fold equipment, a pull-off rate of up to 200 m/min can be achieved according to the required pitches of lay. Assuming that the insulated conductors are drawn continuously from double pay-off stands, in one month about 60,000 km of 0.4 mm diameter conductors can be twisted and stranded

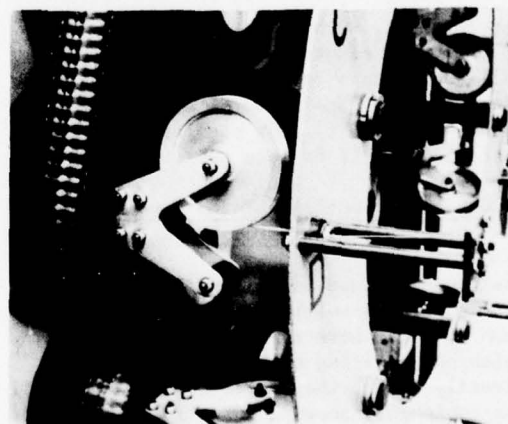


Fig. 8 Twisting support (roller twister)

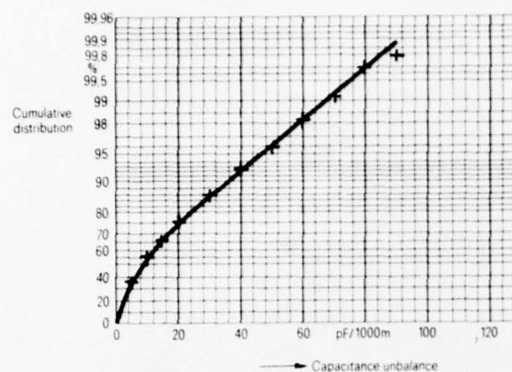


Fig. 9 Capacitance unbalances within 10-pair units (all combinations)
Conductor diameter: 0.5 mm
Length: 1000 m N = 675

in a single operation to form 10-pair units, using only one equipment setup. At present, the SZ equipment is operated together with a conventional bunching machine (Fig. 6).

The capacitance unbalances of units stranded from SZ twisted pairs match the results achieved when using conventional twisting methods. A typical cumulative distribution of unbalances within 10-pair units having a conductor diameter of 0.5 mm is shown in Fig. 9.

Units comprising 7 star quads with 0.6 mm conductor diameter were also experimentally manufactured for cables according to French specification PTT 88. For the capacitance unbalances k_1 within the quad an average of 30 pF/600 m was achieved (max. 180 pF/600 m), while unbalances between adjacent star quads reached an average value of 20 pF/600 m (max. 75 pF/600 m). The permissible limits specified in PTT 88 were thus easily met.

Other applications of the double twister principle with straight accumulator

The new SZ method is also suitable for certain applications involving power cables. Frisch GmbH Ratingen have developed equipment with which house wiring cables can be stranded directly before they enter a sheathing line. The equipment, shown in Fig. 10, is designed for conductor cross sections of $2 \times 1.5 \text{ mm}^2$ to $5 \times 6 \text{ mm}^2$, and there is another version for conductor cross sections up to $5 \times 16 \text{ mm}^2$.

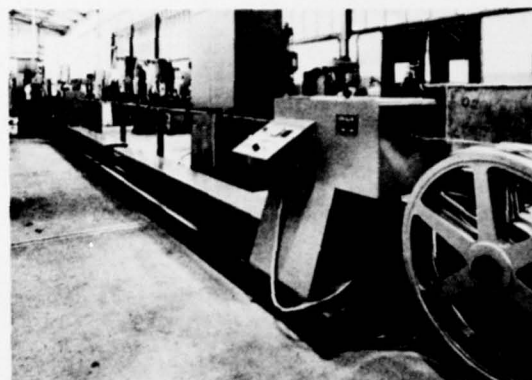


Fig. 10 SZ stranding machine for house wiring cables, also suitable for SZ stranding of telephone cable units (Frisch Kabel- und Verseilmaschinenbau GmbH, Ratingen)

In Fig. 10 the stand at the exit end of the double twister setup can be seen on the right with the control console. The twisted wires are guided via a pull-off device and a rotating lay-plate (not shown here) to a subsequent extruder line. The SZ equipment can perform about 1000 twists per minute on insulated conductors with a cross section up to 4 mm^2 (max. pull-off rate 300 m/min).

Experiments have shown that a shortened version of this equipment can also be used advantageously for unit stranding of communication cables. A particularly attractive possibility is that of equipping twisting strander lines with this type of SZ equipment. This would allow the use of a stationary double winder or a bundle packer 7, for instance, in continuous operation, thus eliminating further machine downtimes. The pull-off rate is determined primarily by the preceding SZ pair or star quad twisting equipment.

Conclusion

Twisting strander lines based on the double-twister SZ principle operate virtually uninterrupted at high speeds and can be used with pay-off reels or pail-packs of any size. Because of the low personnel demand and the simple machinery involved, very economic production is guaranteed. The lines are easy to operate, require little maintenance, and are reliable.

Initial fears that frequent disturbances would occur as a result of conductor breaks, for instance, have been dispelled, especially as continuous processes have been introduced in the preceding operations, thus reducing drastically the number of irregularities and joints in the conductor material.

High-speed twisting strander lines have therefore come to play an important role in the rationalization of communication cable manufacture.

References

1. Vogelsberg, D.: Combined Pair Twisting and Stranding of Telephone Cables. *Wire Journal*, 9 (1976) 1, pp. 78 to 85
2. Vogelsberg, D.: SZ Twisting and Stranding of Communications Cables Using Rotating Accumulators with Periodically Changing Capacity. *20th International Wire & Cable Symposium Proceedings*, 1971, pp. 145 to 155
3. Vogelsberg, D.: Progress in SZ Twisting and Stranding of Communications Cables. *23rd International Wire & Cable Symposium Proceedings*, 1974, pp. 7 to 12
4. Oberender, H. and Spinler, K.: SZ Twisting and Stranding of Telecommunications Cables Using Roller-Twisters. *Wire*, May/June 1975, pp. 94 to 98
5. Braun, D.: SZ Stranding of Telecommunications Cables. *Wire World International*, Febr. 1977

6. German-Patent No. 2 230 972
US-Patent No. 3 823 536
7. Matousek, H.: New wire working methods in the cable industry. *Wire*, July 1976, pp. 160 to 164



Dieter Vogelsberg
Siemens AG
NK E 2
Austrasse 101
D-8632 Neustadt/Coburg
Germany

Dieter Vogelsberg was born in 1930. From 1948 to 1955 study of communications engineering at Technische Universität Berlin. In 1955 he joined Siemens AG, where he has been engaged in the development of communications cables. He was responsible for communications cables research, design and measuring technique. He is currently head of the production engineering department.

Leaky Coaxial Cable with Helical Membrane

Polyethylene Insulation by Direct Extrusion

Y. Saito, H. Kumamaru, K. Sakamoto, and S. Shimada

Sumitomo Electric Industries, Ltd.

Yokohama, Japan

SUMMARY

A new extrusion process for stable production of air-dielectric-type insulation of the coaxial cable has been developed in which both a helical plastic string around the inner conductor and a plastic pipe over the helical insulation are simultaneously extruded directly through two independent passages formed inside a special extrusion-die.

This paper describes the new extrusion process and its application to a new wide band leaky coaxial cable (LCX) for a vehicular communication system. This new technique is widely applicable to production of various types of high quality coaxial cables, including LCX.

1. INTRODUCTION

Recently, in Japan, the LCX has widely been used for vehicular communications and other inter-communications in tunnels, high-rise buildings, underground shopping centers and so on. The most difficult of all about these communication systems is how to establish effective inter-communications between moving stations and ground stations. One of the conventional systems for vehicular communication depends on radio wave. Such a system, however, has a serious disadvantage for use in areas where direct radio waves can be interrupted by complex topography or man-built structures. The LCX is a most suitable transmission line for vehicular communications in the undesirable situations mentioned above, since the cable provides a uniform distribution of electromagnetic waves not extending far from the LCX. This uniformity of electromagnetic waves is brought about by a specially designed slots array on the outer conductor of the LCX.

The LCX has been utilized in Japan, in the 150/400 MHz frequency bands. In the near future the range of band will be extended to the 800 MHz band for a vehicular communication system. The Japanese National Railways (JNR), above all, has decided to install two LCXs on each side of the tracks, both up and down, over several hundred kilometers for the automatic train control system of future trunk lines including the Tohoku and the Joetsu New Trunk Lines.

Mechanical properties as well as initial electrical properties of the LCX are important especially in such severe surroundings where the LCX vibrates incessantly in the violent blast of wind caused by passing fast trains. Development of new LCX with stronger mechanical properties than that of the conventional LCX has been in progress to cope with the harsh conditions of use by applying direct extrusion technique to produce helical membrane insulation.

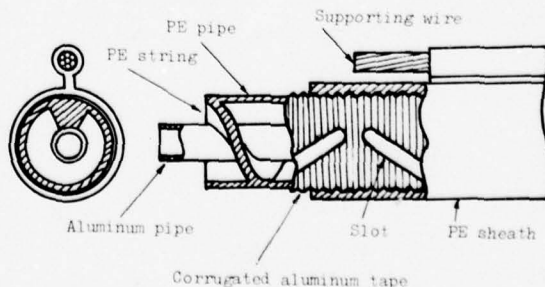
2. ADVANTAGES OF NEW TECHNIQUE

The new technique has been applied to our production of LCX. Fig. 1 shows a cross-sectional view and partial cutaway view of the LCX. The inner conductor is usually made of an aluminum or copper pipe for large diameter LCX and copper wire for LCX of small diameter. The outer conductor is corrugated aluminum tape with a slanted, zigzag array of slots which is longitudinally applied to coaxial structure. Cable sheath is jacketed by extruding black polyethylene over the outer conductor and supporting wire to form a self-supporting type LCX.

The insulation is composed of polyethylene string wound helically around the inner conductor and the polyethylene pipe extruded around the helical string. This type of insulation has been ordinarily produced by three separate processes—making a plastic string by extrusion, winding the rigid plastic string helically around the inner conductor, and extruding a plastic pipe over the helical insulation. The conventional processes, however, have the following disadvantages.

- (1) It is necessary to make plastic string having a special trapezoid cross-section so as to prevent the helical string from tumbling during production.
- (2) The unit length is limited by a pay-off length of the plastic string.
- (3) It is extremely difficult to wind the rigid plastic string helically around such a soft conductor as aluminum pipe, without deforming the conductor.

Fig. 1 Cable structure of LCX



(4) The production procedure is complicated.

To rectify these disadvantages, the development work on new extrusion process was undertaken for stable production of the helical membrane polyethylene insulation. In the new process, both the helical polyethylene string around the inner conductor and the polyethylene pipe over the helical string are simultaneously formed by direct extrusion. This process offers the following advantages as compared with the conventional processes.

- (1) It is easy to apply helical polyethylene string having an optional, rectangular cross-section without impairing the structure.
- (2) It is possible to produce cables with a very long unit-length under normal production conditions.
- (3) It is possible to wind helically one or more polyethylene string(s) without deforming the soft inner conductor.
- (4) Substantial cost savings can be expected through the tandem process of polyethylene string extrusion, polyethylene string winding, and polyethylene pipe extrusion.

This new technique is applicable extensively to the production of various types of high quality coaxial cables, which have such advantages as small impedance irregularities, excellent mechanical stability and flexibility, and easy jointing or connecting work.

3. NEW MANUFACTURING PROCESS

3-1 Outline of extrusion facilities

Fig. 2 shows a scheme of extrusion facilities for manufacturing helical membrane polyethylene insulations or LCX cores. The facilities include a pay-off drum supported by any conventional means, such as jackstands, which permits free rotation of the drum as the inner conductor is pulled by a pay-off capstan, caterpillar capstan, for example. The inner conductor is passed through a straightener, cleaning bath, preheater, and then an extrusion apparatus, wherein the helical polyethylene string and polyethylene pipe are extruded directly around the inner conductor to form a uniform diameter of LCX core while passing through a sizing die. The LCX core is then fed to a take-up drum through a

cooling trough and a capacitance monitoring apparatus wherein the capacitance of the LCX core is monitored successively along the entire length.

3-2 Direct extrusion process

In the new process, both the helical polyethylene string and the polyethylene pipe are simultaneously extruded directly over the inner conductor and are instantly bonded with each other. A cutaway view of the extrusion apparatus is shown in Fig. 3. The inner conductor is fed through a rotary-die holder centrally located within a cylindrical die block and passes from this holder through the central orifice of a rotary die. Polyethylene, on the other hand, is fed by a screw to a cavity inside the extrusion head and is extruded through two independent passages. One passage is formed inside the rotary die and is led to an aperture at its exit end extending radially outward from the central orifice to produce the helical polyethylene string. The other passage is formed cylindrically between a sleeve and the die block, tapering from the entrance side of the extrusion apparatus toward its exit end and forming an aperture to produce the pipe over the helical string.

In order to provide rotary motion to the rotary die having the holder, a sprocket is secured to the entrance side of the holder with bolts. The drive sprocket is adapted to be driven by a variable speed motor through a chain. The rotary die is rotated by the motor, resulting in the formation of a uniformly extruded string winding about the inner conductor over its length. A lay length of the helical string, the

Fig. 3 Extrusion-die arrangement

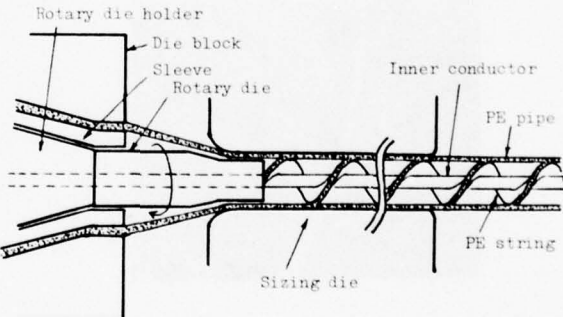
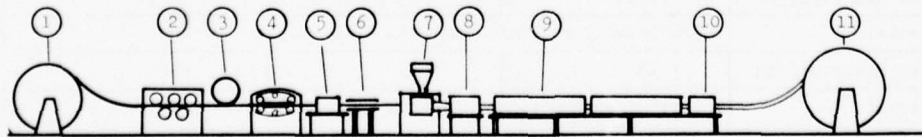


Fig. 2 Extrusion line



- | | |
|----|---------------------|
| 1 | Pay-off |
| 2 | Straightener |
| 3 | Counter |
| 4 | Pay-off capstan |
| 5 | Cleaning bath |
| 6 | Preheater |
| 7 | Extruder |
| 8 | Sizing die |
| 9 | Cooling trough |
| 10 | Capacitance monitor |
| 11 | Take-up |

Fig. 4. Close-up view of direct extrusion

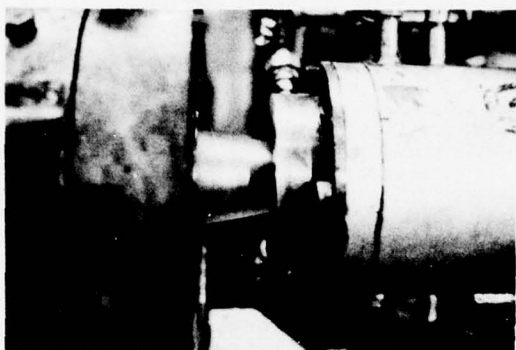
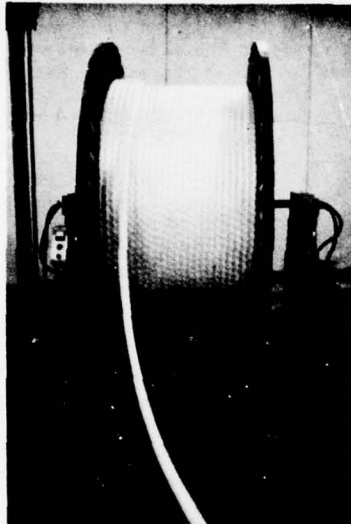


Fig. 5. Take-up drum



pitch, is determined by a line speed and a rotation speed of the rotary die. Any desired pitch is provided by merely adjusting the relative speeds of the line and the rotation. Both the helical string and the pipe are fed to a sizing die just after extrusion to provide not only uniformity in diameter but also good bonding between them.

In the new process, any desired string shape can be provided by merely varying the cross-sectional shape of the aperture of the rotary die. Various sizes of LCX cores can be extruded by interchanging the rotary die, the sleeve, the die block and the sizing die.

Fig. 4 shows a close-up view of the direct extrusion.

Fig. 5 shows an extruded LCX core being taken up by a drum.

4. PROPERTIES OF LCX PRODUCED BY NEW PROCESS

4-1 Cable design

The new LCX design utilizes a directly extruded polyethylene insulation. This design offers improved electrical characteristics, improved mechanical stability and flexibility and easy jointing or connecting work compared with conventional LCX.

We have produced three standard types of new LCX, and they have been on the market for two years. Table 1 shows the construction of the three types. Their insulation diameters are 20 mm, 32 mm and 43mm respectively. The design for inner conductor does not employ hard conductor such as hard copper wire or pipe of conventional design. The inner conductors of the type 43D and 32D are softened aluminum pipes. Further, 20D type LCX design permits the use of softened aluminum wire bringing about the advantages of not only being lighter but also economy of resources. The design of outer conductor isolates the problems of electrical conduction and radiation from that of mechanical strength by laminating adhesive, thin plastic films on aluminum tape with a slanted array of slots which is longitudinally applied to coaxial structure. Corrugations are added to the laminations for flexibility and crush resistance.

Fig. 6 shows photographs of three standard type LCXs.

Table 1. Cable construction of three new LCXs

| Type | | 43D (LCX 50 - 17.3) | 32D (LCX 50 - 13.0) | 20D (LCX 50 - 8.0) |
|-----------------|--------------------|---|------------------------|-----------------------------------|
| Description | Material | Softened Aluminum Pipe | | Softened Aluminium or Copper wire |
| | Outer Diameter, mm | 17.3 | 13.0 | 8.0 |
| Insulation | Material | Low Density Polyethylene with M.I. 0.3 | | |
| | Outer Diameter, mm | 43 | 32 | 20 |
| Outer Conductor | Material | Corrugated Laminated Aluminum Tape with Slots | | |
| Cable Sheath | Material | Ethylene Copolymer with M.I. 0.2 | | |
| | Outer Diameter, mm | 50 | 40 | 27 |

Fig. 6 View of three standard types of new LCX

Left : 20D (LCX50-8.0)
Right : 32D (LCX50-13.0)
Center: 43D (LCX50-17.3)

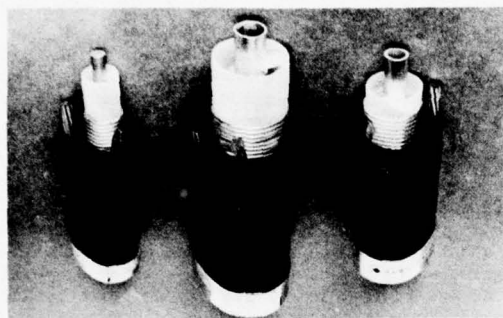
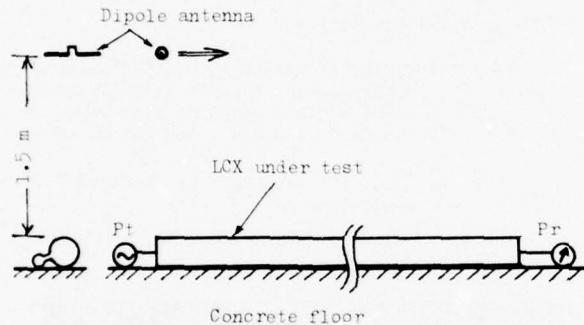


Fig. 7 Standard construction method



4-2 Electrical properties

From the point of view of transmission system, the transmission loss, coupling loss and impedance uniformity are principal properties of LCX. These electrical properties of new LCX for the use in frequency bands of 150 MHz and 400 MHz or 400 MHz and 800 MHz are shown in Table 2. From the result of these measurements, new LCX was found well suited to the use not only for 400 MHz band but 800 MHz band. Measurements of all these properties were carried out with the LCX laid on a concrete and by the standard construction method as shown in Fig. 7.

Typical electrical properties of 43D type LCX with 55 dB of coupling loss for the bands of 400 MHz and 800 MHz are shown in Figs. 8, 9 and 10.

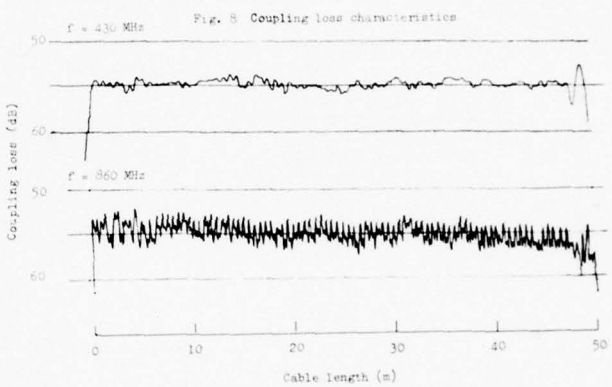
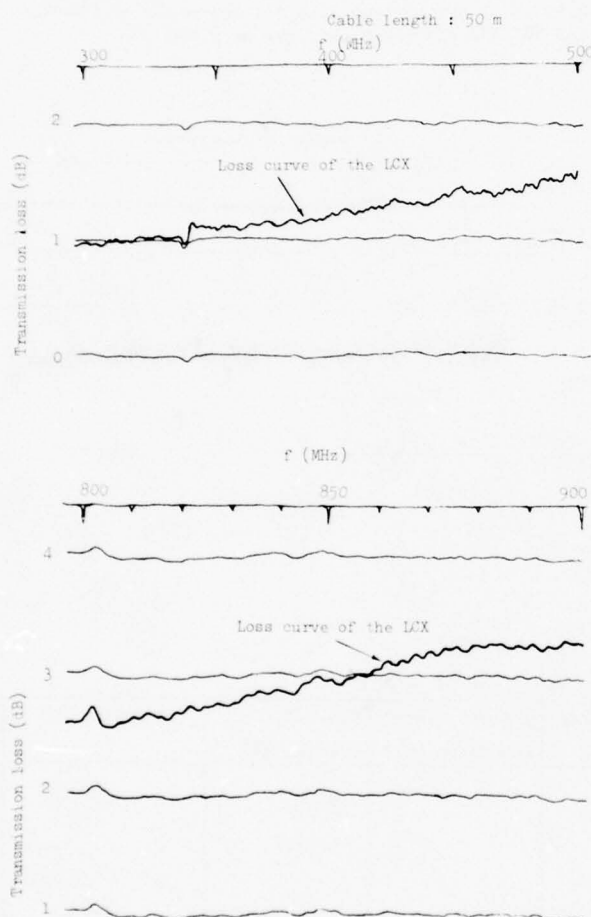


Table 2. Typical electrical properties (at 20°C)

| Type of the LCX | Frequency Band (MHz) | Coupling Loss (dB) | Attenuation Constant (dB/Km) | Characteristic Impedance (Ω) | V.S.W.R. (S.R.L. dB) | Permittivity |
|---------------------|----------------------|--------------------|------------------------------|---------------------------------------|----------------------|--------------|
| 43D (LCX50-17.3) | 140 | 80 | 22 | 50 ± 1 | <1.2 (>21) | 1.23 |
| | ~ 470 | 70 | 22 | | | |
| | 470 | 60 | 25 | | | |
| | | 50 | 40 | | | |
| | 380 | 75 | 34 | | | |
| | ~ 900 | 65 | 36 | | | |
| 32D (LCX50-13.0) | 380 | 55 | 60 | 50 ± 1 | <1.3 (>18) | 1.25 |
| | ~ 900 | 50 | 120 | | | |
| | | | | | | |
| 20D (LCX50-8.0) | 140 | 75 | 32 | 50 ± 1 | <1.2 (>21) | 1.38 |
| | ~ 470 | 65 | 35 | | | |
| | 470 | 55 | 40 | | | |

Fig. 8 illustrates an example of coupling levels measured at the frequencies of 430 MHz and 860 MHz respectively. The magnitude of coupling loss is usually defined as the ratio of the power to be transmitted in the LCX to the power received by a standard half wave length dipole antenna located 1.5 m away from the LCX. Therefore, coupling

Fig. 9 Transmission loss v.s. frequency



loss was measured by moving the antenna along a 50 m long LCX. It is observed from the experimental result in the Figure that new LCX has not only small fluctuations of coupling loss but much the same coupling level for the frequency bands of 400 MHz and 800 MHz.

Fig. 9 shows the comparison of transmission loss against frequency characteristics of the LCX measured by the swept-frequency method using the Ratio Meter. The dimensional uniformity of the LCX is so good that the transmission loss curve is very smooth. In the long-distance transmission system, smooth loss curve eliminates or at least modifies the repeater design requirement in respect of linearity.

Fig. 10 illustrates the frequency characteristics of structural return loss. Measurement was taken by the swept-frequency method using the SWR bridge over the frequency range of 10 - 1200 MHz. Two large peaks of the return loss at the frequencies of about 500 MHz and 1000 MHz are noticeable in the Figure, which are caused by the resonance of reflections due to the slots array on the outer conductor. The return loss characteristics, other than the above mentioned resonance effect, are extremely good in the entire frequency range and, as a result, good connection of the LCX to radio equipment may be expected.

4-3 Mechanical properties

For radiotelephone system of new JNR's trunk lines, it is planned to use two LCXs aerially installed along each side of the tracks of both ways. Besides vibration due to the wind, the LCX vibrates

Fig. 11 Residual stress in the helical PE string
Above : Conventional type
Below : New type

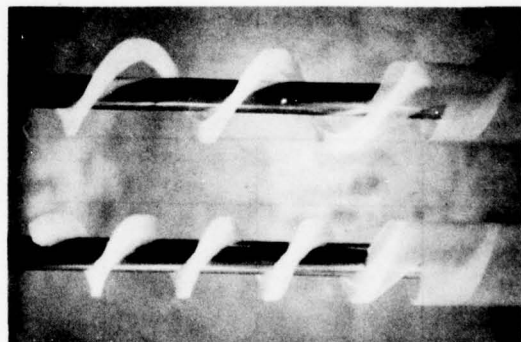
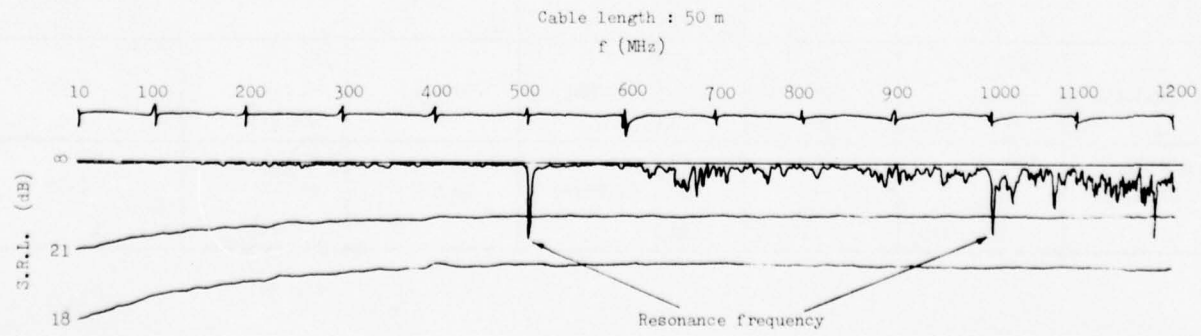


Fig. 10 Structural return loss v.s. frequency



at certain regular intervals because of the air blasts of the passing of fast trains. It is imperative, therefore, that the LCX should be able to work as long as a few decades under such conditions.

Fig. 11 illustrates the comparison of stability between the helical polyethylene string of new LCX core and that of conventional LCX core. The residual stress in the helical polyethylene string of conventional LCX is noticeable in the Figure, even after several years of practical use, as a relaxation of the string around the inner conductor. The new LCX core, on the other hand, has no residual stress in the polyethylene string and a good bonding between the polyethylene string and polyethylene pipe is obtained. A helical pitch just after extrusion is maintained throughout. Dimensional stability of the insulation is responsible for excellent mechanical properties of the cable as described below.

- (1) Flexibility of the cable increases because no residual stress is present in the polyethylene string (and because annealed conductor can be used as inner conductor).
- (2) The cable's resistance to vibration increases because stress concentration is reduced to the inner conductor which is free from distortion.
- (3) Jointing or connecting work can be easily carried out because the polyethylene string does not stick out of the cable end.

Fig. 12 illustrates the comparison of flexibility between the new and conventional LCXs. Flexibility, in this case, was considered to be proportional to the drooped distance of the free end with a weight of the cantilever as shown in the Figure. Both types of new 20D LCX which use the annealed aluminum wire and copper wire for the inner conductor seem several times more flexible than the conventional LCX whose inner conductor is semi-hard-drawn copper wire. The new 20D LCX with softened

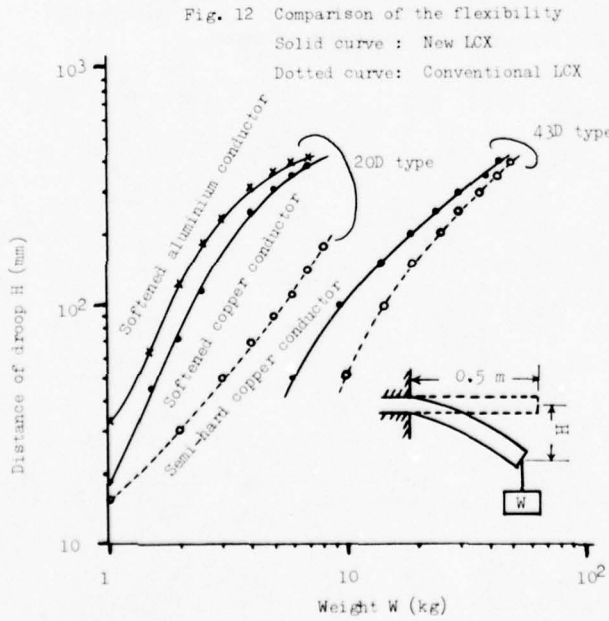
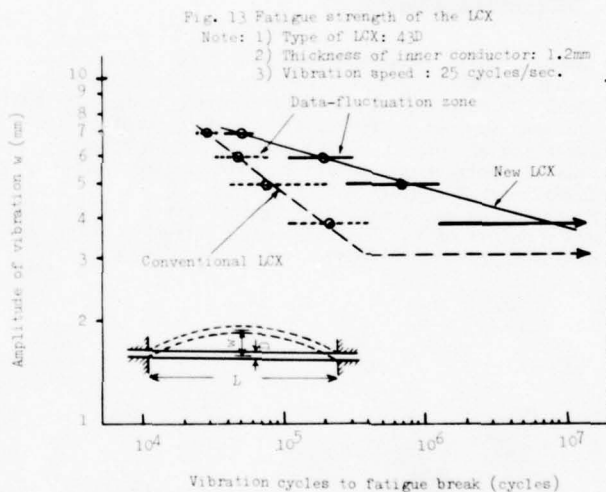


Fig. 12 Comparison of the flexibility
Solid curve : New LCX
Dotted curve: Conventional LCX

aluminum inner conductor has, in particular, the advantages of not only being flexible but also light. The new 43D LCX is fairly good with respect to flexibility compared with the conventional LCX.

Fig. 13 compares fatigue strength measurements of new LCX and conventional LCX. Vibration test, by the accelerative method using short pieces of 43D LCX, was carried out at a constant speed of 25 cycles per second and variable amplitude from 3 to 7 mm. Specimens of 1 m long LCX were fixed on both ends of testing bench in parallel and made to oscillate compulsively in the middle of the cables longitudinally, the type of oscillation which is most aggravating to the vibration fatigue of the LCXs. Neither specimen of new LCX or conventional LCX was damaged until the inner conductors of aluminum pipe came to a fatigue break point by contact with the edge of the polyethylene string. So far as the condition of the amplitude remains under 5 mm, vibration enduring strength of the new LCX seems 10 times greater than that of the conventional LCX.

It appears from the above that the increased mechanical properties of flexibility, stability and vibration endurance of the LCX make it possible to minimize the degradation of cable in the course of processing at factory and installation, and also keep field failures at minimal after installation even under harsh field conditions as typified by the site along railway tracks.



5. CONCLUSION

We have developed a new manufacturing process for extruding helical membrane polyethylene insulation for coaxial cables and applied its process to a new wide band LCX for vehicular communication system. This process makes it possible to apply rigid polyethylene string helically around the soft inner conductor without deforming the conductor. This new technique is widely applicable to production of various types of high quality coaxial cables.

The new LCX with a helical membrane insulation made by this technique has advantages of small impedance irregularities, excellent mechanical stability, flexibility and vibration endurance and making jointing or connecting work easy. The new LCX has been on the commercial market for two years in Japan.

6. ACKNOWLEDGEMENTS

The authors wish to express their thanks to the Japanese National Railways for valuable advice and suggestions. They are grateful to the Sumitomo Chemical Company, Ltd. for granting permission to publish this paper. The cooperation of the staff of the company is greatly appreciated.



Katsuji Sakamoto

Sumitomo Electric Industries, Ltd.
1 Taya-machi,
Totsuka-ku, Yokohama,
Japan

Katsuji Sakamoto finished the Mechanical Engineering Course of Tsurumi Industrial High School in Kanagawa Prefecture in 1962. He then joined Sumitomo Electric Industries and has been engaged in development and design of manufacturing processes of communication cables.
Mr. Sakamoto is a member of Communication R & D Group.



Yasunori Saito

Sumitomo Electric Industries, Ltd.
1 Taya-machi,
Totsuka-ku, Yokohama,
Japan

Yasunori Saito received his B.S. degree in Electrical Communication Engineering from Tohoku University in 1969. He then joined Sumitomo Electric Industries and has been engaged in research and development of various kinds of coaxial cables such as long-distance coaxial cable, superconducting coaxial cable and leaky coaxial cable.

Mr. Saito is now a member of Communication R & D Group, and a member of the Institute of Electronics & Communication Engineers of Japan.



Shin Shimada

Sumitomo Electric Industries, Ltd.
1 Taya-machi,
Totsuka-ku, Yokohama,
Japan

Shin Shimada received his B.S. and M.S. degrees both in telecommunication engineering from Waseda University in 1970 and 1972, respectively. He then joined Sumitomo Electric Industries and has been engaged in development and design of communication cables.
Mr. Shimada is a member of Communications, and also a member of the IEEE and the Institute of Electronics and Communication Engineers of Japan.



Hiroyuki Kumamaru

Sumitomo Electric Industries, Ltd.
1 Taya-machi,
Totsuka-ku, Yokohama,
Japan

Hiroyuki Kumamaru received his B.S. degree in Electrical Engineering and Ph. D. degree in Engineering from Tokyo University in 1957 and 1971 respectively. In 1957, he joined Sumitomo Electric Industries and has been engaged in research and development of communication cables.

Dr. Kumamaru is now a Manager of Communication R & D Group, and a member of the Institute of Electronics & Communication Engineers of Japan.

EC GRADE FULLY ANNEALED ALUMINIUM CONDUCTORS
IN PAPER INSULATED TELEPHONE CABLE

R.J. Lewis and N.W. Peters
Telecom Australia Headquarters, Melbourne, Australia

Summary

An earlier paper presented to the Nineteenth International Wire and Cable Symposium in 1970 reported on the manufacture, installation and economic application of large size helical paper insulated EC grade aluminium cable in Telecom Australia's network. The paper was based on experience gained from laboratory work and early field trials.

The purpose of the present paper is to report on the developmental work and field installations that have taken place since 1970, and the extent of savings that are being made by the use of paper insulated aluminium cable. The majority of the work since 1970 has been concerned with the development of a range of wire jointing connectors to joint 0.53mm, 0.81mm and 1.15mm EC grade fully annealed (FA) aluminium conductors. These connectors are also suitable for jointing certain combinations of aluminium and copper conductors. Information of the service history of aluminium cables installed from as early as 1965 is provided.

The purchase price savings for aluminium cable compared with copper during 1977-78 is expected to be about 8%, and no significant installation or maintenance cost penalty is expected in the sizes which will be used.

It is anticipated that this development will prolong the use of helical and longitudinal paper insulation in Australia.

Introduction

The 1970 paper detailed Telecom Australia's interest in aluminium cable for use as a substitute for copper during periods of copper shortage, and as a means of saving money where aluminium cable is cheaper. Cable manufacturing installation and maintenance experiences were described, together with details of the Series 1 field trials with 0.63mm FA and $\frac{1}{2}$ H conductors, and the Series 2 trials with 0.52mm FA conductors. The paper reported on the unacceptably high level of open circuit faults which had occurred at the wire jointing connectors of one 0.52mm installation. The cause of these failures is detailed in the present paper. Further field trials during 1970-72 with 0.52mm and 1.15mm cables were foreshadowed and the possibility of routine use of aluminium cable, where it is economically attractive, from January 1972 was reported.

The present paper is concerned with the development and use of 0.52mm, 0.81mm and 1.15mm aluminium cable by Telecom Australia from 1970.

Field Trials Since 1970

The basic cable design had been established by 1970 as, EC grade FA aluminium conductors, helical paper insulation, unit twin core construction and a moisture barrier sheath; although at that time only 0.63mm and 0.52mm cable had been used. The field trials since 1970 have been primarily to provide experience with aluminium cables to the Australian cable industry and to confirm the performance of wire jointing connectors applied to them. Each connector system was subjected to an extensive laboratory evaluation before field trial and details of the development and evaluation of

connectors, for each conductor gauge, are provided in other Sections of this paper.

The Series 3 field trials of 0.52mm and 1.15mm cable foreshadowed in the 1970 paper, were installed during 1971-74. A connector designed and manufactured in Australia was used for 0.52mm cable and the 1.15mm cables were jointed by a twist and weld technique using a specially developed welding tool. The 0.52mm gauge was seen as attractive because a large quantity could be used in the subscriber network without the larger diameter of the aluminium cable incurring a significant duct penalty. The duct penalty costs with 0.52mm cable are very small because cable larger than 1800 pairs is seldom required, and 1800/0.52mm cable can be installed in Telecom Australia's 100mm diameter ducts. The 1.15 mm trials were conducted because this gauge offered the greatest percentage savings, compared with copper, and a significant quantity was required for installation in the junction network at that time. At the 1970 prices of aluminium, \$A586/tonne and copper, \$1,480/tonne, the saving on maximum size 0.52mm cable was 30%, but was 48% for 1.15mm cable.

An economic study conducted in 1974 showed that with the large quantity of 0.64mm copper cable being installed in metropolitan junction networks there was a large potential saving in the substitution of 0.81mm aluminium cable for 0.64mm copper; even though the maximum size aluminium cable for installation in 100mm ducts contained only 800 pairs compared with 1200 for the copper cable. Consequently, a fourth series of field trials comprising 10 projects and 32,000 Pkm of 0.81 cable were installed in 1974-1976. Three types of connectors were used including one of Australian design and manufacture. In this application the connectors had to provide for jointing the 0.81mm aluminium to 0.64mm copper (at exchange terminations) and to 0.50mm copper (at loading coils). Sufficient of these cables had been satisfactorily completed by March 1976, for the decision to be taken to start routine use of 0.81mm cable in the junction cable network under the general surveillance of six State Co-ordinators; one for each of the six States of Australia. These co-ordinators had been appointed to generally co-ordinate planning and installation, and to provide feedback to Headquarters during the initial stages of routine use. Although paper insulated junction and subscribers cables used in Australia are identical, 0.81mm cables were not, at that stage, introduced into the subscriber main cable network. The range of conductors that would have had to be jointed to the 0.81mm aluminium included 0.40mm and 0.90mm copper. By March 1977 suitable connectors became available and 0.81mm aluminium began being used for subscribers cables.

The Series 3 field trials, with 0.52mm and 1.15mm cable, were completed by 1974 and although the results of the two 0.52mm projects were satisfactory, it was considered that this was not sufficient to justify starting routine use. In addition, some doubts were held regarding the ability of connector jointed 0.52mm EC grade FA conductors to withstand the stresses imposed during cable joint re-arrangements, that would be required during the life of some cables. A fifth series of field trials comprising 9 projects, and 15,300 Pkm of 0.52mm cable was, therefore, organised. In addition, a 300 pair cable installation was set up at Telecom Australia's Maidstone (Victoria) Test Site to obtain data on the incidence of faults, particularly

open circuits, in 0.52mm cable joints following re-arrangement work. Fortunately at about this time it also became necessary to re-arrange a 600 pair joint in one of the early 0.52mm cables, due to development in the area served by the cable. Both re-arrangements were judged to be successful with the level of faults not significantly different to that expected for copper. By March 1977, sufficient of the 0.52mm cables installed in the Series 5 field trials had been satisfactorily completed for the decision to be taken for routine use of 0.52mm cable to start; again under the general surveillance of the State Co-Ordinators.

A larger size connector of Australian design and manufacture has been developed and laboratory tested for the 1.15mm gauge. The laboratory tests were satisfactory and even though the connectors have not been used in field trials there is sufficient confidence in this robust, large gauge conductor for routine use to start as soon as bulk supplies of the connector become available.

We have thus reached the stage where satisfactory jointing methods are available for all three gauges and two are already in routine use.

During the period 1973-1976, a separate development project for longitudinally applied sealed paper insulation (SPI) was proceeding for both copper and aluminium conductor cable. Technically satisfactory cable has been produced in each gauge with a mutual capacitance of 45 nf/km, the standard mutual capacitance for voice frequency cable in Telecom Australia. However, for the larger gauges, higher manufacturing costs will probably restrict the use of SPI with aluminium to 0.52mm.

Conductor Jointing

Aluminium cable is used by Telecom Australia in conjunction with existing copper cables for network extension purposes. It is jointed to copper tail cables to permit termination at field cabinets and exchange main frames. Thus the associated jointing system must be capable of handling copper to aluminium connections.

The corrosion potential of the combination of metals is controlled by making the application of a dry air pressure protection system mandatory for paper insulated aluminium conductor cables. This has not presented a problem since gas pressurisation of main subscriber and junction cables is already standard practice in Australia.

The difficulties with jointing aluminium lie in :-

1. The rapidly forming insulating coating of oxide Al_2O_3 which must be removed to effect electrical connection.
2. The relative fragility of small gauge aluminium (0.52mm) conductors compared with their copper counterparts.
3. The notch sensitivity of aluminium.
4. A wider variability of the tensile and elongation characteristics of cable conductors manufactured from aluminium in comparison with copper.

Jointing Methods

The simple unsoldered crank twist joint which has a population in the hundreds of millions in existing copper networks is not directly applicable to aluminium because of the oxide film. However, with

the addition of specialised soldering techniques including zinc enriched solder and non corrosive oxide removing fluxes, twist joints may be made to provide satisfactory electrical connections. This method is not considered an adequate solution to jointing aluminium cables today because of the escalation of labour costs.

Jointing methods which have been examined and field trialled during the aluminium cable development project include :-

1. Soldering
2. Cold Pressure Welding
3. Electric resistance welding
4. Machine applied in line connectors
 - a. Wire in slot type
 - b. Tang type

The preference for mechanical connectors which has emerged from the work is based on :

1. The uniformity of the electrical connection which they produce.
2. The inherent productivity of the jointing machines with which they are applied.

In line connectors however produce a variable mechanical performance between individual joints. This characteristic can become a serious disadvantage particularly where the conductor material is EC grade aluminium which is very sensitive to notching.

A breakdown of the jointing methods used in the trials is shown in Table 1.

| Trial Group | Conductor | Jointing Method |
|-------------------|--|--|
| Series 1 65/66 | 0.63mm FA EC Al 0.63mm $\frac{1}{2}$ H Al | Twist and weld or sleeve and crimp |
| Series 2 69/70 | 0.52mm FA EC Al | A-MP (Green)* |
| Series 3 71/74 | 1.15mm FA EC Al 0.52mm FA EC Al | Al/Al twist and weld Al/Cu twist and solder Utilux H2561** |
| Series 4 74/75 | 0.81mm FA EC Al | A-MP (Red)* A-MP (Mini Brown)* Utilux H2562** |
| Series 5 75/ | 0.52mm FA EC Al | A-MP (Mini Pink)* Utilux H2562-1** Egerton No. 6** |

* Wire in slot Connector - ** Tang type connector

TABLE 1 - SUMMARY OF JOINTING METHODS

Summary of Jointing Experience

The jointing experience gained from the Series 1 and 2 trials has been reported previously. Series 2 had confirmed that the smaller diameter 0.52mm fully annealed conductor could be made into cable on the existing cable making plant and that by using connectors the jointing productivity could be lifted significantly; to higher levels in fact than pertained with manual jointing of copper. They also showed that handling this conductor after jointing with A-MP standard green connectors carried the risk of an

unacceptably high percentage of open circuits in a completed cable installation. Investigation showed that this was the result of the variability and notch sensitivity of the material in combination with the wire entry geometry and absence of a stress relieving mechanism in the connector. Work was commenced to establish an improved connector and to investigate alloy materials for this small gauge conductor.

It is of interest to note that the Series 2 trials involved the first usage of any magnitude of machine applied connectors in the Australian main cable network; and indeed expedited mechanisation of large size copper cable jointing. There are sufficient machines available today to handle collectively the 2 and 3 wire jointing of all gauge combinations and there is little residual need for hand jointing in copper main subscriber or junction cables.

Series 3 trials conducted during 71/74 were initially mounted in order to give design and manufacturing experience with 1.15mm EC aluminium conductors. At that time none of the existing connector systems were capable of accommodating this large diameter conductor and recourse was made to an improved welding technique. Tooling was developed specifically for the purpose. Figure 1 refers.

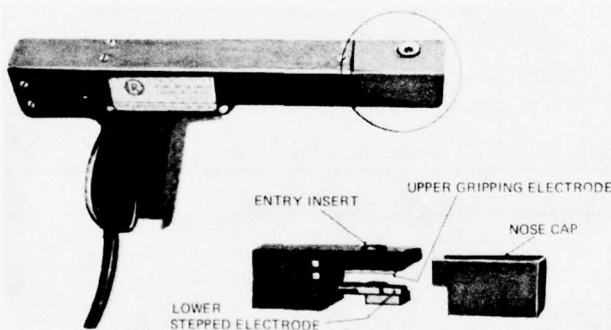


Figure 1 - Conductor Welding Tool

Al to Al joints were twisted and welded by this method and for the Al to Cu joints at loading coil and terminating cable tails, twisting and aluminium-soldering was used. It was recognised that the jointing productivity would not be great but this was accepted to gain the required design, manufacturing and installation experience with this cable type.

The trial results showed that the welding equipment plus its power supplies and charging facilities, were relatively expensive to provide in quantity. The welding handtool required frequent cleaning of the electrodes during usage and was prone to malfunction. Its inability to handle Cu/Al joints was an obvious disadvantage. The electrical performance of the Al joints produced was very good however, and their mechanical behaviour presented no problems as could perhaps be expected with this wire diameter.

The results of laboratory evaluation work on a Utilux (Australian) connector applied to the two wire jointing of 0.52mm FA aluminium conductors became available during the course of the Series 3 trials. Two additional projects with this conductor were included. Results showed that under field conditions the mechanical performance of this connector was marginally better than the A-MP standard connector with the same conductor. With some modifications it was

expected this performance improvement could be optimised. Figure 2 refers.

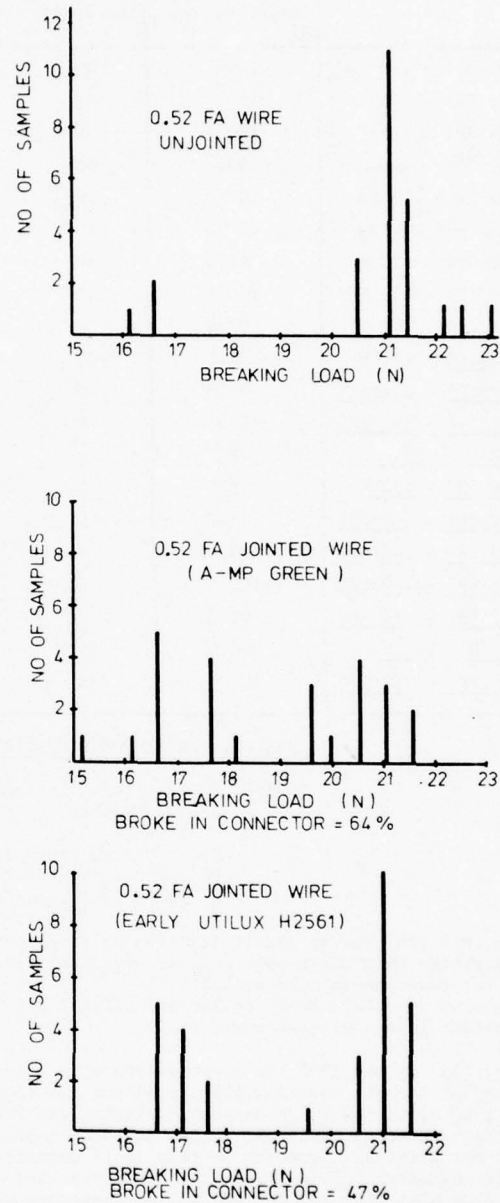


Figure 2 - Breaking Strength 0.52mm FA Aluminium Conductor

Series 4 trials in 74/75 covered the mid range 0.81mm diameter aluminium conductor which is the electrical equivalent of 0.64mm copper, the most commonly used conductor in our junction cables. The additional cross section of conductor over an 0.52mm wire offered a higher confidence level with respect to the notching problem and some installations were jointed out with A-MP (Standard Red) connectors. A series of smaller A-MP Mini connectors with different wire entry geometry to the standard was then becoming available in addition to an improved Utilux connector and projects covering 0.81mm wire and both of those connectors were included. The results led to a decision to release

| Type of Conductors | Ratio of Joint Mean B/S to Conductor Mean B/S | % of Batch Which Failed Within The Joint | Joint Mean B/S (N) | | | | Ratio of Standard Deviation to Mean ($/ \bar{x}$) | Mean Conductor Breaking Strength (N) |
|---------------------------------|---|--|--------------------|-------|------|------|---|--------------------------------------|
| | | | Min. | Mean | Max. | S.D. | | |
| .32 SPI - .40 Pe | 100 | 70 | 20.0 | 20.35 | 21.0 | 0.36 | 0.018 | 20.08 |
| .32 SPI - .40 Pe | 100 | 30 | 20.0 | 20.53 | 21.0 | 0.19 | 0.009 | 20.08 |
| .64 SPI - .64 Pe | 100 | 0 | 77.5 | 79.35 | 81.0 | 1.07 | 0.013 | 79.00 |
| .40 SPI - .40 SPI | 99.8 | 65 | 29.0 | 31.18 | 31.5 | 0.66 | 0.021 | 31.25 |
| .64 Pe - .64 Pe | 100 | 0 | 78.0 | 80.30 | 82.0 | 1.16 | 0.014 | 79.00 |
| .40 Pe - .40 Pe | 100 | 55 | 30.0 | 31.65 | 33.0 | 0.63 | 0.020 | 31.25 |
| .32 SPI - .32 SPI | 96.0 | 60 | 13.0 | 19.28 | 20.5 | 1.68 | 0.087 | 20.08 |
| .64 SPI - .64 SPI | 100 | 15 | 80.0 | 80.13 | 80.5 | 0.22 | 0.003 | 79.00 |
| <u>.81 SPI</u> - .64 Pe | 95.4 | 0 | 34.5 | 37.10 | 43.5 | 2.34 | 0.063 | 38.89 |
| <u>.52 SPI</u> - .40 Pe | 91.8 | 25 | 12.0 | 17.68 | 20.5 | 2.48 | 0.140 | 19.25 |
| <u>.52 SPI</u> - <u>.81 SPI</u> | 89.5 | 45 | 13.5 | 17.23 | 20.0 | 2.53 | 0.146 | 19.25 |
| <u>.81 SPI</u> - <u>.81 SPI</u> | 90.3 | 0 | 34.5 | 35.10 | 37.0 | 0.58 | 0.017 | 38.89 |
| <u>.52 H</u> - <u>.52 H</u> | 100 | 10 | 12.0 | 14.73 | 16.5 | 1.19 | 0.081 | 14.68 |
| <u>.40 SPI</u> - <u>.32 H</u> | 99.1 | 5 | 9.2 | 9.38 | 9.8 | 0.16 | 0.017 | 9.47 |
| <u>.40 SPI</u> - .40 SPI | 93.2 | 0 | 8.5 | 8.83 | 9.0 | 0.24 | 0.027 | 9.47 |
| <u>.40 SPI</u> - .40 Pe | 93.4 | 0 | 8.5 | 8.90 | 9.0 | 0.25 | 0.028 | 9.47 |
| <u>.52 SPI</u> - .40 Pe | 100 | 0 | 15.5 | 16.47 | 21.0 | 1.10 | 0.067 | 15.95 |
| <u>.52 SPI</u> - <u>.81 SPI</u> | 100 | 0 | 15.9 | 16.78 | 22.0 | 1.40 | 0.083 | 15.95 |
| <u>.81 H</u> - <u>.81 H</u> | 98.6 | 55 | 47.5 | 48.75 | 50.0 | 0.64 | 0.013 | 49.42 |
| <u>.52 SPI</u> - <u>.52 SPI</u> | 100 | 55 | 15.3 | 16.03 | 16.8 | 0.34 | 0.021 | 15.95 |

TABLE 2 - BREAKING STRENGTH TEST RESULTS FOR UTILUX H2562-1 CONNECTORS

NOTES: In each case, 20 samples were tested. Aluminium conductors are underlined.

SPI = Sealed Paper Insulation
 Pe = Polyethylene Insulation
 H = Helical Paper Insulation

the cable for general use in junction applications. Subscribers main cable applications were excluded as it was not then possible to reliably joint 0.81mm aluminium to 0.40mm PEIUT pillar and cabinet tails to specified levels of performance.

Series 5. By mid 1975 the optimisation of a Utilux Connector biased toward 0.52mm aluminium had produced the type H2562-1 which under bench testing exhibited better mechanical performance than had been achieved with any previous connector on this small diameter EC grade conductor.² (Refer Table 2). This type and also the A-MP Mini Pink and the BPO No. 6 connectors were used on a series of projects to establish whether the notching problem could be controlled in the field to a level where routine use of the conductor could be established. All of the results are not in for these trials but the early indications were such that controlled usage under surveillance was undertaken.

Connector Design

The function of a connector are :-

1. To penetrate the in situ conductor insulation.
2. To enter into the conductor material removing by abrasion any oxide film.
3. To provide a high integrity electrical connection.

4. To maintain the connection for the life of the cable plant, by virtue of stresses produced in the metal elements during crimping.
5. To provide insulation of the connection from other conductors etc., in the cable.

A connector is very much a device tailored to the conductors it is to joint. Its critical dimensions are determined by the conductor diameter, material characteristics, and the thickness and type of its insulation. As an indication it is generally accepted that three sizes of connectors with overlapping diameter ranges are needed to joint paper insulated copper telephone conductors in the diameter range between 0.32mm and 0.90mm.

To accept aluminium wires manufactured on a resistance equivalence to copper basis requires an extension upwards of approximately 30% in the capacity of each connector size or else the ability to joint certain commonly required gauge combinations in mixed Al/Cu networks will be lost.

Preferred sub ranges are thus : 0.32 - 0.52mm
 0.40 - 0.81mm
 0.51 - 1.15mm

The Australian Specification (No. II33) for connectors to joint large size gas protected cables has the following requirements :-

1. Initial Resistance

The connection resistance measured between two points 50mm apart on the jointed conductors shall not exceed the following values :

| | |
|--------------------------|-------------------------|
| 0.32mm Cu - 14 milliohms | 0.64mm Cu - 5 milliohms |
| 0.40mm Cu - 10 milliohms | 0.81mm Al - 5 milliohms |
| 0.52mm Al - 10 milliohms | 0.90mm Cu - 4 milliohms |
| 0.51mm Cu - 7 milliohms | 1.15mm Al - 4 milliohms |

2. Resistance After Thermal Cycling

The connection resistance measured similarly shall not exceed the initial value plus 2 milliohms for any conductor combination after the joints have been submitted to 25 thermal cycles. Each cycle shall consist of 45 minutes at 65°C followed by the same period at -35°C with a transfer time between the two temperatures of not more than 3 minutes.

3. Mechanical Strength of Connection

The mean breaking strength of a sample of twenty joints shall not be less than 80% of the mean breaking strength of a sample of ten unjoined wires. The minimum not being less than 70%.

4. Insulation Resistance

The insulation resistance of joints shall be not less than 100,000 Megohms.

5. Dielectric Breakdown

The dielectric breakdown strength of joints shall not be less than 1000V DC.

The jointing experience gained during the trials with locally manufactured connectors on aluminium has been progressively incorporated in connector designs to establish a range of 3 Utilux connectors designated for simplicity as Yellow, Red and Blue. These are small "in-line" type connectors some 15mm long. The material is brass post plated with tin after the punching and forming operations are complete. A connector joint is shown in Figure 3 and their wire jointing capability with respect to copper and aluminium conductors of Australian origin are shown in Table 3.

| YELLOW CONNECTORS H2564-1 (S114/144) | | RED CONNECTORS H2562-1 (S114/143) | | BLUE CONNECTORS H2563-1 (S114/145) | |
|--------------------------------------|----------|-----------------------------------|-----------|------------------------------------|-----------|
| WIRE DIAMETER (M) | | | | | |
| WIRE 1 | WIRE 2 | WIRE 1 | WIRE 2 | WIRE 1 | WIRE 2 |
| 0.32 Cu | 0.32 Cu | 0.40 Cu | 0.40 Cu | 0.51 Cu | 0.51 Cu |
| 0.32 Cu | 0.40 Cu | 0.40 Cu | 0.51 Cu | 0.51 Cu | 0.64 Cu |
| 0.32 Cu | 0.51 Cu | 0.40 Cu | 0.52 Al | 0.52 Cu | 0.81 Al |
| 0.40 Cu | 0.40 Cu | 0.40 Cu | 0.64 Cu | 0.51 Cu | 0.90 Cu** |
| 0.40 Cu | 0.51 Cu | 0.40 Cu | 0.81 Al | 0.51 Cu | 1.15 Al |
| 0.40 Cu | 0.52 Al* | 0.51 Cu | 0.51 Cu | 0.64 Cu | 0.64 Cu |
| 0.52 Al*0.52 Al* | 0.51 Cu | 0.52 Al* | 0.54 Cu | 0.81 Al | 0.90 Cu** |
| | 0.51 Cu | 0.64 Cu | 0.64 Cu | 0.64 Cu | 1.15 Al |
| | 0.51 Cu | 0.81 Al | 0.64 Cu | 0.64 Cu | 0.81 Al |
| | 0.52 Al* | 0.52 Al | 0.81 Al | 0.81 Al | 0.81 Al |
| | 0.52 Al* | 0.64 Cu | 0.81 Al | 0.81 Al | 0.90 ** |
| | 0.52 Al* | 0.81 Al | 0.81 Al | 0.81 Al | 1.15 Al |
| | 0.64 Cu | 0.64 Cu | 0.90 Cu** | 0.90 Cu** | 0.90 Cu** |
| | 0.64 Cu | 0.81 Al | 0.90 Cu** | 0.90 Cu** | 1.15 Al |
| | 0.81 Al | 0.81 | 1.15 Al | 1.15 Al | 1.15 Al |

TABLE 3 - JOINTING CAPABILITY OF UTILUX CONNECTORS

NOTE:

- I. * Use limited to installation of cable under surveillance of State Aluminium Co-ordinators.
- II. ** The H2563-1 connector cannot be used to joint 0.90mm copper conductor with polythene insulation thicker than 0.35mm.

The mid range Red connector which accepts 0.40mm to 0.81mm wires is shown in Figure 4 and again with its side walls lowered to show the contact arrangement in Figure 5. Tangs of reducing height and flattened profile at the outer edges of the connector provide stress relief for the parts of the conductors significantly notched to form the electrical connection. The hardness of different areas of the connector is controlled during manufacture to achieve the desired performance of the tangs during crimping.

The crimp is of a full roll configuration to prevent relaxation of the contacts with time and temperature variation.

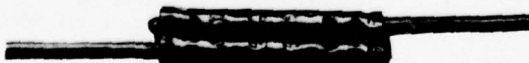


FIGURE 3 - Crimped Connector (H2562-1 RED)

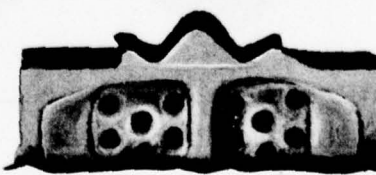


Figure 4 - Utilux H2562-1 Red Connector

Service History

A total of 38 individual field trial cables including both subscriber and junction cables have been installed since the first 0.63mm lead sheathed cables in 1965. All have been maintained under gas pressure and all are still in service. There fault history has not been different to similar copper cables.

During 1976 one of the original 1965 lead sheathed cables developed a gas leak in the lead sheath due to corrosion and it was necessary to replace a length of cable. Conductors from a section of the recovered cable were metallurgically examined and no corrosion or other deterioration was detected in any of the conductors examined.

Savings

The extent of savings offered by aluminium cable depends primarily on the cost differential between copper and aluminium. The price of copper has fluctuated for most of the period since 1964 and an average Australian price of \$A1,300/tonne has been forecast for 1977-78. The average price of aluminium has risen each year since 1973 and an average price of \$A955/tonne is expected for 1977-78. (The rate for the Australian \$ for August 1977 is approximately \$A1.00 equals \$US1.1025). At these prices attractive savings in the purchase price of aluminium cable compared with copper as shown in Table 4, are available.

| Cable Size | Saving (%) |
|-------------|------------|
| 400/1.15mm | 12 |
| 150/1.15mm | 7.5 |
| 800/0.81mm | 11.5 |
| 150/0.81mm | 6.5 |
| 1800/0.52mm | 7.5 |
| 800/0.52mm | 6.5 |
| 150/0.52 | -1 |

TABLE 4 - Savings Related to Cable Size

The savings on maximum size cables i.e. 400/1.15mm, 800/0.81mm and 1800/0.52mm, can be obtained from Figures 7, 8 and 9 respectively for metal prices in the ranges, copper \$A700-2,000/tonne and aluminium \$A800-1,200.

It is considered that the savings derived from the figures are conservative and will increase when a greater proportion of cable used is aluminium.

It is worth noting that at 1973 average prices of copper \$A1,240/tonne and aluminium \$A580/tonne the savings on a 1,800/0.52mm cable was 23% on an 800/0.81mm cable 33%, and on a 400/1.15mm cable 36%.

Since routine use has started 110,000 Pkm of 0.81mm and 20,000 Pkm of 0.52mm aluminium cable has been supplied at a saving of approximately \$A265,000. Currently Telecom Australia's monthly large size paper cable order contains on an average over 20% aluminium cable. This will increase as the field user gains experience and confidence in aluminium cable. The introduction of 1.15mm cable will further increase the proportion of aluminium cable used.

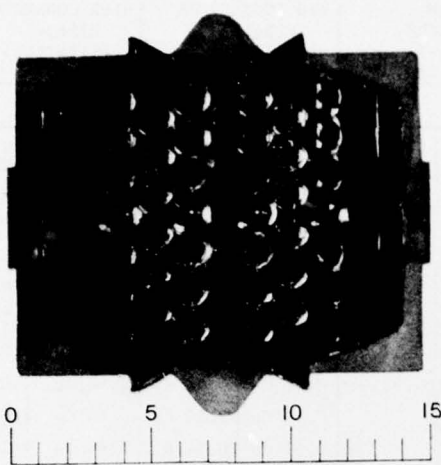


FIGURE 5 - H2562-1 Connector with Side Walls Lowered

A choice of manually operated or electro-hydraulically operated machines is available to crimp the connectors which are supplied in reels of 1000 in strip form. A manual machine is illustrated in Figure 6.



FIGURE 6 - Jointing Machine (Manually Operated)
Quality Control of Field Jointing

A simple field instrument which measures the resistance of joint samples made prior to commencing a large size cable joint provides "field" quality assurance by checking that the machine type in use is in correct adjustment and is producing joints of satisfactory electrical performance within resistance limits specified for the type of cable conductors concerned.³

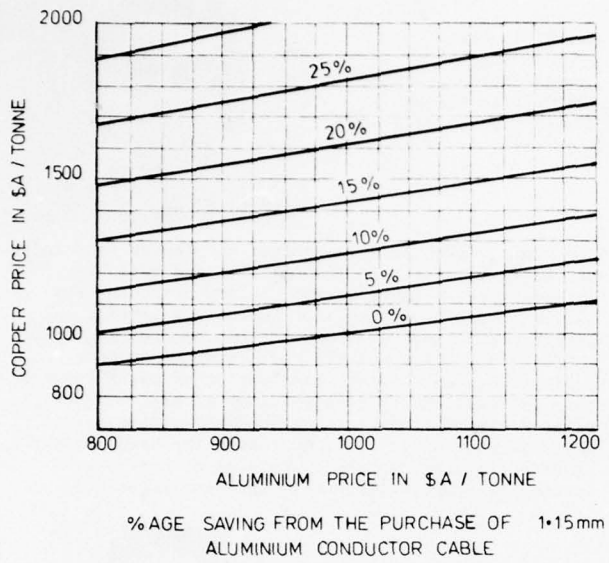


FIGURE 7

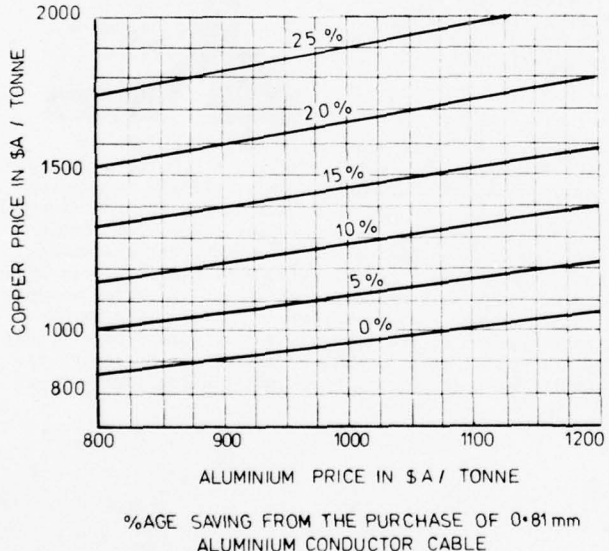


FIGURE 8

Duct Costs

Aluminium cables occupy more duct space than the same pair size copper cables. This extra space is of little consequence except where a project would have used copper cable containing more pairs than the largest useable aluminium cable. Here the cable savings would often be more than offset by a need to carry out subsequent cable installations more frequently, thereby using more duct space and advancing the date at which additional ducts would have to be provided. PV of AC methods, as discussed in the 1970 paper, provide tools for studying such situations, but are tedious to apply to individual projects and provide results that are heavily dependent on predicted interest and inflation rates and on

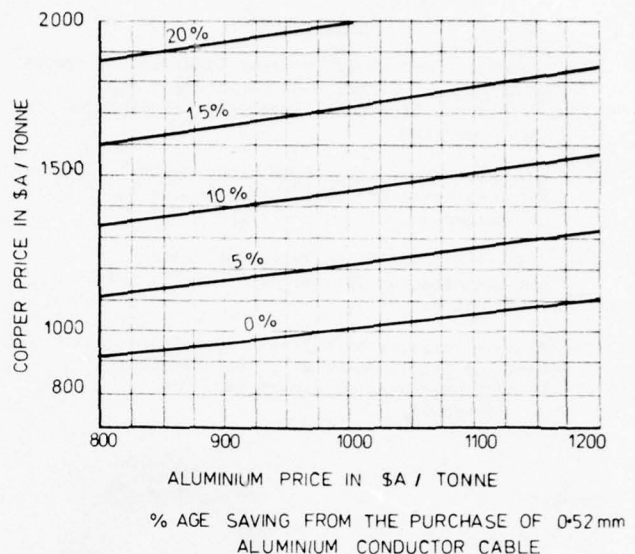


FIGURE 9

predicted duct installation costs. The latter have risen rapidly from an average of \$5,600/duct km in 1970 to \$9,900/duct km in 1976. To overcome these problems the principle being adopted in Telecom Australia is to use aluminium whenever the installed cost of the cable per pair is less for aluminium than for copper provided the use of aluminium does not result in the duct route requiring augmentation in less than 15 years. This principle is expected to adequately allow for the value of the additional duct space used by aluminium and will result in a continuing use of large pair size copper cables.

Future

We have thus reached the stage in Telecom Australia where we have a range of large size aluminium cables, and their accompanying installation practices, that will continue to be used while metal prices and other cable manufacturing costs are such that the use of these cables is economically attractive. The processes for paper insulated copper and aluminium cables are so similar that it is possible to change the proportion of aluminium used quite quickly should the price differential change significantly, or should a shortage of either metal occur.

It is anticipated that the use of EC grade FA aluminium conductors with paper insulation will prolong the use of both helical and longitudinal paper insulation in Australia. The decision to use this material for the smaller 0.52mm conductor cables in lieu of a more robust alloy wire⁴ has been based on cost coupled with the experience which has demonstrated an ability to joint the conductor in the field. However, as labour costs increase, the slower paper insulating processes become less competitive, compared with high speed cellular plastics extrusion. As the tensile properties of EC grade aluminium are not suitable for high speed extrusion processes, cellular plastics insulation will require the use of alloy which would be more expensive than EC grade. Cellular plastics will therefore only become economically attractive when the cost of aluminium alloy or copper insulated with this material is comparable to EC grade FA aluminium insulated with paper.

References

1. "Aluminium Conductors in Paper Insulated Telephone Cables". R.A. Clark, M.A. Rheinberger and A.W. Sisson. Nineteenth International Wire and Cable Symposium.
2. "A Connector for Large Size Cable Joints". Telecom Australia Research Laboratories Report No. 7108, B.A. MacLennan.
3. "Connector Jointing of Telephone Cables". Telecommunication Journal of Australia Volume 23, No. 3, October 1973.
4. "Machine Jointing of Helical Paper Insulated Aluminium Alloy Conductor". Telecom Australia Research Laboratories Report No. 7064, B.A. MacLennan.

Speaker

Mr. A. W. Sisson
Superintending Engineer,
Lines Construction Branch,
Headquarters,
Telecom Australia.



After qualifying as an Engineer in 1950, Mr. Sisson spent 10 years in the field working on external plant. He moved to Headquarters in 1960 to establish Telecom's Cable Design Group. He was Senior Engineer, Cable Design, for eight years and initiated the earlier trials for aluminium conductor cable. In 1975 he took over as the Superintending Engineer, Lines Construction Branch, where he is responsible for the design and development of outside plant and the associated construction practices.

Mr. R. J. Lewis
Telecom Australia
Communication House
199 William Street
Melbourne, Victoria 3000,
Australia



Bob Lewis worked as a Technician and Senior Technician on the installation of transmission and switching equipment for a short period, before attending the Royal Melbourne Institute of Technology (RMIT). He obtained a Diploma of Communication Engineering from RMIT in 1959 and spent the next seven years as a project engineer on the installation of major cables; this was followed by five years as an area engineer responsible for the installation and maintenance of external plant. In 1972, he joined the Headquarters staff of Telecom Australia where he is currently Section Manager, Cable Design and Specifications.

Mr. N. W. Peters,
Telecom Australia,
Communication House,
199 William Street,
Melbourne, Victoria 3000,
Australia



Noel Peters joined Telecom in 1946 After the war service with the Royal Australian Air Force on radio system maintenance. He was progressively Technician, Senior Technician and Technical Instructor in Telephone Switching and Long Line Equipment areas. Following completion of a Diploma of Communication Engineering at the Royal Melbourne Institute of Technology in 1964 he worked as a Field Engineer installing major conduit routes in the city of Melbourne. Since 1968 he has been engaged in the design and development of external plant installation practices at Telecom Headquarters where he is Senior Engineer Installation Engineering.

STAIRCASE TO ALUMINIUM
THE BRITISH POST OFFICE PROGRAM FOR A NEAR-COMPLETE SUBSTITUTION
OF ALUMINIUM FOR COPPER CONDUCTORS IN LOCAL LOOP CABLES

H J C SPENCER

British Post Office Telecommunications Headquarters
London, England

Abstract

The British Post Office plan for a near complete change to aluminium conductors in local loop cables is described. The long term aim is a true unigauge network using only 0.5mm aluminium cables. The economic case for changing to aluminium conductors is restated. The designs of cable used are discussed with particular reference to ways of overcoming the problem of the extra size of aluminium cables. For the aluminium equivalent of 0.4mm (26 gauge) copper cables the mutual capacitance is being increased, this having no operational disadvantage in the United Kingdom network. Larger gauge copper conductors will be substituted by 0.5mm aluminium conductors with their performance enhanced by loop electronics. The solutions adopted to solve a number of practical problems are described. An indication is given of the reduction of cable costs already achieved and to be expected in the future. No counter increases in operating costs have been experienced and none are foreseen.

Introduction

1 Use by the British Post Office (BPO) of cables with aluminium conductors on a large scale started in 1968 when they became a standard for some local loop filled distribution cables. Since a change to aluminium alloy conductors experience with these has been wholly satisfactory and in 1976 the BPO, with the cooperation of the United Kingdom (UK) telephone cable industry, formulated a 5 year plan for an almost complete change to aluminium conductor cables for local loops. The ultimate aim is to move gradually to a true unigauge network using only cables with 0.5mm (24 gauge) aluminium conductors. The 1976 plan for the change to aluminium conductors, shown in Figure 1, recognised that there were still problems to solve before the change could be completed, and that there were doubts about the timing of individual steps in the program and even in the order of the steps.

Why Use Aluminium?

2 The case for changing from copper to aluminium conductors is largely economic and is made by Figure 2. For equal conductivity, over the last 20 years the cost of aluminium has

always been less than half that of copper, and a reasonable projection would suggest a future cost as low as one-quarter that of copper. The dramatic difference in cost between aluminium and copper is, of course, reduced when complete cables are compared. Figure 3 shows a typical cost breakdown and indicates that a cost reduction for complete cables of 20-25% is to be expected. The precise value would depend upon conductor gauge, number of pairs, etc.

Cable Design Considerations

3 A general problem posed by the use of aluminium conductors in telephone cables is that, for equal conductivity, they are 60% greater in cross-sectional area than copper conductors. For a given mutual capacitance insulation thickness is directly proportional to conductor diameter, so that complete aluminium cables with the same primary electrical constants also have 60% greater cross-sectional areas than copper cables, ie they are about 25% greater in diameter. The increased cost of insulating and sheathing materials is not very important, assuming the use of polyethylene sheaths, because the combined costs of insulation and sheath are small when compared with other costs, as indicated by Figure 3, but the increased cable diameter has economic disadvantages when cables are to be installed in an existing duct network which has been dimensioned with the expectation that smaller copper cables were to be used.

4 The problem of increased size of aluminium conductors can be alleviated by suitable choice of the primary cable constants in some circumstances. Local loop cables have traditionally been manufactured with a mutual capacitance of 50-55nF/km regardless of gauge. This is presumably because such a design resulted in the most cost effective cables when conductors were paper insulated copper, and sheaths were made of lead. Figure 4 indicates, however, that for cables made from modern materials a mutual capacitance of 50-55nF/km is not ideal for copper conductors, and that cables with aluminium conductors should be manufactured with a mutual capacitance considerably higher than the ideal for copper.

5 A corollary of constant mutual capacitance design is that the ratio of resistance to attenuation, for unit length, the characteristic impedances of cables vary with gauge. The UK telephone system, and probably many others, has been designed with line limits based on the ratio of resistance to attenuation of cables of larger gauge than are now commonly used. In consequence cables with 0.32mm (28 gauge) and 0.4mm (26 gauge) copper conductors, which it is now possible to use for many loops because of increases in telephone sensitivity, are resistance limited when manufactured with the traditional mutual capacitance. Advantage can be taken of this when designing aluminium equivalents of cables of these gauges by increasing the mutual capacitance, and so reducing cable diameters, without operational penalty. It is to be noted that the device of increasing the mutual capacitance of cables is not applicable in the UK network when substituting aluminium conductors for copper gauges larger than 0.4mm and other means have to be adopted for overcoming the size disadvantage of aluminium, as discussed later.

6 The change in cable impedance which follows from increasing the mutual capacitance of aluminium equivalents of the small gauge copper cables benefits telephone side tone. The BPO standard telephone circuit was designed to provide minimum side tone when connected to a limiting line of 0.5mm (24 gauge) copper and the use of smaller gauge copper conductors with the traditional mutual capacitance results in an undesirable increase in side tone. Recent BPO research into subjective telephone assessment indicates that the importance of side tone is seriously under-estimated by standards based on loudness alone, and control of local network impedances is likely to become increasingly important in the future, favouring the use of aluminium as a substitute for copper in the smaller gauge cables.

Problems and Solutions

7 It is convenient to consider the problems posed by the program outlined in Figure 1, and the solutions adopted or proposed, in 5 basic steps.

Step 1 - Distribution Cables

8 In the UK local network these are cables of 100 pairs or less connecting subscribers to cross connection points (ready access terminals).

Size. Because these cables contain relatively few pairs and are provided in duct of ample capacity, or are directly buried, their size is relatively unimportant.

Moisture Penetration. Aluminium is vulnerable to moisture in the presence of a polarising voltage. However, experience has demonstrated that such conditions are equally disastrous for copper conductors, even when insulated with

polyethylene. The solution for small cables, now thoroughly proven, is to insulate the conductors with cellular polyethylene and to completely fill the cable interstices with petroleum jelly.

Wire Jointing. Traditional twist joints are unacceptable for aluminium. Welded joints and soldered joints have been tried by the BPO with limited success. Joints made with "B-wire" connectors have, however, been proven fully satisfactory by accelerated life tests and by nearly 10 years of field experience. Since the B-wire connectors are also now the standard method of jointing copper conductors in the distribution network their use does not constitute an extra requirement for aluminium.

Termination at Cross Connection Points. The latest standard BPO practice for cross connection cabinets is to pass the cable conductors through identification holes in fanning strips, and to interconnect them, either directly or indirectly by jumpers, using B-wire connectors. Early aluminium cables with conductors made from $\frac{3}{4}$ hard electrical conductivity (EC) grade material were not considered sufficiently ductile for this practice. Aluminium alloy conductors have, however, proved fully satisfactory and are now terminated in exactly the same way as copper conductors.

Screw Terminations. Aluminium conductors are not suitable for direct termination beneath screw heads because of problems with relaxation and oxidation. The long term solution will be the development of new type terminals, but as an interim measure aluminium conductors are being terminated indirectly by interposing a short copper tail connected with a B-wire connector.

Step 2 - Main Feeder Cables

9 These are cables of 100 pairs or more, connecting cross connection points to telephone exchanges (central offices).

Size. If the cables were electrical copies of copper cables the 25% increase in cable diameter would be unacceptable. The solution for replacement of 0.4mm copper, now the most common feeder cable gauge, is to increase the mutual capacitance, as discussed in paragraph 5. By using a mutual capacitance of 60nF/km with 0.5mm aluminium conductors an operational replacement has been achieved with negligible size penalty.

Moisture Penetration. Experience with aluminium distribution cables has proved petroleum jelly filling to be a completely satisfactory solution. However, the 10% increase in cable diameter necessary to maintain the required mutual capacitance was considered unacceptable for main feeder cables in the UK circumstance of an existing and limited duct network. Also, the additional insulation and sheath materials would

have reduced the cost advantage of aluminium by about 5%, which was undesirable. Fortunately analysis of maintenance statistics for the main feeder network revealed that modern polyethylene sheathed cables protected by an air pressure system are largely immune from moisture penetration. Bearing in mind the improvement to be expected from the introduction of injection-welding sheath closure techniques it was considered that non-filled (dry) feeder cables were the most cost effective solution, for the UK. It is recognised, however, that in other circumstances filled cables would be the preferred solution for both copper and aluminium cables.

Wire Jointing. Use of B-wire connectors, as for distribution cables, is a possible solution to the problem of jointing aluminium main feeder cables, but the connectors are rather bulky when used in large numbers. As a preferred alternative a new crimp has been developed for use with the BPO in-line jointing machine. The crimp is multi-purpose, suitable for both copper and aluminium conductors with diameters in the range 0.32-0.63mm. Its performance has been proved in accelerated life tests and field trials.

Termination at Cross Connection Points. Although the termination of filled distribution cables in the new fanning-strip cross connection points is a proved practice the termination of dry feeder cables was open to question. Accelerated life tests and field trials have removed the doubts, however, and the termination of dry aluminium conductors is now a standard practice. The use of filled B-wire connectors is a beneficial factor.

Termination on Exchange Main Frames. It is believed that satisfactory wire wrapping techniques will be developed for aluminium alloy conductors. However, field tests have not been in progress long enough for the technique to be introduced as a standard practice, and copper tail-cables are being used as an interim measure.

Step 3 - Armoured Cables

10 These are standard distribution cables additionally protected by a layer of steel wires and a further polyethylene sheath. They are used when cables are buried directly in the ground, without duct.

Low Extensibility. Early distribution cables using $\frac{3}{4}$ hard EC grade aluminium conductors were not considered suitable for protection with steel wire armour. Because of the low extension of the material, of the order of 1%, it was feared that if installation practices were abused conductor breaks could occur before possible excessive pulling loads were taken by the armouring wires. The problem was solved by the change to aluminium alloy conductors which have an extension of about 10% before break.

Step 4 - Aerial Cables

11 Self-supporting aerial distribution cables of "figure-of-eight" construction are used by the BPO in rural areas.

Fatigue. Tests on cables using $\frac{3}{4}$ hard EC grade aluminium conductors showed that, unlike copper, these had a finite fatigue life when tested in conditions simulating aerial use. Aerial cables with these conductors were not, therefore, adopted as a standard despite some satisfactory initial experience. This problem was also solved by the change to aluminium alloy conductors. Tests on cables with alloy conductors indicated that they had an apparently unlimited life when subjected to the tests which had revealed the shortcomings of the $\frac{3}{4}$ hard EC grade material.

Step 5 - Cables for Long Loops

12 Some subscribers loops require the use of copper conductors of 0.5mm (24 gauge), 0.63mm (22 gauge) or 0.9mm (19 gauge) diameter for part, and in the extreme, the whole of routes, to allow transmission and signalling limits to be met.

Size. The device of increasing the mutual capacitance of operationally equivalent cables with aluminium conductors is not applicable because cables of gauges greater than 0.4mm are transmission limited. Cables with aluminium conductors must, therefore, carry the full size penalty inherent in the material, and this is unacceptable for the UK feeder network. The solution proposed is to eliminate the need for gauges larger than 0.5mm aluminium by the use of loop electronics. At present day costs, and for UK loop lengths, it is uneconomic to use electronic devices on all pairs in a cable. Their use can be justified, however, where they enable gauges to be reduced not only on the long loops to which they are connected but also to many shorter loops which would otherwise be over-gauged because of the presence of a few long loops. It might be thought that aluminium conductors, being cheaper than copper, reduce the competitiveness of loop electronics. However, since in the UK main network the choice is between copper conductors and small aluminium conductors with electronics the two developments compliment each other.

Progress with the Implementation of the Program

13 Progress has been broadly in line with the timescale of Figure 1. The change to aluminium conductors in distribution cables is substantially complete, 88% of the non-armoured cables purchased in 1976 having aluminium conductors. The residual is accounted for by 2 pair cables terminated on screws in subscribers premises, for which copper conductors will be used until a terminal suitable for aluminium has been developed, and by cables

for which the larger gauge copper conductors are essential for transmission and signalling pending the availability of loop electronics.

14 The change to aluminium conductors in armoured and aerial cables has been initiated too recently to be reflected in purchases. A penetration similar to that for unarmoured distribution cables should be achieved in about a year.

15 The change to 0.5mm aluminium conductors in place of 0.4mm (26 gauge) copper conductors in main feeder cables is being made on a Region by Region basis. All Regions are now planning to use 0.5mm aluminium main cables and over half the Regions are now actively installing them.

16 Overall, approaching half the loop kilometres of local cables installed by the BPO now have aluminium conductors. Completion of the remaining steps in the program is dependent upon the development of MDF termination techniques and of electronic loop extender devices. The development of MDF wire wrapped terminations has already been referred to. Development of loop extender devices is now almost complete and a range including 6dB amplifiers and line current boosters allowing increases of about 1000 ohms in signalling resistance limits are being purchased. The extent to which it will be economic to use these to eliminate the need for conductors larger than 0.5mm aluminium will depend upon the costs of the devices when bought in quantity and to the study of individual applications as they arise. It may be that the timescale for this step will be increased from that shown in the program.

Savings Achieved

17 Very substantial savings have been achieved since 1968 by the substitution of aluminium conductors in distribution cables. For the year 1976, for example, cables with 0.5mm aluminium conductors cost 35% less than the copper cables which would otherwise have been used. However, this is a distorted comparison because the very large saving is in part due to the BPO policy of not using conductors of a lower gauge than 0.5mm in distribution cables, irrespective of transmission and signalling requirements, for handiability reasons. For distribution cables, therefore, the comparison is between 0.5mm aluminium and 0.5mm (26 gauge) copper conductors which are not electrically equivalent.

18 A fairer comparison is that between 0.5mm aluminium conductors and 0.4mm (26 gauge) copper conductors in main feeder cables. In 1976 both these types of cable were purchased in substantial quantities and the cost per loop kilometre of the aluminium cables was only 80% of the cost of the copper cables. Savings are, of course, sensitive to the price of copper and, because of the present depression in the price, the savings from the use of aluminium for the current year will undoubtedly be less than 20%.

A long term indication is given by Figure 5, which estimates the savings which would have been achieved at the metal prices existing over the last 20 years. The lowest saving would have been 10% in 1958, the highest 37% in 1966, 1973 and 1974, and the average 23%.

19 It is of interest that in 1976 the cost of 0.5mm aluminium cables was slightly less than that of 0.32mm (28 gauge) copper cables so that, as the performance of 0.5mm aluminium is superior, the only justification for using 0.32mm copper cables is their small size. The program for change to aluminium assumes that the small size of 0.32mm copper will be the overriding factor for about 5% of cables.

20 Analysis of cable costs and material prices for 1976 suggests that the total cost of converting the raw materials, copper and polyethylene, into finished cables is about 5% higher for aluminium than for copper, indicating that even at the present state of the cable making art there is an adequate margin between the lower material and higher manufacturing costs for aluminium.

Are There Off-Setting Operating Costs?

21 The attitudes of cable layers and splicers are encouraging. Cable layers are showing a definite preference for aluminium cables because of their light weight, only half that of copper. Cable splicers have, since the change from $\frac{3}{4}$ hard EC grade to alloy material, come to look upon aluminium as merely silver coloured copper.

Installation. The works practices for the installation of both distribution and main feeder cables with aluminium conductors are identical to those which would be used for an exclusively copper network. With the exception of a modest, once-and-for-all, Headquarters directed training program in Regions, no additional installation costs which can be attributed to the use of aluminium have been identified.

Maintenance. The use of aluminium distribution cables has been standard practice long enough to demonstrate that even in the hostile environment in which these small cables are placed the service given by aluminium is indistinguishable from that of copper. Sufficient experience has yet to be accumulated to allow the same to be said of feeder cables but that acquired to date has been wholly satisfactory.

Conclusions

22 The BPO has, after some years of experience with small jelly-filled aluminium conductor cables in its distribution network, embarked on a program to use aluminium conductors for the vast majority of its local loop cables. The program is progressing satisfactorily with about half of all the local loop cables now being installed having aluminium conductors.

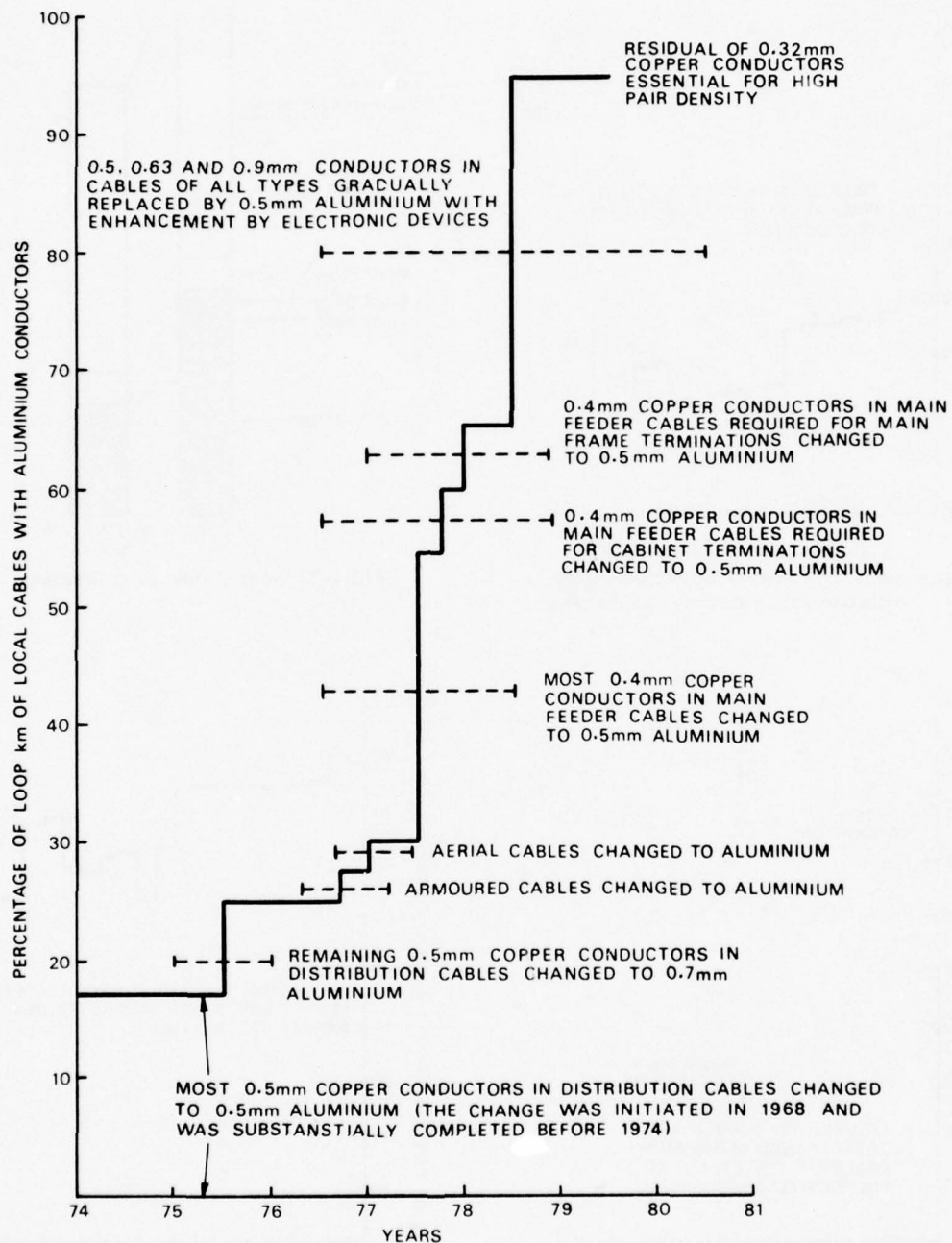


FIG.1 Provisional Program for Conversion of Supply of Local Cables to Aluminium : April 1976

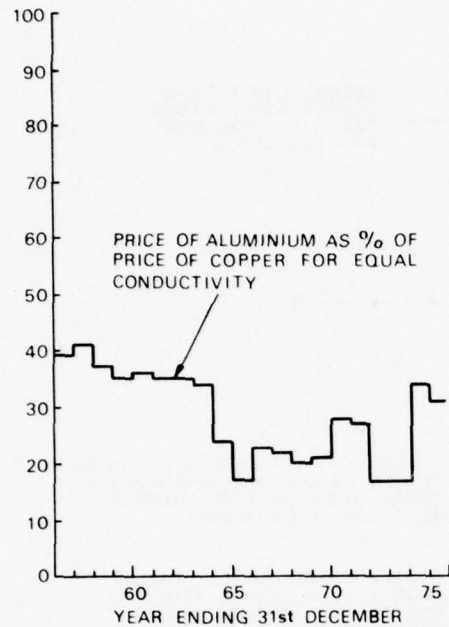


FIG.2 20 Year Copper/Aluminium Price relationship—Annual Averages

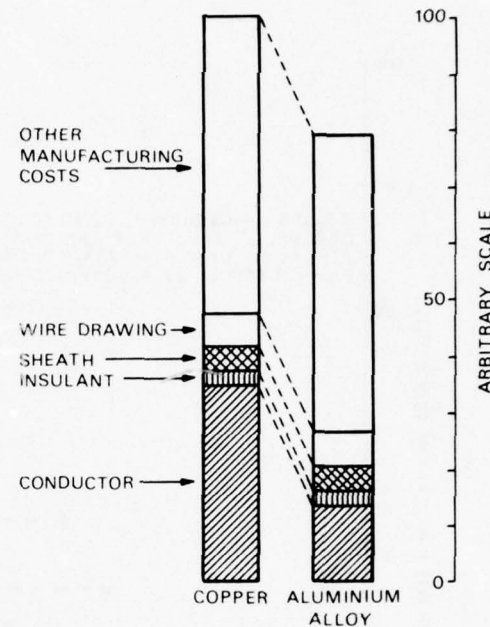


FIG.3 Typical Cable Cost Analysis

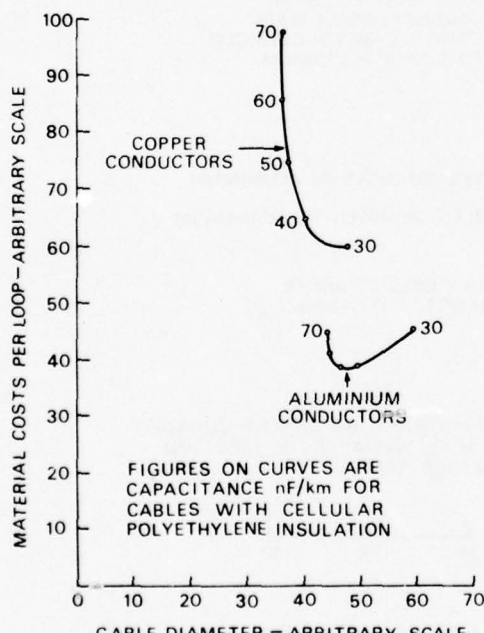


FIG.4 Material Costs and Cable Diameters for Constant Attenuation with Varying Capacitance

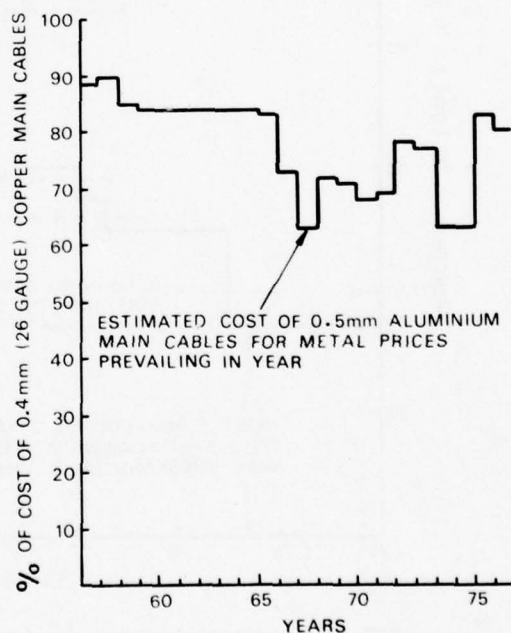


FIG.5 Cost of 0.5mm Aluminium Main Cables as Percentage of Cost of 0.4mm (26 gauge) Copper Main Cables



H J C Spencer,
British Post Office
Telecommunications
Headquarters,
OP2,
Lutyens House,
1-6 Finsbury Circus,
LONDON, EC2M 7LY
England

(01) 432 5470

Mr Spencer is the Head of the Local Line and Junction Planning Division of the Operational Programming Department. He is responsible for the management of, and plant standards in, the local loop network and the junction network, with a particular interest in cable design. He is a Member of the Institution of Electrical Engineers.

Acknowledgement

Acknowledgement is made to the Senior Director of Planning and Provisioning of the Post Office for permission to make use of the information contained in this paper.

ALUMINIUM ALLOY CABLE CONDUCTORS - A PROVEN SUBSTITUTE FOR COPPER

D R Bissell

Post Office Telecommunications Headquarters, London, England

Abstract

The British Post Office decision to utilise aluminium alloys as a substitute for copper cable conductors followed successful laboratory tests and field trials to assess their suitability. Earlier trials with cables using 3/4 H aluminium conductors had resulted in a number of conductor failures attributable to the mechanical characteristics of the aluminium wire. A decision was therefore made to develop alloys of aluminium which were known to be capable of conversion into a more suitable wire. Accordingly development work in co-operation with the wire and cable makers was put in hand. This work is now complete and cables manufactured with this aluminium alloy are now specified and installed as a standard practice. Field reaction has been very favourable with the staff accepting the alloys as being just like copper from the handling aspect.

sufficient of its physical properties to be used as a conductor.

As well as this more unusual use of aluminium in Telecommunications the BPO had themselves experimented with aluminium in the underground network and had installed cables containing paper insulated aluminium conductors in the early 1950's. Some of these cables are still in use and are continuing to give satisfactory service.

During the 1960's the increasing price differential between copper and aluminium provided incentive for further exploitation of aluminium on the grounds of economy. Consequently a cable specification was prepared and large quantities of aluminium cable up to 100 pairs for use in the distribution network were purchased and installed^{3,4}. These cables were manufactured using 3/4 H aluminium conductors of 0.6 mm or 0.8 mm diameter insulated with cellular polyethylene, fully filled with petroleum jelly and sheathed overall with black polyethylene.

Introduction

This paper outlines the development of aluminium alloy conductor cable with particular reference to the wires themselves, and shows how the successful manufacture and introduction to the field has been accomplished.

As described in a companion paper¹, the motivation for change to aluminium from copper was based on sound economic grounds and was aided by the uncertainty of guaranteed copper supplies at that time. The choice of aluminium was not completely novel because as early as 1900 the British Post Office has experimented with aluminium wires as a direct replacement for the bronze wires then used in overhead telegraph circuits. Aluminium wire had also been supplied by the National Telephone Company to Captain R F Scott's ill fated expedition to the Antarctic. There wires were laid directly over the snow to provide the physical link for field telephones.

Samples of this wire recovered from the Antarctic have been tested both physically and metallurgically² and show that the aluminium used was in fact an alloy containing some 0.5% of iron and 0.3% of silicon, possibly one of the earliest aluminium alloys to be used commercially. It is interesting to note that despite its long exposure to the adverse conditions for some 50 years, the wire when tested still retained

Studies on the optimum sizes of conductor and insulation⁵ resulted in the adoption of 0.5 mm in place of 0.6 mm diameter conductors. This change, although small, produced difficulties in both the manufacture and installation of cable. From a manufacturing aspect the wire required a minimum tensile strength for the insulating and laying-up processes and the achievement of this minimum strength resulted in low elongation values down to the 1% mark. This low elongation figure made cable installation more critical and several cases of cable failure occurred. These failures, although not large in number, were considered very significant because they showed a source of potential trouble and undermined the confidence of the field staff in aluminium. Consequently a decision was made to improve the characteristics of thin aluminium wire and it became obvious that an alloy would have to be developed.

Aluminium Alloy Conductors

In 1970 the BPO set up a special committee to review the known alloy materials available on the market and to investigate any likely alloys under development. The findings of this committee were made known to the cable and wire making industry and a joint effort on the development of a suitable wire was commenced.

As a basis for this development work the essential physical requirements of a cable conductor were decided.

There are listed as follows:-

1. Conductivity

The wire must possess adequate conductivity in order to meet planning requirements and to provide an effective transmission loop. For this reason a lower limit of 61% IACS (Internationally Agreed Copper Standard) was specified.

2. Elongation

Good elongation consistent with adequate tensile strength would appear to be the most desirable of physical characteristics. The ability of a cable to share the installation loads equally among all conductors greatly reduces the possibility of individual conductor failures. A minimum elongation value of 5% was considered adequate to achieve this result.

3. Ultimate Tensile Load or Stress

The tensile performance of a wire is critical for certain manufacturing processes and the subsequent installation of economic cable lengths. Wire drawing and insulating operations demand a minimum strength in the order of 15 Newtons, and up to 90 MN/m² for cabling lengths of 500 m (depending on pair count and duct conditions).

4. Proof Stress

A specified value of 0.1% proof stress is considered essential in order to fix the shape of the tensile test envelope and to ensure that thinning of the wire does not occur during manufacture or installation. A minimum value of 90 MN/m² is considered to be necessary in order to meet the installation requirements.

5. Handleability

Ease of handability although difficult to specify is an essential property if jointing, terminating and cable setting operations are to be performed without failure of the conductor. Particular tests for these characteristics have been developed and the most important of these are the 180° Reverse Bend Test and the Wrap Test.

Included in this requirement are:-

- (a) good surface finish and low sensitivity to local stress raising notches, kinks or impurities.
- (b) freedom from embrittlement due to ageing.
- (c) resistance to vibration fatigue
- (d) freedom from intercrystalline corrosion attack.

6. Jointing

Aluminium, unlike copper, produces an insulating skin as it oxidises. This oxide accounts for the poor jointing performance of connections involving aluminium. Any jointing technique used must therefore ensure that this skin does not interfere with the joint performance. To meet this requirement the crimp and compression connections have been developed. For such joints it is essential for the conductor material to have good resistance to cold flow and stress relaxation up to the normal operational temperature.

In order to achieve a common target for the individual development effort that was required, a set of target values was produced. These values were based on the above criteria but were modified in the light of experience to provide a workable and achievable list of objectives.

These values were set as follows:-

1. Tensile strength

110 MN/m² over a gauge length of 250 mm.

2. Elongation before Fracture

5% over a gauge length of 250 mm.

3. 0.1% Proof Stress

90 MN/m² minimum average.

4. 180° Reverse Bends

9 complete bend cycles before fracture.

5. Helical Wraps

3 complete cycles before fracture.

6. Stress Relaxation

Not less than 80% of original test results when subjected to a sustained load equal to the 0.1% proof load value.

7. Intercrystalline Corrosion

Not less than 80% of original results after treatment.

8. Ageing

Tensile, elongation and 0.1% proof load values after ageing shall be equal to original results.

These parameters are now specified as standard values and cables manufactured to these requirements are in service. Typical test results obtained from these cables are shown overleaf.

Test Results

The test results shown in Table 1 have been compiled from data obtained from the cable manufacturers and from BPO type approval tests. These have been averaged out to give mean values except where minimum values have been quoted.

Table 2 shows the approximate composition of the alloys and it can be seen that several different types of alloy have been supplied. For convenience these alloys have been shown as three separate family groups.

No test results for stress relaxation and intercrystalline corrosion have been shown but tests so far have shown the alloys to be completely satisfactory within the limits set.

Vibration fatigue has also been tested but as this criteria does not appear in the manufacturing specification it has not been included in Table 1. However experimental results show that the alloys are vastly superior to 3/4 H aluminium and approach the values obtained for copper.

Manufacturing Experience

The alloys being supplied are heat treatable and respond to both batch and in-line annealing processes⁶. Unlike copper or aluminium - which are fully annealed before being processed to the required hardness - the alloys are partially annealed and require a close control of the variables to achieve consistent results.

For the batch annealing process small ovens are utilised and recirculating fans are installed to produce equalised temperatures throughout the charge. An inert gas is introduced, after initial heating, to ensure that oxidisation is kept to a minimum. Annealing temperatures are in the order of 250°C and the process time is approximately 4 hours.

Good results have been obtained with this method but it has the disadvantage of adding an extra stage into the processing cycle.

For the in-line process a tandem drawing annealing and insulating system is operated. The wire is first drawn down to size then passed

| PROPERTY | UNIT | EC GRADE ALUMINIUM | | COPPER | ALUMINIUM ALLOY | | |
|---------------------|-------------------------|--------------------|----------------|----------|-------------------|-------------------------------|--|
| | | BPO SPECIFICATION | 99.7% EC GRADE | SUPPLIED | BPO SPECIFICATION | *IRON ENRICHED EC GRADE ALLOY | *MODIFIED IRON ENRICHED EC GRADE ALLOY |
| BREAKING LOAD | NEWTONS | 24-36.5 | 29.5-31 | 32.6 | 22(MIN) | 23-26.5 | 27-30 |
| ELONGATION AT BREAK | % | - | 1-3 | 21.6 | 5(MIN) | 10-20 | 10-20 |
| 0.1% PROOF STRESS | NEWTONS/mm ² | - | - | - | 90(MIN AVE) | 100 | 101 |
| 180° REVERSE BEND | BENDS TO FAILURE | 9(MIN) | 10 | 12 | 9(MIN) | 12 | 15 |
| WRAP TEST | CYCLES TO FAILURE | 3(MIN) | 4 | 4 | 3(MIN) | 5 | 6 |
| CONDUCTIVITY | % IACS | 60.66 | 63.4 | 100 | 60.66 | 62.2 | 61.0 |

TABLE 1 RESULTS OBTAINED FROM PRODUCTION CABLE
(*batch annealed)

| FAMILY GROUP | UNIT | S _i | M _g | Z _N | M _N | F _e | C _u | A _L |
|---------------------------------------|------|----------------|----------------|----------------|----------------|----------------|----------------|----------------|
| GROUP 1 IRON ENRICHED | % | UP TO 0.1 | UP TO 0.1 | UP TO 0.1 | UP TO 0.05 | 0.6-1.0 | UP TO 0.1 | REST |
| GROUP 2 IRON/COPPER ENRICHED | % | 0.1 | 0.2 | 0.1 | 0.05 | 0.5 | 0.3 | REST |
| GROUP 3 IRON/MAGNESIUM ENRICHED | % | 0.1 | 0.25 | 0.05 | 0.03 | 0.25-0.75 | 0.1 | REST |
| EC GRADE | % | 0.06 | 0.004 | 0.03 | TRACE | 0.27 | 0.004 | REST |

TABLE 2 COMPOSITION OF ALLOYS

through the annealer where the wire is heated either by an induction process or a resistance method. It is then quenched in water and passes on to the extrusion head. As the annealer is inline with the other processes the heating time is short and consequently higher temperatures are utilised. Control of the operation is more critical and the properties of the annealed wire are marginally less than for the batch annealed wire. Conductivity is reduced by approximately 3% which is due to the different annealing mechanism and is related to the final metallurgical structure of the alloy. The advantages of this method are the comparatively high process speeds combined with the reduction in handling effort.

The remaining cabling processes do not present any unusual problems and conventional plant is utilised.

Installation Experience

Initial reaction to the new alloys was one of caution but as experience grew the planners and installation crews became to accept them with little reservation. Cables manufactured with aluminium alloy are now fully accepted and are installed as common practice. The fault rate of these cables is certainly no worse than their copper equivalent but insufficient statistics are available to detect whether or not their performance is better.

The cable at present in use is manufactured to BPO specification CW 218 and is of the twisted pair layer type construction, fully filled with petroleum jelly, cellular polyethylene insulated and sheathed overall with polyethylene compound impregnated with carbon black. Pair sizes range from 1 up to 100 and the cables are utilised in the Exchange Area network. Some 4 million loop kilometres of this cable have been installed up to the present at an annual rate of 1 million lkm.

Further Use of Aluminium Alloy

As described by Mr Spencer¹ the BPO are now introducing aluminium alloy conductor cables into the pressurised part of the Exchange Area network. The progress of this has been good and no undue problems have been encountered. The cable is being manufactured to BPO specification CW 251 and is of unit construction, cellular polyethylene insulated and sheathed overall with natural polyethylene. The sheath incorporates an aluminium moisture barrier to prevent osmosis, and to minimise the likelihood of corrosion the internal relative humidity is limited to 50% during manufacture and the cable is supplied with sealed cable ends.

The application of aluminium alloy to star quad cables for use in the junction network is also being studied and prototype cables will be manufactured for evaluation. The use of aluminium in coaxial cables has been considered but the cost

savings are not seen to be sufficient to justify the design effort which would be involved. The rapid development of optical fibre cables may well reduce the future demand for coaxial cables.

Suggestions have also been made for the use of aluminium alloy for internal cables to be used in exchanges and even customers premises. These projects however are still only tentative and it is too early to judge their possible outcome.

Conclusions

The development of aluminium alloy conductors has been described and comparisons with copper given. To date the alloys appear to compare favourably with copper and they have been fully accepted by the field staff. Failures of aluminium alloy cables have been rare and no more frequent than those of their copper counterparts. The use of aluminium alloys in cables is being extended and development of suitable working practices is also in progress.

For the BPO network aluminium alloys have come to stay and can truly be looked upon as a proven substitute for copper.

References

1. H J C Spencer, "Staircase to Aluminium, The British Post Office programme for near complete substitution of aluminium for copper conductors in local loop cables". International Wire and Cable Symposium 1977.
2. F G McDonald, "Test made on 50-year-old wire from the Antarctic". British Communications and Electronics, March 1961.
3. E L Winterborn, "Aluminium-Conductor Cables in the Telephone Distribution Network". Post Office Electrical Engineers J64 October 1971, P161.
4. K I Kincaid and D K Smith, "Aluminium Conductors for Polyethylene-Insulated Telephone Cables". Electrical Communications 46 No. 1 1972, P72.
5. H J C Spencer, "Optimum Design of Local Twin Telephone Cables with Aluminium Conductors". Proc IEE, 116 April 1969, P481.
6. J Prichett "Aluminium Cables:
G W Argus Design and Manufacture
J R Osterfield in the UK". 2nd
D M Salamon International Symposium
C E Wilbude on Subscribers Loops
 and Services. London
 3-7 May 1976.



D R Bissell C Eng MI Mech E
British Post Office
Telecommunications Headquarters
OP10
Carlton House
Carlton Avenue East
Wembley, Middlesex
HA9 8QH
England
(01) 908 1176

Mr Bissell works for the British Post Office in the External Plant Development Division and is Head of Group responsible for the mechanical aspects of cable design. He has had many years of practical experience on both development and field work. He is a Chartered Engineer and a Member of the Institution of Mechanical Engineers.

Acknowledgement

Acknowledgement is made to the Senior Director of Planning and Provisioning of the Post Office for permission to make use of the information contained in this paper.

LIFE PREDICTION OF INSULATIONS FOR FILLED CABLES IN PEDESTAL TERMINALS

G. A. Schmidt
General Cable Corporation
Research Center
Union, New Jersey

IPCEA WORKING GROUP 434 (REA ADVISORY COMMITTEE)
Chairman: K. W. Brownell, Brand-Rex Co.

Members of IPCEA Working Group 434 Participating in Round Robin Test

M. C. Biskeborn
W. A. Fallon
M. Farago
J. G. Henderson
I. Kolodny, G. A. Schmidt
J. S. Lizotte
E. D. Metcalf
J. Ruskin, D. Cretney

Phelps Dodge Communications Co.
Okonite Company
Northern Telecom Limited
Canada Wire & Cable Limited
General Cable Corporation
Independent Cable, Inc.
Anaconda Telecommunications
Phillips Cables Limited

ABSTRACT

The utility of the DTA test was explored by Working Group 434 of the REA Advisory Committee in comparison with an air oven aging method as a means to predict the life of insulations. The air oven method is proposed to REA as an initial qualification test for a system of filling compound and insulation.

Factors other than the pedestal environment can affect the life of insulations. If direct sunlight enters the terminal housings, the insulations will crack and fade. This will result in noise, shorts and loss of transmission.

The resistance of the insulation to mechanical damage during termination and reentering will influence the life of insulations. Conductors with cellular insulations require considerably more care than conductors with solid coverings.

BACKGROUND AND PURPOSE

During 1975, REA included a test for the determination of the oxidative stability of insulated conductors in their specification PE-39 that covers filled telephone cables. Details of the test method of the differential thermal analysis were reviewed by the members of the REA Advisory Committee, Working Group 434, but one question remained. This was the establishment of a meaningful DTA test requirement. As much as a short duration test was desired, past experience has shown that DTA data cannot be used to predict the useful service life of insulated telephone singles. The DTA test conditions of 200°C in pure oxygen are too far removed from the most severe service conditions of telephone singles. These service conditions exist in environments where insulated conductors are exposed to sun, draft and moisture and to temperatures that do

not exceed 80°C. In addition, the DTA test records only oxidative polymer failure. Embrittlement due to crystallizations cannot be detected.

Working Group 434 decided to set up a Round Robin Test, utilizing both an air oven aging method that was presented to the IWCS in 1973¹ and DTA tests in order to determine if there is any correlation between the results from these two different tests. Since solid and cellular insulations based on the same polymer of high density polyethylene and propylene-ethylene copolymer were selected for the Round Robin Test, additional information could be obtained regarding the performance of these two polymers in solid and cellular form. Working Group 434 decided to use two commercial petrodatum based cable filling compounds as the immersion media. One of these materials, compound A, is a typical domestic compound while compound B is a typical Canadian compound. The demonstration of the effect of these filling compounds on the insulations and the determination of the relative life expectancy of solid versus foam were expected to be significant parts of the Round Robin Test.

SAMPLES

A. Insulated Conductors

A 500 ft. length of each of the No. 22 AWG insulated conductors listed below were distributed to each of the eight participating members of the REA Advisory Committee.

| Sample No. | Type | Insulation Polymer | Color | Wall Thickness, Inches |
|------------|---------------------|--------------------|-------|------------------------|
| I | Solid | HDPE | White | 0.0134 |
| II | Cellular, 35% blown | HDPE | White | 0.0099 |
| III | Solid | HDPE | Green | 0.0134 |
| IV | Cellular, 35% blown | HDPE | Green | 0.0099 |
| V | Solid | Prop-Eth. Cop. | White | 0.0144 |
| VI | Cellular, 35% blown | Prop-Eth. Cop. | White | 0.0099 |
| VII | Solid | Prop-Eth. Cop. | Green | 0.0144 |
| VIII | Cellular, 35% blown | Prop-Eth. Cop. | Green | 0.0099 |

Samples I through IV were manufactured by General Cable Corporation, samples V through VIII by Northern Telecom, Limited.

B. Filling Compounds, Petrolatum Based, Commercial

1. Filling Compound A
2. Filling Compound B

TEST METHODS

A. Method for Life Prediction of Filled Cable Insulations, Utilizing Air Oven Aging

1. Correlation Between Service Life and Life Prediction Based on Accelerated Air Oven Aging

In 1971 when the problem with cracked insulations in pedestals surfaced, it became apparent that a test was needed that would allow the prediction of the service life of insulations so that adequately stabilized compounds could be selected for use.

Cracking of insulations in pedestals causes noise, especially when the humidity is high. In severe cases, shorts occur that result in loss of transmission. The only effective solution to the problem is to splice in a new section of cable.

In an effort to develop a meaningful test, it was found that by determining the time at 100°C in turbulent air that causes the loss of flexibility of insulated conductors, and that by progressively doubling the time for each 10°C reduction in temperature starting at 100°C the service life at an average temperature of 35°C can be calculated. This method for predicting the useful life of insulations was accepted, because laboratory data correlated satisfactorily with actual cracking of first generation polyethylene insulations in pedestals.

These first generation low density polyethylenes, stabilized with < 0.1% Santonox R, had been cracking in pedestals under severe climatic conditions in less than five years. The predicted life for this type of insulation was found to be in the range of 0.8 years to 1.7 years when evaluated by the oven aging elongation test method, described in Reference 1. Additional data determined by this laboratory method on the same type compound are presented in Table 1.

Table 1

| | Air Oven Aging in Turbulent Air (Linear air speed approx. 400 ft/min.) | | Air Oven Temperature 90°C 100°C | |
|--|--|-----|---|-----|
| | Insulated Conductor, No. 24 AWG solid copper, 0.0075 inches of insulation* | | White | Red |
| Days to embrittlement determined by loss of elongation | 22 | 18 | 17 | 12 |
| Calculated Life of Insulations, Years, at 35°C | 2.9 | 2.4 | 2.2 | 3.2 |

*Stabilizer: < 0.1% Santonox R

Density: 0.924

Melt Index: 0.12

Good agreement was found in calculated values of service life of LDPE, HDPE and propylene-ethylene copolymer by testing to embrittlement at 70C, 85C, 90C and 100C. However testing at 70C and 85C are impractical and only of academic interest because times to embrittle at these lower temperatures are very long.

2. Air Oven Aging Test: Procedure and Discussion

- a. Preheat telephone cable filling compound precisely to 110°C and dip coat 12 inch sections of 15 inch long specimens by immersing for 10 seconds. This dip coating procedure simulates the process of hot filling telephone cables.

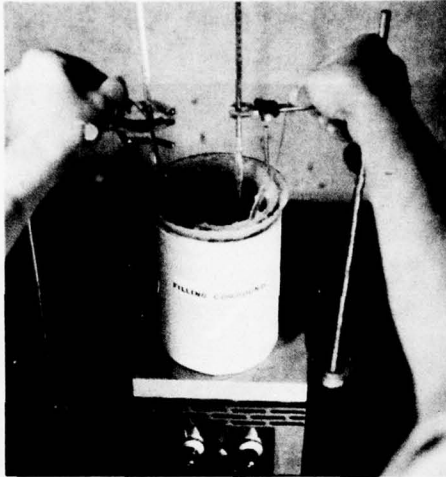


Figure 1: Wire sample just prior to a 10 second immersion in the filling compound at 110°C.

Previously¹ the insulated conductors were immersed in an excess of filling compound and conditioned for two weeks at 85°C. However, conditioning temperature of 70°C was chosen for the round robin test as being more in line with actual service conditions.

An extensive evaluation was completed at the GCC Laboratories regarding the effect of filling compound on solid and cellular filled cable insulations with respect to time to embrittlement, swelling and absorption. It was found that the amount of filling compound that is present in an actual cable or on dip coated insulation is in great excess of the amount of filling compound that can be absorbed by or will react with the insulations. Consequently the time to embrittlement, absorption and swelling of solid and cellular filled cable insulations is practically the same, whether the sample was dip coated and conditioned or conditioned in a simulated cable or in great excess of filling compound.

- b. Hang the coated insulations in an air oven for two weeks at 70°C.
- c. At the completion of the two week period, wipe the filling compound from the insulations with soft paper towels and hang the insulated conductors in an air oven at 100°C with the fresh air vent in the fully open position and with turbulent air flow.

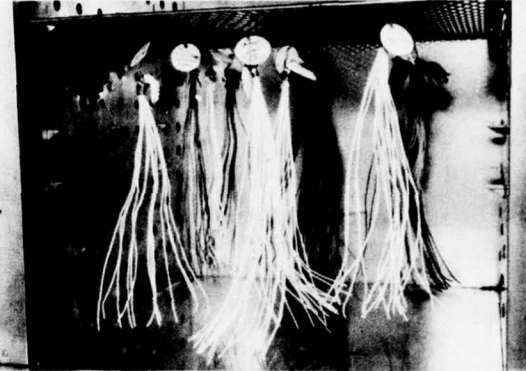


Figure 2: Insulated conductors exposed in an air oven to turbulent air at 100°C.

When the air flow is measured with a flow meter that indicates linear air speed, readings of approximately 400 ft/min. should be obtained. Place enough specimens into the ovens so that testing to embrittlement is possible. In order to make testing in monthly intervals possible, start a second set of samples one month after the first batch. The second set of samples will be used after embrittlement of the samples from the first set in order to pinpoint the failure date.

- d. Sections of insulated conductor, as discussed under (b) above are prepared for elongation testing as follows: place the sections of insulated conductor on a stone table top or a cutting board and hold it firmly by the end next to the operator. Take an industrial razor blade and cut the top layer of the insulation off in a smooth uninterrupted motion.



Figure 3: Demonstration of preparation of a segmental test specimen. In order to achieve smooth surfaces, one industrial razor blade should be used for three cuts only.

Should the razor blade cut into the conductor, discard the specimen. Use the larger segment for the elongation test. Using an initial tensile tester grip separation of 1.5 inches, a testing area of one inch and a rate of grip separation of 2 inches per minute, determine the unaged elongation first. As the aging of the insulation progresses, the adhesion of the insulation to the conductor increases to the point when it is no longer possible to separate the larger segment from the conductor. The smaller segment will then be used for elongation testing.

While the use of segmental test specimens was brought about by necessity due to the adhesion between the copper conductor and the insulation after extended aging, it was found that unaged segmental specimens have increased sensitivity to processing imperfections. It is demonstrated in Table 2 below that the utilization of segmental specimens will spot insulations with limited life considerably earlier than when tubular specimens are used for processing control elongation testing. Three insulations were prepared for this test.

Insulation 1: satisfactorily processed
 Insulation 2: processing not satisfactory
 Insulation 3: compound temperature and conductor preheat considerably lower than used for production.

Table 2
 ELONGATION AT BREAK, %

| Sequen-tial Order | No. 22 AWG Propylene-Ethylene Copolymer Filled Cable Insulations | | | |
|-------------------|--|-------------|------|-------------|
| | 1 | | 2 | |
| | Tube | 3/4 Segment | Tube | 3/4 Segment |
| Ori - 1 | 640+ | | 500 | 550* |
| gr - 2 | | 570+ | | 0* |
| ndl - 3 | 670 | | 610 | 500* |
| 4 | | 590+ | | 0 |
| 5 | 640 | | 550 | 540 |
| 6 | | 600+ | | 480 |
| Avg | 650 | 590 | 550 | 510 |
| | | | | 530 |
| | | | | 0 |
| 6 Days at 100°C | | | | |
| | 550 | 500+ | 220 | 0* |
| | 610+ | 520 | 410* | 0* |
| Avg. | 580 | 510 | 320 | 0 |
| % of Original | 89 | 86 | 58 | 0 |
| | | | | - |

Legend: * = Jaw Break
 * = Break between the jaw and the bench (gage) mark
 + = Break at the bench mark.

B. Differential Thermal Analysis (DTA)

1. General

The differential thermal analysis determines the time that a small section of insulated conductor can resist oxidation when

exposed to pure oxygen at 200°C.

2. Test Equipment



Figure 4: DU PONT INSTRUMENTS 990 Thermal Analyzer with cell

3. Test Procedure - Test Conditions:

Sample: 5 mg of 22 AWG insulated conductor
 Calorimetric Sensitivity: 0.5 mcal/sec/in.
 Temperature Program: isothermal at 200°C ± 1°C
 Zero Shift: 0 in.
 Time Base: 5 min/in.
 Inert Gas: nitrogen, purified grade
 Reactive Gas: oxygen, purified grade
 Gas Flow Rate: 200 cc/min.

- a. The sample of insulated conductor is placed in an open (uncrimped) pan in the DSC cell at ambient temperatures. A nitrogen gas purge is supplied to the cell and the cell is sealed.
- b. The temperature is set at 200°C and the sample is equilibrated at that temperature.
- c. The purge gas is switched from the inert nitrogen to the reactive oxygen and simultaneously the recorder time base is started.
- d. The scan is continued until the sharp upward movement of the pen, that indicates the oxidation, has gone through the maximum and is sloping downward.
- e. The elapsed time between zero and the extrapolated oxidation onset is the polymer induction time and it is recorded as a measure of oxidative stability. The oxidative exotherm is extrapolated to the base line by drawing a straight line (tangent) through the change in slope (position to negative) of that curve to the base line.

ANALYSIS OF ROUND ROBIN TEST RESULTS

A. Air Oven Aging Data, Comparison of Results from Participating Laboratories

The test results that were obtained to date are recorded in Tables 3 and 4 and they were utilized to calculate the life of the insulations in years at 35°C. This information is shown in form of bar charts in Figures 5 and 6.

TABLE 3
A COMPARISON OF THE DAYS TO EMBRITTLEMENT AFTER AIR OVEN AGING AND THE INDUCTION TIMES OBTAINED BY DIFFERENTIAL THERMAL ANALYSIS ON HIGH DENSITY POLYETHYLENE INSULATED CONDUCTORS (22 AWG) BY THE SEVERAL PARTICIPANTS IN THE IPCEA-REA ROUND ROBIN

| HDPE SAMPLE & TEST METHOD | ROUND ROBIN PARTICIPANTS | | | | | | | |
|---------------------------------------|--------------------------|------|------|------|------|------|------------|------|
| | 1 | 2 | 3 | 4 | 5 | 6 | 7 | 8 |
| I SOLID WHITE Oven Aged, Days* | | | | | | | | |
| Dry | 160 | - | - | - | - | - | - | - |
| Compound A | 70 | 175 | >168 | >168 | 178 | >454 | >410 | >460 |
| Compound B | 98 | 85 | - | >168 | >360 | 167 | 350 to 379 | 460 |
| DTA, Minutes** | | | | | | | | |
| Dry Copper Pan | - | 62.0 | 53.0 | 78.2 | 55.6 | 71.1 | - | 64.3 |
| Al Pan | - | 58.5 | 66.9 | 78.7 | 68.2 | 72.8 | - | 66.5 |
| Compound A | - | - | 7.2 | - | - | 44.4 | - | 54.0 |
| Compound B | - | - | - | - | - | 44.9 | - | 41.5 |
| II CELLULAR WHITE Oven Aged, Days* | | | | | | | | |
| Dry | *** | - | - | - | - | - | - | - |
| Compound A | 56 | 68 | 124 | 84 | 360 | 274 | 260 to 320 | 460 |
| Compound B | 63 | 61 | - | >175 | 44 | 57 | 139 to 200 | 115 |
| DTA, Minutes** | | | | | | | | |
| Dry Copper Pan | - | 12.0 | 13.4 | 15.2 | 34.4 | 12.7 | - | 8.2 |
| Al Pan | - | 15.8 | 50.0 | 15.2 | 43.6 | 21.8 | - | 9.1 |
| Compound A | - | - | 2.4 | - | - | 4.7 | - | 7.9 |
| Compound B | 5 | - | - | - | - | 7.5 | - | 6.5 |
| III SOLID GREEN Oven Aged, Days* | | | | | | | | |
| Dry | *** | - | - | - | - | - | - | - |
| Compound A | 126 | >186 | >168 | >175 | 360 | >454 | >410 | >460 |
| Compound B | 112 | 170 | - | >175 | 190 | 240 | 379 to 410 | 460 |
| DTA, Minutes** | | | | | | | | |
| Dry Copper Pan | - | 73.0 | 47.6 | 72.7 | 62.1 | 66.8 | - | 67.0 |
| Al Pan | - | 67.5 | 68.0 | 74.5 | 69.3 | 75.2 | - | 74.5 |
| Compound A | - | - | 2.2 | - | - | 41.9 | - | 48.0 |
| Compound B | - | - | - | - | - | 57.9 | - | 59.6 |
| IV CELL. GREEN Oven Aged, Days* | | | | | | | | |
| Dry | 133 | - | - | - | - | - | - | - |
| Compound A | 49 | 49 | 116 | 84 | 360 | 274 | 292 to 320 | 460 |
| Compound B | 56 | 95 | - | >175 | 52 | 60 | 139 to 200 | 111 |
| DTA, Minutes** | | | | | | | | |
| Dry Copper Pan | - | - | 11.1 | 8.0 | 26.4 | 7.4 | - | 7.2 |
| Al Pan | - | 35.5 | 50.0 | 11.2 | 34.8 | 19.1 | - | 10.5 |
| Compound A | - | - | 3.1 | - | - | 1.9 | - | 4.5 |
| Compound B | - | - | - | - | - | 3.2 | - | 4.0 |

* To embrittlement of the insulation after air oven aging at 100°C.

** Induction time in oxygen at 200°C, obtained with Differential Thermal Analysis

***Test was not run because insulation stuck to conductor. Data not included in Figures 7 and 13.

9/30/77

TABLE 4

A COMPARISON OF THE DAYS TO EMBRITTLEMENT AFTER AIR OVEN AGING AND THE INDUCTION TIMES OBTAINED BY DIFFERENTIAL THERMAL ANALYSIS ON PROPYLENE-ETHYLENE COPOLYMER INSULATED CONDUCTORS (22 AWG) BY THE SEVERAL PARTICIPANTS IN THE IPCEA-REA ROUND ROBIN

| PROP-ETH. SAMPLE & TEST METHOD | ROUND ROBIN PARTICIPANTS | | | | | | | |
|--------------------------------------|--------------------------|------|------|------|------|------|------------|------|
| | 1 | 2 | 3 | 4 | 5 | 6 | 7 | 8 |
| V SOLID WHITE Oven Aged, Days* | | | | | | | | |
| Dry Compound A | >175 | - | - | - | >360 | >454 | >410 | >460 |
| Compound B | 161 | >186 | 166 | >175 | 178 | 296 | 320 to 350 | 460 |
| DTA, Minutes** | | | | | | | | |
| Dry Copper Pan | - | 32.0 | 37.0 | 46.7 | 45.6 | 48.6 | - | 50.3 |
| Al Pan | - | 33.0 | 47.0 | 59.0 | 50.6 | 46.5 | - | 54.0 |
| Compound A | - | - | 7.0 | - | - | 26.5 | - | 27.6 |
| Compound B | - | - | - | - | - | 31.7 | - | 40.8 |
| VI CELL, WHITE Oven Aged, Days* | | | | | | | | |
| Dry Compound A | *** | - | - | - | >360 | 321 | 379 to 410 | 460 |
| Compound B | 70 | 98 | 128 | 126 | 94 | 107 | 139 to 200 | 145 |
| DTA, Minutes** | | | | | | | | |
| Dry Copper Pan | - | 7.5 | 9.1 | 8.0 | 21.8 | 17.4 | - | 19.3 |
| Al Pan | - | 14.0 | 32.9 | 13.5 | 32.9 | 34.3 | - | 23.2 |
| Compound A | - | - | 1.6 | - | - | 9.2 | - | 15.6 |
| Compound B | - | - | - | - | - | 2.8 | - | 16.8 |
| VII SOLID GREEN Oven Aged, Days* | | | | | | | | |
| Dry Compound A | 168 | - | - | - | >360 | >454 | >410 | >360 |
| Compound B | 154 | 158 | 166 | >161 | 178 | 296 | 320 to 350 | 460 |
| DTA, Minutes** | | | | | | | | |
| Dry Copper Pan | - | 50.5 | 53.6 | 45.0 | 56.4 | - | - | 49.6 |
| Al Pan | - | 57.0 | 51.6 | 49.2 | 57.3 | - | - | 53.0 |
| Compound A | - | - | - | - | 43.6 | - | - | 39.5 |
| Compound B | - | - | - | - | 11.1 | - | - | 38.0 |
| VIII CELL, GREEN Oven Aged, Days* | | | | | | | | |
| Dry Compound A | *** | - | - | - | >360 | 321 | 379 to 410 | 460 |
| Compound B | 70 | 73 | 124 | 98 | 75 | 117 | 139 to 200 | 164 |
| DTA, Minutes** | | | | | | | | |
| Dry Copper Pan | - | 37.0 | 29.7 | 10.0 | 27.6 | 13.1 | - | 18.4 |
| Al Pan | - | 41.0 | 38.7 | 24.2 | 37.1 | 31.5 | - | 22.8 |
| Compound A | - | - | 7.2 | - | - | 5.5 | - | 17.2 |
| Compound B | - | - | - | - | - | 2.0 | - | 14.8 |

* To embrittlement of the insulation after air oven aging at 100°C.

** Induction time in oxygen at 200°C., obtained with Differential Thermal Analysis

***Test was not run because insulation stuck to conductor. Data not included on Figures 7 and 13

9/30/77

FIGURE-5

LEGEND

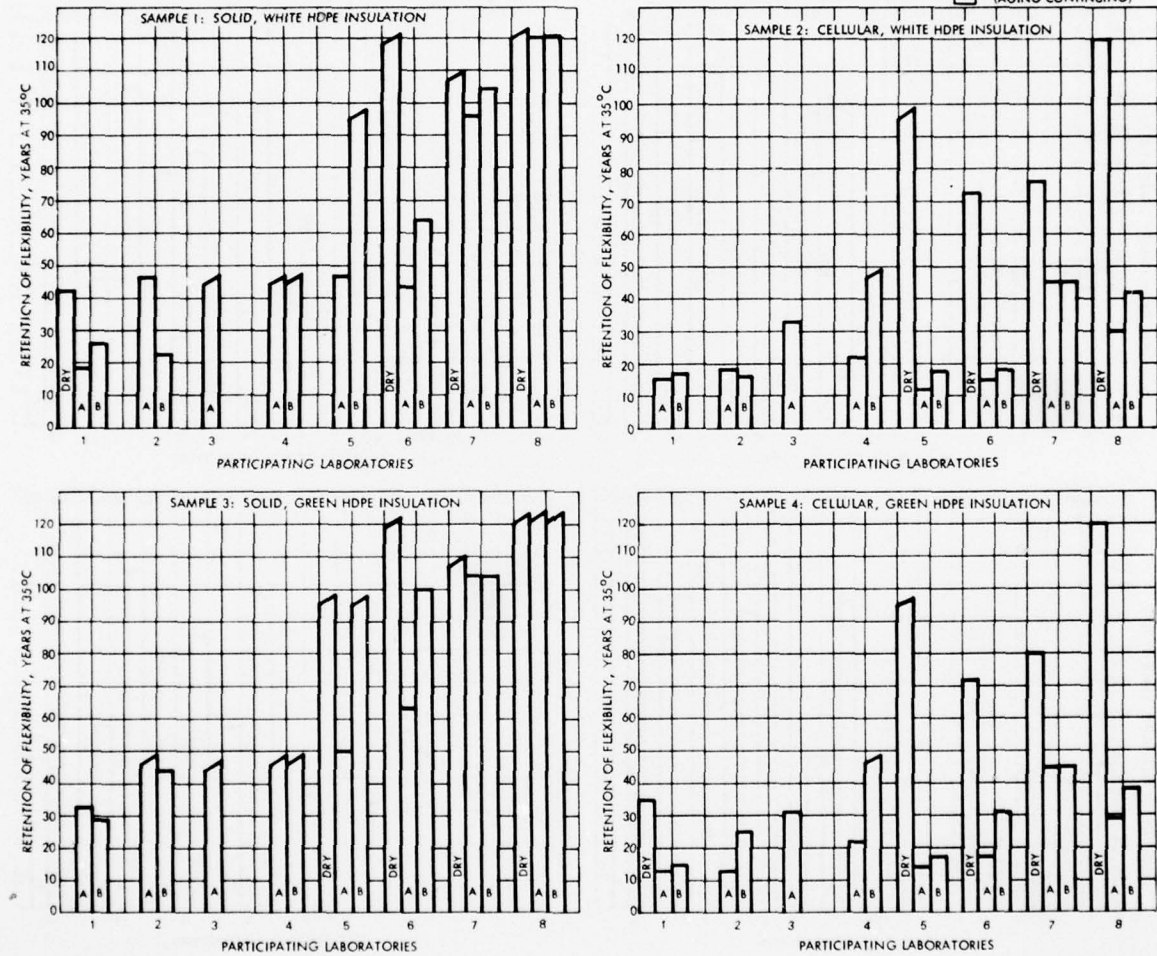
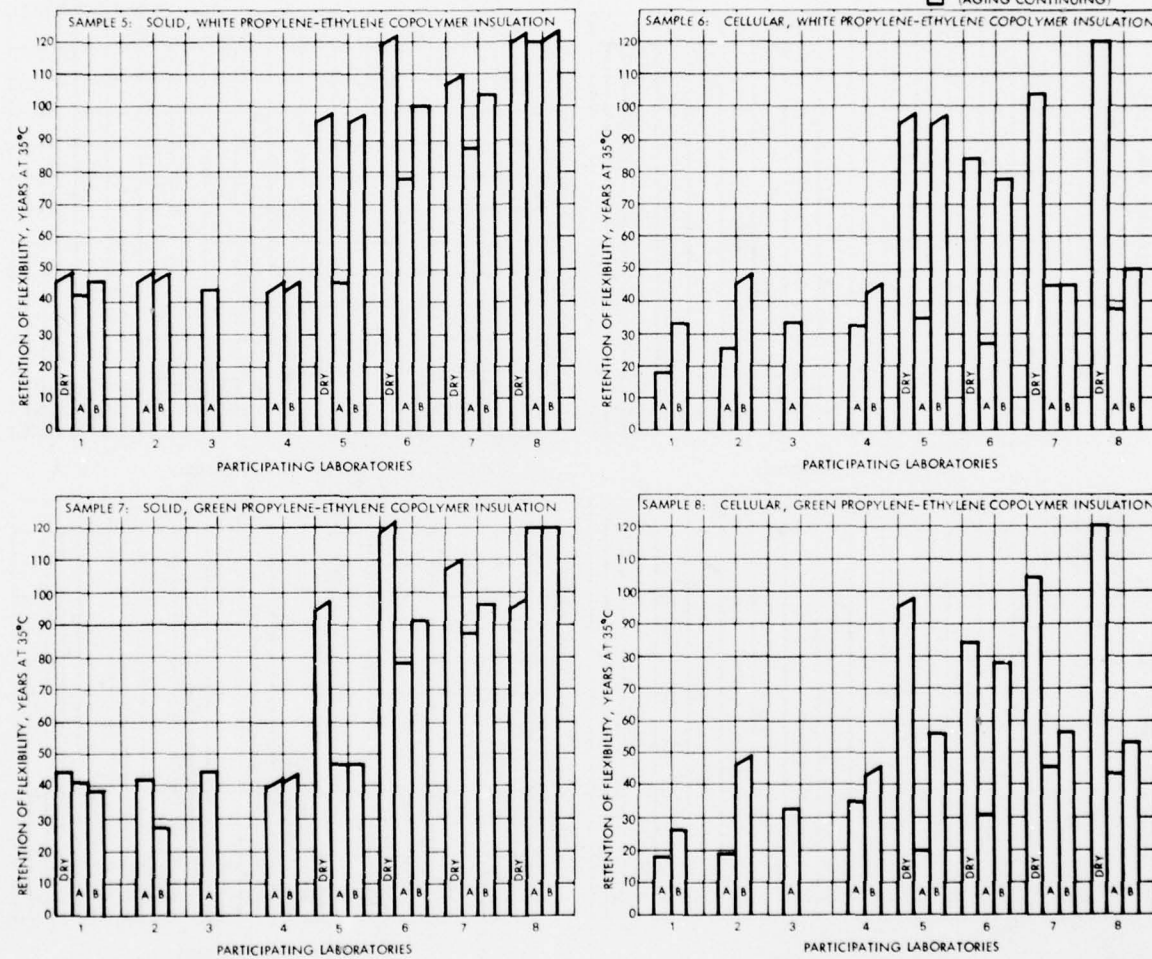


FIGURE-6

LEGEND □ SAMPLE EMBRITTLED
 □ SAMPLE NOT YET EMBRITTLED
 (AGING CONTINUING)



After analyzing the results from the eight participating companies, it became apparent that significant differences must have existed in testing techniques or in conditions during oven aging. These differences are particularly noticeable when comparing interlaboratory results from tests on the four propylene-ethylene copolymer insulations.

Table 5 below lists the round robin participants in order of increasing calculated life of insulations obtained from their testing.

The two factors that have the greatest influence on the air oven aging test are temperature and air flow in the oven. Based on the information that was received from the eight participants, it was

found that the companies that obtained the shorter life times of the insulations exceeded the maximum acceptable aging temperature of 100.5°C by up to 2.5°C.

The air flow in the ovens of the participants was high, the fresh air vents were kept open, and based on the information received it appears that the air velocities were satisfactory and they did not cause major differences in the test results. It is possible, however, that the actual air flow differences are greater than reported by the participants due to the difficulties associated with velocity measurement in turbulent air flow. The results indicate the importance of standardization of oven aging conditions. A practical approach in solving this problem would be the selection of one commercial oven design that has proven useful and reliable for long duration air oven aging programs.

TABLE 5
TEMPERATURE FLUCTUATIONS, AIR VELOCITIES AND INFORMATION ON INSTRUMENTS USED FOR MEASURING AIR VELOCITIES

| Participant in the Round Robin Test | Air Oven Conditions | | Instrument Used for Measuring Air Velocity |
|-------------------------------------|---|--|---|
| | Temperature Fluctuations °C | Air Velocity, ft./min. | |
| 1 | 99.0 to 102.0 | 250 to 500 | Alnor Velometer, Type 6000-P with Pitot Tube Probe |
| 2 | 99.0 to 103.0 | 360 to 440 | Anemotherm, Model 60 Air Meter |
| 3 | possibly to 102°C reported 1.1 to 2.3 | For four ovens ranging from 330 to 550 | Anemotherm, Model 60 Air Meter |
| 4 | 98.0 to 102.0 | 180 to 200 | Bacharach Instrument Co., Florite Model MLD |
| 5 | 99.5 to 100.5 | 630 to 650 | Digital Anemometer, Model AM 5000, Air Flow Development Co., (UK) |
| 6 | 99.5 to 100.5 | 360 to 440 | Anemotherm, Model 60 Air Meter |
| 7 | * Oven temperature possible slightly below 100°C | 300 | Thermo-Anemometer, Wallac OY, Type GGA 23F |
| 8 | 99.0 To 101.0 | 400 to 440 | Alnor Velometer, Type 6006-P and Pitot Probe Type 6060-P |

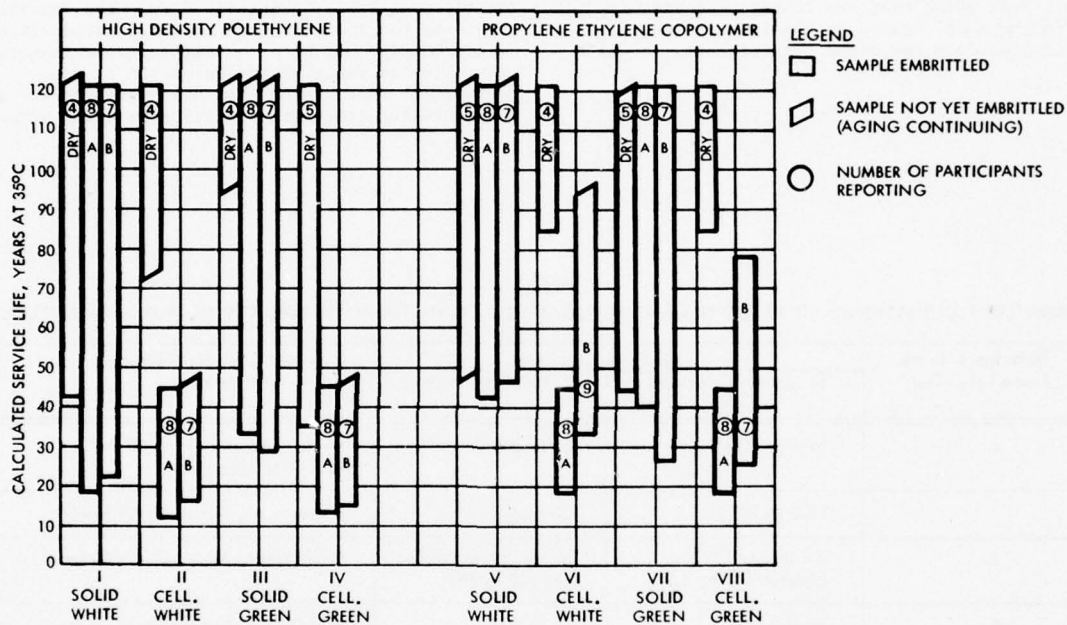
*No information

B. Influence of Petrolatum Based Filling Compound on the Life of the Insulations

The test results that were displayed in Figures 5 and 6 are combined in Figure 7. In addition, the number of participants that supplied test results for the specific sample is shown.

FIGURE-7

RANGE OF AIR OVEN AGING DATA AMONG ALL ROUND ROBIN PARTICIPANTS REPORTED AS OF SEPT. 30, 1977



Realizing that the wide spread in test results is due to excessively high aging temperature that was employed by at least three participants and a temperature slightly below 100°C that may have been utilized by one participant, it is clear that the insulations that were aged in contact with the filling compounds prior to air oven aging embrittle considerably earlier than the same insulation that did not have contact with filling compound. It is known that filling compounds will extract stabilizers from the insulations². Cellular insulations are affected by the filling compounds more severely than the respective solid insulations. Part of the reason for the earlier embrittlement of the cellular insulations is due to the higher ratio of surface area to material that promotes the harmful activity of the petrolatum based compound. The same is true for thin wall solid insulations, for instance for the 0.008 inch wall of No. 26 AWG solid copper conductor.

In addition, it was found that the original cellular HDPE insulations have only one third of the primary stabilizer Irganox 1010 present when compared with their solid counterparts. The same was

not found with the propylene-ethylene copolymer insulations. Precise quantitative methods for the remaining stabilizers and copper inhibitors are not available to date.

Table 6

| Sample No. | Sample | Primary Stabilizer Irganox 1010 |
|------------|------------------------------------|---------------------------------|
| I | Solid White HDPE | 0.072% |
| II | Cellular White HDPE | 0.022% |
| III | Solid Green HDPE | 0.093% |
| IV | Cellular Green HDPE | 0.033% |
| V | Solid White Prop-Eth. Copolymer | 0.19% |
| VI | Cellular White Prop-Eth. Copolymer | 0.20% |
| VII | Solid Green Prop-Eth. Copolymer | 0.19% |
| VIII | Cellular Green Prop-Eth. Copolymer | 0.21% |

An observation was made with an X-ray dispersive system that supplies an additional reason for the poorer aging performance of insulations that had been in contact with filling compound prior to aging.

Copper was found to be present not only on the inner surface of the insulation, but also 60 microns from the inner surface in the insulation. It appears that the filling compound dissolves sulfur from the stabilizer system, most likely from DLTPD, when it diffuses through the insulation towards the conductor. It is theorized that the sulfur reacts with the copper conductor and it forms a complex which diffuses into the insulation and causes copper catalyzed degradation of the insulation.

The original insulation and the insulation that had been immersed in petrodatum based filling compound for two weeks at 85°C and that were subsequently air oven aged for 28 days at 100°C were observed and analyzed by a scanning electron microscope (SEM) that is equipped with an X-ray energy dispersive spectrometer. The top layer of the insulation was longitudinally sliced from the conductor and the inner surface that had been adjacent to the conductor and a spot in the insulation wall, 60 microns from the inner surface were examined by the SEM/X-ray technique.

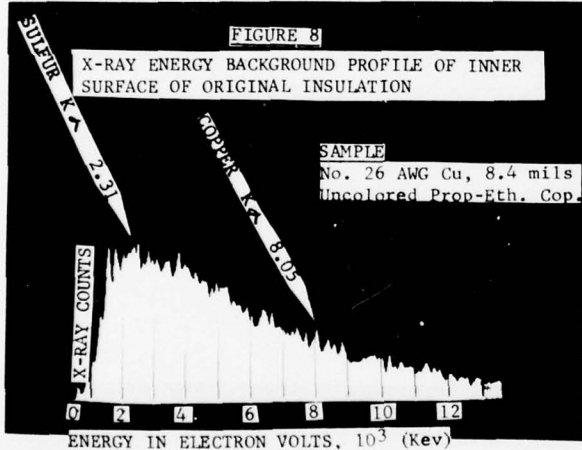


Figure 8: The X-ray analysis indicates that only traces of copper and sulfur were detected on the inner surface of the original insulation

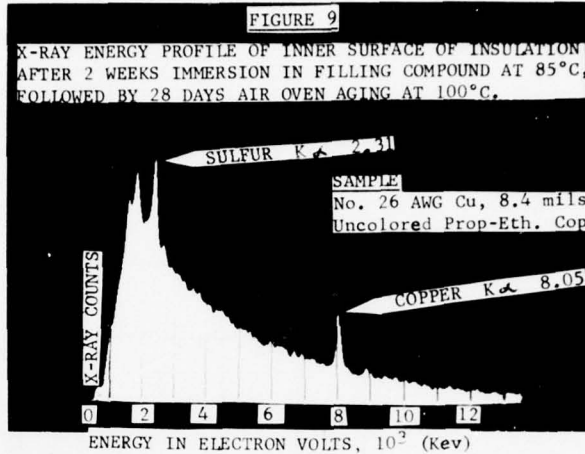


Figure 9: The two main peaks indicate the presence of substantial quantities of copper and sulfur in the insulation that had been immersed in filling compound and that was subsequently air oven aged.

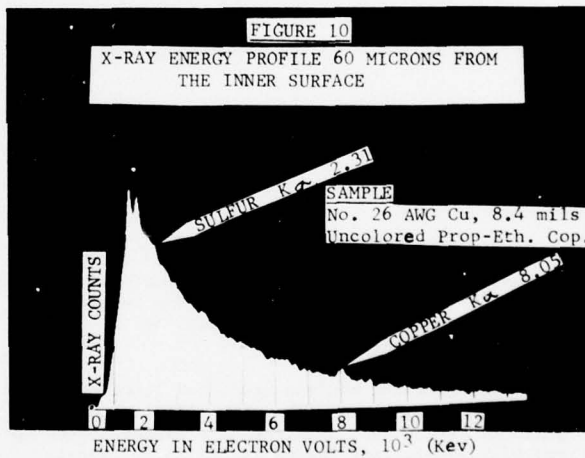


Figure 10: It can be seen that the amount of copper and sulfur is considerably less than the amount that is present on the inner surface.

Copper and sulfur were not found near the outer surface of the insulation.

C. Life Predictions of Insulations

Table 7 shows the calculated minimum and maximum lifetimes of the eight samples of filled cable insulations. The calculations are based on all test results after air oven aging that were obtained by the participants that were reporting on the specific samples as of August 19, 1977. As pointed out in paragraph A, the range of results obtained would have been considerably smaller if the temperature in the air ovens of all participants would have been maintained precisely at 100°C ± 0.5°C.

Table 7

PREDICTED LIFE OF THE EIGHT FILLED CABLE INSULATIONS BASED ON THE TEST RESULTS
OF THE REPORTING PARTICIPANTS

| Sample No. | Type | Insulation | Color | Detail | Predicted Life, Years at 35°C | | Number of Participants Reporting |
|------------|----------|----------------|-------|--------|-------------------------------|---------|----------------------------------|
| | | | | | Minimum | Maximum | |
| I | Solid | HDPE | White | Dry | 42 | >121 | 4 |
| | | | | A | 18 | 121 | 8 |
| | | | | B | 22 | 121 | 7 |
| II | Cellular | HDPE | White | Dry | 72 | 121 | 4 |
| | | | | A | 12 | 44 | 8 |
| | | | | B | 16 | >46 | 7 |
| III | Solid | HDPE | Green | Dry | >94 | >121 | 4 |
| | | | | A | 33 | >121 | 8 |
| | | | | B | 29 | >121 | 7 |
| IV | Cellular | HDPE | Green | Dry | 35 | >121 | 5 |
| | | | | A | 13 | 44 | 8 |
| | | | | B | 15 | >46 | 7 |
| V | Solid | Prop-Eth. Cop. | White | Dry | >46 | >121 | 5 |
| | | | | A | 42 | 121 | 8 |
| | | | | B | 46 | >121 | 7 |
| VI | Cellular | Prop-Eth. Cop. | White | Dry | 84 | 121 | 4 |
| | | | | A | 18 | 44 | 8 |
| | | | | B | 33 | >94 | 7 |
| VII | Solid | Prop-Eth. Cop. | Green | Dry | 44 | >19 | 5 |
| | | | | A | 40 | 121 | 8 |
| | | | | B | 26 | 121 | 7 |
| VIII | Cellular | Prop-Eth. Cop. | Green | Dry | 84 | 121 | 4 |
| | | | | A | 18 | 44 | 8 |
| | | | | B | 25 | 78 | 7 |

By observing the minimum predicted lifetimes, it must be realized that the values would have been higher if the aging temperature of the insulations would have been maintained precisely at $100 \pm 0.5^\circ\text{C}$ by all participants.

Comparing the minimum predicted lifetimes of the solid insulations with their cellular counterparts it can be seen that the life expectancy of the cellular insulations tested is 30% to 50% shorter than their solid counterparts.

D. Appearance of Insulations After Air Oven Aging

During the Round Robin Test Program, it was observed that the appearance of the embrittled "dry" aged HDPE insulations is different from the embrittled "dry" aged propylene ethylene copolymer insulations. While the cellular HDPE insulations show circumferential cracks when they embrittle, the cellular propylene ethylene copolymer insulations break open and large sections of almost bare conductor are exposed.

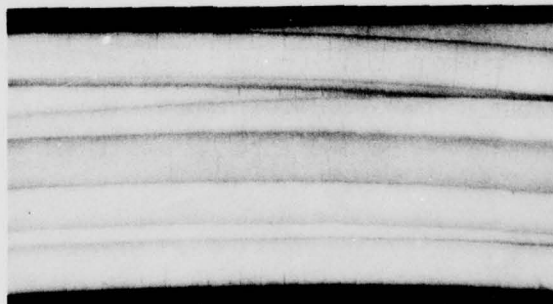


Figure 11:

Magnification 8X

Sample No. II: No. 22 AWG solid copper conductor with 0.0099 inches of white cellular HDPE insulation with circumferential cracks after 274 days air oven aging at 100°C .

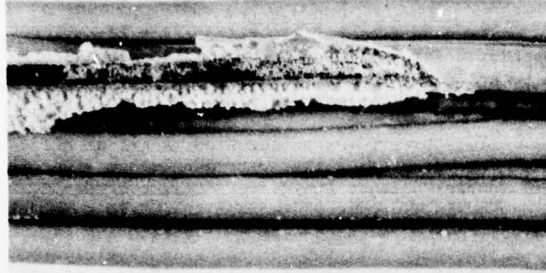


Figure 12 Magnification 8X

Sample VIII: No. 22 AWG solid copper conductor with 0.0099 inches of green cellular propylene-ethylene copolymer insulation with an exposed section of conductor after 330 days of air oven aging at 100°C.

It was also noted, that in general the aged embrittled cellular HDPE insulations that had been immersed in filling compounds show less cracking at the time when they lose their ability to elongate than the dry aged samples. In the case of the cellular propylene ethylene copolymer insulations, the samples that had been immersed in filling compound A have most of their conductor exposed when they embrittle, while the samples that had been immersed in filling compound B show considerably less damaged insulation. The following is a summary of the observations:

TABLE 8

APPEARANCE OF INSULATIONS AFTER AIR OVEN AGING WHEN ZERO ELONGATION IS REACHED

| Sample Number | Identification | "Dry" Aged | Aged at 100°C After 2 Weeks Contact at 70°C With Filling Compound | |
|---------------|--------------------------------|--|---|--------------------------------------|
| | | | A | B |
| I | HDPE, Solid White | * | * | * (1) |
| II | HDPE, Cellular White | Circumferential cracks partial ivory discoloration | Circumferential cracks partial ivory discoloration | |
| III | HDPE, Solid Green | * | * (1) | * (1) |
| IV | HDPE, Cellular Green | Circumferential cracks, partial discoloration | * (1) | * (1) |
| V | Prop.-Eth. Cop. Solid White | * | * (1) | * |
| VI | Prop.-Eth. Cop. Cellular White | Sections of insulation split open, no circumferential cracks | Most of conductor exposed, insulation fell off | Section of insulation split open (1) |
| VII | Prop.-Eth. Cop. Solid Green | * | Section of insulation split open, some circumferential cracks | Some circumferential cracks |
| VIII | Prop.-Eth. Cop. Cellular Green | Section of insulation split open, no circumferential cracks | Most of conductor exposed, insulation fell off | * |

* = Insulation intact

(1) = Circumferential cracks in the upper bent section only

The aging periods that were required to produce the effects recorded in Table 8 above, are as follows:

TABLE 9

DAYS TO ZERO ELONGATION AFTER AIR OVEN AGING AT 100°C

| Sample Number | Sample Identification | "Dry" Aged | Aged at 100°C After 2 Weeks Contact at 70°C With Filling Compound | |
|---------------|--------------------------------|------------|---|-----|
| | | | A | B |
| I | HDPE, Solid White | 483 + | 167 | 243 |
| II | HDPE, Cellular White | 274 | 57 | 67 |
| III | HDPE, Solid Green | 483 + | 240 | 380 |
| IV | HDPE, Cellular Green | 274 | 60 | 116 |
| V | Prop.-Eth. Cop. Solid White | 454 + | 296 | 378 |
| VI | Prop.-Eth. Cop. Cellular White | 321 | 107 | 296 |
| VII | Prop.-Eth. Cop. Solid Green | 454 + | 296 | 346 |
| VIII | Prop.-Eth. Cop. Cellular Green | 321 | 117 | 296 |

+ = Sample still flexible, test continues

In conclusion, the information shown in Tables 8 and 9 emphasizes the need for selecting a system of most suitable and compatible materials for insulation and filling compound. It should be noted that production material that is represented by Samples V through VIII is not used in combination with Filling compound A.

E. Evidence of Oxidation by Infrared Analysis

Flexible sections from Figure 11 (Sample No. ID) that could be pressed into a thin film for infrared analysis, showed evidence of oxidation due to the presence of the carbonyl absorption at 1720 cm^{-1} .

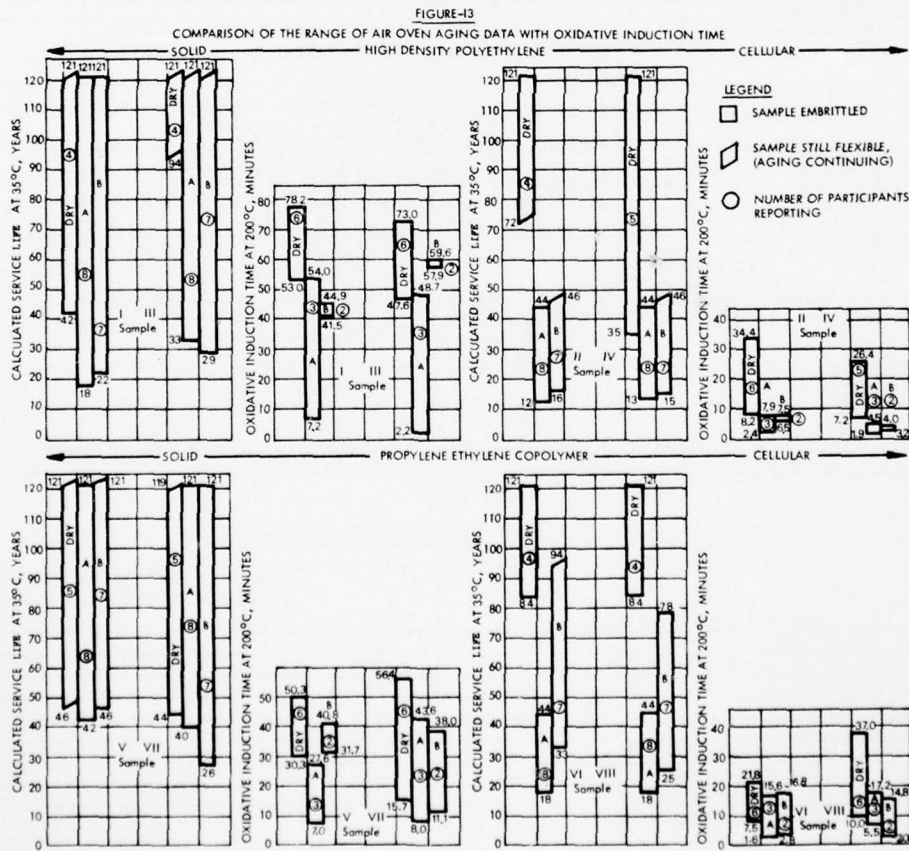
The insulation shown in Figure 12, (Sample No. VIII) showed oxidation by infrared analysis only where it was in contact with the copper conductor or in the areas that split open.

It was found that oxidation cannot be seen on the eight Round Robin test samples with the gravimetric oxygen absorption test that is described in detail in Ref. 1. This information correlates with the data from Ref. 1 where oxidation could be very nicely demonstrated with the gravimetric method on LDPE, but not on HDPE or propylene ethylene copolymer insulation.

F. Differential Thermal Analysis and Predicted Life Based on Air Oven Aging: Comparison of Test Data

The ranges of oxidative induction times and predicted life of the eight insulations are demonstrated in Figure 13. The number of participants in these tests is recorded also.

It is surprising to see wide ranges of oxidative induction times that were obtained on identical samples because the differential thermal analysis is a very well defined test. In some cases, the correlation between laboratories is good, but then only two laboratories participated in the test. An effort was made to find a significant correlation between the DTA data and the air oven results, but it does not exist. It was found that the results from both test methods are related only in the very broadest sense.



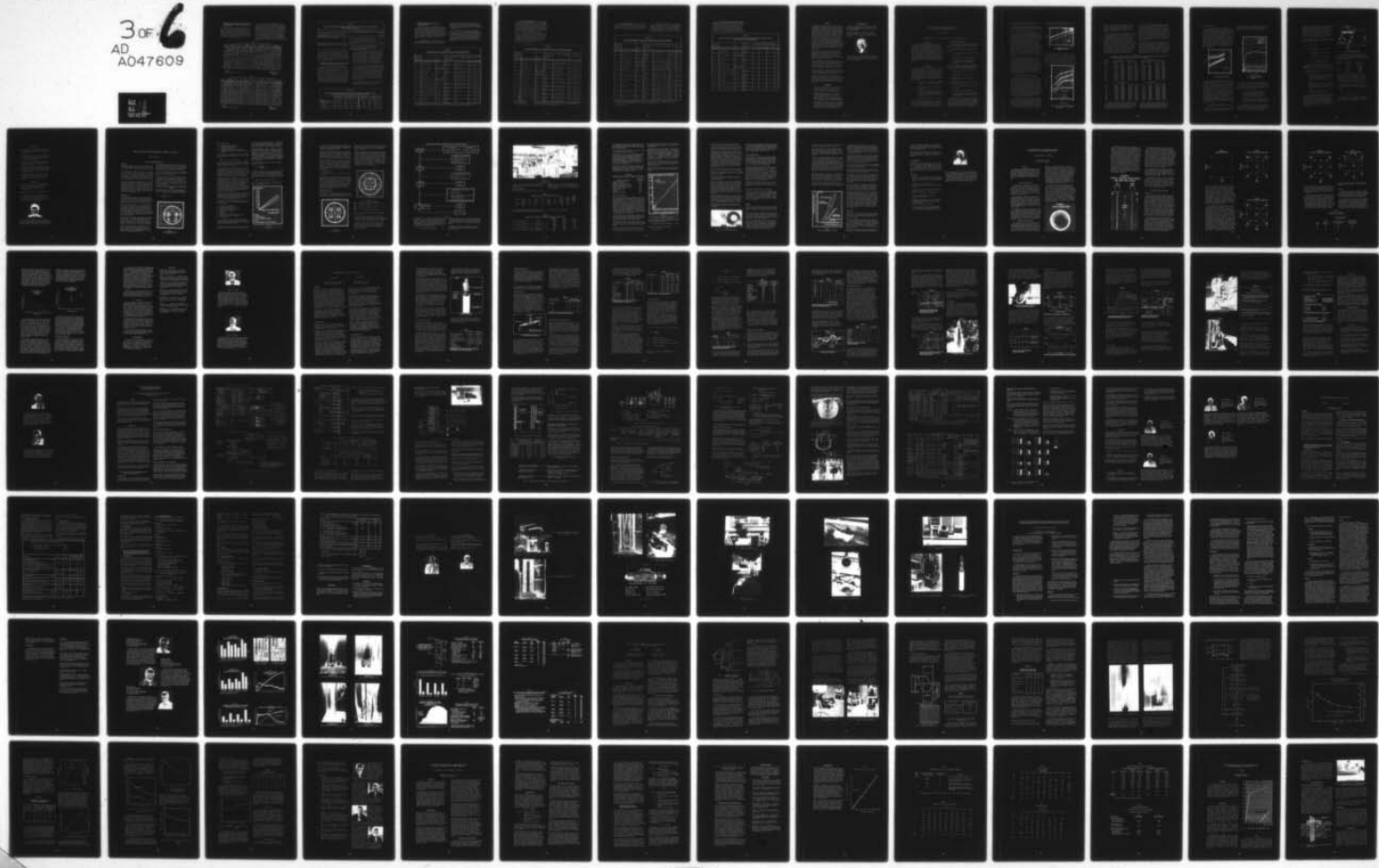
AD-A047 609

ARMY COMMUNICATIONS RESEARCH AND DEVELOPMENT COMMAND --ETC F/G 9/1
PROCEEDINGS OF INTERNATIONAL WIRE AND CABLE SYMPOSIUM (26TH) CH--ETC(U)
NOV 77 E F GODWIN

UNCLASSIFIED

3 OF 6
AD
AD47609

NL



G. Determination of the End Point of Air Oven Aged Insulations by Oxygen Induction Time and by Elongation

One of the participating Laboratories determined the oxygen induction times of the eight samples of insulated conductors after various periods of exposure to circulating air at 100°C. The test results are shown in Tables 10 and 11 and they show that during aging at 100°C, the stabilizer system is being consumed as demonstrated by a decline in oxygen induction time.

It was of interest to determine if the end points, as indicated by oxygen induction times, would correlate with the end points as determined by elongating the specimens. The corresponding elongation values from one of the other participating Laboratories were inserted in Tables 10 and 11. Based on 20 tests that were completed as of 9/30/77, good correlation between end points of OIT and elongation is indicated 11 times, while 5 times the oxygen induction time exceeded the time to embrittlement and 4 types of specimens continued to elongate after failure had been indicated by oxygen induction time. A summary is shown in Table 12.

TABLE 10
COMPARISON OF OXYGEN INDUCTION TIMES WITH ELONGATION OF AGED SPECIMENS OF HDPE INSULATIONS

| Days of Aging at 100°C | Sample #1 HDPE Solid White | | | | | Days of Aging at 100°C | Sample #2 HDPE Cellular White | | | | | Days of Aging at 100°C | Sample #3 HDPE Solid Green | | | | | Days of Aging at 100°C | Sample #4 HDPE Cellular Green | | | | | | | | |
|------------------------|----------------------------|---------|---------|------|------|------------------------|-------------------------------|---------|---------|------|------|------------------------|----------------------------|---------|---------|------|------|------------------------|-------------------------------|---------|---------|------|-----|------|-----|------|-----|
| | Dry | Comp. A | Comp. B | OIT | E | | Dry | Comp. A | Comp. B | OIT | E | | Dry | Comp. A | Comp. B | OIT | E | | Dry | Comp. A | Comp. B | OIT | E | | | | |
| 0 | 66.5 | 720 | 720 | 720 | 0 | 9.1 | 407 | 407 | 407 | 0 | 74.5 | 703 | 703 | 703 | 0 | 10.5 | 380 | 380 | 380 | 0 | 10.5 | 380 | | | | | |
| 76 | 45.7 | 707 | 32.5 | 633 | 39.0 | 720 | 76 | 5.0 | 400 | 2.0 | 8 | 2.0 | 400 | 76 | 37.0 | 590 | 39.8 | 710 | 42.1 | 660 | 76 | 3.0 | 397 | 2.0 | 380 | 2.0 | 450 |
| 100 | 42.5 | 730 | 2.5 | 733 | 2.0 | 720 | 100 | 5.3 | 400 | <1.0 | - | 1.8 | 8 | 100 | 41.2 | 593 | 8.3 | 707 | 3.2 | 697 | 100 | 4.1 | 383 | <1.0 | 8 | 2.1 | 67 |
| 111 | 22.0 | 2.2 | 3.2 | 111 | 5.1 | <1.0 | - | <1.0 | - | 111 | 36.8 | 5.7 | 4.3 | 111 | 3.5 | <1.0 | - | <1.0 | 50 | 111 | 3.5 | <1.0 | - | 1.4 | 40 | | |
| 115 | 35.0 | 3.3 | 3.0 | 115 | 5.2 | <1.0 | - | <1.0 | - | 115 | 37.2 | 7.0 | 5.0 | 115 | 3.8 | <1.0 | - | <1.0 | 50 | 115 | 3.8 | <1.0 | - | 1.0 | 50 | | |
| 122 | 31.2 | 720 | 3.4 | 700 | 2.2 | 720 | 122 | 4.8 | 403 | <1.0 | - | <1.0 | - | 122 | 35.3 | 617 | 5.8 | 700 | 3.3 | 703 | 122 | 4.1 | 387 | <1.0 | - | <1.0 | 8 |
| 132 | 28.5 | 2.2 | 1.5 | 132 | 5.2 | - | - | <1.0 | - | 132 | 36.3 | 6.5 | 5.5 | 132 | 3.7 | - | - | <1.0 | - | 132 | 3.7 | - | - | <1.0 | - | | |
| 145 | 26.3 | 627 | 1.9 | 700 | 1.1 | 720 | 145 | 5.2 | 430 | - | - | - | - | 145 | 33.5 | 650 | 8.2 | 707 | 5.0 | 716 | 145 | 3.7 | 417 | - | - | <1.0 | - |
| 160 | 30.0 | - | 2.1 | 575 | <1.0 | - | 160 | 6.0 | - | - | - | - | 160 | 36.0 | 7.5 | 5.2 | 160 | 3.9 | - | - | - | - | 160 | 3.9 | - | - | - |
| 175 | 42.0 | - | <1.0 | B | <1.0 | - | 175 | 3.5 | - | - | - | - | 175 | 41.0 | 5.2 | 3.0 | 175 | 2.5 | - | - | - | - | 175 | 2.5 | - | - | - |
| 179 | 40.1 | 647 | <1.0 | - | <1.0 | 770 | 190 | 2.9 | 493 | * | - | * | - | 190 | 34.5 | 627 | 6.7 | 790 | 3.8 | 730 | 190 | 1.7 | 437 | * | - | * | - |
| 202 | 30.5 | <1.0 | - | <1.0 | - | 202 | 3.2 | - | - | - | - | - | 202 | 38.5 | 6.5 | 2.9 | 202 | 2.0 | - | - | - | - | 202 | 2.0 | - | - | - |
| 216 | 35.0 | 633 | * | - | * | 100 | 216 | 2.1 | 450 | * | - | * | - | 216 | 34.0 | 630 | 4.8 | 697 | 3.2 | 837 | 216 | 3.1 | 383 | * | - | * | - |
| 231 | 29.6 | * | - | * | 70 | 231 | 2.6 | - | - | - | - | - | 231 | 36.3 | 6.2 | 700 | 2.8 | 231 | 2.4 | * | - | * | - | * | - | * | |
| 247 | 31.2 | 797 | * | - | * | 8 | 247 | 2.0 | 217 | * | - | * | - | 247 | 33.5 | 667 | 5.8 | 8 | 2.1 | 813 | 247 | 1.6 | 367 | * | - | * | - |
| 258 | 28.5 | * | - | * | - | 258 | 2.0 | - | - | - | - | - | 258 | 30.6 | 4.5 | 2.4 | 258 | 1.5 | * | - | * | - | 258 | 1.5 | * | - | * |
| 273 | 27.3 | 807 | * | - | * | 273 | 1.8 | 37 | * | - | * | - | 273 | 26.0 | 690 | 2.8 | 1.5 | 733 | 273 | 1.5 | 30 | * | - | * | - | * | |
| 460 | 4.5 | 517 | <1.0 | - | <1.0 | - | 460 | <1.0 | B | <1.0 | - | <1.0 | - | 460 | 7.3 | 537 | <1.0 | - | <1.0 | B | 460 | <1.0 | B | <1.0 | - | <1.0 | - |

* = Not Tested
B = Brittle
- = Testing discontinued due to embrittlement of the insulation

LEGEND:
OIT = Oxygen Induction Time
Reported in Minutes.
E = Elongation, %

TABLE 11
COMPARISON OF OXYGEN INDUCTION TIMES WITH ELONGATION OF AGED SPECIMENS OF PROPYLENE-ETHYLENE COPOLYMER INSULATIONS

| Days of Aging at 100°C | Sample #5 Prop. Eth. Cop. Solid White | | | | | Days of Aging at 100°C | Sample #6 Prop. Eth. Cop. Cellular White | | | | | Days of Aging at 100°C | Sample #7 Prop. Eth. Cop. Solid Green | | | | | Days of Aging at 100°C | Sample #8 Prop. Eth. Cop. Cellular Green | | | | | | | | | |
|------------------------|---------------------------------------|---------|---------|-----|------|------------------------|--|---------|---------|------|------|------------------------|---------------------------------------|---------|---------|------|------|------------------------|--|---------|---------|------|------|------|------|------|-----|---|
| | Dry | Comp. A | Comp. B | OIT | E | | Dry | Comp. A | Comp. B | OIT | E | | Dry | Comp. A | Comp. B | OIT | E | | Dry | Comp. A | Comp. B | OIT | E | | | | | |
| 0 | 54.0 | 510 | 510 | 510 | 0 | 23.2 | 393 | 393 | 393 | 0 | 53.0 | 513 | 513 | 513 | 0 | 22.8 | 403 | 403 | 403 | 0 | 22.8 | 403 | | | | | | |
| 76 | 28.5 | 440 | 10.3 | 503 | 8.5 | 490 | 76 | 7.2 | 303 | 2.2 | 320 | 6.5 | 260 | 76 | 22.8 | 403 | 6.8 | 507 | 7.7 | 490 | 76 | 10.5 | 257 | 2.3 | 260 | 2.2 | 230 | |
| 100 | 19.8 | 383 | 9.3 | 507 | 7.0 | 100 | 100 | 8.5 | 327 | 2.2 | 270 | 2.0 | - | 100 | 21.4 | 417 | 7.0 | 507 | 5.3 | - | 100 | 10.5 | 347 | 2.1 | 260 | 2.0 | - | |
| 111 | 23.8 | - | 7.0 | 52 | 111 | 11.7 | 1.8 | 8 | 8 | 1.8 | 8 | 1.5 | - | 111 | 19.5 | 5.6 | 3.0 | - | 111 | 10.5 | 2.2 | 1.8 | - | - | - | - | | |
| 115 | 20.1 | - | 7.3 | 7.5 | 115 | 9.7 | <1.0 | - | <1.0 | - | 115 | 18.5 | 7.0 | 5.2 | 115 | 8.5 | 1.6 | 287 | 1.2 | - | 115 | 8.5 | 1.6 | 287 | 1.2 | - | | |
| 122 | 21.0 | 377 | 5.3 | 503 | 6.8 | 447 | 122 | 9.5 | 340 | <1.0 | - | <1.0 | 300 | 122 | 17.2 | 350 | 5.7 | 500 | 4.0 | 497 | 122 | 9.2 | 300 | 2.1 | 8 | <1.0 | 197 | |
| 132 | 20.0 | - | 5.8 | 6.7 | 132 | 8.0 | <1.0 | - | <1.0 | - | 132 | 18.5 | 4.5 | 3.5 | 132 | 6.2 | 1.5 | - | <1.0 | - | 132 | 6.2 | 1.5 | - | <1.0 | - | | |
| 145 | 20.8 | 497 | 6.7 | 513 | 5.4 | 500 | 145 | 8.3 | 347 | <1.0 | - | <1.0 | 260 | 145 | 19.2 | 350 | 6.0 | - | 4.5 | 483 | 145 | 8.0 | 333 | 1.7 | - | <1.0 | 183 | |
| 160 | 19.7 | - | 4.6 | 4.6 | 160 | 8.5 | - | - | - | - | 160 | 17.7 | 5.8 | 4.5 | 160 | 7.4 | 1.4 | - | <1.0 | - | 160 | 7.4 | 1.4 | - | <1.0 | - | | |
| 175 | 18.0 | 503 | 1.9 | 530 | 1.8 | 530 | 175 | 7.0 | 397 | * | - | * | 277 | 175 | 16.0 | 513 | 1.8 | 523 | 1.6 | 557 | 175 | 5.0 | 371 | <1.0 | - | * | 223 | |
| 190 | 19.0 | - | 2.8 | 1.6 | 190 | 6.5 | - | - | - | - | 190 | 17.8 | 3.0 | 2.1 | 190 | 5.9 | 1.4 | 1.0 | - | * | 190 | 5.9 | 1.4 | 1.0 | - | * | | |
| 202 | 16.0 | - | 3.0 | 1.8 | 202 | 6.2 | - | - | - | - | 202 | 16.8 | 2.8 | 1.3 | 202 | 3.7 | <1.0 | - | * | - | 202 | 3.7 | <1.0 | - | * | - | | |
| 216 | 15.2 | 493 | 2.0 | 533 | 2.1 | 543 | 216 | 5.3 | 403 | * | - | * | 190 | 216 | 15.1 | 487 | 3.1 | 547 | 2.1 | 527 | 216 | 4.7 | 360 | * | - | * | 203 | |
| 231 | 13.8 | - | 2.2 | 2.2 | 231 | 5.4 | - | - | - | - | 231 | 14.3 | 2.7 | 1.6 | 231 | 4.6 | * | - | * | - | 231 | 4.6 | * | - | * | - | | |
| 247 | 14.5 | 490 | 1.6 | 506 | 2.2 | 547 | 247 | 4.0 | 380 | * | - | * | 247 | 247 | 15.1 | 487 | 2.4 | 527 | 1.9 | 550 | 247 | 4.6 | 357 | * | - | * | 107 | |
| 258 | 12.6 | - | 2.1 | 533 | 2.3 | 258 | 3.9 | - | - | - | - | - | 258 | 11.8 | 1.9 | 1.7 | 500 | 258 | 3.5 | * | - | * | 258 | 3.5 | * | - | * | - |
| 273 | 14.3 | 503 | 1.8 | 507 | 1.3 | 500 | 273 | 3.3 | 363 | * | - | * | 40 | 273 | 11.1 | 477 | 1.7 | 497 | 1.5 | 477 | 273 | 2.3 | 343 | * | - | * | 03 | |
| 460 | 5.0 | 463 | <1.0 | B | <1.0 | B | 460 | <1.0 | B | <1.0 | - | <1.0 | 8 | 460 | 3.5 | 417 | <1.0 | B | <1.0 | B | 460 | <1.0 | B | <1.0 | - | <1.0 | B | |

* = Not Tested
B = Brittle
- = Testing discontinued due to embrittlement of the insulation

LEGEND:
OIT = Oxygen Induction Time
Reported in Minutes.
E = Elongation, %

TABLE 12

CORRELATION BETWEEN FAILURE POINTS AS INDICATED BY OXYGEN INDUCTION TIMES AND ELONGATION
AFTER AIR OVEN AGING AT 100°C

| | Out of 20 tests that were completed by 9/30/77 No. of Tests | ? |
|--|--|----|
| Correlation between Oxygen Induction Time and Elongation | 11 | 55 |
| Oxygen Induction Time > 1.0 minute at the time when the insulation embrittled | 5 | 25 |
| Detail: Three of the five tests reached < 1.0 minute OIT at the next test period. Thirty and 38 days were needed between embrittlement and < 1.0 minute OIT for the remaining two insulations. | | |
| Insulations continue to elongate after the Oxygen Induction Time is < 1.0 minute | 4 | 20 |
| Detail: One of the four tests reaches embrittlement at the next test period, while 87, 338 and 345 days were needed to embrittle for the remaining three specimens. | | |

It is concluded that the correlation between the two types of end point determinations on the samples tested is fair. The elongation test is preferred since it requires less time and expense and, in addition to indicating end points that are due to oxidation, it will detect also end points that are caused by changes in the crystalline structure of the insulation.

H. Sunlight and Its Effect on the Life of Insulated Conductors Exposed in Pedestal Terminals

The life of insulated conductors in pedestal terminals can be shortened when direct sunlight enters the terminal housings. The results of sunlight exposure are severe color fading and cracking of the insulations which results in noise and in severe cases in shorts, followed by loss of transmission. Filled cable insulations to date are by design not stabilized against UV radiation and the pigments that are employed for color coding are not light stable. The best solutions of this problem are properly designed pedestals and well trained craftsmen that will place the top covers onto the pedestals after completion of their assignments.

Filled cable insulations can be designed to be light stable, however, the cost of the insulation compounds and the color concentrates would be significantly increased. A lightfast red color concentrate that contains a suitable red pigment but no UV absorbers, costs four times as much as the standard red pigment, and due to the low opacity of the lightfast concentrate, twice as much would be needed so the actual usage cost would be eight times that of the standard pigment.

A comparison of standard PE color concentrates with experimental concentrates that contain lightfast pigments was made. Molded slabs, 0.050 inches in thickness, of HDPE with one percent of lightfast red and orange pigments were exposed outdoors in a direction 45° to the Southern horizon in Union, New Jersey from June 2, 1976 to December 2, 1976. While the lightfast pigments show only a very slight change in color during the six months exposure period, the molded slabs with the standard pigments are noticeably faded after two weeks of outdoor exposure.

The physical properties of all exposed specimens indicate the need for UV stabilizers, if resistance to sunlight is required.

TABLE 13

ELONGATION OF MOLDED COLORED HDPE, 0.050 INCHES IN THICKNESS AFTER OUTDOOR EXPOSURE
AT UNION, NEW JERSEY FROM JUNE 2, 1976 TO DECEMBER 2, 1976

| | Standard Orange Elongation, % | Lightfast Orange Elongation, % | Standard Red Elongation, % | Lightfast Red Elongation, % |
|-------------------------------|----------------------------------|-----------------------------------|-------------------------------|--------------------------------|
| Original | 880 | 950 | 920 | 800 |
| Exposed Outdoors - 2 Weeks | 960 | 610 | 940 | 930 |
| 4 Weeks | 560 | 570 | 640 | 910 |
| 3 Months | 0 | 0 | 0 | 0 |

I. Mechanical Strength of Insulation in Pedestal Terminals

The service life of even the highest grade of properly manufactured insulated conductor can be impaired if mechanical damage is inflicted during the initial or subsequent termination process. Insulations having the greatest resistance to abrasion and compression have the best chance for survival. Foam and foam skin insulations require much more care when being terminated than either solid propylene-ethylene copolymer or HDPE insulations.

a. Scrape Abrasion - Insulations from the Round Robin test program and additional samples of HDPE foam skin and solid LDPE were subjected to an

abrasion test, utilizing the GE scrape tester. Briefly, the test consists of abrading 3/8 inches of insulation at 60 cycles per minute with a 0.016 inch OD steel mandrel that has a load of 700 grams attached to it.

The test results obtained are recorded in Table 14 in the order of increasing resistance to scrape abrasion. It can be seen that cellular HDPE, the HDPE foam skin and the solid LDPE insulations have the least resistance to abrasion, while the cellular propylene ethylene copolymer insulations are noticeably better, however, solid HDPE and propylene-ethylene copolymer insulations are far superior.

TABLE 14
SCRAPE ABRASION OF SOLID, CELLULAR AND FOAM SKIN TELEPHONE INSULATIONS

| Order of Increasing Resistance to Scrape Abrasion | Insulation Type Over No. 22 AWG Solid Copper | Wall Thickness, Inches | Color of Insulation and Round Robin Test Sample Number if Applicable | Scrape Abrasion Test, Cycles to Failure at R.T. (25°C)* | | |
|---|--|-------------------------|--|---|----------|---------|
| | | | | Individual Results | Range | Average |
| 1 | Cellular HDPE | 0.0099 | White Sample II | 6, 6, 4, 3, 3, 3, 5, 5, 5, 8 | 3 to 8 | 4.6 |
| 2 | Foam Skin, HDPE | Foam 0.0108 Skin 0.0023 | Green - | 7, 6, 5, 9, 7, 11, 6, 10, 5, 10 | 5 to 11 | 7.6 |
| 3 | Cellular HDPE | 0.0099 | Green Sample IV | 11, 9, 13, 10, 12, 13, 12, 7, 11, 14 | 7 to 14 | 11.2 |
| 4 | Solid LDPE | 0.009 | Green - | 21, 9, 11, 10, 12, 14, 8, 8, 13, 10 | 8 to 21 | 11.6 |
| 5 | Foam Skin, HDPE | Foam 0.0103 Skin 0.0041 | White - | 16, 9, 18, 7, 11, 9, 7, 13, 11, 18 | 7 to 18 | 11.9 |
| 6 | Cellular Prop. Eth. Cop. | 0.0099 | Green Sample VIII | 27, 19, 31, 33, 36, 19, 35, 11, 24, 21 | 11 to 36 | 25.6 |
| 7 | Cellular Prop. Eth. Cop. | 0.0099 | White Sample VI | 20, 16, 36, 13, 34, 42, 29, 19, 21, 27 | 13 to 42 | 25.7 |
| 8 | Solid Prop. Eth. Cop. | 0.0144 | Green Sample VII | 4778 | - | 4778 |
| 9 | Solid Prop. Eth. Cop. | 0.0144 | White Sample V | 5732 | - | 5732 |
| 10 | Solid HDPE | 0.0134 | Green Sample III | 6313 | - | 6313 |
| 11 | Solid HDPE | 0.0134 | White Sample I | 6527 | - | 6527 |

*GE Scrape Tester, 700 gram load on 0.016 inch steel mandrel, abrading 3/8 inches of insulation, 60 cycles per minute, readings taken 12 inches apart, insulated conductor rotated 120° after each test.

b. Knife Edge Compression - The knife edge compression test is performed in an Instron Machine. The insulated conductor is placed on a horizontal grounded steel support, the conductor is connected to a low voltage current and the knife edge is compressing through the insulation at 0.05 inches per minute and the force required is recorded in pounds. As soon as the knife edge comes in contact with the conductor, the test is terminated.

The results obtained are recorded in Table 15. The range of results is rather narrow, all results are within 4.6 and 27.5 lbs. The solid propylene-ethylene copolymer insulation is most resistant to knife edge compression. The cellular propylene ethylene copolymer is superior to the solid HDPE. Solid LDPE is most susceptible to damage by knife edge compression.

TABLE 15
KNIFE EDGE COMPRESSION OF SOLID, CELLULAR AND FOAM SKIN TELEPHONE INSULATIONS

| Order of Increasing Resistance to Knife Edge Compression | Insulation Type Over No. 22 AWG Solid Copper | Wall Thickness, Inches | Color of Insulation and Round Robin Test Sample Number if Applicable | Knife Edge Compression, lbs., at R.T. (25°C)* | | |
|--|--|----------------------------|--|--|------------|---------|
| | | | | Individual Results | Range | Average |
| 1 | Solid LDPE | 0.009 | Green - | 4.4, 4.5, 4.3, 4.7, 4.3, 5.0, 4.6, 4.7, 4.2, 5.3 | 4.2 to 5.3 | 4.6 |
| 2 | Cellular HDPE | 0.0099 | White Sample II | 6.5, 4.5, 6, 6, 6, 6, 6, 5, 4.5 | 4.5 to 6.5 | 5.7 |
| 3 | Foam Skin, HDPE | Foam 0.0108 Skin 0.0023 | Green - | 6, 5, 6, 6.5, 6, 6.5, 6, 6, 6, 5 | 5 to 6.5 | 5.9 |
| 4 | Foam Skin, HDPE | Foam 0.0103 Skin 0.0041 | White - | 6, 6.5, 5, 6.5, 6.0, 6, 5, 6.5, 6, 7 | 5 to 7 | 6.1 |
| 5 | Cellular HDPE | 0.0099 | Green Sample IV | 8, 7, 6, 7, 7, 7, 6, 6, 7, 6 | 6 to 8 | 6.7 |
| 6 | Solid HDPE | 0.0134 | White Sample I | 13, 14, 13, 13, 12, 12, 12, 12, 12, 12 | 12 to 14 | 12.5 |
| 7 | Solid HDPE | 0.0134 | Green Sample III | 14, 13, 13, 13, 12, 12, 13, 12, 13, 12 | 12 to 14 | 12.7 |
| 8 | Cellular Prop. Eth. Cop. | 0.0099 | Green Sample VIII | 22, 19, 21, 19, 21, 22, 23, 15, 21, 21 | 15 to 23 | 20.4 |
| 9 | Cellular Prop. Eth. Cop. | 0.0099 | White Sample VI | 21, 23, 19, 24, 32, 26, 27, 22, 25, 25 | 19 to 32 | 24.4 |
| 10 | Solid Prop. Eth. Cop. | 0.0144 | White Sample V | 28, 27, 29, 22, 28, 29, 26, 28, 28, 30 | 22 to 30 | 27.5 |
| | | 0.0144 | Green Sample VII | 30, 26, 31, 24, 27, 25, 31, 31, 29, 21 | 21 to 31 | 27.5 |

*0.010 inch edge compression test is performed in an Instron Machine. The insulated conductor is placed on a horizontal grounded steel support, the conductor is connected to a low voltage current that is connected to a 0.05 inch per minute. The test is terminated when a low voltage current makes contact with the grounded steel support. Readings are taken 12 inches apart. The insulated conductor is rotated 120° after each test.

c. Flat Plate Compression - The flat plate compression test determines the force in pounds that is required to crush 2.25 inches of insulation between two steel plates at 0.05 inches per minute. The test is performed with the Instron Machine.

The range of the results for all samples tested is between 275 and 2720 lbs. The best performance is shown by the solid propylene-ethylene copolymer insulations, followed by solid HDPE insulation with the cellular propylene-ethylene copolymer ranking third. The details of all tests are recorded in Table 16.

| Order of Increasing Resistance to Flat Plate Compression | Insulation Type Over No. 22 AWG Solid Copper | Wall Thickness, Inches | Color of Insulation and Round Robin Test Sample Number if Applicable | Flat Plate Compression, lbs., at R.T. (25°C)* | | |
|--|--|----------------------------|--|--|--------------|---------|
| | | | | Individual Results | Range | Average |
| 1 | Cellular HDPE | 0.0099 | Green Sample IV | 295, 255, 275(1) | 255 to 295 | 275 |
| 2 | Cellular HDPE | 0.0099 | White Sample II | 300, 340, 350(1) | 300 to 350 | 330 |
| 3 | Foam Skin, HDPE | Foam 0.0108 Skin 0.0023 | Green - | 360, 405, 345, 285, 295, 340, 345, 340, 400, 450 | 285 to 450 | 357 |
| 4 | Foam Skin, HDPE | Foam 0.0103 Skin 0.0041 | White - | 460, 520, 290, 455, 285, 360, 315, 305, 295, 340 | 285 to 520 | 363 |
| 5 | Solid LDPE | 0.009 | Green - | 690, 590, 760, 600, 680, 860, 950, 720, 590, 630 | 590 to 950 | 707 |
| 6 | Cellular Prop. Eth. Cop. | 0.0099 | Green Sample VIII | 910, 1110, 1040, 960, 840, 830, 1090, 1060, 840, 840 | 830 to 1110 | 952 |
| 7 | Cellular Prop. Eth. Cop. | 0.0099 | White Sample VI | 945, 985, 910, 950, 1010, 1100, 900, 1170, 880, 1100 | 880 to 1170 | 995 |
| 8 | Solid HDPE | 0.0134 | White Sample I | 1600, 1250, 1170, 1390, 1570, 1330, 1530, 1070, 1510, 1470 | 1070 to 1600 | 1389 |
| 9 | Solid HDPE | 0.0134 | Green Sample III | 1740, 1410, 1340, 1300, 1260, 1240, 1480, 1340, 1460, 1450 | 1260 to 1740 | 1422 |
| 10 | Solid Prop. Eth. Cop. | 0.0144 | Green Sample VII | 2050, 2050, 2750, 2800, 2850, 2400, 3050, 3025, 2725, 2400 | 2050 to 3050 | 2610 |
| 11 | Solid Prop. Eth. Cop. | 0.0144 | White Sample V | 2250, 2150, 2775, 2750, 2350, 3050, 2750, 2550, 3250, 3325 | 2150 to 3325 | 2720 |

*2.25 inches of insulation are crushed between two steel plates at 0.05 inch/minute. The test is terminated when the conductor makes contact with the flat steel plates. The readings are taken 12 inches apart and the insulated wire is rotated 120° after each test.

(1) Sample depleted.

d. Summary of Mechanical Strength Performance Ratings - By combining the ratings of the insulations tested for scrape abrasion, knife edge and flat plate compression, it is clearly demonstrated in Table 17 that the solid propylene-ethylene copolymer and HDPE insulations have the greatest resistance to mechanical damage, while the HDPE all foam and foam skin insulations need the greatest care when they are installed in pedestal terminals.

| Order of Increasing Mechanical Strength | Insulation Type Over No. 22 AWG Solid Copper | Wall Thickness, Inches | Color of Insulation and Round Robin Test Sample No. if Applicable | Rating of Performance from Lowest, (Rating 1) to Highest (Rating 11) | | | | Summary |
|---|--|----------------------------|---|--|------------------------|------------------------|----|---------|
| | | | | Scrape Abrasion | Knife Edge Compression | Flat Plate Compression | | |
| 1 | Cellular HDPE | 0.0099 | White Sample II | 1 | 2 | 2 | 5 | |
| 2 | Foam Skin, HDPE | Foam 0.0108 Skin 0.0023 | Green - | 2 | 3 | 3 | 8 | |
| 3 | Cellular, HDPE | 0.0099 | Green Sample IV | 3 | 5 | 1 | 9 | |
| 4 | Solid LDPE | 0.009 | Green - | 4 | 1 | 5 | 10 | |
| 5 | Foam Skin, HDPE | Foam 0.0103 Skin 0.0041 | White - | 5 | 4 | 4 | 13 | |
| 6 | Cellular Prop. Eth. Cop. | 0.0099 | Green Sample VIII | 6 | 8 | 6 | 20 | |
| 7 | Cellular Prop. Eth. Cop. | 0.0099 | White Sample VI | 7 | 9 | 7 | 23 | |
| 8 | Solid HDPE | 0.0134 | White Sample I | 11 | 6 | 8 | 25 | |
| 9 | Solid HDPE | 0.0134 | Green Sample III | 10 | 7 | 9 | 26 | |
| 10 | Solid Prop. Eth. Cop. | 0.0144 | Green Sample VII | 8 | 11 | 10 | 29 | |
| 11 | Solid Prop. Eth. Cop. | 0.0144 | White Sample V | 9 | 10 | 11 | 30 | |

SUMMARY

The members of working group 434 and their chairman have made a great and successful effort in conducting the round robin test in order to appraise the validity of air oven aging of insulations vs differential thermal analysis as a means to predict the service life of the filled cable insulations. When an explanation was sought to explain the wide ranges of test results that were obtained, they made information available that helped to explain the differences in test results. It was demonstrated that the selected test temperature in the air ovens must be precisely maintained within $\pm 0.5^{\circ}\text{C}$. It was found that the solid insulations displayed satisfactory aging performance, before and after contact with the petroleum based filling compounds. The cellular insulations tested were found to embrittle earlier than their solid counterparts, their service life is approximately 30% to 50% shorter.

Comparing the test data from the differential thermal analysis with results from the air oven aging test, it was found that the test data are related only in the very broadest sense. An answer has not been found why the test results from the well defined DTA test vary so widely between the various laboratories.

Based on the results of the Round Robin Test, a carefully defined air oven method has been proposed to the REA as an initial qualification test for oxidative stability of high density polyethylene or propylene-ethylene copolymer insulated conductors which are utilized in filled telephone cables.

The life of insulation in pedestals is shortened if sunlight enters the pedestals, since neither the insulation compounds nor the color concentrates are designed to be resistant to UV radiation.

Another factor that can affect insulation life in pedestals is mechanical damage that may occur during termination or reentering. All foam and foam-skin insulations require considerably more care than solid HDPE and propylene-ethylene copolymer insulations.

REFERENCES

1. "Methods for Life Prediction of Insulations of Air Core Cables and Filled Cables" by G. A. Schmidt, General Cable Corporation, 22nd International Wire & Cable Symposium 1973.
2. "Non-Extractable Stabilizers for Polypropylene and Polyethylene Insulation of Fully-Filled Cables" by S. Verne and R. T. Puckowski, BICC, London, England, B.R.O. Pointer, ICI, Ltd., Welwyn Garden City, Hertfordshire, England, 21st International Wire & Cable Symposium 1972.
3. "Evaluation of Thermal Degradation in Polyethylene Telephone Cable Insulation, B. B. Pusey, M. T. Chen, W. L. Roberts, Superior Continental Corporation, Hickory, North Carolina, 20th International Wire & Cable Symposium 1971.

ACKNOWLEDGEMENTS

The author wishes to express her thanks for the effort and contributions of the chairman and the participating members of Working Group 434 and their Laboratories.

Due acknowledgement is made to her colleagues Messrs K. J. Virkus, J. N. D'Amico, J. Fech, S. Lutwin, and R. Lang for their valuable contributions.



Miss G. A. Schmidt, Assistant Director of Research and Development, Material Science, General Cable Corporation, Research Center, 800 Rahway Avenue, Union, New Jersey 07083

IMMUNITY TO WATER OF FOAM, FOAM-SKIN AND SOLID
INSULATED FILLED TELEPHONE CABLES.

J. A. Olszewski

Research Center, General Cable Corporation, Union, New Jersey 07083

Abstract

Self-capacitance stability tests on foam, foam-skin and solid insulated wires immersed in water show the first two types to be substantially less stable. Three and one-half years duration water immersion tests on filled cables, however, show all three basic types of insulation to have practically equivalent performance, both in measured mutual capacitance and loss tangent stability. The accuracy of measured loss tangent though appears to be questionable and so is the interpretation of its values as measured. The knowledge of true loss tangent behaviour is most important in assessing cable attenuation, especially at carrier frequencies.

Introduction

Foam or foam-skin insulated filled telephone cables are preferred by the users because of favorable economics compared to conventional solid insulated filled cables. To illustrate this point more clearly, about 30% expanded (by volume) foam insulation permits the reduction of filled cable dimensions to the same values as in the air core cables. Adoption of these newer designs, however, raises several questions relating to their performance, namely:

- i. Immunity to water in terms of stability of electrical transmission characteristics.
- ii. Conductor to conductor voltage withstand level.
- iii. Immunity to insulation cell filling by oils contained in the petrolatum based filling compounds or electrical transmission stability with in-service aging.
- iv. Mechanical strength of the insulation.

This study addresses itself to the first question only, namely, the stability of open circuit admittance when filled cables employing foam, foam-skin and solid insulations are subjected to the industry standardized water immersion test.

Test Method and Results

The study presented in this paper was limited to No. 22 AWG singles of filled cable dimensions and No. 22 AWG filled cables.

The singles employed the following types of insulation:

- a. Solid propylene-ethylene copolymer (PP).
- b. Solid HDPE.
- c. 30% expanded (by volume) HDPE foam.
- d. 50% expanded (by volume) inner layer with 0.002" thick solid skin HDPE foam-skin.

Three, 50 pair cables studied were covered with our standard FPA sheath and were filled with the following filling compounds respectively:

- i. 85/15 compound - 85% PJ + 15% PE + stabilizers.
- ii. 92/8 compound - 92% PJ + 8% PE + stabilizers.
- iii. ICMAC compound - 100% PJ blend + stabilizers.

Each cable had unit core construction with unit insulation types as given below:

- a. Solid propylene-ethylene copolymer (PP).
- b. Solid HDPE.
- c. 30% expanded (by volume) MDPE foam.
- d. 50% expanded (by volume) inner layer with 0.002" thick skin - propylene-ethylene (PP) foam-skin.

The length of all samples of singles was 100 feet. These were coiled and one set was immersed in tap water bath at room temperature. A second set was immersed in tap water which was maintained at 65°C and so was the third set of samples but after prior aging for one week in petrolatum at 70°C. Self-capacitance (C_s) of each sample was

measured periodically at 1000 Hz, using a capacitance bridge having an accuracy of 0.1%.

The measured change in self-capacitance of singles with time of immersion at room temperature is shown in Figure 1, and that for singles immersed in water at 65°C is shown in Figure 2.

All filled cable samples were 30 feet long with 26 feet of their length immersed under a 3 foot head of tap water at room temperature. Holes, 3/8" in diameter, were cut through the cable sheaths and core tape. The holes were 12 inches apart and rotated 90° from each other in a fixed direction. Tip to ground, ring to ground, and tip plus ring to ground capacitance and dissipation factor measurements were made periodically at 1000 Hz, using a ratio arm transformer type capacitance bridge. The changes in pairs capacitances of each type of insulation and in each type of cable were determined over a 3-1/2 year period of immersion. For brevity, only the average measured values for each insulation type and only for 92/8 compound filled cable are given. These results are shown in Table 1. Calculated 1000 Hz mutual capacitance and mutual dissipation factor are shown graphically in Figure 3.

Apart from the above, additional two 25 pair No. 22 AWG cables were prepared and tested under industry standardized water immersion. Each of these cables employed solid HDPE insulation, but one was filled with our production filling compound Q9, while the other had 85/15 filling compound. Both cables were allocated to carrier frequencies studies and Figure 4 shows their per cent changes in 772 kHz attenuation with time of immersion in water at room temperature. Attenuation values were determined by calculation from measured resistance, inductance, capacitance and conductance of pairs at 772 kHz.

Discussion of Capacitance Test Data

The concern with change in open-circuit admittance characteristics on water entry or moisture ingress into foam or foam-skin insulated filled cable core is justified because foam and foam-skin insulations can be expected to absorb water into their cells through a known mechanism of water vapour permeation and condensation. This phenomenon is similar to that already observed in air core type cables, when water vapour was found to permeate through the polyethylene jacket and condense in the cores of these cables.¹ On the other hand, solid insulations change to much lesser degree and theoretically should be immune, since solid polyethylenes or propylene-ethylene copolymers can absorb water only in parts per million.²

The behaviour of the three types of insulated singles studied, i.e. solid, foam and foam-skin, immersed in water at room temperature, is shown in Figure 1. This self-capacitance stability data is difficult to judge because of the slow rate of moisture ingress into the insulations under study due to low vapour pressure. In general, however, it is apparent that the difference in performance

between solid and expanded insulations is small, with solids being somewhat more stable.

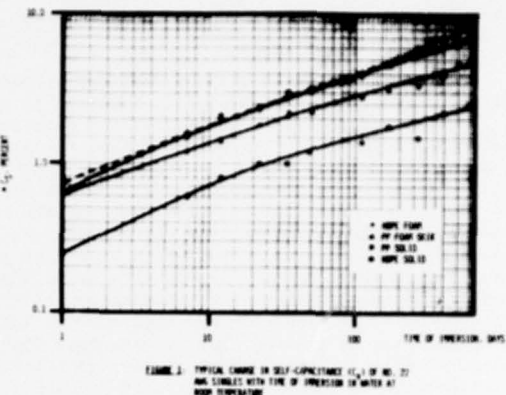


FIGURE 1. TYPICAL CHANGE IN SELF-CAPACITANCE (C_s) OF NO. 22 AWG SINGLES WITH TIME OF IMMERSION IN WATER AT ROOM TEMPERATURE

The temperature accelerated test on the singles, conducted at 65°C - see Figure 2, shows very significant differences. While the self-capacitance of solid insulated conductors stabilizes at 1 to 5% level of increase, the self-capacitance of singles with cellular insulations is far less stable and in tests to-date, did not reach equilibrium with an observed capacitance increase of up to 40%. The outer solid plastic skin of foam-skin

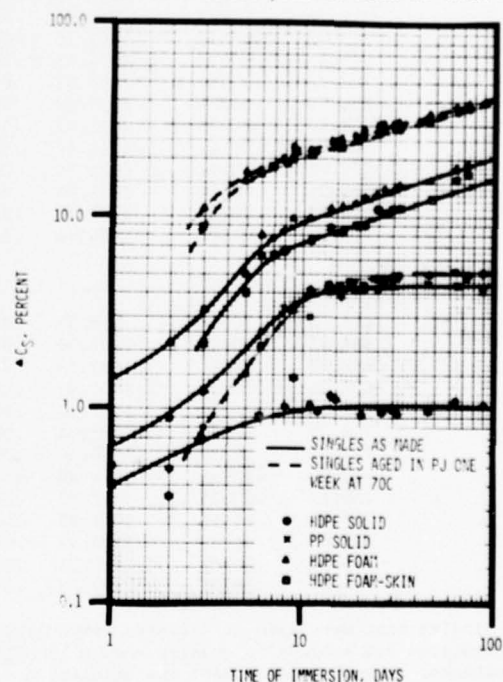


FIGURE 2. TYPICAL CHANGE IN SELF-CAPACITANCE (C_s) OF NO. 22 AWG SINGLES WITH TIME OF IMMERSION IN WATER AT 65°C.

type, as expected, is not an important factor in retarding moisture ingress. Complete filling of cellular insulations with water, theoretically can result in significantly higher increase in the dielectric constant than 40% observed in tests to-date.

Of special interest are two distinct slopes in self-capacitance change of singles immersed in water at elevated temperature. The inflection points on the curves more or less coincide in time for all types of insulations studied. This appears to signify bridging by condensed water of small air gap that is practically unavoidable around the metal conductor. This is the primary, if not the only, reason for the increase in self-capacitance of solid insulated singles, and implies limited or no adhesion of the insulation to the conductor. The small space between the conductor and the inner wall of any insulation is inherent for all standard insulation materials and can often be made substantial by an inadequate insulation extrusion process through improper cooling in the water trough.

After reaching the inflection point indicated above, the solid insulated singles tend to stabilize in self-capacitance while the expanded insulations continue to increase in self-capacitance due to the continued ingress of moisture into the insulation cells and its condensation. Moisture ingress into insulation cells is the cause of the greater rate of change in self-capacitance of foams up to the inflection point and its higher level in general. The effectively thinner polymeric membrane of cellular walls, results in the inflection point occurring somewhat earlier in time than for solid insulations.

It is interesting to note the finding that the theorized air gap around the conductor apparently causes an early change in self-capacitance. This appears to be due to highly conductive surface of the conductor which bridges condensed tiny droplets of water that collect on the conductor or on the inner wall of the insulation tube. This gives the equivalent of an increase in conductor diameter. Lower temperature of the conductor, through air

TABLE I
Experimental 1000 Hz Average Partial Capacitance and Dissipation Factor Data for No. 22 AWG
92/8 Filled Cable in Water Immersion Test at Room Temperature.

| Immersion Time t, days | Solid PP | | | | Solid HDPE | | | |
|------------------------|-------------|--------|--------------|--------|--------------|--------|--------------|--------|
| | 1 Wire to G | | 2 Wires to G | | 1 Wire to G | | 2 Wires to G | |
| | C,pF | tanδ | C,pF | tanδ | C,pF | tanδ | C,pF | tanδ |
| ≤ 0 | 729.80 | .00062 | 1033.16 | .00075 | 715.09 | .00046 | 1005.66 | .00075 |
| 17 | 735.91 | .00192 | 1045.96 | .00254 | 724.93 | .00123 | 1030.70 | .00208 |
| 32 | 740.56 | .00250 | 1058.69 | .00392 | 731.16 | .00198 | 1044.03 | .00377 |
| 47 | 742.33 | .00272 | 1062.10 | .00441 | 733.20 | .00225 | 1049.93 | .00420 |
| 89 | 747.45 | .00325 | 1074.48 | .00582 | 740.48 | .00258 | 1068.63 | .00503 |
| 129 | 753.29 | .00359 | 1086.02 | .00644 | 747.32 | .00282 | 1082.72 | .00552 |
| 194 | 756.83 | .00386 | 1093.52 | .00710 | 751.87 | .00304 | 1096.37 | .00617 |
| 255 | 757.12 | .00395 | 1095.42 | .00746 | 751.85 | .00317 | 1098.67 | .00643 |
| 325 | 764.49 | .00441 | 1114.34 | .00848 | 761.50 | .00367 | 1123.47 | .00745 |
| 390 | 771.08 | .00476 | 1128.24 | .00920 | 768.77 | .00382 | 1140.88 | .00773 |
| 607 | 781.56 | .00549 | 1151.98 | .01064 | 778.74 | .00451 | 1165.95 | .00920 |
| 987 | 791.79 | .00770 | 1177.68 | .01434 | 784.48 | .00575 | 1182.22 | .01135 |
| 1270 | 799.95 | .00884 | 1194.44 | .01604 | 793.82 | .00682 | 1202.48 | .01322 |
| | Foam MDPE | | | | Foam-Skin PP | | | |
| ≤ 0 | 677.20 | .00081 | 959.57 | .00107 | 711.44 | .00062 | 987.15 | .00085 |
| 17 | 688.85 | .00182 | 985.36 | .00312 | 724.71 | .00158 | 1017.74 | .00317 |
| 32 | 696.83 | .00221 | 1003.68 | .00418 | 731.74 | .00190 | 1034.44 | .00395 |
| 47 | 698.76 | .00236 | 1008.93 | .00443 | 733.44 | .00210 | 1037.97 | .00422 |
| 89 | 703.88 | .00264 | 1021.97 | .00512 | 737.43 | .00230 | 1048.08 | .00483 |
| 129 | 707.25 | .00244 | 1025.14 | .00487 | 740.17 | .00248 | 1053.75 | .00507 |
| 194 | 712.03 | .00271 | 1040.50 | .00535 | 745.60 | .00231 | 1063.48 | .00512 |
| 255 | 712.04 | .00324 | 1041.48 | .00612 | 746.47 | .00234 | 1064.85 | .00498 |
| 325 | 718.19 | .00375 | 1057.82 | .00710 | 751.87 | .00308 | 1082.45 | .00598 |
| 390 | 727.04 | .00418 | 1077.95 | .00812 | 760.03 | .00347 | 1102.07 | .0072 |
| 607 | 737.83 | .00487 | 1104.42 | .00943 | 771.02 | .00392 | 1126.63 | .00858 |
| 987 | 750.65 | .00587 | 1134.23 | .01138 | 781.31 | .00524 | 1152.60 | .01095 |
| 1270 | 764.03 | .00777 | 1162.75 | .01445 | 794.20 | .00586 | 1179.95 | .01227 |

Singles that were aged at elevated temperature in petrolatum are subject to greater change in self-capacitance, as such aging causes the insulation to swell, especially away from the conductor, and consequently increases the gap at the conductor.

cooling of conductor ends which protruded out of the water bath, may be responsible for more efficient condensation of water vapour in the air space around the conductor of relatively short samples that were under study in the

experimental set-up.

The greater immunity to water ingress, in terms of capacitance stability, of solid insulated filled cables than of foam or foam-skin types, was not observed on actual filled cable samples selected for test. The test data taken at room temperature for about 1300 days of immersion - see Figure 3 - indicate that the expanded insulations are as stable as solid insulations. In test not reported here, small relative differences in performance between studied insulations were observed in other filling compounds and in some cases expanded insulations appeared to be somewhat more stable. The overall level of mutual capacitance (C_m) increases, however, varied from one filling compound to another, as it was already pointed out in reference 3.

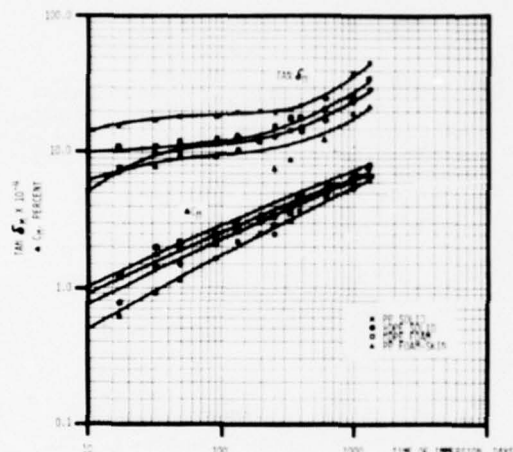


FIGURE 3: CALCULATED 1000 Hz MUTUAL CAPACITANCE AND DISSIPATION FACTOR OF FOAM, FOAM-SKIN AND SOLID INSULATIONS IN 90/15 FILLED CABLE.

The comparable performance of cellular and solid insulations in filled cables appears to be in part due to limited access of water to the singles since the cable core is filled and in part due to testing at room temperature when even performance in water of singles with various insulations is only slightly different. Probably, the most important factor is the limited duration of testing as data shown in Figure 2 suggest strongly that, given enough time and suitable environment, cellular insulated filled cables will change more with water ingress than the solid insulated cables. Longer time testing or accelerated testing is required to prove or disprove the latter and to determine whether the mutual capacitance of cellular cables at full saturation with water will be larger than the half value of the self-capacitance of singles, or $C_s/2$.

Discussion of Dissipation Factor Test Data

The interest in the behaviour of the dissipation factor of cable pairs (loss tangent), stems from the known fact that water entry into the

filled cable core, can substantially increase the dielectric loss of the core medium (filling compound) and this will increase the attenuation of the cable, especially at carrier frequencies.

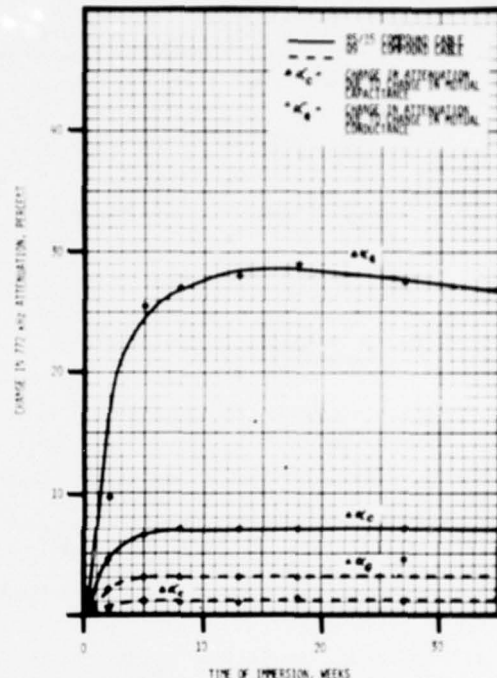


FIGURE 4: CHANGE IN 772 kHz ATTENUATION OF NO. 22 AWG FILLED CABLES IN WATER IMMERSION TESTS.

A typical example of attenuation change at T1 carrier frequency of 772 kHz, for water immersed No. 22 AWG solid insulated filled cables with 85/15 and Q9 filling compounds is shown in Figure 4. This data, which was derived from measured primary parameters R, L, C and G, show that:

- The increase in carrier frequencies attenuation due to moisture induced increase in the dissipation factor is significantly higher than that due to increase in mutual capacitance.
- The moisture ingress into poorly designed filled cables can cause significant increase in attenuation at carrier frequencies.

The mutual dissipation factor data graphed in Figure 3 suggests that foam, foam-skin and solid insulated filled cables have similar stability, but the analysis of the 1000 Hz loss tangent test results, given in Table 1, points to a serious

anomaly. Practically immediately upon immersion of filled cable samples in water, computed by conventional method loss tangent of wire-to-wire branch, is found to be negative. The measured loss tangent values of tip-to-ground, ring-to-ground and tip plus ring-to-ground circuits in each case are positive but the magnitude of computed loss tangent of wire-to-wire circuit is not only negative but increases with time of immersion.

The reasons for the calculations yielding negative result can readily be seen from the following accepted relationship:

$$G_d = \frac{G_t + G_r - G_{t+r}}{2}$$

where G_d = conductance of wire-to-wire circuit.

G_t = conductance of tip-to-ground circuit.

G_r = conductance of ring-to-ground circuit.

$G_t + r$ = conductance of tip plus ring-to-ground circuit.

The above indicates that if the sum of measured conductances of tip-to-ground and ring-to-ground is smaller than that measured for tip plus ring-to-ground, G_d will calculate to be negative.

The above described finding tends to imply the following possibilities:

- a. The assumed conventional admittance circuit for the telephone cable pair is not valid for cables with elements of core medium having high dielectric loss, at least as far as conductances are concerned.
- b. Conventional interpretation of measured conductance results on cables with wet filling compound or "semi-conducting" cable core medium appears to be not correct.
- or c. Capacitance bridges used in the tests do not yield correct results.

The test program described herein was carried out using bridges of the ratio arm transformer type. Their simplified circuit diagram is shown in Figure 5 for tip, ring or both wires to ground measurements. Mutual admittance was measured with ground taken off terminal b and only specimen point e grounded, while wire-to-wire measurements were made with specimen point e connected to terminal d of the bridge with ground point switched from b to d.

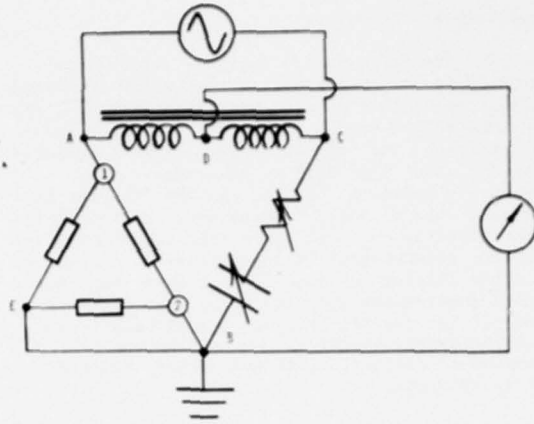


FIGURE 5. SIMPLIFIED SCHEMATIC OF CAPACITANCE BRIDGE EMPLOYED IN THE TEST PROGRAM.

The example of calculated values of capacitance and dissipation factor, from measured data shown in Table 1, for No. 22 AWG cable filled with 92/8 compound and employing solid HDPE insulation, is illustrated below:

| Time of Immersion, Days | Wire-to-Wire Capacitance, pF | Wire-to-Wire tan δ |
|-------------------------|------------------------------|---------------------------|
| 0 | 212.26 | -.00023 |
| 47 | 208.24 | -.00267 |
| 194 | 203.69 | -.00538 |
| 607 | 195.77 | -.00946 |
| 1270 | 192.58 | -.01316 |

Directly measured results on wire-to-wire branch, made the observed anomaly even more puzzling, since the obtained values were negative and confirmed in general the figures calculated from the standard three measurements to ground. Measured negative loss tangent on any passive circuit indicates incorrect procedures.

The implication of the above findings is that the calculated mutual loss tangent may also be incorrect, since the conventional interpretation specifies

$$G_m \approx G_d + \frac{G_t + r}{4}$$

where G_m = mutual conductance.

Thus, the test data validity, including that shown in Figure 4, is questionable. The subject requires further studies, especially on cables before and after immersion in water.

Conclusions

1. Foam and foam-skin insulated filled cables in water immersion tests of 3-1/2 years duration are as stable in capacitance as solid insulated cables.
2. Foam and foam-skin singles in temperature accelerated water immersion tests show significantly less stable self-capacitance than their solid insulated counterparts.
3. Solid skin in foam-skin insulation type is not a significant factor in mitigating moisture ingress into the underlying foam layer.
4. Small air gap between the insulation and the conductor appears to be the reason for changes in self-capacitance of solid insulated singles measured in water. These changes, however, are relatively small.
5. Measured dissipation factor values on filled cables that have moisture in their cores, using the procedure described, appears to be incorrect. This subject requires further studies.

References

1. H. W. Friesen and A. S. Windeler, "Moisture Permeation and Its Effect on Communication Cable", 15th International Wire & Cable Symposium, Atlantic City, New Jersey December 1966.
2. "Modern Plastics Encyclopedia", McGraw-Hill, 1976-1977.
3. J. A. Olszewski, "Capacitance Relationship in Filled Telephone Cables and Equilibrium Prediction from Water Immersion Tests", 24th International Wire & Cable Symposium, Cherry Hill, New Jersey, November 1975.



J. A. Olszewski, Assistant Director of Research in charge of research and development of communication wires and cables, General Cable Corporation, Research Center, 800 Rahway Avenue, Union, New Jersey 07083

ANALYSIS AND CONTROL OF CAPACITANCE UNBALANCE TO GROUND IN FILLED CABLE

Joaquin Prósper

CABLES DE COMUNICACIONES S.A.

ABSTRACT

One of the greatest problems in the manufacture of filled cable today is that of reaching the specified requirements in the capacitance unbalance to ground.

This paper shows a study in which all the changes that in one way or another can interact in the capacitance unbalance to ground are analyzed. Unfortunately it is not possible to control many of these at present, but by them we can detect those that have greater effect on the unbalance, thus enabling us to concentrate our efforts in improving them.

Experimental cables were made to conduct this study and the samples show that 70-80% of the capacitance unbalance to ground are explained by changes in the coaxial capacitance, this means that the control of the coaxial capacitance is the most important. The unbalance to ground on the experimental cables was well within the specified limits, obtaining a better accumulative distribution of the unbalance than in the air-core standard PIC cable.

INTRODUCTION

Historically from the beginning of multipair cable one of the greatest problems the manufacturer has had, has been to obtain a satisfactory balance of the pairs. This characteristic is important as it determines the pick-up noise in the pair circuits.

After a study around 1972 on the maximum metallic noise that could be accepted from a paired circuit transmission viewpoint, the maximum medium value acceptable was determined on the capacitance unbalance to ground in a multipair cable. In this way the manufacturer's specification was established at 150 pF/Kft for the 19-22 (AWG), at 200 pF/Kft for the 24-26 (AWG), and an individual maximum of 435 pF/Kft for any gauge.

At that time filled cable was becoming very popular. The methods of insulating, pairing and stranding were the same as in non filled cable but with a greater effective dielectric constant than non filled, therefore the increase in the capacitance unbalance to ground was in the range of 30-70%.

On the other hand with the introduction of the T-carrier system the control of pick-up noise has become more important, consequently the level of unbalance to ground should be minimum or at least within the required specifications.

Subsequently other effects ⁽¹⁾ such as insertion loss peaks and special forms of crosstalk appear in high frequencies (T2 carrier), thus making them unacceptable in the transmission of pairs with a high level of capacitance unbalance to ground.

This has led to great efforts by the cable industry to meet (in filled cable) the specified values of capacitance unbalance to ground.

To the present date there has been very little published on the way to reduce the unbalance level to ground on a normal production of multipair filled cable. The object of this "paper" is to present the result of a study showing the correlations of the capacitance unbalance to ground with different parameters.

THE PARAMETERS WHICH MOST EFFECT THE UNBALANCE TO GROUND

According to Maupin ⁽²⁾ the individual capacitance to ground of a wire in a balanced shielded pair (Fig.1) is expressed by a complicated function:

$$C_g = -\frac{\epsilon_m}{f_g} \frac{d}{(\frac{d}{2s})^{\frac{1}{2}}} = \epsilon_m F_g \quad (1)$$

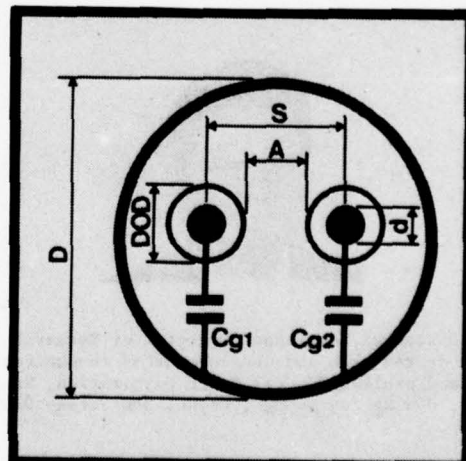


Figure 1
Balanced shielded pair

where in formula (1):

- ϵ_m = Medium dielectric constant
- d = Diameter of the conductor
- S = Interaxial distance
- D = Effective diameter of the shielding
- F_g = Dimensional and geometrical function of the cable

In conclusion it is indeed quite simple to deduce that the unbalance of capacitance to ground described as:

$$C_{ug} = C_{g1} - C_{g2} = \epsilon_m (F_{g1} - F_{g2}) \quad (2)$$

Is directly proportional to the dielectric constant of the medium and of the difference in the dimensional or geometrical functions of one of the wires in the structure of the cable.

As it is well known the manufacturing process for filled and unfilled cable is the same. It is in fact identical to non filled cable if we omit the filling process. Consequently the difference in the dimensional function (2) will stay unchanged and the unbalance to ground will increase according to the increase in the dielectric constant of the medium.

Due to the fact that the effective dielectric constant of the medium is between 1.75 - 1.81 in non filled cable and 2.23 - 2.3 in filled cable, the increase that should be expected in the capacitance unbalance to ground of filled cables compared to non filled would be about 30%. Nevertheless it is a fact that the unbalance to ground increases in the order of 30-70%. This shows us that the differences in the geometrical functions do not stay constant or that other parameters exist which are not considered in the expression (1).

Evidently a multi-pair cable is of an extremely complex geometrical structure which cannot exactly be resembled to the "shielded balanced pair" model, due to there being many variables which can interact with the capacitance unbalance to ground.

Principally the following parameters are considered to have the most effect on the capacitance unbalance to ground:

- a. Diameter of the conductor
- b. Diameter over insulation
- c. Dielectric constant of insulation
- d. Eccentricity of insulation
- e. Interstitial air spaces
- f. Twisting
- g. Stranding
- h. Expansion percentage (foam insulation)
- i. Dielectric effective of medium
- j. Pair position

It is self-evident that all these parameters do have an influence upon the unbalances to ground, but to establish how important each one is on the unbalances to ground is quite a task.

Nevertheless we do assume beforehand that there will exist a strong interaction in the parameters them-

selves which we have just mentioned. Consequently it will indeed be very difficult to try to sum up the relations between the unbalances to ground and each and every one of the individual parameters.

We think therefore it is more logical to obtain dependent relations with some of the master characteristics which interrelate in various of these parameters. To this effect one of the most important master characteristics which can be found is the coaxial capacitance. This coaxial capacitance is in fact known to be a function of the dimensional parameters such as: conductor diameter, diameter over insulation, dielectric constant of insulation and eccentricity.

The coaxial capacitance can be expressed approximately as follows:

$$C_{coax} = \frac{16.93\epsilon}{\ln \frac{DOD}{d}} \text{ pF/ft} \quad (3)$$

A dependent relation between the unbalance to ground (C_{ug}) and the coaxial capacitance variations (ΔC_{coax}) can be constructively obtained through expressions (1) and (3). This relation for filled cable with solid insulation is approximately given by:

$$C_{ug} (\text{pF/Kft}) = 150 \cdot \Delta C_{coax} (\text{pF/ft}) \quad (4)$$

Figure 2 represents the various dependence relations for 4 different cases.

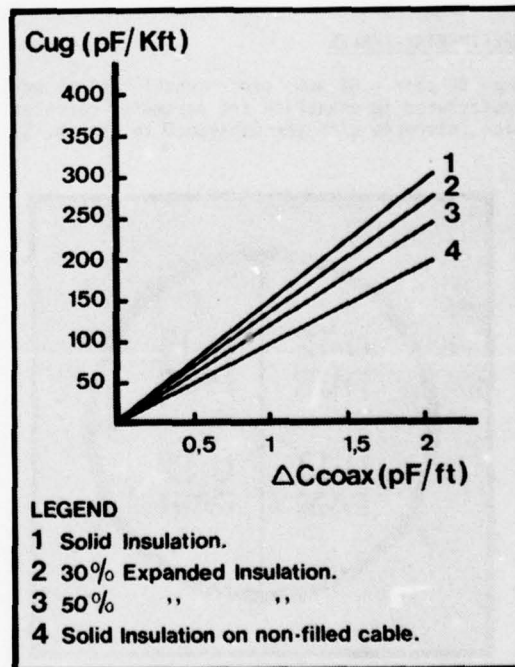


Figure 2
Unbalance to ground versus unbalance of coaxial capacitance

It is actually possible therefore to theoretically foretell the capacitance unbalance to ground value based on the deviations of coaxial capacitance produced during the manufacture.

We have only considered the dimensional variations which have influence upon the coaxial capacitance, therefore the values of unbalance to ground will only be approximate. The possible effects in the processes after the manufacture such as pairing, cabling, filling etc. are not taken into account.

Unfortunately there exists no other master characteristic as easy as this one to monitor and control in a continuous manner during the manufacturing process. Under these circumstances the analysis on the influence of the capacitance unbalance to ground of the various steps in the manufacture can only be performed if the total process is divided in two areas:

1. Insulation area
2. Remainder of the process area during the manufacture

Logically the first area will be controlled by the fundamental characteristic of coaxial capacitance, while the second area which is at present uncontrollable will not be relatively unknown due to the fact that if the influence of the first area is known, then that of the second area (rest of the process) should equal the percentage not explained (variation of the capacitance unbalance to ground) by means of the master characteristic in the first area (coaxial capacitance).

EXPERIMENTAL CABLES

Three 50 pair - 22 AWG experimental cables were manufactured to establish the parameter correlation which interacts with the unbalance to ground. Single

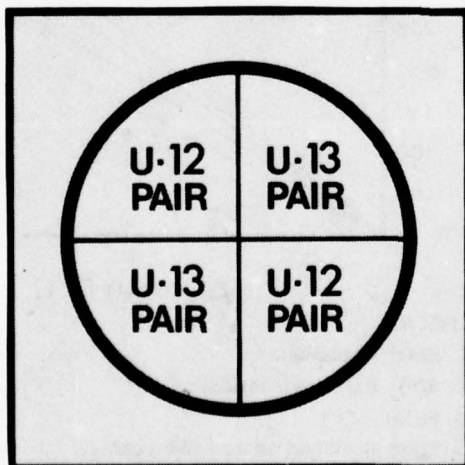


Figure 3
Core Configuration

conductors were insulated with solid HDPE and with dimensions of 86 NF/m target mutual capacitance. The core configuration in all the cables was as shown in Figure 3.

Although these cables were manufactured in normal production condition a preliminary measurement and control program was established prior to its manufacture, and was therefore undertaken throughout. A few deliberately unbalanced pairs were put in the 13 pair units with solid HDPE insulation, in this way the amount of influence of certain changes upon the capacitance unbalance to ground could be established. The exact penalty value of the above mentioned pairs was known to us. Figure 4 shows the defective pairs which were put in.

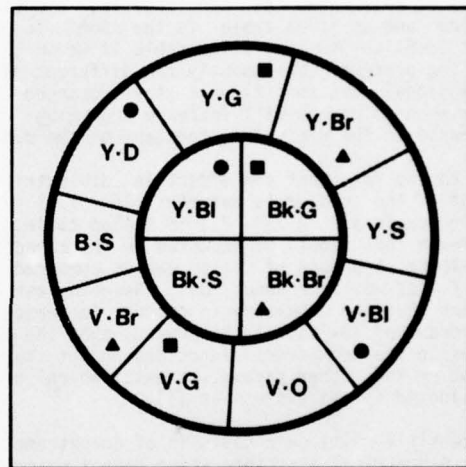


Figure 4

Known special pair arrangement

- = Pairs with considerable difference in conductor diameter (d)
- ▲ = Pairs with considerable difference in coaxial capacitance between wires
- = Pairs with distorted pair twist

Figure 5 on the following page shows the schedule of controls used.

A different length of stranding lay was used in each of the cables manufactured, in this way we could observe any possible influence of unbalance caused by the core being more or less compact.

As shown in Figure 5 the control during the wire insulation process is given. The control was performed with a coaxial capacitance monitor, in this way deviation in wires of $\pm 0.5 \text{ pF/ft}$ ($\pm 1.7 \text{ pF/m}$) was obtained.

CONTROLS CARRIED DURING THE MANUFACTURE OF THE EXPERIMENTAL CABLES

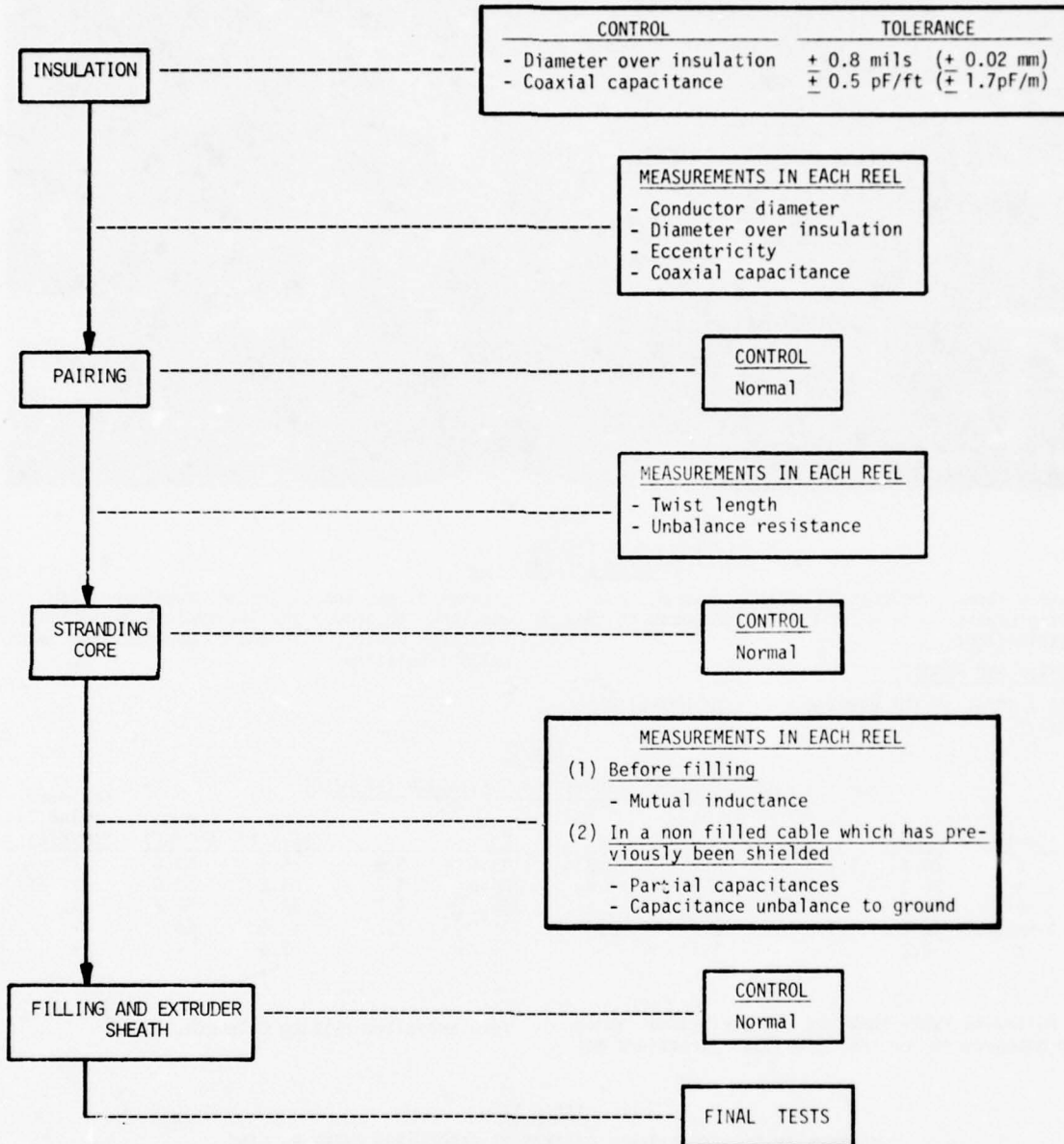


Figure 5

The inductance at 800 Hz was measured in each pair before filling, in this way the existence of any change in interaxial spacing during the filling process would show up. The inductance at 800 Hz is independent of the proximity effects caused by the other wires and the interaxial spacing can be calculated by the standard equation:

$$L = 1.482 \log \frac{2S}{d} + 0.1609 \text{ mH/mile} \quad (5)$$

Prior to filling, one of the cables was shielded. The partial capacitances and capacitance unbalance to ground were measured. The next step was to remove the shield, fill the cable and recover once again.

The object of the above mentioned method was to establish the changes in parameters before and after filling.

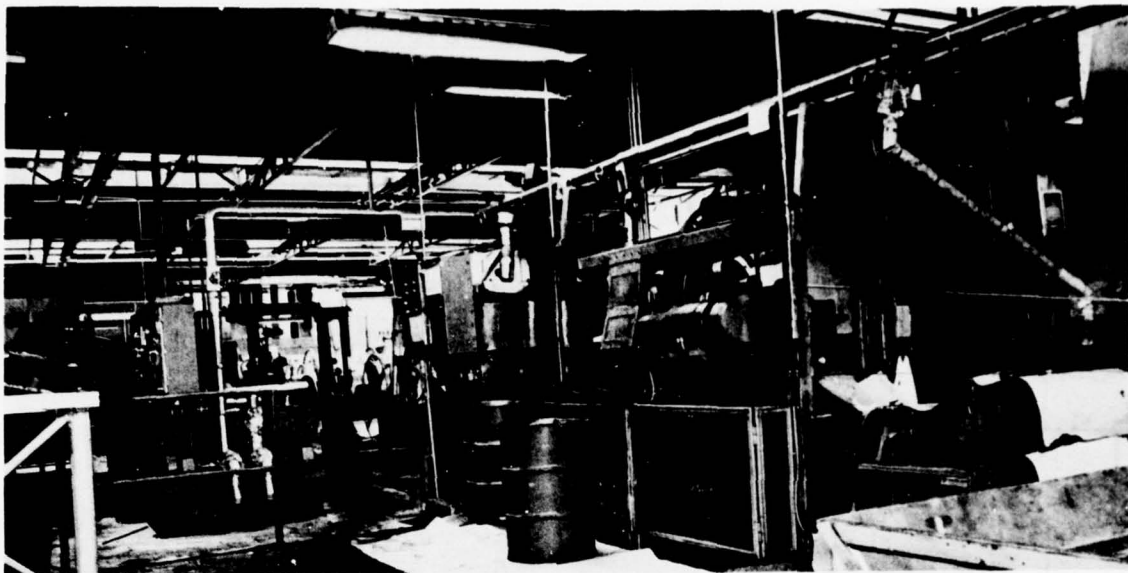


Figure 6
Cable filling line

Figure 6 shows a photograph of the equipment for filling cables with a petrolatum compound at the sheathing line.

ANALYSIS AND RESULTS

Table I shows us the average values of mutual capa-

citance direct and to ground, together with the unbalance to ground and its typical deviations, on the three cables, A, B and C manufactured with solid insulation.

TABLE I
AVERAGE VALUES AND TYPICAL DEVIATION (NF/MILE)

| Cable | C_m | σ | C_d | σ | C_g | σ | C_{ug} (pF/Kft) | σ_{ug} (pF/Kft) | Maximum Value (pF/Kft) |
|----------|-------|----------|-------|----------|-------|----------|----------------------|---------------------------|------------------------------|
| A | 86.4 | 1.5 | 34.1 | 2.6 | 104.6 | 3.9 | 59.5 | 59.2 | 223 |
| B | 86.2 | 1.5 | 33.8 | 3.4 | 104.8 | 4.1 | 54.6 | 52.8 | 227 |
| C | 86.0 | 1.4 | 32.7 | 2.3 | 105.8 | 4.2 | 58.7 | 58.2 | 222 |
| Average | 86.2 | 1.5 | 33.5 | 2.4 | 105.0 | 4.1 | 57.6 | 56.7 | - |
| σ | 0.2 | - | 1.1 | - | 1.2 | - | 2.6 | - | - |

The following table shows us the variations which were encountered on the previous parameters be-

fore and after filling C length.

TABLE II
CHANGES IN THE CAPACITANCE PARAMETERS BEFORE AND AFTER FILLING

| | | Before filling | Filled | Change |
|--|-----------------------|-------------------|--------|--------|
| C_m - Mutual capacitance | (NF/Mile) | 71.9 | 86.0 | 19.6% |
| σ | (") | 1.61 | 1.5 | - |
| C_g - Capacitance to ground | (NF/Mile) | 84.3 | 105.8 | 25.5% |
| σ | (") | 4.54 | 4.2 | - |
| C_d - Direct Capacitance | (NF/Mile) | 29.8 | 32.7 | 10% |
| σ | (") | 2.70 | 2.3 | - |
| C_{ug} - Capacitance unbalance to ground | (pF/Kft) | 48.8 | 58.2 | 19.3% |
| σ | (pF/Kft) | 46.9 | 56.7 | - |

The capacitance unbalance to ground in Table I and II was averaged on 38 pairs, in other words the 12 pairs which were inserted with intentional mismatch were not computerized.

It can be appreciated from Table I that the level of unbalance to ground was excellent.

The standard deviation of the average parameters in filled cable as we had foreseen decreased with respect to the non-filled cables (see Table II). This consequently means that greater evenness of parameter capacitance is achieved during the filling process, the reason is that the dielectric medium is more homogeneous and consequently due to this the gaps are equalized.

A sample of all the pairs in all the cables were taken for its subsequent dimensional evaluation. The parameters were also correlated with the capacitance unbalance to ground. The result of these correlations can be seen in Table III.

TABLE III
CORRELATION BETWEEN Cug AND A NUMBER OF PARAMETERS

| Parameter unbalance | Correlation Coefficient |
|-----------------------------------|-------------------------|
| Conductor diameter | 0.40 |
| Diameter over insulation | 0.45 |
| Coaxial capacitance calculated | 0.51 |
| Coaxial capacitance measured | 0.90 |
| Dielectric constant of insulation | 0.37 |
| Interstitial air gap | 0.13 |
| Eccentricity | 0.20 |
| Twisting | 0.10 |
| Unbalance resistance | 0.37 |

DOD and d correlation

The coefficient correlation obtained on 0.45 and 0.40 are actually rather weak, this therefore indicates that there is no significant correlation with the unbalance to ground. Nevertheless this weak correlation is mainly due to the measurements as carried out with the usual processes of micrometer and optic microscope on DOD and d giving us little reliance. This is clearly demonstrated when one tries to correlate the unbalance to ground with the coaxial capacitance unbalance, which are calculated from the measurement of DOD and d. The correlation is much lower in this case to that obtained through the measured coaxial capacitance.

On the other hand we did obtain an extremely high correlation coefficient ($\rho=0.74$) when only the pairs were considered with a known diameter difference (Δd) and were purposely put into the cable.

The high coefficient ($\rho=0.74$) obtained is very easy to explain, as in this case there is greater difference in diameter, this way improving the measurements.

Correlation in the coaxial capacitance unbalance

The high correlation coefficient obtained $\rho=0.90$,

does demonstrate that the best control of unbalance to ground is obtained by means of a coaxial capacitance monitor.

The coefficient correlation square is statistically demonstrated ("') to be equivalent to the total variation percentage which is explained through the variations of the independent variables. In other words 81% of the capacitance unbalance to ground in our case is explained by the coaxial capacitance unbalance. The remaining 19% is due to random variations or some other variables which have not been taken into account.

The highest coefficient obtained was $\rho=0.9$ and the lowest $\rho=0.83$. This indicates that 70% of the unbalance in this case was due to the variations of coaxial capacitance.

Figure 7 shows us the graph on the correlation of unbalance to ground with coaxial capacitance unbalance.

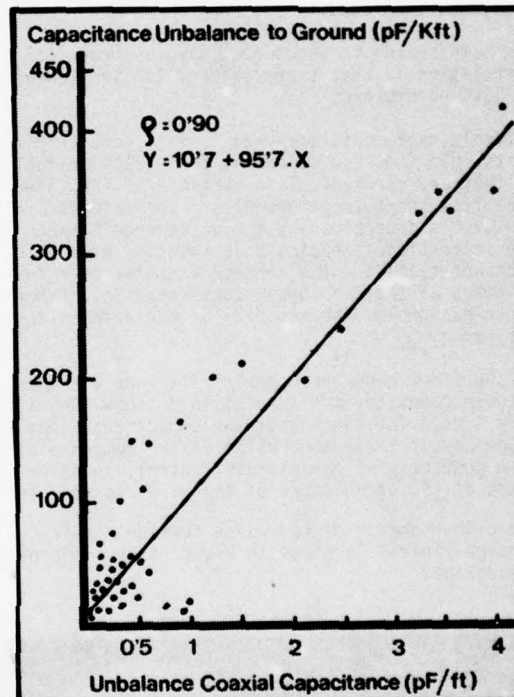


Figure 7
Correlation between unbalance to ground and unbalance of coaxial capacitance

The lineal regression curve obtained by the least square method corresponds to:

$$Y \text{ (pF/Kft)} = 10.7 + 95.7 \cdot X \text{ (pF/ft)} \quad (6)$$

and with an estimated typical error:

$$S_{yx} = 51.5 \text{ pF/Kft}$$

Dielectric constant of insulation correlation

The existing correlation between the unbalance to ground and the deviations in the dielectric constant of the insulation was quite weak ($\rho=0.37$).

Nevertheless it was established that the dielectric constant did vary in approximately 1% from wire to wire depending on the colors. This in turn produced a change of approximately 0.6pF/ft . in the coaxial capacitance. Consequently through the lineal regression curve (6) this 1% change in the dielectric constant will contribute in approximately 69pF/Kft . to the unbalance to ground. This therefore does indicate deviations in the dielectric constant from wire to wire, contributing to the capacitance unbalance to ground at a higher level than could be expected by the coefficient correlation found.

Eccentricity and interstitial air gap correlation

Both of these correlations are very low, indicating that there is no apparent correlation in capacitance unbalance to ground.

The main reason for not obtaining a practical correlation is that there is very little accuracy in both parameters.

Optical instruments are used in the eccentricity tests, but the results cannot be totally reliable, as they are carried out in sections of insulated wire from short length samples. The interstitial air gap is determined by the difference between the interstitial spacing S (arrived at by the inductance test) and the average diameter over insulation of the pair under consideration. Experience has proven the accuracy of these tests to be very poor.

On the other hand the eccentricity and air gap between conductor and insulation do show to have very little influence upon the capacitance unbalance to ground if these abnormalities are compensated by a good coaxial capacitance control, in other words if the capacitance of the wires is the same.

The cross-section of two wires forming a pair (orange-violet) is shown in Figure 8 by a micro-photograph.



Figure 8
Micro-photograph of mismatched pair

This pair had a capacitance unbalance to ground of 30 pF/Kft , notwithstanding the high eccentricity in the orange wire and the air gap between the conductor and the violet insulation. These wires on the other hand between them showed a difference in coaxial capacitance of only 0.31 pF/ft .

Twisting Correlation

The correlation of twisted pairs with the capacitance unbalance to ground was unexpectedly very weak ($\rho=0.10$) to such a point that even negative correlations were found to be had. We expected that the tendency would be that the greater the pair twist the greater the unbalance to ground would be, but this was not experienced.

As we all know pair lay distortion affects the unbalance to ground in a pair due to its geometric configuration being unsymmetrical or one wire longer than the other in a pair. The resistance unbalance in the pair was measured to obtain the twist distortion level. This method is not quite accurate in as much as the difference in the diameter of the copper conductor will influence the results. However the capacitance unbalance to ground and the resistance unbalance remain somewhat weak in the correlation found.

Without doubt we cannot generally admit as valid this negative result (e.g. uncorrelated) since different pairing machines can be used by manufacturers.

Stranding and pairing position correlation

There can be found no significant tendency between the unbalance to ground and the stranding and pair position variables. On the other hand this does not mean there is generally no influence, since manufacturers can have different packing factors in so much as stranding, cabling and filling operations are concerned.

SUMMARY

The general dimensional tolerance of the insulated wires in standard air-core PIC cables were established at ± 1 mils. for "DOD" and ± 0.2 mils for "d".

The same manufacturing procedure and tolerance were used on filled cables, nevertheless there did exist an increase in the dielectric constant of the medium, and the increase expected in the capacitance unbalance to ground was around 30%.

On the other hand high density polyethylene was used on the insulation making it in this way compatible with the filling compound. High density polyethylene does although present certain difficulties in processing⁶ and to maintain the same tolerance, the quality of the wire was poorer compared with that of other insulations.

This could possibly have been the reason why the unbalance to ground increased by over 30%.

We have observed in the above mentioned analysis that there does exist a clear influence of the dimensional parameters in the unbalance to ground, while the remaining formation parameters do not show a significant contribution towards the unbalance.

It can be appreciated that the individual correlations of the various parameters is not as good as could be expected due to the difficulties in accuracy and reliance or the high interaction which exists between them. However the coaxial capacitance correlation which was measured did indeed present conclusive results. This result is mainly due to the coaxial capacitance which inter-relates all the dimensional parameters, consequently controlling all its variations and maintaining at the same time a greater uniformity of the insulated wire.

It can practically be said that the capacitance unbalance to ground is proportional to the coaxial capacitance unbalance between the two wires in a pair. Therefore if one maintains at a constant level the coaxial capacitance of the insulated wires the level of unbalance should be very low.

Figure 9 compares the unbalance cumulative distribution between the experimental filled cables - PIC, standard air core cable and typical filled cables.

An approximate 60% reduction in the specified average maximum level was obtained on the experimental filled cables which were manufactured. This reduction clearly shows to be more than sufficient to assure the continuity of these average values in current production, if a strict coaxial capacitance control is kept.

On the other hand the rest of the parameters which consequently result from the manufacture (pairing, stranding, cabling and filling) have less importance. Only 30% in the level of capacitance unbalance to ground is due to distortion pair twist, stranding, filling operations, etc....

We ask ourselves if in the long run these parameters will have the same importance in the case of filled cable with expanded insulation.

In answer to our question, two filled cables with 30% expanded insulation were manufactured and an unbalance evaluation was performed.

Unfortunately in this case, due to difficulties on the insulation line the coaxial capacitance at $\pm 0.5 \text{ pF/ft}$. could not be controlled as in the case of solid insulation. The coaxial capacitance could only be kept at $\pm 1.5 \text{ pF/ft}$., for this reason the maximum average unbalance expected was 190 pF/Kft.

135 pF/Kft. was the true average value found in this case, through the correlation carried out on the coaxial capacitance unbalance, we found that 75% in the level of unbalance to ground was explained by the coaxial capacitance deviations.

However a certain increase in the coaxial capacitance unbalance between the wires in a pair which had already been paired could be appreciated compared with the same wires before pairing. This increase in coaxial capacitance unbalance is probably due to distorted wires (crushing) during its pairing, since expanded insulation is softer than solid. On pairs with short pair twist this increase was slightly higher. Consequently stricter control should be kept on expanded insulated filled cable with regards to tension and a reduction of same should be kept in mind during the pairing process.

CONCLUSIONS

It can be observed from the results of the analysis carried out that the dimensional parameters were the greatest contributors to the capacitance unbalance to ground.

Definite conclusions cannot possibly be obtained if one tries to individually analyze each and every one of the parameters, due to the high interaction which exists between them. The clearest conclusions can be obtained from the Master characteristics analysis, in which various of these parameters are grouped together.

The analysis show that approximately 70-80% of the unbalances to ground are due to the variations in

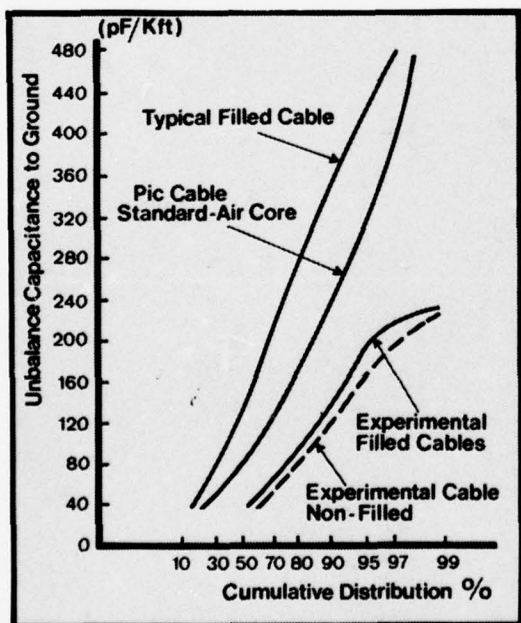


Figure 9
Capacitance unbalance to ground

coaxial capacitance between wires. The remaining 20-30% is due to the influence of the formation parameters (not dimensional) which exists in the rest of the manufacture.

A good control in the quality of the wire during the extrusion process is therefore essential to meet the requirements of capacitance unbalance to ground.

ACKNOWLEDGMENT

The author is sincerely grateful to Mr. F.W. Horn for his assistance, ideas, suggestions and correction of this paper. Acknowledgment is also due to Mr. F.J. Viñuales and Mr. C. Pérez for their help in the laboratory tests and to all the people who have kindly contributed in the manufacture of the cables.

REFERENCES

1. "Effect of pair unbalance on carrier frequency insertion loss and crosstalk in multipair cable"
By: A.F. Judy and J.J. Refi, I.W.C.S. November 1976.
2. "Measurements in multipair cables"
By: J.T. Maupin, B.S.T.J. Vol. 30 July 1951, pp 652-667.
3. "Controlling polyethylene insulated wire capacitance"
By: A.E. Hartman I.W.C.S. December 1965
4. "Statistic" book by Murray R. Spiegel,
Schaum's outline series.
5. "Capacitance relationship in filled telephone cables and equilibrium prediction from water immersion tests"
By: J.A. Olszewski I.W.C.S. 1975
6. "The extrusion of high density polyethylene insulated wire for filled telephone cable"
By: J.C. Remley and B.M. Brooke, I.W.C.S. 1975.



J. Prósper obtained his Technical Engineering degree in Telecommunication in 1973 from the university School of Technical Engineers (E.U.I.T.T.) in Telecommunication in Madrid. He joined the Research and Development Department of Cables de Comunicaciones S.A., Zaragoza, Spain in 1974. He is at present responsible for the Electrical Measurement Laboratory and the Outside Telephone Plant.

THE MANUFACTURING CAUSES OF CAPACITANCE UNBALANCE TO GROUND IN FILLED TELECOMMUNICATIONS CABLE

W. M. Flegal and B. C. Vrieland

Western Electric Company
Norcross, Georgia

Abstract

The major cable manufacturing operations have been studied experimentally to determine the cause of capacitance unbalance to ground. Two previously undetected twister-related variables are shown to influence the unbalance of a pair. The relative importance of the manufacturing variables are determined from the experimental data.

Historical Perspective

The importance of maintaining pair balance in multipair transmission lines has long been recognized. This need for pair balance has been critical not only in maintaining isolation from external noise¹ but also in influencing the insertion loss and crosstalk loss of pairs at newer carrier frequencies due to interactive effects within the cable.²

The maintenance of the required pair balance has been made more difficult with the introduction of filled cable. By adding filling compound the capacitance to ground and consequently the unbalance to ground has been increased because of the higher dielectric constant of the compound compared to air.³ A new process step also introduces additional variability into the final product.

To maintain the necessary pair balance, very tight specifications have been imposed on filled cable. Meeting these specifications has required that close control of every manufacturing process be maintained. The goal of this project was to identify the most significant causes of capacitance unbalance to ground and then to determine acceptable control limits for each manufacturing process.

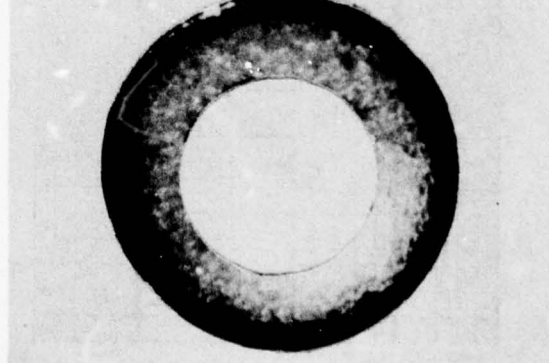
Manufacturing Techniques

The manufacture of filled telecommunications cable consists of four distinct operations: (1) tandem wire drawing and plastic insulating; (2) twisting of single insulated wires to form pairs; (3) stranding of pairs into cable cores; and (4) application of filling and sheathing materials. Each of these operations introduces

a unique set of variables which can affect the capacitance unbalance of pairs in the cable. To determine quantitatively the contribution of each important variable to the unbalance of a pair required that a series of carefully designed and controlled experimental cables be manufactured. Previous experiments have demonstrated the difficulty in obtaining good correlation between the manufacturing variables and the capacitance unbalance of a pair, primarily because of the interdependence of many of the variables. To overcome this problem, the experimental cables were manufactured with variation in only one or two independent parameters per cable.

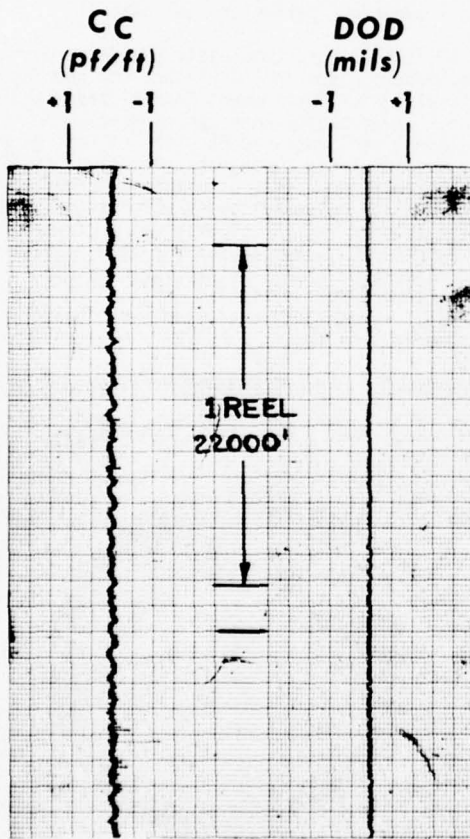
All cables were completely manufactured in the Western Electric Co. Product Engineering Control Center Development Capabilities Laboratory. These cables were approximately 2000 feet in length and contained 25 pairs of dual expanded plastic insulated conductors (DEPIC). This insulation, which consists of a thin layer of solid high density polyethylene (HDPE) extruded concentrically over a layer of expanded or foamed HDPE (Figure 1), was chosen for study because of the conversion of all filled cable manufactured by Western Electric to this design.⁴ A standard ALPETH (polyethylene over aluminum) sheath was used on all cables.

FIGURE 1
DEPIC INSULATION



The DEPIC conductors were manufactured on a tandem wire draw-insulate line at 5000 feet per minute. The control of the variation in the insulated wire was achieved by using consecutively insulated lengths of orange and yellow wire to form "pseudo-mated" pairs. Two colors were used to preserve individual wire identity. Typically three reels containing 22,000 feet of wire were made of each color insulated for a particular cable. Since the time required to insulate the wire was approximately 30 minutes, large variations in insulation properties were eliminated. The coaxial capacitance and diameter over dielectric (DOD) were monitored and recorded on line. A typical trace (Figure 2) shows a variation in coaxial capacitance of ± 0.2 pf/ft and in DOD of ± 0.1 mils. Recordings of coaxial capacitance and DOD were made for all wire manufactured. Any wire exhibiting more than ± 0.3 pf/ft capacitance variation or ± 0.2 mils DOD variation was rejected.

FIGURE 2
**TYPICAL COAXIAL CAPACITANCE
AND DOD TIME TRACES**



All pairs were twisted on the same twister. It is of Western Electric design incorporating a single bow with a fixed carriage, internal supply. The tension on the singles is maintained mechanically by means of the wire paying off over a sheave on the end of an arm before entering the bow. Since each single reel has its own tension arm, the backtensions on the singles are independent of each other. The appropriate tension is set by a maintenance operator when the twister is not running. The wire is pulled through the twister by a multi-grooved capstan. Up to nine 2000 foot lengths of twisted pairs were obtained from a pair of reels. Since the insulated wire comes from the same pair of reels, variations between pairs are greatly reduced.

All stranding was also done on one machine. The same powered supply and face plate positions were always used for a given numbered pair. Cables were normally made in groups of three to six with all cables being stranded consecutively onto the same core truck.

Each group of cables was filled and sheathed in one continuous run at 100 fpm. The filling compound, a single component petroleum jelly (SCPJ) was injected under pressure at a temperature of around 190° (880C). Individual cables were re-reeled onto smaller reels for testing. The capacitance unbalance of each pair was measured using a capacitance test set.

Manufacturing Process Studies

Insulating

Historically most of the effort to meet capacitance requirements has been directed toward obtaining better control of the insulating process. This improved capacitance control has been achieved primarily through the use of on-line capacitance monitors to measure and control the coaxial capacitance.^{5,6} For solid insulations, either line speed or extruder screw speed can be varied to maintain a constant coaxial capacitance; the DOD will vary accordingly. With expanded insulations, variations in screw speed, line speed, barrel zone temperatures, wire temperature and water trough position affect the insulation weight per unit length or the degree of expansion or both. These variables must be controlled to meet simultaneously specifications on two dependent variables - coaxial capacitance and DOD.⁷

Taken together, the coaxial capacitance (C_C) and DOD specifications define an operating window or square into which all insulated wire must fall (Figure 3). From a manufacturing viewpoint, it is desirable to know what magnitude of capacitance unbalance can be expected in those pairs formed from wires manufactured at the extremes of the specifications (i.e., corners of the square). This information is especially important since a maximum individual pair capacitance unbalance limit has been imposed on filled cable.

**FIGURE 3
OPERATING WINDOW**

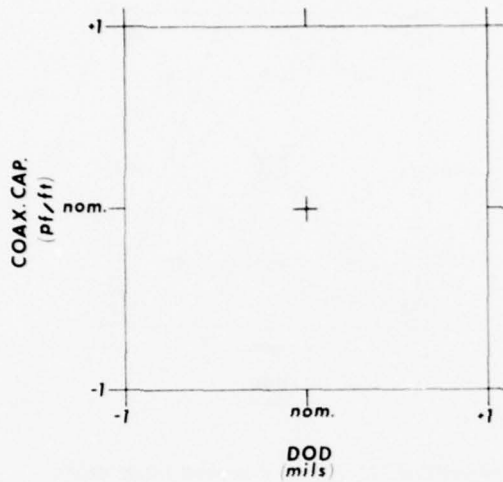
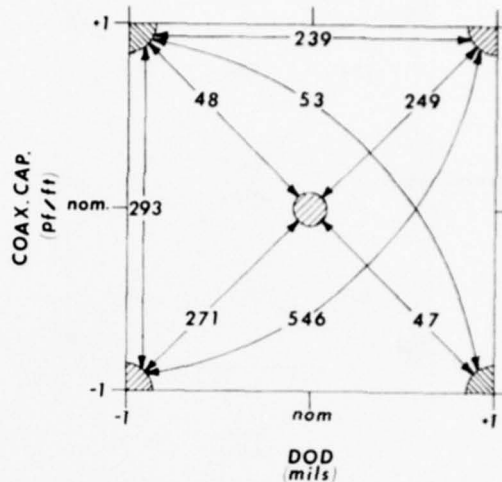


**FIGURE 4
22 AWG CAPACITANCE UNBALANCE**



Wire was purposely insulated at various positions in the C_c-DOD square and was mated selectively to create pairs having known C_c and DOD differences. A series of three experimental cables was made for each of three wire gauges - 22, 24 and 26. One cable in each set had all wire insulated to nominal conditions and served as the control. For the second cable, pairs were made by mating a wire from a corner of the square with a nominal or center of the square wire. The third cable included pairs created from wires at the corners of the square twisted together to represent the diagonals and sides of the square. Five nominal pairs were included as a secondary control in each of these cables.

The measured capacitance unbalances for the various combinations are shown in Figures 4, 5 and 6 for 22, 24 and 26 gauges, respectively. The values shown in the figures represent the average of five pairs in each cable. The average unbalances for the control cables and control pairs are shown in Table 1. These cables demonstrate that the capacitance unbalance of a pair is very sensitive to the differences in C_c and DOD between the wires of the pair. Some C_c and DOD differences produce little unbalance; others produce very large unbalances. This effect can be explained best by examining Figure 7 which shows lines of constant percent foam expansion superimposed over the 24 gauge data. The greater the difference in the degree of expansion between the wires of the pair, the greater the capacitance unbalance. Since the lines of constant expansion are inclined, preferential directions are created. The increase in unbalance for the

**FIGURE 5
24 AWG CAPACITANCE UNBALANCE**

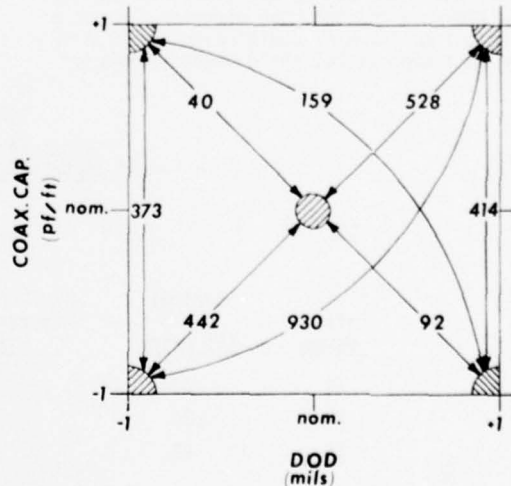
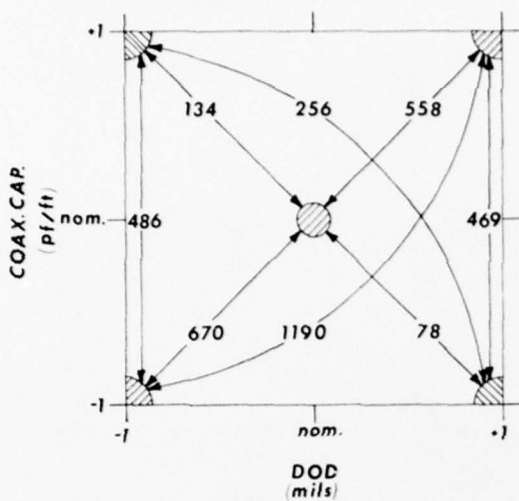


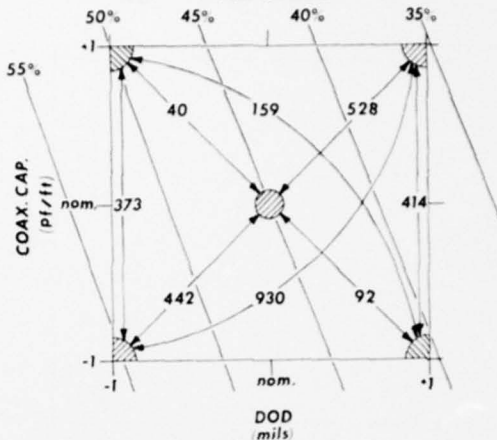
FIGURE 6
26 AWG CAPACITANCE UNBALANCE



same C_C and DOD differences with finer gauges can also be explained by their greater variations in expansion. These cables establish that the expansion should be controlled within tight limits if capacitance unbalance is to be maintained at low levels.

Another insulating variable that was studied was the conductor diameter. A 22 gauge cable was made with the coaxial capacitance and DOD held at their nominal values. Three conductor diameters were used to achieve differences of 0, 0.1, 0.2 and 0.3 mils in this cable. Results from this cable indicate that approximately 30 pf/kft capacitance unbalance can be attributed to each 0.1 mil difference in conductor diameter. Since an electrical resistance specification is also imposed on filled cable, the conductor diameter

FIGURE 7
**LINES OF CONSTANT EXPANSION
FOR 24 AWG**



must be controlled within a narrow range making large capacitance unbalances from this effect unlikely.

Twisting

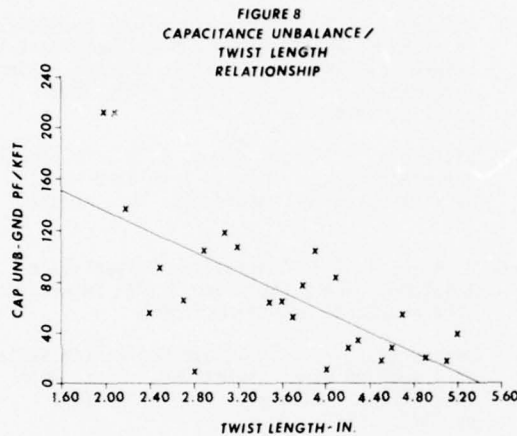
The twisting process has long been considered a contributor to capacitance unbalance, but very little has been proven because of the interaction of insulation parameters. In these experiments two twister-related effects were identified.

At the outset of the experiments, a reference cable was made from six reels of wire insulated consecutively. These pairs were then twisted from consecutive reels providing 8 to 9 twisted pairs per reel - a very mated pair design. When tested, this cable revealed a relationship of capacitance unbalance to ground with twist length as shown in Figure 8. When a linear best fit is

TABLE 1
**Capacitance Unbalance
of Control Pairs and Cables**

| Wire Gauge | Control Cable (25 pairs) | Capacitance Unbalance (pf/1000 ft) | |
|------------|-----------------------------|---|---|
| | | Control Pairs Center-Corner Cable (5 pairs) | Control Pairs Diagonals Cable (5 pairs) |
| 22 | 32 | 36 | 47 |
| 24 | 36 | 80 | 78 |
| 26 | 29 | 60 | 53 |

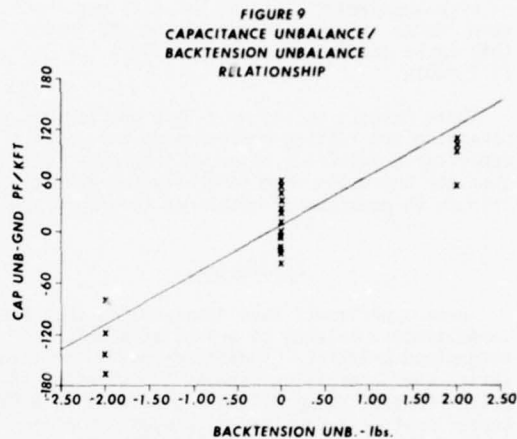
made, the line shown on the figure results and the data are linearly correlated with a coefficient of -0.70. Although subsequent cables made on different twisters (of the same basic design) also demonstrated a similar relationship to that of Figure 8, the correlation was poorer with coefficients ranging between -0.50 and -0.61. When analysis of variance techniques were applied to the data for each of the four cables of this group, however, the effect of twist length was determined as significant at the 0.01 level for each cable. It might be noted that in addition to the linear behavior is what appears to be a sinusoidal variation with twist length.



The cable was tested by the Bell Laboratories group in Atlanta for the amount of "twist eccentricity" in the various pairs. By "twist eccentricity" is meant the distance the axis of the pair helix is from the center of the "shield" that surrounds the pair. An exaggerated case of eccentricity is when one of the singles of a pair is straight while the other is wrapped around it in a "barber pole" fashion. The analysis of the Bell Laboratory data did indicate some increased eccentricity in the shorter twists and a model based on a helical pair with twist eccentricity within a cylindrical shield predicts an increased capacitance unbalance to ground for eccentric pairs.

The idea that twist eccentricity contributes to capacitance unbalance to ground leads naturally to the consideration of backtension unbalance. This experiment consisted of making a cable in which the tension applied to the single insulated wire reels varied from its normal setting of 1.5 pounds. The high tension setting was 2.75 pounds, while the low tension was 0.75 pounds; both settings represent about the limits that can reasonably be reached without wire breakage. The 25 pairs of the cable were subdivided into 5-pair groups which in turn were given backtensions of

high-low, low-high, low-low, normal-normal and high-high. The 5-pair groups spanned uniformly the twist length range from 2 inches to 5.2 inches. The results are shown in Figure 9 where the tension unbalance of zero applies to 15 pairs and the positive unbalance indicates that the orange single has the high tension. The linear best fit produced a correlation coefficient of 0.89 and a slope that predicts 58 pf/kft for every pound of tension unbalance.



The effect of twist length and backtension unbalance does not appear to be a large contributor to capacitance unbalance to ground when considered in the light of the strong contribution of such parameters as coaxial capacitance, DOD, and percent expansion. The twist length effect produces only large unbalances for twists around 2 inches and the oscillating appearance of the data can show some quite low unbalances for short twists. Capacitance unbalance to ground shows a stronger correlation to backtension unbalance on the other hand, but the slope of the line relating the two is not great nor is the twister likely to be out of adjustment by more than a pound.

Stranding and Sheathing

Although the effect of stranding lay direction was not expected to be great, there were two cases in which the first length of core was stranded in a left hand direction with a 36" helix while the second length of the same setup was stranded with a right hand helix of 36". In neither of these two cases (2 cables for each) was any significant difference noted in capacitance unbalance to ground. There were no experiments conducted on different types of strander.

For the process of filling and sheathing, however, there was the expectation that some contribution to capacitance unbalance to ground might be found. The experiment conducted in this case was to vary the temperature of the filling compound on consecutive cores run through the sheathing process. The first cable was filled with SCPJ at a temperature of around 170°F (77°C), while the second cable was filled with 230°F (110°C) SCPJ. The cable with the cooler fill actually had the higher average unbalance (54 pf/kft) than the hot fill cable (46 pf/kft), but with standard deviations of 38 pf/kft, this difference in means is not significant. The unbalance improvement for the hot fill resulted even though the average capacitance to ground for this cable was 2.5 nf/kft higher than the cool fill cable.

These results do not mean that problems in the stranding and filling processes do not cause a capacitance unbalance to ground increase, but that the processes when correctly run do not contribute to capacitance unbalance to ground.

Conclusions

These experiments have demonstrated that the capacitance unbalance to ground of a pair is determined primarily by differences in the insulation characteristics between the wires of the pair. Control of capacitance unbalance in DEPIC cables must be accomplished through close control of the coaxial capacitance, DOD and percent expansion at insulating. Such control reduces the magnitude of the capacitance unbalance which can be produced by an unfortunate combination of insulated wires having coaxial capacitance, DOD and percent expansion differences.

Although insulation characteristics are dominant, twisting does contribute to the unbalance of a pair through the twist lengths and backtension differences. An increase in twist lengths is not possible because of the deleterious effect on crosstalk. Twister brake tensions should be maintained as equal as possible through a periodic maintenance program.

Stranding and sheathing were found to have little effect on capacitance unbalance. Efforts in these areas should be directed toward maintaining normal operating conditions.

Acknowledgements

The authors wish to thank Messrs. H. T. Folger, J. C. Clark, E. C. Akins and A. S. Hamilton for their assistance in manufacturing the experimental cables. The assistance of Messrs. W. M. Newton, R. J. Brown and T. G. Hardin is also acknowledged. The measurement of twist eccentricity was done by Messrs. W. T. Anderson and J. M. Pace of Bell Laboratories.

References

1. Brewer, M. L. and Price, H. P., "Effect of Cable Unbalances on Power Induced Circuit Noise," 25th International Wire and Cable Symposium, pp. 108, 1976.
2. Judy, A. F. and Refi, J. J., "Effect of Pair Unbalance on Carrier Frequency Insertion Loss and Crosstalk in Multipair Cable," 25th International Wire and Cable Symposium, pp. 91, 1976.
3. Olszewski, J. A., "Capacitance Relationships in Filled Telephone Cables and Equilibrium Prediction from Water Immersion Tests," 24th International Wire and Cable Symposium, pp. 399, 1975.
4. Mitchell, D. M., "Material Savings by Design in Exchange and Trunk Telephone Cable Part I-Waterproof Cable with Dual Insulation," 23rd International Wire and Cable Symposium, pp. 216, 1974.
5. Biskeborn, M. C. and Kempf, R. A., "A Capacitance Monitor for Plastic Insulated Wire," Bell Laboratories Record, pp. 308, August, 1957.
6. Hartman, A. E., "Controlling Polyethylene Insulated Wire Capacitance," 14th International Wire and Cable Symposium, 1965.
7. Dougherty, T. S., "A Unique Monitoring System for Expanded Wire Insulations," Proc. 25th International Wire and Cable Symposium, pp. 387, 1976.



William M. Flegal

William M. Flegal received the Bachelor of Mechanical Engineering, Master of Science in Mechanical Engineering, and Doctor of Philosophy degrees from the Georgia Institute of Technology. He joined Western Electric's Cable and Wire Product Engineering Control Center in 1970 as a Senior Development Engineer working on plastic insulating developments. For three years he was on active duty with the U. S. Navy as an Engineering Duty Officer, returning to Western Electric in March, 1974. He is a Registered Professional Engineer.



Bruce C. Vrieland

Bruce Vrieland is a Senior Development Engineer with the Western Electric Cable and Wire Product Engineering Control Center. During the past seven years he has been involved in the measurement and characterization of transmission properties for both standard product and development multipair cables. He has received both B.S.E. and M.S.E. in Electrical Engineering degrees from the University of Michigan.

A NEW GENERATION OF FILLED CORE CABLE

BY

T.K. McMANUS

Northern Telecom Canada Ltd.
Montreal Quebec Canada

R. BEVERIDGE

Sask. Tel.
Regina Saskatchewan

ABSTRACT

This paper presents a new approach to the prevention of water ingress in plastic insulated cables. It addresses a concept which has resulted in the development of a new cable design capable of blocking the flow of water along the core, while maintaining transmission properties. The filling medium employed to achieve the objectives is an inert powder. It ensures water blocking capability and removes the problems associated with handling conventional grease filled cable. Because of its inert nature, it eliminates the question of the impact of filling compounds on insulation and other outside plant hardware.

The paper reviews the development test program concentrating on those aspects considered vital to establishing the acceptability of the new concept. A description of experiences with the cable in field trials and as a standard telephone network element is included.

INTRODUCTION

Water poses a serious problem when it gains entry to a cable core. It degrades transmission, and in some cases results in complete failure of the pairs.

Pulp and paper insulated cables short out as water enters, however the phenomenon of swelling, unique to these insulations, prevents further penetration along the core. In air-core PIC Cable, the water is free to travel and can result in a large capacitance increase if it entirely fills the interstices in the core.

Grease filled cable was introduced to prevent water ingress and, together with sealed sheath, has, in general, met that objective. There are inherent problems associated with grease filled cable. To maintain the same mutual capacitance as air-core cable, larger diameters are necessary. Handling of the filled cable becomes more involved, resulting in reduced splicing efficiency. Increased stiffness in cold weather creates problems in

placing, and at elevated temperatures the flow characteristics of the grease are such that the use of filled cable in aerial installations can lead to maintenance difficulties.

As reported in earlier papers (Ref.1), some of these problems have been overcome by intelligent design and handling techniques. The problems associated with splicing remain as a major concern, and, since 100% fill cannot be achieved in grease filled cable in all instances, complete protection against water ingress has not been attained.

This paper is addressed at a solution to these and other problems. The cable described has been termed a new generation of filled cable, because the means by which the prime objectives are accomplished, differs greatly from the conventional grease filled approach. It uses a dry filling material which, on contact with water forms an impervious block and prevents further ingress of the water into the core.

This approach guarantees protection against water travel in cables, and as reported in this paper, the results of prolonged and extensive trials have demonstrated that powder filled cable not only meets but exceeds the objectives for conventional filled cable.

FILLING MEDIUM

In 1973 the concept of dry core filling was examined as a viable alternative to grease. Selection of a suitable material was made after extensive laboratory tests were performed on mixtures of materials. Handmade models were used to determine suitability of the medium as a practical water blocking agent, and a final choice was made for shop manufacturing trials.

The material chosen is a two component system consisting of a surface treated calcium carbonate and a high molecular weight polymeric resin. (Ref.2).

Both components are chemically inert, safe to handle under all conditions, non-flammable, and have no noxious properties. These qualities ensure operator and craftsman protection, and were the first prerequisites in the choice of materials.

When water penetrates the cable core in sufficient quantity to break down the surface tension of the coated calcium carbonate, the resin dissolves rapidly in the water forming a viscous solution. The solution travels only a short distance along the cable core, dependent upon the degree of fill and the water pressure. The blocking action occurs within a short distance, ensuring maintenance of transmission capability and preventing further water travel along the core.

The degree of fill required to achieve water blocking is less than 100%, which is necessary with grease filled cable. Hence the new design is a marked deviation from the accepted view of filled cable. This emphasizes the change in concept from that of keeping water out of the core, as in the case of grease, to that of self sealing protection, as in the case of powder.

The actual degree of fill is governed by the balance required between short water blocking distance, and the desired transmission characteristics. In the prototype production a level of 60%, (based on the bulk density of the powder), was used and, as shown in later sections, provides the desired features.

POWDER FILLED PRODUCT

The powder is applied to the pairs of the cable core, and over the core wrap to ensure that no leakage path exists between the core wrap and the sheath. The sheath consists of a coated aluminum tape which is formed into a tube, overlapped and sealed during the jacketing process. (Fig 1)

The application of the powder in a uniformly distributed manner within the core, is a major requirement to ensure consistent electrical quality. Early vintage product had a variation in powder distribution and hence a wide coefficient of capacitance deviation. Advances have been made in the manufacturing techniques which ensure an even application of powder. This is reflected in a low coefficient of deviation ($\leq 2.0\%$) obtained on present day production. The uniform fill has also meant an improved water blocking capability, and current production consistently meets the 3'-fourteen day water penetration test requirement.

The new cable is lighter, much easier to handle, and has electrical performance approaching that of air-core cable. It meets the water penetration test every time.

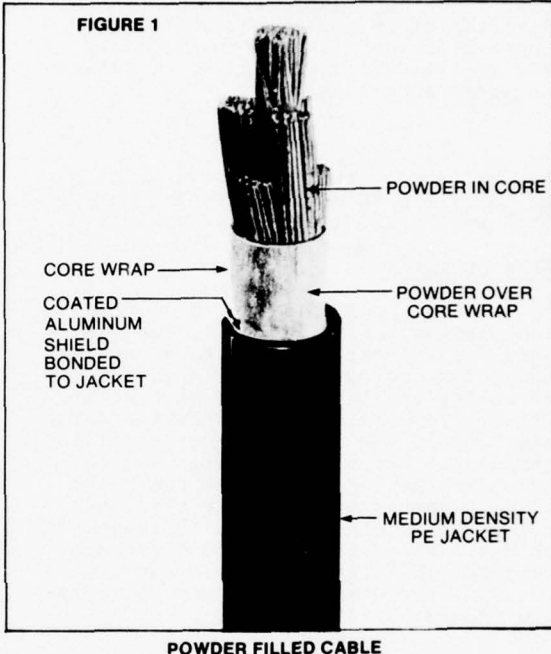


Table 1 provides a comparison of typical physical and electrical parameters of a powder filled cable with the equivalent grease filled cable.

| | GREASE | POWDER |
|--|--------------|--------------|
| MUTUAL CAPACITANCE | 83NF/MILE | 83NF/MILE |
| CAP. DEVIATION | 1.5% | 2.0% |
| CAP. UNBAL. TO GROUND | 175 PF/1000' | 90 PF/1000 |
| ATTENUATION @ 772 KIIZ | 21.5 dB/MILE | 21.5 dB/MILE |
| WEIGHT | 243 LB/1000' | 220 LB/1000 |
| DIAMETER | 0.64" | 0.65" |
| STIFFNESS @ 0°C LB CONSTANT 6° DEFLECTION | 7.5 | 51 |

TABLE 1
COMPARISON OF TYPICAL PHYSICAL AND ELECTRICAL PARAMETERS FOR 25 PAIR 22 AWG CABLE

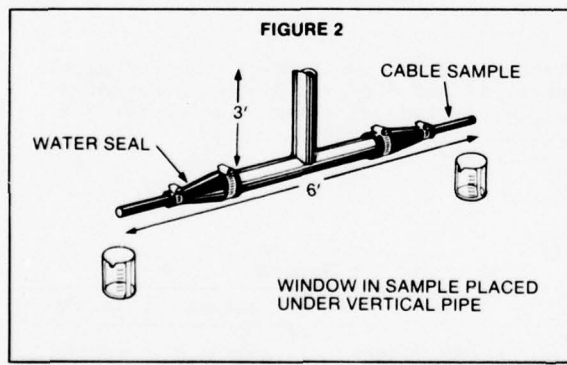
PRODUCT EVALUATION

Prior to entering into field trials, the new cable was subjected to a series of laboratory tests to ensure it met the design objectives. The program included; water blocking capability, transmission characteristics, mechanical stability, compatibility, and long term stability, as well as standard cable characterization and acceptance testing.

This section of the paper will address the major elements of the test program which were vital to the development.

WATER BLOCKING

The new concept in prevention of water transmission, using a dry core medium, means a different approach to assessing the product performance. With grease filled cable, the intent is to keep water out. Dry core filling uses the fact that water enters the core to change state and prevent the water from progressing further into the core. The distance which the water penetrates, before blocking action occurs, is therefore the main criterion in assessing water blocking performance. This characteristic was examined using the standard "T" type penetration apparatus. (FIG 2)



"T" TYPE PENETRATION APPARATUS

The water blocking tests were carried out on cable samples with windows cut into the sheath and core wrap. The samples were inserted into the apparatus with the window under the vertical pipe. Typical openings ranged from 2"x1" to a 3/16" nail hole. Other forms of damage were simulated by uneven openings subjected to differing heads of water. Multiple sheath rupture was also examined with varying hole separations to simulate the effect of lightning damage.

The penetration of water into the cable sample was monitored using a time domain reflectometer connected to one of the pairs, and the distance was later verified by dissection. A typical penetration distance of three feet was obtained with the nominal three feet head of water. The distance was found to vary non linearly with head of water applied and the degree of fill. Using a constant level of 60% fill, the penetration distance approached a limit of 15' under conditions of extreme pressure. (i.e. 20 psi air pressure super imposed on a 6' head of water). The results of tests on more than 500 samples are summarized in Table 2.

TABLE 2

| HEAD OF WATER | PENETRATION | |
|---------------|-------------|---------|
| | AVERAGE | MAXIMUM |
| DROPLETS | 0 | 0 |
| 1" | 3" | 8" |
| 3' | 2.5' | 5' |
| 6' | 4' | 9' |
| 50' | - | 15' |

SUMMARY OF WATER PENETRATION RESULTS

TRANSMISSION CHARACTERISTICS

The transmission characteristics of the cable were designed to be identical to those of conventional filled cable. Under conditions of single sheath rupture with subsequent water entry and blocking the local mutual capacitance (in the blocked section) increases 86% with a corresponding increase in attenuation of 40% at 772 KHz.

Translated into a 6000' repeater section, a single sheath rupture results in less than 0.1% increase in mutual capacitance. Using a 5% level of capacitance increase in a repeater section as the guiding criterion, this would mean approximately 50 ruptures, each subjected to 3 feet head of water, would have to occur before the capacitance approached the critical level.

Since a major problem experienced with undetected water in cable is associated with digital carrier performance, a number of tests were carried out to define the ability of the new cable to meet carrier requirements.

Crosstalk measurements were performed on cable in the dry state and deviations from this base were examined on cables with single and multiple damage conditions. Table 3 summarizes the results on a selection of damaged cables.

TABLE 3

| TEST CONDITION | CROSSTALK dB | | | |
|----------------|--------------|----------|---------|----------|
| | NEAR END | | FAR END | |
| | MEAN | σ | MEAN | σ |
| DRY | 72.6 | 11.3 | 74.2 | 8.7 |
| 17.5' WET | 72.9 | 11.5 | 74.0 | 8.7 |
| DRY | 72.6 | 11.3 | 74.2 | 8.7 |
| 80' WET | 73.1 | 11.1 | 73.2 | 8.2 |
| DRY | 70.2 | 9.9 | | |
| WET EVERY 300' | 70.8 | 9.2 | | |
| WET EVERY 50' | 70.7 | 9.0 | | |
| WET EVERY 25' | 70.9 | 9.1 | | |
| DRY | 73.3 | 10.4 | | |
| 80' WET END | 74.2 | 10.5 | | |

CROSSTALK RESULTS ON CABLES SUBJECTED TO VARIOUS DAMAGE CONDITIONS

Four sets of wet conditions were examined in this test. The first two consisted of wet sections of 17.5', and 80' being spliced into the middle of a 5200' cable. The entire length was then measured for near and far end crosstalk. The third situation simulated lightning damage by inserting a 300' long section of cable which was damaged at various points along its length. The fourth case used an 80' section of water logged cable spliced to one end to determine the effects of a wet section close to a repeater.

Near and far end crosstalk were measured at 150KHz, 772KHz, and 3.1MHz. The results in table 3 show that under the various damage conditions simulated, no significant change in crosstalk level or spread was detected.

Additional crosstalk measurements were performed using a prototype digital crosstalk measurement apparatus. The digital test set consists of a T1 carrier simulator which transmits pseudo-random signals down a number of the pairs in the cable under test. The resulting crosstalk in one of the unused pairs is then picked up and added to a pure carrier signal and fed to an error detector. The gain or loss added to the crosstalk signal needed to just exceed the system error rate, is monitored. Table 4 lists the results which confirm the earlier analogue crosstalk findings that no significant difference exists between "dry" and "wet" performance.

TABLE 4

| EXCITOR PAIR | DETECTOR PAIRS | | | |
|--------------|----------------|------|------|------|
| | # 18 | | # 25 | |
| | DRY | WET | DRY | WET |
| 1 | 8.4 | 8.9 | 19.7 | 19.5 |
| 3 | -5.6 | -5.4 | 16.0 | 16.1 |
| 5 | -3.9 | -3.9 | 0.7 | 1.4 |
| 7 | 5.5 | 6.1 | 0 | 0 |
| 9 | -1.6 | -4.1 | 24.0 | 23.8 |
| 11 | 11.7 | 11.5 | 26.5 | 26.5 |
| 13 | 10.9 | 11.9 | 8.7 | 9.1 |
| 15 | 11.2 | 12.5 | -1.4 | -1.4 |
| 17 | -2.2 | -1.8 | 18.0 | 18.0 |
| 19 | -0.2 | -0.7 | 13.1 | 13.0 |
| 21 | 11.7 | 12.1 | 20.0 | 20.4 |

GAIN/LOSS FIGURES - DIGITAL CROSSTALK

LIGHTNING DAMAGE

One area of concern with the introduction of the powder filled cable, was that pinholes, due to lightning damage, might result in a series of blocked sections, which in aggregate form could impair the transmission quality. An examination of the factors determining the probability of fault conditions occurring in a cable was carried out, and the impact of such damage was determined.

The probability of lightning damage to buried cable is a function of the earth conditions, the proximity to other buried plant, and the distance from the stroke point. If a cable is within the critical distance, where the earth potential exceeds the breakdown strength of the cable jacket, pinholes will occur.

The critical distance is expressed: (Ref.3)

$$R_C = \frac{I \cdot \epsilon}{2 \cdot \pi \cdot V_0} \quad \dots \dots \dots \quad 1$$

R_C = Critical distance

I = Impulse current magnitude

V_0 = Impulse breakdown voltage (jacket)

ϵ = Earth resistivity

The degree of pinhole damage may be expressed:

$$P = 100 \cdot N \cdot A \cdot \frac{\pi}{2} R_c \% \dots 2$$

P = % cable subject to pinholes/year

N = Strokes to ground / unit area

A = Area of vulnerability/unit length

$$A = 2 \cdot R_c \% \dots 3$$

Hence;

$$P = 100 \cdot \frac{N \cdot I^2 \cdot \rho^2}{4 \cdot \pi \cdot V_0^2 \% \% \dots 4}$$

Hence substituting the relevant earth resistivity and thunderstorm frequency data provides an estimate of likely damage statistics for a given region. Employing this technique, the suitability of powder filled cable was assessed from a system security point of view.

The rate at which fault conditions appear depends on the number of lengths vulnerable to the pinholing phenomenon, which are situated in a wet environment. The water penetration into the core through the pinholes results in a capacitance increase which was considered to reach critical proportions at a 5% level.

The penetration of water into the core through pinholes of the size normally encountered with lightning damage, (other than direct strikes or arcing to the cable), was found to be much shorter than the 3' length discussed in an earlier section on mechanical damage effects. Results of experiments to determine the typical penetration distance in the event of a pinhole occurring in the sheath are shown in table 5.

TABLE 5

| PINHOLE DIAMETER | WATER HEAD (FEET) | | | |
|------------------|-------------------|-----|-----|----|
| | 0.5 | 1 | 2 | 3 |
| 0.021" | 6" | 5" | - | 5" |
| 0.032" | 8" | 10" | 22" | - |
| 0.052 | 12" | 17" | 29" | - |

WATER PENETRATION DISTANCE THROUGH PINHOLES IN THE CABLE SHEATH

Using these typical blocking distances as a base, and applying the level of damage as calculated using equation 4, a view of the fault rate expected in

a number of areas in North America was obtained. The mean time to reach fault conditions, (defined as a 5% change in capacitance), due to lightning damage was calculated and the results for Canada are shown in table 6.

TABLE 6

| PROVINCE | AVERAGE ANNUAL % OF CABLE SUBJECT TO JACKET PINHOLES | MEAN TIME TO A "FAULT CONDITION" YEARS |
|---------------|--|--|
| ALBERTA | 0.003 | 2.000 |
| MANITOBA | 0.009 | 2.000 |
| SASKATCHEWAN | 0.003 | 10.000 |
| B.C. | 0.03 | 300 |
| ONTARIO | 0.06 | 200 |
| QUEBEC | 0.09 | 300 |
| NEWFOUNDLAND | 0.95 | 50 |
| NEW BRUNSWICK | 0.5 | 50 |
| NOVA SCOTIA | 0.5 | 50 |
| P.E.I. | 0.1 | 200 |

Hence the mean time to a "fault" condition approaches the normal life expectancy of cable in areas where extremely high earth resistivities are prevalent, and far exceeds it in areas of low resistivity. In the majority of applications, there is a low degree of risk, therefore the principal conclusion of the study was that the transmission characteristics of powder filled cable would not be significantly degraded as a result of lightning damage in the form of pinholes.

PHYSICAL TEST PROGRAM

The nature of the filling material is such that it may be easily removed from the cable core. The ease with which it can be removed posed a further question. - Will the powder shift within the cable during shipping and installation? Three experiments were performed to test for this effect.

A - An actual shipping test was performed which transported a reel of powder filled cable over 1500 miles, held in a truck in the same position.

B - Samples of prototype cable were subjected to a vibration test as per ref. 5. In this test the samples were preconditioned by temperature cycling, humidity exposure, and heat aging. The samples were then

vibrated for 20 minutes in a varying cycle that ranged from 5 Hz to 20 Hz and back to 5 Hz in one minute. Table 7 lists the results obtained.

TABLE 7

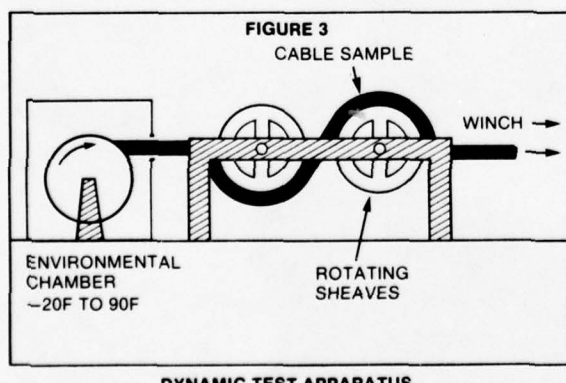
| PAIR I.D. | % CHANGE MUTUAL | SAMPLE # | PENETRATION IN FEET | |
|-----------|-----------------|----------|---------------------|-------|
| | | | LEFT | RIGHT |
| B-W | 0 | 1 | 3.5 | 4.0 |
| G-W | 0.5 | 2 | 3.5 | 2.5 |
| BR-R | 0.8 | 3* | 3.0 | 3.0 |
| B-BK | 0.1 | 4 | 0 | 0 |
| G-BK | 0.4 | 5* | 0 | 3.5 |
| B-Y | 0.2 | 6 | 0 | 0 |
| O-Y | 0 | 7* | 4.0 | 4.5 |
| G-V | 0.1 | 8 | 4.5 | 0 |
| S-V | 0.2 | 9* | 0 | 0 |
| | | 10 | 0 | 4.5 |

*SAMPLES WHICH WERE VIBRATED

EFFECT OF VIBRATION ON MUTUAL CAPACITANCE AND WATER BLOCKING CAPABILITY.

The results shown in table 7 were obtained on consecutive lengths cut from prototype cable. The penetration results indicate a variability of filling material content in the prototype cables. As discussed earlier, the variability has been corrected with advances in manufacturing technique.

C - Cable samples were subjected to a dynamic test apparatus. (FIG 3). The cables were pulled through the apparatus at speeds of 250 FPM and were preconditioned at temperatures ranging from -30C to +30C.



In all of the tests, the mutual capacitance, capacitance unbalance, and water blocking capability were measured before and after. A T.D.R. was also used to examine before and after impedance characteristics. Changes detected, were of a minor nature, well within the experimental error. It was concluded that a redistribution of powder does not occur when handling the cable under normal shipping and installation conditions.

LONG TERM STABILITY

The diffusion of moisture through the sheath into the core is a possibility recognized by many researchers active in the communication field. (Ref. 4) Permeation of the exterior polyethylene jacket is a well documented fact, and cables without metallic barriers have encountered such a phenomenon. With the sealed sheath of modern day construction, the rate of permeation into the core has been so drastically reduced as to be insignificant. Because of the nature of the filling compound, the question of moisture diffusion becomes important, and hence a program of tests to verify the performance of the new cable over extended periods was carried out. Various accelerated aging tests were performed on samples of cable with sheath construction ranging from jacket only to a properly bonded sheath. Table 8 lists the samples and the tests to which they were subjected. Each situation represents a different acceleration factor and combined with the presence or absence of metallic barrier, a wide range of factors were covered.

TABLE 8

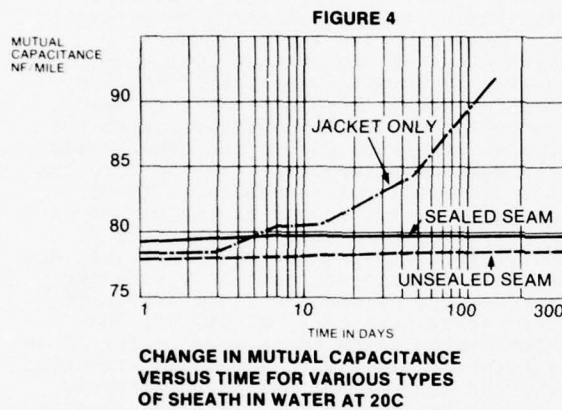
| | ROOM TEMP. | 50C | 70C | CYCLED 40C - 60C |
|-----------------|------------|-----|-----|------------------|
| STANDARD SHEATH | | | * | * |
| UNSEALED SEAM | | * | * | * |
| JACKET ONLY | * | * | * | * |
| DAMAGED SHEATH | * | * | * | |

*SAMPLES SUBJECT TO VARIOUS AGING CONDITIONS.

The highest acceleration factor resulting from cycling, elevated temperature, and absence of metallic barrier was determined to be 5000 to 1. The results from this test showed that it would take in excess of 200 years before a powder filled cable with regular sheath would experience a

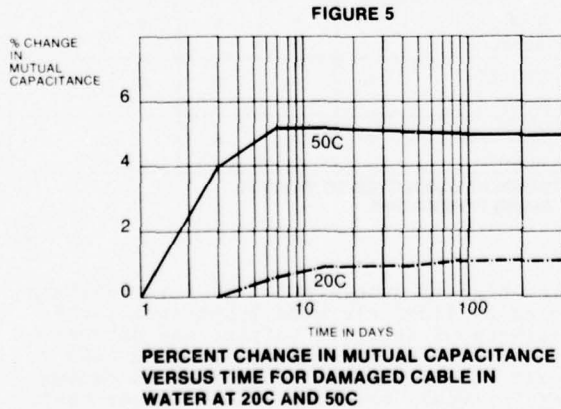
capacitance increase of 5%, if the cable was situated in a permanently wet environment.

Figures 4 and 5 illustrate the results of two of the experiments aimed at confirming the ability of the new cable to perform over long periods. Three samples of cable were used: - One with the standard sealed sheath, one with a poor bond at the overlap, and one having only a jacket. As expected, the "jacket only" sample increased in capacitance, while both the others remained stable over the time frame of the test.



The rate of increase in capacitance of the "jacket only" sample agreed with the results obtained in earlier cycling and elevated temperature tests.

Cables with damaged sheaths were also immersed and monitored. The mutual capacitance increased in the initial stages as water entered the cable and blocked. Once blocking occurred, the mutual capacitance levelled off and remained constant. FIG 5



Summarizing the results of the lab. test program, it was concluded that the powder filled cable would perform electrically in an identical manner to grease filled cable. Physically the new cable outperforms the grease filled cable and guarantees protection against water travel in the core. The cable will retain its electrical characteristics over the normally expected lifetime for telephone cable, and in the event of sheath damage, it will seal itself against the further penetration of water in such a manner as to retain transmission quality.

APPLICATION TESTING

As part of the normal evaluation program on a new cable, a number of "real life" trials were held. They may be divided into three basic categories: "In house", Technology, and Field trials.

"IN HOUSE"

Two lengths of powder filled cable, together with a reference length of grease filled cable were buried in the grounds of Northern Telecom's Kingston cable manufacturing plant. The area was chosen because of the tendency to flood in spring, and hence provide a severe test for the cables. Fig. 6 illustrates the wet conditions which prevailed during the placing operations which were performed in December 1975.

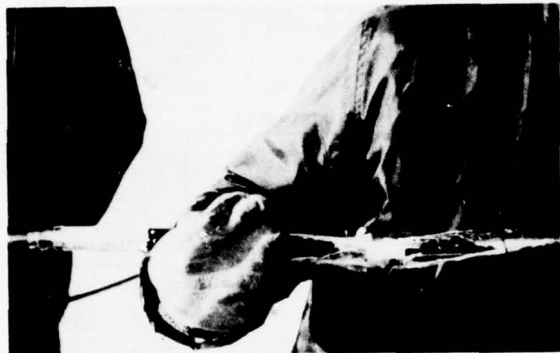
FIGURE 6



"IN HOUSE" FIELD TRIAL AT KINGSTON

Two buried splices were performed on the powder filled cables, and all ends were terminated in a pedestal for ease of access. One of the powder filled cables was damaged in 9 separate locations with the damage ranging from slits in the sheath to a complete ring of sheath being removed. One of the damage conditions is shown in Fig. 7.

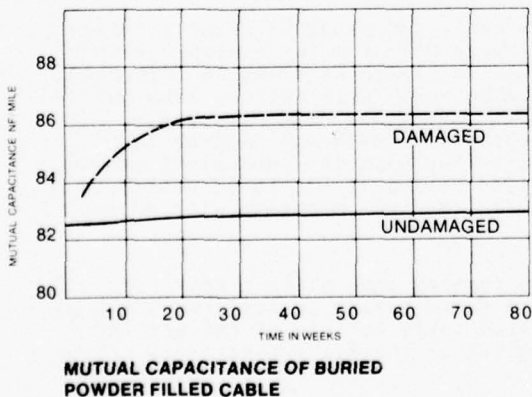
FIGURE 7



EXAMPLE OF THE DAMAGE CONDITIONS ON THE POWDER FILLED CABLE

Once installed the cables were monitored to determine if a change in transmission parameters occurred. It was found that the undamaged cable remained stable over the entire period. The damaged cable showed an increase in the early stages as water entered the cable and blocked. After 10 weeks the capacitance levelled out and has remained stable since. (A period of 90 weeks). Fig. 8 shows the results of mutual capacitance over the period.

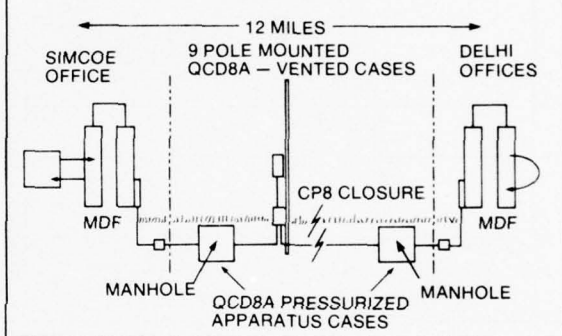
FIGURE 8



TECHNOLOGY TRIAL

A technology trial was held with Bell Canada to verify the performance of powder filled cable on a digital carrier link. A 25 mile loop of cable was installed between two offices in Southern Ontario. The cable was ploughed over the major portion of the route with apparatus cases installed on poles as shown in Fig. 9. Splices at the repeater points were above ground in CP-8 closures, as shown, and intermediate splices were buried. The repeaters close to the offices were installed in pressurized apparatus cases in manholes.

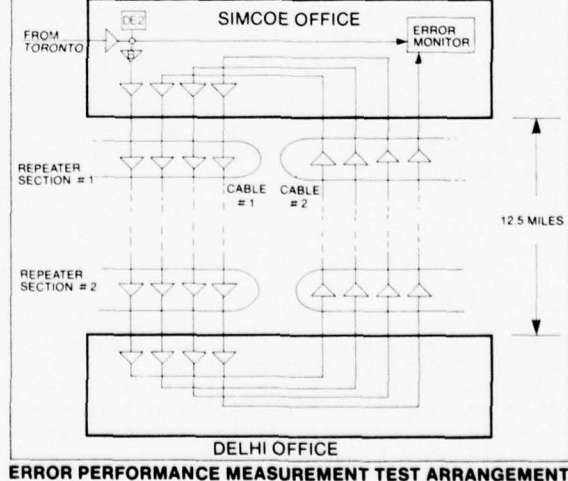
FIGURE 9



TECHNOLOGY TRIAL APPARATUS CONFIGURATION

The main objective of the tests, performed on the cable, was to monitor for any degradation in digital transmission quality that could be attributed specifically to the cable. A 100 mile span was simulated by looping back four times between the two offices, as shown in figure 10.

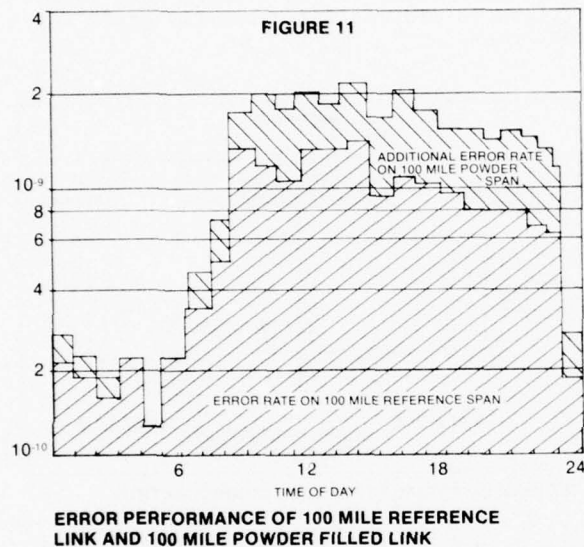
FIGURE 10



ERROR PERFORMANCE MEASUREMENT TEST ARRANGEMENT

From the results of standard measurements taken over the period of testing, (winter to summer), it was seen that the transmission characteristics remained stable.

The error rate performance was measured on a working LD-1 carrier system which was rerouted over the new cable facility. The errors were monitored with automated test equipment at the input and output of the span, over a period of six weeks. The results, averaged for a 24 hour period, are shown in Figure 11.



The actual errors appearing in the 100 mile span of powder filled cable were of the same order as those generated in the 100 mile Toronto/Simcoe span.

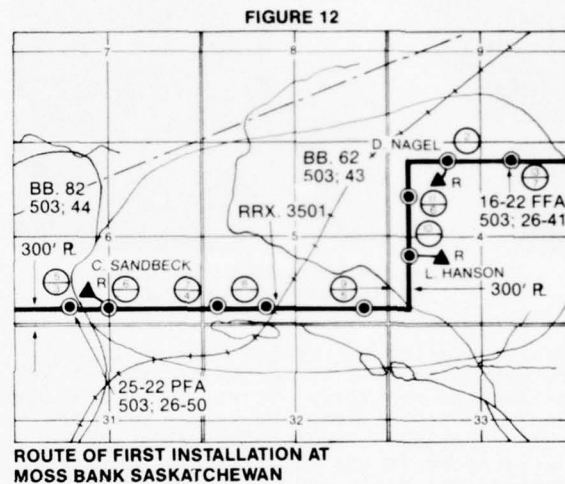
The errors were correlated with the telephone activity, exhibiting peaks during daylight hours and low levels at night. It was concluded from the trial that the powder filled cable performed satisfactorily on the system. The cable will be cut over as a permanent link on digital carrier between Delhi and Simcoe at a later date.

FIELD TRIALS

A major field trial of the new product was initiated by Saskatchewan Telecommunications in late fall 1976. The cable was supplied from Northern Telecom's plant in Regina, where it was manufactured on a standard production line.

The first 3.5 miles of cable were installed in October 1976 to examine the performance of the cable over the winter and spring seasons. Following verification of satisfactory performance, the second phase of the field trial was set in motion, and shipments of powder filled cable as standard production was commenced in June 1977.

A special program of product testing and operator reaction was performed on the initial installation at Moss bank in Saskatchewan. (Figure 12)

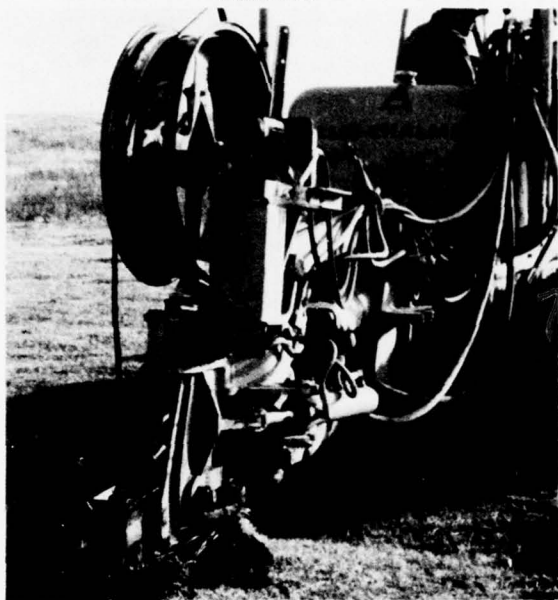


The tests carried out on the cable included normal V.F. performance and carrier capability at 150KHz, and 772KHz. Each span was checked prior to splicing in the loading coils.

The cable was ploughed using an Allis Chalmers HD11 tractor equipped with a standard plough as shown in figure 13. Loading coils were spliced into the cable at regular 4500' intervals. Because the cable was lighter in comparison with the equivalent grease filled cable, it was found easier to handle, and was ploughed with no trouble.

The testing and splicing operations were found easier to perform on the powder filled cable because of the ease of removal of the filling material. (Figure 14).

FIGURE 13



PLOUGH USED IN FIELD TRIAL INSTALLATION

FIGURE 14



SPLICING OPERATION IN PROGRESS

A series of questionnaires were issued to the field personnel to obtain their reaction to the new product. The questionnaires (Figure 15) attempted to obtain information pertinent to the human aspects of the installation and splicing as well as the performance characteristics.

FIGURE 15

| |
|--|
| <p>QUESTIONNAIRE #2 O.P. FIELD TRIAL #26 TO BE COMPLETED BY: SPLICING CREW</p> <p>1. WERE THERE ANY NOTICEABLE DIFFERENCES IN THE SHEATH, CONDUCTOR INSULATION, COLOUR CODE, ETC. BETWEEN THIS NEW CABLE AND THE NORMAL "GREASE" FILLED CABLE?</p> <p>2. WAS THERE A GOOD BOND BETWEEN OUTER PE JACKET AND THE ALUMINUM SHIELD.</p> <p>3. (Wavy line)</p> <p>8. WERE THERE "ANY" DETRIMENTAL QUALITIES OF THE NEW CABLE? (IRRITATION ETC.)</p> <p>9. WOULD YOU RATHER WORK WITH "GREASE" FILLED OR THIS NEW "COMPOUND" FILLED CABLE? EXPLAIN WHY.</p> <p>10. ADDITIONAL COMMENTS</p> |
|--|

The data obtained from the questionnaires were summarized as follows:

- The new cable was found to be more flexible and lighter than the equivalent grease filled cable. In other respects it handled in a similar manner as grease filled cable.
- Because of the lack of grease to act as a lubricant, the removal of the sheath from long sections was found to be more difficult. It was estimated however that the sheath could be removed with approximately the same ease as air-core cable.
- When opening the cable it was found best to use typical air-core techniques to prevent the occurrence of split pairs. The method employs the application of tape at the end of the cable core just after the sheath has been removed.
- The filling compound was easily removed by shaking the core, leaving very little residue on the conductors and facilitates splicing.

- Examples of comments received on the questionnaire were:-

No worse than grease - in fact better.
Comes off the clothes easy, and does not bother the eyes.

It is far superior in handling and splicing,... and on clothes.

- A definite preference was expressed by the craftsmen for powder filled cable.

The data obtained from the electrical testing are summarized in table 9.

TABLE 9

| STANDARD V.F. TESTS | |
|--|------------------|
| RESISTANCE | MET REQUIREMENTS |
| RESISTANCE UNBALANCE | MET REQUIREMENTS |
| LOSS AT 1000 Hz | MET REQUIREMENTS |
| INSULATION RESISTANCE | MET REQUIREMENTS |
| SINUSOIDAL LOSS/4500' SECTION* | |
| AT 16 KHz | 5.5 dB |
| AT 56 KHz | 7.0 dB |
| AT 76 KHz | 8.0 dB |
| AT 112 KHz | 9.5 dB |
| PSEUDO-RANDOM DIGITAL LOSS/4500' SECTION** | |
| T1 | 17.5 dB |
| * USING WILCOM T236/T237 | TEST SET |
| ** USING LENKURT 91100 | TEST SET |

RESULTS OF FIELD TRIAL MEASUREMENTS

The results show that the cable met all the electrical requirements per standard acceptance procedures. The carrier capability was also ascertained, and all special test results were positive. The reaction of the splicers and field craftsmen indicated their preference for the product over grease filled cable.

A second field trial of powder filled cable was performed by Commonwealth Tel, Pennsylvania. The cable was used in an aerial application and was found to perform up to all expectations. The lighter weight of powder filled cable meant longer spans in aerial sections and the smaller diameters predicted for the larger pair sizes, introduced the possibility of less bulky outside plant hardware.

Once again, all electrical testing, performed as per R.E.A. specification PE 39, met requirements, and craftsman reaction to the product was favourable.

CONCLUSION

A new generation of filled cable has arrived with the introduction of powder filled cable. The results of extensive laboratory tests have demonstrated the capability of the new product to perform in most conditions encountered in the outside plant environment. These results have been confirmed by the successful use of cable in buried and aerial installations in a number of field trials.

With the conclusion of these trials, the new cable is now considered a tried and proven member of Northern Telecom's standard portfolio.

The reaction of personnel to the new cable has been favourable and estimates of productivity improvement have shown advantages to be gained from the use of the new product. There is little doubt that this new generation of filled cable will answer the needs of today's technology, and will move forward into tomorrow's environment with the confidence of a proven background.

ACKNOWLEDGMENTS

The authors wish to thank the management of Northern Telecom and Sask Tel for their encouragement and permission to publish this work. Special recognition must be given to those members of Cable Division R&D Northern Telecom, who provided significant contributions to this development. Sincere gratitude is also expressed to the personnel in Bell Canada, and Commonwealth Tel., who provided valuable input to this paper.

REFERENCES

1. E.J. Gouldson, Mrs. M. Farago, G.D. Baxter. "Foam Skin, a composite expanded insulation for use in telephone cables" 21st Annual Wire & Cable Symposium 1972.
2. Leo V. Woytiuk, "Water Blocked Cables", U.S. Patents 4,004,077, and 4,002,819.
3. D.O. Lawrence, "Next Generation Filled Cable - Lightning Study", Internal NTCL Report TR-4090-76-12.
4. H.W. Friesen and A.S. Windeler : "Moisture permeation and its effect on communication cable". 15th Annual Wire & Cable Symposium 1966.
5. Rural Electrification Agency : "Guidelines for the long-term electrical stability of telephone wires and cable" 1974.



T.K. McManus graduated from Queen's University of Belfast in 1966 with an Honour's degree in Physics. He immigrated to Canada shortly after, and joined Northern Telecom as a member of the Research and Development group at the Communications Cable division. He is presently a Product Manager in Northern Telecom Canada Ltd., responsible for H.F. and Pic cables.



R.E. Beveridge graduated in 1959 from the University of Saskatchewan with a degree in Mechanical Engineering. He joined Sask. Tel. after graduation and has been involved mainly in outside plant staff engineering. He is presently Manager of the outside plant group in Sask. Tel.

DEVELOPMENT OF FLAME RESISTANT CABLES
FOR NUCLEAR POWER PLANT AND
THEIR QUALIFICATION TEST RESULTS

J. Matsuo, M. Hanai, Y. Yamamoto, T. Sakurai, I. Nishikawa
Showa Electric Wire & Cable Co., Ltd.
Kawasaki, Japan

Summary

Qualification tests on cables for nuclear power plants have been performed in the United States and Japan on the basis of IEEE std 383 which was established in 1974.

This report shows the results of detailed qualification tests on the cables that have been developed and manufactured by us for use in nuclear power plants according to the standard. Tests were performed for flame resistance and environmental resistance including radiation resistance, and evaluation of properties probably needed in the future were also done.

In the test results, it was confirmed that cables supplied for the qualifications satisfied the standard, and some new facts were affirmed from the results of the qualification tests.

Introduction

For nuclear power plants, complete protections for safety must be provided from the viewpoint of special environmental conditions including radiations and some kinds of design basis events. Cables for nuclear power plants are not the exception, and the flame resistant properties and the environmental resistant properties under the peculiar environmental conditions including radiation are required as the special performance of the cables.

Nowday in the United States and Japan, the qualification of these cables are being put in practice on the basis of IEEE std 383 which requires these performances.

In the United States, many cable manufactures have done the qualification tests at authorized test organizations, but cable manufactures in Japan have done these tests using their own test equipment, on the basis of users' specification which refers to the standard, because there is no such authorized organization in Japan. The qualification tests consist of flame resistant tests including a vertical tray flame test which is specified in the standard and of environmental tests which ensure the performance over the life under the normal service conditions for 40 years and additionally under any accidental conditions possible during the service life that is design basis event.

This report shows the results of the qualification tests required in IEEE std 383 and of some new flame tests for cables which we have developed.

Qualification tests of flame resistant cables
for nuclear power plants

Cable samples

Table 1 shows a list of cable samples for the qualification tests. This table shows only the outline of materials used for cable specimens and of cable con-

structions, and the details of actual cables are shown for each test result.

Cables used inside primary containment vessel (PCV) are required flame resistant properties and superior environmental properties including radiation resistance and other cables used outside PCV are required flame resistant properties.

For most cables, all materials have flame resistance, but for some exceptional cables, such as high voltage power cables, coaxial cables and the like, it is too difficult to provide flame resistant property to the insulation because of required superior electrical property. In this case, by providing higher flame resistance to the jacket material, the flame resistant cables are achieved.

And additionally, materials with properties necessary for environmental performance, such as heat resistance, steam resistance, radiation resistance, and the like, as well as flame resistance, are used for the cable inside PCV.

Outline of qualification tests

Fig. 1 shows the outline of qualification tests concerning cables for nuclear power plants. About environmental test, the mechanical property and the insulation resistance after each environmental condition are measured in addition to the test items required by IEEE std 383, and additionally the capacitance of coaxial cables are measured. As evaluations of combustion for materials, oxygen index and quantity of hydro chloric (HCl) acid gas generation in combustion are measured.

Qualifications for flame resistant properties

The flame tests required in this standard consist of the IPCEA vertical flame test for coaxial cables in their completed shape and insulated conductors of other cables and of the vertical tray flame test for completed cables. In this report, oxygen index and quantity of HCl gas generation in combustion of materials and the effect of the carbonized layer related to the combustion of high voltage power cables are also shown.

Results of oxygen index measurements

This measurement is mainly used for selecting materials of flame resistant cables. Table 2 shows the oxygen indexes of materials used in the cable specimens. Most materials used for cable constructions have so high oxygen index that the cables meet the requirement of IPCEA and UL FR-1 flame test with exception of insulations of coaxial cables and high voltage power cables.¹

The measurement of the oxygen index includes a few problems which the oxygen index changes to some extent with the form of specimens and the forming condition of the carbonized layer of specimens in combustion.

Table 1 Summary of various cable constructions

| Zone | Class | Cable specimen | Material | Cable construction |
|---|---|---|---|---|
| Inside containment vessel (Radioactive Zone) | High voltage cable Low voltage cables (for control power and instrumentation etc.) (600 V grade) | *1 FR-PH (6 ~ 15 KV) | Insulation EP rubber Jacket FR-Hypalon *3 | |
| | | FR-PH | Insulation FR-EP rubber Jacket FR-Hypalon Filler KAINOL *4 | |
| | | FR-PN | Insulation FR-EP rubber Jacket FR-Neoprene *5 Filler KAINOL | |
| | | FR-CH | Insulation FR-crosslinked PE(XLPE) Jacket FR-Hypalon Filler KAINOL | |
| Outside containment vessel | Low voltage cable (600 V grade) | TEFZEL *2 insulated cable | Insulation TEFZEL 280 Jacket TEFZEL 280 | |
| | | Radiation resistant silicone rubber insulated cable | Insulation Radiation resistant silicone rubber Braid treated glass fiber | |
| | High voltage cable (6 ~ 15 KV) | FR-CV (6 ~ 15 KV) | Insulation crosslinked PE Jacket special FR-PVC | Same construction as high voltage FR-PH cable |
| | | FR-CV (600 V) | Insulation FR crosslinked PE Jacket low HCl PVC *7 | Same construction as low voltage FR-PH cable |
| Inside and outside containment vessel Coaxial and tri-axial cables | (A) RG 59 B/u | | | |
| | | | | |
| | | (B) RG 216 /u | Insulation Radiation crosslinked PE including "anti-rad" Jacket FR-XLPE | |
| | (C) RG 114 /u | | | |

*1 FR: flame resistant

*2 TEFZEL: Du pont's trade name ethylene tetrafluoro-ethylene copolymer

*3 Hypalon: Du pont's trade name chloro-sulphonated polyethylene

*4 Kainol: Japan KAINOL Co., Ltd. trade name novolac type phenol resin fiber

*5 Neoprene: Du pont's trade name poly chloroprene

*6 Insulation: Radiation cross-linked foamed polyethylene including "anti-rad"

*7 Low HCl PVC: Refered to the sub-heading measurement of the quantity of hydrochloric acid gas generation in combustion

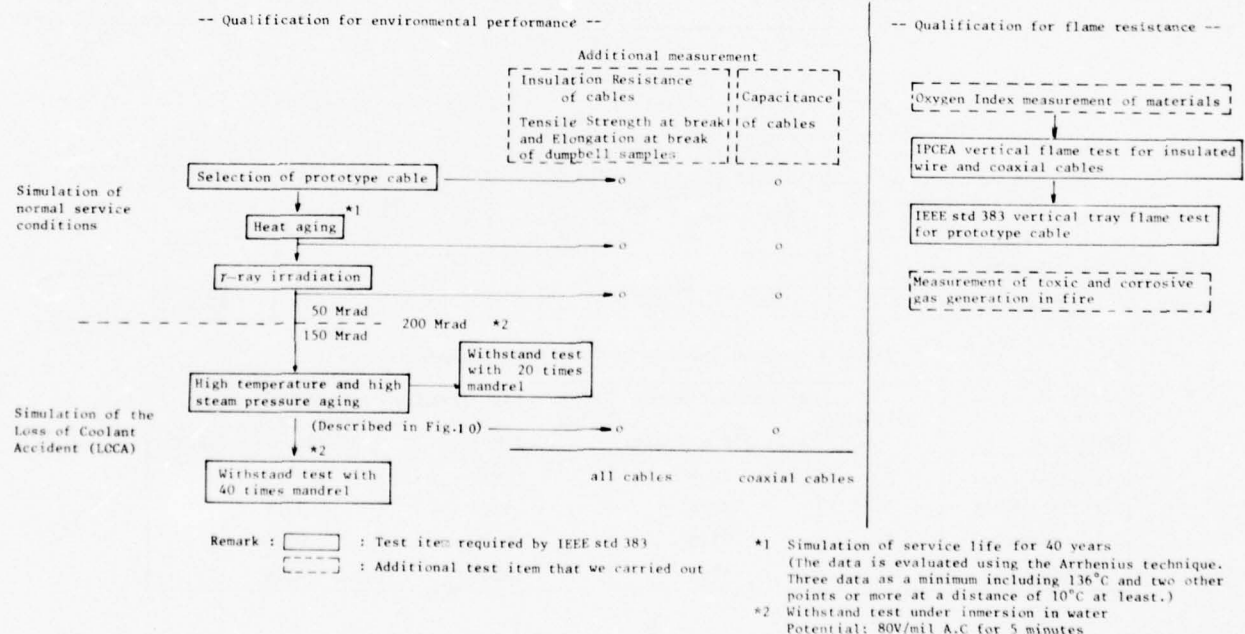


Fig. 1 Diagram of qualification tests for Nuclear Power Plant Cables

Table 2 Oxygen index of materials

| Appli-cation | Material | Oxygen Index | | | | |
|--------------|-------------------------------------|----------------|----|----|----|----|
| | | 10 | 20 | 30 | 40 | 50 |
| insulation | Ethylene-propylene(EP) rubber | 19.2 | 1 | 1 | 1 | 1 |
| | Crosslinked polyethylene (XLPE) | 17.6 | 1 | 1 | 1 | 1 |
| | F.R - EP rubber | 32.5 | 1 | 1 | 1 | 1 |
| | F.R - XLPE | 30.3 | 1 | 1 | 1 | 1 |
| | Radiation resistant silicone rubber | 29.0 | 1 | 1 | 1 | 1 |
| | TEFZEL | higher than 80 | 1 | 1 | 1 | 1 |
| jacket | F.R - Neoprene | 43.4 | 1 | 1 | 1 | 1 |
| | F.R - Hypalon | 49.1 | 1 | 1 | 1 | 1 |
| | Special FR - PVC | 43.4 | 1 | 1 | 1 | 1 |
| | Low HC1 PVC | 27.8 | 1 | 1 | 1 | 1 |
| filler | Kainol | 32.5 | 1 | 1 | 1 | 1 |

Remark * A, B and C are values specified hereinunder.¹

- A: oxygen concentration in air
 B: minimum value for passing IPCEA vertical flame test
 C: minimum value for passing UL FR-1 test

As an example, Table 3 shows the comparison between the oxygen index of the standard form specimen shown in ASTM D-2863 and the oxygen index of specimens sampled from cables using FR-XLPE. These oxygen indexes are greatly changed by the structure, as shown in this table.

In the case of flame resistant materials used for the cables for nuclear power plants, it is said that the change of oxygen index by each environmental test must be considered.²

The changes of oxygen index by the environmental tests related to representative specimens are shown in Table 4.

As shown in Fig.10, accelerated conditions were used as the environmental conditions.

The results showed that some lowering of the oxygen index is found after irradiation of gamma ray in most materials, except for FR-Neoprene, and it was considered that this might be due to the decomposition of the additive by the radiation.

In conclusion, the lowering of the oxygen index did not occur even after the series of environmental tests was completed.

Table 3 Oxygen index variety due to sample shape (FR-XLPE)

| | ASTM D2863 | Tube sample cut from insulated wire | | | Tube samples cut from coaxial cable jackets | |
|--------------------|------------|-------------------------------------|----------------|-------------|---|----------------|
| | | Outer diameter(mm) | Thickness (mm) | Length (mm) | Outer diameter(mm) | Thickness (mm) |
| Outer diameter(mm) | 6 | 1.8 | 3.6 | 4.8 | 11.3 | 6.2 |
| Thickness (mm) | 3 | 0.8 | 1.0 | 1.0 | 0.85 | 0.85 |
| Length (mm) | | | | 150 | | |
| Oxygen index | 30.3 | 36.2 | 34.2 | 33.8 | 25.4 | 32.5 |

Table 4 Oxygen index change by environmental tests

| Sample | Original | After heat aging (121±1°C x 7 days) | After γ-ray irradiation (200 Mrads) | After LOCA simulation (described in Fig.10) |
|--------------|----------|-------------------------------------|-------------------------------------|---|
| FR-XLPE | 30.3 | 29.8 | 28.9 | 30.7 |
| FR-EP rubber | 32.5 | 32.9 | 32.5 | 32.9 |
| FR-Neoprene | 43.4 | 47.8 | 55.7 | 62.3 |
| FR-Hypalon | 49.1 | 49.1 | 43.9 | 47.4 |

IEEE std 383 vertical tray flame test

Tests related to the qualification of flame resistant cables before setting up the vertical tray flame test were almost small scale tests, and could easily be done in laboratories, such as flame tests for materials and horizontal or vertical flame tests for insulated conductors. With the setting of the standard,

cable manufactures in Japan have prepared facilities for flame tests.

The following paragraph shows the results of vertical tray flame test for the developed cables in Table 1 and additionally the results of comparison between this test and vertical duct flame test which has been lately adopted by one of users in Japan.

IEEE std 383 vertical flame test method and its facility

Fig. 2 shows the main test room which has a height 4m in the test area (3m x 3m). This room is equipped with an air-flue monitoring and ventilating system capable of replacing air in the test room once every 2 (two) minutes.



Fig. 2 Room for vertical flame test

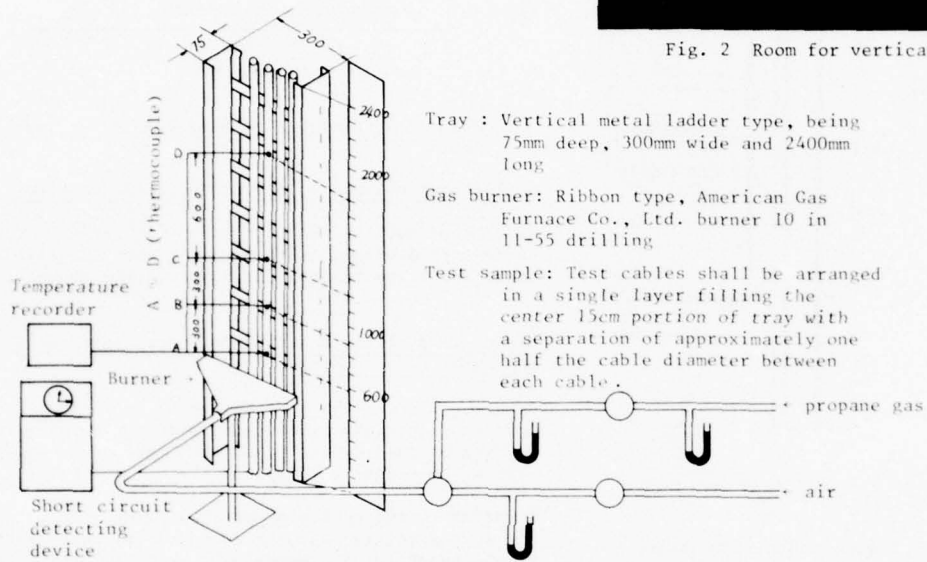


Fig. 3 Vertical tray flame test apparatus

Test results for the developed cable

Results of tray tests for the representative cables are shown in Table 5 with the oxygen index of materials used and results of IPCEA vertical flame tests.

All samples satisfied the vertical tray flame test, but burning behavior of each sample was somewhat different due to materials used and by the difference of cable sizes.

In the case of high voltage power cable, the carbonized layer of the jacket created in combustion has adiabatic and protective effect against the insulation and prevents the fire spread of the cable, as described later, thus resulting in shorter flame distance of the insulation as compared to other cables.

But because of the flammability of the insulation, when some parts of the jacket broke during the burning time, the insulation caused decomposition, melting, and combustion, thus resulting in some afterburning even after removing the burner.

Comparing low voltage FR-PH cable with FR-CH cable showed that, as described by results of oxygen index and IPCEA vertical flame test, higher flame resistant FR-PH cable had shorter distance burned of the insulation and the jacket in the case of vertical tray flame test.

On the contrary, comparing low voltage FR-PH cable with FR-PN cable showed that FR-PH cable used Hypalon, which has higher oxygen index than that of Neoprene, as the jacket, showed longer flame distance in the case of vertical tray flame test.

The result showed that the evaluation for flame resistant cables could not be performed by only the oxygen index.

Comparison of burning behavior between the vertical tray flame test and the vertical duct flame test

Recently, as a more severe flame test, the vertical duct flame test has been done in Japan.

The figures of both test methods are shown in Fig. 4. Results of both tests for representative cables in Table 5 are shown in Table 6.

The results showed that the vertical duct test was a more severe flame test than the vertical tray test. Reasons for the severity were suggested by the following two items.

- (1) Flame promotive effect by a flue; Very fast up-welling air stream was generated in the inside of the duct, and the flame stretched to the upper part because it was pulled up by the stream.
- (2) Effect of temperature increasing; Temperature comparison between the vertical tray and the vertical

closed duct, where samples were not burnt, is shown in Table 7. The point at which the temperature was measured was about 1m above the burner. The test result showed that the temperature of the vertical closed duct increased to some extent with the increased duration of combustion.

Concerning the above description, a test result that the rise of temperature of materials resulted in considerable lowering of oxygen indexes of materials was reported.³

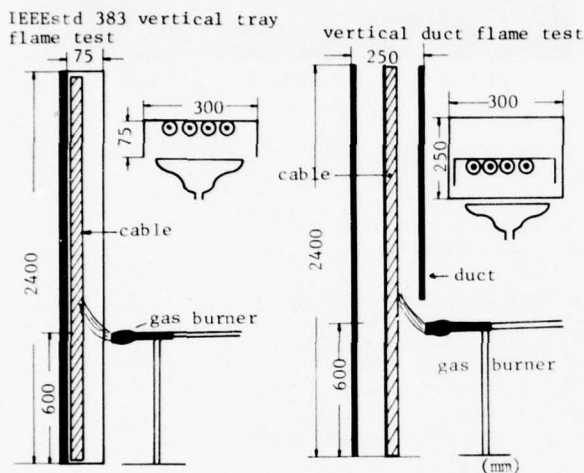


Fig. 4 Apparatus of vertical tray and duct

Table 6 Comparison between both flame tests

| Test Sample | IEEE std 383 vertical flame test | | Vertical duct flame test | |
|--------------------------------------|-------------------------------------|----------|-----------------------------|----------|
| | Length of jacket burned(cm) | Decision | Length of jacket burned(cm) | Decision |
| 6kV FR-CV 1c x 100mm ² | 70 | passed | 180 | failed |
| 6kV FR-CV 3c x 38mm ² | 50 | passed | 100 | passed |
| 600V FR-CV 7c x 2mm ² | 130 | passed | 180 | failed |
| 600V FR-PH 7c x 2mm ² | 100 | passed | 150 | passed |

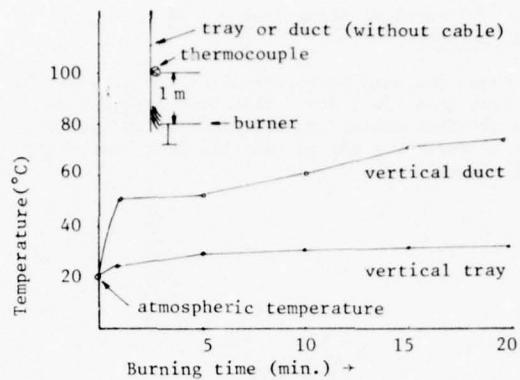


Fig. 5 Temperature rise of both flame tests

Evaluations related to other combustion behaviors

We carried out two evaluations on combustion behavior, as described below, in addition to three qualification tests for flame resistance, as described above.

Measurement of the quantity of hydrochloric acid gas generation in combustion

Recently, attentions have been paid to suppression of toxic and corrosive gases generated from burning cable in fire because of the detrimental effect to human beings and electrical devices.

In order to reduce the quantity of generation of toxic and corrosive gas as much as possible, measurement of the quantity of hydrochloric acid gas generated in combustion was added as a qualification.

In Japan, this kind of research and development was first performed for low HCl PVC including in Table 1, and at present considerable quantity of this material are used as a cable jacket material. Several methods for hydrochloric acid measurement in combustion have been already shown; here the results by JCS 56* method, which was temporarily published, were shown. The outline of the test device and the method is shown in Fig. 6 and 7. Measurement results are shown in Table 7. The quantities of HCl from most materials varied from about a third to about a half of that from conventional PVC material.

*JCS56: Japan Cable Makers Association
Standard No. 56

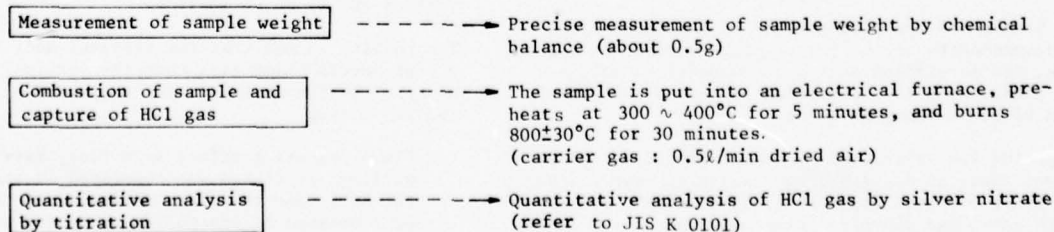


Fig. 6 Measurement of the quantity of HCl gas generation in combustion

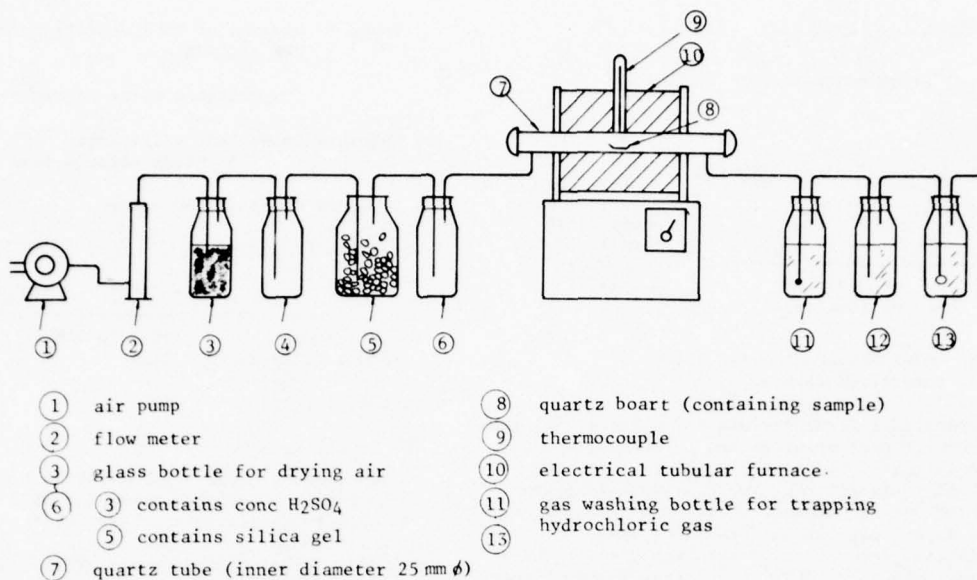


Fig. 7 Diagram of combustion and HCl trapping apparatus

Table 7 Weight of HCl evolution by material

| Material | (reference) conventional PVC for cables | low HCl PVC jacket of low voltage FR-CV cable | Special FR-PVC jacket of high voltage FR-CV cable | FR-EP rubber insulation of low voltage FR-PH and FR-PN cable | FR-XLPE insulation of low voltage FR-CH cable and jacket of coaxial cable | FR-Neoprene jacket of low voltage FR-PN cable | FR-Hypalon jacket of low voltage FR-PH and FR-CH cable |
|--|--|--|---|--|---|---|--|
| Weight of HCl evolution * (mg/g) | 300 ~ 350 | 80 ~ 90 | 230 ~ 250 | 70 ~ 80 | 50 ~ 60 | 140 ~ 150 | 90 ~ 100 |

Remark * mg/g (weight of HCl gas/weight of sample)

From the point of view of ingredients of materials, there are two methods of HCl suppression. One is the addition of HCl capture agent to the material, for example low HCl PVC, and another is that the addition of halogenated compounds as flame-retardants, is kept to a minimum in selecting ingredients of a material.

carbonized layer formation from the viewpoint of materials, the jacket material of high voltage power cable was obtained by using a special combination of polymers and additives that strengthens the carbonized layer. Flame tests for the special flame resistant high voltage power cable are shown in Table 5 and 6.

Fig. 8 and 9 show an experimental result about the adiabatic effect of the carbonized layer.

Formation of carbonized layer

As described above, the method of providing flame resistance to high voltage power cables must be achieved by using flame resistant jacket.

When a conventional XLPE insulated PVC jacketed cable (CV) is burnt in vertical tray test, cracks generate on the surface of the jacket and then the PE insulation is intensely burnt at the part of the cracks, so that the flame reaches the top of the tray within 10 minutes. Simply increasing oxygen index of PVC jacket by the addition of flame retardants provides little protection effect against the combustion and if these cracks generate, the cable does not pass the flame test. Therefore, carbonized layer formed in combustion is required, so that it is very tough, and cracks do not generate. And the layer has protection effect and adiabatic effect for the insulation.

As the result of the investigation that focuses on the

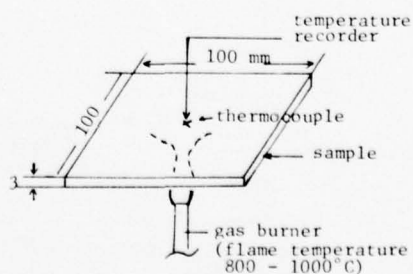
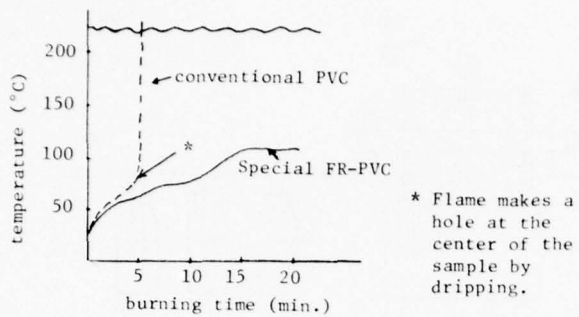


Fig. 8 Diagram of the test for adiabatic effect of carbonized layer of special FR-PVC



With a conventional flame resistant PVC plate, melting of flame contact part occurred and a large hole was created at the part, but on the contrary, with the special flame resistant PVC, the considerable expansion occurred during carbonizing and the expanded carbonized layer acted as an adiabatic layer, which resulted in the temperature of the back side of the burner being only about 100°C even after twenty minutes of the flame test.

Qualifications related to environmental conditions

Outline of environmental test

Environmental tests related to cables for nuclear power plants have been done on the basis of conditions shown in IEEE std 323 attached table, but, in Japan, these tests often have been done under each condition of the boiling water reactor or the pressurized water reactor.

The outline of test conditions related to the both reactors shown in the attached table is shown in Table 8. This table shows that the condition of the pressure water reactor is rather severe from the viewpoint of total dose and that of the boiling water reactor is rather severe from the viewpoint of heating condition.

Consequently, it may be possible that performance required to materials varies according to the type.

The test, described here, simulates the combined conditions of the boiling water reactor, and the pressurized water reactor. And it is considered that cables which succeed in the test, satisfy the performance required by both types of reactors. Test conditions are shown in Fig. 10.

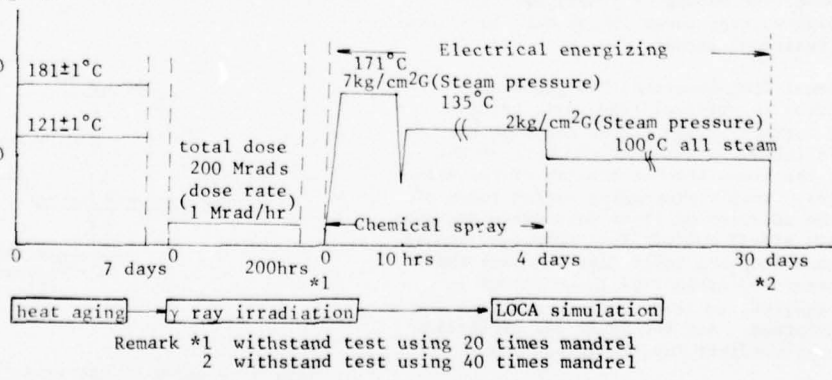


Fig. 10 Diagram of environmental test conditions

Table 8 Diagram of LOCA condition for BWR and PWR

--Pressure water reactor--

(1) Exposure to Nuclear Radiations
150 Mrads after 1 year

(2) Exposure to Steam and Spray

(a) Steam Exposure

| Time | (°C) | (1bf/in ² , gauge) |
|------------------------|---------------|-------------------------------|
| 0 to 10 seconds | 48.9 to 148.9 | 0 to 70 |
| 10 seconds to 10 hours | 148.9 | 70 |
| 10 hours to 4 days | 98.9 | 40 |
| 4 days to 1 year | 75.0 | 5 |

(b) Spray Exposure

Continuously spray for first 24 hrs with a solution of the following composition at a rate of 6.1 ((ml/min)/m²) of area of the test chamber.

0.28 molar H₃BO₃ (3000 parts per million boron)
0.064 molar Na₂S₂O₃

NaOH to make a pH of 10.5 at 77°F (about 0.59 percent)
Dissolve chemicals, on a one-liter basis, in the following order:

--Boiling water reactor--

(1) Exposure to Nuclear Radiations

26 Mrads integrated over the accident

(2) Exposure to Steam and Spray

(a) Steam Exposure

| Time | Temperature (°C) | Pressure (1bf/in ² , gauge) |
|---------------------|------------------|--|
| 0 to 20 seconds | 57.2 to 137.8 | 0 to 62 |
| 20 seconds to 5 min | 137.8 to 171.1 | 62 |
| 5 min to 3 hours | 171.1 | 40 |
| 3 hours to 6 hours | 160.0 | 40 |
| 6 hours to 4 days | 121.1 | 25 |
| 4 to 100 days | 93.3 | 10 |

(b) Spray Exposure

Continuously spray with demineralized water at a rate of 6.1 ((ml/min)/m²) of area of the test chamber.

Accelerated thermal aging was performed, under a condition of $181 \pm 1^\circ\text{C} \times 7$ days for silicon rubber insulated cable and TEFZEL insulated cable, for which heat resistance is required, and under a condition of $121 \pm 1^\circ\text{C} \times 7$ days for other cables.

After thermal aging, 200 Mrads γ -ray was irradiated at about 1 Mrad/hr dose rate by ^{60}Co γ -ray source for all samples.



Fig. 11 Example of ^{60}Co γ -ray irradiation

The electrical energizing was performed, in accordance with the electrical loads suggested in Table 9, during the LOCA test, and the chemical spray shown in the attached table of IEEE std 323 was sprayed for first 4 days of the LOCA test.

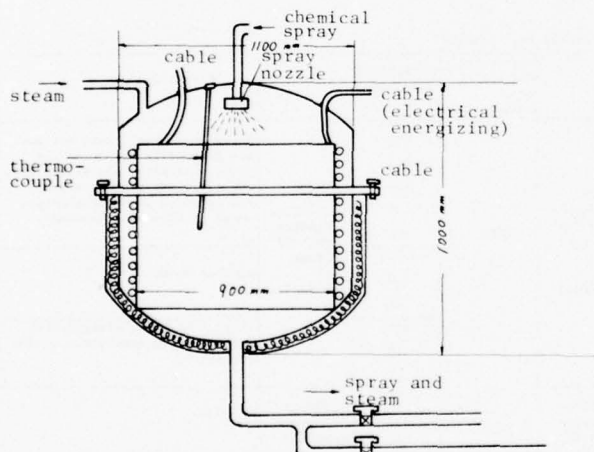


Fig. 12 Test vessel for LOCA test

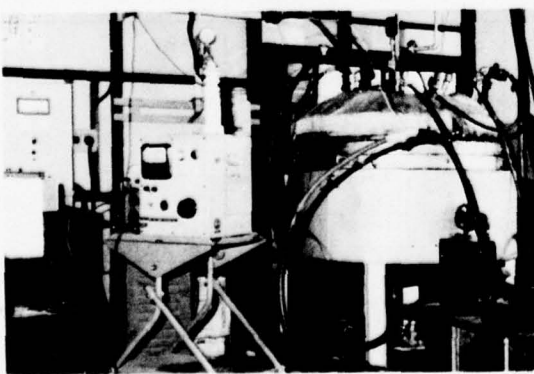


Fig. 13 Equipment for LOCA test

The judgement of pass or failure in this qualification test depends on the withstand voltage test with a cable wound around a mandrel with twenty times the outer diameter of cable after γ -ray irradiation, and another withstand voltage test with cables wound around a mandrel with forty times after LOCA test.

In this test, mechanical properties and insulation resistance of the cables were measured as references.

For most cables, dumbbell specimens taken from a 1mm plate were used for tension test because sampling the specimens from cables after γ -ray irradiation was very difficult.

Test results for the developed cables

Environmental test results of the representative cables are shown in Table 9. The results show that all cables in Table 9 satisfied the required environmental performance.

Comparing FR-XLPE with FR-EP gives some larger lowering of the elongation in FR-XLPE by γ -ray irradiation and some larger lowering of the insulation resistance in FR-EP after LOCA test, but the difference of the property change for both materials was small and the both had approximately similar environmental property.

Comparing FR-Hypalon with FR-Neoprene gives larger lowering of elongation of FR-Neoprene by γ -ray irradiation.

After LOCA test, some cracks generated in the jacket of FR-PN cable. On the contrary, in FR-PH and FR-CH cable used FR-Hypalon as the jacket, no cracks were generated, even after the cables were bent up into small diameter around the cable diameter.

With most materials except FR-Neoprene, after LOCA test the elongation at break recovered higher value than that after γ -ray irradiation.

Though TEFZEL insulated cable and silicone rubber insulated cable passed both the withstand test, the elongations at break after the γ ray irradiation was nearly zero.

Consequently, judgement of pass or failure for these cables cannot be done by the value of elongation at break.

Tests of coaxial cables include the measurement of the electrostatic capacity, as well as the tension test and the insulation resistance measurement. Since the large lowering of insulation resistance after the γ -ray irradiation considerably recovered after LOCA test, it is considered that the lowering depends, not on the permanent deterioration of the insulation, but on the temporary effects of secondary electrons created in the insulation by the γ -ray irradiation. The increase of electrostatic capacity after the heat aging might be due to the change which occurred in cable structure by the heating above the melting point of PE.

XLPE including antirad for the insulation showed approximately same mechanical property change as FR-XLPE of the jacket.

Table 5 Results of flame tests

| Classification | Cable (size) | Oxygen Index (O.I.) | | IPCEA vertical flame test | | IEEE std 383 vertical tray flame test *1 | | |
|---------------------|---|-------------------------|-----------|---------------------------|--------------------------------------|--|--------------------------------|---|
| | | Material | O.I. | Distance burned (mm) | Decision | Cable length burned (cm) | Time of after*2 burning (min.) | Decision |
| High voltage cables | 6kV FR-PH (15x100mm ²) | Insulation EP rubber | 19.2 | 50 100 30 100 | passed passed passed passed | about 5 about 3 | passed passed | After the burner was put out, some parts of the jacket which contacted the flame were found to be cracked and the insulation in that parts kept burning with weak flames. |
| | Jacket FR-Hypalon | 49.1 | | | | | | |
| Low voltage cables | 6kV FR-CV (15x100mm ²) | Insulation XLPE | 17.6 | 30 100 | passed passed | about 3 | passed | When the burner was put out, the cables were scarcely burning so that there was no after burning. |
| | Jacket Special FR-PVC | 43.4 | | | | | | |
| Coaxial cables | FR-PH 7c x 2mm ² | Insulation FR-EP rubber | 32.5 | 90 ~ 120 | passed | 90 100 | 0 | passed |
| | Jacket FR-Hypalon | 49.1 | | 70 ~ 90 | passed | 50 60 | | |
| | FR-PH 2c x 38mm ² | Insulation FR-EP rubber | 32.5 | 115 ~ 140 | passed | 100 | 0 | passed |
| | Jacket FR-Hypalon | 49.1 | | | | 120 | | |
| | FR-CH 7c x 2mm ² | Insulation FR-XLPE | 30.3 | 115 ~ 140 | passed | 100 | 0 | passed |
| | Jacket FR-Hypalon | 49.1 | | | | 120 | | |
| | FR-PN 7c x 2mm ² | Insulation FR-EP rubber | 30.3 | 90 ~ 120 | passed | 70 | 0 | passed |
| | Jacket FR-Neoprene | 43.4 | | 80 | | | | |
| | FR-CV 7c x 2mm ² | Insulation FR-XLPE | 30.3 | 115 ~ 140 | passed | 90 | 0 | passed |
| | Jacket Low HCl PVC | 28.0 | | | | 130 | | |
| (A) RG 59 B/u | Insulation Irradiated XLPE including anti-rad | 17.6 | 90 ~ 100 | passed | | | 0 | passed |
| | Jacket FR-XLPE | 30.3 | 100 ~ 120 | passed | | | | |
| | | | 90 ~ 100 | passed | | | | |

Remark : *1. Evaluation Standard: Unacceptable when the cable burned completely up to the top of the tray or when cable did not self-extinguish after the burner had been put out.

*2. Time required for self-extinguishment of cable after the burner has been put out.

Table 9 Summary of environmental test results

| Proto type cable | Property | Original | After heat aging | After γ ray irradiation | | Electrical energizing level during LOCA | After LOCA simulation | | Visual change |
|--|-------------------------------------|---------------------|---------------------|--------------------------------|-----------------------------|---|---------------------------------|-----------------------------|---|
| 600V FR-PH (7c x 2mm ²) | I.R.*1 (MΩ·km) | 2,200 | 6,800 | 6,900 | | 600V | 900 | 0.6 | After LOCA Test, there was not any detectable change of the jacket visually. No cracks when the cable was bent by a small radius which was approximately equal to the cable diameter. |
| | FR-EP T.S.(kg/mm ²) | 0.7 | 0.7 | 0.8 | | | 140 | | |
| | E.I. (%) | 480 | 470 | 90 | | | 2,600V (80V/mil) x 5 minutes | | |
| 600V FR-CH (7c x 2mm ²) | FR-EP T.S.(kg/mm ²) | 1.4 | 1.7 | 2.5 | | 3A | 2,600V (80V/mil) x 5 minutes | 0.9 | Same as above. |
| | XLPE E.I. (%) | 460 | 200 | 40 | | | withstand voltage test (passed) | | |
| | | | 510 | 30 | | | 120 | | |
| 600V FR-PN (7c x 2mm ²) | I.R. (MΩ·km) | 1,600 | 6,500 | 4,900 | | | 850 | 1.0 | After LOCA test, cracks were discovered on some parts of the jacket. |
| | FR-EP T.S.(kg/mm ²) | 1.5 | 1.0 | 2.2 | | | - | | |
| | Neoprene E.I. (%) | 580 | 200 | 20 | | | 10 | | |
| 600V *2 TEFZEL insulated cable (7c x 2mm ²) | I.R. (MΩ·km) | 4.5x10 ⁵ | 5.2x10 ⁵ | 5,300 | | | 4,200 | 4.2 | Nothing. |
| | T.S. (kg/mm ²) | 5.2 | 5.5 | 4.5 | | | 1,300V x 5 minutes (passed) | | |
| | E.I. (%) | 285 | 290 | 0 | | | 0 | | |
| 600V *2 Radiation resistant silicone rubber insulated cable (7c x 2mm ²) | I.R. (MΩ·km) | 5.4x10 ⁴ | 6.8x10 ⁴ | 1.2x10 ⁴ | | | 7,800 | 0.46 | Nothing. |
| | T.S. (kg/mm ²) | 0.95 | 0.98 | 0.48 | | | 3,500V x 5 minutes (passed) | | |
| | E.I. (%) | 450 | 435 | 0 | | | 0 | | |
| 15kV FR-PH (1c x 100mm ²) | I.R. (MΩ·km) | 1.2x10 ⁴ | 3.5x10 ⁴ | 9,500 | 19.6kV x 5 minutes (passed) | 8,600V 270A | 8,400 | 19.6kV x 5 minutes (passed) | Nothing. |
| Coaxial cable (A) RG 59B/u | I.R. (MΩ·km) | 4.6x10 ⁷ | 1.0x10 ⁶ | 1.6x10 ³ | | 600V | 5.5x10 ⁵ | 7.000V x 5 minutes (passed) | Nothing. |
| | Capacitance (nF/km) | 65.3 | 72.4 | 72.4 | | | 71.7 | | |
| | Radiation T.S.(kg/mm ²) | 2.2 | 2.6 | 1.3 | | | 1.0 | | |
| (B) RG 216/u | XLPE E.I. (%) | 620 | 650 | 40 | | | 70 | 2.3x10 ⁵ | 5,000 x 5 min. (pass) |
| | I.R. (MΩ·km) | 7.1x10 ⁶ | 2.2x10 ⁵ | 1.2x10 ⁴ | | | 77.0 | | |
| | Capacitance (nF/km) | 67.5 | 77.5 | 76.9 | | | - | | |
| (C) RG 114/u | I.R. (MΩ·km) | 7.7x10 ⁶ | 7.7x10 ⁵ | 9.9x10 ³ | | | 1.6x10 ⁶ | 2,000V x 5 min. (passed) | 39.7 |
| | Capacitance (nF/km) | 34.7 | 37.8 | 38.2 | | | - | | |

Remark : *1. I.R.: Insulation Resistance

*2. For these two cables, samples for T.S. and E.I. measurements are cut from the insulated wires.

Effect of chemical spray on the degradation of materials

After LOCA test, deterioration e.g. traces of swelling and crazing was found on the surface part of materials, such as FR-XLPE, FR-EP and XLPE, which were directly exposed to steam atmosphere.

However, such a phenomenon was not found on the surface of FR-Hypalon, FR-Neoprene, silicone rubber, and TEFZEL.

Since it was considered that the phenomenon might be due to chemical spray, model experiments using dumbbell specimens were performed under the following conditions.

Specimens: For XLPE, FR-XLPE, FR-EP, and FR-Hypalon dumbbell specimens were cut from 1mm thickness plate of these materials. For each material, unirradiated specimen and irradiated specimen on which 200 Mrads γ -ray was irradiated, were supplied.

Test condition: All specimens were put into an autoclave including an aqueous solution as described below and held for twenty hours in 170°C steam (7kg/cm²G steam pressure). And then they were taken out of the autoclave and the observation of the external appearance and the tension test were carried out.

Solution : Each 100cc of the following three kinds of aqueous solutions was respectively poured into the autoclave to investigate the effect of ingredients in the chemical spray.

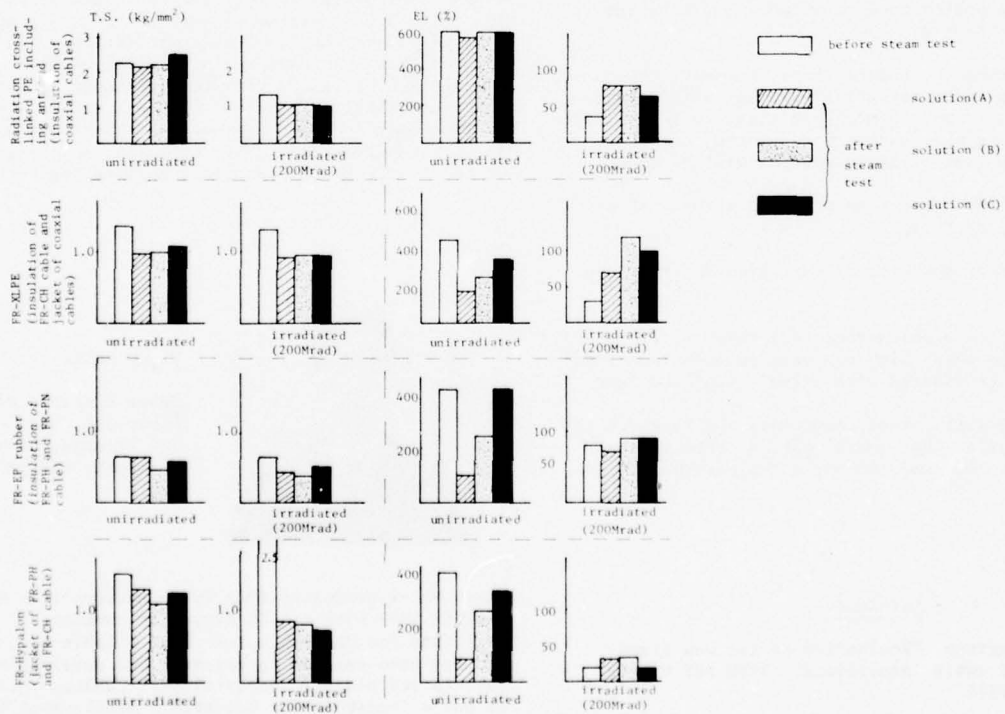


Fig. 14 Effect of elements of chemical spray on the mechanical properties of materials

A: demineralized water

B: 173g H₃BO₃ (0.28 mol/l) and 158g Na₂S₂O₃ 5H₂O (0.064 mol/l) are dissolved into 10L demineralized water.

C: 62g NaOH is added to B solution to adjust the aqueous solution at pH10.
(Chemical spray components in IEEE std 323 attached table)

Results of the tension test are shown in Fig. 14.

With the unirradiated specimens, change of the tensile strength at break and the elongation at break were hardly found for XLPE which contained only little amount of the antioxidant, even after the steam tests including A, B or C solution respectively. With the other three kinds of materials containing considerable amounts of additives, the tensile strength at break and the elongation at break were lowered, and the lowering of elongation at break was largest in the test that use demineralized water (A).

With specimens after the irradiation, there was a tendency of the lowering of tensile strength of each specimen; on the contrary, there was a tendency of the increasing of the elongation.

Comparison with these three kinds of aqueous solutions showed less increase of the elongation in the case of solution C which contain NaOH, as compared to other solutions.

Concerning the external appearances, any detectable change was not found in the unirradiated specimens after the steam test; on the contrary, with the

irradiation specimens except FR-Hypalon, deterioration like swelling and crazing was found, and it was especially remarkable in the case of solution C containing NaOH.

The conclusion of above results is that the deterioration phenomenon is created on the surface part of irradiated specimens, and the deterioration is mainly caused by NaOH in chemical spray.

With specimens examined here, the deterioration occurs on the surface of polyolefines such as PE and EP rubber; but not occur with Hypalon, Neoprene, TEFZEL and silicon rubber.

It is considered that the deterioration is surface deterioration, and does not have large effect on the mechanical properties of the materials by the fact that the elongation at break, which has large effect on the results of the environmental test, reversely increased by the steam tests. It was confirmed by cables such as FR-PH and FR-CH that the deterioration of the insulation did not occur when a jacket layer was used.

The reason that the deterioration is limited only to the surface part, is as follows. When polymer materials were irradiated by γ -ray in air, the degradation of materials is often accelerated in existence of oxygen and is especially remarkable on the surface area in contact with air.⁴

Conclusion

Qualification tests of cables developed for the nuclear power plant were performed on the basis of IEEE std 383. As the test results, it was affirmed that all cables examined have performance required for cables for nuclear power plants.

When considering the future trend, however, these qualification tests may not always be satisfactory, and therefore it may be probable that, in future, the test conditions will become more severe, and additionally, new qualification methods will be added.

And further, there are some problems which must be investigated, as follows.

- o the effect of the kind of radiation and the dose rate
- o the effect of simultaneous test which perform γ -ray irradiation under high temperature and steam conditions, as considered more actual simulated test

In future, we will intend to promote the research for the qualification test positively in order to deal with such problems and improve cable materials.

Reference

- (1) J.W. Robertson "Evaluation of two new flame resistant cable insulations" IEEE PES Winter Meeting 1974
- (2) VAN L. CANADY "Evaluation of radiation resistance of polymer for nuclear power plant application" Raychem corp report No. 73CH0777 - 3EI-17

(3) E.C. Lupton Jr. et al. "Some differences noted in the flammability of wire constructions between testing at room temperature and at elevated conductor temperature" 24th International Wire and Cable Symposium 1975.

(4) M. Kuriyama, J. Ogura et al. "Dose rate effect to radiation degradation of polymers" Meeting of the Institute of Electrical Engineering of Japan 1976 report No. EIM-76-66



JUN-ICHI MATSUO

Showa Electric Wire & Cable Co., Ltd.
1-1 2-chome, Odasakae,
Kawasaki, Kanagawa,
Japan

Jun-ichi Matsuo graduated from Kyoto University in 1957 with a B.Sc degree in electric engineering. Then he joined The Showa Electric Wire & Cable Co., Ltd. and has been engaged in research of high voltage cables, and a technical engineer of high voltage cables. Mr. Matsuo is now a section leader of The Electric Power Engineering Department of Showa Electric Wire & Cable Co., Ltd. or a member of The Institute of Electrical Eng'g of Japan.



MISAO HANAI

Showa Electric Wire & Cable Co., Ltd.
1-1 2-chome, Odasakae,
Kawasaki, Kanagawa,
Japan

Misao Hanai graduated from Tokyo Metropolitan University in 1959 with a B.Sc degree in chemistry. Then he joined The Showa Electric Wire & Cable Co., Ltd. and has been engaged in research and development of rubbers and plastic materials for cables. Mr. Hanai is now a leader of The Research & Development Section of rubber and plastic materials for cables of Showa Electric Wire & Cable Co., Ltd. and a member of The Society of Polymer Science of Japan.



YUUJI YAMAMOTO

Showa Electric Wire &
Cable Co., Ltd.
1-1 2-chome, Odasakae,
Kawasaki, Kanagawa,
Japan



ICHIRO NISHIKAWA

Showa Electric Wire &
Cable Co., Ltd.
1-1 2-chome, Odasakae,
Kawasaki, Kanagawa,
Japan

Yuuji Yamamoto graduated from Musashi Institute of Technology in 1963 with a B.SC degree in electrical engineering. Then he joined The Showa Electric Wire & Cable Co., Ltd. and has been engaged in technical engineering of rubber and plastic cables. Mr. Yamamoto is now a section chief of The Electric Power Engineering Department of Showa Electric Wire & Cable Co., Ltd. and a member of The Institute of Electric Engineering of Japan.

Ichiro Nishikawa graduated from Waseda University in 1969 with a B.SC degree in applied chemistry. Then he joined The Showa Electric Wire & Cable Co., Ltd. and has been engaged in research and development of rubbers and plastics materials for cables. Mr. Nishikawa is now a member of The Research & Development Section of rubber and plastic materials for cables of Showa Electric Wire & Cable Co., Ltd. and a member of The Society of Polymer Science of Japan.



TAKAKO SAKURAI

Showa Electric Wire &
Cable Co., Ltd.
1-1 4-chome,
Minami-Hashimoto
Sagamihara, Kanagawa,
Japan

Takako Sakurai graduated from University of Electro-communications in 1972 with a B.SC degree in applied physics. Then she joined The Showa Electric Wire & Cable Co., Ltd. and has been engaged in research and development of telecommunication cable manufacturing process. Miss Sakurai is now a member of Telecommunication Development Department of Showa Electric Wire & Cable Co., Ltd. and a member of The Institute of Electronics & Communication Engineers of Japan.

SPECIAL TELEPHONE CABLES AGAINST FIRE HAZARDS

G. Beretta

P. Calzolari

Industrie Pirelli S.p.A.

Milan, Italy

ABSTRACT

PVC telephone cables can become a dangerous fire propagation path; therefore special PVC compounds were studied to obtain cables with high self-extinguishing properties and also with the reduction of HCl in the gases emitted when the cables are burnt.

In the first part of the paper new switchboard cables, manufactured with the above mentioned properties, are described and the obtained results are given in comparison with usual Specifications.

In the second part of the paper a single quad 1.3 mm high frequency telephone cable is described, for use in underground railways with a very high safety degree: in case of fire the cable should maintain service continuity, without flame propagation and with low fume emission.

On the experimental lengths of cable many tests were carried out and the results are given in the paper.

1. Special PVC switchboard cable with very high self-extinguishing properties and with low HCl emission in case of fire

1.1 - Introduction

The danger of fire propagation is present where there are cables laid in bundles, particularly in risers. When subjected to the heat produced by a prolonged fire, they can become an extremely dangerous fire propagation path.

In these conditions fire can propagate with speeds of the order of some meters per minute and can produce dense and suffocating fumes. The use of this material, which is well known as having flame retarding properties, does not eliminate the danger described before, when intense heat is present and the cables are laid in a way that favours convection (e.g. cables laid vertically in duct).

In addition to the obvious danger of fire propagation itself, also the opacity and toxicity of the gases produced during fire, are important. Such gases are harmful both for persons and equipment particularly in presence of water or moisture.

A research program aimed at the reduction of the danger described above has been carried out in connection with PVC insulated switchboard telephone cables. The cables here described are the result of this research program.

1.2 - Properties of special switchboard cables

The switchboard cable, object of this research, has the same constructional characteristics of the standard cables used in exchanges and in the private premises for telephone distribution.

Also the physical, mechanical and electrical characteristics of these cables should not differ from the ordinary ones. It is pointed out that the characteristics of the new type must fully comply with the requirements of IEC Spec. 189-2, to which the Italian Standards are harmonized.

Two peculiar qualities of the new cables must be emphasized.

1.2.1 - Non Propagation

The problem of obtaining PVC compounds that do not propagate the flame even in severe fire conditions was already solved some years ago and the final results obtained in Italy were described also in a contribution presented at the 22nd Atlantic City's Symposium¹.

A testing procedure for flame propagation has been established in cooperation with ENEL (Ente Nazionale per l'Energia Elettrica)². This test, which is particularly severe, is carried out in the laboratories of CESI in Milan. (fig. 1)

Now the test has been standardized by CEI (Italian Electrotechnical Committee) and consists in evaluating the amount of fire propagation on a bundle of cables (figs. 2 - 3) having a height of approx 5 m fixed to a vertical steel frame and heated for a period of one hour at a temperature of approx 500°C.

This test is considered as passed if the cables have burnt for a length not greater than 3.5 m or 1.5 m for corresponding quantities of 10 and 5 kg/m respectively of non-metallic material contained in a bundle of cables.

The PVC cables of usual construction, subjected to the same test, burn completely in a few minutes.

1.2.2 - Reduction of toxicity

It is well known that the switchboard PVC insulated cables release fumes containing toxic gases like HCl, CO and CO₂ during fire. The new type of cable insulated and sheathed with special PVC compounds, reduces this danger, firstly as a result of their high self-extinguishing properties; secondly, the new PVC compounds used for insulation and sheaths incorporating special additives, allow a further drastic reduction of HCl emission.

Particularly, the PVC compounds, used for these cables, have an HCl emission which is about 60% lower as compared with standard PVC compounds when they

are tested by an appropriate method 3.

Studies on this subject are under consideration at IEC.

1.3 - Results obtained

Up to now, many km of switchboard telephone cables of the new type are manufactured with the aim of evaluating the possibility of an industrial production; particularly, cables with sizes up to pairs 52, 0.5 and 0.6 mm tinned copper conductor, screen ed and unscreened, are considered.

Many tests have been carried out and the results obtained have been compared with the standard production ones.

The physical characteristics of these cables have

Table 1: Typical measurements carried out on special PVC insulated switchboard cables and characteristics of the insulation and sheathing materials.

| Properties | Test method | Required values | Insulation | Sheath |
|--|-------------|-----------------|----------------|------------------|
| | | | Typical values | |
| Min. tensile strength N/cm ² | | 1250 | 1650 | 1600 |
| Min. elongation at break % | | 125 | 165 | 269 |
| Min. tensile strength after ageing (168 h at 80°C). Percentage of the initial value | IEC 189 | 80 | 80 | 115 |
| Min. elongation at break after ageing (168 h at 80°C). Percentage of the initial value | 1) | 80 | 96 | 112 |
| Cold bend: 2 h at -10°C 16 h at -10°C | IEC 189 | no cracks | no cracks | — |
| Cold flexibility T _f | ASTM D 1043 | | — | no cracks -10 |
| Specific gravity g/cm ³ | | | 1.49 | 1.51 |
| Heat shock (1 h at 150°C) | IEC 189 | no cracks | no cracks | no cracks |
| Min. shrinkage after 15 min. at 150°C % | IEC 189 | 3 | 1 | 1 |
| Oxygen Index O.I. | ASTM D 2863 | | 31 | 30 |
| Max. emission of HCl during combustion % | 2) | | 11 | 13 |
| Resistance to fire propagation | CEI 20-22 | | pass | |
| D.C. voltage test V | | 1500 | pass | |
| Minimum insulation resistance Mohm.km | IEC 189 | 500 | 3900 | |
| Minimum mutual capacitance of any pair nF/km | | 120 | 88 | |

1) Mean of minimum measured values. No one value is out of specified requirements.

2) According to Doc. 18A(Italy)26

been evaluated also after a period of many months to check the influence of a prolonged stocking in an industrial environment.

In Table 1 typical data are given, as obtained by measurements on special cables, in comparison with the relevant requirements of IEC 189-2.

1.4 - Conclusions

The results obtained demonstrate the manufacturing possibilities of special switchboard cables with high self-extinguishing properties, together with the emission of low-toxic fumes in case of prolonged exposure to fire.

The compound formulation allows high extrusion speed of both sheathing and insulation, at a rate comparable with the normal formulations; the use of the new compounds does not affect greatly the switchboard cable cost.

In Italy an extended use of these cables would be possible in many applications, mainly in the exchange distribution.

2. Special high frequency telephone cable, one quad 1.3 mm for underground railway, with a very high degree of safety in case of fire

2.1 - Introduction

In cooperation with technicians of ATM (Milan Tram way and Subway Board), a 1-quad 1.3 mm telephone cable was studied to provide a high safety degree when used in subways and in other similar laying situations (such as for railways and motorway tunnels, underground passages in factories and so on).

This cable, designed for high-frequency long distance communications up to 160 MHz, is screened against electromagnetic noise effects. This cable is also armoured with steel tapes to provide a great mechanical robustness.

The cable construction complies with all the requirements for a laying along an underground railway in open trench or on the walls. Such requirements are flexibility, high robustness, protection against rodent attack and electromagnetic noise.

The cable is manufactured with special compounds to obtain the following main properties in case of fire:

- Continuity of service (telephone and data transmission) up to the replacement of the damaged parts
- Non-propagation of flame
- Low fume emission

The design of this cable and the trial phase, carried out during 76/77, mainly had the aim of verifying the properties described above.

2.2 - Cable characteristics

The cable characteristics are given in Table 2.

Table 2: Constructional details of special telephone cable one quad 1.3 mm (fig.12)

- a) Conductor
Annealed copper wire, diam 1.3 mm
- b) Insulation
Special silicone rubber
- c) Fire proofing textile protection over each insulated conductor
- d) Quadding
- e) Wrapping
Fire proofing tape
- f) Inner sheath
Special silicone rubber
- g) Screening
Copper tape 0.1 mm thick
- h) Wrapping
Special non-burning tape
- i) Armouring
2 steel tapes 0.2 mm thick
- j) Outer sheath
Self-extinguishing special PE compound with very low fume emission in case of fire
 - Inner sheath: outer diam. approx 15 mm
 - Copper screen: outer diam. approx 16 mm
 - Cable outer diam. approx 24 mm
 - Weight per km approx 900 kg
 - Nominal length: 500 m
 - Delivery on standard wooden drums

The electrical characteristics are given in Tab. 3

Table 3: Electrical characteristics of special telephone cable one quad 1.3 mm

- a) Electrical D.C. resistance
at 20°C max 14. = ohm.km
- b) Nominal mutual capacitance 43 nF/km
- c) D.C. voltage test between conductors with earthed screen (duration: 1 min.) 1500 V
- d) Insulation resistance min 1000 Mohm.km
- e) N.E.X.T. at 160 kHz more than 56 dB/230 m*
- f) F.E.X.T. (equal level)
at 160 kHz more than 68 dB/230 m*
- g) Typical values:
 - Attenuation at 20°C
 - Frequency
 - Characteristic impedance at 20°C

| | | | |
|---------------------|------------|------------|------------|
| Frequency | 60 kHz | 120 kHz | 160 kHz |
| Attenuation at 20°C | 1.55 dB/km | 2.20 dB/km | 2.40 dB/km |
| Impedance at 20°C | 142 ohm | 139 ohm | 138 ohm |

* In accordance with CCITT Green Book Vol. III Rec. G 321.

It is pointed out that the outer sheath is manufactured by extrusion of a special thermoplastic compound, based on a PE copolymer basis, non flame propagating and with low emission of toxic fumes in case of fire.

The latter characteristic is very important for the safety in tunnels where the emission of dense and suffocating fumes in large quantities could create danger for persons and difficulties for emergency interventions.

Many laboratory and field tests were carried out also with fire simulation to evaluate the cable behaviour.

2.3 - Jointing

A joint was designed to withstand mechanical strains and very high temperatures when subjected to a direct fire. Fig. 4 shows the joint and also its constructional details.

2.4 - Measurements program

In the following Table the tests carried out in laboratory are listed.

Table 4: Laboratory tests

a) Electrical characteristics of the cable

Conductor resistance

Insulation resistance

Voltage test

Mutual capacitance

N.E.X.T. and F.E.X.T.

b) Physical and mechanical characteristics of the insulation and sheath

Tensile strength

Elongation

Cold flexibility

Oxygen Index

Fume Emission

Water absorption (only for the sheath)

Burning field test

A first field test was carried out on a complete length of cable, a part of which approx 6 m long, including a complete joint, was put to fire in a trough with alcohol flame for at least 30 minutes.

(figs. 5 - 6 - 7)

At the end of the test the fire was extinguished by

the water of a fire hose directly launched on the cable and the joint contained in the trough.
(figs. 8 - 9)

During and at the end of the test the following parameters were checked:

- Conductor resistance
- Dielectric strength
- Insulation resistance
- N.E.X.T. and F.E.X.T.
- Characteristic impedance

A second test was carried out, as indicated above, after laying the cable for about 150 m along the rails, to check the transmission behaviour.

(fig. 10)

Data were transmitted on one pair at a rate of 1200 bit/sec (with level of 40 dBm) and the error rate was checked.

On the other pair remote controls were transmitted at a rate of 9600 baud and with frequency modulation (95 and 105 kHz with max signal amplitude of 2 V).

Bending tests and impact tests were carried out on samples taken from the burnt cable.

The sample was completely bent at least 5 times on a mandrel with 50 cm diameter and during the test a D.C. voltage of 1000 V was applied between the conductors.

In the impact test a shaped tool with a mass of 2.8 kg was dropped on the burnt cable from a height of 1 m.

A D.C. voltage of 200 V was applied during the impact test between conductors to check the short circuit.

2.5 - Measurements results

- Electrical characteristics

The measurements fully comply with the values given in Table 3.

- Physical characteristics

The insulation and outer sheath characteristics are given in Table 5.

Burning field tests

The duration of the two tests was respectively of approx 45 and 35 minutes.

- The outer sheath is completely burnt by fire but with very low fume emission and without flame propagation outside the trough.

- A low quantity of white smoke is developed only after approx 15 min. when the inner insulation material is fired.

- The electrical parameters, that is, conductor and insulation resistance, N.E.X.T. and F.E.X.T., im

Table 5: Typical characteristics of silicone rubber insulation and polyethylene ther thermoplastic sheath, as determined on some experimental lengths

| Properties | | Silicone rubber insulation | Thermoplastic sheath |
|--|-------------------|----------------------------|----------------------|
| Tensile strength, min | N/cm ² | 700 | 500 |
| Elongation at break, min after ageing (240 h at 200°C) | % | 270 | 350 |
| T.S., percentage of initial value, min | | 70 | - |
| E.B., percentage of initial value, min after ageing (160 h at 80°C) | | 70 | - |
| T.S., percentage of initial value, min | | - | 70 |
| E.B., percentage of initial value, min | | - | 70 |
| Oxygen Index, min | O.I. | 22 | 34 |
| Smoke Evolution, max | Dm | 118 | 82 |
| Water Absorption, after 2 h in boiling water, max mg/cm ² | | - | 5 |
| Specific Gravity, | g/cm ³ | 1.2 | 1.50 |

T.S. and E.B. - Tensile Strength and Elongation at Break ASTM D 638

Oxygen Index ASTM D 2863

Dm = Specific Optical Density - NBS Smoke Density Chamber Flaming Mode

Water Absorption ASTM D 570

(fig. 11)

pedance are comparable with the original ones with no practical differences.

- The bending test does not reveal short circuits.
- The impact test reveals short circuits only after 30 impacts.
- During the transmission test no troubles affected the quality of the transmitted remote controls and the error rate was at the normal level.

Conclusions

After the trial phase a possible application of this cable is under consideration not only for the existing underground railways, but mainly for the new ones planned in some of the most important Italian towns.

Acknowledgments

The Authors wish to thank the management of Industrie Pirelli S.p.A. for the kind permission to publish this paper.

A very important contribution to the experimental work, described in the second part of the paper, was given by A.T.M. and also by S.I.R.T.I. - Milan that designed the joint and carried out the electrical field test.

References

- 1) G. Beretta-P. Calzolari "Self-extinguishing PVC for telephone and signalling cables" - 22nd Atlantic City's Symposium
- 2) Specifications "Norme CEI 20 - 22: Prova dei ca vi non propaganti l'incendio"
- 3) Document 18A(Italy)26:"Italian proposal of test method and requirement for the maximum allowable development of hydrochloric acid by sheathing compounds under fire conditions"

Dr. G. Beretta
Dir. Ricerca e Sviluppo Cavi
Industrie Pirelli S.p.A., Milan (Italy)
Director of Special and Low Voltage Cables Group

Born in 1930. He received his degree in chemistry at the University of Pavia in 1955.
In 1957 he gained the Research Laboratories of Industrie Pirelli S.p.A. where he has been involved in research into insulating materials for cables.



Ing. P. Calzolari
Dir. Progettazione Telecomunicazioni
Industrie Pirelli S.p.A., Milan (Italy)
Director of the Telephone Cable Planning and Development Department

Born in 1931. He has a master degree in Electrical Engineering achieved at the University of Bologna.
He has been with Pirelli since 1956.



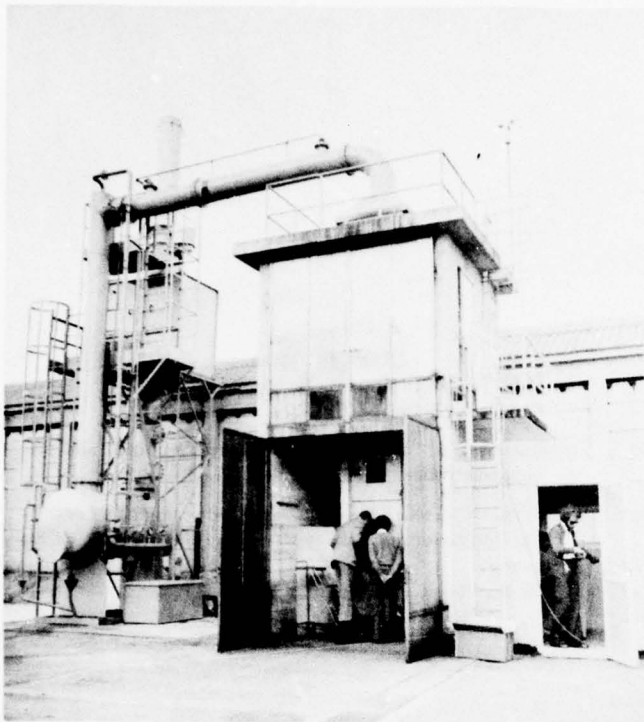


Fig. 1 - Test ring where cables are fired
and flame propagation is measured

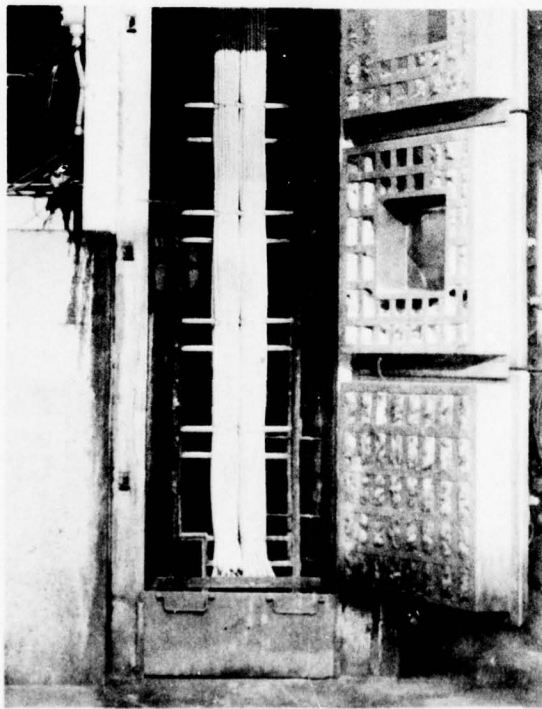


Fig. 2 - Cable arrangement before the test

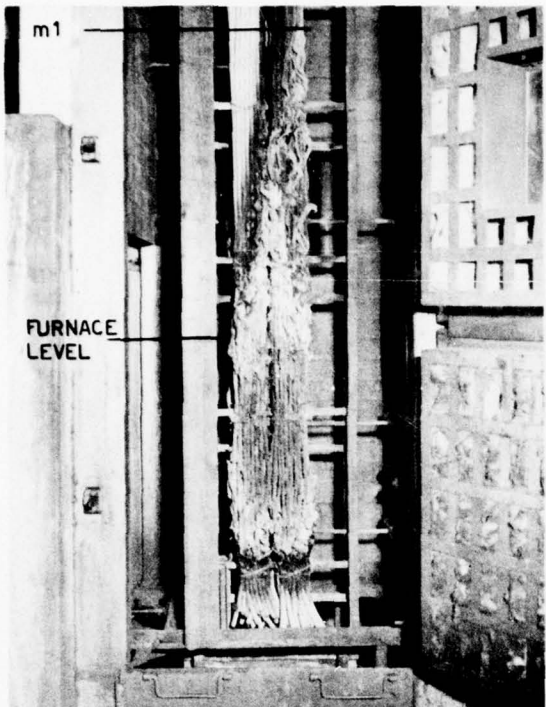
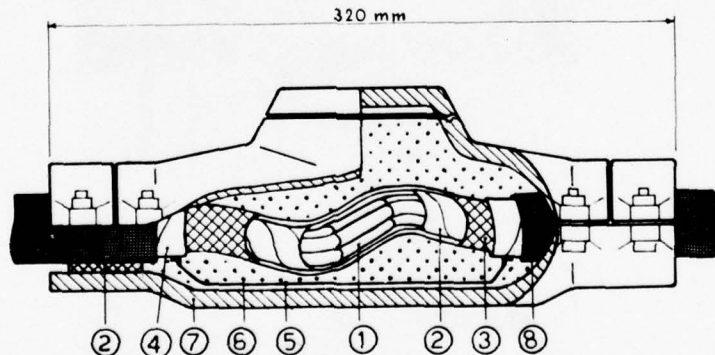


Fig. 3 - Cables after fire test



Fig. 5 - Burning field test
Detail: the joint is burning



- | | |
|------------------------|--------------------------------|
| ① conductor splice | ⑤ continuity armour wire |
| ② glass tape | ⑥ silicone filling compound |
| ③ copper tape | ⑦ iron-cast sleeve |
| ④ steel tape armouring | ⑧ special thermoplastic sheath |

Fig. 4 - Cable joint



Fig. 6 - Burning field test
Detail: the cable is burning



Fig. 7 - Burning field test
Cable and joint are burning

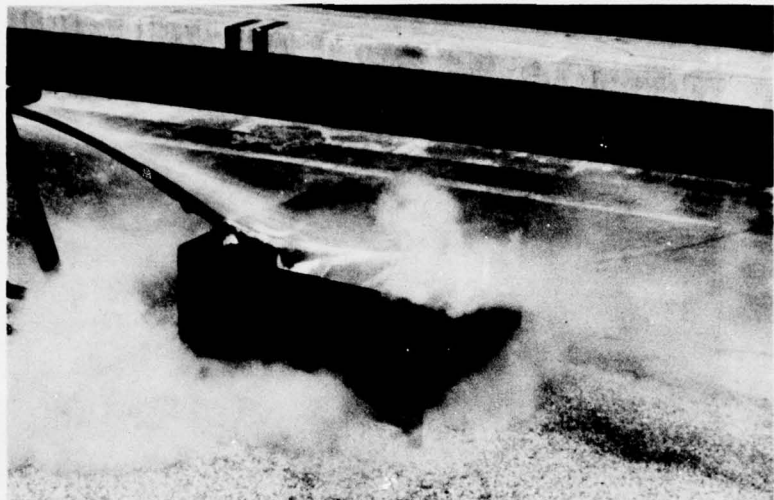


Fig. 8 - Fire extinguished

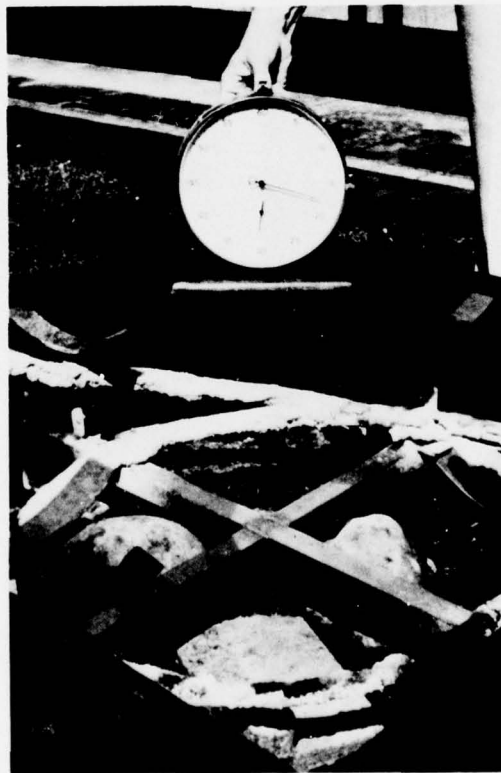


Fig. 9 - The cable after fire extinction

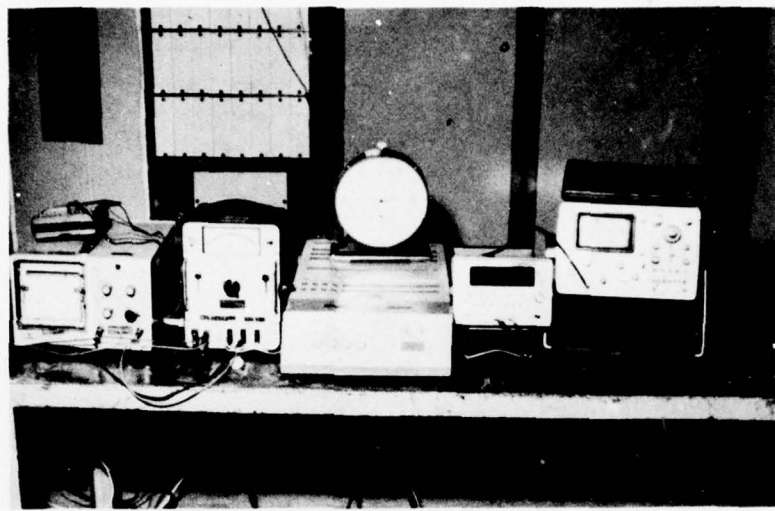


Fig. 10 - The equipments for data transmission and control

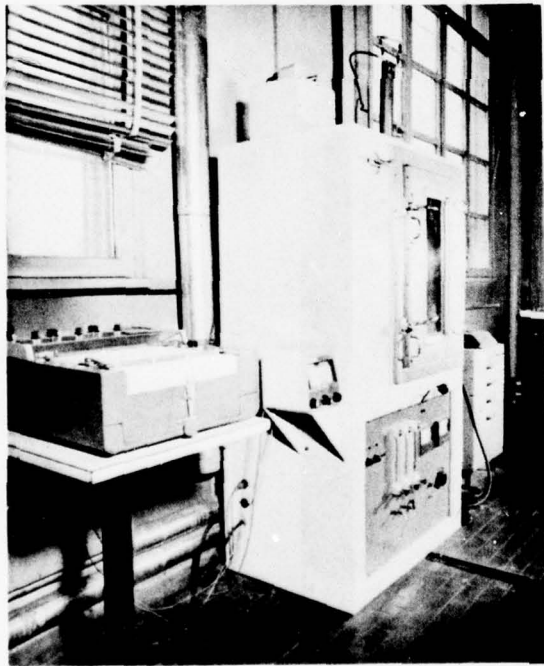


Fig. 11 - NBS Smoke Density Chamber Flaming Mode



Fig. 12 - Special high frequency telephone cable
one quad 1.3 mm

PERFORMANCE OF FLUOROPOLYMER WIRE AND CABLE INSULATION IN LARGE SCALE TESTS FOR FLAMMABILITY, SMOKE, CORROSIVE OFF-GASES AND CIRCUIT INTEGRITY

E. W. Fasig, Jr., D. B. Allen, J. C. Reed

Plastic Products and Resins Department
E. I. du Pont de Nemours & Co., Inc., Wilmington, Delaware

Large scale fire tests are described and results are reported that illustrate the advantages of fluoropolymers in resistance to flame propagation, low evolution of corrosive off-gases, and low smoke production. Cables that maintain circuit integrity in long term flame exposure are described; testing results, cost and property trade offs are given.

INTRODUCTION

In recent years, greater emphasis has been placed on analyzing the overall hazards of using one or another material as insulation for wire and cable. As a result, specifiers and users are demanding more information on performance characteristics such as flammability, aging, evolution of smoke and corrosive off-gases, and fuel value (heat of combustion).

This paper deals with tests and results obtained in evaluating flammability, smoke generation and corrosive off-gases. It also includes information on materials which help provide insight into performance of various insulations in these areas.

FIRE SAFETY

Studies are now underway that seek to quantify and mathematically describe uncontrolled fires in buildings, transit vehicles, and aircraft. Until such work results in reliable models which can be used to analyze overall hazards, industry is faced with the need to make judgments on the basis of tests which have limited scope. Designers must take into account properties of materials and use realistic tests to help predict behavior in a fire that may occur at any time in the design life of a facility (power plant, factory), transit car or aircraft. Concerning wire and cable, the following factors bear directly on the question of fire safety:

- Insulations should resist burning. As part of this equation, insulations should have oxygen indices above ambient levels, high flash and auto-ignition temperatures, and demonstrable flame retardancy.

- Once exposed to fire, insulations should contribute little as a fuel source (low heat of combustion).
- Insulation weight should be minimized. Thin insulations over the smallest practical conductor size offer one solution. Using multiplexing where applicable saves on the number of circuits actually needed.
- Properties of the insulation should not change with time. The logical choice is to use materials with inherent thermal stability and fire retardance over those made useful only after extensive compounding.
- Overall costs must be considered. Cables used extensively 10 years ago in some industries are now considered unacceptable because their safety performance is considered inferior by today's standards. Responsible designers shun their use even though their purchase cost is low. A good example of the protection afforded by newer designs can be seen in the nuclear power industry.

Higher prices for better cable designs may add a fraction of a percent to construction costs but save millions of dollars in costs and lost revenues by preventing the spread of fire. Some of these concepts are illustrated in Table I.

The example shows how proper design can take advantage of thin walls, low fuel value and a high temperature index (ampacity) to save about 84 percent of the fuel load per foot of tray in a plant. Similar analyses can be done to show safety advantages in transit cars, aircraft and occupied spaces.

FIRE TESTS

There is no universally acceptable test but there are some tests which appear to have merit. Again, a rationale should be used to choose realistic fire exposures:

- Specimens in the test should closely match those

in actual use. Reasonably long lengths of multi conductor cables in horizontal and vertical runs should be tested if this is how an actual facility is to be wired. Conversely, if analysis shows that a high concentration of single wires in a vulnerable location represents a real hazard, tests on single wires or unjacketed bundles may be needed.

- Fire sources should be quantified, reproducible and available at a variety of locations.
- Large- or full-scale tests should receive greater weighting than small, bench-scale analyses. Tests of a single wire stretched horizontally or at some angle may give a false idea of performance of cables in a filled tray.

Among several tests that appear to meet reasonable criteria are the modified ASTM E-84 tunnel test covered at last year's Symposium⁽¹⁾ and the vertical tray test of IEEE 383. Both use large samples and high output flame sources. Modifications to the IEEE test add even more stringent demands including still higher flame size, corner location, and higher density of cables.

To illustrate the effects of such tests, Du Pont ran a cooperative study with General Electric Nuclear Energy Division in September 1976, and a full report was issued on the results.⁽²⁾ Comparative tests were conducted on cables insulated with Tefzel® fluoropolymer and a representative cross-linked, flame-retarded polyethylene (XLPE-FR). Table 2 lists these tests and illustrates the variables considered.

- Location in a corner for vertical tests (chimney effect).
- Vertical and horizontal tests with cables spaced one-half cable diameter apart (per IEEE 383).
- Flame sources of 210,000 and 400,000 British Thermal Units (BTU) per hour, premixed gas and air for vertical tests; 300,000 BTU/hr. diffusion gas flame, horizontal tests.
- Spacing between cable tray and flame source in vertical tests according to flame intensity.

- Orientation of the vertical tray with either the rungs facing toward the fire or away from it.

We found large differences in performance in this series of tests. Figures 1-4 show how adjusting conditions in vertical tests intensified the damage to cables using the same premixed gas flames. The results agree with the general concepts on fire safety listed earlier. In the case of "Tefzel" fluoropolymer, less damage was sustained, fewer pounds of jacket and insulation were consumed, and flame height above the source was less. This material is used in thin insulations and has a low fuel value (6,100 BTU/lb.), an oxygen index of about 30, a 150 temperature index, high flash and auto-ignition temperatures (1,026°F and 1,028°F, respectively), and exhibits these properties without compounding.

In the horizontal test, we gained new insights not predicted by the vertical tests. Both "Tefzel" and the XLPE-FR are quoted as having oxygen indices about 30. Yet, the inherently high fuel value of polyethylene (20,000 BTU/lb.) overshadowed the beneficial effects of compounding. Damage to "Tefzel" was limited to an area just beyond the 4-1/2 foot long igniter flame. Flame travel during the 20-minute test ran only 3-1/2 feet past the flame source while the XLPE-FR carried flames 17.5 feet, which was within two feet of the end of the 25 foot tunnel. The XLPE-FR cables were fully involved and burned completely after the end of the test period. Results are shown in Table 3. Table 4 lists data on other constructions tested earlier in 15 minute exposures. Note that both "Teflon" fluorocarbon (OI > 95) and "Tefzel" fluoropolymer, performed about the same.

Another set of tests were conducted on "Tefzel" at Southwest Research Institute in San Antonio, Texas in March 1977. In these tests, filled trays (40 percent theoretical based on cross-sectional areas of cables and trays) were tested using a variable output flame source. Trays were placed in a corner and reached from floor to ceiling, a distance of 12 feet. Silicone fire seals were installed at the top and bottom to simulate penetrations through the floor and ceiling. The test design was according to a fire scenario developed by G. E. Nuclear, its architect/engineer, C. F. Braun, and Southwest Research Institute (SwRI). Solid trays were used in the four tests. In two of these the lower half of the front cover was removed exposing cables to the fire source. Instruments measured temperatures in up to 14 locations, including the flame, and composition of off gases, i.e. CO, CO₂, O₂, hydrocarbons, in the closed tray test. The latter showed conditions within the trays where no visual record was available.

On the advice of SwRI, the fire sources were wooden cribs. These are widely used and understood by fire protection engineers, are covered in standards, and can

be duplicated in many laboratories. SwRI measured the heat evolved in a room-sized calorimeter. Figures 5 and 6 reveal these cribs liberate intense heat. In one case, heat was measured at 360,000 BTU/hr. with an average of about 300,000 BTU/hr. for 15 or so minutes in the 20 minute tests.⁽³⁾

Several concerns were addressed in these tests. Would heat build up in closed trays when exposed to externally applied flame. Would full tray tests with random cable fill be more difficult to pass than those with cables spaced as in IEEE 383. Finally, would the corner location intensify the severity of exposure by the natural chimney effect. The results answer these questions.

Figures 7 through 10 show typical test setups and results. Table 5 shows that even in the most severe case (test #3), cables exposed to the flames were damaged to a height of less than four feet but there was no propagation after the fire source was removed. With the cover on, damage was limited to only those cables in direct contact with the cover and only to a height of 16 inches.

CORROSION

This is an area of concern where instruments can be damaged in an emergency or where liberated off-gases are considered a stress-cracking hazard to stainless steel vessels and piping. In the September 1977 tests, we sought to measure the corrosive effects of off-gases generated by burning cable insulations. As shown in Figure 11, test coupons of stainless steel and copper were placed in locations exposed to off-gases in the vertical tray tests. Others were placed at the end of the 25 foot tunnel (modified ASTM E-84). In all cases, corrosive damage to the coupons was less with "Tefzel" fluoropolymer even though this material contains 62.5 percent by weight fluorine. These results are most probably related to the following:

- Halogens in "Tefzel" are an integral part of the structure which is highly resistant to breakdown.
- Evolved halides from thermal and flame exposure are low in "Tefzel". By contrast, flame retardants added to rubber, polyethylene, polyvinyl-chloride (PVC), and other materials are inherently thermally unstable. They release halogen containing gases in high temperature exposures to quench the flames.
- Less "Tefzel" was available to be burned and less was consumed using identical flame exposure conditions.

Results are shown in Figure 12 for copper coupons at the top center location in vertical tests. Coupons at all locations showed weight loss with about the same ratio, "Tefzel" versus the XLPE-FR. Damage to the stainless steel was less and all coupons to the side of the vertical trays sustained less damage than those closer to the rising

column of gases above the flame source.

Two other examples of tests for corrosive off-gases are detailed below:

Copper Mirror Test: Industry specifications often call for "copper mirror" tests in which corrosive gases from heated materials are allowed to condense on a copper surfaced glass specimen. In a typical test, "Tefzel" and "Teflon" fluorocarbon resins caused no discoloration or removal of copper at 175°C for 16 hours. By contrast, two widely used rubbers removed 50 percent of the copper and PVC took it all off. Even at 250°C, there was little or no copper removal with "Teflon" fluorocarbon or "Tefzel" fluoropolymer, only slight discoloration.

Pyrolysis: Compared with PVC and two other halogen containing plastics, "Tefzel" liberated lower detectable halides when heated to 400°F in air (15 ml./min.) at 5°C per minute heat rise. At 200°C, the PVC had evolved 0.1 milligram HCl hydrogen chloride per gram of sample. By the time 400°C had been reached, PVC had liberated 70 milligrams per gram (mg./gm.). One of the halogen containing plastics yielded 30 mg./gm. detectable fluoride ions and the other, 47 mg./gm. of combined fluoride and chloride ions. "Tefzel" at 400°C had liberated only 1.5 mg./gm. detectable fluoride.

There is a final area of discussion that is important—the distinction between stress-cracking which has been induced by various halides. It is widely documented that chloride ions cause stress-cracking in unsensitized austenitic stainless steels even in concentrations as low as 1 part per million (ppm). By contrast, Ward, Mathis, and Staehle⁽⁴⁾ showed stress-cracking with fluoride ions did not occur without sensitizing austenitic stainless steel. They listed one or more of the following as prerequisites to stress-cracking with fluoride ions:

- Tensile stress, applied or residual;
- Cold work, with or without appreciable residual macro stress;
- A crevice;
- Visible oxide film formed by elevated temperature exposure in air.

They reported that no attack occurred on annealed specimens and drew distinctions between the mode of attack with fluoride ions compared with chloride ions.

Theus and Cels⁽⁵⁾ showed that fluoride ion stress-cracking of sensitized 304 stainless occurs only under acidic conditions and depends on the concentration (their "open circuit potential" data). No cracking occurred with 1 ppm fluoride ion from pH of one to eight. With 10 ppm, no cracking occurred above pH of

0.75. It took 100 ppm to cause cracking between pH of 0.75 to 2.5, and 1,000 ppm between pH of 2.5 to 3.5. Above pH of 3.5, even 1,000 ppm of fluoride ions failed to cause cracking. In no case did unsensitized samples crack.

Du Pont conducted similar studies as shown below:

• Samples

- Strip of 304 stainless steel bent into a "C" and clamped in that position; stress on the outside radius was 110 percent of yield.
- Sensitized 304 plate with weld bead deposited on it.
- Unsensitized 304 plate with weld bead.

• Conditions

Thermal: Rapid rise to 143°C; hold for 17 minutes; decline over 2.8 hours to 65°C; hold at 65°C for seven months.

- Environment: pH from 2.2 - 9.35; borated solution (0-2,000 ppm); fluoride ion concentration, 0-1,000 ppm in water.

• Results

- No cracking under any conditions.
- Intergranular attack, only, at two of 16 conditions -- and then only on the "C" ring (2.2 and 4.2 pH, 1,000 ppm fluoride ion, no borate solution).

One last point: We are not aware of cases in which fluoride ions were suspected of being a problem except where chloride ions also were present. The latter probably could have been the cause.

SMOKE

Results are widely available on various materials tested according to National Fire Protection Association (NFPA) 258-T ("NBS smoke chamber"), the Rohm & Haas XP-2 chamber, and a method advanced by Arapahoe Chemicals Corp.⁽⁶⁾ In this paper, we concern ourselves only with the relative performance of various materials in a variety of tests using the modified ASTM E-84 tunnel test. Data in Table 6 list results for 15- and 20-minute exposures of various insulations with values expressed as percentages of the smoke evolved by a standard red oak sample in the normal E-84, 10-minute test. Figure 13 shows a graphical comparison in one test between "Tefzel" fluoropolymer and XLPE-FR. The area under each curve was used to calculate percentages in each case. As shown in Table 6, smoke produced by "Tefzel" or "Teflon" fluorocarbon was considerably lower than that from the

other materials listed.

OTHER

Other questions apply in the choice of electrical insulations which have not been addressed in this paper. As a sidelight, however, we ran a series of tests to study one other performance characteristic in emergency situations, circuit integrity. Because of their bulk and cross-linked nature, cables insulated with conventional rubbers and XLPE-FR show some time delay before electrical failure of conductors exposed to flames. However, it is also recognized that the thermosets, once involved, can enter the "deep seated" burning mode in which they exhibit afterglow or continue to propagate as live embers even when the fire source is removed. Such behavior is distinctly different from what we found in our tests on "Teflon" and "Tefzel". For example, in vertical fire tests, we found that "Teflon" and "Tefzel" were damaged in the area of intense flame but, just inches above that, insulations were functional. The total area damaged was limited. There was no afterglow to cause re-ignition or propagation as glowing embers, and the height of the flames was less than that for XLPE-FR in one set of tests (Figure 1). In the modified ASTM F-84 test, we found that cables insulated with "Teflon" fluorocarbon and "Tefzel" fluoropolymer burned in the fire zone and beyond to a distance of about a foot. Yet, material fully engulfed in fire as far as 3-1/2 feet past the igniter flame was sound. Data reported by Sandia Laboratories⁽⁷⁾ on horizontal filled tray test indicated temperatures of cables involved in flames 10-1/2 inches above the source registered only 300°F while the flame temperature registered 1800°F. Mere exposure to fire does not mean cables undergo damage. The severity of exposure, including fuel contributed by the insulation, helps to determine the extent of damage.

Another factor in this question is design. Critical circuits should be duplicated in remote locations to prevent loss of function. Critical leads in a transit vehicle, for instance, could be damaged by collision, failure of other components, or vandalism as well as by fire. Redundant circuits in remote locations could pick up the function. This practice is widely used in the design of nuclear power plants as defined in Regulatory Guides of the U.S. Nuclear Regulatory Commission.

Nevertheless, we did some work in this area and had cables produced and tested to demonstrate extended circuit integrity. Successful candidates had mica tapes applied to the conductors followed by insulation with "Teflon" or "Tefzel". Multi-conductor cables were then fabricated and jacketed with the same resin as used on the primaries. These cables endured up to one hour of flame exposure at 210,000 BTU/hr. in the same vertical test described earlier (13-1/2 inch spacing). Cables maintained circuit function even after being forcefully struck and deformed. Only when a metal object was rammed into individual cables could shorts be

produced. These tests show that, where necessary, cables that combine extended circuit integrity, the thin insulation and safety benefits of "Teflon" and "Tefzel" can be employed.

CONCLUSION

This paper is intended as a review of safety factors and tests to demonstrate performance in fire or other emergency situations. The subjects are of current interest but do not represent a complete analysis of hazards and safety-related items. We feel intelligent design must address other subjects, as well, and urge that all adoptions of one or another cable insulation be made on a sound analysis of hazards, useful life, and overall benefits related to costs.

REFERENCES

- (1) "A Test Method for Measuring and Classifying the Flame Spreading and Smoke Generating Characteristics of Communications Cable", J. R. Beyreis, J.W.Skjor-dahl, Underwriters Laboratories and S. Kaufman, W. M. Yocom, Bell Laboratories; 25th Annual Wire and Cable Symposium, Cherry Hill, N.J., November 16-18, 1976.
- (2) "Fire Tests - Insulated Wire and Cable", tests sponsored by General Electric Nuclear Energy Systems Division and E.I. Du Pont de Nemours & Co., Inc., conducted September 27-29, 1976; report issued January 1977 by Joseph R. Perkins, Du Pont and Paul J. Ryan, Sr., General Electric.
- (3) "Fire Tests on "Tefzel" Insulated Cables", William R. Herrera, Jesse J. Beitel, Final Report Project No. 03-4685-115, Southwest Research Institute, March 1977, PP. 12 and 13.
- (4) C. T. Ward, D. L. Mathis, and R. W. Staehle, Corrosion 25 (1969) page 394.
- (5) Technical paper presented to the Electrochemical Society Meeting, N.Y., N.Y., October 13-17, 1974: "Fluoride Induced Intergranular Stress Corrosion Cracking of Type 304 Stainless Steel", G. J. Theus and J. R. Cels.
- (6) New Smoke Test - Fast, Simple, Repeatable, Jack Kracklauer, Charles Sparkes, Rod Legg, Plastics Technology, March 1976
- (7) Leo Klamerus, Sandia Laboratories, report to the Insulated Conductors Committee of the Power Engineering Society of the Institute of Electrical and Electronic Engineers, April 13, 1977.

EDWARD W. FASIG, JR.
Senior Marketing Representative
Fluorocarbons Division
Plastic Products and Resins Department
E. I. du Pont de Nemours & Co., Inc.
Wilmington DE 19898

Edgar W. Fasig, Jr., Senior Marketing Specialist in the Fluorocarbons Division of Du Pont's Plastic Products and Resins Department, joined Du Pont in 1963 as a chemical engineer in the former Plastics Department's Research and Development Division. He has held a variety of jobs in technical services and marketing, including assignments in the Los Angeles and Chicago District Sales Offices. In 1976, he was made a Senior Marketing Representative handling developing markets for fluorocarbon products, film and tubing. Mr. Fasig holds B.S. and M.S. degrees in chemical engineering from Ohio State University.



DAVID B. ALLEN
Senior Marketing Specialist
Fluorocarbons Division
Plastic Products and Resins Department
E. I. du Pont de Nemours & Co., Inc.
Wilmington DE 19898

David B. Allen, Senior Marketing Specialist in the Fluorocarbons Division of Du Pont's Plastic Products and Resins Department, joined Du Pont in 1954 as a salesman. He has held a variety of assignments in technical services and marketing in Chicago, New York, Washington, D.C., before returning to Wilmington to his present assignment. In 1976, he was made a Senior Development Specialist in Fluorocarbons and the following year was made a Senior Marketing Specialist for Fluorocarbon products. Mr. Allen holds a B.S. degree in chemistry from Georgetown University.



JOSEPH C. REED
Technical Specialist
Fluorocarbons Division
Plastic Products and Resins Department
E. I. du Pont de Nemours & Co., Inc.
Wilmington DE 19898

Joseph C. Reed, Technical Specialist in the Fluorocarbons Division of Du Pont's Plastic Products and Resins Department, joined Du Pont in 1948 as a power supervisor at the company's Belle, W. Va., plant. He has held a variety of assignments in the company's Plastic Products and Resins Department including instrument engineer and supervisor, technical representative and marketing analyst. In 1976, he was made a Technical Specialist working with Du Pont's Fluorocarbon products. Mr. Reed holds a B.S. degree in electrical engineering and M.S. degree in power and fuel engineering from Virginia Polytechnic Institute and State University.



Figure 1
Flame Height
(Modified IEEE 383 Flame Test)

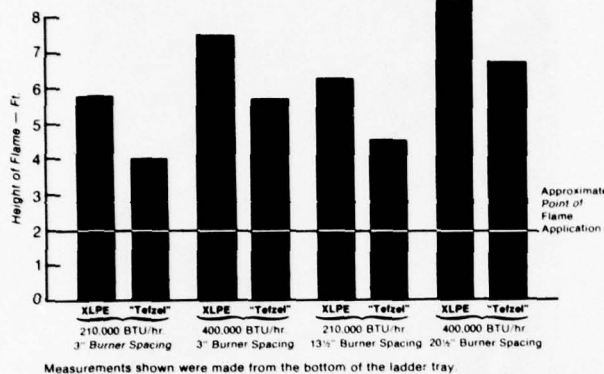


Figure 4
IEEE 383 Test
(Modified) Comparison of Results

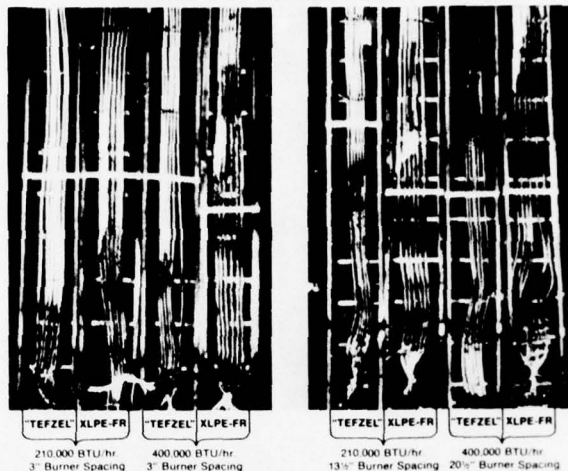


Figure 2
Length Burned
(Modified IEEE 383 Flame Test)

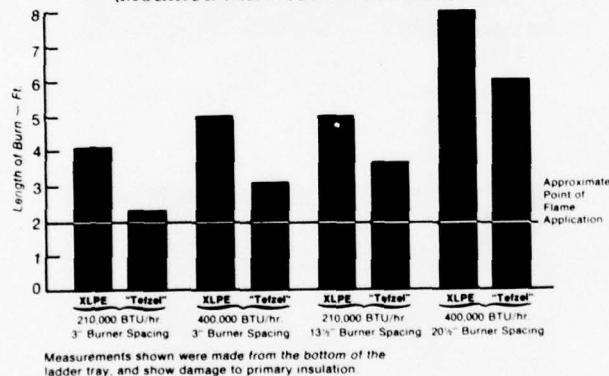


Figure 5
**Energetics of Burning Crib Test 22.4 lbs.
03/09/77**

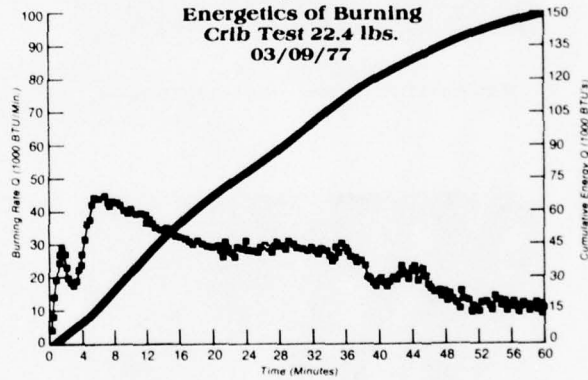


Figure 3
Weight Burned (Jacket + Primary)
(Modified IEEE 383 Flame Test)

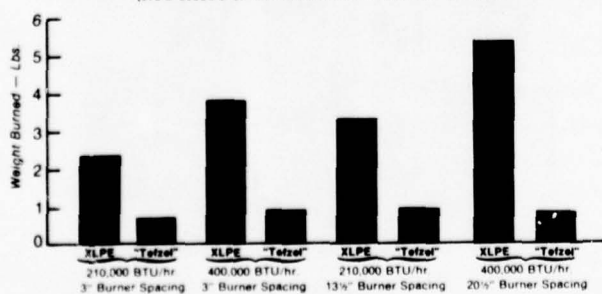
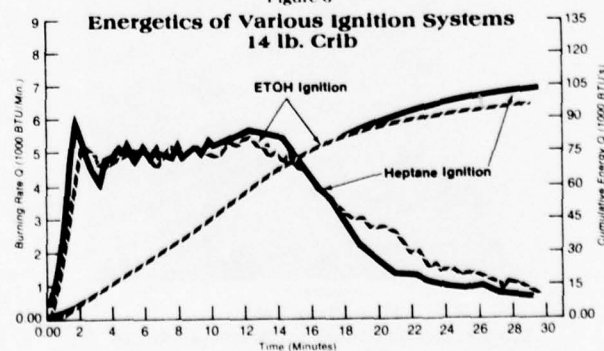


Figure 6
**Energetics of Various Ignition Systems
14 lb. Crib**



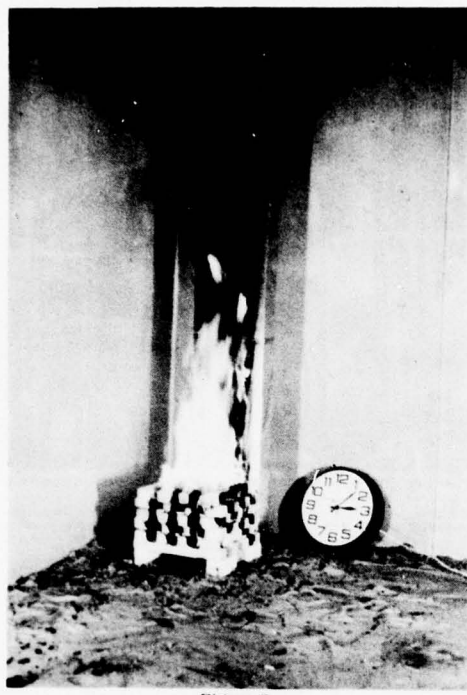


Figure 7
Filled Tray Test
14 lb. Wood Crib — Lower Half of Cover Removed



Figure 9
Filled Tray Test
14 lb. Wood Crib — Tray Fully Covered



Figure 8
Filled Tray Test
Damage to Cables During the 20 Minute Exposure

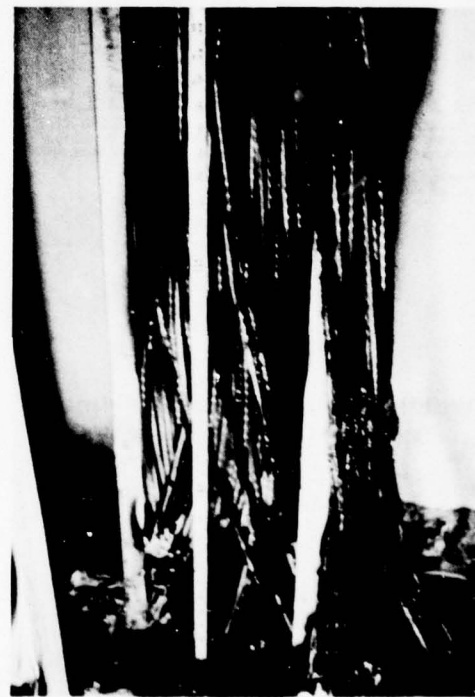


Figure 10
Filled Tray Test
Limited Damage to Cables in Fully Closed Tray

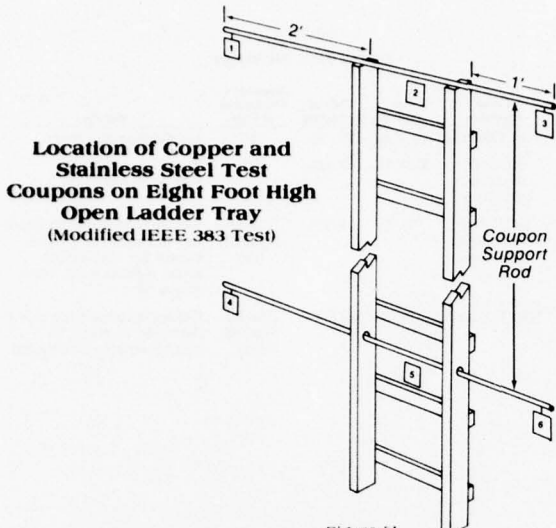


Figure 11

Figure 12
Corrosion (Modified IEEE 383 Flame Test)
(Copper Exposed to Offgases from Burning Insulation)

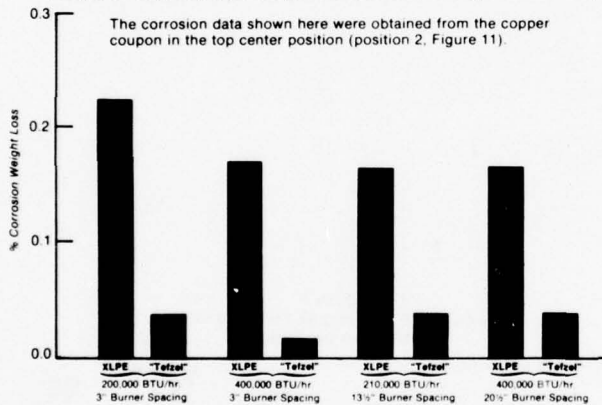


Table 1
Effects of Designing Around Materials
Properties to Lower Fuel Load

| | "Tefzel" | Typical XLPE |
|----------------------------------|----------|--------------|
| Conductor size, AWG | 12 | 10 |
| Number of 19/C cables in tray | 36 | 36 |
| Conductor ampacity, amperes | 7.5 | 6.2 |
| Comparative cross section area | 40% | 100% |
| Comparative weight | 54% | 100% |
| Weight of insulation + jacket | | |
| lbs./ft. of tray | 4.56 | 12.35 |
| kg./m. of tray | 6.82 | 18.6 |
| Fuel value BTU/lb. | 6,100 | 14,000* |
| MJ/kg. | 14.2 | 32.6 |
| Fuel contributed BTU/ft. of tray | 27,800 | 172,900 |
| MJ/m. of tray | 96.3 | 598.8 |
| Comparative fuel contribution | 16% | 100% |

*Typical fire retardant XLPE estimated at about 2/3 fuel value of unadulterated polyethylene

This "equal ampacity" case is based on calculations using the method of IPCEA 54-440 second edition and NEMA WC 51-1975

Table 2
Tests Conducted September 27-29, 1976
Cables Insulated with "Tefzel" Fluoropolymer and XLPE-FR

| Vertical Test (Modified IEEE 383, 8 foot open vertical tray placed in a corner, one foot from each wall) | | | |
|--|-------------------|-------------------------|---|
| Flame Intensity, BTU/hr. | Tray Rungs Facing | Burner-to-Tray Distance | Comment |
| 210,000 | To Fire | 3" | Flames blasted through cables |
| 210,000 | Away From Fire | 13 1/2" | Hottest part of flame applied to cables |
| 400,000 | To Fire | 3" | Flames blasted through cables |
| 400,000 | Away From Fire | 20 1/2" | Hottest part of flame applied to cables |

Horizontal Test (Modified ASTM E-84 Tunnel Test)

- 300,000 BTU/hr. diffusion gas flame
- Cables spaced one-half cable diameter apart
- Method and apparatus per reference (1)
- Test duration: 20 minutes

Figure 13
Graphical Illustration of Smoke
Produced in Modified ASTM E-84
Tunnel Test
September 29, 1976

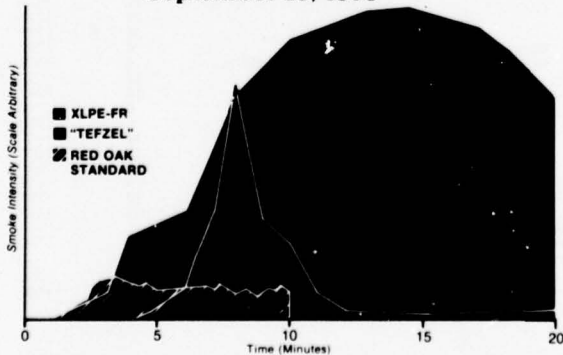


Table 3
Modified ASTM E-84 Tunnel Test
20 Minute Flame Exposure

| | "Tefzel" | XLPE-FR |
|--|----------|-----------------------------|
| Flame spread, maximum in 20 minutes, ft. | | |
| Total distance burned, ft. | 8 | 22 |
| Burner flame length, ft. | 4 1/2 | 4 1/2 |
| Flame spread, feet | 3 1/2 | 17 1/2 |
| Total amount of cable damaged, including any continued burning after 20 minutes, ft. | 9* | 25 (completely consumed) |
| Maximum outlet temperature including time after 20 minute period | 480°F | 800°F |

*Damage to jacket. Primaries intact at about one-half to one foot past igniter flame. No continued flaming or afterglow after igniter flame extinguished.

Table 4
Modified ASTM E-84 Tunnel Tests
15 Minute Flame Exposure

| Primary Insulation | Jacket | Cable O.D. | Number of Cables in Test | Flame Spread | Test | Cable Exposure | Fire Source | Time of Exposure | Spacing - Fire Source of Tray | Results |
|------------------------------|--------------------|-------------------|--------------------------|--------------|------|-------------------------------|-------------|------------------|-------------------------------|---|
| Polyethylene | "Teflon" FEP | 10.8mm (.425 in.) | 9 | 3.0 ft. | 1 | Tray Covered | 22.4 lb. | 25 min. | 2" | No damage to cables |
| | | | 12 | 4.5 ft. | | | | | | |
| | | | 18 | 4.5 ft. | | | | | | |
| | | | 24 | 3.0 ft. | 2 | Bottom 6' of cables Uncovered | 22.4 lb. | 20 min. | 2" | Slight scorching of cables in front row |
| Polyvinyl Chloride | Polyvinyl Chloride | 12.2mm (.480 in.) | 6 | 19.5 ft. | | | | | | |
| | | | 6 | 19.5 ft. | | | | | | |
| | | | 9 | 19.5 ft. | | | | | | |
| | | | 12 | 19.5 ft. | 3 | Bottom 6' of cables Uncovered | 14 lb. | 20 min. | Source Against Tray | Cables extensively damaged within tray to 41" height except for nine cables along right siderail intact above 16" |
| Silicone Rubber | Silicone Rubber | 7.87mm (.310 in.) | 6 | 19.5 ft. | | | | | | |
| | | | 9 | 19.5 ft. | | | | | | |
| | | | 12 | 19.5 ft. | | | | | | |
| | | | 24 | 19.5 ft. | | | | | | |
| Polyvinyl Chloride | Polyvinyl Chloride | 11.4mm (.450 in.) | 36 | 19.5 ft. | | | | | | |
| | | | 6 | 19.5 ft. | 4 | Tray Covered | 14 lb. | 20 min. | Source Against Tray | Cables in contact with cover damaged to about 16" height; others undamaged |
| | | | 9 | 19.5 ft. | | | | | | |
| | | | 12 | 19.5 ft. | | | | | | |
| Polyvinyl Chloride | "Teflon" FEP | 10.2mm (.400 in.) | 6 | 19.5 ft. | | | | | | |
| | | | 9 | 19.5 ft. | | | | | | |
| | | | 12 | 19.5 ft. | | | | | | |
| | | | 18 | 19.5 ft. | | | | | | |
| Polyvinyl Chloride | "Teflon" FEP | 9.53mm (.375 in.) | 6 | 17.5 ft. | | | | | | |
| | | | 9 | 19.5 ft. | | | | | | |
| | | | 12 | 19.5 ft. | | | | | | |
| | | | 18 | 19.5 ft. | | | | | | |
| Reference Material | | | | | | | | | | |
| Red Oak (10 minute exposure) | | | | 19.5 ft. | | | | | | |

Table 5B
Tests and Results

Table 5A
Full Tray Fire Tests at Southwest Research Institute,
San Antonio, Texas on March 9 & 10, 1977

Setup: Vertical tests; trays one foot from each wall in a corner location.

Trays: Galvanized steel, solid back and sides with cover, 4" x 12" x 12' high. Silicone fire stops were foamed in place at top and bottom to simulate penetrations through floor and ceiling.

Cables: 202 7/C #14AWG conductors (40% fill)

Insulation: 10 mils of "Tefzel" fluoropolymer

Jacket: 20 mils of "Tefzel" fluoropolymer

Fire Source: Wood cribs ignited with ethanol. The 22.4 lb. source closely duplicated burning debris typical of that in nuclear facilities (gloves, clothing, masks, etc., used in radiation areas). The 14 lb. source was more energetic being constructed of smaller lumber elements.

Table 6
Modified ASTM E-84 Tunnel Tests
Results on Smoke

| 15 Minute Exposure Data | | | | |
|-------------------------|---------------------|---------------------|--------------------------|--------------|
| Primary Insulation | Jacket | Cable O.D. | Number of Cables in Test | Smoke Factor |
| Polyethylene | "Teflon" FEP | .425 in. | 9 | 41.9 |
| | | | 12 | 55 |
| | | | 18 | 109 |
| | | | 24 | 224 |
| Polyvinyl Chloride | Polyvinyl Chloride | .480 in. | 6 | 1500 |
| | | | 6 | 1386 |
| | | | 9 | 1745 |
| | | | 12 | 1889 |
| Silicone Rubber | Silicone Rubber | .310 in. | 6 | 449 |
| | | | 9 | 823 |
| | | | 12 | 1042 |
| | | | 24 | 1772 |
| Polyvinyl Chloride | Polyvinyl Chloride | .400 in. | 36 | 2119 |
| | | | 6 | 1822 |
| | | | 9 | 2018 |
| | | | 12 | 818 |
| Polyvinyl Chloride | "TEFLON" FEP | .375 in. | 18 | 1942 |
| | | | 6 | 719 |
| | | | 9 | 1056 |
| | | | 12 | 1461 |
| Polyvinyl Chloride | "TEFLON" FEP | .375 in. | 18 | 1535 |
| | | | 6 | 461 |
| | | | 9 | 699 |
| | | | 12 | 865 |
| Reference Material | | | | 1112 |
| | | | | 100 |
| 20 Minute Data | "Tefzel" XLPE-FR | "Tefzel" XLPE-FR | 0.510 0.690 | 350 1500 |

THE EVALUATION OF COMMUNICATIONS CABLE FLAMMABILITY
USING THE RELEASE RATE APPARATUS

by

E.J. Gouldson
G.R. Woollerton

E.E. Smith
H.C. Hershey

Northern Telecom Limited
Montreal, Quebec

Ohio State University
Columbus, Ohio

ABSTRACT

The Ohio State Release Rate Apparatus has been modified so that simultaneous measurement of heat, flame spread, smoke, toxic and corrosive gases and circuit integrity are possible.

Data from the release rate apparatus collected over a range of heat fluxes have been used in conjunction with simulation of the Steiner Tunnel Test to predict the behaviour of cables in the tunnel. The results of the simulation have been compared with actual tests in the tunnel.

INTRODUCTION

Within the cable industry, committees have been set up to evaluate the response of wires and cables to fire, working with the primary emphasis on flame spread, smoke, toxic and corrosive gases and circuit integrity.

Because of the need for more severe flame spread tests, large scale tests have now been developed in many countries. All but one of those known to the authors are vertical tests using several cables and a large heat source together with natural ventilation. The exception is the method for testing cables in the Steiner Tunnel¹ which is a horizontal test using forced ventilation.

There are important differences in the vertical tests, making comparison difficult. The cables are mounted in an open room, or in a special enclosure. The enclosure may be thermally insulated or conducting. The ignition sources vary from electrically heated furnaces with piloted ignition to propane gas or alcohol, the test temperatures vary from 600-900°C, the calorific input from the sources differ, and the test times vary from 15 to 60 minutes. Even the quantities of cable per test vary as do the pass/fail criteria.

A weakness of these tests is that they were designed to measure only flame spread, even though the Steiner Tunnel can measure smoke. None of the tests have methods for toxic and corrosive gas analysis. Methods to measure smoke and some gases are available, but these tests were designed as research and quality control tools for relative ranking of materials under defined conditions and could be misleading if related to the large scale test.

In this paper, we are making a fresh approach to the problem of cable flammability. It is shown that release rate data may be used to model large scale tests such that one set of data can be collected and used to simulate any large scale test. As an example, the Steiner Tunnel Test has been modelled and the results from the computer simulation compared to actual tests. The technique is not limited to flame spread alone; smoke and various gases are included in the simulation.

THE RELEASE RATE APPARATUS

In the 1975 I.W.C.S. paper, "Fire Hazard Evaluation of Cable and Materials"¹, the method for testing wires and cables in the Ohio State University Release Rate Apparatus was described. The cables could be tested for flame spread, heat release and smoke.

Referring to Fig. 1, the apparatus consists of an environmental chamber which has a constant flow of air passing through it. The radiant panel is adjustable over a range of heat fluxes to give the necessary exposure to the sample under test. The change in temperature and optical density of the air leaving the apparatus is measured, and from these the rates of heat and smoke release are calculated.

For testing cable, the sample is mounted in the holder and positioned vertically so that the small pilot flame can

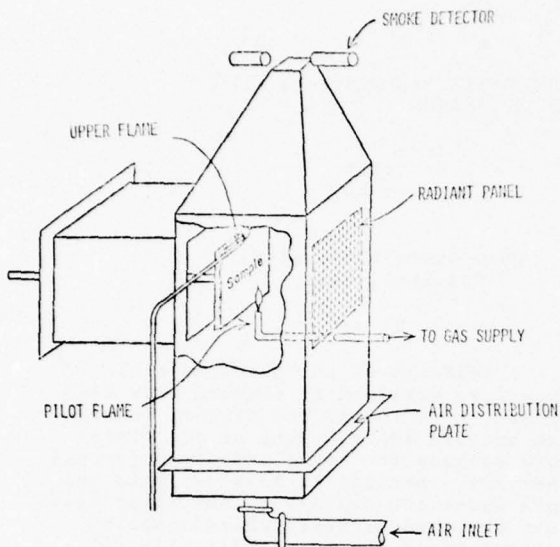


FIG. 1 SCHEMATIC OF RELEASE RATE APPARATUS

impinge on its bottom surface. The test can be performed without the pilot flame, with the pilot flame at the bottom, or with the pilot flame together with another small flame at the top to burn off ignitable gases. All three types of test obviously give different results and are required for different evaluations. (For detailed descriptions of the basic apparatus and its operation, and method of test for cables see Refs. 1, 2 and 3).

Gas Analysis

The capabilities of the release rate apparatus have been extended with the addition of methods to analyse hydrogen chloride and total acid gases, nitrous oxides and carbon monoxide during a test.

A dual system is presently employed for acid gas analysis based on the use of specific ion electrodes. The first system records HCl rate of release and the second system records the total acidity of the gases evolved. The two systems are identical, except for the specific ion electrode, and only the HCl method is described here (Fig. 2).

The specific ion electrode has been adapted to a Fisher-Milligan bubbler and a specific ion meter is used to monitor 0.2% of the stack gas from the release rate apparatus. A small ministatic pump and flow meter maintain a constant air flow through the system. The feed is a length of 1/4" Teflon tube, with a 1/8"

bore which is inserted into the top of the inner chimney of the release rate apparatus. The tube is centred and fixed in position.

The volume of liquid in the bubbler is 274 ml, chosen so that with the flow condition set at 0.2% of the stack gases, the system is direct reading, i.e. Normality $\times 10 =$ g. of HCl in the bubbler. Dividing by 2 and adjusting the decimal point makes the system direct reading in grams of HCl produced during the test. In order to be able to read the HCl generated at the start of the test, or when levels are so low that they are beyond the detection level of the electrode system, 5×10^{-5} N HCl is used in the bubbler. This acts as a starting solution and enables the monitoring of the total HCl generated. It also gives a very convenient calibration before every run.

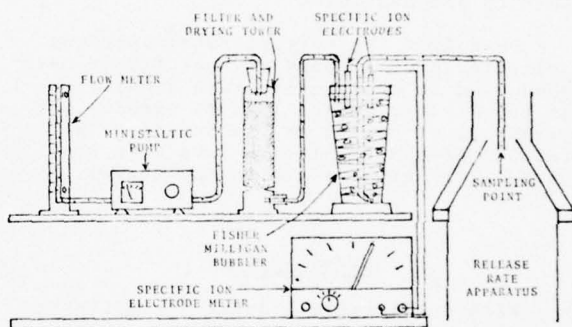


FIG. 2 HCl DETECTION SYSTEM

Tests performed indicate that because of the small sample tube and relatively high flow rate, the line is essentially self heating and minimal loss or delay of HCl due to condensation or absorption occurs before the gas is measured by the sensing apparatus. It has also been shown that results from this method compare very well with results using a combustion boat in a tube furnace.

The second system measuring total acid gas uses the same Teflon tube and results are expressed in change of pH, equivalent normality of HCl or grams per square metre of sample area.

The total nitrogen oxides present in the gas stream are analyzed using a commercial nitrogen oxide chemiluminescence analyzer (NO/NO_x). Sampling in the chamber is made using the same Teflon tube used for the HCl.

A commercially available electro-chemical type carbon monoxide analyzer is used for measurement of the carbon monoxide gas during the test. A similar Teflon tube is positioned with its end just inside the exit stack of the release rate apparatus. Dual ranges on the analyzer of 0 to 250 and 0 to 2,000 ppm are required, the higher range being most desirable for cables subjected to high heat fluxes.

Filtering systems to eliminate soot are important, but must be applied at different points for the different gases. For HCl and acid gases, the bubblers receive unfiltered combustion products and a combination water trap, fibreglass filter and indicating grade silica gel drying towers treat the gases prior to their passage through the ministatic pumps and flow meters. The sample line to the NO_x meter has rough fibreglass and 5 micron disc filters prior to the gases entering the meter. The carbon monoxide meter is similarly protected with filters.

Computerization of Data

The release rate apparatus now monitors the rate of production of four gases as well as simultaneously recording other flammability properties. Thus a

large amount of data is generated which must be processed, and reported in terms which can be interpreted as meaningful results. The addition of analysis apparatus to the system to monitor other gases will produce further complications to the point where the analysis of the data would require considerably more time than the test itself.

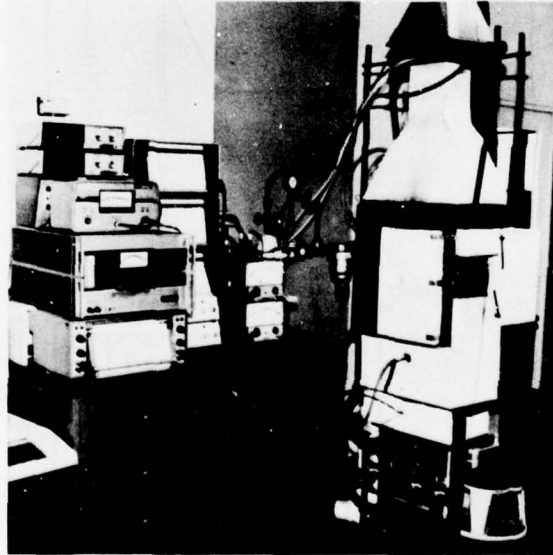
For this reason a mini-computer system has been added to the apparatus. It contains a dual floppy disc memory facility and is programmed to enable the computer to use on-line data from monitoring transducers on, or associated with, the release rate apparatus. At present, the data is stored from six channels with provision for up to ten additional input channels as the systems are developed.

Data is sampled from every channel every half second and the average values are stored every three seconds. Correction factors are now applied to the smoke results using the instantaneous heat readings to correct for both the constant error caused by heat from the radiant panel and the variable effect of heat released from the burning sample.

The computer integrates data from channels whose signals are proportional to the rates of release. It reports these as totals at discreet time intervals, maximum rates of release, and times at



A - COMPUTER CONSOLE



B - GENERAL VIEW OF EQUIPMENT

FIG. 3

which these occur. For channels whose signals are proportional to those total amounts collected (e.g. HCl, pH), the system will differentiate the results and report rates of release and maxima, and total time periods selected. Other reports are generated which present the data in forms suitable for modelling other tests.

Circuit Integrity Test

During flammability studies of cable using the release rate apparatus, samples are subjected to simulated testing ranging from extreme service conditions (75°C) to fully developed fire situations (600-700°C). To be able to study the

effect these have on the circuit integrity of the cables, the apparatus has been modified to allow connections to be made to the ends of the conductors of the cables under test. The general arrangement is shown in Fig. 4, but the actual physical placement of the cable in the sample holder will depend on the size of the cables.

In the example shown, the cable is about 1 cm diameter. It is bent through 180° alternatively left and right and placed in the holder with the connecting ends protruding to the rear. These ends are placed through holes made in the corners of the holders, and through corresponding holes in the pressure back plate. The bared conductor ends are divided into two groups, bound with wire and connected to corrosion resistant Teflon covered leads which pass through air-tight holes drilled in the outer door, to a 6-volt buzzer circuit. The time from the start of the test to buzzer ringing is a measure of circuit integrity.

The system gives reasonably repeatable results and is sufficiently discriminating to detect changes in cable design. It indicates the time that a cable would remain serviceable in the type of fire situation corresponding to the heat flux used in the test.

As an example of its use, a study was made on cable models with heat barrier tape and HCl scavenger powder. The tests were carried out at 20 kW/m² (approximately 500°C at the cable surface), and the results are shown in Table 1.

TABLE 1

RESULTS FROM CIRCUIT INTEGRITY TEST

| CABLE TYPE | TIME TO FAILURE (secs.) |
|------------------------|----------------------------|
| Standard Inside Cable | 104 |
| With Heat Barrier Tape | 158 |
| With HCl Scavenger | 70 |

THE RELEASE RATE APPARATUS AND LARGE SCALE TESTS

During the development phase of new inside wires, the objective was set that the cable should be capable of passing the draft Canadian medium scale flame test.⁴

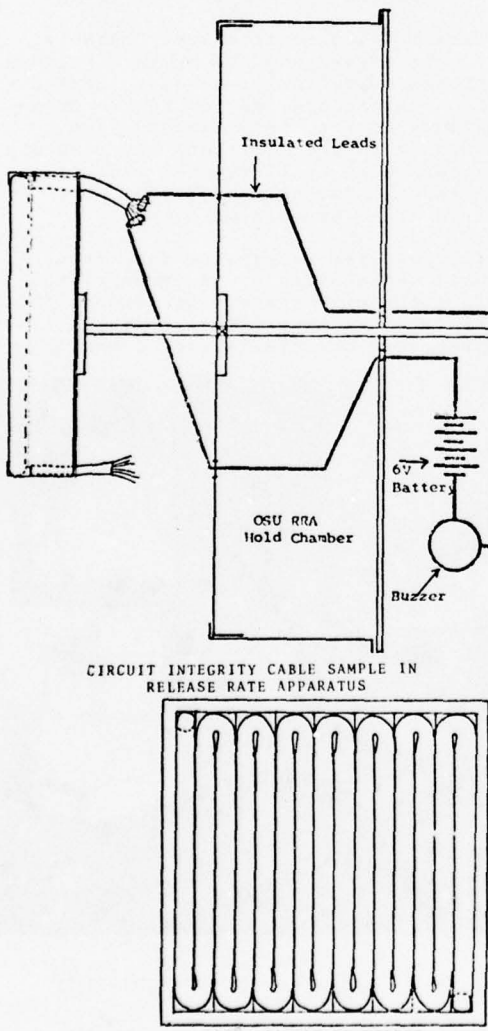


FIG. 4 CIRCUIT INTEGRITY TEST

This is similar to the I.E.E.E. 383 test but is carried out in a smaller room with a narrower cable mounting rack. The burner size is the same at 70,000 BTU/hour (20.5 kW). A significant reduction in smoke and corrosive gases was also a goal.

Cables were manufactured with experimental compound and tested in the release rate apparatus using the lower pilot flame only. Typical results are shown in Table 2 from which it was concluded that sufficient improvement had been made to warrant large scale testing. When tested, the standard inside cable burned very quickly to the top of the cable rack (see Fig. 5). The improved cable only burned 450 mm (18") above the point of flame impingement (Fig. 6) and was considered a good pass.

TABLE 2
COMPARATIVE DATA FROM
RELEASE RATE APPARATUS

| PROPERTY | CABLE A (%) | CABLE B (%) |
|-------------------|----------------|----------------|
| Heat Release | 100 | 63 |
| Flame Spread Time | 100 | 270 |
| Ignition Time | 100 | 600 |
| Acid Gas | 100 | 50 |
| Smoke | 100 | 56 |
| Carbon Monoxide | 100 | 100 |

Samples of these cables were then tested in the Steiner Tunnel by the method described in Ref. (6). Both cables burned to the end of the tunnel, although the new cable had a longer time to total involvement. Disturbing was the fact that the improvements in smoke predicted from the release rate apparatus were not found in the Steiner Tunnel Test.

These results led to a study of the variables involved in large scale testing and the feasibility of using data from the release rate apparatus to accurately predict the results of testing in large scale facilities by means of mathematical simulation.

Application of Release Rate Data

A developing fire, whether it be a room fire or a cable test, can be con-

sidered an unsteady state chemical reaction system. As is the case in this type of reaction system, it can be analyzed using basic chemical reaction rate data for the burning materials and physical reaction rates, i.e. heat and mass transfer.

It may be assumed that hazard levels which are present in a real fire are indicated by concentration vs. time information for heat, smoke and toxic and corrosive gases. Since the concentrations which develop in an unsteady state system are dependent on both rate and quantity of heat, smoke and gases released, the release rates are important information needed to analyze a fire system.

Methods for obtaining these release rate data^{2,3} and their use for predicting performance of materials and products in real fire situations⁷ have been described elsewhere. Before illustrating the application of these release rate data, two points should be emphasized:

- 1) Release rates are a function of exposure; there is no single release rate that is characteristic of a material.
- 2) Release rate data, using the Ohio State University Release Rate Apparatus and suggested operating procedures are obtained at a number of well-defined, constant exposures.

These exposures do not, nor are they intended to, simulate a "real" fire exposure. To determine performance of a material in a real fire, its release rate over a range of exposures is needed from which its performance can be predicted if the exposure generated by the fire is known. In other words, the performance of a product in a real fire depends both on its release rate characteristics and on the fire system in which it is found since both contribute to the conditions to which it is exposed.

It is to this latter point that mathematical simulation (modelling) of fire systems is directed. The relationship of an item to its surroundings requires that the interdependence of each item in a fire system be considered and the individual contributions be integrated to predict their exposure conditions.

The Steiner Tunnel Test can be used to illustrate the point. The burner generates an exposure which will ignite a combustible sample. As the sample burns, it releases heat at a rate characteristic of the sample and exposure. The heat

released by the sample and burner, minus that absorbed by the walls of the tunnel and sample, raises the temperature of the gases flowing down the tunnel, thereby changing the exposure to which the downstream portion of the sample is exposed. Thus, exposure conditions are developed by both the burner and the sample, and the key to the enhanced exposure is the rate at which heat is released by the sample. Amounts of smoke and gases leaving the tunnel are also a function of the release rate of smoke and gases from the sample. By using a computer to make heat and material balances over incremental lengths of the tunnel, temperatures of gas and walls can be calculated in each length increment as a function of time.

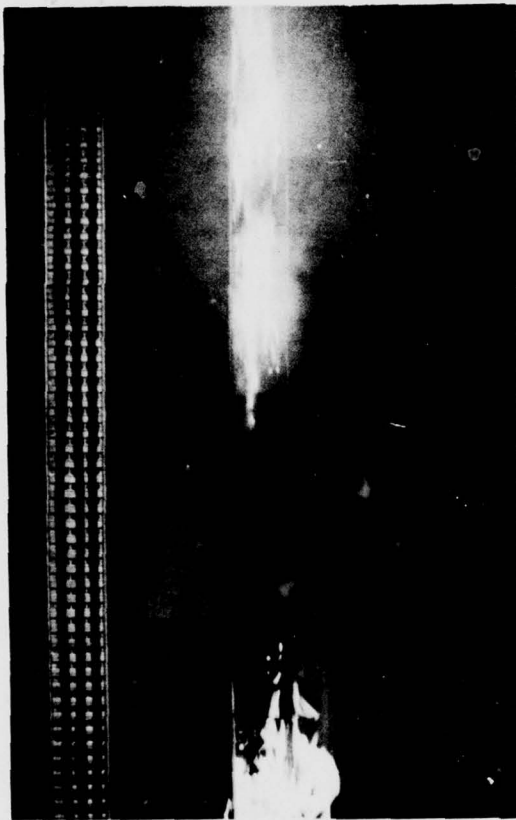


FIG. 5 VERTICAL TEST - STANDARD CABLE

Modelling the Steiner Tunnel Cable Test

Basic assumptions made in modelling the tunnel were: Air flow through the tunnel is divided into two parts, A and B. The upper layer, Gas A, includes the combustion gases and smoke. This gas is heated by the heat released from the

sample and is cooled by convection and radiation losses to the surrounding walls. Gas B is air only, heated from surrounding walls. At each length element an amount of B is shifted into A as calculated by an entrainment equation. It was assumed that all methane burns in the first 600 mm (2 feet) of the tunnel; 45% in the first 150 mm (0.5 foot) and 20, 20 and 15% in subsequent 150 mm (0.5 foot) sections.

Appropriate view factor and flame emissivities were used to calculate the radiant heat interchange from flame to the walls, and from walls to the sample. A combined radiant and convective heat transfer coefficient for the upper and

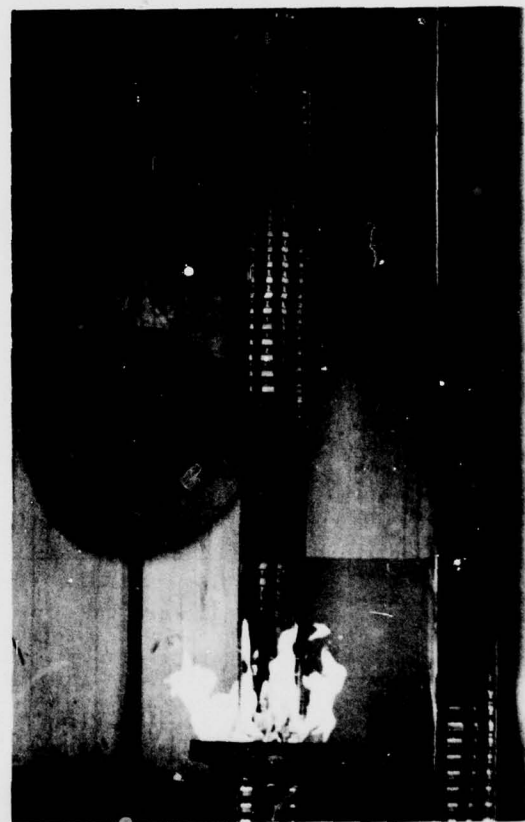


FIG. 6 VERTICAL TEST - IMPROVED CABLE

lower sections of the tunnel was determined and used for calculating heat flux to the "upper" and "lower" walls. From this heat flux, the wall surface temperature and temperature gradient into the walls were calculated using the Schmidt method as referenced in McAdams⁸ for unsteady state heat transfer.

The heat balance made on each length element is represented by Figure 7.

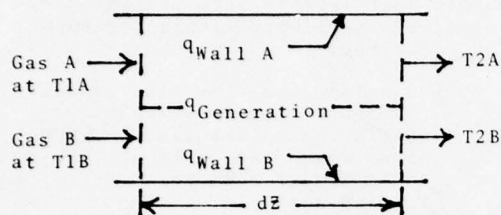


FIG. 7 HEAT BALANCE SCHEMATIC

Gas A and Gas B entering the volume element at a temperature of T_{1A} and T_{1B} , exit at T_{2A} and T_{2B} respectively. A value of T_{2A} is assumed, T_{2B} calculated based on this assumption, and heat losses by convection and radiation to Wall A and Wall B ($q_{Wall\ A}$ and $q_{Wall\ B}$) calculated. Then the sum of the heat losses to the walls plus the sensible heat gain to Gas A and Gas B are added and compared to the total heat generated within the volume element. If the heat losses from the element are equal to the heat added, T_{2A} and T_{2B} are set equal to the T_{1A} and T_{1B} entering the next length element, and the same heat balance performed for this and all remaining elements. If not equal, a new value of

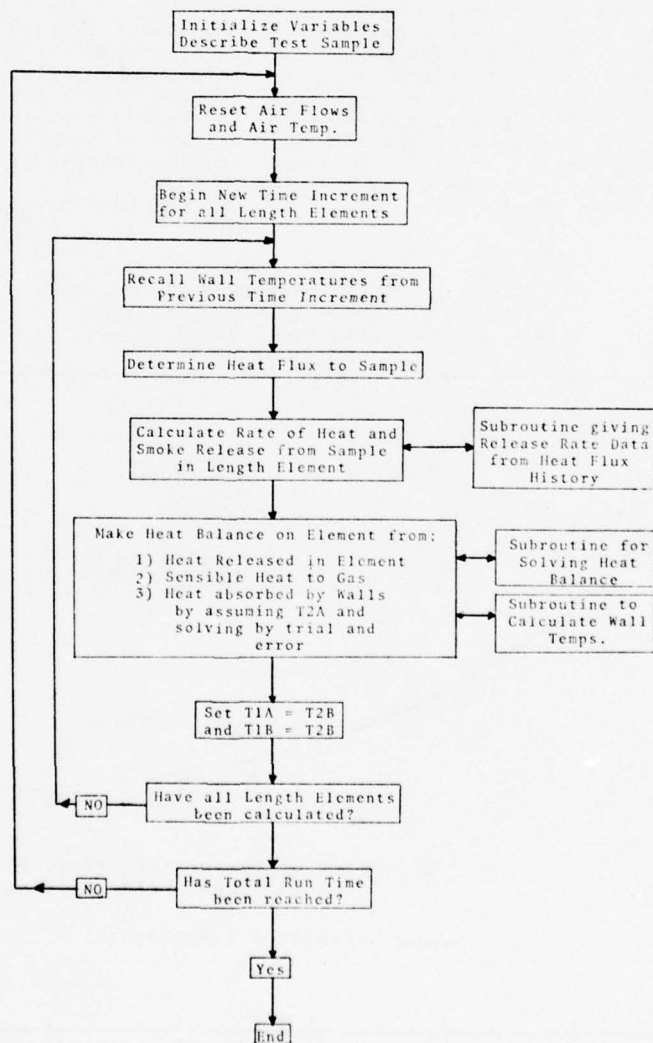


FIG. 8 FLOW DIAGRAM

T_{2A} is assumed using an interpolation subroutine, and the balance repeated until heat losses from the element are equal to the heat added to the element. Between each element, the air entrained from Gas B to Gas A is added to A and T_{1A} corrected for this mixture.

Figure 8 is a flow diagram illustrating the computer calculations for each length element at a given time increment, and the successive time increments taken to determine conditions within the tunnel as a function of time. Figure 9 compares the calculated temperature distribution in the tunnel with that observed by Parker⁹ when an asbestos cement board is tested.

One of the critical features of the model is the heat release rate data used in calculating the heat generated. Heat release rate data obtained in the release rate apparatus must be properly interpreted and put into a form that can be utilized by the model. For the cable material reported in this paper, a time-flux product must be exceeded before the sample will release heat. In addition, the heat release rate is a function of prior heat released because of char formation,

and a function of the incident heat flux and oxygen concentration.

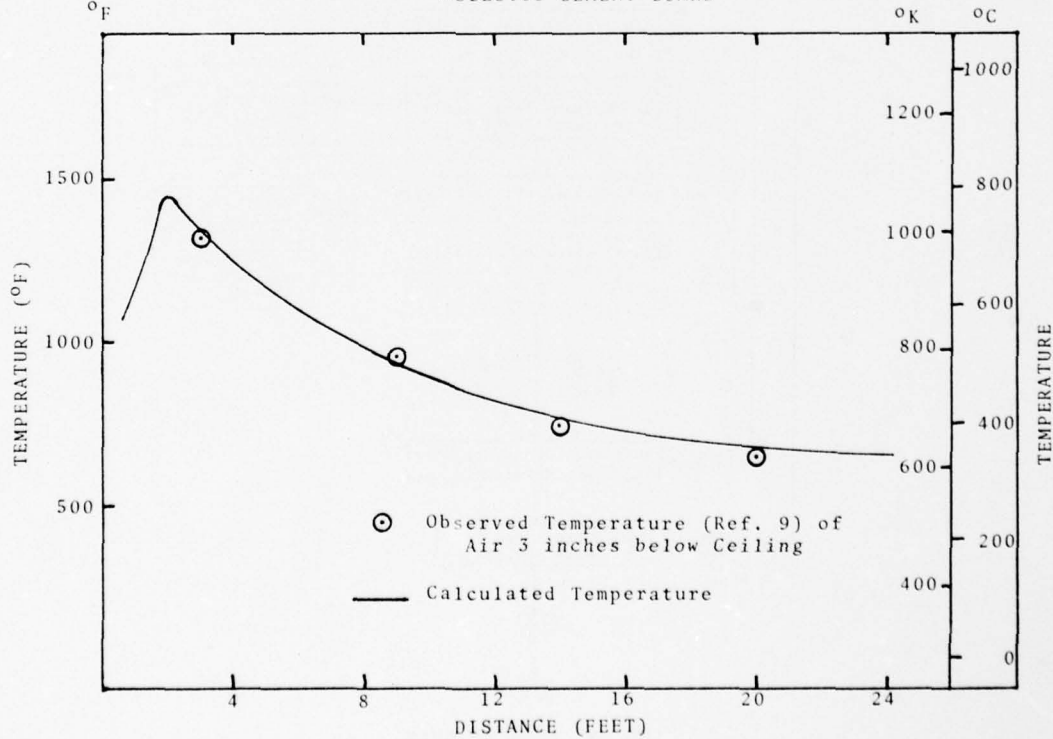
The model and equations used to calculate heat release rate for the varying exposures developed within the tunnel do the following:

- A. Calculate the time-flux product (exposure time in seconds multiplied by the flux in kW/m^2 above which the cable will burn) to determine when the cable will release heat.
- B. Calculate the rate of heat release as a function of prior heat release from that surface, incident heat flux, and oxygen concentration.

Smoke release rates are calculated as a function of the flux-time product and incident heat flux from equations developed from a group of release rate curves. The minimum flux-time product for release of smoke is different than that for the release of heat.

It must be noted that the model is

FIG. 9 AVERAGE TEMPERATURE OF GAS A
AFTER 10 MIN. TEST WITH
ASBESTOS CEMENT BOARD



not yet "fine tuned". For example, only coarse adjustments have been made for the relative effect the thermal diffusivity of walls, the heat capacity of sample, and the entrainment of Gas B into Gas A have on the temperature distribution in the upper section of the tunnel. Effect of oxygen concentration on release rates has been virtually ignored. Results thus far are preparatory and are presented to illustrate concepts and techniques used in applying release rate data to modelling cable tests in the Steiner tunnel.

Applying the Model

Performance in the tunnel test was predicted for four types of communications cable. Data was collected from the release rate apparatus over a range of heat fluxes, using both the pilot and the upper flame. This data was prepared in the form required for use in the model and the programme run. The calculated (predicted) performance for time to total involvement is compared in Table 3 to that observed in tests performed by Underwriters Laboratories Inc., Northbrook, Illinois.

TABLE 3

COMPARISON OF PREDICTED AND OBSERVED PERFORMANCE

| CABLE DESIGNATION | TIME TO TOTAL INVOLVEMENT | |
|-------------------|---------------------------|--------------------|
| | CALCULATED (MINUTES) | OBSERVED (MINUTES) |
| A | 7:18 | 9:00 |
| B | 13:30 | 13:16 |
| C | 13:12 | 12.48 |
| D | 13:42 | -- |

Smoke and toxic gas produced in the tunnel test can be predicted by the model if basic release rate data are available. The predicted smoke and carbon monoxide concentration in the exhaust gas from the tunnel for Cable B are shown in Figures 10 and 11. Smoke release rates were not corrected for oxygen concentration and flaming combustion throughout the tunnel was assumed.

Because visible smoke from this type of sample reduces the % Transmission of light through the exhaust gas to very low values soon after the cable becomes in-

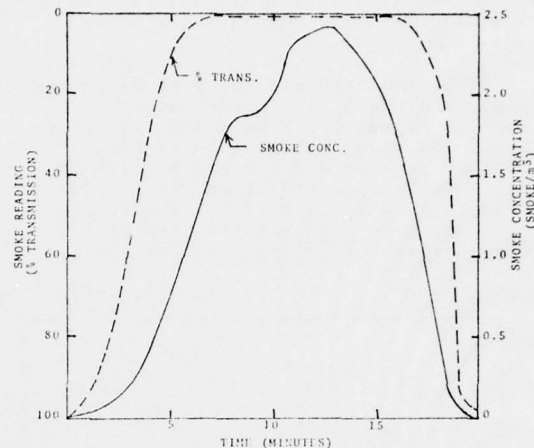


FIG. 10 SMOKE RELEASE

volved, smoke evolution as indicated by "Smoke Contributed" values from the tunnel test have little significance. The model's prediction of smoke concentrations illustrates the advantage of using Optical Density rather than % Transmission for monitoring smoke produced. Significant differences in smoke produced by different cables are indicated by integration of smoke concentration (optical density) curves. These differences are not shown when smoke is monitored by % Transmission.

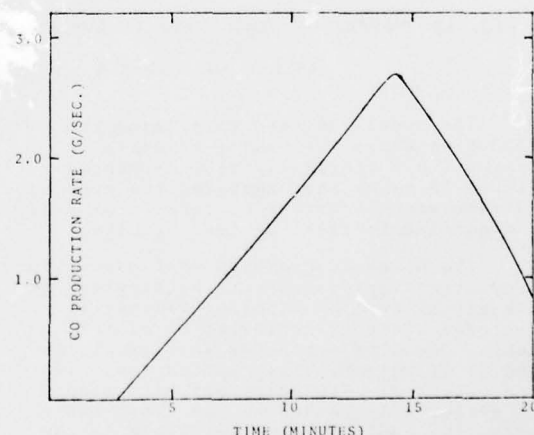


FIG. 11 CARBON MONOXIDE GAS RELEASE

The model is also useful for predicting the effect changes in testing procedures will have on cable test results and for predicting how the changes

in flammability characteristics of cable will influence results from the tunnel test.

The predicted effect of changing the quantity of fuel gas to the burner is shown in Figure 12. The model indicates that a 20% change above and below the standard rate of 270,000 BTU/hr. (79 kW) will have a major effect on results for a sample such as Cable B. For materials which are more "combustible", results are less sensitive to changes in fuel gas rates.

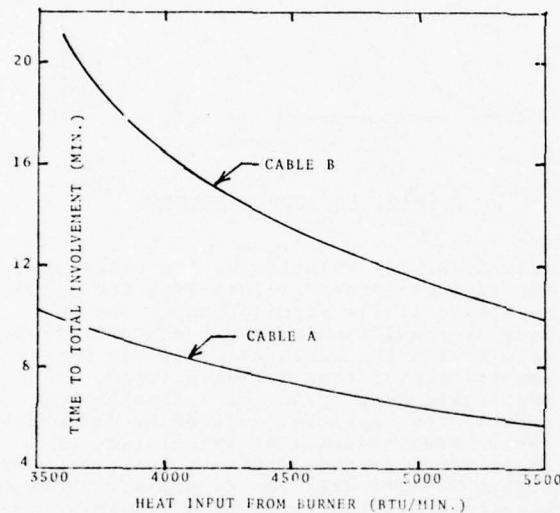


FIG. 12 EFFECT OF HEAT INPUT TO BURNER FOR CABLE A AND CABLE B

The model was used to examine the situation where the number of cable tested (in a single layer) was changed. Figure 13 shows that changing the exposed surface area or number of cable tested has a significant effect on test results.

The model is probably most useful for predicting improvements to be expected in the tunnel test by altering flammability (release rate) characteristics of the cable. Results presented in Figures 14 and 15 illustrate this application. If the weight of insulation per unit length of cable is increased by 20% above and below the nominal value for Cable B, the time to total involvement will change significantly.

An important material characteristic is the flux-time product built into the insulating material, i.e. the time a cable must be exposed to a given flux (above the minimum self-propagation flux) before the

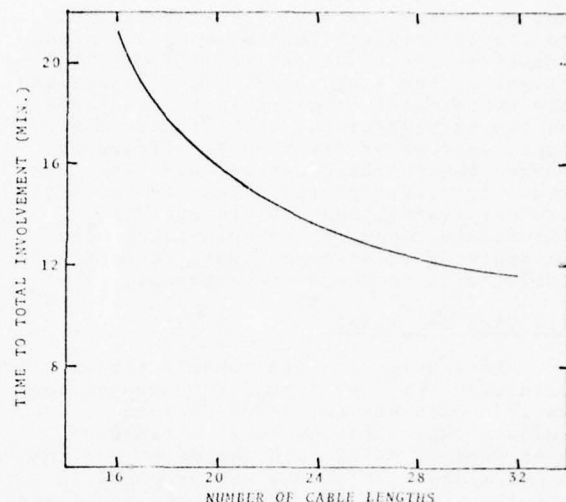


FIG. 13 CHANGE IN NUMBER OF CABLE LENGTHS TESTED FOR CABLE B

material will start to release heat. Change in time to total involvement for cable having different time-flux products indicate that the flux-time product is an important design parameter of cable. The data also show that accurate measurement of the minimum time-flux product is necessary for reliable prediction using the model.

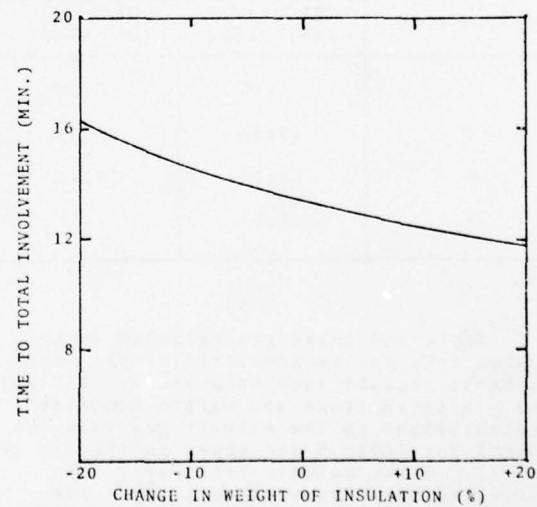


FIG. 14 CHANGE IN WEIGHT OF INSULATION FOR CABLE B

Performance Criteria

The model can be used to find basic flammability criteria needed to meet specific performance levels in the Steiner tunnel test. For example, the heat release rate characteristics for a cable that will have a desired Flame Travel Distance can be estimated. Three characteristics of the cable must be considered:

- 1) The minimum incident heat flux before the cable will release heat (burn).
- 2) The rate and amount of heat released at flux levels above the minimum.
- 3) Minimum flux-time product for the cable.

If a cable releases heat at a negligible rate after it becomes involved, the heat flux at any distance down the tunnel after a 20-minute blank run represents the minimum incident heat flux the cable must withstand, so that it does not become involved beyond that point. A flame length of four feet beyond the point of involvement was assumed.

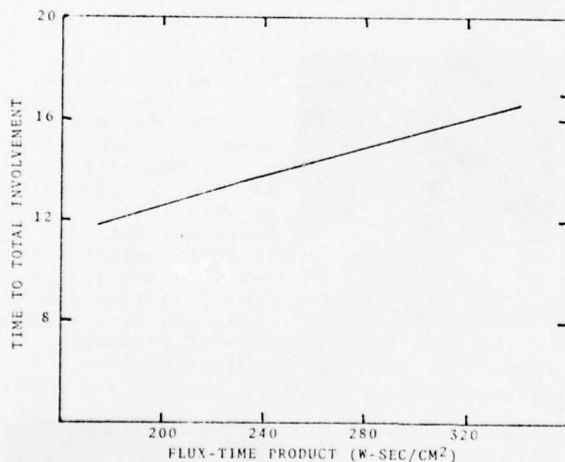


FIG. 15 CHANGE IN FLUX-TIME PRODUCT FOR CABLE B

At a distance of 5.5 feet in a blank run, the incident heat flux on a sample after 20 minutes was calculated to be approximately 30 kW/m^2 . In other words, for the cable to have a Flame Travel Distance under five feet (flame reaching to 9.5 feet), the cable should not burn when exposed to a heat flux of 30 kW/m^2 and release negligible heat at heat flux above 30 kW/m^2 .

Most cables will have a significant rate of heat release when involved so that the heat flux vs. distance distribution in the tunnel will change, requiring a higher level of resistance to burning to meet the same Flame Travel Distance rating.

TABLE 4
PERFORMANCE CRITERIA

| CABLE | DESIRED FLAME DISTANCE RATING (feet) | AVE. HEAT RELEASE RATE (kW/m^2) | MIN. HEAT FLUX FOR BURNING (kW/m^2) |
|-------|--------------------------------------|--|--|
| X | 5 | 0 | 30. |
| Y | 5 | 55 | 60. |
| X | 15 | 0 | 12. |
| Y | 15 | 55 | 40. |
| X | 19.5 | 0 | 10. |
| Y | 19.5 | 55 | 35. |

While the shape of the release rate vs. heat release curve, the total heat release, and flux-time product should be considered (and are in the model), approximate criteria, based on only minimum heat flux and an average heat release rate have been listed in Table 4. The criteria are for two cables, X and Y, one which has a negligible heat release rate and another which has an average heat release rate of 55 kW/m^2 .

CONCLUSIONS

A test method is available which can measure simultaneously all of the flammability properties required over the range of heat fluxes found in a fire. By suitable modelling techniques, it has been possible to use the data collected from the release rate apparatus to predict flame spread in the Steiner Tunnel. Simultaneously determined is the amount of smoke and gases generated during the test.

These same basic release rate data can be used to model other types of cable tests. The approach is similar, i.e. the contribution the sample under test makes to the conditions to which the sample is exposed is obtained from release rate information. But the physical description of other test systems would require modification of this model for calculating heat and mass flows within and out of the system.

ACKNOWLEDGEMENTS

The authors wish to thank Ontario Hydro Research Laboratories for testing

cables in their medium scale flame test facility and Underwriters Laboratories, Inc., Northbrook, Illinois for testing cables in the Steiner Tunnel.

They also wish to thank their colleagues at Northern Telecom Limited and Ohio State University who contributed to this paper.

References

- (1) Gouldson, E.J., Woollerton, G.R. and Checkland, J.A., "Fire Hazard Evaluation of Cables and Materials" 1975 International Wire and Cable Symposium Proceedings, pp. 26-36.
- (2) Proposed "Test for Heat and Visible Smoke Release Rates for Materials and Products", submitted to Committee E.05, American Society for Testing and Materials, Philadelphia, PA. (June 1977).
- (3) Smith, E.E., "Measurement of Heat, Smoke and Toxic Gas Release", Fire Tech., Vol. 8, No. 3 (1972).
- (4) Ontario Hydro Specification No. L-891 SM-77, "Specification for Test to Determine Fire Retardancy and Acid Gas Evolution of Insulated Power and Control Cable".
- (5) IEEE Standard 383, Para. 2.5, Flame Tests - Specification on Electric Cables, Field Splices and Connections.
- (6) Beyreis, J.R., Skordahl, J.W., Kaufman, S. and Yocum, M.M., "A Test Method for Measuring and Classifying the Flame Spreading and Smoke Generating Characteristics of Communications Cable", 1976 International Wire and Cable Symposium Proceedings, pp. 291-295.
- (7) Smith, E.E., "Relation of Performance Tests to Actual Fires", Fire Tech., Vol. 12, No. 1 (1976).
- (8) McAdams, W.H., "Heat Transmission", 3rd Edition, pp. 46-49, McGraw-Hill, New York (1954).
- (9) Parker, W.J., "An Investigation of the Fire Environment in the ASTM E-84 Tunnel Test", NBS Tech. Note 945, Center for Fire Research, National Bureau of Standards (1977).



Eric Gouldson graduated from London, England, with an Engineering Degree in 1960. Until he emigrated to Canada in 1967, he was employed by AEI Ltd. working on EHV cables. Since 1967 he has been at Northern Telecom Ltd. where he is now

Manager of Cable Development in the R&D laboratories of the Cable Division.

Greydon R. Woollerton was born in Sherbrooke, Quebec and obtained a B.Sc. degree at Bishop's University. He is presently a member of R&D staff of Northern Telecom, with experience in spectroscopy and flammability research since 1956. He is a member of the Order of Chemists of Quebec, the Chemical Institute of Canada, the Spectroscopy Society of Canada, and several fire research committees of A.S.T.M. and the Canadian Standards Association.



Edwin E. Smith was born in Sugarcreek, Ohio and received his academic degrees in chemical engineering at the Ohio State University; his Ph.D. in 1949. Major fields of interest include flammability research and industrial pollution control. He is a member of the American Institute of Chemical Engineers, American Chemical Society, National Fire Protection Assoc., and ASTM.

Harry C. Hershey was born in Baton Rouge, Louisiana, and received his B.S., M.S., and Ph.D. degrees in chemical engineering from the University of Missouri at Rolla in 1960, 1963 and 1965 respectively. He worked for Union Carbide from 1960 to 1962. He has been at Ohio State University since 1966, where his present title is Associate Professor, Chemical Engineering. His publications are in the areas of rheology, turbulence, applied mathematics and thermodynamics.



INTERLABORATORY EVALUATION AND CORRELATION STUDIES
WITH THE ARAPAHOE AND NBS SMOKE CHAMBERS

C.J. Sparkes, J.J. Kracklauer, & R.E. Legg

Arapahoe Chemicals, Inc.
Boulder, Colorado

ABSTRACT

Requirements for large-scale testing are pending for the evaluation of fire and smoke safety of wire and cable products. But small-scale tests such as the NBS or Arapahoe Chambers are needed for smoke research programs to screen materials prior to submitting them for large-scale testing.

An interlaboratory evaluation was conducted to determine the statistical variability of the two instruments. Smoke data was obtained under flaming conditions for a series of typical jacketing or insulation materials used by the wire and cable industry. Superior precision was shown by the Arapahoe method, and gravimetric smoke measurements from the instrument appear to correlate with specific optical density measurements in the NBS Chamber. The Arapahoe Chamber offers speed and simplicity of operation for high sample throughput.

INTRODUCTION

Smoke has been defined as a primary concern for life safety with construction products. Substantial loss of visibility has been shown to occur minutes before temperature and oxygen depletion become a significant threat in full-scale test fires.¹ A fire victim's ability to see escape routes and successfully egress is usually lost in the early stages of a fire. This is supported by fire statistics that show a relationship between smoke and fatalities in building fires.^{2,3}

As a result of a growing sense of urgency about the need to control smoke generation considerable attention is being given to the development of test methods. It is anticipated that the wire and cable industry, as with other industries in the building construction area, will require large-scale testing to adequately evaluate products for fire safety. But development of low smoke materials will require screening of large numbers of trial materials before a low smoke optimum is found. Since large-scale tests are expensive and difficult to run, a suitable laboratory scale method is needed.

Several laboratory scale tests have been developed to measure smoke from burning materials. Most have been found to lack good repeatability or to be prohibitively time consuming and expensive to run. Two of the more widely accepted small-scale test methods are the NBS-Aminco⁴ and the Arapahoe Smoke⁵ Chambers. Smoke is determined optically under flaming or smoldering conditions in the NBS instrument. Light transmittance measurements are made of the attenuation of a collimated beam of light. Scattering or absorption of the light beam is caused by the particulate matter which is confined to an 18 cubic foot chamber during the duration of the test. Although a number of smoke parameters can be determined from the optical data, one of the most useful is the maximum specific optical density D_m , which will be used herein.

Smoke weight is measured gravimetrically under flaming conditions in the Arapahoe Chamber by filtering the particulates. Combustion products from a small sample are continuously drawn through a glass fiber filter. At the end of the test both smoke particulates and char are determined gravimetrically and are reported as percentages of amount of the original sample burned. The method is particularly convenient and simple and the results can be shown to correlate with optical smoke values.

Both the gravimetric and the optical method have been used to measure smoke generation from a series of typical jacketing or insulation materials used in the wire and cable industry. A Round Robin evaluation of the test methods was conducted in which eight labs ran slab samples in the Arapahoe Smoke Chamber and 10 labs evaluated both wire and slab samples in the NBS unit. Variability estimates were obtained for smoke results from both instruments using statistical analysis. The purpose of the interlaboratory study reported herein is to compare the variability that occurred in smoke results and to show correlation between gravimetric and optical smoke values.

MATERIALS AND EQUIPMENT

A variety of polymers representing typical jacketing and insulation materials were evaluated in the interlaboratory evaluation. Silicone rubber, flame retardant crosslinked polyethylene, chloroprene, chlorosulfonated polyethylene, polyvinyl

chloride, flame retardant ethylene propylene rubber, and a fluorocarbon were supplied in wire and in 20 to 30 mil slab configurations. A rigid PVC reference material in 125 mil thickness, plus eight different slab samples were supplied to the laboratories that ran the gravimetric chamber. Nine slab and eight wire samples were sent to the laboratories that obtained the optical data.

Gravimetric smoke measurements were made with Arapahoe Smoke Chamber model 705. Optical data was obtained with NBS-Aminco Model J4-5800B instrument. Four Arapahoe Chambers were shared among six of the gravimetric Round Robin participants in the study. Two of the laboratories had instruments in house and had previous experience in operating the unit. Approximately 4 to 8 hours of learning time were required from those labs with no prior experience. In contrast, all participants that obtained optical measurements had instruments and experienced operators in their laboratories prior to beginning the Round Robin evaluation.

TEST PROTOCOL

Along with the learning period for the gravimetric method, other procedural modifications were necessary to complete the interlaboratory study. For example, the NBS Chamber is most suitable for slab samples. A new procedure was devised to evaluate wire composites in the instrument. The remainder of the work in the optical method was done with standard procedure under flaming conditions. The D_m was calculated from the following equation as an average of 3 replicate runs per sample material

$$D_m = \frac{V}{AL} \left(\log_{10} \frac{100}{T_m} \right) \quad (1)$$

Where V = Volume of the NBS Chamber occupied by smoke.

A = Exposed area of the sample from which smoke is generated.

L = Length of light beam path in the Chamber.

T_m = Minimum light transmittance.

It should be noted that in the interest of reducing the work load, none of the 8 laboratories were required to evaluate all of the materials in both the flaming and nonflaming modes in the NBS-Aminco Chamber.

The procedural changes for the Arapahoe Chamber were more extensive. The instrument is best suited for 125 mil thick slab samples. Most polymers will produce a measurable quantity of smoke without overloading the filtration system when burned for 30 seconds under standard conditions. The slabs were supplied in 20 to 30 mil thickness. Doubling or tripling of the sample or the flame exposure time was required in most instances to obtain a measurable quantity of smoke. This probably increased the variability seen in the gravimetric test results. Table 1

shows the procedure changes required for the eight samples (materials 1, 3, 5, 7, 9, 11, 13, 15) evaluated in the Arapahoe Chamber.

In addition to changes in the test protocol, the calculation procedure was modified for samples 3 and 5. The materials dripped under flaming exposure and burned cleanly without charring. To maintain consistency in the calculation of the percentage smoke, the drips were considered to be unburned material and the calculation of percent char was not carried out. Most of the laboratories were able to finish the entire series of samples in 8 to 16 hours. The data reported represents an average of 5 sample replicates per material.

RESULTS AND DISCUSSION

The average smoke values for each material were obtained. Tables 2, 3 and 4 contain the data for each material and lab. This is the background information used in the statistical analysis herein. The procedure was developed by Dr. John Mandel at the National Bureau of Standards⁶ and has been used by the ASTM to analyze Round Robin data from other smoke test programs. The procedure yields a relative repeatability and reproducibility estimate within and between labs by material.

The first is defined as the relative repeatability. It is the percentage difference within a one instrument lab with one operator required to establish (with good confidence) that materials are distinguishable from one another in average smoke value. The second is the relative reproducibility. It is the percentage in the mean smoke value required to discriminate (with good confidence) between materials run in different machines at different laboratory locations. Good confidence is defined as being 95% sure of the correctness of the decision. The repeatability and reproducibility within and between labs for data from the NBS and Arapahoe Chambers by material is shown in Table 5.

Comparison of the gravimetric and the optical slab results shows the Arapahoe Chamber to offer greater within laboratory precision than the optical chamber. The relative repeatability within labs is slightly better for the gravimetric method. This could indicate that the gravimetric chamber is a better ranking tool for comparing smoke values from a consistent series of materials within any given lab.

But the NBS Chamber shows better reproducibility. The optical data is more consistent between laboratories than gravimetric data from the same set of slab samples run under similar flaming conditions. This is probably related to the experience factor explained in the materials and equipment section of this report. The operators of the optical smoke measurement instruments had more time to standardize their procedure and equipment before beginning the test series.

A more valid comparison is to look at the gravimetric results for the 125 mil rigid PVC reference samples. This material was usually run before the samples in the interlaboratory evaluation to verify the proper function of the gravimetric hardware. As displayed in Table 5, a substantial reduction in variability within and between laboratories occurred relative to all other slab or wire samples in the study. This is an indication of the type of variability that should occur under good conditions, (i.e. non-dripping 125 mil thick material) in the gravimetric chamber. Furthermore, the variability for the reference material is lower than the historical results of interlaboratory evaluations of the optical test method as shown in Table 6.

This is the result of several inherent factors in gravimetric smoke measurement. First, the equipment is much more simple and easy to operate. No complicated optical apparatus is present. Smoke loss by deposition on the walls and floor of the combustion chamber is held to a minimum in the flow through system.

But the relevance of smoke weight percentage determinations remains to be established. To obtain the benefits of speed, simplicity and precision the smoke mass, a primary result of combustion is measured. However, light obscuration, as secondary effect of combustion, is of the most interest. Therefore, correlation of the gravimetric results with light obscuration as measured by optical density is essential.

CORRELATION OF OPTICAL AND GRAVIMETRIC METHODS

Several methods have been used to relate gravimetric smoke results from the Arapahoe Chamber with optical results from the NBS-Aminco instrument. Data obtained by Kracklauer, Sparkes, and Legg⁵ shows that D_m is directly proportional to the percent smoke measured in the Arapahoe Chamber. But separate curves are required for each material. Application of this theory led to the use of the gravimetric method as a ranking tool for screening consistent series of samples of the same material type. No attempt was made to directly predict D_m since a separate correlation was required for each material.

Samples of polymethyl methacrylate, polyvinyl chloride, polyester, and polystyrene were evaluated by Hilado and Cumming at the Fire Safety Center of the University of San Francisco. Data was obtained from both the Arapahoe and the NBS-Aminco Chambers. Correlation was established between percent smoke and D_m in both the flaming and nonflaming modes of exposure.

More recent work by Seader and Ou at the Flammability Research Center of the University of Utah⁶ has led to a generalized theory applicable to a wide variety of materials. The use of radiative transport theory for light attenuation by scattering and absorption together with particle coagulation theory resulted in an equation relating

particle mass concentration to optical density as follows for flaming and nonflaming combustion:

$$D/L = (POD) C_s \quad (2)$$

Where D = Optical density
 $\log_{10} (100/T_m)$.

C_s = Mass concentration of particles.

POD = Particulate optical density = 33,000
 cm^2/gm

L = Light path length.

The theory can be applied to nondripping materials that behave similarly under flaming combustion in both the NBS and Arapahoe Chambers. According to Ou and Seader⁹ concentration of particles C_s can be determined from the percent smoke value in the Arapahoe Chamber and the weight loss in the optical method as follows:

$$C_s = \frac{T_1 M}{V} \quad (3)$$

Where T_1 = M_p/M_a = Arapahoe percent smoke when char is deleted from the calculations.

M_a = Airborne mass loss in the Arapahoe Chamber.

M_p = Smoke particulate mass determined in the Arapahoe Chamber.

M = Airborne mass loss of the specimen as measured in grams in the NBS Chamber.

V = Volume of the NBS Chamber.

Rearrangement of equation (2) together with substitution of the proper value for POD, V , C_s , and L yields the following predictive equation (4) for determination of D_m . The assumptions used to arrive at this equation are:

1. The weight of smoke particulates in the NBS Chamber is not reduced by settling, and
2. The weight of smoke produced per amount of sample burned (T_1) is the same for both instruments.

$$D_m = (7.8) (M) (T_1) \quad (4)$$

An estimation of M can be obtained by assuming that all exposed material in the NBS Chamber is completely consumed during the test. This assumption appears to be most valid for thin samples such as the 20 to 30 mil slabs supplied for the interlaboratory evaluation discussed herein if no charring occurs.

But char formation occurs during the combustion of most polymer systems such that a better approximation of M could be obtained if percent char measurements from the Arapahoe Chamber are taken into account. This yields the following application of the theory proposed by Seader and Ou for prediction of D_m .

$$D_m = (7.8) (M) (T_2) \quad (5)$$

Where T_2 = Smoke mass percentage of the total airborne loss and char produced in the Arapahoe Chamber.

Application of this equation to the smoke and char data from the slab samples in the interlaboratory evaluation yields the correlation in Figure 1. The data used for this is the average smoke result across all laboratories for each material. If material 15 is dropped from the series, an excellent correlation with a coefficient of 0.88 is shown between the D_m predicted values and those actually measured by the Round Robin participants.

Material 15 was dropped because of dissimilar burning that occurred in the two instruments such that a basic assumption of the correlation theory was violated. Sample 15 was doubled in thickness before being run in the gravimetric chamber. Unlike the other slab samples in the series, doubling the thickness changed the burning characteristics. Melting and dripping occurred at single thickness in the NBS Chamber, but did not occur at double thickness in the Arapahoe instrument. This led to a disproportionately low smoke value in the NBS Chamber which cannot be accounted for by this predictive method.

CONCLUSIONS AND RECOMMENDATIONS

Good correlation is shown between Arapahoe gravimetric smoke values and NBS Chamber optical data for slab samples run in the flaming mode if burning characteristic of the material are similar. This confirms the work by Seader and Ou at the University of Utah and Hilado and Cumming at the University of San Francisco. Although the correlation is particularly good for nondripping solid materials, it appears to be valid for samples that drip under flaming exposure.

Comparison of the variability in the slab data shows the gravimetric unit to have superior average repeatability within labs and the optical chamber to have superior average reproducibility between labs. But the gravimetric instrument was run by relatively inexperienced operators on thin samples that required substantial technique development. When a learning situation existed and nonstandard procedures were required from both instruments, the gravimetric chamber showed better reproducibility and repeatability than the optical method. An indication of the improvement that could be seen in the precision of the gravimetric results is reflected in the data from the rigid PVC reference material.

The data presented herein establishes the gravimetric method as a useful screening tool for smoke evaluation. It provides superior precision to the optical method with the advantage of speed and simplicity for higher sample throughput in smoke research programs.

ACKNOWLEDGEMENTS

The authors are indebted to the members of the IEEE Power Engineering Society WG 12-36 Subgroup on Smoke for the release of the interlaboratory data from both the NBS and Arapahoe Chambers for outside publication. This paper is published by the consent of Arapahoe Chemicals, Inc., a Syntex Company in Boulder, Colorado.

REFERENCES

1. Kracklauer, J.J., Sparkes, C.J., "A Critical Review of Smoke Hazard Criteria for Construction Products," *Plastics in Building Conference* of the SPE Regional Technical Conference, November 9-10, 1976.
2. Anon, "Three Studies of Smoke and Gas Fatalities Funded," *NBS Dimensions*, Dec., 1974 pg. 283.
3. Berl, W.G., Fristom, R.M., Halpin, B.M., "Fire Problems," *APL Technical Digest*, The Johns Hopkins University, 14, No. 2, (1975).
4. Lee, T.G., "Interlaboratory Evaluation of Smoke Density Chamber," *NBS Tech. Note 708*, U.S. Government Printing Office, Washington, D.C., December, 1971.
5. Kracklauer, J.J., Sparkes, C.J., Legg, R.E. "New Smoke Test--Fast, Simple, Repeatable," *Plastics Technology*, Volume 22, No. 3, March, 1976, pp. 46-49.
6. Results of the 1975 Smoke Density Chamber Round Robin Conducted by ASTM E5.02, Working Document, pg. 1.
7. Hilado, C.J., Cumming, H.J., "Studies with the Arapahoe Smoke Chamber," *The Journal of Fire and Flammability*, Volume 8 (July '77) pp. 300-308
8. Seader, J.D., Ou, S.S., "Correlation of the Smoking Tendency of Materials," *Fire Research*, Volume 1, 1977, pg. 3.
9. Seader, J.D., Ou, S.S., "Correlation of Gravimetric Smoke Measurement by the Arapahoe Chamber with Optical Smoke Measurement by the NBS Chamber for Flaming Combustion," in press *Fire Research*, Volume 3, 1977.

BIOGRAPHIES

Jack J. Kracklauer obtained a B.A. and B.S. in Chemical Engineering in 1964 from the University of Notre Dame. Industrial experience includes two years in process development and engineering with Union Carbide Corporation in silicone manufacture with three years of product development and technical services for silane coupling agents with Union Carbide at Tarrytown, NY. Joined Arapahoe in 1969 and has spent the last 8 years in product and market development, primarily in the plastics additives area. Currently manager of the Market Development Department with Arapahoe.

Charles J. Sparkes was born in England and obtained a B.S. degree in Chemistry in 1966. Initial industrial experience in the pharmaceutical industry with Glaxo Laboratories. In February 1968, moved to the Bahamas to work with the Syntex Corporation in Steroid Chemistry. In 1972, transferred to Arapahoe Chemicals, Inc., a Division of Syntex Corporation, to work in the development and commercial introduction of smoke suppressant/flame retardant technology in the plastics industry.

Rod E. Legg obtained a B.S. in Chemical Engineering in 1973 and an MBA in 1975 from the University of Colorado. Joined Arapahoe Chemicals, a Syntex Company in Boulder, Colorado in 1972 to work on the development of smoke test equipment and flame retardant/smoke suppressant plastics additives. Currently a product development engineer in the Market Development Department.

FIGURE 1

Predicted Versus Actual Dm For Slab Sample

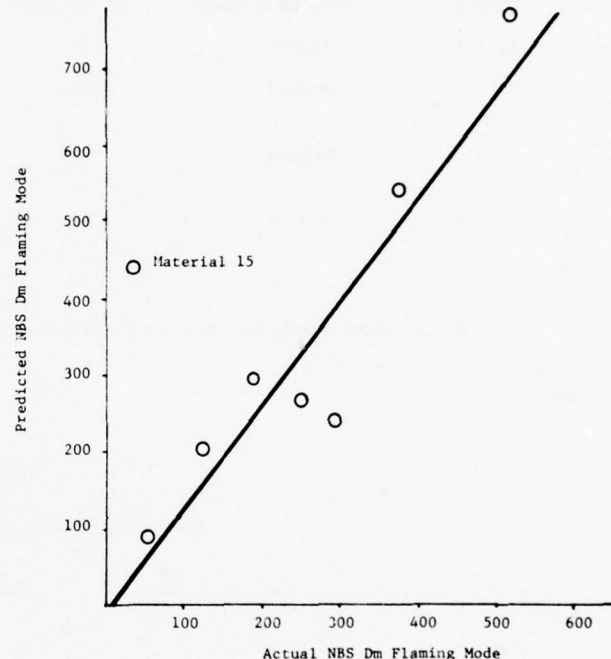


TABLE 1
PROCEDURAL REVISIONS FOR THE GRAVIMETRIC CHAMBER*

| <u>Sample Number</u> | <u>Required Thicknesses of Standard Samples</u> | <u>Sample Burn Time in Seconds</u> | <u>Comments</u> |
|----------------------|---|------------------------------------|--|
| 1,11,13 | Single | 30 | Char delaminated during combustion. |
| 3 | Double | 60 | Drips were caught in a preweighed dish. No char was produced. |
| 5 | Triple | 60 | Sample burned cleanly and dripped. Preweighed dish was used to catch drips. |
| 7,9,15 | Double | 60 | Char delaminated during combustion. Preweighed dish was necessary to prevent char losses. |

* Standard conditions are a 30 second burn time for a 1 1/2 inch x 1/2 inch sample.

TABLE 2
ARAPAHOE PERCENT SMOKE FOR SLAB SAMPLES

| Lab | MATERIAL | | | | | | | | |
|---------|----------|----------|----------|----------|----------|-----------|-----------|-----------|------------|
| | <u>1</u> | <u>3</u> | <u>5</u> | <u>7</u> | <u>9</u> | <u>11</u> | <u>13</u> | <u>15</u> | <u>Ref</u> |
| 1 | 7.28 | 4.65 | 1.75 | 7.50 | 7.38 | 11.03 | 16.92 | 18.45 | 10.50 |
| 2 | 7.48 | 6.22 | 2.60 | 6.74 | 6.86 | 10.08 | 14.84 | 9.63 | - |
| 3 | 8.02 | 4.70 | 2.17 | 7.05 | 7.48 | 12.30 | 15.24 | 15.06 | 10.70 |
| 4 | 7.58 | 2.83 | 2.95 | 6.86 | 6.32 | 10.58 | 13.94 | 10.58 | 10.67 |
| 5 | 9.45 | 6.18 | 3.30 | 8.38 | 8.23 | 16.15 | 18.20 | 16.70 | 11.00 |
| 6 | 8.18 | 3.80 | 3.28 | 6.59 | 6.30 | 9.97 | 13.53 | 7.65 | 12.15 |
| 7 | 10.13 | 1.67 | 2.20 | 7.55 | 9.18 | 10.57 | 16.77 | 17.63 | 12.50 |
| 8 | 8.78 | 5.93 | 3.00 | 8.68 | 7.80 | 9.53 | 19.68 | 19.03 | - |
| Overall | 8.37 | 4.33 | 2.65 | 7.33 | 7.43 | 11.06 | 15.84 | 14.08 | 11.16 |

TABLE 3
D_m FOR SLAB SAMPLES

| <u>Lab</u> | FLAMING MODE MATERIAL | | | | | | | | | |
|------------|--------------------------|----------|----------|----------|----------|-----------|-----------|-----------|-----------|--|
| | <u>1</u> | <u>3</u> | <u>5</u> | <u>7</u> | <u>9</u> | <u>11</u> | <u>13</u> | <u>15</u> | <u>17</u> | |
| 1 | 249 | 156 | 62 | 200 | 306 | - | - | - | 248 | |
| 2 | 258 | 126 | - | - | - | 415 | 614 | 50 | - | |
| 3 | - | - | 59 | 190 | 301 | 407 | 645 | 41 | - | |
| 4 | 252 | - | 38 | 177 | - | - | - | 33 | 222 | |
| 5 | 257 | - | - | - | 278 | 360 | 441 | 34 | 246 | |
| 6 | - | 111 | 57 | 210 | 325 | 406 | - | - | 231 | |
| 7 | 266 | 146 | 69 | - | - | - | 409 | 60 | 252 | |
| 8 | - | - | - | 207 | 297 | 363 | 434 | 23 | 241 | |
| 9 | 252 | 119 | 65 | 227 | 300 | - | - | - | - | |
| 11 | 251 | - | 65 | 169 | 283 | 328 | 578 | 44 | - | |
| Overall | 255 | 132 | 59 | 193 | 298 | 378 | 520 | 41 | 240 | |

TABLE 4
D_m FOR WIRE SAMPLES

| <u>Lab</u> | FLAMING MODE MATERIAL | | | | | | | |
|------------|--------------------------|----------|----------|----------|-----------|-----------|-----------|-----------|
| | <u>2</u> | <u>4</u> | <u>6</u> | <u>8</u> | <u>10</u> | <u>12</u> | <u>14</u> | <u>16</u> |
| 1 | 293 | 924 | 743 | 924 | 426 | - | - | - |
| 2 | 264 | 924 | - | - | - | 369 | 194 | 662 |
| 3 | - | - | 924 | 894 | 485 | 502 | 292 | - |
| 4 | 228 | 924 | 879 | 924 | - | - | - | 809 |
| 5 | 282 | - | - | - | 451 | 456 | 345 | 839 |
| 6 | - | 924 | 924 | 924 | 447 | 558 | - | - |
| 7 | - | 355 | 374 | - | - | - | 146 | 377 |
| 8 | - | - | - | 529 | 403 | 383 | 233 | 456 |
| 9 | 409 | 799 | 751 | 857 | 519 | - | - | - |
| 11 | 245 | - | 628 | 762 | 357 | 213 | 126 | 690 |
| Overall | 289 | 835 | 743 | 834 | 445 | 410 | 224 | 627 |

TABLE 5

RELATIVE PRECISION: SLAB AND WIRE SAMPLES

| Material | Repeatability Within Labs | | | Reproducibility Between Labs | | |
|----------------------|---------------------------|-------------------|----------|------------------------------|-------------------|----------|
| | NBS-Slabs | Arapahoe Slabs | NBS-Wire | NBS-Slabs | Arapahoe Slabs | NBS-Wire |
| 1 | 12.81 | 15.88 | 14.43 | 16.99 | 34.48 | 62.48 |
| 3 | 16.23 | 23.10 | 1.49 | 39.62 | 109.22 | 66.09 |
| 5 | 26.30 | 23.75 | 6.75 | 48.54 | 60.35 | 74.98 |
| 7 | 27.89 | 16.15 | 14.35 | 28.09 | 27.65 | 49.13 |
| 9 | 12.83 | 10.92 | 8.72 | 14.17 | 38.86 | 31.16 |
| 11 | 9.91 | 15.73 | 63.84 | 25.36 | 45.66 | 79.09 |
| 13 | 14.97 | 21.98 | 27.78 | 55.27 | 34.00 | 107.27 |
| 15 | 59.96 | 17.08 | 26.31 | 82.33 | 89.08 | 81.24 |
| 17 | 11.53 | - | - | 12.99 | - | - |
| * | - | 4.84 | 20.46 | - | 22.90 | 68.93 |
| Averaged Variability | 21.38 | 16.60 | 41.69 | 35.93 | 51.36 | 52.08 |

* 125 mil thick rigid PVC reference material.

TABLE 6

INTERLABORATORY EVALUATIONS
OF THE ARAPAHOE AND THE NBS-AMINCO CHAMBERS:
ROUND ROBIN VARIABILITY RESULTS

| Organization | Average Repeatability | Average Reproducibility |
|--------------------------------------|--------------------------|----------------------------|
| <u>ASTM: E5.02 Subgroup</u> | | |
| NBS Flaming Slabs | 31.2% | 62.3% |
| NBS Nonflaming Slabs | 21.5% | 44.8% |
| <u>BSI (Great Britain)</u> | | |
| NBS Flaming Slabs | 24.8% | 50.8% |
| <u>Current Interlaboratory Study</u> | | |
| NBS Flaming Slabs | 21.4% | 35.9% |
| NBS Flaming Wire | 20.5% | 68.9% |
| Arapahoe Slabs | 16.6% | 51.4% |
| Arapahoe Rigid PVC Reference | 4.8% | 22.9% |

EFFECTIVE METHODS OF RETARDING FIRE PROPAGATION THROUGH
CABLE PENETRATIONS IN TELEPHONE EXCHANGES

by

R.L. Medynski

BELL-NORTHERN RESEARCH
MONTREAL, QUEBEC

ABSTRACT

Changing technology has rendered obsolete most present designs of vertical cable penetrations in telephone exchanges. The application of available materials to provide a universal approach to this problem, building code considerations, design and application variables are discussed in the context of the eighteen typical samples submitted to a controlled ASTM E119 type fire test. The conclusions drawn from the tests have resulted in a relatively simple method to effectively seal cable penetrations.

INTRODUCTION

Recent changes in technology coupled with the necessity to economize have resulted in difficulty of application and, proliferation of designs for cable penetrations in telephone exchanges. The proliferation of designs has led to a difficult administrative problem which in turn has manifested itself into a hard look at the existing closures, in an attempt to rationalize this area and arrive at an acceptable alternative. The ideal would be one basic method for all applications, which would meet the building code requirements and application requirements of the telephone company.

Eighteen representative samples were constructed for two separate series of tests. Data collected were analysed to formulate recommendations to Bell Canada for one basic universal system which would be compatible with existing cabled and uncabled penetrations, as well as provide a design basis for future applications.

Testing was carried out by the ULC-S101-1975 "Standard Methods of Fire Endurance Tests of Building Construction and Materials", see Appendix I. From the conclusions it is shown that a relatively simple method satisfying the set design criteria is feasible, both technically and economically, using the facilities and with the technical assistance of the Underwriters' Laboratories of Canada (U.L.C.). The tests were small scale for comparison purposes of closure materials.

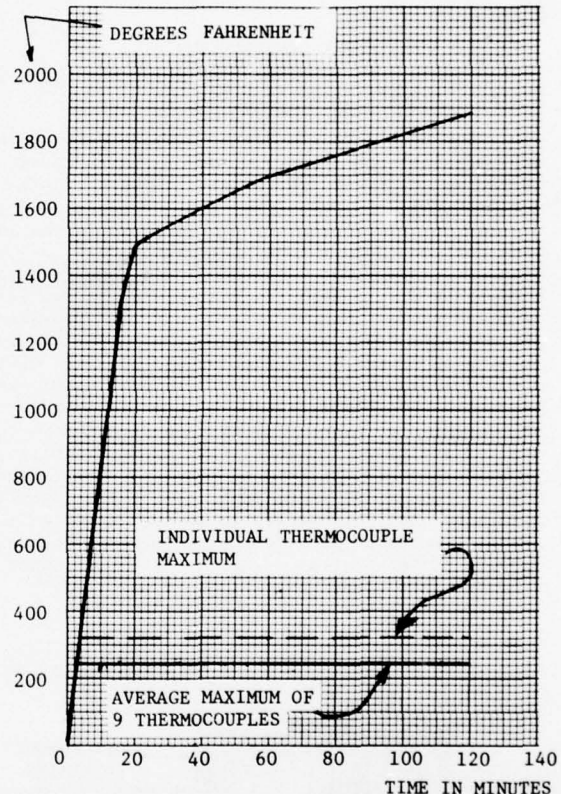


FIG. 1 - TEST FURNACE TIME-TEMPERATURE CURVE.

SCOPE

The scope of the program was to arrive at a method or design of cable penetration closure which will, under recognized test conditions, retard fire propagation for a specified time, given the conditions and variables encountered in telephone exchanges. Types of cables were not considered to be relevant, other than to ensure the use of a typical sampling in the tests.

Study Objectives

The objectives were to evaluate and/or record the suitability of available systems and materials and their effectiveness in the proposed application designs; the effectiveness of cable and wire insulation in group cable configurations to impede flame and gas penetration; and finally to determine to what extent correlations exist between cable decomposition rate through a closure and (i) closure materials used, (ii) closure depth, (iii) the cross-sectional mass of Central Office Equipment (C.O.E.) cable groups. Data gained from the results would be used to standardize on an acceptable cable penetration closure system.

CABLE PENETRATIONS

Design Considerations - Application

The necessity for flexibility, to provide for variable conditions, dimensions and changes in technology precluded a rigid closure design, see Appendix 2 for clarification. Because of the density of cables required in telephone exchange applications, provisions for individual cable openings are not practical. Application conditions also prohibit a design with a myriad of piece-parts. Rather, slots must be provided for multiple cable passage thus assuring flexibility of capacity for the future, coupled with a closure system capable of effecting a seal at any stage of cable fill. Such a system must also be compatible with existing penetrations, to avoid a proliferation thus assuring applicability in all cases of additions of cables, which can occur frequently. Additions require that such a system be easily re-enterable and re-sealable in restricted access locations with minimum tools, labour, administration, and be free of dust, vibration and conditions which may adversely

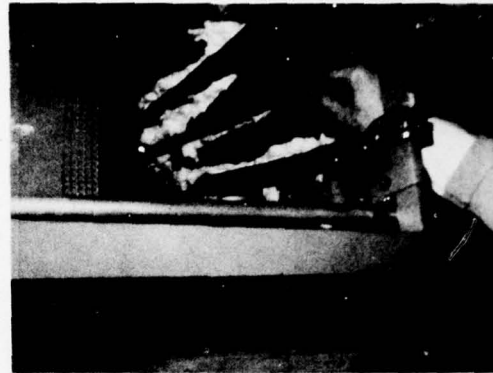


FIG. 3 - SHOWING CERAMIC FIBRE PLACEMENT BETWEEN STUB CABLES IN A TELEPHONE EXCHANGE.

effect adjacent equipment. During the cabling phase of a telephone exchange (central office) extension which may last a number of weeks, it is necessary to keep the penetrations closed as much as possible, a desirable feature of any closure system. The closure top should be sufficiently rigid to withstand normal maintenance activities and, of course, the existing cost levels should not be exceeded.

After a process of elimination it was concluded that a bulk type of material was required which may be packed, or which could flow to fill voids in a cabled penetration.

Building Code

Regardless of the telephone company's design considerations, the building code regulations, Ref. 1, had to be satisfied. Briefly, telephone exchanges fall into a category of building requiring that a floor assembly have a 2 hour rating, in the most severe case. This would be the floor between the basement and the first storey in a building having 4 storeys and over. Other floors and buildings with a lesser number of storeys have less severe ratings. It was decided not to differentiate these variables as administration and control would impose a burden, but to provide a closure system with a 2 hour rating.

TEST SAMPLES

Test samples were constructed of poured reinforced concrete with a specified compressive strength of 3000 lbs., Ref. 2. The external dimensions of the sample slabs were 39 inches x 39 inches x 6 inches deep, this depth being the minimum that may be expected in the telephone exchanges in question. In reality, most critical areas have a greater depth due to additional structural requirements. These slabs were intended to fit the small scale test furnace at the U.L.C. The penetration dimensions were, nominally, 10 inches x 20 inches for C.O.E.

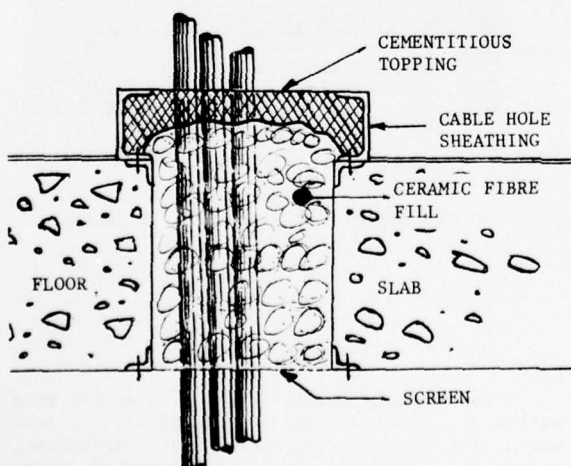


FIG. 2 - CONCEPT OF SEALING AN INTER-FLOOR CABLE PENETRATION.

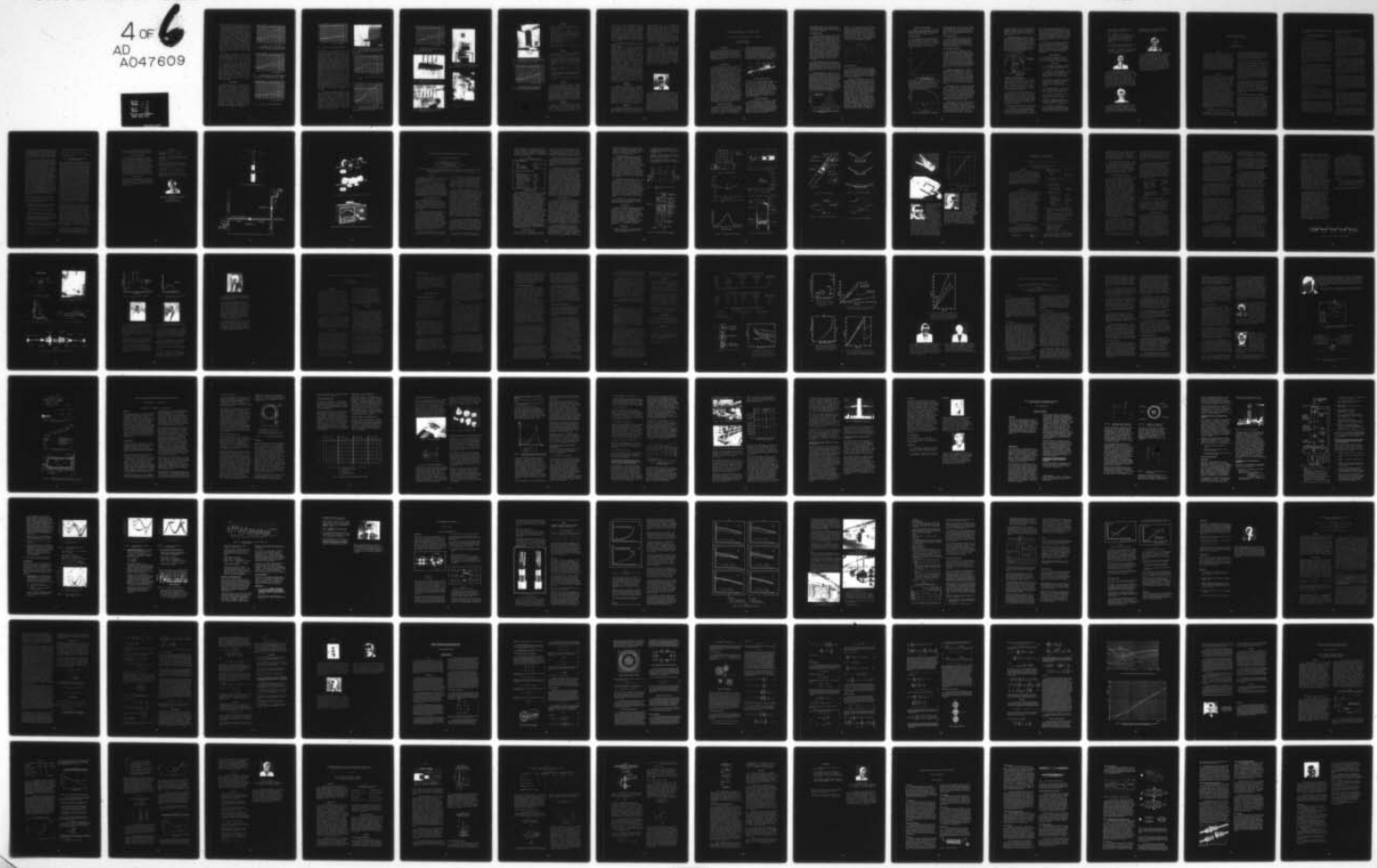
AD-A047 609

ARMY COMMUNICATIONS RESEARCH AND DEVELOPMENT COMMAND --ETC F/G 9/1
PROCEEDINGS OF INTERNATIONAL WIRE AND CABLE SYMPOSIUM (26TH) CH--ETC(U)
NOV 77 E F GODWIN

UNCLASSIFIED

4 OF 6
AD A047609

NL



cables; 10 inches x 32 inches for stub cables. It may be questioned as to the necessity of using concrete slabs to accomodate sample closures, but it would be unrealistic to do otherwise, as the cooling effect of the concrete on a penetration is considerable. Metal, or any substitute material, may produce conditions not encountered "in situ", or become structurally deficient during the course of the test causing premature destruction of the test sample. The dimensions of the penetrations in the slabs were typical, so that the assembled test samples complete with cable racks, cables, etc., were representative of any that may be found in a telephone exchange. Our last sample, Fig. 15 & 16, was estimated to weigh 1200 lbs. At the time of assembly of the test samples, thermocouples were disposed symmetrically onto the closure surface, along the edges of the closure, and into the cable groups as well as cable surfaces. The interior furnace temperatures were similarly monitored and controlled.

One aspect of testing actual size samples that had to be considered was the effect of the cables protruding into the test furnace interior. They would undoubtedly interfere with the normal flow of the gas flames, but to what extent? Would the emissions interfere with combustion? Would the fire retardants in the cable and wire insulation effect the furnace operation? These did occur but were corrected by the introduction of a supplementary air supply through the base of the furnace which enabled the furnace temperature to follow the curve. The following graphs illustrate some of the results. In all cases the highest temperatures recorded are shown and are not the average. The heavy horizontal line at 390°F represents the maximum individual permissible temperature recording which is the 325°F plus 65°F ambient. The variables start at 65°F, and are a solid line for the closures' unexposed surface, and a dotted line for the cable temperatures.

TEST RESULTS

The findings after test indicate that a closure depth of 10 inches is required of a combination of Alumina-Silica Ceramic fibre, see Appendix 3 for a description, as the tightly filled bulk-pack material and a vermiculite, Appendix 4, cement topping. Eight inches of fibre plus two inches of the cement topping. The resiliency of this fibre, even under extreme heat, is retained, thus filling in cavities left by melting cable insulation, and impeding further degradation through the closure. A rigid type of fill would not likely function this way. The vermiculite cement acts as the last thermal barrier and an excellent seal against the passage of smoke & hot gases. In many cases the degradation of the cables was markedly less at the level of the vermiculite cement after they had deteriorated through the ceramic fibre.

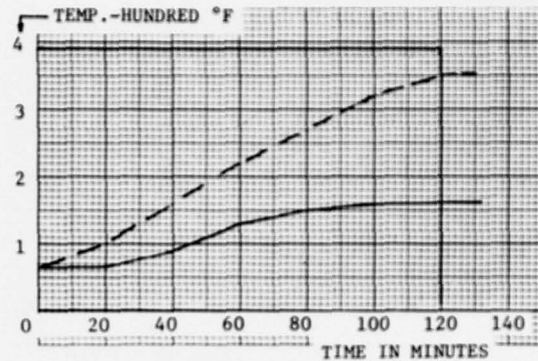


FIG. 4 - TEMPERATURE RESULTS OF CONCEPT APPLIED TO AN EXISTING TYPE OF PENETRATION WITH C.O.E. CABLES. ALL OTHER CRITERIA SATISFACTORY.

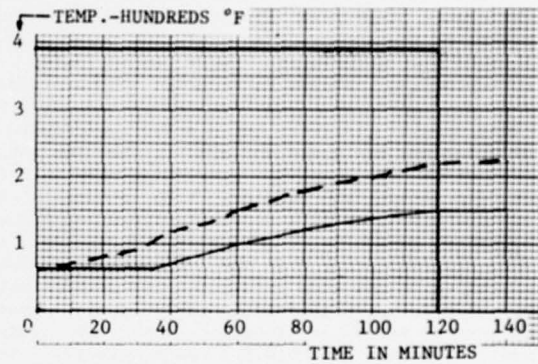


FIG. 5 - TEMPERATURE RESULTS OF A CLOSURE INITIALLY SEALED, RE-OPENED TO ADD C.O.E. CABLES, THEN RESEALED. ALL OTHER CRITERIA SATISFACTORY.

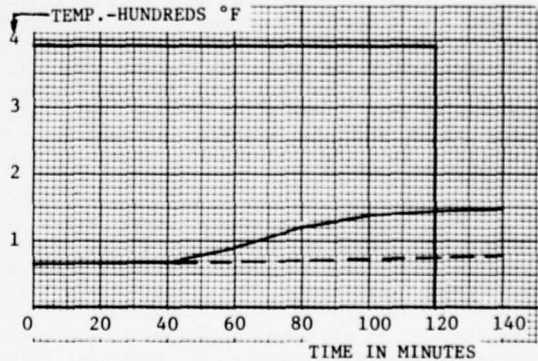


FIG. 6 - AS FOR FIG. 4, BUT WITH STUB CABLES.

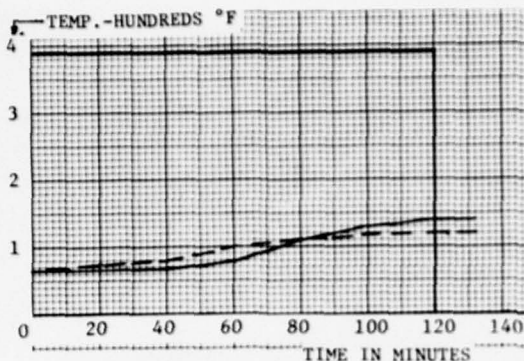


FIG. 7 - AS FOR FIG. 5, BUT WITH STUB CABLES.

Examination after test showed that only 4 inches of ceramic fibre was insufficient because the cables on the unexposed side of the test sample started to deteriorate much sooner with a corresponding increase in recorded temperatures. This was especially noticeable in the C.O.E. cable groups. In these cases a too rapid passage of flame and hot gases appeared to char the cable insulation too rapidly preventing the intermescent effect from forming. With 8 inches of ceramic fibre, small amounts (wispings) of smoke appeared initially, gradually subsiding to nothing, indicating that the intermescent effect of the cable and wire insulation had effectively blocked all openings between cable layers. This, of course, varied in duration with the cross-sectional size of C.O.E. cable groups. The approximate 2 inches of vermiculite cement topping is easily pierced when cable must be added; it may easily be cut with a knife. Cable may then be fed down through the fibre without the necessity of removing it for small numbers of cables. Thus in effect the penetration remains almost intact for the duration of the cabling. To seal, a small amount of vermiculite cement is required around the cable or cables that have been added. Samples that were initially cabled and sealed were opened after curing and cables were added and the closure re-sealed. No sacrifice to the closures' integrity was recorded.

For those penetrations where fibre and vermiculite cement may be placed between cables, even as little as 0.25 inch, no further treatment was found necessary. For penetrations with C.O.E. cable groups, see Appendix 5 for description, it was found necessary to add a fire retardant mastic, Appendix 6, coat or "skin" around the exterior of the cable column. This extended for 4 feet above the unexposed surface of the test sample, and for the 1 foot into the furnace. This "skin" successfully resisted the penetration of smoke and hot gases except in the minutest quantities. Surface temperatures remained at an acceptable level.



FIG. 8 - A FUTURE DESIGN CONCEPT FOR STUB CABLES UTILIZING CONCRETE BLOCK UNITS WITH THE HOLES PLUGGED WITH VERMICULITE CEMENT IN THE UNCABLED MODE.

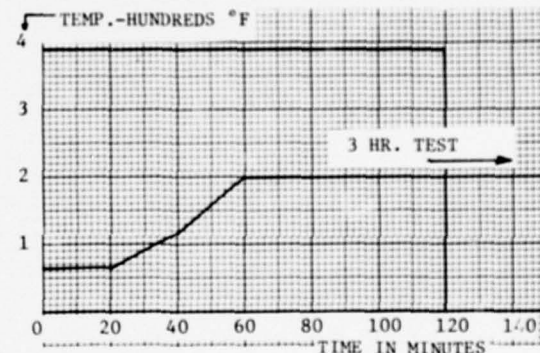


FIG. 9 - TEMPERATURE RESULTS OF TESTING FOR FIG. 8 SAMPLE.

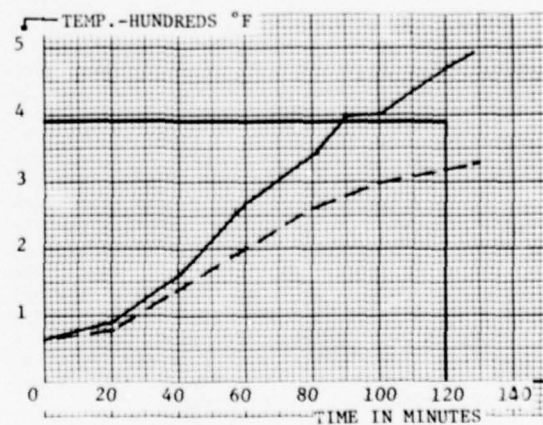


FIG. 10 - TEMPERATURE RESULTS OF TESTING A FIG. 8 SAMPLE WITH 56 STUB CABLES, WITH MINIMAL CERAMIC FIBRE AND VERMICULITE CEMENT.

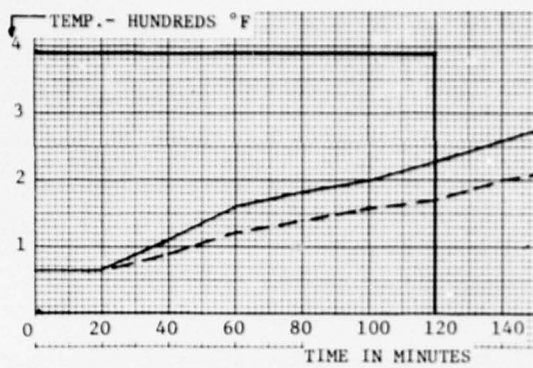


FIG. 11 - TEMPERATURE RESULTS OF A STUB CABLE CLOSURE WITH INCREASED DEPTH OF CERAMIC FIBRE AND VERMICULITE CEMENT.

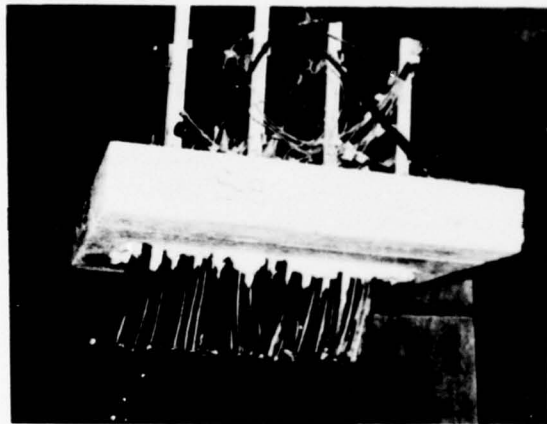


FIG. 12 - STUB CABLE SAMPLE BEING HOISTED ONTO TEST FURNACE.

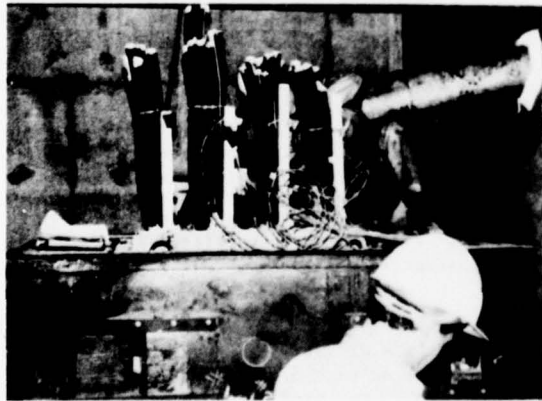


FIG. 13 - SAMPLE ON TEST FURNACE, THERMOCOUPLE LOCATIONS BEING VERIFIED.

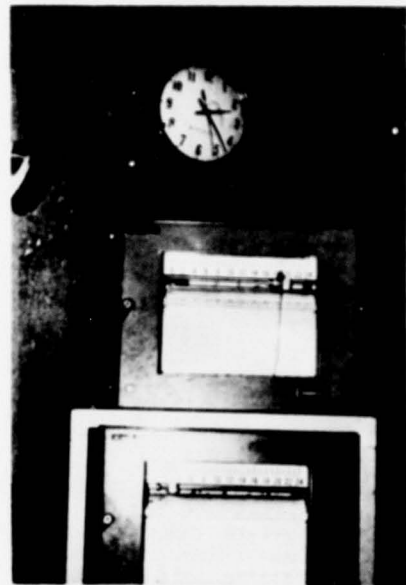


FIG. 14 - VIEW OF RECORDERS, TOP FOR FURNACE TEMPERATURE, BOTTOM FOR SAMPLE SURFACE. WALL CLOCK DENOTES TEST DURATION OF 2 HOURS, 22 MINS.



FIG. 15 - SAMPLE CLOSURE FOR C.O.E. CABLES BEING PREPARED.

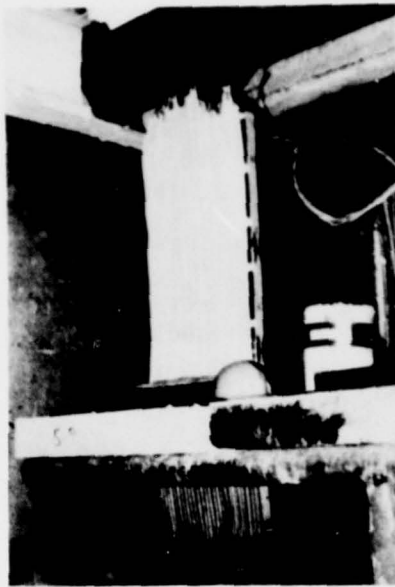


FIG. 16 - SAMPLE COMPLETE, CABLES OF BOTTOM PORTION REQUIRE MASTIC COAT. NOTE THERMOCOUPLE WIRES EMANATING AT TOP OF CABLE COLUMN.

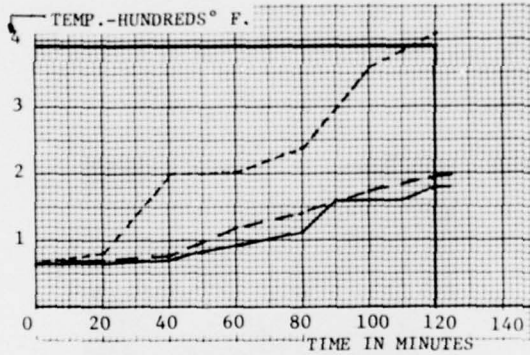


FIG. 17 - TEMPERATURE RESULTS OF LAST SAMPLE. THE TWO HIGHEST CABLE THERMOCOUPLES FROM INTERIOR OF CABLE COLUMN ARE SHOWN.

REFERENCES

- 1) National Building Code of Canada - 1975,
Page 1, Subsection 1.2 "Interpretation of Test Results"
Page 2, Subsection 1.3 "Aggregates Used in Concrete"
Page 3, Subsection 1.4 "Types of Concrete"
Page 36, Table 3.1.2.A "Classification by Group or Division of Typical Occupancies".
Page 39, Table 3.1.3.A
Page 53, (9); and sub-section 3.1.10 "Flame Spread Rating"
Page 70, 3.2.2.29 (1), 3.2.2.30 (1)
Page 71, 3.2.2.31 (1)
Page 72, 3.2.2.32 (1)
- 2) Three samples tested at 3340, 4040, 3620, P.S.I. at 29 days.

APPENDIX 1

This standard is similar to the ASTM-E119, the time-temperature curve is identical. The test criteria applied were as follows:

- 1) The average temperature rise on any part of the unexposed surface may not exceed 250°F (120°C) above ambient, with an individual temperature rise of 325°F (163°C) above ambient. A minimum of 9 thermocouples must be used;
- 2) There should be no penetration of flame or hot gases through or around the closure assembly;
- 3) The cables emanating on the unexposed side of the test samples should not decompose for the test duration;
- 4) The closure must maintain its structural integrity.

APPENDIX 2

The telephone company required a closure system to meet dimensional variations from 6 inches to 10 inches wide and 4 inches to 16 feet long with penetrations at various stages of cable fill, as well as uncabled penetrations provided but not yet used. C.O.E. type of cable penetrations with up to 400 cables representing a cross-sectional area of approximately 225 square inches are frequently encountered. Stub cable penetrations may be found with up to 12 cables per 8 linear inches of 10 inch wide slot, with a potential of 16 cables. Restricted accessibility is a constant in most cases.

APPENDIX 3

Alumina - Silica Ceramic Fibre in bulk form resembles cotton batten. It is a white, light, fibrous, easy to handle material that lends itself to packing into small openings. It is non-allergenic and may be safely handled without

gloves etc. It is a refractory material suitable for continuous exposure up to 2300°F. It retains its resiliency in this temperature range, and thermal stability. In the tests it appeared unaffected by the furnace temperature (1875°F), and could be re-used. Thermal conductivity is very low and it is unaffected by water and most chemicals except for hydrofluoric and phosphoric acids and strong alkalies. In severe thermal applications, up to 2300°F continuous exposure, it will not contaminate or emit offensive odours, since it remains stable and contains no corrosion promoting agents.

The principal constituent elements of this material, depending on the supplier, vary as follows:-

Alumina (Al_2O_3) 45.1% - 46.3%; Silica (SiO_2) 51.9% - 53.2%; and some trace elements. In blanket form it is available in various thicknesses (0.25 in to 2.0 in), widths (12 in to 48 in), lengths, and densities (3 to 24 p.c.f.). This material's primary commercial use is as a refractory product in such high temperature industrial applications as expansion joints and wall linings in kilns and furnaces, high temperature boiler wall insulation etc. The recommended application is to pack voids around and between cables passing through inter-floor cable openings. The resiliency of this product, and its ability to retain this property under extreme heat, is important. This allows the fibre to be packed through a small opening; if a void exists on the other side the fibre will expand to fill that void until its resiliency causes it to "spring" back through the opening if packing continues. This way voids between cables can be filled in the closure reducing the chances of a "chimney" effect in case of fire. Similarly in case of fire the cable sheaths melt or otherwise destruct leaving a void which then promotes further destruction of the cables through the closure. This fibre's resiliency would cause such void to be filled thus reducing further cable destruction.

APPENDIX 4

Vermiculite is available as "expanded vermiculite" from commercial insulation suppliers in the "plaster aggregate" consistency required. Vermiculite is a micalike clay mineral which in its natural state has little commercial use. When heated rapidly to about 570°F, vermiculite can expand to 20 times its original thickness. In this state exfoliated (or expanded) vermiculite is extremely light (specific gravity as low as 0.09) and is used in lightweight concrete or plaster, for thermal and acoustic insulation etc. The application of this material is as the major aggregate in the vermiculite cement which provides the "topping" for the closure method.

APPENDIX 5

These cables are secured to the bars of the ladder type cable racks with cord. Two or more cables, depending on size (for approximately 2 square inches in cross-section), are secured

tightly under one stitch, thus constricting any potential passage of air, gas, etc. Stitches are continuous where a large number of cables are involved or, each succeeding stitch is anchored to the preceding one. The first layer, of course, is also anchored to the bars of the cable rack, these bars being on 9 inch centres. Cables secured thereto must be free of crosses, twists etc., these requirements being quite strictly enforced in the author's experience. This manner of securing has the added advantage of optimizing the cable rack capacity. Thus the vertical cable column becomes a rigid unit with the cable mass constricted at every 9 inches.

APPENDIX 6

Fire retardant mastics are available from several sources and a typical description would be that the material is viscous, fibre-containing, and may be applied by brush, spray or painter's mitt. Its principal commercial use would be as a high-build mastic coating designed to protect group cable against fire propagation. It would be tested in various tests such as Fire Propagation of Free Film, Insulation Tests, Temperature Stabilization, Salt Water Immersion, Thermal Shock, Fire Test, and Dielectric Strength. This material would allow a relatively easy method of increasing fire-stopping capability in some difficult areas.



Roman L. Medynski was born and educated in Montreal, Canada. Since 1955 he was employed by Northern Telecom until 1974, except for a 2 year period with Sperry Gyroscope in quality control, and some military service. During this time he acquired considerable field experience with telecommunications equipment before entering the engineering department of Northern Telecom. This latter experience included Installation Engineering, Equipment Application Engineering- Building Studies. Since 1974 Roman has been with BNR-Systems Consulting. Involvement with the cable penetrations started in 1975 and was quite propitious as this item was a perennial problem during his Northern Telecom days.

DESIGN AND PERFORMANCE OF AN OPTICAL CABLE

M. J. Buckler, M. R. Santana and S. C. Shores

Bell Laboratories
Norcross, Georgia

Abstract

The design and performance of an exploratory optical cable is discussed. The emphasis is placed on current cable design; optical performance - loss, bandwidth and long term aging; mechanical performance - tensile, bend and low temperature handling; and future design and performance directions.

Introduction

Bell Laboratories has in recent years been very active in the development of lightwave communications technology.¹ In 1976 an experimental optical fiber transmission system (designated FT3) operating at 44.736 Mb/s (DS3), the third level of the Bell System Digital hierarchy, was tested at the Bell Labs/Western Electric facility in Atlanta, Georgia.² The DS3 signal is the equivalent of 28 T1 signals, or a capacity of 672 voice channels per fiber. For the Atlanta Lightguide System Experiment, the optical cable, which has a 12mm OD, contained 144 optical fibers with a potential capacity of nearly 50,000 two-way voice channels. The advantages offered by this new transmission medium over conventional copper links are many. For example, optical cables can provide large information carrying capacity, and at the same time can be smaller in size, lighter in weight, more immune to interference, more difficult to tap, and hold promise of being more economical than their equivalent metallic counterparts. This paper will consider the design and performance of the high capacity exploratory optical cable used in the Atlanta Lightguide System Experiment.

Optical Cable Design

The major consideration in the Bell Labs optical cable design was the simplification of the task of splicing the optical fibers.³ This concern provided the impetus for a planar type assembly for holding the fibers. The linear array

ribbon⁴ concept is attractive from the splicing standpoint since groups of fibers can be handled at once with relaxed alignment requirements needed to accomplish mass field splicing. In the Bell Labs optical cable design, 12 of the fiber ribbons (see Figure 1) are stacked in a rectangular array which facilitates the application of factory-applied cable connectors. Each of the 12 ribbons

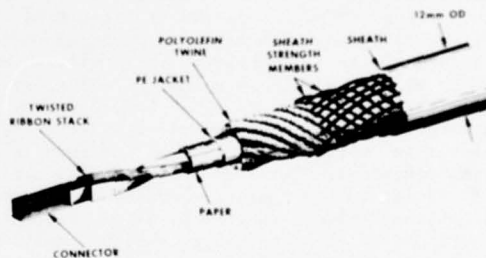


FIGURE 1. LIGHTGUIDE CABLE DESIGN

contained 12 low-loss germania-doped borosilicate multimode optical fibers, for a total of 144 fibers within a single optical cable. The developed view (in Figure 1) of the fiber optic cable shows the various cable components and construction used to achieve a design that exhibits good bending characteristics, thermal and mechanical isolation, and high strength. Optical, mechanical, and long term aging performance results for this cable design will be discussed in the following sections.

Optical Performance

During packaging, microscopic perturbations of the fiber axis from straightness can cause mode coupling and, thus, add loss (microbending loss⁵) and reduce pulse delay distortion.⁶ For our particular fiber design, coupling between guided modes and the light-radiation field occurs when the fiber's axis is deformed with periods of the order of 1mm, and amplitudes as small as a micrometer.

Field-worthy cables must inhibit fiber axis deflections of this microscopic nature and yet allow for normal installation and handling procedures.

Transmission Loss

The Bell Labs fiber optic cable made for the Atlanta system experiment, which was 1023m in length, had 134 fibers (out of the original 144) survive ribbon and cable fabrication. A 658m section of this cable (with 138 transmitting fibers) was installed in a standard plastic underground duct system. In the process of ribbon and cable fabrication, the inherent losses of the fibers were increased⁷ because of microbending. For loss measurements between 0.63μm and 1.05μm, made with an incoherent source, the microbending loss was essentially independent of wavelength, as expected.⁵ The mean increase in loss due to packaging was 1.3 dB/km with 50 percent of the fibers having an added loss less than 1.2 dB/km and 90 percent having an added loss less than 2.9 dB/km.⁷

Light sources used in the system experiment were gallium-aluminum-arsenide lasers operating at 0.82μm. At this wavelength the mean loss was 6.0 dB/km for the installed-cabled fibers, where 50 percent of the fibers had a loss less than 5.8 dB/km and 90 percent had a loss less than 8.3 dB/km.⁷

A basic prerequisite for a Bell System cable transmission medium is that it be a long-life product. Therefore, aging studies under actual field conditions are an integral part of the overall Bell Labs evaluation of fiber optic components for a complete fiberguide transmission system. Thus, the total optical attenuation at 0.63μm (He-Ne) was remeasured for the installed cable, 20 months after the completion of installation. The measurement repeatability using this He-Ne loss set was ±0.2 dB/km for these measurements. Figure 2 shows a histogram of the change in 0.63μm loss over this 20 month time

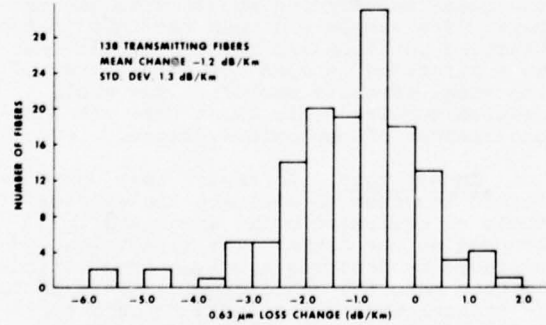


FIGURE 2. HISTOGRAM OF 0.63 μm CABLE LOSS CHANGE DUE TO 20 MONTHS' AGING

interval. The effects of this 20-month aging of the installed cable was to reduce the mean fiber loss by 1.2 dB/km (with a standard deviation of loss change of 1.3 dB/km), with maximum reduction in packaging added losses occurring in outside ribbons in the cable core, and in central fibers within a ribbon. Table I presents a chronological listing of the 0.63μm loss data and fiber yield for the unpackaged fibers to the installed-aged cable.

Table I
Loss and Fiber Yield Versus Manufacturing Processes

| Fiber State | Measurement Date | Fiber Length | Test Set Used | Number of Transmitting Fibers | 0.63μm Loss (dB/km) |
|---------------|------------------|--------------|---------------|-------------------------------|---------------------|
| Unpackaged | 9/75 | 1-2km | Spectral | 144 | 10.9 0.9 |
| ASR Ribbons* | 10/75 | 1km | He-Ne | 137 | 11.7 1.0 |
| Cable on Reel | 11/75 | 1023m | He-Ne | 134 | 12.2 1.1 |
| Cable in Duct | 12/75 | 658m | Spectral | 138 | 13.0 2.1 |
| Cable in Duct | 9/77 | 648m | He-Ne | 138 | 11.8 1.3 |

*Measurements just before cable manufacture.

Impulse Response

The pulse spreading characteristics of 72 of the 144 fibers in the experiment cable were obtained from impulse response measurements taken before and after cable manufacture and again after cable installation. The impulse response was measured at 0.82μm using techniques and equipment described elsewhere.⁸

Assuming the bandwidth to be inversely proportional to length for the 72 unpackaged fibers (incomplete mode mixing), the mean measured fiber bandwidth at the optical 3 dB point was 438 MHz·km. For the manufactured cable the mean 3 dB point bandwidth was 553 MHz for the 1023m on-reel length, and 690 MHz for the 658m installed length. Using the measured bandwidth data for the 1023m length of cabled fibers and the 658m length of installed-cabled fibers, the 3 dB bandwidth was calculated to be proportional to $(\text{length})^{-0.50 \pm 0.17}$. This result agrees with previous predictions of square root of length dependence for complete mode mixing.⁹ Using this square root of length dependence the mean 3 dB bandwidth for the cabled fibers was $559 \text{ MHz} \cdot \sqrt{\text{km}}$. Thus, the 3 dB bandwidth increase in going from uncabled to cabled fibers was 121 MHz (27.6%) for a 1km length. However, this increase in bandwidth was accompanied by a mean increase in loss of 1.3 dB/km.

Mechanical Performance

As part of the mechanical evaluation of the Atlanta Experiment Cable, several segments were subjected to tensile, bend and low temperature handling tests.

Tensile Strength

Two cable segments approximately 15m long were loaded in steps of about 220 N up to a maximum load of 4448 N. Elongation of a 3.0m gauge length was measured and light continuity checks were performed at each load step. Figure 3 shows a typical load-strain curve obtained.

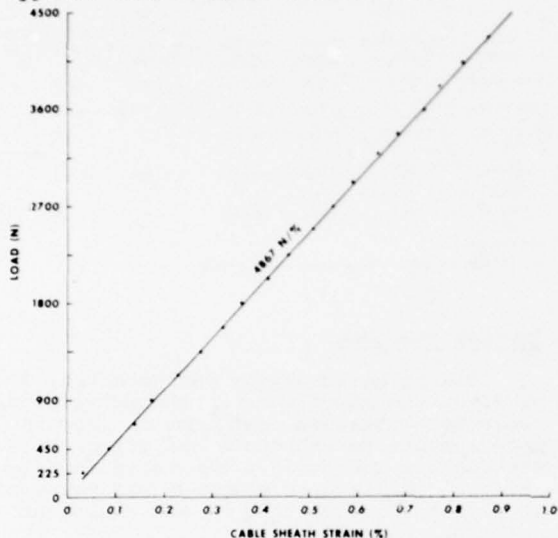


FIGURE 3. LOAD-STRAIN BEHAVIOR OF THE ATLANTA EXPERIMENT CABLE

The behavior is linear up to approximately 4226 N after which the reinforcing strength members in the sheath yield and the tensile stiffness of the cable is lowered. Figure 4 gives the fiber survival versus load and cable sheath strain for the two samples combined.

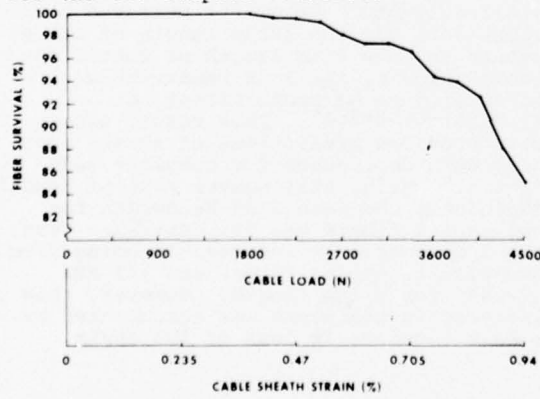


FIGURE 4. PERCENT FIBER SURVIVAL VS CABLE LOAD

No fiber breaks occurred until the cable load exceeded 1779 N. At a load of 4448 N, more than 85% of the fibers survived. These results are encouraging in view of the fact that the cable weighs about 934 Newtons per kilometer.

Bending Properties

A 15m segment of the fiber optic cable was subjected to 20 reverse bends over a 76, 51 and 25cm diameter drum. Continuity checks of the cabled fibers before and after these tests showed no fiber breakage as a result of this room temperature handling.

Low Temperature Handling

In anticipation of possible cold weather installation conditions, such as the Bell System's Chicago Lightwave Communications installation¹⁰ in March 1977, a number of 0°F mechanical tests were performed. These tests were intentionally designed to be more rigorous than the expected field handling, so as to prove-in the mechanical protection characteristics of the cable sheath at low temperatures. Four separate tests were performed on the cable at 0°F with fiber continuity checks made at the conclusion of each test.

Mandrel Strength Test. A mandrel strength test was performed to evaluate the effects of simultaneous bending and tension on the optical cable. In this test a maximum of 1045 N of tension was applied to the cable sample as the sample was formed 90 degrees around a 15cm diameter pulley. The sample was left under load for 10 minutes with no load decay during the test. No mechanical damage occurred to the cable samples during this test.

Twist Test. This test evaluated the effects of torsional loads about the cable axis. In these tests the cable samples were twisted a full 360 degrees per 30cm in a direction to close the spiral wrap of the steel reinforcing sheath strength members. The sample was then returned to the starting position and twisted 360 degrees in a direction to open the spiral wrap of the steel strength members. The cable samples survived this twist test with no occurrences of mechanical damage.

Impact Test. An impact test was performed in order to evaluate the effects of tools or equipment being accidentally dropped on the cable. The impact load was produced by dropping a weight from various heights onto the cable sample. This force is transmitted to the cable through a 0.64cm radius impact head. These tests were performed at 22.7 N-m loads and each

sample was struck ten times. Normal cable samples showed no signs of sheath splits. Moreover, samples which were purposely abraded on rough concrete, such as might occur on a city street, still showed no sheath splits.

Reverse Bend Test. This test evaluated the effects of tensile and compressive forces when the cable sample was bent around small diameters. Tensile forces were produced in one longitudinal half of the cable and compressive forces were produced in the other half when the cable was bent 90 degrees around a pulley. The cable was then returned to the starting position and bent 90 degrees around a second pulley which was parallel to the first pulley (see Figure 5).

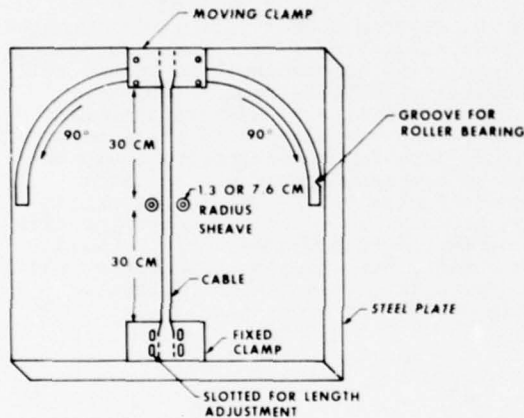


FIGURE 5. REVERSE BEND FIXTURE

This reversal changed the position of the cable so that the tensile side of the cable became the compressive side, thereby completing one cycle of the test. Two test conditions were used at 10 cycles each; one around a 1.3cm radius and the second around a 7.6cm radius. In both cases the cable sheath kinked and finally split at the bend location.

For the four different mechanical tests performed at 0°F, there was no fiber breakage, even in the cases of reported sheath splits. It should also be noted that similar tests at 70°F did not produce any sheath splits or fiber breaks. These tests show that some care must be exercised to retain the mechanical integrity of the cable when handling it in a cold weather environment.

Future Design and Performance Directions

To produce an optical transmission system, the optical cable described here had to be integrated with other required optical transmission components. This integration was successfully accomplished in

the Atlanta Fiberguide Experiment.^{1,2} In fact, the Atlanta Experiment was the stepping stone to the installation of optical fiber cables for the Bell System's Chicago Lightwave Communications Project. For the Chicago project the cables are of the same design as described here (except that they have only two ribbons); these cables are being evaluated under actual live-traffic conditions.

As a result of the design and evaluation of the Atlanta Experiment optical cable, designs and material changes are being investigated. The goal of these efforts is to advance from a technically proven design idea to an environmentally stable, economical design which remains compatible with real-world handling conditions.

Acknowledgement

The successful fabrication of the Atlanta Fiberguide Experiment Cable is due to the efforts of many individuals at Bell Laboratories and Western Electric.

References

1. S. J. Buchsbaum, "Lightwave Communications - An Overview," Physics Today, 29, No. 5 (May 1976), pp. 23-27
2. J. S. Cook, J. H. Mullins and M. I. Schwartz, "An Experimental Fiber Optics Communications System," 1976 IEEE/OSA Conference on Laser and Electro-Optical Systems, San Diego, May 1976.
3. M. I. Schwartz, "Optical Fiber Cabling and Splicing," Technical Digest of Papers of the Topical Meeting on Optical Fiber Transmission I, Williamsburg, Virginia, January 1975, p. WA2.
4. M. J. Saunders and W. L. Parham, "Adhesive Sandwich Optical Fiber Ribbons," B.S.T.J. Brief, 56, No. 6 (July-August 1977), pp. 1013-1014.
5. W. B. Gardner, "Microbending Loss in Optical Fibers," B.S.T.J., 54, No. 2 (February 1975), pp. 457-465.
6. D. Marcuse, "Losses and Impulse Response of a Parabolic Index Fiber With Random Bends," B.S.T.J., 52, No. 8 (October 1973), pp. 1423-1437.
7. M. J. Buckler, L. Wilson and F. P. Partus, "Optical Fiber Transmission Properties Before and After Cable Manufacture," Technical Digest of Papers of the Topical Meeting on

Optical Fiber Transmission II,
Williamsburg, Virginia, February
1977, pp. WA1-1 - WA1-4.

8. J. W. Dannwolf, S. Gottfried,
G. A. Sargent and R. C. Strum, "Optical-Fiber Impulse-Response Measurement System," IEEE Transactions on Instrumentation and Measurement, IM-25, No. 4 (December 1976), pp. 401-406.
9. S. D. Personick, "Time Dispersion in Dielectric Waveguides," B.S.T.J., 50, No. 3 (March 1971), pp. 843-859.
10. A. R. Meier, "'Real-World' Aspects of Bell Fiber Optics System Begin Test," Telephony, 192, No. 15 (April 11, 1977), pp. 35-39.



Michael J. Buckler received his B.S. in Electrical Engineering (3/71) and his M.S. in Electrical Engineering (12/71) from the Georgia Institute of Technology. After graduation in 1971, Mike began work at Bell Telephone Laboratories in the Digital Transmission Division where he worked on high speed digital multiplexers and test equipment. Since 1975, he has been working on exploratory development of optical waveguide transmission media in the Loop Transmission Division. He is a member of IEEE and OSA.



Manuel R. Santana received his B.S. Degree in Electrical Engineering in 1970 from the University of Hartford and his M.S. Degree in Electrical Engineering in 1971 from Georgia Institute of Technology. Since 1970, he has worked on cable design

and development in the Bell Telephone Laboratories Loop Transmission Division. He is a member of the IEEE.



S. Clayton Shores (Clay) was educated at the University of Baltimore, majoring in Industrial Management. He joined Bell Laboratories in 1952 from the Quality Assurance Division of Western Electric Company, and was engaged in the development of capacitance monitoring equipment used in the manufacture of the first Trans-Atlantic cable. He has experience in multipair cable design, central office main distributing frames where he holds one patent, outside plant apparatus, and is presently involved with lightguide cable design and processing.

OPTICAL FIBER CABLE PLACING
TECHNIQUES - LONG SECTION LENGTHS

by

RON SOYKA

GTE California
Santa Monica, California

Abstract

On April 25, 1977, a PCM Trunk Carrier System began carrying commercial telephone traffic over 5.6 miles of optical fiber cable. This was accomplished through a joint experimental venture in Long Beach, California between General Telephone & Electronics Corporation and General Cable Corporation. The cable was placed through a series of 56 manholes in an existing conduit trunk route which joins a central office to a Class 4 toll office. This paper reviews the cable placing techniques used for pulling in unusually long cable sections, some up to one-kilometer in length, with a maximum cable pulling tension restraint of 900 pounds.

Introduction

It has become apparent that the many recent studies undertaken to establish the feasibility of communication systems employing an optical fiber design has produced significant advances in related technology. The GTE experimental project is a testimony to the feasibility and accelerated progress that has been made in the field of optical fiber cable use and from all trend indications will continue¹. It has been established through this project that long underground sections pulls of optical fiber cable can successfully be made utilizing existing conduit systems. Because the attenuation (dB) loss of an optical fiber splice averages .5 dB, and the fiber splicing process and testing requires considerable time, it is desirable at the present time to minimize the number of splice points in an optical cable installation. Placing long uncut lengths of optical cable tends to reduce the number of required splice points. Long section optical cable pulls reflects the viability of technology to provide cost-effective alternatives to the currently conventional cable designs through use of fiber optics². These technology trends and potential applications for an optical cable design have been the subject of many worldwide studies.

Experimental Optical Fiber Cable Design

The experimental optical fiber cable was developed specifically for the GTE California project. This optical communication system changes the traditional

electrical form of carrying people's voices to a radically new system whereby speech is converted into streaming invisible light pulses that travel over hair-thin strands of ultra pure glass contained in a cable assembly designed expressly for optical communications³. (See Figure 1)

Inner Cable Properties of Optical Fiber Assembly

The inner cable design consists of six graded-index optical fiber strands encapsulated in a flat plastic tape. The core of each fiber is .0025 of an inch in diameter; the diameter is .005 of an inch with the cladding, and .006 of an inch with the EVA protective coating. Two fiber strands are assigned to carrier system #1 used for public telephone traffic, two are held as spares and the remaining two fibers are assigned to carrier system #2 used for testing, training and demonstrations. The cable contains an extruded plastic core with two helical channeled grooves and a center wire for additional strength.

The six-fiber assembly (ribbon tape) is placed in one groove, and three pairs of 22-gauge insulated copper wires in the other groove. One pair of wires supplies power to the two regenerative repeaters installed along the cable route, another pair serves as an order wire circuit and the third pair is for fault locating. The extruded plastic core which houses the optical fibers and the three 22-gauge pairs, is wrapped with an asbestos-glass laminated tape.

Structural Properties of Cable Jacket Sheath

Over the laminated tape covering the fiber assembly is a welded .055 of an inch (55 Mils) thick aluminum tube covered with a polyethylene jacket. Covering this inner plastic jacket is a corrugated steel armor, serving as the primary strength member, which is flooded with an asphaltic compound thereby providing a moisture barrier. The exposed surface of the cable consists of an outer polyethylene jacket; the cable diameter is 1.125 of an inch and weighs .45 pounds per foot. The overall characteristics of this cable design prevents shifting of the fiber assembly relative to the sheath, and provides adequate protection from reasonable bending and external impacts. Prior to being shipped from the factory, the cable is pressurized with nitrogen at 10 PSI which prevents

moisture penetration, and also enables monitoring of the cable's physical integrity before and after it is installed.

Planning, Coordinating and Implementing Stages of Cable Installation

Conduit Route Selection

An existing conduit route was selected for the optical cable installation, chosen primarily on the total length of cable required to be tested in the experiment and also that existing conduit and route conditions be reasonably accommodating and typical. The route connected a central office to a Class 4 toll office (see Figure 2) and supported the placing of approximately 5.6 miles of cable through a series of 56 manholes. The route provided several types of conduit material: PVC, MCD and ACD (Transite). Inconsistency of conduit in/out wall position, within some manholes, suggested possible cable pull through problems since ducts were staggered, in some cases, both horizontally and vertically. This condition, however, later proved to be of minor consequence and surprisingly did not present any real handicap even during one-kilometer length pulls.

One of the more significant considerations of the project's preparation and planning was the decision to verify the integrity of the conduit route in detail. An extensive inspection was made of the entire conduit route using a mandrel and washing when necessary; placement of a 3/8-inch polypropylene fish line (used for placement of the primary cable pull line) was also provided at this time. During inspection of the conduit system, it was found that numerous 90-degree bends existed including a 300-foot bridge crossing with three sweeping 90-degree bends at each end of the crossing. The bridge condition was initially considered to be the most adverse cable placing problem. However, analysis of a test pull provided the necessary data to effectively deal with the condition and provide a smooth transition plan for the optical cable pull.

Cable Staging and Testing

The experimental cable, on 11 reels (including one spare reel), was delivered to the staging area loading dock, located at the starting point of job (Long Beach toll office). Upon delivery, each reel was inspected for damage, and the factory pressurization was checked. On-the-reel attenuation (dB) was measured for each fiber; the cable was then re-pressurized after attenuation measurements were made.

It should be noted that the cable was manufactured in approximately one-kilometer lengths because of the processing characteristics involved with the glass material. Test results generally indicated that most fiber joining techniques will cause some attenuation (dB) loss. This loss, however, cannot exceed certain attenuation levels within the cable system, therefore, long section pulls provide fewer splices and less chance of splicing error. It was

agreed early in the project that maximum cable length pulls would be attempted, wherever route conditions made it possible.

Preparation for Cable Pulls

An investigation was made in the area of long cable section pulls and related coefficients of friction, especially since the cable manufacturer established a maximum allowable cable pulling tension of 900 pounds. In attempting to deal with one-kilometer length pulls, the 900-pound tension limit presented an interesting hurdle. A major manufacturer of line tension monitoring instruments was contacted to explore the ways to accurately monitor cable and pulling line tension. The relation of coefficient of friction values between cable, pull line and conduit was explored with a great deal of reservation, primarily because of the assorted and intermixed conduit materials and many 90-degree bends that would be encountered throughout the conduit route⁴⁸.

In addition to the various conduit materials reviewed, regarding friction, the cable pull line selection was found to be one of the essential ingredients for maintaining constant tension smoothness during each section pull. Several types of pull lines were considered and tested: 3/8-inch polypropylene, 1/4-inch wire rope and 1/2-inch dacron rope. It was decided that a 13/16-inch dacron rope (3500 feet - continuous length) would be used based on acceptable elongation properties and that the rope design had been used by underground cable placing personnel for many years as a company standard.

Based on the established cable tension monitoring requirements, which were arrived at from preliminary investigation work, it was agreed that the tensiometer company would provide a running line tensiometer unit, equipped with a meter readout instrument and automatic line tension limit control (see Figures 3 and 3A). A sample of the actual 13/16-inch dacron pull rope was provided for proper calibration of the tensiometer unit. The pulling vehicle was modified to accommodate installation of the tensiometer unit.

Cable Test Pull

Although considerable preliminary information had been accumulated regarding the handling and pulling tension characteristics of the optical cable, there was still a degree of doubt as to the actual optical cable pulling performance outcome. In addition to this apprehension, the cable manufacturer pointed out that the total package cost for the experimental cable represented a sizable investment. It was therefore agreed that a test pull be scheduled in an attempt to assure favorable cable placing results.

A coaxial CATV cable similar to the optical cable in weight and size was provided for the test pull. The initial pull consisted of 2000 feet into the Long Beach toll office. The duct route was encumbered with a long 250-foot sweeping 90-degree approach into the vault with approximately 130 feet

of cable required to be pulled around a 26-1/2-inch X 4-inch pulling wheel, then up three floors to the terminating equipment. During the 2000-foot pull, at speeds upwards to 80 feet per minute, the cable tension remained under 550 pounds; the pulling exercise provided the first positive indication that the cable tension limits would not be exceeded.

Upon recovery of the test cable, by use of a power dolly, a second test pull was scheduled, particularly since there was considerable concern with the previously mentioned bridge crossing located midway in a 3000-foot section. During this pull, excessive line tension was experienced numerous times requiring detailed investigation work. However, because the pull was under a test situation, important data was obtained from the unsuccessful pull and carefully analyzed for modifying of the upcoming optical cable pull. The results of the test pull suggested that the bridge section be made in two pulls; the many sweeping 90-degree bends created excessive drag which even when doubling the amount of lubricating compound the established 900-pound tension limit was exceeded. The excessive tension nevertheless provided an opportunity to observe the pull line tensiometer's automatic limit control feature under actual field conditions. A preset audible alarm with warning light activates when the line tension reaches 80 percent of the 900-pound allowable tension; then a second warning light is activated and automatically turns off the pulling vehicle's engine when line tension reaches 900 pounds. It was generally agreed that a dependable safety factor had been built into the pulling system through use of the tensiometer device, thereby eliminating potential cable damage due to over pulling.

Primary Equipment, Material and Tool Selection

The following equipment, material and tool items are those used for the test pulls and were also used for the optical cable pulls:

1. Pulling Vehicle - Hydraulic constant drive (level wind) bed winch equipped with 3500 feet of continuous length dacron rope.
2. Cable Pulling Grip - 40-inch length with 1/2-inch band clamps for securing grip on cable.
3. Connector Link - Pull rope to cable grip (swivel type 10,000-pound ball bearing action).
4. Running Line Tensiometer - Equipped with meter readout instrument and automatic limit control: complete package adapted to pulling vehicle with separate 12-volt power supply.
5. Lubricant - Approximate use - 5-gallon can for each one-kilometer length of cable: Base make-up consists of a non-drying gel neutral oil.
6. Plastic Collar - For cable protection from conduit at manhole locations.
7. Cable Feed Tube - With split collar.
8. Communication - Two-way hand radio units.

9. Sheave - Pulling wheel 26-1/2-inch X 4-inch.
10. Fish Line - 3/8-inch polypropylene rope.
11. Pull Line - 13/16-inch dacron rope (3500 feet continuous length).

Placing Long Sections of Optical Fiber Cable Becomes Routine

The preliminary cable test pulls provided sufficient performance results to optimistically set in motion the placing routine for the optical cable. The placing crew consisted of six craft construction personnel and one placing supervisor; splicing was performed by laboratory technicians with craft splicing personnel assisting. The first optical cable section pull was generally considered a repeat of the first test pull; line tension readings were approximately the same at 550 pounds during the 2000-foot pull. After the initial pull, most feelings of apprehension became low profile and concern was generally directed more to the physical handling of the cable, i.e., loading reels and positioning at job site in an attempt to avoid any unnecessary damage. Most of the longer pulls of 3000 feet appeared to have similar pulling patterns; line tensions averaged approximately 800 pounds. Probably the most critical period during each section pull was when the cable entered and left intermediate manholes. Each of these locations was observed by placing personnel equipped with radio; pulling speed was reduced when the cable entered the manhole and was increased on instructions of the observer as the cable left the manhole; most cable pulling speeds averaged 90 feet per minute. Cable slack for splicing at each pulling end was obtained by pulling around a 26-1/2-inch X 4-inch pulling wheel. Slack for intermediate manhole racking was obtained usually by two personnel physically pulling the cable by hand starting at the center manhole location; the slack pulling was considerably easier than first anticipated.

The techniques used for placing the optical cable generally paralleled those of conventional cable. Preliminary job difficulty anticipation was focused on unknowns such as damage to the cable from over pulling; once underway however, the tensiometer device provided developing line tension patterns, thereby providing for total control of all section pulls. It was found that maintaining a constant pulling speed eliminated excessive pulling line elongation and cable surging; also, lower and more constant line tension was experienced during higher pulling speeds of 80 - 100 feet per minute. Probably the most significant contribution in obtaining the relatively smooth pulling operation was the liberal application of a newer type of pulling compound, consisting of a non-drying gel neutral oil base. The compound is quite slippery, and adheres well to the cable.

It should be pointed out that each cable section pull had with it a contingency plan for dealing with excessive line tension, should it build up, which could ultimately require the cable to be cut and spliced at the nearest intermediate manhole.

as a last resort. The total cable placing work effort required approximately eleven working days with no serious cable placing damage experienced.

Summary and Conclusion

The experiment has established that an optical fiber assembly housed in a ridged, heavily structured cable sheath can be pulled without damage into existing underground conduit, in uncut lengths up to one-kilometer. The experiment also established that, although the optical fiber cable design dictates greater awareness of handling characteristics compared to conventional cable, conventional placing methods nevertheless can be used. The successful cable placing performance was primarily attributed to the use of a sophisticated running line tensiometer device (operationally simplistic) which provided constant cable tension observation throughout the cable placing operation.

Acknowledgements

The author takes this opportunity to express appreciation for the sincere cooperation and work efforts extended on the part of all associated Outside Plant Construction personnel who made possible the success of the one-kilometer length optical fiber cable pulls.

References

1. Military and Commercial Fiber Optical Application:
GTE Sylvania, Paper by R. J. Gomperts
2. Development of a Robust Optical Fiber Cable and Experience to Date with Installation and Jointing:
Paper from 1976 IWCS P.P. 247
3. Worlds First Optical Communication System to Provide Regular Telephone Service to Public:
GTE News Release 4/25/77 by J. B. Lawrence, Jr.
4. Inferring Duct-Run Geometry from Cable - Tension Data:
A Case History Paper from 1976 IWCS P.P. 152
5. Engineering and Pulling Long Cable Lengths Through Conduit Systems:
Reprint from Telephone Engineer and Management 4/15/74



Ron Soyka
General Telephone Company of California
Engineering and Construction Department -
Outside Plant
100 Wilshire Boulevard
Santa Monica, California 90406

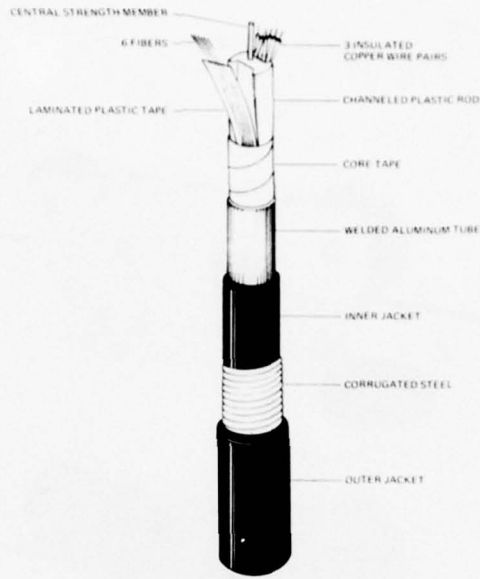


Figure 1 Cutaway Drawing of Optical Fiber Cable

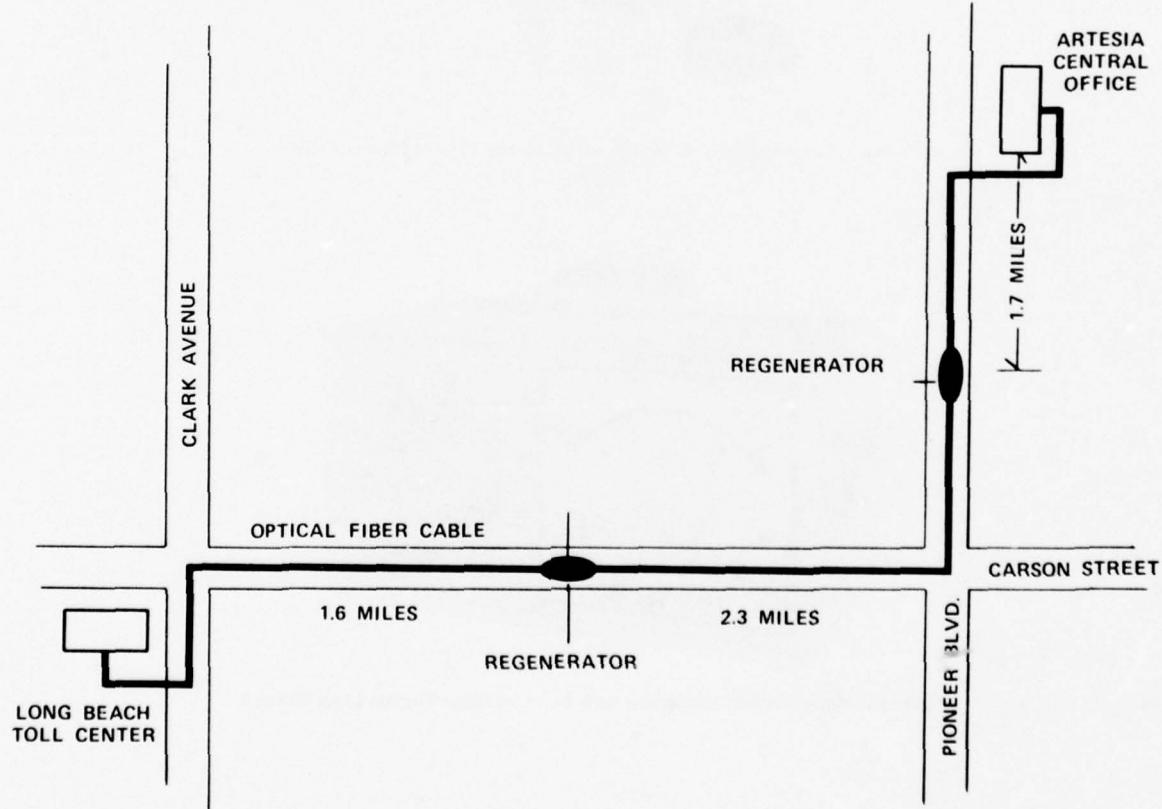


Figure 2 Route of GTE Optical Fiber Communication System Long Beach – Artesia, California

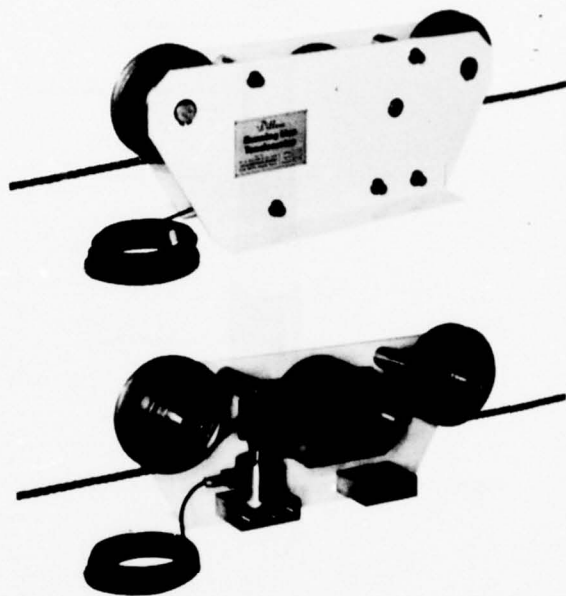


Figure 3: Running Line Tensiometer with Exposed View of Internal Design

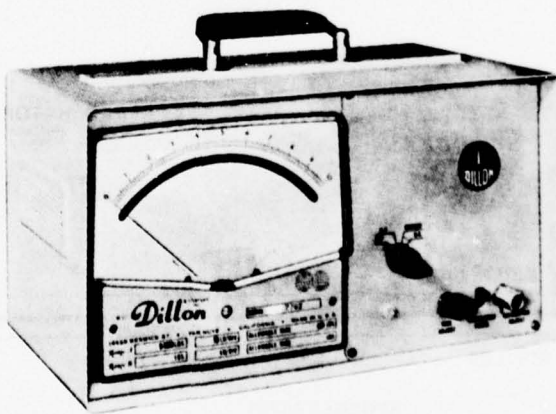


Figure 3A: Meter Readout Instrument with Automatic Line Tension Limit Controls

APPLICATION OF OPTICAL TRANSMISSION IN OUTSIDE PLANTS

E.E. Basch and R.A. Beaudette

GTE Laboratories Incorporated
a subsidiary of
General Telephone & Electronics Corporation
40 Sylvan Road
Waltham, Massachusetts 02154 USA

Index Terms - Fiber Optic Communication, Optical Fiber Splicing, Optical Fiber Cable, Fiber Optic Repeaters, Fiber Optic Transmission, Optical Cable Pressurization

Abstract

The rapid development of optical guided wave technology has proven its feasibility in communication systems.¹ GTE Labs in cooperation with General Telephone of California, GTE Service Corporation of Stamford, Connecticut and General Cable of Union New Jersey has installed a digital voice, telephone transmission facility, connecting two central offices between Long Beach and Artesia, California. The cable was installed in 3-1/2 inch subterranean ducts connecting 55 manholes using conventional pulling methods. This paper briefly describes the system installed and discusses the transmission facility in some detail.

The Implemented System

A simplified block diagram of the optical transmission system is shown in Figure 1. The terminal equipment of the system at Long Beach and Artesia includes a 24 voice channel T-1 bank and optical interface equipment. The latter equipment is located in the Line Terminating Shelf (LTS).

Figure 1 also shows two transmission lines which are kept fully operational. Line #1 carries live telephone traffic and line #2 is maintained on standby. A total of 9.1 km of fiber cable connects the two central offices. Twenty splice points and two repeaters were required to complete the span. The transmission system was implemented to achieve a 10 dB signal margin. This design goal, although somewhat conservative, was calculated to insure that the experimental system would remain useful during the life of the test, even under severe degradation of components or line losses.

Also shown in Figure 1 are the power feed pairs which supply dc power to the span repeaters. One repeater is supplied

from each end office. An order wire line is also provided for service communication. In line with GTE objectives to maintain the highest quality of service, the optical transmission system is backed up by an independent metallic transmission system which is automatically switched in if an emergency occurs. The metallic facility used five repeaters to span the distance.

Two of the voice channels in the experimental system are reserved for test purposes, with an additional channel dedicated to error monitoring equipment. Figure 2 illustrates the layout of equipment in the Long Beach C.O. The four hardware shelves above the optical fiber shelf provide the necessary dc power, fusing and lightning protection. The fiber shelf is used for dressing the fiber lines prior to entering the optical shelf below. The optical terminating shelf and the line terminating shelf contain the electrical/optical interface equipment. The modem interfaces one of the voice channel with error detection equipment. The latter provides a bit by bit error checking in a transmission path that leaves the Long Beach C.O., is looped in Artesia C.O. and returns to L.B. Error records are provided by a hard copy printer at the L.B. end only. No error monitoring equipment is necessary at Artesia.

Figure 3 shows the essential parts of the span repeater. Each line consists of an avalanche photodetector (APD)-amplifier, electronic regeneration circuits and an LED optical line driver in each direction. DC to dc converters are used to convert the single dc voltage input to the low voltages necessary to supply the repeater circuits. Also included is a standard fault locating filter.

The typical attenuation/wavelength characteristics for the cabled fibers are

shown in Figure 4. A point of minimum loss occurs at 820 nm. This matches the LED emission wavelength to optimize transmission as shown in Figure 5. Table 1 illustrates the operating characteristics of experimental system's longest link.

TABLE 1
Typical Line Characteristics

| FIBER PARAMETERS | |
|--|-------------------------|
| Type | Graded Index |
| N.A. | 0.16 |
| Core Diameter | 62.5 μm |
| Fiber Diameter | 125 μm |
| Line Attenuation | 6.2 dB/km (AVG) |
| PARAMETERS FOR LONGEST LINK | |
| Line Length | 3.6 km |
| Operating Temperature | $\leq 60^\circ\text{C}$ |
| Bit Error Rate | 10^{-8} |
| Receiver Sensitivity | -66 dBm |
| Transmitter Output (Out of 2 m Fiber) | -23 dBm |
| Line Power Budget | 43 dB |
| Line Loss | 27 dB |
| Splice Loss | 5 dB |
| Total Transmission Loss | 32 dB |
| Transmission Margin | 11 dB |

The Optical Cable

The optical cable consists of six graded index fibers mounted in a laminated plastic tape.² Figure 6 shows that the tape is loosely fitted in one of two channels created by a channeled porous plastic rod. The center of the resilient plastic rod is reinforced by a 0.1 inch diameter copper strength member which can also be used as a conductor. Three pairs of #22 insulated copper lines are provided in the other channel. These are used for power feed and maintenance service. A welded aluminum tube encases the core components and an inner PVC jacket acts as a moisture seal. A corrugated steel wrap over the inner jacket protects the latter against damage during installation. Finally, an outer layer of PVC helps to reduce pulling friction. The cable obtained in one km lengths, was pulled break-free through 55 manholes and is kept under a dry air pressure of 10 psi. The average loss in the fibers is 6.2 dB/km. The optical system cable route is illustrated in Figure 7. This shows the splice points and the two repeater locations at 2.7 and 6.4 km. Repeater site assignments were influenced by practical considerations (such as working space) as well as transmission performance objectives.³

Cable Termination

Pressurization requires that the cable ends be air tight. Consequently, an end

seal was installed immediately above the optical rack as shown in Figure 8. The cable was brought up from the cable vault and routed directly to the rack where it was stripped back about 8 feet to expose the core, fiber tape and metallic lines.

The laminated fiber tape was reinforced by slipping 3/8 inch PVC tubing over its exposed length. The end seal or pressure dam was installed and fastened above the rack with the fiber tape and metallic pairs routed to the fiber shelf as shown in Figure 8.

The pressure seal is formed by installing a plastic tube on the end of the cable to contain an epoxy sealing compound. Figure 9 illustrates the construction of the pressure seal. The assembly is held together with electrical tape. The latter also seals the lower end of the pressure dam while the contents are curing. Before pouring, the sealer cable preparation consists of stripping the end of the cable so that each layer is exposed to the sealing material to produce a good seal. The fiber tape is composed of two laminated plastic strips enclosing the fibers and sealed only at the edges. This fabrication contributes to easy handling of individual fibers but also results in an air space between layers conducive to pressure leaks. Preparation of the tape for splicing the fibers in the splice case includes sealing of the fiber tape ends. This not only prevents pressure leaks but also protects the tape against internal pressure which could destroy it.

Cable Splicing

The laminated plastic tape shown in Figure 6 acts as a carrier for the individual glass fibers. In the splicing process, the top layer of tape is stripped back about 3 feet to expose individual fibers. Three foot lengths of #24 PVC tubing are installed over each fiber to improve handling. Then, the tape and fibers are secured in a "FIBER TRANSITION" assembly as shown in Figure 10. A support pallet made of fiberglass board 1/2 inch wide by 1-1/2 inches long forms a base to which the protected fibers are secured. An epoxy adhesive holds and seals the fiber tape in place. A short length of plastic heat shrink tubing provides strain relief for the transition assembly. Once assembled in this fashion, the handling characteristics of the fibers approaches that of wire.

The splicing technique used in the California experiment is illustrated in Figure 11.⁴ After stripping the ends to be joined the two fibers are butted in a V-groove milled out of a small copper block. The resulting splice is shown in exploded view in Figure 12. An aluminum splint supports the splice components. The fiber/

V-block as well as the end of the vinyl tubing are cemented to the splint and a section of shrink tubing encases the entire assembly to complete the splice. The resulting connection is 3/16 inch in diameter and 3 inches long.

A diamond cleaving tool is used to face the fiber prior to splicing. The cleaver shown in Figure 13 resembles a wire stripper. In practice, the fiber to be faced is inserted to span the whole width of the opening at the head of the tool. Upon depressing the cleaver arms two small rubber pads are lowered to hold the fiber under tension and at the proper cleaving angle. Activating the knife release lever in the center of the tool drops the diamond cutter to nick the fiber. The tension on the fiber then creates a break which is perpendicular to the fiber axis. Three of these devices were used with excellent success in the field system installation.

Joining of the two fibers for splicing is accomplished with the help of the splicing tool as shown in Figure 14. The photograph shows two fibers butted on a small V-block. The small blocks are small magnets which hold the fibers in place during the operation. A micromanipulator is provided at one end to carefully position the fibers. The splicer also contains a heater beneath the V-block surface to cure the splice adhesive. Curing time is about two minutes. A small lever, shown at the lower left of the V-block releases the completed splice assembly from the curing block.

A graph of typical splice losses is shown in Figure 15. Splice losses were obtained which remained below 0.5 dB for more than 95% of the splices.

Conclusion

The 9 km optical transmission facility installed in California has been operational since April 22, 1977. This experimental system handles live telephone traffic between a class 5 end office and a class 4 switching center. The optical cable was placed in existing underground ducts using conventional placing practices. The intricate problems of handling the small fiber and splicing in manholes was successfully solved. The methods employed offer a promising solution to future applications in telephone transmission systems.

References

1. D. King, O. Szentesis, "Fibre Optics: A New Technology for Communications," Telesis (February 1977).

2. G. Bahdev, J.A. Olszewski, "Experience with Fiber Optic Cable," 1977 International Wire and Cable Symposium (November 1977)
3. R. Soyka, "Optical Fiber Cable Placing Techniques," 1977 International Cable Symposium (November 1977).
4. J.F. Dalgleish, "A Review of Optical Fiber Connection Technology," Telephony (January 1977).

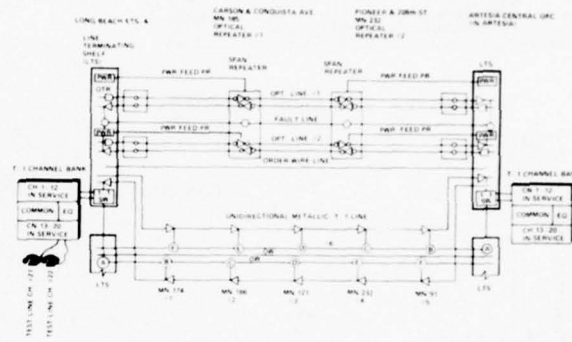


Figure 1. Experimental T-1 Fiber Optic System

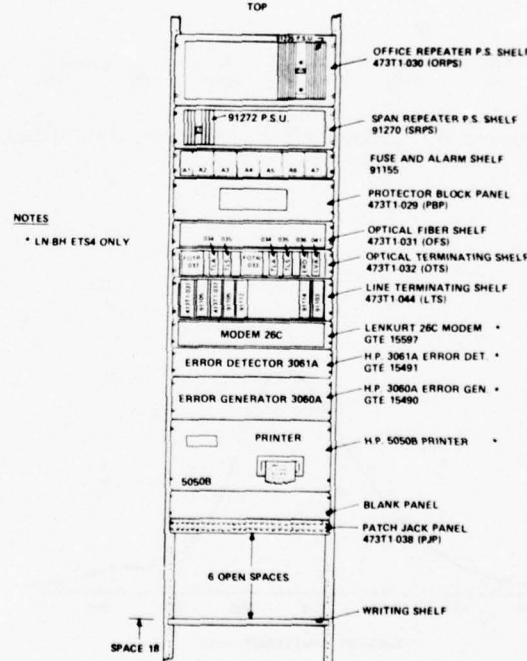


Figure 2. Central Office Equipment

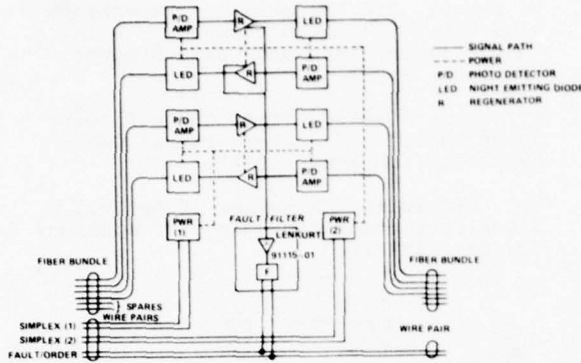


Figure 3. Span Repeater

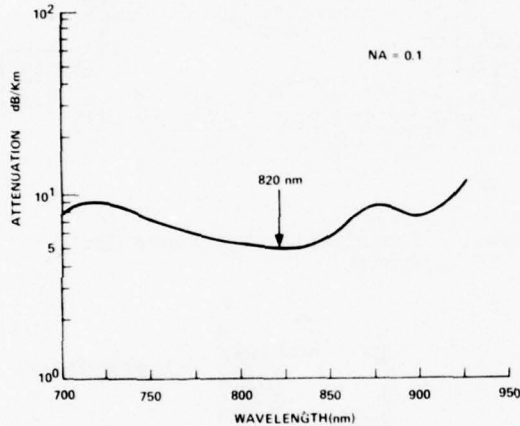


Figure 4. Attenuation Spectrum of Cabled Fiber

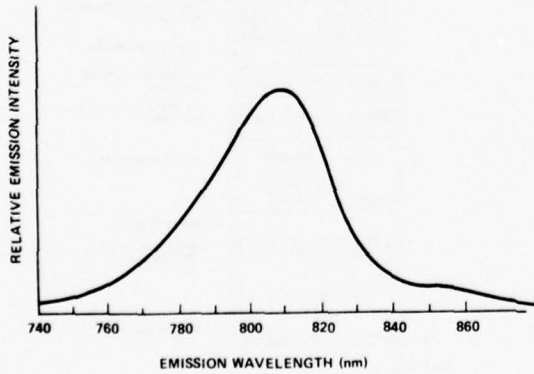


Figure 5. LED Emission Wavelength

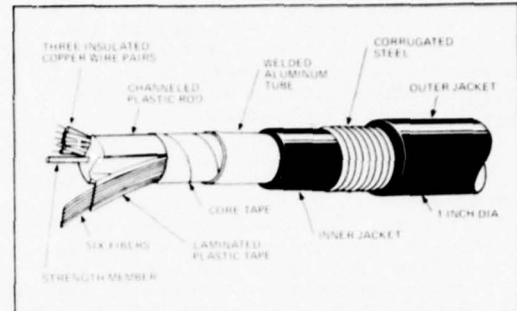


Figure 6. Optical Cable Construction

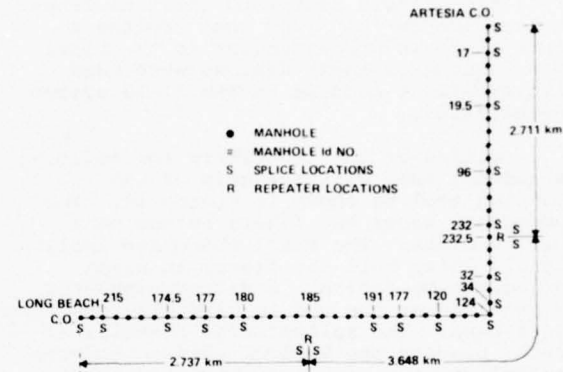


Figure 7. Optical System Cable Route

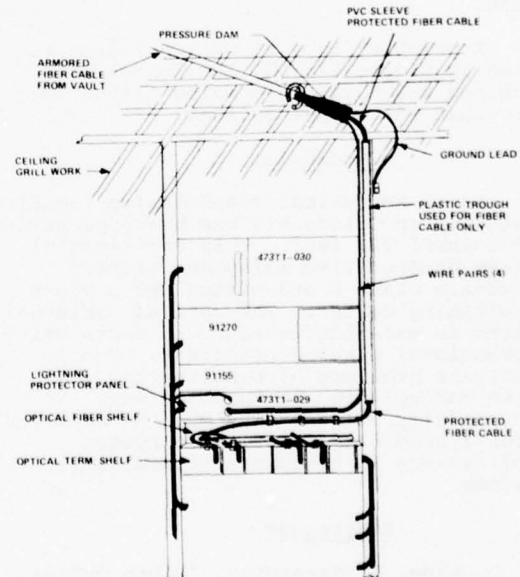


Figure 8. Fiber Cable Routing

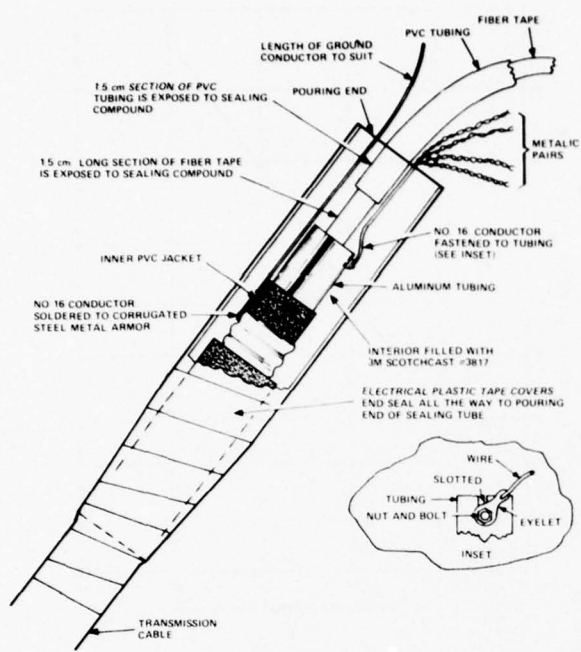


Figure 9. Cable End Seal

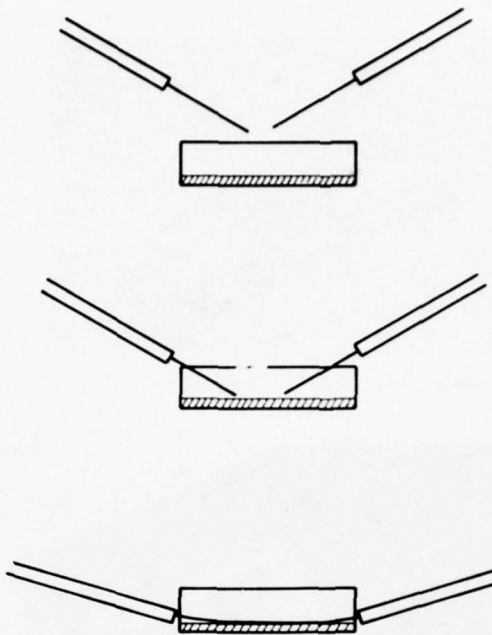


Figure 11. Splicing Principle

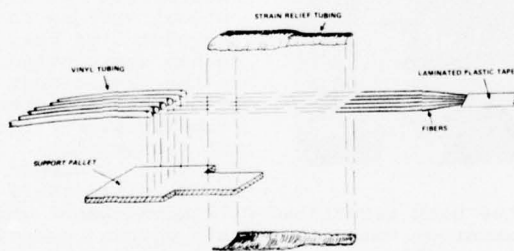


Figure 10. Fiber Transition Assembly

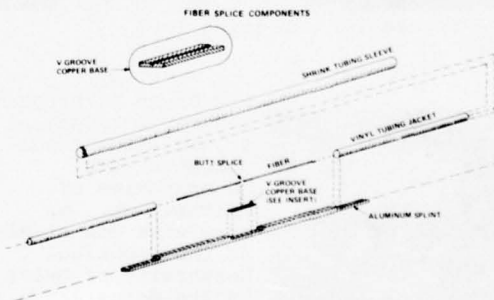


Figure 12. Fiber Splice Assembly

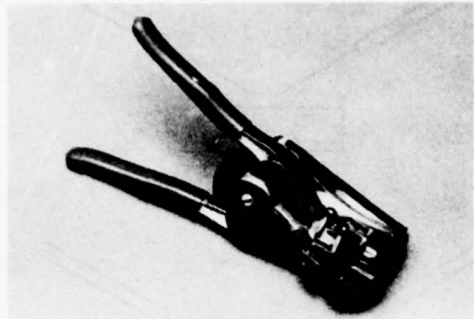


Figure 13. Fiber Cleaving Tool

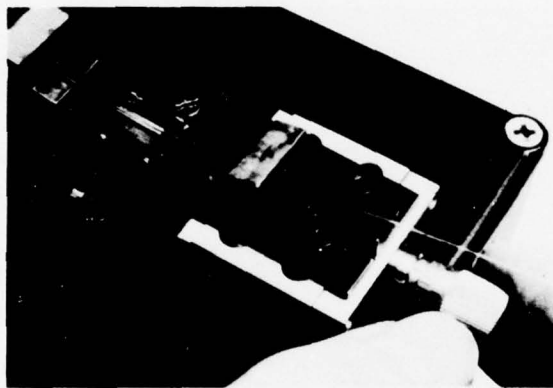


Figure 14. Splicing Tool



Mr. Basch is Program Manager for Optical Transmission Development at GTE Laboratories of Waltham, MA. He completed his studies at the Technical University of Delft in the Netherlands where he was awarded the MS degree in Electrical Engineering.

He has an extensive background in the communications field. This includes video telephones, broadband communications and error correction coding. He has also performed studies in digital transmission techniques as applied to telephone trunking and subscriber loops. In the past few years he has provided the technical leadership in the development of optical transmission system. He also has performed comprehensive studies in the application of fiber optic cable to outside telephone plants.

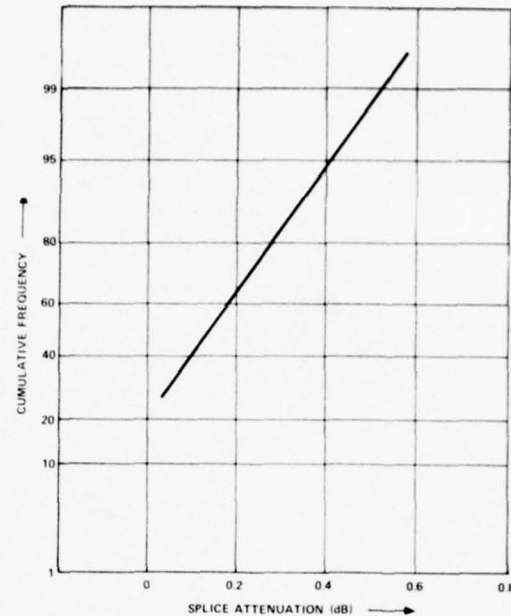


Figure 15. Splice Losses



Richard A. Beaudette is a Member of Technical Staff at GTE Laboratories, Waltham, MA. He has been affiliated with optical systems for the past five years. He has contributed to the development of optical splicing techniques, receiver and transmitter designs. A member of GTE since 1957,

he has been associated with development work on numerous communications projects including data processing systems, telephone conferencing systems, telephone outside plant system, cable television and broadband communication systems. He received his bachelor's degree in electronics from Northeastern University and is a member of the Institute of Electrical and Electronic Engineers. He has received two patents.

INSTALLATION OF AN OPERATIONAL TWO-KILOMETER FIBER OPTIC CABLE

G. J. Wilhelmi, J. C. Smith, and G. W. Bickel

ITT ELECTRO-OPTICAL PRODUCTS DIVISION
P. O. Box 7065
Roanoke, Virginia 24019

Abstract

Six 1-km fiber optic cables have been installed in a 10-cm PVC duct system. Evaluation of the cables after installation verified that no fibers were damaged and a small decrease in fiber attenuation occurred. The best six fibers from each cable were then field terminated with single fiber demountable connectors. Loss measurements performed on these connectors resulted in an average loss of approximately 2 dB.

Introduction

The potential use of fiber optics for the transmission of digital data over long distances is apparent. However, widespread use of such systems is contingent upon the availability, installability, reliability, and maintainability of the various system components. Such a system has been designed, built, installed, and is now operational. This fiber optic data transmission system utilizes a single fiber per channel to form an operational link between a satellite receiving station and the associated data processing center. This system, which is the largest (and possibly the first major) operational one to date, is composed of eighteen links, each approximately 2 km in length. The basic system specifications have been reported elsewhere.¹ Therefore, this paper only briefly discusses these specifications for completeness with the primary emphasis placed on reporting on the fiber optic cable design, installation, and termination.

System Description

The fiber optic data transmission system operates over 2 km with an NRZ data rate from 100 Kb/s to 20 Mb/s. The overall data channel performance specifications are:

- Distance 2 km
- Data Rate 100 Kb/s to 20 Mb/s

| | |
|------------------------------------|-------------------|
| ● Bit Error Rate | <10 ⁻⁸ |
| ● Mean Time Between Failure | |
| 0-30°C | 7000 hours |
| 70°C | 3000 hours |
| ● Input/Output Electrical Signal | |
| Data Format | NRZ |
| ● Output Electrical Signal-Digital | |
| Rise/Fall Time ^a | <15 nsec |
| Pulse Spread ^b | <20 nsec |
| ● Output Electrical Signal-Analog | |
| SNR _C | >30:1 |
| Peak-to-Peak Voltaged | 3±1V |
| Rise/Fall Time ^a | <25 nsec |
| Pulse Spread ^b | <15 nsec |
| Overshoot | <10% |
| Droop ^e | <10% |
| Optical Crosstalk (1 km) | <50 dB |

- a. 10% to 90% peak-to-peak amplitude.
- b. Change from input pulse width to output pulse width measured at 50% points.
- c. Ratio of peak-to-peak 10 MHz square wave signal amplitude out of 10 MHz filter to RMS noise out of filter with source constantly on.
- d. Measured across 10K Ω load.
- e. Measured for 100 consecutive logic ones at 100 Kb/s, NRZ.

The components of the system are:

- transmitter module
- receiver module
- multi-fiber cable
- buffered fiber
- one-way optical connector

Figure 1 is a diagram of the data channel configuration. The TTL input to the transmitter module is used to modulate a light emitting diode (LED)

operating at 0.82 μm . Two-meter buffered fibers are used to couple light from the transmitter modules to the multi-fiber transmission cable. The buffered fibers have optical connector plugs on each end for mating with the module jacks and multi-fiber cable.

At the receiving end of the system, the cable fibers are terminated with the optical connector jacks. Similar to the transmitting end, two-meter buffered fibers are used to couple light to the receiver modules. An avalanche photodiode detector (APD) is used to maximize sensitivity in the receiver. The receiver module supplies the required digital and analog outputs.

Multi-Fiber Optical Cable

The cable designed to meet the transmission and duct installation requirements of this system is an external strength member, eight-fiber, graded index cable. As shown in the cable cross section diagram in Figure 2, the cable is formed around a 0.2cm optical fiber bundle. This bundle is composed of eight fibers helically laid around 0.099cm fiber in the center. At least six of the fibers were to be operational after installation. In the formation of the cable, a layer of polyurethane is extruded over the optical fiber bundle. To safely pull a 1 km length of this cable through a system of conduit, pipes, and ducts, the tensile strength of the cable must be greater than the maximum anticipated pull force. To provide the necessary tensile strength, Kevlar[®] 49 strength member yarns are helically laid around the polyurethane cover of the fiber bundle. Finally, the Kevlar[®] is covered with Teflon[®] tape. An outer jacket of polyurethane is then extruded over the tape. The outer jacket and the strength members protect the fiber bundle from damage due to crushing as well as providing the necessary tensile strength. Also, the outer polyurethane jacket provides abrasion resistance and protection against water.

The graded index fibers for the cables are fabricated using a chemical vapor deposition (CVD) process. The finished fiber is composed of three basic layers. The core is composed of doped silica with a refractive index profile which approximates a parabolic distribution from the center of the core to the edge of the cladding. The cladding around the core is formed by a layer of borosilicate.

The cladding provides the index of refraction difference necessary to con-

fine the optical power to the fiber core. The glass fiber is protected against abrasion and the degrading effects of water by a double coating consisting of RTV Silicone and an extruded polyester elastomer (Hytreel[®]). This double coating also reduces the microbending losses of the fiber.

To meet the system power link budget, the maximum attenuation was specified to be less than 10 dB/km with an average attenuation of less than 9 dB/km per cable. In addition, each of the fibers was required to have a multimode and material dispersion less than 6 ns/km and 4 ns/km respectively, yielding a total dispersion of less than 7.2 ns/km (root sum square addition). Note that the material dispersion assumes a 300 Å spectral width. A complete list of cable specifications are:

| | |
|-------------------------------------|--------------------------------|
| Glass Fiber Diameter | 0.13 ± 0.013mm |
| Cable Diameter | 6.1 ± .3mm |
| Tensile Strength | 130 Kg |
| Number of Fibers | 8* |
| Isolation Between Fibers | ≥50 dB |
| Attenuation | ≤10 dB/km max, 9 dB/km ave. |
| Dispersion (Multimode and Material) | ≤7.2 nsec/km |
| Min Bending Radius | 5cm |
| Length | 1 km |

*6 guaranteed after installation

A total of six cables was installed for this system: 3 from each terminal to the midpoint. The average fiber attenuation for the installed cables was 6.84 dB/km. A histogram of the fiber attenuation for the cables is given in Figure 3. The average multimode dispersion for the fibers was 3.48 ns/km.

Cable Installation

A total of eight 1-km cables was supplied for this program; six of which were installed in an underground 10cm PVC duct system. The installation involved pulling three cables from each terminal to an interconnect hut located at approximately the midpoint of the run. The total duct run was approximately 1.8 km in length with manholes located every 100m. At the processing center, the cables were pulled up the side of the building through a metal duct, laid across the roof, routed through the roof to a cable tray, and then brought into the terminal rack. At the antenna site, the cables entered the building through the floor and were routed under a false floor to the terminal rack.

To allow the three cables to be pulled simultaneously, a rack was built to support and pay off the cables (see Figure 4). The rack was positioned directly over the starting manholes which were located just outside the two terminal buildings. The three cables passed down into the manhole through a funnel which was filled with cable lubricant to reduce the coefficient of friction of the cables.

In each of the manholes, pulleys were used to align the cable in both the input and output ports of the manholes. This allowed the cables to be pulled by a winch from the midpoint rather than having to use a series of shorter pulls to each manhole in which a change in direction occurred. The cables were pulled to the winch which was located above the first manhole beyond the midpoint and then back pulled to provide the necessary excess cable for dressing in each manhole and for termination.

A spring gauge was attached to the cable to monitor the tensile load at the winch. In addition to monitoring the force at the end point, a reading was taken in each manhole when the cable reached that point to determine the force on the pull cord and the force actually on the cables. The maximum force exerted on the cables for this installation was between 18-27 Kg per cable.

A continuity check, performed after the cables were installed, verified that no fibers were damaged as a result of the installation. Loss measurements were then performed on each fiber. An LED source was used to inject light into one end of a fiber, while an optical power meter was used to measure the light out of the other end. The fiber was then cut approximately one meter from the injection end to measure the power injected into the fiber. The difference in the readings was the cable attenuation. Note that the substrate light was removed prior to these measurements. The resulting fiber attenuations in all cases were slightly less than the attenuations measured in the laboratory before installation.

Cable Termination

After the installation and check-out of the six cables, the best six fibers from each cable were terminated with single fiber demountable connectors. The connector used for this system was designed by ITT Optical Equipment Division (Leeds, U.K.). The fiber alignment mechanism for the connector consists of a watch jewel bearing located within

a precision machined stainless steel ferrule (see Figure 5). In the center of the jewel bearing is a precision hole into which the optical fiber is inserted.

The terminated ferrules are placed in a precision alignment sleeve which aligns the two fiber cores. Both of the ferrules are spring loaded to ensure that the fibers are abutted. As shown in Figure 6, the alignment sleeve is housed in the connector body, while the ferrules are screwed into the body through the use of the knurled caps and threaded sleeves.

Two installation techniques were examined during the field terminations: (1) scribe and break, and (2) polishing. Both techniques followed the same procedure except for the final end preparation. Basically, this procedure involved stripping the outer jackets from the fiber, measuring the fiber diameter, selecting a jeweled ferrule of the appropriate size, "fire polishing" the end of fiber to ensure all of the plastic coatings have been removed, and epoxying the fiber inside the ferrule.

In using the scribe and break technique, the fiber end was prepared prior to epoxying the fiber in the ferrule. To prepare the fiber end, a small scratch was made in fiber using a diamond scribe. The fiber was then broken at the point of the scratch. This procedure yielded flat mirror finished ends perpendicular to the fiber axis. With the aid of a mechanical fixture, the fiber was positioned in the ferrule with the end within a few microns of, but recessed from, the end of the ferrule. Using this technique, the termination was completed as soon as the epoxy cured. However, preparation time, difficulties in use of mechanical system, and yield (~60%) made this approach unacceptable for field use.

The second approach employed for the field terminations, polishing, proved to be somewhat more acceptable. In this approach, the fiber was cut approximately 0.8cm from the Hytrex[®] coating, epoxied into the ferrule with approximately 0.2cm of fiber extending beyond the end of the ferrule, and then polished to yield a flat mirrored finish on the fiber. The polishing procedure used 600 grit polishing paper to grind the fiber end down to the ferrule surface. A 1 μm polishing solution was then used to produce the mirror like fiber end. Note that all of the polishing was performed with the ferrule in a special fixture to ensure that the end would be perpendicular to the fiber axis. The polishing

technique resulted in an easier procedure for both field and factory implementation, and gave a higher yield (>90%).

The attenuation of each field installed connector was then measured. The technique used for these loss measurements was: (1) inject light from an LED source into the fiber of interest; (2) measure the light out of the terminated fiber; (3) connect a short "standard" fiber to the terminated fiber; and (4) measure the power out of the short fiber. The connector loss was the difference in the two measurements. By transmitting the light through approximately 1 km of fiber, all of the substrate light was removed prior to the connector. In addition, the short "standard" fiber also had the substrate light removed so that the connector loss measurements only related the optical power in the fiber core before the connector to the light in the core after the connector. Typical results of these measurements are given in the histogram in Figure 7. These results show that in most cases that the connector losses were below 1.5 dB.

As a final check, the end-to-end attenuation for the cables and field installed connectors was measured for each of the eighteen data channels. These measurements were made using an LED transmitter connected to a short buffered fiber. The power was measured out of the buffered fiber and then connected to the transmission cable fiber. A second buffered fiber was connected to the transmission cable at the receiver end. The optical output of the receiver buffered fiber was then measured. The end-to-end loss was the difference in the two measurements. The results of these measurements are summarized in Figure 8. The link power budget specification allowed for a total end-to-end attenuation of 23 dB. As seen in Figure 8, the worst case loss was approximately 3 dB less than the maximum allowable loss of 23 dB with a 5 dB improvement being more typical.

Conclusions

This field installation has shown that the eight-fiber external strength member cable can be duct installed without degrading cable performance. It was found that for both field and factor demountable single fiber connectors, polishing for end preparation was preferable to the scribe and break technique. In addition, the field installation verified that the same termination results were achievable in both the field and laboratory environments. The results of this system installation, termination, and check-out substantiate the fact that many types of fiber optic systems are realistic today.

References

- ¹T. Eppes, J. Goell, and R. Gallenberger, "A Two Kilometer Optical Fiber Digital Transmission System for Field Use at 20 Mb/s," AGARD Symposium, London, England, 16-20 May 1977.

This program was conducted under NRPO Contract No. N00123-76-C-0724.

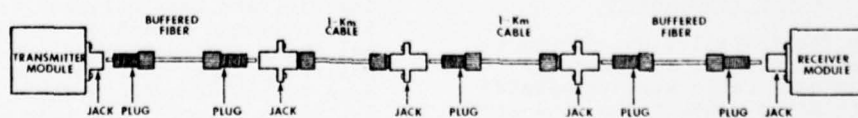


Figure 1. Data Channel Configuration

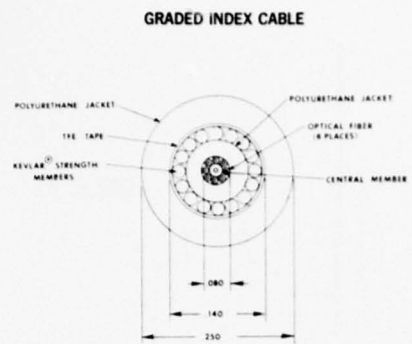


Figure 2. ITT Eight-Fiber Cable
(Dimensions in inches)

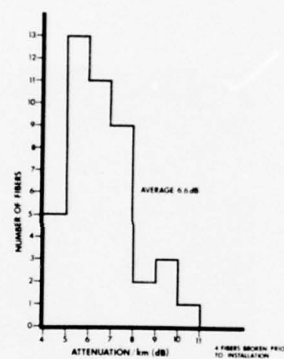


Figure 3. Attenuation of Installed Cables



Figure 4. Cable Installation Rack Assembly

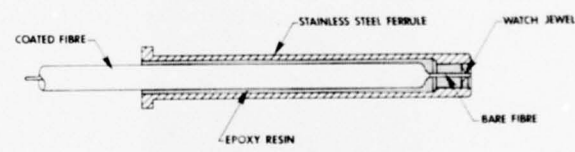


Figure 5. Jewelled Ferrule

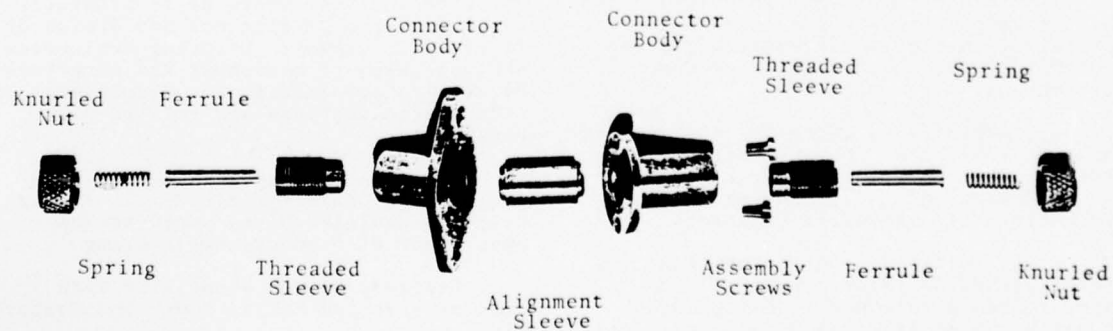


Figure 6. Single Channel Connector Components

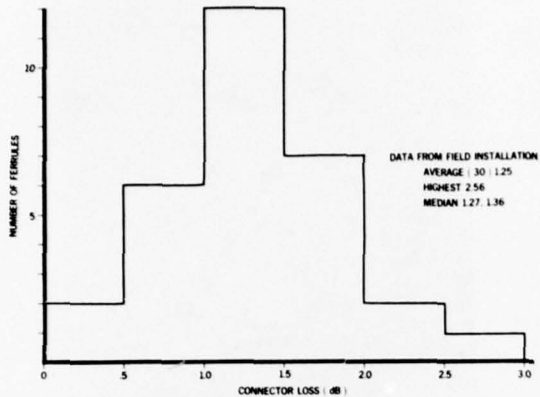


Figure 7. Field Installed Connector Losses

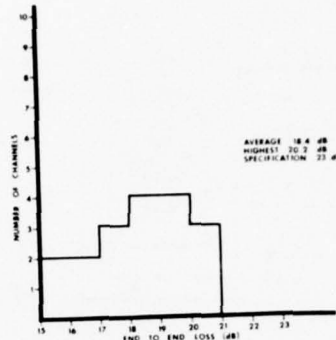


Figure 8. End-to-End Loss Measurements After Installation



Gary Bickel received his BS degree in physics from MIT in 1961 and his PhD in physics from the University of Minnesota in 1974. He has been a member of the Fiber Optics Laboratory of ITT Electro-Optical Products Division since 1973, with initial responsibility for fiber and cable optical evaluation. Currently he is Project Leader for Measurements and Coupling development.

Dr. Bickel is a member of the Optical Society of America. He currently is a member of the Fiber Optics Task Group of the A2-H Wire and Cable Subcommittee of the Society of Automotive Engineers.

Prior to his graduate education, Dr. Bickel worked in laser component and laser system development. His graduate research was on linear and nonlinear optical properties of visible and infrared materials.



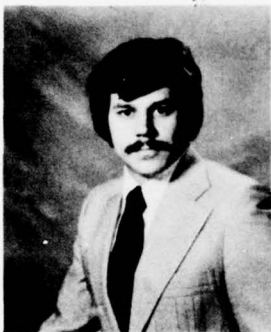
John C. Smith graduated from the Universidad Tecnica del Estado - Santiago, Chile in 1958.

He joined ITT Electro-Optical Products Division in 1974, where he is presently engaged in the development and design of fiber optic cables, including evaluation and selection of equipment and materials. He is also involved in the development of fiber optic coatings and related processes.

Prior to joining ITT, he was associated with General Cable Corp. (Philadelphia Insulated Wire) where he was Supervisor of Products Engineering.

Earlier, he was associated with Simplex Wire and Cable, Power and Control Division.

From 1960 to 1966, he held the position of Supervisor of Compounding Laboratory in MADECO, Santiago, Chile, where he was responsible for compounds development for wire and cable.



Gary Wilhelm was awarded a BS and an MS degree in Electrical Engineering from Texas A&M University in 1971 and 1973, respectively.

Mr. Wilhelm joined ITT Electro-Optical Products Division in 1976 and is currently the manager of the Aerospace and Ground Systems Section of the Fiber Optics Laboratory. He is engaged in the design and development of new fiber optic communication systems as well as the fabrication, installation, and check-out of standard systems. He has also conducted research fiber termination techniques for use in either laboratory or field environments and evaluation of single fiber demountable connector loss mechanisms.

Prior to joining ITT, he was associated with McDonnell Aircraft Co. where he was responsible for an electro-optical sensor design for remote sensing applications, electromagnetic scattering theory development and the development of a digital flight control system which included redundancy management.

REINFORCED SINGLE FIBER CABLES FOR OPTICAL DATA LINK APPLICATIONS

L. L. Blyler, Jr.
A. C. Hart, Jr.
Bell Laboratories
Murray Hill, New Jersey 07974

ABSTRACT

Many applications for optical fibers such as data bussing in telephone switching systems require large numbers of short (up to 1000 ft. long) single fiber links having high performance standards and reliability. The numerical aperture (NA) and physical dimensions of the fiber are often governed by such factors as the brightness of the light source, the sensitivity of the detector, the data rate of the link, etc. These properties impact upon the materials and structure chosen for cabling the fiber in a major way. For example added losses due to microbending during cable fabrication are strongly dependent on fiber NA and diameter, as well as on the properties of the materials used for coating and packaging the fiber. We have studied the added losses associated with jacketing coated fibers with extruded thermoplastics such as PVC and thermoplastic elastomers of different modulus value.

The strength of the optical fiber data links bear importantly on their reliability. We present typical strength distributions obtained for coated furnace-drawn data link fibers. Minimum strengths, guaranteed by proof testing, are used as parameters for the design of aramid yarn-reinforced cables. We have evaluated the tensile load bearing capabilities of these reinforced cables as well as their bending characteristics under load. Failure mechanisms under these deformations are described.

INTRODUCTION

When an optical fiber is placed in a structure which imposes random bends on its axis, added losses result due to coupling of guided modes to radiation modes. This phenomenon, known as microbending, is strongly dependent upon fiber dimensions and NA and also on the properties of the material(s) used to coat the fiber. Experience has shown that soft coatings with moduli of 10,000 psi and below are very effective in reducing microbending loss¹, particularly in the case of fibers with reasonably high NA (>0.10). These coatings serve to cushion the fiber axis from irregularities imposed by the outside structure. Of course it is important that the fiber coating be as smooth as possible so that these irregularities do not arise from the coating itself.

In the case of single fiber cables the "structure" into which the coated fiber is placed is normally an extruded jacket. The jacket can

produce axial distortion of the fiber as a result of stresses caused by shrinkage of the jacket around the fiber during cooling. Such stresses are likely to be non-uniform on a small scale owing to the presence of non-uniform residual elastic strains, filler particles and other solid inclusions and the morphology of the bulk material. Additionally any non-uniform contact between the jacket and the coated fiber, which is influenced by voids at the interface and surface irregularities of the coating, would be expected to produce axial distortion of the fiber.

EXPERIMENTAL

Materials

The jacket compounds chosen for study in this work were principally low modulus materials. Preliminary experiments demonstrated that large added losses result when small diameter fibers (~100μm OD) are packaged in jackets of high modulus materials (>50,000 psi). Consequently two classes of soft materials were investigated--thermoplastic elastomers and plasticized PVC. The thermoplastic elastomers were block copolymers of two types--polyolefins and polyesters. In the polyolefin type polypropylene blocks form the crystallizable segment and the amorphous segments are ethylene-propylene copolymers. The polyester type consists of crystalline and amorphous segments of poly(ether-ester) entities. These materials are available with a range of elastic modulus and hardness values. Generally properties are controlled by varying the amount of crystalline component present in the copolymer.

The plasticized PVC materials used were compounds typical of wire and cable grades. Modulus is controlled by varying the amount and type of plasticizer incorporated in the material.

Jackets were reinforced with aramid filament yarn to increase the load bearing capabilities of the cable structures studied. These yarns consist of individual continuous filaments having a diameter of 0.47 mils, a tensile modulus of 1.9×10^7 psi, and an ultimate elongation of 2.8%. The ultimate breaking load of a yarn is determined by the number of filaments it contains, which is conventionally expressed in terms of denier (= weight in grams of 9 km of yarn).

Cable Constructions

Three different reinforced cable structures were investigated in this work as depicted in Fig. 1. Plasticized PVC was used as the principal jacket material here, and the modulus and thickness of the PVC were varied. Two aramid yarn contents were tried, one consisting of low denier yarns, the other high denier yarns. In all cases the yarn was incorporated straight through the cable, without stranding helically about the fiber.

RESULTS AND DISCUSSION

Cabling (Microbending) Losses

Experiments were performed to evaluate the effect of extruded jacket materials on fiber loss. A long (2250m) length of transmission fiber having a graded germanium-borosilicate core with an NA of 0.23 was obtained. This fiber had a 55 μ m diameter core and an outer diameter of 110 μ m and was coated with a UV-cured epoxy-acrylate polymer⁴ at a nominal thickness of 2.3 mils. The spectral loss curve of this fiber was measured using a launch NA of 0.30, as shown in Fig. 2. At this launch NA the fiber was slightly over-filled which tends to emphasize the microbending contribution.

The fiber was jacketed in 200-300 meter lengths to an outer diameter of 40 mils with various thermoplastic elastomers listed in Table I. The spectral loss curves for these shorter lengths were measured in the same manner as for the long length and a comparison is shown in Fig. 2. It was assumed that the loss of the original fiber was uniform with length. All of the extruded jackets increase the loss of the fiber and large differences in added loss among the materials are evident.

In Fig. 3 we plot the added loss at 820 nm, a typical wavelength of a GaAlAs injection laser, against the flexural modulus of the jacket material. A strong correlation is evident. The polyester elastomers show more rapid decay of added loss after the fiber is stored on a drum for several days. This decay, shown in Fig. 3, is caused by the time-dependent relaxation of stresses imposed on the fiber by the viscoelastic jacket.

The resistance of fibers to microbending is strongly dependent upon their dimensions and NA. Gloge's² and Gardner's¹ analyses predict that microbending loss is approximately inversely proportional to the 4th power of the NA and the 2.5th power of the fiber outer diameter. Thus large diameter, high NA fibers useful for data links employing low brightness LED's should be particularly resistant to packaging losses. This fact is illustrated in Table II which shows data for four nylon coated fibers with NA's ranging from 0.34 to 0.38 and outer diameters of 220 μ m. These fibers were jacketed to an O.D. of 80 mils with a semi-rigid plasticized PVC having a flexural modulus of 50,000 psi. Despite the high modulus and thickness of this jacket, within experimental error no added loss could be measured. On the other hand a smaller diameter (110 μ m O.D.) lower NA (0.23) nylon coated fiber was jacketed with a much lower modulus (<1000 psi) plasticized PVC of somewhat greater thickness. In this case an added loss of 4 dB/km was incurred.

Fiber Strength

The load carrying ability of an optical fiber cable may be taken as the maximum load it will support over its entire length without sustaining fiber breakage at some point. Thus the load rating one assigns to a cable is dependent upon the proof strength of the fiber. Fiber strength is determined by the degree of surface damage imparted to it during fabrication. Surface damage arises from a number of sources, the principal ones being flaws present on the surface of the preform which are not healed by the drawing process, particulate contamination in the atmosphere of the heat source, e.g. the furnace, particulate impurities in the coating material applied to the fiber, and fiber contact with the coating die. Most of these factors can now be dealt with effectively. Preform flaws may be reduced by fire polishing and careful handling, and a flexible die applicator³ provides a non-contacting technique for producing concentric coatings. Furnace contamination remains a difficult problem but progress is being made.

A typical strength distribution for an optical fiber drawn with a Zirconia induction furnace is represented by the data displayed in Fig. 4. This is a Weibull plot of the strength distribution for a 600 meter long, 110 μ m diameter germanium-borosilicate core, graded-index fiber broken in 20 meter gauge lengths. The coating in this case was a commercial silicone resin, with an outer layer of extruded nylon. The preform was handled carefully, and a flexible applicator die was used to apply the silicone coating. The strength distribution shows a high strength mode to the 30% failure level below which there exists a lower strength tail. The tail, relatively steep, is attributed to furnace contamination.

The weakest break on the 600 m long fiber occurred at 246 ksi. Such fibers would readily pass a 100 ksi proof test over kilometer lengths in the great majority of cases. In production, however, 35 to 50 ksi proof tests are more normal due to less well controlled processing and handling. Thus cables must be designed such that the fiber experiences strains below the 0.3 to 0.5% range under the highest loads applied.

Cable Strength Characteristics

Cable tensile strength characteristics on short gauge lengths are conveniently evaluated with an Instron machine. In Fig. 5 a load vs. strain curve at a strain rate of 2.0%/min is displayed for a cable consisting of a 220 μ m O.D. fiber coated with UV cured epoxy-acrylate polymer, jacketed with plasticized PVC (flexural modulus = 1500 psi) to an outer diameter of 0.095 in. Imbedded within the PVC are strands of aramid yarn via Structure B. In the range of very small strains, below 0.1%, there is some curvature in the load-strain curve as the individual filaments of yarn begin to support the load. Above 0.1% strain the load rises approximately linearly with strain until the yarn breaks, usually at a strain level near 2.0%. In the case of this cable, the load supported is greater than 100 lb. After the yarn breaks the load drops to a lower value, which may be quite high since the fiber remains unbroken. Because the yarn is usually broken only at one point along the gauge length, it continues to offer partial reinforcement. Thus subsequent deformation is quite localized and concentrated in the vicinity of the yarn break. As a result the strain axis no longer reflects the actual strain on the fiber. Further deformation results ultimately in fiber breakage with an attendant drop in load.

The load bearing capabilities of the various constituents of the cable (fiber, jacket, reinforcing yarn) may be analyzed by fabricating the structure with one of the components absent. Thus in Fig. 5 are displayed curves for the same cable structure without the fiber and without the yarn present. The cable without the fiber behaves very similarly to the real cable, and the load carried by the fiber is given by the difference between these two curves. The cable without the yarn supports loads which are very close to this difference. This means that the PVC jacket contributes very little support in this structure. The cable without the yarn may be strained to values of about 7%, where the fiber breaks.

The expected load carried by each component of the cable at a given strain may be calculated by assuming each component acts independently in parallel so that loads are additive. Table III therefore compares the calculated loads carried by yarn, fiber and jacket at 1% strain with those measured in the above experiment. Each individual filament in the yarn is assumed to act independently. As may be seen the calculation correctly predicts the loads carried by the fiber and jacket but the actual load carried by the yarn is about 25 to 30%

lower than expected. This effect is probably caused by a number of factors including the initial curvature in the load-strain curve where the yarn filaments are being straightened out and the lack of effectiveness of some of the yarn filaments due to breakage. As a consequence of this effect more aramid yarn must be incorporated in a fiber cable than expected to achieve a given degree of reinforcement.

The load rating of a reinforced fiber cable depends upon the proof test which the fiber passes. For example a 35 ksi proof stress corresponds to a proof strain of approximately 0.33%. Thus the load rating of the cable shown in Fig. 5 would be 15 lbs. When fiber proof strengths are low it is especially important to minimize the initial curvature in the load-strain curve so that adequate load ratings may be achieved. This is accomplished by insuring that the reinforcing yarn lies in an extended condition in the cable structure, so that it offers effective reinforcement at as low a tensile strain level as possible.

Evaluation of Cable Structures

The cable structures displayed in Fig. 1 were fabricated and evaluated mechanically. In all cases the cables contained nominally 220 μ m diameter nylon coated fibers and equal amounts of aramid filament yarn in the cross-section. The PVC material used was a transparent semi-rigid compound with a flexural modulus of 50,000 psi.

Load-strain curves are compared in Fig. 6. Very similar tensile behavior is exhibited by the three structures. All show yarn rupture at a strain of 1.8 to 2.0% at loads between 65 and 75 lb. Some differences are apparent, however. Structure A exhibits a tendency for the fiber to break when the yarn ruptures. Just why this occurs is not clear, but it is worth noting that in this structure the fiber lies freely in a bed of yarn, and therefore may be stressed independently of the cable jacket. Such stress may be incurred at a cable termination. Structure C shows excessively high initial compliance at low strains. This behavior probably results from the poorer extension of the reinforcing yarn in the structure caused by longitudinal shrinkage of the ETFE outer jacket when it is tubed over the cable. Another deficiency of Structure C is evident when the cable is bent. The reinforcing yarn is relatively free to move in this structure because the thin ETFE sheath is not bonded to the yarn or to the PVC layer below it. When bent, the yarn on the tension side of the cross-section slips around the circumference to reduce the tensile stress. This usually occurs suddenly as the bending radius is reduced. When it occurs the cable becomes very easy to bend locally at the point where the yarn has slipped, which puts the fiber in danger of breaking.

The above mentioned deficiencies of Structures A and C make Structure B more viable for data link development. It exhibits good strength

characteristics and is relatively easy to fabricate. It is also possible to mechanically strip the PVC with simple tools leaving both the coated fiber and reinforcing yarn free for termination.

The tensile characteristics of Structure B are dependent on the amount of reinforcing yarn incorporated, the modulus of the jacket material used, the outer diameter of the jacket, and the diameter of the fiber cabled. Fig. 7 shows the effect of some of these parameters on the load-strain curve. Comparison of Curves b and c demonstrates the combined effect of increasing fiber size from 110 μm to 220 μm O.D. and jacket modulus from 1000 psi to 50,000 psi. The major contribution here is the increase in fiber size since the jacket contributes little to the load bearing capabilities of these cables. The pronounced initial curvature in Curve c may be caused in part by compliance of the lower modulus PVC in the grips of the Instron machine during the test.

The effect of increasing aramid-yarn content is seen by comparing Curves a and b. The load-strain curve is most sensitive to this parameter.

Bending

The bending characteristics of a single fiber cable around a radius under a tensile load are important for applications in which the cable is pulled through troughs, ducts, etc. which contain sharp corners. Even though the cable is designed to support the tensile load applied, locally high tensile stresses due to bending may cause the fiber to fail. The short gauge length breaking strength for fibers may be taken as approximately 750 ksi. This stress is reached at bending radii of 30.6 and 61.2 mils for 110 and 220 μm diameter fibers respectively. Therefore in order to keep the fibers from breaking it is essential to prevent them from conforming to these small radii.

We have found there are several approaches which may be taken to reduce the susceptibility of single fiber cables to breakage by bending under load. Use of a small diameter fiber capable of sustaining small bending radii if the system permits it is most helpful. Beyond that the cable jacket thickness and stiffness may be increased. For small diameter fibers the jacket may be made so thick that even when the cable is forced to conform to the sharpest bend, the fiber bending radius remains above its critical value. This approach is not completely satisfactory for large diameter fibers, however. As an example 220 μm diameter fibers would require a jacket diameter of at least 0.125 in. for such protection, which may be undesirably large.

Increasing jacket stiffness is helpful in reducing the degree of conformance with sharp bending radii under low tensile loads, e.g. a few pounds. At higher loads even stiff jackets yield under the high local tensile stress and the cable bends sharply. However compliant jackets deform locally at the bend, where the sharp radius presses into the material so that the bending radius experienced by the fiber

decreases with time until the fiber ultimately breaks. Stiff jackets offer much higher resistance to this local time-dependent deformation and thereby may be of great advantage.

CONCLUSIONS

1. Low modulus thermoplastic elastomers and PVC are effective jacketing materials for small diameter (110 μm) moderate NA (0.23) fibers. Added losses as low as 1dB/km are possible for such fibers when the jacket modulus is less than 10,000 psi. Large diameter (220 μm), high NA (0.35) fibers are so resistant to microbending that high modulus materials may be used for their jacketing.
2. Aramid yarn reinforcement of single fiber cables provides high breaking loads on short gauge length specimens. For long gauge lengths the load rating of a cable depends upon the proof strength of the fiber and the ability of the yarn to reinforce the cable at as low a tensile strain as possible (<0.1%). Direct imbedding of the yarn within the cable jacket provides the most effective reinforcement.
3. The susceptibility of fiber cables to fiber breakage by bending around a sharp radius under a tensile load may be reduced by decreasing fiber O.D., and by increasing jacket diameter and stiffness.

ACKNOWLEDGMENTS

We wish to thank H. Schonhorn and H. G. Vazirani for providing the epoxy-acrylate-coated fibers used in this study, M. Grasso and J. R. Simpson for spectral loss measurements on several fibers, and F. V. DiMarcello for providing the fiber strength results displayed in Fig. 4.

BIBLIOGRAPHY

1. W. B. Gardner, B.S.T.J., 54 No. 2, 457(1975)
2. D. Glege, B.S.T.J., 54 No. 2, 245(1975)
3. A. C. Hart, Jr. and R. V. Albarino, Technical Digest, Topical Meeting on Optical Fiber Transmission II, Williamsburg, Va., Optical Society of America, 77CH 1227-8QEC, Feb. 22-24, 1977, pp TuB2-1-4
4. H. N. Vazirani, H. Schonhorn and T. T. Wang, ibid, pp TuB3-1-4

TABLE I: Cabling Loss Experiments with Thermoplastic Elastomers

| Material | Type | Flexural Modulus (psi) | Fiber Length Jacketed (m) | Added Loss at 820 nm (dB/km) |
|----------|------------|---------------------------|------------------------------|---------------------------------|
| TPE-A | Polyester | 7,000 | 207 | 1.1 |
| TPE-B | Polyolefin | 10,000 | 250 | 3.0 |
| TPE-C | Polyolefin | 18,000 | 259 | 4.4 |
| TPE-D | Polyester | 30,000 | 211 | 7.3 |
| TPE-E | Polyolefin | 35,000 | 130 | 14.6 |

* 40 mil O.D. extruded jacket on 110 μ m O.D., epoxy-acrylate-coated, 55 μ m graded index, germanium-borosilicate core fiber

TABLE II: Added Loss for PVC Jacketed, Nylon-Coated Fibers

| Fiber No. | Fiber O.D. (μ m) | Fiber NA | PVC Jacket O.D.(mils) | PVC Flexural Modulus (psi) | Added Loss at 820 nm (dB/km) |
|-----------|--------------------------|-------------|--------------------------|-------------------------------|---------------------------------|
| 10-12-3 | 220 | .34 | 80 | 50,000 | 0.0 |
| 10-18-1 | 220 | .38 | 80 | 50,000 | -1.3 |
| 11-1-1 | 220 | .34 | 80 | 50,000 | +0.9 |
| 11-3-1 | 220 | .37 | 80 | 50,000 | +0.1 |
| 3-17-2 | 110 | .23 | 115 | 1,000 | +4.0 |

TABLE III: Load Carried by Single Fiber Cable Components at 1% Tensile Strain

| Components | Calculated Load (lb) | Measured Load (lb) |
|--------------------------|----------------------|--------------------|
| Aramid yarn | 65.9 | 47 |
| Fiber (220 μ m O.D.) | 6.3 | 7 |
| PVC Jacket (95 mil O.D.) | 0.7 | ~0 |
| Total | 72.9 | 54 |

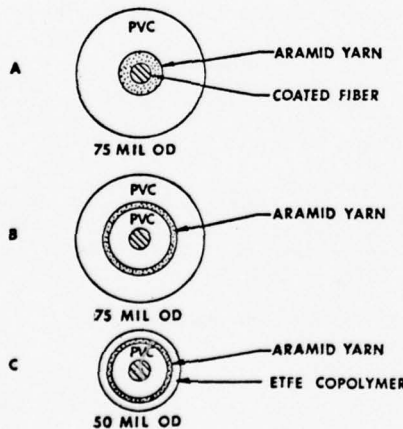


Fig. 1: Schematic of reinforced cable structures investigated.

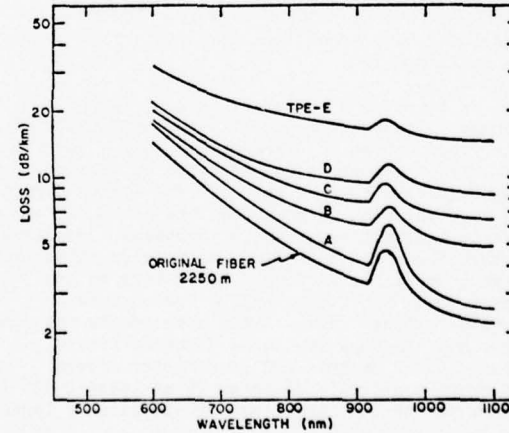


Fig. 2: Spectral loss curves for an 0.23NA, 55 μ m diameter graded germanium-borosilicate core, 110 μ m OD fiber with UV-cured epoxy-acrylate coating, jacketed with thermoplastic elastomers to an O.D. of 40 mils. Refer to Table I.

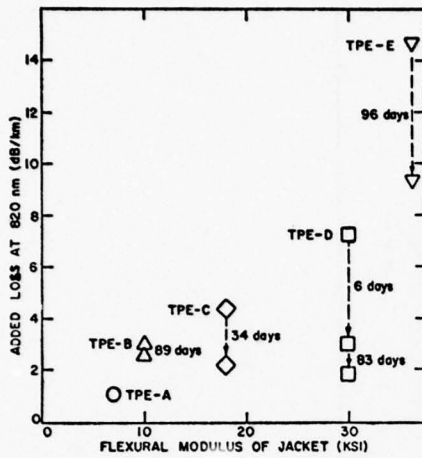


Fig. 3: Added loss at 820 nm for the fibers of Fig. 2 as a function of jacket modulus. Dashed lines indicate decay of added loss with time.

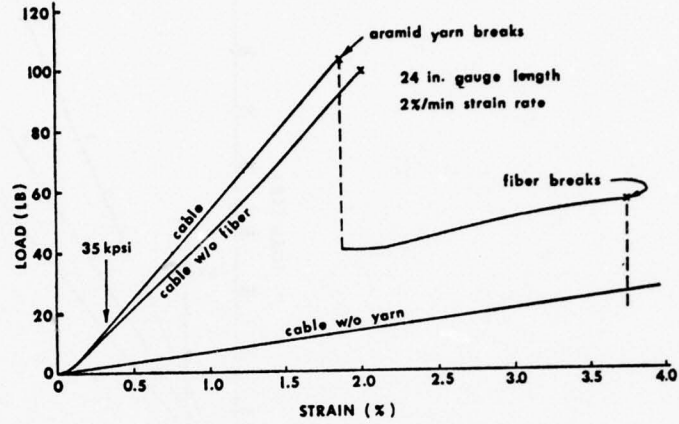


Fig. 5: Load vs tensile strain for a cable containing a 220 μm OD fiber and a plasticized PVC jacket reinforced with aramid filament yarn.

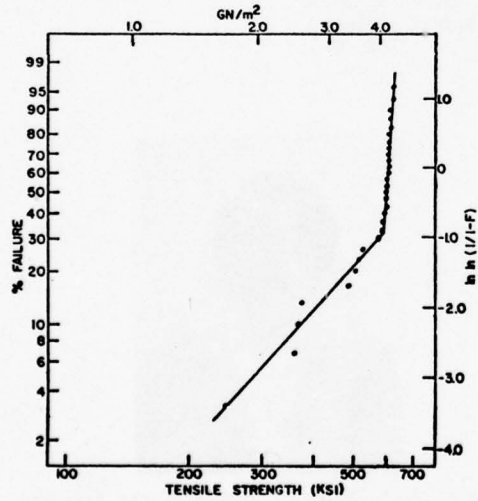


Fig. 4: Weibull plot of 20 m gauge length tensile strength distribution for 600m long, 110 μm OD fiber drawn with a Zirconia induction furnace and coated with a silicone resin.

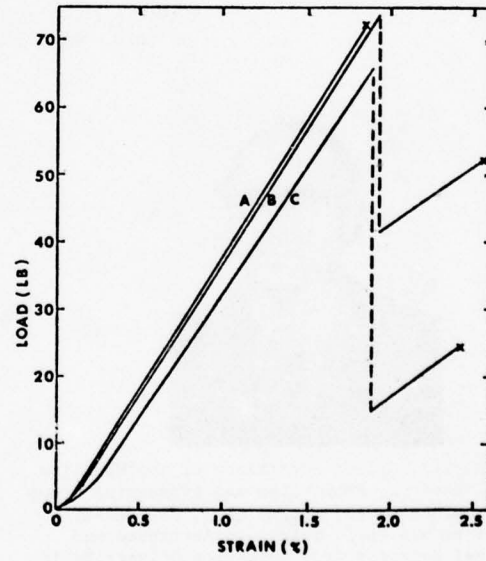


Fig. 6: Load vs tensile strain for the reinforced cable structures depicted in Fig. 1. All cables contain a 220 μm OD nylon coated fiber and the same amount of aramid filament yarns.

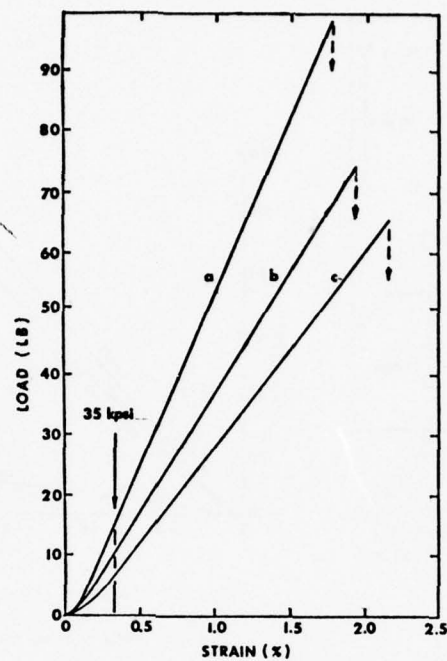


Fig. 7: Load vs tensile strain for reinforced cable structure B; curve a: 220μm OD fiber, high yarn content, 1500 psi PVC flexural modulus; curve b: 220μm OD fiber, low yarn content, 50,000 psi PVC modulus; curve c: 110μm OD low yarn content, 1000 psi PVC modulus.



Lee L. Blyler, Jr. is supervisor of the Plastics Applied Research, Properties and Processing Group at Bell Laboratories, Murray Hill, New Jersey. He received his Ph.D. degree in Aerospace and Mechanical Sciences from Princeton University in 1966. He joined Bell Laboratories in 1965 and has worked in the areas of polymer rheology and processing and polymer materials studies relevant to optical fiber technology.



Arthur C. Hart, Jr. is a member of the Plastics Research & Development Department, Bell Laboratories, Murray Hill, New Jersey. He received a Master of Science in Engineering from Princeton University in 1964. In 1968 he joined Bell Laboratories and since 1971 has been involved with plastic coatings for optical fiber waveguides.

SOME FIELD APPLICATIONS OF FIBER OPTIC CABLE SYSTEMS

D.F. Hemmings* and J.B. Wise

(Canada Wire & Cable Co. Ltd., Toronto, Ontario, Canada)

and

F.R. McDevitt

(Harris Corporation, Electronic Systems Division,
Melbourne, Florida, USA)

Summary

Fiber optic cable systems technology has advanced significantly over the past few years; early expectations of its usefulness have now developed into reality. System and cable designs have progressed for ducted, aerial and ploughed cable installations in urban and rural environments. Some field applications of fiber optic cable systems are being realized in power utilities, transportation utilities, industrial control, and telecommunications. In particular, some details of field trials in Winnipeg (Manitoba), London (Ontario) and Edmonton (Alberta), Canada are presented in this paper.

Introduction

The development of fiber optic cable systems has progressed much more rapidly than could have been anticipated five years ago, when the first major breakthroughs in the research laboratories occurred. This technology is already competing successfully against coaxial cable and microwave systems for some applications in 1977 - a year which will probably be heralded as the start of the growth phase of fiber optics as a real business opportunity. Significant long-haul and local broadband contracts will have been let in North America by the end of this year. The first major optical fiber supply deal has been consummated and fiber optic cabling has passed through its first phase design for duct, aerial and ploughing applications. Injection laser diodes and avalanche photodiodes are now commercially available with respectable guaranteed lifetimes.

Decisions on the development of

improved cable and other component designs are expected to come not from the beleaguered research scientist in a fiber optics laboratory but from a combination of field experience and the participation of production cable engineers. Canada Wire has therefore conducted field trials in difficult environments where ducted, aerial, and ploughed cables are being evaluated to collect long-term performance data.

Duct Installation:

In 1976, available cables were only adequate for installation in ducts or conduits. Tests on these cables were primarily laboratory results and indicated little about performance in wide ranges of the year-round field conditions found in Canada. In September 1976, a multi-purpose fiber optic system was installed in the Dorsey Converter Station near Winnipeg, Canada. The cable route, shown in Figure 1, was tortuous and the cable was installed in three phases - from the center of the switchyard to each of the two buildings (the DC Converter Station and the AC Rectification Station) and through the ducts and trays on three stories of the DC Converter Station. Cable installation was performed by a standard crew; other than loosening the cable in a snag, no special instructions were given. The crew had had no prior knowledge or experience with fiber optic components; the installation, for the 600-meter route was completed by 5 technicians and 2 supervisors in 10 hours, principally because of the complexity of the route in the DC Converter Station.

The fiber optic system, shown in Figure 2, employs a 6-fiber cable. Each fiber has a crush-coating of nylon; the strength member is a stranded high-tensile rope; the cable jacket is polyurethane. Unless jacket is greased, dusted or dirty, the polyurethane material has the undesirable characteristics of high surface friction; this is particularly significant

* D.F. Hemmings is now with Harris Corporation, Electronic Systems Division, Melbourne, Florida.

for indoor (clean) installations in already-crowded trays or ducts. Installation caused no fiber breakage or degradation in the cable performance. However, the high flexibility and small size of the cable in crowded and open trays outdoors may lead to an installer's heavy boot inadvertently causing fiber breakage.

The transmission capability of the system is three double half-duplex links; there is no redundancy in the cable. The links transmit telemetry information at 1.5 Mb/s. The digital links are operating at better than 10^{-11} B.E.R. through a very high interference environment.

The system has played through one year when the cable was exposed to temperatures in the range of at best -40°C to +50°C. Some cable is located in water and/or oil. Temporary variations in cable attenuation have been less than 5 dB/km (the measuring instrument error is ± 1 dB/km for this project). There is no apparent permanent degradation of the cable performance after one year on site.

In implementing the successful operation of this system, it has been found necessary to change suppliers of injection laser diodes and avalanche photodiodes because the reliability and operating parameters of devices available in mid-1976 have been rapidly superseded.

During the preparation for this project, two multi-fiber connectors were evaluated. One such connector is employed in this system; however, it is the present consensus of opinion that link availability eliminates these connectors from use in this type of application in the future. Both connectors evaluated are time-consuming to assemble and disassemble (in case of failure) and their current designs lead to unnecessary risk of fiber breakage in or near the ferrule.

Aerial Installation

An understanding of the elements of fiber optic cabling has been reached in 1977 sufficient to make a significant step forward in the design of self-supporting aerial cable for the Canadian environment. In October 1977, a one-kilometer length of self-supporting, 8-fiber cable was installed in London, Ontario, Canada as part of the first major cable television supertrunk system being built for an urban environment by Canada Wire and Harris.

This system, which is essentially a Canadian cable television industry project, will be commissioned in mid-1978 to carry 12 television and FM stereo by digital transmission at a typical rate of 322 Mb/s. Figure 3 shows the terminal and repeater, of which there are two each in the system. The system offers extended broadband services to satellite communities or suburbs presently too distant to serve economically with coaxial cable systems. Each fiber channel has the capability of transmitting three television channels and either three FM channels or three DS2 streams (i.e. a total of 288 voice circuits).

The cable route, shown in Figure 4, runs parallel to an existing trunk line. The fiber optic approach to CATV trunking will be evaluated directly against a pressurized one-inch coaxial cable of the best performance available today. Cable installation again employs a standard crew with no special instructions which would make fiber optic cable less economical to install than coaxial cable.

The fiber optic cable, in this case, has its fibers tubed and protected to withstand a wide temperature range (-55°C to +55°C) and the effects of wind (i.e. vibration). The cable also has to maintain its performance under severe ice-loading conditions.

The injection laser diodes and avalanche photodiodes are being screened to meet guaranteed MTBF's in excess of 10,000 hours. All connectors are of the single-fiber type. The cable is being spliced at two points in each 3-kilometer section along the link. The cable fabrication process in 1977 does not allow for large volumes of fiber optic cable significantly greater than one kilometer with a satisfactory yield.

Ploughing Installation

The progress in fiber optic cable development has enabled Canada Wire to conduct the first known, worldwide, cable-ploughing field trial. In September 1977, Canada Wire ploughed four one-kilometer fiber optic cables, each of different design, to a depth of 1.1 meters at a rural site near Edmonton, Alberta, Canada - See Figure 5. All cables were installed successfully without any apparent damage to fiber transmission.

During ploughing, optical attenuation was monitored continuously; the results indicate less than 0.1 dB/km variation, which is within the error of the measuring

equipment. Of the four cables, two designs enabled ploughing, splicing and testing in the field to be relatively easy. The other two cables will require some design improvements to satisfy specifications which are being generated for this type of installation.

Continuity data have been collected; optical dispersion and transmission information are forthcoming. Harris has built DS4-rate and CATV supertrunk-type transmission electronics, with repeater, to allow monitoring of these cables under the stringent Canadian winter conditions. The effects of cable relaxation, lightning, frost heaving and moisture ingress are being considered. Field splicing has been conducted and is being perfected to meet standard maintenance practice and expectations.

Other Considerations

Cable designs for these applications indicate that, until it may be otherwise proven, the need for pressurization of fiber optic cables to maintain an MTBF of 30 years is not justified. The double polymer sheath and a silicone-filled tube (around each fiber) is probably sufficient to minimize moisture ingress and maintain cable strength for duct and aerial installations. The effect of moisture at the fiber surface is not presently considered a significant source of fiber performance degradation provided the residual stress on each fiber in the cable and the fiber surface parameter are controlled.

For ploughing installation, an aluminum sheath in the cable offers an improved moisture barrier and the opportunity to conduct the standard high-voltage-to-ground test after installation and lightning strikes; but a non-metallic cable has the advantage of being "lightning-proof" provided certain installation rules are observed.

The fiber used in broadband transmission networks of high bandwidth (e.g. 300 Mb/s) is typically better than 6 dB/km, 600 MHz-km to support the economic benefits of this technology. Canada Wire's results indicate less than 0.2 dB/km excess optical loss due to cabling is readily achievable on, say, a 12-fiber cable; there is also insignificant variation in dispersion in the same fabrication process.

In conclusion, fiber optics technology is successfully meeting the short-term technical requirements of field applications in several market segments,

such as power utilities, transportation utilities, industrial control, and telecommunications. Projections for the longer term indicate that fiber optics is becoming the technically superior transmission medium; technical credibility in this technology will be existent and demonstrable by 1980. The economic advantages of fiber optics over copper cable and microwave is related to production volumes, but there is sufficient evidence in 1977 that fiber optics will be a competitive and preferred technology within three years in major markets. In North America, there are motivations to use this technology extensively as soon as technical credibility has been established by such field trials as have been outlined in this paper.



David Hemmings was born in England in 1946. He was educated at the University of Wales where he gained a Bachelor's degree in Physics and Master's degree in Electronics. Since 1972, Mr. Hemmings has been working in fiber optic technology and market development. He participated in the establishment of the glass fiber, and cable development program for Canada Wire from 1972 to 1976. Mr. Hemmings has since been the Product/Market Manager, Fiber Optic Systems for Canada Wire.



John Wise was born in Australia in 1947. He was educated at the University of New South Wales where he gained a Bachelor's degree in Engineering in 1968. Mr. Wise worked for eight years with Telecom Australia in planning and engineering development department. He developed computer-peripheral fiber optics hardware during this time. Mr. Wise is now an Applications Engineer, Fiber Optic Systems for Canada Wire.

(Mailing address: Canada Wire and Cable Co. Ltd., Technology and Development Division, 80 Bloor Street West, Suite 606, Toronto, Ontario M5S 2V1, Canada)



Ray McDevitt was born in the U.S.A. in 1944. He was educated at Auburn University where he gained Bachelor's and Master's degrees in Electrical Engineering. Mr. McDevitt has been with Harris Corporation since 1968, where he has been a leader in fiber optics technology. He has been involved in a number of state-of-the-art fiber optic systems projects. Mr. McDevitt is now Manager of Engineering, Fiber Optic Systems for Harris Corporation.

(Mailing address : Harris Corporation, Electronic Systems Division, P. O. Box 37, Melbourne, Florida 32901, U.S.A.)

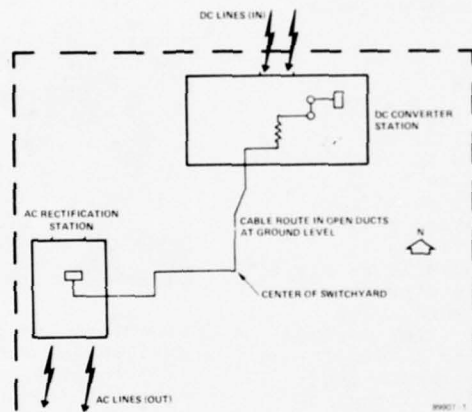


Figure 1 - Dorsey 1 Link Near Winnipeg, Manitoba
September 1976 - Cable Route

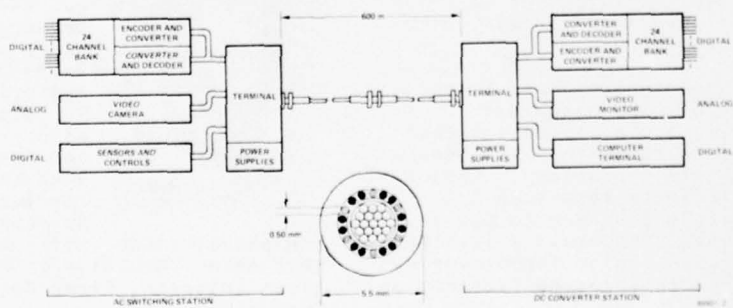


Figure 2 - Operating Fiber Optic System at Dorsey Converter Station

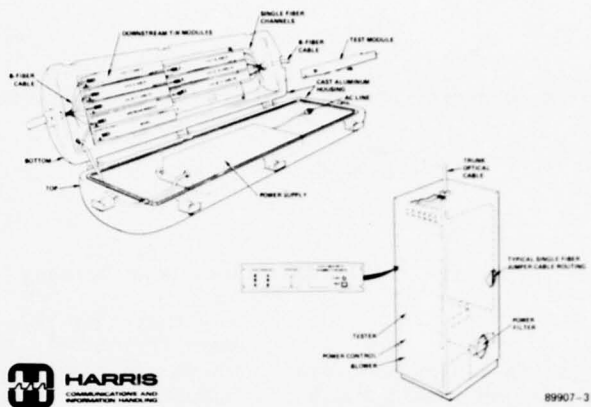


Figure 3 - Fiber Optic Cable Television Supertrunk System

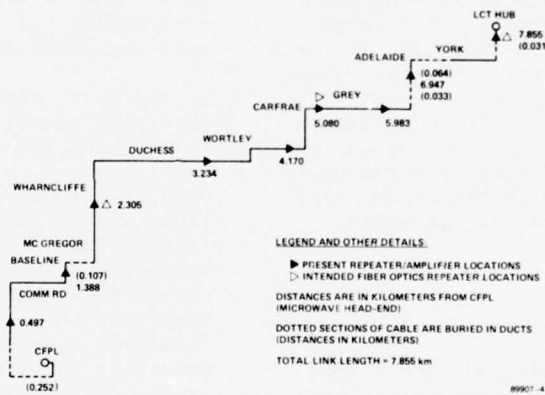


Figure 4 - Cable Television Supertrunk In London, Ontario

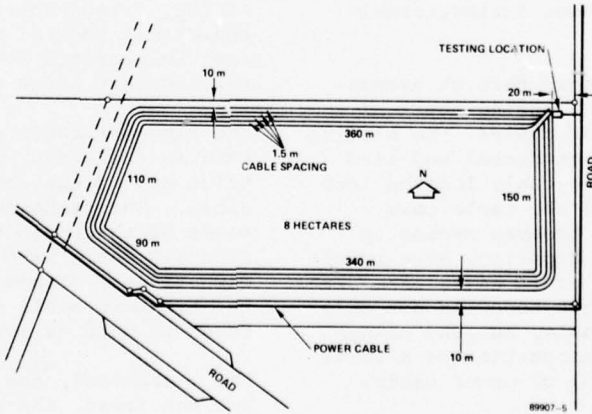


Figure 5 - Ploughing Field Trial of Four 1 - km Fiber Optic Cables Near Edmonton, Alberta

A NEW CABLE JACKET DESIGN WITH BUILT-IN AXIAL STRESS RELIEF

Wolfgang Lynen - Robert Ney

Lynenwerk K.G., Eschweiler, West Germany

Abstract

The described cable jacket design combines high tensile strength, light weight and substantial cost savings. The axial strength is achieved by embedding into the polyethylene cable jacket, during the extrusion operation, at spaced intervals concentric to the cable core, bundles of glass fibers. Upon cooling, the polyethylene shrinks and thereby tightly locks the glass fiber bundles within the jacket. This cable type is now being installed at a rate of about 20,000 miles per year in Europe. In addition to telephone cables, the new design can be used in other cable types which have to withstand high axial stress such as CATV cables for aerial installation.

Introduction

A cable is normally designed for a specific application. This applies to the conductor elements as well as to the jacket which usually has to provide mechanical support and protection against the environment and wear during normal use.

Cables are often damaged through excessive axial stress, e.g. during the installation of aerial cables, the plowing of cables during direct burial and also in the pulling of long cable lengths into ducts. Protection of the cable core against axial stress becomes necessary whenever the cable elongation, as a result of the axial stress, could cause permanent damage. Damage in this sense is not only the rupture of the cable, but any change in the transmission properties of a telecommunication, control or power cable.

Protection against this kind of damage is provided by stress relief elements which have to be designed and applied in such a

way that they relieve the endangered cable core effectively from stress. Cables which are temporarily or frequently exposed to high axial stresses are mainly aerial cables as well as mine and bore hole cables. These cables are installed over medium or long distances without any intermediate mechanical support. They have to carry their own weight and often even additional loads. Aerial cables must also withstand high tensile forces.

In the past, metals and especially steel were used almost exclusively as materials for tension relief elements. For some time, however, a new material is being used in Europe with great success: glass fiber yarn. At the 1975 IWCS a paper on "Glass Fibre Armoured PIC Trunk Cable Assembled with Connecting Plugs"¹ was presented by AEG Kabel, Germany. The described so-called bandage construction, developed by AEG, is, however, designed primarily for plow-in or duct installations and is still in a testing stage. By contrast, the cable jacket design presented here is a technically advanced solution which has received the approval of the German Post Office Authorities and the German Federal Railway System, after long and careful tests and is in actual service on a large scale.

The Figure-8 cable construction is widely used in the U.S.A. and in many other countries around the world as aerial telephone cable. The technical and economic advantages of the Lyniport cable over the Figure-8 cable were analyzed in numerous comparisons. Depending on the cable size, the Lyniport cable can save the manufacturer as much as 30%.

The mechanical, the electrical and, last but not least, the economic advantages led to the success of the Lyniport cable. The cable design and the manufacturing process are protected by patents in the U.S.A. and

many other countries.

I am going to present and explain the new design in this paper. The mechanical properties and the advantages are illustrated with data from an actual installation. Finally, other possible applications for the Lyniport cable jacket will be discussed.

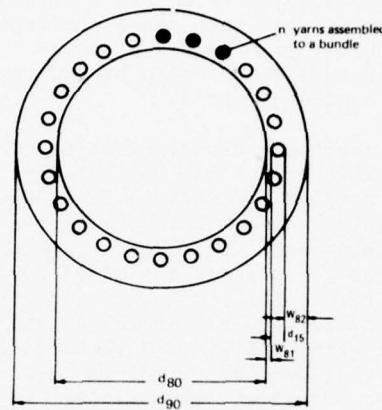
The design of the tension relief construction depends to a large extent on the supporting hardware. It is desirable to have hardware which can be applied to any piece of the cable, if possible without special preparation of the cable surface. The hardware such as clamps, spirals and similar devices are to be applied to the cable, that is to the outside of a preferably round cable. This requires a reliable force-fit between the cable jacket and the strength elements within the cable. Conventional designs employed a steel braid or steel rope through the interstices of which an interlock to the cable jacket and, therefore, the hardware was accomplished.

Design of the Cable Jacket

As mentioned before, we have introduced the use of glass fiber yarn instead of the traditional metals as tension relief elements in cable jackets. Because of its brittleness until it is embedded, the glass yarn must be fed longitudinally to the jacket. It is not possible to work the glass yarn by braiding or twisting as is customary for steel wire.

The glass fiber tension relief elements are embedded in the cable jacket as a concentric ring as shown in Figure 1. The jacket material above and below this ring is connected through bridges between the glass yarn bundles. The wall thickness of the outer part of the cable jacket - above the glass yarn layer - corresponds to the sheath thickness normally used in conventional cable jackets. A force-fit between the glass yarns and the surrounding polyethylene is achieved as a result of the shrinkage of the polyethylene during the cooling. This volume shrinkage can amount to 10%. Crystalline and amorphous areas develop during the cooling whereby especially the zone crystallization is responsible for the volume shrinkage. This shrinkage causes the glass yarn bundles inserted to the molten jacket

material to become firmly enclosed and undulated. If used with suitable hardware, this mechanical (and not chemical!) connection can be considered as absolutely safe.



d₈₀ = Diameter of the cable core, diameter under the sheath
d₉₀ = Overall diameter
d₁₅ = Diameter of a yarn bundle (composed of n yarns)
w₈₁ = Inner section of the cable sheath (portion under the yarn bundles)
w₈₂ = Outer section of the cable sheath (portion over the yarn bundles)

Figure 1 — Cross sectional view of the jacket design

Materials

Type E glass yarn which is used predominantly for textiles is just as suitable for our application. We work presently with a glass yarn with glass elements of 9 µm thickness. In the sizing process during the manufacturing of the glass yarn the individual fibers are surrounded with a starch base layer to prevent the scratching and breaking of the fiber. Also successfully tested were yarns with a plastic sizing. The glass can be obtained in various sizes or diameters, measure in "tex" or "denier." It is not necessary to process the glass yarn further, e.g. into a strand. The yarn comes normally on bobbins with a capacity of up to 4 kg (8.8 lbs), corresponding to a length of about 30 km (18 miles) for 1360 tex size yarn. This is a standard size yarn available from any glass yarn manufacturer around the world.

The plastic compound for the cable jacket is polyethylene. This, again, is a standard compound available in almost identical quality from any supplier of

cable jacket materials. We have used BASF Lupolen in large quantities.

The Cable Construction

The glass yarn bundles as tension relief elements are arranged on a circle with a space between each other corresponding to about the yarn bundle diameter. If necessary, this space could be reduced to half the bundle diameter.

The shrinking characteristics of the polyethylene affect the way the glass yarns are bundles. A maximum of 10,000 tex glass yarn per bundle can be locked into polyethylene. This key figure determines number and size of the glass yarns, e.g. 7 yarns of 1360 tex or 14 yarns of half this size. So far cable jackets have been made with 4, 5, 6 or 7 yarns of 1360 tex size per bundle. Figure 2 illustrates other possible combinations. Depending on the outer diameter of the cable, we have incorporated 12, 18, 24 or 36 yarn bundles in the jacket.

Requirements for the Cable Core

There are no special requirements for the cable core. Normally a plastic tape is wrapped around the core before the jacket extrusion. The heat developed during the extrusion is about the same as during the application of a non-reinforced PE jacket. The glass fiber yarn reinforced cable jacket can also be put over a cable with a metal sheath or outer conductor, e.g. a CATV coaxial cable. It is also feasible to apply the Lyniport jacket over a petro-jelly filled core or in conjunction with a laminated plastic metal sheath.

The Application of the Cable Jacket

The cable jacket is applied in a single extrusion step with a conventional single screw extruder suitable for polyethylene. The extruder can be operated to its full capacity. If required, a plastic or a metal tape, with or without a copolymer layer, can be applied longitudinally in the same operation.

| | $n_{015} = 4$ Recommended value for | | | | $n_{015} = 5$ Recommended value for | | | | $n_{015} = 6$ Recommended value for | | | | $n_{015} = 7$ Recommended value for | | | | | | | |
|---------------|--|----------|----------|----------|--|----------|----------|----------|--|-------|----------|----------|--|----------|-------|----------|----------|----------|----------|-------|
| | d_{50} | w_{81} | w_{82} | d_{15} | P_B | d_{50} | w_{81} | w_{82} | d_{15} | P_B | d_{50} | w_{81} | w_{82} | d_{15} | P_B | d_{50} | w_{81} | w_{82} | d_{15} | P_B |
| $n_{15} = 6$ | | | | | | 3.0 | 0.3 | 0.8 | 0.6 | 200 | 3.0 | 0.3 | 0.8 | 0.6 | 250 | 3.0 | 0.4 | 1.0 | 0.7 | 300 |
| $n_{15} = 12$ | 3.0 | 0.3 | 0.8 | 0.4 | 300 | 3.5 | 0.3 | 1.0 | 0.6 | 400 | 3.5 | 0.3 | 1.0 | 0.6 | 500 | 4.0 | 0.5 | 1.2 | 0.7 | 600 |
| $n_{15} = 18$ | 5.0 | 0.3 | 1.0 | 0.4 | 500 | 6.0 | 0.3 | 1.0 | 0.6 | 600 | 6.0 | 0.5 | 1.2 | 0.6 | 700 | 7.0 | 0.5 | 1.2 | 0.7 | 800 |
| $n_{15} = 24$ | 7.0 | 0.3 | 1.0 | 0.4 | 650 | 8.0 | 0.3 | 1.2 | 0.6 | 800 | 8.0 | 0.5 | 1.2 | 0.6 | 950 | 9.0 | 0.5 | 1.4 | 0.7 | 1,100 |
| $n_{15} = 30$ | 12.0 | 0.3 | 1.4 | 0.4 | 800 | 13.0 | 0.5 | 1.6 | 0.6 | 1,000 | 13.0 | 0.5 | 1.6 | 0.6 | 1,200 | 14.0 | 0.5 | 1.8 | 0.7 | 1,400 |
| $n_{15} = 36$ | | | | | | 15.0 | 0.5 | 1.6 | 0.6 | 1,200 | 15.0 | 0.5 | 1.6 | 0.6 | 1,450 | 16.0 | 0.5 | 1.8 | 0.7 | 1,700 |

Explanation of abbreviation codes:
 d_{50} = diameter over taping (total taping) (all values are reference values)
 w_{81} = fractional thickness of sheath (inner part)
 w_{82} = fractional thickness of sheath (outer part)
 d_{15} = diameter of bundles
 n_{15} = number of glass yarn bundles
 n_{015} = number of yarns in one bundle
 P_B = breaking load at 2% elongation at break

Figure 2 — Constructional principles for the use of glassyarn 1360 TEX

The Extruder Head and Tools

A special extruder head has been developed which permits the extrusion of the inner and the outer part of the cable jacket in one process and also places the glass yarn exactly in the correct position. The polyethylene, as it comes from the extruder screw, is divided into different channels thereby supplying the compound to the extruder head tools above and below the glass yarn bundles. Figure 3 shows the extruder head from the front, while Figure 4 gives a cross section view.



Figure 3 — View of the extruder head

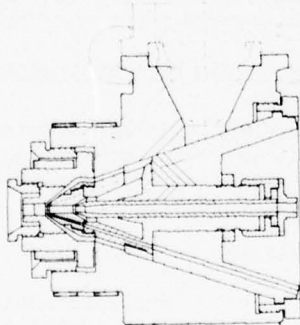


Figure 4 — Extruder head, cross-sectional view

The two flows of jacket compound are each channeled to a combination tool consisting of two guide nipples and one nozzle whereby the second guide nipple doubles as nozzle for the inner jacket part. This second nipple contains also the guide channels for the glass fiber yarns. The glass yarns leave these channels in the front of the nipple in a low pressure zone and are then embedded in the polyethylene coming up from the inner jacket.

The tool consists of three basic parts, however, the inner guide nipple is made of four parts for manufacturing reasons. The front part of this nipple can be exchanged and permits to cover a diameter range of about 5 mm. Figure 5 shows such a tool set.

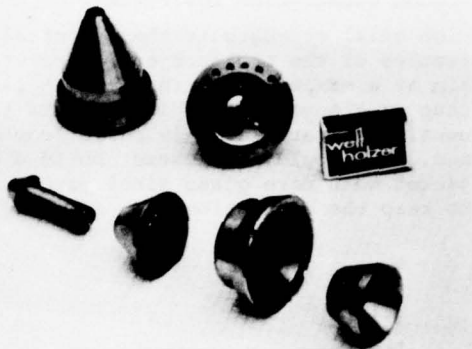


Figure 5 — Special tools for 18 glassyarn bundles

Special Equipment for the Jacketing System

In addition to the aforementioned special extruder head, a pay-off system and a pre-heater for the glass yarn are necessary. The size and shape of the pay-off system depend on the required breaking load of the cable jacket, i.e. the number and the size of the glass yarns. The number of pay-off bobbins goes down as larger size glass yarn is used.

The preheater serves to heat the glass yarn before it is fed into the extruder head if the yarns do not get enough heat while passing through the channels in the extruder head. Preheating is necessary for production speeds of more than 20 m (65 ft) per minute. About 100 W per yarn in the infrared heater is required for production speeds of up to 100 m (328 ft) per minute.

The pay-off frame must have one brake system for each yarn to keep it under tension. If the end of the yarn is brought to the outside of the bobbin, it can be connected to the beginning of the next bobbin with a fast drying glue while the first bobbin is still paying off. This assures continuous production and permits the use of only one brake for each two bobbins.

The Mechanical Properties of the Cable Jacket

The main properties of our cable jacket are:

- high axial strength and low elongation
- good bendability
- good oscillation resistance.

High axial strength is the essential feature of the Lyniport cable jacket. We aim at a maximum breaking load at less than 2% elongation. This protects the usually vulnerable cable cores from damage. One could, of course, build a cable jacket with more glass fiber yarns so as to keep the elongation even lower.

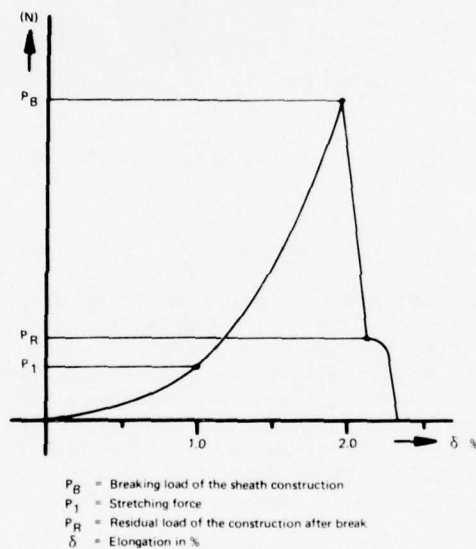


Figure 6 – Testing of the LYNIPORT cable jacket construction typical diagram of elongation due to traction effort

A stress-elongation diagram is shown in Figure 6. In the lower load range the elongation increases rapidly to 0.5%. Thereafter, as can be clearly recognized, the elongation increases more slowly, proportionally to the steadily increasing load to the breaking point of the stress relief elements. The flat portion of this curve represents the range during which the undulated yarns are stretched until they are straight. The curve drops sharply after the stress relief elements are broken - which proves that all glass yarns were engaged to absorb the applied load.

The German Federal Postal system specified

that the residual load P_R may not exceed one third of the breaking load P_B of the cable jacket.

The bendability of cables with our new jacket, despite the brittleness of the unsupported glass fiber, does not change appreciably as compared to a cable without glass stress relief elements. This results from the glass yarn undulation which, upon bending, enables the yarn to react like a bellows. Both the stress relief elements and the cable core will be damaged only if the cable is bent over a radius smaller than permitted for cables without stress relief elements. The minimum permissible bending radius should be no less than 20 times the cable diameter.

The cable is not susceptible to oscillations which occur normally with aerial cables, especially the Figure-8 cable. This property results from the fact that this cable is round and that the glass yarns as supporting elements are firmly embedded in the jacket compound.

Extensive oscillation or dancing tests have been conducted in special outside test bays with 50 m (164 ft) long spans of aerial cables in Europe under summer and winter conditions. The main result was that the tested samples passed more than 10^7 oscillations without any damage.

Advantages of the New Cable Jacket Construction

The Lyniport cable jacket offers in comparison to cable with conventional metallic stress relief elements the following advantages:

1. Easy handling in production

The glass yarn is incorporated into the cable jacket during the jacket extrusion, while conventional stress relief elements (e.g. braided or stranded steel wire) require one additional process step. External support elements have to be manufactured and installed separately. Glass yarns are supplied ready to use in the pay-off devices in long lengths. A simple joining technique permits continuous production. Lyniport cables are light weight and easy to handle in production and during testing. By contrast the bulky conventional steel stress relief elements are difficult to handle and can easily cause accidents.

2. Good strength to weight ratio

Support elements of glass yarn feature a much better strength to weight ratio than steel wire. The total weight of a cable is thus lower than the weight of a comparable cable with steel wire reinforcement.

3. Easy installation

The cross section of the new cable is round. A round and lightweight cable is easier to install than the Figure-8 cable. The mounting hardware is simply a wedge-type clamp or a spiral wire. The splicing of a drop wire to the cable in midair can be done easily and fast.

4. Good electric properties

The transmission properties of an electric cable are normally affected by metallic stress relief elements. If an electric shield is not required, the use of glass yarn instead of steel wire yields a considerable improvement. If an electric shield has to be incorporated in a cable with a glass yarn reinforced jacket, such shield can be placed in an optimally effective position around the cable core.

5. Glass is best suited chemically

Glass yarn is noncorrosive, does not rot and even outlasts the plastic jacketing materials in resistance to temperature extremes.

6. Lower production cost

The new cable jacket is more economical to make. The cost advantage in production has been discussed briefly before and should not be neglected.

The Application of the Lyniport Cable Jacket to Aerial Telephone Cable for the German Federal Postal System (DBP)

The development of the new cable jacket originated from special requirements of the DBP which also supported the development program. The DBP telephone cable network is one of the main applications for our cable and shall, therefore, be used as illustration. We also initiated some contacts with postal administrations and cable manufacturers in other countries and numerous test programs were conducted successfully or are under way.

The DBP installs approximately 30,000 km (19,000 miles) of telephone cable with axial stress relief elements each year. These cables are supplied by five cable manufacturers, four of which are Lynenwerk licensees. Although these cables are used as dropwire, they must have the transmission quality of an exchange cable. As a rule, they are installed in lengths from about 100 m (330 ft) to several kilometers, in certain cases for remote customers even in longer lengths. The cores of these cables contain 2, 4, 6 or 10 pairs, stranded into star quads. Cables with more conductors can be easily designed and manufactured.

The conductor has a diameter of 0.6 mm (23 AWG) and is insulated with 0.25 mm (0.010") polyethylene. The stranded star quads are usually wrapped with a polyethylene tape over which an inner polyethylene jacket is applied. The core is then jacketed. However, on request of the DBP, a shield of a plastic bonded aluminum tape with a drain wire of 0.6 mm copper is folded over the core longitudinally. Figure 7 shows the dimensions of the cable jacket with the embedded glass yarn bundles in columns 2 to 6.

| 1 Number of pairs | 2 d_{80} Diameter of the cable cores (mm) | 3 W_{81} Thickness of the inner section (mm) | 4 W_{82} Thickness of the outer section (mm) | 5 Number of bundles x number of yarns per bundle | 6 d_{90} Overall diameter (mm) | 7 Breaking load (mean value) (N) |
|----------------------------|--|---|---|---|--|---|
| 2 | 4.6 | 0.3 | 1.0 | 12 x 6 | 8.6 | 5500 |
| 4 | 7.3 | 0.3 | 1.2 | 18 x 5 | 11.3 | 8000 |
| 6 | 7.5 | 0.3 | 1.2 | 18 x 6 | 11.7 | 9000 |
| 10 | 9.0 | 0.3 | 1.4 | 24 x 6 | 13.6 | 11000 |
| 16 | 12.1 | 0.3 | 1.4 | 24 x 7 | 16.9 | 12500 |
| 20 | 13.1 | 0.3 | 1.4 | 24 x 7 | 18.1 | 12500 |

d_{10} = Diameter of the conductor = 0.6 mm

d_{20} = Diameter of the core = 1.1 mm

d_{80} = Diameter after twisting + 2 · thickness of the inner sheath + thickness of the screen

Figure 7 — Installation cable with strain relief
Data of the cable jacket

The cable jacket for the 2 pair cable is applied by an extruder with a 90 mm screw. On this line we succeeded recently in applying simultaneously the inner polyethylene jacket over the cable core. Such a tandem operation is very desirable for a continuous production in 3 shifts as we have set up for the cables for the DBP. This line operates continuously at a speed of 80 m/min (250 ft/min).

The essential elements of this line are shown in Figures 8 and 9.

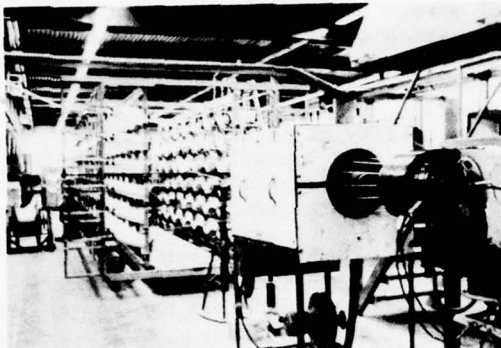


Figure 8 — View from the extruder towards the pay-off

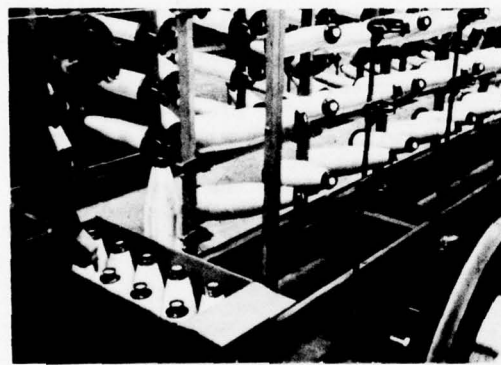


Figure 9 — Partial view on the feeding frame for the glassyarn

Cables with larger numbers of pairs are jacketed on an extruder with 120 mm screw diameter. The production speed for cable with up to 10 pairs is 50 m/min (155 ft/min).

We use glass yarn of 1360 tex size as tension relief elements. This yarn comes in lengths of about 30 km on each bobbin. The continuous pay-off change from an empty to the next full bobbin is possible through the use of our so-called double pay-off frame. The end of one and the beginning of the next glass yarn are joined with a fast drying glue.

The Lyniport cable must meet demanding mechanical requirements. The test load figures are the same as for aerial cables with steel strength members, though the actual weight and the diameter of our cable are much smaller.

Figure 10 shows the respective figures for a 10-pair cable. The mechanical safety factor for the new cable jacket construction is now 10.

| | LYNIPORT cable J 2 Y(St)(Zg) 2Y 10 x 2 x 0.6 | Installation cable with supporting braid of steel wires J 2 Y(Z)Y 10 x 2 x 0.6 | Figure - B cable A.2Y2YT 10 x 2 x 0.6 |
|---|--|--|---|
| cable core ϕ (mm) | 9.0 | 11.6 | 8.5 |
| overall ϕ of the cable (mm) | 13.6 | 14.4 | 11.5 x 19.5 |
| weight of the cable core (kg/km) | 89.3 (up to and including the screen) | 108 (without steel wire braid) | 77.3 (without screen) |
| total weight (kg/km) | 178 | 292 | 190 |
| theoretical breaking load (N) | 11500 | 10500 | ~9000 |
| construction of the traction relieving device | 144 yarn à 1360 tex | 24 steel wires 0.8 Ø flat shaped | steel rope 7 x 1 mm ² |
| weight of the traction relieving device (kg/km) | 20 | 95 | 55 |
| admissible maximal traction load (N) | 7200 | 6750 | 4000 |
| traction load in 50m span width at 20°C (N) | 850 | 1570 | 900 |

Figure 10 — Comparison between various designs of self-supporting cables with 10 pairs

The tests for these cables are done on a selective basis for the test load, the breaking load and the residual load, as was indicated in Figure 2. These tests are outlined by the DBP in a special publication as required according to VDE 0472 specification.

The new cable jacket construction was - following a DBP request - subjected to several special tests at the Lynenwerk, by outside test laboratories and at technical universities. These tests concerned mostly the oscillation behavior of the cable and its resistance to high and low temperature extremes. The latter tests were conducted with the wedge type clamps which are used in Germany as mounting hardware. The Institute for Application of Plastic Materials at the Technical University Aachen issued a test report according to which the axial stress is transmitted satisfactorily between the mounting hardware and the glass yarn embedded in the cable jacket even at cable temperatures in excess of 60° C (140° F).

The DBP has aerial telephone cables with the Lyniport jacket installed in their network by means of wedge type clamps, as shown in Figure 11. Each supporting point is also a fixed point. At the same time, a so-called "plus loop" or spare loop is provided, which can be used later on for the connection of additional drop wires. The linemen of the DBP are acquainted with this type of installation technique.

The sag of the cable is defined in tables as a function of the outside temperature and is adjusted for each span length individually. These tables are set up to provide the sag depth for each span length/temperature combination. They were established from the cable data based on the so-called starting condition at a temperature of -5° C (21° F) and a sag of 1% of the span length.

A different type of mounting hardware as alternative to the conventional wedge type clamp has been developed and is already in use. This new hardware is based on the well-known spiral concept of Preformed Line Products in Cleveland, Ohio and was developed and is made by a licensee of PLP in Germany.

Further Possible Applications of the New Cable Jacket

The new cable jacket is not only suitable for aerial cables, but also for applications where price or weight prohibited the incorporation of conventional stress relief elements in the past. We developed a complete line of exchange cables for duct installation with stress relief elements of glass yarn as "feed-in" or "pulling help." This subject has already been discussed at previous meetings. I refer to the paper "Engineering for Cable Installation" by Mr. Pehrson² from General Cable Corporation where problems with the installation of exchange cables were discussed and to the paper by Mr. Dagefoerde from AEG which was already cited once before. In that design the axial stress is transmitted from the mounting hardware through the cable jacket to a copolymer coated aluminum tape to which in turn the stress absorbing glass yarns are bonded. The same applied to glass yarn bonded to a textile strip which again has to be bonded to the jacket.

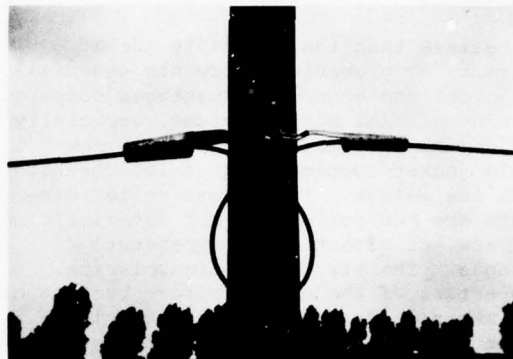


Figure 11 – Suspension point for a 10 pair cable

We are cooperating with an American cable manufacturer and the REA to install, before the end of this year, two sizes of standard U.S. aerial telephone cables equipped with the Lyniport jacket in two different locations in the United States.

Further Development of the Lyniport Principle

So far, because of certain conditions described earlier, only polyethylene has been used as material for the Lyniport jacket. This has been based on the concept that a suitable compound must develop a zone crystallization after passing the solidification temperature. There are some other compounds with this feature, but they are not used for cable jackets, mainly because of their price.

We succeeded recently in combining glass yarns with cable jacket compounds other than polyethylene with a good axial stress transmitting mechanical bond. A different technology was required because the necessary undulation of the glass yarn has to be created in a different way. It is now possible to utilize PVC and EPR or natural rubber in conjunction with the glass yarn as cable jacket, thus opening new applications where polyethylene jackets could not be employed for reasons of safety.

Conclusion

We believe that the new cable jacket concept, as presented today has essential technical and economic advantages compared to conventional cable designs, especially for aerial telephone cables. The new cable jacket combines high axial strength with low weight. The stress relief elements are non-corrosive, not deteriorating and are not affected by temperature changes. The electrical transmission properties of the cable improve because of the absence of metallic parts causing attenuation or electrical reflections. The cable jacket can be manufactured easily and economically. Special tools were developed and the process and cable design are protected by U.S. and foreign patents. The ease in handling and installation of these cables offers additional cost savings. The new cable jacket can be used for many applications where a cable must withstand axial stresses.

Acknowledgments

We thank Messrs. D. R. Stein and G. F. Stoeckl of Cable Consultants Corp. for their assistance in the preparation of this paper.

References

1. H. G. Dagefoerde, Glassfibre Armoured PIC Trunk Cable Assembled With Connecting Plugs," IWCS, 1975, pp 136-142.
2. V. W. Pehrson, "Engineering for Cable Installation," IWCS, 1975, pp 260-267.

Biography



Wolfgang Lynen received an MBA degree from the University of Fribourg, Switzerland in 1967. After further studies at the University of Oklahoma, Norman, he was employed by Monsanto Co., first in St. Louis then in Brussels. He joined Lynenwerk, cable works, West Germany, in 1973. He is managing director for all commercial activities of the company since 1975.



Robert P. Ney is technical director of Lynenwerk and responsible for all major technical activities. He was graduated from the Universities of Aachen and Cologne as a mechanical and electrical engineer. Mr. Ney has substantially participated in the development of the new cable jacket construction.

STATE OF THE ART TEST FOR MECHANICALLY INDUCED
NOISE VOLTAGE IN ELECTRONIC CABLE

J. W. KINCAID, JR.

BELDEN CORPORATION
GENEVA, ILLINOIS

ABSTRACT

The need for standardization of low noise cable test methods is discussed. A review of certain aspects of NBS, ISA and MIL-C-17 test methods is presented. Test apparatus which yields repeatable triboelectric charge generation in cable is described. The technique involves twisting one end of a cable and measuring charge output at opposite end while controlling and monitoring axial tension, rate and magnitude of twist.

The low noise cable is often used to interconnect crystal-type transducers to high input impedance instrumentation amplifiers⁶. In these applications the triboelectric charge⁷ output from the cable must be negligible compared to the charge output from the transducer. Thus the maximum permissible triboelectric charge output level at which a cable ceases to qualify as "low noise" is dependent on the requirements of the application. Efforts to refine the definition of "low noise cable" are further complicated by the variety of mechanical treatments employed to excite the triboelectric charges and the usage of both cable charge output and noise voltage registered on read-out instruments as measures of low noise cable performance.

The main purpose of this paper is to call attention to the need for establishing a standardized mechanical treatment method which gives repeatable results. A standardized means of measuring, recording, and classifying triboelectric charge generation in electronic cable is also needed. Through reporting on a test fixture which gives repeatable results, the feasibility is established and guidelines are provided along which future standardization efforts may proceed.

INTRODUCTION

The cornerstone for standardization of low noise cable testing was set in May 1955 with the appearance of the National Bureau of Standards Report "A Simple, Objective, Test for Cable Noise Due to Shock, Vibration, or Transient Pressures" by T. A. Perls¹. Subsequent to and largely based on the NBS report, formalized test methods have appeared in MIL-C-17² and the Instrument Society of America publications³.

The NBS method* has been used with general success over the years. However, it is known that private industry has often developed alternative test procedures for in-house use⁴. Additionally, it is known that the NBS method does not yield repeatable results from which a rigorous study of the noise generation may easily be made. Perls' claimed results which are repeatable within 30% for the same cable sample with a possible variation of 3 to 1 for different samples of the same cable⁵. Greater repeatability is not claimed in the ISA* or MIL-C-17 methods*.

A QUANTITATIVE INTERPRETATION OF
TRIBOELECTRIC CHARGE GENERATION
DYNAMICS.

For the NBS and MIL-C-17 methods, cable motion (see figure 1) commences from a horizontal plane which is parallel to plane "K" at height "h".

* Here reference is made to the appropriate NBS, MIL-C-17 or ISA test method described in reference 1, 2, or 3 respectively.

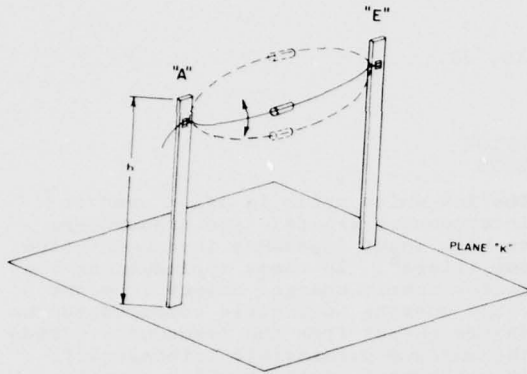


Figure 1. Sketch of Cable Motion in NBS and MIL-C-17 Methods.

Because the cable is clamped at points "A" and "E" and is weighted down at midspan point "B", twisting moments are generated at these points as the cable swings back and forth prior to coming to rest in a plane perpendicular to plane "K". Pre-positioning the cable in the horizontal plane establishes non-zero initial values for the twisting moments, provided the cable is clamped at points "A" and "E" while in a vertical plane.

It is theorized that triboelectric charge generation during the test is primarily due to relative motion at the conductor-insulation interface (see figure 2). The motion at the interface is due to the axial twisting moments and is accompanied by a slowly changing axial tension in the cable. Triboelectric charges are also generated as a result of a possible "jerky" motion of the cable during the first swing or two. It is theorized that these charges arise from a relative motion at the interface due to bending moments about an axis which is at right angles to the cable axis. This mode of charge excitation is accompanied by rapidly changing axial tension.

The ISA method recommends that cable motion be initiated in a plane which is perpendicular to plane "K" and passes through points "A" and "E". (see figure 3). The cable is weighted down at midspan point "B" and clamped at points

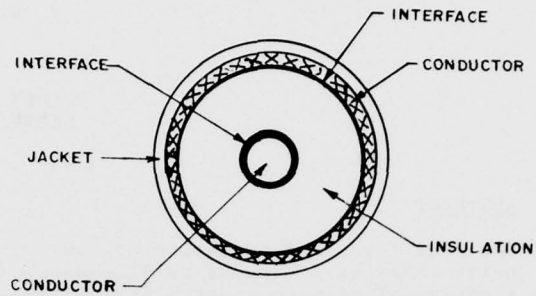


Figure 2. Location of Conductor-Insulation Interface.

"A" and "E". Point "B" is raised distance "d" above points "A" and "E" and released to initiate the cable motion. The resulting cable motion is quite "jerky" and it is theorized that triboelectric charge generation arises from bending moments at right angles to the cable axis and is accompanied by rapidly changing axial tension.

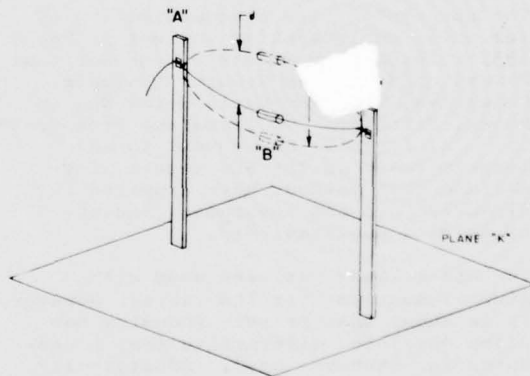


Figure 3. Sketch of Cable Motion in ISA Method.

According to this quantitative interpretation, triboelectric charge generation is induced (for the considered test methods) by either or both of two

forms of mechanical treatment. These forms are designated as the twisting mode and the bending mode and are characterized, respectively, by twisting motion about the cable axis and bending motion at right angles to the cable axis.

The NBS, ISA, and MIL-C-17 test methods do not specify that axial tension changes in the cable are to be monitored during the test. There is no provision for commencing the test with known initial values of axial tension, twisting moment, or bending moment.

CHARACTERISTICS OF AN IMPROVED TEST SYSTEM

The purpose of an improved test system is to provide a display of triboelectric charge which is a repeatable function of the variables and parameters of the mechanical treatment. Furthermore, the generated triboelectric charge is a rather complicated function of the entire cable design and fabrication process. Attainment of a repeatable relationship between triboelectric charge and mechanical treatment is a prerequisite for rigorous study of the influence of cable design, materials, and fabrication processes.

Analysis of the preceding quantitative interpretation indicates the following items to be essential in a test system which would provide for a systematic study of triboelectric charge generation:

1. Controlled and monitored axial tension.
2. Controlled and monitored twist of the twisting mode.
3. Controlled and monitored displacement of the bending mode.

STATE OF THE ART TEST

Discussion

To obtain a reasonably simple test apparatus it was decided a test cable should be subjected to only one mechanical treatment, i.e., twisting mode or bending mode. The twisting mode treatment seems to excite charge generation more efficiently than does the bending mode treatment. Consequently, development efforts have focused on a twist test apparatus. However, development of a bending mode excitation apparatus is being pursued and will be reported on in the future.

A photograph of the twist test apparatus is presented in figure 4. The apparatus is considered to be state of the art because of the new techniques used in

applying and monitoring the twist, tension and generated charge output.

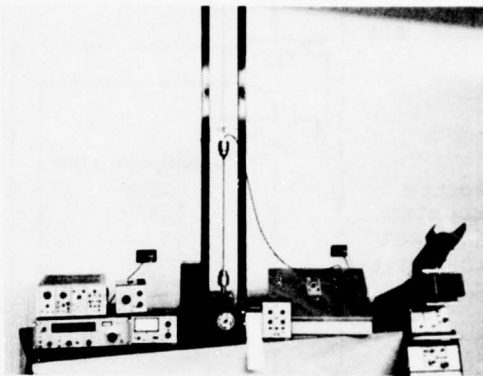


Figure 4. Twist Test Apparatus.

The apparatus is relatively simple and provides a mechanical treatment which primarily excites the twisting mode of triboelectric charge generation. Frequency response studies of the apparatus have shown the presence of a mode which was not a consideration in the quantitative interpretation of triboelectric charge generation dynamics. This mode is due to the pulsations of the stepper motor which are transmitted to the cable at the fundamental rate of twist (steps/second). With this apparatus, detection of the twisting mode component is unhindered by the presence of the weak pulsation mode component. The twisting mode component has been found to be independent of the rate of twist (steps/second). The pulsation mode component, on the other hand, is a function of both the rate and magnitude of twist.

Equipment Used in the Twist Test Apparatus

The functional components are diagrammed in figure 5. The pertinent characteristics are listed below.

1. Stepper motor (Superior M093-FD07).
Step size: 1.8°
Holding torque: 450 oz.-in.
Step rate: 3 steps/second to 500
steps/second
Potentiometer adjustment
on control panel.
Constant motion speed: greater than
40 steps/second.

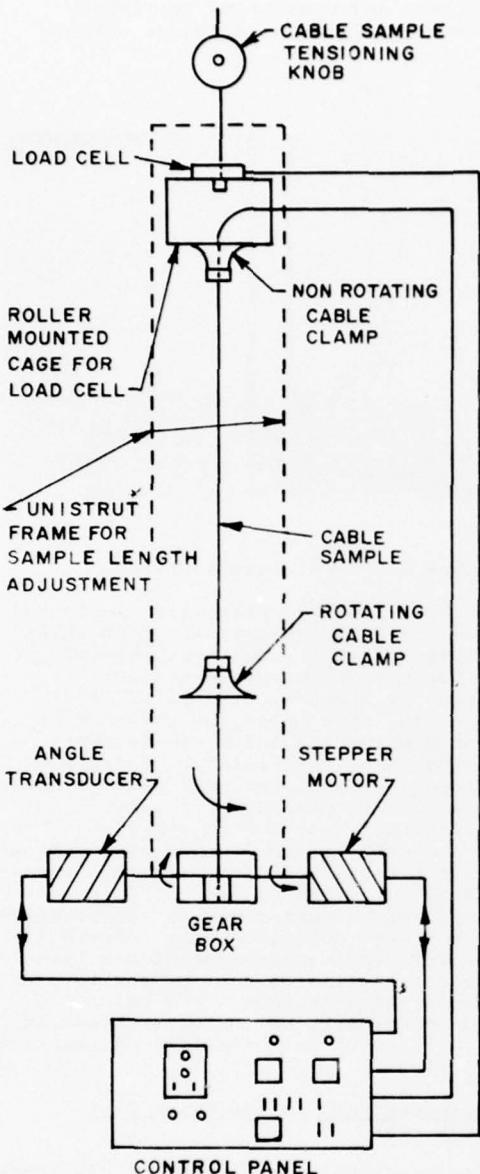


Figure 5. Equipment Diagram.

2. Headstock chuck cable clamps (Jacobs 56B)
Maximum cable diameter: .5"
Compression marks on jacket are circumferentially spaced 1" long grooves parallel to cable axis.
Lower chuck has closed interior which shields rotating end of cable.
Clockwise rotation is defined looking into lower chuck jaws.
Upper chuck is static with feed-

* Registered trademark of Unistrut Corp.

through feature for cable connection at termination point.

3. Angle transducer (Transtek-603)
Linear range: $\pm 60^\circ$.
4. Gear box
Three shafts, right angle drive 1:1 ratio.
5. Load cell(Kristal 9011)
Sensitivity: 19 pc/lb.
Maximum load: 300 lbs.
6. Charge amplifier (Kristal 5002)
Static and dynamic charge measurement capability.
7. Control panel (Belden)
Houses charge amplifier and logic-circuitry used to program stepper motor.
Switch selectable functions:
Direction and number of steps of rotation. (2-199 steps)(bilateral or unilateral)
Number of cycles (continuous, 1 to 99)

The inclusion of component manufacturers' names is not intended as an endorsement. It is assumed that similar products from other manufacturers could function equally well.

Procedure for Mounting the Cable Sample in the Test Fixture and Selecting the Initial Conditions.

Prior to conducting a test the cable sample must be mounted and the initial cable tension, twist, number of steps, directional sequence of rotation and step rate must be selected. The following procedure is followed:

1. Sample length up to 54" is selected.
2. Sample is secured in lower chuck jaws.
3. Sample is secured in upper chuck jaws.
4. Sample is terminated at load cell cage or control panel and shielded as necessary.
5. Sample is placed under tension by adjusting tensioning knob and monitoring load cell output through charge amplifier and oscilloscope.
6. "Initial twist" is obtained by single step rotation of lower chuck. Zero twist condition (within 1.8°) is obtained (for cable constructions without an inherent longitudinal twist) when equal

tension changes are produced by equal clockwise and counterclockwise rotation of lower chuck. For cables with an inherent longitudinal twist the following technique is used. Triboelectric charge polarity is observed for single step rotation in both directions. Increasing tension is accompanied by the opposite charge polarity from decreasing tension. The neutral position is reached by single step rotation in the direction of decreasing tension until a charge polarity reversal is obtained.

7. Number of steps of clockwise and counterclockwise twist are entered on separate thumbwheel switches.
8. Direction of first step is switch selected.
9. Directional sequence of rotation is switch selected. The motion can be unilateral or bilateral. Bilateral implies both clockwise and counterclockwise rotation about the neutral position. Unilateral implies rotation on either the clockwise or counterclockwise side of the neutral position.
10. The number of cycles, continuous, or 1 to 99 is switch selected.

Test Results

As discussed earlier in this paper, the amount of twist and the axial tension are unmonitored and only nominally controlled in the NBS, ISA, and MIL-C-17 test methods. In this section, test results are given which show the dependence of generated triboelectric charge on the values of "initial twist and tension".

1. Initial twist. The triboelectric charge generated during one cycle for three sets of "initial twist" conditions is given in figure 6. The numbered traces correspond to the initial conditions as follows:

 - 1) Zero "initial twist".
 - 2) 10 steps clockwise from zero-twist.
 - 3) 10 steps counterclockwise from zero-twist.

Figure 7 shows the change in axial tension which occurs during one cycle for these "initial twist" conditions.

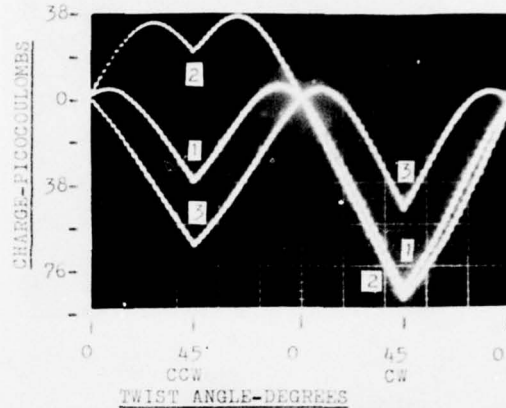


Figure 6. Generated Charge versus Twist Angle.

Other parameters of the experiment are as follows:

Cable type: RG-59/U
 Cable length: 48 inches
 Twist rate: 10 steps/second
 Angular twist: 25 steps bilateral (45°)
 Starting direction: Counter-clockwise.
 Initial axial tension: 4 pounds.

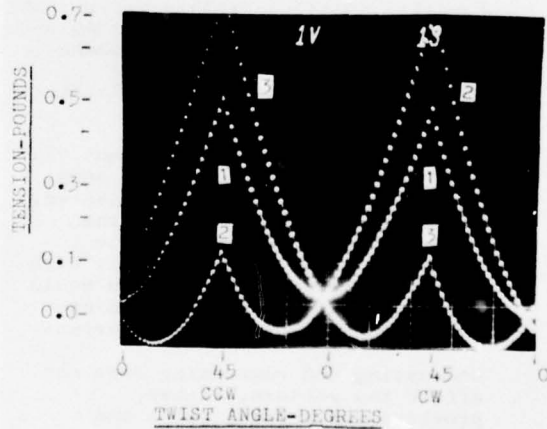


Figure 7. Axial Tension versus Twist Angle.

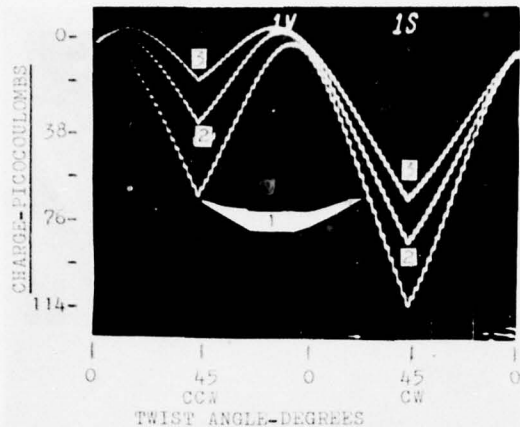


Figure 8. Generated Charge versus Twist Angle.

2. Initial Axial Tension. The triboelectric charge generated during one cycle for three sets of "initial axial tension" is given in figure 8. The numbered traces correspond to the initial conditions as follows:

- 1) 2 pounds
- 2) 4 pounds
- 3) 6 pounds.

The other parameters of the experiment are the same as for the "initial twist" variation experiment except zero initial twist was maintained. Figure 9 shows the change in axial tension which occurs during one cycle for these "initial axial tension" conditions.

Figures 6 and 8 show generated charge for 1 cycle of motion only. However, as the motion is repeated, subsequent cycles reproduce the same charge versus twist angle pattern. After a sufficiently high number of cycles, the pattern would change due to aging phenomena at the conductor-insulation interface.

Demounting and remounting does not affect the pattern, either, provided the initial twist and tension have been carefully adjusted.

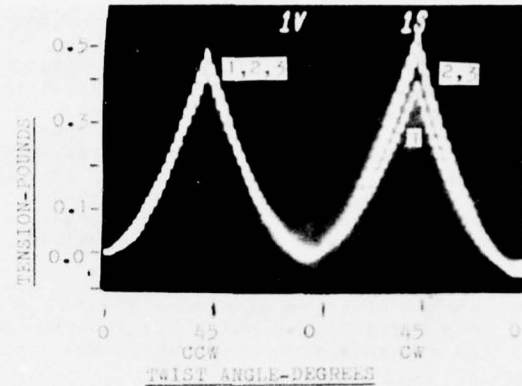


Figure 9. Axial Tension versus Twist Angle.

3. Pulsation Mode Characteristics.

Figure 10 presents an amplitude spectrogram of generated charge for the following experiment:

Cable type: RG 59/U.
Cable length: 48 inches.
Twist rate: 30 steps/second.
Angular twist: 6 steps, unilateral (10.8°).
Initial axial tension: 2 pounds.
Initial twist: zero.

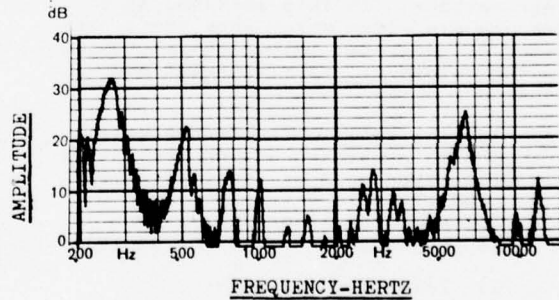


Figure 10. Amplitude Spectrogram.

The spectrogram shows the fundamental of several harmonics due to the cable twist frequency of 2.5 cps (30 steps/sec/12 steps/cycle). The pulsation mode component is evident at 30 hz. The peak at 60 hz is due to the second harmonic of the

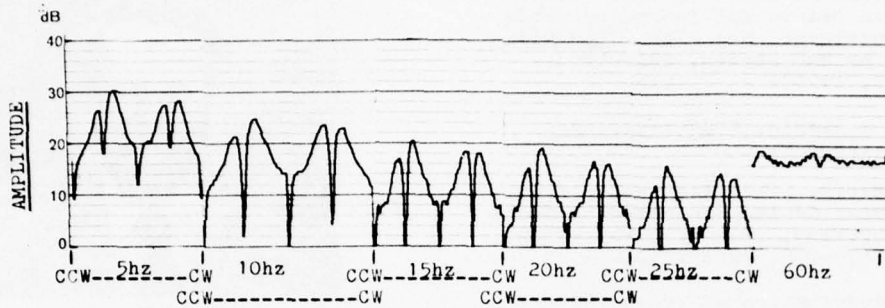


Figure 11. Harmonic Amplitude Variation with Twist Angle.

pulsation mode and 60 hz power frequency interference.

Figure 11 shows the amplitude variation during one cycle of twist for the fundamental and first four harmonics for the following experiment:

Cable type: RG 59/U.
Cable length: 48 inches.
Twist rate: 5 steps/second.
Angular twist: 100 steps, bilateral (180°)

Initial axial tension: 3 pounds.
Initial twist: zero

Also shown is the 60 hz power frequency interference level. The data in figures 10 and 11 were obtained with the following equipment. B&K No. 2511 vibration meter, No. 1621 1/3 octave bandpass filter, and No. 2306 level recorder.

SUMMARY AND RECOMMENDATIONS

A test fixture which provides for repeatable triboelectric charge generation in electronic cable has been described. The technique involves holding one end of the cable stationary while the other end is twisted about the longitudinal cable axis. Axial tension, rate and magnitude of twist are monitored and controlled with state of the art techniques.

Careful adjustment of the "initial twist" and axial tension insures reproducibility of results for the same cable sample, even after demounting and remounting on the fixture. However, consistency of results, from sample to sample, even with identical initial conditions is

dependent on the uniformity of cable construction materials and manufacturing processes.

As described in this paper, a fixture which excites triboelectric charge generation in the "bending mode" is being developed. Study and characterization of cable triboelectric charge generation properties with the "twisting mode" and "bending mode" test fixtures is being planned. Findings will be reported on in the future.

A variety of fixtures, and methods are currently used by the industry for characterizing "low noise" cable performance. There is a need for standardization. This paper has reported on the feasibility of obtaining repeatable test results and, it is hoped will be of value in establishing a future standard.

ACKNOWLEDGEMENTS

The author acknowledges the dedicated efforts of the Technical Research Center staff. In particular, recognition is due Terry Koehn and Scott Lehman for their important contributions in the design of the twist test apparatus.

REFERENCES

1. T. A. Perls, A Simple, Objective, Test for Cable Noise Due to Shock, Vibration or Transient Pressures, (National Bureau of Standards Report, May 1955).
2. Military Specification Sheet, MIL-C-17/126 or MIL-C-17E paragraph 4.8.15.

3. Instrument Society of America,
Standard S37.10, paragraph 6.2.
4. This trend is noted in test requirements on prints for low noise cable constructions. See also: Low Noise Cables by Don Styles, (Electron, April 8, 1976).
5. Perls, A Simple, Objective, Test for ... page 9.
6. T. A. Perls, Electrical Noise from Instrument Cables Subjected to Shock and Vibration, (J. Appl. Phys., 23, No. 6, 674-680. June 1952).
7. For a description of triboelectrification theories see D. A. Seanor, Triboelectrification of Polymers, (Electrical Properties of Polymers, Technomic Publishing Co., 1972).



John W. Kincaid received the MSEE and BSEE degrees from the University of Oklahoma in 1967 and 1966, respectively. He is a Product Development Engineer at Belden Technical Research Center and is engaged in long range development studies.

A STUDY COMPARING PAIRS AND QUADS

Valentin Abadia

CABLES DE COMUNICACIONES S.A.

INTRODUCTION

Cable users do not seem to agree on the most desirable type of cable construction, whether it be pairs or quads. One cannot be said to be superior to the other, nevertheless there does exist advantages and disadvantages in each case. Our aim is to try to analyze them focused on three different points of view; first, transmission quality; second, conductor joining (splicing) and last but not least, cost. We feel qualified to make such a study since our factory can produce either construction and so we do not have a bias in either direction.

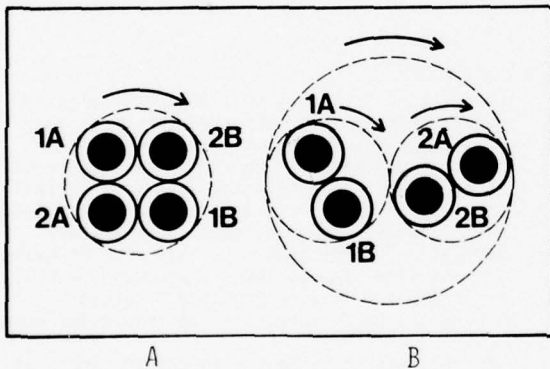


Figure 1
a) Star Quad
b) D.M. Quad

Figure 1 shows the two different types of quad constructions that exist, namely star quad (or spiral four quad) and the multiple twin quad, which is also called D.M. Quad. The D.M. consists of two pairs which are in turn twisted together. In the star quad the four wires are twisted at the same time, the pairs being formed by the wires diametrically opposed. We have used this type of quad in our comparisons due to its reduced mutual capacitance having economical advantages which we shall evaluate.

The pairs and quads used in the tests were manufactured using the same technology and production controls, in this way the study was objectively possible. The plastic insulated pairs and quads were insulated using a coaxial capacitance monitor. All the quads were bound individually thus reduc-

ing the distortions during the stranding process.

Tests were made on pair and quad cables up to a frequency of 1024 KHz which is the main PCM system of 30 channels.

The possibility of obtaining higher quality cables with other types of manufacture and controls is not debated in this study. The fundamental idea consists in comparing the two constructions when the same techniques have been used in both.

1. THE TECHNICAL CHARACTERISTICS OF BOTH CONSTRUCTIONS

1.1

The use of phantom circuits

Phantom circuits allow an increase of 50% in the capacity of the circuits in a cable when two pairs are used as an additional new circuit can be obtained by using special repeating transformers. This simple arrangement is shown in Figure 2.

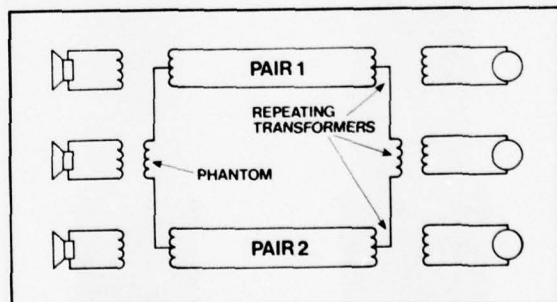


Figure 2
Physical and phantom connections

This however does not work on two adjacent pairs because the pairs themselves have to be transposed or twisted in order to obtain a balance to ground and reduce interference between two adjacent phantom circuits.

One advantage of quad cable is that of the phantom circuits being able to be used, however this technique is not commonly used in exchange areas and it is in fact quite obsolete with the use

of carrier systems. These are actually circuits which have poor balance and offer bad transmission quality. Well balanced quads are needed if one is to use the phantom circuits at high frequencies.

1.2

Mutual capacitance and size

As the pair in a quad is formed by the wires which are diametrically opposed, less diameter over insulation is needed to obtain the same mutual capacitance and consequently the same attenuation.

The construction therefore of quads presents less diameter than that of pairs having an equal number of circuits. This reduction depends upon the size and mutual capacitance and is between 8 and 10 percent. In Figure 3 two equal cables one constructed with pairs and the other with quads are shown.

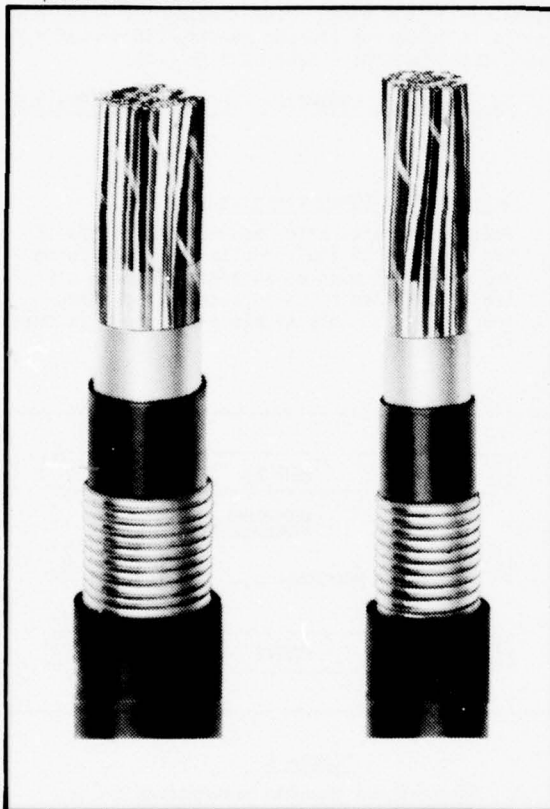


Figure 3
Sizes of pairs and quads

If on the other hand we should wish to obtain as many circuits as possible in a specific cable diameter, the quad construction would allow us more circuits than that of the pair with the same attenuation. The increase percentage depends on the gauge and mutual capacitance. This

is shown in Table 1 for one capacitance level.

TABLE 1

Increase in the number of circuits in quads (percent) for 52nF/Km. (0.083 μF/mile)

| GAUGE IN MM. (AWG) | | | |
|--------------------|-----------|----------|-----------|
| 0.9 (19) | 0.64 (22) | 0.5 (24) | 0.40 (26) |
| 20% | 23% | 29% | 30% |

One last point I would like to mention is that star quads of large gauges (16 AWG) and low mutual capacitance (up to 32nF/mile) have been normally used for toll cables. It is very difficult and sometimes even impossible to obtain this capacitance with pairs, especially if the insulation is pulp or paper. The use of electronic equipment has made this type of cable quite obsolete and the tendency is small gauges and higher capacitance.

1.3

Attenuation

The degree of attenuation a telephone signal suffers when it is transmitted through a pair of wires at low frequency depends upon the mutual capacitance and conductor resistance of the two wires. Consequently as a lower mutual capacitance can be obtained for the same insulation thickness the quad cable shows a lower attenuation at low frequency than that of pairs with the same diameter over dielectric (D.O.D.). This reduction is between 5 and 7 percent depending on the thickness of the insulation used.

This relation nevertheless is not so simple at carrier frequencies, due to the fact that a star quad cable has a smaller diameter than that of pairs of the same mutual capacitance. When the frequency rises the increase of resistance in the quad cable is greater than that of the pair, due to the so called proximity effect. The attenuation at high frequencies is therefore greater.

An example of the above mentioned can be seen on the next page in Figure 4.

We can see from Figure 4-A the attenuation measured on two 22 AWG pulp cables which had the same D.O.D. At voice frequencies the quad cable had a lower attenuation than that of the pair cable. This is in fact due to its lower mutual capacitance, but as the frequency was increased the resistance of the wires in the quad cable also increased above that of the pair cable (approximately 13% at 1 MHz). This in turn made the quad cable give a higher attenuation than the pair cable, although the

pair cable has had a higher mutual capacitance.

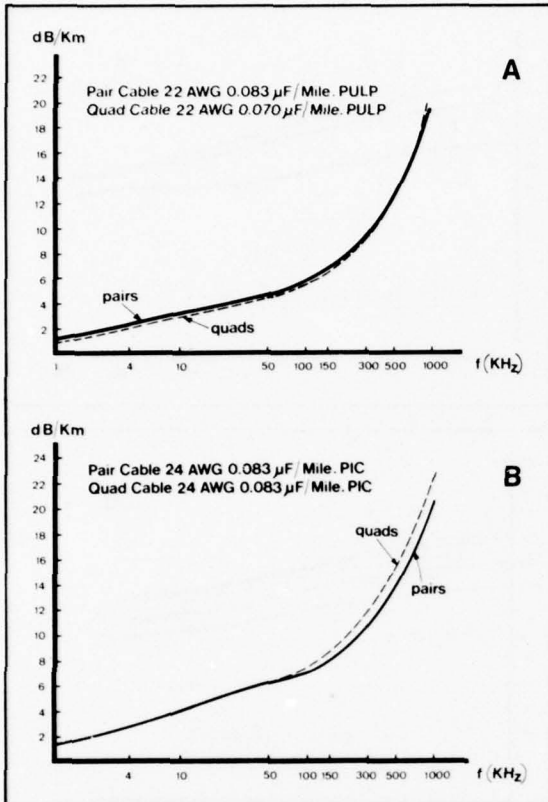


Figure 4
Attenuation of quad and pairs as a function of frequency

The same effect can be seen in Figure 4-B but with two 24 gauge PIC cables of the same nominal capacitance (83 nF/mile). The attenuation was the same on both constructions at low frequencies. At high frequencies the higher resistance in the quad cable (increased by approximately 14% at 1 MHz) also made the attenuation rise, at 1 MHz becoming 1.6db/Km. higher.

Consequently we can say that due to the extra resistance increase the advantage of the quad cable in respect to obtaining less attenuation with the same insulation material is completely lost when it rises above approximately 300 KHz.

This data should be kept in mind when one is to use this cable on high frequency systems.

1.4

Crosstalk

Needless to say we all know that the crosstalk

between pairs in the same quad is quite high. This has led to the practice of nearly always balancing them when installing, by means of systematic reversals. The greater the frequency the closer the reversal should be. Nevertheless this operation is very complex, needs trained personnel and takes up a lot of time and money. Further on in the paper we shall take a closer look.

Crosstalk can be reduced in pair cable if the correct choice of pair twists is made. The crosstalk between pairs in different quads in quad cable can be reduced by the proper choice of twist, but this situation is quite different in the case of the pairs of the same quad.

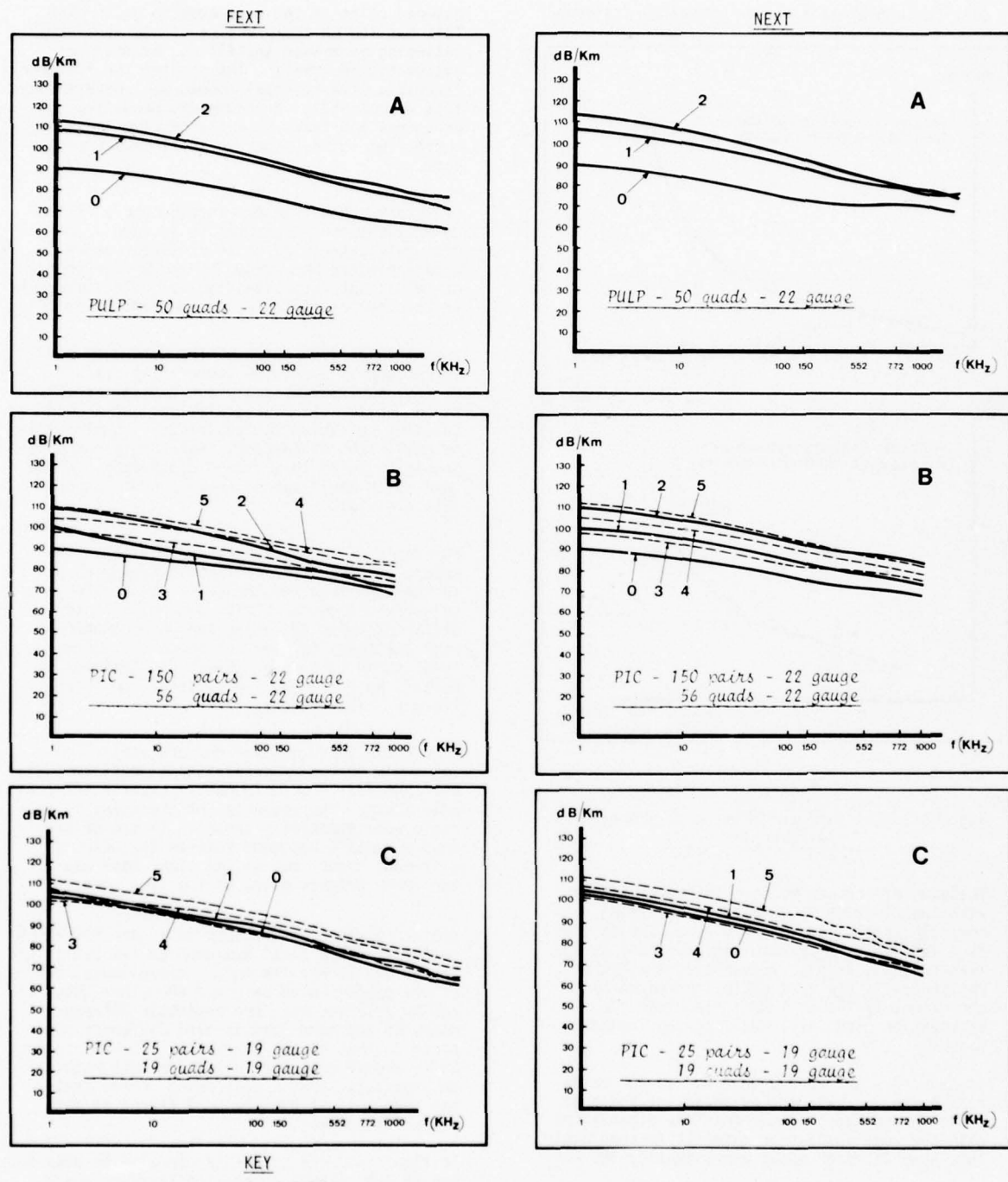
Crosstalk between pairs of the same quad can be reduced by carefully controlling its dimensions. Consequently the coaxial capacitance monitor (in PIC insulation) and a good quadding operation is fundamental. Cabling also originates distortion, therefore great care should be taken in avoiding distortions in the quad which would subsequently produce unbearable crosstalk.

To enable us to analyze the crosstalk in the quad cables we differentiated between the pairs in the same quad and the pairs which belonged to different quads. Tests were made on three different types of cables and were compared with the tests carried out on pairs. The results can be seen in figure 5. To simplify matters we only show the crosstalk on three types of combinations.

Figure 5-A shows the far end crosstalk (Fext) and the near end crosstalk (Next) performed on a 22 AWG and 70 nF/mile mutual capacitance quad pulp cable. The sequence of the quads in this cable were especially chosen. It can be seen that crosstalk was good between the pairs of different quads, but on the other hand was very poor between pairs of the same quad.

Another example can be seen in Figure 5-B which shows "Fext and Next" measured on two cables of 22 AWG and 83 nF/mile mutual capacitance, one of the cables being pair and the other quad. It can be observed that the crosstalk between pairs of the same quad is also different compared to that of the pair cable. In this gauge it is indeed much more effective with regards to crosstalk, that a pair twist scheme that has been well studied be used than a strict dimension control.

In figure 5-C the crosstalk can also be seen in two 19 AWG cables. A great difference which should be mentioned is that the crosstalk between the pairs of the same quad equals more or less the results obtained on pair cable. Crosstalk data is not shown between alternate quads because these quads had like twists and this does not represent normal construction.



KEY

Quad Cable

- 0 - Pairs of the same quad
- 1 - Pairs of adjacent quads
- 2 - Pairs of alternative quads

Pair cable

- 3 - Adjacent pairs
- 4 - Alternative pairs
- 5 - Pairs separated by two

Figure 5
Crosstalk comparison between pairs and quads

This does in fact certify our observations: if we measure the capacitance unbalance on pairs of the same quad having sufficient thickness in gauge (0.8mm. and over) - The results are quite low compared to that of small gauges. The explanation of this phenomenon is that the quad formation with heavy gauges is much better than with small gauges, moreover it is also much more resistant to deformation.

It has been observed, although the measurements were only carried out up to 1 MHz, that the crosstalk on the pairs of the same quad decreases with the frequency more rapidly than in normal pairs, whatever the gauge may be. This is described in references (1) and (2). The maximum frequency of our study as we have already stated is of 1 MHz, consequently we cannot judge the exact rate at which it decreases.

To summarize we can say with the exception of large gauges that the crosstalk in quad cable is higher than in pairs. At high frequencies the crosstalk between pairs of the same quad increases more rapidly than in the normal pairs.

2. COST

As we have already mentioned previously, the quad formation offers a few economical advantages due to the savings in material.

In order to obtain the same mutual capacitance less insulation thickness is needed. Apart from this advantage, less cable diameter is achieved which represents a savings in jacket material.

Nevertheless we should bear in mind the entire manufacturing process which leads to the true savings. With regards to the manufacture the main difference arises in the pairing or quadding process. Figure 6 shows two types of quadding machines while Figure 7 shows a standard pairing machine.

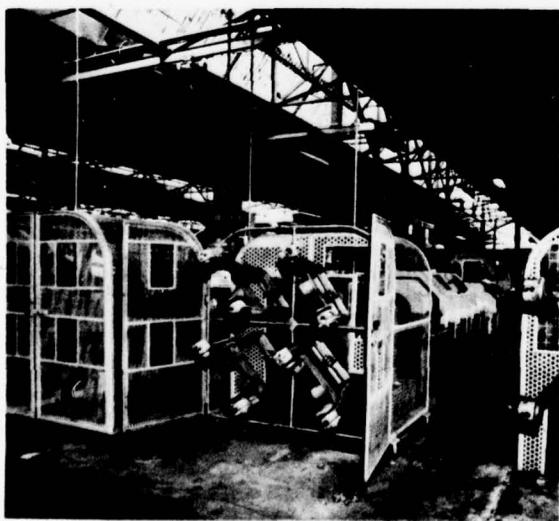


Figure 6A
Conventional quadding machine



Figure 6B
High speed quadding machine

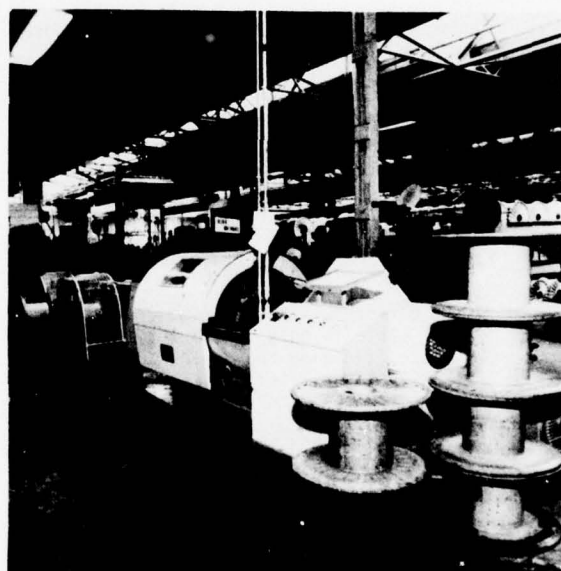


Figure 7
Standard pairing machine

A quadding machine costs more than a pairing machine and its speed is different. Therefore if the quadder is slower this in turn leads to an increase in the labor cost which in turn could completely cancel the savings in material.

The main savings in cost between pairs and quads are the following:

- Insulation material

- Core Wrap

- Jacket materials

We have previously mentioned that with the same mutual capacitance the final core diameter is less in the quad cable by approximately 13-15%.

The final cost depends mainly on the type of jacket required and the size of the cable. The greatest advantage is obtained from the small cables with reinforced jackets.

- Binders

(Additional cost if each quad is bound)

- Labor cost

This greatly depends on the speed of the quadding machine against that of the pairing machine. It could well be a high percentage in the final cost of the cable.

- Power consumption

- Return on investment

We have calculated the approximate cost of three cables in order to examine what has been stated up until now. These cables have been manufactured using two different methods: In the one case with modern quadders at a high speed and in the other case with a conventional quadder which is much slower. The cables which we compared were:

- 100 pair cable 22 AWG 0.083 μ F/Mile - FPA jacket
- 50 quad cable 22 AWG 0.083 μ F/Mile - FPA jacket

This cable will however show a saving in material cost compared to the above cable due to the fact that it has less insulation thickness.

- 50 quad cable 22 AWG 0.070 μ F/Mile - FPA jacket

The difference in cost compared with the pair cable is only due to its manufacture. Due to it having the same insulation thickness the materials are exactly the same with the exception of the binders.

The results can be seen in Table 2.

TABLE 2
COST COMPARISON IN MONETARY UNITS

| | PAIRING | HIGH SPEED QUADDING | LOW SPEED QUADDING |
|-----------------------------|---------|---------------------|--------------------|
| Pairs 0.083 μ F/Mile | 100 | -- | -- |
| Quads 0.083 μ F/Mile | -- | 96 | 104 |
| Quads 0.070 μ F/Mile | -- | 103 | 108 |

In fact it is actually possible to obtain a saving in the quad cable of up to approximately 4%

with the modern machinery now available, and even more if the jacket is complex.

Quadding machines with the same speed as the pairing machines are needed if we are to lower the cost of quad cable. The savings in material with the conventional quadder is completely absorbed by the manufacturing costs.

The inconvenience of high speed quadders is that you cannot work with heavy gauges (19 AWG and over), consequently these quad cables will have a much higher manufacturing cost which will cancel the savings obtained from the materials. Furthermore in these cases the overall cost of the copper in the cable is much higher, therefore the savings in material has less influence upon the total cost.

It is necessary to mention one last point: As there is a need sometimes to balance the quads when splicing cable lengths in order to reduce its unbalance, some customers request the capacitance unbalance to be measured on all the pairs, together with a detailed written instruction on splicing. This is in fact quite easily carried out by means of automatic equipment, but it does take more time which in turn increases the cost of the cable.

3. INSTALLATION AND SPLICING

A very important point in all cable projects is that of the installation. Generally the price of the actual cable is only 40 to 50% (and sometimes less) of the total cost of an installed cable. From the remaining a significant amount is taken up by the placing and splicing.

Labor cost is extremely high, consequently the time a splice takes is of a fundamental importance. For instance if the splice on an installation of large feeder pulp cable is undertaken manually, the labor cost of splicing is greater than the cost of the cable. This information is an example and will orientate those who are not familiarized with the subject, reminding them of how important splicing is.

Naturally the cost of splicing varies depending on the type of jacket, the number of pairs and the installation. On cables with few pairs the cost of splicing is relatively small. On pulp cable with a large number of pairs used for subscriber loops the cost of splicing is very high. In general terms it accounts for between 20 to 45 percent of the total cost of installation.

We should differentiate between two types of splices in quad cable:

1. The first comprises only the connections of the conductor and the jacket splice, as in that of pairs.
2. The second one is performed when it is

necessary to balance the quad. In this case the capacitance unbalance on each end to be spliced should be measured and a written instruction on how to splice should be made which will join the conductors in such a way as to reduce the unbalance.

The telephone company has studied the time required to splice pair cable in comparison with that of quads and this is shown in Table 3. All the cables used were of 19 AWG, paper insulated with lead sheath, a type not manufactured by our company. The conductors were joined manually by twisting.

TABLE 3
AVERAGE TIME NECESSARY TO PERFORM A SPLICE (IN HOURS)

| TYPE OF CABLE | | | | | | |
|--------------------------|-------------|----------|-------|----|----|----|
| | Pairs | | QUADS | | | |
| | No. Balance | Balanced | | | | |
| No. of pairs or quads | 100 | 150 | 50 | 75 | 50 | 75 |
| TIME IN HOURS | | | | | | |
| Aerial Installation | 22 | 25 | 23 | 27 | 51 | 62 |
| Underground Installation | 23 | 26 | 25 | 28 | 53 | 63 |

The above information is sufficient to give us an idea but is of course approximate and therefore will change depending on the number of pairs.

It can be appreciated from this data that a quad splice needs approximately 7% more time than its equivalent in pairs. Part of the explanation is that the solid color code of pairs is easier to identify than that of the color bands normally used in quads.

An added influence is the time it takes to identify the pairs which form the quad. With plastic quads the difference should be smaller as the color code is easier to identify. Nevertheless the color code of pairs is simpler and easier to distinguish. Besides, the most modern splicing techniques have been designed for pair cable, consequently at the moment it is by far the fastest and cheapest method.

Our aim is not however to debate this point. Quads can also be stranded in units and given a color code easier to identify, in this way the modern splicing methods could be applied. Nevertheless the loss of time in the identification of both pairs in the quad will still exist and will without doubt make the splicing operation slightly longer. If the quad should also

have to be balanced, then the time taken up by the splicing is even greater. The above Table does indeed show the time that is necessary to balance a splice which is generally two and a half times greater. The number of pairs to be balanced depends on the type of system to be used. The higher the frequency of transmission the more splices that will have to be balanced. This fact also depends on the length of installation. On long lengths where there is bad crosstalk the splice is balanced, while on short lengths this is not practical.

4. USAGE

We have just shown that the electrical characteristics of pairs are better than that obtained with quads, with this in mind therefore, the only reason for using quads is "Price".

When are quads more economical than pairs? In the first place one should observe the total installation. Generally it should be a compromise between the cable price and the splicing cost. An exact calculation however cannot be made as a detailed study is needed in each individual case. In general practice high frequency systems are being introduced to increase cable capacity and this would be a compelling reason for using pairs.

We have analyzed below the characteristics of both constructions depending on the type of installation.

4.1

Subscriber loops

This type of network joins the control terminal with the subscribers. It generally works with voice frequencies at short distances. The level of crosstalk is very low, consequently the quad does not need to be balanced. Phantom circuits are not generally used and small gauges are employed on this type of installation.

Duct installations are used in urban areas with manholes keeping equal distances. The compromise between the price of the cable and that of the splices should decide the use of either one or the other type.

Figure 8 on the following page shows the comparative cost of this type of installation with a distance of 125 m. (410 feet) between manholes, assuming that the cost of a quad cable is 4 percent less than that of its equal capacitance in pair cable and that the splice of this cable needs 7 percent more time. It is quite clear that there is a small difference in favor of pairs.

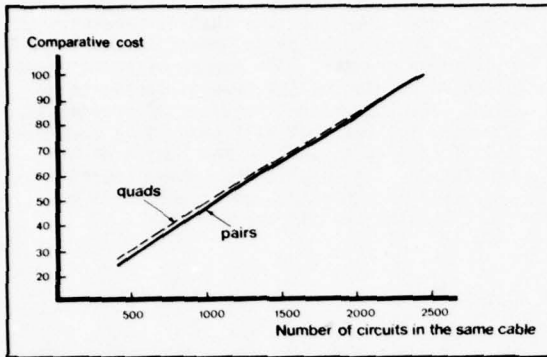


Figure 8
Cost versus cable size (subscriber)

This total cost is mostly based upon the labor cost and the distance between splices. Cables with a large number of circuits are more economical the greater this distance is. Nevertheless this point is rather doubtful where pulo insulated cable is concerned, the reason being that to obtain quads with $0.083 \mu\text{F}/\text{mile}$ means lowering the dielectric strength to an unacceptable level, although there are no such problems where PIC or DEPIC cables are concerned.

Existing ducts could be taken advantage of by the installation of quads, and the increase in cost of the splice would be compensated for by the number of circuits, therefore lowering quite considerably the cost per circuit.

In the case of large gauges (19 AWG and over) the choice of pairs is quite clear as there is no possible savings with quads.

4.2

Interoffice trunks

This type of link is used between central terminals either in voice or carrier frequencies.

Pair cable is the most economical when gauges of 19 AWG and over are to be used. There is now nevertheless a general tendency experienced everywhere towards the use of electronic equipment, abandoning in this way large gauges.

The convenience of using voice frequencies depends entirely on the length. As there is no subscriber service the distance between splices can be greater.

Figure 9 shows the comparative cost in these cases with a distance in length of 460 m. (1513 feet) between splices. In this case quads could be more economical if they are not balanced, however they should be balanced if they are to be used for long distances.

It can be seen that curves A and B remain approximately parallel regardless of cable size.

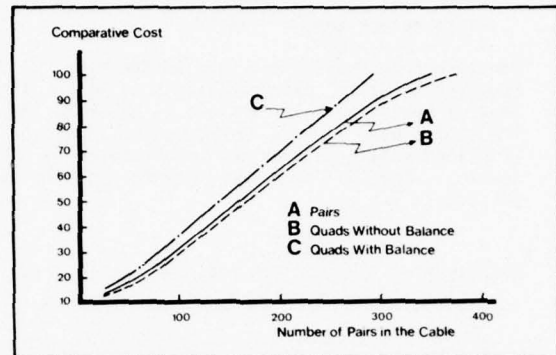


Figure 9
Cost versus cable size (Trunks)

The use of phantom circuits is the most economical system, even if they have to be balanced, as in this way you have 50% more circuits in the same cable. However this practice has become quite obsolete with the use of carrier frequency.

Two points already mentioned should be kept in mind when one is to use carrier frequency:

- Attenuation for quads is slightly higher than for pairs of the same capacitance.
- Crosstalk is worse between the pairs of the same quad.

Quads could evidently be more economical than pairs if we were to use for instance systems of up to 12 channels (108 KHz) and not all the pairs in the cable were used for high frequency.

Quads do not seem to be advisable if one is to use all the pairs and a higher frequency system. This is also the case for PCM systems where high frequency (772 KHz for T1 and 1024 KHz for 30 channel PCM) is used. It is very difficult to use all the pairs in the cable on a PCM system when a quad cable is employed.

4.3

Toll Trunks

These are links with great capacity and number of channels. Coaxials are used on heavily used routes. Symmetric pairs are used with the carrier or PCM system, therefore quads are not the most suitable for this type.

CONCLUSION

Our intention in this paper has been to try to highlight the characteristics of pairs and quads, together with their advantages and disadvantages. Pairs with regards to splicing do have advantages over quads and they are indeed electrically better. From an economical viewpoint quads have the advantage if large gauges are not used, but they do present higher crosstalk and attenuation at high frequencies.

Quads are therefore economically more attractive on low frequency circuits when:

- Many circuits are needed in a certain diameter and the crosstalk is low
- Phantom circuits are used

At high frequencies quads do not show advantages with regards to pairs, except maybe when a limited capacity is needed. Due to the high frequency of PCM the pairs are much better.

ACKNOWLEDGEMENT

I would like to especially express my gratitude to Mr. F.W. Horn for his kind comments and text corrections. I would also like to thank C.T.N.E.'s C.I.E. (Centro de Investigación y Estudio) for their kind help. Acknowledgment is also due to the people who have carried out the tests especially Mr.J.C.Romay, who has shown great enthusiasm.

REFERENCES

1. Multipair cables for broadband transmission
By: Hiroshi Kaiden and Shoro Inao - 17th
I.W.C.S. 1968
2. Cables & Transmission - Transmission Numeriques
December 1975.
3. Symmetric Telephone Cable either for loading
without balancing or for PCM-transmission.
By: D.J. Dekker, H.G. Dageforde and P. Zamsow
22nd I.W.C.S. 1973.
4. Third volume of the green C.C.I.T.T. recommendation book.
5. Instrucción de Ingeniería No. 330.001 de C.T.N.E.



Valentin Abadia graduated from the Superior Telecommunication Engineering School (E.T.S.I.T.) in Madrid in 1974, obtaining a degree in telecommunication engineering. He joined Cables de Comunicaciones's Research Department in Zaragoza, Spain soon after, where he is now responsible for improving the electrical characteristics of all communication cables and proving in new test equipment and procedures.

ON THE COMPUTATION OF PRIMARY PARAMETERS OF CIRCUITS
IN TWISTED MULTIWIRE CABLES

V. Belevitch

MBLE Res. Lab., 2, av. Van Becelaere, 1170 Brussels, Belgium

G. C. Groenendaal

Philips Res. Labs, Eindhoven, Netherlands

R. R. Wilson

NKF Kabel BV, 26 Delft, Netherlands

Summary

Several papers (published or in course of publication) by the authors are devoted to the computation of the primary parameters of circuits in multiwire cables. Two papers^{1,2} deal with the proximity effect in uniform cables and are based on Carson's³ quasi-stationary approach. In the meantime essentially equivalent equations have been derived by Lenahan⁴ on the basis of Kuznetsov's theory⁵. Kuznetsov's claim that his theory is more rigorous than Carson's is refuted here. For the effect of twisting on the self-capacitance of a circuit, the basic results of Martin⁶ have been corrected by us⁷ and extended to the mutual capacitance⁸, thus altering substantially the accepted theory of capacitive cross-talk. The foundation of our theory is discussed and our main results are summarized.

Introduction

Because the pairs or quads forming a multiwire cable are generally twisted, a rigorous derivation of the propagation parameters from Maxwell's equations is hopeless. In engineering practice, the secondary (propagation) parameters are thus deduced from the primary (R, L, C, G per unit-length) parameters by elementary line theory (generalized telegraph equations) and only the primary parameters are computed by field theory, using the transverse, quasi-stationary approximation. These approximations are justified because of the relative orders of magnitude of the main geometric parameters of the problem : a typical transverse dimension d (wire diameter, distance between wires of a pair) is of the order of 1 mm, the twisting pitches h range from 5 cm to 1 m so that one has

$$h \gg d \quad (1)$$

whereas the shortest wave-length λ to be transmitted satisfies

$$\lambda \gg h \quad (2)$$

else the useful consequences of the twisting (cage effect on the electric field and averaging of the magnetic coupling) disappear, and the crosstalk is so large that the cable cannot be used.

From (1) and (2) one deduces

$$\lambda \gg d \quad (3)$$

For perfect parallel conductors in a homogeneous dielectric, condition (3) only allows to propagation of TEM waves, and the transverse field is independent of z (direction of propagation). This is the only case where the telegraph equations can be rigorously deduced from Maxwell's equations; moreover the resulting inductance (L) and inverse capacitance ($K = C^{-1}$) matrices per unit-length are related by

$$L/\mu = \epsilon K \quad (4)$$

For imperfect conductors a pure TEM wave is impossible because the currents in the wires generate longitudinal electric fields; this means that the TEM mode is coupled to other modes. Owing to (3), the attenuation per unit-length of the higher modes is, however, enormous (of the order of $1/d$) whereas, for good conductors, the attenuation and phase-shift of the TEM mode over a distance of the order of d is negligible, else the cable would again be useless. Consequently the small coupling per unit-length between the TEM mode and the other modes can be computed as if the TEM field was not propagating, so that the transversal penetration problem is almost separated from the longitudinal propagation. This is the essence of Carson's quasi-stationary theory, and of the equivalent Kuznetsov's theory discussed in the Appendix. The transversal problem is solved from Maxwell's equations with the quasi-stationary approximation (the magnetic field produced by the displacement current is neglected everywhere) and is only used to compute the impedance matrix Z per unit-length. The telegraph equations based on that Z and on the electrostatic capacitance matrix C hold as an excellent approximation, and the propagation parameters are derived by elementary line theory. Moreover, with $Z = R + j\omega L$, the asymptotic value L_∞ of L at high-frequency is still related to

$$L_\infty/\mu = \epsilon K \quad (5)$$

similar to (4).

Carson's theory, as summarized above, was only established for good parallel conductors in a homogeneous dielectric. For a heterogeneous dielectric, nothing is changed as regards the computation of Z since the quasi-stationary equations do not involve ϵ at all. As regards the computation of K , it is now a separate electrostatic problem, so that (5) no longer holds in the heterogeneous case.

So far we have only discussed parallel wires. Qualitatively, the effects of the twisting are most clearly understood if one considers one energized straight pair of parallel wires around which a second idle pair (twisted or not on itself) is helically wound. The magnetic field is established by the currents in the energized pair and is hardly affected by the eddy currents in the idle wires, if the latter are thin, since the reaction magnetic field has only a multipolar nature. By contrast, if one considers the electrostatic field established by the central pair as if it existed alone, it is obvious that the wires of the second spiralling pair occupy places of different potentials along the z -axis in that field, whereas they should be equipotential. Equipotentiality can

only be restored if the total zero charges on the idle wires separate longitudinally into positive and negative charges per unit length according to the position of the idle wires in the field of the energized pair. This phenomenon of longitudinal charge separation alters considerably the original electrostatic field, because the reaction field is now caused by true charges and not by multipoles as in the magnetic reaction.

The above remarks hold for a general multiwire cable. The modification of the electric field by the twisting is important because all adjacent pairs from a Faraday cage around any given pair. The cage, being equipotential, gets charged by longitudinal separation, and this increases the capacitance per unit length of every pair by some 10 to 15 %. By contrast, the magnetic field is hardly modified by the cage, so that the inductance per unit length is almost unaffected by the twisting. These remarks hold for the primary parameters of a single circuit, but the effects of the twisting on the mutual inductances and capacitances, which affect cross-talk, must also be estimated. Here again, there is a considerable difference between the electric and magnetic effects of the twisting. Since the cage is an almost perfect electrostatic screen, except for some (multiply) periodic field patterns (along z) of periodicities related to the twisting pitches and thus capable of leaking through the cage, the capacitive cross-talk between non-adjacent circuits is destroyed in general, i.e. except for some critical pitch combinations. By contrast, the twisting almost cancels the inductive cross-talk by an averaging process along the z-axis, except again for some critical pitch combinations where the averaging is replaced by a systematic increase proportional to z. Since, however, the averaging process is different from the cage effect, the dangerous pitch combinations for inductive and capacitive cross-talk may be different or unequally critical.

For a single twisted pair in free space, a spiral field theory has been developed and applied to the computation of the inductive cross-talk. This theory will not be discussed here because it is hardly susceptible of further generalization and does not handle the cage effect which is much more important. In fact, the older cross-talk theories were based on the transverse field approximation where the field of an energized pair in a given cross-section is computed as if the geometry of that section extended to all z, the resulting fields being then rotated in accordance with the twisting of the energized pair. In such a theory, the values of the elements of the Z and K matrices are taken from the theory of parallel wires with the local values of the geometric parameters and thus become (multiply) periodic functions of z because the mutual distances between individual wires vary with the twisting. The matrix relation between the charges Q per unit length and the voltage V is

$$V = K Q \quad (6)$$

and the charges on the idle wires are zero in a system of parallel wires. By contrast, for twisted wires, the cage effect produces zero voltages on the idle wires, and non-zero charges are generated by longitudinal separation; consequently the inversion of the linear system (6) yields different values for the self- and mutual capacitances in the two cases. The above approach was followed by Martin⁶ in a paper which seems to have been largely ignored. Martin's

computation, limited to the effect of twisting on the self-capacitance, has been improved by us⁷; moreover, we extended the theory to the computation of the mutual capacitance⁸.

Parallel wires

The Z-matrix is deduced from the relations between the voltage drops per unit length and the currents in the wires. These relations are given in sec. 2 of our paper² and are reproduced here with a minor change of notation making dimensionless the arguments of all logarithms. As stated in our first paper¹ (there is some confusion in this respect in Lenahan⁴) we use j for the imaginary unit in jw but i for the 90° rotation in the complex plane of the cable cross-section; the notations^{1,3} and Re denote the conjugate and the real part with respect to i.

We consider a number N of parallel wires and call a_s and σ_s the radius and conductivity of wire s. The screen is a cylinder of internal (external) radius $a_0(b)$ and has conductivity σ_0 . The complex distance from centre of wire s to centre of wire t is called D_{st} and this also applies to the screen for $s = 0$. We assume a uniform permeability μ throughout. We define the following notations

$$d_{st} = \frac{D_{st}}{D_{os}} ; \quad d_s = \frac{D_{os}}{a_0} \quad (7)$$

$$k_s^2 = -jw\mu\sigma_s \quad (8)$$

$$\lambda_{ns} = -\frac{n J_{n-1}(k_s a_s)}{J_{n+1}(k_s a_s)} \quad (9)$$

$$w_p = \frac{J_{p-1}(k_o a_o) Y_{p-1}(k_o b) - J_{p-1}(k_o b) Y_{p-1}(k_o a_o)}{J_{p-1}(k_o b) Y_{p+1}(k_o a_o) - J_{p+1}(k_o a_o) Y_{p-1}(k_o b)} \quad (10)$$

$$F_{nm}(u) = n \sum_{r=0}^{\infty} w_{m+r} \frac{(m+r-1)}{(m-1)} \left(\frac{m+r}{n} u \right)^{m+r} \quad (11)$$

$$f_m(u) = \sum_{r=0}^{\infty} w_{m+r} \frac{(m+r-1)}{(m-1)} u^{m+r} \quad (12)$$

$$T_{nm} = \frac{(m+n-1)!}{(n-1)!(m-1)!} \quad (13)$$

If I_s is the total current in wire s and hence $I_0 = - \sum_{s=1}^N I_s$ the current in the screen, the corresponding voltage drops per unit length are

$$U_0 = -\frac{jw\mu}{2\pi} \sum_{s=1}^N I_s \left[\ln \frac{a_0}{a_s} + \frac{1}{k_o a_s} \frac{J_0(k_o a_s) Y_1(k_o b) - J_1(k_o b) Y_0(k_o a_s)}{J_1(k_o a_s) Y_1(k_o b) - J_1(k_o b) Y_1(k_o a_s)} \right] \quad (14)$$

$$U_s = -\frac{j\omega u}{2\pi} \operatorname{Re} \left(\frac{I_s J_0(k_s a_s)}{k_s a_s J_1(k_s a_s)} \right) + \sum_{t=1}^N I_t \ln \left| \frac{D_{st}}{a_t} \right| + \sum_{q=1}^N I_q \sum_{p=1}^{\infty} \frac{w_p}{p} (d_s d_q^*)^p + \sum_{t \neq s}^{\infty} \left[\sum_{n=1}^N \frac{A_{nt}^*}{d_{ts}^n} - \sum_{q=1}^N A_{nq} f_n(d_s d_q^*) \right] \quad (s=1,2,\dots,N) \quad (15)$$

In the last equation, the coefficients A_{nt} are the solutions of the infinite linear system

$$\sum_{m=1}^{\infty} \left[\sum_{t=1}^N \frac{A_{mt} T_{nm}}{d_{ts}^m d_{st}^n} - \sum_{q=1}^N A_{mq} F_{nm}(d_s d_q^*) \right] + \lambda_{ns} A_{ns} | \frac{D_{os}}{a_s} |^{2n} = \sum_{t=1}^N \frac{I_t}{d_{st}^n} - \sum_{q=1}^N I_q f_n(d_s d_q^*) \quad (s=1,2,\dots,N; n=1,2,\dots,\infty) \quad (16)$$

together with the conjugate system.

We now assume that each wire of radius a_s (except the screen) is surrounded by an insulation of radius b_s and dielectric constant ϵ_s , whereas the rest of the dielectric has the constant ϵ_0 . The K-matrix is deduced from the relations between the wire voltages V_s and the charges Q_s per unit length. The notations are the same as above except that (9) and (11) are replaced by

$$\lambda_{ns} = n \frac{\frac{\epsilon_s - \epsilon_0}{\epsilon_s + \epsilon_0} (\frac{a_s}{b_s})^{2n}}{1 + \frac{\epsilon_s - \epsilon_0}{\epsilon_s + \epsilon_0} (\frac{b_s}{a_s})^2} \quad (17)$$

$$F_{nm}(u) = nm \sum_{r=0}^{\min(n,m)} \frac{(m+n-r-1)!}{(n-r)!(m-r)!r!} \frac{u}{1-u}^{m+n-r} \quad (18)$$

The relations are

$$V_o = -\frac{1}{2\pi\epsilon_0} \sum_{s=1}^N Q_s \ln \frac{a_s}{a_s} \quad (19)$$

$$V_s = \frac{Q_s}{2\pi} \left(\frac{1}{\epsilon_s} - \frac{1}{\epsilon_0} \right) \ln \frac{b_s}{a_s} - \frac{1}{2\pi\epsilon_0} \left(\sum_{t=1}^N Q_t \ln \left| \frac{D_{st}}{a_t} \right| - \sum_{q=1}^N Q_q \ln \left(1 - \frac{d_s d_q^*}{a_s} \right) + \operatorname{Re} \sum_{n=1}^{\infty} \left[\sum_{t=1}^N \frac{A_{nt}^*}{d_{ts}^n} - \sum_{q=1}^N A_{nq} \left(\frac{d_s d_q^*}{a_s} \right)^n \right] \right) \quad (s=1,\dots,N) \quad (20)$$

In the last equation, the coefficients A_{nt} are the solutions of the infinite system

$$\sum_{m=1}^{\infty} \left[\sum_{t=1}^N \frac{A_{mt}^* T_{nm}}{d_{ts}^m d_{st}^n} - \sum_{q=1}^N A_{mq} F_{nm}(d_s d_q^*) + \lambda_{ns} A_{ns} \left| \frac{D_{os}}{a_s} \right|^{2n} \right] = \sum_{t=1}^N \frac{Q_t}{d_{st}^n} - \sum_{q=1}^N Q_q \left(\frac{d_s d_q^*}{a_s} \right)^n \quad (s=1,2,\dots,N; n=1,2,\dots,\infty) \quad (21)$$

and of its conjugate.

The above results have not been established in our papers but are almost a particular case of the relations (14-16) when the latter are written for perfect conductors and transposed from L to K. In particular, one then has $w_p = 1$ in (10), and (11) reduces to (18); similarly (12), and the other sums in w_p appearing in (15-16) have simple closed form expressions. Finally, the replacement of (9) by (17) results from the replacement of the skin-effect equation in the metal by the Laplace equation in the annular insulation of constant ϵ_s .

In our two papers¹² we have specialized the equations (14-16) for various modes (side, phantom, asymmetric) in a screened pair or quad and have derived series expansions for the solutions in terms of various parameters. It is impossible to summarize here all our contributions and we only comment on one important point.

At high frequency, the skin-effect limits the current to a thin layer on the surface of the conductors, and the asymptotic value of the impedance can be computed by surface impedance considerations. The first order effect on the impedance can then be deduced from the derivative of the h.f. inductance with respect to the radius. This, so-called incremental inductance rule, was discovered by Wheeler⁹ and established more rigorously by Alessandrini¹⁰. We have shown that, if the rule is modified so as to allow a complex increment of the wire radius, its validity extends to second order effects. Finally, a similar rule (first order only) holds for the effect of a thin insulation with $\epsilon_s \neq \epsilon_0$: it is sufficient to consider the dielectric as homogeneous with the value ϵ_0 and adopt for the wires the fictitious radii

$$a'_s = \frac{\epsilon_0}{\epsilon_s} a_s + (1 - \frac{\epsilon_0}{\epsilon_s}) b_s \quad (22)$$

This rule immediately results from the first-order approximation of (17) for $b_s \approx a_s$, which yields $\lambda_{ns} / a_s^{2n} \approx n/a_s^{2n}$ in (21).

Twisted wires

For the estimation of the cage-effect on the self capacitance of a twisted circuit, it is essential to take into account at least all adjacent circuits. For a compact quad cable, these are the six quads surrounding any quad. The total of seven quads contains 28 wires, hence 27 independent circuits. It is convenient to take as circuits the 14 side circuits (2 per quad), the 7 phantom circuits (1 per quad) and the 6 super-phantoms formed by the 6 peripheral quads with the central quad. An analytic solution of the corresponding linear system (6) is out of question, even for thin wires, but a series expansion in the parameter

$$s = b/D \quad (23)$$

($2b$ = distance between opposite wires in a quad; D = distance between centres of adjacent quads) up to terms in s^4 has been obtained. At that order, the effects of the phantoms are negligible, whereas the matrices corresponding to the side- and superphantom circuits are circulant and can be inverted analytically. For a side-circuit in a homogeneous dielectric, and assuming that all wires are thin, i.e. for

$$w = a/b \ll 1 \quad (24)$$

(a = wire radius), the result is

$$C = \frac{2\pi\epsilon_0}{g_S - \frac{12s^2}{g_A} - \frac{96s^4}{g_S} \left(1 - \frac{3}{2g_A} + \frac{17}{8g_A^2}\right)} \quad (25)$$

where

$$g_S = 2 \ln \frac{2}{w}; \quad g_A = \ln \frac{6^{1/2}}{sw^{1/4}} \quad (26)$$

The expression (25) gives the cage-correction to the formula $C = 2\pi\epsilon_0/g_S$ valid for parallel wires. In Martin's paper, the factor between parentheses in the denominator of (25) is erroneously replaced by 1. Additional corrections to (25) in powers of w , for thick wires, are also given in our paper.

As regards the effect of the twisting on the mutual capacitance, we have only treated the simplest case of two pairs at constant relative distance D . If one denotes by $\beta(\gamma)$ the angle between the line joining the centres of the wires of the first (second pair) with respect to the line joining the centres of the pairs, our result to order s^2 is

$$C_{12} = \frac{8\pi\epsilon_0 s^2}{g_S^2} \left[\left(1 - \frac{1}{2g_F}\right) \cos(\gamma + \beta) - \frac{1}{2g_F} \cos(\gamma - \beta) \right] \quad (27)$$

where g_S is still (25) and where

$$g_F = \ln \frac{1}{2ws^2} \quad (28)$$

The terms in $1/2g_F$ of (27) are the corrections due to the twisting. In particular, the term in $\cos(\gamma - \beta)$ produces additional critical pitch combinations with respect to the theory of capacitive crosstalk in parallel wires.

Appendix

In Kuznetsov's book⁵ (pp. 6-7) it is shown that under certain approximations the transverse field is the gradient of a scalar function satisfying the two-dimensional Laplace equation and taking constant values on the wire boundaries. In terms of the scalar (ϕ) and vector (A) potentials, one has

$$E_{tr} = -\text{grad}_{tr} \phi - j\omega A_{tr} \quad (A1)$$

and it is claimed that A_{tr} is far from being equal to zero so that ϕ is not constant on the wire boundaries. Since in Carson theory, one has $A_{tr} = 0$ and $\phi = C^t$ on the wire boundaries, Kuznetsov's theory is apparently more general.

But the potentials are only defined within an arbitrary gauge-invariant transformation : the new potentials

$$\phi' = \phi + \theta$$

$$A'_z = A_z$$

$$A'_{tr} = A_{tr} - \frac{1}{j\omega} \text{grad}_{tr} \theta \quad (A2)$$

where θ is an arbitrary harmonic function, leave all fields invariant. Since E_{tr} is a gradient in Kuznetsov's theory, so is A_{tr} by difference in (A1). One thus can choose θ in (A2) so as to make $A'_{tr} = 0$. In conclusion, Kuznetsov's theory is absolutely equivalent to Carson's theory as regards all results and only adds unnecessary complications obscuring the essential issues.

References

1. V. Belevitch, Theory of the proximity effect in multiwire cables, Philips Res.Repts., vol. 32, pp. 16-43 and 77-148; Jan. and Apr. 1977.
2. G. C. Groenendaal, R. R. Wilson and V. Belevitch, Calculation of the proximity effect in a screened pair or quad, Philips Res.Repts., vol. 32, to appear, 1977.
3. J. R. Carson, The rigorous and approximate theories of electrical transmission along wires, B.S.T.J., vol. 7, pp. 11-25; Jan. 1928.
4. T. A. Lenahan, The theory of uniform cables, B.S.T.J., vol. 56, pp. 597-625; Apr. 1977.
5. P. I. Kuznetsov and R. L. Stratovich, The propagation of electromagnetic waves in multiconductor transmission lines, New York : Pergamon Press, 1964, Chap. 1.
6. H. E. Martin, Die Berechnung der Übertragungseigenschaften symmetrischer Leitungen unter Berücksichtigung der Verdrallungseffektes, Arch. Elektr.Übertr., vol. 18, pp. 293-308; 1964.
7. V. Belevitch, R. R. Wilson and G. C. Groenendaal, The capacitance of circuits in a cable with twisted quads, Philips Res.Repts., vol. 32, pp. Aug. 1977.
8. V. Belevitch, On the theory of cross-talk between twisted pairs, Philips Res.Repts., vol. 32, to appear, 1977.
9. H. A. Wheeler, Formulas for the skin-effect, Proc. IRE, 30, pp. 412-424; Sept. 1942.
10. V. Alessandrini et al., The skin effect in multiconductor systems, Int.J.Electron., vol. 40, 1, pp. 57-63 1976.

Authors



Vitold Belevitch was born in Helsinki (Finland) on 2 March 1921. His degrees are electr.-mech. engineer Louvain (Belgium) 1942, Dr Sc. Louvain 1945, fellow IRE 1961, Dr honoris causa Munich 1975. He worked from 1942 to 1953 at Bell Telephone (Antwerp). He was lecturer (since 1952), then professor (1960) at Louvain Univ. Since 1963 he is director of MBLÉ Res. Lab. Brussels. He has written three books on circuit theory and numerous articles in various fields of applied mathematics.



René R. Wilson received his electrical engineering degree from Delft University of Technology, The Netherlands, in 1951. From 1951 to 1961, he was with Draka Kabel, Amsterdam. From 1961 to 1971 he was head of the Telecommunication Laboratory of NKF Kabel, Delft, The Netherlands. He is currently engaged in research and development activities on telecommunication cables at NKF Kabel. He is a member of the Royal Netherlands Institute of Engineers.



Gradus C. Groenendaal was born in Est, The Netherlands, on March 14, 1943. He received the degree in electrical engineering from Eindhoven University of Technology, in 1968. From 1968 to 1970 he served with the Royal Netherlands Air Force. In 1970 he joined the Philips Research Laboratories, Eindhoven, The Netherlands, where he is engaged in research on systems for broadband transmission via cables including related electromagnetic field problems and computer-aided-design tools. He is a member of IEEE and of the Netherlands Electronics and Radio Society.

PARAMETRIC DESIGN OF FLEXIBLE COAXIAL CABLES BASED ON A NEW MULTIWIRE IMPEDANCE THEORY

Dr. techn. Gerhard H. Nowak

ITT Cable-Hydrospace
San Diego, California

Abstract

Conductive surfaces within communication lines for electromagnetic broadband signal propagation are commonly made of properly arranged wire arrays. This paper presents an electromagnetic field perturbation theory for multiwire arrays and cylindrical shields. Fundamental equations resulting from this theory lend themselves to the exact impedance evaluation of practical wire array configurations frequently employed in flexible communication lines. Implementing these results into the transmission line theory yields all characteristic propagation parameters necessary for the parametric design of practical flexible transmission lines.

Introduction

Nowadays, underwater cable applications necessitate electromagnetic cables with extensive intrinsic flexing capabilities. Consequently, flexible mechanical design configurations of electrical conductor elements incorporated within such cables becomes mandatory. Performance optimization of electromagnetic signal propagation is one of the main topics in design of modern electromechanical cables. In support of a meaningful design effort, the need for accurate design tools becomes evident. Conventional mathematical formulations derived from simplified model assumptions often prove to be unsatisfactory in predicting signal propagation performance along flexible conductor lines.

This paper shows how prediction of electromagnetic signal propagation along flexible conductors can be improved considerably by introducing more realistic model concepts. In order to demonstrate the method of approach, only circular coaxial line configurations are considered. However, the method described in this paper lends itself to the treatment of more complex transmission line configurations, such as shielded twisted pair problems or conductive tape arrangements over served outer conductors.

Related to EM cable application, frequencies are confined to the range less than 200 MHz which implies negligibly small displacement currents and wavelengths many times larger than the transmission line diameter. Since small signal attenuation per wavelength typifies communication lines in general, spatial field rate in the axial direction becomes many orders of magnitudes smaller than spatial field rates in transversal directions. These intrinsic system restraints qualify to assume quasi-stationary electrodynamic field conditions.

Classical electrodynamics explains self-consistent transport phenomena of electromechanical signal energy through dielectric media enclosed by coaxial conductors. The existence of time-varying field distributions of electrical field strength, \mathbf{E} , in conjunction with magnetic field intensity, \mathbf{H} , are the underlying reasons in supporting this phenomenon.

A complete mathematical representation of electromagnetic phenomena is obtained by means of Maxwell's field equations. Investigation of Maxwell's equations for *rotational* symmetric field configurations shows that two independently excitable field modes may exist which are known as the TM and TE modes. In reality, only the TM mode field propagates along the conductive surfaces with a relatively low attenuation. Any excited TE mode field energy dissipates within a very short distance from its point of excitation. This field type is associated with local eddy currents generated within the solid conductors.

For nonrotational symmetric field configuration, TE and TM modes cannot exist independently from each other. Propagation of a TM mode signal along nonrotational symmetric cylindrical conductors causes increased signal power loss due to power dissipation by some eddy currents associated with the concurrent TE mode field. To a certain extent, this effect takes place within helically formed wire elements. TM mode power dissipation occurring within nonrotational symmetric field configurations is affected by certain current density distributions in direction of the wire axis. However, the increase in power dissipation related to the TM mode field structure is usually much larger than the accompanying TE mode power loss rate. Thus, electromagnetic field propagation along flexible (nonrotational symmetric) coaxial lines is basically of TM mode nature.

Solid Conductor Coaxial Lines

Coaxial communication lines with solid circular cylindrical conducting surfaces maintain electromagnetic fields of TM mode only. Electrical and magnetic field distributions are sufficiently defined by Maxwell's equations. In axis-centered polar coordinates (r, ϕ, z), Maxwell's equations for TM mode field configurations are as follows:

$$-\frac{\partial H_\phi}{\partial z} = \epsilon_0 \epsilon \frac{\partial E_r}{\partial t} + \sigma E_r \quad (1)$$

$$\frac{1}{r} \frac{\partial(rH_\phi)}{\partial r} = \epsilon_0 \epsilon \frac{\partial E_z}{\partial t} + \sigma E_z \quad (2)$$

$$\frac{\partial E_r}{\partial z} - \frac{\partial E_z}{\partial r} = -\mu_0 \mu \frac{\partial H_\phi}{\partial t} \quad (3)$$

$$\frac{1}{r} \frac{\partial}{\partial r} (rE_r) + \frac{\partial E_z}{\partial z} = 0 \quad (4)$$

Herein are: ϵ the dielectric constant, μ the magnetic permeability, and σ the electrical conductivity of the medium.

In obtaining electrical and magnetic field distributions (E_r, E_z , and H_ϕ), solutions derived from the system of equations must be specialized for the electrically conductive regions as well as for the dielectric region. The method of

integration in obtaining solutions can be accomplished in two ways:

Phenomenological Approach. By introducing distributed network parameters resulting in solutions amenable to direct electrical measurement techniques.

Analytical Approach. By analytical methods in satisfying electrodynamic boundary conditions.

Phenomenological Solutions (Kelvin's Method)

The electromagnetic properties of the conductors as well as the dielectric medium are sufficiently described by introducing distributed network parameters R , L , C , and G (Figure 1). Electromagnetic field quantities are directly related to transversal line voltage V and longitudinal line current I . By virtue of this field equivalent line representation, the above system of Maxwell's equations reduces to the system:

$$-\frac{\partial V}{\partial z} = RI + L \frac{\partial I}{\partial t}, \quad (5)$$

$$-\frac{\partial I}{\partial z} = GV + C \frac{\partial V}{\partial t}. \quad (6)$$

Parameter R combines the distributed resistances of the inner and outer conductors:

$$R = R_1 + R_2 \text{ (ohms/m)}. \quad (7)$$

Similarly, parameter L combines the distributed inductivities of the inner and outer conductors as well as the so-called space inductivity L_o :

$$L = L_1 + L_2 + \frac{\mu_0 \mu^{(2)}}{2\pi} \ln \frac{r_2}{r_1} \text{ (H/m)}. \quad (8)$$

The capacity between inner and outer conductor per unit line length follows from:

$$C = \frac{2\pi\epsilon_0 \epsilon^{(2)}}{\ln \frac{r_2}{r_1}} \text{ (F/m)}. \quad (9)$$

In the same fashion, the dielectric shunting admittance is represented by:

$$G = \frac{2\pi\sigma^{(2)}}{\ln \frac{r_2}{r_1}} \text{ (S/m)}. \quad (10)$$

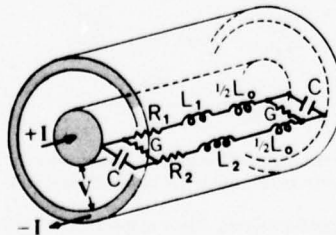


Figure 1. Distributed Network Parameters

Considering periodic signal propagation along an infinitely long line, solution of Equations (5) and (6) render the following relationships for voltage and current distribution along the line:

$$V(z, t) = V_o e^{-\gamma z + \omega t}, \quad (11)$$

$$I(z, t) = I_o e^{-\gamma z + \omega t}. \quad (12)$$

Herein is $\omega = 2\pi f$ the circular signal frequency and γ the propagation constant of the line which is obtained from the relationship:

$$\gamma = \sqrt{PQ}, \quad (13)$$

where

$$P = R + i\omega L, \quad (14)$$

$$Q = G + i\omega C. \quad (15)$$

Signal response along an infinitely long transmission line and a finite length line becomes identical if the characteristic impedance

$$Z_o = \sqrt{\frac{P}{Q}}, \quad (16)$$

is matched by the far end output impedance.

Both parameters γ and Z_o characterize the transmission line completely since they enter theory as two independent parameters of the general solution of the system (5) and (6). However, no explicit evaluation of either parameter can be performed since no explicit representation of P exists. This relates to the fact that R_1 , R_2 , L_1 , and L_2 cannot be obtained explicitly within the scope of the phenomenological approach.

Analytical Solutions

Solutions of the set of Equations (1) through (4) can also be obtained by direct methods of analysis. It is required that general field solutions satisfy certain boundary conditions established to match field discontinuities along interfaces between conductors and dielectric media. In doing so, a system of linear homogeneous equations for the constants of integrations remains to be solved. By enforcing the associated system determinant to become zero, an eigenvalue h is obtained which directly corresponds to parameter γ such that

$$\gamma = ih. \quad (17)$$

The value of h can be evaluated in terms of configuration parameters specifying the coaxial line. From field equations the characteristic impedance Z_o can be derived, again explicitly related to coax configuration parameters. Through the relationship

$$P = \gamma Z_o \quad (18)$$

it follows that

$$P_1 = R_1 + i\omega L_1 = \frac{k^{(1)}}{2\pi\sigma^{(1)}} \frac{J_0(k^{(1)}r_1)}{J_1(k^{(1)}r_1)}, \quad (19)$$

$$P_2 = R_2 + i\omega L_2 = \frac{-k^{(3)}}{2\pi\sigma^{(3)}} \frac{H_0^{(1)}(k^{(3)}r_2)}{H_1^{(1)}(k^{(3)}r_2)} W(r_2, r_3). \quad (20)$$

Herein define $J_0(x)$ and $J_1(x)$ Bessel functions of the zero and first order. Furthermore, it means that $H_0^{(1)}(x)$ and $H_1^{(1)}(x)$ represent first kind Hankel functions of zero and first order. Parameter $k^{(i)}$ stands for the complex wave number (skin effect parameter) of the region (i). There are four different field regions associated with a coaxial cable (Figure 2).

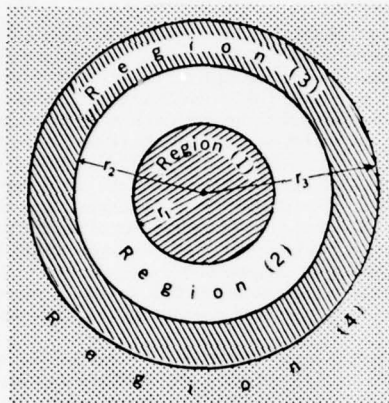


Figure 2. Cross Section of a Solid Coaxial Cable

For the metallically conductive regions ($i = 1$, inner conductor; $i = 3$, outer conductor) it is

$$k^{(i)} = \sqrt{-i\omega\mu_0\mu^{(i)}\sigma^{(i)}} \quad (i = 1, 3) \quad . \quad (21)$$

Within the dielectric regions ($i = 2$, interior dielectric; $i = 4$, exterior dielectric) this parameter is representable by

$$k^{(i)} = \sqrt{\omega^2\epsilon_0\mu_0\epsilon^{(i)}\mu^{(i)} - i\omega\mu_0\mu^{(i)}\sigma^{(i)}} \quad (i = 2, 4) \quad . \quad (22)$$

The radii r_1 , r_2 , and r_3 are explained in Figure 2. Parameters $\epsilon^{(i)}$, $\mu^{(i)}$ and $\sigma^{(i)}$ are the regional dielectric constant, magnetic permeability, and electrical conductivity, respectively. Factor $W(r_2, r_3, k^{(2)}, k^{(3)}, k^{(4)})$ reflects the influence of the current distribution within the outer conductor limited by the outer dielectric region (4).

The results obtained by the relationships (19) and (20) can be obtained by direct impedance evaluations of the individual conductor elements. This means that the theory of electromagnetic wave propagation along cylindrical structures depends on the knowledge of the unit length impedances of the inner as well as outer conductors.

Flexible Coaxial Configurations

Flexibility of transmission lines requires other than solid conductor configurations. The most common arrangement to achieve flexible conducting surfaces is an array of wires confined within some fictitious cylinder surfaces. In order to enhance flexibility, all wires are bent helically by maintaining a uniform helix geometry. Because of the helix-shaped wire configuration, electromagnetic fields within flexible coaxial lines are of semi-cylindrical nature. In this connection, it can be shown that electromagnetic fields around helically twisted conductor elements of common lay length are basically helically transformed cylindersymmetric fields.¹ Therefore, it is adequate to consider

a certain equivalent structure formed by an array of parallel wires. Since any array of cylindrical wires represents a cylindrical configuration, electromagnetic field propagation can be expressed in terms of conductor impedances as indicated above. Figure 3 shows the ladder network of distributed parameters for a general coaxial line made of cylindrically arranged wires.

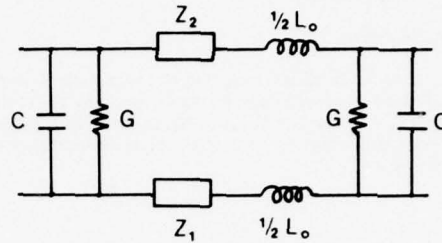


Figure 3. Distributed Network Parameters of Flexible Cable

Both the distributed capacity C , as well as conductivity L_0 , can be directly obtained from static and stationary field conditions. In particular, it is C the unit length capacity measured between the inner and outer array of wires. A mathematical representation of C , as well as L_0 , can be obtained through methods related to conformal mapping.

The transmission line parameters P and Q are in this case:

$$P = i\omega L_0 + Z_1 + Z_2 \quad , \quad (23)$$

$$Q = G + i\omega C \quad . \quad (24)$$

Herein are the impedances of the inner and outer conductor, Z_1 and Z_2 , the only remaining quantities subject of determination. Consequently, the problem of electromagnetic field propagation along wire structures rests upon finding the unit length impedance for each wire element of the conductor forming array.

Impedance of Multiwire Arrays

The unit length impedance of a wire being a member of an array of parallel circular cylindrical wires can be determined from the electromagnetic field distribution related to the individual wire current density distributions. In turn, each wire current density distribution is affected by the external field distribution, thus strongly influenced by the intensity and geometry of all other wire current density distributions.

For general wire arrays, this multiwire array problem has been solved in a rigorous manner. It is the purpose of this section to outline the method of the approach.

Single Wire Impedance

A general wire impedance representation can be obtained in terms of electromagnetic field quantities at the surface of the wire. This relationship can easily be derived from the complex Poynting theorem by expressing the wire's rate capability of storing as well as dissipating electromagnetic field energy. For a wire segment of one meter length and radius a , its impedance Z can be evaluated by the complex valued relationship

$$Z = \frac{a}{I I^*} \int_0^{2\pi} E_z(a, \phi) H_\phi^*(a, \phi) d\phi . \quad (25)$$

In this formula there are I the total wire current, $E_z(a, \phi)$ the wire axial electrical field strength, and $H_\phi(a, \phi)$ the azimuthal magnetic field strength on the wire surface. The asterisks symbolize the conjugate complex quantity.

Wire Array Geometry

An array of N wires arranged in an axis parallel fashion is uniquely defined by specifying each wire's center by the complex number $\xi_i = \xi_i + i\eta_i$ ($i = 1, 2, \dots, N$), together with the corresponding wire radius a_i ($i = 1, 2, \dots, N$). Figure 4 illustrates this situation for $N = 4$.

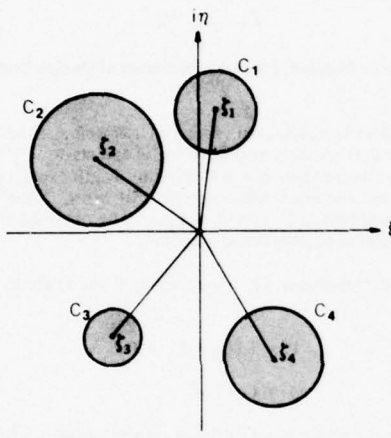


Figure 4. Array of Parallel Wires

Within the wire boundaries C_i defined by the circle of radius a_i about its center ξ_i the electric conductivity of the wire material shall be $\sigma^{(i)}$ and the magnetic permeability $\mu^{(i)}$. The total current within the i -th wire is denoted by symbol I_i . Furthermore, all electromagnetic field symbols associated with the field quantities within the i -th wire can be identified by the superscript (i) . Non-superscripted field symbols refer to the wire external field region. The wire external field region, or dielectric region, is of homogeneous nature. Its electromagnetic field properties are specified by the dielectric constant ϵ and the magnetic permeability μ . Dielectric losses within the external region are considered to be zero. Consequently, no electric current will be present within that region since any displacement current is considered to be nonexistent for reasons mentioned above.

Wire External Magnetic Field

All electric current paths within wires are parallel and perpendicular to the ξ, η plane, thus the magnetic field \mathbf{H} excited is of plane type expressible in terms of components lying within the ξ, η plane. The magnetic field \mathbf{H} is composed of two components:

- The fundamental (unperturbed) magnetic field \mathbf{H}_o .
- The multipole (perturbing) magnetic field \mathbf{h}_o .

In this way it is

$$\mathbf{H} = \mathbf{H}_o + \mathbf{h} . \quad (26)$$

For any point within the dielectric region, the magnetic field is certainly free of sources, hence

$$\operatorname{div} \mathbf{H} = 0 . \quad (27)$$

This implies that an associated vector potential exists which can only exist within the interior of the wires. The vector potential distribution must be identical with the current density distribution within each wire. For the fundamental magnetic field component, a scalar contour line integral performed around the i -th wire contour line (magnetic circulation) must be equal to the total wire current I_i . Since perturbation of current distribution does not affect the amount of magnetic circulation around each wire, the nature of the perturbing magnetic field \mathbf{h} corresponds to the presence of an infinite set of fictitious current n -tuples at each wire center. This n -tuple generating the external magnetic field component \mathbf{h} is equivalent with the actual current density distribution which, in turn, is responsible for perturbing the unperturbed current density distribution.

From mathematical considerations, it is derived that the external magnetic field can be conveniently expressed in a complex valued orthogonal coordinate system. For any point, $\xi = x + iy$, within the dielectric region there exists the following representation of components:

$$H_x(x, y, z, t) = \frac{1}{2\pi} e^{i(hz+\omega t)} \operatorname{Im} \sum_{i=1}^N \frac{I_i}{\xi - \xi_i} , \quad (28)$$

$$H_y(x, y, z, t) = \frac{1}{2\pi} e^{i(hz+\omega t)} \operatorname{Re} \sum_{i=1}^N \frac{I_i}{\xi - \xi_i} , \quad (29)$$

$$h_x(x, y, z, t) = e^{i(hz+\omega t)} \operatorname{Im} \sum_{i=1}^N \sum_{n=1}^{\infty} \frac{n c_n^{(i)}}{(\xi - \xi_i)^{n+1}} , \quad (30)$$

$$h_y(x, y, z, t) = e^{i(hz+\omega t)} \operatorname{Re} \sum_{i=1}^N \sum_{n=1}^{\infty} \frac{n c_n^{(i)}}{(\xi - \xi_i)^{n+1}} . \quad (31)$$

The set of coefficients $c_n^{(i)}$ [$i = 1, 2, \dots, N$; $n = 1, 2, \dots$] relates to the n -tuple current distribution and will be subject to solution.

For the sake of convenience, the total external magnetic field can be expressed in terms of polar coordinates with the origin at the center of the k -th wire. In this way, the radial and azimuthal field components become

$$H_r(r, \phi, z, t) = e^{i(hz+\omega t)} \operatorname{Im} \left\{ e^{i\phi} \sum_{i=1}^N \left[\frac{I_i}{2\pi} \frac{1}{\xi + \xi_k - \xi_i} \right. \right. \\ \left. \left. + \sum_{n=1}^{\infty} \frac{n c_n^{(i)}}{(\xi + \xi_k - \xi_i)^{n+1}} \right] \right\} , \quad (32)$$

and

$$H_\phi(r, \phi, z, t) = e^{i(hz+\omega t)} \operatorname{Re} \left\{ e^{i\phi} \sum_{i=1}^N \left[\frac{I_i}{2\pi} \frac{1}{\xi + \xi_k - \xi_i} \right. \right. \\ \left. \left. + \sum_{n=1}^{\infty} \frac{n c_n^{(i)}}{(\xi + \xi_k - \xi_i)^{n+1}} \right] \right\} . \quad (33)$$

In both formulas

$$\xi = r e^{i\phi} \quad (34)$$

with $r \geq a_k$.

Wire Internal Fields

The total electromagnetic field within each wire consists of some unperturbed field components to which perturbing components are superimposed. Within the boundary circle C_k of the k -th wire, the electrical field can be expressed as follows:

$$E^{(k)} = E_o^{(k)} + e^{(k)} . \quad (35)$$

Similarly, the magnetic field:

$$H^{(k)} = H_o^{(k)} + h^{(k)} . \quad (36)$$

Both field distributions are interrelated by virtue of Maxwell's equations:

$$\operatorname{curl} H^{(k)} = a^{(k)} E^{(k)} , \quad (37)$$

$$\operatorname{curl} E^{(k)} = -i\omega \mu_0 \mu^{(k)} H^{(k)} . \quad (38)$$

Because of the wire geometry, there is $E_x^{(k)} = E_y^{(k)} = 0$. In combining the last two equations and introducing polar coordinates with origin at the wire center, one obtains the following differential equations for both components of axial electrical field strength:

$$\frac{\partial}{\partial r} \left(r \frac{\partial E_z^{(k)}}{\partial r} \right) + k^{(k)2} r E_z^{(k)} = 0 , \quad (39)$$

$$\frac{\partial}{\partial r} \left(r \frac{\partial h_z^{(k)}}{\partial r} \right) + \frac{1}{r} \frac{\partial^2 h_z^{(k)}}{\partial \phi^2} + k^{(k)2} r h_z^{(k)} = 0 . \quad (40)$$

The complex wave number $k^{(k)}$ is defined with reference to Equation (21).

From the solutions of Equations (39) and (40), the magnetic field components are obtained as follows:

$$H_r^{(k)}(r, \phi) = 0 , \quad (41)$$

$$H_\phi^{(k)} = \frac{1}{i\omega \mu_0 \mu^{(k)}} \frac{\partial E_z^{(k)}}{\partial r} , \quad (42)$$

and

$$h_r^{(k)} = -\frac{1}{i\omega \mu_0 \mu^{(k)}} \frac{1}{r} \frac{\partial h_z^{(k)}}{\partial \phi} , \quad (43)$$

$$h_\phi^{(k)} = \frac{1}{i\omega \mu_0 \mu^{(k)}} \frac{\partial e_z^{(k)}}{\partial r} . \quad (44)$$

By selecting proper solutions of differential Equations (39) and (40) the electrical and magnetic field distributions within the wire can finally be written:

$$E_z^{(k)}(r, \phi, z, t) = e^{i(hz+\omega t)} \times \\ \times \sum_{n=0}^{\infty} J_n(k^{(k)} r) \{ a_n^{(k)} \cos n\phi + b_n^{(k)} \sin n\phi \} , \quad (45)$$

$$H_r^{(k)}(r, \phi, z, t) = \frac{1}{r} \frac{e^{i(hz+\omega t)}}{i\omega \mu_0 \mu^{(k)}} \times \\ \times \sum_{n=0}^{\infty} n J_n(k^{(k)} r) \{ a_n^{(k)} \sin n\phi - b_n^{(k)} \cos n\phi \} , \quad (46)$$

$$H_\phi^{(k)}(r, \phi, z, t) = e^{i(hz+\omega t)} \left[\frac{I_k}{2\pi a_k} \frac{J_1(k^{(k)} r)}{J_1(k^{(k)} a_k)} + \right. \\ \left. + \frac{k^{(k)}}{i\omega \mu_0 \mu^{(k)}} \sum_{n=0}^{\infty} J'_n(k^{(k)} r) [a_n^{(k)} \cos n\phi + b_n^{(k)} \sin n\phi] \right] . \quad (47)$$

The wire external magnetic field distribution as well as the electrical-magnetic field within the wire depend on the knowledge of three sets of complex valued coefficients, $a_n^{(k)}$, $b_n^{(k)}$, and $c_n^{(k)}$ ($k = 1, 2, \dots, N$; $n = 1, 2, \dots$). All coefficients can be evaluated in terms of solutions derived from a set of linear equations. The set of equations is obtained by meeting well-known boundary conditions.

Boundary Conditions

The external and wire internal magnetic field distributions are related to each other since certain field continuity requirements must be met along the wire interface surface common to both regions. In defining a point $\xi = \xi_k + a_k e^{i\phi}$, at the surface of the k -th wire, compulsory magnetic field boundary conditions are as follows:

$$H_\phi^{(k)}(a_k, \phi) = H_\phi(a_k, \phi), (k = 1, 2, \dots, N) ; \quad (48)$$

$$\mu^{(k)} H_r^{(k)}(a_k, \phi) = \mu H_r(a_k, \phi), (k = 1, 2, \dots, N) . \quad (49)$$

Both boundary conditions are conveniently met by confronting Equations (33) and (47) as well as Equations (32) and (46), respectively. In this manner, the following two identities become established:

$$\frac{I_k}{2\pi a_k} + \frac{k^{(k)}}{i\omega \mu_0 \mu^{(k)}} \sum_{n=1}^{\infty} J'_n(k^{(k)} a_k) [a_n^{(k)} \cos n\phi + b_n^{(k)} \sin n\phi] = \\ \operatorname{Re} \left\{ e^{i\phi} \sum_{i=1}^N \left[\frac{I_i}{2\pi} \frac{1}{\xi_k - \xi_i + a_k e^{i\phi}} + \sum_{n=1}^{\infty} \frac{n c_n^{(i)}}{(\xi_k - \xi_i + a_k e^{i\phi})^{n+1}} \right] \right\} \\ (k = 1, 2, \dots, N) ; \quad (50)$$

$$\frac{1}{i\omega\mu_0\mu} \frac{1}{r} \sum_{n=1}^{\infty} n J_n(k^{(k)} a_k) [a_n^{(k)} \sin n\phi - b_n^{(k)} \cos n\phi] =$$

$$\text{Im} \left\{ e^{i\phi} \sum_{i=1}^N \left[\frac{I_i}{2\pi} \frac{1}{\xi_k - \xi_i + a_k e^{i\phi}} + \sum_{n=1}^{\infty} \frac{n c_n^{(i)}}{(\xi_k - \xi_i + a_k e^{i\phi})^{n+1}} \right] \right\}$$

$$(k = 1, 2, \dots, N) . \quad (51)$$

Both equations are valid for any wire which requires that N such pairs of equations exist. From this system of equations, both coefficients, $a_n^{(k)}$ as well as $b_n^{(k)}$, can be easily expressed in terms of the coefficient, $c_n^{(k)}$. This is accomplished by virtue of the orthogonality property of the eigen function set $\cos n\phi$ and $\sin n\phi$. In performing the analysis, all resulting integrals can be expressed in terms of complex valued contour integrals which, in turn, are easily evaluated by applying the residue theorem. After some lengthy but elementary algebraic modifications, a final set of linear equations for the set of complex valued coefficients

$$x_m^{(i)} = m c_m^{(i)} \quad (i = 1, 2, \dots, N; m = 1, 2, \dots) \quad (52)$$

can be obtained:

$$x_m^{(s)*} = g_m^{(s)} \sum_{h=1}^N h \neq s \left[\frac{I_h}{(\xi_h - \xi_s)^m} + 2\pi(-1)^m \times \right.$$

$$\left. \times \sum_{q=1}^{\infty} \frac{\binom{m+q-1}{m-1}}{(\xi_h - \xi_s)^{m+q}} x_q^{(h)} \right]$$

$$(s = 1, 2, \dots, N; m = 1, 2, \dots) . \quad (53)$$

Together with its conjugate complex set of equations

$$x_m^{(s)} = g_m^{(s)*} \sum_{h=1}^N h \neq s \left[\frac{I_h}{(\xi_h^* - \xi_s^*)^m} + 2\pi(-1)^m \times \right.$$

$$\left. \times \sum_{q=1}^{\infty} \frac{\binom{m+q-1}{m-1}}{(\xi_h^* - \xi_s^*)^{m+q}} x_q^{(h)*} \right]$$

$$(s = 1, 2, \dots, N; m = 1, 2, \dots) \quad (54)$$

a complete set of linear equations for the parameter $x_m^{(s)}$ is established. The abbreviation symbol, $g_m^{(s)}$, appearing in both equations stands for

$$g_m^{(s)} = \frac{a_s^{2m}}{2\pi} \frac{\left(1 - \frac{\mu}{\mu^{(s)}}\right) J_{m-1}(k^{(s)} a_s) + \left(1 + \frac{\mu}{\mu^{(s)}}\right) J_{m+1}(k^{(s)} a_s)}{\left(1 + \frac{\mu}{\mu^{(s)}}\right) J_{m-1}(k^{(s)} a_s) + \left(1 - \frac{\mu}{\mu^{(s)}}\right) J_{m+1}(k^{(s)} a_s)} . \quad (55)$$

For many practical wire configuration cases, the infinite set of linear equations, Equations (53) and (54), may be simplified by truncation of higher order terms without impairing the accuracy of the solutions.

The remaining sets of coefficients, $a_m^{(i)}$ and $b_m^{(i)}$, are obtained in terms of $x_m^{(i)}$ by means of the relationships:

$$a_m^{(i)} = -\frac{4i\omega\mu_0\mu}{a_i^{m+1} k^{(i)}} \frac{\text{Re}\{x_m^{(i)}\}}{\left(1 - \frac{\mu}{\mu^{(i)}}\right) J_{m-1}(k^{(i)} a_i) + \left(1 + \frac{\mu}{\mu^{(i)}}\right) J_{m+1}(k^{(i)} a_i)}$$

$$(i = 1, 2, \dots, N; m = 1, 2, \dots) \quad (56)$$

and

$$b_m^{(i)} = -\frac{4i\omega\mu_0\mu}{a_i^{m+1} k^{(i)}} \frac{\text{Im}\{x_m^{(i)}\}}{\left(1 - \frac{\mu}{\mu^{(i)}}\right) J_{m-1}(k^{(i)} a_i) + \left(1 + \frac{\mu}{\mu^{(i)}}\right) J_{m+1}(k^{(i)} a_i)}$$

$$(i = 1, 2, \dots, N; m = 1, 2, \dots) . \quad (57)$$

With the knowledge of the set of coefficients $x_m^{(s)}$ all electromagnetic field quantities can be evaluated at any field point. Thus, evaluation of any wire impedance can easily be performed by means of Equation (25). Inspection of coefficients associated with the linear set of Equations (53) and (54) reveals that solutions $x_m^{(i)}$ are strongly influenced by wire array geometry. Consequently, current distribution as well as wire impedance represent quantities depending on wire array configuration. For an array with large enough spacings between wires, all coefficients, $x_m^{(i)}$, approach zero as spacings increase beyond any limit. For this situation, only the zero order term of the current distribution remains being related to the self-imposed wire internal skin effect. As the wire spacings decrease, higher order current terms become dominant affecting distribution of current density within the wire conductor. This effect is commonly known as proximity effect. For this reason, the system of Equations (53) and (54) shall be called current perturbation equations (CPE).

Impedance of a Linear Wire Array

For some special symmetric configuration cases, solutions to Equations (53) and (54) become accessible to closed form evaluation methods. Such a case represents the infinite linear array of wires with equal radius, a , and uniform spacing, $2d$ (Figure 5).

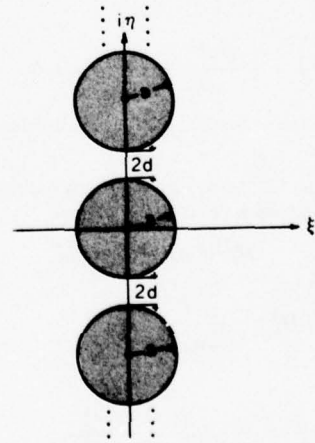


Figure 5. Infinite Linear Wire Array

Filing the wire centers along the imaginary axis yields

$$\xi_n = 2i(na + d) \quad (n = 0, \pm 1, \pm 2, \dots) . \quad (58)$$

After some elementary modification, CPE for the linear wire array becomes:

$$y_{2n} = B_{2n-1} + 2\pi \sum_{p=0}^{\infty} \frac{(-1)^p \gamma_{2p}}{1 + \frac{p}{n}} B_{2(n+p)-1} \left(B_{2p-1} + 2\pi \sum_{q=0}^{\infty} \frac{(-1)^q \gamma_{2q}^*}{1 + \frac{q}{p}} B_{2(p+q)-1} y_{2q} \right), \quad (n = 1, 2, \dots) \quad (59)$$

where

$$\gamma_{2m} = \frac{1}{2\pi[(2m)!]^2} \left[\frac{\pi a}{a+d} \right]^{4m} \frac{J_{2m+1}(ka)}{J_{2m-1}(ka)}$$

The numbers B_{2n-1} ($n = 1, 2, \dots$) are Bernoulli's numbers ($B_1 = 1/6, B_3 = 1/30, B_5 = 1/42, B_7 = 1/30, \dots$). A fast converging series representation for the coefficients is obtained by repetitive resubstitution of the relationship (59) upon itself. Finally, evaluation of the wire impedance according to Equation (25) renders:

$$Z = \frac{k}{\pi a \sigma} \left\{ \frac{1}{2} \frac{J_0(ka)}{J_1(ka)} - \sum_{m=1}^{\infty} \frac{B_{2m-1}^2}{[(2m)!]^2} \left[\frac{\pi}{1 + \frac{d}{a}} \right]^{4m} \frac{J_{2m}(ka)}{J_{2m-1}(ka)} \times \left[1 - \frac{k^* a}{2m} \frac{J_{2m}(k^* a)}{J_{2m-1}(k^* a)} \right] \left[1 - \frac{\pi^4 B_{2m+1}}{24 \left(1 + \frac{1}{m} \right) \left(1 + \frac{d}{a} \right)^4 B_{2m-1}} \frac{J_3(ka)}{J_1(ka)} \right] \times \left[1 - \frac{\pi^4 B_{2m+1}}{24 \left(1 + \frac{1}{m} \right) \left(1 + \frac{d}{a} \right)^4 B_{2m-1}} \frac{J_3(k^* a)}{J_1(k^* a)} \right] \right\} . \quad (60)$$

The first term within the bracket represents the well-known single wire impedance. By this representation, single wire impedance is formally established in performing the limit $d \rightarrow \infty$.

Served Wires

Arrays of wires representing N served (or braided) wire arrangements can be treated by centering N wires at the apexes of a regular N sided polygon with the diagonal $2R$. The n -th wire center coordinate representation in the complex plane becomes:

$$\xi_n = R e^{\frac{2i\pi}{N}(n-1)} \quad (n = 1, 2, \dots, N) . \quad (61)$$

Again, the corresponding CPE can be derived by specialization of Equations (53) and (54). The final set of linear coefficient equations can be written in the form

$$\left(\sin \frac{\pi}{N} \right)^p \left\{ -N \binom{N+p-1}{p-1} \left(\frac{a_0}{R} \right)^{2N} + (-1)^p \left[\frac{I_0}{I_1} + \sum_{n=1}^{N-1} \frac{1}{\left(1 - e^{\frac{2i\pi n}{N}} \right)^p} \right] \right\} =$$

$$= \sum_{q=1}^{\infty} \left[\binom{p+q-1}{p-1} \left(\frac{a_1}{R \sin \frac{\pi}{N}} \right)^{2q} \times \sum_{n=1}^{N-1} \frac{\left(\sin \frac{\pi}{N} \right)^{p+q}}{\left(1 - e^{-\frac{2i\pi n}{N}} \right)^p \left(1 - e^{-\frac{2i\pi n}{N}} \right)^q} + \delta_{pq} \right] \eta_q \quad (p = 1, 2, \dots) . \quad (62)$$

Complex valued solutions η_p ($p = 1, 2, \dots$) derived from the linear system of Equation (62) allow impedance evaluation of a unit length wire situated at the circumference of the array. In this manner the formula

$$Z = \frac{k^{(1)}}{2\pi a_1 \sigma} \left\{ \frac{J_0(k^{(1)} a_1)}{J_1(k^{(1)} a_1)} - 2 \frac{\mu^{(1)}}{\mu} \sum_{n=1}^{\infty} \left(\frac{a_1}{R} \right)^{2n} \frac{\eta_n^2}{\left(\sin \frac{\pi}{N} \right)^{2n}} \times \frac{J_n(k^{(1)} a_1)}{J_{n-1}(k^{(1)} a_1)} \left[1 - \frac{n}{k^{(1)*} a_1} \frac{J_n(k^{(1)*} a_1)}{J_{n-1}(k^{(1)*} a_1)} \right] \right\} \quad (63)$$

is obtained.

In utilizing this served wire impedance theory a numerical program has been derived to evaluate practical served wire configurations commonly used in flexible coax structures. Figure 6 displays the computed frequency response curve of a 56- and a 300-wire serve arrangement. The numerical representation is made in a dimensionless parametric manner. The skin effect parameter related to the inner enveloping cylinder has been chosen for the dimensionless frequency variable x . Real part R_s as well as imaginary part ωL_s of the served wire impedance are normalized with respect to the real part R_t and imaginary part ωL_t impedance of a solid conductive tube. This tube of reference is made of the same conductive wire material and its inner and outer cylinders correspond with the inner and outer enveloping surfaces of the served wire structure. At a certain specific frequency, the real part impedance ratio assumes a minimum which is smaller than one. For this frequency, the power loss within the served wire is less than the corresponding loss within the solid reference tube. This phenomenon is qualitatively explainable by the fact that crowding of current density lines shifts toward higher frequency, less power dissipation is experienced when subdividing a homogeneous conductive domain into smaller subdomains. However, with frequency further increased, proximity effect becomes noticeable as current crowding advances progressively. Consequently, for high enough frequencies, power dissipation within the served wire arrangement will exceed the power loss taking place within the reference tube and a transition minimum will develop. This phenomenon is well described in literature.²

The multiwire impedance theory has been extended toward numerical evaluation of braided wire structures as well as wire strands.

Flexible Coaxial Line Program

Based on the multiwire impedance theory, a series of numerical computer programs have been developed to aid the coaxial cable design effort. Figure 7 shows the calculated attenuation response for the flexible coaxial line RG 58U. Calculation is based on configuration data taken from MIL Handbook 216. The broken line shows the nominal mean line

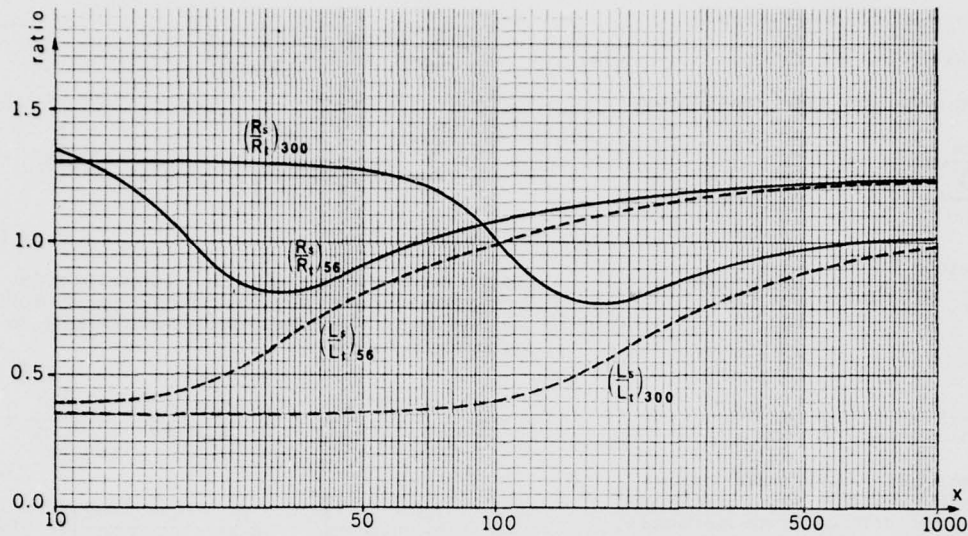


Figure 6. Normalized Representation of Served Wires Impedance (56 and 300 Wires)

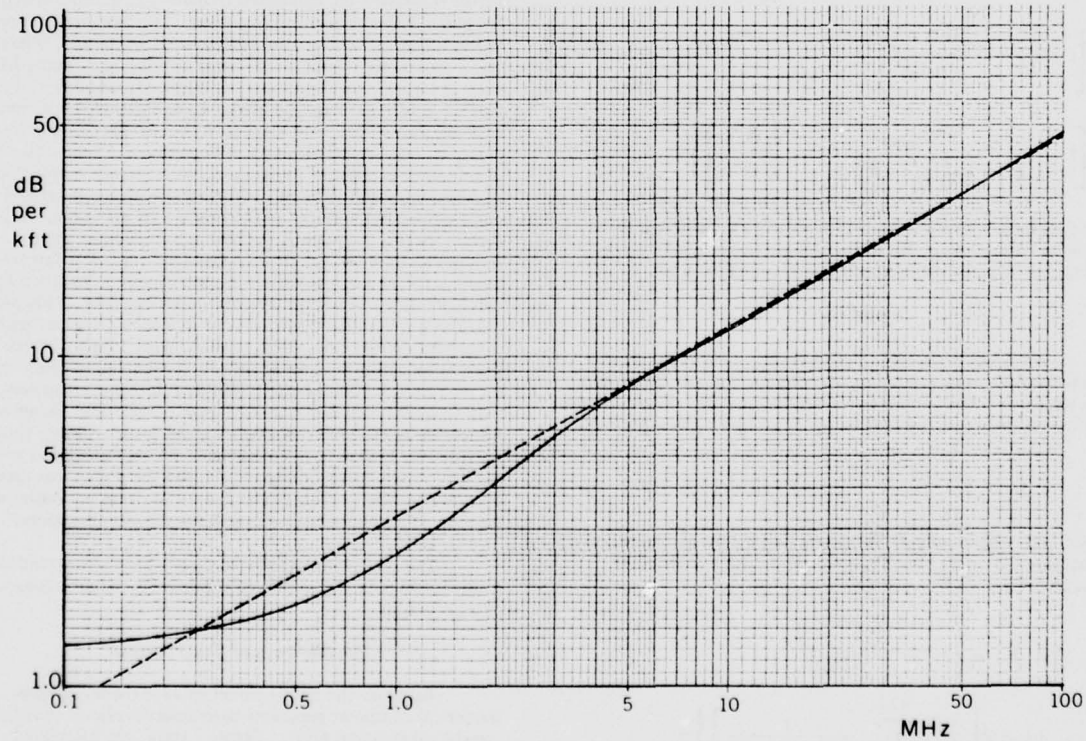


Figure 7. Computed Attenuation Response of Coaxial Line RG 58C/U (Solid Line = Computed Curve, Broken Line = Mean Value Curve Taken From MIL Handbook 216)

of attenuation response as indicated in the handbook. Transition minimum of flexible conductor impedance response can be recognized by inspection of the attenuation response curve.

Calculation shows that the value of minimum becomes less pronounced as wire coverage increases. Therefore, stranded inner conductor wires which are deformed into a closely packed array, indicate an impedance response with shallow transition minimum. Numerical as well as experimental investigations of corresponding line attenuation studies certainly reflect this trend by displaying less undulatory attenuation response curves.

Practical coaxial cable design work requires parametric evaluations of structures made of various flexible conductor elements. For this purpose, a set of numerical routines has been developed utilizing the wire impedance method on the principle of combining different types of coaxial inner and outer conductor configurations. Outer conductor designs include multilayer served and braided wire constructions as well as multiconductive layers of solid metals. Served wire constructions with cylindrical shielding can also be investigated by this routine. Inner conductor types relate to multilayer wire strand configurations and multilayer solid metals.

Required input parameters for all programs are design-oriented configuration data such as number of wires, picks per inch, etc. All necessary conversions to geometric configuration parameters required by the numerical program are carried out internally, such as wire diameter ratios, wire lay angles, wire coverage, etc. Output data obtained from the program relates to frequency response of the complex valued characteristic impedance, signal attenuation, phase velocity, and distributed line parameters.

Program coding has been done in FORTRAN IV. In utilizing high-speed data processors, computation time for a set of output data per given frequency is less than 0.5 second. Particular attention has been directed toward the numerical evaluation of both kinds of Hankel functions for complex arguments extending over almost their entire validity range. A special Hankel function subroutine has been developed which is based

on certain integral representations. This subroutine renders high accuracy combined with computer time efficiency in performing numerical evaluations requested by the algorithm.

Conclusion

The problem of quasistationary electromagnetic field distribution in the vicinity of parallel circular cylindrical arrays of conductive surfaces can be treated in a general manner. As indicated in this paper, results of the theory have been specialized successfully for electromagnetic field problems related to flexible coaxial cable systems. Further specialization of this theory allows electromagnetic field representation along non-coaxial cylinder conductors. Particularly, parametric field representations can be derived for a shielded array of noncoaxial conductive wires. The case of shielded pair of wires represents the most simple case and has been investigated successfully. Results obtained have been applied in the development of a computer design program for shielded twisted pair lines.

The electromagnetic field representation along a parallel wire array can be applied toward many other cable-related field problems of significant technical importance. One group of problems relates to cross talk through cylindrical shields. By proper application of the multiwire impedance theory, evaluation of mutual impedance can be achieved for many configuration cases.

Another application of the multiwire impedance theory has been extended to the study of distortion of coaxial fields due to a certain eccentricity deviation of two nominally coaxial cylinder conductors.

References

1. H. Buchholz, "Die hochfrequente Wirbelströmung im kreiszyklindrischen Schirmleiter verdrillter Leiterpaare," Archiv für Elektrotechnik, Bd 31, 1937.
2. H. Kaden, "Wirbelströme und Schirmung in der Nachrichtentechnik," Second Edition, Page 36, Springer, Berlin 1959.



Gerhard H. Nowak
ITT Cable-Hyrospace
Box 81446, San Diego,
California 92138

Biography:

Dr. Nowak is a native of Vienna, Austria. He studied Mathematics and Physics at the University of Technology Vienna where he earned his academic degrees, "Diplom Ingenieur" (1950) and "Dr. techn." (1955). Since joining ITT Cable-Hyrospace in 1974, Dr. Nowak has made many important contributions in design theory of electromechanical cables. His fundamental work has established the basic concept and software for a comprehensive electromechanical design routine which is presently used within ITT Cable houses.

DUCTILE PLASTIC OPTICAL FIBERS WITH IMPROVED VISIBLE AND NEAR INFRARED TRANSMISSION

Henry M. Schleinitz

E. I. du Pont de Nemours & Company
Plastic Products and Resins Department
Wilmington, Delaware 19898

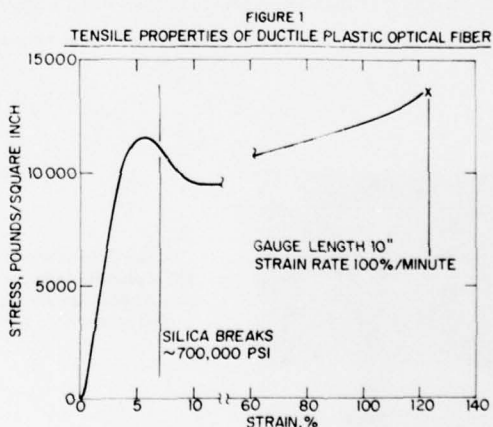
Summary

Optical fibers with a poly(methyl methacrylate), P(MMA), core and a glassy polymer cladding have been prepared with attenuation less than 300 dB/km at 650 nm wavelength. Ductility is achieved by molecular orientation of the polymer in the fibers which exhibit elongation exceeding 100%. Tough fibers can be produced with large core diameter and high numerical aperture which augment coupling to opto-electronic devices. The absorption spectrum of P(MMA) includes bands in the near infrared, but the absorption bands of poly(perdeuteromethylmethacrylate), P(MMA-d₈), are displaced to longer wavelengths providing windows for transmission in the near infrared. Fibers with a P(MMA-d₈) core retain the mechanical property advantages of the protonated counterpart and are suitable for optical transmission links of 100 meters length.

Glassy organic high polymers can be processed to fibers with axial molecular orientation which imparts ductility to the fiber. The tensile properties of a typical fiber with an oriented poly(methyl-methacrylate) core and a thin cladding of a lower index glassy polymer are compared to a silica fiber in Figure 1. Although the modulus and strength of the plastic are significantly lower than the silica, the plastic fiber exhibits a distinct yield point at 11 500 psi (79.3 MPa) stress and 5.7% elongation. The fiber elongation at failure substantially exceeds 100%. This ductile failure mode makes it possible to fabricate large diameter fibers with superior toughness. The apparent deficiency in strength is readily offset with supplementary tensile members in a cable structure such as PFX-P140R in which Kevlar® aramid reinforcing fibers provide a breaking strength exceeding 25 kg.

Fibers for Visible Transmission

Although remarkable advances have been realized in producing high strength optical fibers from inorganic glasses¹, the low elongation of these brittle materials imposes a limit to the fiber diameter for practical bend radii. Most glass fiber manufacturers have selected fiber diameters of less than 150 μm with active core diameters of multimode, step index guides on the order of 60 μm .^{2,3} High insertion losses from light emitting diodes are typical for doped silica fibers due to the small core diameter and low numerical aperture. Fibers from compound glasses can be produced with higher numerical aperture⁴, and plastic clad silica fibers offer both larger core diameter and higher numerical aperture⁵, but both classes incorporate other disadvantages.



The configuration of the optical fibers discussed in this paper is described in Table I. Diametral variation is small, and both circularity and concentricity are excellent.

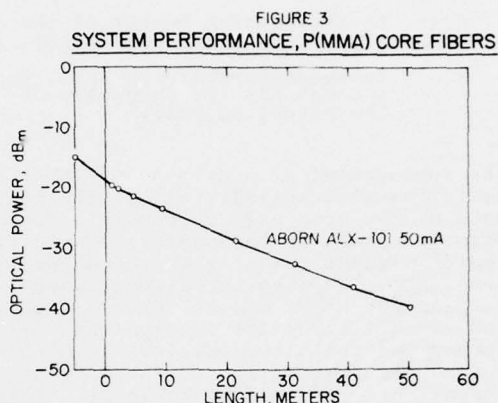
TABLE I
CONFIGURATION OF PLASTIC OPTICAL FIBERS

| Parameter | Units | Mean | St'd Dev. |
|--------------------|-------|-----------|-----------|
| Outside Diameter | μm | 400 | 10 |
| Core Diameter | μm | 368 | 9 |
| Cladding Thickness | μm | 16 | 2 |
| Eccentricity | μm | 2 maximum | |

The refractive index of the core polymer, 1.49, and the low refractive index of the cladding polymer, 1.39, provide a numerical aperture of 0.54 at 650 nm. The numerical aperture at the -10 dB power points is 0.55 at steady state. The large diameter and high numerical aperture are the bases of high coupling efficiency which provide fabricators and end users more facile and less expensive connector technology than required for glass optical wave guides.

The near infrared spectrum of P(MMA) core optical fibers is dominated by absorption from higher harmonics of the carbon-hydrogen stretching vibration at 900, 740, and 622 nm. These spectral absorption peaks are inherent to the material and do not arise from impurities. At wavelengths below 600 nm, scattering contributes increasingly to attenuation. The spectrum of Figure 2 shows that the optimum carrier wavelength is 650 nm at which the attenuation is well below 300 dB/km. The performance of these fibers in simulated communications systems is indicated in Figure 3. Coupling efficiency

is high vis-a-vis doped silica fibers, and transmission links in excess of 50 meters at -40 dBm are possible with these fibers and inexpensive LED's.



Fibers for Near Infrared Transmission

Near infrared carrier wavelengths are preferred to visible for many optical communications systems because⁶

- silicon detectors are somewhat more sensitive in the near infrared,
- GaAs or GaAlAs infrared LED's and diode lasers provide higher power and faster operation than currently available visible emitters, and
- most inorganic glass fibers have attenuation minima between 800 and 900 nm.

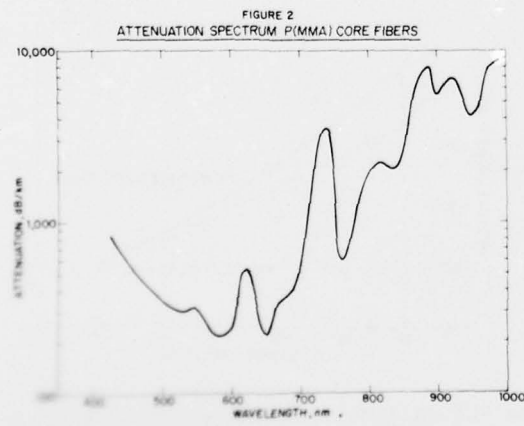
Plastic optical fibers compatible with these more highly developed components would be desirable.

The fundamental oscillation frequency of a covalently bonded atom pair is determined to a first approximation by the bond force constant and the reduced mass⁷ of the system.

$$\omega_0 = \frac{1}{2\pi c} \sqrt{\frac{k}{mM}} \quad (1)$$

The harmonic frequencies can be calculated by quantum theory for anharmonic diatomic oscillators⁸

$$v_{n-1} = \frac{E_n - E_0}{hc} = n\omega_0 [1 - (n+1)x] \quad (2)$$



in which

- ω_0 is the fundamental frequency,
- k is the bond force constant,
- m, M are the masses of the atoms in the bonded pair,
- v_{n-1} is the frequency of the harmonic,
- n is the quantum number of the higher quantum energy level, and
- x is the anharmonicity ratio to account for the asymmetry of the potential well.

The replacement of hydrogen in P(MMA) by deuterium substantially alters the reduced mass of the atom pair responsible for absorption peaks in the preferred spectral region without changing the bond force constant. The theoretical peak wavelengths for P(MMA-d₈) calculated from (1) and (2) utilizing the fundamental frequency and the anharmonicity ratio observed experimentally for the conventional polymer are reported in Table II. The data imply useful transmission windows at about 700 nm and 800 nm.

TABLE II

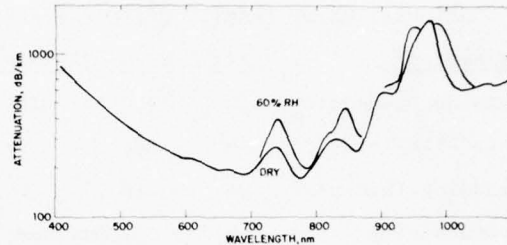
ABSORPTION PEAK WAVELENGTHS
C-D OVERTONES

$$\begin{aligned} x &= 0.0162 \\ M &= 12, m = 2 \\ \omega_0(C-H) &= 3048 \text{ cm}^{-1} \end{aligned}$$

| n | v_{n-1} cm^{-1} | λ_{n-1} nm |
|---|-------------------------------|-----------------------|
| 1 | 2164 | 4621 |
| 2 | 4256 | 2350 |
| 3 | 6275 | 1594 |
| 4 | 8222 | 1217 |
| 5 | 10096 | 990 |
| 6 | 11898 | 840 |
| 7 | 13628 | 734 |
| 8 | 15285 | 654 |

Perdeuterated poly(methylmethacrylate) was synthesized (99.7% isotopic enrichment by 60 MHz H NMR) by routes described previously⁹, and processed into optical fibers. The attenuation spectrum of these experimental fibers, Figure 4, essentially duplicates the theoretical predictions.

The spectrum of glass fibers includes overtone absorption peaks from residual O-H impurities at 970 and 740 nm. Similar peaks are expected in plastic fibers. Since organic polymers are permeable to water, the magnitude of the absorption due to hydroxyl is related to

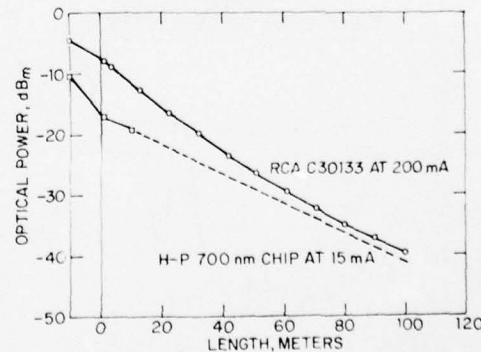


the exposure conditions. The influence of dissolved water on a P(MMA-d₈) core optical fiber equilibrated at 23°C and 60% R.H. is indicated in Figure 4. Absorption peaks occur at the expected wavelengths and have little influence on the attenuation at the optimum wavelengths for transmission. The process is completely reversible.

The refractive index of P(MMA-d₈) is 1.48 at 650 nm. The numerical aperture is essentially identical to conventional P(MMA) fibers with the same cladding. As expected, the thermal and mechanical properties of the polymer, except density, are almost unaffected by isotope exchange. Optical fibers with P(MMA-d₈) core retain the toughness of the protonated counterpart.

Figure 5 demonstrates the compatibility of P(MMA-d₈) core fibers with near infrared sources.

FIGURE 5
SYSTEM PERFORMANCE, P(MMA-d₈) CORE FIBERS



The RCA gallium aluminum arsenide LED can power transmission links of 100 meters at -40 dB_m at rates to 150 MHz (3 dB point) although the emission wavelength, 820 nm,

is not ideally matched to the fiber attenuation minimum at 790 nm. The Hewlett-Packard device, based on inexpensive gallium arsenide phosphide technology, is suitable for data transmission at rates to 5 MHz and may provide equal transmission length because the peak emission wavelength is more closely matched to a fiber attenuation minimum at 690 nm.

Conclusion

Optical fibers from organic high polymers have been developed with attenuation in the visible and in the near infrared spectrum below 300 dB/km. Ductility and outstanding toughness in large diameter fibers is achieved through molecular orientation. Good coupling efficiency and lower attenuation than reported heretofore establish these fibers as candidates for transmission media in short length optical communications systems.

References

1. C. R. Kurkjian, et al. "Tensile Strengths of Long Lengths of Coated Silica Fibers", Optical Fiber Transmission II, Optical Society of America, TuA2-1, (1977).
2. F. L. Thiel and W. B. Bielawski, "Optical Waveguides Look Brighter Than Ever", Electronics, March 21, 1974, p 89.
3. R. Love, "Fiber Optic Developments Spark Worldwide Interest", Electronics, August 5, 1976, p. 88.
4. H. Aulich, et al., "High Aperture, Medium-Loss Alkali-Lead-Silicate Fibers Prepared by the Double Crucible Technique", Optical Fiber Transmission II, Optical Society of America, TuC5-1, (1977).
5. G. C. Adams, to be published.
6. J. P. Wittke, "Designer's Guide to: Optical-Fiber Communications Systems", EDN, May 20, 1975.
7. Chemical Applications of Infrared Spectroscopy, C.N.R. Rao, Academic Press, N.Y., 1963, pp 8,9.
8. Introduction to Infrared and Raman Spectroscopy, N. B. Colthup, L. H. Daly, and S. E. Wiberley, Academic Press, N.Y., 1964, pp 10 et seq.
9. Nagai, et al., J. Poly. Sci., 62, S95 (1962).



Henry M. Schleinitz
E. I. du Pont de Nemours & Company
Plastic Products and Resins Department
Wilmington, Delaware 19898

Henry M. Schleinitz is a Research Associate at the Du Pont Experimental Station Laboratory where he has conducted research on optical transmission in plastic wave guides. He has investigated various aspects of polymer characterization and compounding and plastics processing for Du Pont since receiving his Ph.D. in Chemical Engineering from Cambridge University in 1965. Dr. Schleinitz is a member of the ACS and the SPE.

STRESS STRAIN AND OPTICAL TRANSMISSION DATA ON PLASTIC CLAD
SILICA FIBER OPTIC CABLES WITH AND WITHOUT CONNECTORS

G. C. Adams

E. I. du Pont de Nemours & Company
Plastic Products and Resins Department
Wilmington, Delaware 19898

ABSTRACT

Plastic clad silica fiber optic cable of a single fiber reinforced with high strength aramid fibers has been found sufficiently rugged and resistant to fiber break to allow ordinary handling practices upon cable installation. The strength and transmission performance is defined by specialized tests on cable while under tension and during bending. A connector assembly of high strength and low loss is identified.

INTRODUCTION

An increasingly optimistic future is predicted for fiber optics in a host of noteworthy applications from computer data links to kilovolt power distribution systems. It is apparent that practical transmission systems employing optical fiber cables can be designed, built and installed without developing long term stability problems. Commercial use is a foregone conclusion, and there have been a number of developments that could result in large scale use. As commercialization becomes more imminent, many practical questions arise. Designers want to know the amount of transmission loss in fiber optic cable under tension, the tolerance of core material to tension upon pulling long lengths into and out of ducts, flexibility and resistance to crush of cable and the sensitivity of cable to bending, twisting and flexing and other physical abuse aspects of handling. While comprehensive evaluations of the actual transmission properties of cable have been reported by Lebduska⁽¹⁾ and Sigel⁽²⁾, there seems to be a dearth of information on practical cable.

The practical aspects of handling cable on installation or short term basis are presented on the left side of Table I while the analogous cable property for testing purposes is seen on the right side. In general this paper is concerned with two practical aspects of testing on cable to

Table I

REQUIREMENTS FOR PRACTICAL
FIBER OPTIC CABLE

| <u>Installation</u> | <u>Short Term Tests</u> |
|---------------------|-------------------------|
| • pull into conduit | • tensile strength |
| • flexibility | • low modulus |
| • bend/twist | • low bend radius |
| • impact and crush | • impact strength |

determine the susceptibility to transmission loss and breakage of silica fiber under harsh conditions of handling. These two aspects are cable tension and cable bending. Cable bending was studied with and without tension.

CABLE CONSTRUCTION

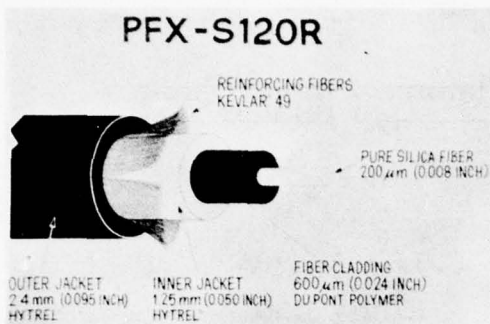
The fiber optic cable under study, PFX-S120R, as depicted in Figure 1, is composed of a single silica fiber core, suitable plastic cladding, and an interlayer of polyester elastomer -- Kevlar® aramid fiber -- polyester elastomer which comprise the cable jacket. The Kevlar® aramid fibers, hereafter referred to as aramid fibers, assure high strength at low cable elongation and the Hytrel® provides cable bulk, chemical resistance, impact protection, and support in the multicomponent construction.

RESULTS

Cable Tensile Properties

Since the elongation of silica optical fibers before breakage is low, incorporation of selective cable components is necessary to protect the fiber during installation and end use. The configuration of cable components shown in Figure 1

Figure 1



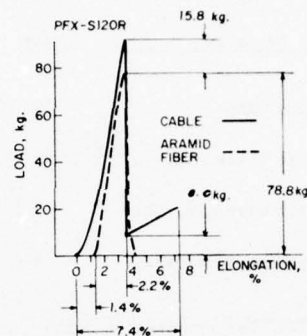
is designed to meet loading requirements of 90 kg. (200 lbs.), which is considered to be twice or more the typical maximum loading on single fiber cable being pulled by a person.

The load-elongation curve of such 1 meter length cable stretched at 10 percent per minute is shown in Figure 2. Also presented are data for the aramid fiber tested in amount in the fiber optic cable. The aramid fibers are loaded and brought to the point of breakage at 90 kg. and 3.5 percent elongation. The abrupt load reduction results in total aramid fiber breakage leaving the load carried by the intact silica fiber at 3.5 percent cable elongation. Loading of silica fiber continues until it breaks at 7.3 percent elongation and 20 kg. The aramid fibers assure that a high load is attained before breakage of the silica fiber at twice the elongation to break of the aramid fibers. Since loads of 80-90 kg. are unlikely in cable installation, the aramid fibers protect the silica fiber from premature breakage, thus meeting an important installation requirement of maintaining transmission while pulling cable through conduits and over other load requiring conditions.

Superposition of the break points of aramid fibers in Figure 2 enables understanding of loading of multicomponent cable. Cable elongation at aramid fiber break exceeds aramid fiber elongation by 1.4%. At this elongation, the aramid fibers, which were incorporated into the cable during processing, begin to carry the load.

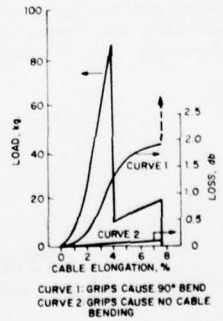
A compilation of several possible physical measurements from Figure 2 is seen in Table II and a comparison is made with published property data of aramid fiber and silica.

FIGURE 2
ANALYSIS OF LOAD-
ELONGATION CURVE OF CLADDED
SILICA FIBER OPTIC CABLE
AND OF ARAMID REINFORCING FIBER



Two methods of cable gripping were employed for monitoring of light transmission of cable under tension. A self-tightening grip which incorporates increasingly sharper bending at 90 degrees results in up to two decibels light loss during initial loading before aramid fiber breakage (Figure 3). However, cable wrapped and clamped 180 degrees in a wide radius of 3.75 cm. with no sharp bending as used in tensile testing, shows little loss during loading.

FIGURE 3
LOAD AND TRANSMISSION LOSS vs CABLE
ELONGATION FOR SILICA FIBER CABLE
TRANSMISSION LOSS IS GREATER FOR CABLE
GRIPPED BY 90° BENDING



Cable Bending Properties

The amount of light transmitted by an optical fiber is exponentially related to bending: the greater the bending, the greater the loss until all transmission is

TABLE II
TENSILE PROPERTIES OF FIBER OPTICS CABLE, ARAMID FIBERS
AND CLAD SILICA FIBER

| Property | Cable | Aramid Fiber tested as 5400 denier (1) | Literature | Silica tested as clad silica | Literature |
|------------------------|-------|--|------------|------------------------------------|------------|
| Modulus, GPa | 59 | 82 | 130 | 85 | 73 |
| Load to break, kg. | 90 | 78 | | 21 | |
| Tensile strength, GPa | 2.1 | 1.8 | 3.6 | 4.9 | |
| Elongation to break, % | 3.5 | 2.2 | 2.8 | 7.4 | |

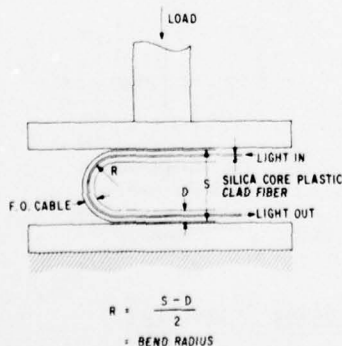
(1) 5400 denier fiber in cable

lost at the fiber break point. Loss due to bending may be studied in any of several bending tests including cable wrap on various size mandrels, cable loading while bent, and bending of cable in a 180 degree or U configuration. Results from two of these tests will be discussed in detail. These tests partially simulate insertion of cable through restricted openings and pulling of cable around corners of different radius of curvature.

The 180 Degree Bend Radius Test

A schematic representation of cable bending is shown in Figure 4. Initially cable bent to 1.25 cm. bend radius, R, is inserted between the platens of an

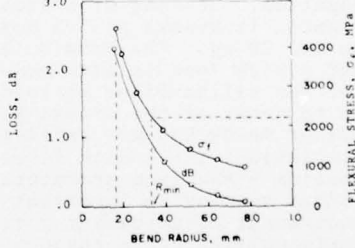
FIGURE 4
REPRESENTATION OF BEND RADIUS TEST OF
FIBER OPTICS CABLE COMPRESSION
CONTINUES UNTIL SILICA BREAKS



Instron machine. Platen movement or closure of 1.25 cm. per minute is maintained

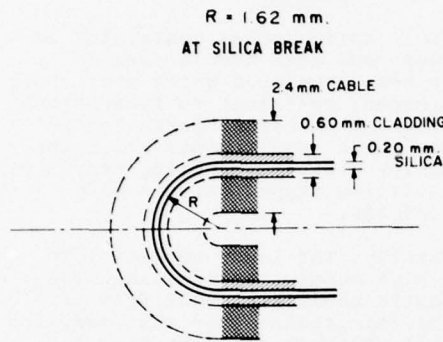
while load and light transmission is monitored. Increasing loss occurs simultaneously with increasing load (Figure 5).

FIGURE 5
LIGHT LOSS AND FLEXURAL STRESS VS.
FIBER OPTIC CABLE BEND RADIUS FROM 180°
BEND RADIUS TEST



No significant loss occurs until the cable is bent to about 5.0 mm. radius -- about twenty-five silica fiber diameters or 2.0 cable diameters separation between fibers. Loss then increases exponentially to silica fiber break. Silica fiber breakage due to bending occurs when the polyester copolymer jacket of 2.4 mm diameter is folded just short of contact and a silica-to-silica separation of twice the bend radius (1.62 mm) or 3.25 mm is reached (Figure 6). This separation between cable surfaces is 0.3 cable diameters and indicates superior break resistance to high curvature of silica. The absence of fiber breakage at high curvature is attributed to a technique of fiber preparation which leaves a clean fiber surface free from cracks, voids and flaws.

FIGURE 6
TO SCALE REPRESENTATION OF CONFIGURATION OF CABLE, CLADDING AND SILICA AT SILICA BREAK ON 180° BEND RADIUS TEST



A formula for calculating flexural stress, σ_f , of bent fiber from fiber diameter, D, and bend radius, R, is given from structural mechanics⁽³⁾ as

$$\sigma_f = \frac{E D}{2 R} \quad (1)$$

where E is the modulus of glass fiber, 73.1 GPa. Insertion of bend radius at break given above of 1.62 mm. gives a flexural stress at break of 4.5 GPa., a value close to the tensile strength at break of silica fiber of 4.9 GPa. given in Table II. Upon stretching by bending, silica fiber breaks at the outside curvature of the bend at a stress comparable to fiber tensile strength. The bend radius study verifies that silica fiber possesses a tough surface essentially free from cracks and voids.

The above analysis enables a procedure for establishment of a recommended short term minimum bend radius, R_{min} , for cable. Flexural stress from equation (1) is plotted in Figure 5 versus bend radius, R. As an illustration, assume that 50 percent of the breaking stress is allowed in cable use, short term. A minimum bend radius of 3.2 mm. is dictated by the calculation for 2.41 mm. diameter cable.

The decibels loss, dB, of light intensity, I, transmitted through curved fiber has been shown to conform approximately to the relationship⁽³⁾

$$dB = C_1 e^{-C_2 R}$$

$$\text{where } dB = 10 \times \log_{10} \frac{I_0}{I_1}$$

C_1 and C_2 are constants (to be determined for a given cable type)

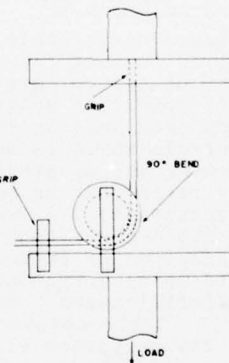
$$R = \text{bend radius.}$$

Appropriate curve fitting of experimental data show that assessment of cable quality is indicated by the magnitude of C_1 and C_2 . These values are approximately 18 and -15, respectively for plastic clad silica fiber cable. For low loss plastic fiber cable, C_1 is lower and C_2 is higher.

Mandrel Bend Test With Load

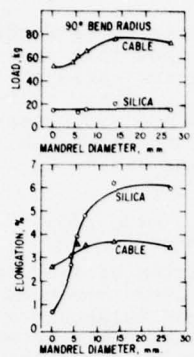
Installation of fiber optic cable of necessity involves movement of cable around corners and bulkheads of various curvature. Because cable movement involves feeding and pulling, there are a variety of load bearing configurations encountered. Test results from a simulation of the loading of cable around corners are discussed below. The mandrel bend test incorporated a 90 degree bend of cable around mandrels of diameter 4.2, 5.3, 7.3, 13.4 and 25.8 mm in a manner shown in Figure 7. Results are shown in Figure 8.

FIGURE 7
REPRESENTATION OF 90° BEND WITH LOAD. CABLE ELONGATION CONTINUES UNTIL SILICA BREAKS.



Aramid fiber elongation to break averages 3.2 percent for all mandrel diameters. Elongation to break of silica ranges from 0.7 to 3.2 percent for mandrel diameters up to 4.6 mm. and higher elongations for larger mandrel diameters. Provided 5.0 mm. diameter or greater is maintained at a 90 degree bend configuration, cable may be loaded over short term, as on installation, to 60 kg. before the silica fiber is no longer protected. These results illustrate a practically unrestricted silica fiber and cable bend radius range without fiber breakage and a high elongation capability of clad silica fiber when reinforced with aramid fiber in a multicomponent cable construction.

FIGURE 8
LOAD AND ELONGATION OF SILICA AND
OF CABLE AT BREAK vs DIAMETER OF
MANDREL OVER WHICH CABLE IS LOADED
AT 90° ANGLE



Zero bend radius data points in Figure 8 are established by loading of cable over a square cross-sectioned steel bar incorporating a 90 degree bend radius. The continuity between data points is gratifying. The identical test, run in a 60 degree bend configuration, results in protection by aramid fibers above 1.52 mm. diameter.

Connected Cable Strength Tests

Use of fiber optic cable requires an understanding of connector technology and establishment of appropriate tests to verify a suitable connector system. The AMP connector employed in this study is a polypropylene ferrule which is suitable for fine grain polishing and adapted for adhesion to cable by resin potting material. With careful preparation, 1-3 decibels light loss are obtained per connector. A strong bonding adhesive of ferrule to cable is possible using a cyanoacrylate high strength material known commercially as "Loctite 414".* Cable components bonded to adhesive are the polyester elastomer jacket and the aramid fibers which support much of the load. Connector strengths were measured by mounting two such connectors in a connected configuration midway between Instron jaws which gripped the fiber optic cable. Values obtained were 30 kg. or 35% of cable strength. Slightly higher values of 37 kg. were obtained by gripping directly one connector. That this type adhesive provides strong bonds was evident by failure principally by the ferrule in cross section and less often by pullout of the cable from connector.

Under normal installation conditions, cable connectors are connected after the rigors of cable movement and loading are completed. Loading requirements on connected cable not being great under such

circumstances, a break load of 30 kg. is considered high. A connector system of suitable strength is identified, and others are currently being evaluated.

SUMMARY

Fiber optic cables containing a high strength and high modulus aramid fiber have been developed which over short term are rugged, resistant to fiber break upon bending and withstand large loads while bent. Such requirements are necessary to employ ordinary handling practices upon installation around corners and through conduits.

Firstly, the loads necessary to break the high modulus reinforcing fiber in fiber optic cable are found from this study to be far greater than that required to pull cable through straight line conduit. As an example, in tension fiber optic cable exhibits excellent transmission properties. The presence of a high strength aramid fiber, which breaks at over 80 kg. at 3.5 percent elongation, assures protection against silica fiber breakage which occurs at over 7 percent cable elongation and a load of 20 kg. The analysis illustrates how advantage is taken of high elongation to break of silica and the high modulus and low elongation to break of the aramid fiber. A safe cable load on installation of straight line pull of PFX-S120R fiber optic cable is established.

Secondly, cable transmission while bent and under no load is also excellent. Cable transmission is maintained while in a U shape or 180 degree bent configuration until fiber breakage at 0.3 cable diameters separation between cable surfaces or 3.0 mm. This bend radius is unlikely to be reached in end use. Loss previous to breakage is between two and three decibels. No compression of jacketing occurs at breakage. Unjacketed clad silica breaks at an identical bend radius.

Finally, high light transmission and silica fiber integrity are maintained for cable when loaded while in a 90 degree bent configuration over various size mandrels. No premature silica breakage with loading occurs for mandrel diameters above 5.0 mm. Loads of 60 kg. and above are sustained.

The above results illustrate how proper consideration of cable construction leads to superior transmission characteristics of fiber optic cable.

REFERENCES

1. R. L. Lebduska, Optical Engineering, 13, 49 (1974).
2. G. H. Sigel, Jr., Fiber Optics for Naval Applications: An Assessment of Present and Near-Term Capabilities, Naval Research Laboratory Report 8062, Sept. 1976.
3. M. K. Barnoski, Fundamentals of Optical Fiber Communications, p. 67, Academic Press, N. Y. (1976).

Hytrel® and Kevlar® are registered trademarks of E. I. du Pont de Nemours & Company, Wilmington, DE.

**Loctite" is a registered trademark of the Loctite Corporation, Newington, CT.



George C. Adams
E. I. du Pont de Nemours & Company
Plastic Products and Resins Department
Wilmington, Delaware 19898

George C. Adams has been with the Du Pont Company since 1967. He has a B.S. in Chemical Engineering from Northeastern University and a Ph.D. from the University of Massachusetts in the physical chemistry of polymer. His past experience in the solid state structure of polymers has been broadened to include the fracture of glass and the testing of fiber optic cable. Dr. Adams is a member of the American Physical Society.

DESIGN CONSIDERATIONS FOR SINGLE FIBER CONNECTORS

William L. Schumacher

AMP Incorporated

ABSTRACT

Small single optical fibers are difficult to handle, and introduce junction losses due to their own characteristics. Compounding these losses by the addition of connector losses is undesirable. Central fiber axis to fiber axis alignment through elimination of connector tolerance build up and fiber protection and maintainability features are desired. Such a connector design is compared with other designs.

INTRODUCTION

Fiber connector design faults usually fall into two major categories. The first is excess alignment tolerance or high control cost required to control the precise alignment. The second is a high probability of fiber damage or interface damage and contamination. This paper discusses various connector designs to illustrate the problems involved in obtaining minimal connector insertion losses. A design solution to eliminate connector tolerance build up and protect the fiber is included. This design has a single fiber alignment feature that accepts the normal fiber size variations while holding losses to the minimum by aligning the central axis of one fiber to the central axis of the second fiber.

PERMANENT SPLICES

Probably the single item that has received the most thought and attention in optical connectors and splices is fiber-to-fiber alignment. What is the best way to aim one fiber at the other in order to provide maximum transfer of light? Probing this area has created many different approaches. Unfortunately, what appears to be an excellent solution causes undesirable side effects.

Hot Splices

Direct, permanent splicing of fibers (no future disconnection) has probably reached the highest degree of perfection and success. Optical fibers have been successfully spliced by aligning silica fibers and then fusing in an electrical arc.^{1,2} A plasma and an oxyhydric torch³ have also been used for splicing fibers by using the heat fusing technique. The fusing of the same materials eliminates the interface losses due to

the light having to travel through another material with a different index of refraction. Without refraction index changes and with good mechanical alignment prior to fusing, low losses can be obtained. The hot splice method can be used in fiber manufacturing to increase total fiber lengths.

Bonding Agents

Rather than fusing the fibers together, an index matching material that also acts as a permanent bonding agent is another method used. There are quite a few splices using a bonding agent. The difference between these various styles is in the mechanical means of aligning the fibers during the setting up cycle of the bonding agent.

Aligning Rods

An alignment method such as three rods with diameters chosen to provide just the right size in order to accept the fiber in the small hole in their center has several variations^{4,5}. Some rods are chosen to have a slip fit for the largest fiber. Others have a tight fit on the fiber such as would be applied to the rods by a heat shrinkable tube or an elastomeric tube. By using plastic rods or plastic coated rods, a very tight fit rod style gives slight deformation of the three rods and thus helps to center fibers of different diameters (as is found in normal production). The bonding agent provides an index match for this permanent splice.

Aligning Tubes

Loose and tight fitting tubes have also been used with an index match material to provide good splices. Tight tubes⁶ can be straight or capillary. They can be formed from a large metal tube to have a small controlled size center section. One loose tube technique snugs the fibers up in a corner as shown in Figure 1.



Figure 1. Loose Tube Splice

Open Grooves

In a similar fashion to the corner of a loose tube, an open air "V" groove can be used to align the fibers. Either the fiber is bent slightly and holds itself into bonding position, or it is pressed down into the groove by a hard or possibly soft cover. The groove can be "V" shaped at various angles, be made by pressing a fiber into a soft substitute¹⁰, or be flat bottomed "V" shape¹¹. When dealing with fibers from different production runs (as opposed to splicing a broken fiber) and thus different fiber diameters, the "V" angle can introduce fiber alignment variations. When aligning different fiber sizes, the absurd, yet best, "V" angle is 180° or a flat plate. At the other extreme, a small angle, or deep "V", would catch the large fiber at the top and let the small fiber drop down out of sight. The angle chosen then becomes a matter of tradeoff as to results, methods and construction.

In general, permanent fiber optic splices have seen quite a bit of design effort and new excellent results are still being reported. The fixed splice has many advantages over a connector that must be disconnectable. It permits easy use of index matching materials with their multiple benefits. This material and other splice elements are not subject to later exposure and contamination. Being fixed, subsequent position, etc. variations are eliminated providing unchangeable low losses. The spliced fiber is buried and safe from harm both at the interface and along its length. These are all desirable benefits and would enhance the connector design if possible to achieve.

CONNECTOR CONSIDERATIONS

Almost all of the successful fixed splice methods have an overlapping member. This overlapping member contacts both fibers along at least one straight surface. This becomes more difficult with a fiber end in each connector half. How do you align it, protect it, keep it clean and do all the necessary good things when you are operating with two vs. one piece? As with splices, many many ways have been created.

Tube Connector

Just as in a splice, a tube can be utilized to align the fibers. Here an additional consideration must take place. The fiber ends must be positioned with reference to a positive stop so that they always come into close controlled proximity. Figure 2 shows such a connector¹² in two stages of engagement. Not indicated is the threaded coupling nut nor the index matching fluid that fills the alignment hole in the plug. The outside of the plug entering the jack provides the initial alignment.

The small alignment hole is made slightly larger than the largest fiber and has a tapered entry. The tapered entry provides the final guidance of the hooded loose jack fiber into alignment in the plug. The plug is formed vs. machined, and has room for the matching fluid to escape past the pushing piston action of

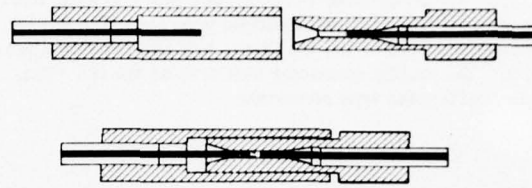


Figure 2. Tube Alignment Style Connector

the jack fiber. The alignment here is on the fiber vs. through the cumulative connector tolerances. Only the connector half to connector half alignment might cock the various diameter fibers slightly.

Straight Sleeve Alignment Connector

Some connector designs encase the single fiber in each connector half to fully protect it. The sleeve in which this is accomplished must have its central hole located very accurately in the center. The machining of metal connectors, such as SMA type, for single fibers now becomes a more taxing manufacturing problem to hold diameters and their concentricity. The fiber diameter variation requires slight clearance for the passage of the largest fiber. Rotation of a concentric sleeve connector of this type¹³ showed a tolerance build up from one side of the connector to the other that resulted in high and low insertion loss readings about 1.5 db apart.

Instead of trying to make the straight sleeves as concentric as possible, the opposite approach has also been taken. A double eccentric connector¹³ has been designed with everything off center on purpose. The fiber is fixed in the center member and then the eccentrics are adjusted to move the fiber into the connector true center.

Taper Sleeve Alignment

By using a tapered tip on the fiber containing sleeve, fit tolerances can be removed. The tapered sleeve is pressed into a polishing tool that sets up the fiber separation dimension. Providing the fiber is located in the true center of the tapered sleeve and providing there is good concentricity throughout the center biconical alignment tube, there will be no insertion loss variation when the parts are rotated.

Another theme of the tapered sleeve connector¹⁴ is to use three rods as an integral part of the sleeve. These rods then compress down on the single fiber as they enter the biconical alignment tube. If material density, rod diameters, etc. are controlled, the centering of the fiber will take place.

Grooved Connectors

By integrating a row of rods into one unit, one connector¹⁵ has provided multiple grooves. These "V" grooves are used to lay the fibers into and provide alignment. The mating connector half acts as the lid. This is an overlapping type connector.

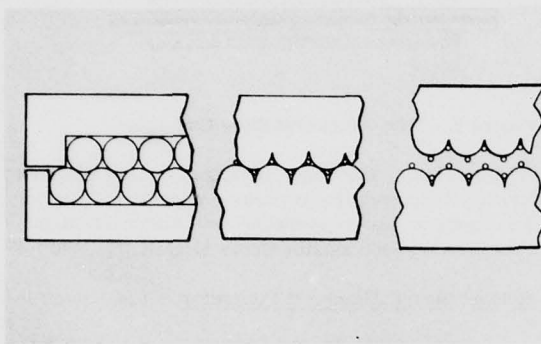


Figure 3. Overlapping "V" Groove Connectors.

On one side of the connector half, the fiber is contained in the "V" groove. On the other side, the mating fiber rides on top of the curved surface of the lid until it is mated with the overlapping base. A feature of this connector is its fiber accumulation region. Here the fiber bends to absorb slight length variation resulting from the butting of the two fibers in the overlap region. This always assures the smallest possible fiber separation. Because of minimal forces, the fiber ends are not damaged. The mating action of the connector is to close the two halves lid-to-base and then slide the halves together along the fiber axis, butting and accumulating excess fiber length.

Optical Self Centering Overlap Style Connector

A recently tooled connector¹⁶ has incorporated a device into it that aligns the central axis of the fiber vs. an edge. It does this while protecting the fiber in a groove. The basic principle of this connector can easily be utilized in single or multiple fiber connectors, housed in plastic or metal and scaled up or down to accommodate other fiber basic sizes. The many different operating conditions and requirements will dictate differently constructed connectors. All plastic, plastic-clad silica, and all glass fiber each have their own areas of use, cable construction and handling techniques. Although the connector design being shown here was designed for commercial use, the basic fiber alignment technique can be converted to many uses.

Resilient Heart

Two identical resilient members constitute the basis for this connector. The fibers in each connector half are positioned just short of the connector centerline. This positioning is accomplished by fixturing in a scribe-and-break tool, or a polishing tool¹⁷. In this

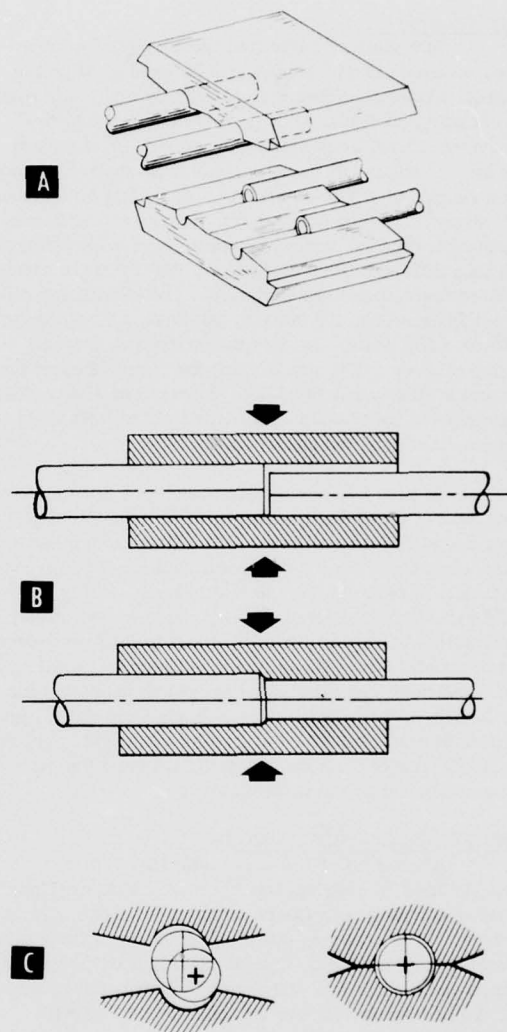


Figure 4. Fiber tolerances are absorbed by the two mirror-image elastomeric support members which conform, under pressure, to the diameter of each fiber.

overlap section, both fibers are resting in a protective groove in their respective connector half. (See Figure 4a.) These are further protected by the hood effect of the housing.

The mating mechanism keeps the fibers separated as they approach each other to prevent stubbing the fibers and eliminate the shovel effect of accumulating any foreign matter along the way. Once the connector halves position the fibers longitudinally

the mating action moves them perpendicular to the fiber axis to complete the closure.

During the closure action any connector tolerance build up results in an increase or decrease of the force being applied to the resilient insert. The compliancy of this resilient insert absorbs the tolerance variations. More importantly, it absorbs fiber-diameter variations while aligning the centers of the fiber (see Figure 4b, 4c). When the inserts reach equilibrium, they are overlapping and cover the fibers from both connector halves. Thus, in addition to aligning the fiber centerlines, the insert also encloses and protects the fibers from atmospheric contamination.

Repeatability of Multiple Engagements

A wealth of test effort and information is available on the initial fiber used (PFX-P, 400 μm O.D.) in a connector of this type. When a fiber is cut, and a connector (without any index matching material) is inserted into the line joining this fiber to itself, loss indications are less than 1 db. Upon repeated engagement and disengagement, the insertion loss reading holds very steady. A maximum standard deviation of 0.02 db is typical before and after repeated engagements. An excursion from the original reading as low as 0.05 db has indicated some type of contamination.

Joining fibers of the same size is not what is normally encountered in every day use. The plastic fiber diameter range is reported to be from 380 μm (.0150") to 420 μm (.0165"). Mating any fiber size to any other fiber size in this range should result in an insertion loss of under 2 db. This includes the light escaping when joining a large to a small fiber plus other normal losses encountered in a dry (no matching index-material) connection. Engaging many other connector halves containing various fiber diameters to one specific connector has resulted in repeatable readings with only 0.07 db maximum standard deviation. Tests have been conducted joining fibers ranging in diameter from 330 μm (.0120") to 445 μm (.0175"). No insertion loss has been over 3 db when joining such a wide range of fiber diameters.

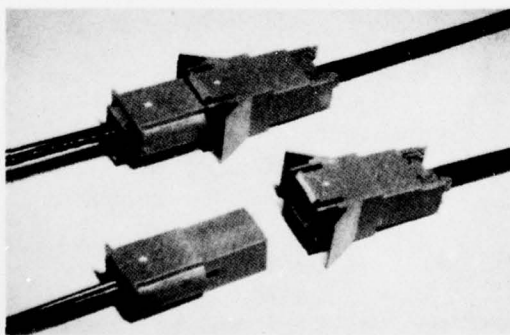


Figure 5. Duplex Optical Self Centering Overlap Style Connector.

Fiber Construction Design Demands

The end finishing of the fiber varies from one type to another and within the same types. The all-plastic fiber can be just cut, or cut and treated or polished. The author has found that for the plastic fiber, the polish technique gives reliable consistent results. The fiber is confined, trimmed and polished with 600 grit, then 3.0 μm , and finished with 0.3 μm silicone carbide paper. It is a relatively easy task, taking a total of under five minutes to terminate a dual channel cable. Just a plain razor cut will give decent results but the polish finish is preferred for the more sophisticated applications.

The all-glass fiber is very easy to scribe and break. Good clean square breaks may be consistently accomplished along with the accurate location of the point of break. A tool has been built and used for prototype and test use, that breaks the fiber at a specific location from a datum surface on the connector. Location control is about .0005". While polish of small glass fibers is possible, the scribe and break technique is the least tedious.

Plastic-clad silica comes in many forms. Some have fairly hard cladding that can be at least gently held. Other clads are soft and easily destroyed in handling. Problems show up in gripping, bonding, polishing, scribing and breaking, and aligning that are different to some degree for each manufacturer's product. For a scribe and break of plastic-clad silica, the flaw is put into the core vs. the cladding in an all glass fiber. Polish grit creeps between core and cladding. How do you hold a fiber where the core slides in and out of the cladding? But, the big core is favored and it will be used.

CONCLUSIONS

Various designs and methods of aligning single optical fibers have been discussed. The many variations themselves indicate the ardent search for a better or improved method. The optical self-centering overlap style connector technique of fiber alignment has been presented in this paper. It has shown promise of consistently low insertion loss values. Testing of different size and type fibers in this alignment feature are continuing. Other connector configurations utilizing this alignment method are being designed and considered for additional field requirements.



William L. Schumacher is the innovative type engineer. His exposure to the many facets of the termination and connector industry have sparked a broad range of patented products. Basic crimps, mass termination techniques, high-voltage connectors, coaxial cable, coaxial connectors, and assembly methods are typical patent areas. The fiber optic field is one of his latest areas of concentration and contribution.

Bill is a Senior member of IEEE and has participated with the Parts Hybrids and Packaging Groups, E/EIC and the IEEE Computer Society. He obtained his BSEE from the University of Missouri, Columbia. He has authored offered and invited technical papers .

REFERENCES

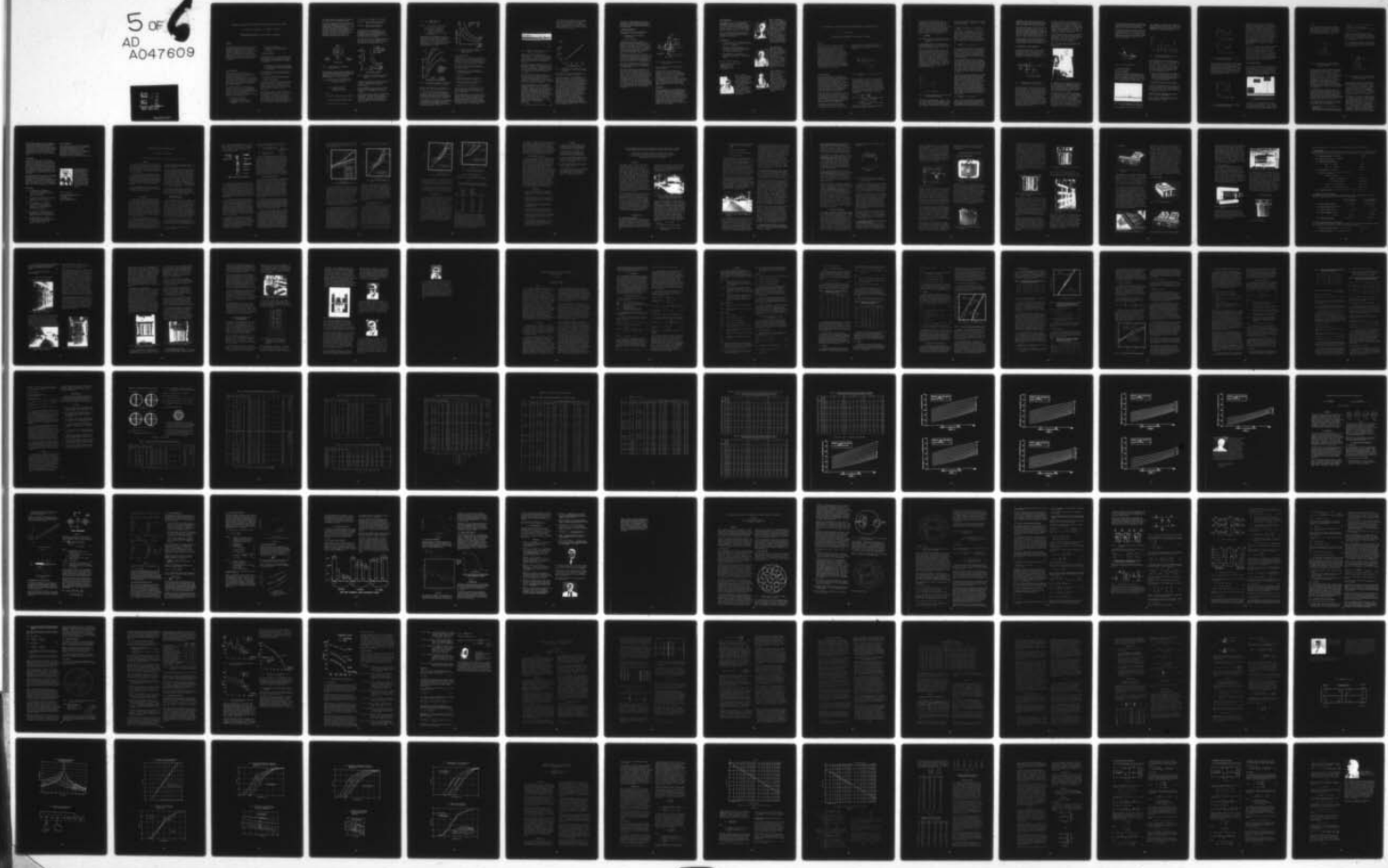
1. Y. Kohanzadeh, HOT SPLICES OF OPTICAL WAVEGUIDE FIBERS, March 1976, Volume 15, No. 3 APPLIED OPTICS pages 793-795.
2. D. L. Bisbee, SPLICING SILICA FIBERS WITH an electric arc, March 1976, Volume 15, No. 3 APPLIED OPTICS pages 796-798.
3. A. Tardy, R. Jocteur, OPTICAL FIBER SPLICING WITH PLASMA TORCH AND OXYHYDRIC MICRO-BURNER, Sept. 1976, 2nd European Conference on Optical Fiber Communication, V111. 5.
4. T. Kemura, Sohara, RECENT ADVANCES IN OPTICAL FIBER TRANSMISSION TECHNOLOGY, January 1976, Japan Telecommunications Review.
5. F. L. Thiel, R. M. Hawk, OPTICAL WAVEGUIDE CABLE CONNECTION, November 1976, Volume 15, No. 11 APPLIED OPTICS.
6. D. Pinnow, U.S. Patent 3,810,802, May 1974.
7. J. F. Dalgleish, H. H. Lukas, J. D. Lee, SPLICING OF OPTICAL FIBERS, London, Sept. 1975, First European Conference on Optical Fiber Communication.
8. C. M. Miller, LOOSE TUBE SPLICES FOR OPTICAL FIBERS, Sept. 1975, Volume 54, No. 7 BSTJ page 1215.
9. C. G. Someda, SIMPLE LOW LOSS JOINTS BETWEEN SINGLE-MODE OPTICAL FIBERS, April 1973, B. S. T. S.
10. C. M. Schroeder, ACCURATE SILICON SPACER CHIPS FOR AN OPTICAL FIBER CABLE CONNECTOR, Feb. 1977, Optical Fiber Transmission II Technical Digest, Williamsburg, Va., WA6.
11. S. F. Dalgleish, CONNECTIONS: WELL DESIGNED SPLICES CONNECTORS MUST ALIGN FIBERS EXACTLY, August 5, 1976, ELECTRONICS page 96.
12. K. Miyazaki, M. Honda, T. Kudo and Y. Kawamura, THEORETICAL AND EXPERIMENTAL CONSIDERATIONS OF OPTICAL FIBER CONNECTOR, January 1975, Optical Fiber Transmission, Williamsburg, Va. WA4.
13. H. Tsuchiya, H. Nakagome, N. Shimizu, S. Ohara, DOUBLE ECCENTRIC CONNECTORS FOR OPTICAL FIBERS, May 1977, Volume 16, No. 5, APPLIED OPTICS page 1323.
14. K. Fenton, R. McCartney, CONNECTING THE THREAD OF LIGHT, Ninth Annual Connector Symposium Proceedings, October 20-21, 1976, pages 64-72.
15. F. L. Thiel, R. M. Hawk, OPTICAL WAVEGUIDE CABLE CONNECTION, APPLIED OPTICS, November 1976, Volume 15, No. 11 pages 2785-2791.
16. W. L. Schumacher, FIBER OPTIC CONNECTOR DESIGN TO ELIMINATE TOLERANCE EFFECTS, Tenth Annual Connector Symposium Proceedings, October 1977.
17. Assembly Instruction Sheet, AMP Incorporated IS 1732.

AD-A047 609 ARMY COMMUNICATIONS RESEARCH AND DEVELOPMENT COMMAND --ETC F/G 9/1
PROCEEDINGS OF INTERNATIONAL WIRE AND CABLE SYMPOSIUM (26TH) CH--ETC(U)
NOV 77 E F GODWIN

UNCLASSIFIED

5 of 6
AD
A047609

NL



INFLUENCE OF JACKETING ON THE TRANSMISSION LOSS OF LOW-LOSS OPTICAL FIBERS

B. Hillerich, P. Rautenberg, D.S. Parmar, P. Schlang

AEG-TELEFUNKEN KABELWERKE AG 4330 Mülheim, W. Germany

Summary

The attenuation increase of tight jacketed optical fibers due to eccentricity and diameter fluctuations of the jacket are estimated. Loss increase is further caused by bubbles between the fiber and the jacket. Tolerances due to these inhomogeneities are specified so that only small loss increase occurs. Possibilities are mentioned to control the eccentricity, the diameter's constancy and the formation of bubbles.

- c) to set the limits
- d) to control the limits with the help of special devices and processes

2. System analysis

Microbendings caused due to inhomogeneities in the jacket are considered as the only relevant reason for attenuation-increase. The following inhomogeneities are taken into account:

- a) Diameter fluctuation of the jacket
- b) Void formation on the fiber surface
- c) Contamination like burnt particles in the melt

The inhomogeneities mentioned under item 3 are rare and do not cause any remarkable loss increase.

3. Theoretical and empirical relations

Diameter Fluctuation

As already reported /1/ diameter fluctuations alone do not cause high attenuation increase but these in addition to eccentricity of the fiber in the jacket lead to additional loss. The reasons for this effect are described in the following.

Thermoplastics used for the jacketing of optical fibers shrink during cooling from the processing temperature to room temperature. For Nylon-12, for example, the shrinkage value lies between 0.5% and 1.6%. The shrinkage value depends upon the cooling process after the extrusion. After reheating at a later stage, for instance during the jacketing process of

1. Introduction

Before cabling optical fibers are generally provided with a plastic jacket either in form of a hollow tube or a tightly extruded layer of 0.1 ... 0.6 mm thickness. It depends more or less on the cable construction which of the two types of jacket is to be selected. We prefer the tight jacket and hence our investigations were conducted basing on this type and are discussed hereby.

It is known that tight jacketing of optical fibers may cause an attenuation increase. For the cable manufacturer it is not a question to avoid these additional losses at all, but somehow to find out an economical optimized technique to achieve a permissible attenuation increase. Therefore it is necessary

- a) to know the reason for attenuation increase
- b) to quantify the correlation attenuation increase/causing parameters

the cable itself, the amount of shrinkage may change due to recrystallization.

If during jacketing, the optical fiber is not exactly centred within the jacket, the neutral axis defined by theory of elasticity is not congruent with the center of the cross-section of the jacket, because of the much higher Hook's modulus of silica compared to the jacketing material. But it lies between the axis of the jacket and the axis of the fiber, which do not coincide in case of an eccentric extruded jacket (Fig. 1).

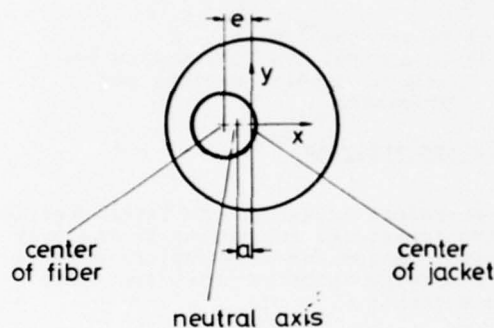


Fig. 1: Cross-section of eccentric jacketed fiber

The stresses induced by the shrinkage cause forces which are compensated by elasical forces of fiber and jacket. This leads to bending of the fiber. The resulting bending radius R is calculated as:

$$(1) \quad R = \frac{4e^2 [(E_1 - E_2)(B-1)^2 + E_2 R_2^2 B^2 / R_1^2]}{4e \epsilon [E_2(1-A) + E_1 A]} + \frac{(E_1 - E_2)R_1^2 + E_2 R_2^2 / R_1^2}{4e \epsilon [E_2(1-A) + E_1 A]}$$

Where

$$A = E_2(R_2^2 - R_1^2) / [E_1 R_1^2 + E_2(R_2^2 - R_1^2)]$$

$$B = R_1^2(E_1 - E_2) / [E_2 R_2^2 + R_1^2(E_1 - E_2)]$$

ϵ = eccentricity of the fiber

ϵ = relative shrinkage of the jacket

E_1 and E_2 = Hook's moduli of the fiber and jacket respectively

R_1 and R_2 = Radii of the fiber and jacket respectively

It follows that the curvature C, the reciprocal of the bending radius, is proportional to the shrinkage ϵ of jacketing material and nearly inversely proportional to the eccentricity e of the fiber within the jacket.

If Nylon 12 is taken as jacketing material the curvature can be calculated as a function of the jacket radius R_2 and the eccentricity e as shown in Fig. 2.

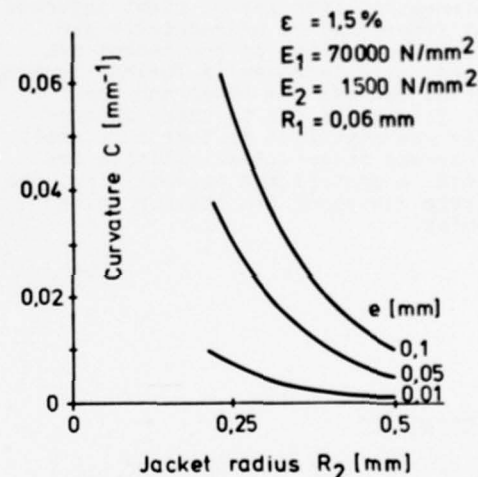


Fig. 2: Curvature of eccentric jacketed fiber as function of jacket radius

In case of a larger eccentricity a change in jacket radius leads to a greater change in curvature as by lower eccentricity.

Thus fluctuations in the jacket diameter in case of any eccentricity cause fluctuations in curvature, i.e. micro-bendings.

As shown by several authors microbendings induce mode-coupling and can lead to attenuation increase. To approximate this attenuation increase α , in case of multimode fibers with parabolic index profile a formula given by Marcuse /2/ can be used:

$$(2) \quad \alpha = \frac{1.45 \cdot a^2 \cdot K_c}{\bar{\Lambda} \cdot \Delta^2}$$

with
 a: core radius of the fiber
 K_c : variance of curvature
 $\bar{\Lambda}$: mean period length of diameter fluctuation
 Δ : relative refractive index difference

The variance of curvature K_c can be calculated with the help of equation (1) with given eccentricity and diameter fluctuations. Some results are plotted in Fig. 3. It can be seen that an eccentricity of 0.1 mm leads to 100times higher variance of curvature than an eccentricity of 0.01 mm.

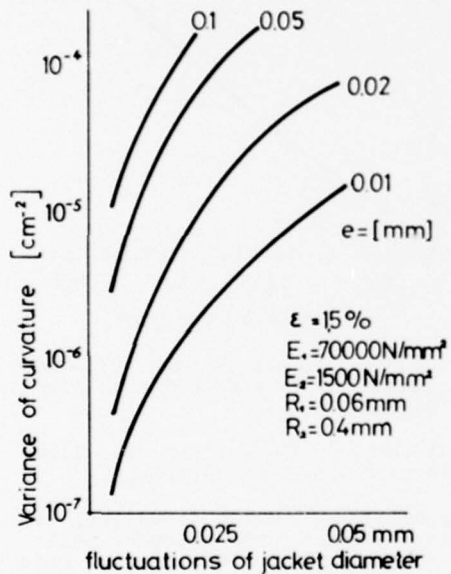


Fig. 3: Variance of curvature as function of jacket diameter fluctuations

Beside other reasons the parameter $\bar{\Lambda}$ depends upon line speed and screw speed.

With the used machinery $\bar{\Lambda}$ amounts to 1...10 cm. If the melt stream coming out of the die head is turbulent, jacket diameter fluctuations of a period-length in mm-range sometimes occur. This usually causes very high attenuation increase.

If an attenuation increase of 1 dB/km due to jacketing is accepted, with help of this theory upper limits concerning eccentricity and jacket diameter fluctuations are stated as shown in Fig. 4.

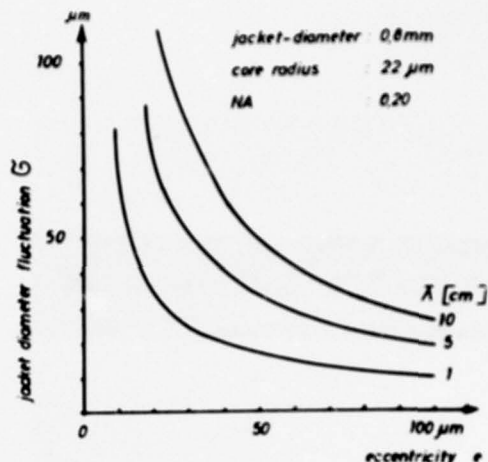


Fig. 4: Jacket diameter fluctuation vs. eccentricity for 1 dB/km additional loss

Voids and bubbles

How far voids in the jacket give rise to additional loss, is being examined at present. Up to now it was found that voids with less than 0.3 mm length usually do not lead to a perceptible loss increase.

Following reasons are considered as causes for void and bubble formation at the fiber surface:

- a) Vapourization of the unreacted pre-coating solvents or decomposition of the pre-coating
- b) Humidity
- c) Faulty vacuum setting in case of a particular extrusion process
- d) Turbulence in the melt coming out of the extruder cross head
- e) Quenching of the jacketing /3/

The typical shape and appearance of the void or bubble can help in finding out which of the above five reasons cause bubble formation.

The unreacted solvents or decomposition of pre-coatings normally cause drop-shaped bubbles which stand with their tip on the fiber's surface. Bubbles formed due to humidity, quenching, and faulty vacuum setting are of very irregular shape and partly enclose half of the fiber and have a scattered range of length (Fig. 5).

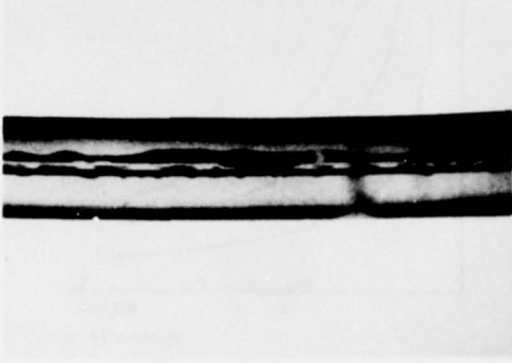


Fig. 5: Bubbles in fiber jacket due to faulty vacuum setting

Finally the bubbles caused due to turbulence in the extruded melt occur rather regular and enclose the fiber fully. Such a jacketed fiber seems to be partly hollow and partly tight jacketed with a period length in the range of few cms.

Bubbles, caused by vapourization of the unreacted solvents in the pre-coating can be easily avoided by pretempering of the fiber to be jacketed. In order to prevent decomposition of the pre-coating it has to be chosen for sufficient temperature stability.

High attenuation increase has been measured in case of bubbles caused due to wet fiber surface. These bubbles can be avoided using pretreatment like dry storage, air-conditioning of the extrusion line hall, or even tempering the fiber just before it enters the cross-head.

The third possibility namely faulty vacuum setting, can only be avoided by respective measures during extrusion. Thereby it has to be noted that in order to prevent unnecessary melt pressure, tube extrusion is preferred. The tubing die produces a tubular shape which is then drawn down in conical shape to contact the fiber shortly after its exit from the die. The die permits the use of vacuum to obtain tight jacket and to control the length of the extruded cone. Best results can be performed adjusting the vacuum so that a constant correction is maintained.

Fig. 6 shows an optimal setting of vacuum

for various fiber diameters to guarantee a constant cone length. It can be seen that a slight fluctuation in fiber diameter or an uneven fiber surface can cause irregularities in the cone length which could give rise to bubble formation and diameter fluctuation.

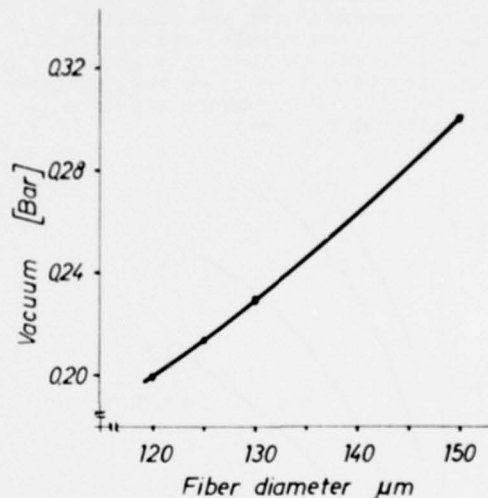


Fig. 6: Optimal vacuum setting for fiber jacketing as a function of fiber diameter

Obviously for a different extruder line, the above plot would be different.

The fourth type of bubble formation, i.e. due to turbulence in the extruder melt appears as soon as the melt outflow rate exceeds a certain velocity: At this point the laminar flow changes to turbulent flow. The extruded melt partly touches the fiber and hence the air gap which is not yet evacuated is enclosed by the melt. This prevents the complete evacuation of the gap. The result is, as stated before, a periodically hollow and tight jacket causing an extremely high increase of attenuation. This can be avoided by reducing extrusion line speed. However, for the line speed a lower limit is determined by the fact that other periodicities as diameter fluctuations induced by the screw revolution have critically low spatial period-length. As mentioned above, diameter fluctuations with low spatial period-length could give rise to additional loss.

The type of bubble formation which is caused by a cooling-shock can be avoided by using a sufficiently slow cooling procedure, e.g. a modified water cooling or air cooling.

5. Measuring devices

As discussed above, the influencing parameters to be controlled are

- a) Eccentricity and diameter fluctuations
- b) Bubble formation

Special devices were developed for controlling both. The eccentricity in two planes is controlled with help of TV cameras. The TV monitors are placed just beside the extruder, so that the operator is able to adjust the line for optimal eccentricity. Due to optical distortion the fiber appears thicker than in reality within the transparent jacket.

Therefore the eccentricity can not be measured by this device. On the other hand, a concentric jacketed fiber would, in any case, appear concentric on the monitor too, i.e. the optical distortion does not prevent the adjustment of concentricity.

Once the eccentricity of the fiber within the jacket is optimized, it would not alter normally, even for the jacketing of the next fiber.

For fine adjustment and examination for bubbles, another device has been built. Fig. 7 shows a schematic sketch of the device. It is a projector whereby the fiber under test is illuminated and projected onto a screen at two perpendicular planes. The cell is filled with a liquid whose refractive index is matched to the refractive index of the jacketing material. Therefore the jacketing material appears very faint on the screen whereas the fiber is clearly visible. Due to index matching by the liquid, optical distortion does not occur and eccentricity can be exactly evaluated.

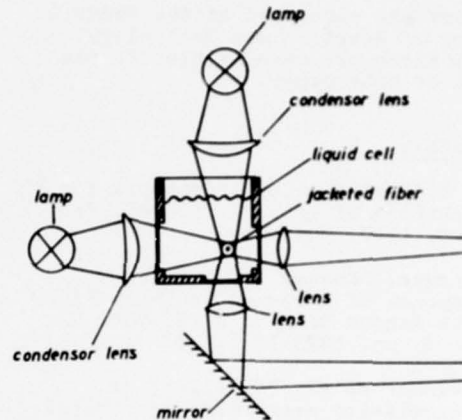


Fig. 7: Device for quality check of fiber jacket

The same device is used to check the bubble formation.

In this case, it is necessary to investigate the fiber not in motion. Otherwise the bubbles would appear as shadows on the screen. A short length of jacketed fiber in the beginning of the extrusion procedure is cut and investigated in static position. It has not been noticed that a bubble free jacket in the beginning, showed bubbles at a later stage of the jacketing, unless diameter fluctuations of the precoated fiber occur.

Conclusion

The tight jacketing of optical fibers without remarkable loss increase demands very high quality standard concerning the jacket. Usually the eccentricity should not exceed $10 \mu\text{m}$, and fluctuations of the outer diameter should remain below about $30 \mu\text{m}$. These requirements which are reaching the limits set by the extrusion process lead to new special extrusion heads, new measurement devices, and, compared to the jacketing of copper wires, unusual low line speeds.

Acknowledgement

The authors wish to thank the staff of the development centre of AEG-TELEFUNKEN KABELWERKE for helpful discussions and help in the experimental work. The authors are also obliged to the AEG-TELEFUNKEN Research Institute at Ulm for providing optical fibers to carry out this research.

This work was sponsored by the Federal Ministry of Research and Technology. The authors alone are responsible for the content of this paper.

References:

- /1/ B. Hillerich et al, "Criteria for the jacketing of optical fibers", Proc.III. ECOC, 1977, München
- /2/ Marcuse, "Losses and Impulse Response of a Parabolic Index Fiber with Random Bends", BSTJ, Vol. 52, No. 8, pp. 1423-38 (1973)
- /3/ Rokunohe et al, "Stability of transmission properties of optical fiber cables", Proc. II. ECOC, 1976, Paris

Authors' mailing address:

AEG-TELEFUNKEN KABELWERKE AG
Development Center
Sommerfeld 22-28
D-4330 Mülheim/Ruhr
W. Germany



Peter Schlang, born in 1944, studied Electrical Engineering at the RWTH Aachen. 1970 he graduated as Diplom-Ingenieur. Since joining AEG-KABEL he has worked in the laboratories for communication and coaxial cables, later on for fundamental development. Now he is responsible for the section of fundamental development.



Daljit S. Parmar, born in 1945, received his B. Tech. degree in Chemical Engineering from the University of Madras (India) in 1968 and M.Sc. in Chemical Engineering from the University of Bradford (U.K.) in 1970. He joined AEG-KABEL as a member of the Development Centre in 1971. He is engaged in the process development in various fields of cable manufacture, specially the jacketing of optical fibers.



Peter Fautenberg was born in 1948. After qualifying as radio-TV technician in 1970, he joined Fachhochschule Düsseldorf and received his Ing.(grad.) in Communication Engineering in 1973. In the same year he joined AEG-KABEL as development engineer. He is engaged in the development and testing of optical fiber cables.



Bernd Hillerich, born in 1950, studied Physics at Bonn University and graduated as Dipl.-Phys. in 1974. He joined AEG-KABEL development centre in 1975. Since then he is engaged in development of measuring and testing methods for optical fiber cables and in fundamental problems concerning optical fiber cable design.

ON SITE LOCATION OF OPTICAL FIBER DEFECTS AND EVALUATION OF TRANSMISSION LOSS

B. Hillerich

AEG-TELEFUNKEN KABELWERKE AG 4330 Mülheim, W.Germany

Abstract

Methods for checking optical fibers concerning faults and transmission loss are described and compared. It is reported about an optical measuring apparatus, by means of which fiber faults can be analyzed and located and the transmission loss can be evaluated by the pulse reflection or backscattering method. The measured loss values for some fibers are compared with the loss values obtained with the conventional 2-point-measurement. Whereas the pulse reflection method seems to be well suited for on site measurement with laid cables, the backscattering could become the standard method for loss measurement in laboratory because of its advantages compared with other methods.

fractures has already been described two years ago /1/. In this case (fig. 1) light pulses are launched into the fiber under test.

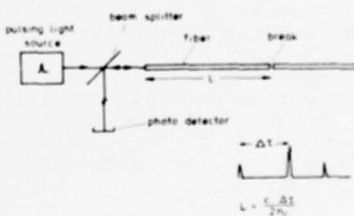


Fig. 1: Principle of optical fiber break location

1. Introduction

For the development and production of optical fiber cables it is necessary to measure the fiber parameters which can be influenced during the processing of optical fibers to cables. One of these parameters is the transmission loss. The loss can change extensively during the individual production stages. For example a loss increase over the whole fiber length may occur due to microbendings or local loss increase may be caused by fiber fractures or other defects.

Hereby methods will be described to locate such local defects. Moreover it will be discussed which methods suit for quick loss measurement. Finally an apparatus is described which since last year has been in use for laboratory and on site fiber fault location and loss measurement. Practical results are reported.

2. Methods to locate fiber defects

The "reflection method" to locate fiber

At the position of a break, a small part of the incident light is reflected. The reflected amount of the light pulses reappears at the input end of the fiber and is detected by a sensitive photo detector. This method corresponds to TDR with high frequency cables. The distance L between the input end of the fiber and the position of break is evaluated from the time interval Δt between pulse emission and re-appearance of the reflected light pulse as follows:

$$(1) \quad L = \frac{c \cdot \Delta t}{2} \approx \frac{c_0 \cdot \Delta t}{2 n_c}$$

where c = Effective propagation velocity of light in the fiber

c_0 = Vacuum light velocity

n_c = Refractive index in the centre of fiber core

For silica fibers of $n_c \approx 1.46$, Δt approximates to $1 \mu s$ for $L = 100 m$.

The power of light reflected from a fracture as per Snellius law amounts to a maximum value of 3.5% (7% in case of constructive interference between both fiber surfaces) of incident power. In case of an inclined fracture, the reflected power is lower. Marcuse showed /2/ that above a critical angle α_t no reflection from the fracture can be detected. The critical angle can be approximated:

$$(2) \quad \alpha_t \approx \sqrt{2\Delta}$$

where Δ is the relative refractive index difference between fiber core and cladding.

In such cases and also in case of some splitted fractures it is not possible to locate the position of fracture with the help of pulse-reflection.

These faults can be located by means of the back scattering method. Barnoski and Morrison suggested this method for loss measurement /3/. Herby light pulses are launched into the fiber likewise. The power of backscattered light within the fiber due to Rayleigh scattering is recorded as a function of the time delay in respect to pulse emission. At the time delay, which corresponds to a position of a fracture, an abrupt change in the backscattered power occurs. Fig. 2 shows the backscattering of a fiber with non-reflecting fracture.

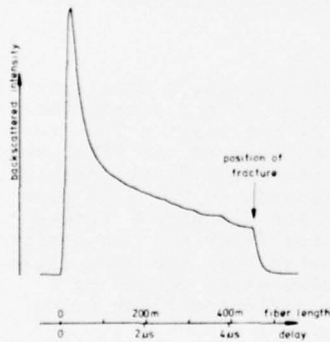


Fig. 2: Backscattered light of a fiber with a non-reflecting break

The power of backscattered light is very small in comparison to the incident light. It is 40 ... 50 dB lower, depending on the loss induced by scattering of the fiber, its numerical aperture, and the duration

of the light pulses. Therefore the signal/noise-ratio should be improved e.g. using a boxcar-averager.

3. Methods to measure the transmission loss

The "2-point measurement" is the conventional method of evaluating the transmission loss of optical fibers. The light power I_1 , coming out at the far end of the fiber is compared with the light power I_0 coming out after a few meters without changing the launching condition at the input end. The loss then amounts to

$$(3) \quad \alpha [\text{dB}] = 10 \log (I_1/I_0)$$

Since the light coupling at the input end is unchanged in both cases, the measurement is very accurate. A disadvantage is that the fiber has to be cut some meters behind the input end for measuring the power I_0 . This method, therefore, is not non-destructive and hence less suited for field measurement.

This disadvantage can be avoided if the power coupled into the fiber is measured only once to obtain I_0 , and for every loss measurement an optimal adjustment of light power launching is done at the input end ("Insertion-loss method"). The adjustment of optimal launching requires a measurement-value transfer from the far end of the fiber, which is mostly unsuitable in case of buried cable sections or cables in ducts.

Such difficulties can be omitted, if light power launching and detection can take place at the same fiber end as with the pulse reflection method /4/. The same apparatus as for fault location can be used. At the far end of the fiber a plane mirror is fixed perpendicular to the fiber's axis, which reflects the light pulses coming out of the fiber back into the fiber. The light pulses coming out of the input fiber end have suffered an attenuation which corresponds to twice the fiber length. Comparing the height of these pulses I_1 with the pulse height I_0 for a short fiber lenght the loss can be evaluated as

$$(4) \quad \alpha [\text{dB}] = 5 \log (I_1/I_0)$$

With the above mentioned backscattering method only one fiber end is needed for measurement. From the decrease of the backscattered signal as function of the time-delay, the transmission loss can be

evaluated, considering that the ratio between incident and backscattered light power is constant over the fiber length (which should be true in most cases).

With this method the uniformity of loss over the fiber length can be checked, and defects as scattering centers can be localized. Another advantage in comparison with the insertion loss method proves to be that incorrect measurement results because of non-optimal adjustment of light power launching are nearly impossible.

A disadvantage is the low measurement range because of the extremely low power of backscattered light. Therefore a costly signal averager seems to be necessary.

4. Description of the apparatus

A measuring apparatus has been developed, by means of which fiber fractures and other faults can be localized and the transmission loss can be evaluated by pulse reflection and backscattering. The principle of operation is shown in fig. 3.

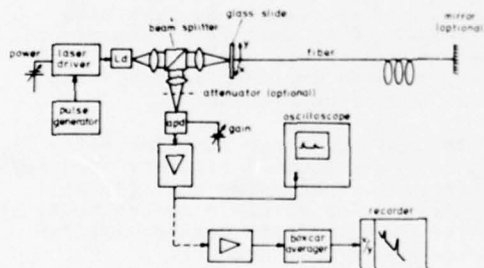


Fig. 3: Apparatus for fiber fault location and loss measurement

A SHJ-laserdiode (Ld) with an emission wavelength of 904 nm is driven by current pulses of $I_{peak} = 10 \text{ A}$ and a repetition rate of 3 kHz. The light pulses emitted by the laserdiode have a halfwidth of 50 ns and are launched into the fiber by two microscope lenses ($NA = 0.25$). The light power coupled into the fiber amounts 50 ... 150 mW depending on core diameter and numerical aperture of the fiber under test. The light power reappearing at the input end of the fiber due to backscattering and reflection is splitted by a beam splitter, a part is focussed on an avalanche photodiode (apd).

The gain of the avalanche photodiode and the light power of the laserdiode is variable in order to avoid overload and nonlinearity, if the set is used for loss measurements. If necessary, an additional 20 dB-optical attenuator can be used. The signal - after amplification - is displayed on an oscilloscope, which provides a digital display of the delay.

With the help of this feature the distance between the input end of the fiber and fractures or other faults can be evaluated very easily. In order to improve the signal/noise-ratio the signal can be processed by a boxcar averager.

Fig. 4 gives an idea of the rather compact and rugged optical assembly of the apparatus.

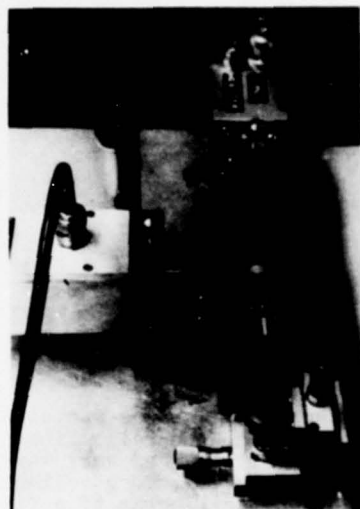


Fig. 4: Optical assembly

The dimension of the base plate is 20x26 cm. The laserdiode together with the laserdriver and the avalanche photodiode with a preamplifier are placed within well shielded housings in order to avoid signal interference by strong current pulses of the laser driver.

The input end of the fiber is put into a micropositioner of the "v-groove-type" which is adjustable in x- and y-direction. A coated glass slide serves as stop in z-direction. By this a well defined position of the fiber in z-direction and also a small amount of reflection at the fiber input end is obtained. Only 0.4% of the light power coupled into the fiber is reflected. This is a rather low value compared with the 3.5% - reflection at a

single glass/air-boundary. Strong reflections at the fiber input cannot be tolerated with backscattering measurement because of the very low signal level.

For loss measurement by pulse reflection a plane mirror is fixed at the far fiber end perpendicular to the fiber axis by a mount shown in fig. 5. If index matching liquid is attached between mirror surface and fiber a reflection nearly without loss is obtained.

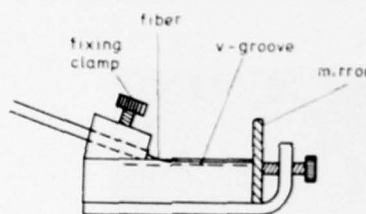


Fig. 5: Fiber mirror mount

5. Practical results

5.1 Fault location

During 12 months the apparatus was used for fracture location, non-reflecting breaks (as in fig. 2) occurred very rarely. Typically, breaks showed strong reflections. A reflection oscillosogram of a fiber with several breaks is shown in fig. 6.

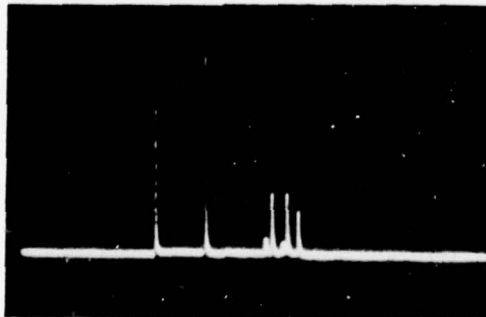


Fig. 6: C.r.t. display of a fiber with several breaks (Hor.: 1μs/div.)

Sometimes multiple reflections between

two fractures or between the fiber's end and a fracture, which simulate additional fractures, are observed. Fig. 7 gives an example. Such multiple reflections can be identified in the following way:

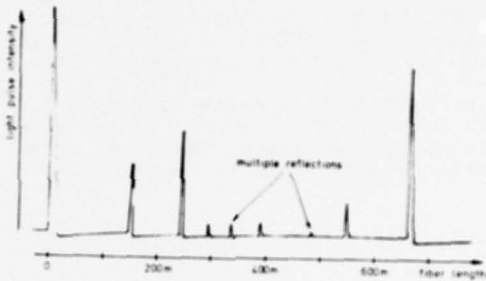


Fig. 7: Pulse reflection display with multiple reflections

The time delay of the n reflections of a fiber shall be $T_1 \dots T_n$. The differences $\tau_{ij} = |T_i - T_j|$ with $1 \leq i, j \leq n$ are evaluated. τ_{0j} is stated as $\tau_{0j} = T_0$. If (3) $\tau_{ij} = \tau_{ijk}$ for any i, j, k with $0 \leq i < j < k \leq n$, then T_j is assumed to represent a multiple reflection. There are two reasons why this analysis can lead to erroneous results:

1. With this apparatus the time delay T_i cannot be evaluated with any accuracy. Therefore, when using equ. (3) as criterion for multiple reflections, the error of time-delay measurement has to be taken into account.
2. A position, where equ. (3) is valid, can coincide with a real fracture.

Besides fiber fractures other defects may occur, for example local defects, which originate from the fiber drawing process, or fiber sections of high loss caused due to improper jacketing.

Such defects are localized by analysis of the backscattering-signal.

In fig. 8 the backscattering of a fiber with a defect, originating from the drawing process is shown.

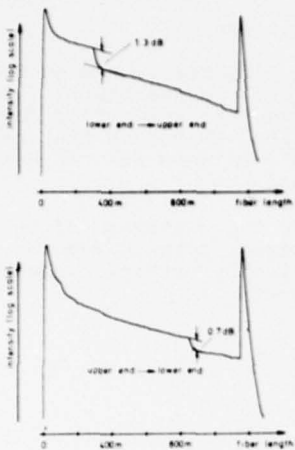


Fig. 8: Backscattered power of a fiber with a local defect

It is interesting that this defect causes a higher jump of intensity in one direction (lower end \rightarrow upper end) along the fiber than in the other direction. Fig. 9 represents the backscattering of a fiber, which is improperly jacketed at one end section. The loss at this section equals 10 dB/km, whereas the loss of the main part amounts to 3.6 dB/km.

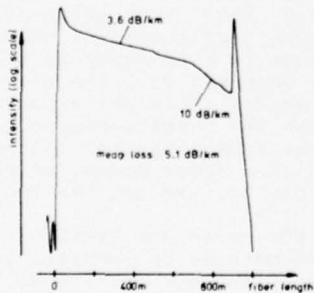


Fig. 9: Backscattered power of a fiber with lossing section

The accuracy of fault location mainly depends on the accuracy of time-delay evaluation. Because with the oscilloscope used along with this apparatus (HP 1722) the delay is generated and measured by analog circuits (only the display is digital), the accuracy is not better than $\pm 0.3\%$ or $\pm 1\text{ m}$, if the delay is below $3\text{ }\mu\text{s}$. So, a fracture, which has a distance of about 600 m from the fiber's end, can be localized within $\pm 2\text{ m}$. In practice this error often is sufficiently small [A fiber fault locator with digital delay measurement is under development at AEG-TELEFUNKEN. The accuracy of delay measurement is expected to be within $\pm 0.01\%$].

The dynamic range of our apparatus amounts to 60 ... 70 dB for a $(S+N)/N$ -ratio of more than 2:1, depending on the core radius and numerical aperture of the fiber to be examined. So, with fibers of $NA = 0.21$, core radius $a = 20\text{ }\mu\text{m}$ and transmission loss $\alpha = 6\text{ dB/km}$ fractures within a distance of about 4 km can be localized. By means of a boxcar-averager the $(S+N)/N$ -ratio is remarkably improved, whereby the dynamic range rises up to 75 ... 85 dB.

5.2 Loss measurement

The pulse reflection method proved to be well suited for the fast loss measurement in the field. Only a few components (a pulsing laser diode, some simple optical components, and an oscilloscope) are needed. In fig. 10 an example of a pulse reflection oscillogram is shown.

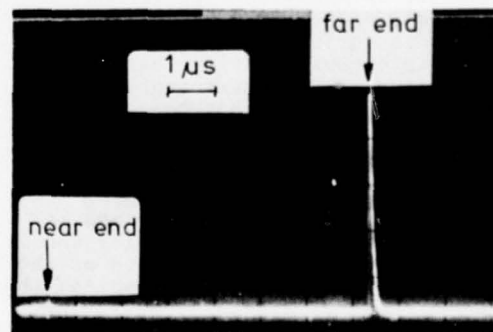


Fig. 10: Loss measurement with pulse reflection. Display on c.r.t.

The fiber has a length of 707 m. This results in a time delay of $7\text{ }\mu\text{s}$ between input (pulse at the left in fig. 10) and the pulse reflected by the mirror at the far end of the fiber (high pulse at the

right).

For some fibers with step- and graded-index profile the agreement of the loss value evaluated by the pulse reflection method and the conventional 2-point-method was tested. The histogram of the loss value differences is shown in fig. 11.

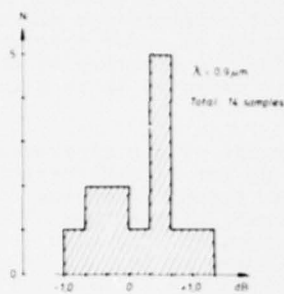


Fig. 11: Difference in loss measurement between conventional and pulse reflection method

For the 2-point-method a wavelength-filtered incoherent light source was used. The low launching aperture of $NA = 0.15$ did not fill the NA of the fibers, which amounted to $0.17 \dots 0.26$. The differences in loss value between the two methods are within -1.0 dB and $+1.2$ dB. The mean absolute difference is 0.53 dB. So the agreement is quite acceptable. It has to be taken into consideration that the average error of 2-point-measurement amounts to 0.2 dB and that the different launching conditions can lead to different loss values in the order of several tenths of one dB /%.

The apparatus has a measuring range of 25 dB. This figure seems to be low and is caused by the go- and return path of the light pulses along the fiber. Besides the measuring range of a 2-point-measuring apparatus with wavelength-filtered tungsten lamp as light source and lock-in-detection-technique has about the same value.

Loss measurement by analysis of the back-scattering exhibits following advantages in comparison to other methods:

1. Only one fiber end is required for measurement
2. Reproducible and accurate results even with non optimal light power launching

3. Display of the length dependence of loss
4. Evaluation of fiber length
5. Faster than other methods (see 1. and 2.)
6. Non-destructive

Due to these advantages this method competes with the conventional 2-point-measurement as standard method for fiber-loss evaluation. Therefore the agreement of loss values between the two method is of interest.

Fig. 12 shows the histogram of the loss-value differences between 2-point-method and backscattering method, evaluated for a lot of fibers.

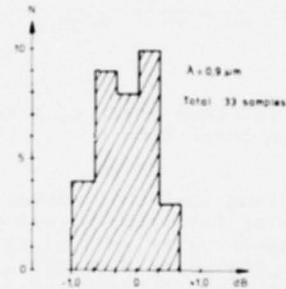


Fig. 12: Difference in loss measurement between conventional and back-scattering method

These fibers, produced by 4 different manufacturers, have core radius $a=20 \dots 35 \mu\text{m}$ and numerical apertures of $NA=0.2 \dots 0.3$. There is a tendency to higher loss values measured with the back-scattering method. This was expected because, with the 2-point-measurement, the NA of the fibers was not filled and therefore higher order modes, which are sometimes lossier, are not excited.

Altogether the agreement between these so different methods is remarkably good. The maximum difference is -1.0 dB and $+0.7$ dB respectively, the mean absolute difference amounts to 0.35 dB. This agreement is far better than with the first results reported by Barnoski et al /3/. It may refer to the different launching conditions. Barnoski launched the light pulses by a tapered fiber section into the fiber thus exciting mainly the lossier higher order modes.

The measuring range of our set amounts to 12 dB, mostly restricted by the dynamic range of the logarithmic amplifier. It is desirable to blend out parts of the signal, mostly the input reflection, that in spite of the low dynamic range fibers with total loss higher than 12 dB can be analyzed part by part. Modifications concerning this point are under development.

Conclusions

It has been shown that with a single rather simple apparatus as well fiber faults like fractures, scattering centers and lossy sections can be detected and located, as the transmission loss can be measured. This apparatus mainly consists of a pulsed laserdiode, some simple optical components and an oscilloscope. For exact analysis of backscattering, however, an additional signal averaging device is necessary.

For loss measurement, the pulse reflection method proved to be suited for laid optical fiber cables, thus for on site measurement. The backscattering method has, compared to other methods, several advantages, which give rise to the expectation that this method will become the standard method for loss measurement in laboratory.

References

- /1/: J. Guttmann, O. Krumpholz, "Location of imperfections in optical glass-fibre waveguides", Electron.Lett., Vol. 11, pp. 216-217 (1975)
- /2/: D. Marcuse, "Reflection losses from imperfectly broken fiber ends", Appl.Opt., Vol. 14 (1975)
- /3/: M.K. Barnoski, R.M. Morrison, "Fiber waveguides, a novel technique for investigating attenuation characteristics", Appl.Opt., Vo. 15, No. 9, pp. 2112-2115 (1976)
- /4/: B. Hillerich, "Measurement of the attenuation of optical fibers by pulse reflection", Technisches Messen atm (1976) No. 9,pp.269-270
- /5/: R. Olshansky et al, "Length dependent attenuation measurements in graded-index fibers, Proc. II. Europ. Conf. on Optical Commun., Paris (1976)

Acknowledgement

The author wishes to thank Dr. Krumpholz for valuable references and the director of the development centre of AEG-TELEFUNKEN KABELWERKE AG for the permission of this publication. This work was partially sponsored by the German Federal Ministry for Research and Technology. The author alone is responsible for the content of this paper.



Bernd Hillerich studied physics at Bonn University. He graduated as Dipl.-Phys. in 1974 and joined AEG-KABEL in 1975. Since then he is engaged in developing measuring and testing methods for optical fiber cables and in fundamental problems of optical fiber cable design.

Author's address:

AEG-TELEFUNKEN KABELWERKE AG
Development Center
W. Germany
22-28 Sommerfeld
4330 Mülheim/Ruhr-Saarn

EXPERIENCE TO-DATE WITH OPTICAL FIBER CABLES

G. Bahder and J. A. Olszewski

Research Center, General Cable Corporation, Union, New Jersey 07083

Abstract

A low loss multi-fiber cable has been developed suitable for duct and buried installations using conventional installation methods and equipment. Trial lengths of this cable, up to one kilometer in length, have been produced in the factory, installed in the field and are operating satisfactorily in commercial service.

This paper describes the cable design, the test results achieved and discusses the mechanical and optical properties of these cables. The comparatively large volume of cables produced to-date permitted statistical treatment of their most important optical characteristics with high confidence level in results obtained. Some results confirm, while others appear to contradict established theories.

It is apparent that as the optical quality of the fibers improves, it will be more difficult to maintain the low level of loss due to the cabling operation with present technology.

Introduction

Since about 1970 the world-wide development of low-loss optical fibers has advanced to such an extent that their application in long distance optical communication systems has become feasible. Early in the development, it was anticipated that ten or more years of R&D work would be required to reduce the cost of optical fibers to the level at which the fibers would be economically competitive with metallic conductors. It was also anticipated that the development of optical cables and their evaluation under normal field conditions would also take ten or more years and, therefore, the development work on optical fibers and cables should be carried out concurrently.

In 1974 General Telephone & Electronics and General Cable Corporation established a joint project for the development of an optical communication system for installation in a commercial telephone network and evaluation under field conditions. GT&E undertook principally the development of electro-optical carrier equipment and splices, while GCC undertook the development of the optical cable. Rapid progress in optical fiber development

obsoleted the originally established project objectives and new, more stringent project requirements were introduced.

One of the basic requirements for this project was the development of an optical cable having less than 10 dB/km attenuation at 820 nm wavelength which could be installed in lengths up to 1 km in existing ducts or buried directly using conventional methods and equipment.¹ For the initial trial installation it was decided to use T-1 carrier and to install a link, about 9 km long between two telephone offices, one in Long Beach, and one in Artesia, California. This system was put in operation by General Telephone of California in April 1977.² Following this project, other similar fiber optic cables have been made for other applications.

The purpose of this paper is to describe the basic construction and properties of optical cables that have been developed and constructed to-date for a series of projects that have either been completed or are presently underway.

Cable Construction and Mechanical Properties

The construction of the optical cables that were produced and are described herein is shown in Figure 1. The optical fibers are laid parallel to each other inside a flat plastic ribbon lamination about 6 mm in width. The ribbon lamination incorporates 6 or 10 graded-index fibers*, depending on customer requirements. The fibers are either buffered or coated with a few microns thick polymeric layer. Color coding is accomplished either by having one fiber with colored buffering, or in case of unbuffered fibers, one edge of ribbon lamination colored. The polymeric laminants were so made as to be pealable apart to expose the fibers for splicing or terminating purposes.

The fiber lamination is placed inside one of two diametrically opposite helical grooves which were produced in a plastic core extruded over a solid copper wire to an overall diameter of 11 mm.

* Fibers were made by Corning Glass Works, Corning, New York.

Three or seven polyethylene insulated color-coded pairs having metallic conductors 0.64 mm in diameter, as required by the customer, are placed in the second groove. The core assembly is bound by a helical wrap and covered with parallel folded core tape similarly bound.

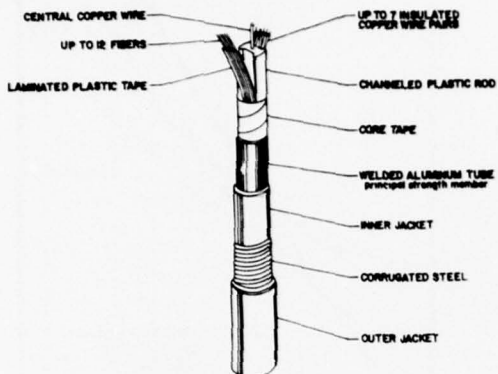


FIGURE 1: CUTAWAY VIEW OF OPTICAL FIBER CABLE

The sheath of each cable is constructed from 1.3 mm thick aluminum strip which is formed into a tube longitudinally welded and subsequently drawn down in a continuous process to form a pressure tight, loose fitting tube over the cable core. The diameter over the aluminum is 19 mm. The outside surface of the tube is flooded with an asphaltic compound followed by a polyethylene jacket, followed by 0.15 mm thick corrugated steel tape with overlap, asphaltic flooding compound and outer polyethylene jacket to an overall diameter of approximately 2.5 cm.

The cable construction described above is based on our concept that optical fiber cables, to be practical, must be capable of being installed in long lengths using equipment and methods familiar, and available to the cable users. The aluminum tube is the strength member required for placement of cables and together with the steel armor and jackets protects the cable core during installation operations and during service life of the cable against crushing, cutting, impact and water or moisture entry. The electrical shielding efficiency for metallic circuits incorporated in the core, is also high.

The design of the cable core has built-in flexibility as far as fiber count is concerned since placement of laminations in each groove, or more than one lamination per groove, is feasible. In the optical cables manufactured to-date, 0.64mm (No. 22 AWG) polyethylene insulated pairs were positioned in one of the grooves and these were employed by the cable users for repeater power feed, order, fault locating, etc.

The mechanical properties of the cables were experimentally determined to be as follows:

| | | |
|------|----------------------------------|----------------------------------|
| i. | Minimum bending radius | 30 cm |
| ii. | Maximum compressive force | 240 kg per 10 cm of cable length |
| iii. | Maximum permissible tensile load | 400 kg |

The above maximum compressive force of 240 kg per 10 cm of cable length was taken at 28 per cent aluminum tube deformation when the aluminum tube inner wall just touches the outer periphery of the core. Under this condition, the core movement, or fiber lamination movement within the core, was not restricted. Maximum permissible tensile load of 400 kg was derived from tests on the cable sheath alone which at 0.2% elongation showed a load of about 540 kg. The strain of 0.2 per cent was taken as a safe maximum value from the point of view of the optical fibers. Another safety precaution consisted of taking 75 per cent of measured 540 kg load, or about 400 kg, as the maximum permissible axial tensile load during installation.

Cable Attenuation Analysis

A number of cable production runs were made for projects that are either completed or are presently under construction. The discussion of optical properties is mainly based on production runs of eleven cables for GT&E/GCC T1 trial which employed six buffered fibers and a run of three cables for T3 link which employed seven unbuffered fibers. Fibers used in the GT&E/GCC trial had a minimum bandwidth of 200 MHz, while in the T3 trial the fiber minimum bandwidth was 400 MHz. All fibers made by Corning Glass Works were of graded-index type and their nominal dimensions were 62.5 μ m core and 125 μ m diameter over cladding. Buffered fibers had 200 μ m nominal diameter over the EVA type buffering.

A summary of attenuation results is shown in the form of statistical plots in Figure 2. These results indicate that in the case of the cables for GT&E/GCC trial the 50% probability attenuation at 820 nm wavelength and 0.1 launch NA of fibers before cabling was 5.1 dB/km while after cabling it was about 6.1 dB/km; corresponding results for T3 link were 4.4 dB/km and 5.1 dB/km.

In the case of unbuffered fibers, the cabling operations caused a 0.7 dB/km increase in the 50 per cent probability attenuation and practically no increase in its 3σ limits, while in the case of buffered fibers the cabling operations increased the 50 per cent probability attenuation by 1.0 dB/km and also substantially increased the 3σ attenuation limits. It is apparent that non-uniformity of the buffering is the primary cause of the difference in behavior of unbuffered and buffered fibers. Figure 2 also shows that the cabling operation improves the attenuation of 6 per cent of buffered fibers. This is an indication that the attenuation values as measured on

fibers before cabling comprise some losses caused by microbending, and this microbending in some fibers during the loss measurement is larger than in the finished cables.

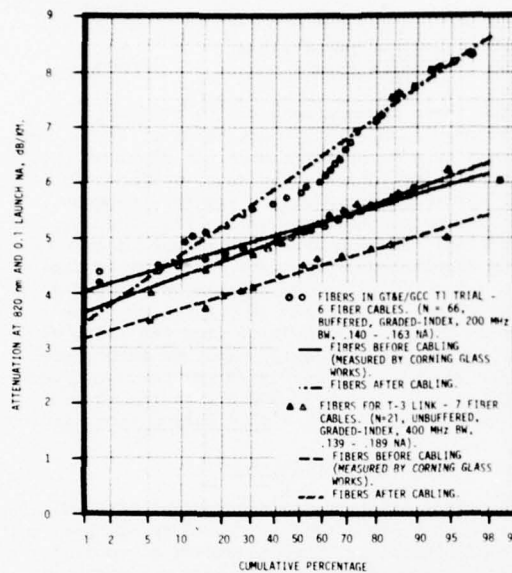


FIGURE 2. STATISTICAL DISTRIBUTION OF BUFFERED AND UNBUFFERED FIBER ATTENUATION BEFORE AND AFTER CABLING.

In order to analyze the increase in attenuation due to the cabling operation, the unbuffered fibers used for manufacture of cables were divided into two categories: the first having an attenuation of 3.5 to 4.3 dB/km and the second having an attenuation of 4.3 to 5.0 dB/km. Similarly the buffered fibers were divided into categories having an attenuation of 4 to 5 dB/km and 5 to 6 dB/km. An increase in attenuation due to the cabling operation is statistically plotted for each group of fibers in Figure 3. Figure 3 shows that in case of both unbuffered and buffered fibers, the increase in the attenuation due to the cabling operation is higher for the fibers having lower attenuation before the cabling operation.

On an average basis, the difference in attenuation of the two selected groups of buffered fibers utilized in the GT&E cable is 1 dB/km (5 to 6 minus 4 to 5 dB/km) and the average difference in the attenuation increase due to cabling operation is approximately 0.5 dB/km. Similarly for the considered two groups of unbuffered fibers, the average difference in the attenuation before the cabling operation is 0.75 dB/km (4.3 to 5.0 minus 3.5 to 4.3 dB/km) and the difference in the average increase in attenuation due to cabling operation is 0.4 dB/km. On the basis of the above results, one can postulate that the high value of attenuation as measured on some fibers before the cabling operation is mainly caused by the high core to cladding interface losses which may be introduced by the geometrical non-uniformity of the fiber and/or by the

microbends of the fibers in the configuration at the time of the attenuation measurements.

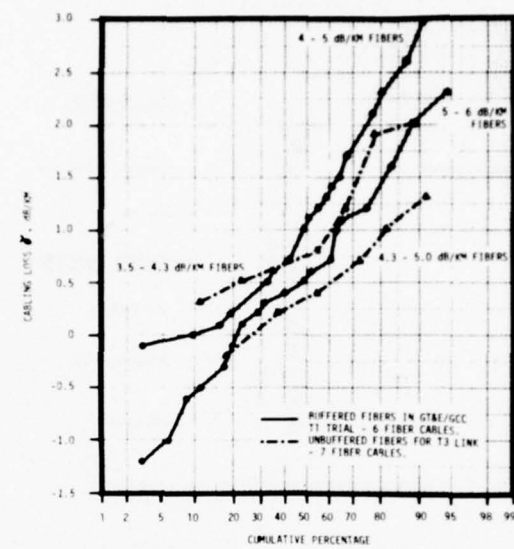


FIGURE 3. STATISTICAL DISTRIBUTION OF BUFFERED AND UNBUFFERED FIBER CABLING LOSS AS A FUNCTION OF FIBER ATTENUATION BEFORE CABLING.

The above results indicate that buffering of the fibers with EVA compound causes additional microbending of the fibers and hence higher losses in finished cables as compared with cables made of unbuffered fibers. Higher order modes are stripped from the higher attenuation fibers due to the imperfections at the core/cladding interface and only small number of additional modes is stripped by the microbending distortion introduced by the cabling operations. The reverse explanation can be postulated for the lower attenuation fibers with lesser interfacial irregularities.

Effect of Numerical Aperture on Cabling Loss

The statistical distribution of cabling losses for buffered and unbuffered fibers for various numerical apertures (NA) is shown in Figure 4. Similarly as above, the fibers are divided into two categories: unbuffered fibers having NA 0.139 to 0.150 and 0.150 to 0.180 and buffered fibers having NA 0.140 - 0.150 and 0.150 - 0.163. Figure 4 indicates that fibers having higher numerical aperture have higher increase in attenuation due to cabling operation (higher cabling loss χ). In other words, the measured results show that the smaller is the NA, the less is the added loss due to the microbending. These results do not confirm but rather contradict the theoretical analysis given in references 3 and 4.

The results of Figure 4 appear to be logical and imply that while it is true that high NA

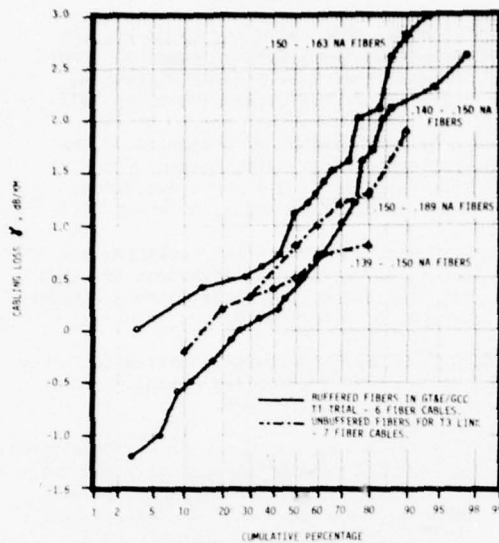


FIGURE 4. STATISTICAL DISTRIBUTION OF BUFFERED AND UNBUFFERED FIBER CABLEING LOSS AS A FUNCTION OF FIBER NUMERICAL APERTURE.

fibers are less sensitive to microbending, they also accept more light power at the input, and higher order modes travelling close to high critical angle are attenuated more in traversing the fiber core. The net results is the sum of both effects.

The lesser disparity, in the case of unbuffered fibers, appears to be due to lesser degree of microbending in these cables resulting from more uniform lamination as compared to buffered fibers.

Effect of Attenuation on Bandwidth

In order to demonstrate the effect of attenuation on the bandwidth of completed optical cables, a statistical plot of bandwidth is made for 600 MHz minimum bandwidth class buffered fibers with an attenuation range 4.5 to 5.8 dB/km and separately with an attenuation range 5.8 to 7.0 dB/km - Figure 5. These fibers were used for high speed data link and were not previously described. Figure 5 indicates that fibers with higher attenuation exhibit broader bandwidth. 400 MHz minimum bandwidth unbuffered fibers, previously described, did not indicate dependence of the bandwidth on attenuation. It is worthwhile to emphasize that in case of both buffered and unbuffered fibers, at 50 per cent probability, the cabling operation did not significantly affect the bandwidth of the fibers. At higher probabilities, the effect of the cabling operation was pronounced and the bandwidth decreased on some fibers and increased on other fibers.

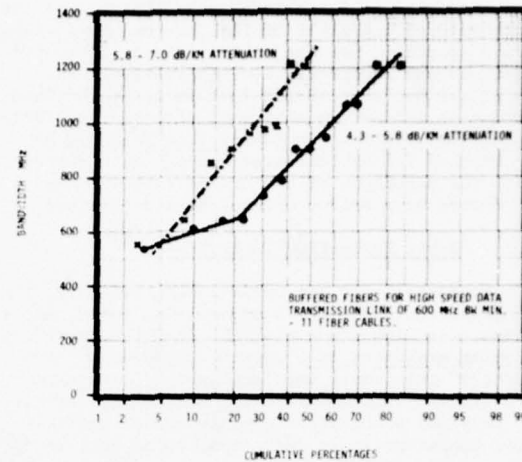


FIGURE 5. STATISTICAL DISTRIBUTION OF BUFFERED FIBER BANDWIDTH AS A FUNCTION OF ATTENUATION IN COMPLETED CABLES.

Effect of Non-Equilibrium Loss

The effect of non-equilibrium loss is demonstrated in Table 1. Column B shows the results of

Table 1

Measured Attenuation on Installed and Fused-Spliced Link with 820 nm LED Source, dB/length

| A | B | C | D |
|--------------|---|---|-----------------------|
| Fiber Number | Sum of Two Separate Section Losses (1180 + 805 Meters) | Completed Length Losses (1985 Meters) with Fused Splices) | Difference (B - C) |
| 1 | 14.07 | 12.40 | 1.67 |
| 2 | 15.15 | 13.94 | 1.21 |
| 3 | 13.50 | 13.11 | 0.39 |
| 4 | 12.29 | 11.61 | 0.68 |
| 5 | 13.80 | 12.98 | 0.82 |
| 6 | 15.12 | 14.47 | 0.65 |
| 7 | 14.65 | 13.01 | 1.64 |
| 8 | 11.92 | 11.08 | 0.84 |
| 9 | 12.29 | 11.54 | 0.75 |
| 10 | 12.21 | 11.28 | 0.93 |
| Average | 13.50 | 12.54 | 0.96 |

attenuation measurements performed separately on two lengths of installed optical fiber cables, while Column C shows the results of attenuation measured after splicing of these two lengths. The difference between Columns B and C represents the non-equilibrium loss augmented by the loss in one additional splice. Since the average loss in the fused type splice is 0.2 dB, it can be anticipated that the average non-equilibrium loss is in the order of 1.2 dB when a commercial LED of 820 nm wavelength is used as a light source.

It should be taken into account that a splice introduced into a fiber optical system provides two loss components: one the splice loss as indicated above and two additional non-equilibrium loss. The splice non-equilibrium loss is not taken into account in the determination of the non-equilibrium loss of the system. Therefore, its loss can be higher than 1.2 dB indicated above. At the present time, the magnitude of the non-equilibrium loss introduced by a splice has not been determined.

Cable Evaluation In Service

The details of the cable installation by GT&E are given in references 1 and 5. The cable, in conjunction with other electro-optical components, is being evaluated in a commercial network. Two fibers of this cable were employed to form a test loop 3.6 km long, containing 7 mechanical splices. The loop LED stability (input power) as well as fiber output power is under continuous surveillance by two detectors and recorders. During 12 weeks of operation, the LED output power was stable, while the power transmitted through the loop dropped by about 20 per cent or about 1 dB. This is equivalent to about 0.27 dB/km increase in loss. During this time, on one occasion an abrupt drop in transmitted power of about 0.6 dB was momentarily recorded. However, a week later the power recovered to the previous level. It is expected that continuous monitoring of this test loop, together with monitoring of other optical cable systems, will provide extensive information relating to the optical cable stability and to its performance in service. This information is essential for the full commercialization of optical fiber cables.

Conclusions

1. It has been demonstrated that cables with 5 dB/km average attenuation can be regularly manufactured using unbuffered, graded-index, fibers.
2. The average non-equilibrium loss for utilized graded-index fibers and for commercial LED light source is estimated to be approximately 1.2 dB or higher.
3. The cabling losses are smaller for higher attenuation fibers and are higher for lower attenuation fibers.
4. It has been found that the cabling losses of the manufactured optical cables are higher for fibers having high numerical aperture.
5. The progress in development of low loss fibers (3 dB/km or less) will necessitate development of new cable constructions insuring lower cabling losses.
6. It is expected that within next 3 to 5 years sufficient data will be obtained on optical cables in service to establish the cable design and the installation procedures for commercial optical systems.

References

1. R. Soyka, "Optical Fiber Cable Placing Techniques (Long Section Lengths)", 26th International Wire & Cable Symposium, Cherry Hill, New Jersey, November 1977.
2. E. E. Basch and R. A. Beaudette, "The California Fiber Optic System", 26th International Wire & Cable Symposium, Cherry Hill, New Jersey, November 1977.
3. D. Gloge, "Optical-Fiber Packaging and Its Influence on Fiber Straightness and Loss", The Bell System Technical Journal, Volume 54, No. 2, February 1975.
4. R. Olshansky, "Distortion Losses in Cabled Optical Fibers", Applied Optics, Volume 14, No. 1, January 1975.
5. J. A. Olszewski and G. H. Foot, "Development and Installation of an Optical Fiber Cable for Communications" to be published at National Telecommunications Conference (NTC'77), Los Angeles, December 1977.

ACTIVE PROTECTION DEVICE FOR SUPPRESSION OF INDUCED LONGITUDINAL VOLTAGES
IN TELECOMMUNICATION CABLES IN THE FREQUENCY RANGE FROM 16 TO 3,400 HZ.

W. Baum, Baum-Elektrophysik GmbH, Nuernberg, West Germany
A. Silberhorn, Deutsche Bundespost, Darmstadt, West Germany
M. Still, Kabel-und Metallwerke Gutehoffnungshuette A.G.
(Kabelmetal), Hannover, West Germany

Abstract

This paper describes the Active Reduction System (ARS), a device for the suppression of induced longitudinal voltages in telecommunication cables. It consists of an amplifier, a transformer and a power supply. The first experimental installation took place in Munich in 1972, where telephone cables were subjected to considerable interference by the new rapid transit facilities. This large-scale experiment was carried out for about 5 years. It has led to product improvements. The German Posts and Telecommunication Administration (DBP) recently indicated that it considered the tests as completed. The Active Reduction System has thus become an approved device which may be used wherever permanent interference is present.

The test program has confirmed the validity of the principle on which the ARS is established and nothing prevents its application to other technical areas or its use in foreign countries. New applications will no doubt call for changes in the parameters of the device. However, the ARS is flexible and lends itself to a wide range of adaptations. Furthermore, the ARS is suitable not only for new installations but it can be economically retrofitted into existing systems.

1. Introduction

1.1 Interference sources.

There are three types of interference in telecommunication cables induced by electric power equipment. These are called capacitive, inductive or ohmic interference, depending on the type of coupling between the telecommunication cables and the power line.

Capacitive interference is caused by the electrical field of the power line. Interference of this type can be avoided through simple shielding of the telecommunication circuit.



Fig.1 Rapid transit motor car type
ET 420 (German Railroads), using
thyristor-controlled traction.

Inductive interference is caused by the magnetic field around a current-carrying conductor. This magnetic field can induce considerable voltages into telecommunication cables within its vicinity. This is particularly so in power systems in which the go and return conductors form a large loop, as is the case with electric railroads which use ground for the return path. These voltages are generated in the circuit between the telecommunication conductor and ground and are therefore called longitudinal voltages. They can be calculated according to the following equation:

$$E_1 = 2\pi f M I r$$

wherein:

E_1 = Induced longitudinal voltage

f = Frequency of the interfering power system

M = Mutual inductance between power system and telecommunication lines

l = Length of parallel path

I = Current in the power system

r = Screening factor

Ohmic interference is generated wherever a common ground is shared between power and telecommunication systems, as is the case when telecommunication cables are located in the vicinity of the power system. The current flow in the power system through ground resistance generates voltage gradients which are effective between the neutral ground and the telecommunication lines. This voltage appears in the circuit between conductor and ground as a longitudinal voltage.

The inductive and ohmic coupling between power systems and telecommunication lines is particularly close when both transmission systems are geographically located next to one another, if the distance over which they are in close proximity is long, if the current in the power system is of high magnitude or if both systems use ground for their return path.

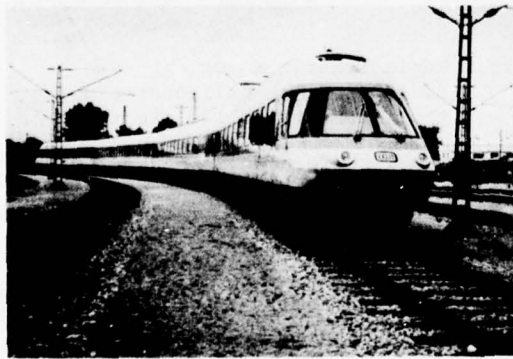


Fig.2 Motor car type ET 403 (German Railroads) for traction of Inter-City trains.

As far as power lines are concerned, electric railroads are particularly troublesome. This holds true for either AC- or DC-operated lines, where harmonics from the rectifiers or high frequency parasitic signals from chopper-operation of the locomotives may generate interference. Symmetrically laid out 3-phase AC systems interfere with telecommunication lines

only in the case of faults (short-circuit between phases or short-circuit to ground) and these are usually only of short duration. However, this is true only if the telecommunication circuit is located at a sufficient distance from the 3-phase system where no resulting field exists. If, on the other hand, the telecommunication cables are sufficiently close to the AC-system so as to create unequal distances with respect to the individual phases, a steady longitudinal voltage will be induced into these cables by the resulting field. This is known to be the case in 50 Hz and 60 Hz systems, in particular within high-voltage power transmission corridors.

1.2 Effects on telecommunication cables.
We shall consider here only those parasitic, induced voltages which lie outside of the danger zone (65V limit, according to German VDE Spec.) and are of long-time duration, that is, more than 0.5 sec.

Longitudinal voltages can lead to operational interference in telecommunication lines even at relatively low magnitude. This magnitude limit depends on the type of operation and on the operational voltage. The German Post Office uses two systems for 60 VDC battery voltage: the "Rotarysystems" (HDW- and EMD-System). The limits for 16 2/3 Hz are about 10 V and 15 V, respectively. Induced longitudinal voltages of higher magnitude can lead, for example, to dialing distortions because dialing pulses are transmitted in the circuit between conductor and ground. Furthermore, in DC-systems there exists the possibility of interruption of existing telephone communications.

Another effect of the longitudinal voltage, especially within the audio frequency range, is interference created by dissymmetries in the grounding of the terminals. If one assumes that the symmetry of a telecommunication system is 40 dB and considering a permissible noise voltage of 0.5 mV (per CCITT Specs.), a longitudinal voltage of 0.2 V (measured in accordance with the psophometrical curve of CCITT) can already lead to an inadmissible noise interference of 1 mV.

1.3 Protective devices used in the past.
In the past, passive devices were used to reduce or eliminate induced longitudinal voltages in cables.

Greater physical separation between the telecommunication and power systems is a simple way to reduce the interference. There are many cases, however, where such separation cannot be implemented as, for example, in valleys, along power lines or if an existing railroad is electrified.

A known passive protective measure is the improvement of the screening factor of the telecommunication cable. This is difficult in cases where the cables are subjected to low-magnitude longitudinal voltages which, when integrated over longer distances, may become quite considerable. Furthermore, this kind of protection can be implemented only through the installation of new cables.

Another protective measure is the use of isolating transformers. These are suitable only in AC-operated telecommunication systems and, furthermore, they affect the transmission characteristics. There is a limit to the quantity of isolating transformers that may be built into a telecommunication line.

Another known method consists of improving the coupling between the cable sheath (or a spare conductor) and the cable conductors through a transformer. This device is called a neutralizing transformer. This transformer derives the required power for the reduction of the longitudinal voltage from a pilot wire of high conductivity which is grounded at both ends of the protected telecommunication system. The pilot wire current (primary of the neutralizing transformer) induces a compensating voltage in the conductors of the cable. This voltage, however, can never attain the amplitude of the induced voltage because of losses due to the pilot wire resistance and ground resistance.

2. Physical background

2.1 Generation of the longitudinal voltage. As already mentioned above, it is the magnetic field, which is generated e.g. by the loop formed by the overhead wire and rail return path of electric railroads, that is responsible for the voltage induced into telecommunication cables. In the case of single-phase operated railroads the return flow divides up into parts which are conducted through the rails and through the ground. Therefore, in the case of telecommunication cables located, in particular, in the vicinity of railroad stations, the

ohmic interference will likewise become effective.

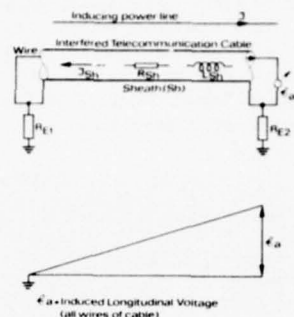


Fig.3 Effect of interference: induced longitudinal voltage in all wires of the cable.

Both types of interference cause induced longitudinal voltage to appear in the conductors of the telecommunication cable. This voltage can be measured at one end of the cable against local ground if the conductor is grounded at the other end.

The longitudinal voltage is directly proportional to the current of the inducing system and is also a function of its frequency. The mutual inductance (that is, the transformer coupling) between the loop created by the overhead wire and ground on the one hand, and the loop created between the telecommunication cable conductor and ground, on the other hand, determines the amplitude of the induced voltage.

The amplitude and the phase of the longitudinal voltage are continuously variable as a function of the inductive or ohmic components which, in turn, depend on the current drawn by the locomotive, its location, etc.

2.2 Principle of operation of the Active Reduction System (ARS).

It is therefore not possible to use a voltage of predetermined amplitude and frequency (such as, for example, from the supply system of the overhead wire)

for the compensation of the longitudinal voltage. Instead, one uses the voltage which appears in a conductor pair of the affected telecommunication cable. This pair, which is grounded at one end, will reveal at the other end the induced longitudinal voltage. This pair is called pilot wire. The voltage which is integrated over the whole length of the cable, corresponds to the magnitude and phase of the induced longitudinal voltage in all conductors of the cable.

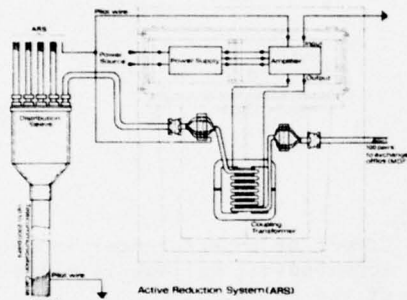


Fig.4 ARS principle.

The ARS consists of an amplifier, a transformer and a power supply. The amplifier is driven by the pilot wire. The cable is treated as the secondary winding of the transformer, whereas the primary winding (an insulated copper conductor) is connected to the output of the amplifier. The primary voltage is induced into the conductors of the cable with equal amplitude but opposite phase as a compensating longitudinal voltage to cancel the effect of the induced longitudinal voltage.

This principle is known from the neutralizing transformer applications. However, there is a difference: the power available for neutralizing transformers consists merely of what is induced into the pilot wire with respect to ground. This power is not sufficient to cover the losses in the primary circuit of the transformer and therefore it is not possible to attain good screening factors.

With the ARS, these transformer losses are compensated by a regulated AC-amplifier which is energized by an independent source, such as a battery. The amplifier is designed to feed to the coupling transformer a voltage of precise amplitude

and phase as dictated by the pilot wire. This is the only way to achieve proper compensation.

3. Technical concept of the ARS

3.1 Coupling transformer.

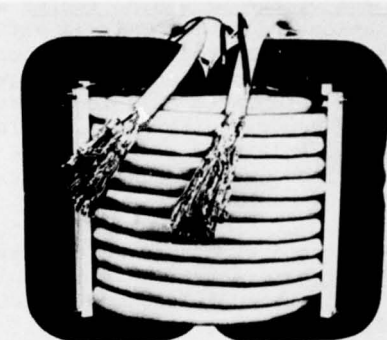


Fig.5 Coupling transformer: core with windings.

A laminated core of high permeability is wound with about 30 windings of a 100-pair, plastic-insulated telecommunication cable (0.6 mm dia. copper conductors). This cable makes up the secondary. The primary winding consists of an insulated, stranded (16mm² cross-section) copper conductor. The transformation ratio is 1:1 and the laminated core has a precisely defined air gap to eliminate DC effects. The windings are arranged in a way to minimize stray inductance so that the effective inductivity in the telecommunication cable pairs is negligibly small.

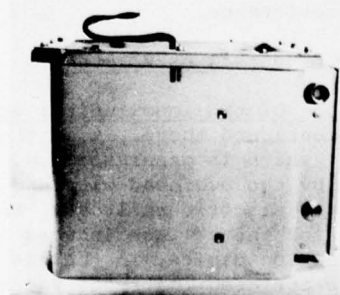


Fig.6 Coupling transformer, complete in housing.

The dimensions of the ARS were guided by a simple fact: it is often necessary to install the ARS in the basements of telecommunication exchanges and these are frequently old buildings. It was therefore necessary to design the coupling transformers so that they may suitably be carried down narrow, winding stairs by 2 to 3 workers. A square housing with a circumferential grip design was therefore selected. It is made from glass-fiber reinforced, polyester resin. Its dimensions at the base are 46 cm x 46 cm. Its height is 44 cm and it weighs about 170 kg with the transformer. The housing is tapered toward the top, where the length of a side is about 56 cm. The transformer is cast into the housing with plastic foam.

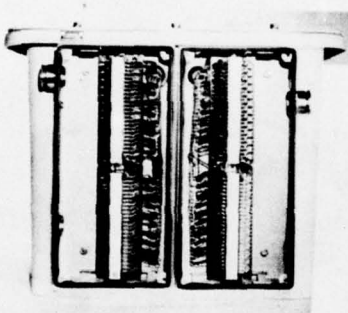


Fig.7 Coupling transformer (terminal strips exposed)

Two insulated terminal boxes with extendable terminal strips are attached to one side of the housing. The ends of the 100 pairs of the wound cable (i.e.: the transformer secondary) are soldered to terminal lugs and can be solder-connected to the telecommunication cable they are designed to protect. The cable sections are fed into the terminal boxes through watertight feed-throughs. The cables lead on one side to the distribution sleeves and on the other side to the main distribution frame.

A steel mounting frame for the power supply and amplifier is located on top of the coupling transformer. A short-circuit relay is also located there for the purpose of short-circuiting the primary winding of the transformer in the event of amplifier failure. This is to prevent the transmission of parasitic impulses.

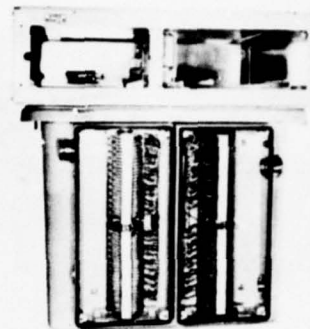


Fig.8 Coupling transformer with mounting frame.

The size of the mounting frame is 52 x 58 x 18 cm. It weighs about 25 kg. This results in a space requirement of about 0.3m² area with about 62 cm height.



Fig.9 Earlier generation ARS in operation in Munich.

The housing and mounting frame are designed so that three units can be stacked together vertically, as the required overall height of about 2 m is available in most basements. Furthermore, the mounting frame can be offset by 90° with respect to the housing in order to afford convenient access to the amplifier and power supply, irrespective of where the equipment is located.

3.2 Amplifier.

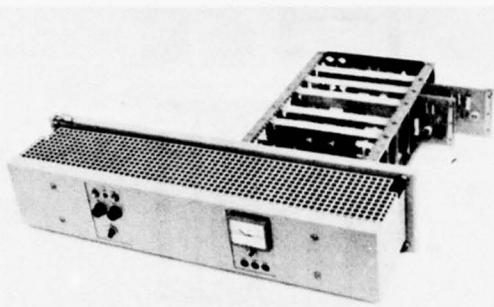


Fig.10 ARS amplifier of most recent design.

The amplifier is a regulated AC-amplifier consisting of a preamplifier and a power amplifier stage. The shape of the mounting frame dictates that it be L-shaped. Its depth is 34 cm. The power amplifier stage with its 60 cm-wide front extends by about 20 cm over the coupling transformer. The weight of the amplifier is about 9 kg.

The result of the interference reduction is a differential voltage between the original induced longitudinal voltage and the compensating voltage which is being fed into the cable through the amplifier and coupling transformer. This differential voltage should always be as close to null as possible. One recognizes the fact that control of this differential voltage calls for an amplifier design of outstanding properties. In particular, the amplifier must have an excellent non-linear distortion factor within the 16 Hz to 4 kHz range if one is to reduce the longitudinal voltage by a factor of 100.

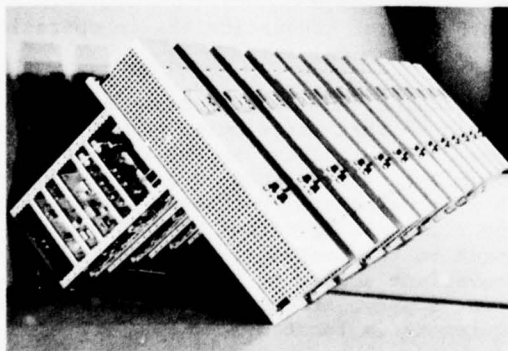


Fig.11 ARS amplifiers in production.

In order to provide for rapid corrective action in the case of rapid increases of the interference voltage (i.e.: short-circuit condition in the interfering power circuit) it is necessary to get fast regulation in the amplifier, even in the event of step-by-step changes in the load. Furthermore, the amplifier must be so designed as to render impossible continuous overload which would be harmful to the amplifier. Finally, the amplifier must be protected from the possibility of self-excitation caused by capacitive coupling between the cable pairs and the pilot wire, over its whole operating range. Steps must be taken to keep it below the critical phase shift which would lead to oscillations. The fully transistorized amplifier of the ARS, which is designed as a plug-in unit, possesses all of these characteristics.

3.3 Power supply.

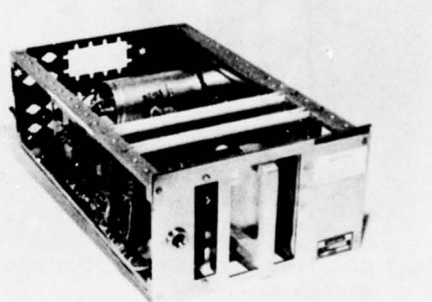


Fig. 12 60 VDC power supply.

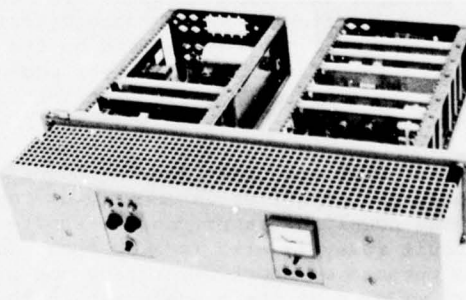


Fig.13 ARS amplifier with power supply

The left-hand side of the mounting frame provides the space (about 33 cm deep and 20 cm wide) for the power supply. ARS installations in use within the telecommunication system of the German Post Office Administration (DBP) derive their power from a standard 60 V battery. It is of course possible to design the system for use with other power sources (for example: 28 VDC, 48 VDC, 110 VAC, etc.). The weight of a DC power supply is about 3 kg and that of an AC supply, for either 50 Hz or 60 Hz, about 7 kg.

3.4 Monitoring unit.

In the event of a continuous overload (for example: induced voltage 50 V at 16 2/3 Hz), the reduced voltage, which is continuously being monitored will exceed the preset threshold (for example: 3V). If this occurs, the protective device can no longer handle the requirements, causing the ARS to be disconnected and an alarm to be initiated. The alarm is also initiated in case of failure of a sub-unit or if the amplifier is switched off or removed from its mount.

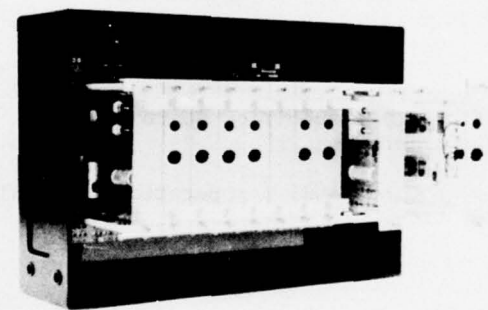


Fig.14 Monitoring unit (PC boards removed).

The monitoring unit also contains a monitoring circuit for the pilot wire, since a break of the pilot wire would lead to wrong voltages being fed to the amplifier. A pilot wire break will therefore result in an alarm.

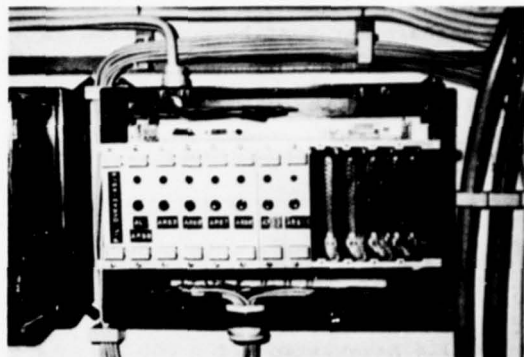


Fig.15 Monitoring unit, installed.

The monitoring unit is of plug-in type and it measures 36 x 25 x 21 cm. It weighs about 5 kg. The system provides 12 empty spaces for insertion of either the pilot wire monitoring circuit or the alarm unit. Furthermore, the monitoring unit contains multiplexing circuitry for the pilot wire. There is only one pilot wire per cable, even in the event where more than one ARS system protects the cable. Each pilot wire monitor and each ARS has its proper alarm circuit, which includes a visual alarm status indicator and the circuitry for consolidated remote monitoring.

4. Electrical data

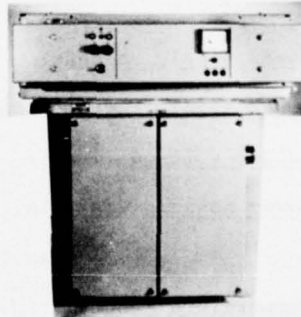


Fig.16 ARS, complete.

The ARS system described herein has the following electrical characteristics:

4.1 Transformer.

The transformer must be considered as a cable, since it is built into a cable. The described version is stranded in star quads. Stranding in pairs is, of course, possible.

4.1.1 Loop resistance, DC measured: 6 ohms

4.1.2 Mutual capacitance ($f = 800$ Hz): 5 nF

4.1.3 Capacitance unbalances:

pair - to - pair: 74 pF

pair - to - ground: 222 pF

4.1.4 Attenuation ($f = 800$ Hz): 0.07 dB

4.1.5 Dielectric strength ($f = 50$ Hz, $t = 2$ min.):

secondary winding:

conductor-to-conductor: 500 V rms

conductor-to-shield: 2,000 V rms

primary - to - secondary: 2,000 V rms

primary - to - control winding: 2,000 V rms

4.1.6 Screening factor (passive), 16 2/3 Hz @ 35 V rms: 0.015

4.2 Amplifier and power supply.

The German Posts and Telecommunication Administration (DBP) specifies 60 VDC. If AC were to be used, 220 VAC (50 or 60 Hz) would be specified.

| | Operation (nominal) at 60 VDC: | Operation (nominal) at 220 VAC: |
|--|-----------------------------------|------------------------------------|
|--|-----------------------------------|------------------------------------|

4.2.1 Power supply voltage: 54 to 72 VDC 200 to 240 VAC

4.2.2 Power supply current (max.): 3 A 1.6 A

4.2.3 Output voltage (max.): 35 V rms 35 V rms

4.2.4 Power consumption (min.): 60 W 70 VA

(max.): 260 W 380 VA

4.2.5 Temperature range: 0 to 40° C 0 to 40° C

4.3 Overall characteristics of the ARS.

The data shown are valid for the very low frequency of 16 2/3 Hz. More favorable figures are obtained with the described system, using higher frequencies.

4.3.1 Maximum reducing voltage ($f = 16$ 2/3 Hz): 35 V rms

4.3.2 Screening factor (@ 16 2/3 Hz, 35 V rms): 0.01

4.3.3 Screening factor for psophometrically weighted longitudinal voltage within the frequency range up to 4 kHz: 0.025

4.4.4 Permissible total DC current load: 3 A

5. Experience with the ARS

5.1 Large-scale use by the DBP.



Fig.17 ARS of most recent design, in operation at the DBP.

In connection with the 1972 Munich Olympics the DBP conducted an experiment with about 380 ARS systems over a period of several years. For reasons already mentioned, these systems were designed for operation at 60 VDC, for 100 pairs and for 35 V(@ 16 2/3 Hz) max.induced voltage. In addition, several units were fabricated



Fig.18 Rapid transit motor car at Essen railroad station.

for use at 220 VAC, 50 pairs and 70 V (@ 16 2/3 Hz) max. induced voltage. The latter units were for mobile use.

The requirement for the ARS arose because the German Railroads built a new urban rapid transit system for the Olympics. This system (S-Train) operates on 15 kVAC with a frequency of 16 2/3 Hz. For the operation of the S-Train, 120 thyristor-controlled AC-motor cars of the most modern design were implemented. These motor cars require about 3 to 4 times the current of conventional locomotives during the acceleration phase. Furthermore, harmonic currents of substantial amplitude occur with this thyristor control. These are the source of parasitic voltages whose magnitude is a factor of 20 to 30 times greater than the signals generated by conventional motor cars which use amplitude control and single-phase collector motors.

The good experience made with the ARS by the DBP over the past few years during this experiment have led to further use of the ARS, for instance, in areas of heavy S-Train concentration (Frankfurt, Stuttgart, Ruhr region, Etc.). Today, the ARS is in use in the whole territory of the German Federal Republic with about 500 systems in service.

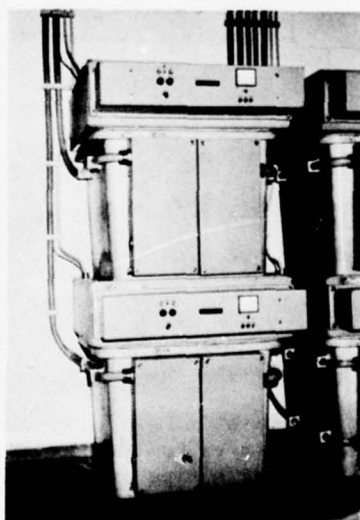


Fig. 19 ARS in operation at the DBP.

The DBP uses the ARS only in existing telecommunication cables which are subject to interference by new interference sources, rather than to incur the additional expense and technical problem of replacing these cables by new cables with improved screening factor. Furthermore, the ARS can be used not only against interference from railroads but also against continuous interference from high-voltage transmission lines. This is especially the case where the telecommunication cables are laid parallel to high-voltage transmission lines.

5.2 Assembly and installation.

The use of a pilot wire for the capture of the parasitic voltage permits the selection of the location of the ARS irrespective of the location of the interference source. For this reason the location of the ARS is considered most suitable in the basement of telecommunication exchanges. This permits the units to be designed for indoor operation and the hitherto heavy, sealed, cast-metal housings of the reducing transformers could be exchanged for lighter plastic housings. Indoor cables (100-pairs) can be routed from the distribution sleeve directly to the apparatus located in the same room and from there to the main distribution frame.

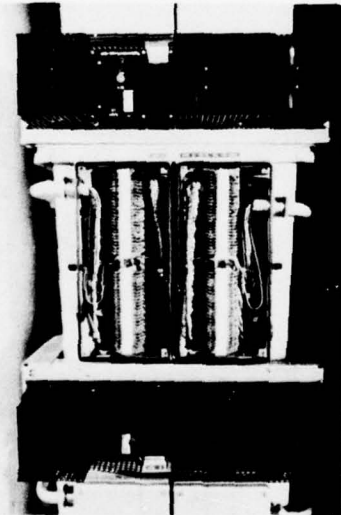


Fig.20 Early-generation ARS installation (terminal strips exposed).

There is no problem in assembly but it is recommended that this be performed by skilled technicians to prevent mistakes

that could affect the good working order of the equipment. The Munich experiment has shown that unskilled personnel made mistakes which required considerable expenditure to correct. To detect gross errors during assembly, the ARS is now equipped with a pilot monitor and an automatic quick-disconnect.

In order to provide for uninterrupted service, the power supply is connected to a battery. The battery must be properly designed, since each unit draws an average of 2 to 3 A.

If several ARS units are connected in parallel on one cable, experience has shown that one pilot wire is adequate for up to 500 pairs. If more pairs are to be protected in one cable, two pilot wire groups should be used.

The DBP has also successfully investigated the use of connectors (50 pairs) between the ARS and the cables. This special design is reserved for mobile use, since it is not customary for the units to be disconnected from the cables.

In the event where cables are subjected to continuous longitudinal voltages in excess of 35 V at 16 2/3 Hz, these can be reduced to acceptable values by connecting two ARS systems in series. Such an arrangement is in actual use by the DBP and experience has shown that it is good practice to connect the two devices to the same end of the cable.

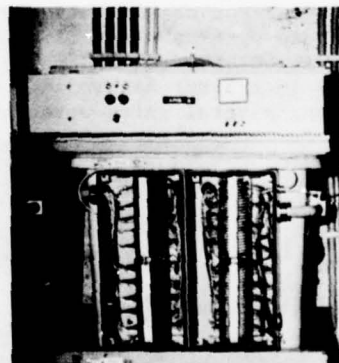


Fig.21 ARS installation in Duesseldorf (terminal strips exposed).

5.3 Operational experience.

As already mentioned, there are currently about 500 ARS systems in operational use

with the DBP. The broadband amplifier reduces the fundamental frequency, thus eliminating operational disturbances. It also reduces harmonics which are noise sources affiliated, in particular, with thyristor-controlled traction.

These noise voltages are diminished by the ARS, by preventing their build-up along dissymmetries of the terminals. The ARS does not improve the terminal symmetry and neither is it effective against noise voltages caused by poor cable symmetry. This protective measure does not reduce existing noise but it rather serves to prevent the generation and build-up of noise in the switching system.

It has been shown that the expected reduction of longitudinal voltages within the range of 16 Hz to 3.4 kHz can be obtained with the ARS. The ARS does not in any way affect the characteristics of the cable. The failure rate is extremely small, given proper design and installation.

The good experience made with the ARS has motivated the DBP and the German Railroads to retrofit the ARS into existing telecommunication networks, when faced with new interference sources. This is considered more efficient and economical rather than to attempt correcting the problem at the interference source.

6. Further developments and new applications

The present ARS generation is the result of customary practice dictated by the German Post Office Administration. The Post Office specifications are mainly based on requirements for the local telecommunication system of Munich, since a portion of that network was severely disturbed in 1972, rendering impossible proper telephone communications.

Results obtained to date show that the system presents the proper technical solution to the problem. It is, however, possible to start designing a system based on different parameters than those used in Germany.

As a result of the relatively low frequency requirement of 16 2/3 Hz the transformer is rather bulky and it could be considerably reduced if it were to be

designed for 60 Hz (or, alternately, the reducing voltage could be increased by a corresponding amount). The same reasoning also holds true if 0.4 mm conductors rather than 0.6 mm conductors were used for the windings.



Fig. 22 ARS amplifier with power supply during inspection.

The amplifier lends itself to be adapted to any suitable AC- or DC-source. The amplifier and power supply could also be centrally located on a rack, as specified by another customer.

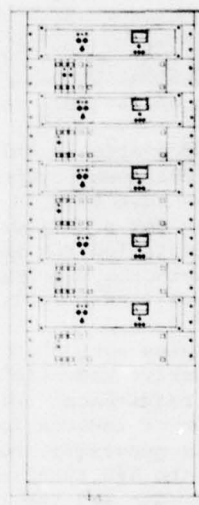


Fig. 23 Group of ARS amplifiers in proposed centrally-located stacked layout (conceptual design).

If the parasitic interference is within the audio frequency range (i.e.: harmonic generation by rectifiers of DC-traction railroads or chopper-controlled

vehicles), the transformer could be replaced by the transforming property of the cable sheath which must be insulated from ground, as is the case in installations using welded, corrugated steel sheath design (Wellmantel). The amplifier output increases with decreasing frequency. Tests have shown that the available ARS-amplifier can be successfully used within the frequency range starting at 300 Hz. A cable length of 500 m is already sufficient for the reduction of induced longitudinal voltages amounting to several volts.

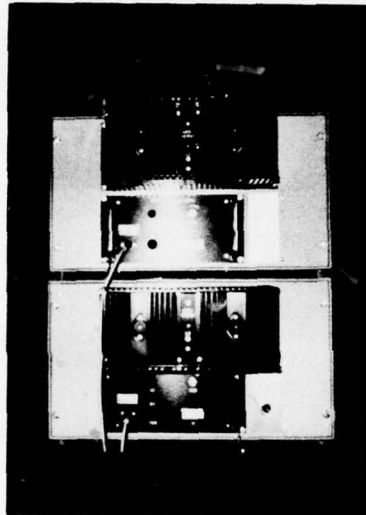


Fig.24 ANFS in operation.

This particular system is called the "Active Noise Frequency System" (ANFS) and a few units have been in successful experimentation for a period of some years. It is installed for noise reduction in secondary networks which are spread out over large areas (industrial applications).

These few examples show that it is possible to design an Active Reduction System for virtually any requirement which calls for the elimination of induced longitudinal voltages. It is necessary, however, that the design of the ARS take into consideration the bandwidth and the level of the interference voltage. Also, transverse voltages which may be caused by unsymmetrical design of the terminal network may be a source of noise and these, too, can be reduced by the ARS.

It is not uncommon today to find many countries where telecommunication lines are laid out parallel to power trans-

mission lines. Continuous interference may therefore be expected if the power line is subject to load unbalances or if the telecommunication cables are not laid out symmetrically with respect to the power line phase cables. The ARS system can also be used beneficially in this kind of environment.



Mr. Walter Baum is general manager of Baum-Elektrophysik GmbH, Nuernberg, West Germany, a subsidiary of the Kabelmetal group. He graduated in 1960 as a physicist from the University of Wuerzburg. He joined Baum-Elektrophysik in 1960, where he has been active in measurement and control techniques for industrial applications.



Mr. Armin Silberhorn is head of the section for interference technology in the Telecommunication Engineering Centre of Deutsche Bundespost at Darmstadt. He graduated in 1970 as an electrical engineer from the University of Munich. He joined Deutsche Bundespost and has since been active in the protection of telecommunication lines and equipment against inductive interference, lightning and corrosion.



Mr. Michael Still is technical manager for telecommunication products in the sales office of Kabel-und Metallwerke Gutehoffnungshuette A.G. (Kabelmetal) in Hannover, West Germany. He graduated in 1964 as an electrical engineer from the University of Aachen and has since been active in the development of telecommunication cables and related measurement and noise suppression technologies. He has been affiliated with Kabelmetal since 1969.

CROSSTALK CONSIDERATIONS IN PAIRED COMMUNICATION
CABLES FOR PCM USE

R. Hauschmidt

Phillips Cables Limited
Brockville, Canada

Abstract

Crosstalk requirements for communication cables intended for PCM carrier systems are usually stated in terms of limitations on the mean and standard deviation of pair-to-pair crosstalk measurements performed at a single frequency. Assuming independent, normally distributed measurements allows an analytical computation of the total interfering power and the subsequent translation of system error rate objectives into bounds for the statistics of individual crosstalk values. By means of extensive measurements at 772 kHz and 1.576 MHz on a variety of cable types, the unreliability of current crosstalk criteria as derived by the preceding method is demonstrated. Traditional assumptions about crosstalk values are examined. Alternative methods of treating crosstalk data are discussed, and a superior procedure for evaluating crosstalk performance is developed. This is then applied to cable acceptance testing and system design using a set of graphs and tables that utilize statistics readily obtained from pair-to-pair single frequency crosstalk measurements. Comprehensive tables of cable measurements and derived statistics are included to provide reference data for representative paired cable designs.

1. Introduction

A prime source of interference in paired communication cables is crosstalk. In the design of PCM carrier systems, the crosstalk power coupled into a transmission line is a factor limiting the repeater span length, the number of pairs assigned to PCM usage, or both. The need for a reliable criterion to gauge the crosstalk performance of a cable becomes evident.

Instead of directly applicable digital crosstalk or error rate measurements, single frequency sinusoidal signals at the Nyquist frequency are usually employed to measure a pair's crosstalk susceptibility. Simple statistics (e.g. mean, standard deviation) of these measurements are then used to judge the cable's suitability for T-carrier systems. Requirements for these statistics have traditionally been derived from system error rate objectives assuming independent, normally distributed measurements.^{1,2,3,4} This assumption allows an analytical computation of the total interfering power and the subsequent translation of error rate specifications into a cable crosstalk criterion.

Several areas of research into improved crosstalk characterization of cables in digital systems are immediately evident: the validity of using single frequency sinusoidal signals to describe disturbances in a pulse system; the accuracy of analytically summing individual crosstalk values to quantify the actual total interfering power; the effects of the measurement technique (equipment sensitivity, shielding problems, terminations) on the obtained values; the validity of length and frequency corrections.

This paper essentially restricts itself to a data processing problem. It is assumed that accurate single frequency, pair-to-pair crosstalk measurements are available on either a 100% testing or a representative sampling basis. It is further assumed that the limits on the power sum of these interfering sources as derived from error rate considerations are developed satisfactorily in the literature. Only the intermediate step of transforming the individual measurements or some simple statistics characteristic of them into a value quantifying the worst case of total interfering power encountered is examined.

For small cables where 100% testing is feasible, and especially where this testing is done on some kind of automatic test set with direct access to a computing facility, actual power sums can be calculated, the worst case identified and then compared with a requirement for maximum interfering power. For larger pair count cables, where only sampled data is available, it is necessary to make certain assumptions about the nature of the statistical distribution of the individual cross-talk measurements. This usually takes the form of various normality assumptions, both to facilitate summing operations and to describe percentiles of the sum in terms of its mean and standard deviation.^{1,2,3} More complicated formulae are derived by considering the crosstalk measurements to have a truncated normal distribution.⁴ By means of data from 100% tested cables (which enables calculation of the actual power sums), the truncated normal method will be demonstrated to be less inaccurate than the others, but still to have an unnecessarily pessimistic bias. The method will be refined by allowing a variable truncation factor for the distribution of the crosstalk measurements, its precise value dependent upon the nature of the data set. After proving the superiority of the new

method using the completely tested cables, it will be applied to partially sampled large pair count cables to demonstrate its use in cable acceptance testing and carrier system design.

2. Measurements

All measurements were made manually using a Siemens Pegelsender W2007 and a Siemens Pegelmesser D2007 as oscillator and level meter, respectively. Only the two pairs under test were terminated in their characteristic impedances, and 110Ω pure resistances were found to be a good approximation to the expected impedances of the pairs at the carrier frequencies. All pairs not under test were left floating, as was the internal screen in the case of cables with separately shielded compartments. To facilitate switching between test pairs, all pairs were fanned out and connected to a specially designed board which provided at least 120 dB isolation between test circuits at the frequencies involved (772 kHz, 1.576 MHz).

3. Terminology and Equations

The following terminology will be adhered to throughout this paper:

| | |
|----------|--|
| NEXT | = near-end crosstalk loss in dB |
| FEXT | = input-output crosstalk loss in dB |
| ELFEXT | = equal level far-end crosstalk loss in dB |
| a | = attenuation in dB |
| α | = attenuation in nepers |
| log | = logarithm (base 10) function |
| exp | = exponential (natural) function |

The terms "crosstalk" and "crosstalk loss" will be used interchangeably and will always be stated in positive dB.

The following length correction formulae will be used to relate crosstalk values at different lengths, L_o and L_1 :

$$\text{ELFEXT} (L_1) = \text{ELFEXT} (L_o) - 10 \log (L_1/L_o) \quad (1)$$

$$\text{FEXT} (L_1) = \text{FEXT} (L_o) - 10 \log (L_1/L_o) + a (L_1) - a (L_o) \quad (2)$$

$$\text{NEXT} (L_1) = \text{NEXT} (L_o) - 10 \log [(1 - \exp (-4\alpha L_1)) / (1 - \exp (-4\alpha L_o))] \quad (3)$$

Also,

$$\text{ELFEXT} (L) = \text{FEXT} (L) - a (L).$$

It is seen that the length corrections are done on a power basis, corresponding to random coupling with length, an assumption generally made at the lengths under consideration (> 1000 ft.). For a few of the cables (PCM terminating cables) where shorter lengths were measured, the length corrections were done on a systematic coupling basis:

$$\text{NEXT} (L_1) = \text{NEXT} (L_o) - 20 \log (L_1/L_o) \quad (4)$$

$$\text{ELFEXT} (L_1) = \text{ELFEXT} (L_o) - 20 \log (L_1/L_o) \quad (5)$$

It is important to note here that the type of length correction used has no bearing at all on the conclusions reached in this paper or on the analysis on which these are based. The problem of converting individual pair-to-pair crosstalk values to crosstalk power sums is independent of the problem of the validity of the length corrections. Furthermore, in the case of the linear length correction functions described above, all the statistical operators described below can be applied to original measurements, with any desired length corrections being executed subsequently. It is only for the sake of comparison and reference that figures are quoted for fixed lengths (usually 7800 feet or 1000 feet).

Denoting individual crosstalk measurements by x_{ij} (from i th circuit into j th circuit), the following statistical quantities are defined for n pair combinations (i,j):

$$\text{average crosstalk } \bar{x} = \sum_{i,j} x_{ij}/n \quad (6)$$

$$\text{crosstalk standard deviation } s = (\sum_{i,j} (x_{ij} - \bar{x})^2 / (n-1))^{1/2} \quad (7)$$

$$\text{rms crosstalk } \bar{x}_{\text{rms}} = -10 \log (\sum_{i,j} 10^{-x_{ij}}/10 / n) \quad (8)$$

$$1\% \text{ worse than } (1 \text{ percentile}) \quad 1\%WT = \bar{x} - 2.33s \quad (9)$$

minimum crosstalk x_{\min} = lowest measured value.

Where 100% testing is done, actual power sums can be calculated as below (N = no. of circuits):

$$\text{i}^{\text{th}} \text{ power sum } P_i = -10 \log \sum_{j=1, j \neq i}^N 10^{-x_{ij}}/10 \quad (10)$$

$$\text{average power sum } \bar{P} = \sum_i P_i/N \quad (11)$$

$$\text{power sum standard deviation } s_p = (\sum_i (P_i - \bar{P})^2 / (N-1))^{1/2} \quad (12)$$

The formula (9) for the 1st percentile ($1\%WT$) assumes a normal distribution. Since actual crosstalk data usually admits of a slightly positively skewed distribution, the formula will tend to estimate high. However, this statistic of the individual measurements is not used in any analysis. More importantly, the $1\%WT$ value of the power sums ($= \bar{P} - 2.33 s_p$) is an integral part of the derivation of crosstalk requirements. All indications are, though, that the power sum, being the sum of a large number of random variables, behaves essentially normally, and no appreciable error is incurred using the above formula.

4. Data Base

To provide a workable data base to test theories about crosstalk power sums and develop more reliable methods of estimating them, a number of cables were measured completely. Tables 7-11 in Appendix 2 list all relevant statistics of the measurements. The following notation is used:

Cable Types

- FTC: Filled Twin Core - solid polyethylene insulation, filled core, internal D-shield surrounding half the core, overall Alpeth sheath.
- FTCAL: Filled Twin Core (Aluminum) - aluminum conductors, cellular polyethylene insulation, internal D-shield surrounding half the core, filled core, overall Alpeth sheath.
- TERM: PCM Terminating Cable - pairs individually screened with either a braided or an aluminum foil shield, individually jacketed and assembled under a common sheath.

Type of Crosstalk

- N772: NEXT at 772 kHz, corrected to infinite length.
- F1576: FEXT (Input-Output) at 1.576 MHz, in dB/7800 feet.

Pair Location

- WSU: within sub-unit
- BASU: between adjacent sub-units
- BOSU: between opposite sub-units
- ALL: all possible pair combinations
- I/S D: inside of the internal D-shield in the Twin Core cables
- O/S D: outside of the internal D-shield in the Twin Core cables
- IE: measured from the inside end of the cable reel
- OE: measured from the outside end of the cable reel.

Notes:

- (i) For Twin Core cables, only pair combinations with one pair on each side of the internal D-shield are tested for NEXT, and combinations with both pairs on the same side of the D-shield are considered for FEXT.
- (ii) For the terminating cables, all possible combinations within the cable are measured for both FEXT and NEXT.

- (iii) For a further explanation of BASU, BOSU and WSU, reference should be made to Appendix I which describes the core structures of the test cables.

Statistics

- $X_{.5}$: median or 50th percentile of the distribution
- s_m : below mean standard deviation
- $s_{.5}$: below median standard deviation
- P_{min} : minimum calculated power sum.

The below mean (or median) standard deviation is obtained by assuming a perfectly symmetric distribution whose segment below the mean (or median) is identical to that of the actual distribution. Since the power sum is determined primarily by the low crosstalk values, some references prefer using a below mean deviation to the true deviation.

It should be emphasized that P_{min} , the minimum calculated power sum, actually represents the worst case, i.e., the maximum total interfering power, because of the sign convention for crosstalk values chosen in Section 3.

For NEXT measurements, two sets of power sums (their minima are denoted by $P_{min}(1)$, $P_{min}(2)$) are obtained for each set of crosstalk values. Depending upon what unit is considered the disturbed or disturbing one, different power sums are calculated, while the set of crosstalk measurements remains the same due to the reciprocal nature of the coupling.

5. Evaluation of Traditional Crosstalk Requirements

In this section we examine some previously published crosstalk requirements that are often quoted in cable specifications. The derivation of the actual requirements will not be questioned; only the assumptions made about the total interfering power will be scrutinized and compared with the measured total power.

5.1 Cravis and Crater¹

The authors develop engineering equations for the design of repeatered lines in T1 carrier systems (772 kHz):

$$\text{NEXT: } \bar{X} - s \geq 68 + 10 \log n \quad (13)$$

$$\text{ELFEXT: } \bar{X} \geq 21 + a_n + 2.33 s_n \quad (14)$$

where:

$$a_n = 5 \log [n^3 \exp(h^2 s^2) / (\exp(h^2 s^2) + n - 1)] \quad (15)$$

$$s_n = 6.593 [\log(\exp(h^2 s^2) + n - 1) - \log n]^{1/2} \quad (16)$$

$$h = 1/10 \log e$$

e = base of natural logarithms

n = number of interfering systems.

Equation (13) assumes a 32.5 dB repeater section loss, and includes a 9.5 dB safety margin for incomplete knowledge of crosstalk data. It also assumes that the average power sum of n NEXT values is $P_n = \bar{X} - s - 34 - 10 \log n$, its standard deviation is 3.2 dB, and hence its 1%WT value is given by

$$1\%WT = \bar{X} - s - 41.5 - 10 \log n \quad (17)$$

The following table compares the margin by which the measured NEXT values exceed the requirement (13) with the margin by which the measured minimum NEXT power sum exceeds the assumed power sum (17) used in obtaining that requirement.

Table 1: Evaluation of Cravis and Crater NEXT Requirement at 772 kHz

| CABLE | MEASURED VALUES \bar{X} -s P_{min} | (A) MARGIN OF (\bar{X} -s) OVER REQUIREMENT (13) | (B) MARGIN OF P_{min} OVER REQUIREMENT (17) | B-A |
|----------------|--|--|--|--------------|
| 100/22 FTC | 108.3 108.3 | 83.4 81.6 | 23.3 23.3 | 33.5 31.7 |
| | | | | 10.2 8.4 |
| 54/22 FTC | 99.9 99.9 | 81.0 82.5 | 17.6 17.6 | 36.9 38.4 |
| | | | | 19.3 20.8 |
| 54/22 FTC | 97.6 97.6 | 73.8 73.4 | 15.3 15.3 | 32.0 31.6 |
| | | | | 16.7 16.3 |
| 52/20 FIC A1 | 106.4 106.4 | 86.2 86.8 | 24.3 25.3 | 35.4 36.0 |
| | | | | 11.1 20.7 |
| 26/22 FTC (IE) | 92.7 92.7 | 77.5 77.0 | 13.6 13.6 | 37.4 36.9 |
| | | | | 23.8 23.3 |
| 26/22 FTC (OE) | 94.7 94.7 | 80.0 80.8 | 15.6 15.6 | 37.9 38.7 |
| | | | | 22.3 23.1 |
| 26/22 FTC (IE) | 94.7 94.7 | 81.0 82.2 | 15.6 15.6 | 38.9 40.1 |
| | | | | 23.3 24.5 |
| 26/22 FTC (OE) | 93.4 93.4 | 82.1 81.2 | 14.3 14.3 | 41.3 40.4 |
| | | | | 27.0 26.1 |
| 26/22 FTC | 97.1 97.1 | 82.5 82.3 | 18.0 18.0 | 38.0 37.8 |
| | | | | 20.0 19.8 |

The final column indicates that on the average, the minimum measured power sum exceeds the 1%WT power sum calculated from assumptions in Cravis and Crater by 19.8 dB more than the margin by which the NEXT X-s requirement is met. Even when the 9.5 dB safety factor is omitted from (13), in 17 of the 18 cases in Table 1 the requirement (13) is seen to be overly pessimistic.

The ELFEXT limitations incorporated in equations (14) - (16) are usually displayed graphically. They are derived assuming that individual crosstalk readings in dB are distributed normally and that the resulting power sum (in dB) of n interfering sources is distributed normally. This is similar to the procedure followed by Murthy³, and a detailed examination of the validity of these assumptions is made in Section 5.3.

5.2 Jacobsen²

Jacobsen derives crosstalk limits for low capacity PCM systems using slightly more complicated formulae. For NEXT, using what he calls a

"peak and bulk" method, he approximates the first percentile of the total interfering power by

$$1\%WT = m - [10 \log (n-1) + 0.115 s^2] \oplus [F^{-1}(P)(0.01/n) s] \quad (18)$$

where:

m = median of the individual crosstalk values

F⁻¹ = inverse of the normal probability distribution function, and

⊕ denotes addition on a power basis.

A similar method is applied for the FEXT values, except that the "bulk" and "peak" contributions are added on a voltage basis, and special allowances are made for sample size. Again, the results are best presented graphically and reference should be made to the original paper for details².

Table 2 summarizes the accuracy of the approximation to the power sums made by Jacobsen.

Table 2: Evaluation of Jacobsen Crosstalk Requirements at 772 kHz

| CABLE | NEXT 1% WT POWER SUM | | | FEXT 1% WT POWER SUM | | |
|-------------|------------------------------|------------------------------|----------------------------------|----------------------|--------------|---------------|
| | MEASURED | JACOBSEN | DIFFERENCE | APPROX. | MEASURED | JACOBSEN |
| 100/22 FTC | 83.4 81.6 | 72.3 72.3 | -11.1 -9.3 | 66.9 68.2 | 58.4 57.6 | -8.5 -10.6 |
| 54/22 FTC | 81.0 82.5 | 59.5 59.5 | -21.5 -23.0 | 69.4 66.2 | 56.9 56.7 | -12.5 -9.5 |
| 54/22 FTC | 73.8 73.4 | 69.9 69.9 | -3.9 -3.5 | 65.4 68.5 | 60.3 60.9 | -5.1 -7.6 |
| 52/20 FICAL | 86.2 86.8 | 61.4 61.4 | -24.8 -25.4 | 74.2 73.1 | 65.7 62.6 | -8.5 -10.5 |
| 26/22 FTC | 77.5 77.0 80.0 80.8 | 65.9 65.9 68.9 68.9 | -11.6 -11.1 -11.1 -11.9 | 68.7 74.7 | 57.6 65.2 | -11.1 -9.5 |
| 26/22 FTC | 81.0 82.2 82.1 81.2 | 68.1 74.1 66.1 66.1 | -12.9 -14.1 -16.0 -15.1 | 70.7 71.1 | 60.1 61.2 | -10.6 -9.9 |
| 26/22 FTC | 82.5 82.3 | 71.9 71.9 | -10.6 -10.4 | 66.1 68.3 | 61.6 64.1 | -4.5 -4.2 |

Again, it is seen that the approximations used in the derivation of the formulae are unduly conservative, especially when considering the recommendation that further safety margins of 6 dB or more are tacked onto the requirements solely to account for lack of complete knowledge of cross-talk behaviour.

5.3 Murthy³

In formulating crosstalk loss requirements for PCM systems that are applicable to both T1 and TIC, Murthy assumes normally distributed crosstalk values in calculating their power sums and first percentiles of these sums:

$$1\%WT = \bar{X} - a_n = 2.33 s_n \quad (19)$$

where:

$1\%WT$ = 1st percentile of the power sum distribution (either NEXT or FEXT)

\bar{X} = crosstalk mean (NEXT or FEXT)

n = number of interfering circuits

and a_n , s_n are defined by (15), (16).

Although further refinements to account for items like different pulse shapes are included in the overall method, Table 12 in Appendix 3 (under "Normal XT Dist.") shows that a consistent bias is introduced in the power sum approximation alone.

5.4 Bradley⁴

Bradley considers crosstalk effects in 48 channel PCM systems (T1C). Again, the critical assumption is that the individual crosstalk values in dB are distributed essentially normally, with the improvement of adding a truncation factor c . This effectively restricts crosstalk values to the range $(\bar{X} - cs, \bar{X} + cs)$. The first percentile of the power sum distribution is now given by

$$1\%WT = \bar{X} - a'_n = 2.33 s'_n \quad (20)$$

where:

$$a'_n = 5 \log [T(s)^2 n^3 \exp(h^2 s^2) + n-1] / (U \exp(h^2 s^2) + n-1) \quad (21)$$

$$s'_n = 6.593 [\log(U \exp(h^2 s^2) + n-1) - \log n]^{1/2} \quad (22)$$

$$U = T(2s)/T^2(s) \quad (23)$$

$$T(s) = [\phi(c-hs) - \phi(-c-hs)] / [\phi(c) - \phi(-c)] \quad (24)$$

ϕ is the normal probability distribution function, and h , n , X and s are as defined earlier.

A truncation factor of $c = 3.5$ (i.e., all crosstalk values fall within 3.5 standard deviations of the mean) is usually selected. Table 12, under "Truncated XT Dist.", lists the results of the $1\%WT$ power sum calculated under this assumption. A marked improvement over similar computations using non-truncated normal distributions for the crosstalk is evident; however, an unnecessary bias towards lower than actually recorded values is still present.

6. Development of Crosstalk Model

The preceding section has shown that the process of predicting the power sum (and its first percentile) of the individual interferences from statistics of the distribution of the pair-to-pair crosstalk values introduces a significant error into the derivation of crosstalk requirements.

Furthermore, this error is not random, but induces consistent underestimates of the $1\%WT$ power sum value, in some cases by as much as 13 dB. A necessary assumption in this analysis has been the nature of the distribution function of the crosstalk measurements. Normal distributions have traditionally been used, with the addition of a truncation factor proving beneficial. An improved characterization of the crosstalk distribution function was sought as the key to improved specification of crosstalk requirements.

6.1 Crosstalk Distribution Functions

For all cables investigated, crosstalk measurements were plotted on normal probability paper and consistent and significant deviations from normality were noted. Figure 1 exemplifies the typical pattern observed.

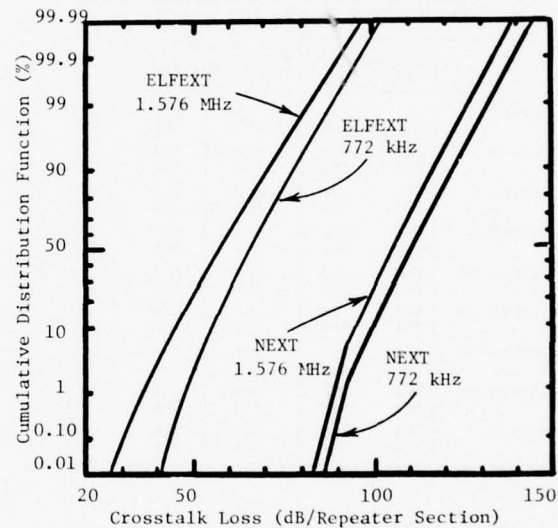


Figure 1: Crosstalk Loss Distribution Functions

The bulk of each distribution is normal, with some tendencies towards positive skewness. The lower tail of the curve (the part dominating the power sum calculations) is definitely truncated, and the upper tails range from truncation to excessive spreading. The degree of truncation at the lower end varies considerably from cable to cable, and very rarely approaches the value of 3.5 assumed by Bradley.

Two possibilities were considered for an improved characterization of the distribution function: take into account the small amount of skewness observed in many cases, or use a truncated normal model incorporating a better estimate of the true truncation factor. Since formulae already exist for the power sum of truncated normal random variables (see equations (20)-(24)), and since this method (with $c = 3.5$) has shown promising results, it was decided to follow the latter course.

6.2 Truncation Factor

To find suitable estimates for the truncation factor of the crosstalk distribution, the exact value of c which, when substituted into equations (20)-(24), yields the exact minimum measured power sum was computed for each set of measurements. As expected, most values were considerably lower than 3.5. Table 3 summarizes the results.

Table 3: Average Truncation Factors Required to Yield Exact 1%WT Power Sum

| CABLE TYPE | NEXT | | FEXT | |
|--------------|-------------|-------------|-------------|-------------|
| | 772 kHz | 1.576 MHz | 772 kHz | 1.576 MHz |
| 12/22 TERM | 2.03 (0.71) | 1.98 (0.18) | 2.44 (0.48) | 2.80 (1.17) |
| 26/22 FTC | 2.88 (0.84) | 2.46 (0.21) | 2.23 (0.59) | 2.63 (0.51) |
| 52/20 FTC AL | 2.21 (0.05) | - | 2.47 (0.04) | - |
| 54/22 FTC | 3.57 (1.65) | 3.73 (1.49) | 2.73 (0.52) | 3.27 (0.68) |
| 100/22 FTC | 4.02 | 3.61 | 2.82 | 2.84 |

The figures in brackets denote the standard deviations of the calculated factors.

Larger pair count cables, where multi-unit constructions are employed, display a wider spread of crosstalk values (larger c) due to the mixture of within unit and between unit results (cf. Tables 7-9). Generally speaking, considerable variation in the truncation factors is observed, sufficient to make the use of an average figure unattractive.

For sampled data, where calculation of exact power sums is impossible, the minimum recorded crosstalk value was expected to provide a simple and logical estimate for the truncation point of the distribution, which, when normalized and subsequently substituted into equations (20)-(24), will yield the correct 1%WT power sum. To test the effectiveness of this procedure, the truncation factors defined by the minimum measured crosstalk value, c_m , were correlated with the truncation factors required to calculate the exact measured power sum, c_p . Remarkable correlations were obtained ($\rho = 0.91$), and the resulting regression lines for FEXT and NEXT are plotted in Figure 2.

The entire procedure was repeated using different statistics for the centrality and dispersion parameters of the crosstalk distribution; e.g. the median instead of the mean, and the below mean and below median deviations instead of the standard deviation. The original combination of (mean, standard deviation) proved to provide the most consistent and accurate final estimate of the 1%WT power sum.

Summarizing, the following procedure was used to estimate worst case power sums:

- Measure pair-to-pair crosstalk for a representative sample of pair combinations. Record \bar{x} , s , x_{\min} .

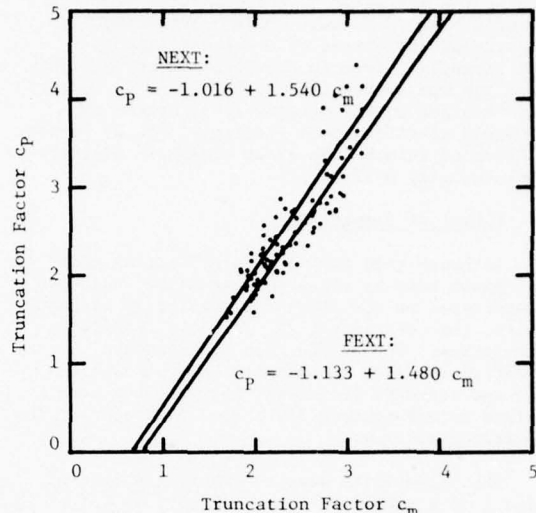


Figure 2: Regression of truncation factor required for exact 1%WT power sum, c_p , on truncation factor defined by minimum crosstalk value, c_m .

$$(ii) \quad c_m = (\bar{X} - X_{\min})/s \quad (25)$$

(iii) From Figure 2:

$$c_p = -1.016 + 1.540 c_m \text{ (NEXT)} \quad (26)$$

$$c_p = -1.133 + 1.480 c_m \text{ (FEXT)} \quad (27)$$

- From equation (20)-(24) and using $c = c_p$, calculate the expected 1%WT.

The computations for the data set of the 100% tested cables are listed in Table 12 under the column "VTN XT Dist." (for Variably Truncated Normal).

6.3 Model Evaluation

Table 12 reveals that the VTN method yields results superior to those obtained assuming non-truncated or fixed truncated normal distributions for the crosstalk. Table 4 compares the performances of the three methods.

Table 4: Comparison of Accuracies of Power Sum Approximations Assuming Different Crosstalk Distributions

| | NON-TRUNCATED NORMAL | | FIXED TRUNCATED NORMAL ($c=3.5$) | | VARIABLY TRUNCATED NORMAL | |
|-----------------------|----------------------|-------|------------------------------------|------|---------------------------|------|
| | NEXT | FEXT | NEXT | FEXT | NEXT | FEXT |
| Average Deviation | +5.9 | -5.9 | +2.6 | -3.5 | +0.1 | -0.1 |
| Maximum Deviation | +3.7 | -0.9 | 5.3 | +1.6 | 3.8 | +1.7 |
| Minimum Deviation | -13.7 | -10.6 | -9.7 | -7.2 | -2.9 | -2.1 |
| Maximum Absolute Dev. | 13.7 | 10.6 | 9.7 | 7.2 | 3.8 | 2.1 |
| No. of Positive Dev. | 5 | 0 | 11 | 3 | 26 | 20 |
| No. of Negative Dev. | 43 | 44 | 37 | 41 | 22 | 24 |

The VTN method has essentially randomized the sign of the deviation of the predicted from the measured 1%WT power sum. More importantly, it has reduced the spread of these deviations significantly. Even in the cases where the 1%WT power sum was overestimated, the error is comfortably absorbed in the margins incorporated into crosstalk specifications precisely for the purpose of "lack of information about crosstalk distribution" (usually 6-12 dB).

6.4 Effect of Sample Size

Although good accuracy in predicting worst case power sums by the preceding method has been demonstrated on the data from completely tested cables, the question of the effect of sample size arises. The sample mean and standard deviation are good estimates of the population mean and standard deviation; however, the sample minimum is not necessarily a good indicator of the population minimum.

The probability density function q of the range R of a sample of size n drawn from a population with probability density function f truncated at a and b is given by

$$q(R) = n(n-1) \int_a^{b-R} f(u) f(u+R) \left[\int_u^{u+R} f(x) dx \right]^{n-2} du \quad (28)$$

Even for the case of a normally distributed population, this expression is best evaluated numerically, and Tippett⁸ compiled comprehensive tables of the probability integral of the distribution of the maximum (obtained from the range by assuming symmetry) in samples of size n taken from a normal distribution. The expected value of the extreme (measured in terms of the standard deviation) is plotted as a function of sample size n in Figure 3.

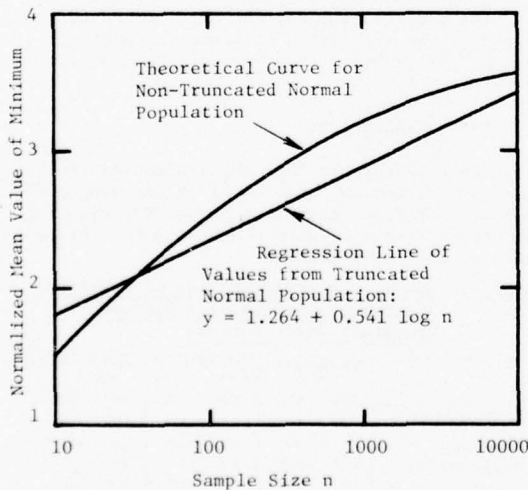


Figure 3: Expected Value of Minimum of Sample

For crosstalk data, where the population has a truncated normal distribution, the expected value of the extreme value of the sample will fall below this curve. The regression line obtained from the 100% tested cables (sample size n = total number of combinations) is included in Figure 3 and has the equation

$$c_m = 1.264 + 0.541 \log n \quad (29)$$

Hence, for a partially sampled cable, the truncation factor c_m will be the larger of the two values obtained by equations (25) and (29), where n = total number of pair combinations for 100% testing.

6.5 Multi-Unit Cables

Large pair count cables of multi-unit construction require special attention. Usually, sufficient crosstalk isolation exists between adjacent units to enable the use of within-unit measurements alone in determining FEXT performance. Similarly, for NEXT only the crosstalk between the two Go and Return units in closest proximity to one another needs to be considered.

It has been demonstrated using available crosstalk data that the above is not only a time-saving sampling procedure but also an absolute necessity in properly evaluating crosstalk behaviour. Mixing within-unit and between-unit measurements, even if they are properly weighted, can result in a noticeable departure from the assumed truncated normal distribution (e.g. multimodal forms). If the mean and standard deviation from such a mixed population are then inserted into the formulae, an apparent improvement in the worst case power sum over the within-unit 1%WT power sum can actually be indicated. Clearly, this cannot be the case.

On the other hand, in relatively small cables of sub-unit construction, such as the 100 pair Twin Core included in our data base, the effective crosstalk screening between sub-units on the same side of the internal D-shield is not severe enough to distort the distribution function significantly. Therefore, whether or not within-unit and between-unit measurements should be lumped together will depend on the characteristics of the crosstalk distributions involved and the unit sizes. The following approach has been proven to provide accurate results:

- For internally screened cables with units or sub-units smaller than 50 pairs, one representative, properly-weighted sample from the entire population is required to obtain X , s , X_{min} for use in the formulae.
- For large pair count duct cables or smaller cables (internally screened or not) with smallest stranding unit of 50 pairs or more, only statistics from within-unit measurements (for FEXT) or between the two closest units (for NEXT) are used in the formulae. The effects of the other units are determined from tables of correction factors derived below.

6.6 Power Sum Simulations in Multi-Unit Cables

Whether or not adjacent units contribute significantly to the power sums of the within-unit crosstalk alone depends on the magnitudes of the between-unit and within-unit crosstalk means and standard deviations, the sizes of the units and the number of adjacent units. The many variables involved and the fact that we are interested in 1%WT power sums make the analytical solution of this problem formidable. Instead, Monte Carlo simulation techniques were employed in conjunction with a computer to generate tables of factors that quantify the deterioration in the 1%WT power sum. A brief description of the simulation methods and use of the tables follows:

Notation:

- m_1 = mean of within-unit measurements
 m_2 = mean of between-unit measurements
 s_1 = standard deviation of within-unit measurements
 s_2 = standard deviation of between-unit measurements
 n_1 = size of primary unit
 n_2 = number of pairs in adjacent unit(s)
(usually $n_2 = n_1$, or $2n_1$ if two units are adjacent to the primary unit.)
 ΔM = $m_2 - m_1$

Computation: All crosstalk values were simulated using a random number generator and the statistics of the applicable crosstalk distribution assuming a truncated normal distribution. On a power sum basis, $(n_1 - 1)$ within-unit and n_2 between-unit values were added to obtain one power sum. A total of n_1 such sums were generated and the worst case was noted. The entire process was repeated ten times, the results averaged to obtain the expected worst case power sums, and the final number compared with a similar figure derived using only within-unit crosstalk. This difference was observed to depend on s_1 , s_2 , ΔM , n_1 and n_2 , and the simulations were thus conducted for selected values of these variables. Tables 13-15 in Appendix 4 list the results.

Use of Tables: If it has been decided that statistics obtained from within-unit measurements alone have to be used in determining compliance with crosstalk requirements (FEXT, for example), a sufficient number of between-unit measurements should nevertheless be taken to determine valid estimates of m_2 and s_2 . The number n_2 is usually some multiple of the unit size n_1 , depending on how many adjacent units will be dedicated to T-carrier use along with the primary unit. Under the appropriate values of $\Delta M = m_2 - m_1$, n_1 , n_2 , s_1 , s_2 , the tabulated entry indicates the magnitude (in dB) of the expected deterioration in the power sum due to the effect of the adjacent units. This value should be added to the crosstalk requirement obtained for a single unit.

For practical purposes, linear interpolation for non-tabulated values of the parameters will

yield sufficiently accurate results. It should also be noted that for $\Delta M < 8$ dB (approximately) and normally encountered values of s_1 , s_2 , n_1 and n_2 , the preceding method can usually be dispensed with, and one sample of measurements featuring properly weighted within-unit and between-unit pair combinations will be sufficient for application to the crosstalk requirement equations.

7. Crosstalk Requirements

Equations developed in Section 6 for approximating 1%WT power sums are now used in formulating improved crosstalk requirements. Referring to Murthy³ and equations (20)-(27), NEXT and FEXT loss requirements for any transmission rate (with bipolar signalling) and any repeater spacing are:

$$\text{NEXT: } \bar{X}_N - L - \Delta_N \geq M_N + 14.3 + a'_n + 2.33 s'_n \quad (30)$$

$$\text{FEXT: } \bar{X}_F - L - \Delta_F \geq M_F + 13.4 + a'_n + 2.33 s'_n \quad (31)$$

where:

- \bar{X}_N = mean near-end crosstalk loss at the applicable Nyquist frequency
 \bar{X}_F = mean input-output far-end crosstalk loss at the applicable Nyquist frequency
 L = average insertion loss of the cable pairs between repeaters at the Nyquist frequency
 Δ_F, Δ_N = correction factors due to deviations from raised-cosine channel shaping
 M_F, M_N = error margins allocated for various degradations, including insufficient knowledge of crosstalk data (usually 6-12 dB),

and a'_n , s'_n are defined in (21) and (22).

The lower bound for $(\bar{X}_F - L)$ as defined by equation (31), with $\Delta_F = M_F = 0$, is plotted against n , the number of interfering systems, as contours of s and c , in Figures 4-11 (see Appendix 5). Instead of a single curve for each value of s , a band of contours corresponding to a range of likely truncation factors c are generated for each s . Each graph depicts curves for $s = 5$ to 14 for one particular truncation factor c .

Figures 4-11 can thus be used to define minimum allowable crosstalk loss levels. With a suitable margin, e.g. $M = 9$ dB, the curves are directly applicable for FEXT; for NEXT, 0.9 dB is added to the value obtained from the graphs to give minimum allowable levels for $\bar{X}_N - L$. The following examples illustrate use of the graphs.

7.1 Examples

- (i) The following data was collected from a partial sampling scheme on a 100 pair/22 AWG filled core, internally screened cable:

Table 5: Sampled Crosstalk Data from 100 Pair/22 AWG FTC Cable (dB/7800 ft.)

| CROSSTALK TYPE | PAIR LOCATION | \bar{X} | s | X_{min} |
|----------------|---------------|-----------|------|-----------|
| FEXT (I-O) | I/S D | 102.7 | 10.5 | 81.0 |
| | O/S D | 101.4 | 11.4 | 82.4 |
| NEXT | IE | 117.8 | 5.9 | 102.0 |
| | OE | 116.1 | 6.7 | 101.9 |
| F1576 (I-O) | I/S D | 104.9 | 8.7 | 85.5 |
| | O/S D | 106.5 | 10.7 | 87.8 |
| N1576 | IE | 112.7 | 6.9 | 97.2 |
| | OE | 111.7 | 7.6 | 95.0 |

Cable Attenuation in dB/mile: 19.7 (772 kHz), 27.4 (1.576 MHz)

For the F1576 (O/S D) data:

The truncation factor of the sample is, from (25), 1.75.

For 100% sampling (1225 pair combinations), the expected truncation factor would be (from Figure 3 or equation 29) 2.93.

Since it is greater than the sampled truncation factor, we use the expected 100% sample figure for c_m . Substituting in (27) yields $c_p = 3.20$.

Consulting Figure 7 for $n = 49$, $s = 10.7$ and $c = 3.5$, the lower bound for $\bar{X} - L$ is 49.5. For $c = 3.0$ (Figure 8), the bound would be 47.5. Interpolating linearly for the value $c = 3.2$ yields $\bar{X} - L \geq 48.3$. The nominal repeater spacing for this type of cable is 7800 feet, so that $L = 40.5$. Hence, for a very conservative safety margin of $M_F = 12$ dB, the lower bound for the input-output FEXT mean is $48.3 + 40.5 + 12.0 = 100.8$, comfortably below the measured value of 106.5.

For the N1576 (OE) data:

Sampled truncation factor: 2.2.

Expected 100% truncation factor (from (29) for $n = 2500$): 3.1.

From equation (26), $c_p = 3.76$.

From Figure 6 ($c = 4.0$, $s = 7.6$, $n = 50$), $\bar{X} - L \geq 42.7$.

From Figure 7 ($c = 3.5$, $s = 7.6$, $n = 50$), $\bar{X} - L \geq 40.8$.

Interpolating for $c = 3.76$, $\bar{X} - L \geq 41.8$.

For NEXT we add 0.9 to the plotted curves. Hence, the lower bound for mean NEXT at 1.576 MHz becomes $41.8 + 40.5 + 0.9 + 12.0 = 95.2$ ($M_N = 12.0$ dB), well below the measured mean of 111.7 dB.

Incidentally, using non-truncated normal distributions for the individual crosstalk values (Figure 4), the lower bounds for FEXT and NEXT would have been 106.5 and 95.8, respectively. The increase in accuracy achieved by the variable truncation method is obviously more dramatic when

high standard deviations are involved.

(ii) As an example of applying the method to large pair count cables, the following data from a highly-blown cellular insulated, filled core duct cable was analyzed.

Table 6: Sampled Crosstalk Data from 1200 Pair/22 AWG Filled Duct Cable (dB/7800 ft.)

| CROSSTALK TYPE | PAIR LOCATION* | 772 kHz | | | 1.576 MHz | | |
|----------------|-----------------------------|-----------|------|-----------|-----------|------|-----------|
| | | \bar{X} | s | X_{min} | \bar{X} | s | X_{min} |
| FEXT (I-O) | Within Unit | 101.6 | 12.5 | 76.5 | 109.7 | 12.6 | 85.0 |
| | Between Adjacent Units | 118.2 | 7.8 | 105.7 | 126.0 | 8.3 | 107.6 |
| | Non-Adj. Units, 1 Unit Sep. | 132.7 | 8.1 | 118.9 | 140.3 | 8.1 | 127.4 |
| | " " 2 " " | 141.0 | 8.1 | 132.5 | 149.5 | 5.0 | 140.6 |
| NEXT | " " 3 " " | 142.9 | 8.0 | 131.5 | 150.0 | 5.9 | 139.0 |
| | Within Unit | 74.6 | 11.3 | 53.4 | 70.8 | 10.5 | 53.1 |
| | Between Adjacent Units | 93.7 | 6.6 | 83.4 | 90.8 | 6.6 | 79.1 |
| | Non-Adj. Units, 1 Unit Sep. | 108.3 | 6.3 | 95.3 | 103.5 | 6.9 | 91.0 |
| " " 2 " " | " " 3 " " | 118.2 | 6.6 | 110.6 | 122.6 | 5.0 | 102.7 |
| | " " 3 " " | 120.6 | 6.7 | 100.6 | 115.4 | 6.5 | 95.3 |

*All units located in outer layer of cable.

Cable attenuation in dB/mile: 23.6 dB/mi. (772 kHz), 32.7 dB/mi. (1.576 MHz).

Evaluating FEXT performance at 1.576 MHz:

To determine the effect of two adjacent units on the within-unit crosstalk (unit size = 100), we consult Table 15 under $\Delta M = 20$ ($\approx 128.0 - 109.7$), $s_1 = 12.6$, $s_2 = 8.3$, $n_2 = 200$. It is seen that no appreciable deterioration in the ΣX^2 power sum (0.0 dB) is likely; therefore, it is sufficient to consider only within unit FEXT:

Sampled truncation factor (from (25)): 2.0. Expected 100% truncation factor (from (29) for $n = 4950$): 3.3.

From equation (27), $c_p = 3.75$.

From Figure 6 ($c = 4.0$, $s = 12.6$, $n = 99$), $\bar{X} - L \geq 59.5$.

From Figure 7 ($c = 3.5$, $s = 12.6$, $n = 99$), $\bar{X} - L \geq 57.0$.

Interpolating for $c = 3.75$, $\bar{X} - L \geq 58.2$.

For a repeater section of length 7800 feet ($L = 48.3$ dB), $\bar{X} \geq 106.5$ dB. The measured value of the crosstalk meets this with a margin $M_F = 3.2$ dB. If a greater margin (e.g. $M_F = 9$ dB) is desired, the repeater section will have to be shortened by the corresponding amount (note that for a cable of this type, the repeater section will usually be designed for a shorter length anyways, corresponding to a nominal loss of approximately 43 dB). Alternatively, if an even larger margin is demanded, less than 100% PCM fill could be used.

NEXT performance at 1.576 MHz:

Since FEXT is not limiting, it is critical to decide how closely units for opposite directions of transmission can be placed before NEXT becomes a problem. First of all, determine the additional effect that the alternate unit has on the NEXT produced by the adjacent unit:

From Table 15, for $\Delta M = 12$ ($\approx 103.5 - 90.8$), $s_1 = 6.6$, $s_2 = 6.9$, $n_2 = 100$, the expected deterioration is approximately 0.2 dB.

For adjacent units:

Sampled truncation factor: 1.7
100% truncation factor: 3.4

From equation (26): 4.2
From Figure 5 ($c = 4.5$, $s = 6.6$, $n = 100$), $\bar{X}_L \geq 41.2$.
From Figure 6 ($c = 4.0$, $s = 6.6$, $n = 100$), $\bar{X}_L \geq 41.0$.

Interpolating for $c = 4.2$, $\bar{X}_L \geq 41.1$.

For NEXT, 0.9 has to be added to this figure:
 $X_N - L \geq 42.0$.

If a fixed repeater length of 7800 feet (48.3 dB) is required, it is seen that 100% PCM fill is still possible ($90.8 > 42.0 + 48.3 + 0.2 = 90.5$), but only with essentially a zero margin ($M_N = 0.3$). For a properly designed repeater span with nominal loss of 43 dB, this margin increases to 5.6 dB. Normal allocation of T-carrier pairs allows at least one unit separation between opposite directions of transmission, in which case more luxurious margins to allow for various degradations will be available.

In the above cases, the sampled truncation factor was always considerably less than the likely truncation factor for 100% testing, as is to be expected for the relatively small sampling rates employed for such large pair count cables. Although the theoretically expected factor was used in every calculation, the sample truncation factor should nevertheless be computed on the chance that the sample managed to include an unusually bad pair combination. The resulting low crosstalk value will significantly affect the power sums, making use of the sampled truncation factor imperative.

The preceding examples have demonstrated use of the developed improved crosstalk requirements in cable acceptance testing. In a similar fashion, for cables with predetermined crosstalk properties, the tables and graphs can be applied to repeater section design and allocation of T-carrier pairs in cables.

8. Summary

Single frequency measurements of pair-to-pair crosstalk have been examined to determine the validity of traditional crosstalk requirements for cables intended for T-carrier use. On the basis of results from numerous 100% tested cables, it was decided that the approximations to the worst case power sums introduced a consistent, sizable error into the crosstalk limits. New equations were developed on the basis of crosstalk distribution functions that are essentially normal with a variable truncation point. The superior accuracy of this method was demonstrated by comparing it with other published crosstalk criteria. The effects of adjacent units on the within-unit

crosstalk in multi-unit cables were estimated and tabulated. Examples illustrated the use of the graphs and tables in cable acceptance testing and T-carrier system design.

Acknowledgments

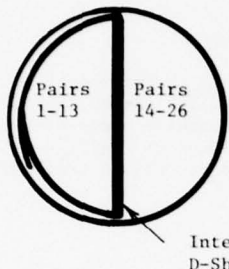
The author wishes to thank the personnel of the Central Laboratory of Phillips Cables Limited for performing the numerous measurements essential to this study, and the management of Phillips Cables Limited for permission to publish this work.

References

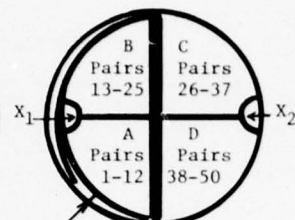
- [1] H. Cravis and T.V. Crater, "Engineering of Tl Carrier System Repeatered Lines", Bell System Technical Journal, p. 431, Mar. 1963.
- [2] B.B. Jacobsen, "Cable Crosstalk Limits on Low Capacity Pulse Code Modulation Systems", Elec. Communication, vol. 48, no. 1 and 2, p. 98, 1973.
- [3] B.R.N. Murthy, "Crosstalk Loss Requirements for PCM Transmission", IEEE Trans. on Commun., vol. COM-24, no. 1, p. 88, Jan. 1976.
- [4] S.D. Bradley, "Crosstalk Considerations for a 48 Channel PCM Repeatered Line", IEEE Trans. on Commun., vol. COM-23, no. 7, p. 722, July 1975.
- [5] R.J. Oakley and R. Jaar, "A Study into Paired Cable Crosstalk", Proc. of Twenty-Second IWCS, p. 136, 1973.
- [6] I. Nasell, "Some Properties of Power Sums of Truncated Normal Random Variables", Bell System Technical Journal, p. 2091, Nov. 1967.
- [7] N.A. Marlow, "A Normal Limit Theorem for Power Sums of Independent Random Variables", Bell System Technical Journal, p. 2081, Nov. 1967.
- [8] L.H.C. Tippett, "On the Extreme Individuals and the Range of Samples Taken from a Normal Population", Biometrika, vol. 17, p. 364.

Appendix 1: Core Constructions of Test Cables

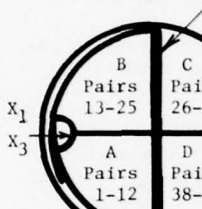
(i) 26/22 FTC:



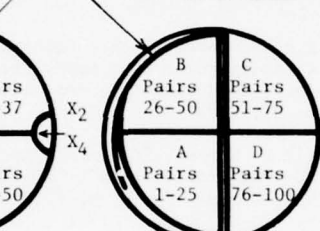
(ii) 52/20 FTICAL:



(iii) 54/22 FTC:



(iv) 100/22 FTC:



X₁, X₂, X₃, X₄ are spare pairs.

Pair combinations for FEXT:

I/S D, ALL: all combinations between pairs in A, B and X.

I/S D, WSU: all combinations between pairs in A alone or all combinations between pairs in B alone.

Similarly, for units outside of D-shield.

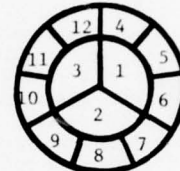
Pair combinations for NEXT:

ALL: all pair combinations from (A,B,X) to (C,D, X).

BASU: all pair combinations from B to C or from A to D.

BOSU: all pair combinations from A to C or from B to D.

(v) 1200/22 Filled Duct Cable:



- (a) In evaluating FEXT performance of the cable, the effect of adjacent units was estimated by considering the deterioration in the 1%WT power sum caused by units 9 and 11 adding further interference to the crosstalk within unit 10.
- (b) In considering NEXT limitations on 100% PCM fill, NEXT between two adjacent units such as 12 and 4 was evaluated. The effect of an alternate unit like 11 further adding to this disturbance in unit 4 was estimated.

Appendix 2: Crosstalk Data

Table 7: Crosstalk in 52 Pair/20 AWG FTICAL Cable (dB/7800 Feet)

| Type of Crosstalk | Pair Location | No. of Combinations | \bar{X} | s | \bar{X}_{rms} | X_{min} | $X_{.5}$ | s_m | $s_{.5}$ | $P_{min}(1)$ | $P_{min}(2)$ |
|-------------------|---------------|---------------------|-----------|------|-----------------|-----------|----------|-------|----------|--------------|--------------|
| N772 | ALL | 676 | 119.9 | 13.5 | 107.1 | 92.0 | 116.5 | 11.4 | 9.5 | 86.2 | 86.8 |
| " | BASU | 144 | 115.7 | 11.0 | 106.2 | 93.0 | | | | 89.9 | 91.0 |
| " | " | 169 | 129.0 | 12.4 | 116.3 | 104.0 | | | | 101.8 | 99.9 |
| " | BOSU | 156 | 114.1 | 10.6 | 105.8 | 92.0 | | | | 87.7 | 87.4 |
| " | " | 156 | 114.6 | 11.4 | 104.8 | 93.0 | | | | 87.6 | 89.7 |
| F772 | I/S D, ALL | 325 | 103.0 | 10.1 | 92.1 | 75.8 | 103.8 | 10.4 | 10.8 | 74.2 | |
| " | " ,WSU | 66 | 97.6 | 8.9 | 89.5 | 75.8 | | | | 74.9 | |
| " | " , " | 78 | 100.1 | 10.0 | 89.3 | 76.8 | | | | 75.6 | |
| " | " , BASU | 156 | 106.9 | 8.9 | 98.3 | 81.8 | | | | 81.1 | |
| " | O/S D, ALL | 325 | 103.8 | 11.1 | 92.8 | 74.8 | 103.6 | 10.3 | 10.5 | 73.0 | |
| " | " , WSU | 66 | 96.3 | 10.0 | 87.7 | 74.8 | | | | 73.2 | |
| " | " , " | 78 | 100.5 | 8.7 | 93.3 | 81.8 | | | | 78.5 | |
| " | " , BASU | 156 | 108.4 | 10.3 | 99.9 | 86.8 | | | | 84.2 | |

Cable Attenuation in dB/mile: 22.5 (772 kHz)

Table 8: Crosstalk in Two 54 Pair/22 AWG FTC Cables (dB/7800 Feet)

| Type of Crosstalk | Pair Location | No. of Combinations | X | s | \bar{X}_{rms} | X _{min} | X _{.5} | S _m | S _{.5} | P _{min(1)} | P _{min(2)} |
|-------------------|---------------|---------------------|-------|------|-----------------|------------------|-----------------|----------------|-----------------|---------------------|---------------------|
| N772 | ALL | 729 | 112.0 | 12.1 | 101.8 | 85.0 | 110.0 | 9.7 | 8.8 | 81.0 | 82.5 |
| | BASU | 144 | 109.7 | 7.6 | 104.6 | 93.0 | | | | 91.5 | 89.3 |
| | " | 169 | 114.4 | 12.7 | 102.4 | 85.0 | | | | 83.2 | 84.6 |
| | BOSU | 156 | 112.7 | 12.6 | 101.6 | 85.0 | | | | 83.7 | 83.7 |
| | " | " | 104.7 | 9.5 | 98.4 | 87.0 | | | | 83.9 | 83.1 |
| | | | | | | | | | | | |
| N1576 | ALL | 729 | 108.1 | 11.3 | 98.2 | 82.0 | 107.0 | 9.6 | 9.1 | 75.5 | 79.3 |
| | BASU | 144 | 106.8 | 8.8 | 100.1 | 86.0 | | | | 84.9 | 85.5 |
| | " | 169 | 108.0 | 12.1 | 97.9 | 82.0 | | | | 79.7 | 81.6 |
| | BOSU | 156 | 109.7 | 9.1 | 103.1 | 89.0 | | | | 87.3 | 79.7 |
| | " | 156 | 101.2 | 9.5 | 94.1 | 83.0 | | | | 77.5 | 86.5 |
| | | | | | | | | | | | |
| F772 | I/S D, ALL | 351 | 96.9 | 10.7 | 86.4 | 72.0 | 97.0 | 10.6 | 10.6 | 69.4 | |
| | " ,WSU | 66 | 90.8 | 9.5 | 83.5 | 73.0 | | | | 70.4 | |
| | " " | 78 | 93.4 | 11.1 | 83.5 | 72.0 | | | | 70.4 | |
| | " ,BASU | 156 | 100.8 | 9.9 | 92.8 | 82.0 | | | | 79.3 | |
| | O/S D, ALL | 351 | 97.1 | 10.8 | 86.9 | 69.0 | 97.0 | 9.8 | 9.9 | 66.2 | |
| | " ,WSU | 66 | 91.1 | 9.6 | 84.7 | 74.0 | | | | 70.9 | |
| F1576 | " " | 78 | 92.0 | 9.2 | 83.3 | 69.0 | | | | 66.7 | |
| | " ,BASU | 156 | 100.6 | 9.2 | 93.0 | 78.0 | | | | 75.6 | |
| | I/S D, ALL | 351 | 99.7 | 10.9 | 89.1 | 73.0 | 99.0 | 10.4 | 9.8 | 68.6 | |
| | " ,WSU | 66 | 95.7 | 11.0 | 87.8 | 77.0 | | | | 72.9 | |
| | " " | 78 | 95.6 | 11.5 | 85.3 | 73.0 | | | | 69.3 | |
| | " ,BASU | 156 | 103.7 | 9.4 | 96.2 | 82.0 | | | | 80.0 | |
| F1576 | O/S D, ALL | 351 | 100.8 | 10.8 | 88.5 | 68.0 | 100.0 | 10.2 | 9.7 | 66.1 | |
| | " ,WSU | 66 | 95.5 | 9.7 | 87.6 | 78.0 | | | | 71.7 | |
| | " " | 78 | 95.1 | 9.8 | 83.6 | 68.0 | | | | 66.3 | |
| | " ,BASU | 156 | 104.8 | 9.8 | 97.0 | 84.0 | | | | 81.0 | |
| | | | | | | | | | | | |
| | | | | | | | | | | | |
| N772 | ALL | 729 | 105.5 | 7.9 | 96.0 | 74.0 | 107.0 | 9.4 | 9.9 | 73.8 | 73.4 |
| | BASU | 144 | 106.6 | 7.5 | 95.5 | 84.0 | | | | 83.2 | 83.8 |
| | " | 169 | 104.1 | 8.3 | 93.1 | 74.0 | | | | 73.7 | 73.8 |
| | BOSU | 156 | 103.6 | 7.5 | 96.6 | 81.0 | | | | 77.8 | 80.8 |
| | " | 156 | 106.8 | 7.4 | 99.2 | 84.0 | | | | 83.2 | 80.5 |
| | | | | | | | | | | | |
| N1576 | ALL | 729 | 102.3 | 8.7 | 91.1 | 71.0 | 104.0 | 9.9 | 10.9 | 70.2 | 70.4 |
| | BASU | 144 | 105.0 | 8.4 | 91.8 | 73.0 | | | | 72.7 | 72.7 |
| | " | 169 | 100.1 | 9.1 | 88.4 | 71.0 | | | | 70.6 | 70.7 |
| | BOSU | 156 | 99.3 | 8.2 | 91.2 | 74.0 | | | | 72.2 | 79.4 |
| | " | 156 | 104.3 | 7.4 | 96.3 | 82.0 | | | | 80.3 | 73.7 |
| | | | | | | | | | | | |
| F772 | I/S D, ALL | 351 | 98.2 | 10.2 | 85.6 | 66.0 | 99.0 | 10.7 | 11.3 | 65.4 | |
| | " ,WSU | 66 | 93.9 | 8.1 | 87.3 | 78.0 | | | | 74.1 | |
| | " " | 78 | 91.0 | 9.2 | 82.5 | 70.0 | | | | 67.0 | |
| | " ,BASU | 156 | 102.4 | 8.7 | 91.6 | 73.0 | | | | 71.2 | |
| | O/S D, ALL | 351 | 97.1 | 9.7 | 88.0 | 74.0 | 98.0 | 10.0 | 10.7 | 68.5 | |
| | " ,WSU | 66 | 92.6 | 9.2 | 85.8 | 77.0 | | | | 72.1 | |
| F1576 | " " | 78 | 92.2 | 9.4 | 85.3 | 74.0 | | | | 71.1 | |
| | " ,BASU | 156 | 102.2 | 7.6 | 94.4 | 78.0 | | | | 77.1 | |
| | I/S D, ALL | 351 | 99.4 | 9.6 | 87.9 | 69.0 | 100.0 | 10.5 | 10.7 | 66.4 | |
| | " ,WSU | 66 | 94.8 | 7.4 | 89.6 | 81.0 | | | | 74.9 | |
| | " ,WSU | 78 | 91.4 | 9.4 | 83.3 | 69.0 | | | | 66.6 | |
| | " ,BASU | 156 | 103.6 | 7.2 | 96.6 | 82.0 | | | | 79.0 | |
| F1576 | O/S D, ALL | 351 | 98.0 | 10.1 | 87.3 | 70.0 | 99.0 | 10.8 | 11.4 | 68.0 | |
| | " ,WSU | 66 | 95.3 | 8.6 | 88.5 | 77.0 | | | | 73.1 | |
| | " " | 78 | 92.7 | 10.0 | 84.1 | 70.0 | | | | 69.0 | |
| | " ,BASU | 156 | 103.7 | 7.5 | 94.5 | 79.0 | | | | 77.7 | |
| | | | | | | | | | | | |
| | | | | | | | | | | | |

Attenuation in dB/mile: Cable 1: 19.9 (772 kHz), 27.9 (1.576 MHz)
Cable 2: 20.0 (772 kHz), 28.3 (1.576 MHz)

Table 9: Crosstalk in 100 Pair/22 AWG FTC Cable (dB/7800 feet)

| Type of Crosstalk | Pair Location | No. of Combinations | \bar{X} | s | \bar{X}_{rms} | X_{min} | $X_{.5}$ | s_m | $s_{.5}$ | $P_{min}(1)$ | $P_{min}(2)$ |
|-------------------|---------------|---------------------|-----------|------|-----------------|-----------|----------|-------|----------|--------------|--------------|
| N772 | ALL | 2500 | 118.4 | 10.1 | 107.1 | 87.0 | 118.0 | 10.2 | 10.2 | 83.4 | 81.6 |
| " | BASU | 625 | 115.6 | 10.0 | 106.4 | 91.0 | | | | 87.8 | 86.8 |
| " | " | " | 115.5 | 10.4 | 105.1 | 87.0 | | | | 83.7 | 84.5 |
| " | BOSU | " | 120.4 | 8.7 | 112.3 | 96.0 | | | | 92.3 | 83.1 |
| " | " | " | 122.2 | 9.7 | 107.5 | 87.0 | | | | 83.9 | 89.5 |
| N1576 | ALL | 2500 | 113.1 | 8.5 | 106.8 | 88.0 | 112.0 | 7.2 | 6.9 | 83.5 | 82.5 |
| " | BASU | 625 | 111.7 | 8.3 | 105.9 | 90.0 | | | | 87.0 | 85.3 |
| " | " | " | 112.4 | 8.6 | 105.8 | 88.0 | | | | 84.8 | 86.7 |
| " | BOSU | " | 114.2 | 7.9 | 109.1 | 98.0 | | | | 90.6 | 84.8 |
| " | " | " | 114.1 | 9.0 | 107.4 | 90.0 | | | | 87.3 | 90.2 |
| F772 | I/S D, ALL | 1225 | 101.3 | 11.0 | 91.1 | 68.7 | 101.7 | 11.0 | 11.3 | 66.9 | |
| " | " ,WSU | 300 | 97.4 | 10.9 | 86.1 | 68.7 | | | | 66.9 | |
| " | " ,WSU | 300 | 96.9 | 10.0 | 87.2 | 69.7 | | | | 68.9 | |
| " | " ,BASU | 625 | 105.3 | 10.1 | 95.0 | 76.7 | | | | 73.8 | |
| " | O/S D, ALL | 1225 | 102.3 | 11.3 | 90.0 | 69.8 | 101.8 | 11.2 | 10.7 | 68.2 | |
| " | " ,WSU | 300 | 98.1 | 11.2 | 87.4 | 71.8 | | | | 68.5 | |
| " | " ,WSU | 300 | 97.8 | 10.1 | 87.5 | 69.8 | | | | 68.8 | |
| " | " ,BASU | 625 | 106.6 | 10.3 | 96.2 | 76.8 | | | | 75.2 | |
| F1576 | I/S D, ALL | 1225 | 105.9 | 10.2 | 94.9 | 76.1 | 106.1 | 10.4 | 10.3 | 73.5 | |
| " | " ,WSU | 300 | 102.2 | 9.7 | 92.1 | 76.1 | | | | 73.5 | |
| " | " ,WSU | 300 | 101.4 | 9.2 | 92.8 | 76.1 | | | | 74.7 | |
| " | " ,BASU | 625 | 109.9 | 9.3 | 100.5 | 82.1 | | | | 79.2 | |
| " | O/S D, ALL | 1225 | 107.5 | 10.8 | 96.1 | 76.4 | 107.4 | 10.5 | 10.5 | 74.5 | |
| " | " ,WSU | 300 | 103.3 | 10.5 | 93.7 | 78.4 | | | | 74.7 | |
| " | " ,WSU | 300 | 102.7 | 9.3 | 93.5 | 76.4 | | | | 75.2 | |
| " | " ,BASU | 625 | 111.9 | 9.8 | 102.2 | 83.4 | | | | 80.9 | |

Cable Attenuation in dB/mile: 19.9 (772 kHz), 28.2 (1.576 MHz)

Table 10: Crosstalk in Three 12 Pair/22 AWG TERM Cables (dB/1,000 feet)

| Type of Crosstalk | Pair Location | No. of Combinations | \bar{X} | s | \bar{X}_{rms} | X_{min} | $X_{.5}$ | s_m | $s_{.5}$ | $P_{min}(1)$ | $P_{min}(2)$ |
|-------------------|---------------|---------------------|-----------|------|-----------------|-----------|----------|-------|----------|--------------|--------------|
| N772 | ALL | 66 | 79.2 | 7.4 | 74.4 | 65.0 | 78.0 | 6.7 | 6.0 | 60.2 | |
| N1576 | " | 66 | 83.2 | 7.7 | 77.4 | 67.0 | 84.0 | 7.5 | 7.8 | 64.0 | |
| F772 | " | 66 | 83.2 | 9.7 | 74.4 | 64.0 | 84.0 | 10.2 | 10.6 | 61.0 | |
| F1576 | " | 66 | 89.4 | 8.7 | 82.0 | 71.0 | 90.0 | 9.1 | 9.3 | 67.7 | |
| N772 | " | 66 | 76.9 | 8.0 | 70.8 | 60.8 | 76.2 | 7.4 | 7.3 | 57.6 | |
| N1576 | " | 66 | 83.4 | 9.0 | 76.9 | 67.8 | 83.2 | 8.4 | 8.3 | 64.1 | |
| F772 | " | 66 | 77.6 | 8.9 | 68.5 | 53.6 | 77.8 | 8.8 | 8.7 | 52.4 | |
| F1576 | " | 66 | 77.2 | 8.7 | 66.0 | 51.2 | 77.0 | 8.9 | 9.0 | 49.4 | |
| N772 | " | 66 | 115.0 | 10.1 | 104.6 | 91.8 | 113.3 | 9.3 | 8.7 | 90.0 | |
| N1576 | " | 66 | 109.1 | 9.8 | 99.7 | 88.2 | 107.2 | 9.1 | 7.9 | 85.0 | |
| F772 | " | 66 | 116.8 | 10.1 | 104.8 | 91.2 | 114.2 | 10.6 | 8.9 | 89.8 | |
| F1576 | " | 66 | 110.0 | 9.7 | 100.8 | 88.7 | 108.7 | 8.5 | 8.1 | 86.1 | |

Attenuation in dB/1,000 feet: Cable 1: 9.0 (772 kHz), 13.2 (1.576 MHz)
 " 2: 11.3 " " 18.4 " "
 " 3: 4.8 " " 7.2 " "

Table 11: Crosstalk in Nine 26 Pair/22 AWG FTC Cables (db/7800 feet)

| Type of Crosstalk | Pair Location | No. of Combinations | \bar{X} | s | \bar{X}_{rms} | X_{min} | $X_{.5}$ | s_m | $s_{.5}$ | $p_{min}(1)$ | $p_{min}(2)$ |
|-------------------|---------------|---------------------|-----------|-----|-----------------|-----------|----------|-------|----------|--------------|--------------|
| N772 | IE | 169 | 100.2 | 7.5 | 93.9 | 79.0 | 100.0 | 7.3 | 7.3 | 77.5 | 77.0 |
| " | OE | 169 | 102.2 | 7.5 | 96.1 | 84.0 | 103.0 | 7.6 | 8.1 | 80.0 | 80.8 |
| N1576 | IE | 169 | 98.1 | 7.7 | 92.5 | 82.0 | 98.0 | 7.2 | 7.4 | 76.9 | 77.1 |
| " | OE | 169 | 100.2 | 8.4 | 92.0 | 78.0 | 101.0 | 9.4 | 9.5 | 76.0 | 76.0 |
| F772 | I/S D | 78 | 91.3 | 9.3 | 83.9 | 70.6 | 91.1 | 8.8 | 8.6 | 68.7 | |
| " | O/S D | 78 | 92.1 | 6.6 | 87.9 | 77.6 | 91.6 | 6.2 | 5.9 | 74.7 | |
| F1576 | I/S D | 78 | 95.7 | 9.7 | 86.9 | 73.4 | 95.4 | 8.9 | 8.9 | 71.1 | |
| " | O/S D | 78 | 96.7 | 7.2 | 91.9 | 82.4 | 96.4 | 6.4 | 6.6 | 77.7 | |
| N772 | IE | 169 | 102.1 | 7.4 | 96.8 | 86.0 | 102.0 | 6.7 | 7.0 | 81.0 | 82.2 |
| " | OE | 169 | 101.2 | 7.8 | 96.1 | 86.0 | 101.0 | 7.1 | 7.0 | 82.1 | 81.2 |
| N1576 | IE | 169 | 100.5 | 7.4 | 95.4 | 86.0 | 101.0 | 7.2 | 7.5 | 80.1 | 80.4 |
| " | OE | 169 | 98.6 | 6.5 | 94.1 | 85.0 | 98.0 | 6.5 | 6.1 | 78.9 | 79.2 |
| F772 | I/S D | 78 | 91.1 | 8.0 | 85.2 | 72.6 | 90.1 | 7.3 | 6.6 | 70.6 | |
| " | O/S D | 78 | 94.2 | 8.8 | 86.3 | 71.6 | 93.1 | 8.5 | 7.8 | 71.1 | |
| F1576 | I/S D | 78 | 96.0 | 8.5 | 89.3 | 76.5 | 95.5 | 7.9 | 7.5 | 73.5 | |
| " | O/S D | 78 | 97.7 | 7.6 | 91.0 | 76.5 | 98.0 | 7.7 | 8.0 | 75.7 | |
| N772 | IE | 169 | 104.0 | 6.9 | 98.8 | 85.0 | 104.0 | 6.9 | 6.9 | 82.5 | 82.3 |
| N1576 | IE | 169 | 103.4 | 8.3 | 96.7 | 85.0 | 103.0 | 7.9 | 7.7 | 80.6 | 79.7 |
| F772 | I/S D | 78 | 92.1 | 8.1 | 82.3 | 68.9 | 91.9 | 7.8 | 8.0 | 66.1 | |
| " | O/S D | 78 | 95.0 | 8.7 | 85.0 | 68.5 | 96.0 | 9.1 | 9.7 | 68.3 | |
| F1576 | I/S D | 78 | 97.7 | 8.2 | 89.4 | 75.0 | 97.0 | 7.7 | 7.5 | 72.5 | |
| " | O/S D | 78 | 101.0 | 9.1 | 90.7 | 74.0 | 101.0 | 9.2 | 9.2 | 73.9 | |
| N772 | IE | 169 | 96.8 | 9.5 | 87.1 | 72.0 | 96.4 | 9.5 | 9.3 | 71.3 | 69.7 |
| " | OE | 169 | 105.7 | 9.0 | 95.5 | 81.0 | 106.2 | 9.5 | 9.7 | 76.9 | 77.4 |
| F772 | I/S D | 78 | 90.2 | 8.2 | 84.3 | 73.4 | 89.7 | 7.2 | 7.3 | 70.0 | |
| " | O/S D | 78 | 93.0 | 8.0 | 86.2 | 75.1 | 94.0 | 8.5 | 8.9 | 71.3 | |
| F772 | I/S D | 78 | 93.2 | 8.8 | 85.8 | 73.6 | 93.2 | 8.3 | 8.4 | 71.4 | |
| " | O/S D | 78 | 92.8 | 7.8 | 87.7 | 79.1 | 93.0 | 7.5 | 7.5 | 74.0 | |
| F772 | I/S D | 78 | 90.2 | 7.7 | 83.9 | 71.8 | 90.8 | 8.1 | 8.3 | 69.0 | |
| " | O/S D | 78 | 91.4 | 7.4 | 86.4 | 75.8 | 90.5 | 6.8 | 6.4 | 71.7 | |
| F772 | I/S D | 78 | 92.0 | 8.7 | 85.4 | 74.8 | 91.9 | 8.3 | 8.3 | 71.9 | |
| " | O/S D | 78 | 91.9 | 8.7 | 85.7 | 75.4 | 91.1 | 7.8 | 7.4 | 71.2 | |
| N772 | IE | 169 | 106.1 | 8.1 | 97.4 | 80.8 | 106.4 | 8.6 | 8.6 | 78.8 | 80.1 |
| " | OE | 169 | 106.1 | 7.7 | 100.7 | 92.0 | 106.2 | 7.5 | 7.6 | 85.9 | 86.0 |
| F772 | I/S D | 78 | 94.3 | 8.1 | 87.8 | 76.8 | 95.1 | 8.9 | 8.9 | 73.5 | |
| " | O/S D | 78 | 91.6 | 6.6 | 87.3 | 75.6 | 91.5 | 6.3 | 6.3 | 72.5 | |
| F772 | I/S D | 78 | 94.9 | 8.4 | 88.3 | 78.1 | 95.7 | 8.4 | 9.0 | 75.1 | |
| " | O/S D | 78 | 90.4 | 6.4 | 86.6 | 74.9 | 89.9 | 5.8 | 5.5 | 72.4 | |

Cable Attenuation in dB/mile: Cable 1: 19.9 (772 kHz), 28.3 (1.576 MHz)

" 2: 20.1 " " 28.5 " "

" 3: 20.5 " " 28.7 " "

" 4: 20.3 " "

" 5: 20.4 " "

" 6: 20.2 " "

" 7: 20.2 " "

" 8: 20.5 " "

" 9: 20.2 " "

Appendix 3: Comparison of Power Sum Approximations

Table 12: Accuracy of Power Sum Approximations at 772 kHz and 1.576 MHz

| Cable | Type of Crosstalk | Pair Location | Measured Minimum PS | Approximations to 1% WT Power Sum | | | |
|--------------|-------------------|---------------|---------------------|-----------------------------------|--------------------|--------------|-------|
| | | | | Normal XT Dist. | Truncated XT Dist. | VTN XT Dist. | |
| | | | | 1% WT | Error | 1%WT | Error |
| 100/22 FTC | N772 | ALL | 83.4 | 80.1 | -3.4 | 83.9 | 0.5 |
| | " | " | 81.6 | 80.1 | -1.5 | 83.9 | 2.3 |
| | N1576 | ALL | 83.5 | 81.0 | -2.6 | 83.2 | -0.4 |
| | " | " | 82.5 | 81.0 | -1.5 | 83.2 | 0.7 |
| | F772 | I/S D | 66.9 | 59.7 | -7.3 | 64.2 | -2.8 |
| | " | O/S D | 68.2 | 59.7 | -8.6 | 64.3 | -3.9 |
| | F1576 | I/S D | 73.5 | 67.3 | -6.2 | 71.3 | -1.4 |
| 54/22 FTC | " | O/S D | 74.5 | 66.6 | -7.9 | 71.0 | -3.5 |
| | N772 | ALL | 81.0 | 69.2 | -11.8 | 73.3 | -7.7 |
| | " | " | 82.5 | 69.2 | -13.3 | 73.3 | -9.3 |
| | N1576 | " | 75.5 | 67.9 | -7.5 | 71.8 | -3.7 |
| | " | " | 79.3 | 67.9 | -11.4 | 71.8 | -7.5 |
| | F772 | I/S D | 69.4 | 58.8 | -10.6 | 62.5 | -7.0 |
| | " | O/S D | 66.2 | 58.7 | -7.5 | 62.3 | -3.8 |
| 54/22 FTC | F1576 | I/S D | 68.6 | 60.7 | -7.9 | 64.4 | -4.1 |
| | " | O/S D | 66.1 | 62.2 | -3.9 | 65.9 | -0.2 |
| | N772 | ALL | 73.8 | 77.1 | 3.3 | 78.8 | 5.0 |
| | " | " | 73.4 | 77.1 | 3.7 | 78.8 | 5.3 |
| | N1576 | " | 70.2 | 71.0 | 0.8 | 73.3 | 3.2 |
| | " | " | 70.4 | 71.0 | 0.6 | 73.3 | 2.9 |
| | F772 | I/S D | 65.4 | 61.6 | -3.8 | 65.0 | -0.4 |
| 52/20 FTICAL | " | O/S D | 68.5 | 62.5 | -6.0 | 65.6 | -2.9 |
| | N1576 | I/S D | 66.4 | 64.9 | -1.5 | 68.0 | -1.6 |
| | " | O/S D | 68.0 | 61.9 | -6.1 | 65.2 | -2.7 |
| | N772 | ALL | 86.2 | 73.0 | -13.1 | 77.0 | -9.1 |
| | " | " | 86.8 | 73.0 | -13.7 | 77.0 | -9.7 |
| | F772 | I/S D | 74.2 | 67.1 | -7.1 | 70.4 | -3.9 |
| | " | O/S D | 73.0 | 64.5 | -8.5 | 68.2 | -4.8 |
| 26/22 FTC | N772 | IE | 77.5 | 74.9 | -2.6 | 76.3 | -1.3 |
| | " | " | 77.0 | 74.9 | -2.1 | 76.3 | -0.7 |
| | " | OE | 80.0 | 76.9 | -3.1 | 78.3 | -1.7 |
| | " | " | 80.8 | 76.9 | -3.9 | 78.3 | -2.5 |
| | N1576 | IE | 76.9 | 72.1 | -4.8 | 73.6 | -3.3 |
| | " | " | 77.1 | 72.1 | -5.0 | 73.6 | -3.5 |
| | " | OE | 76.0 | 71.8 | -4.2 | 73.8 | -2.2 |
| | " | " | 76.0 | 71.8 | -4.2 | 73.8 | -2.3 |
| | F772 | I/S D | 68.7 | 60.4 | -8.3 | 62.1 | -6.0 |
| | " | O/S D | 74.4 | 69.8 | -4.9 | 70.7 | -4.1 |
| | F1576 | I/S D | 71.1 | 63.5 | -7.6 | 66.0 | -5.1 |
| | " | O/S D | 77.7 | 72.8 | -4.9 | 73.9 | -3.8 |
| | N772 | IE | 81.0 | 77.0 | -4.0 | 78.4 | -2.7 |
| | " | " | 82.2 | 77.0 | -5.1 | 78.4 | -3.8 |
| 26/22 FTC | " | OE | 82.1 | 75.1 | -7.0 | 76.6 | -5.5 |
| | " | " | 81.2 | 75.1 | -6.1 | 76.6 | -4.6 |
| | N1576 | IE | 80.1 | 75.6 | -4.5 | 76.9 | -3.2 |
| | " | " | 80.4 | 75.6 | -4.8 | 76.9 | -3.5 |
| | " | OE | 78.9 | 76.5 | -2.4 | 77.3 | -1.6 |
| | " | " | 79.2 | 76.5 | -2.7 | 77.3 | -1.9 |
| | F772 | I/S D | 70.6 | 64.3 | -6.3 | 66.0 | -4.7 |
| | " | O/S D | 71.1 | 64.9 | -6.2 | 67.0 | -4.1 |
| | F1576 | I/S D | 73.5 | 67.7 | -5.8 | 69.6 | -3.9 |
| | " | O/S D | 75.7 | 72.4 | -3.3 | 73.8 | -1.8 |

Table 12: (continued)

| Cable | Type of Crosstalk | Pair Location | Measured Minimum PS | Approximations to 1% WT Power Sum | | | |
|------------|-------------------|---------------|---------------------|-----------------------------------|----------------|----------------|----------------|
| | | | | Normal 1% WT | XT Dist. Error | Truncated 1%WT | XT Dist. Error |
| 26/22 FTC | N772 | IE | 82.5 | 81.0 | -1.5 | 82.0 | -0.5 |
| | " | " | 82.3 | 81.0 | -1.3 | 82.0 | -0.3 |
| | N1576 | " | 80.6 | 75.5 | -5.1 | 77.4 | -3.2 |
| | " | " | 79.7 | 75.5 | -4.2 | 77.4 | -2.3 |
| | F772 | I/S D | 66.1 | 65.2 | -0.9 | 66.8 | 0.7 |
| | " | O/S D | 68.3 | 65.9 | -2.4 | 68.1 | -0.2 |
| | F1576 | I/S D | 72.5 | 70.3 | -2.2 | 72.1 | -0.4 |
| 26/22 FTC | " | O/S D | 73.9 | 70.5 | -3.4 | 72.9 | -1.0 |
| | N772 | IE | 71.3 | 65.0 | -6.4 | 67.5 | -3.8 |
| | " | " | 69.7 | 65.0 | -4.7 | 67.5 | -2.2 |
| | " | OE | 76.9 | 75.4 | -1.4 | 77.7 | 0.8 |
| | " | " | 77.4 | 75.4 | -2.0 | 77.7 | 0.3 |
| | F772 | I/S D | 70.0 | 62.7 | -7.3 | 64.5 | -5.5 |
| | " | O/S D | 71.3 | 66.3 | -5.0 | 68.0 | -3.4 |
| 26/22 FTC | F772 | I/S D | 71.4 | 63.9 | -7.5 | 66.0 | -5.4 |
| | " | O/S D | 74.0 | 66.8 | -7.2 | 68.3 | -5.6 |
| 26/22 FTC | F772 | I/S D | 69.0 | 64.3 | -4.7 | 66.9 | -3.2 |
| | " | O/S D | 71.7 | 66.7 | -4.9 | 68.0 | -3.6 |
| 26/22 FTC | F772 | I/S D | 71.9 | 62.9 | -9.0 | 65.0 | -6.9 |
| | " | O/S D | 71.2 | 63.1 | -8.1 | 65.1 | -6.1 |
| 26/22 FTC | N772 | IE | 78.8 | 79.0 | 0.2 | 80.8 | 2.0 |
| | " | " | 80.1 | 79.0 | -1.1 | 80.8 | 0.6 |
| | " | OE | 85.9 | 80.3 | -5.6 | 81.7 | -4.1 |
| | " | " | 86.0 | 80.3 | -5.7 | 81.7 | -4.3 |
| | F772 | I/S D | 73.5 | 67.3 | -6.1 | 69.0 | -4.4 |
| 26/22 FTC | " | O/S D | 72.5 | 69.5 | -3.0 | 70.4 | -2.2 |
| | F772 | I/S D | 75.1 | 67.0 | -8.1 | 68.9 | -6.2 |
| 26/22 FTC | " | O/S D | 72.4 | 69.0 | -3.4 | 69.8 | -2.7 |
| 12/22 TERM | N772 | ALL | 60.2 | 54.7 | -5.5 | 55.8 | -4.4 |
| | N1576 | " | 64.0 | 57.7 | -6.3 | 59.0 | -5.0 |
| | F772 | " | 61.0 | 51.3 | -9.7 | 53.8 | -7.2 |
| | F1576 | " | 67.7 | 60.6 | -7.1 | 62.6 | -5.1 |
| 12/22 TERM | N772 | ALL | 57.6 | 50.5 | -7.1 | 51.9 | -5.7 |
| | N1576 | " | 64.1 | 53.7 | -10.4 | 55.6 | -8.5 |
| | F772 | " | 52.4 | 48.2 | -4.2 | 50.3 | -2.1 |
| | F1576 | " | 49.4 | 48.5 | -0.9 | 50.5 | 1.1 |
| 12/22 TERM | N772 | ALL | 90.0 | 81.8 | -8.2 | 84.2 | -5.8 |
| | N1576 | " | 85.0 | 76.8 | -8.2 | 79.1 | -5.9 |
| | F772 | " | 89.8 | 83.6 | -6.2 | 86.2 | -3.6 |
| | F1576 | " | 86.1 | 77.8 | -8.3 | 80.3 | -5.8 |

Appendix 4: Correction Factors for Effect of Additional Units on Crosstalk Power Sums

Table 13: Expected Deterioration in 1% WT Power Sums Due to Effects
of Adjacent Units (Monte Carlo Simulation for $n_1 = 25$)

| ΔM | $S_2 \backslash S_1$ | $n_2 = 25$ | | | | | $n_2 = 50$ | | | | | $n_2 = 75$ | | | | |
|------------|----------------------|------------|-----|-----|-----|-----|------------|-----|-----|-----|------|------------|-----|-----|-----|------|
| | | 4 | 6 | 8 | 10 | 12 | 4 | 6 | 8 | 10 | 12 | 4 | 6 | 8 | 10 | 12 |
| 4 | 6 | 0.7 | 1.0 | 1.6 | 3.8 | 8.8 | 0.8 | 1.3 | 3.4 | 5.6 | 10.3 | 0.9 | 2.2 | 3.9 | 7.5 | 11.2 |
| | 8 | 0.0 | 0.4 | 1.2 | 2.0 | 4.4 | 0.0 | 0.1 | 0.9 | 3.0 | 6.8 | 0.9 | 1.0 | 1.7 | 4.0 | 7.4 |
| | 10 | 0.5 | 0.2 | 0.2 | 0.3 | 2.6 | 0.0 | 0.0 | 0.0 | 1.0 | 2.6 | 0.0 | 0.5 | 0.5 | 1.4 | 4.0 |
| | 12 | 0.0 | 0.0 | 0.0 | 0.0 | 1.2 | 0.0 | 0.0 | 0.0 | 0.0 | 0.0 | 0.1 | 0.0 | 0.0 | 0.6 | 1.0 |
| | 14 | 0.0 | 0.0 | 0.0 | 0.0 | 0.0 | 0.1 | 0.0 | 0.0 | 0.0 | 0.0 | 0.0 | 0.0 | 0.0 | 0.0 | 0.0 |
| 8 | 6 | 0.3 | 0.2 | 1.0 | 1.8 | 3.8 | 0.2 | 0.4 | 0.9 | 3.2 | 6.6 | 0.0 | 0.8 | 1.8 | 3.4 | 7.1 |
| | 8 | 0.0 | 0.0 | 0.0 | 0.6 | 1.8 | 0.0 | 0.5 | 0.4 | 1.1 | 3.1 | 0.1 | 0.0 | 0.4 | 1.9 | 4.1 |
| | 10 | 0.0 | 0.1 | 0.0 | 0.4 | 0.3 | 0.2 | 0.1 | 0.0 | 1.2 | 0.6 | 0.3 | 0.0 | 0.2 | 0.0 | 1.7 |
| | 12 | 0.0 | 0.0 | 0.0 | 0.0 | 0.0 | 0.0 | 0.0 | 0.0 | 0.8 | 0.0 | 0.0 | 0.0 | 0.0 | 0.0 | 0.7 |
| | 14 | 0.0 | 0.0 | 0.0 | 0.3 | 0.0 | 0.5 | 0.0 | 0.1 | 0.0 | 0.0 | 0.0 | 0.0 | 0.0 | 0.0 | 0.0 |
| 12 | 6 | 0.0 | 0.0 | 0.1 | 1.0 | 2.0 | 0.1 | 0.1 | 0.8 | 1.0 | 3.0 | 0.2 | 0.7 | 0.7 | 1.4 | 3.7 |
| | 8 | 0.0 | 0.0 | 0.0 | 0.0 | 0.9 | 0.2 | 0.0 | 0.4 | 0.1 | 1.0 | 0.1 | 0.1 | 0.0 | 0.9 | 0.9 |
| | 10 | 0.5 | 0.5 | 0.0 | 0.2 | 0.0 | 0.4 | 0.2 | 0.0 | 0.0 | 0.3 | 0.2 | 0.0 | 0.0 | 0.0 | 0.0 |
| | 12 | 0.3 | 0.0 | 0.0 | 0.7 | 0.0 | 0.0 | 0.0 | 0.0 | 0.7 | 0.0 | 0.2 | 0.0 | 0.0 | 0.0 | 0.0 |
| | 14 | 0.0 | 1.3 | 0.0 | 0.1 | 1.1 | 0.0 | 0.0 | 2.1 | 0.0 | 0.0 | 0.0 | 0.0 | 0.0 | 0.3 | 1.0 |
| 16 | 6 | 0.0 | 0.4 | 0.5 | 0.0 | 0.4 | 0.0 | 0.0 | 0.3 | 0.3 | 1.2 | 0.3 | 0.1 | 0.2 | 1.3 | 1.9 |
| | 8 | 0.0 | 0.0 | 0.3 | 0.6 | 0.0 | 0.0 | 0.0 | 0.0 | 0.0 | 0.0 | 0.0 | 0.0 | 0.0 | 0.0 | 0.7 |
| | 10 | 0.0 | 0.1 | 0.0 | 0.0 | 0.0 | 0.5 | 0.0 | 0.0 | 0.0 | 0.3 | 0.0 | 0.0 | 0.0 | 0.9 | 0.0 |
| | 12 | 0.1 | 0.0 | 0.1 | 0.0 | 0.0 | 0.0 | 0.0 | 0.0 | 0.0 | 0.1 | 0.4 | 1.1 | 0.0 | 0.0 | 0.0 |
| | 14 | 0.0 | 0.0 | 0.0 | 0.0 | 0.0 | 0.0 | 0.0 | 0.0 | 0.9 | 0.0 | 0.0 | 0.0 | 0.0 | 0.0 | 0.0 |
| 20 | 6 | 0.2 | 0.0 | 0.0 | 0.2 | 0.5 | 0.0 | 0.0 | 0.0 | 0.3 | 0.4 | 0.0 | 0.0 | 0.0 | 0.5 | 0.4 |
| | 8 | 0.0 | 0.0 | 0.0 | 0.1 | 0.3 | 0.0 | 0.6 | 0.0 | 0.2 | 0.4 | 0.0 | 0.0 | 0.0 | 0.0 | 0.0 |
| | 10 | 0.0 | 0.0 | 0.0 | 0.6 | 0.0 | 0.0 | 0.2 | 0.2 | 0.4 | 0.0 | 0.0 | 0.0 | 0.0 | 0.0 | 0.3 |
| | 12 | 0.0 | 0.0 | 0.0 | 0.0 | 0.0 | 0.0 | 0.0 | 0.0 | 0.0 | 0.0 | 0.0 | 0.0 | 0.0 | 0.0 | 0.4 |
| | 14 | 0.1 | 0.0 | 0.2 | 0.0 | 0.0 | 0.0 | 0.2 | 0.3 | 0.0 | 0.0 | 0.0 | 0.0 | 0.3 | 0.7 | 0.3 |

Table 14: Expected Deterioration in 1% WT Power Sums Due to Effects
of Adjacent Units (Monte Carlo Simulation for $n_1 = 50$)

| ΔM | $S_2 \backslash S_1$ | $n_2 = 50$ | | | | | $n_2 = 100$ | | | | | $n_2 = 150$ | | | | |
|------------|----------------------|------------|-----|-----|-----|-----|-------------|-----|-----|-----|------|-------------|-----|-----|-----|------|
| | | 4 | 6 | 8 | 10 | 12 | 4 | 6 | 8 | 10 | 12 | 4 | 6 | 8 | 10 | 12 |
| 4 | 6 | 0.7 | 1.1 | 2.2 | 4.4 | 7.9 | 1.2 | 1.7 | 3.3 | 6.1 | 10.0 | 1.5 | 2.3 | 4.2 | 7.1 | 10.7 |
| | 8 | 0.3 | 0.2 | 0.9 | 1.9 | 4.9 | 0.2 | 0.6 | 1.6 | 3.5 | 7.4 | 0.6 | 1.2 | 2.0 | 4.3 | 7.5 |
| | 10 | 0.1 | 0.0 | 0.2 | 0.7 | 2.2 | 0.3 | 0.0 | 0.4 | 1.3 | 3.1 | 0.3 | 0.3 | 0.8 | 2.1 | 4.4 |
| | 12 | 0.7 | 0.0 | 0.3 | 0.0 | 0.4 | 0.0 | 0.0 | 0.2 | 0.0 | 0.6 | 0.0 | 0.2 | 0.1 | 0.0 | 1.5 |
| | 14 | 0.4 | 0.0 | 0.6 | 0.0 | 0.0 | 0.2 | 0.0 | 0.0 | 0.0 | 0.0 | 0.0 | 0.5 | 0.0 | 0.0 | 0.4 |
| 8 | 6 | 0.2 | 0.5 | 0.9 | 2.0 | 4.0 | 0.4 | 0.8 | 1.3 | 3.3 | 5.9 | 0.6 | 1.1 | 1.9 | 4.2 | 7.3 |
| | 8 | 0.2 | 0.3 | 0.3 | 0.6 | 2.1 | 0.3 | 0.1 | 0.6 | 1.4 | 3.5 | 0.3 | 0.5 | 0.7 | 2.0 | 4.0 |
| | 10 | 0.0 | 0.0 | 0.1 | 0.0 | 0.7 | 0.1 | 0.0 | 0.0 | 0.5 | 1.5 | 0.0 | 0.2 | 0.0 | 0.3 | 2.0 |
| | 12 | 0.0 | 0.0 | 0.0 | 0.0 | 0.0 | 0.3 | 0.4 | 0.0 | 0.4 | 0.5 | 0.0 | 0.1 | 0.0 | 0.0 | 0.4 |
| | 14 | 0.0 | 0.0 | 0.4 | 0.0 | 0.0 | 0.1 | 0.2 | 0.0 | 0.0 | 0.0 | 0.0 | 0.0 | 0.0 | 0.0 | 0.0 |
| 12 | 6 | 0.0 | 0.2 | 0.2 | 0.6 | 2.2 | 0.1 | 0.2 | 0.4 | 1.3 | 3.0 | 0.4 | 0.4 | 0.9 | 1.8 | 4.0 |
| | 8 | 0.1 | 0.2 | 0.0 | 0.4 | 0.6 | 0.0 | 0.1 | 0.3 | 0.8 | 1.4 | 0.1 | 0.5 | 0.4 | 0.5 | 2.0 |
| | 10 | 0.0 | 0.0 | 0.0 | 0.2 | 0.3 | 0.3 | 0.0 | 0.1 | 0.3 | 0.6 | 0.0 | 0.0 | 0.0 | 0.3 | 0.5 |
| | 12 | 0.1 | 0.0 | 0.2 | 0.0 | 0.0 | 0.2 | 0.1 | 0.2 | 0.0 | 0.0 | 0.4 | 0.0 | 0.0 | 0.1 | 0.0 |
| | 14 | 0.0 | 0.0 | 0.0 | 0.0 | 0.0 | 0.0 | 0.1 | 0.2 | 0.0 | 0.2 | 0.0 | 0.0 | 0.0 | 0.0 | 0.0 |
| 16 | 6 | 0.0 | 0.1 | 0.1 | 0.4 | 0.9 | 0.0 | 0.3 | 0.3 | 0.6 | 1.2 | 0.2 | 0.2 | 0.1 | 0.9 | 1.7 |
| | 8 | 0.0 | 0.0 | 0.0 | 0.0 | 0.6 | 0.0 | 0.0 | 0.0 | 0.2 | 0.3 | 0.0 | 0.0 | 0.1 | 0.2 | 0.6 |
| | 10 | 0.0 | 0.2 | 0.0 | 0.0 | 0.2 | 0.0 | 0.1 | 0.2 | 0.0 | 0.3 | 0.2 | 0.0 | 0.3 | 0.1 | 0.0 |
| | 12 | 0.1 | 0.0 | 0.0 | 0.1 | 0.0 | 0.1 | 0.0 | 0.0 | 0.0 | 0.0 | 0.0 | 0.0 | 0.2 | 0.0 | 0.5 |
| | 14 | 0.2 | 0.0 | 0.0 | 0.0 | 0.0 | 0.0 | 0.0 | 0.5 | 0.0 | 0.3 | 0.2 | 0.6 | 0.0 | 0.3 | 0.0 |
| 20 | 6 | 0.1 | 0.1 | 0.0 | 0.3 | 0.2 | 0.0 | 0.1 | 0.1 | 0.2 | 0.5 | 0.2 | 0.1 | 0.0 | 0.4 | 0.6 |
| | 8 | 0.1 | 0.0 | 0.1 | 0.0 | 0.1 | 0.0 | 0.0 | 0.0 | 0.0 | 0.1 | 0.0 | 0.0 | 0.0 | 0.2 | 0.2 |
| | 10 | 0.0 | 0.3 | 0.0 | 0.0 | 0.1 | 0.2 | 0.2 | 0.1 | 0.0 | 0.2 | 0.0 | 0.0 | 0.0 | 0.0 | 0.5 |
| | 12 | 0.0 | 0.0 | 0.3 | 0.0 | 0.1 | 0.0 | 0.0 | 0.0 | 0.0 | 0.0 | 0.3 | 0.2 | 0.0 | 0.1 | 0.0 |
| | 14 | 0.0 | 0.0 | 0.0 | 0.0 | 0.0 | 0.0 | 0.0 | 0.1 | 0.0 | 0.1 | 0.0 | 0.2 | 0.0 | 0.0 | 0.2 |

Table 15: Expected Deterioration in 1% WT Power Sums Due to Effects
of Adjacent Units (Monte Carlo Simulation for $n_1 = 100$)

| ΔM | $S_2 \backslash S_1$ | $n_2 = 100$ | | | | | $n_2 = 200$ | | | | | $n_2 = 300$ | | | | |
|----|----------------------|-------------|-----|-----|-----|-----|-------------|-----|-----|-----|-----|-------------|-----|-----|-----|------|
| | | 4 | 6 | 8 | 10 | 12 | 4 | 6 | 8 | 10 | 12 | 4 | 6 | 8 | 10 | 12 |
| 4 | 6 | 0.6 | 1.2 | 2.0 | 4.1 | 7.4 | 1.3 | 2.0 | 3.5 | 6.0 | 9.5 | 1.8 | 2.7 | 4.4 | 7.3 | 10.6 |
| | 8 | 0.4 | 0.5 | 1.0 | 2.2 | 4.8 | 0.6 | 0.9 | 1.7 | 3.5 | 6.4 | 0.7 | 1.5 | 2.4 | 4.5 | 7.7 |
| | 10 | 0.4 | 0.2 | 0.3 | 0.8 | 2.1 | 0.3 | 0.4 | 0.7 | 1.6 | 3.5 | 0.3 | 0.6 | 1.0 | 2.2 | 4.5 |
| | 12 | 0.3 | 0.0 | 0.1 | 0.5 | 0.8 | 0.3 | 0.0 | 0.4 | 0.7 | 1.2 | 0.0 | 0.0 | 0.0 | 0.7 | 2.0 |
| | 14 | 0.0 | 0.0 | 0.0 | 0.2 | 0.0 | 0.2 | 0.1 | 0.1 | 0.2 | 0.2 | 0.0 | 0.0 | 0.0 | 0.2 | 0.4 |
| 8 | 6 | 0.3 | 0.5 | 0.9 | 2.0 | 4.1 | 0.5 | 0.8 | 1.5 | 3.1 | 5.9 | 0.8 | 1.3 | 2.1 | 4.0 | 7.1 |
| | 8 | 0.2 | 0.0 | 0.4 | 0.9 | 2.1 | 0.2 | 0.4 | 0.7 | 1.5 | 3.5 | 0.4 | 0.5 | 1.0 | 2.1 | 4.5 |
| | 10 | 0.0 | 0.0 | 0.0 | 0.3 | 1.0 | 0.0 | 0.1 | 0.2 | 0.7 | 1.3 | 0.0 | 0.2 | 0.6 | 0.7 | 2.2 |
| | 12 | 0.4 | 0.3 | 0.0 | 0.1 | 0.4 | 0.2 | 0.0 | 0.1 | 0.1 | 0.5 | 0.2 | 0.0 | 0.0 | 0.4 | 0.7 |
| | 14 | 0.0 | 0.2 | 0.2 | 0.2 | 0.0 | 0.0 | 0.0 | 0.0 | 0.0 | 0.0 | 0.0 | 0.0 | 0.4 | 0.2 | 0.3 |
| 12 | 6 | 0.1 | 0.1 | 0.3 | 0.8 | 1.7 | 0.2 | 0.5 | 0.7 | 1.4 | 3.0 | 0.5 | 0.5 | 1.0 | 2.0 | 3.8 |
| | 8 | 0.2 | 0.0 | 0.1 | 0.3 | 0.7 | 0.0 | 0.2 | 0.3 | 0.7 | 1.4 | 0.2 | 0.2 | 0.6 | 0.9 | 2.1 |
| | 10 | 0.0 | 0.0 | 0.1 | 0.3 | 0.4 | 0.2 | 0.0 | 0.1 | 0.1 | 0.4 | 0.1 | 0.1 | 0.1 | 0.2 | 0.9 |
| | 12 | 0.0 | 0.0 | 0.0 | 0.0 | 0.1 | 0.3 | 0.0 | 0.0 | 0.0 | 0.1 | 0.1 | 0.0 | 0.2 | 0.0 | 0.1 |
| | 14 | 0.0 | 0.0 | 0.4 | 0.2 | 0.0 | 0.0 | 0.1 | 0.1 | 0.0 | 0.2 | 0.0 | 0.0 | 0.0 | 0.1 | 0.0 |
| 16 | 6 | 0.1 | 0.1 | 0.3 | 0.8 | 1.7 | 0.2 | 0.5 | 0.7 | 1.4 | 3.0 | 0.5 | 0.5 | 1.0 | 2.0 | 3.8 |
| | 8 | 0.1 | 0.2 | 0.1 | 0.2 | 0.4 | 0.0 | 0.0 | 0.0 | 0.3 | 0.5 | 0.1 | 0.0 | 0.3 | 0.5 | 0.9 |
| | 10 | 0.1 | 0.1 | 0.0 | 0.0 | 0.0 | 0.1 | 0.1 | 0.0 | 0.3 | 0.2 | 0.1 | 0.1 | 0.0 | 0.2 | 0.2 |
| | 12 | 0.0 | 0.0 | 0.0 | 0.0 | 0.0 | 0.1 | 0.2 | 0.0 | 0.2 | 0.3 | 0.0 | 0.1 | 0.1 | 0.1 | 0.0 |
| | 14 | 0.1 | 0.3 | 0.0 | 0.2 | 0.3 | 0.1 | 0.0 | 0.1 | 0.0 | 0.0 | 0.0 | 0.0 | 0.0 | 0.0 | 0.0 |
| 20 | 6 | 0.1 | 0.1 | 0.0 | 0.1 | 0.2 | 0.0 | 0.1 | 0.0 | 0.2 | 0.6 | 0.0 | 0.1 | 0.1 | 0.3 | 0.6 |
| | 8 | 0.0 | 0.1 | 0.0 | 0.0 | 0.1 | 0.0 | 0.1 | 0.0 | 0.1 | 0.4 | 0.0 | 0.0 | 0.1 | 0.1 | 0.3 |
| | 10 | 0.0 | 0.1 | 0.0 | 0.0 | 0.0 | 0.0 | 0.0 | 0.1 | 0.1 | 0.0 | 0.0 | 0.0 | 0.0 | 0.1 | 0.2 |
| | 12 | 0.0 | 0.0 | 0.0 | 0.0 | 0.0 | 0.2 | 0.0 | 0.0 | 0.0 | 0.0 | 0.0 | 0.0 | 0.0 | 0.1 | 0.2 |
| | 14 | 0.0 | 0.1 | 0.0 | 0.0 | 0.2 | 0.0 | 0.1 | 0.0 | 0.3 | 0.0 | 0.1 | 0.0 | 0.0 | 0.1 | 0.2 |

Appendix 5: Graphs of Crosstalk Loss Requirements

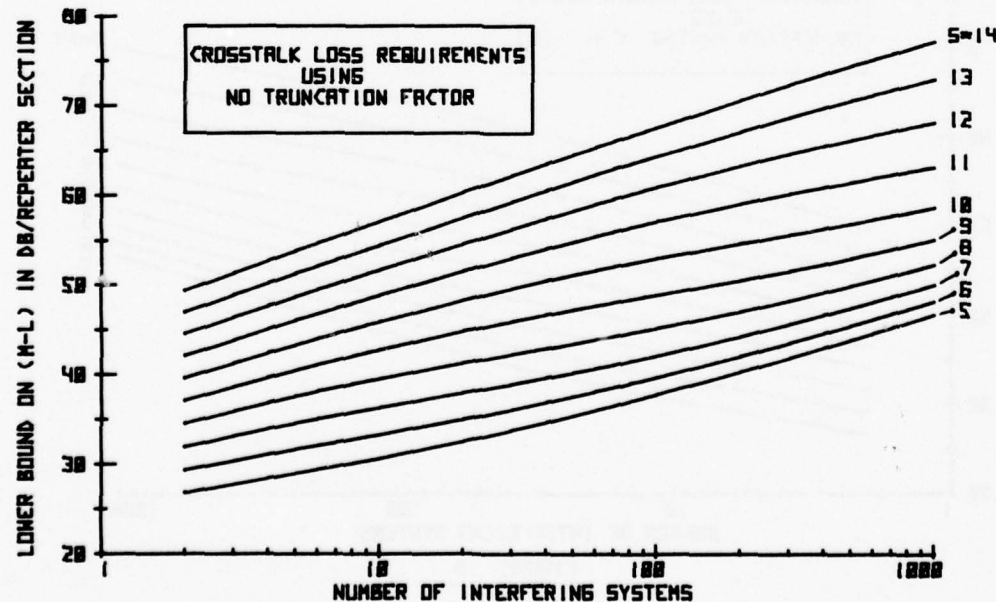


FIGURE 4

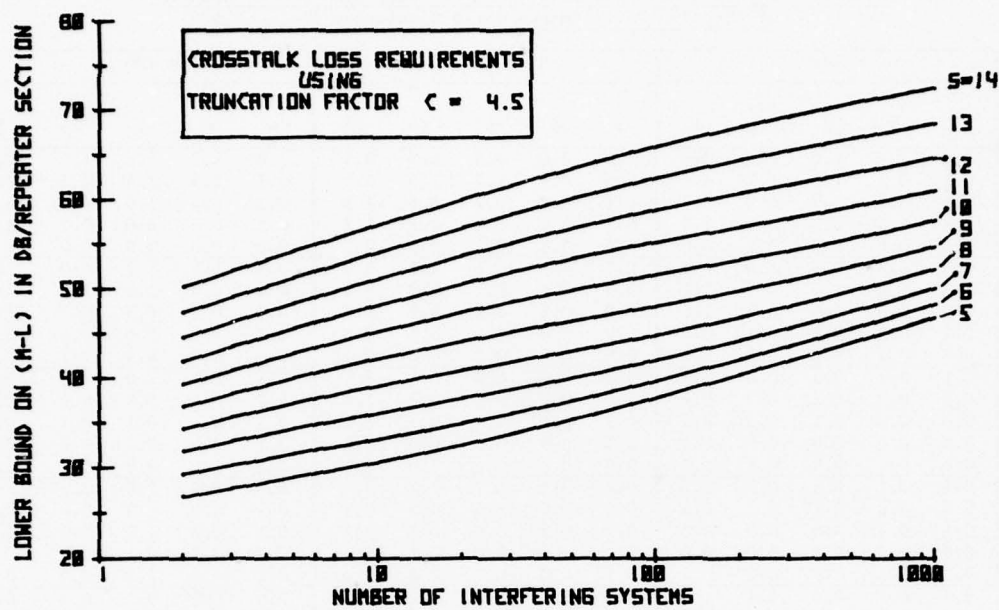


FIGURE 5

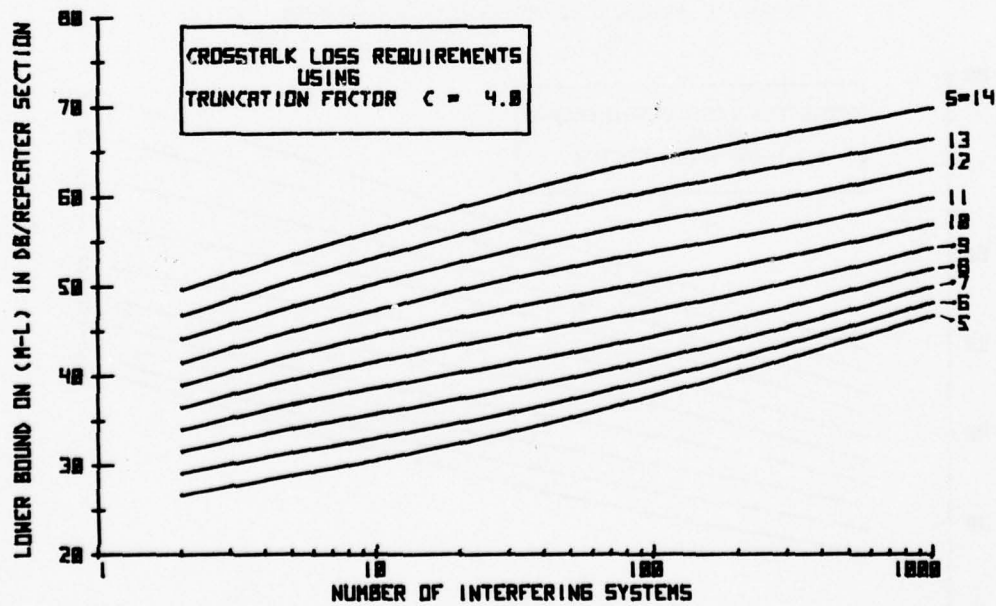


FIGURE 6

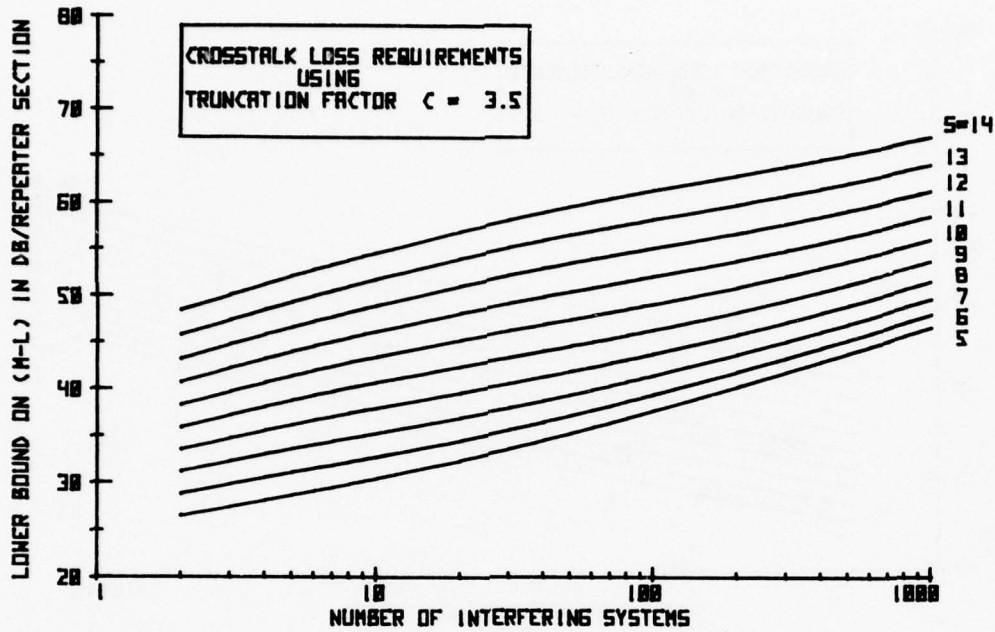


FIGURE 7

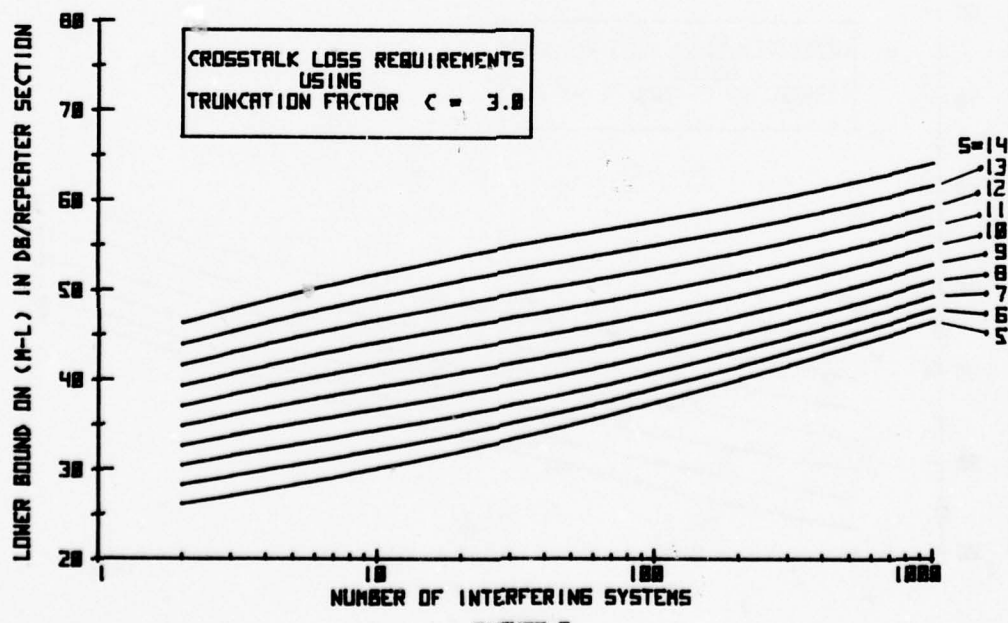
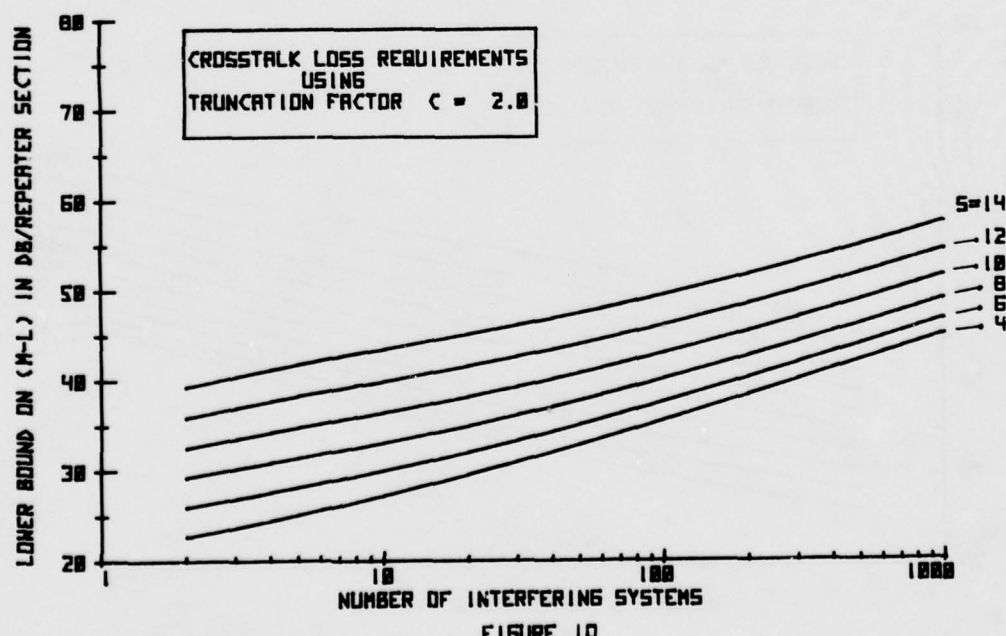
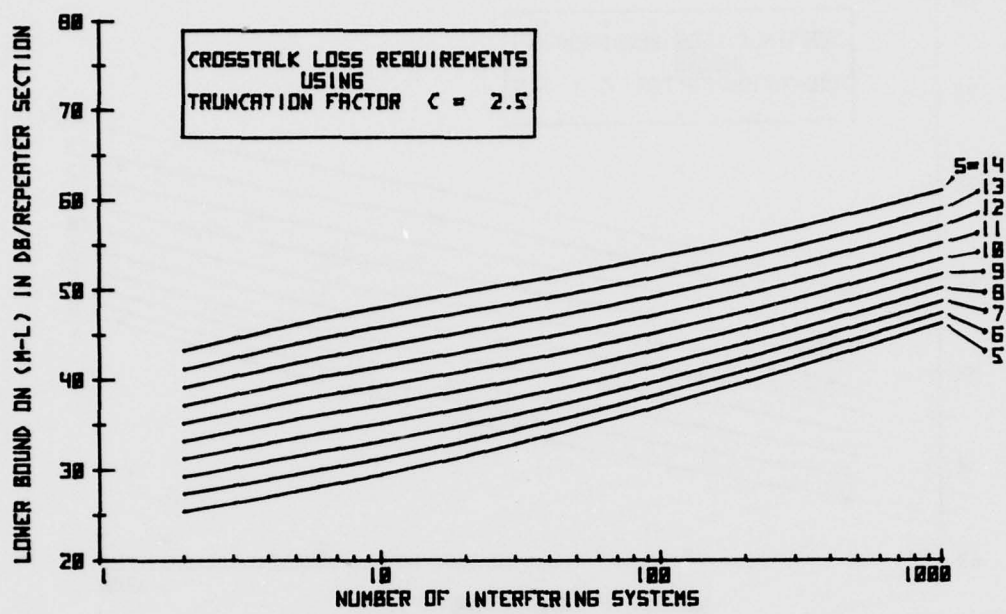


FIGURE 8



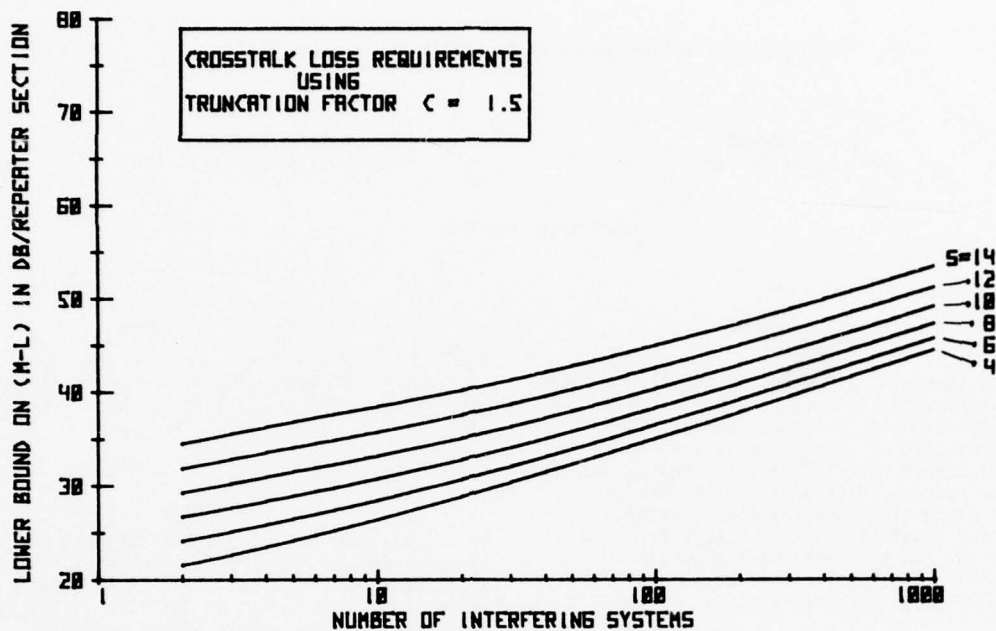


FIGURE II



Reimar Hauschildt graduated in 1967 from Queen's University, Kingston, Canada, with a B.Sc. in Mathematics and Engineering (Communication Theory), and in 1969 from the University of British Columbia, Vancouver, with an M.Sc. in Mathematics and Statistics. After several years with Bell-Northern Research and Northern Telecom Limited in Lachine, Quebec, and Beauchemin-Beaton-Lapointe in Montreal, he joined Phillips Cables Limited in Vancouver in 1975. He is presently development engineer for communication cables and manager of the Central Laboratory for the Communication Products Division.

Phillips Cables Limited,
Post Office Box 2187,
Vancouver, B.C.
V6B 3V7

Parameters Affecting Near-End Crosstalk in Screened Cables

J. P. Savage
Bell Laboratories

T. G. Hardin
Western Electric Co., Inc.

Norcross, Georgia

ABSTRACT

The move to increased bit rates in digital carrier systems has focused attention on the near-end crosstalk of screened, multipair cables. Two near-end crosstalk couplings are: (1) directly through the screen material, and (2) leakage at the cable shield-screen interfaces. Cable design parameters which significantly affect near-end crosstalk are sheath type, screen materials and configuration, and the pair twist algorithm. Improvements in NEXT performance as a result of variations of these parameters are discussed.

I. INTRODUCTION

Evolution of Pulse Code Modulated Carrier Systems such as T1C has generated increasingly more stringent Near-End Crosstalk (NEXT) requirements.^{1,2} Repeater spacings and cable fills for bidirectional operation of these carrier systems are limited by NEXT levels in the cable. The ability to use bidirectional PCM Systems on all pairs within a single cable is advantageous. Near-End Crosstalk considerations require a metallic screen bisecting the cable core for full-fill operations.

The need to meet PCM System NEXT requirements in an efficient manner has generated interest in cross-talk characteristics and the capabilities of various screen designs. Descriptions of screened cables for PCM (and other uses) have been given in previous papers.^{3,4,5} An analysis of the cross-talk mechanisms will allow the cable designer to choose the best screening methods for NEXT isolation.

There are two paths of NEXT coupling in screened cable: (1) directly through the screen material and (2) through any gap between the screen and the cable shield. Four geometric screen configurations used in PCM cables are shown in Figure 1.1

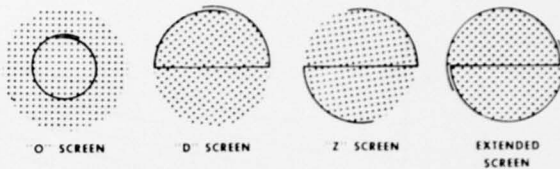


FIGURE 1.1

Previously derived expressions for both mechanisms are reviewed in this paper. The crosstalking field generated by a uniformly twisted pair is expressed as the sum of an infinite series of terms resulting from the separation of variables technique.⁶ The screen leakage mechanism is modeled as a series of waveguide transmission modes.⁹ The screen penetration mechanism is characterized using Schelkunoff's¹¹ approach as a sum of three shielding terms.

Measured data supplement the model to illustrate cable and screen design parameters and their effect on the NEXT performance.

II. NEAR-END CROSSTALK PARAMETERS

2.1 Assumptions

The following model will provide a unifying background for presentation of the parametric data describing Near-End Crosstalk behavior. The following mathematical assumptions are made: homogeneous and isotropic materials, perfect helices of conductor with balanced currents, isolated pairs with no ternary interactions, and wavelengths much longer than cable core periodicities.

Two methods of crosstalk are modeled:

1. Coupling through a gap situated parallel to a z-axis with depth "d" in the y direction and width "b" in the x direction.

2. Coupling directly through an infinite sheet of screen material of good - but not perfect - conductivity.

Method 1 is modeled as a parallel plate waveguide as shown in Figure 2.1. Method 2 is modeled as an infinite metallic sheet with plane wave incidence as shown in Figure 2.2.

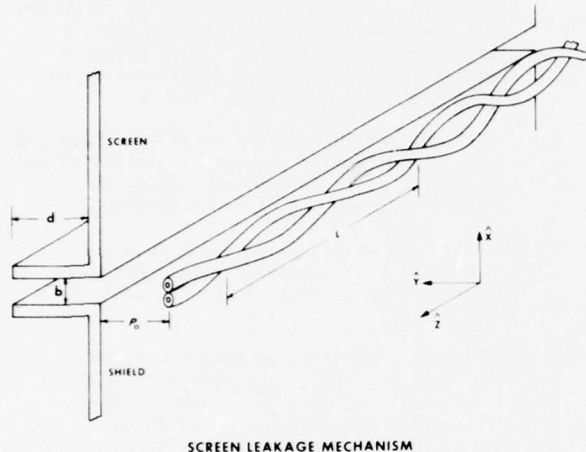


Figure 2.1

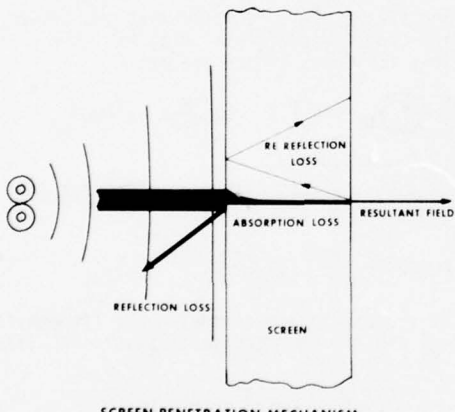


Figure 2.2

2.2 Magnetic Field of Twisted Pairs

Previous work on unscreened cables by Baranov^{6,7} has shown coupling between separated pairs to be dominated by inductive effects. Of particular importance, the z-directed magnetic field, $H(z)$, contributes to the mutual inductance between pairs for well balanced pairs.

$H(z)$ has been derived for a perfect helix of filamentary equal and opposite currents. The geometry and quantities used in the pair model are shown in Figure 2.3.

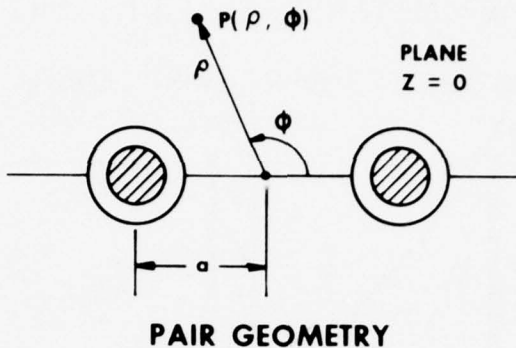


Figure 2.3

Below 10 MHz, the phase shift within one cable period (lay) can be ignored and the field presented by Shenfeld⁸ in M.K.S. units can be used:

$$H(z) = \frac{8\pi a I}{L^2} \sum_{m=1,3,5,\dots} I_m \left(\frac{m2\pi}{L} a \right) K_m \left(\frac{m2\pi}{L} \rho \right) \cos m \left(\phi - \frac{2\pi}{L} z \right) \quad (1)$$

where:

ϕ = phase angle at $z = 0$
 a = distance from current filament to center of pair
 ρ = distance from center of pair to point of observation
 L = pair twist length
 I = current flowing in each filament
 m = index integer

$$\left(\phi - \frac{2\pi}{L} z \right) = \text{helix angle} = \theta \quad (2)$$

$I'_m (\cdot)$ = derivative of the modified Bessel Function of the first kind, order m

$K_m (\cdot)$ = modified Bessel Function of the second kind, order m

$H(z)$ is plotted in Figure 2.4 as a function of distance from the pair (ρ), pair twist length (L), direction along the z axis (helix angle), and distance between wires in the pair ($2a$). All four variables are closely related; changing one will affect the scale and shape of the other curves.

The disturbing magnetic field generated by the twisted pair is a function of wire gauge, twist length and distance from the disturbed pair. The current induced by this field in the disturbed pair is also a series solution. For pairs of equal twist length, separated by a distance C , which is much larger than the wire separation $2a$, the equation for the mutual inductance can be simplified to:

$$M_{12} \approx \frac{\mu}{\pi} \cos \left(\phi_1 - \frac{2\pi z}{L} \right) \cos \left(\phi_2 - \frac{2\pi z}{L} \right) \cos \left(\phi_1 - \phi_2 \right) K_0 \left(\frac{2\pi}{L} C \right) \quad (3)$$

PARAMETERS AFFECTING $H(z)$

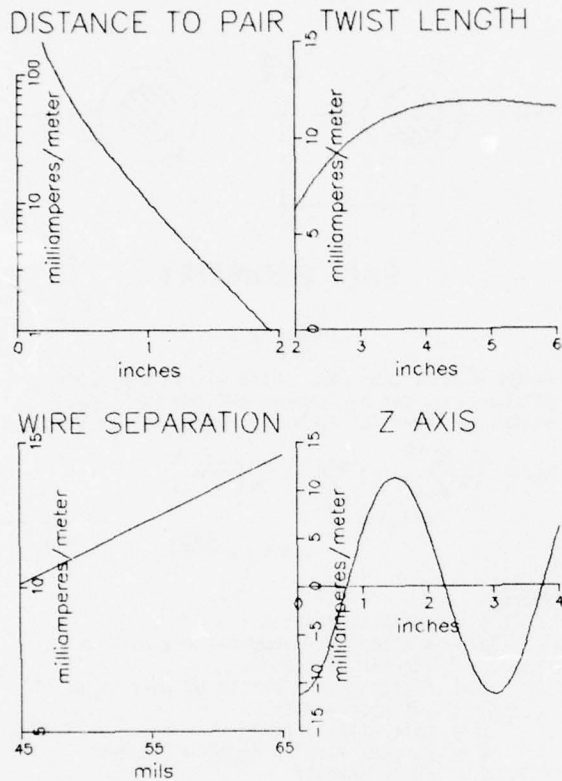


Figure 2.4

The current generated in the disturbed pair is then:

$$I_2 = j\omega M_{12} I_1 \quad (4)$$

The twist phase angle between pairs is a random variable in most manufacturing situations. Reducing twist length can for most orientations reduce the mutual inductive coupling. For unequal twist lengths, the formula describing the mutual inductance is significantly more involved; however, the same parameters of twist length and separation distance are dominant.

2.3 Effects of Intervening Screen

When the screen is placed between crosstalking pairs, the mutual inductance is reduced. For direct coupling through the screen, the $H(z)$ field is reduced due to the shielding effect of the screen. For crosstalk coupling around the screen, the coupling path is extended around the screen-shield gap and the $H(z)$ field is attenuated in the thin gap. This around-screen coupling path will be described first. Then the reduction in field strength (and mutual inductance) caused by the intervening shield material will be covered.

2.3.1 Screen Leakage Model

The gap between the screen and cable shield has been modeled as a parallel plate waveguide with gap opening "b" and depth of screen wrap "d" as shown in Figure 2.1. The following assumptions are made in this model:

1. The gap opening is sufficiently thin that the field is constant in the angular direction and the opening of the gap is everywhere a distance ρ_0 from the pair. This allows a transfer into rectangular coordinates to describe the field behavior in the gap.
2. Field penetration into the metallic screen and cable shield forming the gap is limited to one skin depth. This effectively widens the screen-shield opening at lower frequency.
3. Without loss of generality, we can assume $\phi = 0$. The helix angle, $(\frac{2\pi}{L}z)$, is then proportional to the twist $(\frac{m}{b}x)$ frequency of the pair.

From the source geometry, we know the field in the gap to be periodic in Z . The magnetic field normal derivative H_x must go to zero at the screen and shield boundaries. Use of the Helmholtz equation to determine the field in the source-free gap region will lead to a series solution for propagation modes within the screen-shield gap.

Applying the Helmholtz equation with the above boundary conditions, $(\nabla^2 + \beta^2) H(z) = 0$, the solutions for modes in the gap are:⁹

$$H(z) \sum_{n=1}^{\infty} \sum_{m=1}^{\infty} H_{nm} \cos\left(\frac{n\pi}{L}z\right) \cos\left(\frac{m}{b}x\right) e^{j\beta_{nm}d} \quad (5)$$

$$n=1,3,5,\dots m=1,3,5,\dots$$

where β_{nm} is the propagation constant for the shield and screen structure.

$$\beta_{nm}^2 = \omega^2 \mu \epsilon - \left(\frac{n\pi}{L}\right)^2 - \left(\frac{m}{b}\right)^2 \quad (6)$$

For the screened cable dimension and frequencies, $\omega^2 \mu \epsilon \ll \pi^2$ and the propagation constant simplifies to: $\frac{L^2}{L^2}$

$$\beta_{nm} = j \sqrt{\left(\frac{n\pi}{L}\right)^2 + \left(\frac{m}{b}\right)^2} \quad (7)$$

All modes are below the cutoff frequency of the screen-shield gap and are evanescent modes, leading to attenuation of the field within the screen-shield interface. This basic model predicts that crosstalk coupling around the screen will decrease for thinner screen-shield gaps, extended wraparound, and shorter twist lengths. Data presented in Section III displays these NEXT characteristics.

In addition to the loss within the gap, the cross-talk must couple from the disturbing pair to the gap, thru the gap and from the gap to the disturbed pair. A complete description of this process is beyond the scope of this paper.

2.3.2 Through Screen Coupling

The primary crosstalk mechanism at low frequencies is directly through the screen material. The reduction in magnetic field strength by reflections from and absorption by an intervening metallic barrier has been discussed and described in a considerable body of literature.^{10,14,15,16} Using the approach described by Shelkunoff for shielding of coaxial cables, the reduction in magnetic field strength can be described using three parameters: absorption loss (A), reflection loss (R), and re-reflection loss (N) in thin shields.

This shielding loss S is defined as the ratio:

$$S = 20 \log_{10} \left[\frac{H_0}{H_1} \right]$$

where:

H_0 = magnetic field intensity on the disturbing side of the screen

H_1 = magnetic field intensity on the shielded side of the screen

S = A + R + N

A = absorption loss

$$= 8.686 \sqrt{\mu_0 \sigma g} t \quad (8)$$

R = reflection loss

$$= 20 \log_{10} \left[\frac{(K+1)^2}{4K} \right] \quad (9)$$

N = re-reflection loss

$$= 20 \log_{10} \left[1 - \left[\frac{(K-1)^2}{(K+1)^2} e^{-2\lambda t} \right] \right] \quad (10)$$

$$K = j\omega\mu_0 / \sqrt{j\omega\mu_0} \quad (11)$$

and:

μ = material permeability

g = material conductivity = $1/\sigma$

ω = $2\pi f$, f = frequency

λ = propagation constant in the metal

$$= (1+j) \sqrt{\mu_0 \sigma g} \quad (12)$$

t = screen thickness

p = pair-to-screen distance

For this analysis, N is very small and does not affect NEXT coupling.

Figure 2.5 shows the calculated absorption loss A and the complete shielding loss S for a 4 mil aluminum screen with pairs located 0.10 inches and 1.00 inches from the screen. The reflection loss is the largest portion of S and increases with distance from the screen. The absorption loss is smaller and independent of pair position. Therefore, those pairs nearest the screen benefit least from the overall shielding of the screen material.

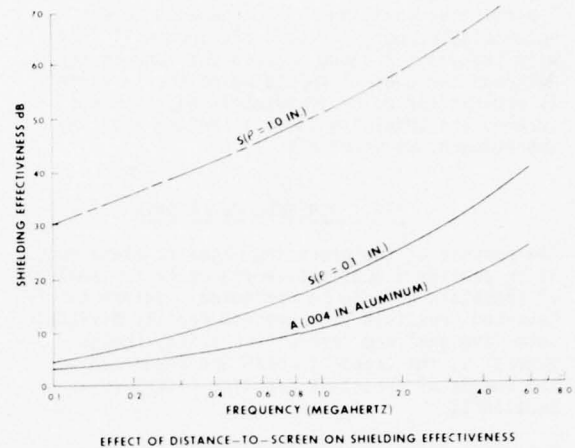


Figure 2.5

2.3.3 Laminated Screens

Since the reflection loss is dependent upon location in the core, improvement of the worst pair coupling can only be achieved by increasing the absorption loss or by laminating the screen material to provide metallic interfaces for reflections within the screen material. At the metallic interfaces of a laminated screen, K is given by:

$$K = \sqrt{\frac{\mu_1 \sigma_2}{\mu_2 \sigma_1}} \quad (13)$$

The reflections within the screen material now are independent of location in the core.

Figure 2.6 displays the shielding provided by various screen materials for a pair located 1/2 inch from the screen.

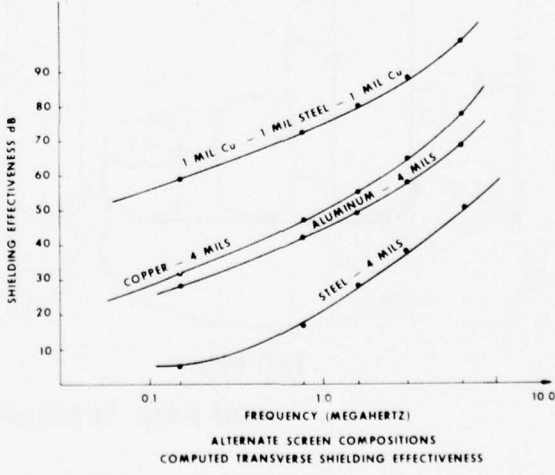


Figure 2.6

The relative positions of homogeneous screen materials, copper, steel, and aluminum will shift with changing distance between pair and screen. Although the overall shielding of the laminate is reduced for pairs immediately adjacent the screen, the shielding is still better than any of the homogeneous materials.

III. SCREENED CABLE DATA

The purpose of the preceding magnetic field models is to provide a qualitative framework for analysis of crosstalk data to be presented. Unfortunately Near-End Crosstalk data are not readily divisible into "leakage" and "direct" coupling, though generally, the trends in NEXT are predicted by the models of crosstalk coupling described in Section II.

3.1 NEXT Behavior with Frequency

The descriptions of NEXT coupling provided by the models predict the through screen coupling to decrease, and the leakage coupling to increase with frequency. Figure 3.1 shows as a function of frequency, the levels of Power Sum crosstalk coupling to units located throughout the core of a 600 pair cable with 120° of screen wrap.

The transmitting group is located at the knee in the screen at all three frequencies.

Crosstalk coupled directly through the screen dominates at 150 kHz. Crosstalk through the screen decreases 3 dB from 150 kHz to 6.3 MHz. Crosstalk coupling should increase 28 dB over this frequency range. The calculated shielding loss for 4 mils of aluminum increases 34 dB for a pair 3/8 inch from the screen. For coupling through the screen, the increased pair susceptibility is offset by the increased shielding of the screen material.

Within the same frequency range, crosstalk coupling via screen leakage does increase linearly with frequency and begins to dominate near 3.0 MHz.

When the gap between screen and cable widens - as occurs in a PASP type sheath - crosstalk coupling via screen leakage begins to dominate at lower frequencies. Figure 3.2 shows the change in location of the most strongly coupled pairs as a function of frequency for 600 pair PASP and ASP sheathed cables. Due to the inner jacket of polyethylene on PASP, the gap between shield and screen can be as much as 5 times as wide. At 6.0 MHz, the Power Sum NEXT of ASP type sheaths is 2.0 to 5.0 dB better than PASP type sheath.

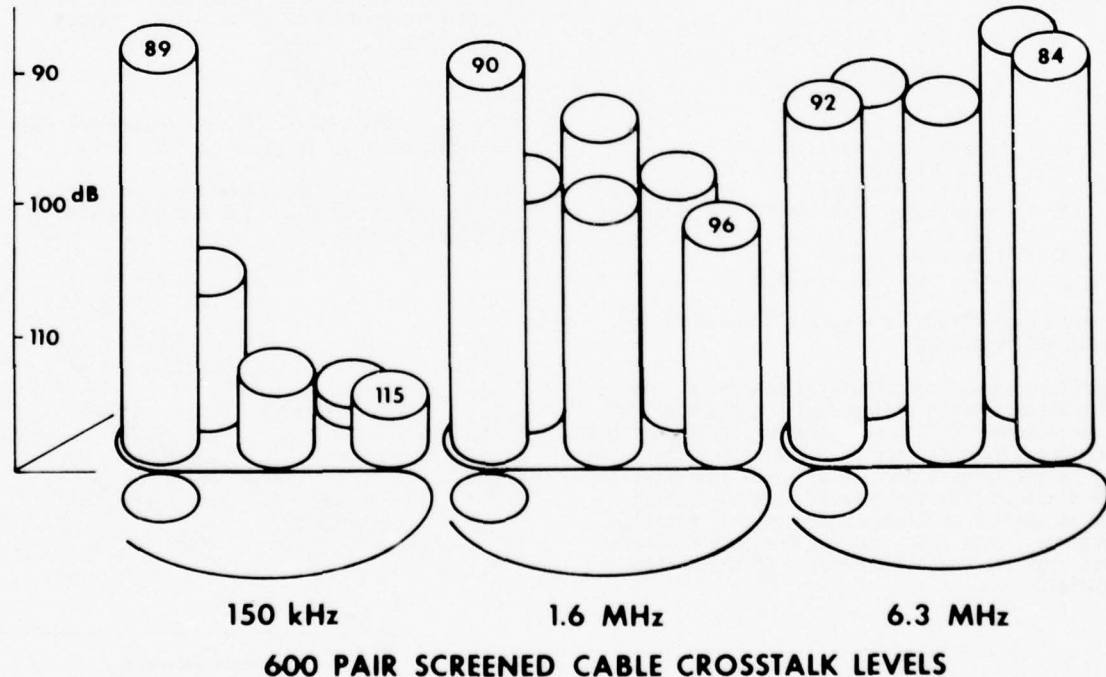


Figure 3.1

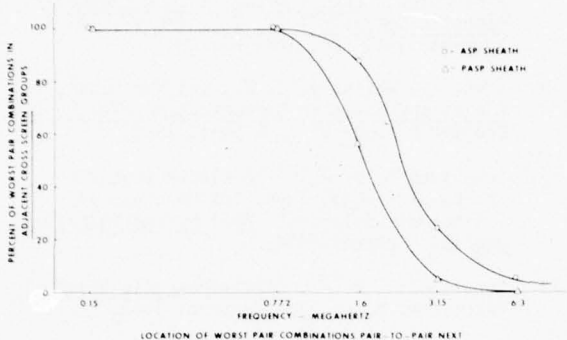


Figure 3.2

3.2 Twist Length Dependence

The NEXT coupling is also affected by the pair twist lengths used in the cable construction. Figure 3.3 shows the regression diagram of Power Sum NEXT vs Twist Length for a typical 22 gauge plastic insulated conductor cable.

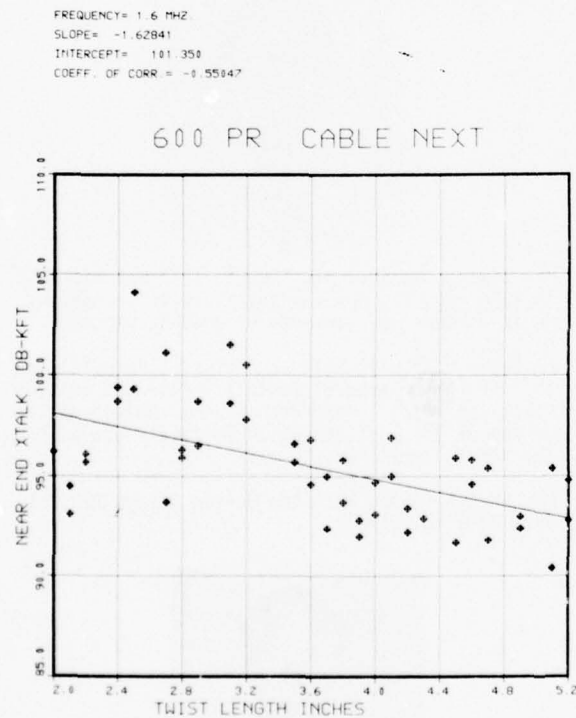


Figure 3.3

This dependence of NEXT on twist length has been observed on several cables over the frequency range 150 kHz to 6.3 MHz and for cables from 100

to 600 pair. For standard unit layups the regression slopes were 1.5 to 2.0 dB per inch of twist and correlation coefficients were 0.53 to 0.65. Using typical dimensions for a 600 pair ASP type cable, the model discussed in Section 2.3 predicts a twist dependency of 1.7 to 2.3 dB per inch of twist.

Alteration of the twist scheme used in cable unit construction can improve the Near-End Crosstalk. A pair twist scheme based on twist frequency spacings and having an average of one third more twists per pair foot was shown to improve worst pair NEXT by 3.0 dB at 1.6 MHz.

3.3 Through Screen Coupling

From the theoretical analysis, it appears that metallic laminate screens can provide improvements in NEXT. An experimental cable with a laminated screen was constructed. Figure 3.4 shows the improvement in worst pair Near-End Crosstalk performance over a similar cable with a 4 mil aluminum screen. This improvement in worst pair performance is significant, particularly for systems sensitive to crosstalk at lower frequencies. Improvement in worst pair performance using homogeneous materials has been limited to the range 1.0 to 3.0 dB.

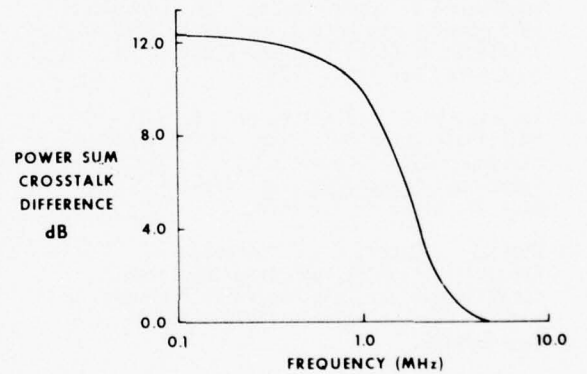


Figure 3.4

IV CONCLUSIONS

PCM systems currently operating on screened cables have Nyquist frequencies of 772 kHz and 1.544 MHz. To improve crosstalk on cables designed for use at 772 kHz, screen penetration considerations are paramount.

To effectively reduce the coupling directly through the screen (1) core constructions which space pairs from the screen (2) screens which improve shielding performance by increased conductivity or permeability and (3) metallic laminates should be considered.

For full-fill operation of systems at 1.544 MHz, the screen penetration and leakage mechanisms are about equal. Improvements in NEXT coupling at higher frequencies can be achieved by extending the screen wrap, particularly on PASP sheaths.

At all frequencies, shortening the twist length will improve NEXT performance.

V. ACKNOWLEDGEMENTS

The authors would like to thank the people in Bell Laboratories and Western Electric who supported this work, particularly T. A. Lenahan, B. C. Vrieland, and the computing sections in Atlanta for numerous crosstalk measurements. D. W. Haake, R. W. Williams and M. J. Kelly provided additional support in preparing and editing the manuscript.

REFERENCES

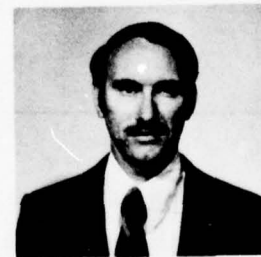
1. Cravis, H. and Crater, T.V., "Engineering of T1 Carrier System Repeatered Lines," *Bell System Technical Journal*, 42: pp. 431-86, March, 1963.
2. Lombardi, J. A., Maurer, R. E., and Michaud, W. P., "The T1C System," 11th International Conference on Communication, San Francisco, 1975, *Conference Record*, pp. 39-1, 39-9, Institute of Electrical and Electronics Engineers, New York, 1975.
3. Roberts, W. L. and Wilkenloh F. N., "Multipair Cable Shielding for PCM Transmission," 19th International Wire and Cable Symposium, *Proceedings*, pp. 175-181, Atlantic City, N. J., 1970.
4. Kbaki, A., Omori, N., Hoshikawa, T., Kobayashi, T., "Balloon Type Insulated Z Screen Cable for Long Range ITV Transmission," *Hitachi Review*, Vol. 25 (1976), No. 11, pp. 387-392.
5. Gabriel, A. P., Peveler, J. and Woods, J. J., "Near-End Crosstalk of Compartmentalized PCM Carrier System Cables," 25th International Wire and Cable Symposium, *Proceedings*, pp. 199-206, Cherry Hill, N.J., 1976.
6. Baranov, N., "Influence of The Twist Length Upon Mutual Inductance Between Two Parallel Spiral Pairs of One Channel Telephone Transmission," *Revue Generale de l'Electricite* Vol. LII pp. 181-188.
7. Baranov, N., "Experimental Verification of the Formulas of Mutual Inductance Between Two Spiralled Parallel Pairs in a Telephone Transmission Channel," *Revue Generale de l'Electricite*, March 1944, pp. 51-56.
8. Shenfeld, S., "Magnetic Fields of Twisted Wire Pairs," *IEEE Transactions on Electromagnetic Compatibility*, Vol. EMC-11, No. 4 November 1969, pp. 164-169.
9. Ramo, S., Whinnery, J. R., and Van Duzen, T., *Fields and Waves in Communication Electronics*, Chapter 8, John Wiley & Sons, 1965.
10. Schelkunoff, S. A., "The Electromagnetic Theory of Coaxial Transmission Lines and Cylindrical Shields," *Bell System Technical Journal*, October 1934.
11. Schelkunoff, S. A., *Electromagnetic Waves*, Princeton, N. J., Van Nostrand, 1943.
12. Kaden, H., *Wirblestrom und Schirmung in Der Nachrichtentechnik*, 2nd Edition, Berlin Springer, 1959.
13. Schulz, R. B., Huang, G. C., Williams, W. L., "R. F. Shielding Design," *IEEE Transactions of Electromagnetic Compatibility*, Vol. EMC-10, No. 1, March 1968.



Mr. Savage received his BSEE in 1975 and his MSEE in 1976 from the Georgia Institute of Technology. He is a member of Tau Beta Pi and Eta Kappa Nu.

He began work with Bell Laboratories in Baltimore in 1969 in the area of Central Office and Outside Plant apparatus. More recently Mr. Savage has worked on the development of multipair cables for carrier transmission.

Mr. Savage served with the United States Marines from 1965 to 1969.



Tommy G. Hardin is a Senior Engineer in the Twisting, Stranding and Cabling Department of the Cable and Wire Product Engineering Control Center. During the past eight years he has worked on the development of multi-pair cables for carrier transmission applications. Mr. Hardin received his BSEE from the Georgia Institute of Technology in 1962 and is a registered Professional Engineer in Georgia.

CALCULATION OF CROSSTALK IN BALANCED PAIR CABLES BY MEANS OF SIMULATION

by

Nils Holte

Electronics Research Laboratory
Trondheim - Norway

ABSTRACT

This paper shows how it is possible to represent realistic twisted pair cables on a computer and how crosstalk may be accurately calculated up to the highest frequencies of practical interest. Both production tolerances and cabling effects are taken into account.

Results show good agreement with general behaviour of practical twisted pair cables. The model predicts that most of the crosstalk observed in practical pair cables is due to deviations from ideal twisting, and a considerable improvement of far end crosstalk may be obtained by narrowing production tolerances.

1. INTRODUCTION

The Norwegian Telecommunications Administration and two Norwegian cable producers are developing new balanced pair cables for 2nd and 3rd order PCM systems (120 and 480 telephone channels). One of the basic problems in this work is to control crosstalk. Thus realistic and accurate crosstalk models are needed. Better crosstalk models will also be important for system design and for improving other types of balanced pair cables.

Crosstalk in practical pair cables can not be successfully calculated from nominal electrical and geometrical parameters. The production processes introduce more or less unavoidable random deviations from nominal geometry which cause the observed crosstalk. Thus a proper description of the cable must contain some statistical parameters characterizing the production processes. Describing the cable turns out to be an essential step in calculating crosstalk for a balanced pair cable.

Calculating crosstalk is not trivial even if the cable is well defined. Existing statistical methods [10], [12], [13] are based upon integrating coupling functions along the cable, assuming weak coupling between pairs. These calculations are relatively fast and thus suitable for finding optimum twist periods. On the other hand this type of method involves several rather rough approximations, and some amount of empiricism has to be used in order to obtain fair agreement with measurements.

Significant improvements may be obtained by solving the generalized telegraph equation numerically (the matrix differential equation characterizing mutually coupled transmission lines). This is done by dividing the cable in short elements and representing each part of the cable by an N-port. The complete cable including terminations is calculated by multiplying the matrix representations of each

element. In principle this method permits us to calculate crosstalk in one specific cable just as accurately as desired by using sufficiently short elements and using sufficiently accurate methods for calculating the coefficients of the generalized telegraph equation. It is just a matter of cost.

Results obtained by this method show correct order of magnitude for both far end and near end crosstalk, and variations with length and frequency are in agreement with practically experienced variations. Calculations predict that the main contribution to crosstalk in practical cables is caused by deviations from ideal twisting.

2. CABLE GEOMETRY

One simple and widely used way of describing a balanced pair cable is that each pair rotates systematically around a fixed point in the cross section. If the wires are just going to touch each other, we will have a cross section as shown in Fig. 1.

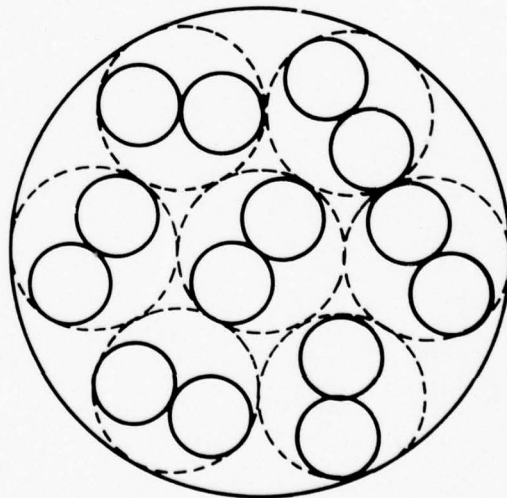


Fig. 1. Cross section of a 7-pair cable having ideal geometry.

This description may be a fair approximation for starquad cables if the geometrical parameters are properly selected. For twisted pairs such a model has little in common with the cable geometry observed in practical

cables. The cabling process gives a smaller cable diameter and leaves the pairs much closer together than shown in Fig. 1. This results in strong mechanical interaction both between pairs in the same cross section of the cable and between pairs in different cross sections. Calculation of the wire positions within a narrow cable sheathing turns out to be a very complicated threedimensional problem governed by the laws of mechanics. In order to obtain practical results we have to introduce some simplifications.

Geometrical measurements [1] show that each twisted pair moves relatively fast within the cross section as we move along the cable. The twist angle of a twisted pair differs from the twist angle of an ideal double helix, but the difference varies relatively slowly along the cable.

Based upon this observation we choose to treat the twist angles separately and neglect mechanical interaction between different cross sections of the cable. The wires of each twisted pair are assumed to have circular cross section and constant separation. Sheathing is assumed to be circular and its diameter is taken from measurements. The problem is now reduced to find the equilibrium positions of all twisted pairs within the sheathing. We assume that this equilibrium is obtained by minimizing the total deformation of insulation (minimizing total overlap between wires).

An iterative algorithm is used to solve this problem:

- 1) The points where the wires of each pair touch each other are placed in fixed positions. The fixed twist angles of each pair have been found by other calculations.
- 2) Overlap between two wires and between a wire and the sheathing is calculated. A displacement vector D is calculated for each overlap as indicated in Fig. 2. The displacement vector is the movement of each wire which is needed to remove the overlap. For overlap between two wires, the wires are given displacement vectors of equal length and opposite direction. The sheathing has a fixed position so that for overlap against the sheathing, only the wire is given a displacement vector D_s . The displacement vectors are directed along the line between the centers of the corresponding circles.
- 3) The vector sum of all displacement vectors for the two wires of each pair is calculated. This is defined to be the displacement vector of each pair.
- 4) The two wires of each pair are both given a movement equal to the displacement vector of that pair.
- 5) 2), 3) and 4) are repeated until equilibrium is reached.

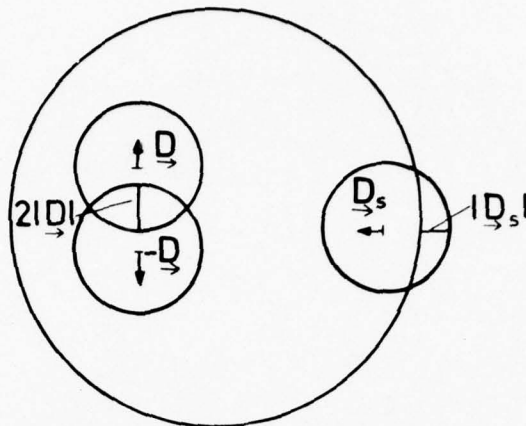
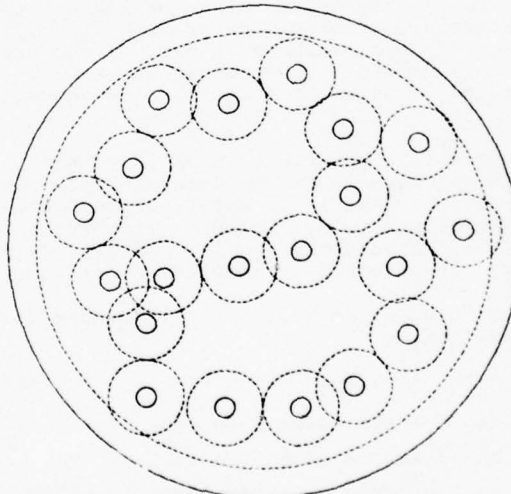


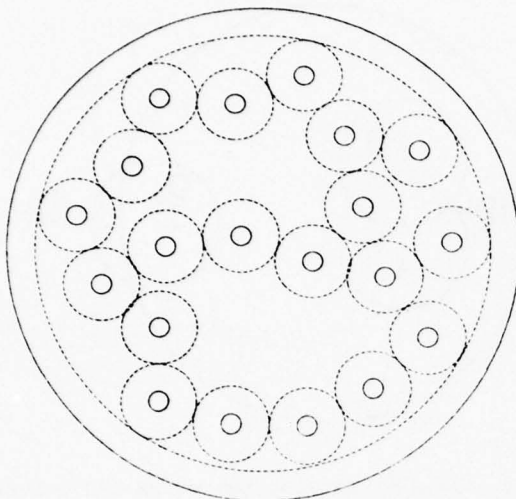
Fig. 2. Overlap between two wires and between a wire and sheathing.

The algorithm is step by step reducing the total overlap. Because only interaction between adjacent wires is treated directly, a considerable number of iterations are needed (for instance 20) in order to simulate the complicated interaction between all the wires of a cable. On the other hand the algorithm is simple and well suited for programming.

In Fig. 3 the start approximation and the final result is shown for a 10-pair cable.



a) Start approximation.



b) Final result.

Fig. 3. Simulation of cabling effects in a cable having 10 pairs.

In a cable having ideal geometry, the twist angles of each pair are increasing linearly along the cable. In practical cables deviations from ideal twist angles are caused both by the twisting process and by the cabling effects. Deviations caused by the twisting are random, and deviations in different pairs are obviously statistically independent. The cabling effects are more complicated. Because a twisted pair transfers a non negligible torque from one part of the cable to another part, the angular deformation of a pair in one cross section is caused by mechanical interaction with adjacent pairs both in the same and different cross sections of the cable.

The interaction between twisted pairs must contain strong elements of deterministic nature. Nevertheless it is a fair approximation to describe the twist angles by stochastic processes, because the angular deviations are sums of large numbers of independent influences.

The resulting twist angle of pair number i is expressed as:

$$\phi_i(x) = s_i x + \theta_i(x) \quad (1)$$

s_i is the average twist frequency of pair i
 x is the distance along the cable

$\theta_i(x)$ is the deviation from ideal twisting

$\theta_i(x)$ is assumed to be a stationary, Gaussian, stochastical process having zero mean and exponential autocorrelation function [14]:

$$R(\tau) \triangleq \langle \theta_i(x) \theta_i(x+\tau) \rangle = \sigma_i^2 \exp(-|\tau|/\tau_0) \quad (2)$$

σ_i is the mean square angular deviation

τ_0 is the correlation length

Cabling effects will produce some amount of correlation between twist deviations in adjacent pairs. This can be taken into account by assuming that all $\theta_i(x)$ are jointly Gaussian. Measurements [1] indicate that this correlation is small and for computational convenience twist deviations $\theta_i(x)$ in different pairs are assumed to be statistically independent.

In this case the joint probability density function of deviations for one pair in two cross sections is given by Papoulis [14]:

$$p(\theta_1, \theta_2; \tau) = \frac{1}{2\pi\sqrt{R^2(0)-R^2(\tau)}} \cdot$$

$$\exp\left[-\frac{R(0)(\theta_1^2 + \theta_2^2) - 2R(\tau)\theta_1\theta_2}{2(R^2(0)-R^2(\tau))}\right] \quad (3)$$

$$\theta_1 = \theta_i(x)$$

$$\theta_2 = \theta_i(x+\tau)$$

For a given deviation θ_1 the conditional p d f of θ_2 is calculated:

$$p(\theta_2|\theta_1; \tau) = \frac{p(\theta_1, \theta_2; \tau)}{p(\theta_1)} = \sqrt{\frac{R(0)}{2\pi(R^2(0)-R^2(\tau))}} \cdot$$

$$\exp\left[-\frac{(R(0)\theta_2 - R(\tau)\theta_1)^2}{2R(0)(R^2(0)-R^2(\tau))}\right] \quad (4)$$

A Gaussian process having exponential auto-correlation function is a first order Marhoff process. Thus the process is uniquely defined by equation (4).

In our simulation the cable is subdivided in elements of equal length. The angular deviation in the first element is drawn from a Gaussian population having a one-dimensional p d f $p(\theta_1)$. Deviations in preceding elements are drawn recursively using the transitional p d f (4).

In practical cables almost all dimensions have random variations around their nominal values. Conductor diameters and insulation thickness are of particular interest.

Different wires in one cable have usually passed through different dies and different extruders. Unavoidable adjustment errors cause small differences in average conductor diameter and insulation thickness. Production processes also generate variations along the cable. In lack of accurate measurements the deviations from nominal insulation thickness and nominal conductor diameter of each wire are assumed to be independent, stationary, Gaussian stochastical processes having exponential autocorrelation function.

Thus variations of the parameters mentioned above may be generated from random distribut-

ions in the same way as deviations from ideal twist angles.

We have described only one way of generating realistic representations of specific pair cables. Real cables are even more complicated than this. Considerable improvements of cable representations may probably be obtained by means of accurate and detailed measurements combined with further theoretical studies.

3. IMPEDANCE AND ADMITTANCE MATRICES

We assume piecewise parallel conductors and homogeneous permittivity between conductors. The per unit length capacitance matrix of each cross section is calculated by means of a method given by Singer et al [2] which simulates the surface charge on each conductor by concentrated line charges inside each conductor.

In most cables permittivity varies across the cross section. We use an average permittivity found by measurements in order to save computing time. More realistic methods are available at the cost of increased computing time. Clements et al [3] calculate the capacitance matrix of dielectric coated cylindrical conductors, and Lenahan [4] describes a method for calculating cables having parallel wires coated with two layers of insulation (foamed skin).

For lossless and parallel conductors and homogeneous permittivity, the per unit length inductance matrix of the wires is proportional to the inverse capacitance matrix as shown by Klein [5]:

$$\underline{L} = \mu_0 \epsilon \underline{\underline{C}}^{-1} \quad (5)$$

$\underline{\underline{C}}$ per unit length capacitance matrix of the wires

μ_0 permeability of vacuum

ϵ permittivity

Dielectric losses are usually negligible for balanced pair cables, but can be taken into account by means of a complex permittivity. We restrict ourselves to frequencies where the skin depth is considerably smaller than the conductor diameters. In this case the effect of finite skin depth is calculated by means of Wheelers incremental inductance rule [6] which has been extended to multipair cables by Alessandrini et al [7].

By means of one additional lossless inductance calculation the resistance matrix and the matrix of inner inductivities are calculated.

4. N-PORT REPRESENTATION OF PAIR CABLES

A multipair cable can be described by the generalized telegraph equation:

$$\begin{aligned} \frac{\delta}{\delta x} \underline{I} &= -\underline{\underline{Y}} \underline{U} \\ \frac{\delta}{\delta x} \underline{U} &= -\underline{\underline{Z}} \underline{I} \end{aligned} \quad (6)$$

\underline{I} is a vector containing the currents of each conductor

\underline{U} is the voltages of each conductor (relative to the shield)

$\underline{\underline{Y}}$ is the admittance matrix of the cable per unit length

$\underline{\underline{Z}}$ is the impedance matrix of the cable per unit length (usually both $\underline{\underline{Y}}$ and $\underline{\underline{Z}}$ vary along the cable).

The equation has been solved by Rice [8] for parallel wires (constant $\underline{\underline{Y}}$ and $\underline{\underline{Z}}$).

Voltages and currents at the ends of a cable are in this case given by:

$$\begin{bmatrix} \underline{U}_0 \\ \underline{I}_0 \end{bmatrix} = \begin{bmatrix} \cosh \ell \underline{\underline{Z}} & \sinh \ell \underline{\underline{Z}} \underline{\underline{Z}}_0 \\ \sinh \ell \underline{\underline{Z}}^T \underline{\underline{Z}}_0^{-1}, \cosh \ell \underline{\underline{Z}}^T \end{bmatrix} \begin{bmatrix} \underline{U}_\ell \\ \underline{I}_\ell \end{bmatrix} = \quad (7)$$

$$\begin{bmatrix} A_{11} & A_{12} \\ A_{21} & A_{22} \end{bmatrix} \begin{bmatrix} \underline{U}_\ell \\ \underline{I}_\ell \end{bmatrix} = \underline{\underline{A}} \begin{bmatrix} \underline{U}_\ell \\ \underline{I}_\ell \end{bmatrix}$$

\underline{U}_0 and \underline{I}_0 are the voltages and currents at the origin. \underline{U}_ℓ and \underline{I}_ℓ are the voltages and currents at the termination. ℓ is the length of the cable.

The hyperbolic functions are defined by the series:

$$\begin{aligned} \cosh x \underline{\underline{Z}} &= \underline{\underline{Z}} + \frac{x^2 \underline{\underline{Z}}^2}{2!} + \frac{x^4 \underline{\underline{Z}}^4}{4!} \dots \\ \sinh x \underline{\underline{Z}} &= \frac{x \underline{\underline{Z}}}{1!} + \frac{x^3 \underline{\underline{Z}}^3}{3!} \dots \end{aligned} \quad (8)$$

$\underline{\underline{I}}$ is the unity matrix

$\underline{\underline{Z}}$ is a square matrix representing a generalization of the propagation constant defined by:

$$\underline{\underline{Z}}_0 = \underline{\underline{Z}}^2 \quad \underline{\underline{Z}} = \sqrt{\underline{\underline{Z}}_0} \quad (9)$$

$\underline{\underline{Z}}_0$ is a square matrix representing a generalization of the characteristic impedance, and it is defined by:

$$\underline{\underline{Z}}_0 = \underline{\underline{Z}}^{-1} \underline{\underline{Z}} = \underline{\underline{Z}} \underline{\underline{Z}} \quad (10)$$

Combining (7), (8), (9) and (10) we obtain:

$$\begin{aligned} A_{11} &= \underline{\underline{Z}} + \frac{\ell^2}{2!} \underline{\underline{Z}} \underline{\underline{Y}} + \frac{\ell^4}{4!} (\underline{\underline{Z}} \underline{\underline{Y}})^2 + \dots \\ A_{12} &= \ell \underline{\underline{Z}} + \frac{\ell^3}{3!} \underline{\underline{Z}} \underline{\underline{Y}} \underline{\underline{Z}} + \frac{\ell^5}{5!} (\underline{\underline{Z}} \underline{\underline{Y}})^2 \underline{\underline{Z}} + \dots \\ A_{21} &= \ell \underline{\underline{Y}} + \frac{\ell^3}{3!} \underline{\underline{Y}} \underline{\underline{Z}} \underline{\underline{Y}} + \frac{\ell^5}{5!} (\underline{\underline{Y}} \underline{\underline{Z}})^2 \underline{\underline{Y}} + \dots \\ A_{22} &= \underline{\underline{Y}} + \frac{\ell^2}{2!} \underline{\underline{Y}} \underline{\underline{Z}} + \frac{\ell^4}{4!} (\underline{\underline{Y}} \underline{\underline{Z}})^2 + \dots \end{aligned} \quad (11)$$

A uniform cable may be regarded as an N-port which is fully described by the A-matrix defined in (11). If the cable-length is

essentially shorter than the wavelength, the series in equation (11) will converge rapidly so that only a few terms are needed for numerical calculations.

Twisted pair cables may be represented by pieces of uniform cables if the wires are approximately parallel with the cable axis and each piece is essentially shorter than the twist periods. Different pieces have got different A-matrices as indicated in Fig. 4.

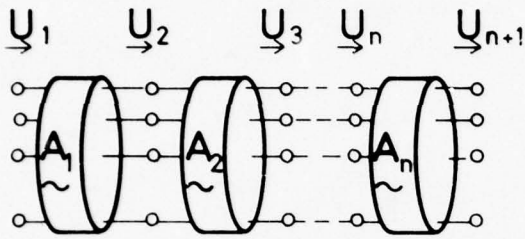


Fig. 4. Different cable sections connected in cascade.

The resulting A matrix for a complete cable is found by matrix multiplication:

$$\begin{bmatrix} U_1 \\ I_1 \end{bmatrix} = A_1 \cdot A_2 \cdot A_n \begin{bmatrix} U_{n+1} \\ I_{n+1} \end{bmatrix} = A \begin{bmatrix} U_{n+1} \\ I_{n+1} \end{bmatrix} \quad (12)$$

5. CALCULATION OF CROSSTALK IN A CABLE HAVING SPECIFIC TERMINATIONS

Each end of a pair is assumed to have an individual termination of the type shown in Fig. 5.

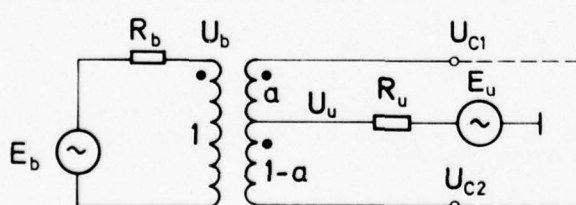


Fig. 5. Terminations for one pair.

Unbalanced terminations may be taken into account by using $a \neq \frac{1}{2}$, and the voltage source E_u permits us to excite longitudinal circuits. The circuit in Fig. 6 is electrically equivalent to the one in Fig. 5, but the latter is more convenient for our calculations:

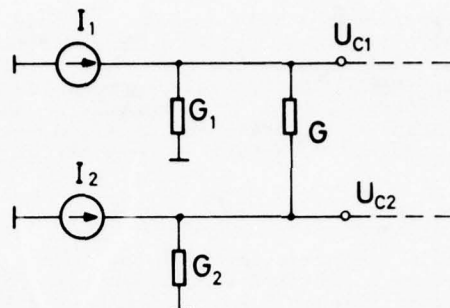


Fig. 6. Equivalent terminations for one pair.

Using elementary circuit theory the relationship between the two representations is found:

$$\begin{aligned} G_1 &= \frac{1-a}{R_u} \\ G_2 &= \frac{a}{R_u} \\ G &= \frac{1}{R_b} + \frac{a^2 - a}{R_u} \end{aligned} \quad (13)$$

The relationship between the circuit voltages U_b , U_u and the wire voltages U_{c1} , U_{c2} in Fig. 5 is:

$$\begin{bmatrix} U_b \\ U_u \end{bmatrix} = \begin{bmatrix} 1 & -1 \\ 1-a & a \end{bmatrix} \begin{bmatrix} U_{c1} \\ U_{c2} \end{bmatrix} = M \begin{bmatrix} U_{c1} \\ U_{c2} \end{bmatrix} \quad (14)$$

Using this notation, the relationship between the current sources of Fig. 6 and the voltage sources of Fig. 5 can be expressed:

$$\begin{bmatrix} I_1 \\ I_2 \end{bmatrix} = \begin{bmatrix} G_1 + G, & -G \\ -G, & G_2 + G \end{bmatrix} M^{-1} \begin{bmatrix} E_b \\ E_u \end{bmatrix} = G_p M^{-1} \begin{bmatrix} E_b \\ E_u \end{bmatrix} \quad (15)$$

G_p is the conductance matrix for the terminations in Fig. 6.

A complete cable is terminated as shown in Fig. 7.

The A matrices of the terminations in Fig. 7b are given by

$$A_1 = \begin{bmatrix} I & 0 \\ G_1 & I \end{bmatrix} \quad A_2 = \begin{bmatrix} I & 0 \\ G_2 & I \end{bmatrix} \quad (16)$$

where G_1 and G_2 are the conductance matrices of the termination networks.

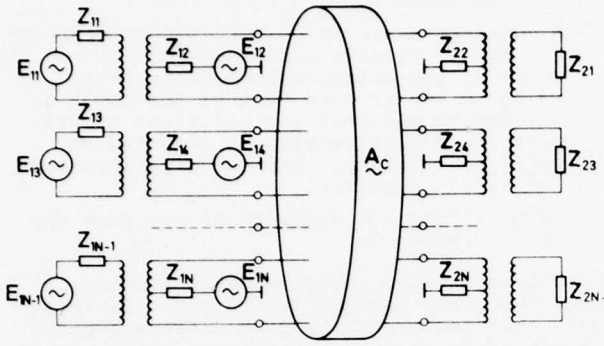
The resulting A matrix for the complete cable including terminations is calculated:

$$A = A_1 A_c A_2 \quad (17)$$

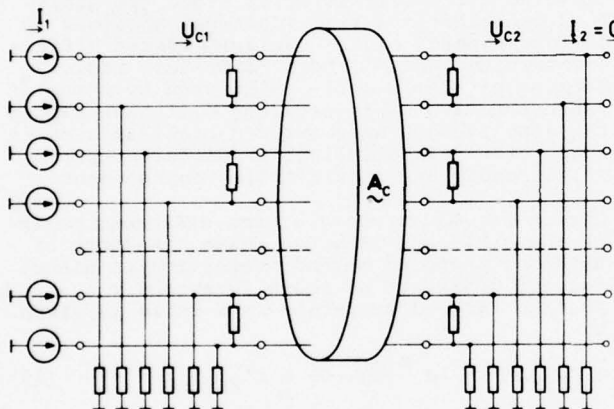
A_c is the A-matrix for the cable.

in the receiving end may be expressed as a function of the circuit voltage sources E_1 in the transmitting end:

$$\underline{U}_2 = M_2 A_{21}^{-1} G_1 M_1^{-1} \underline{E}_1 = Z_1 \underline{E}_1 \quad (20)$$



a) Practical terminations.



b) Equivalent terminations.

Fig. 7. A complete cable including terminations.

The equations governing the conductor currents voltages are:

$$\underline{U}_{c1} = A_{11} \underline{U}_{c2} + A_{12} \underline{I}_2 \quad (18)$$

$$\underline{I}_1 = A_{21} \underline{U}_{c2} + A_{22} \underline{I}_2$$

Transmitting as indicated in Fig. 7b $\underline{I}_2 = 0$.

Thus the conductor voltages in the receiving end are:

$$\underline{U}_{c2} = A_{21}^{-1} \underline{I}_1 \quad (19)$$

We are interested in the transmission between the different circuits in Fig. 7a. Using a straightforward extension of equation (14) and (15) to N wires, the circuit voltages \underline{U}_2

M_i is the conversion matrix between conductor voltages and circuit voltages for the terminations in end no. i of the cable ($i = 1, 2$). M_i for one pair is given in equation (14).

F_1 is the voltage to voltage far end crosstalk matrix for transmission from end 1 to end 2.

Insertion loss for circuit number i in Fig. 7a is defined by:

$$\alpha_i = 10 \lg \left(\frac{P_{li \max}}{P_{2i}} \right) = -20 \lg \left| \frac{2U_{2i}}{E_{li}} \sqrt{\frac{Z_{1i}}{Z_{2i}}} \right| \quad (21)$$

$P_{li \max}$ is maximum power which can be delivered to the cable from the voltage source E_{li} .

P_{2i} is power dissipated in impedance Z_{2i} .

All termination impedances are assumed to be real.

Thus insertion loss can be calculated from element number ii of the F_1 -matrix:

$$\alpha_i = -20 \lg \left| 2F_{1ii} \sqrt{\frac{Z_{1i}}{Z_{2i}}} \right| \quad (22)$$

Usually termination impedances for balanced and longitudinal circuits are different, and different pairs may have different terminations. Thus it is advantageous to use a power ratio rather than a voltage ratio also for the definition of crosstalk.

We define equal level far end crosstalk between disturbing circuit j and disturbed circuit i by:

$$\alpha_{ELFEXT ij} = -10 \lg \left(\frac{P_{2i}}{P_{2j}} \right) = -20 \lg \left| \frac{F_{1ij}}{F_{1jj}} \sqrt{\frac{Z_{2j}}{Z_{2i}}} \right| \quad (23)$$

F_{1ij} is element number ij of F_1 .

Conductor voltages in the transmitting end of the cable are found from equation (18).

$$\underline{U}_{c1} = A_{11} A_{21}^{-1} \underline{I}_1 \quad (24)$$

The voltages \underline{U}_1' across the termination impedances in fig. 7a are the differences between the circuit voltages \underline{U}_1 and the voltage sources E_1 . Using the extended versions of equation (14) and (15) we find:

$$\underline{U}_1' = \underline{U}_1 - \underline{E}_1 = M_1 A_{11} A_{21}^{-1} G_1 M_1^{-1} \underline{E}_1 - \underline{E}_1 = N_1 \underline{E}_1 \quad (25)$$

N_1 is the voltage to voltage near end crosstalk matrix.

In correspondence with the definition of insertion loss and far end crosstalk we define near end crosstalk between disturbing circuit

j and disturbed circuit i by:

$$\alpha_{\text{NEXT } ij} = 10 \lg \left(\frac{P_{ij \text{ max}}}{P_{li}} \right) = -20 \lg \left| 2N_{lij} \sqrt{\frac{Z_{lj}}{Z_{li}}} \right| \quad (26)$$

N_{lij} is element ij of \tilde{N}_1 .

The reflection coefficients at the input ports can be calculated from the diagonal elements of the N_1 matrix:

$$p_{li} = 2N_{lli} + 1 \quad (27)$$

p_{li} is the reflection coefficient for circuit i.

The A-matrix also contains the information about transmission in the opposite direction of the cable.

In this case $I_1 = 0$. Solving equation (18) we find

$$\begin{aligned} \underline{U}_{c1} &= -\underline{A}_{21}^{-1} \underline{A}_{22} \underline{I}_2 \\ \underline{U}_{c2} &= (\underline{A}_{12} - \underline{A}_{11} \underline{A}_{21}^{-1} \underline{A}_{22}) \underline{I}_2 \end{aligned} \quad (28)$$

The near end and far end voltage to voltage matrices for transmission from end 2 to end 1 are:

$$\begin{aligned} \underline{N}_2 &= -\underline{M}_2 \underline{A}_{21}^{-1} \underline{A}_{22} \underline{G}_2 \underline{M}_2^{-1} \underline{I}_2 \\ \underline{E}_2 &= \underline{M}_1 (\underline{A}_{12} - \underline{A}_{11} \underline{A}_{21}^{-1} \underline{A}_{22}) \underline{G}_2 \underline{M}_2^{-1} \end{aligned} \quad (29)$$

6. MODIFICATIONS FOR REDUCING COMPUTING TIME

We have described a method which in principle makes it possible to simulate a complete cable including terminations. Calculating impedance matrices for each element of a cable leads to unmanageable computing time in cables having more than a few pairs. Several methods may be used to reduce the computing time.

- 1) Scaling the results from a short piece of cable.
- 2) Calculating a few cable sections and building a cable by using each section several times.
- 3) Generating admittance and impedance matrices from random experiments.

6.1. Scaling

In a sufficiently short piece of cable direct near end crosstalk and direct far end cross-talk will be dominating. Thus average direct far end and near end crosstalk may be transformed to any cable length using methods published by Cravis & Crater [9]. Double near end crosstalk and other indirect contributions to crosstalk may be scaled as indicated by Holte [10]. Each circuit must be terminated with its characteristic impedance in order to obtain correct results.

6.2. Representative cable sections

The following method has been used:

- 1) A small number of cable sections are calculated. Each section is represented by its A-matrix. Its length must be con-

siderably longer than the correlation lengths of the cable geometry. Twist angles in both ends of each section are approximately equal in order to avoid discontinuities when connecting different sections in cascade.

- 2) A complete cable is constructed by connecting representative cable sections in cascade. Which of the calculated sections we are going to use in each part of the cable is decided by means of a statistical experiment where each section is selected at equal probability. The cable is represented by its A-matrix.
- 3) Terminations are included in the same way as in chapter 5.

If only one representative cable section is used the cable becomes periodical. In this case near end crosstalk from different parts of the cable tends to cancel each other, while far end crosstalk increases proportionally along cable length.

Most of these undesired effects disappear if several representative cable sections are used. Near end crosstalk and multiple crosstalk contributions add up from contributions having traveled different distances along the cable. Thus contributions from identical sections in different parts of the cable have phase differences which tend to be more or less random. Because of this a cable calculated by means of representative cable sections will have almost the same average near end crosstalk as a cable where crosstalk couplings in different parts of the cable are statistically independent.

Direct far end crosstalk from different parts of the cable are added in phase. Because of this the proposed method overestimates direct far end crosstalk as shown in appendix 1. Average far end crosstalk in a cable is given by

$$\alpha_{\text{ELFEXT}} = -10 \lg \frac{N(N+M-1)}{M} + \alpha'_{\text{ELFEXT}} \quad (30)$$

α'_{ELFEXT} is the average direct far end crosstalk in a representative cable section.

N is the total number of cable sections connected.

M is the number of different representative cable sections.

For large cable length (large N) the variation approaches 20 dB/decade of cable length. This differs from the practically experienced 10 dB/decade variation which is caused by statistically independent couplings in different parts of the cable.

In the case where direct far end crosstalk is dominating, equation (30) may be used for corrections. The method gives approximately correct results at frequencies where calculated far end cross talk is dominated by indirect crosstalk contributions.

Using more sophisticated scaling it is possible to compensate far end crosstalk for errors in direct crosstalk at all frequencies. Averaging a large number of different cables is needed to find reliable estimates.

6.3. Generating capacitance and inductance matrices directly from random experiments

Crosstalk coupling per unit length between two lossless transmission lines is given by Klein [5].

Near end coupling:

$$\kappa_{Nij} = \frac{C_{ij}}{\sqrt{C_{ii}C_{jj}}} + \frac{L_{ij}}{\sqrt{L_{ii}L_{jj}}} \quad (31)$$

Far end coupling:

$$\kappa_{Fij} = \frac{C_{ij}}{\sqrt{C_{ii}C_{jj}}} - \frac{L_{ij}}{\sqrt{L_{ii}L_{jj}}}$$

C_{ij} is an element of the per unit length capacitance matrix of the transmission lines \mathcal{C}' .

L_{ij} is an element of the per unit length inductance matrix L' of the transmission lines.

Notice that we are here dividing each pair into two transmission lines, one for the balanced excitation and one for the longitudinal. Conversion formulas between matrices L and C of single wires and matrices L' and C' of transmission lines are given by Klein [5].

It has been shown by Strakhov [11], and the results of this paper confirm that deterministic variations of κ_N and κ_F due to ideal twisting do not contribute significantly to crosstalk in practical cables. Only nonzero mean values and statistical variations of coupling factors are of practical importance.

Correlation lengths of the geometrical stochastic processes in the cable are not longer than a few twist periods. Twisting tends to make the correlation between coupling functions in different cross sections smaller than the corresponding geometrical correlation.

Thus a cable may be simulated by short pieces of uniform cables where coupling in different pieces are statistically independent. Far end and near end coupling in the same pair and in different pairs are for simplicity assumed to be statistically independent. All coupling functions are sums of a large number of random contributions and are thus assumed to have Gaussian p.d.f.

The given assumptions make it possible to draw all coupling factors in a cable from individual Gaussian distributions. All elements of the L' and C' matrices are calculated from the coupling factors. Mean and variance of each coupling factor are estimated from a number of geometrically simulated cables in such a manner that average direct crosstalk remains unchanged when using this simplified method.

Results show that realistic variations of conductor diameters do not affect crosstalk. Thus matrices of resistance and inner conductivities are assumed to be constant and are estimated by averaging calculated matrices.

Using this method the process of calculating impedance and admittance matrices from cable geometry is done only for a limited piece of the cable. Thus considerable computing time is saved. One disadvantage of the method is that deterministic variations of coupling factors have been neglected, so that only cables having considerable deviations from ideal geometry can be calculated.

7. COMPUTER PROGRAMS

The methods described have been implemented in computer programs on a Univac 1108 computer. All programs are written in FORTRAN and are intended for use up to ten pairs.

Computing time depends strongly upon input data, especially the number of pairs. Typical CPU-time for one cable analysis is between 1 minute and several hours.

Only single precision arithmetic is used (36 bits). Numerical accuracy is sufficient for most problems of practical interest.

8. RESULTS

All calculations have been performed for a three pair cable whose cross section is shown in scale in fig. 8.

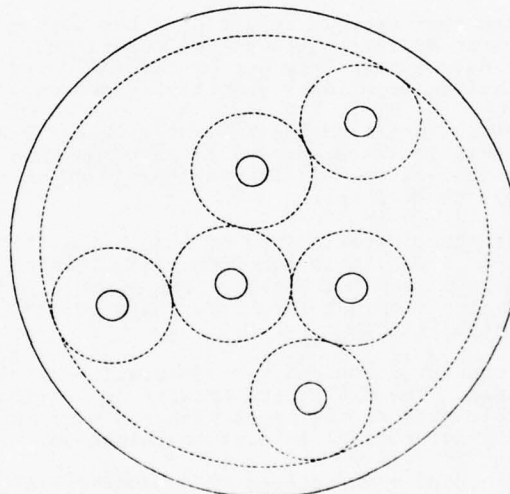


Fig. 8. A cross section of the 3 pair cable used in calculations.

Other specifications:

| | |
|----------------------|----------------|
| Conductor diameter | 0.62 mm |
| Capacitance | 24 nF/km |
| Attenuation at 1 MHz | 8 dB/km |
| Twist periods | $P_1 = 69$ mm |
| | $P_2 = 95$ mm |
| | $P_3 = 125$ mm |

The cable has not been built so that calculations have not been verified by measurements. Nevertheless the results seem to be in good agreement with general behaviour of balanced pair cables.

By using 3 pairs both the complicated mechanical interaction as well as the electrical interaction between different pairs are present. Thus our results are expected to be representative also for other types of twisted pair cables having a limited number of pairs.

8.1. Deviations from ideal geometry

The first calculations are performed for a cable having ideal geometry, that is:

- constant twist periods
- constant and equal conductor diameters in all pairs
- constant and equal insulation thickness in all pairs.

The mechanical interaction between the conductors is taken into account by the iterative algorithm described in chapter 2. Both balanced and longitudinal circuits are terminated with their characteristic impedances. The result is shown in table 1.

In comparison with practical cables a 20-30 dB improvement of far end crosstalk is predicted. It is of course impossible to reach this type of ideal geometry by means of practical cable machinery, but it is demonstrated that significant crosstalk improvement can be reached by narrowing production tolerances.

In the next step we investigate the importance of different production tolerances. In each calculation only one of the following deviations from ideal geometry is present.

- 1) Deviations from ideal twist angles. The deviations are assumed to have rms value $\sigma = 20^\circ$ and correlation length $\tau_o = 200$ mm in all three pairs.
- 2) Stochastic variations of insulation thickness. The deviation from nominal thickness in each wire has an rms value $\sigma_{in} = 6.8\%$ of nominal thickness and a correlation length $\tau_{in} = 1$ m.
- 3) Constant differences of insulation thickness. The difference between insulation thickness of the wires within a pair is 4.3% of nominal insulation thickness.
- 4) Stochastic variations of conductor diameters. The rms value of the deviation from nominal conductor diameter is $\sigma_d = 5\%$ and the corresponding correlation length is $\tau_c = 1$ m. This tolerance produces 0.5% resistance unbalance in average for 500 m of cable.
- 5) Constant differences between conductor diameters. The difference between the diameters of the two wires in a pair is 1% of nominal diameter. This corresponds to 1% resistance unbalance.

Different deviations have been roughly estimated from cable measurements and are assumed to be within correct order of magnitude for practical cables. This accuracy is sufficient to demonstrate general behaviour of pair cables. It is of greater importance that other types of tolerances have not been taken

into account. For instance the present model assumes homogeneous permittivity and thus omits random variations of permittivity along a wire. The effect of random variations in permittivity is probably similar to the effect of random variations on insulation thickness, and may be taken into account by increased insulation tolerances.

| | NEXT (dB) | ELFEXT (dB) |
|--|--------------|----------------|
| Ideal geometry | 73 | 89 |
| Deviations from ideal twist angles | 61 | 69 |
| Stochastic variations of insulation thickness | 70 | 84 |
| Constant differences of insulation thickness | 73 | 91 |
| Stochastic variations of conductor diameters | 72 | 90 |
| Constant differences between conductor diameters | 73 | 89 |
| All tolerances included in one cable | 62 | 69 |

Table 1. Calculated average near and far end crosstalk at 1 MHz for cable length 500 m.

The calculations have been performed by means of the method in section 6.2.

The results of table 1 are obtained by averaging all three pair combinations in only one cable. Thus a tolerance of ± 2 dB must be connected to each of the calculated numbers.

The results show that the main contribution to crosstalk is caused by deviations from ideal twist angles. Random variations in insulation give a small contribution to crosstalk. No significant contribution is caused by the other effects considered here.

Our calculations also indicate that far end crosstalk is more sensitive to deviations from ideal geometry than near end crosstalk.

8.2. Frequency dependency

A realistic cable is assumed to have all the deviations from ideal geometry mentioned in section 8.1. A cable of length 200 m has been simulated by means of the method in section 6.3. The frequency dependency of crosstalk in each pair combination is shown in fig. 9 and fig. 10.

Near end crosstalk exhibits the same type of fast variations with frequency as measured in real cables. Variations of far end crosstalk are also in accordance with typical measurements. At frequencies where direct far end crosstalk is dominating the curve is rather smooth, because all contributions are added in phase. At higher frequencies indirect crosstalk contributions become significant, and variations similar to near end crosstalk are produced.

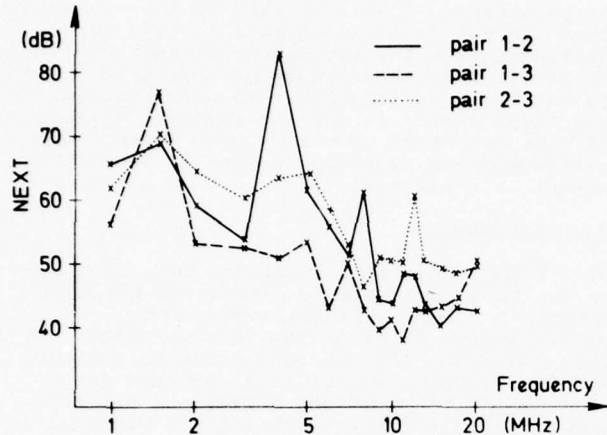


Fig. 9. Near end crosstalk for different pair combinations.

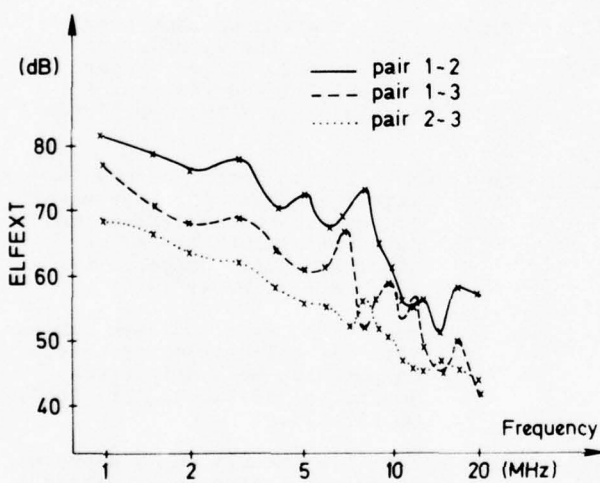


Fig. 10. Far end crosstalk for different pair combinations.

All pair combinations in three different cables have been averaged. For near end crosstalk no significant deviations from 15 dB/decade of frequency are observed. The part of the cable which contributes to near end crosstalk is reduced when frequency increases because of increased attenuation. Thus the near end crosstalk mechanism is the same at all frequencies of interest. The result for far end crosstalk is shown in fig. 11 for cable length 200 m.

Far end crosstalk follows the experienced 20 dB/decade variation with frequency up to 10 MHz. At higher frequencies the frequency dependency is much steeper, and it is even steeper than 35 dB/decade calculated by

Holte [10] for double near end crosstalk. This shows that more complicated types of indirect crosstalk are present. Longitudinal circuits play an important role in connection with indirect crosstalk because their attenuation may be lower than the attenuation of the balanced circuits.

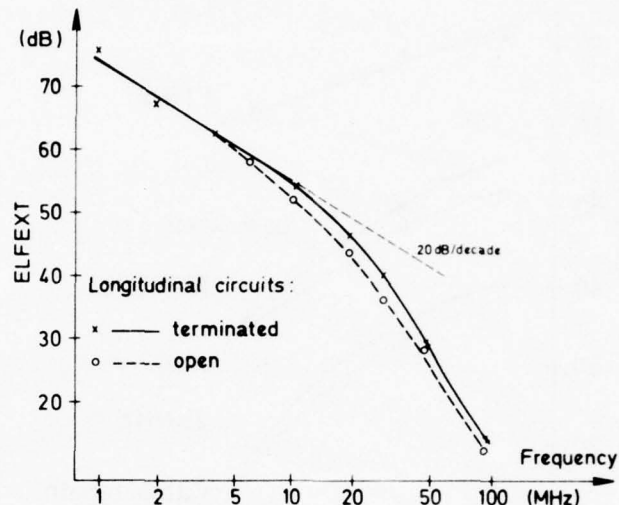


Fig. 11. Average far end crosstalk as a function of frequency.

The results show up to 4 dB difference between the case where all longitudinal circuits are properly terminated and the case where longitudinal circuits are left open. Thus it is advantageous to terminate longitudinal circuits at frequencies above 5 MHz.

8.3. Variations of crosstalk versus cable length

Average far end crosstalk in three cables has been calculated for different cable lengths. The result is shown in fig. 12.

At 1 MHz deviations from the usual 10 dB/decade variation are insignificant. Higher frequencies show steeper variations with cable length. This is probably due to multiple crosstalk coupling combined with lower attenuation in longitudinal circuits. It is demonstrated that scaling of measurements from one cable length to another at high frequencies must be performed with great care.

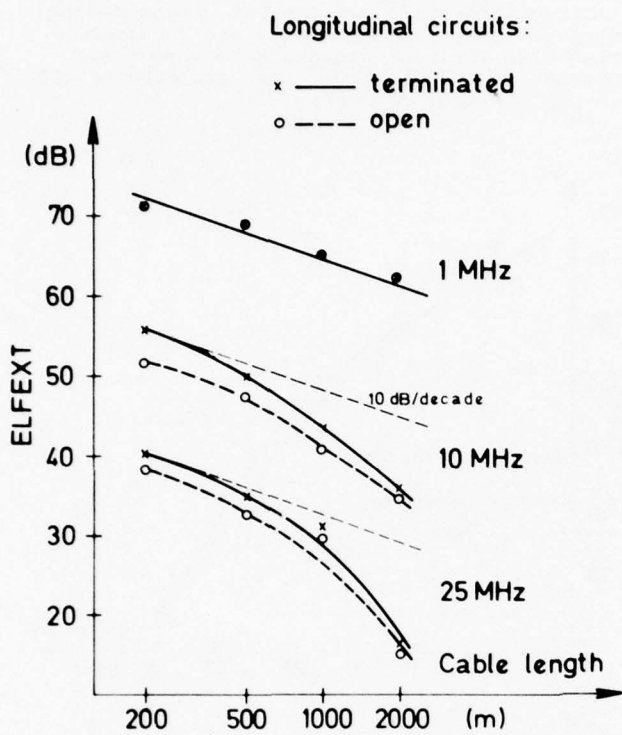


Fig. 12. Average far end crosstalk as a function of a cable length.

9. CONCLUSION

An accurate method for calculating crosstalk in balanced pair cables has been presented. The method calculates specific cables, and it is shown how a realistic cable may be represented on a computer. Both cabling effects and production tolerances are taken into account.

Necessary computing time is large and increases rapidly for increasing number of pairs. The method can be used for crosstalk calculations in cables having up to ten pairs by introducing a few simple modifications.

Calculations have been performed only for a simulated cable containing 3 pairs, but the results show full agreement with the general relationships observed in practical cables. Both near end and far end crosstalk show correct order of magnitude and correct variations with cable length and frequency. Thus the model is a realistic representation of a real cable.

Results show that far end crosstalk in the 3 pair cable for frequencies above 10 MHz increases much faster than 20 dB/decade with frequency and 10 dB/decade with cable length. It is also predicted that the main contribution to crosstalk in practical cables is caused by deviations from ideal twisting, and that a 20 dB improvement of far end crosstalk at 1 MHz may be reached by narrowing the pro-

duction tolerances.

The model may be used for different purposes. Results obtained by means of less accurate methods can be checked. The model makes it possible to look into many of the mechanisms present in balanced pair cables. Production tolerances may be varied and even set to zero. Many experiments of this type would be expensive or impossible to carry out using practical cables in the laboratory. By means of this method we intend to reduce the necessary number of prototype cables in the development of a new cable.

ACKNOWLEDGEMENT

This project has been initiated and supported by the Norwegian Telecommunications Administration, Research Establishment. The author wishes to thank the Telecommunications Administration for the permission to publish it, Dr. T. Røste and Dr. T.A. Ramstad for many helpful discussions during the project and J. Støbakk for programming the methods.

REFERENCES

- [1] N. Holte: Measurements of cable geometry by means of photographic methods, internal communication (in Norwegian).
- [2] H. Singer et al.: A charge simulation method for the calculation of high voltage fields, Paper T 74085-7, IEEE PES Winter Meeting, New York, Jan 27-Feb 1 1974.
- [3] Clements et al.: Computation of the Capacitance Matrix for Systems of Dielectric-Coated Cylindrical Conductors, IEEE Trans. on Electromagnetic compatibility, Vol. EMC-17, No 4, 1975.
- [4] T.A. Lenahan: The theory of uniform Cables Part II: Calculation of charge components, Bell syst. tech. journ. Vol 56, No 4, Apr. 1977, pp 611-625.
- [5] Wilhelm Klein: Die Theorie des Nebensprechens auf Leitungen, Springer Verlag, Berlin 1955.
- [6] H.A. Wheeler: Formulas for the Skin Effect, Proc of the IRE, Sept. 1942, pp 412-424.
- [7] V. Alessandrini et al.: The skin effect in multiconductor systems, Int. J. Electronics, 1976, Vol 40, No 1, pp 57-63.
- [8] S.O. Rice: Steady state solutions of transmission line equations, Bell syst. tech. journal, Vol 20, No 2, April 1941, pp 131, 178.
- [9] H. Cravis and T.V. Crater: Engineering of T1 Carrier System Repeatered Lines, Bell syst. techn. journ. March 1963, pp 431-486.

[10] N. Holte: A statistical model for calculation of crosstalk in a balanced pair cable, 25th Int Wire & Cable symp., Cherry Hill, N.J., Nov 1976, pp 25-31.

[11] N.A. Strakhov: Crosstalk on multipair cable - Theoretical aspects, National telecommunications Conf., Nov. 1973, pp 881-887.

[12] M. Yotsuya, S. Minematsu and A. Itoh: An approach to crosstalk coupling reduction of pair type cable, Int. Wire and Cable symposium, Atlantic City, Dec. 1974, pp 182-193.

[13] R.L. Svarts: Crosstalk on Cables: A communication Theoretic Approach, IEEE trans. on electromagnetic compatibility, Vol EMC 14, No 2, May 1972, pp 64-67.

[14] A. Papoulis: Probability, Random Variables and Stochastic processes. McGraw-Hill, New York, 1965.

APPENDIX 1

Direct far end crosstalk voltage x_T in a cable is the sum of crosstalk contributions from each element of the cable

$$x_T = \sum_{i=1}^N x_i \quad (1.1)$$

Each element has been drawn at equal probability among M representative elements. Far end crosstalk contribution y_i from each representative element has zero mean and variance σ^2 , and different elements are statistically independent.

If n_i specimens of element number i have been chosen the sum is:

$$x_T = \sum_{i=1}^M n_i y_i \quad (1.2)$$

For a given choice of representative elements the average crosstalk power is:

$$\bar{x}_T^2 = \sum_{i=1}^M \sum_{j=1}^M n_i n_j \bar{y}_i \bar{y}_j = \sum_{i=1}^M n_i^2 \bar{y}_i^2 = \sum_{i=1}^M n_i^2 \sigma^2 \quad (1.3)$$

The probability of selecting exactly i specimens of a specific representative element is given by the binomial distribution:

$$P_i = \binom{N}{i} \left(\frac{1}{M}\right)^i \left(\frac{M-1}{M}\right)^{N-i} \quad (1.4)$$

Averaging (1.3) over all possible choices of representative cable elements, mean crosstalk power is found:

$$E(x_T^2) = \sum_{i=0}^N P_i i^2 \sigma^2 = \frac{\sigma^2}{M^{N-1}} \sum_{i=1}^N \binom{N}{i} (M-1)^{N-1} i^2 \quad (1.5)$$

By means of numerical calculations we have found that this sum equals:

$$E(x_T^2) = \frac{(N+M-1)N}{M} \sigma^2 \quad (1.6)$$

Average crosstalk in dB:

$$\alpha_{ELFEXT} = -10 \lg E(x_T^2) = -10 \lg \frac{(N+M-1)N}{M} - 20 \lg \sigma \\ = -10 \lg \frac{(N+M-1)N}{M} + \sigma_{ELFEXT} \quad (1.7)$$



Nils Holte
Electronics Research
Laboratory
The University of
Trondheim
N-7034 Trondheim-NTH
Norway

Nils Holte received his M.Sc. in 1971 and his Dr.ing. degree in 1976 both from the University of Trondheim. He was at the University of Trondheim, department of Electrical engineering from 1970 to 1974 and joined Electronics Research Laboratory in 1975. He has worked on different projects in filter design, digital transmission systems and cable design.

A STATISTICAL METHOD FOR DETERMINING CUSTOMER
NOISE DUE TO WIRE PAIR UNBALANCES

By

D. S. Wilson

Bell Laboratories
Whippany, N. J. 07981

Abstract

Each component of a subscriber loop circuit exhibits certain unbalance properties. The interaction of the series resistive and shunt capacitive unbalances of the wire pair are studied, assuming perfectly balanced terminations. A Monte Carlo approach is used to generate statistical data on subscriber loop balance for large variations in the statistics of the unbalance parameters. It is shown that random splicing of cable reels improves the noise performance of installed cable. Computed balance levels are in excellent agreement with measurements made on cable installed in the field.

Introduction

Each component of a subscriber loop circuit exhibits certain unbalance properties. A program is underway to understand how these unbalances affect overall noise performance. The long term objective of the study is to determine if the present balance requirements for components are reasonable and to determine the costs of meeting noise objectives.

As part of this study, the interaction of the various unbalances in the loop circuit has been investigated. It is important to determine the contribution of each component to the overall noise performance. A statistical model has been developed as a necessary step in characterizing the economic impact of balance requirements and noise objectives.

The loop circuit consists of a wire pair, terminated at the central office (CO) on one end and the customer station set at the other. Two types of wire pair unbalances are relevant: the series resistive unbalance and the shunt capacitive unbalance (to ground). The battery supply relay at the CO can have both resistive and inductive unbalances in the two relay windings. The blocking capacitors located at the CO can also be unbalanced.

At the customer location, unbalances to ground can usually be ignored since there is normally no intentional path to ground

there. However, if one of the protectors at the customer location develops a leakage path to ground, a performance-degrading effect can result. Ringers associated with party lines can also result in performance-affecting unbalances at the customer location.

Normally the customer termination has a large impedance to ground.* This large impedance is essential in order to limit the currents to ground. When these currents are too large, unbalance effects in the loop circuit are magnified, and subscriber noise increases.

This paper focuses on wire pair unbalances. The interaction of the resistive series and the shunt capacitive unbalances are investigated assuming that there are no unbalances at the terminations at either end of the loop circuit -- neither at the CO nor at the customer location. A statistical model based on normal distributions for both the resistive and capacitive unbalances is developed. A Monte Carlo approach is used to generate the statistics of metallic noise present at the customer station set. Cumulative distributions of this noise data are presented for wide ranges of both resistive and capacitive unbalance parameters. As a test case of the applicability of the model, measurements made on new cable installed at North Madison, Connecticut, are analyzed.

Theoretical Approach

Deterministic Model

The solution of any circuit problem, such as the circuit of interest in this study (Figure 1), involves the solution of a system of differential equations subject to certain boundary conditions. In inductive interference problems, the dependent variables of interest are the longitudinal voltages and currents (between tip and ring to ground), and the

* The objective is 10 MΩ.

metallic or differential mode voltages and currents. The conversion of longitudinal signals resulting from power line induction into metallic signals by means of unbalances present in the circuit is known as longitudinal-to-metallic conversion (L/M).

One technique for the solution of L/M problems is application of cascaded circuit theory.¹ In this theory the longitudinal and metallic (LM) response at the far end of a cascade of linear components, under arbitrary conditions of exposure and component unbalance is found in terms of the LM response at the near end. The theory requires that the electrical characteristics of each component of the cascade be known.*

For a single component, such as the wire pair under consideration in Figure 1, no cascading formulas are required. The solution to this circuit problem is obtained by solving the following differential equations written in matrix notation:

$$\frac{d}{dx} \begin{bmatrix} V_1(x) \\ V_2(x) \\ I_1(x) \\ I_2(x) \end{bmatrix} = - \begin{bmatrix} 0 & 0 & Z_1 & 0 \\ 0 & 0 & 0 & Z_2 \\ Y+Y_1 & -Y & 0 & 0 \\ -Y & Y+Y_2 & 0 & 0 \end{bmatrix} \begin{bmatrix} V_1(x) \\ V_2(x) \\ I_1(x) \\ I_2(x) \end{bmatrix} + \begin{bmatrix} \epsilon(x) \\ \epsilon(x) \\ 0 \\ 0 \end{bmatrix}, \quad (1)$$

This equation has the general form:

$$\frac{d}{dx} T(x) = AT(x) + E(x)$$

The solution of the initial value problem for a wire pair of length ℓ is

$$T(\ell) = e^{A\ell} \left[T(0) + \int_0^{\ell} e^{-Ax} E(x) dx \right] \quad (2)$$

where the matrix exponential e^A is the state transition matrix of (1).² In our problem, the boundary conditions are obtained by expressing Ohm's Law at each terminal. This enables us to eliminate current as an unknown, resulting in a 2-point boundary value problem. The unknowns are the longitudinal voltages at

the ends of the line which are obtained from

$$\begin{bmatrix} V_1(\ell) \\ V_2(\ell) \\ \frac{V_1(\ell) - V_2(\ell)}{r_L} \\ \frac{V_2(\ell) - V_1(\ell)}{r_L} \end{bmatrix} = e^{A\ell} \begin{bmatrix} V_1(0) \\ V_2(0) \\ \frac{-V_1(0)}{r_1} \\ \frac{-V_2(0)}{r_2} \end{bmatrix} + \int_0^{\ell} e^{-Ax} E(x) dx, \quad (3)$$

a system of four linear equations in the four unknown voltages. Solution of this system of equations is further discussed in Appendix A.

All impedances at the CO and at the customer location in Figure 1 are assumed to be perfectly balanced. The only unbalances in the circuit are the series resistive unbalance and the shunt capacitive unbalance of the wire pair, ΔR in Ω/mi and ΔC in pF/mi , respectively:^{*}

$$\Delta R = R_2 - R_1$$

$$\Delta C = C_{2g} - C_{1g}$$

Here the subscripts 1 and 2 refer to the two wires of the pair and R and C_g are the resistance in Ω/mi and the capacitance to ground in pF/mi , respectively.

The power influence is assumed to be uniformly distributed throughout the exposure for each frequency of the power spectrum. The magnitude of the exposure at each frequency was chosen in accordance with a noise survey conducted in 1972.³ The assumed "canonical spectrum," based on this survey contains only the fundamental and the odd harmonics thereof, and shows the voltage falling off as $1/N^2$ from the 60 Hz voltage, where N is the order of the harmonic.

The computer program calculates the LM response at the ends of the circuit at each frequency in the spectrum of the exposure. The noise across the customer telephone set is expressed in terms of a balance level (loop or circuit balance in dB) which is defined as

* The output LM responses are given in terms of the input LM responses and the exposure to which the component is subjected.

* $Z_1 = R_1, Y_1 = \frac{1}{j\omega C_{1g}}$, etc.

$$\text{bal(dB)} = 20 \log_{10} \left(\frac{V_L}{V_M} \right),$$

where V_M and V_L are the magnitudes of the metallic and longitudinal voltages, respectively, at the customer location.

The human ear is more sensitive to some noise frequencies than to others. Such differences in the human ear response as well as differences in the response of the telephone set are taken into account by so-called C-message weighting. Appendix B contains a short discussion of C-message weighting and describes how C-message weighted metallic and longitudinal voltages, V_M' and V_L' , are computed from the single frequency results. A new balance level (loop or circuit balance in dB, C-message weighted) is now defined which is independent of frequency and which is representative of the effective noise at the customer's telephone set:

$$\text{BAL(dB, C-message)} = 20 \log_{10} \left(\frac{V_L'}{V_M'} \right).$$

Large values of balance number, BAL, correspond to a well-balanced circuit with V_M' small (low subscriber noise) in comparison to V_L' . C-message weighted balance numbers are plotted in Figure 2 as a function of capacitive unbalance, ΔC . Each curve corresponds to a fixed value of resistive unbalance, ΔR .

Statistical Model - Monte Carlo Method

The deterministic model provides the answer to the following question: A subscriber loop consists of a wire pair with fixed values of resistive and capacitive unbalance and no other unbalances in the loop; what is the balance of the circuit, and what subscriber noise would one expect to find in a given inductive environment?

A more important problem is the following: Using the statistics of resistive and capacitive unbalance for multipair cables, determine the statistics of loop balance and customer noise for the subscriber loop.

A simplified flow diagram of the statistical procedure is shown in Figure 3. The method uses the deterministic model as its foundation as values of loop balance, for fixed values of ΔR and ΔC , are computed and stored. These fixed values of ΔR and ΔC , are selected by the computer according to

prescribed probability distributions.* For the purpose of the analysis, representative distributions were chosen. After enough values of loop balance have been generated, the stored data is, itself, statistically analyzed. This procedure of problem solving comes under the general heading of Monte Carlo simulation.⁴

Two important aspects of the Monte Carlo technique, as employed here, will now be examined. The first of these is the normality of the computer-selected values of ΔR and ΔC . The question is -- are the computer-chosen values normally distributed, with the correct mean and standard deviation? The second aspect concerns the convergence of the final loop balance or noise distribution to its "true" distribution; how many iterations or data points are required to obtain a given desired accuracy?

Computer-generated values of resistive unbalance are plotted on probability paper in Figure 4. The computer was programmed to generate values of ΔR normally distributed about a mean μ_R of zero and having a standard deviation σ_R of 2.2 Ω/mi . The computer-generated data approximates a normal distribution (straight line fit) with a mean and a standard deviation of .04 Ω/mi and 2.18 Ω/mi , respectively. The sensitivity of loop balance to variations in ΔR and ΔC does not require any closer agreement than is achieved here.

For the question of convergence, cumulative distributions of loop balance are plotted in Figure 5, for the first 25, 50, 100 and 200 data points. The standard deviation for the resistive and capacitive unbalances are 2.2 Ω/mi and 100 pF/kft, respectively. Changes of about 0.5 dB result from increasing the number of data points from 100 to 200. On the basis of these and similar curves for other unbalance parameters, it was decided to use 100 data points to generate loop balance distributions. The balance numbers read from such curves are estimated to be accurate to within ±0.5 dB.

* Normal probability distributions about zero mean values were initially chosen. This choice is excellent for resistive unbalances. It is also a good assumption based on an analysis of a small sample of capacitive unbalance data. It has also been assumed that resistive and capacitive unbalances are independent. These assumptions are not limitations of the computer simulation; other distributions can be handled equally well.

Results and Discussion

Cumulative distributions of subscriber noise can now be obtained for the subscriber loop of Figure 1 with $l = 15$ kft for ranges of unbalance parameters of the wire pair. Variations with the standard deviation of capacitive unbalance, σ_C , are given in Figure 6.* For these curves, the standard deviation of the resistive unbalance, σ_R , is kept fixed at $\sigma_R = 2.2 \Omega/\text{mi}$ (chosen as a representative value of resistive unbalance); the means of both unbalance distributions are zero.

For the $\sigma_C = 200 \text{ pF/kft}$ curve, the 80 percentile point corresponds to a loop balance of 73 dB. This means that, if the wire pairs have the unbalance statistics which correspond to this curve ($\sigma_C = 200 \text{ pF/kft}$, $\sigma_R = 2.2 \Omega/\text{mi}$), then 80% of the circuits can be expected to have loop balances that are less than 73 dB for the assumed "canonical" power spectrum.

The cumulative distributions of Figure 6 are used to plot the percentile curve of Figure 7. These curves give the variations in loop balance statistics with variations in the standard deviation of the capacitive unbalance for a fixed σ_R of $2.2 \Omega/\text{mi}$. For example, the median (50 percentile) value of loop balance varies from 69 dB to 63 dB as σ_C varies from 50 pF/kft to 250 pF/kft; the 10 percentile value goes from 62 dB to 56 dB over the same range of σ_C values.

Variations with the standard deviation of the resistive unbalance are given in Figure 8. For these cumulative curves σ_C is kept fixed at 120 pF/kft (chosen as a representative value of capacitive unbalance), while the means of the unbalance distributions are again zero. The percentile curves for these cumulatives are plotted in Figure 9.

The statistics of loop balance presented in Figures 6 through 9 are summarized in Table 1. Included in this table are the computations of the means and standard deviations of loop balance for the indicated unbalance parameters.

Two examples are presented here which illustrate the balance numbers which are typical for a 15 kft wire pair with uniformly distributed unbalances and under uniform exposure. These balance numbers

will be compared to those computed in the next section where the unbalances are not uniformly distributed, but are due to the random splicing of several cable reels.

For both examples the standard deviation of the resistive unbalance is chosen to be $2.2 \Omega/\text{mile}$. A standard deviation of 117 pF/kft (capacitive unbalance) yields median and 10 percentile balance numbers of 67 dB and 60 dB, respectively. If the capacitive unbalance is increased to 180 pF/kft, the median and 10 percentile balance numbers are reduced to 65 dB and 58 dB, respectively.

Unbalance Statistics of an Installed, Multi-Segmented Cable

The unbalance statistics for multipair cables presented in the previous section are for reels of cable right off the production line. The changes that can occur when reels of cable are spliced together in a field installation is the subject of the present section. The section will conclude with a comparison of the theory with experimental measurements made when new reels of cable were installed at North Madison, Connecticut.

When color-coded wire pairs from consecutive manufacturing runs are spliced together, there is a tendency for the uniformity of the cable parameters, including unbalance, to be maintained. Uniformity of cable properties would make it difficult to distinguish this composite cable from one made during a single continuous manufacturing run. The unbalance statistics given in the last section could then be used for the spliced cable; i.e., statistical properties such as the standard deviation of resistive unbalance in Ω/mi would not change.

On the other hand, if the reels of cable are completely independent of one another, splicing them together tends to cancel out unbalances from reel to reel. The unbalance statistics of the composite length of cable are better than for a single reel length.

This is shown in Appendix C where N equal and independent reel lengths are spliced together. Each reel of cable is assumed to have the same unbalance statistics, e.g., normally distributed resistive unbalance with mean equal to zero and standard deviation equal to σ (Ω/mi). It is shown that the resistive unbalance for the total cable length (in Ω/mi) is also normally distributed with mean equal to zero; however, the standard deviation of the composite cable, σ_N , is now given by:

$$\sigma_N = \frac{\sigma}{\sqrt{N}}$$

* All distributions in Figures 6 through 10 are C-message weighted.

TABLE 1
Statistics of Loop Balance
All Loop Balance (BAL) in dB

| $\sigma_R - \Omega/\text{mi}$ ($\mu_R = 0$) | $\sigma_C - \text{pF/kft}$ ($\mu_C = 0$) | BAL (mean) | BAL (Standard Deviation) | BAL 10%ile | BAL 25%ile | BAL median | BAL 75%ile |
|--|---|---------------|-----------------------------|---------------|---------------|---------------|---------------|
| 2.2 | 40 | 70.8 | 7.2 | 62.5 | 65.7 | 69.8 | 74.5 |
| 2.2 | 117 | 68.9 | 7.8 | 60.3 | 63.3 | 67.3 | 73.7 |
| 2.2 | 200 | 66.1 | 7.7 | 57.0 | 60.5 | 64.7 | 71.3 |
| 2.2 | 280 | 63.9 | 8.2 | 55.0 | 58.0 | 62.5 | 68.3 |
| 1.0 | 120 | 71.2 | 8.1 | 61.8 | 65.0 | 69.5 | 75.7 |
| 2.0 | 120 | 69.2 | 8.0 | 60.2 | 63.2 | 67.7 | 73.8 |
| 3.0 | 120 | 66.9 | 7.5 | 58.3 | 61.2 | 65.3 | 71.0 |
| 4.0 | 120 | 65.0 | 7.5 | 56.8 | 59.7 | 63.5 | 68.5 |
| 6.0 | 120 | 62.0 | 7.2 | 54.0 | 56.8 | 60.7 | 65.8 |

The standard deviation (or the spread) of the resistive unbalance is reduced by a factor equal to the square root of the number of cables spliced together.

A computer program was developed to determine the improved balance due to splicing of cable reels. This program was applied to one of the two examples discussed in the previous section. The results are shown in Figure 10 and are summarized in Table 2. The total cable length in each case is 15 kft. consisting of N random segments of equal length. Note that the first few randomizations are the most effective in improving the loop balance.

TABLE 2
Improved Balance Due To Random Splicing*

| NUMBER OF RANDOM SEGMENTS | BALANCE (dB) | | | |
|---------------------------|--------------|------------|--------|--------|
| | MEAN | STAN. DEV. | MEDIAN | 10%ILE |
| NO RANDOMIZATION | 68.9 | 7.8 | 67.0 | 60.0 |
| 4 | 72.7 | 7.1 | 71.5 | 64.0 |
| 8 | 75.3 | 6.5 | 74.5 | 67.5 |
| 12 | 77.1 | 6.0 | 76.0 | 70.0 |

* Total cable length in each case is 15 kft consisting of N random segments of equal length. For each segment, $\sigma_C = 117 \text{ pF/kft}$ and $\sigma_R = 2.2 \Omega/\text{mi}$.

The two cases described above yield the extremes in the values of the standard deviation, σ_N , for the composite cable.

For the reels of cable not completely independent, σ_N will lie between these two values:

$$\frac{\sigma}{\sqrt{N}} < \sigma_N < \sigma.$$

A few general statements can be made about the manufacture and installation of different types of cables. One would expect complete independence for spliced reels of PULP cable because it is not normally color-coded.* Since cable reels are often selected from the cable yard more or less at random to fill a customer's order, one would also expect independence of cable reels in the manufacture and installation of most PIC and waterproof cable.

Some degree of independence may even result because of the manufacturing process. An example of one randomizing mechanism is the periodic replacement of spools of twisted pairs (only about five reels of cable can be made from one set of spools). It may be possible to assume a high degree of independence for all reels of cable.

Application to North Madison, Connecticut

A new No. 2 ESS office was installed in North Madison, Connecticut⁵ to serve the extremities of three existing step-by-step

* Bundle identification by color-coding does not alter the situation.

offices (Guilford, Madison and Clinton). Two new UNIGAUGE (26 gauge), cable runs were installed in the east and west directions from the ESS office to meet up with existing cable runs to N. Clinton and N. Guilford, respectively. Each of these new cable runs was approximately 4.5 miles in length.

Before cutover of the new office, transmission measurements were made on the new cable runs. In particular, loop balance measurements were made using very well-balanced CO terminations, so that the data were indicative of the balance of the wire pairs alone.

Since some limited resistive unbalance data were available from the N. Clinton cable, it was this cable which was chosen for analysis. The standard deviation of the resistive unbalance was found to be 0.84 Ω/mi , a factor of about 2.6 smaller than the expected unbalance for this type of cable. It is assumed that this factor is due to the randomization process discussed in the previous section.* Although no capacitive unbalance data were taken at North Madison, one would expect a similar randomization in the capacitive unbalance statistics. The computer program for random splicing of cable reels was applied to the N. Clinton cable. The cumulative distribution, assuming 7 random segments, is plotted in Figure 11. Also shown in the figure is the cumulative distribution of the measured values of loop balance for a randomly selected sample of 57 out of a total of 600 subscriber lines. The agreement between the measured balance data and loop balance, as predicted by the model, is excellent.

Concluding Remarks

A model is developed for determining subscriber loop balance due to fixed resistive and capacitive unbalances of the wire pair. The terminations at the CO and customer locations are assumed to be perfectly balanced.

A Monte Carlo approach is then used to generate statistical data on loop balance for normally distributed resistive and capacitive unbalances of the wire pair. Subscriber loop balance statistics are given for a range of the unbalance parameters.

* For complete independence of the individual reels of cable, $\sqrt{N} = 2.6$ or $N = 6.8$. This suggests that perhaps 6 or 7 reels of cable were used for this cable run. This is consistent with the fact that the average distance between splice points is less than one mile.

Two examples are presented which illustrate the balance numbers which are typical for a 15 kft. wire pair with uniformly distributed unbalances and under uniform exposure. For both examples the standard deviation of the resistive unbalance is chosen to be $2.2 \Omega/\text{mile}$. A standard deviation of 117 pF/kft (capacitive unbalance) for the first example yields median and 10 percentile balance numbers of 67 dB and 60 dB, respectively. If the capacitive unbalance is increased to 180 pF/kft, the median and 10 percentile balance numbers are reduced to 65 dB and 58 dB, respectively.

Cable unbalance statistics are given for reels of cable right off the production line. It is shown that these are worst case numbers. When reels of cable are spliced together in an installation, unbalances tend to cancel out from reel to reel. The unbalance statistics of the composite length of cable are better than for a single reel length. If σ (Ω/mi) is the standard deviation for a single reel length, it is shown that the standard deviation of a composite cable of N equal and independent reel lengths, σ_N (Ω/mi), is given by:

$$\sigma_N = \frac{\sigma}{\sqrt{N}} .$$

A computer program was developed to determine the improved balance due to random splicing of cable reels. This program was applied to one of the two examples discussed above. For twelve random segments the median and 10 percentile balance numbers for a capacitive unbalance of 117 pF/kft improve to 76 dB and 70 dB, respectively.

The techniques developed in this paper are used to analyze loop balance measurements made on new cable installed at North Madison, Connecticut. Excellent agreement is obtained between measured balance data and balance predicted by the model.

A final comment is in order: The wire pair is a well-balanced component in the subscriber loop. It has been mentioned how unbalances at the customer location, such as carbon block leakage resistances and party line ringers, can seriously degrade service. Unbalances at the CO, especially the battery supply relay, can be even worse offenders.

The balance achieved by the wire pair, with perfectly balanced terminations at both ends, can be considered to be the ultimate or limiting balance of the subscriber loop. Used as a standard of excellence, it is important to have the balance of the wire pair as high as

possible. This is necessary to maintain the present high quality of subscriber loops. And it will be even more important in the future as the inductive environment becomes increasingly hostile.

References

1. W. N. Bell, B.S.T.J. article, in preparation.
2. E. A. Coddington & N. Levinson, Theory of Ordinary Differential Equations, New York, McGraw-Hill, 1955.
3. D. N. Heirman, Time Variations and Harmonic Content of Inductive Interference in Urban/Suburban and Residential/Rural Telephone Plants, IEEE Transaction on Communications, Vol. Com-23, No. 12, December, 1975.
4. N. P. Buslenko, et al., The Monte Carlo Method, Pergamon Press, 1966.
5. H. J. Beuscher, L. W. Richards, No. 2 ESS Design for Operation in High 60-Hz Induction Environments, Conference Record National Telecommunications Conference, 1976, Vol. II., p. 28.1, November, 1976.

Appendix A

Solution of the Wire Pair Differential Equations

The matrix, A , of equation (2) is a constant matrix, and e^A is the state transition matrix of the differential equations (1). Because of the form of A , the solution of the determinant $|(A - \lambda I)| = 0$ for the eigenvalues of A , yields eigenvalues of the form $\pm\lambda_1$, $\pm\lambda_2$.

Since every matrix satisfies its characteristic equation (Cayley-Hamilton Theorem), any power of A can be realized as a linear combination of I , A , A^2 , and A^3 , in which case

$$e^{A\xi} = \sum_{m=0}^{\infty} \frac{A^m}{m!} \xi^m = \sum_{m=0}^3 a_m(\xi) A^m \quad (A1)$$

But $\pm\lambda_1$, and $\pm\lambda_2$ satisfy (A1) by definition; hence the $a_m(\xi)$'s satisfy

$$\begin{bmatrix} 1 & \lambda_2 & \lambda_2^2 & \lambda_2^3 \\ 1 & -\lambda_2 & \lambda_2^2 & -\lambda_2^3 \\ 1 & \lambda_1 & \lambda_1^2 & \lambda_1^3 \\ 1 & -\lambda_1 & \lambda_1^2 & -\lambda_1^3 \end{bmatrix} \begin{bmatrix} a_0(\xi) \\ a_1(\xi) \\ a_2(\xi) \\ a_3(\xi) \end{bmatrix} = \begin{bmatrix} e^{\lambda_2 \xi} \\ e^{-\lambda_2 \xi} \\ e^{\lambda_1 \xi} \\ e^{-\lambda_1 \xi} \end{bmatrix} \quad (A2)$$

Equation (A2) has a unique solution under the reasonable hypothesis of $\lambda_1 \neq \lambda_2$, $\lambda_1 \lambda_2 \neq 0$. The solution is

$$a_0(\xi) = \frac{\lambda_2^2 \cosh \lambda_1 \xi - \lambda_1^2 \cosh \lambda_2 \xi}{\lambda_2^2 - \lambda_1^2} \quad (A3a)$$

$$a_1(\xi) = \frac{\lambda_2^3 \sinh \lambda_1 \xi - \lambda_1^3 \sinh \lambda_2 \xi}{\lambda_1 \lambda_2 (\lambda_2^2 - \lambda_1^2)} \quad (A3b)$$

$$a_2(\xi) = \frac{\cosh \lambda_2 \xi - \cosh \lambda_1 \xi}{\lambda_2^2 - \lambda_1^2} \quad (A3c)$$

$$a_3(\xi) = \frac{\lambda_1 \sinh \lambda_2 \xi - \lambda_2 \sinh \lambda_1 \xi}{\lambda_1 \lambda_2 (\lambda_2^2 - \lambda_1^2)} \quad (A3d)$$

The characterization of a wire pair is now complete since

$$e^{A\xi} = \sum_{m=0}^3 a_m(\xi) A^m \quad (A4)$$

and the column vector

$$\int_0^\xi e^{-Ax} E(x) dx \quad (A5)$$

can be determined for suitably chosen $E(X)$.

Appendix B

C-Message Weighting

Noise at some frequencies is more disturbing to the subscriber than at others. The C-message weighting curve is a measure of the difference of the combined response of the human ear and the telephone set to noise at different frequencies. The curve peaks at 1000 Hz, making this frequency the most disturbing to the subscriber. It falls off at lower frequencies so that, for example, a 200 Hz tone of a given power is 25 dB less disturbing than a 1000 Hz tone of the same power. The fall-off is less rapid at frequencies above 1000 Hz -- to -3 dB at 3000 Hz, and to -30 dB at 5000 Hz.

A factor, $\lambda(f.)$, based on the C-message curve, is defined in order to appropriately weight the single frequency metallic and longitudinal voltages:

$$v_M' = \sqrt{\sum_{i=1}^n \lambda(f_i) v_M^2(f_i)}$$

and

$$v_L' = \sqrt{\sum_{i=1}^n \lambda(f_i) v_L^2(f_i)}.$$

where the i index runs over the single frequencies and the metallic and longitudinal voltages already computed at these frequencies.

The C-message weighted balance number is then defined as follows:

$$\text{BAL(dB, C-message)} = 20 \log_{10} \left(\frac{v_L'}{v_M'} \right).$$

This balance number is frequency-independent and is more representative of the effective noise at the customer's telephone set than the single frequency result.

Appendix C

Unbalance Statistics of an Installed, Multi-Segmented Cable

A total of N reel lengths of cable are spliced together to make up a composite cable. Let

$\Delta R_i \equiv R_{i2} - R_{i1}$, be the resistive unbalance of the i^{th} cable section in Ω/mi , and

$\bar{R}_i \equiv$ average resistance for a single wire of the i^{th} cable section in Ω/mi .

Then the total resistive unbalance of the composite cable is given by:

$$\Delta R_T = (R_{12} - R_{11}) + (R_{22} - R_{21}) + \dots + (R_{N2} - R_{N1}).$$

Also, the average resistance of a single wire through the composite cable is given by:

$$\bar{R}_T = \bar{R}_1 + \bar{R}_2 + \dots + \bar{R}_N.$$

Assumption 1: The average resistance of each cable section are equal, i.e., $\bar{R}_1 = \bar{R}_2 = \dots = \bar{R}_N$. This would be true, e.g., if the sections were of equal length and the same gauge.

With this assumption

$$\bar{R}_T = N \bar{R}_1 = N \bar{R}_1.$$

The percent resistive unbalance of the composite cable is then given by

$$\begin{aligned} \frac{\Delta R_T}{\bar{R}_T} \times 100 &= \frac{1}{N} \left(\frac{R_{12} - R_{11}}{\bar{R}_1} \times 100 \right) + \dots \\ &\quad + \frac{1}{N} \left(\frac{R_{N2} - R_{N1}}{\bar{R}_1} \times 100 \right). \end{aligned}$$

But each of the bracketed terms on the right (excluding, for the moment, the factor $\frac{1}{N}$) is just the percent resistive unbalance of a wire pair from a single reel of cable. Considered as random variables, these terms are normally distributed with zero means and standard deviations, σ_1 .

The random variable is still normally distributed upon multiplication by the factor $\frac{1}{N}$. The new means are again zero, but the standard deviations are now $\frac{1}{N} \sigma_1$.

Finally, the sum of normally distributed random variables (as given by the last equation above) is, itself, normally distributed. The mean of the sum, in the present case, is again zero. The standard deviation of the sum, σ_T , which is now the standard deviation for the composite cable, is given by:

$$\sigma_T^2 = \left(\frac{\sigma_1}{N} \right)^2 + \left(\frac{\sigma_2}{N} \right)^2 + \dots + \left(\frac{\sigma_N}{N} \right)^2.$$

Assumption 2: The standard deviations of the individual cable sections are equal, i.e., $\sigma_1 = \sigma_2 = \dots = \sigma_N$.

With this assumption:

$$\sigma_T^2 = N \left(\frac{\sigma_1}{N} \right)^2 = \frac{\sigma_1^2}{N}$$

and

$$\sigma_T = \frac{\sigma_1}{\sqrt{N}}$$



Daniel S. Wilson
Bell Laboratories
1 Whippny Road
Whippny, N. J.
07981

Cornell. He was on the faculty of the Polytechnic Institute of Brooklyn from 1959 - 1968, first as a Research Associate in Plasma Physics and later as Professor of Aerospace Engineering. He joined Bell Laboratories in 1968 and for several years investigated the effects of electromagnetic radiation due to nuclear detonations (EMP) on communication systems. More recently, he has worked on Inductive Interference problems, specializing in the balance of telephone circuits and its relation to noise performance.

Mr. Wilson received his degrees in Physics: his B.S. degree from Northwestern University and his M.S. and PH.D. from

FIG. 1 SUBSCRIBER LOOP CIRCUIT

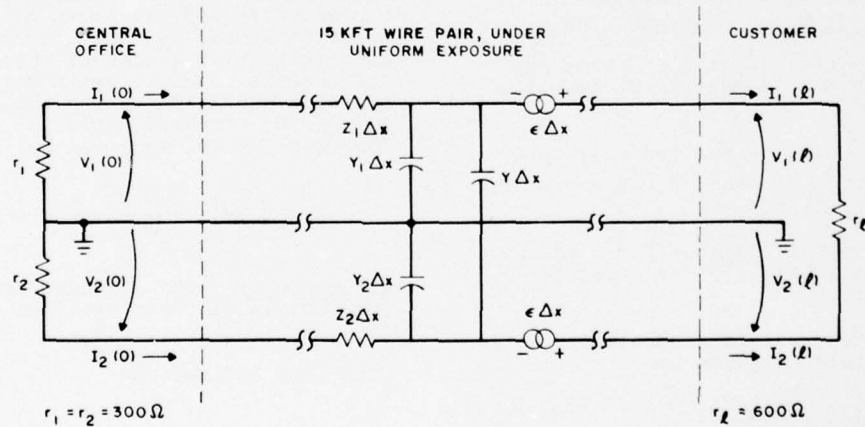


FIG. 2 LOOP BALANCE AS A FUNCTION
OF WIRE PAIR UNBALANCES
(C MESSAGE WEIGHTED)

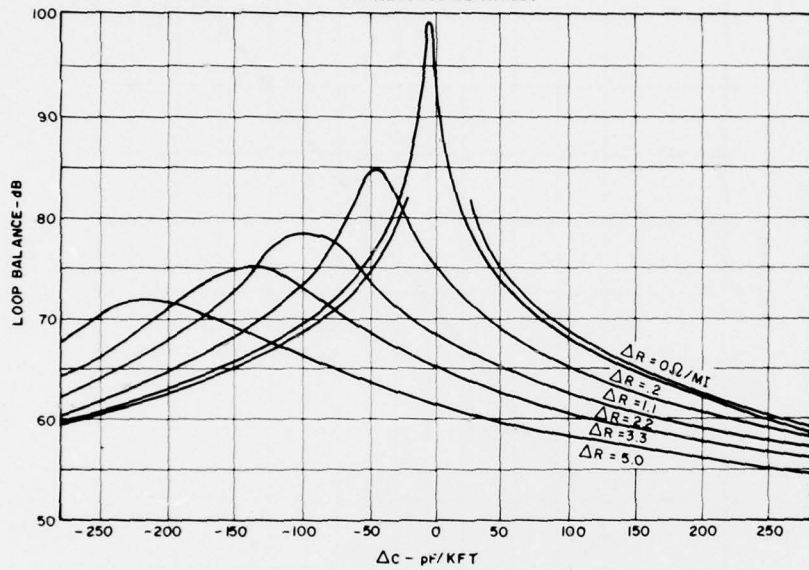


FIG. 3 STATISTICS OF LOOP BALANCE BY
MONTE CARLO SIMULATION

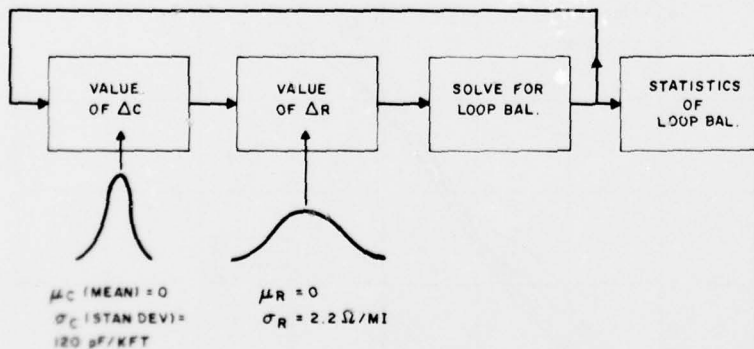


FIG. 4 DISTRIBUTION OF COMPUTER GENERATED
VALUES OF RESISTIVE UNBALANCE

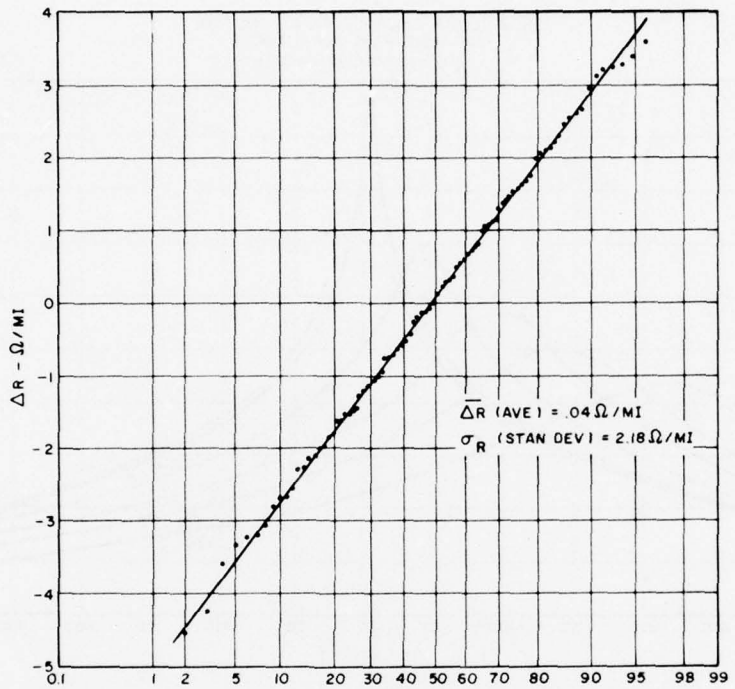


FIG. 5 VARIATIONS OF THE CUMULATIVE
DISTRIBUTION WITH THE NUMBER
OF SAMPLE POINTS

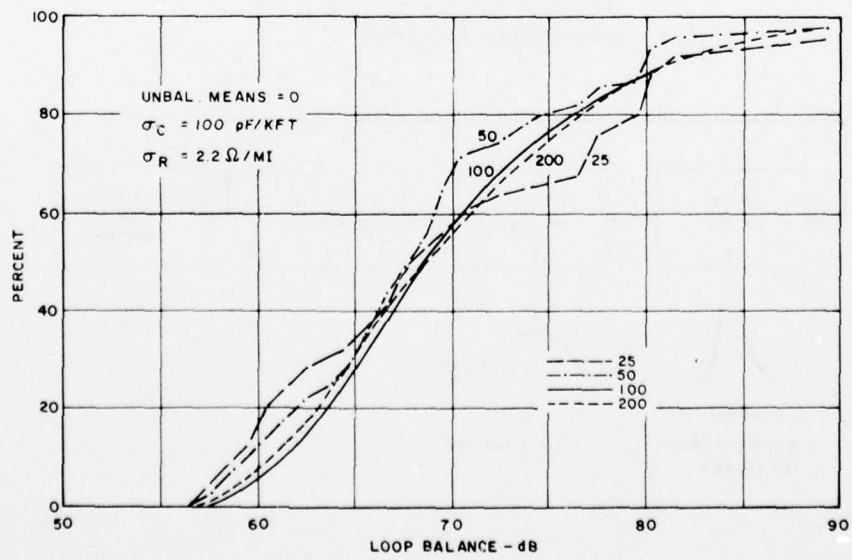


FIG. 6 CUMULATIVE DISTRIBUTIONS - VARIATIONS
WITH STANDARD DEVIATION OF CAPACITIVE
UNBALANCE

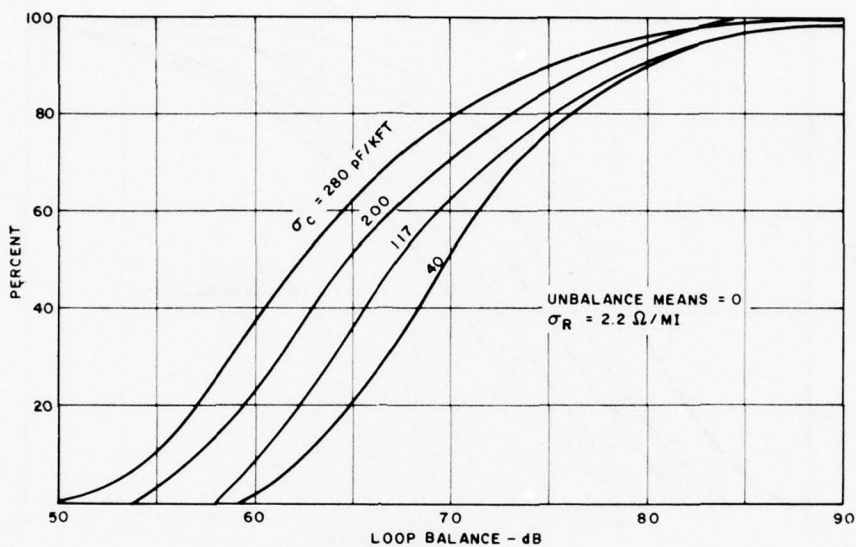


FIG. 7 STATISTICS OF LOOP BALANCE AS A
FUNCTION OF STANDARD DEVIATION
OF CAPACITIVE UNBALANCE

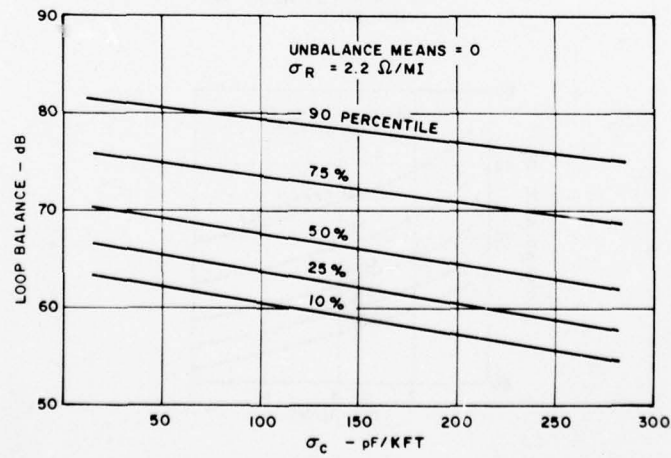


FIG. 8 CUMULATIVE DISTRIBUTIONS - VARIATIONS
WITH STANDARD DEVIATION OF RESISTIVE
UNBALANCE

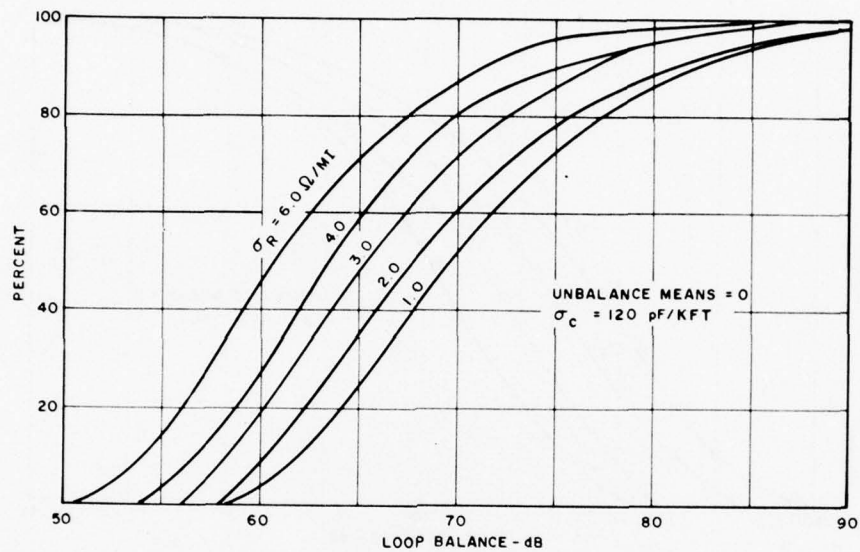


FIG. 9 STATISTICS OF LOOP BALANCE
AS A FUNCTION OF STANDARD
DEVIATION OF RESISTIVE
UNBALANCE

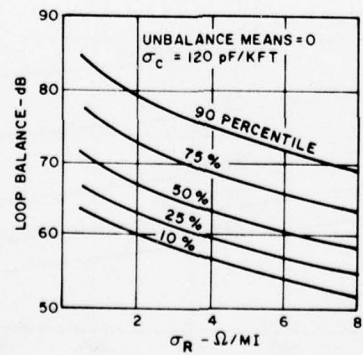


FIG. IO IMPROVEMENT IN LOOP BALANCE DUE TO
RANDOM SPLICING OF CABLE REELS

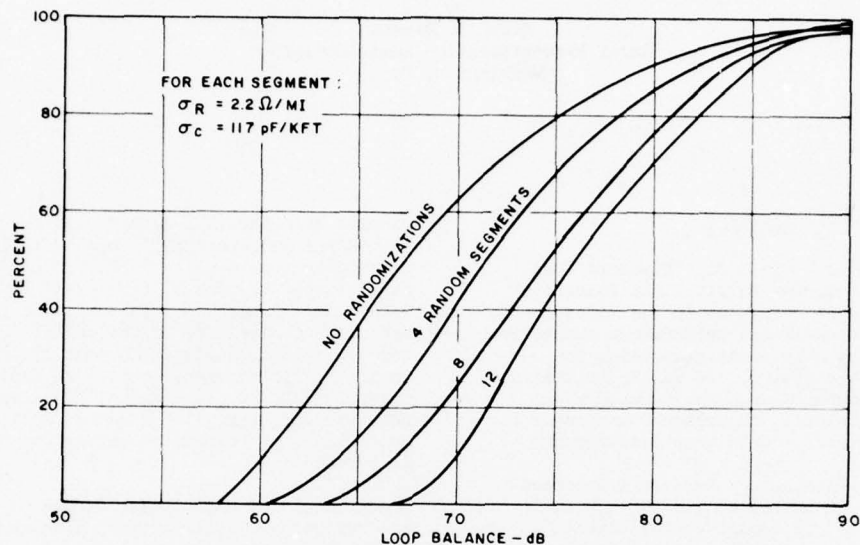
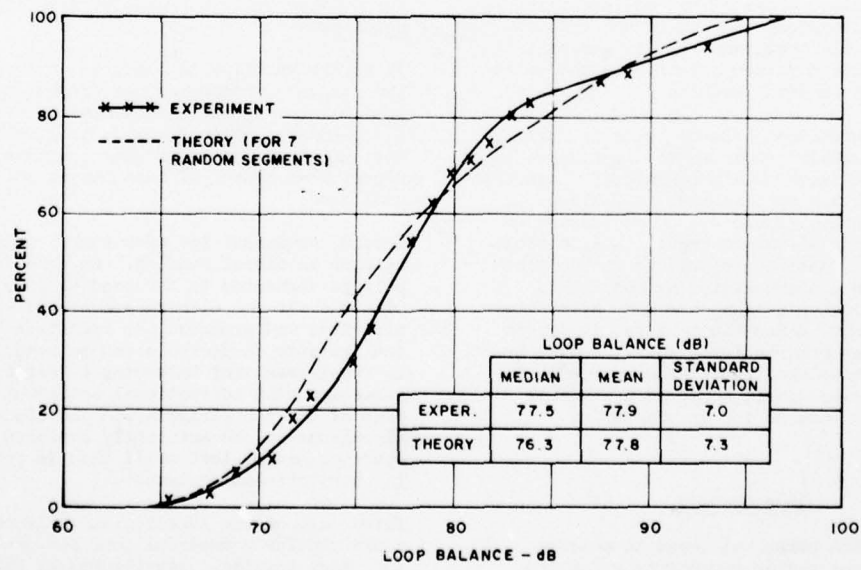


FIG. II THEORY VERSUS EXPERIMENT—
NORTH MADISON, CONNECTICUT



DETERMINING MAGNITUDE OF CABLE CAPACITANCE AND
RESISTANCE UNBALANCE FROM LONGITUDINAL BALANCE
MEASUREMENTS

by
Myron L. Brewer
Rural Electrification Administration
Washington, D. C.

ABSTRACT

IEEE Standard Number 455-1976, "Standard Test Procedure for Measuring Longitudinal Balance of Telephone Equipment Operating in the Voice Band", was developed to determine performance characteristics of various components comprising the telecommunications system. It was found that a relationship exists in a given cable between longitudinal unbalance, capacitance unbalance to ground, and resistance unbalance measurements.

Measurement of resistance unbalance and capacitance unbalance in paired communications cable has often resulted in controversies between manufacturers and purchasers. Resolution of these problems often leads to considerable effort and expense which could be better utilized elsewhere. If such controversies could be reduced everybody would benefit.

Measurement of capacitance unbalance to ground requires expensive equipment operated by a skilled technician. Some of the equipment is designed for laboratory use and is not entirely suitable for field measurements. As a result questions are often raised relative to the validity of field measurement results.

Results of longitudinal balance tests on cable have been accurately converted to capacitance to ground and resistance unbalance values. Inclusion of objective values for longitudinal balance in cable specifications could reduce occurrence of the controversies discussed above. All testing, both in the manufacturing plant and in the field would adhere to a standardized method. This would improve communications and help eliminate misunderstanding. Since the test set is direct reading and does not require either the time or skill needed for a wheatstone bridge or capacitance unbalance bridge it could be a valuable quality control tool in the manufacturing facility.

INTRODUCTION

Early in 1976 REA personnel began to measure various telephone system components using the method described in IEEE Standard 455-1976. The objective of the measurements was to compare

results from the IEEE method with those of the method for measurement of longitudinal unbalance previously recommended by REA. A project was also started to compare results of longitudinal balance measurements on cable in the field with the noise performance of the cable. Since it was not possible to access both ends of installed cable the field measurements were made using a one-port mode of measurement. The far end of the pair was open circuited for the shunt measurements and short circuited and grounded for series measurements.

Measurements of capacitance unbalance to ground and resistance unbalance were also made at each location. Comparative analysis of recorded results from the tests indicated a direct relationship between the one-port longitudinal balance open and short circuited measurements and capacitance to ground and resistance unbalance measurements. Investigation was initiated to determine if measurement of longitudinal balance of cable might provide a practical method for proving cable conformance with applicable specifications.

There are benefits that may be derived from using the standard method for measurement of longitudinal balance in cable measurement. First, the equipment for making longitudinal balance measurements is less expensive than equipment for making direct measurement of capacitance and resistance unbalance.

Second, equipment for measurement of longitudinal balance is direct reading. As soon as the cable pair is connected to the sending port of the set with the far end either open circuited or short circuited and grounded the magnitude of longitudinal balance in decibels can be read. There is no requirement for balancing a bridge as is necessary with conventional equipment for measurement of the two parameters. Therefore longitudinal balance can be accurately measured by an operator having less skill than is required with the conventional equipment.

Third, use of the longitudinal balance test set could provide a powerful tool for quality assurance testing. Results may be obtained in less time than is required with bridge equipment now used. The economics of quality assurance

testing is always an important manufacturing consideration.

A strong point in favor of adopting longitudinal balance tests for cable is the possible elimination of differences of opinion between the purchaser and manufacturer of cable after delivery. The source of these differences is often a question of the validity of measurement results provided by the purchaser. The question of validity is usually due to the complexity of the measurement, especially measurement of capacity unbalance. Use of a direct reading test set would remove the complexity from the measurement. Both manufacturer and purchaser would be speaking the same language because results of measurements would be obtained in the same way with the same test set. Travel and remeasurement to confirm validity of data could thus be reduced.

DATA ANALYSIS

First, it is desirable to establish the direct relationship between results of longitudinal balance measurements (far end open circuited and short circuited grounded) and capacitance and resistance unbalance measurements. The following discussion will develop this relationship. All measurements of capacitance unbalance to ground one-port short and one-port open circuit longitudinal balance were made with all other pairs in the cable grounded and thus at the same potential as the shield. This procedure was used because most cable specifications have capacitance to ground objectives. All longitudinal balance measurements were made at 900 Hertz to satisfy the desire of the IEEE that measurements be made at a harmonic of 60 Hertz. Capacitance unbalance to ground measurements were made at 1000 Hertz.

Derivation of the longitudinal balance equation is shown in Appendix A. Unbalance values have been computed with the equation for 4,998 feet of 22 gauge, plastic insulated, jelly filled cable. Computations are based on 100 pF/kf capacitance to ground unbalance and 0.1Ω/kf resistance unbalance.

Graphic Analysis

There are several methods for analyzing results from longitudinal balance measurements of cable pairs. The method chosen will, to some degree, be determined by the objectives being pursued. The simplest method is to establish a minimum balance objective for satisfactory operational performance. All results are then compared to this objective.

Averaging results in decibels will not provide the same results as averaging actual values of capacitance and resistance unbalance. The purpose of this paper is to establish the relationship between one-port longitudinal balance (shunt and series) measurements and capacitance and resistance unbalance. No attempt will be made to establish the best method of statistical analysis.

Once the decibel unbalance is calculated for a

single unbalance such as 100 pF/kilofoot for capacitance unbalance to ground or 0.1Ω/kilofoot for resistance unbalance the other values for that length cable may be found graphically. Establish this point (either capacitance or resistance) on semi-log paper. When plotting capacitance unbalance the 10pF point will be 20 dB higher and the 1000 pF point 20 dB lower. With resistance unbalance the 0.01 point will be 20 dB higher and the 1Ω point will be 20 dB lower. Figure 3 shows the plot for capacitance unbalance of the 4,998 foot reel of cable for which values have been calculated in Appendix A. Figure 4 shows the plot for resistance unbalance of the same reel. Results of measurement of capacitance to ground and resistance unbalance on twenty-five pairs of this cable have been plotted on these figures to show the excellent fit between calculated and actual values.

Analysis From Computed Balance for Cable Length

The same information can be obtained mathematically, rapidly and accurately. When the decibel balance has been calculated for a given length of cable having a 100pF/kilofoot unbalance, capacitance unbalance to ground can be derived from measured results of one-port shunt (open circuited) longitudinal balance measurements with the equation:

$$C_u = 100 \left(\frac{10^{X_1}}{10^{X_2}} \right) \quad (1)$$

Where:

C_u = Capacitance unbalance in pF/kf
 X_1 = Longitudinal balance for 100pF/kf in (dB/20)
 X_2 = Measured longitudinal balance in (dB/20)

Resistance unbalance for the total cable length has been used as a reference since in manufacturing plants it is usually obtained by measuring the tip and ring conductors and computing the difference. The percentage is then calculated and compared to specification requirements. When the decibel balance has been calculated for a given length of cable having a 0.1 ohm/kilofoot unbalance, resistance unbalance for the total length may be derived from measured one-port series (short circuited and grounded) longitudinal balance with the equation:

$$R_u = \frac{f}{10} \left(\frac{10^{X_3}}{10^{X_2}} \right) \quad (2)$$

Where:

R_u = Resistance unbalance of total length
 f = Cable length in kilofeet
 X_2 = Measured longitudinal balance in (dB/20)
 X_3 = Longitudinal balance for 0.1Ω/kf in (dB/20)

There is a simple method for calculating the resistance unbalance from the short circuit

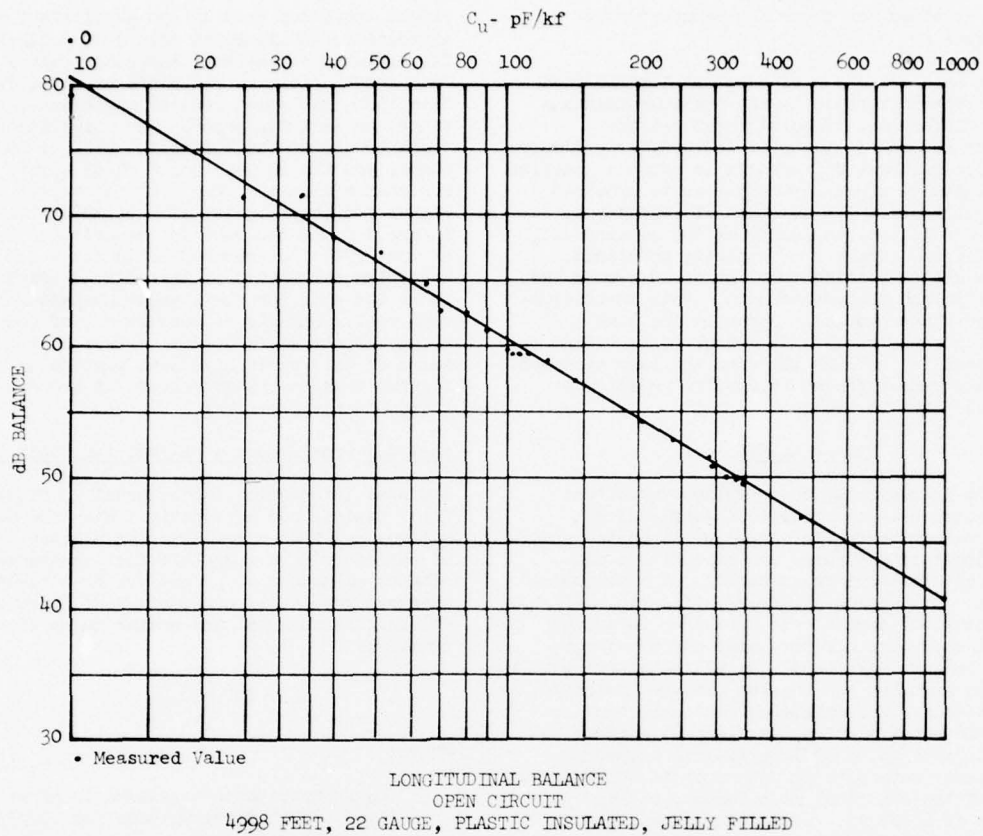


FIGURE 3

grounded measurement. Since the shunt impedance (tip to ring) is the same as the open circuit impedance it is much higher than the conductor resistance. An equation based on conductor resistance only can be developed since frequency does not affect the results. This formula is:

$$R_U = \frac{(368 + R)^2}{(368 \times 10^{12})} \quad (3)$$

Where:

- R_U = Resistance unbalance total length
- R = Average loop resistance/2
- X_2 = Measured longitudinal balance in (dB/20)

Tables 1 and 2 show the measured shunt and series longitudinal balance respectively for twenty-five pairs of the 4,998 foot cable for which calculations have been included in this paper. Actual measured capacitance to ground and resistance unbalance are also shown together with calculated values from formulas (1), (2) and (3).

This method has one undesirable feature. Compu-

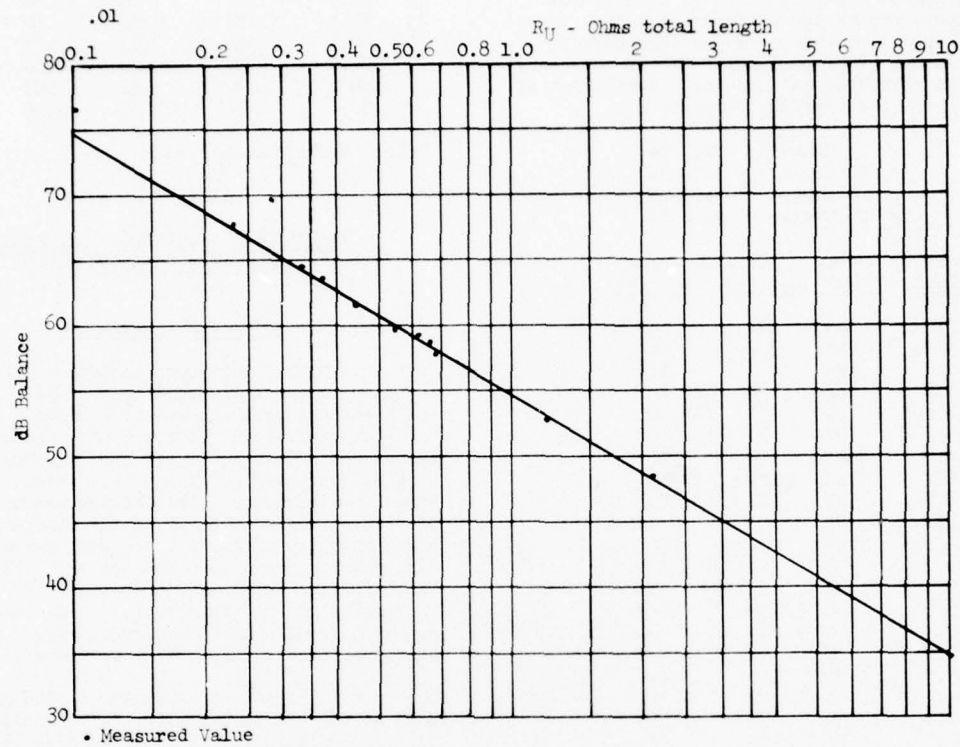
tation of Z_{oc}, Z_{sc} and longitudinal balance would be required for each new length of cable to be measured. This would make it difficult to work with.

Analysis From Longitudinal Balance for One Kilofoot Length

No convenient and simple formula has been found for analysis of results from measured shunt and series longitudinal balance when the decibel balance for a one kilofoot cable length is known. Formulas have been developed for approximating these values with reasonable accuracy. Accuracy of these approximations of less than 1 percent error holds to 6.5 kilofoot maximum cable lengths for all cable gauges.

Beyond this length the error increases rapidly so these should be calculated individually when needed. The 6.5 kilofoot maximum length would appear to cover the majority of the cable lengths manufactured.

Value of capacitance to ground unbalance may be found by the equation:



LONGITUDINAL BALANCE SHORT CIRCUITED AND GROUNDED
4998 FEET, 22 GAUGE, PLASTIC INSULATED, JELLY FILLED
FIGURE 4

$$C_U = 100 \left(\frac{(10^{X_1}) (1/\ell + K_f \ell)}{10^{X_2}} \right) \quad (4)$$

Where:

- C_U = Capacitance unbalance in pF/kf
 ℓ = Length of cable in kilofeet
 X_1 = Longitudinal balance for 100 pF/kf
 in (dB/20)
 X_2 = Measured longitudinal balance in
 (dB/20)
 K_f = Constant for frequency measured:
 Frequency K_f
 900 Hz .0033
 1000 Hz .0039

Magnitude of resistance unbalance for the total length of the cable can be determined from the known balance for a one kilofoot cable with 0.1 ohm/kilofoot unbalance with the equation:

$$R_U = \ell \left(\frac{(10^{X_3}) (1/\ell + K_g \ell)}{10 (10^{X_2})} \right) \quad (5)$$

Where:

- R_U = Resistance unbalance of total length
 ℓ = Length of cable in kilofeet
 X_2 = Measured longitudinal balance in
 (dB/20)
 X_3 = Longitudinal balance for 0.1Ω/kf in
 (dB/20)
 K_g = Constant for cable gauge being meas-
 ured:

| Gauge | K_g |
|-------|--------|
| 19 | .00025 |
| 22 | .001 |
| 24 | .0027 |
| 26 | .0072 |

These equations may easily be programmed into calculators having program capability. Error is less than one percent when compared to results from rigorous computations.

Calculated values of capacitance to ground and resistance unbalance for the twenty-five pairs of the 4,998 foot cable using equations (1) and (4) have been included in Table 1 and (2), (3) and (5) in Table 2.

When using the method described above only a few known values are required. Series resistance is not a factor in open circuit longitudinal balance measurements to the maximum 6.5 kilofoot length. It is necessary to have only the reference balance for one kilofoot of cable at the desired frequency. For 900 and 1000 Hertz, they are:

| | |
|----------|---------|
| 900 Hz. | 73.6 dB |
| 1000 Hz. | 72.7 dB |

Objective values for short circuit longitudinal balance measurements are different for each cable gauge. There is no change due to frequency to the maximum 6.5 kilofoot length. It is necessary to have one reference balance for one kilofoot of cable for each cable gauge. They are:

| | |
|----------|---------|
| 19 Gauge | 71.7 dB |
| 22 Gauge | 72.1 dB |
| 24 Gauge | 72.5 dB |
| 26 Gauge | 73.2 dB |

| Pr. No. | Meas. dB Bal. | Meas. Cu/kf | Calc'd. Eq. (1) | Cu/kf Eq. (4) |
|------------|------------------|----------------|--------------------|------------------|
| 1 | 57.3 | 144 | 141 | 141 |
| 2 | 49.0 | 357 | 367 | 368 |
| 3 | 58.8 | 124 | 119 | 119 |
| 4 | 54.8 | 188 | 188 | 189 |
| 5 | 61.1 | 90 | 91 | 91 |
| 6 | 64.8 | 65 | 60 | 60 |
| 7 | 59.2 | 110 | 114 | 114 |
| 8 | 59.2 | 111 | 114 | 114 |
| 9 | 59.8 | 103 | 106 | 106 |
| 10 | 71.1 | 25 | 29 | 29 |
| 11 | 54.2 | 204 | 202 | 202 |
| 12 | 50.1 | 326 | 324 | 324 |
| 13 | 62.7 | 71 | 76 | 76 |
| 14 | 46.8 | 472 | 473 | 474 |
| 15 | 52.5 | 240 | 245 | 246 |
| 16 | 83.0 | 0 | 7 | 7 |
| 17 | 59.5 | 106 | 110 | 110 |
| 18 | 79.2 | 10 | 11 | 11 |
| 19 | 71.2 | 34 | 29 | 29 |
| 20 | 62.8 | 81 | 75 | 75 |
| 21 | 51.5 | 280 | 275 | 276 |
| 22 | 49.7 | 343 | 339 | 339 |
| 23 | 68.1 | 40 | 41 | 41 |
| 24 | 67.0 | 52 | 46 | 46 |
| 25 | 50.8 | 287 | 299 | 299 |

NOTE: Capacitance values in picofarads

TABLE 1

COMPARISON OF CAPACITANCE UNBALANCE
MEASUREMENTS AND CALCULATIONS

| Pr. No. | Meas. dB Bal. | Meas. R _u /Total | Calculated R _u /Total | | |
|------------|------------------|--------------------------------|----------------------------------|---------|---------|
| | | | Eq. (2) | Eq. (3) | Eq. (5) |
| 1 | 64.6 | .30 | .32 | .32 | .32 |
| 2 | 83.4 | .01 | .04 | .04 | .04 |
| 3 | 63.2 | .37 | .38 | .38 | .38 |
| 4 | 61.5 | .47 | .46 | .46 | .46 |
| 5 | 69.7 | .28 | .18 | .18 | .18 |
| 6 | 59.4 | .58 | .59 | .59 | .58 |
| 7 | 57.6 | .68 | .72 | .72 | .72 |
| 8 | 64.2 | .33 | .34 | .34 | .34 |
| 9 | 58.5 | .65 | .65 | .65 | .65 |
| 10 | 54.9 | .97 | .99 | .99 | .98 |
| 11 | 53.1 | 1.18 | 1.21 | 1.21 | 1.21 |
| 12 | 48.3 | 2.09 | 2.11 | 2.11 | 2.10 |
| 13 | 63.5 | .36 | .37 | .37 | .36 |
| 14 | 65.5 | .28 | .29 | .29 | .29 |
| 15 | 52.7 | 1.24 | 1.27 | 1.27 | 1.26 |
| 16 | 55.0 | .96 | .97 | .97 | .97 |
| 17 | 68.4 | .20 | .21 | .21 | .21 |
| 18 | 58.8 | .62 | .63 | .63 | .63 |
| 19 | 59.6 | .57 | .57 | .57 | .57 |

| | | | | | |
|----|------|------|------|------|------|
| 20 | 58.4 | .66 | .66 | .66 | .66 |
| 21 | 56.5 | .80 | .82 | .82 | .82 |
| 22 | 67.4 | .23 | .23 | .23 | .23 |
| 23 | 76.7 | .11 | .08 | .08 | .08 |
| 24 | 59.1 | .61 | .61 | .61 | .60 |
| 25 | 50.8 | 1.54 | 1.58 | 1.58 | 1.57 |

NOTE: Resistance values in ohms

TABLE 2

COMPARISON OF RESISTANCE UNBALANCE
MEASUREMENTS AND CALCULATIONS

POTENTIAL PROBLEMS

Even though excellent correlations have been found between results of longitudinal balance and unbalance measurements some problem areas have been detected. Others making these same measurements have indicated experiencing some problems but have not found the basic source. Based on experience gained during measurement of fifteen reels of cable at the manufacturing plants and two reels at an operating company warehouse the major problem appears to be in establishing the connection between the test equipment and the cable pair. Data obtained by a fourth manufacturer has been analyzed and the same problem discussed below was detected.

During this series of measurements the method used at the particular plant being visited for fanning and accessing the cable pairs was utilized. This was usually the method used in that plant for quality assurance measurements and permitted the completion of the required number of measurements in the allotted time. Connections to the pairs have been established by plug and jack, switches, alligator clips to terminal blocks, and alligator clips directly to the cable conductor.

Use of plugs and jacks seemed to produce the most reliable results if care was exercised. By twisting the plug slightly after insertion it was possible to determine if the connection was solid. If it was not the plug was removed and cleaned until a solid connection was made. Even then some variance could be seen at high balance readings or low capacitance and resistance unbalance readings. The problem could be detected regardless of the test being made. It was necessary to clean the plug after every four to six measurements.

When switches were used it was impossible to eliminate the problem completely. After extensive cleaning indication of poor connections became quite difficult to detect during measurements. Analysis of the data however revealed a significant variation with some of the switches due to poor connections.

Use of alligator clips connected either to terminal strips or cable conductors seemed to produce good results during measurement. In other words no variation was readily detectable

during the measurements. When results were analyzed there was significant variation between actual measured and calculated balance detected on many of the pairs measured indicating poor connections.

It becomes evident that extreme care must be used when establishing the test connections to cable conductors. At the voltage levels being measured a slight unbalance in the test connection can produce a significant variation in results. There is a possibility that this same problem is producing errors in quality assurance tests. Some method needs to be developed for establishing reliable connections to cable pairs for test purposes.

Another question which has been raised is how to determine whether the unbalance is on the tip or ring side of the cable pair. Most cable specifications have a requirement that distribution of capacitance and resistance unbalance be random between tip and ring conductors. This might easily be determined in a longitudinal balance test set designed to make longitudinal balance tests on cable. The use of switches to add a very small capacitance between tip and ring to ground and a small series resistor in series with the tip and ring conductor would quickly determine where the unbalance was. Improvement of longitudinal balance when one of the capacitors or resistors is switched in would indicate that conductor (tip or ring) has the lowest value of the parameter being measured (capacitance to ground or series resistance).

CONCLUSIONS

This paper has established the relationship of one-port open circuited and short circuited grounded longitudinal balance measurements to capacitance to ground and resistance unbalance. Adoption of longitudinal balance objectives in cable specifications would permit the use of a direct reading test set for both field and laboratory measurements. It also has promise in this application of being a powerful quality assurance tool.

An important advantage can be found when a purchaser finds a need to measure cable and discuss the results with a manufacturer. All tests would have been made in the same test configuration with a test set meeting the IEEE standard method. This could serve to minimize disagreements and doubts on both sides and result in significant monetary savings.

The problem of connecting of the cable pair to the test set common to all tests becomes more critical when very low voltage levels are involved and high degrees of balance are to be measured. Investigation is underway to determine how this connection can be established with minimum problem. Determination of the conductor which contains the unbalance does not appear to be a serious problem.

No attempt is made in this discussion to relate

results of longitudinal unbalance to cable performance in the field. Investigation of this relationship is in progress. A lot of ground has been covered, however, there are still additional areas to explore. Some tentative assumptions have been made but it is too early to present them.

ACKNOWLEDGMENT

The author wishes to extend thanks to Mr. Richard Campbell, Wilcom Products, Inc., and Mr. W. M. Haynes, Jr., South Central Bell, for their helpful discussions and contributions to the mathematics. Thanks are also due Mr. William Carroll, Carroll Communications Services, for his valuable assistance in completing the measurements. Special thanks are extended to REA for granting permission to pursue the investigation to conclusion.

REFERENCES

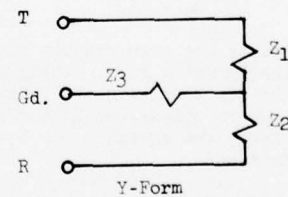
1. "Standard Test Procedure for Measuring Longitudinal Balance of Telephone Equipment Operating in the Voice Band" IEEE Standard Number 455-1976

APPENDIX A

LONGITUDINAL BALANCE

Test Specimen

A test specimen when measuring one-port longitudinal balance may be considered as a three-terminal circuit (tip, ring and ground). Any test specimen can thus be represented by three complex impedances in either Y or Delta form as shown in Figure 1.



OR

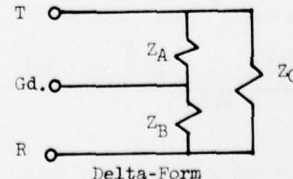


Figure 1

Longitudinal Balance Measurement

The IEEE Standard Driving Test Circuit connected to a Y-Form test specimen is shown in Figure 2.

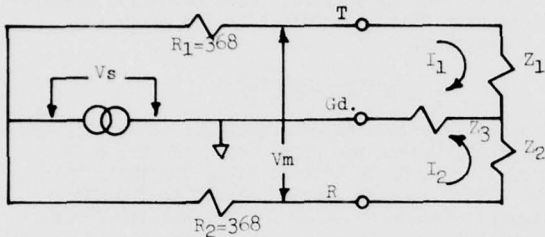


Figure 2

With I_1 & I_2 assumed as shown in Figure 1, the following equations can be written:

$$\begin{aligned} I_1 (R_1 + Z_1 + Z_3) &= V_s - I_2 Z_3 \\ I_2 (R_2 + Z_2 + Z_3) &= V_s - I_1 Z_3 \\ V_m &= I_1 Z_1 - I_2 Z_2 \end{aligned} \quad (6)$$

Solving these equations provides the Longitudinal Balance Ratio.

$$\frac{V_s}{V_m} = \frac{(Z_1 + Z_2)}{Z_1 - Z_2} \left(1 + \frac{Z_3}{R_1} \right) + R_1 + \frac{Z_1 Z_2}{R_1} + \frac{Z_1 Z_2}{Z_3} \quad (7)$$

The equivalent Delta form is:

$$\frac{V_s}{V_m} = \frac{(Z_A + Z_B)}{Z_B - Z_A} \left(1 + \frac{R_1}{Z_C} \right) + R_1 + \frac{Z_A Z_B}{R_1} + \frac{2 Z_A Z_B}{Z_C} \quad (8)$$

Some test specimens are more readily studied in Y form and others in Delta form. Cable as a test specimen seems to fit best with the Delta form. For convenience where comparison of a number of samples is required, the equation may be developed further by putting:

$$Z_A = Z - \frac{\Delta Z}{2}$$

$$Z_B = Z + \frac{\Delta Z}{2}$$

Where:

$$\begin{aligned} \Delta Z &= Z_A - Z_B \\ Z &= \frac{Z_A + Z_B}{2} \end{aligned}$$

Now, neglecting $(\Delta Z)^2$ terms this gives:

$$\frac{V_s}{V_m} = \frac{2Z}{\Delta Z} \left(1 + \frac{R_1}{Z_C} \right) + R_1 + Z^2 \left(\frac{1}{R_1} + \frac{2}{Z_C} \right) \quad (9)$$

Where:

$$R_1 = 368 \text{ ohms in every case.}$$

$$\text{Balance in dB} = 20 \log \left| \frac{V_s}{V_m} \right| \quad (10)$$

Combining equations (9) and (10) we get the following equation for computation of longitudinal balance measured by the one-port mode:

$$\text{Balance in dB} = 20 \log \left| \frac{2Z \left(1 + \frac{R_1}{Z_C} \right) + R_1 + Z^2 \left(\frac{1}{R_1} + \frac{2}{Z_C} \right)}{\Delta Z} \right| \quad (11)$$

Cable Pairs

The values for Z_A , Z_B and Z_C for the Delta form may be determined from the cable parameters for calculation of anticipated longitudinal balance readings. Sending-end impedance of a line with the far end open circuited is given by:

$$\begin{aligned} Z_{oc} &= Z_0 \coth \sqrt{\ell} \\ \text{Where: } Z_0 &= \sqrt{Z/Y} \approx \sqrt{\frac{R}{jwc}} \\ \sqrt{\ell} &= \sqrt{ZY} \approx \sqrt{jwcR} \end{aligned} \quad (12)$$

Assuming shunt conductance and series inductance are negligible, a reasonable approximation may be found by:

$$Z_{oc} = \sqrt{\frac{R}{jwc}} \coth \ell \approx \sqrt{jwcR} \quad (13)$$

Where:

$$\begin{aligned} R &= \text{Loop resistance/kf} \\ C &= \text{Mutual Capacitance/kf} \\ \ell &= \text{Length of cable in kilofeet} \\ w &= 2 \times \pi \times \text{frequency} \end{aligned}$$

One of fifteen reels of cable measured during this investigation contained 4,998 feet of 100 pair, 22 gauge, jelly filled plastic insulated cable. Primary parameters were assumed to be 15.7 nF/kilofoot mutual capacitance and 32.4 ohms/kilofoot loop resistance. Tests were made at 900 Hertz.

Computation by equation (13) using these values yields:

$$Z_{oc} = 53.98 - j 2253.89 \text{ ohms} = Z_A$$

Z_{oc} for a cable pair with 100 pF/kilofoot unbalance may be computed using a value of 15.6 nF/kilofoot mutual capacitance. Computation by equation (13) yields:

$$Z_{oc} = 53.98 - j 2268.33 = Z_B$$

This second calculation is made only to obtain ΔZ for use in computing longitudinal balance in decibels. Subtracting the first result from the second $\Delta Z = 0 - j 14.44$ ohms.

Mutual capacitance of a cable pair may be considered as one-half direct and one-half through ground. The three impedances of the Delta-form specimen may thus be shown as:

$$Z_A = Z_B = Z_{oc} = Z$$

Longitudinal Balance Measurement

The IEEE Standard Driving Test Circuit connected to a Y-Form test specimen is shown in Figure 2.

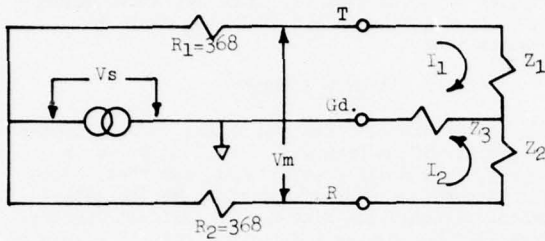


Figure 2

With I_1 & I_2 assumed as shown in Figure 1, the following equations can be written:

$$\begin{aligned} I_1 (R_1 + Z_1 + Z_3) &= V_s - I_2 Z_3 \\ I_2 (R_2 + Z_2 + Z_3) &= V_s - I_1 Z_3 \\ V_m &= I_1 Z_1 - I_2 Z_2 \end{aligned} \quad (6)$$

Solving these equations provides the Longitudinal Balance Ratio.

$$\frac{V_s}{V_m} = \frac{(Z_1 + Z_2)}{Z_1 - Z_2} \left(1 + \frac{Z_3}{R_1} \right) + \frac{Z_1 Z_2}{R_1 + R_2 + Z_3} \quad (7)$$

The equivalent Delta form is:

$$\frac{V_s}{V_m} = \frac{(Z_A + Z_B)}{Z_B - Z_A} \left(1 + \frac{R_1}{Z_C} \right) + \frac{Z_A Z_B}{R_1 + R_2 + Z_C} \quad (8)$$

Some test specimens are more readily studied in Y form and others in Delta form. Cable as a test specimen seems to fit best with the Delta form. For convenience where comparison of a number of samples is required, the equation may be developed further by putting:

$$\begin{aligned} Z_A &= Z - \frac{\Delta Z}{2} \\ Z_B &= Z + \frac{\Delta Z}{2} \end{aligned}$$

Where:

$$\begin{aligned} \Delta Z &= Z_A - Z_B \\ Z &= \frac{Z_A + Z_B}{2} \end{aligned}$$

Now, neglecting $(\Delta Z)^2$ terms this gives:

$$\frac{V_s}{V_m} = \frac{2Z}{\Delta Z} \left(1 + \frac{R_1}{Z_C} \right) + R_1 + Z^2 \left(\frac{1}{R_1} + \frac{2}{Z_C} \right) \quad (9)$$

Where:

$$R_1 = 368 \text{ ohms in every case.}$$

$$\text{Balance in dB} = 20 \log \left| \frac{V_s}{V_m} \right| \quad (10)$$

Combining equations (9) and (10) we get the following equation for computation of longitudinal balance measured by the one-port mode:

Balance in dB =

$$20 \log \left| \frac{2Z \left(1 + \frac{R_1}{Z_C} \right) + R_1 + Z^2 \left(\frac{1}{R_1} + \frac{2}{Z_C} \right)}{\Delta Z} \right| \quad (11)$$

Cable Pairs

The values for Z_A , Z_B and Z_C for the Delta form may be determined from the cable parameters for calculation of anticipated longitudinal balance readings. Sending-end impedance of a line with the far end open circuited is given by:

$$\begin{aligned} Z_{oc} &= Z_0 \coth \sqrt{\ell} \\ \text{Where: } Z_0 &= \sqrt{Z/Y} \approx \sqrt{\frac{R}{jwC}} \\ \sqrt{\ell} &= \sqrt{ZY} \approx \sqrt{jwCR} \end{aligned} \quad (12)$$

Assuming shunt conductance and series inductance are negligible, a reasonable approximation may be found by:

$$Z_{oc} = \sqrt{\frac{R}{jwC}} \coth \ell \sqrt{jwCR} \quad (13)$$

Where:

$$\begin{aligned} R &= \text{Loop resistance/kf} \\ C &= \text{Mutual Capacitance/kf} \\ \ell &= \text{Length of cable in kilofeet} \\ w &= 2 \times \pi \times \text{frequency} \end{aligned}$$

One of fifteen reels of cable measured during this investigation contained 4,998 feet of 100 pair, 22 gauge, jelly filled plastic insulated cable. Primary parameters were assumed to be 15.7 nF/kilofoot mutual capacitance and 32.4 ohms/kilofoot loop resistance. Tests were made at 900 Hertz.

Computation by equation (13) using these values yields:

$$Z_{oc} = 53.98 - j 2253.89 \text{ ohms} = Z_A$$

Z_{oc} for a cable pair with 100 pF/kilofoot unbalance may be computed using a value of 15.6 nF/kilofoot mutual capacitance. Computation by equation (13) yields:

$$Z_{oc} = 53.98 - j 2268.33 = Z_B$$

This second calculation is made only to obtain ΔZ for use in computing longitudinal balance in decibels. Subtracting the first result from the second $\Delta Z = 0 - j 14.44$ ohms.

Mutual capacitance of a cable pair may be considered as one-half direct and one-half through ground. The three impedances of the Delta-form specimen may thus be shown as:

$$Z_A = Z_B = Z_{oc} = Z$$

and

$$Z_C = 2Z_{OC} = 2Z$$

Balance equation (11) (for single port measurement) may be reduced, for application to cable pairs with the far end open, to:

$$\text{Balance in dB} = 20 \log \left| \frac{(Z_{OC}/368)^2 + 3Z_{OC} + 736}{\Delta Z} \right| \quad (14)$$

Using the values from the first Z_{OC} calculation above and ΔZ in formula (14) the anticipated one-port longitudinal balance in decibels for the 4,998 foot cable described above with 100 pF/kilofoot capacitance unbalance is found to be:

60.3 dB

With the far end of the cable pair short circuited and grounded the sending-end impedance is given by:

$$Z_{SC} = Z_O \tanh \sqrt{\frac{R}{jwC}} \ell \quad (15)$$

As with Z_{OC} shunt conductance and series inductance may be assumed to equal zero. A reasonable approximation may be found by:

$$Z_{SC} = \sqrt{\frac{R}{jwC}} \tanh \ell \sqrt{jwCR} \quad (16)$$

Substituting the same parameters used for calculation of Z_{OC} in formula (13) yields:

$$Z_{SC} = 161.82 - j 3.88 = Z_A$$

Recalculating for a cable pair with 0.1 ohm/kilofoot resistance unbalance by setting the loop resistance to 32.3 ohms/kilofoot yields:

$$Z_{SC} = 161.33 - j 3.85 = Z_B$$

Value for ΔZ is now found to be $0.499 - j 0.023$ ohms.

The direct impedance, Z_C , (across the pair tip to ring without going through ground) is the same as it was in the open circuit case. It is thus high enough to be negligible and may be neglected giving:

$$Z_A = Z_B = Z_{SC}/2$$

The balance formula (11) (for single port measurement) may now be reduced, for application to cable pairs with the far end short circuited and grounded, to:

$$\text{Balance in dB} = 20 \log \left| \frac{(Z_{SC}/1472)^2 + Z_{SC} + 368}{\Delta Z} \right| \quad (17)$$

The anticipated series longitudinal balance in decibels is now calculated by substituting the values for normal Z_{SC} (balanced pair) and ΔZ found above in Formula (12). For the 4,998 foot cable with 0.1 ohm/kilofoot resistance unbalance this is found to be:

60.8 dB



Myron L. Brewer
Rural Electrification
Administration
Washington, D. C. 20250

Myron L. Brewer was born in Lincoln, Nebraska on June 24, 1922. He joined General Telephone Company of California in 1947 and held several positions in their engineering department. In 1960 he joined the United States Military Mission to Greece as a consulting engineer for outside plant design and voice frequency transmission. Since 1968 he has been with the Rural Electrification Administration, Washington, D. C. as a Communications Specialist. He is assigned to the Transmission Branch of the Telephone Operations and Standards Division where his primary duties are development of standards and specifications related to voice frequency transmission and inductive coordination.

Mr. Brewer is a member of the Institute of Electrical and Electronics Engineers.

AD-A047 609 ARMY COMMUNICATIONS RESEARCH AND DEVELOPMENT COMMAND --ETC F/G 9/1
PROCEEDINGS OF INTERNATIONAL WIRE AND CABLE SYMPOSIUM (26TH) CH--ETC(U)
NOV 77 E F GODWIN

UNCLASSIFIED

NL

6 OF 6
AD
A047609



END
DATE
FILED
I- 78
DOC

AUTHOR INDEX

| | | | |
|----------------------|----------|-------------------|----------|
| Abadia, V. | 329 | Marechal, M. | 41 |
| Adams, G. C. | 356 | Matsuo, J. | 216 |
| Allen, D. B. | 239 | McDevitt, F. R. | 307 |
| Aono, T. | 32 | McManus, T. K. | 204 |
| Asai, T. | 32 | Medynski, R. L. | 269 |
| Bahder, G. | 380 | Mori, K. | 53 |
| Basch, E. E. | 287 | Ney, R. | 312 |
| Bascou, E. | 41 | Nishikawa, I. | 216 |
| Baum, W. | 385 | Nowak, G. H. | 343 |
| Beaudette, R. A. | 287 | Oh-e, S. | 87 |
| Belevitch, V. | 338 | Ohshima, H. | 102 |
| Beretta, G. | 228 | Ohtomo, S. | 87 |
| Beveridge, R. | 204 | Okada, M. | 1 |
| Bickel, G. W. | 293 | Olszewski, J. A. | 182, 380 |
| Bissell, D. R. | 156 | Orimo, K. | 11 |
| Blyler, L. L., Jr. | 300 | Parmar, D. S. | 367 |
| Bobo, J.-C. | 110 | Patel, A. | 83 |
| Brauer, M. | 24 | Peters, N. W. | 141 |
| Brewer, M. L. | 454 | Prósper, J. | 188 |
| Brownell, K. W., Jr. | 18 | Rautenberg, P. | 367 |
| Buckler, M. J. | 276 | Rebeille, J.-C. | 110 |
| Buerkle, D. H. | 110 | Reed, J. C. | 239 |
| Calzolari, P. | 228 | Sobia, R. | 24 |
| Faber, A. F. | 48 | Saito, Y. | 134 |
| Fasig, E. W., Jr. | 239 | Sakamoto, K. | 134 |
| Flegal, W. M. | 197 | Sakamoto, N. | 87 |
| Gesner, B. D. | 94 | Sakurai, T. | 216 |
| Gouldson, E. J. | 249 | Santana, M. R. | 276 |
| Groenendaal, G. C. | 338 | Sasaki, T. | 32 |
| Hanai, M. | 216 | Savage, J. P. | 420 |
| Hardin, T. G. | 420 | Schlang, P. | 367 |
| Hart, A. C., Jr. | 300 | Schleinitz, H. M. | 352 |
| Hauschildt, R. | 398 | Schmidt, G. A. | 161 |
| Hemmings, D. F. | 307 | Schumacher, W. L. | 362 |
| Hershey, H. C. | 249 | Shimada, S. | 134 |
| Hillerich, B. | 367, 373 | Shimano, T. | 11 |
| Hochon, B. L. | 110 | Shores, S. C. | 276 |
| Holte, N. | 428 | Silberhorn, A. | 385 |
| Hoshikawa, T. | 32 | Smith, E. E. | 249 |
| Hudson, J. A. | 119 | Smith, J. C. | 293 |
| Huszarik, F. A. | 62 | Soyka, R. | 281 |
| Hutson, H. M. | 18 | Sparkes, C. J. | 261 |
| Imaoka, T. | 87 | Spencer, H. J. C. | 149 |
| Kanda, K. | 87 | Still, M. | 385 |
| Kaufman, S. | 24 | Takemori, H. | 1 |
| Kawakubo, S. | 102 | Umetsu, T. | 53 |
| Kincaid, J. W., Jr. | 321 | Vogelsberg, D. | 127 |
| Kiss, K. D. | 68 | Vrieland, B. C. | 197 |
| Kracklauer, J. J. | 261 | Wilhelmi, G. J. | 293 |
| Kroplinski, T. F. | 24 | Williams, J. L. | 24 |
| Kumamaru, H. | 134 | Wilson, D. S. | 440 |
| Kusui, A. | 1 | Wilson, R. R. | 338 |
| Legg, R. E. | 261 | Wise, J. B. | 307 |
| Lewis, R. J. | 141 | Woollerton, G. R. | 249 |
| Long, A. K. | 119 | Yamaguchi, K. | 87 |
| Lynen, W. | 312 | Yamamoto, Y. | 216 |
| Malawer, E. G. | 68 | Yashiro, R. | 53 |
| | | Yoshikawa, T. | 87 |



INTERNATIONAL WIRE & CABLE SYMPOSIUM

SPONSORED BY U.S. ARMY ELECTRONICS COMMAND

14, 15 & 16 November 1978

Cherry Hill Hyatt House, Cherry Hill, N.J.

Please provide in the space below a 100-500 word abstract (12 copies) of a proposed technical paper on such subjects as design, application, materials, and manufacturing of Communications and Electronics Wire & Cable of interest to the commercial and military-aerospace industries. Such offers should be submitted no later than 7 April 1978 to the Commanding General, U.S. Army Electronics Command, Attn: DRSEL-TL-ME, Ft. Monmouth, NJ 07703.

Title: _____

Authors: _____

Company: _____

Address: _____

Stamp

Fold here

Stamp



Commanding General
U.S. Army Electronics Command
Att: AMSEL-TL-ME
Fort Monmouth, N.J. 07703

Fold here

UNCLASSIFIED

SECURITY CLASSIFICATION OF THIS PAGE (When Data Entered)

| REPORT DOCUMENTATION PAGE | | READ INSTRUCTIONS BEFORE COMPLETING FORM |
|--|-----------------------|--|
| 1. REPORT NUMBER N/A | 2. GOVT ACCESSION NO. | 3. RECIPIENT'S CATALOG NUMBER |
| 4. TITLE (and Subtitle) Proceedings of the 26th International Wire and Cable Symposium 1977 | | 5. TYPE OF REPORT & PERIOD COVERED Final 15-17 November 1977 |
| | | 6. PERFORMING ORG. REPORT NUMBER N/A |
| 7. AUTHOR(s) Various Chairman: Elmer F. Godwin | | 8. CONTRACT OR GRANT NUMBER(s) None |
| 9. PERFORMING ORGANIZATION NAME AND ADDRESS Xmsn & Electromech Dvc Team (DRSEL-TL-ME) Electronics Technology & Dvc Lab USA Communications Research & Development Command | | 10. PROGRAM ELEMENT, PROJECT, TASK AREA & WORK UNIT NUMBERS Proj. Element: 62705A Proj/Task: 1L1 62705 AH94 W1 01; Work Unit #: 012C8 |
| 11. CONTROLLING OFFICE NAME AND ADDRESS Xmsn & Electromech Dvc Team (DRSEL-TL-ME) Electronics Technology & Dvc Lab USA CORADCOM, Ft. Monmouth, NJ | | 12. REPORT DATE November 1977 |
| 14. MONITORING AGENCY NAME & ADDRESS (if different from Controlling Office) Same as 11 above. | | 13. NUMBER OF PAGES 463 |
| | | 15. SECURITY CLASS. (of this report) UNCLASSIFIED |
| | | 15a. DECLASSIFICATION/DOWNGRADING SCHEDULE N/A |
| 16. DISTRIBUTION STATEMENT (of this Report) Approved for Public Release: Distribution Unlimited. | | |
| 17. DISTRIBUTION STATEMENT (of the abstract entered in Block 20, if different from Report) | | |
| 18. SUPPLEMENTARY NOTES Proceedings of technical papers presented at 26th International Wire and Cable Symposium sponsored annually by the US Army Communications Research and Development Command. | | |
| 19. KEY WORDS (Continue on reverse side if necessary and identify by block number) Aerospace electronics, cable design, cable evaluation, cable manufacture, cable materials, cable performance, cable testing, electronic wiring, fiber optics, interconnections, military electronics, telephone communications, wire insulation, wire materials, wire testing. | | |
| 20. ABSTRACT (Continue on reverse side if necessary and identify by block number) The International Wire and Cable Symposium is the only symposium of its kind in the world. The proceedings include fifty-five (55) papers in the field of electrical and electronic wire and cable, covering design, materials, testing, evaluation, connections, splicing, installation, applications, fire retardancy, fiber optics, manufacturing, and processing. | | |